Procurement and management of quartzite in the Cantabrian Region:
The Middle and Upper Palaeolithic in the Deva, Cares and Güeña Valleys

Adquisición y Gestión de la cuarcita en la Región Cantábrica:
El Paleolítico medio y superior en las Cuencas del Deva, Cares y Güeña

Tesis doctoral
Alejandro Prieto de Dios
Directores:
Alvaro Arrizabalaga Valbuena
Iñaki Yusta Arnal

Septiembre, 2018

eman ta zabal zazu
Universidad del País Vasco
Euskal Herriko Unibertsitatea

eman ta zabal zazu

Universidad del País Vasco
Euskal Herriko Unibertsitatea

Departamento de Geografía, Prehistoria y Arqueología

Doctorado en Cuaternario: Cambios ambientales y huella humana

Tesis Doctoral

Procurement and management of quartzite in the Cantabrian Region: The Middle and Upper Palaeolithic in the Deva, Cares and Güeña valleys

Adquisición y Gestión de la cuarcita en la Región Cantábrica: El Paleolítico medio y superior en las Cuencas del Deva, Cares y Güeña

Tesis para optar al grado de doctor
Presentada por:

ALEJANDRO PRIETO DE DIOS

Dirigida por:
Alvaro Arrizabalaga Valbuena
Iñaki Yusta Arnal

Vitoria-Gasteiz, 2018

A Mis padres

A mi hermana

A Maite

ÍNDICE

SUPPLEMENTARY INFORMATION III

SUPPLEMENTARY INFORMATION IV

SUPPLEMENTARY INFORMATION V

SUPPLEMENTARY INFORMATION VI

SUPPLEMENTARY INFORMATION VII

AGRADECIMIENTOS

Las líneas que a continuación escribo están dedicadas a todas las personas que, en diferentes momentos, han sido parte de esta Tesis Doctoral. Sin ellas, este trabajo no había sido el mismo, sin ellas, hoy no sería la misma persona. A todas ellas, gracias.

A Álvaro Arrizabalaga tengo que agradecer que me hubiera convencido para venir por primera vez al País Vasco en el año 2009 a excavar los yacimientos que tantas buenas vivencias me han dado, en los que tanto he aprendido y en los que tantas personas he conocido. Por insistir en la realización del Máster de Cuaternario, por aceptar mi trabajo de fin de Máster, por aceptar la dirección de esta Tesis. Por disfrutar de la música juntos, por darme ánimos para seguir, por los consejos durante todo este periodo, por los cafés tomados, por los trabajos que hemos realizado. Por todo ello, muchas gracias.

A Iñaki Yusta, mi director, el que siempre tiene una mañana para mí en la que enseñarme cómo afrontar este trabajo, cómo ver el mundo a través de las piedras y la Geología. Por las mañanas para discutir acerca de la tesis, del tribunal, de los datos, de la fiabilidad del método. A hablar de Ciencia en mayúscula, a discutir de música, a plantear los futuros, a entender la investigación. Por todas las horas dedicadas en formarme delante de un microscopio, a entender las rocas a partir de sus características físicas. Por pensar y poner en práctica la inter-disciplinaridad, por las clases del Máster. Siempre estaré en deuda contigo. Muchas gracias, sin ti esta tesis no hubiera salido adelante.

Al Grupo de Investigación de Alto Rendimiento en Prehistoria (IT-622-13), enmarcado en el Departamento de Geografía, Prehistoria y Arqueología y dirigido por Javier Fernández Eraso, ha supuesto el marco perfecto para el desarrollo de esta investigación. Tanto por el apoyo económico, como por la utilización de las instalaciones allí existentes, gracias. También me gustaría agradecer a todos los miembros que conformamos dicho Grupo, por su acogida y su predisposición para conmigo.

A los cuatro proyectos en los que he participado y participo, muchas gracias por la red de contactos generada, las facilidades económicas aportadas, las reuniones mantenidas. Los proyectos son los siguientes: Entre el Ebro y el Garona, los Pirineos durante el Paleolítico y el Mesolítico, PALMESOPYR (CTP2012-R1). La ruta occidental del poblamiento de la Península Ibérica durante el Paleolítico medio y superior, PALEOGATE (HAR2014-53536-P). ¿Cómo, quién y dónde?: Variabilidad de comportamientos en la captación y transformación de los recursos líticos dentro de los grupos neandertales 2 (HAR2016-76760-C3-2-P). Territorio y movilidad entre los cazadores-recolectores del Paleolítico y Mesolítico Peninsular. Rasgos culturales y factores paleoambientales, PATHFINDER (HAR2017-82483-C3-1-P).

Muchas gracias a la política cultural y científica que el Gobierno Vasco desarrolla a través de becas pre-doctorales como la que yo he recibido. Espero que esta tesis esté a la altura del esfuerzo (económico) que las personas que componen esta sociedad y en la que me he sentido tan bien acogido, han realizado a través de sus impuestos. Muchas gracias al Departamento de Educación, política lingüística y Cultura por haber gestionado este esfuerzo económico a través de la beca predoctoral: BFI-2012-121. La sociedad necesita la Ciencia y la Ciencia a la sociedad, seguid y mejorar vuestra apuesta de futuro, lo necesitamos.

Sin la concesión de los permisos para el estudio de los materiales arqueológicos, esta tesis no se hubiera realizado. Muchas gracias al Museo de Prehistoria y Arqueología de Cantabria (MUPAC) y a la Consejería de Cultura de Cantabria por los permisos recibidos para analizar las colecciones de El Habario y El Arteu y por haberme facilitado el acceso a sus instalaciones. En este apartado, me gustaría agradecer especialmente a Adriana Chauvín las facilidades prestadas tanto dentro como fuera del Museo.

A Javier Baena, muchas gracias por los permisos para analizar las colecciones de El Esquilleu y diversas gestiones. Muchas gracias por estar dispuesto a enseñarme, por tus conversaciones, por tu accesibilidad, por tu forma de entender el mundo, la investigación y la Prehistoria. A él y al Departamento de Prehistoria y Arqueología por haberme abierto las puertas y considerarme uno más dentro del centro. En este apartado, hago especial mención a Irene Ortiz, Víctor Lamas, Guillermo Bustos, Conchi Torres, Sara Díaz, Paloma De La Sota y Felipe Cuartero. Muchas gracias a todos.

Muchas gracias a David Álvarez-Alonso, por las facilidades para el análisis de la colección lítica de la Cueva de Coimbre. Muchas gracias por las conversaciones en medio del río Cares, por aportarme tu visión acerca de la captación de recursos líticos en Asturias, por las charlas en castellano en el centro de Colonia, por tu apoyo en la estancia.

Gracias a Andreas Pastoors, primero de todo por entender las posibilidades de mi trabajo en Alemania, por las conversaciones sobre Ciencia y Sociedad, por el acceso a los materiales de Ravensberg-Troisdorf, por tu accesibilidad, por las gestiones realizadas, por el apoyo económico y por los futuros proyectos que seguimos planteando.

Muchas gracias a todas las personas que hicisteis posible mi estancia en El Neanderthal Museum y el Instituto de Prehistoria y Prehistoria Reciente de la Universidad de Colonia y a las instituciones mismas. Mi forma de entender la investigación y los grupos de trabajo no sería la misma si no fuera por todo lo aprendido allí. Gracias por tanto a Gerd-Christian Weniger, a Marcel Bradtmöller, Isabell Schmidt, María de Andrés, Vivian Bollin, Yvonne Tafelmaier, Manuel Alcaraz y a Natalie. Gracias también al WG Quaternary Research & Appplied Geomorphology del Instituto de Geografía de la Universidad de Colonia por la utilización y supervisión de vuestras instalaciones. Gracias Martin Kehl.

A Javier Fernández Eraso y Josean Mujika, muchas gracias por compartir las asignaturas que tan buenos y malos ratos nos dieron, por enseñarme acerca de la docencia, por mostrarme que, aun en el mundo más competitivo, la sociedad está repleta de personas.

A mis compañeros de “aventuras en la furgo”, también conocidas como las prospecciones geo-arqueológicas. Sin vosotros este trabajo no habría salido adelante. Por ello, gracias Maite García-Rojas, Javier Martín, Maite Iris García-Collado y Blanca Ochoa. Muchas gracias a Raquel, por cortar todas las piedras que te he llevado en este tiempo, por pulir las láminas con tanto detalle, por los consejos que me has dado.

A mis compañeras de laboratorio, Departamento y Facultad, por haber compartido momentos buenos y malos, investigaciones, ánimos, desilusiones, charlas, cervezas, asociaciones, información, metodologías, pisos… me gustaría dedicar esta sección especialmente a Aitor Sánchez, Aitor Calvo (A.K. los Aitores), Cristina Camarero, Maite García-Rojas, Fernando Pérez, Eder Domínguez-Ballesteros, Unai Perales, Joseba López de Ocáriz, Marcos García-Díez, Antonio Romero, Arantzazu Pérez, Miren Ayerdi, Blanca Ochoa, Erik Arévalo, Dario Sigari, Irene, Amaya Echazarreta, Lydia Zapata, Andoni Tarriño y Marcel Bradtmöller. Si tuviera que especificar todas las aportaciones que cada una habéis realizado, escribiría un nuevo bloque de tesis. Muchas gracias por haberme hecho tan feliz en estos años.

A Maite Iris, mi pareja, le doy una y mil gracias. Por aguantarme, por entenderme, por ayudarme cuando no entiendo algo, por supervisar el inglés de este y mil trabajos más, por las conversaciones de Ciencia que tenemos en casa, por ser el azote de las pseudociencias, por darme ánimos cuando ya poco quedaba dentro.

Por suerte, he podido disfrutar de otras muchas personas en este tiempo y que no pertenecen a ámbitos de la investigación. Sin ellas, tampoco podría haber finalizado este trabajo. Sus aportes y vivencias a partir de la convivencia y su apoyo en los momentos más duros de este trabajo ha sido imprescindible para que no perdiera el Norte, para seguir valorando la vida, para seguir entendiendo el mundo presente. Muchas gracias a aquellas personas que me han ayudado en Vitoria-Gasteiz, Lorea, Unai, Tony, Salinero, Imanol, Juan Luis, Vicky… Muchas gracias a mis paisanos de La Vellés, y especialmente a mis Rabones y Rabonas, Dani, Ale, Kike, Héctor, Chechu, Manu, Ana, Tere, Kike, Javi, Nanú, Efrén, Killo, Ezti, Nacho, Nadir, Rubén y Alberto (No te olvidaré, siempre me sacas una sonrisa).

La ayuda que nunca olvidaré es la de mi hermana Rosalía, esa persona que me pide que pare, que me ayuda a levantarme una y mil veces (porque es ella la que más sabe de eso) y no sabemos otra cosa sino es compartir. Por todos los momentos agradables, todos los cigarros que hemos disfrutado juntos, todas tus visitas y todas las veces que me has acogido en casa.

A mis padres, no hay palabras para agradecer todo lo hecho por mí, desde obligarme a dejar de seguir una mosca para hacer los deberes hasta animarme a disfrutar con el conocimiento y seguir los instintos de mi alocada cabeza. Muchas gracias por haber colaborado económicamente con mi carrera, máster y estancia en Vitoria-Gasteiz. Muchas gracias por haberme apoyado en todo momento, por pedirme que me tranquilizara, por aguantarme cuando soy desagradable y animarme cuando ha sido necesario.

A mis cuatro abuelos, a mis tíos y primos, todos los apoyos y felicidad que me habéis dado.

CHAPTER-1

INTRODUCCIÓN

Con piedras nos hemos defendido, hemos cazado, hemos fabricado otros instrumentos, nos han servido para golpear, machacar, cortar, moler, con ellas y por ellas hemos ido alcanzando diversas etapas de desarrollo. Con piedra se ha hecho chispa para encender lumbre en los hogares o para disparar pistolas, fusiles y arcabuces. Con trillos armados de piedras nos hemos servido para separar el grano de la paja (Fernández Eraso, 2015).

De sílice son las piedras que hemos utilizado, por ellas nos hemos movido, con ellas hemos gestionado nuestro entorno, de ellas están hechas nuestras casas, calles y plazas. De sílice son los circuitos del ordenador que estoy utilizando para escribir estas líneas y que junto con otros componentes de diferentes partes del mundo me permiten redactar este trabajo.

1.1. PLANTEAMIENTOS GENERALES

El estudio que plasmamos en esta tesis doctoral, tiene por objetivo general conocer los comportamientos de captación, distribución y gestión de la cuarcita por parte de las comunidades humanas que habitaron la Región Cantábrica entre el Paleolítico medio y el Paleolítico superior. Consideramos que este trabajo puede aportar nuevas perspectivas para entendernos hoy como humanos en el medio natural que estamos modificando continuamente (Bocherens, 2018; Crutzen, 2002; Crutzen and Stoermer, 2000; Steffen et al., 2011; Waters et al., 2016) y que tiene su génesis más remota en los comportamientos y los memes (Dawkins, 2002) que permitieron a nuestra especie la expansión por todas las latitudes de la tierra, excepto en la Antártida.

La extracción de materias primas ha modificado desde el inicio y está modificando la superficie de nuestro planeta y lo esta transformante constantemente, anegando la vida y afectando a la biodiversidad de amplias zonas con el fin de obtener recursos minerales, destruyendo ecosistemas y alterando los paisajes a niveles superiores que los provocados por eventos naturales catastróficos.

La distribución de diferentes materias primas de origen mineral y de productos fabricados con las mismas, está generando un incremento de las emisiones de CO2 y otros productos que alteran la atmosfera en la que nosotros y otros seres vivos habitamos. Además, esta distribución de productos genera la presencia de minerales específicos donde antes no existían, además de la vida que estos llevan aparejada.

La gestión de la producción está generando desequilibrios en las relaciones económicas que afectan de manera clara a todos los seres humanos de la Tierra. Por un lado la fabricación de objetos, generalmente mundializada y fragmentada, provoca el enriquecimiento de ciertos habitantes del planeta y el empobrecimiento de otros muchos, acentuando la desigualdad en el reparto de la riqueza. Por otro lado, la gestión de los residuos de todos los procesos industriales, provoca la destrucción de la vida en amplias zonas del planeta.

A pesar de que estos procesos se hacen más evidentes desde el Siglo-XVIII, durante la Revolución Industrial, I. Wallerstein (Wallerstein, 1974, 1979, 1980) ya plantea el origen del Sistema Mundo Capitalista en el Siglo XVI. La búsqueda de la génesis de este tipo de comportamientos de carácter eminentemente depredador con el medio ambiente (y también con miembros de nuestra propia especie), nos ha llevado a plantear este trabajo y enfocarlo a caballo entre el Paleolítico medio y el Paleolítico superior. De esta forma podemos comparar las pautas de adquisición, distribución y gestión de la materia prima en dos periodos claramente diferenciados y con actores diferentes (Alroy, 2001; Bocherens, 2018; Dayton, 2001; Finlayson, 2004; Gamble, 2001; Martin, 1990; Roberts et al., 2001).

Para ello, nos serviremos de un doble enfoque metodológico y que combina el método hipotético-deductivo y el método inductivo-deductivo. El primero, parte del análisis histórico de las sociedades del Paleolítico como sujeto de estudio para entender las sociedades del presente. El enfoque aportado en este trabajo tiene un componente eminentemente económico y éste se plantea a partir de la captación, gestión y distribución de las materias primas líticas aplicando una visión socio-económica. Hemos utilizado conceptos de diferentes escuelas metodológicas como la Arqueología Procesualista a partir de los Site Catchment analysis (Binford, 1982, 1983; Butzer, 1989; Kelly, 1992; Kelly, 1995; Vita-Finzi, 1978), la escuela de la Human Behavioural Ecology (Borgerhoff Mulder and Schacht, 2012; Cronk, 1991; Hames, 2001; Winterhalder and Smith, 2000), la *Chaîne opératoire*

(Leroi-Gourhan, 1964) o conceptos derivados de la Tipología Analítica (Fernández Eraso and García-Rojas, 2013; Laplace, 1972, 1987). El segundo, el método inductivo-deductivo está claramente presente en esta investigación a partir de la selección de el objeto de estudio, la cuarcita y con el tratamiento de los datos que se realizan en esta tesis. Partiendo del objeto, estático, tratamos de conocer las fuerzas y dinámicas que lo generan: Materia/->Fuerza (Feynman, 2015; Kropotkin, 2015). Caracteres petrológicos + Caracteres tecno-tipológicos + Caracterización geográfica /-> Adquisición, gestión y distribución de la cuarcita.

1.2. HISTORIOGRAFÍA, JUSTIFICACIÓN DEL TRABAJO Y SELECCIÓN DE LA ZONA DE ESTUDIO

El estudio de las materias primas líticas sobre las que se fabricaron las herramientas prehistóricas es un tema de investigación que ha formado parte de la Arqueología prehistórica desde sus inicios como disciplina. Desde finales del siglo XIX, los primeros prehistoriadores, en muchas ocasiones geólogos de formación, ya realizaban descripciones macroscópicas de las rocas utilizadas por las sociedades prehistóricas. Un buen ejemplo de este tipo de investigadores es Juan Villanova y Piera, Catedrático de Geología y Paleontología que ya describía desde perspectivas geológicas y arqueológicas el material lítico que recogía en sus excursiones y campañas arqueológicas (Pelayo López and Gonzalo Gutiérrez, 2012).

La caracterización petrológica de las rocas sobre las que se confeccionaron los artefactos prehistóricos se hace más precisa a partir de los años 50' y 60' del siglo pasado a través de la aplicación de la petrografía y las técnicas de análisis composicional. Estas primeras investigaciones basadas en la aplicación de técnicas derivadas de la Geología estuvieron focalizadas en la obsidiana y permitieron trazar rutas de intercambio de materiales líticos durante la Prehistoria Reciente en el Mediterráneo, Oceanía y América del Norte (Dixon et al., 1968; Earle and Ericson, 1977; Polanyi, 1957). Los llamativos resultados obtenidos en estos trabajos y las mejoras técnicas para la caracterización del material pétreo generaron un aumento de los estudios a nivel cuantitativo y cualitativo durante la década de los 70' (Binns and McBryde, 1969; Kowalski et al., 1972; Sieveking et al., 1972). A partir de los años 80', los estudios petrológicos sobre las industrias líticas se ampliaron a nivel geográfico y cronológico, aumentando igualmente los tipos de materiales estudiados, como el sílex (Luedtke, 1979).

Durante la década de los 80', en Europa y para cronologías paleolíticas, el sílex se convierte en la materia prima lítica más estudiada debido a la importancia que tiene a nivel cuantitativo y cualitativo en las colecciones líticas y a los trabajos pioneros de B. Luedtke, P.Y. Demars, A. Morala, J.M. Geneste o A. Masson, centrados en este material (Demars, 1980; Demars, 1982; Earle and Ericson, 1982; Geneste, 1985; Masson, 1981; Morala, 1979, 1980, 1983; Séronie-Vivien and Séronie-Vivien, 1987; Simonet, 1981). Los interesantes resultados de estos trabajos, pioneros en la caracterización del sílex en Europa para contextos paleolíticos, generaron un incremento de investigaciones en este campo. Desde mediados de los años 80' se realizan diversas tesis doctorales y trabajos especializados en Europa, identificando variedades silíceas que nos permiten conocer las áreas fuente de los materiales recuperados en contextos arqueológicos en buena parte de Europa (Floss, 1990; Jeske, 1989; Normand, 1986; Roebroeks, 1988; Turq, 1989). Complementariamente, la multiplicación de las investigaciones enfocadas al conocimiento de las dinámicas económicas y sociales de las sociedades paleolíticas a partir del análisis tecno-tipológico de la industria lítica (Boëda, 1994; Laplace, 1972, 1987; Leroi-Gourhan, 1964), ha permitido entender los complejos mecanismos de adquisición y gestión del sílex (Andrefsky, 1994; Roebroeks, 1988; Turq, 1996). Asimismo, los aportes teóricos planteados desde corrientes procesualistas y post-procesualistas, modifican la visión eminentemente culturalista de la Prehistoria y las industrias líticas hacia postulados nuevos en los que se prima entender los seres humanos prehistóricos dentro de los procesos económicos y sociales y que relacionan las sociedades prehistóricas con el medio ambiente (Binford, 1982, 1983; Cronk, 1991; Kelly, 1995; Renfrew, 1986; Vita-Finzi, 1978).

A pesar de que las descripciones litológicas básicas sobre las que se confeccionaron los utensilios prehistóricos se venía realizando desde mediados del Siglo XIX en la Península Ibérica, la profundización en la caracterización de la materia prima comienza en la década de los 90', principalmente a partir de los trabajos de X. Terradas, J. Mangado, A. Tarriño y P. Sarabia, principalmente (Mangado, 1998; Sarabia, 1993, 1999, 2000; Tarriño, 1998, 2006; Tarriño and Aguirre, 1997; Tarriño et al., 1998; Terradas, 1995). Estos investigadores, aplicando metodologías

geo-arqueológicas de caracterización del material pétreo, abrirán esta línea de investigación de la Prehistoria en la Península Ibérica, y los dos últimos, específicamente en la Zona Cantábrica. En estos trabajos, al igual que los que se siguen desarrollando en el resto de Europa, se ha primado la caracterización del sílex, la materia prima mejor representada en el Paleolítico superior. Dentro de estas perspectivas, el cambio de milenio supuso la incorporación de nuevas tecnologías, como por ejemplo los Sistemas de Información Geográfica (SIG), que permiten un acercamiento más eficaz a la complejidad económica y social de las sociedades paleolíticas articulada en base a la adquisición, gestión y distribución del sílex. El incremento de estudios enfocados a la caracterización de este material en contextos arqueológicos y geológicos integrado en los análisis tecno-tipológicos de las industrias líticas y en el entendimiento del Paisaje prehistórico, nos está permitiendo delimitar y comprender territorios económicos complejos, así como su articulación a partir de la movilidad humana (Arrizabalaga et al., 2014; Aubry et al., 2012; Baena et al., 2005; Fernández, 2010; Fontes, 2016; Fontes et al., 2016; García-Rojas, 2014; García-Rojas et al., 2017; Prieto et al., 2016; Rissetto, 2012; Sánchez et al., 2016; Soto, 2014; Soto et al., 2017; Turq et al., 2017; Turq et al., 2013).

La cuarcita, a pesar de ser la segunda materia prima lítica más empleada durante el Paleolítico en Europa, no ha sido objeto del mismo desarrollo metodológico que la obsidiana o el sílex, como evidencian los escasos y recientes trabajos geo-arqueológicos focalizados al conocimiento de este material (Blomme et al., 2012; Cnudde et al., 2013; Pedergnana et al., 2017; Pitblado et al., 2008; Pitblado et al., 2012; Roy et al., 2017; Veldeman et al., 2012). Ello ha generado un vacío científico y un sesgo en el conocimiento de las estrategias de adquisición, distribución y gestión de las materias primas líticas (Arrizabalaga, 2010). Este déficit se puede entender a partir de tres

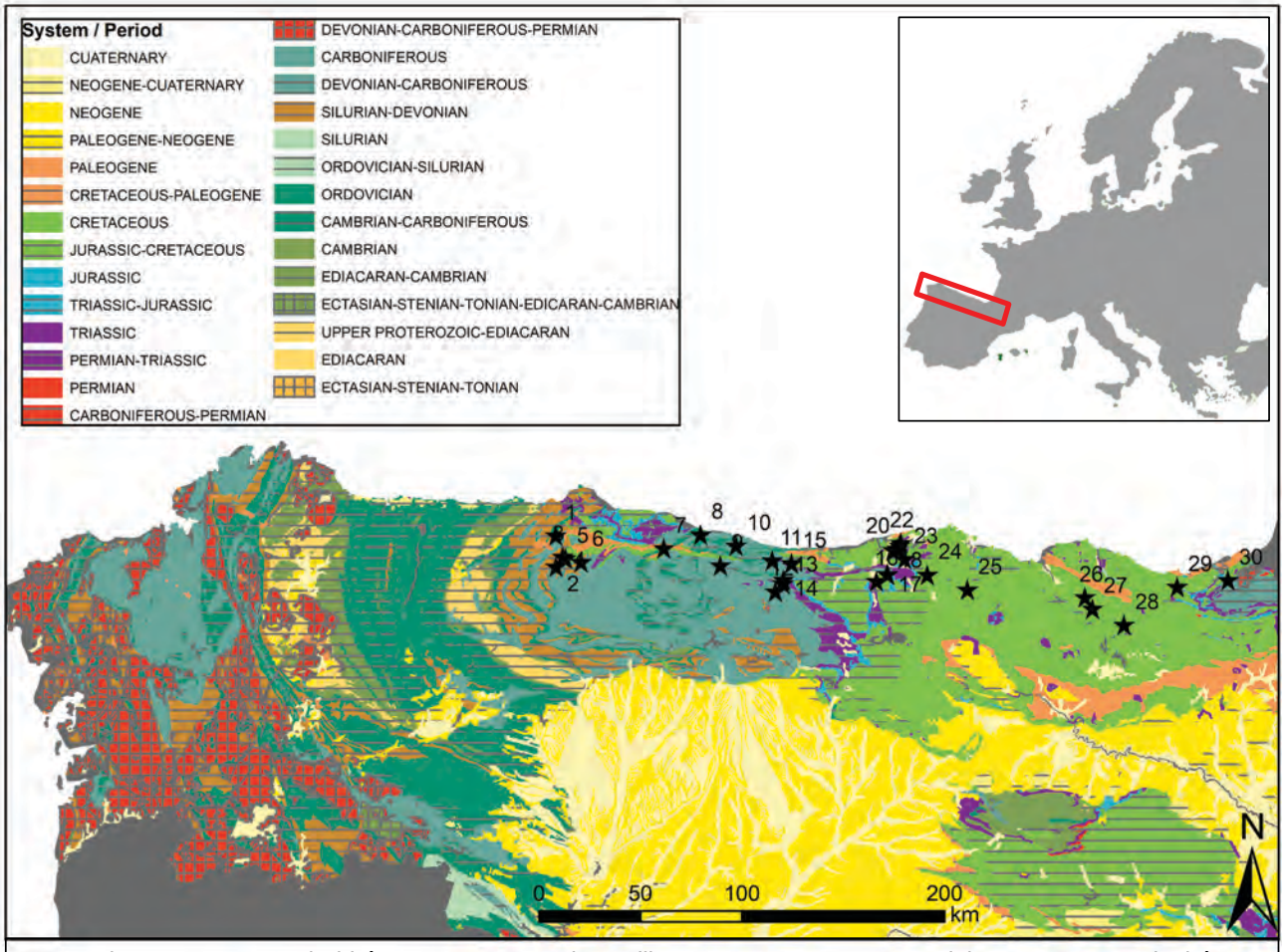

1. La Paloma	7. El Sidrón	13. El Esquilleu	19. Covalejos	25. El Mirón
2. El Conde	8. El Cierro	14. El Arteu	20. El Pendo	26. Arlanpe
3. La Lluera I	9. Sopeña	15. Panes II	21. El Juyo	27. Axlor
4. La Lluera II	10. La Riera	16. Hornos de la Peña	22. El Ruso I	28. Lezetxiki
5. Las Caldas	11. Llonín	17. El Castillo	23. Morín	29. Amalda
6. La Viña	12. El Habario	18. La Flecha	24. Rascaño	30. Aitzbitarte III

Figura-1.1: Mapa geológico a escala 1:1.000.000 de la Cornisa Cantábrica. Sobreimpuesto, la trama de yacimienos utilizados para confeccionar este estado del conocimiento.

ejes interrelacionados. El primero, de carácter geográfico, evidencia que la distribución de los afloramientos rocosos genera una pérdida de información en las zonas con amplia distribución de cuarcitas. El segundo, de carácter crono-cultural, pone de manifiesto la escasez de datos para periodos históricos en los que el sílex o la obsidiana no son cuantitativamente importantes o no están representados. El tercer eje hace referencia a la pérdida de información a nivel interpretativo, consecuencia de la sobrerrepresentación de la información disponible sobre el sílex y la obsidiana, generalmente relacionadas con la movilidad geográfica de larga distancia. Esto impide entender los complejos mecanismos de adquisición, gestión y distribución dentro de zonas económicas más restringidas y, por tanto, los territorios económicos cotidianos de las sociedades prehistóricas.

Para entender cada uno de estos tres ejes y delimitar, dentro de la Región Cantábrica la zona de estudio de esta tesis, hemos elaborado un estado del conocimiento a través de una recopilación bibliográfica. Para ello, hemos seleccionado la información derivada de la descripción litológica básica de los conjuntos líticos de 30 yacimientos arqueológicos entre las cuencas de los ríos del Narcea al Bidasoa. El número de niveles arqueológicos analizados es de 210, circunscritas en cinco asignaciones crono-culturales diferentes: Musteriense (90), Auriñaciense (32), Gravetiense (13), Solutrense (45) y Magdaleniense (30). La bibliografía utilizada es la siguiente (Altuna et al., 1984; Álvarez-Alonso and De Andrés, 2012; Arbizu et al., 2005a, 2009; Arbizu et al., 2005b; Baena et al., 2005; Baldeón, 1993; Barandiarán et al., 1987; Cabrera, 1984; Cabrera et al., 2005; Cabrera et al., 1996; Cabrera et al., 2000; Carrión and Baena, 1999, 2005; Castanedo, 2001; Corchón, 1981; De la Rasilla et al., 2011; Fortea et al., 1992; Fortea et al., 1995; González Echegaray, 1980; González Echegaray and Barandiarán, 1981; González Echegaray and Freeman, 1978; Manzano, 2001; Manzano et al., 2005; Martín et al., 2006; Menéndez, 2006; Menéndez et al., 2009; Montes, 2003; Muñoz and Serna, 1999; Pinto-Llona et al., 2012; Pinto-Llona et al., 2006; Ríos, 2012; Ríos et al., 2013; Rodríguez Asensio and Barrera Logares, 2012; Sanguino and Montes, 2005; Santamaría, 2012; Straus, 1975, 1992; Straus and Clark, 1986). El número de asignaciones crono-culturales en diferentes yacimientos es de 55. Estos datos nos permitirán entender desde un punto de vista cuantitativo la distribución de las materias primas líticas en la Cornisa Cantábrica (Tabla-1.1, al final del capítulo).

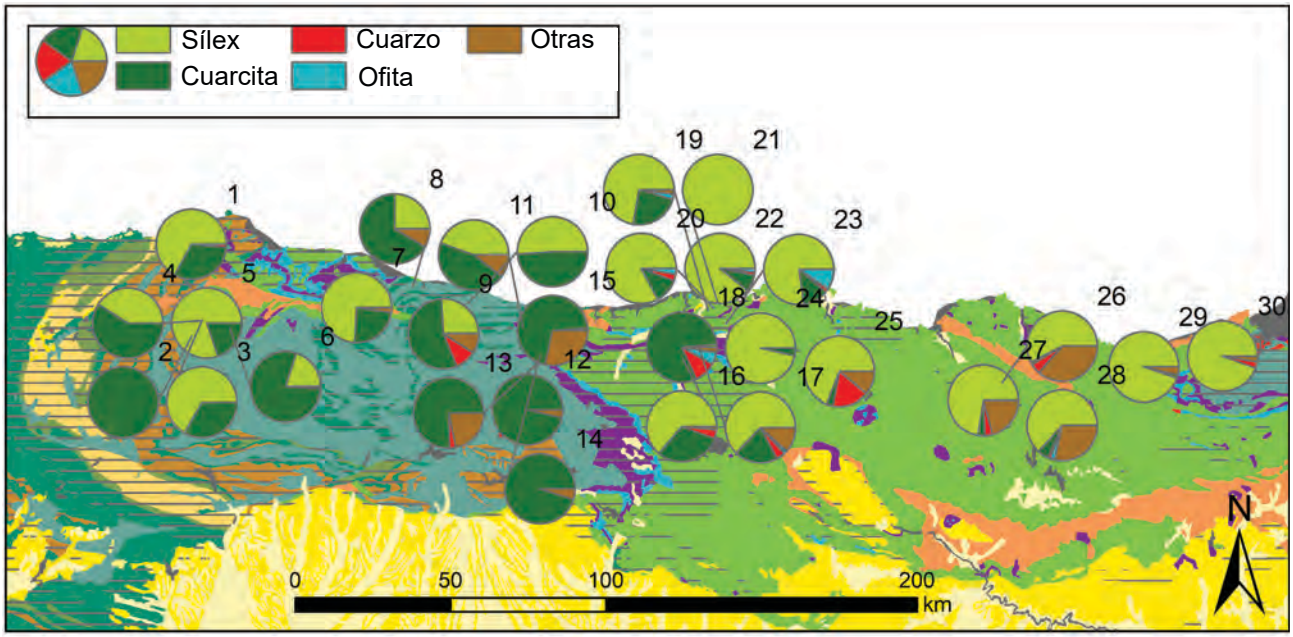

Figura-1.2: Mapa geológico a escala 1:1.000.000 de la Cornisa Cantábrica. Sobreimpuesto, la trama de yacimienos utilizados para confeccionar este estado del conocimiento con los porcentajes de materia prima lítica.

El primero de los ejes previamente comentados, el geográfico, está condicionado por la variabilidad geológica de la zona de estudio. En el caso que nos ocupa, la Región Cantábrica, presenta una alta variabilidad geológica que condiciona y dificulta el conocimiento de nuestro pasado más remoto (Figura-1.1). De forma simplificada, en la Región Cantábrica se observa una sucesión de formaciones geológicas que abarcan de Oeste a Este desde el Precambrico, en la Comunidad Autónoma de Galicia y la zona más occidental del Principado de Asturias, secuencias del Cretácico y el Paleógeno, principalmente representadas en la zona más oriental de esta Región. Las litologías presentes en los yacimientos arqueológicos seleccionados representan, de forma

general, las posibles litologías existentes en estos dominios. En la Figura-1.2 se pueden observar, sobreimpuestos al mapa previamente comentado, los porcentajes de materias primas líticas. En ellos, se observa un predominio de las cuarcitas en la zona occidental de la Cornisa Cantábrica, mientras que en la zona central y oriental, predomina el sílex. El sustrato geológico determina por tanto y de una forma general las litologías identificadas en los yacimientos arqueológicos.

El segundo de los ejes es el cronológico. Utilizando las unidades crono-culturales ya comentadas, observamos una variación en las litologías representadas en los yacimientos (Figura-1.3, Figura-1.4 y Figura-1.5). De forma general apreciamos un paulatino incremento en la adquisición del sílex en detrimento de otras materias primas. En el Musteriense la variabilidad de materias primas seleccionadas es muy alta en todos los dominios, a pesar de existir litologías mayoritarias (Figura-1.3). Éstas se relacionan con el eje geográfico previamente mencionado y de forma general asocia la cuarcita con la zona occidental y central de la Región Cantábrica, mientras que al oriente de la Bahía de Santander, la materia prima predominante es el sílex. La cantidad de otras materias primas es variable, rondando el 25% de cada una de las unidades crono-culturales de cada yacimiento. La presencia de ofita como materia prima secundaria en la zona de la Bahía de Santander responde a la presencia de este material en el sustrato rocoso, especialmente en zonas de diapiros. Por su parte, la presencia de sílex en la zona occidental habría que buscarla en las series sedimentarias que conforman la franja mesozoica asturiana. En la zona más oriental de la Cornisa Cantábrica, la presencia de cuarcita y lutita (contabilizada dentro de la categoría otras litologías) posiblemente se debe a los estratos sedimentarios de origen clástico presentes en la zona y que tienen edades mesozoicas y cenozoicas.

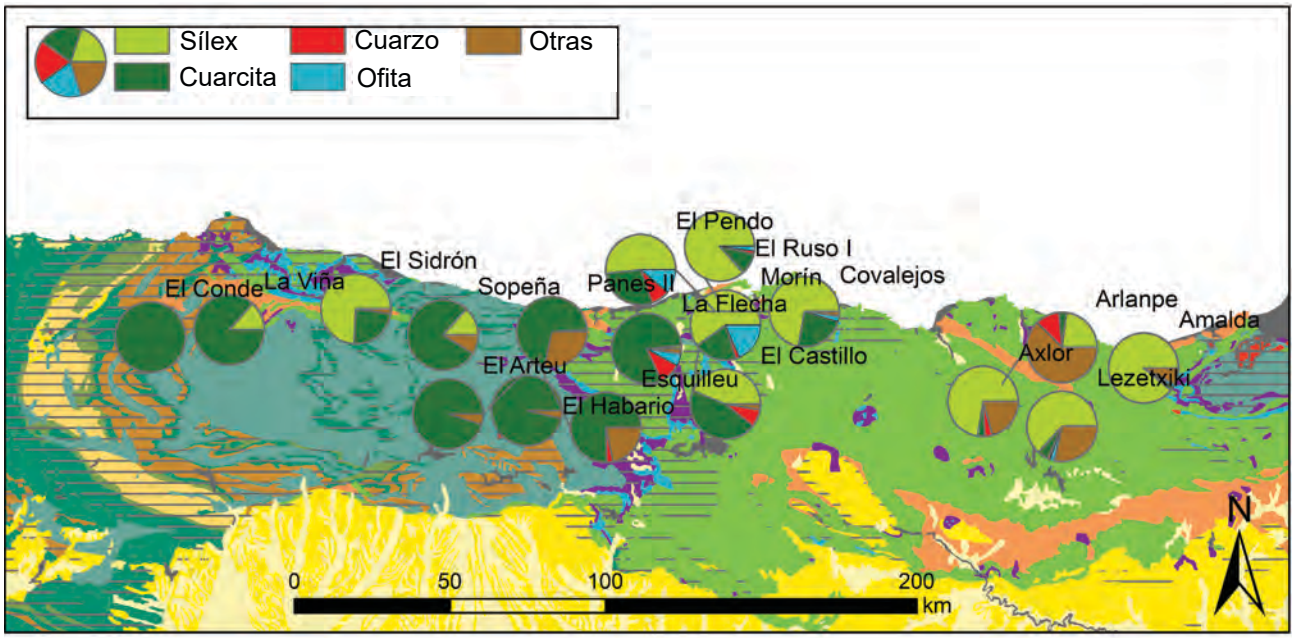

Figura-1.3: Mapa geológico a escala 1:1.000.000 de la Cornisa Cantábrica. Sobreimpuesto, la trama de yacimienos con los niveles crono-culturales musterienses y sus porcentajes de materia prima lítica.

A lo largo del Paleolítico superior se observa un cambio gradual que lleva al sílex a ser la materia prima predominante en todos los yacimientos de la Región Cantábrica. Esta tendencia se observa ya en el Auriñaciense, especialmente cuando se compara con el periodo previo (Figura-1.4a). En la zona más oriental, el sílex es, en Aitzbitarte-III (Gipuzkoa), la materia prima lítica más utilizada, mientras que otras materias primas no llegan ya al 25%, como si se observaba en el Musteriense en otras colecciones arqueológicas de la zona. En la zona central, se observa la misma tendencia, con un aumento generalizado de la proporción de sílex en cada colección. A pesar de ello, la presencia de cuarcitas y otras materias primas en los niveles seleccionados de El Castillo (Cantabria) sigue siendo importante. En la zona más occidental de la Región Cantábrica, las litologías de los yacimientos son diferentes debido a que la materia prima lítica más utilizada sigue siendo la cuarcita. A pesar de ello, vemos que las cantidades de sílex han aumentado respecto a los niveles musterienses.

A pesar de contar con pocos datos de cronología Gravetiense, observamos que la tendencia previamente comentada es más clara, si bien el cuarzo toma un rol importante durante este periodo (Figura-1.4b). En la zona oriental el sílex sigue siendo la materia prima dominante y el resto de materias primas líticas no llegan al 10% de las evidencias líticas en estos yacimientos. Las escasas

unidades crono-culturales analizadas en la zona central muestran una variación importante. Si bien en el Pendo (Cantabria) el sílex es mayoritario y otras materias primas están escasamente representadas, en el Mirón (Cantabria), el porcentaje de sílex es inferior (aun siendo mayoritario) debido a la presencia de cuarzo, mayoritariamente. En la zona occidental de la Cornisa Cantábrica observamos que la cuarcita y el sílex están representados de una forma similar. Por su parte en Sopeña, la cantidad de cuarzo es importante, con porcentajes similares a los expuestos en El Mirón.

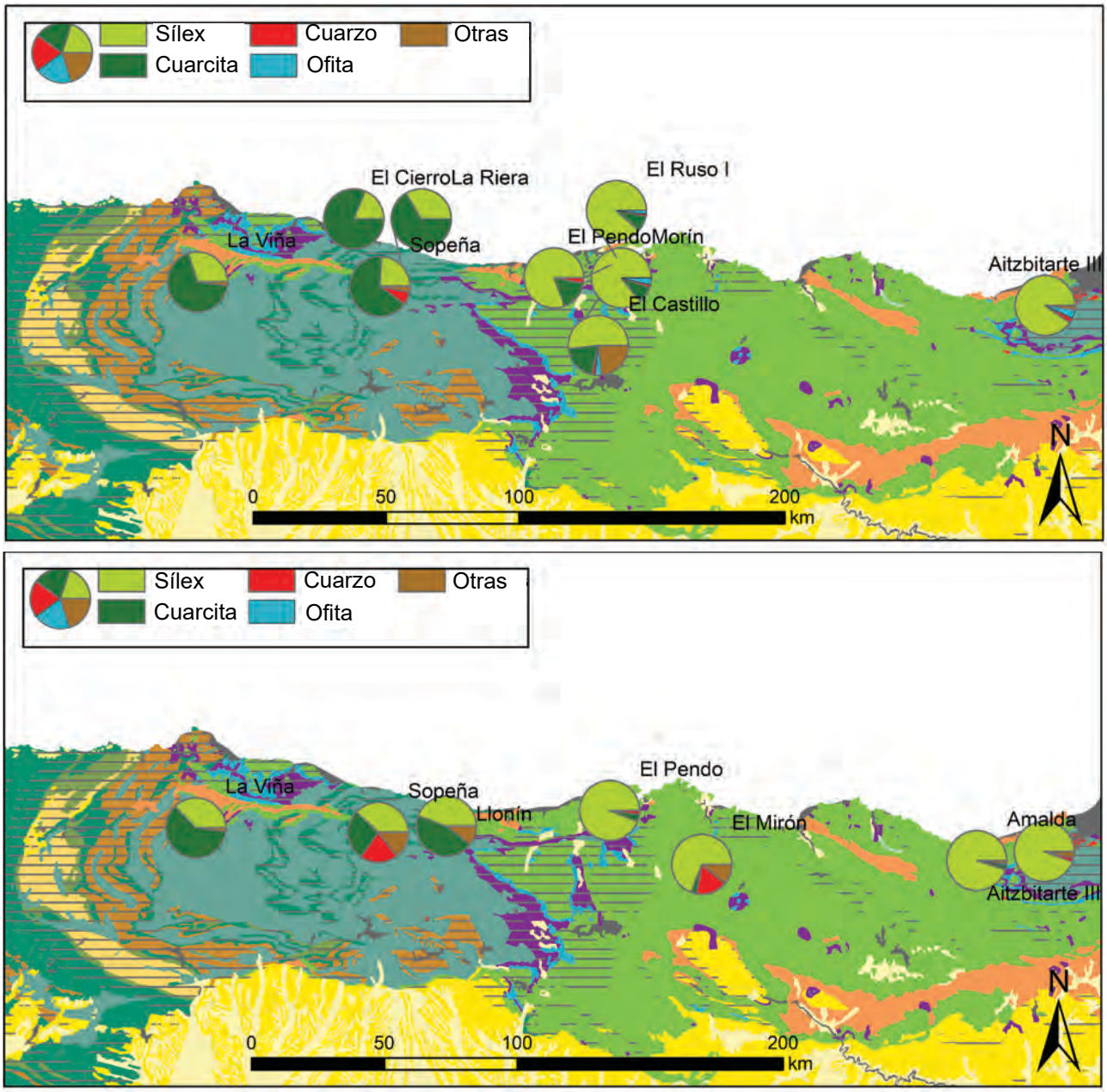

Figura-1.4: Mapa geológico a escala 1:1.000.000 de la Cornisa Cantábrica. Sobreimpuesto, la trama de yacimienos con los niveles crono-culturales auriñacienses arriba y gravetienses debajo y sus porcentajes de materia prima lítica.

En el Solutrense esta tendencia se detiene, especialmente en la zona central y occidental debido al incremento de la cuarcita dentro de las colecciones líticas seleccionadas (Figura-1.5). Este proceso ya ha sido documentado en otros estudios que lo relacionan con la utilización de las cuarcitas para la realización del retoque plano de las foliáceas características de este periodo crono-cultural (De la Rasilla and Fernández de la Vega, 2014; De la Rasilla and Llana, 1994; Schmidt, 2013; Straus, 1983, 2001, 2012). Esta tendencia se aprecia claramente en la zona central, donde, a pesar de ser el sílex la materia prima predominante, la utilización de la cuarcita es mayor que en los periodos crono-culturales anteriores. En esta zona, además, se observa un descenso importante en las cantidades de cuarzo. Por su parte, en la zona occidental, se estabilizan las cantidades de sílex, a pesar de ser en algunos yacimientos la materia prima predominante. Finalmente, en

la zona oriental, el sílex es mayoritario en Amalda, a pesar de que en Arlanpe su proporción sea inferior. Esto se debe probablemente a la pequeña cantidad de industria lítica que compone el nivel solutrense de este yacimiento.

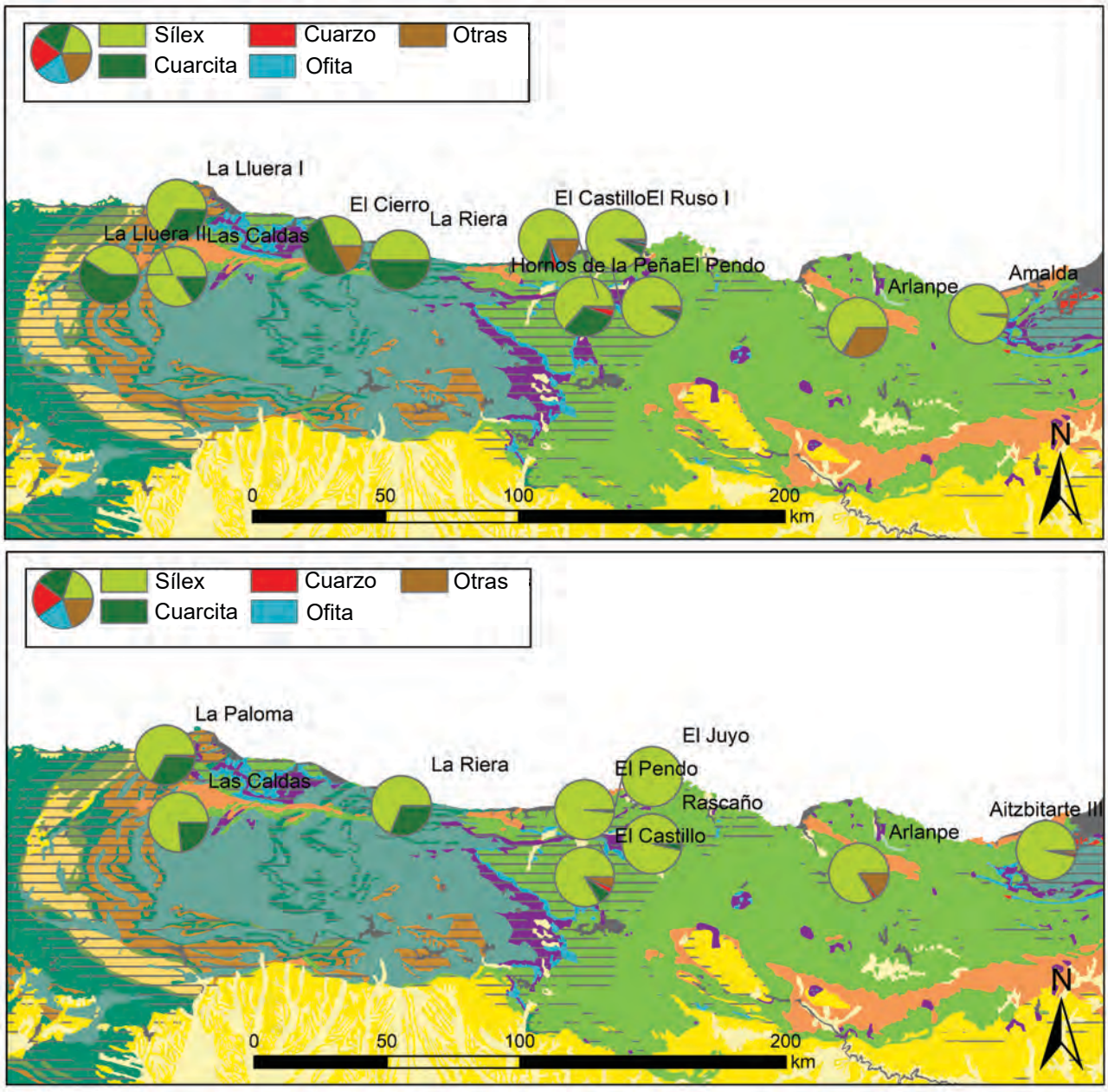

Figura-1.5: Mapa geológico a escala 1:1.000.000 de la Cornisa Cantábrica. Sobreimpuesto, la trama de yacimienos con los niveles crono-culturales solutrenses arriba y magdalenienses debajo y sus porcentajes de materia prima lítica.

Finalmente, en el Magdaleniense observamos el resultado final de la tendencia comentada y el sílex se convierte en la materia prima principal de todos los yacimientos caracterizados en este periodo (Figura-1.5b). A pesar de ello, observamos diferencias geográficas, principalmente entre el área occidental y el área central y oriental. En la primera, a pesar de ser el sílex la materia prima lítica mayoritaria, la cuarcita sigue teniendo importancia en porcentajes superiores al 25%. Por el contrario, en la zona central y oriental, los porcentajes de sílex son siempre superiores al 80% y, excepto en los niveles de El Castillo y de Arlanpe los porcentajes de sílex siempre superan el 95%.

El último de los tres ejes que interesa destacar es el eje interpretativo. Para entender este eje con los datos aportados es importante mencionar que la mayor parte de los trabajos que hemos utilizado para generar este estado de la cuestión acerca de la distribución de las litologías principales en la Cornisa Cantábrica son antiguos y no incorporan los aportes geo-arqueológicos y de detalle. La interpretación que nos aporta esta visión nos acercaría por tanto a una relación dialéctica entre las dos materias primas más utilizadas en el Paleolítico en la Región Cantábrica: el sílex y la cuarcita.

Entendiéndola desde un punto de vista crono-cultural, observamos que existe una paulatina sustitución de la cuarcita por el sílex desde el Paleolítico medio hasta el final del Paleolítico medio. Entendiéndola desde un punto de vista geográfico, observamos dos zonas bien diferenciadas, por un lado la zona occidental, con estratos geológicos más antiguos (Paleozoicos y Precámbricos) y una amplia distribución de cuarcitas en los yacimientos arqueológicos. Por otro, una zona central y oriental, con estratos geológicos más recientes (Mesozoicos y Cenozoicos) con una mayor distribución de sílex. La unión entre ambas tendencias nos plantea los siguientes interrogantes:

- ¿Los estratos geológicos mayoritarios determinan las litologías adquiridas en los yacimientos arqueológicos?
- ¿Qué grado de selección de litologías observamos en los diferentes periodos crono-culturales?
- ¿Existe una tendencia histórica (patrones sociales, culturales o económicos) que promuevan la sustitución de las cuarcitas por el sílex a través de la estandarización de su uso?
- ¿Existe una movilidad mayor de los grupos humanos del Paleolítico superior que en los grupos del Paleolítico medio?
- ¿Cuáles son las zonas de captación de materia prima y los recorridos realizados por los grupos humanos en el Paleolítico para llegar a éstas?
- ¿Existe una movilidad de materias primas en dirección Este-Oeste que va ganando peso conforme avanza el Paleolítico?
- ¿Qué rol juegan los mecanismos de selección de material prima durante el Paleolítico?
- ¿Cuál es el grado de aprovechamiento de cada una de las materias primas líticas?
- ¿Qué papel juega la dispersión y visibilidad de las materias primas?
- ¿Qué papel juega la presentación de las materias primas en los diferentes contextos geológicos?
- ¿Dónde se encuentran las litologías seleccionadas por los grupos humanos dentro de las grandes unidades descritas?
- ¿Cuál es el rol que juegan los agentes erosivos y deposicionales en la dispersión espacial de las potenciales fuentes de materia prima?

Como ya hemos comentado, los trabajos desarrollados desde finales de los años 90 por Andoni Tarriño y otros investigadores que aplican su propuesta geo-arqueológica, están ofreciendo respuestas a algunos de estos interrogantes a través de la caracterización del sílex y el establecimiento de tipos y variedades (Álvarez-Alonso et al., 2017; Arrizabalaga et al., 2014; Barandiarán et al., 2006; Corchón et al., 2007; Elorrieta, 2016; Fernández-Eraso et al., 2017; Fontes et al., 2016, 2018; García-Rojas, 2014; García-Rojas et al., 2017; Herrero-Alonso et al., 2016; Perales, 2015; Perales and Prieto, 2015; Prieto et al., 2016; Rissetto, 2009; Sánchez et al., 2016; Santamaría, 2012; Soto, 2014; Tarriño, 2000, 2006, 2011a, b; Tarriño and Aguirre, 1997; Tarriño et al., 2007a; Tarriño et al., 2013a; Tarriño et al., 2013b; Tarriño et al., 2015; Tarriño et al., 2014; Tarriño et al., 2011; Tarriño and Normand, 2002; Tarriño et al., 2007b; Tarriño et al., 1998). De forma general, plantean:

- La Cuenca Vasco-Cantábrica es el dominio geológico que más cantidad de sílex aporta a los yacimientos arqueológicos de la Región Cantábrica.
- La presencia de, al menos 30 tipos de sílex, agrupados en 14 clases que afloran en esta Región y que están repartidos desde la Cuenca de Oviedo hasta los Pirineos occidentales.
- La existencia de sílex de carácter local, regional, traza y super-traza en función de la distribución de los mismos en periodos prehistóricos.
- La existencia de una economía articulada en torno a esta materia prima durante el Paleolítico superior y que combina la adquisición de sílex de diferentes afloramientos.
- Aporte de sílex en dirección Este-Oeste dentro de la Región Cantábrica.
- La presencia de lugares de agregación entre los diferentes grupos que habitaban la Región donde posiblemente se realizaran intercambios de materia prima.

- Existencia de lugares de captación de sílex en las zonas cercanas a los afloramientos.

Igualmente, están aportando nuevas preguntas con las que plantear nuevas hipótesis de investigación en torno a la adquisición, distribución y gestión del sílex y que nos han servido para plantear objetivos dentro de nuestra investigación:

- ¿Qué importancia tiene el aporte de sílex de dominios ajenos a la Cuenca Vasco-Cantábrica?
- ¿Existen más tipos y variedades de sílex dentro de la Cuenca-Vasco Cantábrica?
- ¿Qué factores determinan que un tipo de sílex tenga un rango de expansión local, regional, traza o súper-traza?
- ¿Cómo son los procesos de captación de materia prima?
- ¿Dónde se producen los procesos de captación de materia prima? ¿Qué grado de selección de tipos específicos se realizan?
- ¿Cómo se moviliza el sílex, en qué formato? ¿quién o quienes movilizan el sílex?
- ¿Cuál es el rol que juegan los agentes erosivos y deposicionales en la dispersión espacial de las potenciales fuentes de materia prima?

A pesar de las respuestas aportadas y las nuevas hipótesis planteadas por esta línea de investigación, seguimos observando un déficit de información en las zonas de amplia distribución de cuarcitas, en periodos crono-culturales específicos y en yacimientos donde el sílex no es la única materia prima lítica. Consideramos que estas carencias requieren de la aplicación sistemática de metodologías de carácter geo-arqueológico que nos permitan entender la cuarcita a través de sus características petrológicas y los patrones de adquisición, gestión y distribución de este material que las sociedades humanas realizaron en el Paleolítico. Para ello, hemos realizado este trabajo. Con el fin de tener un estudio abarcable en el tiempo y factible de realizar dentro de una tesis doctoral, hemos seleccionado una zona específica en la que focalizar nuestro estudio: los valles del Deva, Cares y Güeña. La selección de esta zona se debe a motivos arqueológicos y geológicos. Los motivos arqueológicos se fundamentan en la presencia de yacimientos arqueológicos excavados y accesibles con presencia de cuarcitas y con una variabilidad temporal que nos permita responder a preguntas históricas aplicando una dimensión diacrónica. Los motivos geológicos han condicionado la zona de estudio debido a la presencia de litologías de interés y con un amplio rango cronológico, desde las series Paleozoicas, hasta depósitos cuaternarios y pasando por series Mesozoicas. Finalmente, y con el objetivo de entender la cuarcita en contextos arqueológicos ajenos a la Región Cantábrica, hemos estudiado desde un punto de vista geo-arqueológico las cuarcitas del yacimiento de Ravensberg-Troisdorf (Renania del Norte-Westfalia, Alemania).

1.3. OBJETIVOS

Como ya hemos comentado, el objetivo principal de este trabajo es conocer los mecanismos de adquisición, gestión y distribución de la Cuarcita en las sociedades que habitaron la Región Cantábrica durante el Paleolítico medio y el superior. En esta sección desarrollaremos los objetivos generales y de los que se descolgarán objetivos secundarios. Finalmente, expondremos las diferentes tareas realizadas en esta tesis doctoral. Los objetivos generales de este trabajo son los siguientes:

1. Definir y conocer formalmente la cuarcita arqueológica como roca en la Región Cantábrica a través de:
    a. Las características petrográficas:
        i. La textura y el empaquetamiento de la roca.
        ii. Características de los granos de cuarzo que componen la cuarcita.
        iii. El tamaño, la morfología y la orientación de los granos de cuarzo que componen este material.

iv. La mineralogía de la cuarcita.

b. La composición geoquímica de la cuarcita.

c. Los procesos genéticos de la cuarcita.

2. Establecer tipos y variedades basados en las características físicas de la cuarcita.
3. Establecer una metodología de carácter no-destructivo que permita analizar y clasificar las cuarcitas sin necesidad de realizar analíticas destructivas.
4. Conocer la disposición y la dispersión de la cuarcita en los valles del Deva, Cares y Güeña a través de:

   a. La documentación de los afloramientos masivos compuestos por cuarcitas.

   b. La documentación de los conglomerados donde exista la presencia de clastos de cuarcita.

   c. La documentación de la cuarcita en depósitos no consolidados.

   d. Conocer el ciclo de la cuarcita en la zona de estudio.

5. Conocer las pautas de adquisición de las cuarcitas en la zona de estudio y definir potenciales contextos de captación de esta roca.
6. Identificar las pautas de gestión de la cuarcita a partir del análisis tecno-tipológico de las evidencias líticas estudiadas en los yacimientos seleccionados.
7. Evidenciar la dispersión de la cuarcita realizada a través de la movilidad humana.
8. Definir y caracterizar los territorios económicos paleolíticos en la zona de estudio.
9. Analizar la variabilidad de los comportamientos de adquisición, distribución y gestión de las materias primas líticas en la zona a partir de un eje geográfico y otro cronológico.

Las tareas realizadas han sido las siguientes:

- La delimitación de la zona de estudio.
- Selección de niveles arqueológicos de interés.
- Establecimiento de una metodología de análisis geográfico a partir de los Sistemas de Información Geográfico.
- Creación de fichas de prospección.
- Prospectar geológicamente el área delimitada a través de 116 puntos de prospección.
- La creación de una base de datos geo-referenciada con toda la información disponible.
- Seleccionar criterios de análisis de la industria lítica de diferentes perspectivas metodológicas.
- Establecer bases y criterios uniformes para la caracterización macroscópica de las materias primas líticas.
- Establecer bases y criterios para la caracterización macroscópica de las cuarcitas.
- Establecer bases y criterios para la caracterización microscópica de las cuarcitas mediante técnicas no-destructivas.
- Establecer bases y criterios para la caracterización microscópica de las cuarcitas mediante técnicas petrográficas.
- Observación, caracterización y descripción de las texturas, el empaquetamiento y los granos de cuarzo de 118 láminas delgadas de cuarcita.
- Dibujado y procesado estadístico de 18.855 granos de cuarzo provenientes de 113 láminas delgadas.

- Análisis químico por fluorescencia de rayos-X de 111 cuarcitas.
- Caracterizar más de 10.000 cuarcitas mediante un enfoque macroscópico y microscópico no-destructivo.
- Caracterización tecno-tipológica de 5.237 piezas de industria lítica.
- Establecimiento de una metodología para el análisis de la movilidad a partir de los Sistemas de Información Geográfico.
- Descripción, análisis y síntesis de los datos obtenidos.

1.4. UNA CUESTIÓN DE ESCALA: ORGANIZACIÓN DE LA TESIS DOCTORAL

Este trabajo se estructura en cuatro partes diferenciadas que se articulan a partir de un sistema de escalas que parten de lo más amplio hacia lo más pequeño, para realizar un camino de vuelta que asciende desde las ideas más básicas hasta las más complejas. La primera de las partes está conformada por este capítulo introductorio y los tres siguientes, correspondientes a métodos y materiales. En este primer bloque planteamos la metodología utilizada en este trabajo a partir de una cuestión de escala y enfoque, desde lo más amplio hasta lo más pequeño. La segunda de las partes cambia esta relación y lanza desde lo concreto y minúsculo, un grano de cuarzo, una mayor complejidad de conceptos, hasta entender la dispersión de las cuarcitas a través del ciclo de las rocas. Esta parte corresponde con los dos primeros capítulos de resultados y que sientan las bases para el análisis de los materiales arqueológicos que compone el tercer bloque. El último, presenta los resultados obtenidos de la caracterización de la cuarcita desde un punto de vista geo-arqueológico y tecno-tipológico de las ocho colecciones líticas analizadas en los siguientes siete capítulos de esta tesis, ampliando más si cabe esta jerarquía de conceptos. Finalmente, la cuarta parte de este trabajo corresponde a la discusión y las conclusiones del mismo. En este último bloque evaluaremos la metodología, los resultados y las conclusiones aportadas a partir de la comparación con otros trabajos.

La primera de las partes comentadas presenta, a través de un enfoque cada vez más preciso, la metodología utilizada y los materiales que analizaremos en cada uno de los niveles de profundidad del trabajo. La Geología y la Arqueología van de la mano en cada uno de los capítulos de este primer bloque de trabajo. Partiendo de un análisis bibliográfico a escala regional del Capítulo-1, delimitamos el marco geográfico de estudio y las razones generales de dicha selección. Adicionalmente, en este capítulo planteamos las bases científicas de este trabajo, los objetivos de la tesis, una breve historiografía del estudio de las litologías de los conjuntos industriales prehistóricos y la estructura de esta obra. Una vez especificada la zona de estudio principal y las razones que nos han llevado a ello, en el Capítulo-2 (Materiales y métodos: un enfoque regional para entender las estrategias de captación de materia prima lítica) se especificará la zona de análisis, describiendo la geología de la zona y entendiendo las unidades geológicas a partir de las fuentes disponibles. Asimismo, describiremos los yacimientos arqueológicos analizamos a partir de la bibliografía. En este mismo capítulo expondremos la metodología utilizada para, por un lado, la preparación, realización y el análisis de la información de las prospecciones geo-arqueológicas de campo. Por otro, para entender la dispersión de la cuarcita por parte de los humanos prehistóricos utilizando los Sistemas de Información Geográfica. El Capítulo-3, siguiendo el mismo planteamiento dual, profundiza en el análisis de los materiales procedentes de contextos arqueológicos y geológicos a partir de una metodología de carácter macroscópica. Para ello describimos la propuesta de análisis que hemos seguido para analizar las industrias líticas así como la caracterización macroscópica de las litologías en contextos arqueológicos y geológicos. En el último capítulo de este bloque (Capítulo-4: Materiales y métodos. Un enfoque microscópico para entender la cuarcita en contextos arqueológicos), tomando los materiales seleccionados de los dos anteriores capítulos, plantea los elementos que nos permiten la descripción y caracterización de las cuarcitas a escala microscópica. En este capítulo se aborda la metodología de análisis de carácter destructivo y no-destructivo de la cuarcita.

El segundo de los bloques de este trabajo plantea un enfoque diferente describiendo ya resultados, desde lo más pequeño y esencial a lo más grande y complejo. Estos dos capítulos están

relacionados con el conocimiento de la cuarcita a nivel geológico, sin olvidar las connotaciones arqueológicas del mismo. De esta forma, el Capítulo-5 (Resultados. Definiendo y caracterizando la cuarcita en contextos arqueológicos: de procesos sedimentarios a procesos metamórficos) presenta los resultados obtenidos de la aplicación de la metodología propuesta en el Capítulo-4 y define la cuarcita en contextos arqueológicos, estableciendo tipos y variedades. Por su parte, el Capítulo-6 (Resultados. La cuarcita en los valles del Deva, Cares y Güeña: potenciales zonas de captación), describe las cuarcitas de los valles del Deva, Cares y Güeña en los diferentes ambientes geológicos mediante la metodología explicada previamente. Finalmente, se plantean los potenciales contextos de captación de la cuarcita.

El tercer bloque lo constituye el análisis de las evidencias líticas de los niveles arqueológicos seleccionados desde perspectivas geo-arqueológicas y tecno-tipológicas. Excepto el último de los capítulos, todos comparten la misma estructura y se basan en el análisis cuantitativo de los datos. Éste pasa por la descripción de cada uno de los niveles analizados a partir de las diferentes estructuras de análisis y primando la caracterización de las materias primas. El orden de las estructuras responde a dos factores: por un lado, los objetivos de la tesis que ponen en primer lugar el análisis de la cuarcita. Por otro, la ordenación de las variables en función de su naturaleza: nominal o numérica. Finalmente cada capítulo propone una recopilación de los datos mediante la descripción de los procesos de adquisición y gestión de las materias primas en cada nivel así como la movilidad de las mismas para su incorporación en el registro fósil de cada yacimiento. Los niveles están ordenados cronológicamente. El último capítulo, el Capítulo-13, únicamente incorpora la dimensión descriptiva del análisis geo-arqueológico de la industria lítica. En este capítulo describimos y analizamos las evidencias de la Cueva con arte parietal de la Covaciella y una muestra de las cuarcitas del yacimiento germano de Ravensberg-Troisdorf.

El último bloque corresponde con la discusión y las conclusiones de este trabajo. En el Capítulo-14 hay tres apartados diferenciados. El primero planteará una evaluación de la metodología empleada debido al carácter experimental y metodológico de esta tesis. El segundo tratará de entender y describir la cuarcita como roca, desde su génesis hasta su abandono final por parte de las sociedades paleolíticas. La tercera idea que desarrollaremos evidenciará la variabilidad de los mecanismos de adquisición, gestión y distribución de la cuarcita en la zona de estudio a partir de una visión diacrónica y una visión sincrónica. Finalmente, en el capítulo-15 resumiremos las principales contribuciones de esta tesis, las limitaciones del mismo y las futuras líneas de investigación que abre este trabajo.

Table-1.1: Tabla con los datos utilizados para confeccionar el estado del conocimiento acerca de las materias primas líticas en la Región Cantábrica.

Yacimiento	Nivel	Número de piezas	Sílex	Cuarcita	Cuarzo	Ofita	Otras	Rango crono-cultural
Aitzbitarte III	Vb	1704	96,0	1,1	1,0	1,0	1,5	Auriñaciense
Aitzbitarte III	Vb Superior	403	97,5	0,0	0,0	-	2,5	Gravetiense
Aitzbitarte III	Va	920	95,2	0,4	0,8	-	3,6	Gravetiense
Aitzbitarte III	IV	1077	96,8	0,1	0,6	-	2,6	Gravetiense
Aitzbitarte III	III	1490	92,0	0,0	4,1	-	3,9	Gravetiense
Aitzbitarte III	II	472	88,8	0,6	5,7	-	82,4	Gravetiense
Aitzbitarte III	I	457	96,3	0,4	1,5	-	1,8	Magdaleniense
Amalda	VII	2246	85,5	1,7	0,0	1,3	7,5	Musteriense
Amalda	VI	1962	93,2	2,1	0,4	1,1	1,7	Gravetiense
Amalda	V	799	99,7	0,1	0,0	-	2,1	Solutrense
Amalda	IV	5401	96,8	0,4	0,8	10,0	95,4	Solutrense
Arlanpe	VI (Sector entrada)	221	37,1	1,4	6,3	-	55,2	Musteriense
Arlanpe	V (Sector entrada)	62	48,4	3,2	3,2	-	45,2	Musteriense
Arlanpe	IV (Sector entrada)	144	20,1	0,7	11,8	-	67,4	Musteriense
Arlanpe	5 (Sector central)	30	13,3	0,0	23,3	-	63,3	Musteriense
Arlanpe	4 (Sector central)	94	7,4	2,1	9,6	-	63,8	Musteriense
Arlanpe	3 (Sector central)	209	28,7	0,5	6,2	-	64,6	Musteriense
Arlanpe	E (Sector fondo)	18	5,6	22,2	11,1	-	61,1	Musteriense
Arlanpe	D (Sector fondo)	411	15,1	0,7	20,2	-	61,8	Musteriense
Arlanpe	C/C Cantos	217	25,8	0,5	6,0	-	67,3	Musteriense
Arlanpe	II	1780	65,8	0,0	1,2	-	33,0	Solutrense
Arlanpe	I	470	83,0	0,2	2,1	-	14,7	Magdaleniense
Axlor	3 (Ba)	1059	87,0	1,7	2,9	-	82,3	Musteriense
Axlor	4 (Ba)	13086	84,2	1,8	4,4	0,0	9,6	Musteriense
Axlor	5 (Ba)	2975	79,0	3,0	4,2	0,0	13,8	Musteriense
Axlor	6 (Ba)	1375	61,5	3,5	5,5	0,0	29,5	Musteriense
Axlor	7 (Ba)	208	49,0	5,3	1,4	0,0	44,2	Musteriense
Axlor	8 (Ba)	266	56,0	3,0	2,3	0,0	38,7	Musteriense
Axlor	D	456	80,9	3,7	3,1	0,0	12,3	Musteriense
Axlor	B	305	81,3	3,6	5,9	0,0	9,2	Musteriense
Covalejos	H	-	69,0	20,0	-	1,0	2,0	Musteriense
Covalejos	I	-	68,0	25,0	-	6,0	2,0	Musteriense
Covalejos	J	-	71,0	26,0	-	2,0	1,0	Musteriense
Covalejos	K	-	76,0	20,0	-	1,0	3,0	Musteriense
El Arteu	Recogida	257	-	95,0	0,0	-	5,0	Musteriense
El Castillo	20	1153	43,1	50,6	0,0	-	6,3	Musteriense
El Castillo	16	72	0,0	0,0	0,0	-	0,0	Auriñaciense
El Castillo	22	1010	43,5	45,0	0,0	-	1,1	Musteriense
El Castillo	21	25	40,0	36,0	24,0	-	0,0	Musteriense
El Castillo	18	659	32,9	52,8	0,0	-	14,3	Auriñaciense
El Castillo	14	150	46,0	2,0	0,0	-	30,7	Auriñaciense
El Castillo	12	100	78,0	4,0	6,0	11,0	25,0	Auriñaciense
El Castillo	10	68	70,6	8,8	2,9	2,9	17,6	Solutrense
El Castillo	8	1073	83,9	7,5	3,2	0,0	5,9	Magdaleniense
El Cierro	4	1379	31,0	51,0	1,0	0,0	17,0	Solutrense
El Cierro	7	-	18,8	81,3	-	-	-	Auriñaciense
El Conde	9/8	-	-	100,0	-	-	-	Musteriense
El Habario	Habario B	517	0,5	95,7	-	0,0	3,6	Musteriense
El Juyo	7	156	100,0	0,0	-	0,0	-	Magdaleniense
El Juyo	6	474	99,6	0,2	0,0	0,0	-	Magdaleniense
El Juyo	4	877	11,3	0,2	0,5	0,0	-	Magdaleniense
El Juyo	4 Santuario	63	96,8	1,6	2,5	0,0	-	Magdaleniense
El Mirón	128	-	69,0	3,0	17,0	-	11,0	Gravetiense
El Pendo	XVI	615	79,3	15,9	2,6	3,6	0,8	Musteriense
El Pendo	XIV	339	50,7	32,2	9,5	15,9	0,9	Musteriense
El Pendo	XIII	184	41,3	42,4	23,0	15,2	0,5	Musteriense

Yacimiento	Nivel	Número de piezas	Sílex	Cuarcita	Cuarzo	Ofita	Otras	Rango crono-cultural
El Pendo	XII-XI	473	51,2	35,9	7,6	11,4	0,0	Musteriense
El Pendo	VIIId	560	57,5	28,0	5,0	13,6	0,2	Musteriense
El Pendo	VIIIb	35	62,9	34,3	-	-	0,0	Auriñaciense
El Pendo	VIIIa	189	16,9	81,5	-	1,6	0,0	Auriñaciense
El Pendo	VIII	79	98,7	-	-	1,3	0,0	Auriñaciense
El Pendo	VII	405	89,1	5,7	4,7	0,5	0,0	Auriñaciense
El Pendo	IV Corte Carballo	1608	91,2	5,1	0,6	1,1	2,4	Solutrense
El Pendo	VI	145	97,9	2,1	0,0	-	-	Auriñaciense
El Pendo	Vb	69	95,7	-	4,3	-	-	Auriñaciense
El Pendo	Va	71	94,4	1,4	4,2	-	-	Gravetiense
El Pendo	V	32	93,7	6,2	-	-	-	Gravetiense
El Pendo	IV	356	88,9	1,0	10,1	-	-	Auriñaciense
El Pendo	III	180	90,5	5,6	3,9	-	-	Auriñaciense
El Pendo	IIc-g	258	98,4	1,2	-	0,4	-	Magdaleniense
El Pendo	IIa-b	122	96,8	1,6	0,8	-	0,8	Magdaleniense
El Pendo	II	291	97,4	1,7	-	-	0,9	Magdaleniense
El Ruso I	Va	386	88,1	7,5	2,1	1,8	0,0	Musteriense
El Ruso I	III	602	92,0	5,0	1,5	0,5	0,8	Solutrense
El Ruso I	IVa	267	90,3	4,9	1,1	2,2	1,5	Solutrense
El Ruso I	IVb	266	89,5	8,3	1,5	1,8	0,3	Auriñaciense
El Ruso I	Vc	178	84,8	11,8	1,1	2,2	-	Musteriense
El Sidrón	Unidad 3	373	~75	~20	-	-	5,0	Musteriense
El Sidrón	El osario	399	74,2	23,6	-	-	2,3	Musteriense
Esquilleu	III	-	0,0	58,9	0,0	-	41,1	Musteriense
Esquilleu	IV	-	0,0	71,8	0,0	-	28,2	Musteriense
Esquilleu	V	-	0,0	75,5	0,0	-	24,5	Musteriense
Esquilleu	VI	-	0,0	73,0	0,0	-	27,0	Musteriense
Esquilleu	VIf	-	0,0	71,9	3,5	-	24,6	Musteriense
Esquilleu	VII	-	0,0	72,8	0,0	-	27,2	Musteriense
Esquilleu	VIII	-	0,0	75,4	0,0	-	24,6	Musteriense
Esquilleu	VIIIb	-	0,0	70,4	0,0	-	29,6	Musteriense
Esquilleu	VIIIc	-	0,0	63,3	0,0	-	36,7	Musteriense
Esquilleu	IX	-	0,8	75,1	0,0	-	24,1	Musteriense
Esquilleu	XI	-	0,0	88,1	0,0	-	11,9	Musteriense
Esquilleu	XIF	-	0,0	94,3	0,0	-	5,7	Musteriense
Esquilleu	XIII	-	0,0	90,6	0,0	-	9,4	Musteriense
Esquilleu	XIV	-	0,0	86,4	0,0	-	13,6	Musteriense
Esquilleu	XV	-	0,0	83,5	0,0	-	16,5	Musteriense
Esquilleu	XVI	-	0,0	75,2	0,0	-	24,8	Musteriense
Esquilleu	XVII	-	4,4	57,1	8,0	-	30,5	Musteriense
Esquilleu	XVIII	-	0,0	59,7	0,0	-	40,3	Musteriense
Esquilleu	XIX	-	0,0	62,1	7,6	-	30,3	Musteriense
Esquilleu	XX	-	0,0	85,0	3,9	-	11,1	Musteriense
Esquilleu	XXI	-	0,0	66,8	0,0	-	33,2	Musteriense
Esquilleu	XXII	-	0,0	83,0	3,9	-	13,1	Musteriense
Esquilleu	XXIII	-	0,0	77,8	5,4	-	16,8	Musteriense
Esquilleu	XXIV	-	0,0	71,6	4,5	-	23,9	Musteriense
Esquilleu	XXV	-	0,0	78,7	0,0	-	21,3	Musteriense
Esquilleu	XXVI	-	0,0	77,9	0,0	-	22,1	Musteriense
Esquilleu	XXVII	-	0,0	89,4	9,8	-	0,8	Musteriense
Esquilleu	XXVIII	-	3,9	78,3	13,7	-	4,1	Musteriense
Esquilleu	XXIX-XXX	-	0,0	62,0	29,4	-	8,6	Musteriense
Hornos Peña	C	267	65,5	31,7	4,2	-	1,4	Solutrense
La Flecha	Musteriense	806	1,5	84,0	10,4	6,0	2,5	Musteriense
La Lluera I	IXA (fase I)	28	57,1	42,9	153,1	-	0,0	Solutrense
La Lluera I	VIII	3400	71,4	28,4	0,2	-	0,0	Solutrense
La Lluera I	VII	5761	66,8	32,8	0,4	-	0,0	Solutrense

Yacimiento	Nivel	Número de piezas	Sílex	Cuarcita	Cuarzo	Ofita	Otras	Rango crono-cultural
La Lluera II	II	78	41,0	59,0	-	-	0,0	Solutrense
La Paloma	4	385	80,8	13,2	5,5	-	0,0	Magdaleniense
La Paloma	6	1228	76,8	22,4	0,9	-	0,0	Magdaleniense
La Paloma	Magdaleniense medio (A)	185	55,7	44,3	0,0	-	0,0	Magdaleniense
La Paloma	8	2897	43,1	53,3	0,1	-	0,0	Magdaleniense
La Paloma	Magdaleniense inferior	137	75,9	24,1	0,0	-	0,0	Magdaleniense
La Riera	1	776	31,8	62,6	0,0	-	0,0	Auriñaciense
La Riera	2	139	75,5	11,5	0,0	-	0,0	Solutrense
La Riera	3	508	83,7	13,6	0,0	-	0,0	Solutrense
La Riera	4	1150	77,5	21,2	0,0	-	0,0	Solutrense
La Riera	5	1105	67,1	31,4	0,0	-	0,0	Solutrense
La Riera	6	1354	21,5	77,8	0,0	-	0,0	Solutrense
La Riera	7	2428	45,9	53,3	0,0	-	0,0	Solutrense
La Riera	8	3106	36,4	63,1	0,0	-	0,0	Solutrense
La Riera	9	2361	38,3	60,7	0,0	-	0,0	Solutrense
La Riera	10	2458	36,5	63,2	0,0	-	0,0	Solutrense
La Riera	11	1163	38,4	61,1	0,0	-	0,0	Solutrense
La Riera	12	325	36,6	60,9	0,0	-	0,0	Solutrense
La Riera	13	764	38,1	60,9	0,0	-	0,0	Solutrense
La Riera	14	6117	34,1	65,1	0,0	-	0,0	Solutrense
La Riera	15	3064	34,4	65,2	0,0	-	0,0	Solutrense
La Riera	16	5237	46,3	53,1	0,0	-	0,0	Solutrense
La Riera	17	2402	72,9	26,1	0,0	-	0,0	Solutrense
La Riera	18	4884	75,8	23,7	0,0	-	0,0	Magdaleniense
La Riera	19	4179	68,6	30,3	0,0	-	0,0	Magdaleniense
La Riera	20	2176	81,4	16,6	0,0	-	0,0	Magdaleniense
La Riera	19/20	2330	82,2	15,4	0,0	-	0,0	Magdaleniense
La Riera	21-23	559	79,1	19,9	0,0	-	0,0	Magdaleniense
La Riera	24	3297	71,7	28,2	0,0	-	0,0	Magdaleniense
La Riera	25	54	42,6	55,6	0,0	-	0,0	Magdaleniense
La Riera	26	1374	43,3	56,3	0,0	-	0,0	Magdaleniense
La Viña	IB	953	13,4	86,0	0,0	-	0,5	Musteriense
La Viña	IA	4023	18,7	80,8	0,0	-	0,4	Musteriense
La Viña	XIV	4539	15,8	83,8	0,0	-	0,4	Musteriense
La Viña	XIV + IC	7675	14,2	85,2	0,0	-	0,6	Musteriense
La Viña	XIII basal	68593	4,2	95,7	0,0	-	0,1	Musteriense
La Viña	XIII inf + XIII intrusion	17212	24,5	74,6	0,0	-	0,9	Auriñaciense
La Viña	XIII	23593	32,5	64,2	0,0	-	3,3	Auriñaciense
La Viña	XII	53750	33,0	65,0	0,0	-	2,1	Auriñaciense
La Viña	IX	-	36,3	61,4	-	-	2,3	Gravetiense
La Viña	X	-	38,1	60,3	-	-	1,6	Gravetiense
Las Caldas	16 (sala)	228	89,0	11,0	-	-	0,0	Solutrense
Las Caldas	14 (sala)	244	80,7	18,4	0,8	-	0,0	Solutrense
Las Caldas	15 (pasillo)	354	81,9	18,1	-	-	0,0	Solutrense
Las Caldas	14-A (pasillo)	514	100,0	0,0	-	-	0,0	Solutrense
Las Caldas	12 (pasillo)	729	79,6	20,3	0,1	-	0,0	Solutrense
Las Caldas	11 (pasillo)	2139	96,6	3,4	-	-	0,0	Solutrense
Las Caldas	10 (corte sala I)	68	63,2	36,8	-	-	0,0	Solutrense
Las Caldas	10 (pasillo)	1287	97,0	resto	-	-	0,0	Solutrense
Las Caldas	9 (pasillo)	2123	84,8	15,2	-	-	0,0	Solutrense
Las Caldas	8 (sala)	132	47,7	36,2	2,3	-	0,8	Solutrense
Las Caldas	8 (Pasillo)	730	79,0	10,8	-	-	0,1	Solutrense
Las Caldas	7 (Sala I)	2517	87,3	12,1	-	-	0,0	Solutrense
Las Caldas	6	598	92,5	7,2	-	-	0,3	Solutrense
Las Caldas	5	2306	86,6	13,0	-	-	0,2	Solutrense
Las Caldas	4	1190	68,7	30,6	-	-	0,7	Solutrense
Las Caldas	3	497	85,1	14,7	-	-	-	Solutrense

Yacimiento	Nivel	Número de piezas	Sílex	Cuarcita	Cuarzo	Ofita	Otras	Rango crono-cultural
Las Caldas	II (Sala II)	1080	95,3	4,5	0,2	-	-	Magdaleniense
Lezetxiki	VII	13	53,8	7,7	-	-	38,5	Musteriense
Lezetxiki	VI	112	44,7	5,3	6,1	-	43,8	Musteriense
Lezetxiki	V	50	70,0	6,0	-	2,0	22,0	Musteriense
Lezetxiki	IV	455	71,4	3,1	-	2,2	23,3	Musteriense
Lezetxiki	III	1804	74,1	3,1	-	5,9	14,2	Musteriense
Llonín	V	-	44,4	45,2	-	-	10,4	Gravetiense
Morín	17inf	402	71,6	15,9	4,7	6,2	0,0	Musteriense
Morín	17	2197	67,0	11,1	0,0	19,9	2,0	Musteriense
Morín	16	1803	55,5	20,9	1,4	22,3	0,5	Musteriense
Morín	15	877	53,4	22,5	1,0	23,1	0,0	Musteriense
Morín	13/14	1660	63,0	22,6	0,8	13,7	0,0	Musteriense
Morín	12	1867	49,2	23,6	3,1	23,4	0,2	Musteriense
Morín	11	1672	62,7	22,8	2,4	20,9	0,7	Musteriense
Morín	8a	2187	85,8	7,4	2,0	4,1	0,5	Auriñaciense
Morín	8a en milhojas	497	84,7	10,3	1,4	3,2	0,2	Auriñaciense
Morín	7	-	93,7	3,4	1,7	1,1	-	Auriñaciense
Morín	6	-	93,7	2,1	2,2	1,9	-	Auriñaciense
Panes II	A	81	1,2	70,4	-	-	28,4	Musteriense
Rascaño	2	164	98,8	0,6	0,6	-	-	Magdaleniense
Rascaño	2b	1256	98,3	0,9	0,7	-	-	Magdaleniense
Rascaño	3	3571	98,6	0,9	0,4	-	0,5	Magdaleniense
Rascaño	4	2097	98,7	0,8	0,5	-	-	Magdaleniense
Rascaño	4b	719	98,3	1,2	-	-	0,1	Magdaleniense
Rascaño	5	1457	83,4	16,0	-	-	0,3	Magdaleniense
Sopeña	II	-	37,6	21,0	17,2	-	1,2	Auriñaciense
Sopeña	I	417	38,1	27,1	20,6	-	1,3	Gravetiense
Sopeña	VI	-	13,5	67,6	0,0	-	0,0	Auriñaciense
Sopeña	V	-	28,9	61,5	0,0	-	0,0	Auriñaciense
Sopeña	III	-	34,6	21,0	19,4	-	1,0	Auriñaciense
Sopeña	VII	-	13,9	80,1	0,0	-	0,7	Auriñaciense
Sopeña	VIII	-	11,3	70,6	0,6	-	3,4	Auriñaciense
Sopeña	IX	-	12,5	71,6	0,2	-	7,2	Auriñaciense
Sopeña	X	-	7,8	72,4	0,0	-	5,5	Auriñaciense
Sopeña	XI	-	8,3	69,9	0,0	-	7,3	Auriñaciense
Sopeña	XII	187	7,5	52,5	0,0	-	13,3	Musteriense
Sopeña	XIII	130	10,5	70,6	0,0	-	5,9	Musteriense
Sopeña	XIV	90	13,5	68,3	0,0	-	7,7	Musteriense
Sopeña	XV	229	7,0	86,1	0,0	-	3,0	Musteriense
Sopeña	IV	-	17,5	52,5	0,0	-	7,5	Musteriense

CHAPTER-2

MATERIALS & METHODS. A REGIONAL APPROACH TO UNDERSTAND LITHIC PROCUREMENT STRATEGIES

2.1. Materials. Geological perspectives: Physical Geology of Deva, Cares, And Güeña valleys

2.1.1. Palaeozoic rocks: The Cantabrian Zone

2.1.2. Mesozoic and Cenozoic rocks: The Basque-Cantabrian Basin

2.2. Geological perspectives: Understanding quartzite in the selected area

2.2.1. Preparing a field geology survey: Optimasing information through Digital Cartography and Geographic Information Systems (GIS)

2.2.2. Field Survey: Geological survey for understanding quartzite catchment areas

2.2.3. Systematising geological surveyss: Three quartzite environments, three datasets

2.3. Materials. Archaeological perspectives: The Palaeolithic on the Deva, Cares and Güeña valleys

2.3.1. The Archaeological site of El Esquilleu cave

2.3.2. The archaeological site of El Habario

2.3.3. The archaeological site of El Arteu

2.3.4. The archaeological site of La Cueva de Coímbre

2.3.5. The Cave Art of La Covaciella

2.4. Methodology. Archaeological perspectives: Least Cost Analysis to understand lithic procurement strategies during the Palaeolithic

2.1. GEOLOGICAL PERSPECITVES: PHYSICAL GEOLOGY OF DEVA, CARES, AND GÜEÑA VALLEYS

As previously mentioned, we have selected the proposed area of study due to geological and archaeologica reasons. The first one is based on the variability of the geological domain, probably the highest for Cantabrian coastal area, because this zone is the present limit between the Iberian Massif and the Basque-Cantabrian Basin (Figure-2.1). That situation could open a bigger opportunity to find different types of material. This area is mainly composed of two geological domains. The first one is the eastern part of the Cantabrian Zone, mainly composed of Carboniferous materials. In this zone, two provinces can be clearly distinguished: To the South, the Pisuerga-Carrión Province wich also present Devonian and Silurian remnant, and to the West and North Picos de Europa and Ponga Nappe Province, containing also a Cambrian and Ordovician material. The second one is the western part of the Basque-Cantabrian Basin, in particular, the Navarro-Cantabrian sulcus, mainly dominated by sedimentary Mesozoic rocks and small parts of Cenozoic material (Figure-2.2).

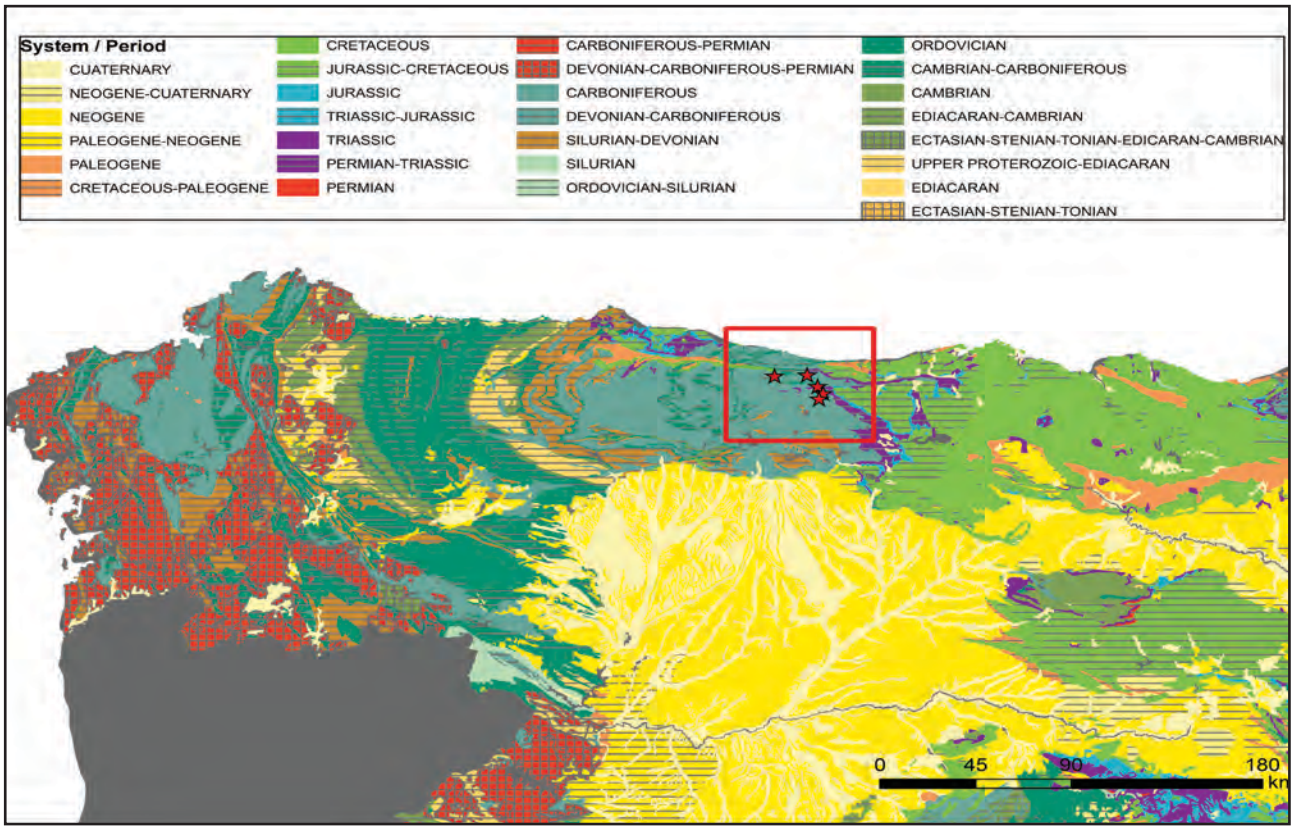

Figure-2.1: Geologic map of northwestern part of Spain, modified from the map/database of Geologic Map from IGME map at 1: 1,000,000 scale (Álvaro et al., 1994). Research area is outlined in red.

2.1.1. PALAEOZOIC ROCKS: THE CANTABRIAN ZONE

The Cantabrian Zone is the outer zone of the Iberian Massif on the Northwest of the Iberian Peninsula, and it is the core of the Iberian-Armorican Arc. The western limit is the Narcea Antiform that separates this zone from the rest of Iberian Massif. It is limited to the North by the sea line, and to south and east it is covered by Mesozoic-Triassic sequences (Figure-2.3). It is characterised by overthrust and folded mantles derived from surface tectonics. Metamorphic process and tectonic foliation are almost absent (Pérez-Estaún et al., 2004).

There are five provinces in this zone: the Southwestern units, grouped into the Somiedo-Correcilla, Aramo and Esla-Valsurvio Units, are characterised by having an almost complete Palaeozoic sequence. The Central Carboniferous Basin is mainly composed of Carboniferous rocks and a band of Cambrian-Ordovician to the East. Ponga Nappe Province, divided into two areas, is characterised by the almost absence of Silurian and Devonian layers, and also by the overthrust of units that create a folded mantle. Picos de Europa Province is a squamous area mainly composed of Carboniferous carbonate rocks. Finally, the Pisuerga-Carrión Province is composed of Carboniferous (mainly), Silurian and Devonian rocks (Bastida, 2004).

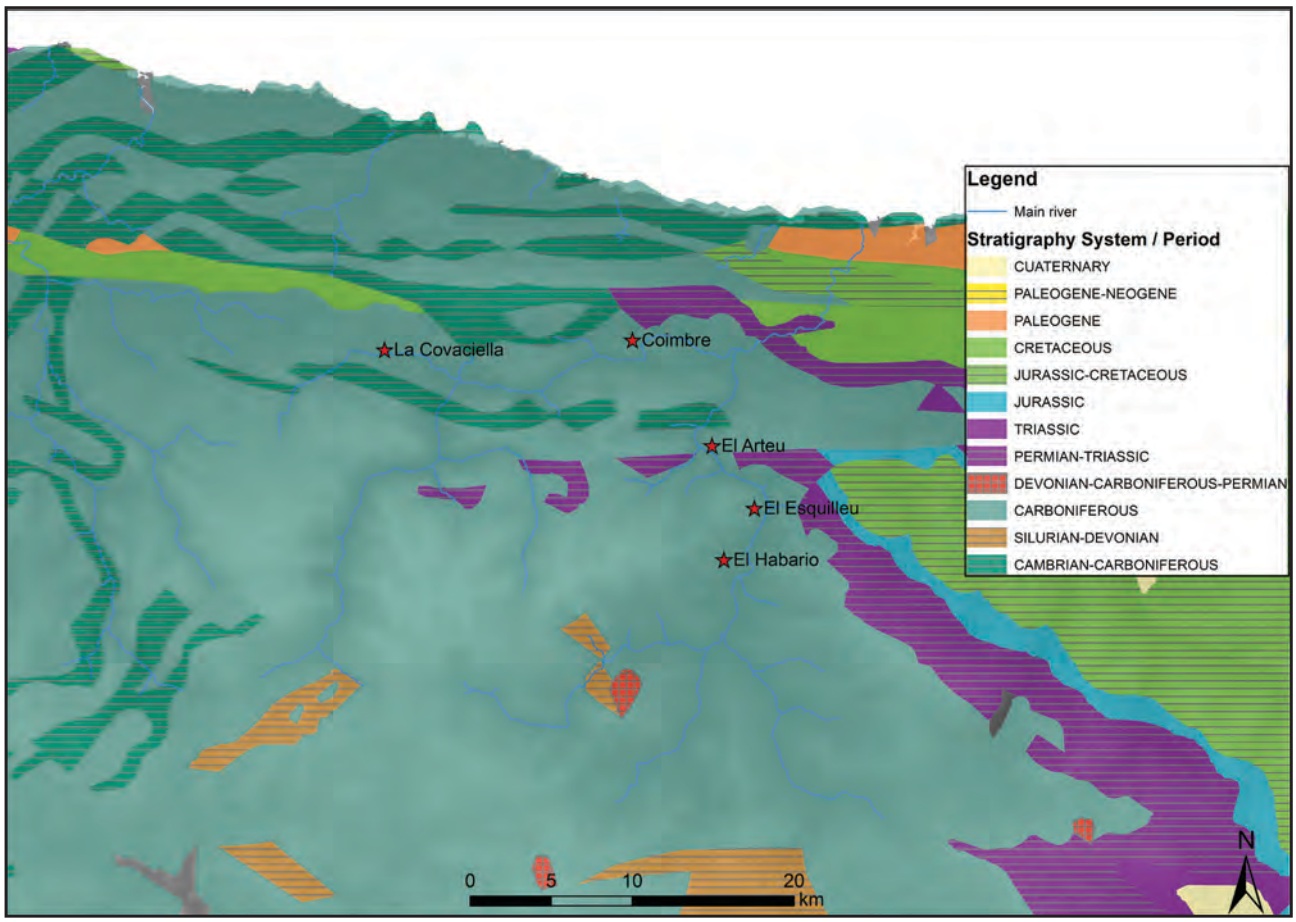

Figure-2.2: Geologic map of research area, modified from the map/database of Geologic Map from IGME map at 1: 1,000,000 scale (Álvaro et al., 1994). Starts represent the archaeological site analysed in this research.

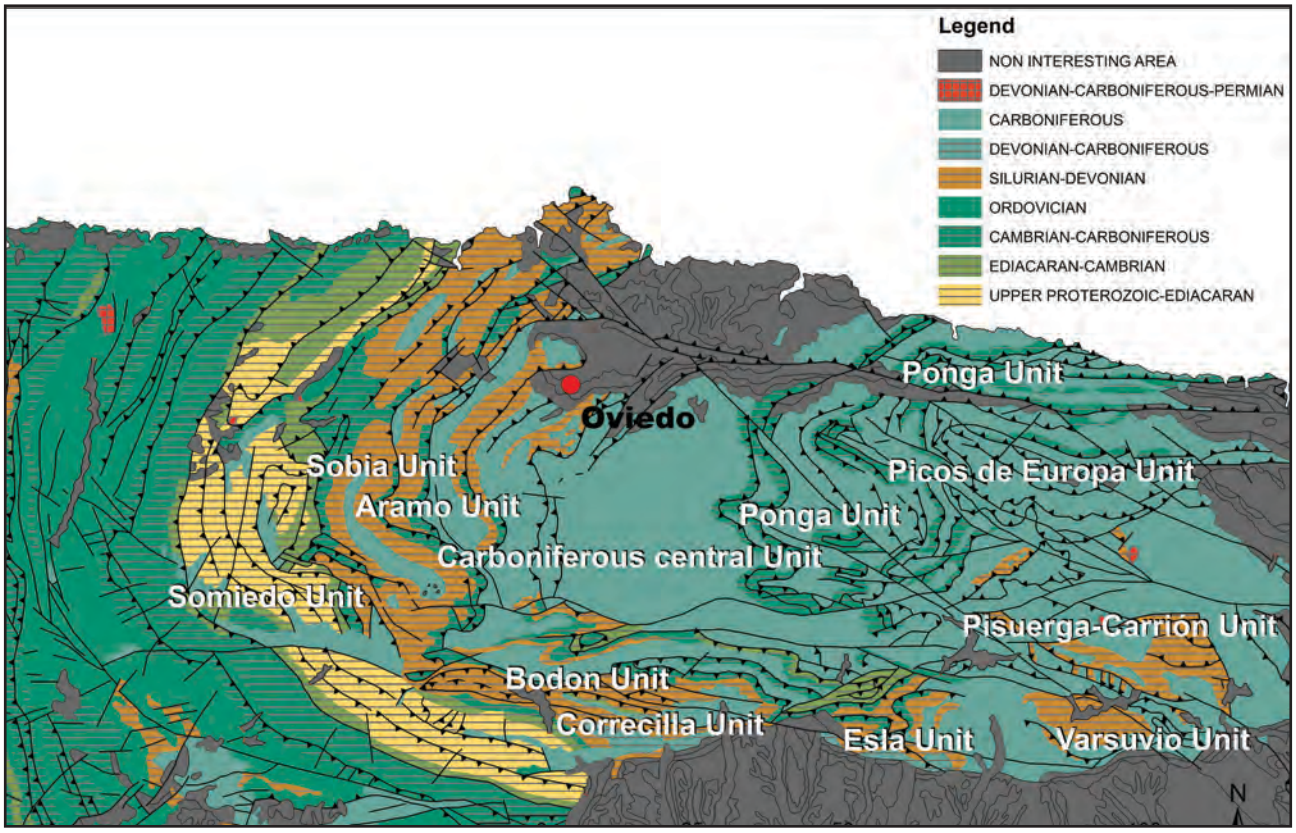

Figure-2.3: Geologic map of Cantabrian Zone with the different units described in text. The map is based on Julivert (1971) and the modification made by Bastida (2004) in figure-2.5.

The stratigraphy of this geological zone is a succession of phases that corresponded with Palaeozoic Domain, with the presence of Precambrian domains only in the western part with the Narcea Formation, Southwestern units (Pérez-Estaún, 2004).

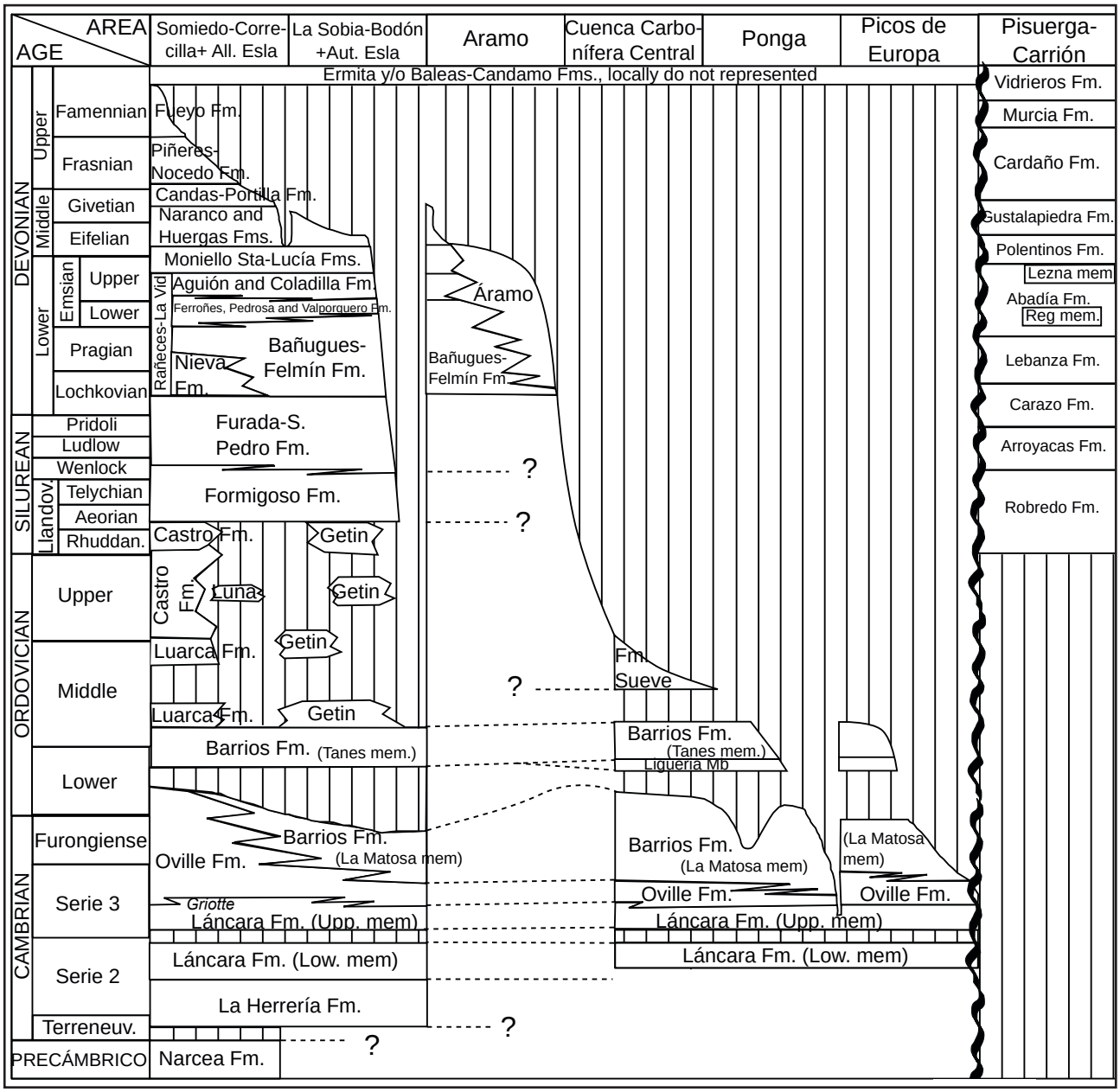

Figure-2.4: Stratigraphy chart from Cambrian to Devonian periods in the Cantabrian Zone. This is modified from figures 2.7 and 2.8 from Aramburu et al. (2004). Striped areas are stratigraphic hiatus, while white areas represent zones without outcrop surface.

The base of the Palaeozoic domain, in the Cambrian-Ordovician period, is almost completely represented in this zone by two siliceous formations, which are divided by a carbonated one (Figure-2.4). The first part is the Herrería Formation that only appears in the Southwestern Units. It is separated by the Lower-Middle Cambrian limestones of the Láncara Formation from two siliceous formations, the Middle Cambrian to Early Ordovician Oville and Barrios Formations (Liñan et al., 2002). The last three, appear in all Cantabrian Zone, but they are thicker on the western zones (Álvaro et al., 2000). Middle and Upper Ordovician are represented by successive and variable types of material, mainly shale and sandstone with a presence of iron oxides. These types of material stay stable along Silurian, and appear, mainly in Southwestern Units and Pisuerga-Carrión Province. In the last unit, the presence of sandstone/quartzarenite is massive in the Robledo, Arroyacas and Carazo Formations (Aramburu et al., 2004). The Devonian mainly appears in Southwestern and Pisuerga-Carrion Units, although it also appears in other units. Lithologically, the Cantabrian Zone is composed of the succession of shale, sandstone, and different carbonate rocks, resulting in sedimentary processes on two parts of the same marine platform: A hemipelagic marine environment

to the east, and marine benthonic to the west. More than 20 formations are dated as Devonian in the Cantabrian Zone, which is fulfilled with Ermita and Vidrieros formations. Along this period (more than 220 M.A.), this area was a big drainage basin in the northern part of Gondwana paleocontinent. There was a gradual increase of grain-size from the beginning of the Cambrian age to the end of Devonian age, also, from the eastern to the western area. This process is in due to sedimentary conditions and the proximity/quantity of source area material to be eroded (Aramburu et al., 1992).

During the Carboniferous, the Cantabrian Zone is influenced by the Variscan orogenic, generating tectonic movements. This situation generates a mixture of new and individualised sedimentary basins and, therefore, discontinuity and variability in the stratigraphy (Figure-2.5). This variability is higher in the Pisuerga-Carrión Province (Pastor-Galán et al., 2014). Overall, the stratigraphy is represented by three phases: The base of the sequence is formed between the Tournaisian and Visean Ages (Lower Carboniferous) and is composed of Vegamian, Baleas, and Alba Formations. These formations consist mainly of shales and different types of limestones, among which radioralite or flint could be found. There is almost no difference in all the Cantabrian Zone. The middle part of the sequence is represented by Namurian carbonate rocks on the first part (Barcaliente Formation), showing continuities with the previous phase, also in the geographical representation. The second part of this sequence is lithologically different from previous phases. It is composed of mixture layers of limestones, shales, conglomerates, sandstones, and coal layers. That situation generates a more complex area, with features similar to the Pisuerga-Carrión Province. The last part of the Upper Carboniferous sequence (Upper Moscovian to Gzhelian) is characterised by a mixed lithology, as seen in the previous phase (Fernández et al., 2004). The stratigraphy shows different formation (e.g. Valdeteja, Picos de Europa, Curavacas and Remoña Formations) due to the diversity of sedimentary environments developed in the Cantabrian Zone by Variscan orogeny. From sedimentary and marine influence on the first part of the sequence to sedimentary alluvial or deltaic formations on the central and late parts of the sequence. This influence is also appreciated in the geographic heterogeneity of the Cantabrian Zone.

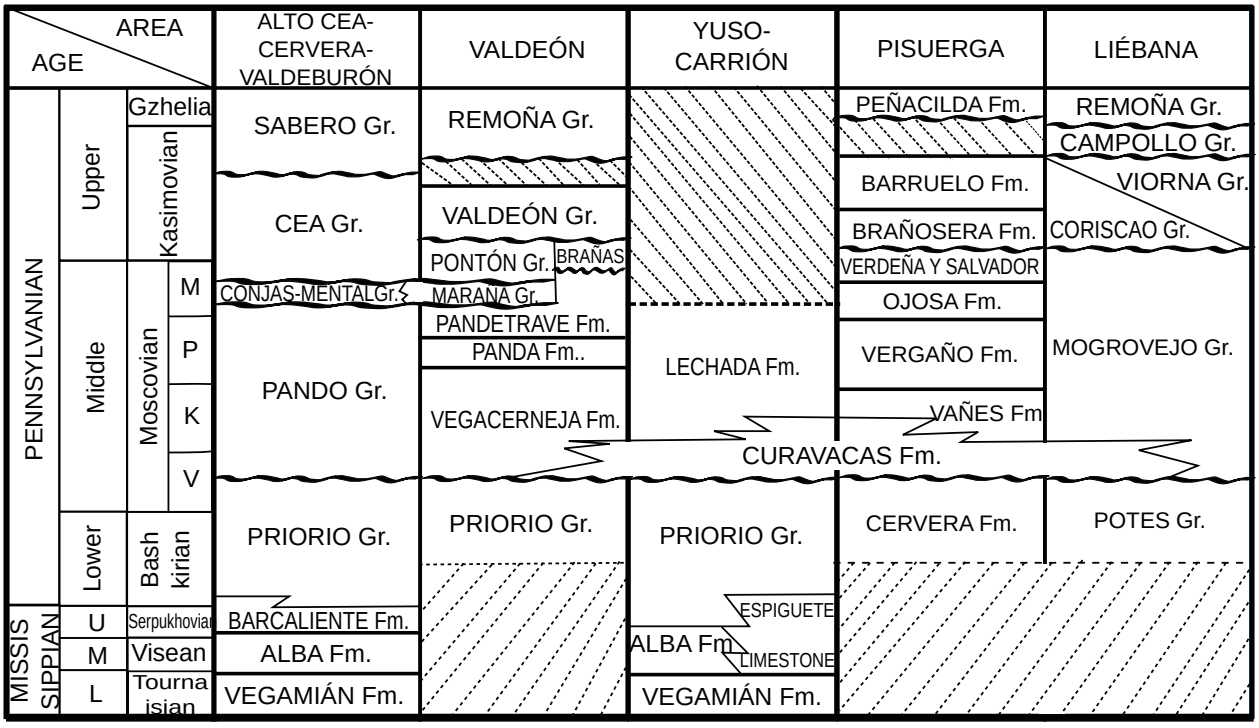

Figure-2.5: Stratigraphy chart of Carboniferous in the Cantabrian Zone (Pisuerga-Carrión Zone). This chart is modified from Figure-2.14 from Fernández et al. (2004).

As we have previously mentioned, the structure of the Cantabrian Zone is mainly based on thrust and folds created by thin-skinned tectonics as a consequence of Variscan Orogenesis during the Carboniferous. These overthrusts are mainly of W/E direction, and they are thicker in the western part. Nevertheless, there are differences in the overthrust of each unit. There are two distinct systems of folds: longitudinal fold system and radial fold system. Both are clearly related with overthrust. Latter Alpine orogenesis reactivated this structure of thrust and fold (Aller et al., 2004). Metamorphism in the Cantabrian Zone is not significant, and it is reduced to areas of very low or low meta-

morphism. These areas are in the Southwestern Units as consequence of Iberian Massif influence and in the central and eastern units through burial metamorphism (Bastida et al., 2002). Additional metamorphic processes could be appreciated as consequence of fault (dynamic metamorphism), contact metamorphism associated with small igneous bodies in the Permian, or cleavage in Eastern and central parts of the Cantabrian Zone (Blanco-Ferrera et al., 2016; Valín et al., 2016).

2.1.2. MESOZOIC AND CENOZOIC ROCKS: THE BASQUE-CANTABRIAN BASIN

The Basque-Cantabrian Basin (CVC) is part of the Pyrenees basin, defined between the Pamplona fault and the limit with the Cantabrian Zone. To the South it is limited by the Duero basin and the Ebro basin, non-deformed Cenozoic domains. To the North is limited by the Cantabrian Sea. This area is characterised by a large Cretaceous sequence generated as a basin in that moment and later Alpine deformation (Robles, 2014).

In this chiefly sedimentary area with minor presence of igneous and metamorphic rocks there are three parts we are going to describe from East to West (Barnolas and Pujalte, 2004). First part is the Basque Trough (Figure-2.6). It is characterised by a deep marine sequence of Jurassic, carbonate a siliciclastic Cretaceous and lower Paleogene on open-sea conditions, and large turbidity deposits, that create a Flysch structure from Albian to Lutetian ages together with the presence of magmatism in the Cretaceous period and little evidence of metamorphic process in the Mesozoic. The second one is the Navarro-Cantabrian sulcus. In this case, the Mesozoic and Cenozoic deposits sequence is shallow, and Cretaceous metamorphism and magmatism are weaker. In that case, sedimentary conditions fluctuated from open and deep-sea conditions to coastal and continental conditions. The third part is the North-Castile zone. It is part of North-Iberian Mesozoic-Paleogene paleomargin. Formative conditions are similar those of the Navarro-Cantabrian sulcus, increasing coastal and continental paleoenvironments in the sedimentary process.

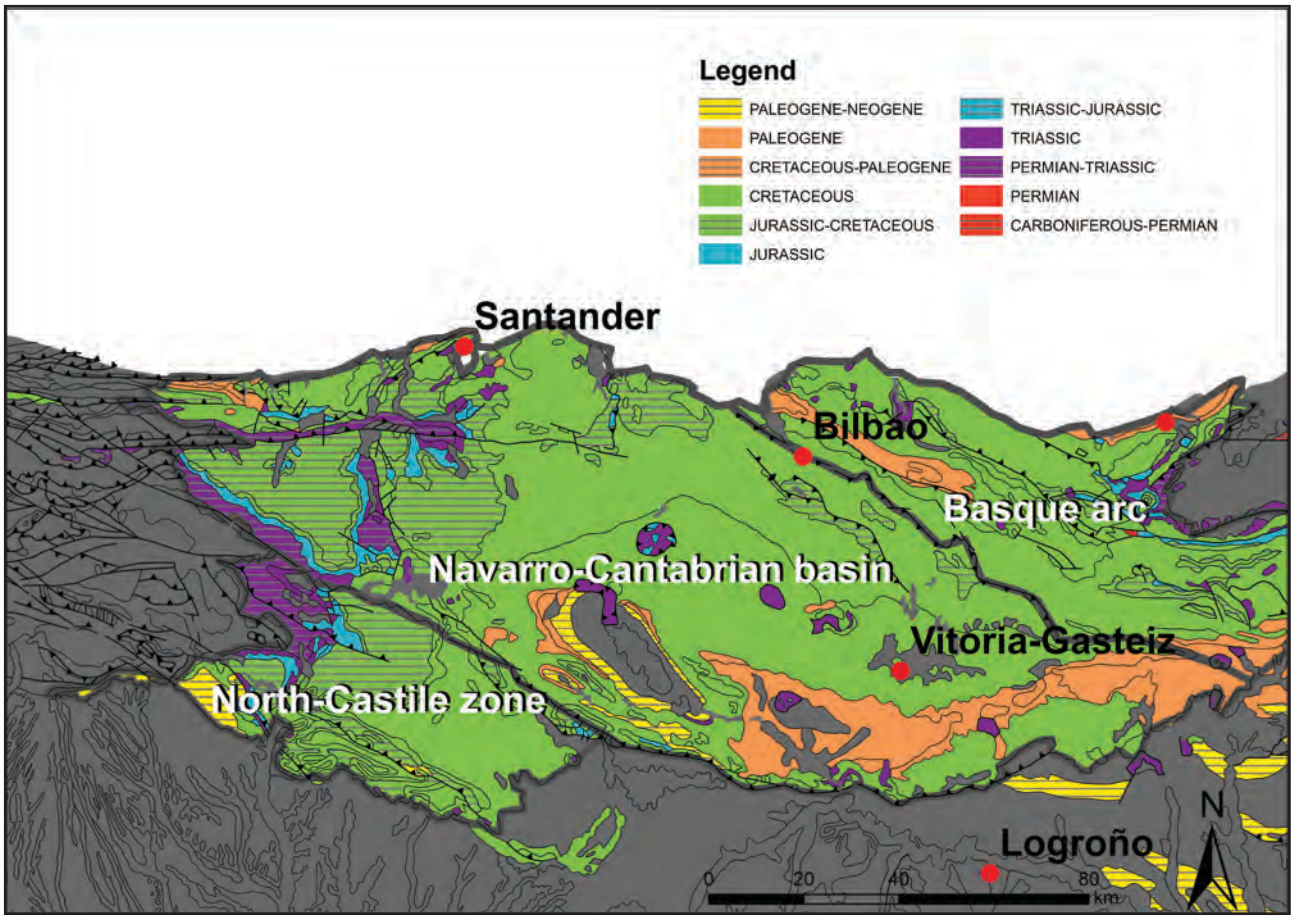

Figure-2.6: Geologic map of the Basque-Cantabrian Basin Zone with the different units described in text. The map is based on figure-3.3 from Barnolas and Pujalte (2004).

The base of the sequence in the Basque-Cantabrian Basin is dated to the late Permian period, with some small outcrops in the Peña Sagra, Peña Labra, Piñeres-Carmona and Salinas de Pisu-

erga areas. In these reduced areas, the Permian is characterised by mixture layers created, mainly, by the erosion of volcanic materials and its later alluvial deposition. Conglomerates, sandstone, and carbonate rocks are also common in these areas (Robles, 2004). At the beginning of the Triassic period, the area started to operate as a rift, which generates an opening basin that is filled with Buntsandstein, Muschelkalk and Keuper facies. The first one is composed of conglomerates, sandstone, and red shales; the second one consists on carbonate rocks (absent from the western areas), and the latter is composed of shale and evaporitic deposits. At the end of the Triassic period and along lower and middle Jurassic, that area became an inter-rift basin where mainly carbonate rocks were deposited due to the predominant marine sedimentary conditions. Only at the beginning and at the end of this period it is possible to find siliciclastic material (Robles et al., 2004). At the end of the Jurassic period, the area became again a big rift zone, creating two different areas. To the west, the Navarro-Cantabrian sulcus and the North-Castile zone, mainly composed of continental deposits (conglomerates, carbonates, sandstone or shales), and the East dominated by limestone or carbonate materials (carbonate sandstone or marlstones) (Pujalte et al., 2004). Along with the Lower Cretaceous, the area is more influenced by marine erosion and deposits as a consequence of the rising of the sea level and the subsidence of the basin. Sedimentary rocks such as sandstone, shales, (underwater/submarine) volcanic and carbonate rocks, filled a complex system of marine influence in this area (García-Mondéjar et al., 2004). In the Upper Cretaceous this area reinforced its marine influence with more flysch formation with limestone, shales, and marls in almost all this area. Flint could also appear, associated to the Basque Trough, as volcanic spread events between the Albian and the Santonian ages (Floquet, 2004). At the end of Maastrichtian, the area starts to change the conditions from an opening area to a closed and compressive one. A period dominated again by limestone and calcareous rocks started, but due to differences in the zone, sandstone or conglomerate deposits could also be found in southern areas (Baceta et al., 2004). From the Ypresian age on, the compressive movement increases, decreasing sedimentary deposits in the area, again formed by calcareous and sandy rocks. These rocks were formed during the Alpine orogenesis without geographic continuity (Robles, 2014).

The structure of this zone is based on three tectonic phases, which have already been mentioned. The first on is associated with the opening movement of the North Atlantic Ocean at the end of the Variscan orogenesis, which generates a network of fractures. The Jurassic ophites (basic volcanic rocks) are related to this movement. The second phase is characterised by the opening of the Biscay Gulf, generated by the displacement of the Iberian massif from Eurasia. This movement generates an echelon folds, and locally lherzolite, alkaline volcanism and contact metamorphism. The third tectonic phase corresponds to the Iberia-Eurasia collision in two different processes that generated the present Pyrenees Range and their western extension through the Cantabrian Mountains. First, crushing/collision structures create a vergence to the North, and second, into South direction (Martínez-Torres and Eguíluz, 2014).

2.2. GEOLOGICAL PERSPECITES: UNDERSTANDING QUARTZITE IN THE SELECTED AREA

2.2.1. PREPARING A FIELD GEOLOGY SURVEY: OPTIMISING INFORMATION THROUGH DIGITAL CARTOGRAPHY AND GEOGRAPHIC INFORMATION SYSTEM (GIS)

We have decided to optimise the survey process using pre-existent information and to use the GIS software ArcGIS v.10.2.2. The materials we have used are:

1. A Digital Elevation Model (DEM) as Base map. It is obtained from the creation of a mosaic raster created by the union of thirteen DEM25 (MDT25, following the Spanish acronym) obtained from the Spanish National Institute of Geography (Instituto Geográfico Nacional, IGN) (IGN, 2017). The number codes used are: 15, 30, 31, 32, 33, 54, 55, 56, 57, 79, 80, 81 and 82. This and later datasets are projected using UTM-ETRS89 30N coordinates system. The raster resolution is 25 meter (Figure-2.7).

2. A geological base map: It is obtained from the selection of MAGNA 1:50.000 shape files, obtained from Instituto Geológico y Minero de España IGME, of the area selected. The thirteen sheets are the following: Lastres nº15 (Pignatelli et al., 2003), Villaviciosa nº30 (Beroiz et al., 2003), Ribadesella nº31 (Navarro, 2003), Llanes nº32 (Martínez García, 2003), Comillas nº33

(Ramírez del Pozo et al., 2003), Rioseco nº54 (Heredia and Rodríguez Fernández, 2003), Beleño nº55 (Julivert and Navarro, 2003), Careña-Cabrales nº56 (Martínez García et al., 2003), Cabezón de la Sal nº57 (Carreras Suárez et al., 2003), Puebla de Lillo nº79 (Alvarez-Marrón et al., 2003), Burón nº80 (Heredia et al., 2003b), Potes nº81 (Rodríguez Fernández et al., 2003) and Tudanca nº82 (Heredia et al., 2003c). As we explain below, for field inspection of geologic units containing highly siliceous rocks the geologic information of these sheets is enough. The updated version of geological cartography from IGME using global and continuous (for Spain) geology, was under construction during this research but it did not introduce more detailed information for our purposes.

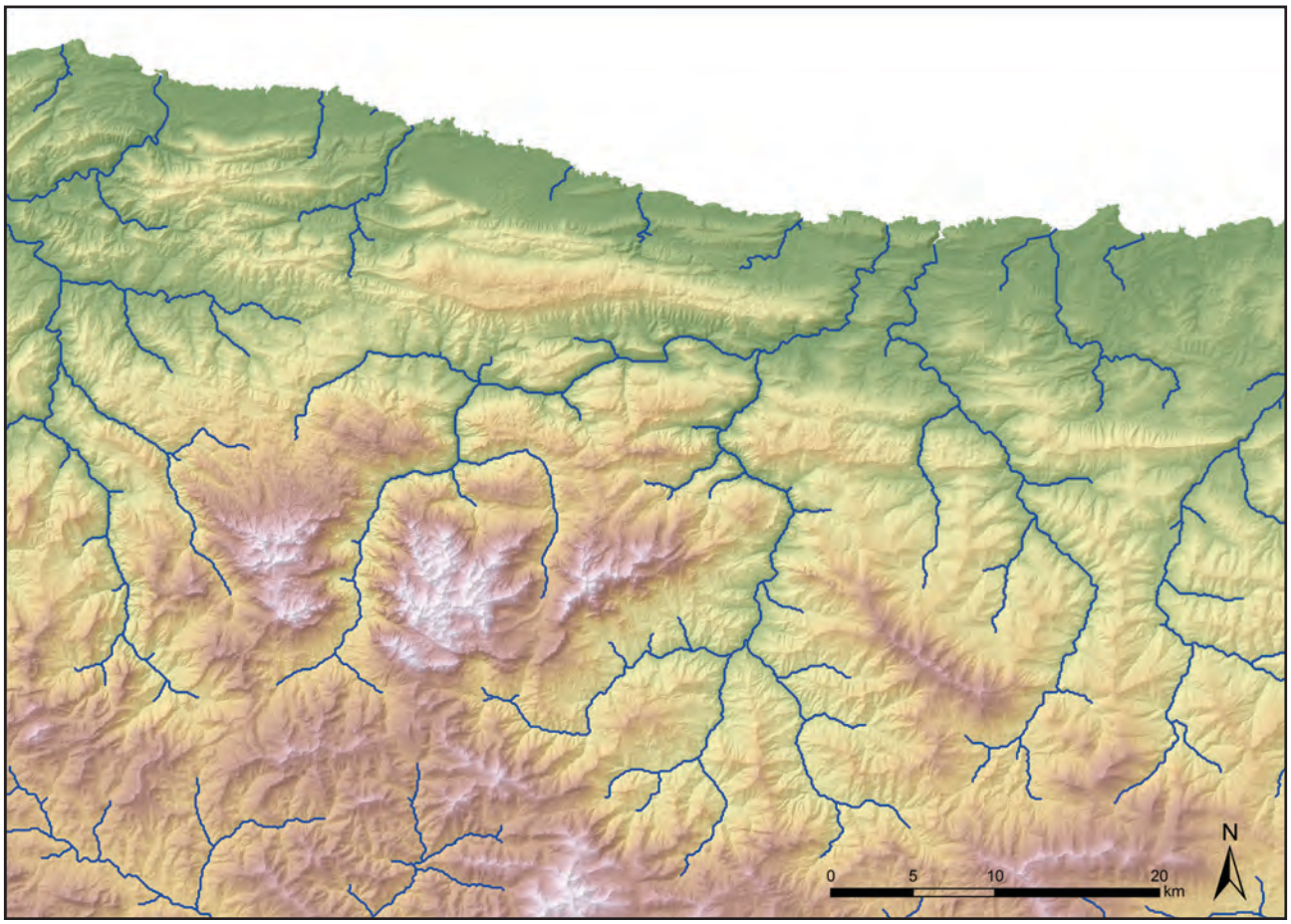

Figure-2.7: Base map of the research area. It was made merging different IGN 25DEM and generating a hillshade map to represent the relief of the area.

3. Geological information derived from the reports of MAGNA sheets maps and stratigraphic columns offered by IGME using the GEODE legend information.

4. Additional geography information derived from the analysis of BTN25 (Base topográfica Nacional) shapefiles. We have selected road, river and municipalities files for a better understanding of the environment.

The methodology used for preparing successive geological surveys (6 field campaigns between 2011-2016) made during this investigation was:

1. First, we have delimitated the corresponding area of each basin analysed, taking as the main research area the Deva-Cares basin and the Güeña river basin. Other basins, such as the Nansa basin to the East, the Sella to the West, the Eastern Coastal Asturian River basin to the North or the Duero river basin to the South are only used for identification and to obtain more information from some outcrops or conglomerates that appear in the main selected area. To create the basin area of each selected river, we have processed the base map using three consecutive geoprocesses/steps:

   a. Delete possible flaws in the DEM base map using the tool: “Fill” from the toolbox (Figure-2.8).

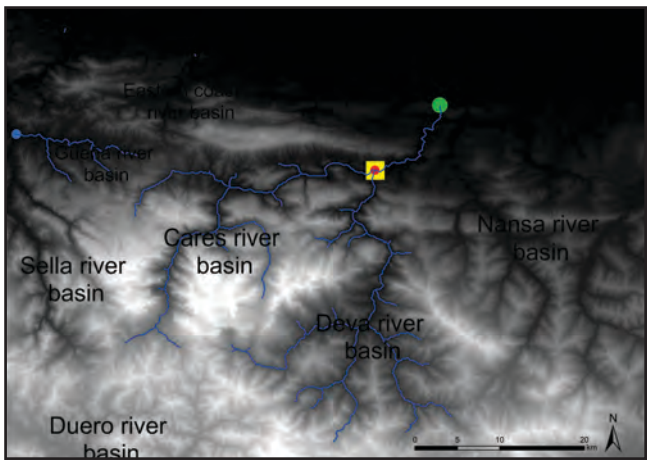

Figure-2.8: Filled DEM with Güeña, Cares and Deva river basins. The points for obtaining different basins are shown using a blue point for Güeña river basin, a yellow square for Deva river basin, a red point for Cares river basin, and a green point for Deva-Cares river basin.

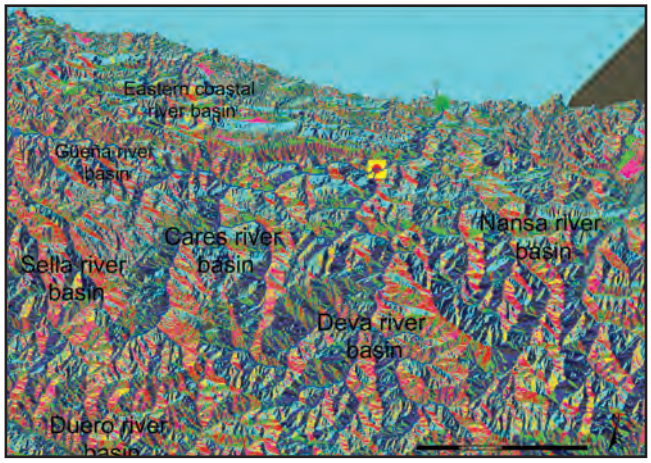

Figure-2.9: Flow direction for the selected area, also showing the points for calculate each river basin.

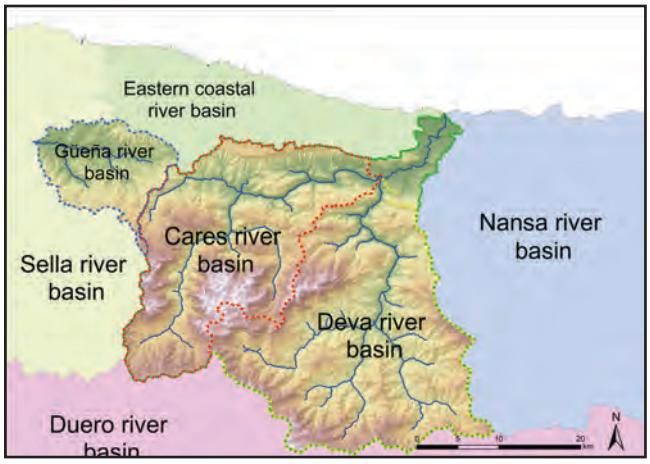

Figure-2.10: Map that represents Deva, Cares, Güeña, and Deva-Cares river basins in the central area and that determines main research area. Others basins are shown at North, East, Duero and Nansa.

b. Determine the flow direction in the resulting DEM using the tool: “Flow direction” from the toolbox (Figure-2.9).

c. Delimit each basin using the resulting DEM and the four interest points represented in point-shapefiles. The points are: 30T 369810/4797851 UTM for the Cares river basin; 30T 369848 4797824 UTM for the Deva river basin; 30T 377474 4805537 UTM for the Cares-Deva river basin; and 30T 327484 4802098 UTM for the Güeña river basin. This process is carried out using the tool “Watershed” from the toolbox. This process selects and extracts the exact area for each basin. The main area is then composed of 1350.51 square kilometres (Figure-2.10).

2. Second, we have created a potential quartzite area in the previous map in order to reduce the area to be surveyed. For this purpose, we have used the previous map and the geological MAGNA 1:50.000 shapefiles. We have selected as the potential areas those with presence of highly siliceous rocks, classified as quartzite, sandstone and quartzarenite. We have differentiated and selected outcrops, represented by a high number of geological units, that is the Barrios, Oville, Murcia or Camporredondo, Arroyacas, Remoña, Lebeña, Campollo, Gamonedo, Cavandi and Carazo Formations and the Potes, Mogrovejo, Valdeón and Pontón Groups (Figure-2.11). Second, the quartzite-containing conglomerates, that are represented by the Cavandi, Puentellés, Maraña, Curavacas, Remoña, Sotres, Cabranes, Caravia, Fuentes, Lechada, Campollo and Peñaferruz Formations and the Valdeón, Brañas, Pontón, Potes, Viorna Groups (Figure-2.12). Finally, we have identified other places where quartzite could appear in recent non-consolidated material, such as river beaches, flank deposits or Quaternary soils (Figure-2.13). We are aware of the fact that some layers may appear both in the prepared maps of conglomerate and outcrops. That is because some geological MAGNA maps include mixed polygons, where conglomerates and outcrops are present.

3. Third, we have combined the previous map with the IGN BTN municipalities, highway, road and unpaved road shapefiles to find the best and most accessible places for the geologic formations with siliceous rocks. This was crucial for obtaining bigger and more representative sections of each formation and for preparing correctly a detailed survey planning to be affordable in time and cost (Figure-2.14).

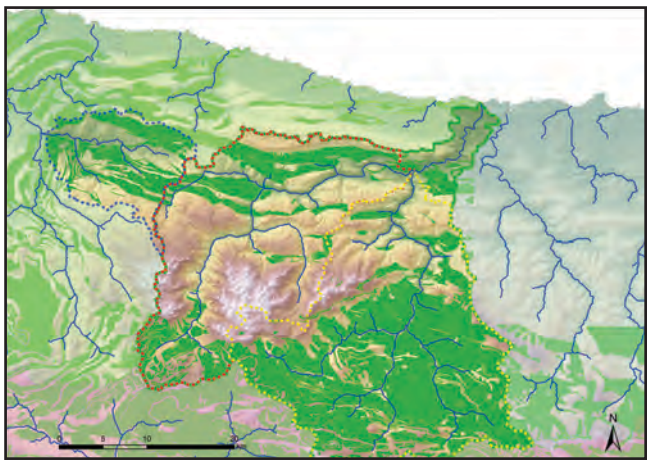

Figure-2.11: Map that represents sandstone and quartzite (green) outcrops on the main research area.

4. Fourth, and after successive prospection that discard layers which do not contain archaeological quartzite, we have systematised formations that are in different MAGNA shapefiles using the GEODE legend and a continuous map of the Cantabrian area Z1100. We have finished processing the information making an association from the chronology proposed by GEODE legend into the shapefiles using starting and finishing chronology. We also made an association of layers with the formations as proposed by GEODE legend.

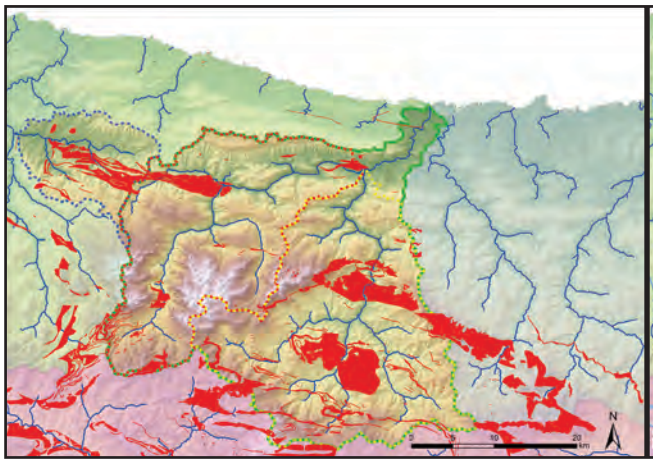

Figure-2.12: Map that represents conglomerates (red) on the main research area.

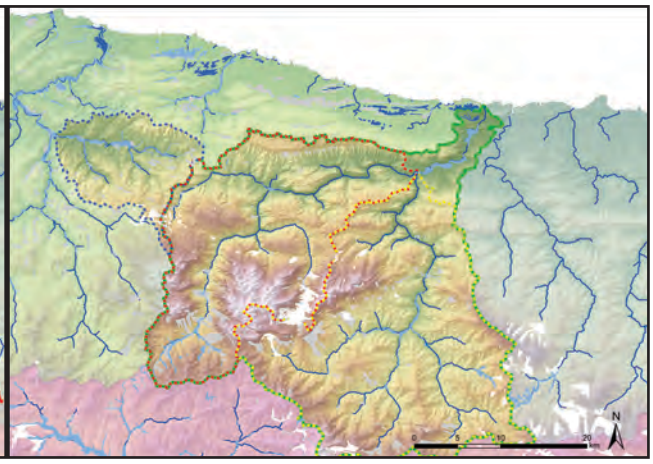

Figure-2.13: Map that represents deposits on the main research area. White for glaciers deposits, grey for gravitational deposit, deep blue for marine deposits, and light blue for fluvial deposits.

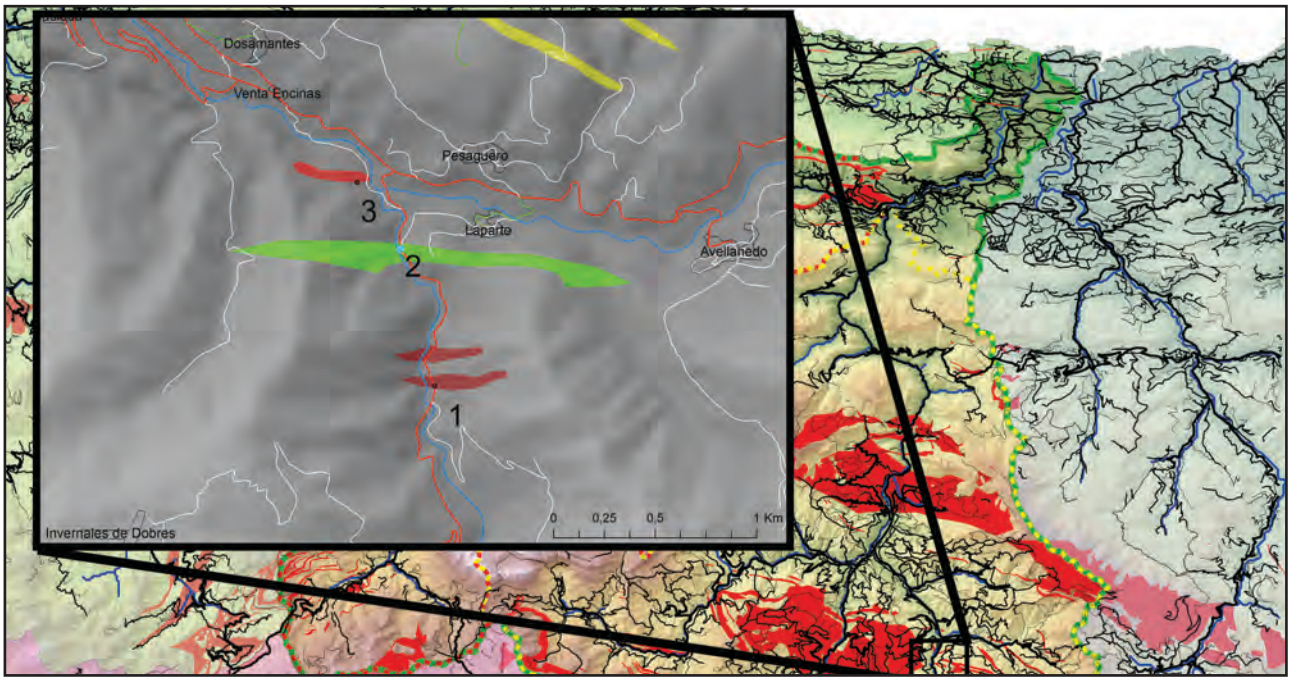

Figure-2.14: Figure showing research area with IGN BTN road map shapefiles and a detailed view of an itinerary proposed for the survey of a small region. Note that road, unpaved road and river intersect with the layer. It helps us to a better understanding of geological features from the formations.

2.2.2. FIELD SURVEY: GEOLOGICAL SURVEY FOR UNDERSTANDING QUARTZITE CATCHMENT AREAS

We have done different geological surveys from the first stage of this research. We have made six surveys (6 field campaigns between 2011-2016) trying to understand the dispersion of quartzite types, its relationship to physical geology and its implication on quartzite procurement strategies. Each survey we have done, solved the questions we had posed, but at the same time opened new ones. For this reason, and also to increase the studied area, we recorded as many elements as possible since the first survey.

At field, we have used a map printed (prepared as described above), a mobile telephone and tablet maps for GPS positioning and orientation in the surveyed area. We have also used the Oruxmaps app (a free offline map viewer) on the tablet for taking points with the tablet GPS. The precision of these points is under 10 meters, an appropriate magnitude for the scale used. We have recorded the points with a consecutive number in each survey, each of which has a reference code called Survey Code I (M_XX, MGR_XX, MIG_XX, J_XX, BP_XX or Last_XX). We have also taken points from general description of areas, to understand the physical geology of the area. The photo cameras Nikon D3100 and Samsung EX1 and several metrical scales were used for taking pictures. We have used different hammers for obtaining fresh cuts in the material, and we have used two magnifying glasses (10x and 20x) for field petrology determination. We have also used diluted hydrochloric acid (HCl 10%) to determine calcitic cement in some sandstones and a Möhs scale.

In order to quantify lithologies of interest, we have counted, at least, 50 pieces of stone in each conglomerate or deposit. In the latter, we have only used the stones inside a one-meter square using parameters similar to those proposed by Roy et al. (2017) (Figure-2.15). In the outcrops, we have quantified each lithology qualitatively. We have selected a stone or chips of stone of each lithological variety for a better petrological characterization in the laboratory, using destructive and non-destructive methodologies. We have used separated sacks for each surveyed point labelled doubly. After the survey, we have sampled the survey in the laboratory re-coding each point with the new one, which is defined using basin code or survey code II (DC_XXX, GU_XXX or SE_XXX). Additionally, each sample we have taken from that site is recoded using that code, followed by a consecutive number (DCXXX_XX). That code is going to be used for later analysis.

Figure-2.15: Data acquisition process on a fluvial deposit

We have used a van for moving and living along the surveys. It was also useful for moving samples from the selected area to the archaeology laboratory. Due to time and economic limitations, we have survey points near to the main highway or road, walking to different sites in case there was no chance to access the geological outcrops. Due to the difficult access to many places and for personal safety, we have decided to do the survey with a colleague. Maite García-Rojas, Blanca Ochoa, Javier Martín and Maite Iris García-Collado were the people who help me in the survey processed. The economic cost of one day of survey is around 50 Euro.

2.2.3. SYSTEMATISING GEOLOGICAL SURVEYS: THREE QUARTZITE ENVIRONMENTS, THREE DATASETS

In order to understand each research point individually and collectively, we have systematised the data collected in a database. The database has been done on Filemaker Pro. Due to the different environments found, we have created three distinct datasets: Quartzite outcrops (Figure-2.17), quartzite that appears on conglomerates (consolidated deposits) (Figure-2.18), and quartzite that is displayed in the sedimentary and non-consolidate deposits (Figure-2.19). We have decided to create these three different databases due to the distinctive characteristics of each environment. However, there are some common fields. These are:

1. Survey code I and II: Original code derived from each survey (M, MIG, BP, J, MGR and Last) and the code used for standardising the data along the research (DC, for Deva-Cares river basin, GU for Güeña river basin, and SE for Sella river basin).

2. UTM coordinate: Reference point where we analysed the environment. All the data included were georeferenced following the UTM-ETRS89 30N system of projected coordinates.

3. Place: Municipality (municipio or concejo) where the point was taken using as reference map the SIANE compilation by the Spanish National Institute of Geography (IGN).

4. Formation: Using the proposal defined by regional geology simplified on the MAGNA series maps-II and modified applying the GEODE maps.

5. Chronostratigraphy: We have defined the timeframe of each survey point by its association with the corresponding geological formation using the Regional Magna 1:50.000 documents and the Regional GEODE map (Zona_Cantábrica: 1000) (Alvarez-Marrón et al., 2003; Beroiz et al., 2003; Carreras Suárez et al., 2003; Heredia et al., 2003a; Heredia and Rodríguez Fernández, 2003; Heredia et al., 2003b; Heredia et al., 2003c; Julivert and Navarro, 2003; Martínez García, 2003; Martínez García et al., 2003; Merino-Tomé et al., 2016; Navarro, 2003; Pignatelli et al., 2003; Ramírez del Pozo et al., 2003; Rodríguez Fernández et al., 2003). We have used the terminology proposed by the International Commission on Stratigraphy for Eon, Era, Period, Epoch and Age (Cohen et al., 2013). We have defined the Subage category using the information from the legend of GEODE map.

6. Lithology: We have differentiated two elements.

    a. First, the items that are inside the stratigraphic sequence we have identified in the survey points for outcrops or conglomerates (below the layer, as an inclusion in the main layer, and above the analysed layer). The lithology is shown using general categories, and listed later.

    b. Second, and using A to C lithological varieties or zonation in case of outcrops and A to E lithological varieties in the case of conglomerates and deposits, we have described existing lithology using different variables. We try to include all quartzite varieties on these variables. In case there are more varieties than 3 for outcrops or five for conglomerates and deposits, we describe them in notes. In cases where lithological variety is high, we decided not to include non-quartzite lithologies. The lithological descriptions for each rock will be described in following sections and it is included in these databases. To quantify the presence of each lithology, we simplified the data acquisition through following criteria:

        i. $x < 1\%$

        ii. $1\% < x > 5\%$

        iii. $5\% < x > 50\%$

iv. x > 50%

7. The joints that are described in outcrops and conglomerates through 3 variables:
   a. To quantify the different directional joints, using these categories:
      i. One
      ii. Two
      iii. Three or more
   b. To define the intensity of joint in the outcrop or conglomerate, with the categories of:
      i. Low-intensity
      ii. Medium-intensity
      iii. High-intensity
   c. To define the composition of the mineral filling the joints, here referred as mineral inclussions:
      i. Silica
      ii. Iron oxide
      iii. Manganese oxide
      iv. Calcareous
8. The bedding of conglomerates or outcrops, simplified through:
   a. Clear
   b. Non-clear
   c. No-bedding
9. Other non-systematized notes

The database of outcrops is completed with the colour hue of the survey points, which is simplified using closed categories: White, Grey, Black, Blue, Green, Orange, Brown, Yellow and Red. Due to the variability of colour in outcrops, we have decided to make two hue colour category.

The database of the conglomerates is completed with characteristics that are related to cement. These are:

1. The cement hue, using same closed categories as for outcrop colour
2. The cement composition, simplified through:
   a. Silica
   b. Iron oxide
   c. Manganese oxide
   d. Calcareous
   e. Argillaceous
   f. Arenaceous
3. The cement compaction, simplified through:
   a. Hard
   b. Medium
   c. Soft

4. The extraction, which determinates the possibility of extracting clasts from the conglomerate. It is simplified through:
   a. Impossible
   b. Hard
   c. Medium
   d. Easy
5. Cement percentage in the conglomerate, defined through:
   a. Less than 5%
   b. Between 5% and 50%
   c. Higher than 50%
6. Packing (Figure-2.16), defined through:
   a) Floating
   b) Isolated
   c) Tangential
   d) Complete

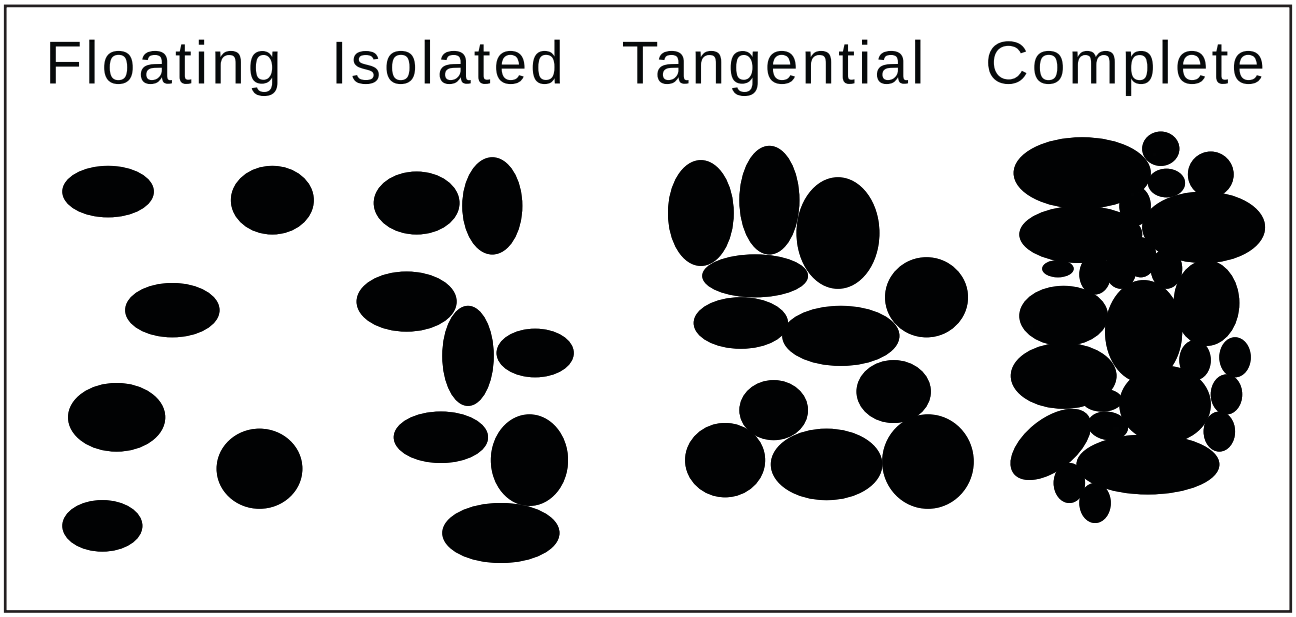

Figure-2.16: Representation of packing categories in conglomerates or outcrops at surveyed points

The deposit types are completed with some additional variable such as:

1. Deposit type, determined by the features of the deposit, and we included:
   a. Fluvial deposit or river beach
   b. Flank deposit
   c. Part of soil
2. Packing, using the same categories as we defined for conglomerate dataset
3. Matrix, defined by two possible types of matrix. Both are defined by the lithological variety, and its quantity. The lithological descriptions will be described in following sections and it is included in these databases. To quantify the presence of each lithology, we simplified the data acquisition through criteria previously exposed.

All variables have been defined using closed categories to use the information quantitatively through GIS and statistics. The variable notes and, finally, the graphic description of the surveyed points are used to illustrate the prospection qualitatively (Figure-2.20). Each main formation described has also been illustrated with a schematic representation.

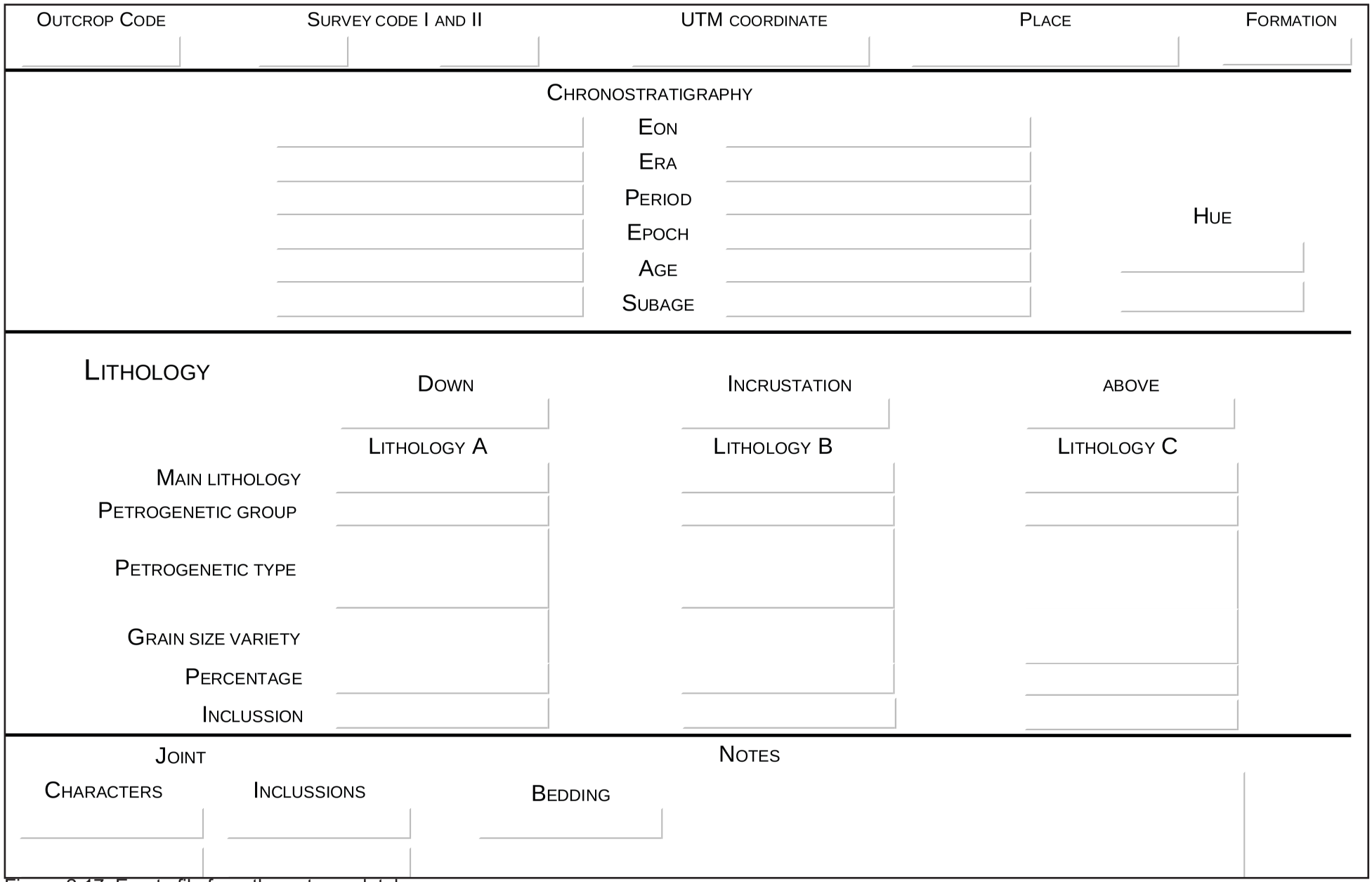

Figure-2.17: Empty file from the outcrop database

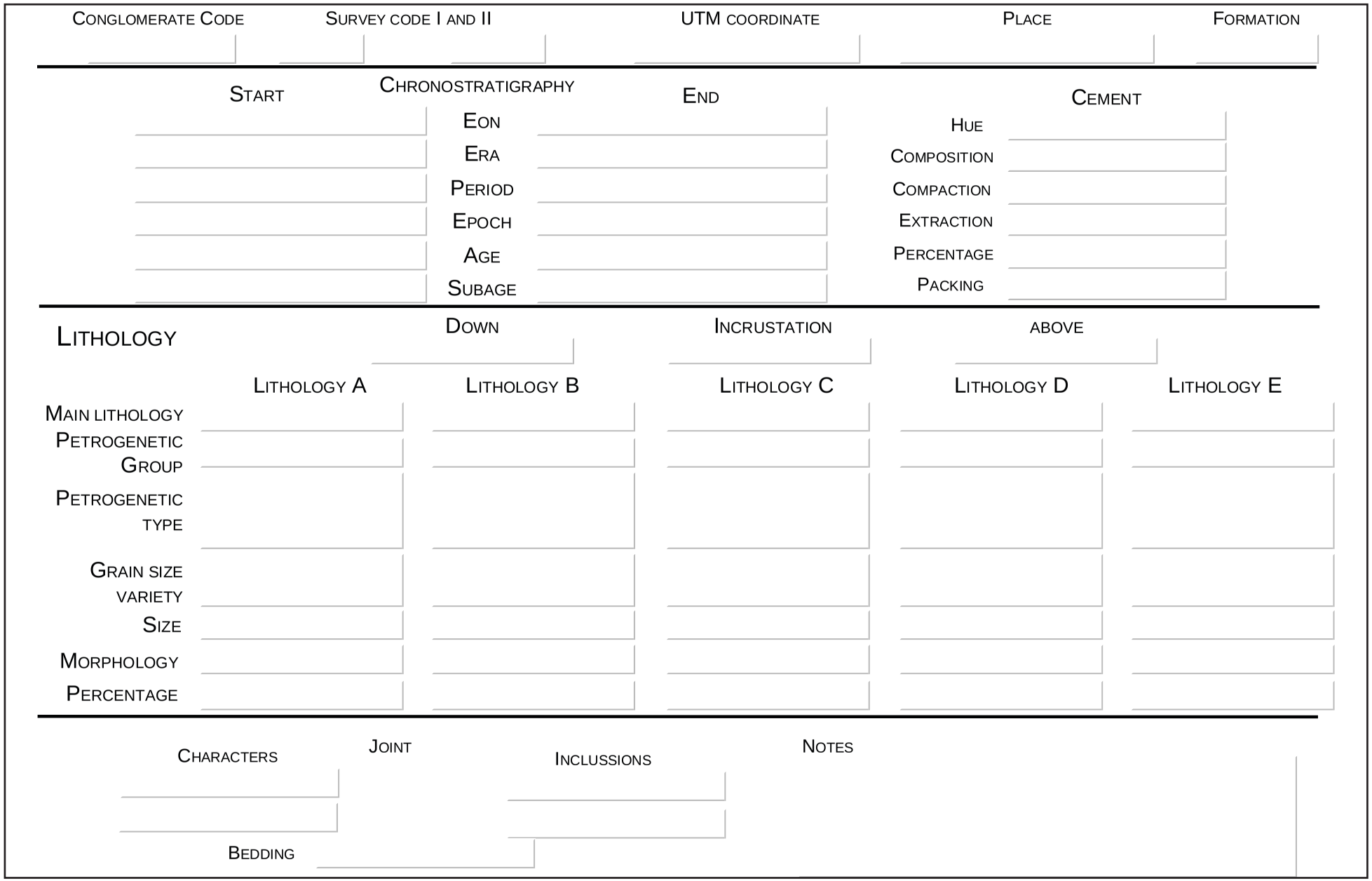

Figure-2.18: Empty file from the conglomerate database

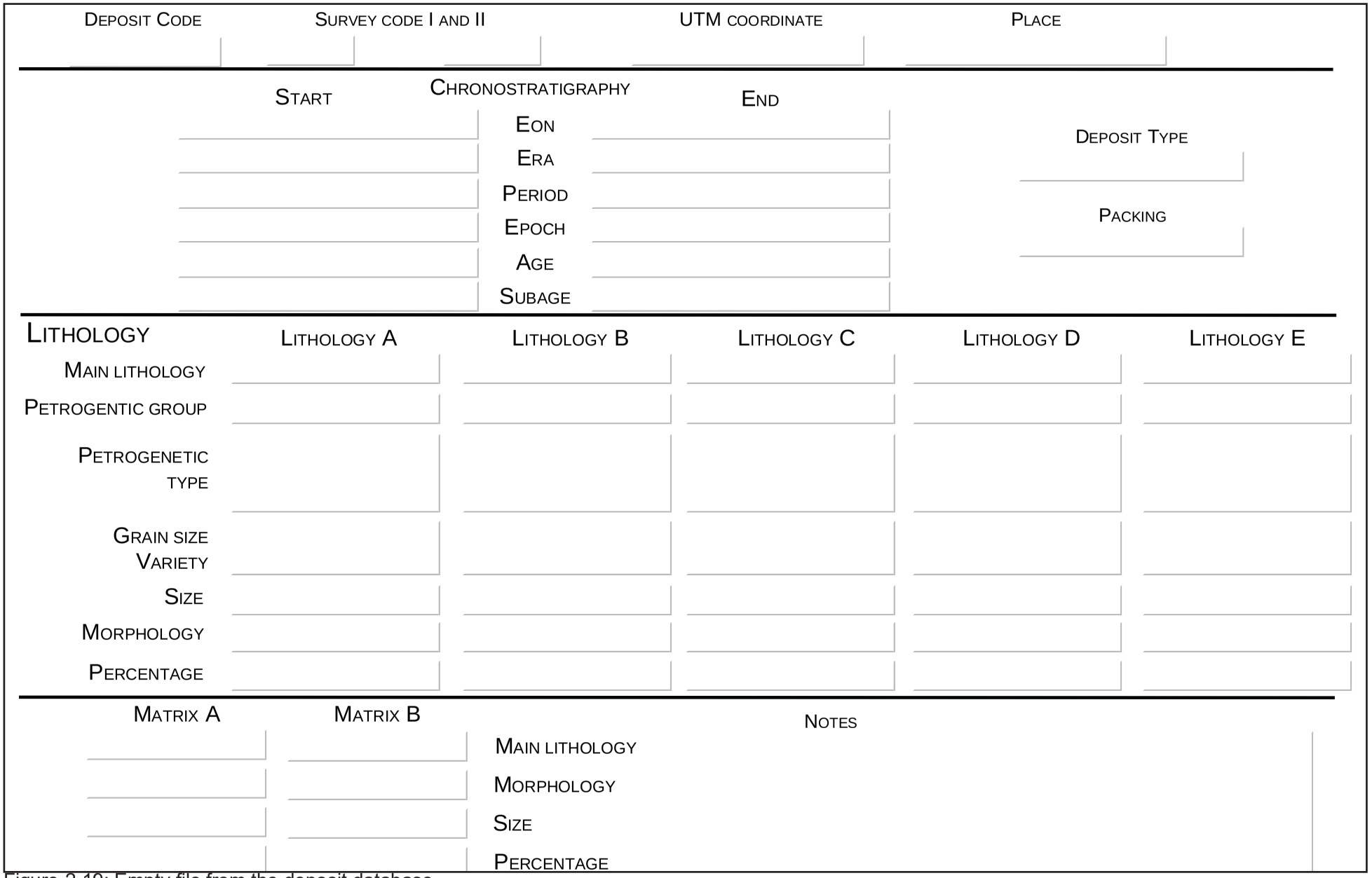

Figure-2.19: Empty file from the deposit database

Figure-2.20: Empty file of graphic information from outcrop/conglomerate/deposit database

2.3. ARCHAOLOGICAL PERSPECTITES: THE PALAEOLITHIC ON THE DEVA, CARES AND GÜEÑA VALLEYS

We selected the proposed area of study due to geological and archaeological reasons. The second one was based on the presence of different archaeological sites from almost all Palaeolithic chronologies in the area. In addition, the presence of other archaeological sites in adjacent valleys opens the possibility to opening new research zones on future research projects. The sites are situated in the northern area, and they are related to the lower altitude of the zone (Figure-2.21). The highest site is El Habario, at 536 a.s.l., in the Liébana valley. However, most of them are in steep relieves as consequence of the mountainous regional geography.

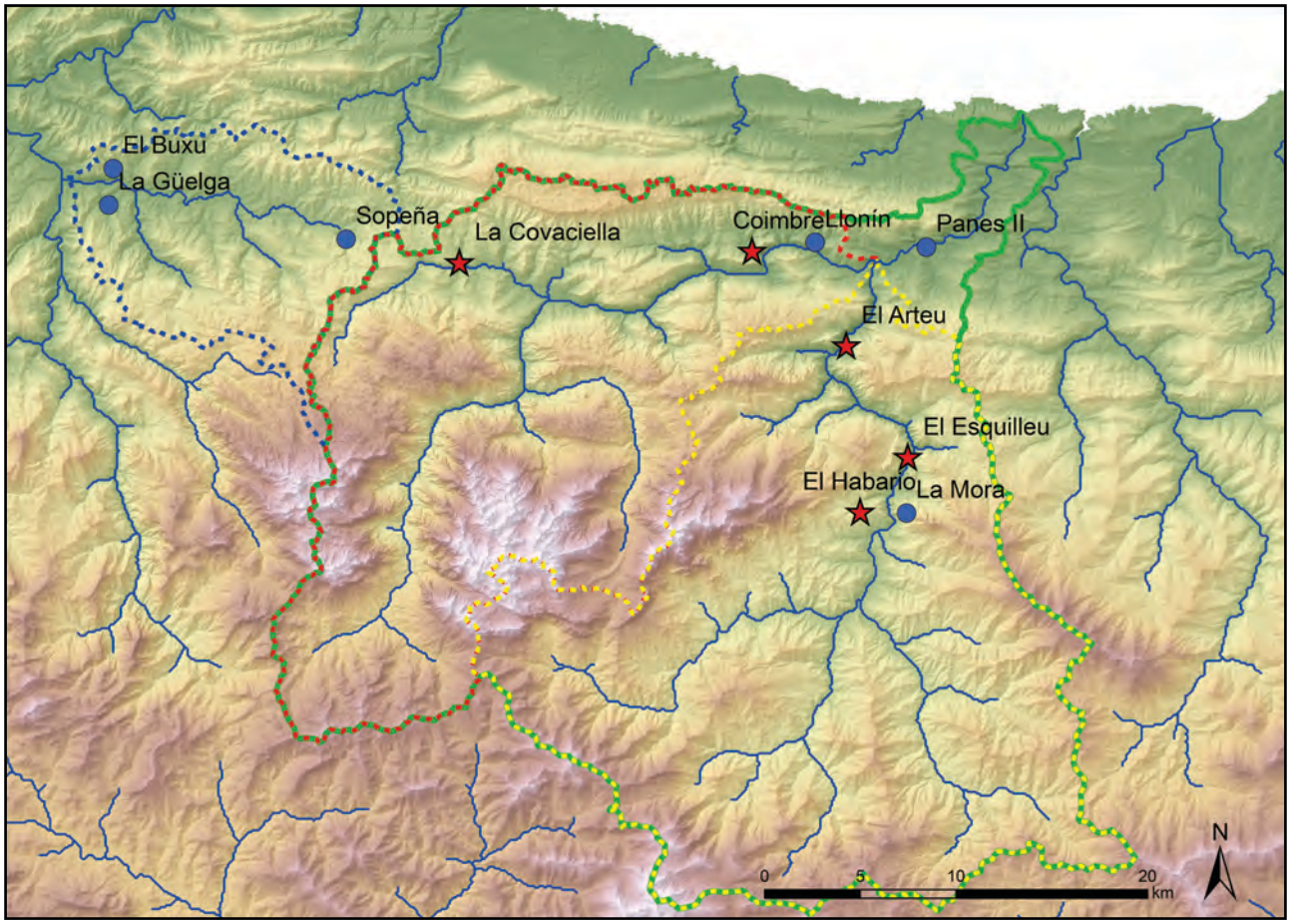

Figure-2.21: DEM map of the area with Palaeolithic archaeological sites. Red-starts represent sites analysed; meanwhile, blue points are other Palaeolithic sites referred in general text.

The Palaeolithic chronological framework of the area starts in the Middle Palaeolithic with the sites of El Habario, Panes II, El Esquilleu Cave, La Mora, the rockshelter of El Arteu, the Güelga cave, and Sopeña rockshelter. Excluding La Mora (González Echegaray, 1957), these Mousterian sites were discovered and excavated from the 1990s due to the increase of research in the area carried out by 1) a research group directed by Javier Baena (from the Autonomous University of Madrid) (Baena et al., 2005), 2) members of C.A.E.A.P (Colectivo para la ampliación de Estudios de Arqueología Prehistórica – Collective for the expansion of research on Prehistoric Archaeology) (Montes and Muñoz, 1992; Muñoz, 2005), 3) the investigation led by Menéndez Fernández on the Sella Valley (Menéndez, 2006), and 4) the discovery of Sopeña by Ana Pinto (Pinto-Llona et al., 2005). These sites are mainly in the Deva Valley or its confluence with the Cares River. La Güelga and Sopeña are in the Güeña Valley. Meanwhile, there is no presence of Middle Palaeolithic sites in Cares valley. The chronology of these sites is focused on the last part of the Middle Palaeolithic period, as shown by the dates from El Esquilleu, Sopeña and La Güelga (Maroto et al., 2012). The presence of a Middle-to-Upper Palaeolithic transitional layer in the last one seems to be clear (De

Andrés and Arrizabalaga, 2014). The sites of Panes II, El Habario, and El Arteu have no numerical dates, but the lithic industry is assigned to the Mousterian.

The Upper Palaeolithic is clearly associated with the Cares and Güeña valleys. The sites of La Güelga (Menéndez, 2006; Menéndez et al., 2009; Menéndez et al., 2014; Quesada and Menéndez, 2009) and Sopeña (Pinto-Llona et al., 2012; Pinto-Llona et al., 2006; Pinto-Llona et al., 2009) show archaeological layers characterised as Early Upper Palaeolithic. The archaeological sites of Coímbre Cave (Álvarez-Alonso et al., 2013a) and Llonín (Calvo et al., 2016; Fortea et al., 1992; Fortea et al., 1995a; Fortea et al., 1999) have Gravettian layers, while the presence of Solutrean findings is restricted to El Buxu (Menéndez, 1986, 1990, 1992, 1999) and Llonín (De la Rasilla and Fernández de la Vega, 2014). Magdalenian layers are present in the archaeological sites of Coímbre, Llonín, and La Güelga (Álvarez-Alonso, 2014); including the lithic findings related to the paintings of La Covaciella Rock Art Cave (Perales and Prieto, 2015).

Due to time restrictions in this research, bureaucracy issues, and other limitations, we could not study each one of the archaeological sites mentioned above. We selected some of them, to have a general overview of the catchment activities in the area. In this way, we selected the El Esquilleu rockshelter, the open-air site of El Habario, the rockshelter of El Arteu, and Coímbre cave. We also studied some findings coming from the Covaciella rock art cave. We are going to describe the sites for a better understanding of the analysis of their lithic collections.

2.3.1. THE ARCHAEOLOGICAL SITE OF EL ESQUILLEU CAVE

The archaeological site of El Esquilleu is a cave situated in the western part of the Cantabria Autonomous Community, within the municipality of Cillórigo de Liébana and near the villages of Lebeña and Allende. The geographic coordinates of the site are X= 371.459 Y= 4.787.705 30T ETRS-1989. It is situated 100 meters away from the left margin of the Deva River and 70 meters above it. The mouth of the Deva River is 18.729 meters away in Euclidean distance. The height is around 270 meters above the sea level (Baena et al., 2005).

Figure-2.22: Surrounding area of El Esquilleu Cave.

The cave is within the Valdeteja Formation, mainly composed of fossiliferous limestones, massive limestones with algal and microbial bioconstructions, and calcareous breccias deposited in Upper Carboniferous (Bashkirian Age). This formation is located in the Eastern zone of the Picos de Europa Province, which is characterised by massive carboniferous limestone affected by different overthrust (Colmero et al., 2002). Lithological composition (mainly carbonate rocks), the affection of Variscan and Alpine orogenesis, and the later fluvial, glacier, gravitational, and karstic erosion generate a sharp relief with slopes of more than 2.000 meters. Cliffs, defiles, talus slopes, moraines, caves and deep gorges are the most important geomorphological features in the area surrounding El Esquilleu Cave. The area is crossed by the Deva River valley that creates a deep and narrow gorge in North-South direction called The Hermida Defile, where the cave is located (Figure-2.22).

The cave, or large rockshelter, is not deep (around 20 meters), while the height is around three metres from the current soil level (Figure-2.23). The excavation of this archaeological site was directed by Dr Javier Baena Preysler between 1997 and 2006. The aim of the excavation was to understand the site from a diachronic perspective, generating an excavation in depth with reduced dimensions on the horizontal surface. The sequence was entirely excavated in a four square meters pit, leaving other ten square meters excavated for surface layers (I-VI) and six square meters for medium layers (VII-XX). The stratigraphic depth was 4.20 meters and was divided into 41 layers, of which 29 have archaeological remains. The amount of faunal remains excavated is 71.815; while 69.899 lithic items were recovered (Cuartero et al., 2015). Although the research processes in El Esquilleu Cave is still in progress, several studies have already been carried out by different specialist.

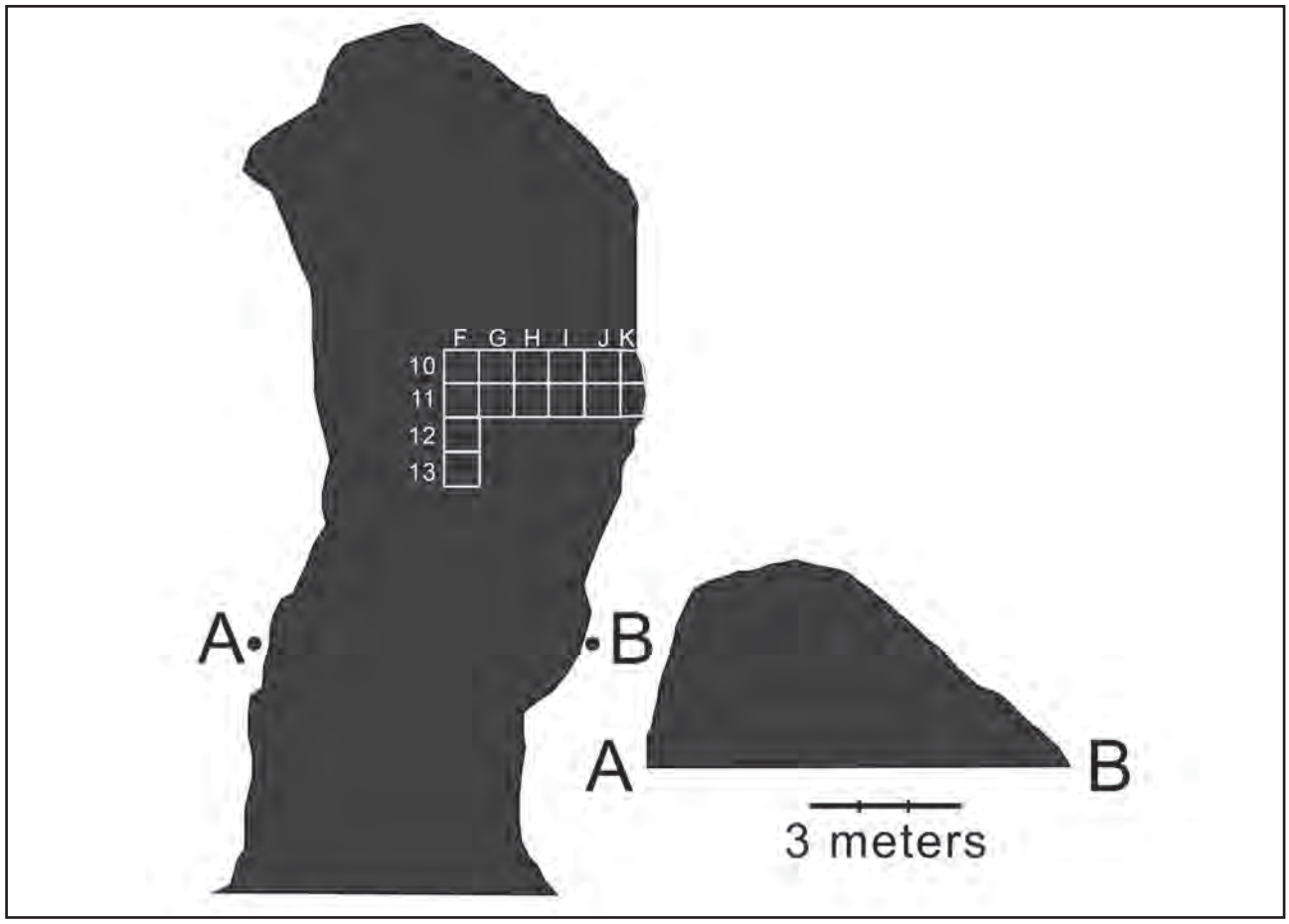

Figure-2.23: Esquilleu plan map and profile of the cave, modified from Jordá et al. (2008).

From a sedimentary point of view, El Esquilleu Cave was analysed by Jesús Jordá and his research group (Jordá et al., 2008). The 42 layers were grouped into four phases (from A to D) according to textural and mineralogical characteristics. The first phase (ESQ-A) was a breccia and speleothem of 20 cm in thickness formed by carbonate precipitation from the cave. There was no human activities or evidence on this first part of the sequence. The second part (ESQ-B) was a sedimentary unit of 180 cm thick, mainly composed of clastic (gravel) autochthonous materials and a small percentage of sandy and calcareous matrix. The sedimentary process that created this unit

was related to frost weathering and widespread flooding activities which affected this open cave. Human activities were present in this part of the sequence. The third part (ESQ-C) was a sedimentary unit (about 70-90 cm thick) mainly composed of thin and dark layers created as consequence of widespread flooding and intensive human activities, represented as fireplaces and other dispersed burned findings. The presence of siliceous material was massive in the sandy and silty matrix. The last part of the sequence (ESQ-D) was a 150 cm thick unit, and it was possible to distinguish two different parts. The upper one was characterised by the presence of calcareous crusts and a later muddy sedimentation with some autochthonous clasts. The lower part of the sequence were mainly muddy sediments, similar to the last part of the previous part of the sequence. Human activities were in clearly decrease, and the last part of the sequence had no archaeological remains.

The micromorphological analysis conducted by Carolina Mallol showed that the Esquilleu sequence was well preserved, although it had been subjected to particular taphonomic processes. The unit ESQ-B showed good preservation but its internal structure had been affected by cryoturbation, as a consequence of the frost weathering previously argued. The unit ESQ-C, which yielded evidence of intensive combustion activities, had been diagenetically altered by a source of dissolved phosphate, which triggered the partial dissolution of bone and ash in the sediments of this anthropogenic-rich layers (Mallol et al., 2010).

From the point of view of absolute chronology, the Esquilleu Cave was dated through two different radiometric methodologies, C14 dating and Thermoluminescence. The first one, using several procedures, such as ultrafiltration, ABOX-SC (acid-base-wet oxidation pre-treatment with stepped combustion) or ABA (acid-base-acid) methods was carried out in different laboratories. Although some of the dates showed discrepancies with the stratigraphy, such as some dates from layer-VI or layer-III, in general terms the sequence showed chronological coherence (Baena and Carrión, 2014; Baena et al., 2012). The proposed chronology for this continuous sequence started around 60Ka, finishing around 37Ka Cal BP, spanning from the beginning of MIS3, including MIS3c and MIS3b, and environmental events H5 and H4, until the H3 event in the middle part of MIS3a (Cuartero et al., 2015). This site is exceptional since the most recent dates of other Cantabrian, northern Spanish sites or European Middle Palaeolithic sites do not exceed 30.000BP (Higham et al., 2014; Maroto et al., 2012). All this underlines the unique nature of El Esquilleu within the last European Middle Palaeolithic.

The data derived from palynological analysis showed the continuity of *Pinus* amounts along the complete palynological record. Herbaceous plants were also relevant. Aquatic and riverbank taxa were present too, as consequence of the geographic proximity to the Deva River. There were three phases according to the palynogram (Figure-3 from Uzquiano et al., 2012). Phase I, layers XXX to XX, was dominated by open landscape species with significant representation of *Pinus*, *Cupressaceae*, and *Betula*. Phase II corresponded to layers XIX to XIV and showed scarce occurrence of *Pinus*, *Betula*, *Cupressaceae*, and *Asteraceae*, due to the affection of hearths and other human activities. Nevertheless, the pollen species were similar to the previous phase. The third phase showed differences with previous phases, due to the presence of mesophilic taxa (*Pinus* is still present), indicating favourable moisture conditions. These taxa were dominant on layers XIII to V.

The anthracological analysis performed on 1341 showed that *Pinus* was the dominant species used for burning activities (Uzquiano et al., 2012). Other species such as *Betula*, *Sorbus*, *Fabaceae*, and *Corylus* were also utilised for these activities in lower layers (XXVII and XXIV to XVII); as well as *Juniperus*, *Betula*, *Sorbus* and a great variety of shrubs in layers XIV to XI. The last one could be a consequence of general decrease of *Pinus* in the environment, that obligated human population to use other wooden fuels; or due to cultural and technical changes on fuel acquisition probably related to the use of different wood fuels for start fire ignition.

Dan Cabanes conducted the last palaeobotany study, focused on phytoliths elements (Cabanes et al., 2010). The quantification and identification of phytoliths in relation to the mineral composition of sediments from the El Esquilleu Cave stratified deposit yielded high-resolution data for reconstructing the behaviour of the late Neanderthal groups that occupied the cave. In unit ESQ-B, phytoliths were poorly preserved due to the calcitic nature of the sedimentary environment. The lower layers from unit ESQ-B and unit ESQ-C showed moderate diagenesis and the presence of well-preserved phytoliths. In unit D, only the uppermost layer showed a high presence of phytoliths, indicating the first human occupation of the cave. The results of this analysis showed the repetitive preparation of grass beds in the centre of the cave in relation with a central hearth area, mainly visible in ESQ-C. Finally, the high presence of inflorescence phytoliths at Esquilleu Cave may pointed to the collection of grass seeds for unknown purposes other than bedding or fuel.

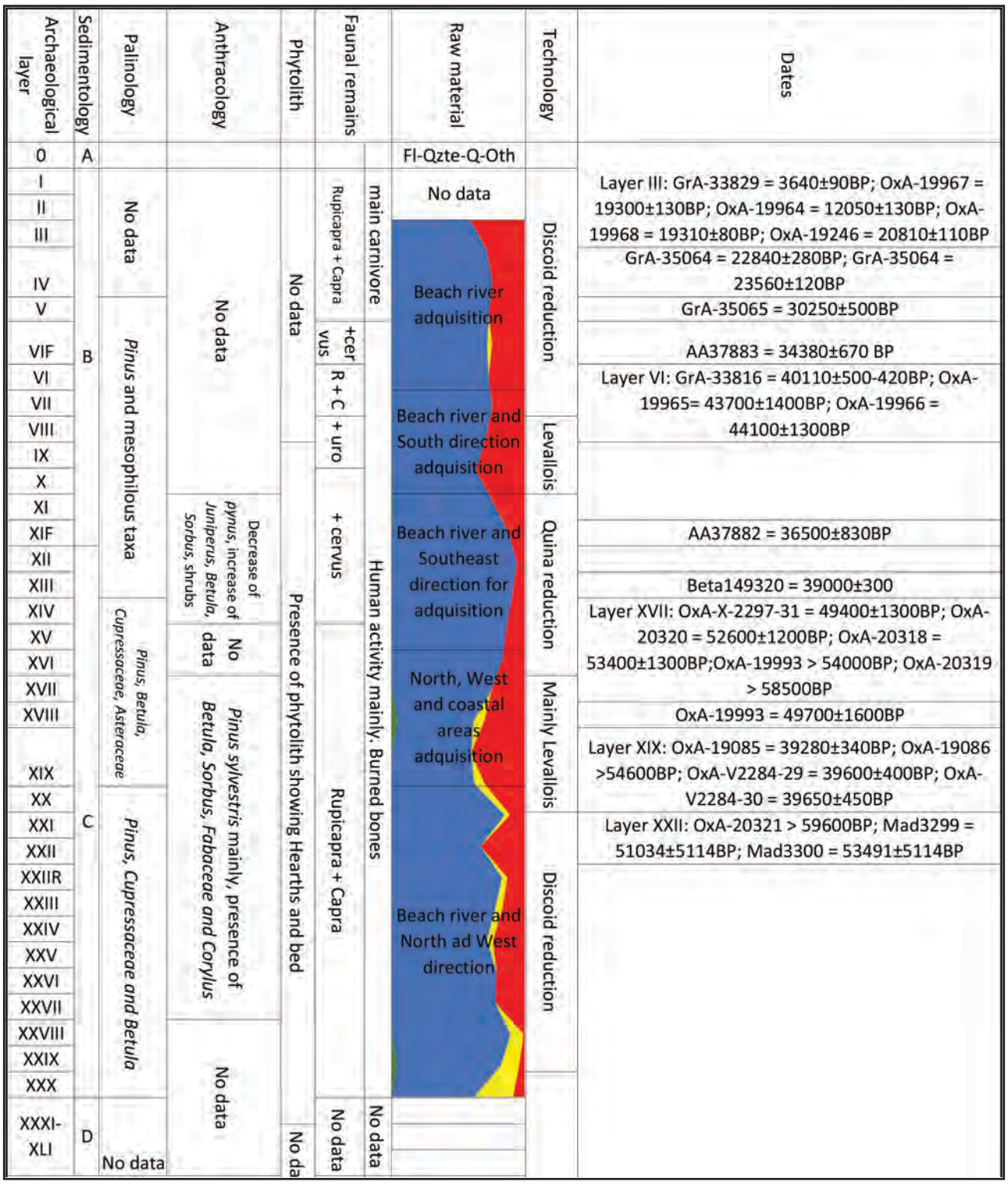

Table-2.1: Chart that summarise the information obtained from different proxis from El Esquilleu.

José Yravedra conducted faunal analysis in two directions: first one, to determine the taxonomy of the bones in El Esquilleu Cave, and the second one, to determine taphonomic agents present on faunal remains. In general terms, *Capra pyrenaica* clearly dominated the faunal assemblages, followed by chamois and deer, whereas *Bos/Bison* was only occasionally found in layers VIII, XI and XIII. Only a few teeth of hyena were recovered in layer-III, as well as some canid remains and small felids bones in layers V to XIII. Seasonality was only recognisable in some layers (from III to XIV) due to fragmentation processes. The data provided allowed to conclude that captures were mainly in summer, also in the first autumn and the last spring periods. On layer-IX, there were also captures on winter (Uzquiano et al., 2012). The animals were introduced into the cave with all the anatomical parts present (Yravedra and Gómez-Castanedo, 2014). The main agent that introduced these animals were humans, although for the first section of the sequence (Layer III to V) there were carni-

vores, as determined by the almost complete absence of cut marks and the increase in the presence of bite marks. Evidence of carcass bite marks was also found in layers VI to XXX, although they were small and the interpretation was related to the secondary/occasional use of the cave by carnivores. Burned bones were present and massive in the layers VI to XXX, where they were also extremely fractured. The use of these bones as fuel could explain this evidence, also the use of fire for cleaning or for sanitary purposes (Yravedra et al., 2005; Yravedra and Uzquiano, 2013).

The lithic raw material was previously characterised by I. Manzano (Manzano, 2001; Manzano et al., 2005). The characterization was mainly done using macroscopic characteristics, although another analysis, such as petrography thin section and compositional analysis was done to describe each type of raw material. In general terms, quartzite was the main raw material in the sequence, followed by ferruginous rocks, diverse kinds of limestones, flints, sandstones, quartz, shales or conglomerate rocks. The investigation proposed a limited catchment area, focused on river beaches and conglomerates (Remoña conglomerates, near El Habario open-site). The author proposed changes in raw material acquisition through the sequence. For the first part (III to VII layers) he proposed a lithic acquisition near river beaches, for the second part (VII to X) also in the river and South direction, for the third one (XI to XV) in the river and to the Southeast, for the fourth (XVI to XIX) to the North, West, and coastal areas and for the last part of the sequence, the fifth part (XX-XXX), in the river and North and West directions.

Lithic Technological characterization of the sequence was conducted by Javier Baena, Elena Carrion, and Felipe Cuartero, mainly. These analyses were made following a technological approach based on qualitative perspective and the application of the concept *Chaîne Opératoire*. These research proposed the presence of different models of lithic reduction, such as Quina, Levallois, Discoid, or blade reduction (Baena et al., 2005). Due to the presence of more than one lithic reduction process in each archaeological layer, the lithic reduction could not be understood as chronological or geographic markers or Mousterian *facies*, showing more relation with site function or raw material availability (Carrión et al., 2008; Carrión et al., 2013). Meanwhile, the sequence of El Esquilleu could be divided in five different sets of layers where a particular knapping conception is dominant: Phase 1 (III-VII) was discoid; phase 2 (VIII to IX) was Levallois; phase 3 (XI-XVI) was Quina; phase 4 (XVII-XXI) was mainly Levallois; and finally phase 5 (XXI-XXIX) was discoid again (Carrión, 2002). Complex recycling processes were appreciated in some layers of El Esquilleu (VI, XIII, and XVII), with different procedures related to previously commented lithic reduction, raw material availability, and site function.

The information provided by all these perspectives in a well excavated sequence offered interesting perspectives about the human groups who inhabited this cave in Prehistoric times during late Middle Palaeolithic. We tried to summarise these studies in table (Table-2.1). In general terms, the sequence of El Esquilleu Cave showed sophisticated strategies of habitat and land use by Neanderthals groups, which were modified through time according to environmental conditions and cultural, social and economic circumstances (Baena et al., 2012). Summing up, we can say that El Esquilleu is one of the most important archaeological sites in the Cantabrian Region for understanding the last Neanderthal groups in the Iberian Peninsula.

Due to time limitations, we selected three archaeological layers to do this research, which offer general and diachronic overview of lithic raw material procurement in El Esquilleu Cave. The selection of these layers was made taking into account the previous studies done and the recommendations of director of the excavation. We selected the layers VIF, XIII and XXIIR:

1. **Layer-VIF:** The first one was situated in the first part of the sequence, where the lithic raw material acquisition was made near river beaches and the lithic reduction was mainly made using discoidal procedures. The numerical date was obtained, also palynological data, and faunal remains. It was in the Sedimentary Sequence B that allowed us to distinguish surface alterations on stone from later analysed layers that correspond with sedimentological phase B. We selected the square J-11 for this study, composed of 301 lithics.

2. **Layer-XIII:** The second one was situated in the middle of the sequence, where the lithic raw material acquisition was made in river beaches and in the Southeast direction, and the lithic reduction was mainly made using Quina reduction. The numerical date was obtained; also data on palynological, anthracological and faunal remains. It was in the sedimentary sequence C, and the presence of phytoliths revealed an intensive use of the cave for residential purposes. We selected the square J-11 for this study, which was composed of 2,444 lithic

fragments.

3. **Layer-XXII-R:** The third one was situated on the lower part of the sequence, where the lithic raw material acquisition was made in river beaches and in North and West directions and where the lithic reduction was made using discoidal procedures. Numerical dates were obtained; also data on palynological, anthracological and faunal remains. We selected the square J-10 for this study, which was composed of 791 lithic remains.

2.3.2. THE ARCHAEOLOGICAL SITE OF EL HABARIO

The archaeological site of El Habario is an open-air site situated in the western part of the Cantabria Autonomous Community, within the municipality of Cillórigo de Liébana, between the villages of Pendes and Cabañes (Figure-2.21). The geographic coordinates of the site are X= 368.973 Y= 4.784.861 30T ETRS-1989. It is situated 1400 meters away from the left margin of the Deva River, 298 meters above it, and it is 18.729 meters away from mouth of the Deva River in Euclidean distance. The height is around 538 meters above the sea level.

The open-air site of El Habario is situated in a small Colluvium of unconsolidated sediments on the top of the Remoña Formation, dated as Gzhelian (Upper Carboniferous) and mainly composed of shales, sandstone, conglomerates, breccia, and limestone lithology olistolith. The last formation is situated in the Northern part of the Pisuerga-Carrión Province, characterised by Carboniferous, Silurian, and Devonian rocks, mainly composed of non-carbonate material; clearly differentiated from the near and mainly calcareous Picos de Europa Province, to the North and West. El Habario is in the area called the Liébana valley, characterised by non-sloped mountains and open valleys created by the Deva River and its tributaries, the Quiviesa and Buyón rivers. This river system erodes material from Peña Sagra and Peña Labra to the East, Sierras Albas and Sierra de las Orpinas to the North, and Sierra Mediana and the Picos de Europa massif to the West. Finally, rivers deposit the material in this open valley, closed to the North by previously mentioned Hermida Defile (Figure-2.4).

Figure-2.24: El Habario site and surrounding area. The place name comes from popular tales that relate the rounded pebbles that spread from the conglomerate in the surrounding area with big beans which were collected by ancient giants. Note that El Habario area is still used by autochthonous people for chestnut providing from surrounding chestnut tree. It is also a recreational area.

The area where El Habario is situated is a small basin almost on the top and relatively flat surface between two small hill tops. The area was prospected in various campaigns: the first one by members of the C.A.E.A.P in the beginning of the 1990s (Castanedo et al., 1993), and later by Elena Carrión and Javier Baena (Carrión and Baena, 1999; Carrión et al., 1995). The first one was carried out by systematic surface material collection and later excavation of a secondary stratigraphy. The second one applied the same methodology, followed by four exploratory excavation pits in high findings concentration surfaces that led to the next excavation in the area around the pit where more and better preserved archaeological remains were found. The excavation was carried out under the direction of Javier Baena and Elena Carrión in 1996. The total excavated surface was around 14 square meters, where two archaeological layers were found after the three first layers clearly affected by vegetation (Figure-2.25). The first four layers had archaeological material clearly affected by erosion, and they were not assigned to any primary deposit. The last layer was composed by silty and yellow sediments formed as a consequence of weathering processes on shale bedrock (Figure-2.26). The archaeological materials from this layer were not as affected by erosion as the material from the previous layers or surface material. The total of pieces recovered from this archaeological layer was 517. No faunal remain was preserved.

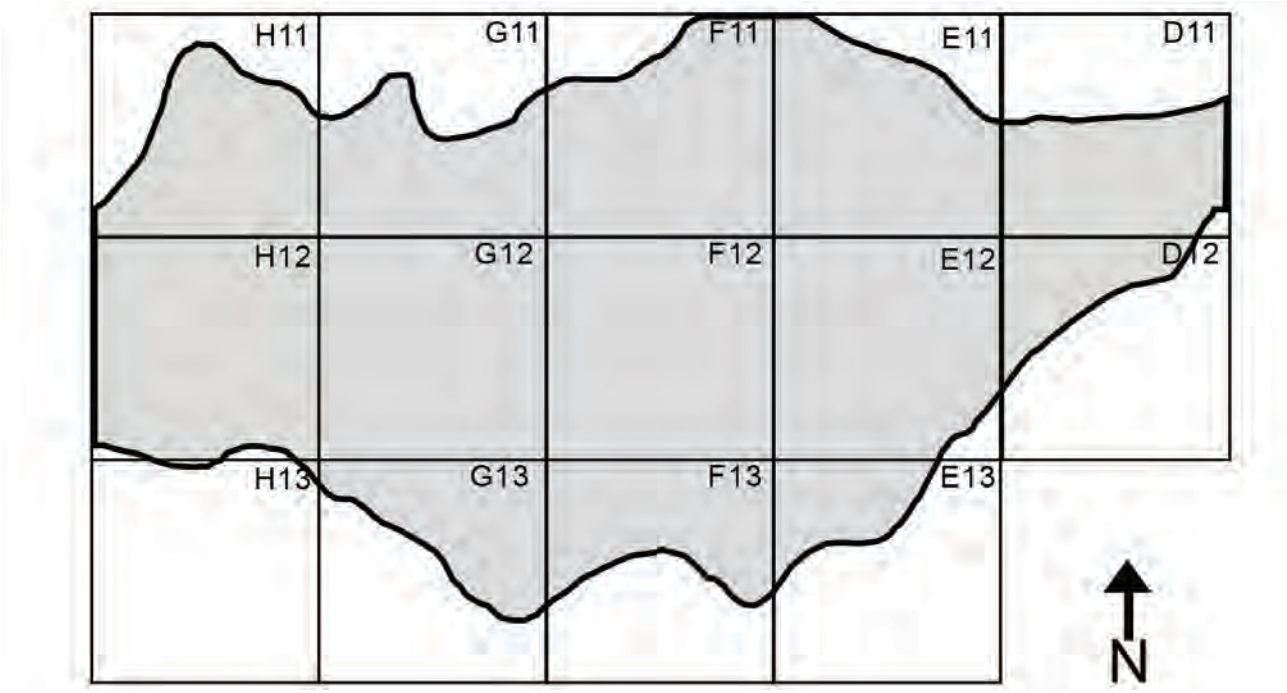

Figure-2.25: El Habario horizontal plan map, modified from Carrión (1998).

Elena Carrion characterised the lithic raw material with macroscopic procedures (Carrión, 1998). Quartzite is the most abundant material (95.7%), while quartzite/arenite (2.9%), sandstone (0.7%), and flint (0.5%) were clearly residual materials. In these studies, the researcher proposed that quartzite was directly collected in adjacent quartzite conglomerates. Other raw materials were probably collected in near river beaches or in other areas that could contain flint.

Elena Carrión and Javier Baena characterised the lithic technology (Carrión and Baena, 1999, 2005). This analysis was made following a technological approach based on qualitative perspectives and the application of the concept *Chaîne opératoire*, as in El Esquilleu Cave. They proposed a dominant lithic reduction model based on a hierarchical centripetal reduction focused on flake production and a tendency to produce pointed flakes. There was an overrepresentation of cores and retouched material. Also material with cortical features (43.5%).

All in all, these features showed that the site was probably used for quartzite catchment activities. The conglomerates near the archaeological site had a significant quantity of high-quality quartzite, as described by previous analyses. The overrepresentation of cores and cortical features pointed out in that direction, but also the underrepresentation of flakes, which was probably carried to other places such as El Esquilleu or El Arteu. Compositional characterization of quartzite made by these researchers pointed in that direction (Figure-10 from Carrión and Baena, 2005). The overrepresentation of retouched material could be related to learning activities or creation of toolkits in a context of raw material abundance, as described in other Mousterian sites (Baena and Carrión, 2006; López

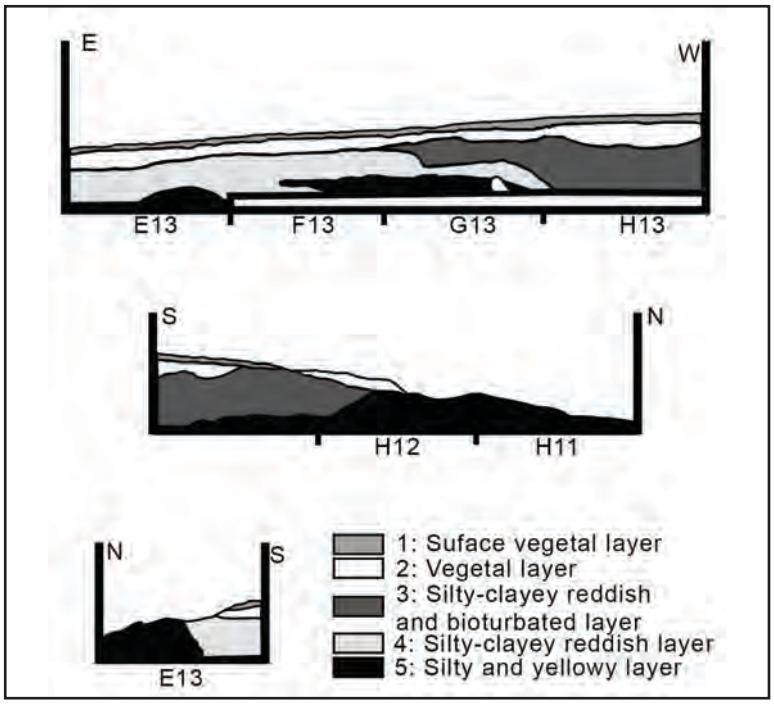

Figure2.6: El Habario excavation profile cuts, modified from Carrión (1998).

and Baena, 2001; Montes, 1988; Ortiz and Baena, 2016; Santonja, 1986).

For the research proposed, we decided to use the material derived from the archaeological site to analyse and understand quartzite procurement activities carried out by Neanderthal groups. Also, to determine other petrological features that could help us to define types of quartzite and to associate them geographically, technically, and according to use features. We selected the material stored at the Archaeological Museum of Cantabria (MUPAC, following the Spanish acronym) coming from the archaeological excavation of El Habario carried out by Elena Carrión and Javier Baena. These materials, although affected by weathering, seem to have internal coherence, and they are on sub-primary position. The total number of pieces analysed is 473 and they are referred in the bibliography and the Museum as El Habario B.

2.3.3. THE ARCHAEOLOGICAL SITE OF EL ARTEU

The archaeological site of El Arteu is a small rockshelter situated in the western part of the Cantabria autonomous community, within the municipality of Peñarrubia and near the village of Rumenes (Figure-2.21). The geographic coordinates of the site are X= 368.247 Y= 4.793.505 30T ETRS1989.

Figure2.27: Surrounding area of El Arteu and the archaeological site of El Arteu.

It is situated 250 meters away from the right margin of the Deva River, 183 meters above it, and it is 15.106 meters away from the mouth of the Deva River in Euclidean distance. The height is around 255 meters above sea level.

The site of El Arteu is in the Barcaliente formation, mainly composed of up to 400 m laminated, thinly bedded micritic limestone and black and fetid black limestone of middle-late Carboniferous (Namurian times; Colmenero et al., 2002). This formation is located in the Eastern zone of the Picos de Europa Province that is characterised by massive carboniferous limestones affected by different overthrusts that repeat the sequences. The Middle Cambrian to Early Ordovician Barrios Formation (mainly composed by quartz-arenite) crosses the massive limestone strata in East-West direction to the South El Arteu site. The area described is partially modified by the siliceous Barrios Formation that reduces the steeped geography, creating an opening area near the archaeological site in The Hermida Defile (Figure-2.27).

The rockshelter of El Arteu is small. No excavation has been carried out in this site and the material was collected in sediments derived from the fallen profiles in the 1990s by Gonzalo Gómez Casares. The sedimentary sequence was about 80 cm deep, and very rich archaeological layers seemed to be present. The collection recovered was small, 247 lithic fragments. Raw material characterization was made by non-destructive procedures by Iván Manzano, showing that quartzite is mainly used as raw material (95% of pieces), followed by ferruginous rocks, flint, sandstone or limestone (Manzano, 2001; Manzano et al., 2005). Elena Carrión conducted technological characterization with previously commented methodological premises, showing that lithic reduction under Levallois or discoid lithic reduction focused on obtaining pointed flakes prevailed (Carrión, 2002; Carrión et al., 2008). El Arteu site seemed to be related to a complex network between the previously described sites of El Habario and El Esquilleu due to similarities in technology and raw material procurement strategies. The prior interpretation of El Arteu for hunting activities inside a complex residential model in the area was suggested (Baena et al., 2005).

For this research, we decided to use this archaeological site taking advantage of the information derived from previous studies, that demonstrated its importance in the area and its relationship with the two archaeological sites previously described. We would like to stress the importance of this type of small places for Palaeolithic Archaeology, which provide different and diverse interpretations of Prehistoric habitat far away from huge or “classic” archaeological sites. We studied this assemblage, composed of 255 lithic fragments in the MUPAC.

2.3.4. THE ARCHAEOLOGICAL SITE OF LA CUEVA DE COÍMBRE

The archaeological site of La Cueva de Coímbre is a cave situated in the eastern part of the Asturias autonomous community, within the municipality of Peñamellera Alta and between Niserias and Besnes villages (Figure-2.21). The geographic coordinates of the site are X= 363.317 Y= 4.798.415 30T ETRS-1989. It is situated 123 meters away from the left margin of the Besnes River (tributary to Cares River) and 42 meters above it. The mouth of the Cares-Deva is 18.822 meters away in Euclidean distance. The height is around 145 meters above sea level.

The cave is located within limestones of the Barcaliente Formation In this area we found siliceous rocks of the Barrios Formation and dark grey carbonate rocks of the described Barcaliente Formation (Carboniferous). This zone is crossed by the Cares River in East-West direction (Figure-2.28).

The Coimbre Cave is a big cave longer than 3.100 meters, with a complete slope of 73 meters. The entrance to the cave is eight meters wide and six to two meters high and opens to the main hall of the cave. The later part of the cave is constituted by ramiform structures with galleries, passages and other small halls. From an archaeological perspective, in 1971, Alfonso Moure and Gregorio Gil have studied the cave due to the presence of engravings attributed to the Initial and Recent Magdalenian (Moure and Gil, 1972, 1974). Later archaeological excavation was carried out in the main hall between 2008 and 2012, conducted by David Álvarez-Alonso and José Yravedra (Álvarez-Alonso et al., 2013a; Álvarez-Alonso et al., 2009; Álvarez-Alonso et al., 2013b). The area was divided into four topographic zones, and two of them were excavated through two excavation pits of 2x1 meters (Zones A and B) Figure-2.29. Later excavation process was focused on the Zone B pit, and during the excavation process, two adjacent square meters were opened. The stratigraphic depth is now around 220 cm. It was divided into seven layers, of which five layers had archaeological remains (Co.B.1, Co.B.2, Co.B.4, Co.B.5, and Co.B.6) (Figure-2.30). High quantity and density of archaeological findings of bone, stone and shell were recovered from this archaeological excavation.

Although the research project at Coimbre cave is still in progress, some studies which have already been carried out are offering contextual information of this archaeological site.

Figure-2.28: Surrounding area of Coimbre.

Cave art is present through engravings that were divided into five groups (Moure and Gil, 1972, 1974). At the entrance of the cave, the first group appears with vertical engravings, triangular signs and the head of an equid. The most interesting engravings are situated in the main hall and are composed of a large bison and the first anatomic part of a horse. The third engraving panel is formed by the heads of two bovids and the representation of a horse at the end of the main entrance, in a small diverticulum. The last two panels are situated in two secondary galleries with animal images. The first one is composed by two goats, two bovids, two cervids, other non-identified animals, and some non-determined figures. The second one consists of some cervid heads and a whole cervid shape.

From the sedimentary point of view, the sequence of Coímbre B was formed through three primary sedimentary processes; two of them of geologic nature and the other the result of the human occupation. The first natural process consisted in the falling of clasts from the roof as a consequence of freeze-thaw shattering and possible paleoseismic events. The second natural process was related to fluvial sedimentation due to accumulation of layers Co.B3, Co.B5 and Co.07 or erosive events, with a partial impact in layers Co.B.6 and Co.B.4, interbedded between layers of fluvial origin. The anthropic processes were also of two kinds: on the one hand the accumulation of numerous remains and, on the other, in the last phase, the elimination of part of the sediments by cleaning up, preparing and structuring the inhabited area in Co.B1 layers (Álvarez-Alonso et al., 2011).

From the point of view of absolute chronology, the sequence in Zone B at Coimbre was dated through C14 AMS methodology (using bone and charcoal) in the same laboratory, and they showed stratigraphy coherence. The proposed chronology for this sequence started in layer Co.B.6 with 29660-28560 Cal BP for the Gravettian occupation of the cave, in line with the warm event of the Greenland Interstadial 1 in one of the cold phases of the MIS 3a. The Magdalenian sequence began with the Archaic Magdalenian layer Co.B.5, at the start of GS2b in the Last Glacial Maximum and with a numerical chronology around 20890-20240 Cal BP. The sequence followed in the Lower Magdalenian layer Co.B.4, after a short hiatus, with dates between 20070-18780 Cal BP, corresponding to

the second half of GS 2b. After a longer hiatus represented by the barren layer of Co.B.3, the Middle Magdalenian layer Co.B.2 was formed in GS2a, with numerical dates between 17220 and 16110 Cal BP. After this layer and in clear stratigraphy continuity, later Co.B.1 Upper Magdalenian numerical dates showed a numerical chronology between 15790 and 14070 cal. BP, proposing the formation of this layer in the last cold phase of GS2a, in the Late Glacial Maximum and the temperate GI1e at the start of GI 1 or Late Glacial Interstadial. All in all, the sequence of Zone B at Coímbre was dated in the final part of the last glacial period, during the late Upper Pleistocene, corresponding to the end of the MIS3 and MIS2 (Álvarez-Alonso et al., 2016).

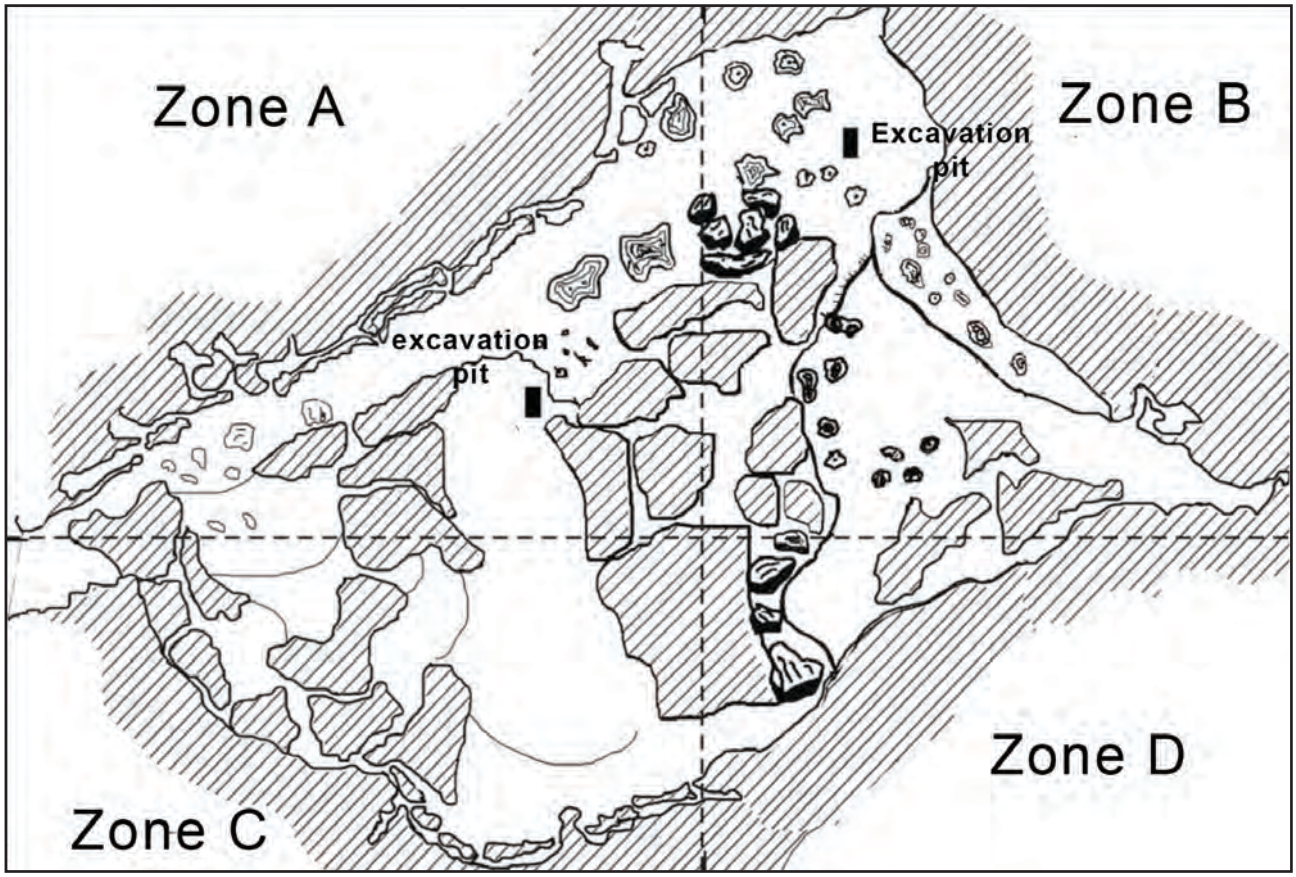

Figure-2.29: The Cave of Coímbre horizontal plan of the main hall, modified from Álvarez-Alonso et al., (2009).

Palaeoenvironmental analyses (from micromammal faunal, anthracology and the study of birds), showed variation in climatic conditions in the sequence of the cave of Coimbre zone B excavation. In Co.B6 layer, the environmental conditions were related to open areas and cold climatic conditions, as micromammal, charcoal, and bird analysis remains demonstrate. There is no more published data for the Magdalenian part of the sequence.

José Yravedra performed faunal analysis, focusing on taxa identification and taphonomic agents affecting bones (Álvarez-Alonso et al., 2016; Yravedra et al., 2016). In general terms, *Bos/Bison*, *Equus ferus*, *Cervus elaphus*, *Capreolus capreolus*, *Capra pyrenaica*, and *Rupicapra pyrenaica* were the most significant species in the sequence. Apparently primary species changed between the Gravettian layer, dominated by first two taxa remains (large bovids, mainly), and the Magdalenian layers, dominated by *Capra* and *Rupicapra*. Age patterns of preys consumed showed that adults are more often hunted than younger preys. They were introduced by humans and were affected by fragmentation and fire, due to the use of bones as fuel for fires, more evident on layer CO.B.6 than in the later Magdalenian layers. Later layers also revealed the consumption of salmonids carried from near rivers. In the first Magdalenian layers rabbits were also hunted.

Lithic, bone, and shell industry are partially published. Quantitatively, the most important lithic raw material was quartzite, followed by flint and radioralite. Meanwhile, and, at least for Magdalenian layers, flint was more used for retouched artefacts. Different types of flint were found in these Magdalenian layers, with a presence of local and long-distance flint types, such as Treviño, Flysch

and Urbasa types from Mesozoic sedimentary sequences of CVC. In the layer Co.B.6, quartzite percentages were much higher in contrast to flint, that was apparently residual. The backed objects such as bladelets, denticulate bladelets and points were found in the sequence, also burins and end-scrapers, with different numerical importance in each layer due to variation in site function and/or cultural changes in the Magdalenian part of the sequence. Meanwhile, in the layer Co.B.6, the presence of retouched material was much more limited. Bone and shell industry were also limited in this layer, only represented by a shell pendant. Bone and shell industry were abundant in the Magdalenian part of the sequence (more important for layers Co.B.1 and Co.B.2 than Co.B.4 and Co.B.5) with different types of decorated and not decorated assegai points, harpoons, and portable art object. Pendants made of teeth and shells appeared in this part of the sequence too.

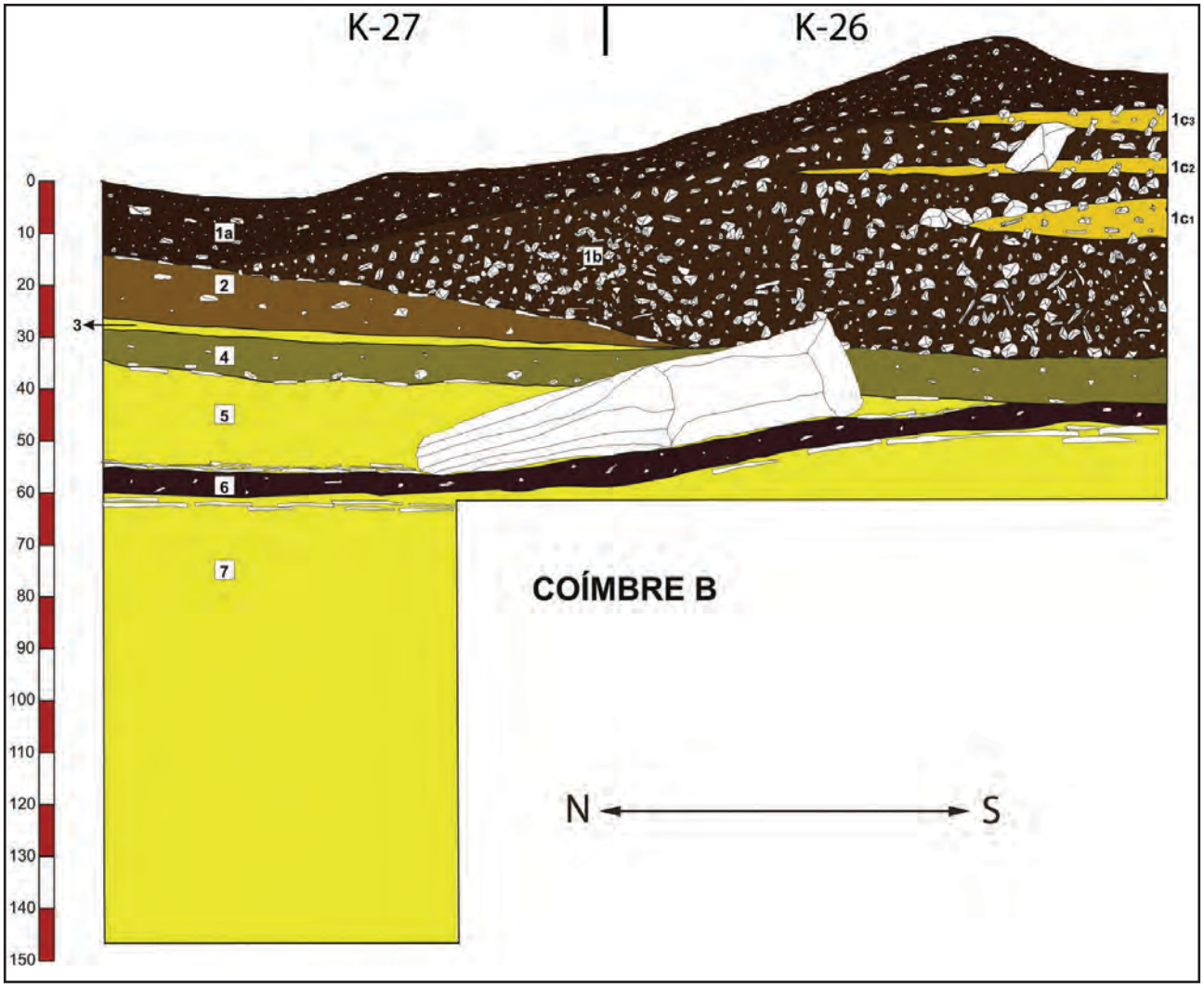

Figure-2.30: The Cave of Coímbre Zone B excavation profile cut modified from Álvarez-Alonso et al., (2016).

In general terms, Coimbre Cave shows an impressive Magdalenian sequence, associated with cave art engravings and an interesting Gravettian layer. The excavation and later provisional but interesting analysis show that Coimbre cave was occupied by Upper Palaeolithic groups during the Gravettian and Magdalenian periods. On the first layer, and Co.B.6, and maybe on the firsts two layers of Magdalenian phase, the occupation was limited and restricted to sporadic visits, as quantity and type of archaeological remains reflected. The last two layers showed that the cave could be used for residential purposes, as faunal consumption and the number and types of archaeological findings shows. The probable chronological association with art engravings also supported this hypothesis.

We selected the Co.B6 layer from the sequence due to the massive presence of quartzite as raw material, but also to obtain an archaeological layer in the first stages of an Upper Palaeolithic sequence. This layer can be compared with previously commented Middle Palaeolithic sites to compare different quartzite catchment and manage strategies. We analysed all non-debris lithic

fragments that are composed of 933 pieces. Additionally, we also took into account the debris lithic remains.

2.3.5. THE CAVE ART OF LA COVACIELLA

The archaeological site of La Covaciella is a cave situated in the eastern part of the Asturias Autonomous Community, within the municipality of Cabrales and between the villages of Pandiello, Puertas, Asiego, Berodia and Inguanzo. The geographic coordinates of the current entrance of the site are X= 347.999 Y= 4.797.811 30T ETRS-1989. It is situated 123 meters away from the left margin of the Casaño River (tributary to Cares River) and 51 meters above it. The mouth of the Cares-Deva is 30.458 meters away in Euclidean distance. The height is around 301 meters above sea level.

The cave is within the Valdeteja and Picos de Europa Formations, mainly composed of fossiliferous limestones, massive limestone with algal and microbial bioconstructions, and calcareous breccia; mainly of later middle Carboniferous (Bashkirian age) (Colmero et al., 2002; Meléndez, 2015). This area is situated between the northern zone of Picos de Europa Province and the Ponga Nappe Province, characterised by a massive carboniferous limestone affected by different overthrust and the almost complete absence of Silurian and Devonian age rocks (Colmero et al., 2002). The presence of the Barrios Formation makes a less abrupt geography. The area is crossed by the Cares and Casaño river valleys that create a restricted basin in West-East direction, where the cave is located (Figure-2.31).

Figure-2.31: Surrounding area of La Covaciella Cave.

The Covaciella Cave is a short cave with less of 184 horizontal meters of itinerary, divided into three layers (Obeso-Amado, 2015). This archaeological site is mainly known due to its impressive cave paintings and was discovered shortly after the serendipitous opening of the cave (previously closed due to geological processes affecting the site) during the construction works derived from the road expansion that is adjacent to the present and artificial entrance of the cave in 1994 (Ochoa et al., 2015). Two research groups have studied the cave in two phases. The first one was directed by J. Fortea after the discovery, showing partial discoveries, focused on the description of the cavity and the rock art (Fortea, 1996, 2007; Fortea et al., 1995b). The second one was carried out between 2014 and 2015 and was done by an interdisciplinary research group led by Marcos García-Díez and Blanca Ochoa. The project focused on cave art, but other studies were done to understand the

context of the cave and other archaeological evidence. The result of the investigation was published in 2015 in a monography about the cave (García-Díez et al., 2015d).

Cave art is limited to the gallery situated in the western part of the cave, accessible through a clayey ramp from the current entrance of the cave. Four panels located on the left part of the gallery are visible. The first panel represents through engraving an incomplete bovid; the second one corresponds to two linear and digital signs, an incomplete and digital drawing of a cervid, the head of a horse drawn with black lines, a complete bison drawn with blank lines and digital drawing, and many digital marks. Panel three is the most impressive one. It is composed of two bisons that were drawn by lines and plain ink, engraved, and finally scraped; a bison drawn in black with a red ochre sign on it; an incomplete bison drawn in black; a carved bison; a digital bovid, a digital goat or reindeer and a triangular sign. The last panel is composed of two (complete and incomplete) black bisons and a big ochre sign. The stylistic features indicate that the painting can be attributed to the Middle Magdalenian, with stylistic similarities with other Cantabrian rock art caves, such as Urdiales and Santimamiñe and Pyrenean caves, such as Niaux. Absolute chronological information is coherent with stylistic criteria: two direct radiocarbon AMS dates on paintings date it between 17733 and 16058 Cal BP (García-Díez et al., 2015d; Ochoa and Vigiola-Toña, 2014).

Researchers found other evidence of human activities in this cave during the last research campaign. They found charcoal wood remains in different parts of the cave. Six fragments of charcoal appeared along the floor of the cave, and another four evidences of charcoal appeared inserted in parts of the wall galleries. The use of different types of wood for lighting is evident, and one of the charcoal fragments was dated in Iron Age chronologies (between 2677 and 2346 Cal BP). It could evidence next visits at the cave in posterior period (Medina-Alcaide and Zapata, 2015). Some vertical and anthropic pits also appear in the cave near the area of panel 3, but no explanation was found by the researcher (García-Díez et al., 2015b). Faunal remains were also found in that cave without marks of human activities on them (García-Díez et al., 2015a). In the lower and small hall of the cave, there are digital marks in a thick clay coverage that appears on the floor and the wall of the hall. No clear interpretation was proposed for this digital marks, that could be related to clay extraction for ceramic, pigments or ritual purposes (García-Díez et al., 2015c).

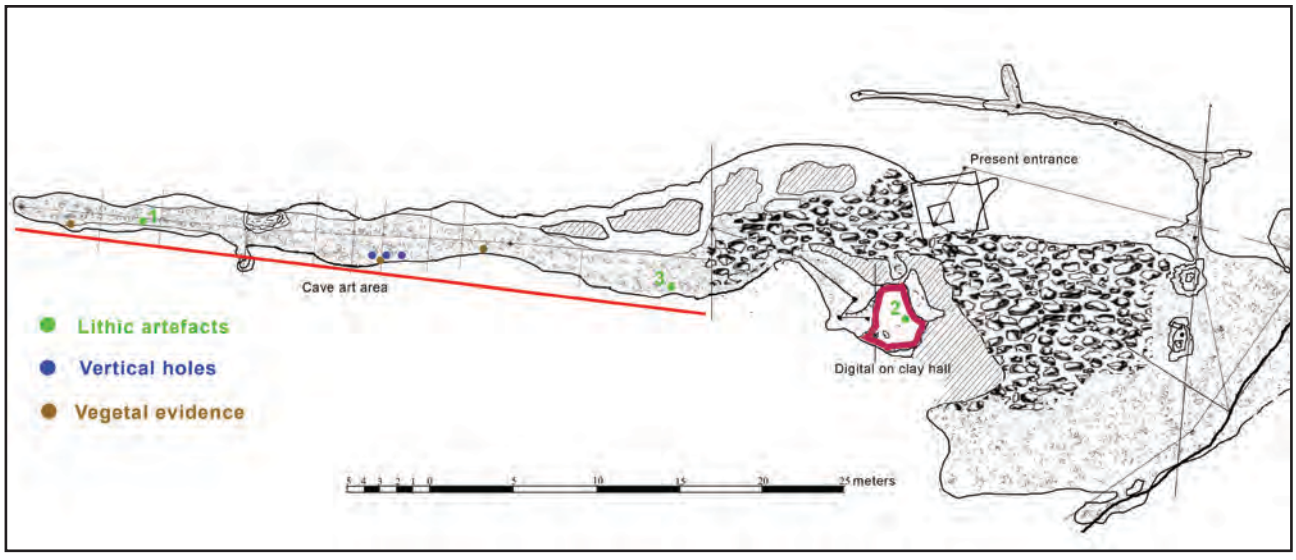

Figure-2.32: Topography of The La Covaciella Cave, created by Ramón Obeso and L'Esperteyu Cavernícola Speleology group. Modified from García-Díez et al., 2015.

There are three lithic artefacts in the cave situated in three different zones (Figure-2.32). Two pieces are quartzite, while the other one is flint. We decided to identify the raw material, typology and technological procedures to understand them concerning main activities carried out in the Cave: Cave painting art. We are aware that the context of the findings is not clear; also that quantity of material analysed is not representative. Nevertheless, these shreds of evidence could help to understand the painting process, the connection with these material and the role that raw material and its study could play in this kind of context (Medina-Alcaide et al., 2014; Plisson, 2007).

2.4. ARCHAOLOGICAL PERSPECTITES: LEAST COST ANALYSIS TO UNDERSTAND LITHIC PROCUREMENT STRATEGIES DURING THE PALAEOLITHIC

In order to understand past human mobility in a heterogeneous and rough region as the research area is, we have decided to use the methodological proposal made by the author and another researcher in recent research publications (García-Rojas et al., 2017; Prieto et al., 2016; Sánchez et al., 2016). This methodology allow us to determine mobility taking into account the variable relief together with distance. In addition, this methodology is also used to determine and identify constraining transit areas or high-mobility transit zones that affected the movement of Palaeolithic societies. In this case, the methodology is adapted to different geography. Doing so, it allows us to compare results of the same methodology applied to different geographical and chronological contexts.

For this research study, we have used the spatial analysis tools offered by the ArcGIS 10.2 software and the Digital Elevation Model developed by the Spanish National Institute of Geography (MDT25, following the Spanish acronym) (IGN, 2017). The number codes used are: 15, 30, 31, 32, 33, 54, 55, 56, 57, 79, 80, 81 and 82. These and later dataset are projected using UTM-ETRS89 30N coordinates system. The raster resolution is 25 meters.

We did not consider bathymetry due to its limitations when applied to the past, although we know it could have provided interesting data on currently submerged Palaeolithic shore and lowlands. The main problem in this respect is access to data, the fluctuations of the sea-level and the differential erosion of its surfaces, which could distort the results of this study. The fact that our spatial analysis deals with current landscape features instead of actual Palaeolithic orography is another limitation, but we consider high-resolution digital cartography is still the best source for our approach. Finally, we are also aware of the fact that effort or cost cannot only be quantified through geographic variables, but we consider these are the only ones based on consistent data we have access to nowadays. Factors such as vegetation, lithology, and the river system or climate constraints could have significantly influenced the mobility of Palaeolithic groups, but being unable to know their exact impact in each period prevents us from including them systematically. Bearing these biases in mind, these are the steps we followed:

First, after having merged all the MDT25 sheets covering the territory under study (figure-2.33a), we created a slope map, measured in degrees, using the Slope tool (Figure-2.33b). Next, this map was reclassified with the Reclass tool. The values of the cells of the new raster output were calculated by assigning average subunits of cost to the movement between specific slope ranges. This calculation was based on the model developed by M. Llobera (2000) after A. E. Minnetti's experiments (Minnetti, 1995) see also López Romero (López Romero, 2005). However, it is worth mentioning there are other valid approaches to calculate the cost of moving, such as those of Pandolf (Pandolf et al., 1977), Langmuir (1984) or Tobler (1993), whose most recent adaptations (Kramer, 2010; Marín, 2009) are currently being debated (Kantner, 2012). The method chosen for this study defines the unitary value of cost as the effort generated by moving at a constant speed of 5 km/h on a different degree of slope (Figure-2.33c). As a result, we obtained a new surface friction map where each pixel contains information on the effort required to cross it, expressed in subunits of cost (Figure-2.33d).

The locations of the archaeological sites were represented by their geographic coordinates, as previously shown. Once these points were located on the friction surface map (slope reclassified), we performed the geoprocess Cost distance tool (Figure-2.33e). The resulting map shows, through a gradient of colours, the accumulated cost of carrying each variety of flint to any given point in the territory. Then we reclassified this map in ranges of 15,000 subunits (Figure-2.33f). Each of these ranges was considered a Cost Unit (CU from now on). This step was performed to make the representation and management of the data clearer and easier. Finally, and with the aim of simplifying the visualisation, we grouped the resulting values in groups of four CU by colour.

The expansion map, as a graphic information for relating easy/difficult movement areas, and the numerical data reported as CU have been used for analysing and comparison between archaeological sites here analysed and other geographic areas.

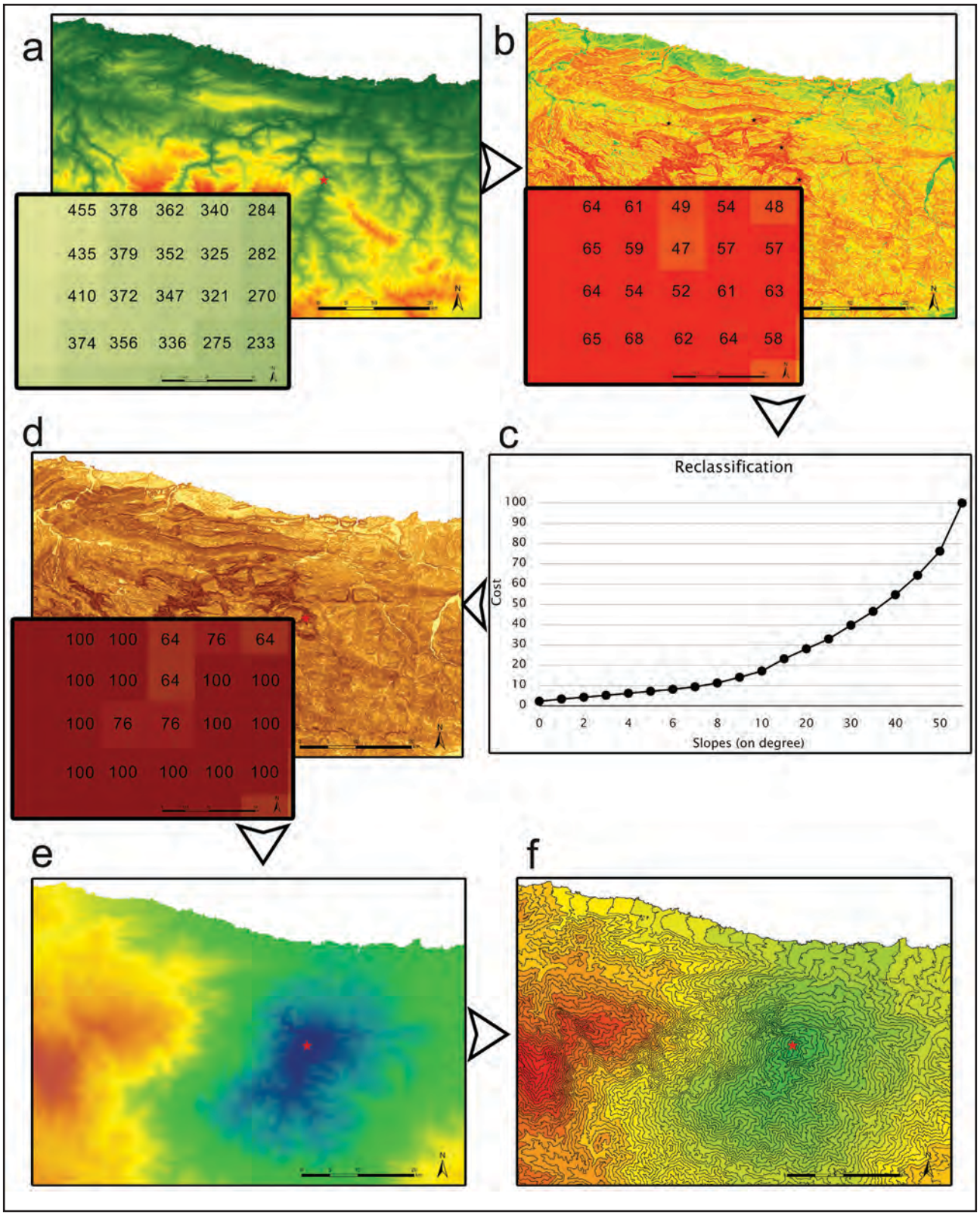

Figure-2.33: Methodological procedures for obtaining cost map from each archaeological site. The analysed site is El Esquilleu.

CHAPTER-3

MATERIALS & METHODS. A MACROSCOPIC APPROACH TO UNDERSTAND LITHIC PROCUREMENT AND MANAGEMENT STRATEGIES

3.1. Methodology. Geological perspectives: Petrological characterisation of stones through macroscopic features

3.2. Mehodology. Archaeological perspectives: Analytical typology, the dialectic and the structural methodology for the characterisation of the lithic products

3.2.1. Petrological structure

2.2.2. Technological structure

2.2.3. Defining the retouch using the morphological and the modal structures

2.2.4. Typometrical structure

3.2.5. Raw data processing: Statistics

3.1. PETROLOGICAL CHARACTERISATION OF STONES THROUGH MACROSCOPIC FEATURES

In this section we define the basic petrological characteristics, the features of the cortical areas, and the general external morphologies of the rocks selected during geological survey exposed above. The total number of samples is 509 stones, selected from the approximate 5000 items observed and analysed on the field survey.

We defined the stones using general petrological and closed categories. These are:

1. Archaeological quartzite (from consolidate sandstone to pure metamorphic quartzites)
2. Flint
3. Limestone
4. Limonite
5. Shale
6. Quartz (either monocrystalline and polycrystalline)
7. Radioralite
8. Volcanic rocks

We distinguished the quantity of the internal different directional joints using the criteria: non-presence, one direction, two directions, or three or more directions categories.

We classified the colour hue of the pieces using closed categories of general colours on two different fields. We observed the colour on fresh-cut. The colours considered are: white, grey, black, blue, green, orange, brown, yellow and red.

We characterised the cortex of the stones using some basic features. These are:

1. Texture: classified as granulate, either coarse or fine grained; or non-granulate, either fine or soapy.
2. Presence or absence of mineral precipitates on the cortex. In case of mineral presence, it is simplified in closed categories: iron oxide, siliceous, or carbonates.
3. Presence or absence of the following features: features derived from plants (such as marks of small roots), features derived from small animals (such as lithophagous), and presence of voids (generally derived from the meteoric alteration of samples in soils/water sources of the sample into water sources).
4. Presence or absence of impact cracks caused by the impact of stones in water courses or by gravitational stone fall.
5. Quantity of different directional joints, using the categories non-presence, one direction, two directions or three or more directions.
6. Colour hue on fresh-cut, using basic descriptions as previously explained.

Finally, we associated to each lithology the size of the rock varieties applying the Udden-Wentworth categories (Wentworth, 1922) and their morphology through the following categories (Figure-3.1):

1. Spherical pebble
2. Flat pebble
3. Tabular pebble
4. Tabular clast

We included and systematised all these features on a form database with closed categories of sampled stones, using the software Filemaker Pro. We also included these features, except the colour hue fields and cortex analysis, in the lithology section of the outcrop, conglomerate, and deposit databases previously commented. This allow us to analyse and understand the geographic dispersion and morphological features of the stones.

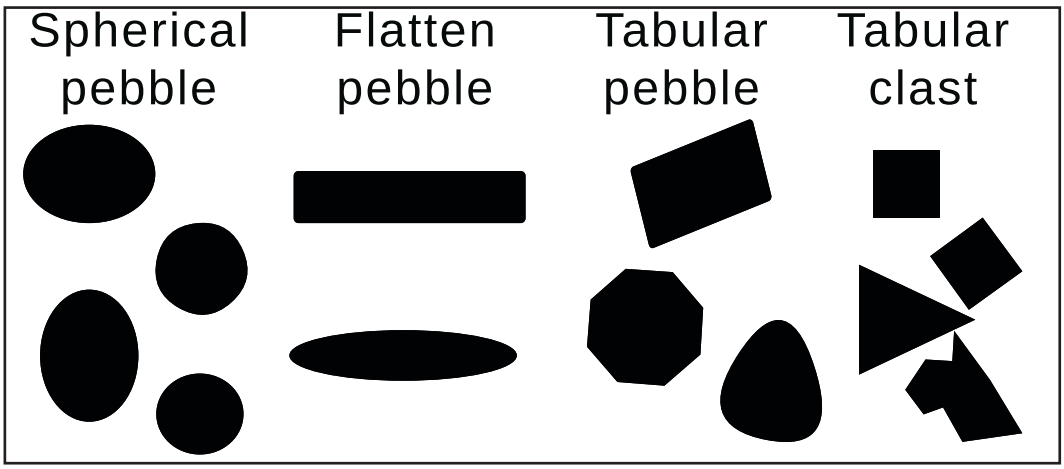

Figure-3.1: Representation of morphology of blocks in conglomerates and deposits

3.2. ANALYTICAL TYPOLOGY: THE DIALECTIC AND THE STRUCTURAL METHODOLOGY FOR THE CHARACTERISATION OF THE LITHIC PRODUCTS

In general, we understand the lithic analysis as the process of knowledge that allow us to observe, measure, quantify and interpret the morphological and technical features of each lithic artefact to understand human, social, behavioural, ecological and economical systems, its continuities or remanences, its modifications or changes. The matter, as the main object analysed, is each lithic implement; the forces, as the aim of the study, the understanding of catchment and management strategies of prehistoric societies. We decided to use the Analytical Typology as the methodological framework that guides this process, applying the dialectic and the structural proposal (Laplace, 1972).

Dialectics is a methodological tool that understands the whole as the relation of dynamic, contradictory and interrelated elements, allowing us to understand each detail into the whole. Its application in lithic analysis is based on the deconstruction of each lithic implement into morpho-technical features that can be defined and measured, and which are later compared with other lithic features, implements and assemblages, and other archaeological evidence to understand each object itself and, through its connections, within its context.

We decided to study every lithic fragment on each analysed unit of study. In the cases of El Arteu, El Habario, and La Covaciella, we studied every lithic fragment, inside each analysed archaeological layer. In the case of El Esquilleu, due to the high quantity of materials recovered in the excavation, we only analysed one square meter from each archaeological layer (J-11 for Layer VIF and XIII, and J-10 for Layer XXII-R). In the case of La Cueva de Coimbre, we analysed every lithic piece except those classified as debris by the study performed by David Álvarez, Aitor Calvo, and Álvaro Arrizabalaga, due to time constraints and their quantity (Álvarez-Alonso et al., 2017). These materials come from the water-screening process.

The structural methodology allowed us to organise and arrange coherently each previously analysed element or feature as accumulative and selective criteria within the different structures. These structures try to understand each morphological and technical features through different approaches: The petrographic or petrological structure focuses on raw material characterisation; the (typo)metrical structure focuses on the measurement of the lithic object; the technological structure focuses on the description of the features derived from technical processes; the modal and the morphological structures define modifications of the pieces after their extraction (retouch), and finally traceology or use-wear structure defines the features modified by the use of each implement (this structure is not commented in this section). The articulation of the criteria within each structure is done through a hierarchical order into four categories: order, group, class, and type.

Once the theoretical framework is exposed, we are going to describe the features or elements analysed within each structure[1].

1 All of the following features are included and systematised in a form database with close categories created with Filemaker Pro.

3.2.1. PETROLOGICAL STRUCTURE

Each lithic implement was petrologically defined using the main lithological categories and the different directional joints previously exposed on the section about the macroscopic definition of stones derived from survey. Colour was also defined as an accumulative feature applying the same parameters.

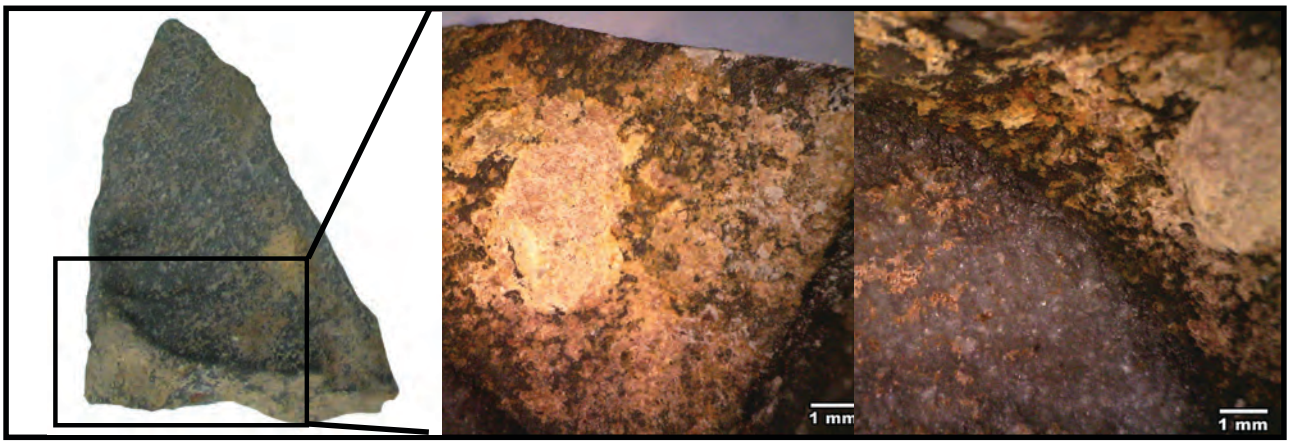

Figure-3.2: Picture of the cortex of ES-407 (Esquilleu, layer-XIII) as an example of cortical areas from conglomerates. From left to right, macroscopic picture of cortical area, microscopy binocular picture at 20x magnification of the cortex and microscopy binocular picture at 20x magnification of the interface between cortex and inner area. In the latter picture it is possible to observe the colour change between cortical areas (darker) and the inner area (lighter).

On this structure we also defined the cortex of each lithic artefact (in case any remains was present covering the implements) as an accumulative feature. We defined the cortex by using the same categories proposed for the macroscopic definition of raw material. The main objective of this process is to understand if the raw material came from outcrops, conglomerates or deposits. We decided to use all the categories for defining the features of every artefact from El Arteu, El Habario and La Covaciella, and of a smaller sample of the artefacts from those archaeological sites with high amounts of lithic implements, such as El Esquilleu and Coimbre. For the non-sampled material, we defined the cortex base on its possible provenance as: unknown, from outcrop, from conglomerate (Figure-3.2) or from secondary deposit (Figure-3.3). Colour, as an accumulative feature, is defined for every cortical elements.

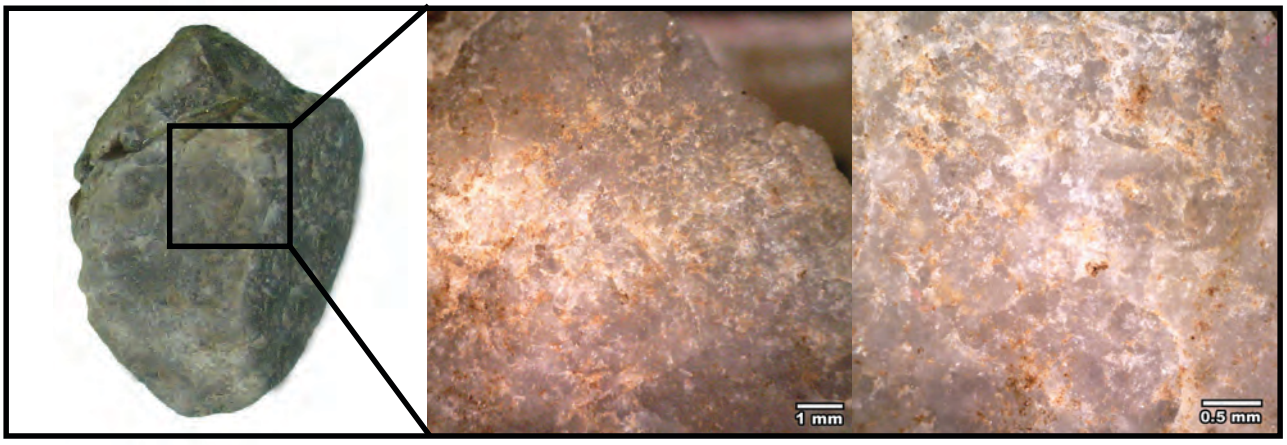

Figure-3.3: Picture of the cortex of ES-378 (Esquilleu, layer-XIII) as an example of cortical areas from fluvial deposits. From left to right, macroscopic picture of cortical area, microscopy binocular picture at 20x magnification of the cortex and microscopy binocular picture at 50x of the cortex.

3.2.2. TECHNOLOGICAL STRUCTURE

For this case of study we followed and adapted the methodological proposal designed by Maite García-Rojas (2010 and 2014).

First, we classified each lithic implement attending to general technological categories and creating the order relation for the artefacts as follows:

1. Cores: Characterised by the presence of one or more knapping surfaces and one or more striking platforms.
2. Knapping products (*débitage* or *Producto Bruto de Talla PBT*): Characterised by the presence of a ventral and a dorsal surface and the presence of a butt of striking platform (García-Rojas, 2014).
3. Chunk: Material that could not be classified in the two previous categories due to conservation or the lack of criteria or features that can assign it to one categories or another.

Secondly, we classified each previous order, with the exception of chunk category, generating the following groups:

The cores are classified attending to their formal characteristics:

1. Discoid core, characterised by centripetal extractions in one or in both faces (Laplace, 1987).
2. Levallois core, characterised by the exploitation for obtaining predetermined flakes following on discoidal procedures (Boëda, 1994).
3. Prismatic core, characterised by a prismatic morphology.
4. Pyramid shaped core, characterised by a pyramidal morphology.
5. Core on flake, a flake with at least one extraction on its ventral face.
6. Irregular or polyhedral core: Non-standardised core.

The knapping products are classified attending to the quantity of planes present on the dorsal surface:

1. Blanks, characterised by the presence of only one plane on the dorsal surface.
2. Core preparation/rejuvenation elements, characterised by the confluence of two or more planes on the dorsal surface. One of them is used as the striking platform and the other one as the knapping surface.
3. Burin spall, characterised by the presence, on the dorsal surface, of a ventral surface and a dorsal surface coming from the original matrix of the stone.

We described and systematised other features that are not included in the structure proposed because they are accumulative. Some of them are restricted to some categories previously commented, while others are accumulative for every type. (Figure-3.4) They are:

Integrity: It evaluates if the lithic implement is complete or not. We systematised it through the following criteria:

1. Complete, if the lithic implement is complete or almost complete.
2. Proximal, if the lithic implement is not complete and the proximal part is present.
3. Medial, if the lithic implement is not complete and the medial part is present.
4. Distal, if the lithic implement is not complete and the distal part is present.
5. Indeterminate, if the lithic implement is not complete and there are not enough features to classify it on any of the categories previously exposed.

Presence of cortex: It evaluates the presence of cortical areas covering the lithic implements through the following criteria:

1. Non-cortical: In case there is no cortical surface covering the lithic implement.
2. Cortical area < 1/3: In case the cortical surface is restricted to 1/3 or less of the dorsal surface for knapping products or less than 1/3 of the complete surface for cores and

chunks.

3. 1/3 < Cortical area > 2/3: In case the cortical surface covers between 1/3 and 2/3 of the dorsal surface for knapping products or between 1/3 and 2/3 of the complete surface for cores and chunks.
4. Cortical area > 2/3: In case the cortical surface covers more than 2/3 of the dorsal surface for the knapping products or more than 2/3 of the complete surface for cores and chunks.

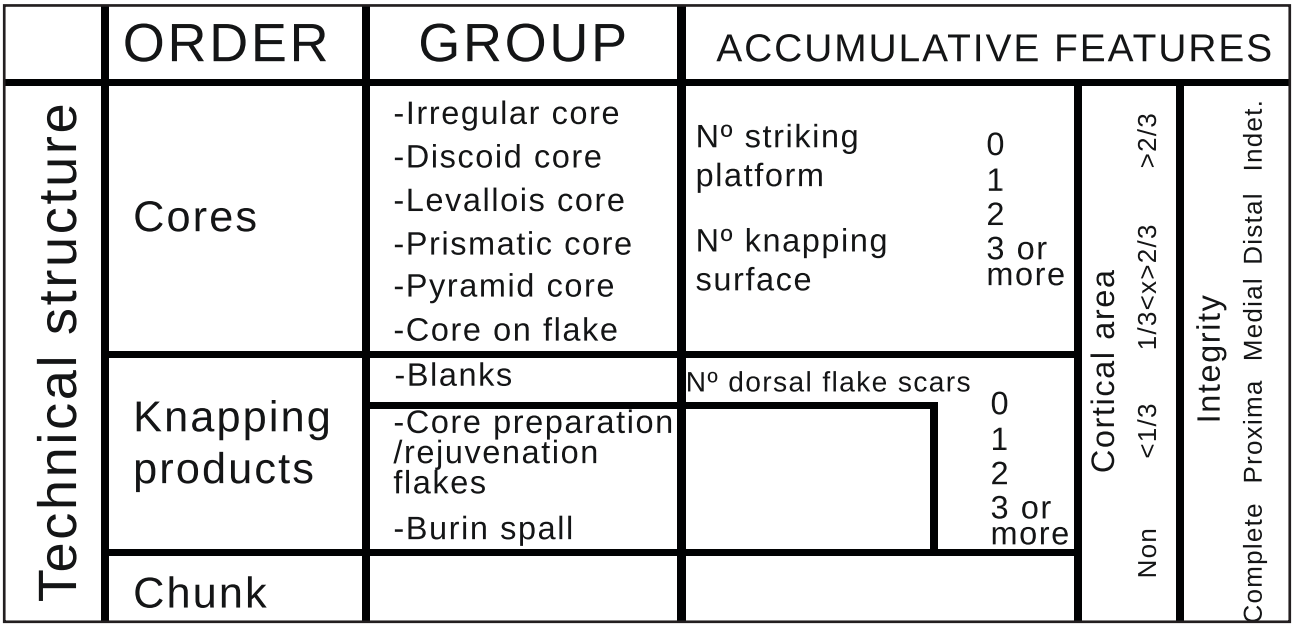

Figure-3.4: Schematic representation of technical structure

Amount of non-consecutive striking platforms, limited to the core order and simplified as:

1. No striking platform
2. One striking platform
3. Two striking platforms
4. Three or more striking platforms

Amount of non-consecutive knapping surfaces, limited to the core order and simplified as:

1. No knapping surface
2. One knapping surfaces
3. Two knapping surfaces
4. Three or more knapping surfaces

Amount of flake negative/dorsal scars on the dorsal surface of blanks, simplified as:

1. No dorsal flake scar
2. One dorsal flake scar
3. Two dorsal flake scars
4. Three or more dorsal flake scars

3.2.3. DEFINING THE RETOUCH USING THE MORPHOLOGICAL AND THE MODAL STRUCTURES

We defined each retouch of each piece as a cumulative element to the technical and petrological structures previously explained. This is based on the definition of retouch as the feature/s that modify the edge/edges of a lithic implement. The modal structure defines five modes or basic types of retouch, based on the degree of modification and the angle formed on the edges. They are:

1. Simple mode (S): Defined by the presence of small negative scars on the preserved edge that generate an angle of around 45˚ in relation to the surface.
2. Abrupt mode (A): Defined by the presence of negative scars caused by the destruction of the edges that generate an angle of around 90˚ in relation to the surface.
3. Plain mode (P): Defined by the presence of longer negative scars on the preserved edge of the lithic implement that generate an angle smaller than 45˚.
4. Burin mode (B): Defined by the presence of negative scars on parallel or sub-parallel position to the edges destructed by the retouch.
5. Splinter (*Écaillé*) mode (E): Defined by the presence of splinter negative scars on clear perpendicular position in relation to its preserved edge.

The morphological structure defines diverse features such as the invasiveness, the direction, the outlining, the morphology, the location, the shape, and the articulation generated by the retouch. The association of different morphological features regarding to previously explained modes can be summarize in new categories, understood as accumulative and selective for each mode. In this way, the structural standardisation based on order and group categories is generated (Figure-3.5).

ORDER Modal structure	GROUP Morphological structure
Simple mode	-Sidescraper -Endscraper -Denticulate -Point
Abrupt mode	-Abrupt -Truncation -Backed blade -Backed point
Plain mode	-Foliates
Burin mode	-Burin
Splinter mode	-Splintered pieces

Figure-3.5: Schematic representation of retouch characterisation through morphological and modal structure

Within the simple mode or order, the groups can be:

1. Sidescraper (R): Defined by the location of the retouch on lateral, perpendicular or lateral-perpendicular position.
2. Point (P): Defined by the articulation of two simple retouches.
3. Endscraper (G): Defined by the location of the retouch on perpendicular position, generating a convex shape.
4. Denticulate (D): Defined by its denticulate outlining.

Within the abrupt mode or order, the groups can be:

1. Abrupt (A): Defined by the presence of an abrupt retouch with denticulate outline.
2. Truncation (T): Defined by the location of the retouch on transversal position.
3. Backed point (PD): Defined by the convergence of a backed blade with the other lateral border.
4. Backed blade (LD): Defined by the location of the retouch on lateral position.

Foliates (F): There are no different groups. It is only characterised by the plain mode of retouch.

Burin (B): There are no different groups. It is only characterised by the burin mode of retouch.

Splintered pieces (*Pièces écaillés*) (E): There are no different groups. It is only characterised by the splinter mode of retouch.

The retouch of each piece is defined attending to the features and structures previously commented, understanding that each piece can present more than one retouch. I defined as maximum three retouches for each piece, differentiating one from each other attending to its retouch group and the discontinuity between retouches.

3.2.4. (TYPO)-METRICAL STRUCTURE

We measured every lithic artefact using a digital calliper with millimeter precision. We took the measurements using the technological axis as primary axis (length or L), in case the lithic artefact had a bulb of percussion or striking platform. We measured the secondary axis (width or W) using the longest distance of the piece in perpendicular position in relation to the primary axis. The third axis (thickness or T) is the thickness of the piece. For the pieces with no primary axis, we measured their longest axis (X-axis) and the Y-axis is the longest axis that cuts the x-axis perpendicularly. The Z-axis was measured as the thickness of each piece. All in all, every lithic implement could be measured as Length/Width/Thickness in case the technological axis was present and X-axis/Y-axis/Z-axis in case there was no technological axis.

We collected these data for two purposes: First to use them as final data for understanding the measurement properties of lithic production. Secondly, for understanding the relationship between the three measurements on each piece. For this purpose, we used the relative Bordes elongation index (RBEI) for every lithic fragment; the relative flatness index Length (RFIL) for the lithic implements where Length is longer than Width (every item measured according to a non-technological axis must be in this category) and the relative flatness index Width (RFIW) for fragments where Width is longer than Length (Tarriño, 2015). We did not use the categories proposed by Tarriño's methodology due to the high quantity of categories proposed. We only used the information provided by the indexes for understanding lithic measurements themselves, making relational statistics using the biplot chart as exposed in the paper. These relational indexes are formulated as follow:

$$RBEI = L / (W + L) \text{ or } RBEI = X / (Y + X)$$

$$\text{If } (L > W)\ RFI_L = T / (T + L) \text{ or } RFI_L = Z / (X + Z)$$

$$\text{If } (W > L)\ RFI_W = T / (L + T)$$

Finally, we classified the blanks using the geometric data according to the analytic proposal made by Javier Fernández-Eraso (2005), that is assigning complete flacking products (defined later) to the following categories:

1. Flake: Length/Width < 3/2
2. Elongated flake: 3/2 > Length / Width < 2
3. Blade: Length / Width >2

We also measured the weight of each lithic implement using a digital scale with milligram precision.

3.2.5. RAW DATA PROCESSING: STATISTICS

We processed the dataset derived from these analyses with statistical procedures using the softwares IBM SPSS v.21 and the Past v.3 following the statistic proposals made by Barceló (2007) and Fernández (2015). We applied categorical (or nominal) descriptive statistics such as frequency tables and its representation through charts (pie chart and bar chart) to understand basic features and the representation of features of the first three structures. We also apply χ-square test and standardised residues analysis to relate variables in and between the first three structures (based on categorical variables). We used basic descriptive statistics such as mean, median, kurtosis, skewness, and variance to understand typometrical variables (numerical and scale variables). In addition, we used frequency and box-plot charts to graphically represent the variables. We used Kolmogorov-Smirnov normality test to prove if numerical variables are or are not normally distributed. We used biplot chart and 95% confidence ellipse to graphically explore the relationship between the Tarriño's indexes. Finally, and because most of numerical variables are not normally distributed, we used

Kruskal-Wallis test to compare variance between proposed nominal variables. We also used median test to compare means. In addition, we used the Grams per Piece ratio to compare medians between variables. The level of significance in every test here exposed is $\alpha = 0.05$.

CHAPTER-4

MATERIALS & METHODS. A MICROSCOPIC APPROACH TO UNDERSTAND "ARCHAEOLOGICAL QUARTZITE"

4.1. Methodology. Binocular characterisation to understand "archaeological quartzite"

4.1.1. Qualitative characterisation of texture and quartz grain features

4.1.2. Qualitative characterisation of quartz grain size and orientation

4.1.3. Qualitative characterisation of non-quartz minerals

4.2. Methodology. Petrography for understanding quartzite in archaeological and geological contexts

4.2.1. Characterisation of packing, texture and quartz grains features for understanding "archaeological quartzites"

4.2.2. Metric characterisation of size, shape and orientation. Digital Image Processing

4.2.3. Non-quartz mineral characterisation

4.3. Methodology. Geochemical characterisation for understanding "archaeological quartzite": X-Ray Fluorescence

4.4. Methodology. Raw data processing: Statistics

4.1. BINOCULAR CHARACTERISATION TO UNDERSTAND "ARCHAEOLOGICAL QUARTZITE"

In this section we define the non-destructive and high-detailed characterization of the items previously classified as "archaeological quartzites", including both those collected during the geological surveys and the lithic implements from archaeological sites. The total of "archaeological quartzites" analysed is 4982, 4511 from archaeological sites and 471 from geological surveys. We recorded all these feature in the database of sampled stones (for those collected during geological survey) or on the lithic artefacts database.

The petrological characterisation of "archaeological quartzites" is founded on four different standardised approaches, depending on the scale of observation. The first one is based on naked eye observation. The second one, uses two 10x and 20x hand magnifiers and the Dino-Lite digital microscope[1] to the same magnification. The third one, employs 50x magnification provided by the Dino-Lite digital microscope. The fourth one applies 250x magnification with the same tool. Most of the pieces were photographed in a flat position to x50 and x250 magnification to create a library of reference pictures. All these different approaches help us to describe and define the features and properties of "archaeological quartzite". We divided the non-destructive petrological characterization into three different elements. These are: a) qualitative characterisation of texture and quartz grain features, b) quantitative-qualitative characterisation of quartz grain size and orientation, and c) characterisation of non-quartz elements.

4.1.1. QUALITATIVE CHARACTERISATION OF TEXTURE AND QUARTZ GRAIN FEATURES

In this section we describe the features considered to understand and distinguish the different types of "archaeological quartzites" using textural features. These features try to resemble those detected in thin section, offering us links to relate the information coming from destructive and non-destructive methodologies. We created two complementary databases for describing texture and quartz grain features. The first one (Database A) was more complex. It contained many fields to try to understand "archaeological quartzites" employing seven initial criteria. This database was used to define every sample collected during the geological survey, every lithic implements from the sites analysed completely (El Arteu, El Habario and La Covaciella), and a sample of material from the sites of El Esquilleu (346/3004 quartzites) and La Cueva de Coimbre (46/739 quartzites). The second database (Database B) is simpler. It was only used once the properties of "archaeological quartzite" were understood after the analysis of the criteria on the first dataset. This latter dataset offers a faster protocol to record big assemblages of lithic artefacts. Summing up, the seven initial criteria were reduced to two criteria, which are explained under the second epigraph of the following section.

4.1.2.1. CHARACTERISATION OF "ARCHAEOLOGICAL QUARTZITE" BASED ON THE CRITERIA FROM DATASET-A:

We systematised the brightness or luster to naked eye on the surface of the "archaeological quartzites" following criteria:

1. Not bright
2. Low bright
3. Moderate bright
4. High bright

We analysed the definition/recognisability of bedding on the surface of "archaeological quartzite" both to naked eye and using low magnification (20x) according to the following criteria:

1. Absence or absence of evidence of bedding

1 We used Dino-Lite model AD7013MZT with polarised light, employed for eliminating most of the bright. The microscope was handled with the MS35B vertical stand. We used the software Dino-Capture 2.0.

2. Non-clear bedding
3. Clear bedding

Coming to the density of surface micro-cracks/chips on the surface of “archaeological quartzite” to naked eye focus, we defined surface micro-cracks as the lighter and sparkling elements with scale morphology that appear on the surface of “archaeological quartzite” (Figure-4.1). We systematised their presence using the following criteria:

1. Absence of surface micro-cracks on the surface of “archaeological quartzite”.
2. Small presence of surface micro-cracks on the surface of “archaeological quartzite”.
3. Medium presence of surface micro-cracks on the surface of “archaeological quartzite”.
4. High presence of surface micro-cracks on the surface of “archaeological quartzite”.

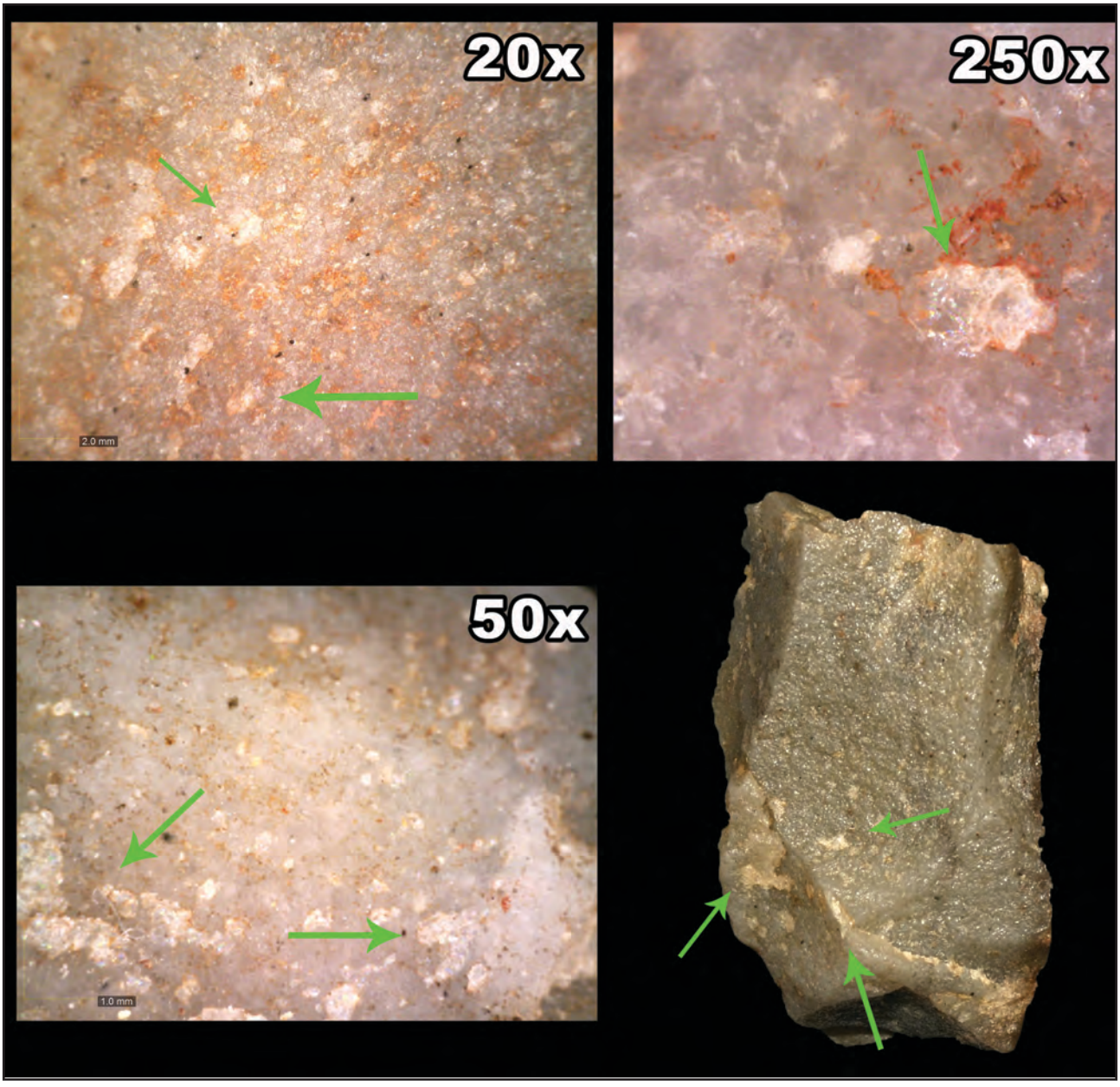

Figure-4.1: Surface micro-cracks on the lithic artefact CoB.K26.37.32. To the naked eye, white, irregular, and lighter superficial areas are identified. To 20x, 50x, and 250x magnification surface micro-cracks are also present and recognisable by similar features. Moderate presence of surface micro-cracks on the “archaeological quartzite” surface.

We distinguished four different types of texture, attending mainly to the superficial relief and the touch of “archaeological quartzites” on flat surfaces following these criteria:

1. Granulated and coarse grained texture forming a very rough surface.
2. Granulated and fine grained texture forming a rough surface.
3. Non-granulate and fine texture.
4. Non-granulate and soapy texture.

We distinguished five different types of packing, defined by similarities with thin section and using the following criteria:

1. **Floating**, if the quartz grains are separated one from each other by cement or matrix. It is easy to recognise *de visu* and at low magnification ranges between 20x and 50x thanks to the presence of saccharoid texture (cement or secondary or tertiary matrix) between the recognised quartz grains, clearly separated one from each other. Between 50x and 250x magnification, it is easy to recognise multiples slopes or three dimensional reliefs, creating numerous steeps and ruffled profiles (Figure-4.2a).

2. **Punctual or isolated**, when the quartz grains are one near another and the contacts between them are restricted to single points. As in the case of the previously commented floating packing type, isolated packing is better recognised de visu and at low magnification ranges between 20x and 50x thanks to the presence of saccharoid texture (cement or secondary or tertiary matrix) between the recognised quartz grains. At ranges between 50x and 250x the grains are closer to each other, but contacts are very small or absent. Steeped, ruffled profiles and three dimensional reliefs are present (Figure-4.2b**).**

3. **Tangential**, in case the grains are joined together, but cement is still present. At low magnification (20-50x) the saccharoid texture decreases and an almost plain relief replaces it. At 50-250x magnification, the saccharoid texture is restricted to a thin layer between the limits of the quartz grains, while the surface of quartz grains is plain with or without the presence of some small points derived from secondary matrix or cement (Figure-4.3a).

4. **Complete**, where there is a very small content of cement or matrix and the grains create an almost complete structure. Matrix or cement is almost absent, limited to small accumulations or small confined areas between grains. The former was observed at low magnification (20-50x) and the latter at high magnification (50-250x). Grains are recognised at 50-250x magnification. They are delimited by very weak, fine, and straight contours. The relief is flat or the result of the overlapping of several flat planes by zones (Figure-4.3b).

5. **Suturated**, when the limits between grains generate a complete and deformed structure (Figure-4.3-a). Matrix or cement is restricted to small points on quartz limits, like in the previously commented packing types. At low magnification (20-50x), the relief is flat or the result of successive and overlapping flat planes, sometimes covered by a thin and bright layer. At high magnification (50-250x) there are almost no quartz limits, which are reduced to very thin and weakly ruffled contours (Figure-4.4a).

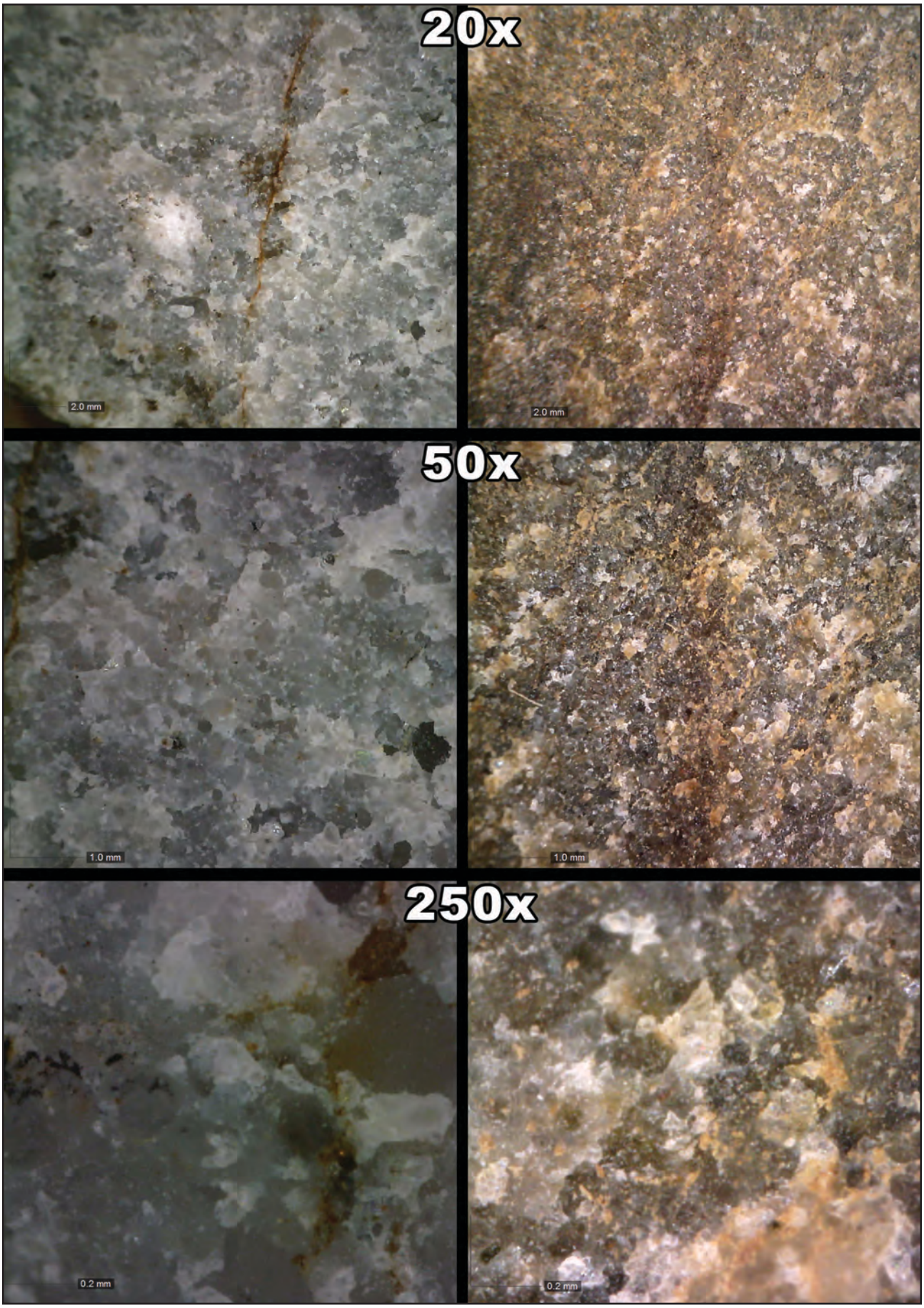

Figure-4.2: Microphotograph of the surface of two “archaeological quartzites” to 20x, 50x, and 250x magnification. On the left side (A), sample DC22_04 exhibits floating packing. On the right side (B), sample DC26_02 shows punctual or isolated packing criteria.

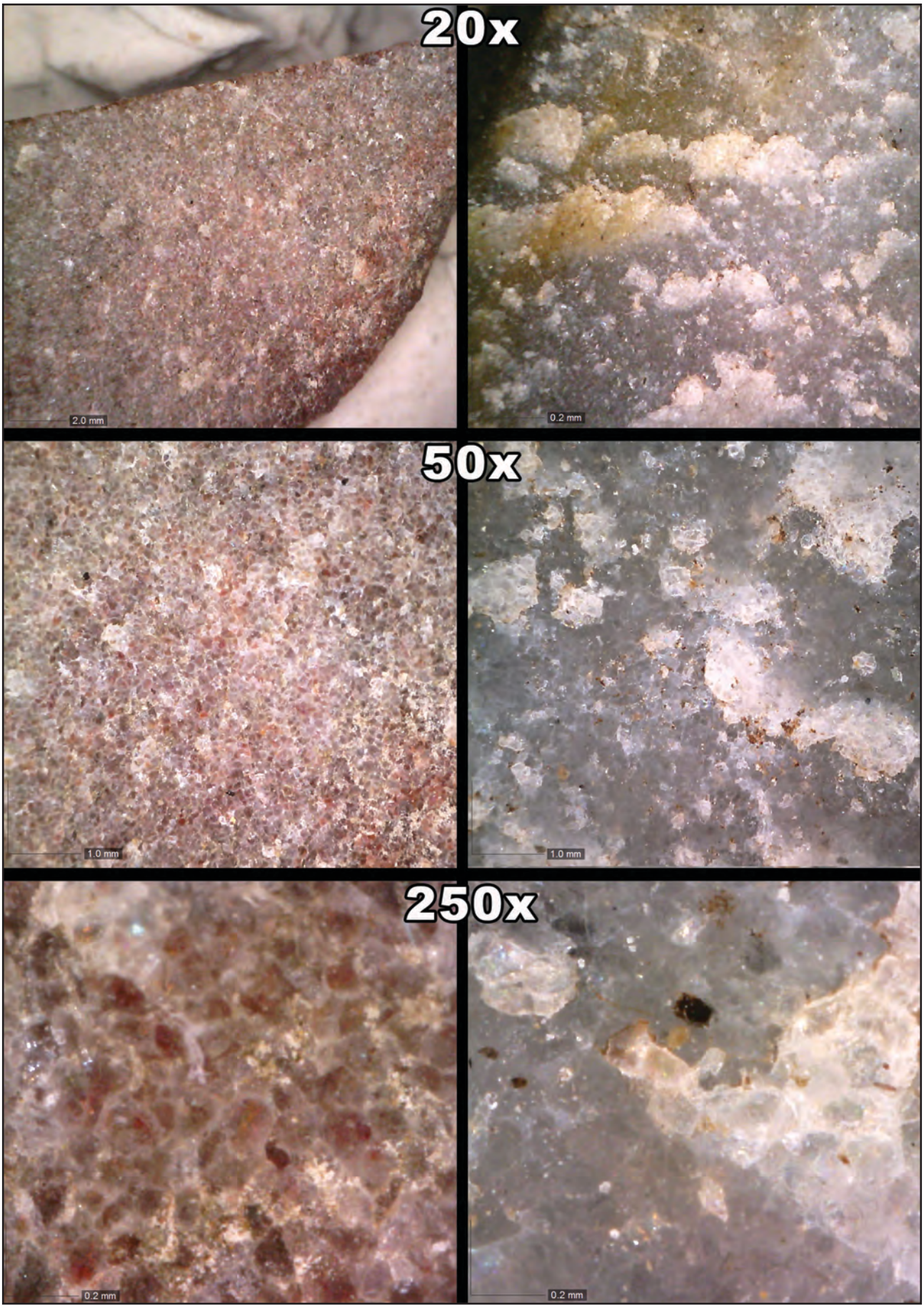

Figure-4.3: Microphotograph of the surface of two “archaeological quartzites” to 20x, 50x, and 250x magnification. On the left side (A), sample ATS-151 exhibits floating packing. On the right side (B), sample ATS-007 shows punctual or isolated packing criteria.

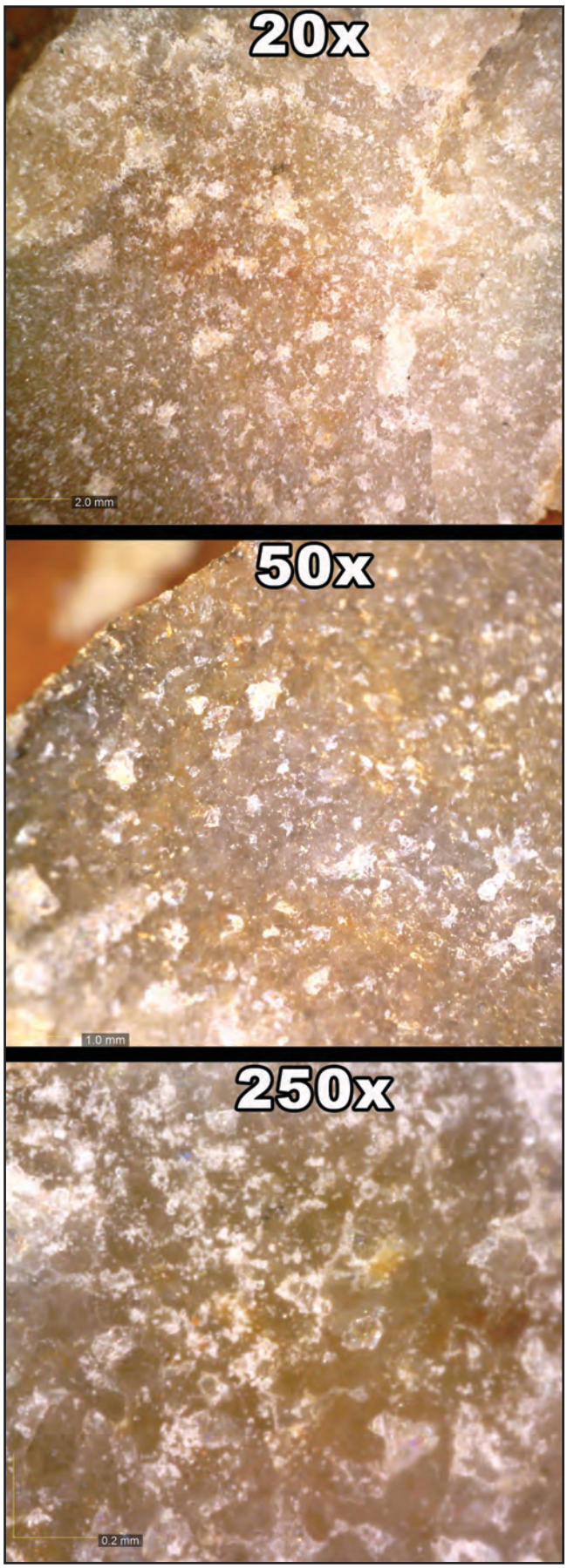

Figure-4.4: Microphotograph of the surface of sample DC74_02 showing suturated packing criteria to 20x, 50x, and 250x magnification.

Quartz grain definition/recognisability was defined using the following criteria:

1. Very easy, in case at least 25 quartz grains were recognisable to 250x magnification screen (approximately 1.6 x 1.3 mm).

2. Easy, in case between 15 and 25 quartz grains were recognisable to 250x magnification.

3. Difficult, in case between 5-15 quartz grains were recognisable to 250x magnification.

4. Impossible, in case less than 5 quartz grains were recognisable to 250x magnification.

We determined quartz grain morphology applying morphological features of the border of the quartz grains that could be matched with the characteristics of quartz grains in thin-section. After the description in depth, we reduced the variability of each “archaeological quartzite” to the two prevailing categories. These were:

1. Quartz grains with plain and angular limits (Figure-4.5a).

2. Quartz grains with plain and rounded limits (Figure-4.5b).

3. Quartz grains with ruffled and irregular limits generated by the affection of matrix or cement (Figure-4.5c).

4. Quartz grains with appearance of regrowth of quartz syntaxial cement, recognisable by the partial or complete dual grain outline that creates a lighter, glossy and curved space between both lines. This feature is associated to the complete packing type and quartz grains with rounded limits that generate concavo-convex lines between grains (Figure-4.5d).

5. Quartz grains with ruffled, irregular and thin limits and surfaces with flat relief. This feature is clearly related to the saturated packing type (Figure-4.5e).

6. Quartz grains with no boundaries detected, where the limits are reduced to small alignments of specks or small saturated lines (Figure-4.5f).

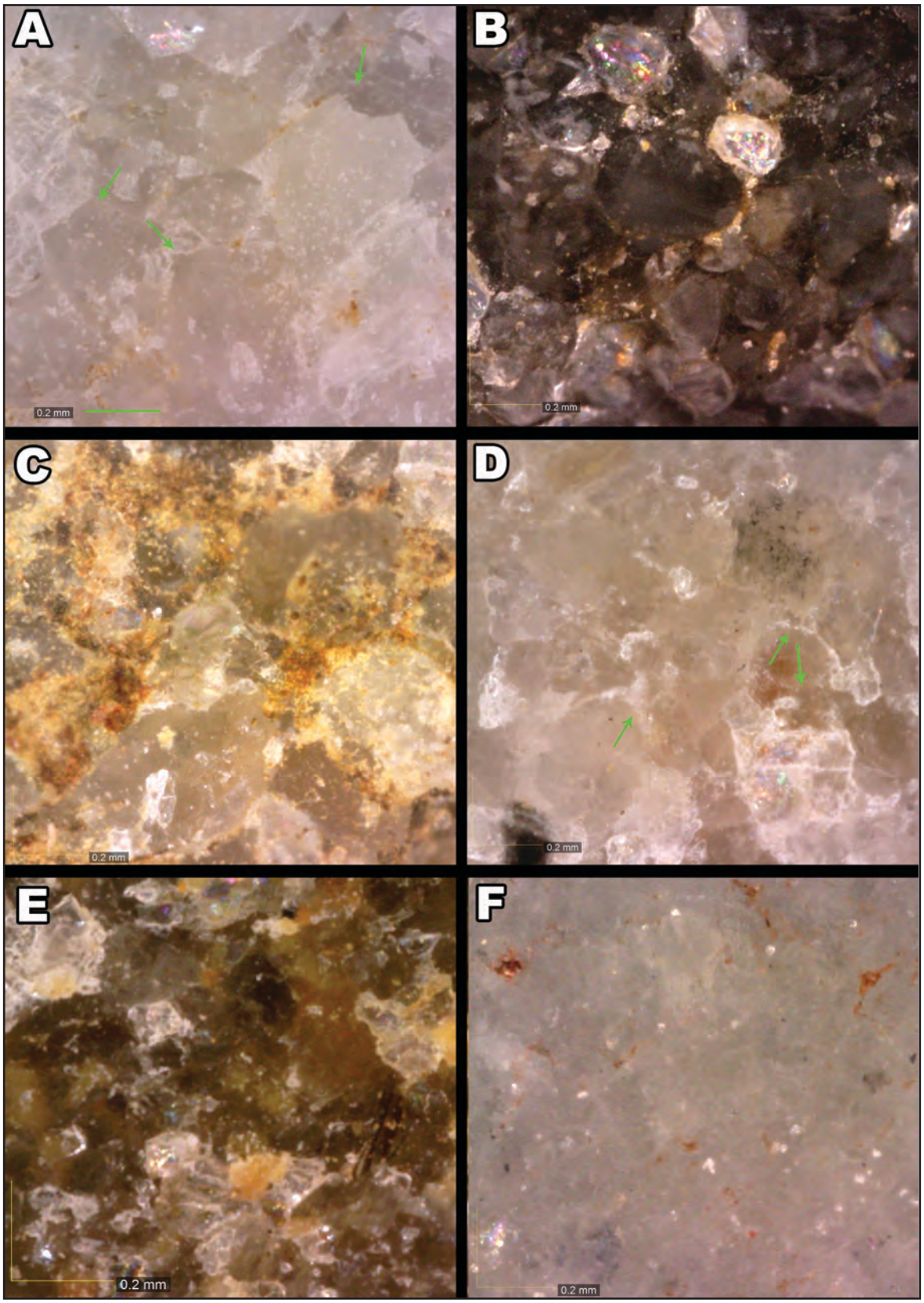

Figure-4.5: Microphotograph of the surface of some “archaeological quartzites” to 250x magnification. The main quartz grain features are: A) Quartz grains with plain and angular limits (arrows on clear angular outlines of the quartz grains), from sample DC20_07. B) Quartz grains with plain and rounded limits, from sample DC46_10. C) Quartz grains with ruffled and irregular limits generated by the affection of matrix or cement, from sample GU01_10. D) Appearance of regrowth of quartz syntaxial cement (arrow on quartz syntaxial cement in the direction of its expansion), from sample GU01_06. E) Quartz grains with ruffled, irregular and thin limits on flat relief surface, from sample DC57_02. F) Quartz grains with no apparent boundaries detected, reduced to small alignments of specks or small saturated lines, from sample CoB. J27.38.294.

4.1.1.2. DEFINITION OF "ARCHAEOLOGICAL QUARTZITE" BASED ON THE CRITERIA OF DATASET-B:

We created the category Texture and Packing (T&P) to simplify and combine the previously texture and packing categories from database A, together with some other features from other criteria. The new T&P category simplified the criteria previously defined in the following groups:

1. **Saccharoid T&P** is defined by the generalised presence of matrix or cement on the surface of the samples. The touch is granular and sandy it is usually heterogeneously coloured to the naked eye. At low magnification (20x) slopes and rough relief are appreciated. At middle magnification (50x) it is possible to observe the presence of isolated to tangential quartz grains surrounded by high amounts of secondary matrix and cement, creating a rough relief. Some quartz grains can sparkle, but brightness or luster is not homogenously distributed. At 250x magnification the quartz grains tend to be isolated and again surrounded by matrix, generally as the sum of small specks that cover the surface of quartz and other mineral grains too (Figure-4.6a).

2. **Granular T&P** is defined by the presence of a granular texture and a tangential to complete packing on the surface of the sample. The quantity of matrix or cement is reduced and its presence is restricted to small areas or the surroundings of the edges of the grain. The touch is granular and coarse and when observed to the naked eye it generally shows heterogeneous colour distribution. At low magnification (20x) softly rough to flat relief is appreciated. At middle magnification (50x) it is possible to recognise quartz grains creating an almost complete or complete packing. Some quartz grains can sparkle, but brightness is not homogenous. At high magnification (250x) the grains of the "archaeological quartzite" are recognisable and create an almost complete to complete packing. Small quantities of cement or matrix (mainly composed by the sum of small specks) fill the small empty areas between quartz grains (Figure-4.6b).

3. **Compact and grainy T&P** is defined by the presence of a very soft granulated texture and complete packing on the surface of the sample. There is no presence of matrix or cement. The touch is still granular although much softer. To the naked eye, the colour is more homogeneous and micro-cracks are recognisable. At low magnification (20x) the relief is softer than on previous T&P and some of the stones shows successive planes of squamous surfaces. At middle magnification (50x) most of the grains are recognisable, although some parts of them are usually negligible. Lighter grains are recognisable, showing lighter and curved outline. The grains create a clear complete packing. At 250x magnification grains are recognisable, especially those with thicker, brighter and curved outlines. Other grains or parts of the outlines are vague or diffused. The previously commented lighter grains are visible (Figure-4.7a).

4. **Fine and grainy T&P** is defined by a fine texture, clearly complete to suturated packing and moderate bright. In general, grains are difficult to observe completely. The touch is fine, with small rough areas, mainly generated by the precipitation of ferruginous, siliceous or carbonated cement or by the presence of joints. To the naked eye colour is relatively homogeneous, except on micro-cracks, generally brighter. At low magnification (20x) the relief is soft without roughness, although some surfaces of the "archaeological quartzites" show squamous surfaces. At middle magnifications (50x) no grains or almost no grains are recognisable and there seems to exist a thin and bright luster covering the surface of the stone. At 250x magnification grains are almost unrecognisable. Only some outlines can be appreciated, creating a suturated packing. Small specks are visible on the outlines of the quartz grains and on the middle part of the grains, but they seem to be on the same level than the rest of the surface, covered by the previously mentioned thin and bright luster (Figure-4.7b).

5. **Fine T&P** is defined by a really fine texture and suturated packing. In general, grains cannot be observed. Only some small relicts from the outlines are observable. The touch is very fine and, as in previous T&P, some areas can be rougher due to cement precipitations. To the naked eye colour is homogenous and shows a high bright. Micro-cracks are much more limited than in previous T&P, although they are present. At low magnification (20x) the relief is very soft and no rugosity is observed, neither the high quantity of squamous surfaces, reduced to very small areas. At middle magnification (50x) no grains are recognisable and only small specks are visible. Thin and bright luster is observed and it

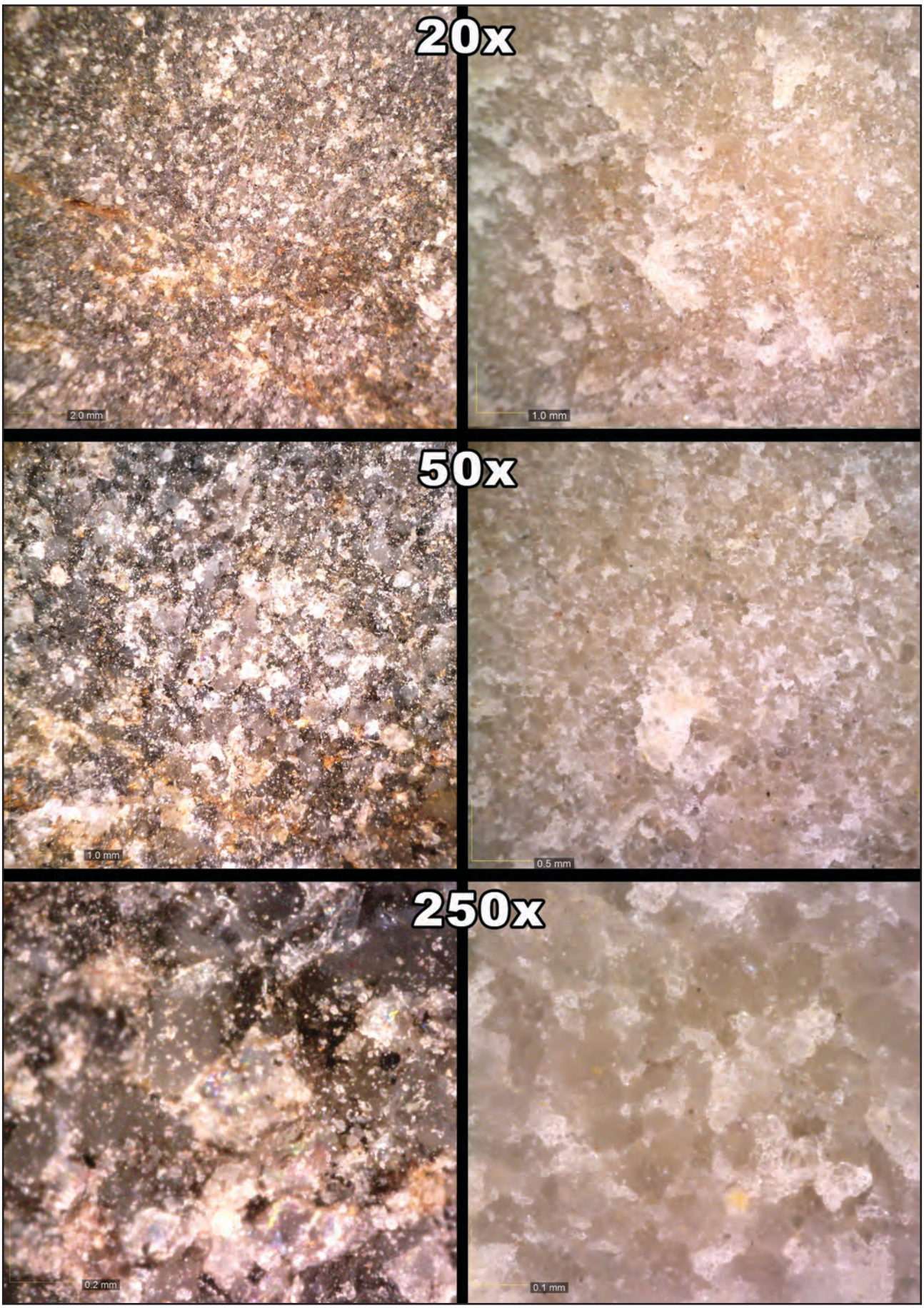

Figure-4.6: Microphotograph of the surface of two “archaeological quartzites” to 20x, 50x and 250x magnification. On the left side, sample DC87_05 shows saccharoid T&P criteria. On the right side, sample DC43_06 exhibits granular T&P criteria.

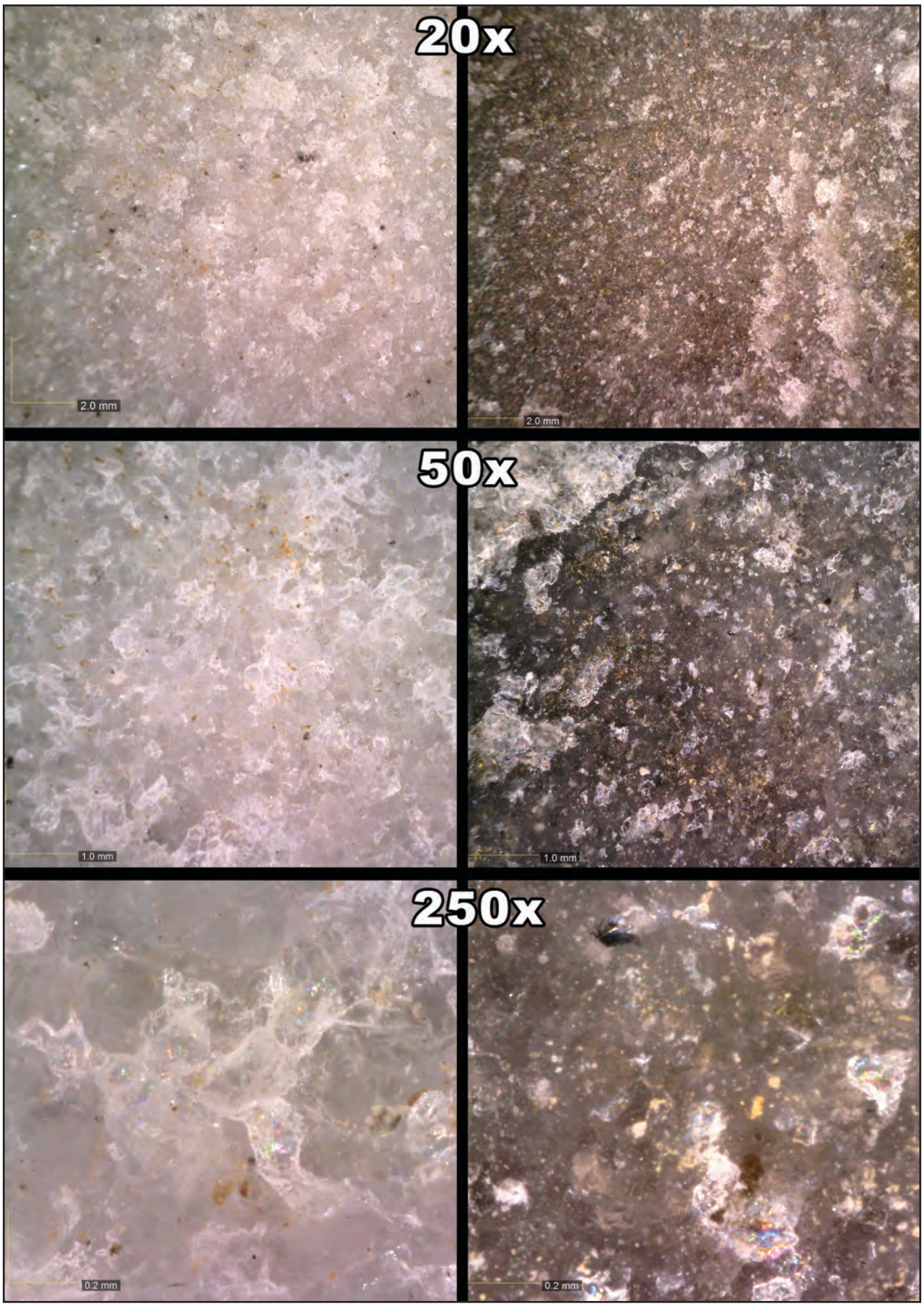

Figure-4.7: Microphotograph of the surface of two “archaeological quartzites” to 20x, 50x and 250x magnification. On the left side, sample DC51_01 exhibits compact and grainy T&P criteria. On the right side, sample DC74_03 shows fine and grainy T&P.

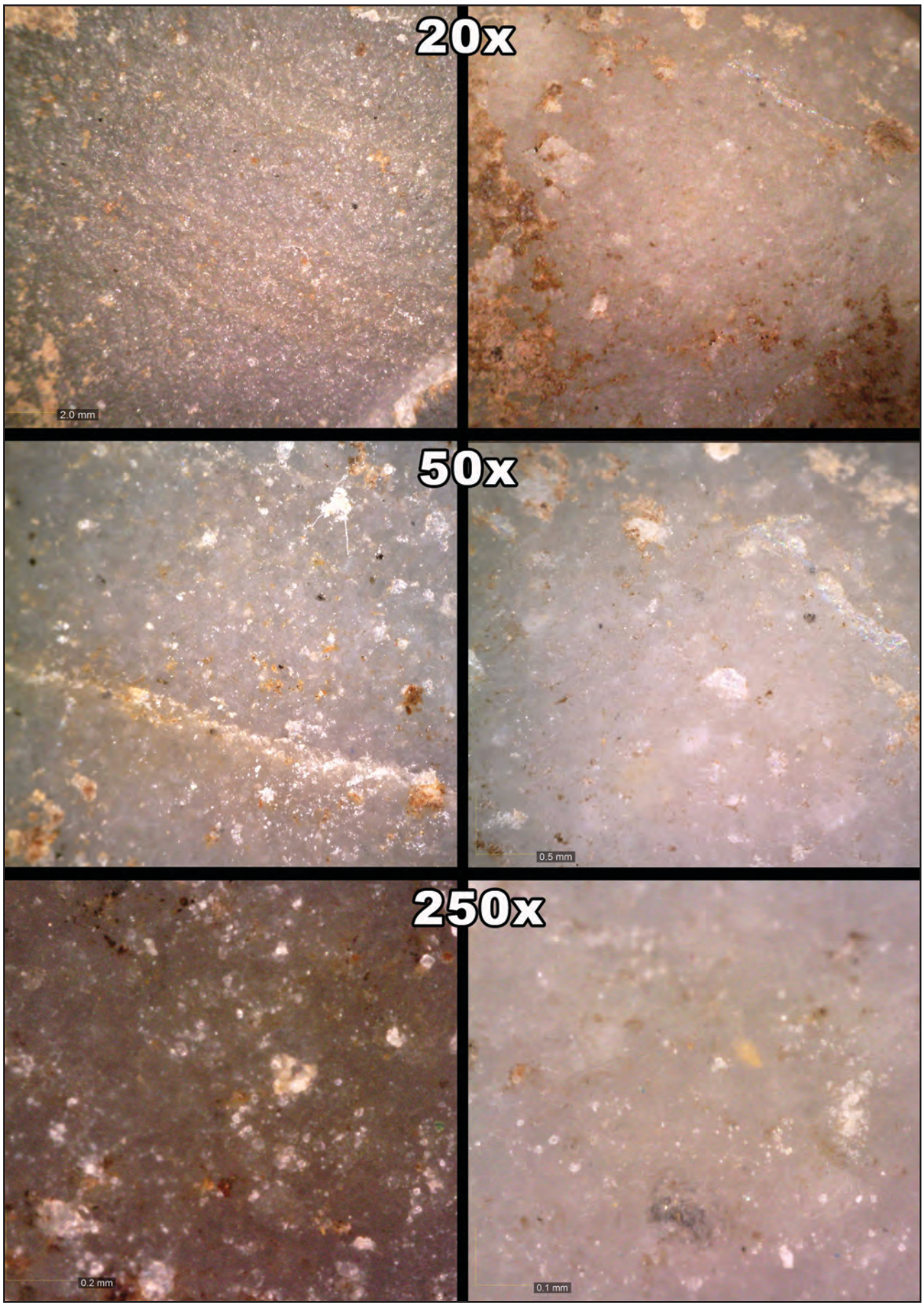

Figure-4.8: Microphotograph of the surface of two “archaeological quartzites” to 20x, 50x and 250x magnification. On the left side, sample ES-441 (Nvl-XIII) exhibits fine T&P criteria. On the right side, sample ES-411 (Nvl-XIII) shows soapy T&P.

clearly covers the entire surface of the “archaeological quartzites”. At high magnification (250x) no grain is observed. Only small specks or associations of them are recognised on the surface, reduced to small areas (Figure-4.8).

6. **Soapy T&P** is quite similar to the preceding T&P. The texture is very fine or soapy and no grain is observed. The touch is soapy, even smoother than in the previous phase. To the naked eye colour is really homogenous, highly bright and, as in previous T&P, micro-cracks are limited. At low magnification the relief is plain and soft and there is almost no plain squamous surface. At middle magnifications (50x) no grain is recognisable, neither the small specks appreciated on the preceding T&P. Previous thin and bright luster is extended onto the entire surface of the “archaeological quartzites”. At high magnifications (250x) only some grains are recognisable, not by the outlines but by a small, thin and almost no recognisable swelling. Almost no small specks are appreciated (Figure-4.9).

Finally, with the aim to understand possible modifications of the T&P criteria defined above, we introduced some small modifications into the definition of the morphology of quartz grains from database A. The result are the following five categories:

1. Quartz grains with plain and angular limits (Figure-4.5a).
2. Quartz grains with plain and rounded limits (Figure-4.5b).
3. Quartz grains with ruffled and irregular limits (Figure-4.5c and Figure-4.5d).
4. Quartz grains with concavo-convex and rounded limits (Figure-4.5c).
5. Quartz grains with no boundaries detected (Figure-4.5e).

4.1.2. QUALITATIVE CHARACTERISATION OF QUARTZ GRAIN SIZE AND ORIENTATION

In this section we describe the features considered to understand and distinguish different types of “archaeological quartzites” according to quartz grain size. This category tries to understand features similar to those analysed on thin section, offering us links to relate the information from destructive and non-destructive methodologies. At the beginning, we decided to use same protocol as the one used for studying quartz grain size, shape and orientation (explained later) on thin section using images obtained with the Dino-Lite digital microscope at 50x and 250x magnification. The application of this protocol of analysis systematically generated very interesting information, but the time required for its application to every single stone item was excessive. In addition, as revealed previously by quartz grain size and textural characterisation, not every quartz grain shape is complete, generating an obvious bias for those samples with a small amount of recognisable grains. Finally, small grains that could be observed at high magnification are generally not recognisable through binocular pictures. For all these reason, the methodology proposed for understanding quartz grain size is based on qualitative description. This allows us to analysed high amounts of material using only two criteria that systematise grain size properties of “archaeological quartzites”:

On one side, we determined grain size using 50x or 250x magnification, obtaining the approximate measurement of the secondary axis of the particles. In general, the measurements were made by comparison with the scale provided by the software Dino-Capture 2.0. If necessary, we used the measurement mode also available in the program. In case the sample was not homogenous, the biggest grain determined the size of the analysed “archaeological quartzite”. We used the following three categories, based on the Udden-Wentworth scale and modified for their application to “archaeological quartzite” quartz grains, to standardize the recording of the quartzite grain sizes:

1. The category **coarse quartz grain size** is used for “archaeological quartzite” containing quartz grains bigger than fine sand. Quartz grain > ±0.25 mm.
2. The category **medium quartz grain size** is used for “archaeological quartzite” containing quartz grains between coarse silt and fine sand, both categories included. 0.031 > Quartz grain < ±0.25 mm.
3. The category **fine quartz grain size** is used for “archaeological quartzite” containing quartz grains smaller than coarse silt. Quartz grain < 0.062 mm.

On the other side, we completed the qualitative analysis of quartz grain size describing the quartz grain size sorting using the following criteria:

1. **Homogenous** quartz grain size distribution
2. **Bimodal** distribution
3. **Heterogeneous** quartz grain size distribution

Finally, we analysed each “archaeological quartzite” using the criterion foliation. It is used to determine the presence or absence of foliation or schistosity affecting at least one surface of the sample. A sample is defined as foliated when its grains are clearly deformed by pressure, creating elongated and deformed grain shapes that clearly distinguish it from the bedding textural categories previously presented (Figure-4.9). This feature is commonly seen in hand specimens.

4.1.3. QUALITATIVE CHARACTERISATION OF NON-QUARTZ MINERAL

In addition to quartz, “archaeological quartzites” contain other minerals in very small proportions. Up to three minerals were identified for each sample and the minerals considered were restricted in order to make comparison between different samples possible. The minerals considered are:

1. Feldspars (Figure-4.10f)
2. White mica (Figure-4.10e)
3. Pyrite (Figure-4.10d)
4. Undetermined black/heavy mineral (Figure-4.10c)

Primary minerals

5. Manganese oxides (Figure-4.10b)
6. Fe-oxides (Figure-4.10a)

Mineral alteration

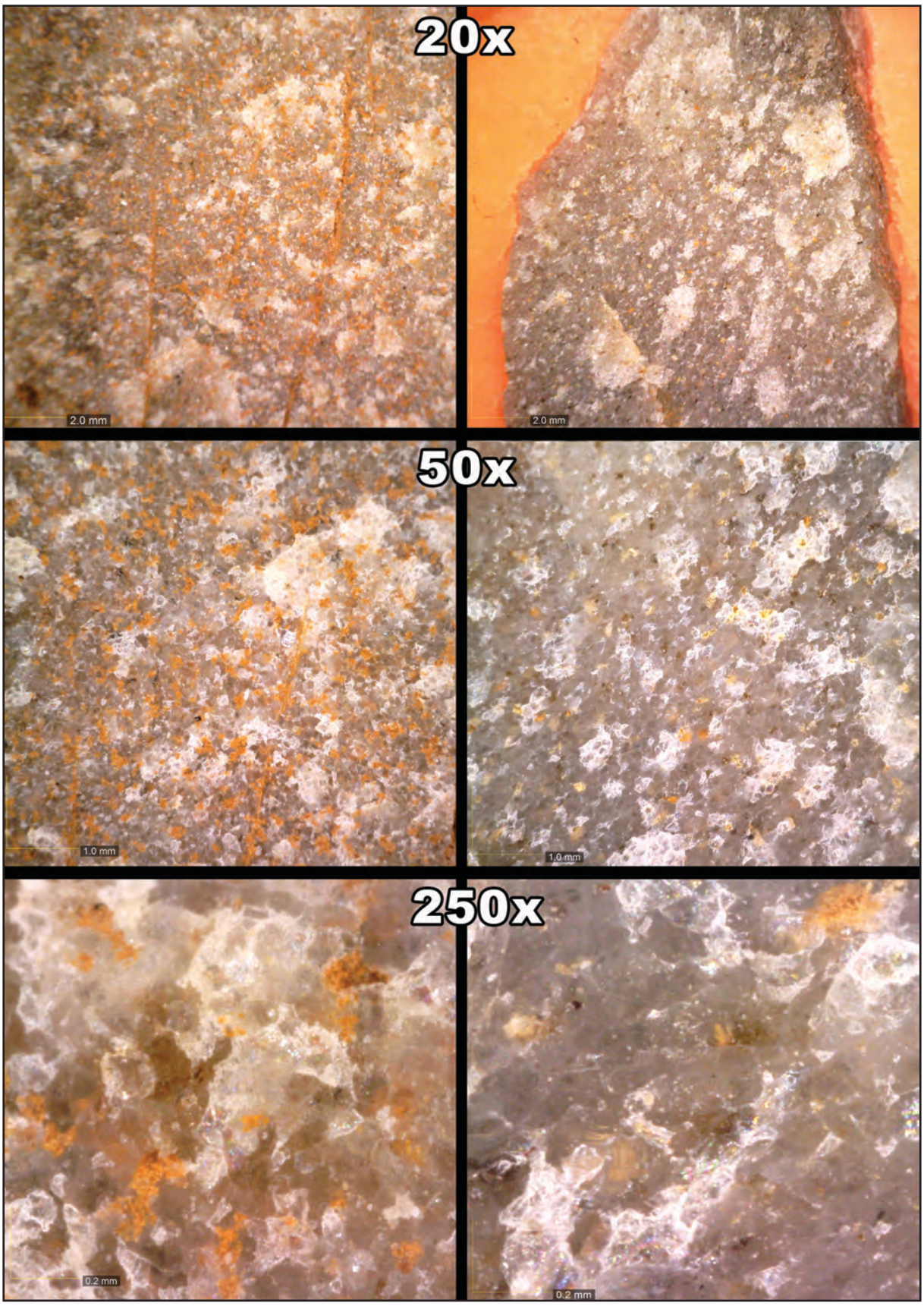

Figure-4.9: Microphotograph of the surface of two “archaeological quartzites” to 20x, 50x and 250x magnification. On the left side, sample DC62_01 exhibits clear bedding of the surface. On the right side, sample DC87_01 shows clear foliation or schistosity. It is easy to distinguish schistosity from bedding thanks to the modification of quartz grain in the former, while on the latter no modification of quartz grain is observable (both observations to 250x magnification). On low magnification, the differences are more subtle, but they could be detected by generally differently coloured layers in the bedding and the absence of colour differences in the schistosity.

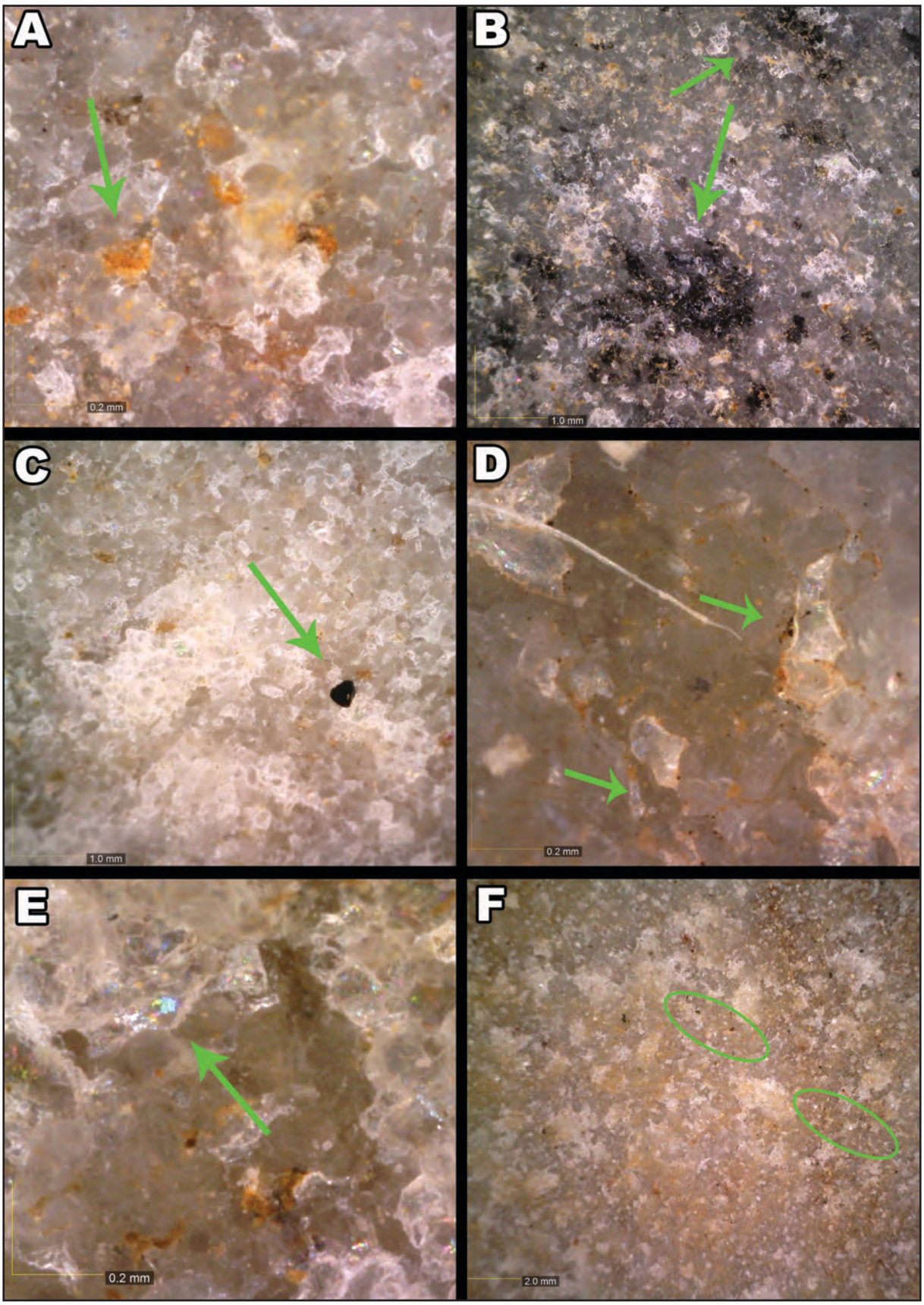

Figure-4.10: Microphotograph of the surface of six “archaeological quartzites”. A) DC89_06 to 250x magnification shows orange and irregular iron oxides. B) DC45_05 to 50x magnification shows black and irregular manganese oxides. C) DC86_04 to 250x magnification shows a big, black, plain and rounded undetermined heavy mineral. D) Co.K26.37.146 to 250x magnification shows very small, black, plain, and angular pyrites. There are iron oxides around the pyrites. E) DC48_01 to 250x magnification shows an elongated, bright, translucent, purple and white mica. F) DC45_06 to 20x magnification shows some small, white and bright feldspars with changeable structures.

4.2. PETROGRAPHY FOR UNDERSTANDING QUARTZITE IN ARCHAEOLOGICAL AND GEOLOGICAL CONTEXTS

The thin sections we studied in this research project came from samples obtained on the geological surveys and from the archaeological sites analysed. The total number of samples obtained from geological surveys is 57 of which, 3 derived from quartzite outcrops, 47 from conglomerates, five from river beaches, and two from offsets or flank deposits. The number of samples we analysed from archaeological sites is 59 of which, twelve came from El Arteu, five from El Habario, 21 from El Esquilleu, eleven from Coimbre, and ten from Troisdorf, Germany (two of the samples from the later site have two different zones, and another two samples have three different zones. Each one of these zones was considered a different sample or unit of analysis). All in all, the total of samples generated is 116, although there are 122 units analysed. The selection of the samples for petrographic thin section preparation, took into account the lithological variability of each piece based on the features obtained through non-destructive characterisation explained in the previous section performed using both the naked eye and a binocular microscope at up to 250x magnification.

Petrological characterisation can refer to diverse features and characteristics of the rock, result of their genesis, and transformations (metamorphic), including sometimes physical, chemical and biological alteration processes in sub-aerial conditions (weathering). The characterisation of these processes can be approached through different types of studies: field relationships, petrographic analyses and geochemical study (Castro, 1989). Here we present the methodological approach applied for understanding quartzite through petrography of thin sections. We divided the petrographic characterization into three categories. These are: a) qualitative characterization of texture and quartz grain features, b) quantitative characterisation of quartz grain size, morphology and orientation, and c) characterisation of non-quartz elements.

All thin sections were prepared at the Laboratory of Sample Preparation of the Department of Mineralogy and Petrology of the University of the Basque Country (UPV/EHU, Spain). Some small lithic artefacts were embedded in proxy resins to properly prepare the sections.

4.2.1. CHARACTERISATION OF PACKING, TEXTURE AND QUARTZ GRAINS FEATURES FOR UNDERSTANDING "ARCHAEOLOGICAL QUARTIZTES"

We distinguished three different types of textures which combine sedimentary and metamorphic features, according to Castro (1989):

1. **Clastic texture with matrix or cement**: Clastic grained texture with the presence of cement or matrix, differentiated from main clastic texture by composition or quartz grain size (Figure-4.11a).
2. **Clastic grained texture**: Clastic completely or almost without matrix or cement (Figure-4.11b).
3. **Mortar texture**: Partially preserved clastic depositional texture with fine, strain-free crystals along grain boundaries caused by metamorphic recrystallization (Figure-4.11c).

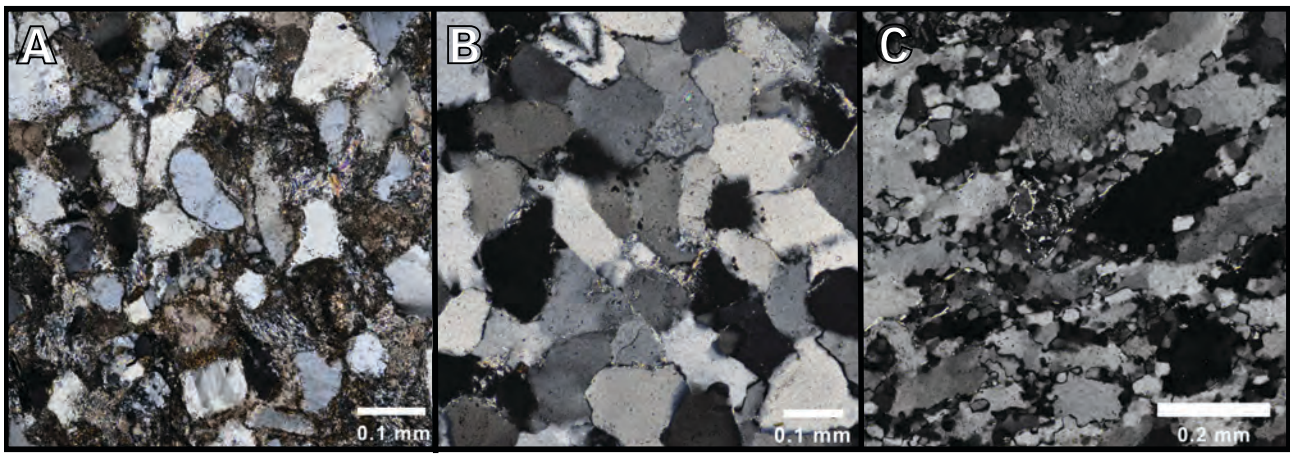

Figure-4.11: Micrographs showing types of textures in quartzites. A: Clastic texture with cement or matrix from sample DC05_02. B: Clastic grained texture from sample ATS-007. C: Mortar texture from sample ATS-195.

We distinguished five different types of packing on archaeological quartzite:

1. **Floating**, if the quartz grains are separated one from another by cement or matrix (Figure-4.12a).
2. **Punctual or isolated**, when the quartz grains are one near another and the contacts between grains are restricted to single points (Figure-4.12b).
3. **Tangential**, in the case where the grains are together, but cement is still present (Figure-4.12c).
4. **Complete**, where there is a very small content of cement or matrix and the grains create a complete or almost complete structure. Matrix or cement is almost absent (Figure-4.12d.
5. **Suturated**, when limits between grains generate a complete and deformed structure (Figure-4.12e).

The quartz grains were characterised applying the criteria proposed by several authors seeking to determine the petrogenesis of quartzite (Bastida, 1982; Folk, 1980; Hirth et al., 2001; Hirth and Tullis, 1989; Howard, 2000, 2005; Stipp et al., 2002a, b; Wilson, 1973). We observed and studied the following diagnostic quartz grain features:

1. **Detrital quartz grains**: Crystal extinguishes as a single unit upon slight rotation of microscope stage (Figure-4.12f).
2. **Grains with concave-convex boundaries**: Interpenetrating grain boundary caused by pressure solution (Figure-4.13b).
3. **Undulose extinction on thin section quartzite**: Crystal extinguishes in irregular sweeping sections as microscope stage rotates several degrees (Figure-4.13c)
4. **Regrowth of quartz syntaxial cement**: Quartz cement added with the same crystallographic orientation as the host crystal (Figure-4.13a)
5. **Stylolites or serrated boundaries**: Irregular, interlocking boundary between two grains, caused by pressure solution (Figure-4.13d).
6. **Böhm/deformation lamellae**: Closely spaced, subparallel band of lighter and darker extinction that terminates at the boundaries of a host crystal (Figure-4.13f)
7. **Presence of recrystallised grains**: Fine, strain-free crystals, mainly along grain boundaries caused by metamorphic recrystallization (Figure-4.13e).

We quantified these textural criteria as:

1. **Very abundant**, when the grain type is over 50% of the total sample.
2. **Major**, with a presence between 5 and 50% of the sample
3. **Minor (or trace)**, if it affects less than 5% of the studied quartz grains.

However, it is common to find grains with several of these characteristics. These criteria enable the assignation of characteristics to determine the type and possible origin of the selected quartzites samples.

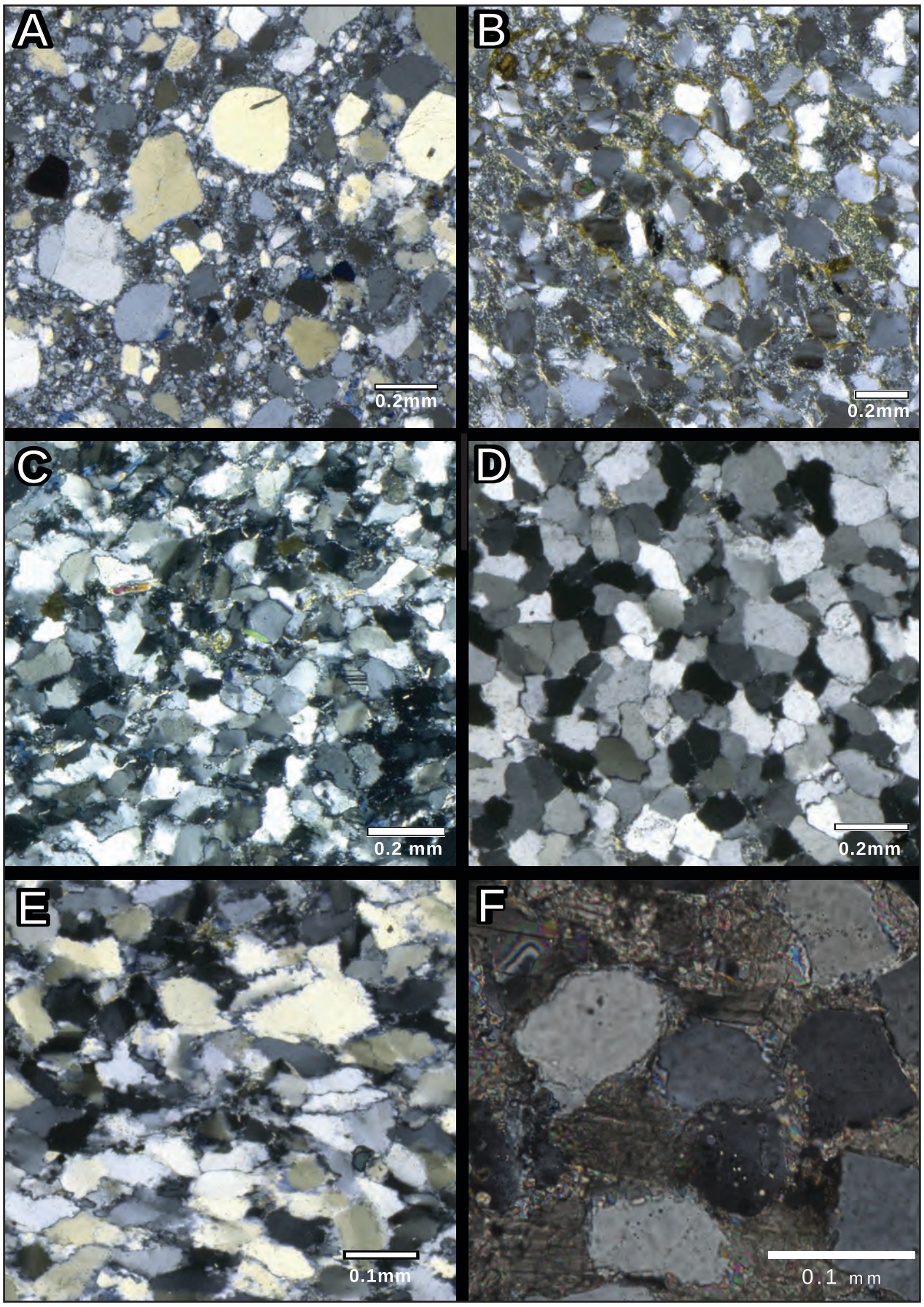

Figure-4.12: Micrographs showing types of packing and grain features in quartzite. A: Floating packing, from sample DC22_04. B: Punctual or isolated packing, from sample DC26_02. C: Tangential packing, from sample ATS-002. D: Complete packing, from sample ATS-007. E: Suturated packing, from sample DC06_05. F. Detrital quartz grains corresponding with the first quartz grain features, from sample DC24_03.

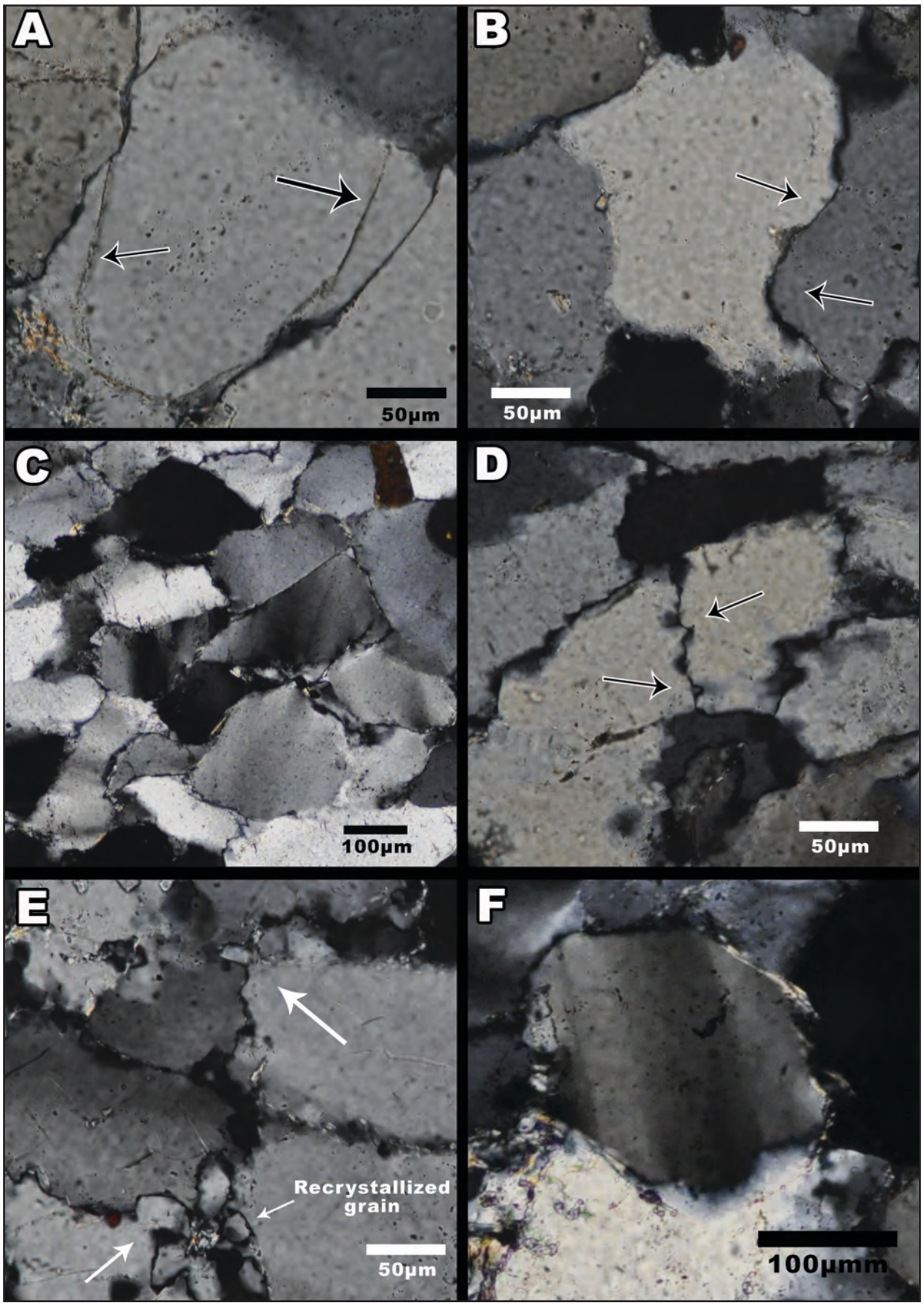

Figure-4.13: Micrographs showing grain features in quartzite: A. Regrowth of quartz syntaxial cement, from sample ATS-023. B: Grains with concave-convex boundaries, from sample ATS-007. C: Undulose extinction of quartzite in thin section quartzite, from sample ATS-310, D: Stylolites or serrated grains boundaries, from sample DC06_05. E: Recrystallised quartz grain, from sample ATS-016. F: Böhm lamellae, from sample ES-435 (Nvl-XIII).

4.2.2. METRIC CHARACTERISATION OF SIZE, SHAPE AND ORIENTATION. DIGITAL IMAGE PROCESSING

Determining the size, shape and arrangement of the quartz grains that constitute most of the sample is another of the objectives of this study, especially considering the importance given to this issue to previous attempts of archaeological quartzite classification (Cuartero et al., 2015; Manzano, 2001; Manzano et al., 2005; Sarabia, 1999). We photographed representative sectors of the thin sections at a high resolution and 200x magnification with a Keyence VH-Z20R/VH-Z20W 3D Scanning optical microscope and a VHX-200E camera at the Department of Geography of the University of Cologne (Germany) and the camera Nikon D90 and a Nikon Eclipse LV100N POL microscope at the Department of Mineralogy and Petrology of the University of the Basque Country. Then, we manually draw the outline of the quartz grains of each thin section, using a graphic tablet. We are aware that it would be possible automatize the drawing process, but after several attempts, the precision of the data obtained was considered not good enough for our analyses (Chang and Chung, 2012; Chung and Chang, 2013; Heilbronner and Tullis, 2006). The next step was the application of the Analyse Particles tool of the freeware ImageJ 1.49p (Rasband, 1997-2016; Schneider et al., 2012), after having carried out the colour contrasts (using the following macro) and having added the scale information. This tool has enabled the data of each of the grains drawn to be obtained simultaneous and automatically (Figure-4.14).

```
run(“8-bit”);

setAutoThreshold(“Default”);

//run(“Threshold...”);

//setThreshold(129, 255);

setOption(“BlackBackground”, false);

run(“Convert to Mask”);

run(“Invert”);

floodFill(3867, 16);

run(“Analyze Particles...”, “size=0.00001-Infinity show=Outlines display exclude clear summarize”);
```

The parameter chosen to quantify grain size is the secondary axis of the particle, termed minor by the software and it is reported in millimetres. This measurement corresponds to the secondary diameter used to determine particle size and systematise them with the Udden-Wentworth scale (Wentworth, 1922) and it allows us to assign the measurements to closed categories.

To quantify the shapes, we used the parameters circularity and roundness, expressed by the software with the followings equations:

$$\text{Circularity} = 4\pi\,[\text{area}]/[\text{perimeter}]^2$$

$$\text{Roundess} = 4\,[\text{Area}]/\pi[\text{Major axis}]^2$$

The first one informs about the degree of irregularity of each particle, whereas the second refers to its elongation, as the relationship between the major and the minor axis. Both are expressed as a coefficient from 0 to 1. More spherical and regular shapes will have a coefficient closer to 1 and more elongated and irregular shapes will have coefficients closer to 0.

The orientation of the particles was quantified with the parameter Angle, which refers to the difference in degrees between the main axis of each particle and the horizontal axis of the photograph. The data were later filtered and only the particles with roundness indexes <0.75 were maintained. This process extracted the particles capable of being oriented in a preferential direction. The data of the orientation of each sample were treated individually. To do this, samples were classified as possessing a preferential orientation if Rayleigh’s R test gave significant values (Davis, 1986; Mardia, 1975).

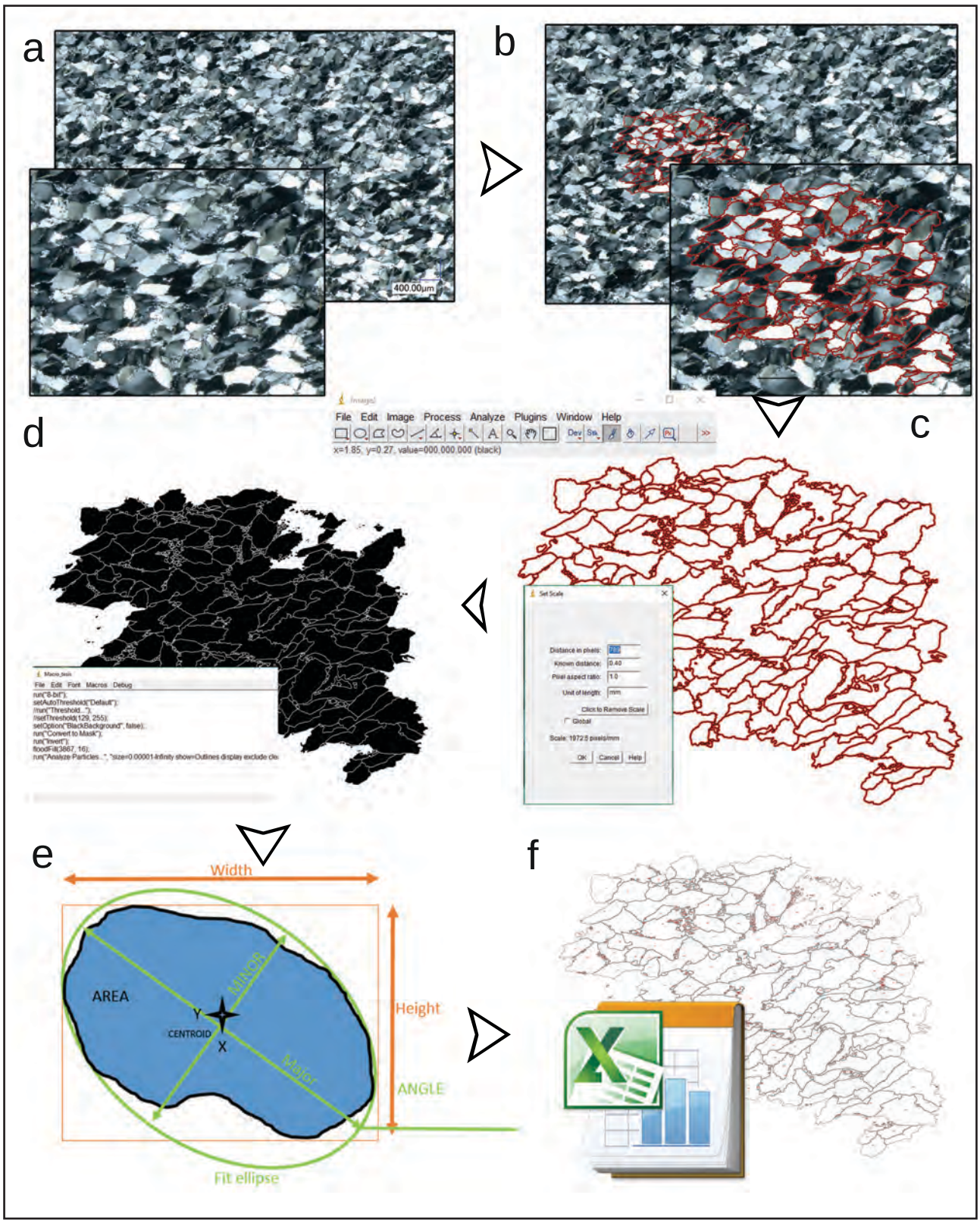

Figure-4.14: Schematic representation of the processing of quartz grains for obtaining numerical values. A: Original picture of thin section with cross polarised light, from sample HA-5847. In detail, a representative area selected for drawing. B: Drawing of the quartz grains from the area selected. C. The process of drawing of the quartz grains and scale application. D: The drawing after the application of the macro for obtaining a binary image. E: Representation of the measurement of one of the quartz grains. The minor (axis) and the angle for the orientation are the selected measurements for the quantification of the grain size. The parameters fit ellipse, major axis, area or perimeter are used for shape description after the application of the formulas proposed. F: Files resulting of the process of analysis of particles: drawing of the grains analysed numbered by the software and Excel sheet with the measurements of the analysed grains (in this case 664 grains analysed).

4.2.3. NON-QUARTZ MINERALOGICAL CHARACTERISATION

Mineral identification of single crystals in thin sections was performed following the criteria described by Adams et al. (1988), Perkins and Henke (2002) and Yardley et al. (1990). In addition to quartz, other minerals are found in quartzite in very small proportions. These were identified according to their optical properties, e.g. phyllosilicates (muscovite, chlorite, biotite, clay minerals) and others, such as feldspar, zircon, tourmaline, rutile, pyrite and other unidentified opaque minerals. The maximum number of minerals identified in a sample is six.

The mineral identification for the matrix is reduced to clayey or siliceous presence of matrix, means the cement type variability is constringed to carbonated or based on microcrystalline quartz. We quantified the composition of matrix/cement according to the following criteria:

1. Very abundant, when the matrix/cement type amounts to over 20% of the total in the sample.
2. Major, with a presence between 20 and 5% in total of the sample.
3. Minor (or trace) if less than 5% of the total of the sample.

4.3. GEOCHEMICAL CHARACTERISATION FOR UNDERSTANDING "ARCHAEOLOGICAL QUARTZITE": X-RAY FLUORESCENCE

Once different methodologies have been developed and adapted for the field relationships and the petrographic characterisation has been performed, here we present the methodological approach for understanding quartzite throughout X-Ray fluorescence analysis. The semi-quantitative chemical composition of the lithic raw material was determined by wavelength dispersive X-ray fluorescence (WDXRF) using a PANalytical Axios Advanced PW4400 XRF spectrometer (4 kW Rh anode SST-mAX X-ray tube) from the SGIker Facilities of the UPV/EHU. The rock chips were placed directly in sample holders without any prior sample manipulation except the selection of non-altered flat surface and smaller than 50 mm in diameter. Finally, the samples were measured with the PANalytical´s Omnian standardless analysis software.

4.4. RAW DATA PROCESSING: STATISTICS

We processed the dataset derived from these analyses with the same statistical procedures exposed on the previous section and using the software IBM SPSS v.21.0 and the freeware Past v.3 (Hammer et al., 2001). We applied categorical (or nominal) descriptive statistics such as frequency tables and its representation through charts (pie chart and bar chart) to understand basic features and the representation of quartz grain or non-quartz mineral features. We also apply χ-square test and standardised residues analysis to relate categorical variables. We used basic descriptive statistics such as mean, median, kurtosis, skewness, and variance to understand numerical and scale variables. In addition, we used frequency and box-plot charts to graphically represent the variables. We used Kolmogorov-Smirnov and Levene's normality test to prove if numerical variables are or are not normally distributed. We used biplot chart to graphically explore the relationship between scale and numerical variables. Because most of numerical variables are not normally distributed, we used Kruskal-Wallis test to compare variance between proposed nominal variables. We also used median test to compare means. We compared samples using parametric and non-parametric tests such as mean and skewness comparison or correlation tests. Finally, we used Principal Component Analysis and dendrogram for understanding associations between variables and grouping variables.

CHAPTER-5

RESULTS. DEFINING AND CHARACTERISING "ARCHAEOLOGICAL QUARTZITE": FROM SEDIMENTARY PROCESSES TO METAMORPHIC REALM

5.1. PETROGRAPHIC CHARACTERISATION OF "ARCHAEOLOGICAL QUARTZITE" THROUGH THIN SECTION

As previously explained, we used the term "archaeological quartzite" to describe what archaeologists or some field geologists describe as "quartzite" (applied generally for macroscopic analysis or as field terminology). Thin section analyses, the most powerful methodological protocol used in this research, show the variability of the rock. In this section we describe the data provided by the analysis made by petrographic analysis in order to understand the genesis, transformation and physical properties "archaeological quartzite". The information obtained is necessary to understand the role of this rock during Prehistory.

5.1.1. CHARACTERISING "ARCHAEOLOGICAL QUARTZITE" APPLYING PACKING, TEXTURAL AND QUARTZ GRAIN FEATURES

Table-5.1 summarises the packing, textural and grain features characterisation of each sample.

The results derived from textural characterisation reveal a great variability within the sample selection we made. The "archaeological quartzites" selected from the archaeological sites and those collected during geological surveys are similarly distributed (χ^2 (2, N = 122) = 1.73, p = .422) (Table-5.2 and Figure-5.1). In general and considering the different provenances, the most represented category is the clastic grained texture, followed by the clastic grained one with cement or texture. Mortar texture is the less represented category. The first two categories are associated with clastic and sedimentary rocks and diagenetic processes, while the third one is clearly associated to metamorphic deformation processes. This general textural characterisation starts to show the variability of genetic processes and subsequent general types of rocks that are inside the term "archaeological quartzite".

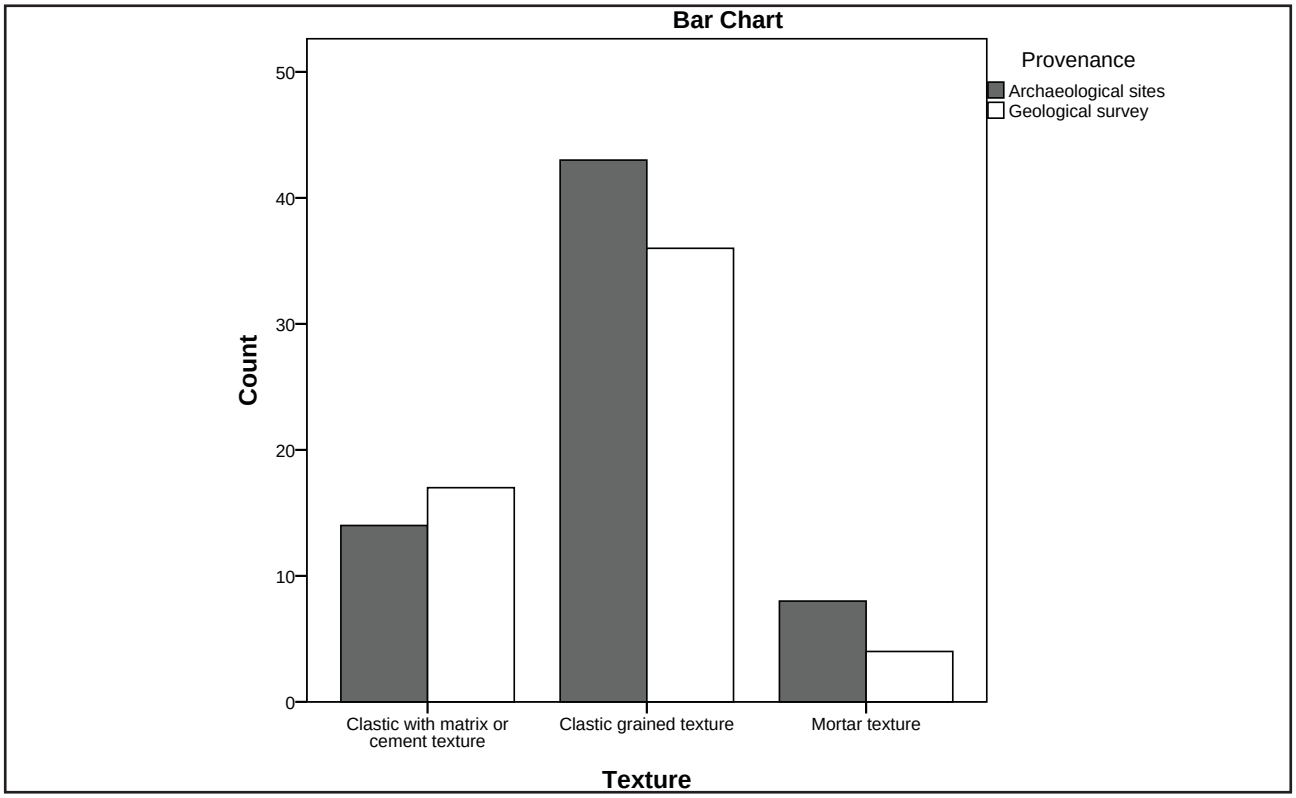

Figure-5.1: Bar chart showing the prevalence of the textures identified on thin section samples, differentiated by provenance (coming from archaeological sites or collected during geological surveys).

Sample	Quartz grain features							Packing	Texture
	Clastic quartz grain	Undulatory extinction quartz grain	Syntaxial overgrowth quartz grain	Concavo-convex limits quartz grain	Suturated/Microstylithic limits quartz grain	Böhm lamellae	Recrystallised quartz grains		
DC02_05	*X*	-	*XXX*	*XXX*	-	-	-	Complete	Clastic grained texture
DC03_2	*XXX*	-	-	-	-	-	-	Tangential	Clastic with matrix or cement texture
DC03_3	-	*X*	*XXX*	*XXX*	-	-	-	Complete	Clastic grained texture
DC04_5	*X*	-	*XXX*	*XXX*	-	-	-	Complete	Clastic grained texture
DC05_1	*XXX*	*X*	-	-	-	-	-	Tangential	Clastic with matrix or cement texture
DC05_2	*XXX*	*X*	-	-	-	-	-	Floating	Clastic with matrix or cement texture
DC06_4	-	-	*XXX*	*XXX*	*X*	-	-	Complete	Clastic grained texture
DC06_5	-	-	-	*XXX*	*XXX*	-	*X*	Suturated	Clastic grained texture
DC06_6	-	-	-	-	*XXX*	*X*	*XX*	Suturated	Mortar texture
DC07_2	*XXX*	*X*	*X*	-	-	-	-	Tangential	Clastic grained texture
DC07_3	*XXX*	*X*	*X*	-	-	-	-	Punctual	Clastic with matrix or cement texture
DC07_7	*XXX*	*XX*	*XX*	-	-	-	-	Complete	Clastic grained texture
DC07_8	*XXX*	-	*XX*	*X*	-	-	-	Tangential	Clastic grained texture
DC16_1	*XXX*	-	*X*	-	-	-	-	Punctual	Clastic with matrix or cement texture
DC18_1	*XXX*	-	-	-	-	-	-	Floating	Clastic with matrix or cement texture
DC18_2	*XXX*	-	*X*	*XX*	-	-	-	Tangential	Clastic with matrix or cement texture
DC21_1	*XXX*	*X*	*X*	-	-	-	-	Punctual	Clastic with matrix or cement texture
DC21_3	-	*XXX*	*XX*	*XXX*	-	-	-	Complete	Clastic grained texture
DC21_6	-	*XXX*	*XXX*	*XXX*	-	-	-	Complete	Clastic grained texture
DC21_7	*XXX*	-	*XX*	*XX*	-	-	-	Tangential	Clastic with matrix or cement texture
DC22_1	*XXX*	*X*	-	-	-	-	-	Tangential	Clastic with matrix or cement texture
DC22_4	*XXX*	*X*	-	*X*	-	-	-	Floating	Clastic with matrix or cement texture
DC24_2	-	*XXX*	*XX*	*XXX*	-	-	-	Suturated	Clastic grained texture
DC24_3	*XXX*	-	-	-	-	-	-	Floating	Clastic with matrix or cement texture
DC24_5	*XXX*	-	-	*XXX*	-	-	-	Tangential	Clastic with matrix or cement texture
DC24_9	-	-	*XXX*	*XXX*	*X*	-	-	Complete	Clastic grained texture
DC25_1	-	*XXX*	*XXX*	*XXX*	-	-	-	Complete	Clastic grained texture
DC25_5	-	*XX*	*XXX*	*XXX*	-	-	-	Complete	Clastic grained texture

Sample	Quartz grain features							Packing	Texture
	Clastic quartz grain	Undulatory extinction quartz grain	Syntaxial overgrowth quartz grain	Concavo-convex limits quartz grain	Sutrurated/Microstylithic limits quartz grain	Böhm lamellae	Recrystallised quartz grains		
DC25_6	-	XXX	-	XXX	XX	-	-	Suturated	Clastic grained texture
DC26_2	XXX	-	X	XX	-	-	-	Punctual	Clastic with matrix or cement texture
DC26_3	-	XX	XXX	XXX	-	-	-	Complete	Clastic grained texture
DC27_1	-	XXX	XXX	XXX	-	-	-	Complete	Clastic grained texture
DC27_12	XXX	-	-	XX	-	-	-	Tangential	Clastic with matrix or cement texture
DC27_3	-	XXX	XX	XXX	-	-	-	Complete	Clastic grained texture
DC27_4	-	XXX	XX	XXX	-	-	-	Complete	Clastic grained texture
DC27_6	XXX	X	-	-	X	-	-	Punctual	Clastic with matrix or cement texture
DC27_9	-	XX	XX	XXX	-	-	-	Complete	Clastic grained texture
DC29_6	XXX	X	-	X	-	-	-	Floating	Clastic with matrix or cement texture
DC39_03	-	-	XXX	XXX	XX	-	-	Complete	Clastic grained texture
DC45_05	-	-	XXX	XXX	XX	-	-	Suturated	Clastic grained texture
DC46_12	-	-	XX	XXX	XXX	-	-	Suturated	Clastic grained texture
DC51_01	-	-	XXX	XXX	X	-	-	Complete	Clastic grained texture
DC61_04	-	-	XXX	XXX	X	-	-	Complete	Clastic grained texture
DC67_05	-	-	-	XXX	XXX	-	X	Suturated	Clastic grained texture
DC68_02	-	-	XXX	XXX	X	-	-	Complete	Clastic grained texture
DC68_05	XXX	XX	-	-	-	X	-	Tangential	Clastic grained texture
DC70_01	-	-	XXX	XXX	-	-	-	Complete	Clastic grained texture
DC71_04	-	-	XX	XX	XXX	-	-	Suturated	Clastic grained texture
DC73_01	-	-	XX	XXX	X	-	-	Complete	Clastic grained texture
DC73_02	-	-	-	XX	XXX	X	-	Suturated	Clastic grained texture
DC73_06	-	-	-	XXX	XXX	-	X	Suturated	Clastic grained texture
DC74_03	-	-	-	-	XXX	X	X	Suturated	Clastic grained texture
DC75_01	-	-	XX	-	XXX	-	XX	Suturated	Mortar texture
DC75_02	-	-	-	-	XXX	X	XX	Suturated	Mortar texture
DC75_03	-	-	XXX	-	XXX	X	-	Suturated	Clastic grained texture
DC75_05	-	-	-	-	XXX	X	XX	Suturated	Mortar texture

Sample	Quartz grain features							Packing	Texture
	Clastic quartz grain	Undulatory extinction quartz grain	Syntaxial overgrowth quartz grain	Concavo-convex limits quartz grain	Suturated/Microstylithic limits quartz grain	Böhm lamellae	Recrystallised quartz grains		
DC77_04	-	-	*XX*	*XXX*	*XXX*	-	-	Suturated	Clastic grained texture
ATS-001	-	*XXX*	*X*	*XX*	-	-	-	Tangential	Clastic grained texture
ATS-002	*XX*	*XXX*	-	*XX*	-	-	-	Tangential	Clastic grained texture
ATS-007	-	*XXX*	*XX*	*XXX*	-	-	-	Complete	Clastic grained texture
ATS-016	-	-	-	-	*XXX*	*X*	*XX*	Suturated	Mortar texture
ATS-023	-	*XXX*	*XXX*	*XX*	-	-	-	Complete	Clastic grained texture
ATS-072	-	-	-	-	*XX*	*X*	*XX*	Suturated	Mortar texture
ATS-151	*XXX*	*X*	-	-	-	-	-	Tangential	Clastic grained texture
ATS-190	-	-	-	*XX*	*XXX*	*XX*	-	Suturated	Clastic grained texture
ATS-195	-	*XX*	-	-	*XX*	-	*XXX*	Suturated	Mortar texture
ATS-302	-	-	-	-	*XXX*	*XX*	*X*	Suturated	Clastic grained texture
ATS-308	-	*XXX*	*XXX*	*XX*	-	-	-	Complete	Clastic grained texture
ATS-310	-	-	-	*XX*	*XXX*	*XX*	-	Suturated	Clastic grained texture
CoB.K26.37.5	-	-	*XX*	-	*XXX*	-	*X*	Suturated	Clastic grained texture
CoB.K26.37.9	*XXX*	*XX*	*XX*	-	-	-	-	Tangential	Clastic with matrix or cement texture
CoB.J27.38.11	-	*XXX*	-	-	*XXX*	-	*X*	Suturated	Clastic grained texture
CoB.K26.37.22	-	*XXX*	*XX*	-	*XX*	-	-	Complete	Clastic grained texture
CoB.K26.37.23	*XXX*	*X*	-	*XX*	-	-	-	Tangential	Clastic grained texture
CoB.J26.38.46	*XXX*	-	-	-	-	-	-	Floating	Clastic with matrix or cement texture
CoB.K26.37.155	-	*XXX*	*XXX*	*XXX*	-	-	-	Complete	Clastic grained texture
CoB.K26.37.201	-	*XX*	-	-	*XXX*	-	*XX*	Suturated	Mortar texture
CoB.J26.38.530	*XXX*	*XX*	*X*	-	-	-	-	Tangential	Clastic grained texture
CoB.J26.38.540	-	*XXX*	*XXX*	*XXX*	-	-	-	Complete	Clastic grained texture
CoB.J26.38.574	-	-	*XX*	-	*XXX*	-	*XX*	Suturated	Mortar texture
ES-199 (Nvl-XIII)	-	*XXX*	-	-	*XXX*	-	*X*	Suturated	Clastic grained texture
ES-239 (Nvl-XIII)	-	*XX*	-	-	*XX*	-	*XXX*	Suturated	Mortar texture
ES-254 (Nvl-XIII)	-	-	*XX*	-	*XXX*	*X*	-	Suturated	Clastic grained texture
ES-290 (Nvl-XIII)	-	*XXX*	-	-	*XXX*	*X*	-	Suturated	Clastic grained texture

Sample	Quartz grain features							Packing	Texture
	Clastic quartz grain	Undulatory extinction quartz grain	Syntaxial overgrowth quartz grain	Concavo-convex limits quartz grain	Suturated/Microstylithic limits quartz grain	Böhm lamellae	Recrystallised quartz grains		
ES-315 (Nvl-XIII)	-	-	*XXX*	*XXX*	*X*	-	-	Complete	Clastic grained texture
ES-378 (Nvl-XIII)	-	-	-	-	*XX*	*XX*	*XXX*	Suturated	Mortar texture
ES-407 (Nvl-XIII)	-	-	*XXX*	*XXX*	*XXX*	-	-	Suturated	Clastic grained texture
ES-411 (Nvl-XIII)	-	-	-	-	*XX*	*X*	*XXX*	Suturated	Clastic grained texture
ES-413 (Nvl-XIII)	-	*XXX*	-	-	*XXX*	-	*X*	Suturated	Clastic grained texture
ES-419 (Nvl-XIII)	-	-	*XXX*	*XXX*	*X*	-	-	Complete	Clastic grained texture
ES-435 (Nvl-XIII)	-	-	*XXX*	*XXX*	*X*	-	-	Complete	Clastic grained texture
ES-441 (Nvl-XIII)	-	-	*XXX*	*XX*	*XXX*	-	-	Suturated	Clastic grained texture
ES-245 (Nvl-XXII)	-	-	*XXX*	*XXX*	*X*	-	-	Complete	Clastic grained texture
ES-246 (Nvl-XXII)	-	-	*XX*	*XXX*	*XXX*	-	-	Suturated	Clastic grained texture
ES-255 (Nvl-XXII)	-	-	*XXX*	*XXX*	*X*	-	-	Complete	Clastic grained texture
ES-263 (Nvl-XXII)	*XXX*	-	*XX*	*XXX*	-	-	-	Tangential	Clastic grained texture
ES-265 (Nvl-XXII)	-	-	-	*XXX*	*XXX*	*X*	-	Suturated	Clastic grained texture
ES-283 (Nvl-XXII)	-	*XXX*	*XXX*	*XXX*	-	-	-	Tangential	Clastic grained texture
ES-293 (Nvl-XXII)	-	-	*XXX*	*XXX*	*X*	-	-	Complete	Clastic grained texture
ES-314 (Nvl-XXII)	-	-	*XXX*	*XXX*	*XX*	-	-	Suturated	Clastic grained texture
ES-328 (Nvl-XXII)	-	-	*XX*	-	*XXX*	-	*X*	Suturated	Clastic grained texture
HA-5827	-	*XXX*	-	-	*XXX*	-	*X*	Suturated	Clastic grained texture
HA-5842	-	-	-	-	*XX*	*X*	*XXX*	Suturated	Clastic grained texture
HA-5847	-	-	-	-	*XXX*	*XX*	*XX*	Suturated	Mortar texture
HA-5848	-	-	-	-	*XXX*	*XX*	*XX*	Suturated	Mortar texture
HA-5855	-	*XX*	*XXX*	*XX*	-	-	-	Complete	Clastic grained texture
Tr-1-18	*XX*	-	*XXX*	*XXX*	-	-	-	Complete	Clastic grained texture
Tr-1-33	*XXX*	-	*XX*	-	-	-	-	Tangential	Clastic with matrix or cement texture
Tr-128-5	*XXX*	-	*XX*	*XXX*	-	-	-	Tangential	Clastic with matrix or cement texture
Tr-129-2-4	*X*	-	*XXX*	*XXX*	-	-	-	Complete	Clastic grained texture
Tr-161-2-3	*XXX*	-	*X*	-	*X*	-	-	Punctual	Clastic with matrix or cement texture
Tr-161-2b-2_Z1	*XX*	-	*X*	*XXX*	-	-	-	Tangential	Clastic with matrix or cement texture

Sample	Quartz grain features							Packing	Texture
	Clastic quartz grain	Undulatory extinction quartz grain	Syntaxial overgrowth quartz grain	Concavo-convex limits quartz grain	Suturated/Microstylithic limits quartz grain	Böhm lamellae	Recrystallised quartz grains		
Tr-161-2b-2_Z2	*XXX*	-	*XX*	*X*	-	-	-	Punctual	Clastic with matrix or cement texture
Tr-161-2b-2_Z3	*XX*	*XX*	*XX*	-	-	-	-	Complete	Clastic grained texture
Tr-161-2b-6	*XXX*	-	*XX*	*XX*	-	-	-	Tangential	Clastic with matrix or cement texture
Tr-222-12_Z1	*XX*	-	*XX*	*XXX*	-	-	-	Complete	Clastic grained texture
Tr-222-12_Z2	*XXX*	-	*XX*	*XX*	-	-	-	Tangential	Clastic with matrix or cement texture
Tr-222-12_Z3	*XXX*	*XX*	*XX*	-	-	-	-	Tangential	Clastic with matrix or cement texture
Tr-223-3-2_Z1	*XXX*	-	*X*	-	-	-	-	Tangential	Clastic with matrix or cement texture
Tr-223-3-2_Z2	*XXX*	-	*X*	-	-	-	-	Tangential	Clastic with matrix or cement texture
Tr-254-2_Z1	*XXX*	-	-	-	-	-	-	Tangential	Clastic with matrix or cement texture
Tr-254-2_Z2	*XXX*	-	*X*	-	*X*	-	-	Punctual	Clastic with matrix or cement texture

Table-5.1: Table showing the features of the quartz grains and the texture and packing characterisation of each sample in thin section. *X*: minor or trace presence; *XX*: Major presence; *XXX*: Very abundant presence.

Texture	Provenance					
	Archaeological sites		Geological survey		General	
	Σ	%	Σ	%	Σ	%
Clastic with matrix or cement texture	14	21,5%	17	29,8%	31	25,4%
Clastic grained texture	43	66,2%	36	63,2%	79	64,8%
Mortar texture	8	12,3%	4	7,0%	12	9,8%
Total	65	100,0%	57	100,0%	122	100,0%

Table-5.2: Table showing the quantity (Σ) and the percentage (%) of the different types of textures recognised in the samples in general and classified by provenance.

The results obtained from the packing characterisation also point to the great variability of the "archaeological quartzites" selected (Table-5.3). As previously verified with texture characterisation, there is no statistic difference between provenances (archaeological or derived from geological surveys; χ^2 (4, N = 122) = 6.9, p = .141). In general, the most represented category is the suturated category, followed by the complete and the tangential packings. Floating and punctual packings are the least represented categories. It is obvious that the most prevalent packing categories are those related with high compaction (Figure-5.2).

Packing	Provenance					
	Archaeological sites		Geological survey		General	
	Σ	%	Σ	%	Σ	%
Floating	1	1,5%	5	8,8%	6	4,9%
Punctual	4	6,2%	5	8,8%	9	7,4%
Tangential	16	24,6%	10	17,5%	26	21,3%
Complete	17	26,2%	21	36,8%	38	31,1%
Suturated	27	41,5%	16	28,1%	43	35,2%
Total	65	100,0%	57	100,0%	122	100,0%

Table-5.3: Table showing the quantity (Σ) and the percentage (%) of the different types of packing recognised in the samples in general and classified by provenance.

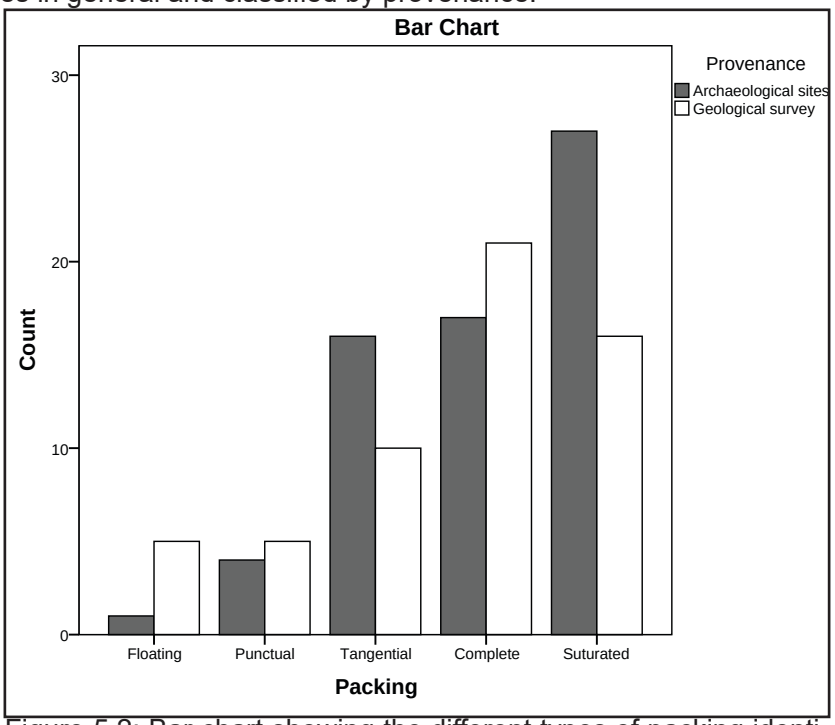

Figure-5.2: Bar chart showing the different types of packing identified on thin section samples, differentiated by provenance (coming from archaeological sites or collected during geological surveys).

The combination of both features reveals the association between both variables (χ^2 (8, N = 122) = 108.96, p < .001). The association of each character is clear, as shown by standardised residues (Table-5.4). Clastic with matrix or cement texture is associated to floating punctual and tangential packing and clastic grained texture to complete and suturated packing. Finally, mortar texture is associated to suturated texture.

	Texture					
	Clastic & Cement		Clastic grained		Mortar texture	
	∑	**res**	∑	res	∑	res
Floating	6	3,6	0	-2,0	0	-0,8
Punctual	9	4,4	0	-2,4	0	-0,9
Tangential	16	3,7	10	-1,7	0	-1,6
Complete	0	-3,1	38	2,7	0	-1,9
Suturated	0	-3,3	31	0,6	12	3,8
Total	31	25	79	65	12	10

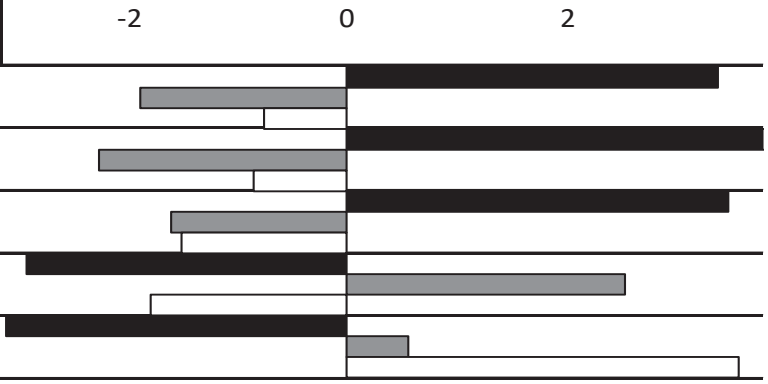

Table-5.3: Frequency table and standardised residues of χ^2 test of the texture categories grouped by packing categories. The last row shows totals, and the second column for each category is its percentage in relation to the total of items analysed.

The results obtained from quartz grain characterisation reveal a great variability in the distribution of the features among the samples (Table-5.5 and Figure-5.3). The most represented feature is the regrowth of quartz syntaxial cement (63.11% of the samples), followed by the grains with concave-convex boundaries (56.56%). The least represented feature is the Böhm/deformation lamellae (16.39%), followed by the presence of recrystallised quartz grains (21.31%). Other quartz grain features such as the presence of detrital quartz grains, undulose extinction and the presence of stylolites or serrated boundaries, are well represented in the samples. Each grain feature too has its own distribution within the samples. Some features are found only in small portions of the samples, such as Böhm/deformation lamellae or recrystallised grains. Others, such as the presence of detrital quartz grains, grains with concave-convex limits quartz grains or serrated/stylolites quartz grain boundaries, are usually very abundant in the samples where they are present.

Quartz-features	Non-presence		Presence							
			General		Minor or traze		Major		Very abundant	
	Σ	%	Σ	%	Σ	%	Σ	%	Σ	%
Detrital quartz grains	76	62,30%	46	37,70%	3	2,46%	4	3,28%	39	31,97%
Undulose extinction on thin section quartzite	74	60,66%	48	39,34%	12	9,84%	13	10,66%	23	18,85%
Regrowth of quartz syntaxial cement	45	36,89%	77	63,11%	12	9,84%	31	25,41%	34	27,87%
Grains with concave-convex boundaries	53	43,44%	69	56,56%	3	2,46%	17	13,93%	49	40,16%
Stylolites or serrated boundaries	63	51,64%	59	48,36%	15	12,30%	11	9,02%	33	27,05%
Böhm/deformation lamellae	102	83,61%	20	16,39%	14	11,48%	6	4,92%	0	0,00%
Recrystallised grains	96	78,69%	26	21,31%	11	9,02%	10	8,20%	5	4,10%

Table-5.5: Table showing the quantity (Σ) and the percentage (%) of the different types of quartz grain features in the samples.

There are clear relationships between some of the quartz grain features, as it can be appreciated in Table-5.6. This χ^2 correlation matrix shows the existence of four positive relationships: 1) the relationship between regrowth of quartz syntaxial cement and grains with concave-convex boundaries, 2) the relationship between Böhm/deformation lamellae and stylolites or serrated boundaries, 3) and also with recrystallised quartz grains; and 4) the relationship between stylolites or serrated boundaries and recrystallised grains. There are several negative relationships as a consequence of the clear differences between the different types of quartzites.

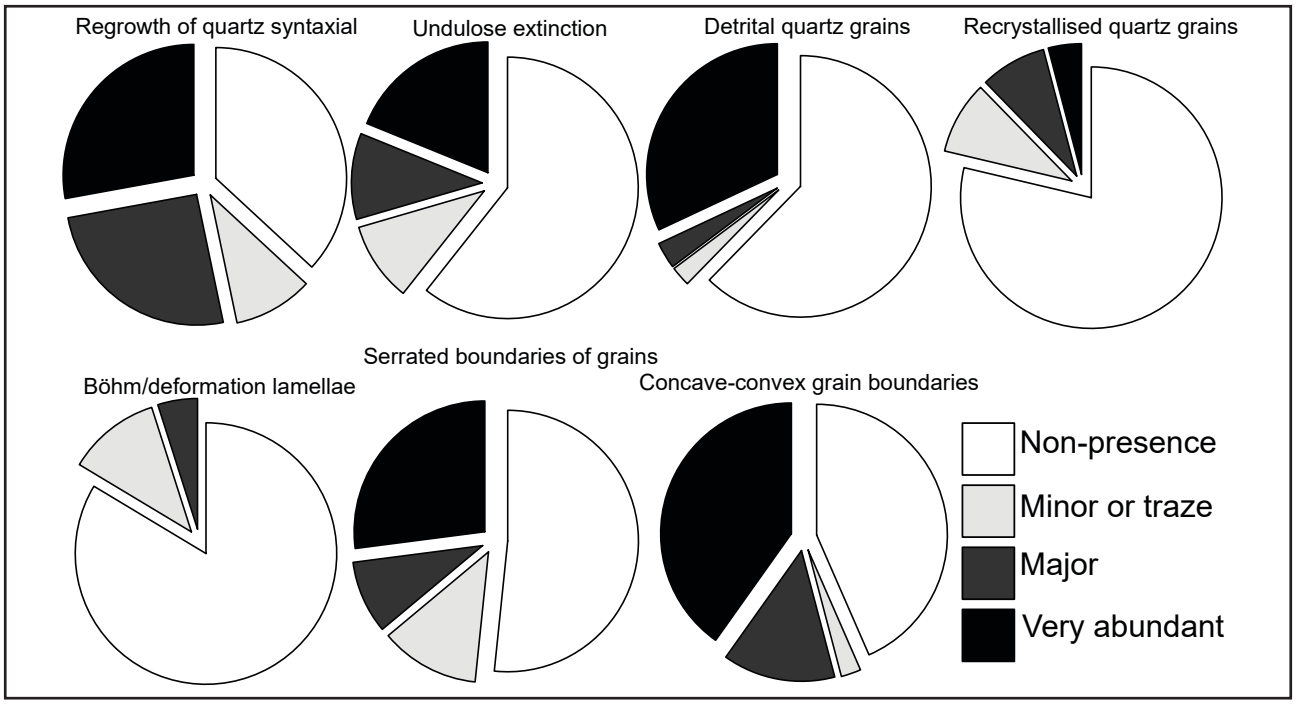

Figure-5.3: Multiple pie chart showing the distribution of the features of quartz grains in "archaeological quartzites". From left to right, Detrital Quartz Grains, Undulose extinction on thin section quartzite, Regrowth of quartz syntaxial cement, Grains with concave-convex boundaries, Stylolites or serrated boundaries, Böms/deformation lamellae and Recrystallised quartz grains.

		Detrital quartz grains	Undulose extinction on thin section quartzite	Regrowth of quartz syntaxial cement	Grains with concave-convex boundaries	Stylolites or serrated boundaries	Böhm/deformation lamellae	Recrystallised grains
Detrital quartz grains	Pearson's r	1	-,153	-,269**	-,358**	-,609**	-,278**	-,354**
	Sig.		,093	,003	,000	,000	,002	,000
Undulose extinction	Pearson's r	-,153	1	,036	-,002	-,233**	-,235**	-,088
	Sig.	,093		,691	,984	,010	,009	,337
Regrowth of quartz	Pearson's r	-,269**	,036	1	,607**	-,287**	-,416**	-,447**
	Sig.	,003	,691		,000	,001	,000	,000
Concave-convex	Pearson's r	-,358**	-,002	,607**	1	-,197*	-,300**	-,445**
	Sig.	,000	,984	,000		,030	,001	,000
Stylolites boundaries	Pearson's r	-,609**	-,233**	-,287**	-,197*	1	,504**	,550**
	Sig.	,000	,010	,001	,030		,000	,000
Deformation lamellae	Pearson's r	-,278**	-,235**	-,416**	-,300**	,504**	1	,459**
	Sig.	,002	,009	,000	,001	,000		,000
Recrystallisd grains	Pearson's r	-,354**	-,088	-,447**	-,445**	,550**	,459**	1
	Sig.	,000	,337	,000	,000	,000	,000	

Table-5.6: Table derived from bivariate Pearson's correlation of the analysis of quartz grain features. * = Correlation is significant at 0.05 (2-tailed). ** = Correlation is significant at 0.01.

The association of these features with the previously commented texture and packing variables were also tested, in this case, applying Discriminant Analysis and grouping by texture categories with 95% ellipses (Figure-5.4). The function created by the two axes could correctly classify the 90.98% of the cases and shows the association between quartz grain features and the textural grouping categories. The first axis solves the 75.57% of the variance and the second one the 24.43%. Table-5.7 shows through a matrix the weight of each variable in the group prediction. The clastic with matrix or cement texture is clearly associated with the high presence of detrital quartz grains in the sample. The group of mortar texture is associated with stylolites or serrated boundaries, deformation lamellae and recrystallised grains. Finally, grains with concave-convex, regrowth of quartz syntaxial cement and, less importantly undulose extinction quartzite surface, are associated to the clastic grained texture group. It is important to mention that clastic grained texture partly overlaps with clastic with matrix or cement texture and also with mortar texture.

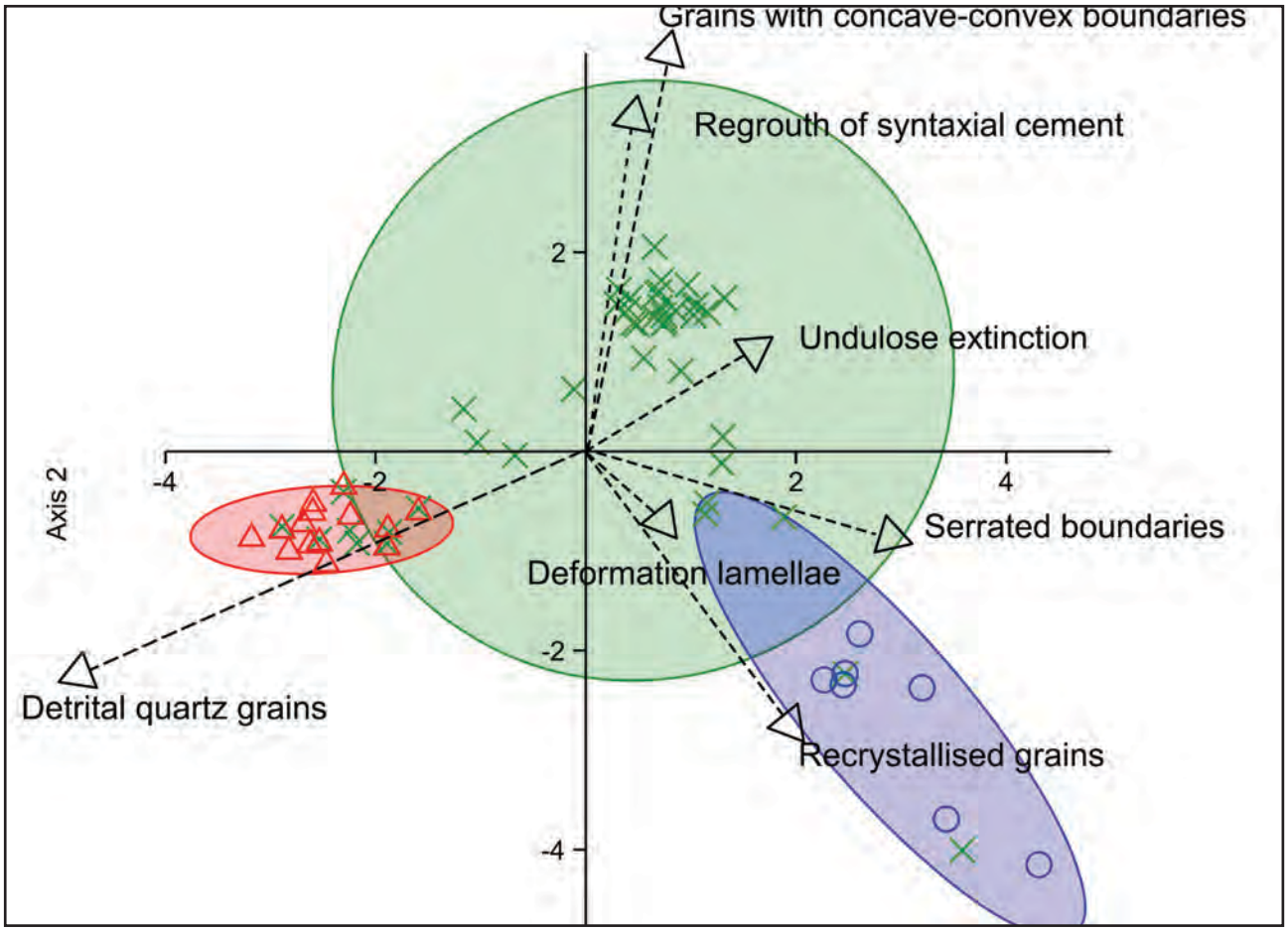

Figure-5.4: Scatter plot result of the Discriminant Analysis of the features of the quartz grains, with the 95% confidence ellipse for each group of texture. Red triangles and ellipse are the samples with clastic and cemented texture. Green crosses and ellipse are the samples with mortar texture.

LOADINGS	Axis 1	Axis 2
Detrital quartz grains	-0,67	-0,34
Undulose extinction on thin section quartzite	0,08	0,20
Regrowth of quartz syntaxial cement	0,07	0,50
Grains with concave-convex boundaries	0,12	0,70
Stylolites or serrated boundaries	0,44	-0,11
Deformation lamellae	0,12	-0,11
Recrystallised grains	0,28	-0,40
Eingevalor	4,72	1,53
Percentage of variance	75,57	24,43

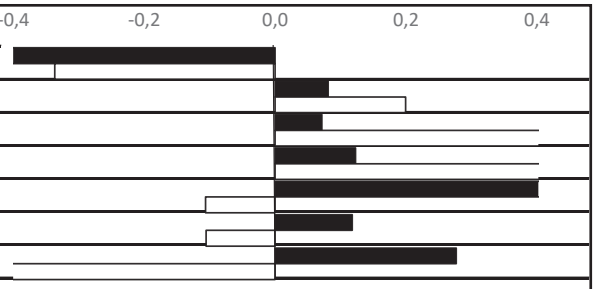

Table-5.7: Each axis represents the loading of the weight of each quartz grain feature generated by the discriminant analysis of texture characterisation.

The Discriminant analysis created using packing as the grouping category reveals an association between quartz grain features and each packing category less marked than in the previous analysis (Figure-5.5). The function created by the four axes could correctly classify the 81.15% of the cases. The first axis solves the 76.74% of the variance, the second axis the 21.79%, the third the 1.21% and the fourth the 0.263%. Table-5.8 shows the weight of each variable in the group prediction matrix. Attending to the first two axes, that represent 98.53% of the variance, there is an association between the feature of detrital quartz grains and the punctual, floating and tangential packing groups. The latter is also associated with undulose extinction and regrowth of quartz syntaxial cement. Complete packing is clearly associated to regrowth of quartz syntaxial cement, to concave-convex quartz boundaries and less clearly to undulose extinction. The latter is also associated to suturated packing, strongly associated with stylolites or serrated boundaries and the existence of recrystallised grains, and, less importantly, to the deformation lamellae feature. The groups generated by 95% ellipses show the similarities between quartz grain features in the groups of punctual, floating and tangential

packing distribution. The overlapping area between the first two is important. The area of complete packing also overlaps on a small surface with the area of tangential packing, attending to the quartz grain features. Finally, the group of suturated packing shows almost no overlapping with the complete packing group and no overlapping at all with other packing groups.

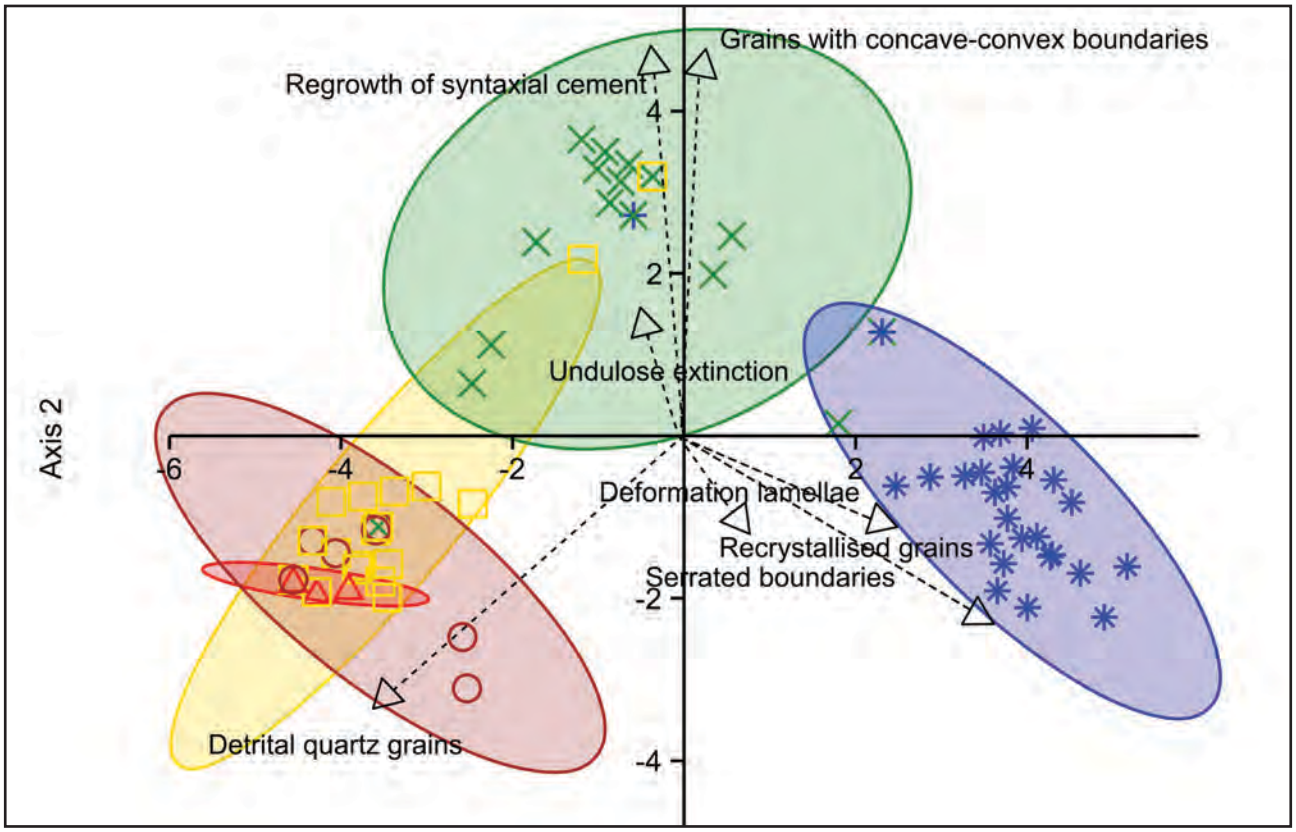

Figure-5.5: Scatter plot result of the Discriminant Analysis of the features of the quartz grains with the 95% confidence ellipse for each group of packing. Red triangles and ellipse are the samples with floating packing. Brown circles and ellipse are the samples with punctual packing. Yellow squares and ellipse are the samples with tangential packing. Green crosses and ellipse are the samples with complete packing. Blue stars and ellipse are the samples with suturated packing.

LOADINGS	Axis 1	Axis 2	Axis 3	Axis 4
Detrital quartz grains	-0,362	-0,363	0,174	0,049
Undulose extinction on thin section qua	-0,023	0,151	0,174	-0,199
Regrowth of quartz syntaxial cement	-0,034	0,531	0,323	0,552
Grains with concave-convex boundaries	0,012	0,530	0,192	-0,463
Stylolites or serrated boundaries	0,366	-0,225	-0,065	0,178
Deformation lamellae	0,078	-0,072	0,026	-0,111
Recrystallised grains	0,150	-0,128	0,002	-0,135
Eingevalue	10,04	2,851	0,158	0,034
Percentage of variance	76,74	21,79	1,21	0,263

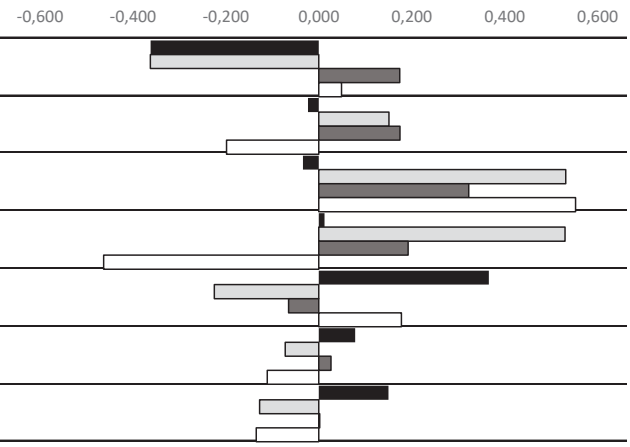

Figure-5.8: Histogram representing the distribution of the circularity index of the analysed quartz grains.

5.1.2. METRIC CHARACTERISATION OF SIZE, SHAPE AND ORIENTATION. DIGITAL IMAGE PROCESSING

The metric and morphological study of the quartz grains has resulted in analysis of 18,855 grains from 118 thin sections[3], which have been summarised with their descriptive statistics in Table-5.9. Supplementary Information-I (from here on, S.I.-I) shows the descriptive statistics of metric, morphological, and directional analysis as represented by bar charts, scatter plots and directional charts.

The size of quartz grains shows high variability, from 0.001 mm to 0.9 mm, although kurtosis is high (Figure-5.6). Skewness is clearly positive, showing high concentration of quartz grains around small sizes < 0.05 mm. At the same time the size of the quartz grains rarely exceeds 0.4 mm. The Udden-Wentworth classification of these data shows a change in skewness, this time clearly negative (Figure-5.7). Very fine sand is the most frequent category, followed by fine sand and coarse silt, which create a well-defined mode. The categories of very fine silt, fine silt and medium silt are well represented too, creating a secondary (and less pronounced) mode. This picture indicates that two types of grains are mainly found in "archaeological quartzites". In general, the former are associated with the framework grains of the original sedimentary rock (deformed or not), whereas the latter forms matrixes and, above all, the newly recrystallized grains. Kolmogorov-Smirnov test demonstrates that grains size, either using numerical values or their conversion through Udden-Wentworth grain scale, is not normally distributed: *KS Numerical* = 0.109; *df* = 18855; $p < 0.01$ and *KS Udden-Wentworth* = 0.229 *df* = 18855; $p > 0.01$.

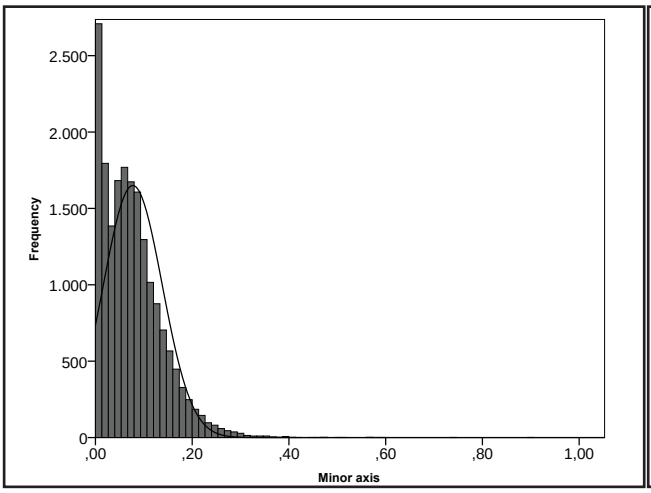

Figure-5.6: Histogram representing the distribution of the sizes, on millimetres, of the minor axis of the analysed quartz grains.

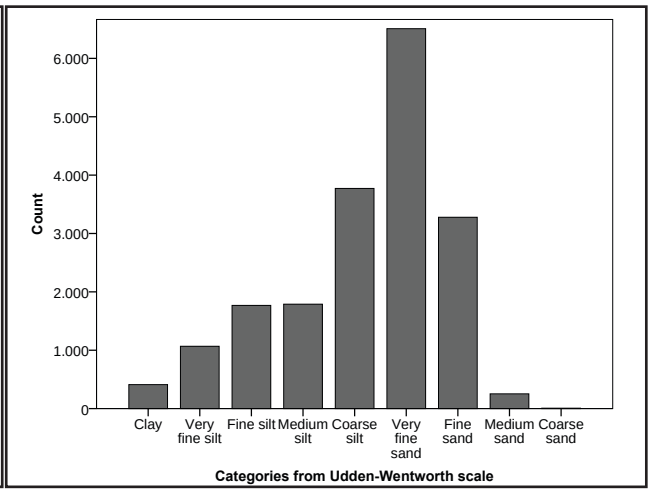

Figure-5.7: Histogram representing the distribution of the sizes of the minor axis of the analysed quartz grains classified according to Udden-Wentworth categories.

The morphology of the quartz grains is approached through two indexes. The first one, the circularity index, has neutral kurtosis and skewness. It shows high variability of the regularity of the shapes, from those near 0, clearly irregular, to the more regular one, nearer to 1 (Figure-5.8). *Kolmogorov-Smirnov* test indicates that circularity is not normally distributed: *KS* = 0.020; *df* = 18855; $p < 0.01$.

The second morphological feature, the roundness index, also has neutral kurtosis and skewness. It shows high variability of the elongation of the particles, from those near 0, clearly elongated, to the non-elongated shapes closer to 1 (Figure-5.9). *Kolmogorov-Smirnov* test indicates that roundness is not normally distributed: *KS* = 0.021; *df* = 18855; $p < 0.01$.

Roundness and circularity indexes are positively and significantly correlated; r (for n = 18,855) = 0.43, $p < 0.01$. Therefore, the deformation of the grains modified the elongation of the particle and the regularity of the perimeter. When these data are classified according to the categories in the Udden-Wentworth scale, it can be appreciated that the circularity and roundness correlation values are higher among the smaller grains and lower among the larger grains (Figure-5.10). This

3 Five samples are not included in the quantitative results but they are included in the thin section qualitative analysis. These are: DC07_08, DC75_01, DC74_03, DC68_02, and DC24_05

demonstrates that there tend to be two types of grain: new grains (smaller and less deformed) and deformed clastic grains (generally larger and more deformed). The Udden-Wentworth categories for the first type of grains are clay, very fine silt, fine silt and medium silt[4]; while for the Udden-Wentworth categories for the second type of grains are those from coarse silt to coarse sand (Figure-5.11).

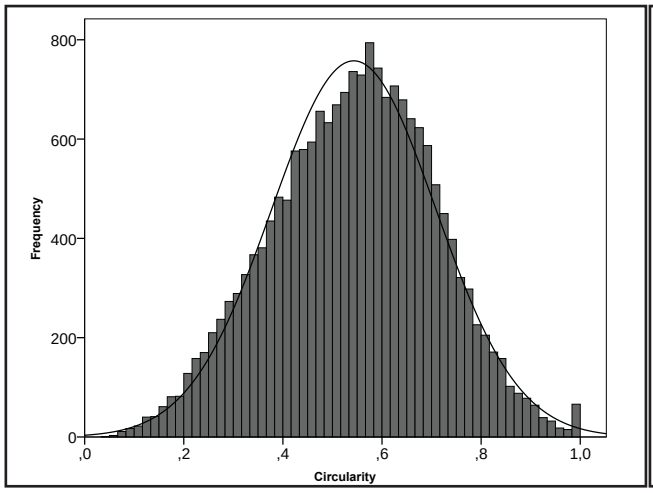

Figure-5.8: Histogram representing the distribution of the circularity index of the analysed quartz grains.

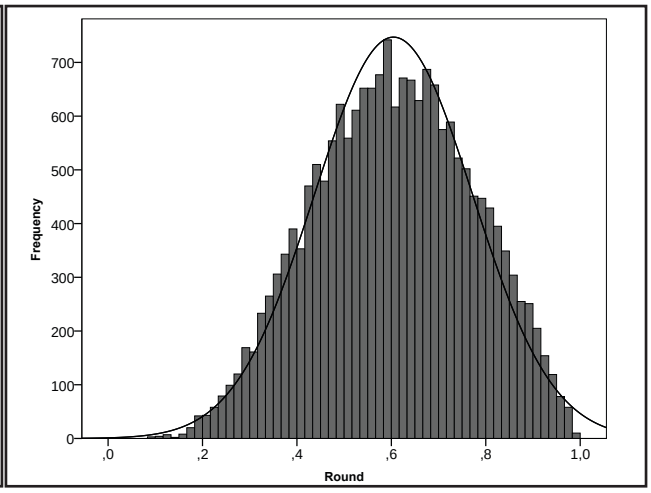

Figure-5.9: Histogram representing the distribution of the roundness index of the analysed quartz grains.

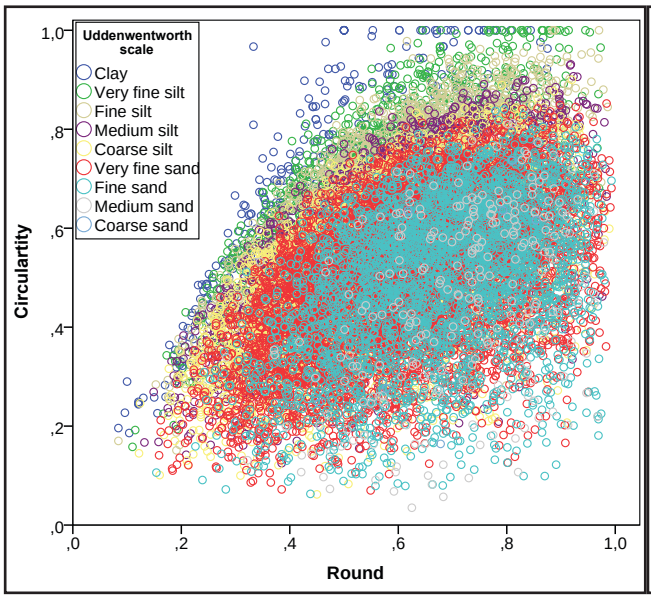

Figure-5.10: Scatter plot representing circularity and roundness indexes. Grains are symbolised with different colours according to the Udden-Wentworth categories.

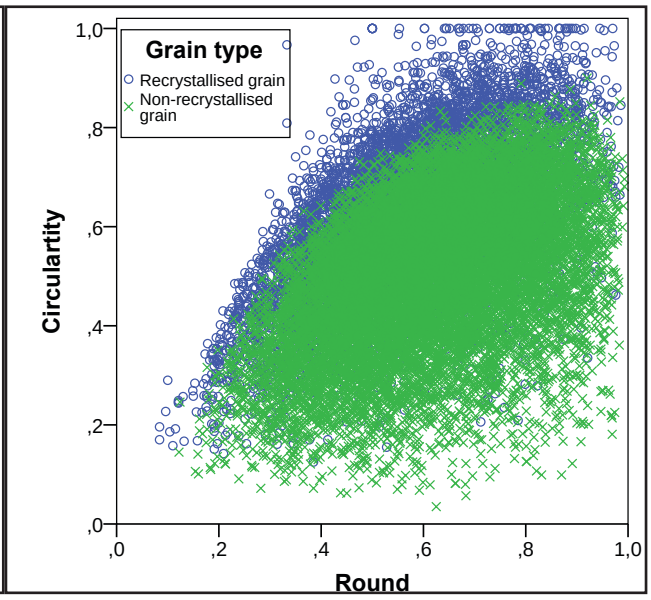

Figure-5.11: Scatter plot representing circularity and roundness indexes. Grains are symbolised with different colours according to the categories non-crystallised grains and crystallised grains (also secondary matrix).

In general, the orientation of all the quartz grains in all the samples is randomly distributed. Using Rayleigh's Index of preferred orientation, it can be seen that there is great variation in "archaeological quartzite" orientation, with values from 0.009 to 0.797. The preferred orientation of the samples from archaeological sites and of those collected during geological survey are similarly distributed for Mardia preferred trend (Mardia, 1975) both with a level of significance of 0.05 (χ^2 (1, N = 118) = 0.113, p = .737) and of 0.01 (χ^2 (1, N = 118) = 0.255, p = .613) (Figure-5.12 and Table-5.10). Using the more robust approach for the preferred orientation test at 0.01 significance level, 44.1% of the samples show preferred orientation. This preferred orientation arises from either bedding as a result of sedimentary processes or schistosity/deformation derived from metamorphic processes.

4 Note that not all the small grains are new grains, smaller matrix may also be present. These grains have not so high circularity and roundness values.

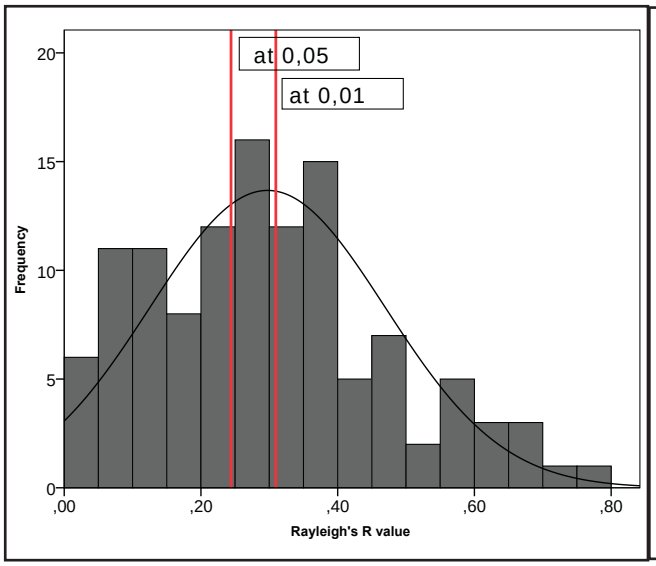

Figure-5.12: Bar chart of the distribution of Rayleigh's index among the samples. Vertical red lines indicate the preferred orientation when more than 50 grains are analysed. Level of significance is represented at 0.05 and 0.01.

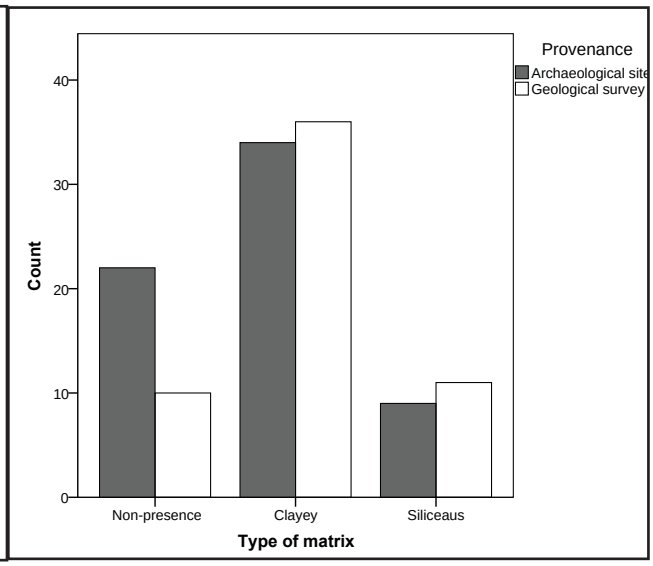

Tabl-5.13: Table showing the quantity (Σ) and the percentage (%) of the quantitative criteria for matrix characterisation, in general and classified by sample provenance.

	Provenance					
	Archaeological sites		Geological survey		General	
	Σ	%	Σ	%	Σ	%
Non-oriented quartzite at 0.05	25	53,2	22	46,8	47	39,8
Oriented quartzite at 0.05	40	56,3	31	43,7	71	60,2
Total	65	56,9	53	43,1	118	100
Non-oriented quartzite at 0.01	35	53,0	31	47	69	55,9
Oriented quartzite at 0.01	30	57,7	22	42,3	54	44,1
Total	65	55,1	53	44,9	118	100

Table-5.10: Table showing the quantity (Σ) and the percentage (%) of preferred orientation at 0.05 and 0.01 levels of significance, in general and classified by sample provenance.

5.1.2. NON-QUARTZ MINERALOGICAL CHARACTERISATION

Table-5.11 summarises mineral identification, the type of matrix and cement and also its quantification in each sample.

The matrix characterisation reveals a small variability among the samples selected. The "archaeological quartzites" chosen from archaeological sites and those taken from geological surveys are similarly distributed ($\chi 2$ (2, N = 122) = 4.251, p<.119) (Table-5.12 and Figure-5.13). The presence of matrix, in general, is high, as reveals the 73.8% of the samples. In general, clayey matrix is the most represented type, with the 57.4% of the sample, while siliceous matrix is not so clearly represented, with the 16.4% of the samples.

	Provenance					
	Archaeological sites		Geological survey		General	
	Σ	%	Σ	%	Σ	%
Non-presence	22	33,8%	10	17,5%	32	26,2%
Clayey	34	52,3%	36	63,2%	70	57,4%
Siliceaus	9	13,8%	11	19,3%	20	16,4%
Total	65	53,3%	57	46,72%	122	100%

Table-5.12: Table showing the quantity (Σ) and the percentage (%) of the different types of matrix, in general and classified by sample provenance.

Sample	Mineral identified								Matrix		Cement	
	Zircon	Tourmaline	Rutile	Mica	Chlorite	Clay	Feldspar	Pyrite	Fe-oxides	Type	%	Type	%
DC02_05	-	-	-	-	X	-	-	-	-	Clayey	X	-	-
DC03_2	-	-	X	-	X	X	-	-	X	Clayey	XXX	-	-
DC03_3	-	-	X	X	X	-	-	-	X	Siliceaus	X	-	-
DC04_5	-	-	-	X	X	X	-	-	-	Siliceaus	X	-	-
DC05_1	-	-	-	X	-	X	-	-	-	Siliceaus	XX	-	-
DC05_2	-	-	-	X	-	X	X	-	X	Clayey	XXX	-	-
DC06_4	X	-	-	X	X	X	-	X	X	Clayey	X	-	-
DC06_5	-	-	X	-	X	X	-	X	X	-	-	-	-
DC06_6	X	-	-	X	-	-	-	X	X	-	-	-	-
DC07_2	X	-	-	-	X	-	-	X	X	Clayey	XX	-	-
DC07_3	X	X	X	-	-	-	-	-	X	Clayey	XXX	-	-
DC07_7	-	-	-	X	X	X	-	-	X	Clayey	X	-	-
DC07_8	-	-	X	-	-	X	-	X	-	Siliceaus	XX	-	-
DC16_1	-	-	-	X	-	X	-	-	X	Clayey	XXX	-	-
DC18_1	-	-	-	X	X	-	-	-	X	-	-	Carbonated	XXX
DC18_2	X	X	X	X	-	-	X	-	X	Clayey	XXX	-	-
DC21_1	X	X	X	X	-	-	-	X	X	Clayey	XXX	-	-
DC21_3	X	-	X	X	-	X	-	X	X	Clayey	XX	-	-
DC21_6	X	X	-	-	-	X	-	X	X	Clayey	X	-	-
DC21_7	-	-	-	X	-	-	X	X	X	Clayey	XX	-	-
DC22_1	X	X	-	X	X	X	-	-	-	Clayey	XX	-	-
DC22_4	-	X	-	X	X	-	-	-	X	Siliceaus	XXX	-	-
DC24_2	X	-	X	X	X	-	X	-	X	Clayey	X	-	-
DC24_3	X	-	-	X	X	-	X	-	-	-	-	Carbonated	XXX
DC24_5	-	-	-	X	-	X	X	-	-	Siliceaus	XX	-	-
DC24_9	-	-	-	X	-	X	-	X	X	Clayey	X	-	-
DC25_1	-	X	-	X	-	X	-	-	X	-	-	-	-
DC25_5	X	-	X	X	-	X	-	X	X	Clayey	XX	-	-
DC25_6	-	-	-	X	X	-	-	X	X	Clayey	X	-	-

Sample	Mineral identified									Matrix		Cement	
	Zircon	Tourmaline	Rutile	Mica	Chlorite	Clay	Feldspar	Pyrite	Fe-oxides	Type	%	Type	%
DC26_2	-	-	-	X	-	X	-	-	X	Siliceaus	XXX	-	-
DC26_3	-	-	-	X	X	X	-	-	-	Siliceaus	X	-	-
DC27_1	X	X	X	-	X	-	-	-	X	Clayey	X	-	-
DC27_12	-	-	-	X	X	X	-	-	X	Siliceaus	XX	-	-
DC27_3	-	X	-	-	X	X	-	-	X	Clayey	X	-	-
DC27_4	X	-	-	X	X	-	-	-	-	Siliceaus	X	-	-
DC27_6	-	-	X	X	-	X	-	-	X	Clayey	XXX	-	-
DC27_9	X	X	-	X	X	-	-	-	X	Clayey	X	-	-
DC29_6	-	-	-	X	-	-	-	-	X	Clayey	XX	Carbonated	X
DC39_03	X	X	-	-	X	-	-	X	X	Clayey	X	-	-
DC45_05	-	-	X	-	-	-	-	-	X	Clayey	X	-	-
DC46_12	-	-	-	-	X	-	-	X	X	-	-	-	-
DC51_01	X	X	X	-	-	-	-	-	-	Clayey	X	-	-
DC61_04	X	-	-	X	-	X	-	-	-	Clayey	X	-	-
DC67_05	X	X	X	-	-	X	-	X	X	Clayey	X	-	-
DC68_02	-	-	-	-	-	X	-	X	X	Clayey	X	-	-
DC68_05	X	X	-	-	-	-	-	X	X	Clayey	X	-	-
DC70_01	-	-	-	-	X	-	-	-	X	Clayey	X	-	-
DC71_04	X	-	-	-	-	-	-	X	X	-		-	-
DC73_01	-	X	-	-	-	-	-	X	X	Clayey	X	-	-
DC73_02	X	-	-	-	X	-	-	X	X	Clayey	X	-	-
DC73_06	X	-	-	-	-	X	-	-	X	Clayey	X	-	-
DC74_03	-	-	-	-	-	-	-	X	X	Clayey	X	-	-
DC75_01	-	X	X	-	-	-	-	X	X	Clayey	X	-	-
DC75_02	-	-	-	-	-	-	-	X	X	-	-	-	-
DC75_03	X	-	-	-	X	X	-	-	X	-	-	-	-
DC75_05	X	-	-	-	X	-	-	X	X	-	-	-	-
DC77_04	X	-	-	-	X	-	-	X	X	Siliceaus	X	-	-
ATS-001	X	-	X	X	-	X	-	X	X	Clayey	X	-	-

Sample	Mineral identified							Matrix		Cement	
	Zircon	Tourmaline	Rutile	Mica	Chlorite	Clay	Feldspar	Pyrite	Fe-oxides	Type	%	Type	%
ATS-002	-	X	-	X	-	-	X	-	X	Siliceaus	X	-	-
ATS-007	-	-	-	X	X	-	-	X	X	Clayey	X	-	-
ATS-016	-	-	-	X	X	X	-	X	X	Clayey	X	-	-
ATS-023	X	-	-	-	-	-	-	X	X	Clayey	X	-	-
ATS-072	X	X	X	X	-	X	-	-	X	Clayey	X	-	-
ATS-151	X	X	-	-	X	X	-	-	X	Clayey	X	-	-
ATS-190	-	X	X	X	X	-	-	-	X	Clayey	X	-	-
ATS-195	X	X	X	X	-	-	-	-	X	Clayey	X	-	-
ATS-302	X	-	X	-	-	-	-	X	-	Clayey	X	-	-
ATS-308	X	-	-	X	X	-	-	-	X	Clayey	X	-	-
ATS-310	-	X	X	X	X	X	-	-	X	Clayey	X	-	-
CoB.K26.37.5	-	X	X	X	X	-	-	X	X	Clayey	X	-	-
CoB.K26.37.9	X	X	X	-	-	-	X	X	X	Clayey	X	-	-
CoB.J27.38.11	-	-	X	X	-	X	-	X	X	Clayey	X	-	-
CoB.K26.37.22	-	-	-	-	-	X	-	-	X	Clayey	XX	-	-
CoB.K26.37.23	-	-	X	X	-	X	-	X	X	Clayey	X	-	-
CoB.J26.38.46	X	-	X	-	X	X	-	X	X	Siliceaus	XX	-	-
CoB.K26.37.155	X	-	-	X	X	-	-	-	X	-	-	-	-
CoB.K26.37.201	X	X	-	-	-	X	X	X	X	Clayey	X	-	-
CoB.J26.38.530	-	X	X	-	-	X	X	X	X	Siliceaus	X	-	-
CoB.J26.38.540	X	-	-	X	X	X	-	-	X	-	-	-	-
CoB.J26.38.574	-	-	-	X	X	-	-	-	X	Siliceaus	X	-	-
ES-199 (NvI-XIII)	X	X	-	-	-	-	-	X	X	Clayey	X	-	-
ES-239 (NvI-XIII)	-	-	-	-	-	-	-	X	X	-	-	-	-
ES-254 (NvI-XIII)	-	-	-	-	X	-	-	-	X	Clayey	X	-	-
ES-290 (NvI-XIII)	X	-	-	-	X	-	-	X	X	Clayey	X	-	-
ES-315 (NvI-XIII)	X	-	X	-	X	-	-	X	X	-	-	Carbonated	X
ES-378 (NvI-XIII)	X	-	-	X	-	-	-	X	X	-	-	-	-
ES-407 (NvI-XIII)	-	-	-	X	-	X	-	-	X	Clayey	X	-	-

Sample	Mineral identified									Matrix		Cement	
	Zircon	Tourmaline	Rutile	Mica	Chlorite	Clay	Feldspar	Pyrite	Fe-oxides	Type	%	Type	%
ES-411 (Nvl-XIII)	-	-	-	X	-	X	-	-	-	Clayey	X	-	-
ES-413 (Nvl-XIII)	-	-	-	-	-	X	-	X	X	Clayey	X	-	-
ES-419 (Nvl-XIII)	X	-	-	-	X	X	-	X	X	Siliceaus	X	-	-
ES-435 (Nvl-XIII)	-	-	-	X	X	X	-	-	X	Clayey	X	-	-
ES-441 (Nvl-XIII)	X	-	X	-	X	-	-	-	X	Clayey	X	-	-
ES-245 (Nvl-XXII)	X	-	-	-	X	-	-	-	X	Clayey	X	-	-
ES-246 (Nvl-XXII)	X	-	X	-	-	-	-	X	X	-	-	-	-
ES-255 (Nvl-XXII)	X	-	-	X	-	-	X	-	X	Clayey	XX	-	-
ES-263 (Nvl-XXII)	X	-	-	X	-	-	-	-	X	Siliceaus	X	Carbonated	X
ES-265 (Nvl-XXII)	X	-	-	X	-	-	-	-	-	Clayey	X	-	-
ES-283 (Nvl-XXII)	X	-	X	-	-	-	-	-	X	Clayey	X	-	-
ES-293 (Nvl-XXII)	-	-	X	-	-	-	-	-	X	Clayey	X	-	-
ES-314 (Nvl-XXII)	-	-	X	-	X	-	-	X	X	Clayey	X	-	-
ES-328 (Nvl-XXII)	X	-	-	X	X	-	-	X	X	Clayey	X	-	-
HA-5827	X	X	X	X	-	X	-	X	-	Siliceaus	X	-	-
HA-5842	X	X	X	-	-	-	-	-	X	-	-	-	-
HA-5847	X	-	X	X	X	-	-	-	X	-	-	-	-
HA-5848	-	-	X	-	X	-	-	X	X	-	-	-	-
HA-5855	-	-	-	-	X	-	-	X	X	Clayey	X	-	-
Tr-1-18	-	-	-	-	-	X	-	-	-	Siliceaus	X	-	-
Tr-1-33	X	-	-	-	-	X	-	-	-	-	-	Microcrystalline quartz	X
Tr-128-5	X	-	-	X	X	X	-	-	X	-	-	Microcrystalline quartz	XX
Tr-129-2-4	-	-	-	-	-	-	-	-	X	Siliceaus	X	-	-
Tr-161-2-3	-	-	-	-	-	-	-	-	X	-	-	Microcrystalline quartz	XX
Tr-161-2b-2_Z1	-	-	-	-	-	-	-	-	X	Clayey	XX	-	-
Tr-161-2b-2_Z2	X	-	-	-	-	-	-	-	X	-	-	Microcrystalline quartz	XX
Tr-161-2b-2_Z3	-	-	X	-	-	-	-	-	X	-	-	Microcrystalline quartz	X
Tr-161-2b-6	X	-	X	-	-	-	-	X	X	-	-	Microcrystalline quartz	XX
Tr-222-12_Z1	-	-	-	-	-	-	-	X	X	-	-	Microcrystalline quartz	X

Sample	Mineral identified								Matrix		Cement	
	Zircon	Tourmaline	Rutile	Mica	Chlorite	Clay	Feldspar	Pyrite	Fe-oxides	Type	%	Type	%
Tr-222-12_Z2	-	-	-	-	-	-	-	-	X	-	-	Microcrystalline quartz	XX
Tr-222-12_Z3	-	-	-	-	-	-	-	-	X	Clayey	X	-	-
Tr-223-3-2_Z1	-	-	X	-	-	X	-	-	-	-	-	Microcrystalline quartz	X
Tr-223-3-2_Z2	-	-	X	-	-	X	-	-	X	-	-	Microcrystalline quartz	XX
Tr-254-2_Z1	-	-	-	-	-	-	-	-	X	Clayey	XX	-	-
Tr-254-2_Z2	X	-	-	-	-	-	-	-	X	-	-	Microcrystalline quartz	XX

Table-5.11: Table showing the minerals identified and the matrix and cement quantity and type in each sample. For matrix and cement quantification in thin section: X: minor or trace presence; XX: Major presence; XXX: Very abundant presence.

Coming to the quantitative analysis of matrix, the “archaeological quartzites” selected from the archaeological sites and those taken from the geological surveys are differently distributed (χ^2 (3, N = 122) = 12.845, p = .005) (Table-5.13 and Figure-5.14). The absence of matrix and the smaller quantities of matrix (represented by the trace category) are relatively similar distributed, although the higher presence of absence of matrix and trace categories are better represented on the samples derived from the archaeological sites. The representation of major and very abundant categories are better represented on the samples derived from the geological surveys, especially regarding to the last category. Then, the presence of matrix is related to small percentages (mainly on samples derived from archaeological sites) and, mainly composed by clay.

	Provenance					
	Archaeological sites		Geological survey		General	
	Σ	%	Σ	%	Σ	%
Non-presence	18	27,7%	10	17,5%	28	23,0%
Minor or trace	39	60,0%	28	49,1%	67	54,9%
Major	8	12,3%	10	17,5%	18	14,8%
Very abundant	0	0,0%	9	15,8%	9	7,4%
Total	65	53,3%	57	46,7%	122	100,0%

Table-5.13: Table showing the quantity (Σ) and the percentage (%) of the quantitative criteria for matrix characterisation, in general and classified by sample provenance.

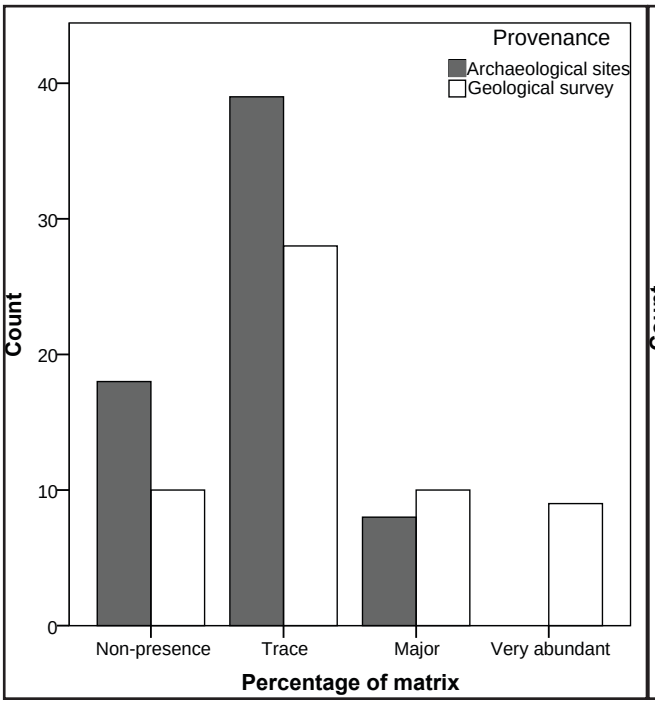

Figure-5.14: Bar chart showing the quantification of matrix identified in thin section samples, differentiated by provenance (coming from archaeological sites or collected during geological surveys).

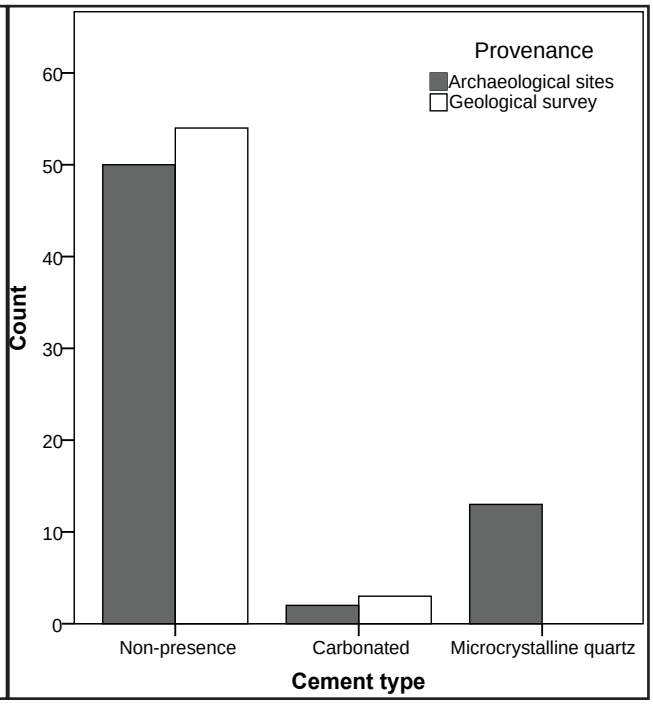

Figure-5.15: Bar chart showing the different types of cement identified in thin section samples, differentiated by provenance (coming from archaeological sites or collected during geological surveys).

Cement characterisation shows higher variability among the samples selected. The “archaeological quartzites” from archaeological sites and those chosen from the geological surveys are differently distributed (χ^2 (2, N = 122) = 12.885, p = .002) (Table-5.14 and Figure-5.15). In general, most of the samples have no cement (14.8% of the samples), with similar representation on the samples from both places. The presence of carbonated cement is also similarly distributed, with small percentages on both types of samples (4.1% of the samples). The biggest differences are on the presence of microcrystalline quartz cement for the samples from the Troisdorf site, without parallel on the samples derived from the geological surveys.

Cement characterisation shows higher variability among the samples selected. The "archaeological quartzites" from archaeological sites and those chosen from the geological surveys are differently distributed (χ^2 (2, N = 122) = 12.885, p = .002) (Table-5.14 and Figure-5.15). In general, most of the samples have no cement (14.8% of the samples), with similar representation on the samples from both places. The presence of carbonated cement is also similarly distributed, with small percentages on both types of samples (4.1% of the samples). The biggest differences are on the presence of microcrystalline quartz cement for the samples from the Troisdorf site, without parallel on the samples derived from the geological surveys.

	Provenance					
	Archaeological sites		Geological survey		General	
	Σ	%	Σ	%	Σ	%
Non-presence	50	76,9%	54	94,7%	104	85,2%
Carbonated	2	3,1%	3	5,3%	5	4,1%
Microcrystalline quartz	13	20,0%	0	0,0%	13	10,7%
Total	65	53,3%	57	46,7%	122	100,0%

Table-5.14: Table showing the quantity (Σ) and the percentage (%) of the different types of cement, in general and classified by sample provenance.characterisation, in general and classified by sample provenance.

Moving to the quantitative characterisation of cement, this feature reveals similar variability within our sample selection. The "archaeological quartzites" selected from archaeological sites and those chosen from geological surveys are differently distributed (χ2 (3, N = 122) = 12.009, p= .007) (Table-5.15 and Figure-15.16). As previously commented, cement is absent on most of the samples. If cement is present, its quantity in samples derived from geological surveys is related with the very abundant category, means on samples derived from archaeological sites is related to trace or major categories (clearly related to the site of Troisdorf).

	Provenance					
	Archaeological sites		Geological survey		General	
Non-presence	52	80,0%	54	94,7%	106	86,9%
Minor or trace	8	12,3%	1	1,8%	9	7,4%
Major	5	7,7%	0	0,0%	5	4,1%
Very abundant	0	0,0%	2	3,5%	2	1,6%
Total	65	53,3%	57	46,7%	122	100,0%

Table-5.15: Table showing the quantity (Σ) and the percentage (%) of the quantitative criteria for cement characterisation, in general and classified by sample provenance.

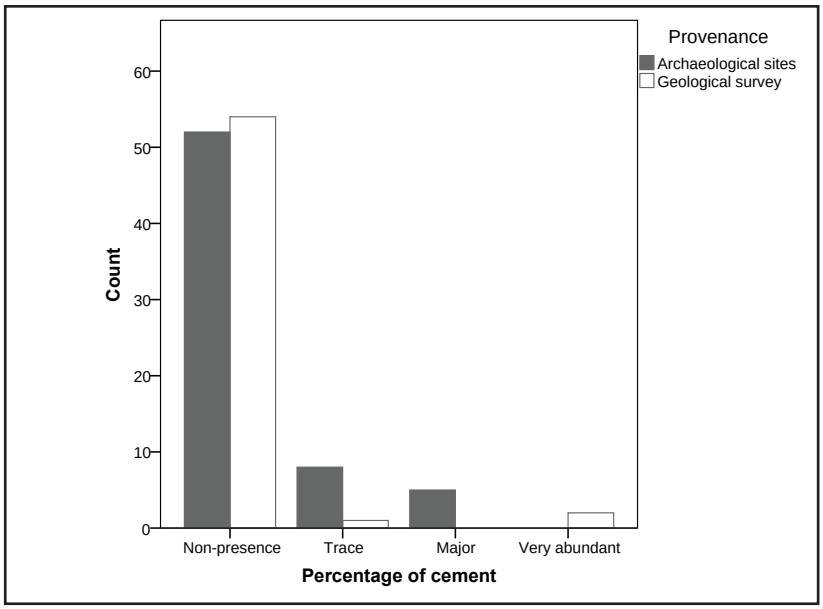

Figure-5.16: Bar chart showing the quantification of matrix identified in thin section samples, differentiated by provenance (coming from archaeological sites or collected during geological surveys).

Mineral identification reveals clear differences in its distribution (Table-5.16). There are no statistically differences between provenances (samples taken from archaeological sites vs samples collected during geological surveys) in the presence of any mineral (Figure-5.17) (χ^2*zircon* (1, N = 122) = .323, p = .570; χ^2*tourmaline* (1, N = 122) = 1.581, p = .209; χ^2*rutile* (1, N = 122) = 1.470, p = .225; χ^2mica (1, N = 122) = 1.951, p = .162; χ^2*chlorite* (1, N = 122) = 1.362, p = .243; χ^2*clay* (1, N = 122) = 1.322, p= .250; χ^2*feldespar* (1, N = 122) = .297, p = .586; χ^2*pyrite* (1, N = 122) = .067, p = .796; χ^2Fe-oxides (1, N = 122) = 1.756, p = .185). In general, Fe-Oxide is the most frequent mineral among those considered, with high presence on every sample as consequence of the weathering process that affects the "archaeological quartzites" on different contexts. Zircon, mica, chlorite, clay and pyrite appear on many samples, while tourmaline, rutile and feldspar are present only in some samples.

	Provenance					
	Archaeological sites		Geological survey		General	
	Σ	%	Σ	%	Σ	%
Zircon	33	55,93%	26	44,07%	59	48,36%
Tourmaline	13	43,33%	17	56,67%	30	24,59%
Rutile	25	60,98%	16	39,02%	41	33,61%
Mica	26	46,43%	30	53,57%	56	45,90%
Chlorite	24	47,06%	27	52,94%	51	41,80%
Clay	23	46,94%	26	53,06%	49	40,16%
Feldspar	5	45,45%	6	54,55%	11	9,02%
Pyrite	27	51,92%	25	48,08%	52	42,62%
Fe-Oxides	58	55,77%	46	44,23%	104	85,25%

Figure-5.16: Bar chart showing the quantification of matrix identified in thin section samples, differentiated by provenance (coming from archaeological sites or collected during geological surveys).

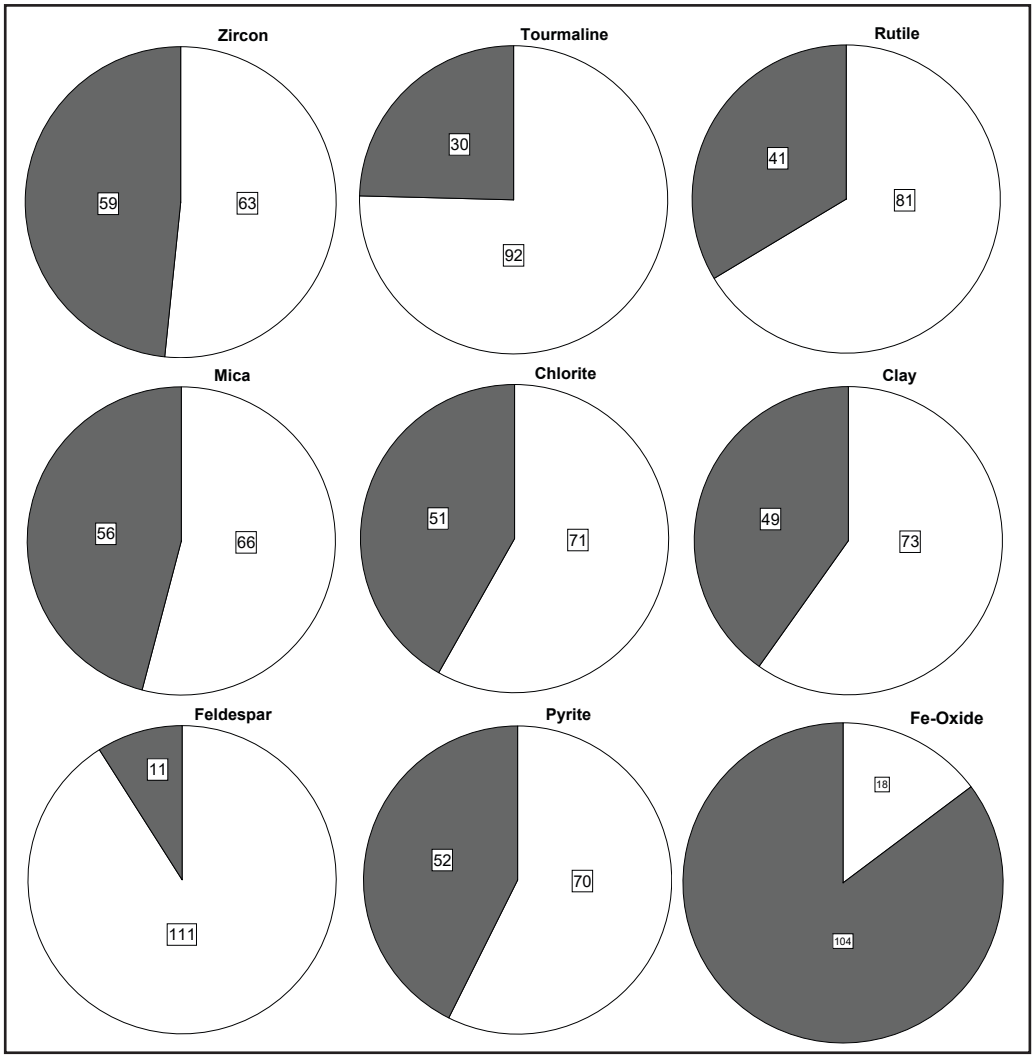

Figure-5.17: Multiple pie chart showing the presence of different mineral in quartzite thin section samples. From left to right Zircon, Tourmaline, Rutile, Mica, Chlorite, Clay, Feldspar, Pyrite, and Fe-Oxides. Shaded areas represent the number of thin sections where the mineral was present, while white areas represent the number of thin sections where that mineral was absent.

5.2. GEOQUEMICAL CHARACTERISATION OF "ARCHAEOLOGICAL QUARTZITES" THROUGH X-RAY FLUORESCENCE

Table-5.17 shows the geochemical characterisation of the 111 "archaeological quartzites" analysed through X-Ray Fluorescence[3]. 45 samples derive from archaeological context, means 66 from geological survey. The data shows differences between the samples that must be explore component by component.

SiO_2 shows the highest values (*M* = 93.99%, *SD* = 6.00). The highest concentration of this component in a sample is 99.66%, while the lowest presence is 61.45%. The samples collected during geological surveys (M = 92.42%, SD = 0.96) and those coming from archaeological sites (*M*= 95.65%, *SD* = 0.51) are different according to the variance and means of this element: *t*(85) = 2.97, *p* = 0.004. Levene's test indicated unequal variances (*F* = 8.140, *p* = 0.005), so degrees of freedom were adjusted from 109 to 85. There are smaller quantities and more variability of SiO_2 component in samples collected from geological surveys than in those chosen from archaeological sites.

Al_2O_3 is present in every sample with smaller and more variable percentages than SiO_2 (*M* = 2.37%, *SD* = 2.15). The minimum value is 0.06% while the maximum is 12.35%. The samples collected during geological surveys (*M* = 2.96%, *SD* = 2.42) and those coming from archaeological sites (*M* = 1.75%, *SD* = 1.65) are different according to their variance and mean: *t*(99) = -3.09, *p* = 0.003. Levene's test indicated unequal variances (*F* = 5.340, *p* = 0.023), so degrees of freedom were adjusted from 109 to 99. There is smaller variability and abundance of Al_2O_3 among the samples coming from archaeological sites than among those collected from geological surveys.

Fe_2O_3 is also present in every sample with diverse percentages (*M* = 0.92%, *SD* = 1.03). Its abundance is small, from 0.03% to 6.43%. The samples collected during geological surveys (*M* = 1.98%, *SD* = 1.24) and those chosen from archaeological sites (*M* = 0.63%, *SD* = 0.63) are different according to their variance and mean: *t*(84) = -3.08, *p* = 0.003. Levene's test indicated unequal variances (*F* = 20.523, *p* < 0.01), so degrees of freedom were adjusted from 109 to 83. As on previously analysed components, there is smaller variability and abundance of Fe_2O_3among the samples coming from archaeological sites than among those collected during geological surveys.

MnO only appears in 32 of the samples from both origins, which reduces its mean (*M* = 0.02%, *SD* = 0.06). Its abundance is small, with values from 0.02%, in the case of presence, to 0.49%. The samples collected during geological surveys (*M* = 0.03%, *SD* = 0.08) and those chosen from archaeological sites (*M* = 0.01%, *SD* = 0.16) are different according to their variance and mean: *t*(61) = -2.21, *p* = 0.031. Levene's test indicated unequal variances (*F* = 12.848, *p* = 0.001), so degrees of freedom were adjusted from 109 to 61. There is smaller variability and abundance of MnO among the samples coming from archaeological sites than among those collected during geological surveys. The quantity of this component is very small and its presence is clearly residual.

MgO is present in every sample with small but diverse percentages (*M* = 0.16%, *SD* = 0.18). Its abundance is always small from 0.02% to 0.81%. The samples collected during geological surveys and those chosen from archaeological sites are similar according to their variance and mean: *t*(109) = -0.28, *p* = 0.20.

CaO is present in every sample with diverse percentages (*M* = 1.03%, *SD* = 3.91). Its abundance is variable, with minimum values of 0.01% to a maximum of 35.09%. The samples collected during geological surveys (*M* = 1.80%, *SD* = 5.36) and those chosen from archaeological sites (M = 0.22%, SD = 0.04) are clearly different according to its variance and mean: *t*(56) = -2.20, *p* = 0.034. Levene's test indicated unequal variances (*F* = 12.726, *p* = 0.001), so degrees of freedom were adjusted from 109 to 56. There is a higher variability and abundance of CaO among the samples collected during geological surveys than among those chosen from archaeological sites. This situation can be explained by the identification of a sample from geological surveys with a concentration of CaO higher than 30% and another two with concentrations higher than 10%.

Na_2O is present in every sample in small and variable percentages (*M* = 0.27%, *SD* = 0.49). Its presence ranges from 0.02% to 2.69%. The samples collected during geological surveys and those chosen from archaeological sites are similar according to their variance and mean: *t*(109) = 0.87, *p* = 0.39.

3 Samples from the archaeological site of Troisdorf have been analysed as a single sample. Samples ES-199 (nvl-XIII), ES-239 (nvl-XIII), ES-246 (nvl-XXII), ES-283 (nvl-XXII) and ES-314 (nvl-XXII) were not analysed.

Sample	X-Ray Fluorescence% Components										
	SiO_2	Al_2O_3	MnO	Fe_2O_3	MgO	CaO	Na_2O	P_2O_5	K_2O	TiO_2	SO_3
DC02_05	97,85	1,36	0,00	0,06	0,17	0,01	0,02	0,02	0,40	0,11	0,02
DC03_2	91,00	4,76	0,02	1,67	0,45	0,13	0,21	0,02	1,18	0,51	0,03
DC03_3	96,82	2,04	0,00	0,10	0,06	0,10	0,08	0,03	0,50	0,20	0,06
DC04_5	97,65	1,35	0,00	0,03	0,08	0,08	0,02	0,04	0,33	0,30	0,07
DC05_2	84,13	4,75	0,08	6,43	0,81	1,90	0,19	0,14	0,93	0,42	0,18
DC05_1	93,15	2,75	0,00	2,35	0,20	0,11	0,12	0,03	0,74	0,36	0,08
DC06_5	98,35	0,90	0,00	0,19	0,03	0,01	0,02	0,01	0,24	0,23	0,01
DC06_4	97,40	1,69	0,00	0,12	0,02	0,04	0,02	0,02	0,42	0,24	0,03
DC06_6	96,85	1,36	0,00	0,45	0,02	0,05	0,05	0,12	0,40	0,16	0,54
DC07_3	81,70	12,35	0,00	2,05	0,72	0,07	0,57	0,04	1,71	0,71	0,07
DC07_2	96,45	2,03	0,02	0,71	0,02	0,11	0,05	0,04	0,09	0,26	0,18
DC07_7	97,88	1,02	0,00	0,13	0,04	0,40	0,02	0,02	0,20	0,19	0,08
DC07_8	95,12	1,95	0,02	2,03	0,28	0,14	0,06	0,03	0,12	0,18	0,06
DC16_1	92,62	4,78	0,00	0,59	0,07	0,13	0,19	0,09	0,58	0,28	0,63
DC18_1	61,45	0,81	0,20	1,60	0,13	35,09	0,10	0,05	0,17	0,18	0,11
DC18_2	86,68	4,40	0,06	1,89	0,16	4,58	0,78	0,05	0,98	0,32	0,02
DC21_1	71,95	8,78	0,15	3,48	0,73	11,20	0,46	0,13	1,75	0,82	0,43
DC21_3	87,36	4,99	0,02	2,63	0,42	2,75	0,34	0,15	0,60	0,52	0,17
DC21_6	96,02	2,09	0,00	0,51	0,04	0,35	0,07	0,03	0,54	0,27	0,03
DC21_7	97,25	1,27	0,00	0,73	0,08	0,13	0,06	0,05	0,17	0,17	0,05
DC22_1	89,27	1,20	0,09	0,31	0,04	8,47	0,02	0,02	0,22	0,17	0,11
DC22_4	98,37	0,88	0,00	0,09	0,02	0,12	0,05	0,02	0,19	0,17	0,06
DC24_2	86,93	6,59	0,00	0,82	0,18	1,47	2,46	0,12	0,75	0,39	0,17
DC24_3	72,98	3,98	0,49	2,32	0,75	17,32	0,97	0,07	0,69	0,33	0,02
DC24_5	83,31	6,56	0,04	1,47	0,44	3,78	2,29	0,12	1,03	0,59	0,30
DC24_9	95,46	2,96	0,00	0,27	0,08	0,07	0,06	0,02	0,85	0,16	0,04
DC25_1	97,28	0,86	0,02	0,76	0,08	0,57	0,06	0,09	0,17	0,04	0,07
DC25_5	92,09	3,26	0,02	1,01	0,09	1,89	0,24	0,27	0,73	0,33	0,03
DC25_6	90,37	3,59	0,00	1,65	0,13	1,89	0,20	0,01	0,92	0,08	1,14
DC26_2	89,06	5,23	0,04	3,05	0,37	0,29	0,10	0,26	1,25	0,26	0,05
DC26_3	97,35	1,82	0,00	0,27	0,05	0,03	0,02	0,01	0,40	0,06	0,01
DC27_1	94,32	3,62	0,00	0,16	0,08	0,09	0,08	0,03	0,93	0,56	0,06
DC27_12	90,41	6,17	0,00	0,50	0,10	0,32	0,12	0,18	1,65	0,42	0,06
DC27_3	93,73	2,49	0,16	2,19	0,06	0,08	0,05	0,11	0,69	0,34	0,03
DC27_4	93,67	3,83	0,00	0,56	0,15	0,19	0,08	0,18	1,00	0,28	0,02
DC27_6	83,65	9,18	0,07	2,83	0,40	0,55	0,21	0,14	2,51	0,36	0,04
DC27_9	89,60	4,10	0,00	3,74	0,64	0,10	0,05	0,05	0,63	0,86	0,06
DC29_6	97,02	2,05	0,00	0,18	0,06	0,09	0,04	0,04	0,20	0,25	0,05
DC39_03	96,44	1,03	0,00	0,70	0,05	0,01	0,02	0,01	0,21	0,41	1,08
DC45_05	94,94	2,16	0,00	1,66	0,20	0,19	0,09	0,10	0,49	0,09	0,07
DC46_12	95,04	1,22	0,00	2,10	0,22	0,17	0,04	0,05	0,09	0,21	0,86
DC51_01	98,30	0,84	0,00	0,40	0,07	0,04	0,02	0,00	0,20	0,08	0,06
DC61_04	97,35	1,54	0,00	0,28	0,07	0,10	0,04	0,05	0,39	0,10	0,07
DC67_05	93,45	3,46	0,00	0,42	0,07	0,82	0,04	0,03	1,03	0,55	0,04
DC68_02	95,68	0,88	0,00	0,13	0,07	2,63	0,02	0,06	0,22	0,30	0,01
DC68_05	94,00	2,09	0,06	2,66	0,11	0,13	0,13	0,04	0,34	0,21	0,17
DC70_01	96,90	2,21	0,00	0,04	0,04	0,01	0,02	0,02	0,67	0,08	0,04
DC71_04	98,74	0,74	0,00	0,09	0,02	0,01	0,02	0,00	0,20	0,19	0,01
DC73_01	89,23	4,04	0,00	2,97	0,30	0,92	1,29	0,03	0,25	0,20	0,74
DC73_02	97,73	0,80	0,00	0,49	0,04	0,15	0,02	0,05	0,22	0,28	0,14
DC73_06	98,54	0,91	0,00	0,14	0,02	0,01	0,02	0,00	0,25	0,10	0,03
DC74_03	97,08	1,08	0,00	0,45	0,07	0,01	0,04	0,02	0,25	0,47	0,51
DC75_01	93,88	2,43	0,00	0,88	0,17	1,22	0,69	0,04	0,31	0,13	0,24
DC75_02	98,11	0,46	0,00	0,31	0,06	0,35	0,16	0,05	0,06	0,24	0,11
DC75_03	96,33	0,72	0,12	1,85	0,12	0,32	0,02	0,28	0,11	0,02	0,10
DC75_05	95,55	2,01	0,00	0,51	0,11	0,38	0,08	0,05	0,57	0,46	0,23
DC77_04	88,30	6,33	0,06	2,35	0,22	0,20	0,15	0,21	1,59	0,46	0,04
HA-5827	93,02	3,43	0,02	0,65	0,18	0,25	0,06	0,13	1,04	0,78	0,31
HA-5842	89,58	5,82	0,02	1,36	0,29	0,16	1,31	0,09	0,71	0,50	0,09
HA-5847	99,31	0,25	0,00	0,10	0,02	0,01	0,09	0,00	0,09	0,04	0,05
HA-5848	96,95	0,90	0,02	1,67	0,09	0,01	0,09	0,02	0,04	0,09	0,08
HA-5855	95,82	0,71	0,00	0,97	0,08	0,15	0,17	0,00	0,10	0,07	1,90
ATS-001	91,94	3,60	0,00	1,34	0,18	0,62	0,91	0,03	0,62	0,48	0,18
ATS-002	89,34	5,29	0,02	1,50	0,33	0,13	2,69	0,08	0,26	0,23	0,05

Sample	X-Ray Fluorescence% Components										
	SiO_2	Al_2O_3	MnO	Fe_2O_3	MgO	CaO	Na_2O	P_2O_5	K_2O	TiO_2	SO_3
ATS-007	98,11	1,14	0,00	0,06	0,04	0,07	0,06	0,01	0,18	0,20	0,08
ATS-016	97,46	1,34	0,00	0,43	0,06	0,12	0,02	0,10	0,33	0,07	0,05
ATS-023	97,78	1,31	0,00	0,07	0,06	0,12	0,11	0,03	0,37	0,07	0,05
ATS-072	93,46	2,15	0,02	1,20	0,16	1,41	0,19	0,04	0,41	0,24	0,62
ATS-151	92,55	3,01	0,03	2,20	0,73	0,16	0,07	0,21	0,55	0,27	0,15
ATS-190	98,03	0,85	0,00	0,28	0,18	0,28	0,04	0,19	0,12	0,02	0,03
ATS-195	96,11	1,31	0,00	0,90	0,13	0,58	0,35	0,04	0,14	0,23	0,06
ATS-302	95,26	1,40	0,00	0,33	0,02	0,14	0,55	0,04	0,58	0,36	1,11
ATS-308	97,56	1,50	0,00	0,28	0,06	0,01	0,05	0,01	0,36	0,11	0,03
ATS-310	98,19	0,96	0,00	0,07	0,03	0,03	0,07	0,02	0,28	0,10	0,14
CoB.K26.37.5	90,09	3,83	0,00	1,18	0,25	1,06	0,98	0,91	0,66	0,51	0,15
CoB.K26.37.9	85,12	7,70	0,04	1,18	0,40	0,68	1,68	0,49	1,35	0,61	0,19
CoB.J27.38.11	92,95	3,00	0,03	0,59	0,18	0,70	0,85	0,37	0,56	0,07	0,16
CoB.K26.37.22	93,23	3,24	0,00	0,64	0,20	0,20	0,80	0,22	0,72	0,13	0,10
CoB.K26.37.23	93,01	3,34	0,03	0,67	0,24	0,47	0,81	0,24	0,54	0,09	0,16
CoB.J26.38.46	91,06	2,35	0,00	2,93	0,36	0,11	0,02	0,07	0,15	0,18	0,08
CoB.K26.37.155	89,86	4,29	0,00	0,34	0,26	0,15	0,72	0,17	0,51	0,26	0,08
CoB.K26.37.201	93,03	2,86	0,02	0,84	0,40	0,20	1,16	0,23	0,22	0,29	0,11
CoB.J26.38.530	87,17	4,91	0,05	1,53	0,40	0,69	0,90	1,01	0,71	0,41	0,16
CoB.J26.38.540	98,26	0,50	0,00	0,10	0,05	0,09	0,23	0,01	0,12	0,36	0,05
CoB.J26.38.574	85,90	1,67	0,08	1,81	0,13	1,07	0,09	1,55	0,46	0,47	0,19
Tr-1-18	99,37	0,19	0,00	0,13	0,04	0,03	0,02	0,03	0,04	0,05	0,09
Tr-128-5	98,48	0,26	0,00	0,27	0,02	0,30	0,02	0,02	0,02	0,10	0,04
Tr-129-2-4	99,54	0,13	0,00	0,08	0,02	0,01	0,04	0,01	0,02	0,12	0,04
Tr-1-33	99,11	0,07	0,00	0,12	0,02	0,16	0,02	0,00	0,02	0,11	0,02
Tr-161-2-3	99,63	0,09	0,00	0,19	0,02	0,01	0,02	0,00	0,02	0,06	0,02
TR-161-2b-2	99,37	0,12	0,00	0,18	0,08	0,01	0,02	0,01	0,02	0,10	0,07
TR-161-2b-6	99,63	0,12	0,00	0,13	0,02	0,01	0,02	0,01	0,02	0,05	0,03
TR-222-12	99,40	0,15	0,00	0,27	0,02	0,04	0,02	0,02	0,02	0,10	0,01
TR-223-3-2	99,57	0,11	0,00	0,09	0,02	0,01	0,02	0,06	0,02	0,13	0,02
TR-254-2	99,66	0,06	0,00	0,17	0,02	0,04	0,02	0,00	0,02	0,05	0,01
ES-254 (Nvl-XIII)	98,46	0,71	0,00	0,25	0,05	0,05	0,10	0,03	0,13	0,10	0,05
ES-290 (Nvl-XIII)	96,66	1,73	0,00	0,51	0,12	0,07	0,12	0,03	0,50	0,13	0,07
ES-315 (Nvl-XIII)	95,83	1,17	0,00	0,13	0,06	0,01	0,09	0,04	0,35	1,95	0,09
ES-378 (Nvl-XIII)	97,27	0,84	0,03	0,41	0,06	0,49	0,09	0,29	0,29	0,13	0,05
ES-407 (Nvl-XIII)	98,15	0,66	0,00	0,21	0,04	0,10	0,19	0,03	0,17	0,20	0,12
ES-411 (Nvl-XIII)	98,16	0,83	0,00	0,14	0,05	0,06	0,22	0,02	0,29	0,07	0,04
ES-413 (Nvl-XIII)	96,35	1,14	0,00	0,44	0,05	0,48	0,07	0,02	0,33	0,06	0,06
ES-419 (Nvl-XIII)	97,35	0,70	0,00	0,41	0,08	0,27	0,23	0,24	0,26	0,20	0,11
ES-435 (Nvl-XIII)	97,27	1,53	0,00	0,19	0,06	0,01	0,06	0,04	0,47	0,31	0,04
ES-441 (Nvl-XIII)	96,81	1,68	0,00	0,21	0,06	0,01	0,02	0,02	0,52	0,48	0,05
ES-245 (Nvl-XXII)	97,92	0,77	0,00	0,11	0,05	0,06	0,02	0,03	0,23	0,48	0,08
ES-255 (Nvl-XXII)	94,57	2,46	0,00	1,46	0,38	0,07	0,24	0,03	0,55	0,18	0,02
ES-263 (Nvl-XXII)	94,68	2,31	0,00	1,29	0,35	0,11	0,04	0,13	0,74	0,23	0,07
ES-265 (Nvl-XXII)	97,97	1,05	0,00	0,22	0,05	0,01	0,15	0,01	0,28	0,12	0,06
ES-293 (Nvl-XXII)	97,76	1,04	0,00	0,40	0,06	0,11	0,08	0,08	0,29	0,02	0,02
ES-328 (Nvl-XXII)	95,94	2,11	0,00	0,50	0,09	0,05	0,12	0,05	0,66	0,32	0,07

Table-5.17: Table showing the results of X-Ray Fluorescence of "archaeological quartzites". All data as wt. % oxides.

K_2O is present in every sample in diverse percentages (M = 0.47%, SD = 0.43). Its abundance ranges from minimum values of 0.02% to a maximum of 2.51%. Samples collected during geological surveys (M = 0.60%, SD = 0.06) and those chosen from archaeological sites (M = 0.28%, SD = 0.03) are clearly different according to their variance and mean: t(89) = -3.36, p = 0.001. Levene's test indicated unequal variances (F = 10.341, p = 0.002), so degrees of freedom were adjusted from 109 to 89. There is a higher variability and abundance of K_2O among the samples coming from geological surveys than among those from archaeological sites.

TiO_2 is present in every sample with small and diverse percentages (M = 0.26%, SD = 0.24). Its abundance is always small, with values from 0.02% to 1.95%. The samples collected from geological surveys and those coming from archaeological sites are similar according to their variance and mean: t(109) = -1.08, p = 0.28.

P_2O_5 is present in almost every sample with small and diverse percentages (M = 0.10%, SD = 0.20). Only eight samples have no P_2O_5 at all. In the cases where Phosphorous pentoxide is present

its abundance is variable, ranging from minimum values of 0.01% to maximum values of 1.55%. The samples collected during geological surveys (*M* = 0.07%, *SD* = 0.01) and those coming from archaeological sites (*M* = 0.14%, *SD* = 0.27) are clearly different according to their variance, as indicated by Levene's test (*F* = 12.10, *p* = 0.001). For this reason degrees of freedom were adjusted from 109 to 89. Meanwhile, there are no significant differences between their means *t*(59) = 1.85, *p* = 0.07. There is higher variability of P_2O_5 among samples coming from archaeological sites than among those from geological surveys, which can probably be explained by the different sedimentological composition of the archaeological layers.

Finally, SO_3 is present in every sample in small and diverse percentages (*M* = 0.16%, *SD* = 0.28). Its abundance is always small and reduced to values from 0.01% to 1.90%. The samples collected during geological surveys and those coming from archaeological sites are similar according to their variance and mean: *t*(109) = -0.51, *p* = 0.61.

Once each main component detected by X-Ray Fluorescence is understood, we tried to explain the relationships between the elements through a Pearson bivariate correlation matrix (Table-5.18). It is clear that the presence of silicon dioxide, as the main component, is negatively related to the all other components, except for sulphur trioxide. The latter is not significantly related with any other component, as a consequence of its very small presence. Although calcium oxide is present in every sample, it is only correlated with iron and manganese oxides. This last one is positively correlated with iron, magnesium and potassium oxides. The others components, that is, aluminium oxide, iron(III) oxide, magnesium oxide, potassium oxide and sodium oxide are positively correlated with each other, with the exception of phosphorous pentoxide and titanium dioxide.

		SiO_2	Al_2O_3	Fe_2O_3	MnO	MgO	CaO	Na_2O	K_2O	TiO_2	P_2O_5	SO_3
SiO_2	Pearson's r	1	-,682**	-,627**	-,666**	-,678**	-,751**	-,437**	-,572**	-,364**	-,287**	-,091
	Sig.		,000	,000	,000	,000	,000	,000	,000	,000	,002	,340
Al_2O_3	Pearson's r	-,682**	1	,552**	,216*	,708**	,095	,543**	,871**	,454**	,224*	,033
	Sig.	,000		,000	,022	,000	,321	,000	,000	,000	,018	,730
Fe_2O_3	Pearson's r	-,627**	,552**	1	,404**	,781**	,217*	,203*	,448**	,259**	,203*	,140
	Sig.	,000	,000		,000	,000	,022	,033	,000	,006	,033	,144
MnO	Pearson's r	-,666**	,216*	,404**	1	,430**	,695**	,152	,208*	,096	,153	-,051
	Sig.	,000	,022	,000		,000	,000	,110	,028	,314	,109	,598
MgO	Pearson's r	-,678**	,708**	,781**	,430**	1	,229*	,394**	,538**	,357**	,216*	,012
	Sig.	,000	,000	,000	,000		,016	,000	,000	,000	,023	,904
CaO	Pearson's r	-,751**	,095	,217*	,695**	,229*	1	,099	,073	,058	,003	,007
	Sig.	,000	,321	,022	,000	,016		,299	,449	,545	,976	,945
Na_2O	Pearson's r	-,437**	,543**	,203*	,152	,394**	,099	1	,243*	,188*	,222*	,085
	Sig.	,000	,000	,033	,110	,000	,299		,010	,048	,019	,378
K_2O	Pearson's r	-,572**	,871**	,448**	,208*	,538**	,073	,243*	1	,441**	,198*	-,007
	Sig.	,000	,000	,000	,028	,000	,449	,010		,000	,037	,939
TiO_2	Pearson's r	-,364**	,454**	,259**	,096	,357**	,058	,188*	,441**	1	,158	,036
	Sig.	,000	,000	,006	,314	,000	,545	,048	,000		,098	,704
P_2O_5	Pearson's r	-,287**	,224*	,203*	,153	,216*	,003	,222*	,198*	,158	1	-,021
	Sig.	,002	,018	,033	,109	,023	,976	,019	,037	,098		,826
SO_3	Pearson's r	-,091	,033	,140	-,051	,012	,007	,085	-,007	,036	-,021	1
	Sig.	,340	,730	,144	,598	,904	,945	,378	,939	,704	,826	

Table-5.18: Table derived from the bivariate Pearson's correlation from the components analysed through X-Ray fluorescence. * = Correlation is significant at 0.05 (2-tailed). ** = Correlation is significant at 0.01.

To finish, we create a PCA (Figure-5.18 and Table-5.19) with the aim of better understanding the behaviour of the variables. The first two components explain the 97.68% of the variance. The main differences are based on the quantity of silicon dioxide, calcium oxides and aluminium oxide. Secondary differences are related to the quantity of manganese oxide, sodium oxide and phosphorous pentoxide. Finally, SO_3, TiO_2, K_2O, MgO and Fe_2O_3 have no statistical weight in the variance expressed by the first two principal components.

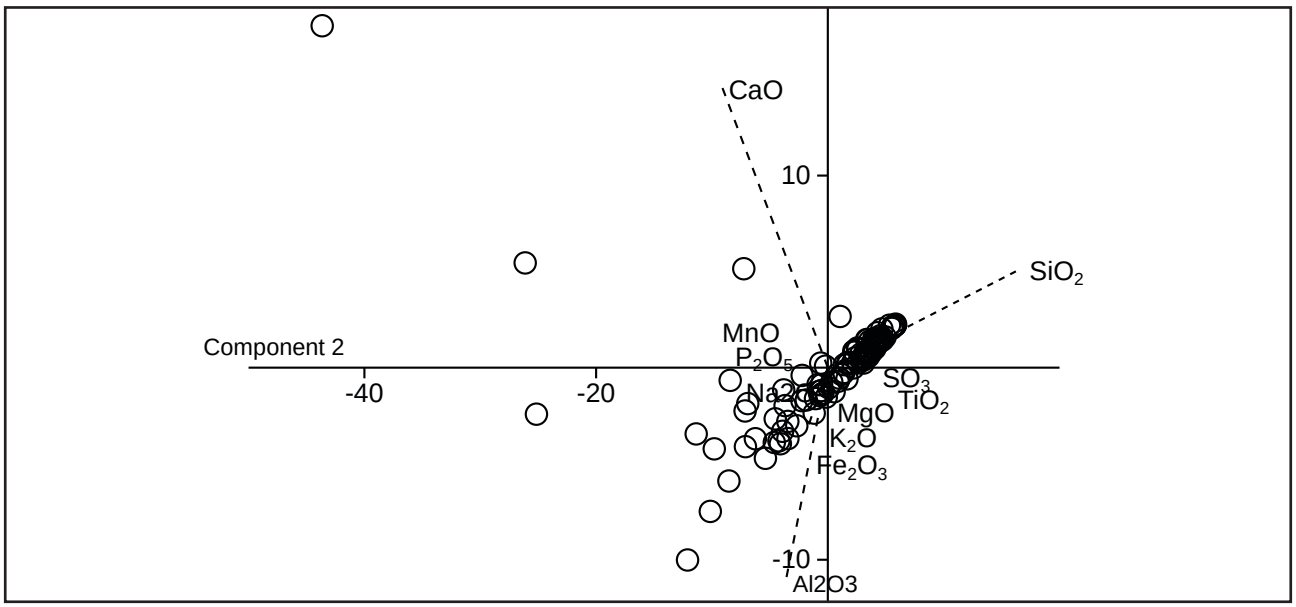

Figure-5.18: Scatter plot results of the PCA of the components of the X-Ray Fluorescence, showing PC1 and PC2.

	Principal component 1	Principal component 2
SiO_2	0,858	0,265
Al_2O_3	-0,186	-0,570
MnO	-0,085	-0,154
Fe_2O_3	-0,006	0,004
MgO	-0,016	-0,031
CaO	-0,469	0,751
Na_2O	-0,028	-0,069
P_2O_5	-0,031	-0,099
K_2O	-0,011	-0,031
TiO_2	-0,007	-0,019
SO_3	-0,003	-0,006
Eigenvalue	48,097	8,269
% variance	83,353	14,330

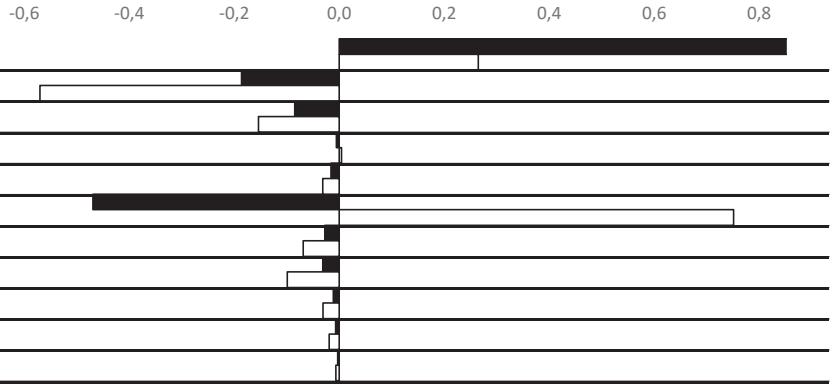

Table-5.19: Loading of each component detected by X-Ray Fluorescence on each axis generated by the PCA.

5.3. UNDERSTANDING "ARCHAEOLOGICAL QUARTZITE" VARIABILITY THROUGH PETROGENESIS: DEFINITION OF GROUPS AND TYPES

The characterisation of texture and packing of "archaeological quartzites"; the description and quantification of their quartz grains features; their textural relationships, determined by their size, shape and orientation; the mineral detection through petrography; and, finally, the geochemical characterisation provide diagnostic information and associations of characters enabling the identification of diagenetic and metamorphic processes conducting to the genesis of "archaeological quartzites". The types of quartzite can be grouped through a gradation that relates petrogenesis with a series of petrographic characters, in accordance with several geological studies (Bastida, 1982; Folk, 1980; Hirth and Tullis, 1992; Howard, 2000, 2005; Skolnick, 1965; Stipp et al., 2002; Wilson, 1973). In this way, we identified seven types of quartzite according to their petrogenetic stages that can be assorted into three main groups. The first two types belong clearly to the sedimentary realm and consist of quartz-arenite or sandstone. The third and fourth types can be included into the group of the orthoquartzites and, although they are sedimentary, their textures display deformations in the quartz grains. The last three types correspond to clearly metamorphic origins and, therefore, it is appropriate to name them as quartzites. Summing up, the petrogenetic types are the following:

Clastic and Cemented Quartz-Arenite, CC: It is characterised by clastic texture with matrix or cement and floating or punctual packing. The presence of detrital quartz grains is big, although it is possible to observe some other features, such as grains with concavo-convex limits in zones where grains are adjacent. In addition, it is possible to recognise quartz grains or fragments from deformed rocks with metamorphic features, for example stylolites quartz grain limits, deformation lamellae or mortar textures. It corresponds to the immature stage or sub-mature quartz-arenites of Folk (1980).

Clastic Grained Quartz-Arenite, CA: It is characterised by clastic texture and tangent or complete packing. The grain boundaries are made of flat or slightly concave-convex surfaces, adapted to the characteristics of the contiguous grains. The quartz grains that form this type, lack elements indicating metamorphic stress and quartz grains are mostly clastic. As the previously defined type, it is possible to recognise grains or fragments from deformed rocks with metamorphic features. It corresponds to the sub-mature, mature and super-mature quartz-arenites of Folk (1980).

Syntaxially Overgrown Orthoquartzite, OO: It is characterised by clastic grained texture and tangent-complete or complete packing. This type of orthoquartzite and the following type represent more advanced diagenetic stages of cementation and/or deformation by lithostatic pressure, with gradual steps towards changes by metamorphism. The quartz grains in this texture display syntaxial cement which grows in optical continuity over the original grain, adapting to the spaces between contiguous grains, and some grains may appear slightly deformed. Syntaxial overgrowth may generate large protrusions in the boundaries of the grains with concave-convex planes. This texture is produced by diagenetic processes or low-grade regional metamorphism, with little effect on the quartz or rock texture. It corresponds to microstructure A in the detrital grain quartzite of Wilson (1973) or the scarcely deformed quartzite of Bastida (1982).

Sutured Grain Orthoquartzite, SO: It is characterised by clastic grained texture and complete-sutured to completely sutured packing. The quartz grain boundaries are clearly deformed by an increase in pressure. This type of contact between grains can lead to microstylolitic forms and sporadically to bulges, which may lead to the appearance of new recrystallized grains of smaller size, although in very small proportions. The presence of the original morphology of detrital grains is insignificant, unlike the grains with syntaxial cement, also accompanied by a sutured texture. The quartz grains display clear undulatory extinction, in many cases generating deformation lamellae. It is possible to observe some microfissures inside the quartz grains. It corresponds to the detrital grain type B of Wilson (1973) and the quartzite with deformed and slightly or non-recrystallized grains of Bastida (1982).

Bulging Recrystallized Quartzite, BQ: It is characterised by the presence of mortar texture and suturated packing. There is a combination of two grain types that are clearly different. One consists of the old grains with signs of metamorphic deformation, with sutured edges, microfractures, undulose extinction and Böhm lamellae. These are surrounded by new very small, undeformed recrystallized grains, which are grouped around the old grains and occasionally in their fracture zones. They do not display signs of metamorphic stress and appear in variable amounts, usually without exceeding 50% of the sample. They are formed by processes of mi-

gration of the grain boundaries, which generate serrated boundaries or a microstylolitic texture. When these boundaries break, new grains are generated. They are formed under metamorphic conditions at low to medium temperatures (250-400 ˚C; Stipp et al. 2002) and low pressure. They correspond to part of the quartzite types with foam texture described by Howard (2005), microstructure regime 1 of Hirth and Tullis (1992) and the BLG of Stipp et al. (2002).

S**ubgrain Rotation Recrystallized Quartzite, RQ**: This type is characterised by the presence of mortar texture and suturated packing. It is related with the previous petrogenetic type by the presence of two different grain types. The old quartz grains display serrated and concave-convex edges and small recrystallized grains, clearly more abundant than in the previous type. They are formed by the recrystallization of grains associated with migration processes of the grain boundaries and accompanied by the rotation of their bulging edges. These characteristics derive from an increase in pressure and temperature (400-500 ˚C; Stipp et al. 2002) and correspond to the types described by Howard (2005) with mortar texture, microstructure regime 2 of Hirth and Tullis (1992) and the SGR of Stipp et al. (2002).

Grain Boundary Migration Recrystallized Quartzite, MQ: This type is characterised by the presence of a clastic grained texture (more related with foam texture) and suturated packing. There is high presence of recrystallised grains that make it impossible to differentiate between the original grains and those formed by metamorphic recrystallization, which is more important than in the previous types. There is almost no indication of the grains to have suffered metamorphic deformation processes, as they have been erased by the general recrystallization that affecting the rock. The boundaries between new grains are easily recognisable, with suturated to interdigitated forms. The small quantity of old grains are suturated and most of them exhibit deformation lamellae. The type of crystallisation that has led to this microstructural type occurred at relatively high temperature (>500 ˚C; Stipp et al. 2002). This, and the pressure effect, caused conditions favouring very rapid migration of the boundaries and their fracture due to rotation processes or rapid migration. They correspond to part of the types of grain enlargement described by Wilson (1973) and Bastida (1982), the microstructure regime 3 of Hirth and Tullis (1992) and the GBM of Stipp et al. (2002).

Principal Components Analysis, based on the quantification of quartz grains and supported by textural and packing criteria (only used for graphic representation), helped us visualise the proposed petrogenetic types (Figure-5.19 and Table-5.20). In addition, it reinforced the previously commented association of features understood through petrogenesis. The first two axes explain 69.82% of the variance and the first four 93.36%. This association of quartz grain features, texture and packing is also important to understand the features that could be analysed through non-destructive microscopic characterisation.

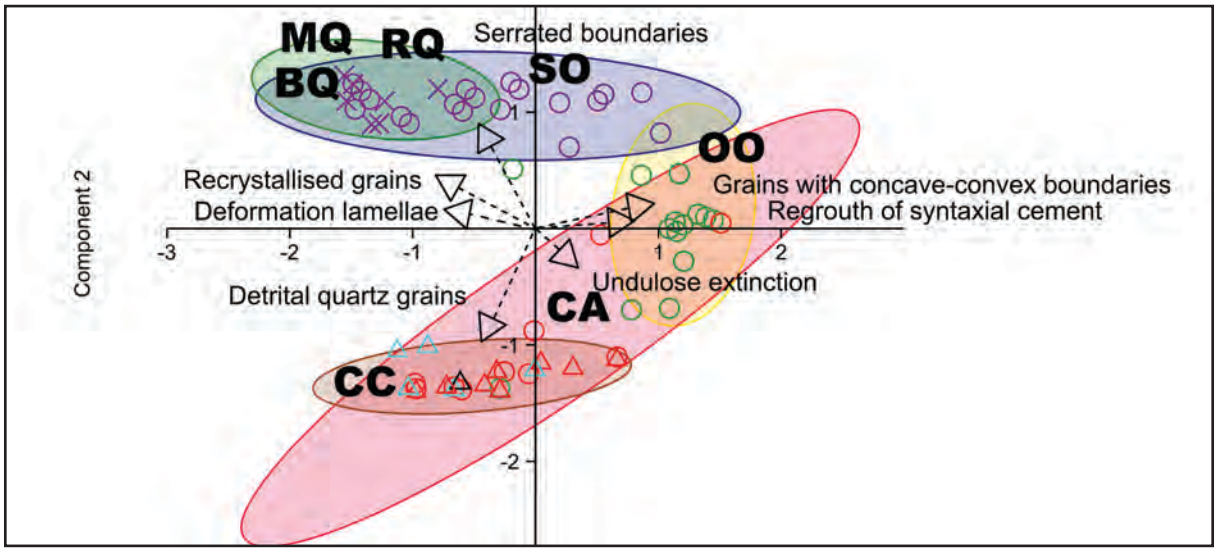

Figure-5.19: Scatter plot result of the PCA of the quantitative information about the features of quartz grains. 95% confidence ellipses are depicted for each petrogenesis type. Note that the 95% grouping ellipses of types MQ and RQ are not represented due to the reduced number of samples available (only two and three respectively). Different symbols represent texture categories: triangles for clastic texture with matrix or cement, circles for clastic grained texture and crosses for mortar texture. Different colours symbolise packing categories: black for floating packing, light blue for punctual packing, red for tangential packing, green for complete packing and purple for suturated packing.

	PC 1	PC 2	PC 3	PC 4
Detrital quartz grains	-0,216	-0,722	-0,208	-0,057
Undulose extinction on thin section quartzite	0,116	-0,046	0,941	-0,070
Regrowth of quartz syntaxial cement	0,576	0,026	-0,098	0,759
Grains with concave-convex boundaries	0,669	0,130	-0,193	-0,637
Stylolites or serrated boundaries	-0,283	0,622	-0,140	0,013
Deformation lamellae	-0,131	0,127	-0,050	-0,062
Recrystallised grains	-0,252	0,236	0,057	0,077
Eigenvalue	3,451	3,191	1,573	0,667
% variance	36,278	33,551	16,538	7,015

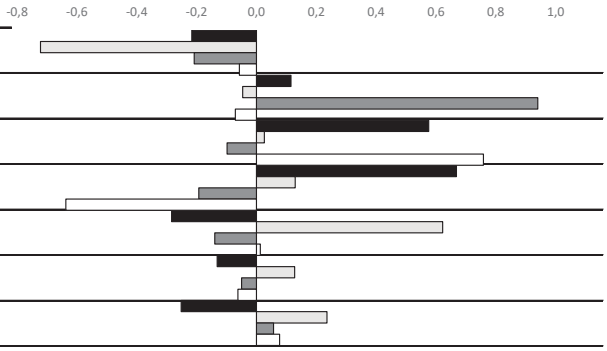

Table-5.20: Loading of each quartz grain features on each axis generated by the PCA. Only the first four principal components are shown.

Once the types are defined, we will discuss their characterisation and influence on quartz grain size, morphology and orientation and also on the presence of non-quartz minerals and chemical composition by X-Ray fluoresce.

The size and morphology of quartz grains is clearly influenced by the petrogenetic types of quartzite, according to the comparison of means and variance. Levene's test from the four variables (size synthetized by minor axis, classification of size using Udden-Wentworth scale, circularity and roundness) reveals different variance between groups: Levene's test of minor axis $F = 79.945$, $p < 0.001$; Levene's of U-W scale $F = 175.749$, $p < 0.001$; Levene's test of circularity $F = 135.319$, $p < 0.001$; Levene's test of roundness $F = 6.930$, $p < 0.001$. *H* Kruskal Wallis test also shows differences between the variance of different petrogenetic types: *H* for minor axis $\chi 2$ (6, N = 18855) = 3067.057, $p < 0.001$; *H* for Udden-Wentworth scale $\chi 2$ (6, N = 18855) = 3137.265, $p < 0.001$; *H* for circularity $\chi 2$ (6, N = 18855) = 580.913, $p < 0.001$; *H* for roundness $\chi 2$ (6, N = 18855) = 348.350, $p < 0.001$. (Table-5.21 and Figure-5.20). Quartz grain orientation is also influenced by the petrogenetic types, as revealed by $\chi 2$ (6, N = 118) = 27.319, $p < .001$. Standardized residues analysis shows the petrogenetic types with significant preferred orientation (Figure-5.21).

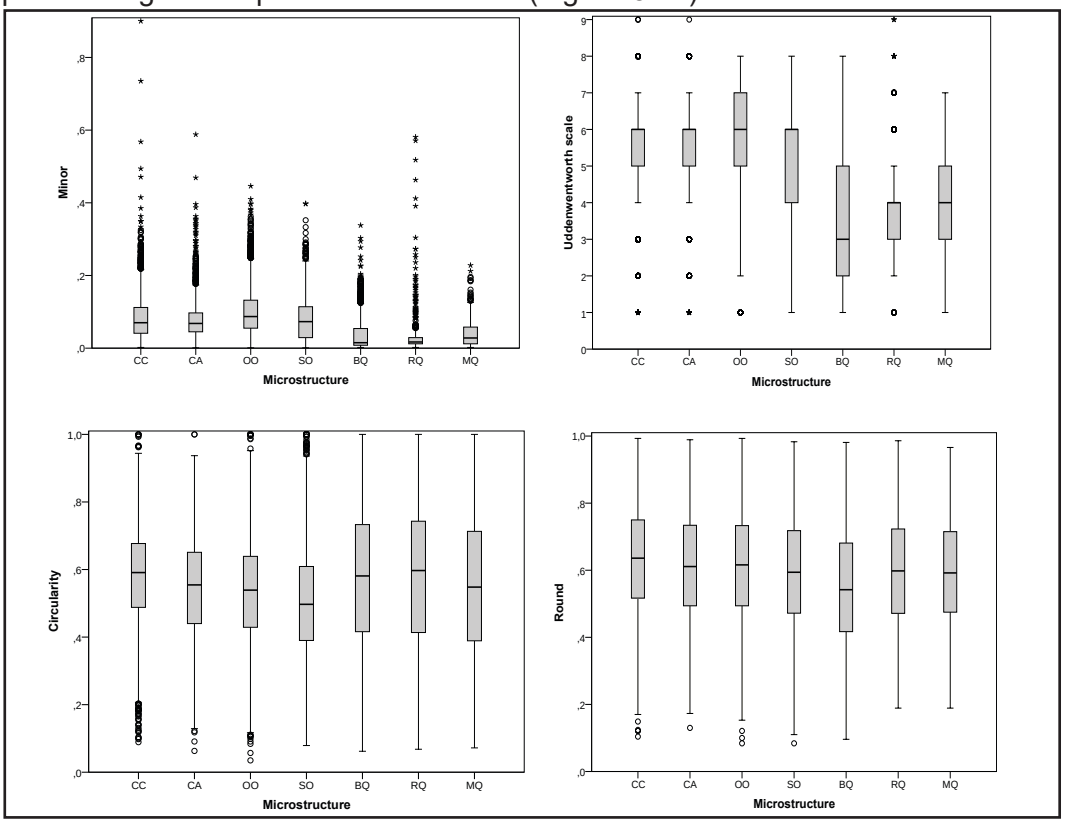

Figure-5.20: Four boxplots representing size and morphology of quartz grains for each petrogenetic type (Microstructure). Size is analysed using the measurements of the minor axis, afterwards classified applying Udden-Wentworth categories (1 for clay, 9 for coarse sand). Morphology is synthetized through the circularity and roundness indexes.

		Minor	Udden-Wentorth	Circularity	Round
Clastic and Cemented Quartz-Arenite	Mean	,08340	5,4995	,57483	,62966
	Median	,07000	6,0000	,59100	,63600
	Variance	,004	1,546	,020	,026
	Std. Deviation	,060389	1,24323	,142470	,161008
	Minimum	,002	1,00	,089	,104
	Maximum	,900	9,00	1,000	,993
	Range	,898	8,00	,911	,889
	Interquartile Range	,071	1,00	,189	,233
	Skewness	2,154	-,815	-,441	-,194
	Kurtosis	14,245	,856	,149	-,454
Clastic Grained Quartz-Arenite	Mean	,07867	5,4609	,54197	,61271
	Median	,06800	6,0000	,55450	,61100
	Variance	,003	1,398	,022	,026
	Std. Deviation	,055428	1,18218	,149922	,162405
	Minimum	,001	1,00	,063	,130
	Maximum	,588	9,00	1,000	,989
	Range	,587	8,00	,937	,859
	Interquartile Range	,052	1,00	,211	,240
	Skewness	2,204	-1,073	-,254	-,067
	Kurtosis	9,127	2,095	-,221	-,579
Syntaxially Overgrown Orthoquartzite	Mean	,09723	5,7546	,52998	,61364
	Median	,08700	6,0000	,53900	,61600
	Variance	,004	1,625	,023	,027
	Std. Deviation	,061449	1,27471	,151574	,165173
	Minimum	,001	1,00	,035	,084
	Maximum	,446	8,00	1,000	,993
	Range	,445	7,00	,965	,909
	Interquartile Range	,077	2,00	,210	,239
	Skewness	1,012	-1,250	-,163	-,083
	Kurtosis	1,490	2,057	-,128	-,545
Sutured Grain Orthoquartzite	Mean	,07808	5,1764	,50609	,59634
	Median	,07300	6,0000	,49700	,59400
	Variance	,003	2,786	,028	,028
	Std. Deviation	,057063	1,66902	,166643	,168507
	Minimum	,001	1,00	,079	,084
	Maximum	,398	8,00	1,000	,983
	Range	,397	7,00	,921	,899
	Interquartile Range	,085	2,00	,219	,246
	Skewness	,762	-,937	,380	-,025
	Kurtosis	,683	-,037	,060	-,611

		Minor	Udden-Wentorth	Circularity	Round
Bulging Recrystallized Quartzite	Mean	,03662	3,7557	,57262	,54913
	Median	,01500	3,0000	,58100	,54200
	Variance	,002	2,827	,041	,031
	Std. Deviation	,043492	1,68140	,201430	,176796
	Minimum	,002	1,00	,062	,096
	Maximum	,338	8,00	1,000	,981
	Range	,336	7,00	,938	,885
	Interquartile Range	,046	3,00	,317	,264
	Skewness	1,910	,343	-,191	,133
	Kurtosis	4,288	-,949	-,826	-,675
Subgrain Rotation Recrystallized Quartzite	Mean	,03350	3,7705	,57242	,59547
	Median	,01700	4,0000	,59700	,59800
	Variance	,003	1,824	,047	,029
	Std. Deviation	,057172	1,35061	,215920	,169206
	Minimum	,002	1,00	,068	,189
	Maximum	,581	9,00	1,000	,986
	Range	,579	8,00	,932	,797
	Interquartile Range	,017	1,00	,330	,252
	Skewness	5,516	,887	-,399	-,057
	Kurtosis	39,145	1,225	-,696	-,648
Grain Boundary Migration Recrystallized Quartzite	Mean	,04143	4,2186	,54842	,59348
	Median	,02800	4,0000	,54800	,59200
	Variance	,002	2,262	,037	,026
	Std. Deviation	,039081	1,50401	,191788	,161266
	Minimum	,002	1,00	,072	,189
	Maximum	,228	7,00	1,000	,966
	Range	,226	6,00	,928	,777
	Interquartile Range	,047	2,00	,324	,241
	Skewness	1,679	-,244	-,017	-,051
	Kurtosis	3,151	-,693	-,914	-,576

Table-5.21: Descriptive statistics of quartz grain size and morphology for each petrogenetic type.

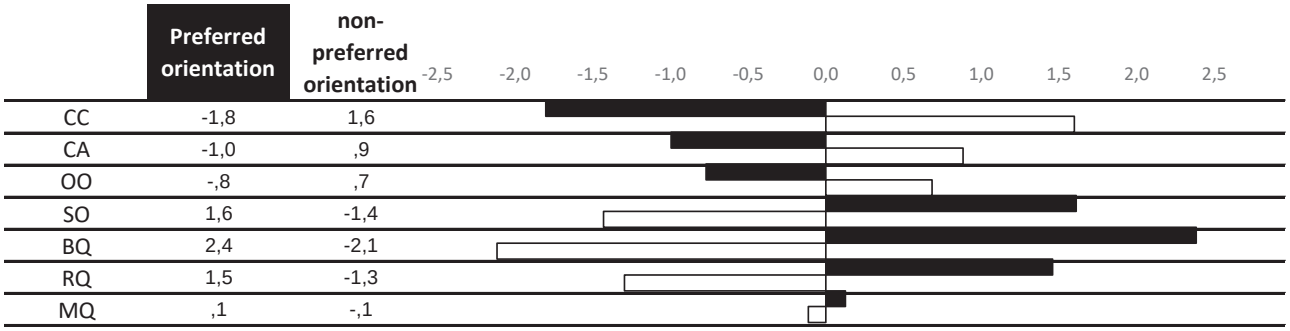

Figure-5.21: Standardised residues derived from χ2 test of the samples with preferred orientation, showing the weight of each category in the different petrogenetic types.

Within the group of quartz-arenite, the types clastic and cemented quartz-arenite and clastic grained quartz-arenite are similarly distributed according to the commented parameters. Most of the quartz grains are situated around sizes of 0.07 mm with very high kurtosis and clearly positive skewness, as most of the quartz grains are situated within the values of very fine sand. It is important to note the presence of big grains as outliers in both petrogenetic types, clearer in the CC type (e.g. DC16_01 for CC or DC07_07 for CA in S.I.-I). The presence of a matrix in the samples (represented by the values from clay to medium silt) is obvious, and shows general continuity with the values of the minor axis and the roundness and circularity indexes (e.g. samples DC27_03 and DC03_02 in S.I.-I). In general, and keeping in mind small differences, the roundness index shows more elongated forms for the secondary matrix, as a consequence of its adaptation to the framework grains (Figure-5.22). This is more evident in the type CA than in the type CC, because of its specific packing characteristics. Meanwhile, the circularity index reveals that the matrix is slightly more regular than the framework grains. This is a clear difference with other petrogenetic types such as BQ or RQ types. Coming to the orientation of quartz grains, there are clear differences between these two petrogenetic types and the more deformed ones. Some samples exhibit a preferred orientation due to sedimentary bedding.

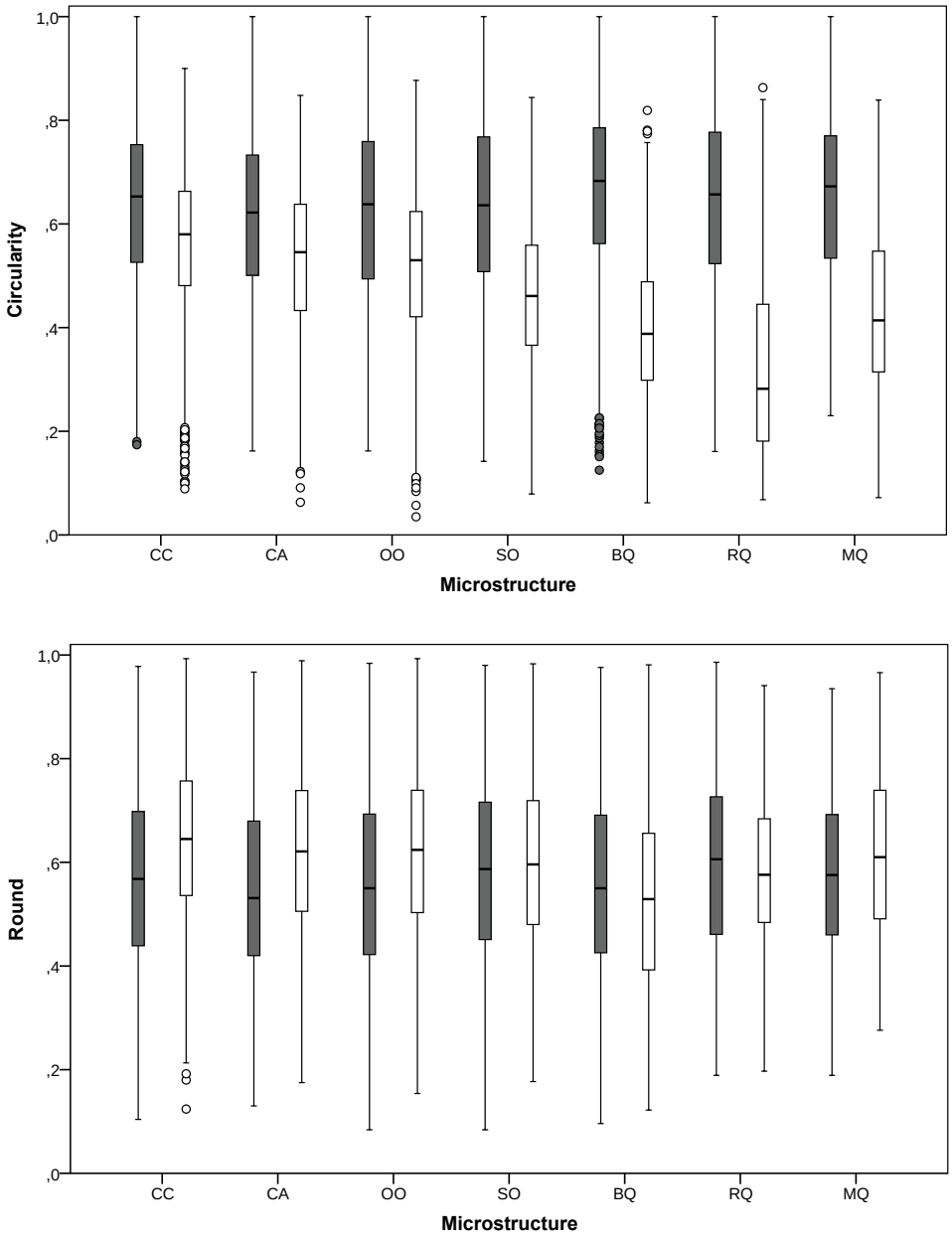

Figure-5.22: Double boxplot showing the distribution of circularity and roundness indexes of quartz grains for each petrogenetic type and grouped by type of matrix. Primary matrix in white for grains bigger than or equal in size to U-W category of coarse silt and secondary matrix in grey for grains smaller than or equal in size to U-W category of medium silt.

In the group of orthoquartzites, both types are different from each other according to their size and morphology. Syntaxially overgrown orthoquartzite is clearly different from any other type based on quartz grain size as a consequence of the quartz overgrowths that fill the holes between grains. Its circularity values are slightly smaller than in the previous group due to the modification of the original quartz grains. Nevertheless, their roundness index values are similar. Remains of matrix are still present, generally exhibiting similar size and morphology to the ones observed in the previous types (e.g. DC39_03, in S.I.-I). The preferred orientation of the type OO is uncommon and it only appears in a few deformed samples or in those that still exhibit bedding as a consequence of the primary sedimentary conditions.

The type of suturated grained orthoquartzite is distinctively different from the previous type. The size of the particles is smaller than in the previous type and they are more related with the size of the group of quartz-arenites. The morphology of the grains clearly differs from the previous type, with smaller circularity and roundness values as a consequence of the increase of the deformation process. The differences in circularity of the particles between the framework grains and the matrix are emphasized by the appearance, in some of the samples, of new non-deformed grains, similar on grain size than matrix (<5% of the sample). This situation evidences the starting point of the recrystallization processes (i.e. ATS-302 in S.I.-I). In this type the original matrix is still present, generating similar roundness indexes for both matrix and framework grains (lower roundness values than in previous types) (e.g. ATS-190 in S.I.-I, without recrystallised grains). Preferred orientation is major in this group as a consequence of deformation and processes related with metamorphic schistosity.

The three types of the quartzite group do also show differences in quartz grain size and morphology when compared to the previous groups due to the recrystallization generated by metamorphic process. Bulging recrystallised quartzite exhibits two clear modes in the distribution of grain size and morphology (Figure-5.23). The new, small and recrystallised quartz grains display high values of circularity and roundness and, considering size, are grouped around fine silt (e.g. ATS-016 in S.I.-I). The old grains are similar in size to the previously commented types, but they are more deformed, as shown by circularity and roundness indexes. The presence of these two modes generates, in general, a decrease of the mean of the minor axis and Udden-Wentworth scale, while the means for circularity and roundness values increase. Schistosity is present as a consequence of the rise of pressure, as demonstrated by the preferred orientation (most of the samples) and the small roundness index of the matrix.

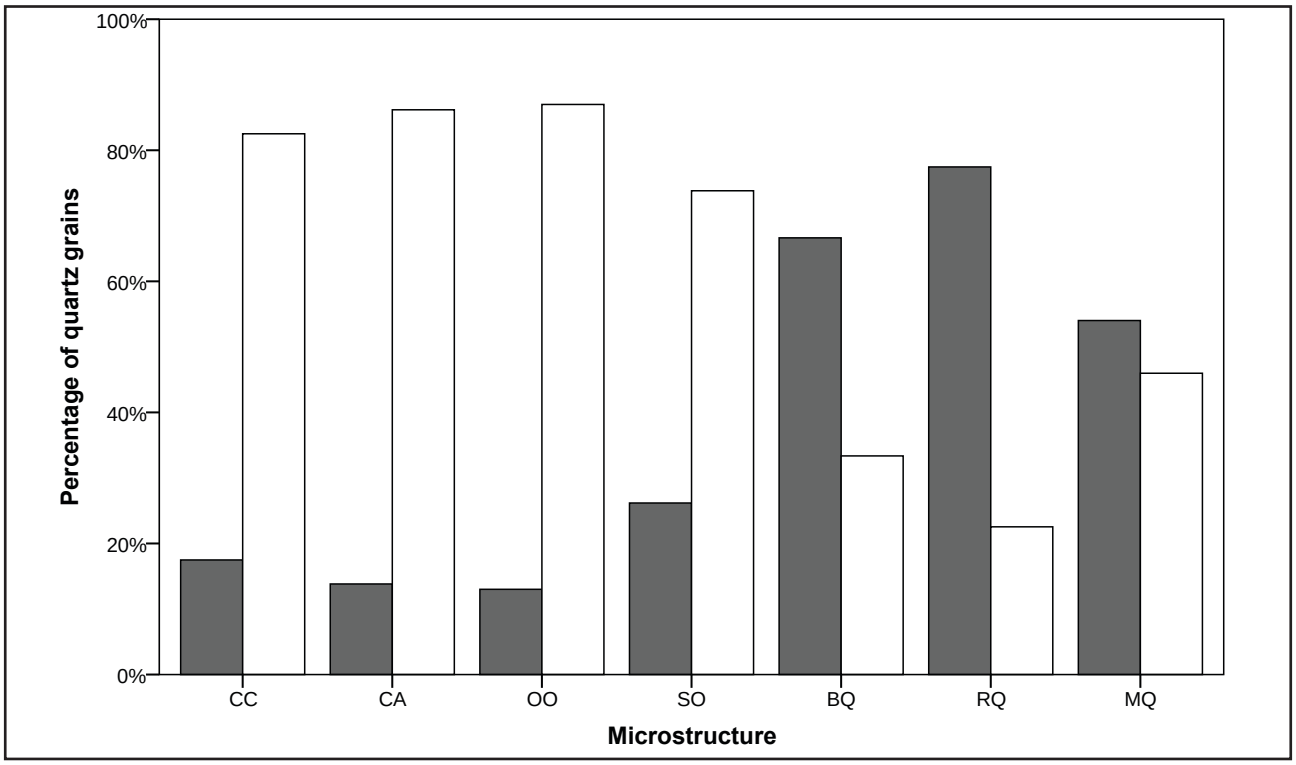

Figure-5.23: Bar chart showing for each petrogenetic type the percentage of primary matrix from coarse silt to coarse sand Udden-Wentworth categories) and secondary matrix of quartz grains (from clay to medium silt). Primary matrix in white and secondary matrix in grey. There is a increase on percentage of secondary matrix due to recrystallization processes on the SO, BQ and RQ types.

The type of subgrain rotation recrystallised quartzite shows similar bimodal distribution of circularity and roundness indexes, but this is not so clear for size. There are many more new recrystallised grains that are, in general, bigger in size than in the previous phase. They exhibit no irregularities, which contrasts with the old grains with higher irregularity in their shapes (e.g. ATS-195 in S.I-I). Some of the old grains are also bigger, as a consequence of deep deformation of the quartz grains (e.g. Es-378 (Nvl-XIII) in S.I.-I). Therefore, the mean of grain size is higher than in the previous type and it has a very positive skewness. Preferred orientation and lower roundness index indicate a high degree of schistosity, verifiable in every sample as a consequence of the increase of deformation and metamorphic processes.

The quartz grains of the type grain boundary migration recrystallized quartzite are different from those previously commented. In this type, the previously bimodal distributions of size and morphology becomes single mode distributions (e.g. HA-5842 in S.I.-I). The circularity index is also different. However, the roundness index reveals an inversion of means and distribution, with more similarities with the CC, CA or OO types than with the deformed types. Schistosity is only present in one of the two samples.

Once the general effects of the petrogenetic types on quartz-grain size and morphology are understood, we will describe its influence on non-quartz minerals.

The statistical treatment of the presence and quantification (categorical) of matrix reveals that its presence is significantly associated to petrogenetic types (χ^2 (18, N = 122) = 77.333 p < .001). Standardised residues show a positive relationship of major and very abundant categories with the CC type (+3.5 and +4.4) and also a positive relationship of the CA, OO, and SO types with trace matrix (+1.4, +1.5, and 1.7). Coming to the type of matrix, there is no statistically significant relationship between types (χ^2 (6, N = 90) = 6.329, p = .412). The cement quantification also reveals its association with the petrogenetic types χ^2 (18, N = 122) =.034. Standardised residues mainly show this relationship with the CC petrogenetic type. Regarding to the cement type, there is no evidence of association to any petrogenetic type (χ^2 (2, N = 18) = 2.927, p = .231).

Non-quartz mineral identification does not reveal any statistical differences within the proposed petrogenetic classification. Only the presence of high quantity of different non-quartz minerals could be related to the types CC or CA. According to Kruskal-Wallis test, the values from X-Ray fluorescence do not show any clear relation with petrogenetic types either. Only the presence of Fe_2O_3 and MnO display different distributions based on the petrogenetic type (χ^2 (6, N = 111) = 18.952, p = 0.004 and χ^2(6, N = 111) = 18.221, p = 0.006 respectively).

The petrogenetic groups and types proposed, summarised in Figure-5.24 and Figure-5.25, relate the information based on quartz grain features and textural and packing properties with grain size, morphology and orientation, and matrix quantification. They also offer a coherent explanation of diagenetic and metamorphic processes affecting the properties of quartzites, simplifying and defining the variability of “archaeological quartzites”. In contrast, variability in the presence of cement, mineral characterisation, mineralogical characterisation of the matrix, non-quartz mineral characterisation, X-Ray Fluorescence, and internal differences in grain size could not be only understood through petrogenesis. The former unconsolidated sediment and/or post-depositional weathering could explain the variability appreciated on the non-petrogenetic characterisation. For these reasons, in the following chapters these attributes will be analysed and contextualized as cumulative elements to the initial classification, in order to better understand their variability and influence in the catchment and management of “archaeological quartzite”.

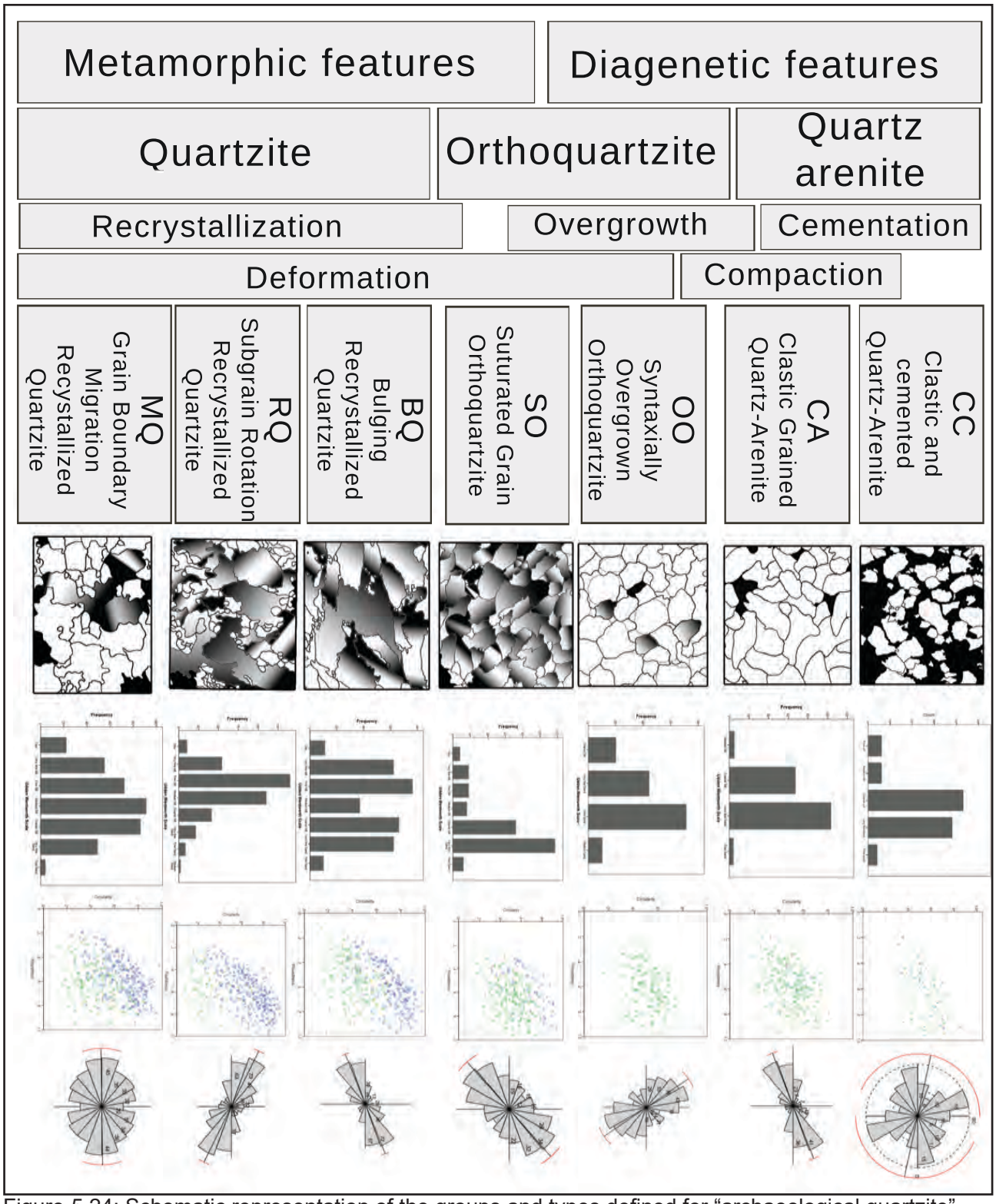

Figure-5.24: Schematic representation of the groups and types defined for “archaeological quartzite”.

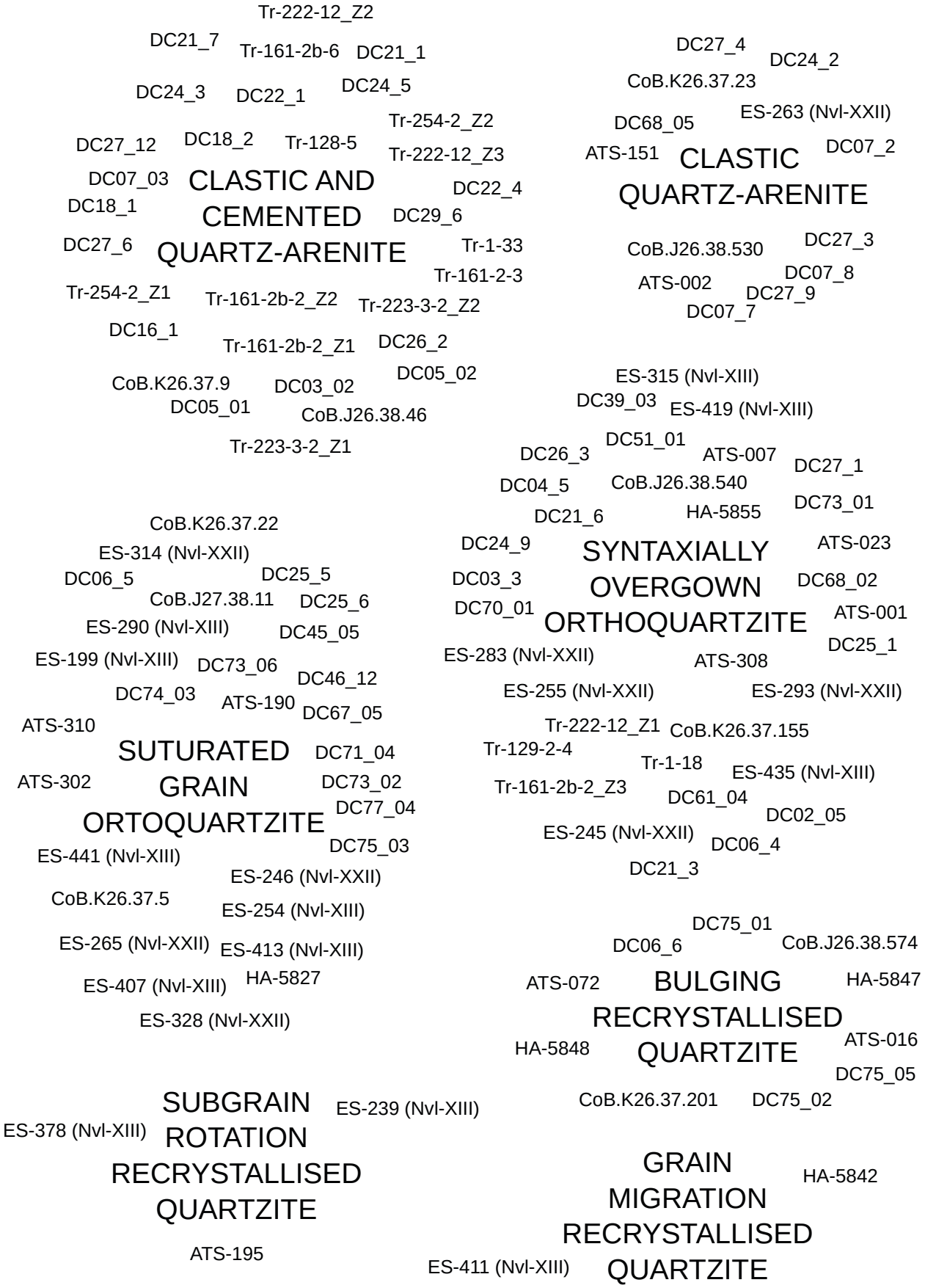

Figure-5.25: “Archaeological quartzite” samples grouped around their petrogenetic types.

5.4. FROM PETROGRAPHIC TO BINOCULAR CHARACTERISATION: DEFINITION OF GROUPS AND TYPES THROUGH NON-DESTRUCTIVE ANALYSES

The groups and types established and defined through thin section analysis were applied to non-destructive characterisation by using similar qualitative criteria for the analysis of texture and quartz grain features. The use of two databases of criteria, previously explained in the methodology section, is the consequence of evolution of this research over time. The simplification from database-A to database-B was carried out in order to simplify data acquisition and to get rid of multiple non-diagnostic features that only hindered the analysis. The description of all these features during the data acquisition process, the comparison with the remains of the samples once were got to prepare thin section, and the comparison with the reference collection of micro-photographs, helped us to assign petrogenetic groups and types to every artefact (Figure-5.26).

CC type is characterised through thin section by the association of clastic and cemented texture and floating or punctual packing, as well as by the presence of clastic quartz grains. This is reflected in database-B on the association between saccharoid T&P and the presence of flat and angular, rounded or ruffled grains. In database-A this type is defined by coarse grained texture, floating or punctual packing, flat and angular or rounded quartz limits and irregular quartz grain limits caused by the effect of matrix or cement. There is no presence of brightness, neither of micro-cracks. Some of the stones show bedding on the surface. In general, in this type it is easy to recognise, at least, 25 different grains, although sometimes this task is complicated by a high frequency of matrix or cement.

CA type is characterised through thin section by the association of clastic grained texture, tangent or tangent-to-complete packing, the presence of clastic grains delimited by concave-convex quartz limits, and occasional undulatory extinction. This is reflected in database-B on the association of granular T&P and the presence of flat and angular (in lesser proportion than in the samples from the previous type) or rounded quartz grains. In database-A, CA type is associated to coarse grained texture, tangent or sometimes complete packing, and flat and rounded or angular quartz grain limits. Brightness or luster is present, but it is of low intensity. There is a small increase in the presence of micro-cracks. Bedding appears in some samples and it is generally easy to recognise more than 25 quartz grains in the samples.

OO type is characterised through thin section by the association of clastic grained texture, complete packing, and the presence of a higher degree of undulatory extinction, concavo-convex quartz limits, and syntaxial quartz overgrowth. This is reflected in database-B on the association between compact and grainy T&P and the presence of concave-convex quartz grain limits. In database-A, this type is defined by fine grained texture, complete packing, and flat and rounded quartz grain limits, surrounded by the halo of quartz overgrowth. Most of the samples have medium bright, while others are more variable, with small to high degrees of brightness. The presence of micro-cracks is also variable. It is easy to recognise grains, although not as easy as in the previous quartz-arenite.

SO type is characterised through thin section by the association of clastic grained texture, suturated grained packing, stylolites boundaries, high presence of undulatory extinction, and occasional presence of recrystallised grains or deformation lamellae. It is related to fine and grainy T&P and the presence of ruffled and irregular quartz grain limits in database-B. In database-A, SO type is associated to fine grained and occasionally to fine texture, suturated packing, flat and ruffled grain boundaries, and no boundary detection. As on the previous type, the intensity of brightness is variable, as well as the presence of surface micro-cracks. Grains are less recognisable than in the previous type. Foliation structures are easy to recognise on some of the samples.

BQ type is characterised through thin section by the association of mortar texture, suturated packing, and presence of stylolitic quartz grains, deformation lamellae, clear undulate extinction, and significant presence of recrystallised grains. It is associated to the fine T&P and the presence of irregular grains or the absence of quartz grain boundary detection in database-B. In database-A, it is associated to fine texture, suturated packing, flat and ruffled limits of quartz grains, and the non-detection of quartz grains. The quantity of recognisable grains is smaller than five to 250x magnification and the presence of surface micro-crack is again variable. The intensity of brightness is high. Finally, and as in the previous type, foliation is obvious in most of the samples.

RQ type is characterised through thin section by the association of mortar texture, suturated packing, presence of stylolitic quartz grains, and high presence of recrystallised quartz grains. It is related to soapy T&P and absence of quartz grain boundary detection of quartz grain feature in database-B. In database-A, it is defined by soapy texture and absence of quartz grain boundary detection. The intensity of brightness is high. As in previous types, foliation is obvious on some samples. There are almost no micro-cracks on the surface.

MQ type is characterised through thin section by the association of clastic texture, suturated packing, concavo-convex quartz grain limits, presence of deformation lamellae, and stylolitic quartz grain limits. It is related with soapy texture and absence of quartz grain boundary detection in database-B. In database-A, it is defined by soapy texture and the absence of quartz grain boundaries. Intensity of brightness is high, and there is an almost complete absence of micro-cracks on surface. Foliation is not present, neither bedding.

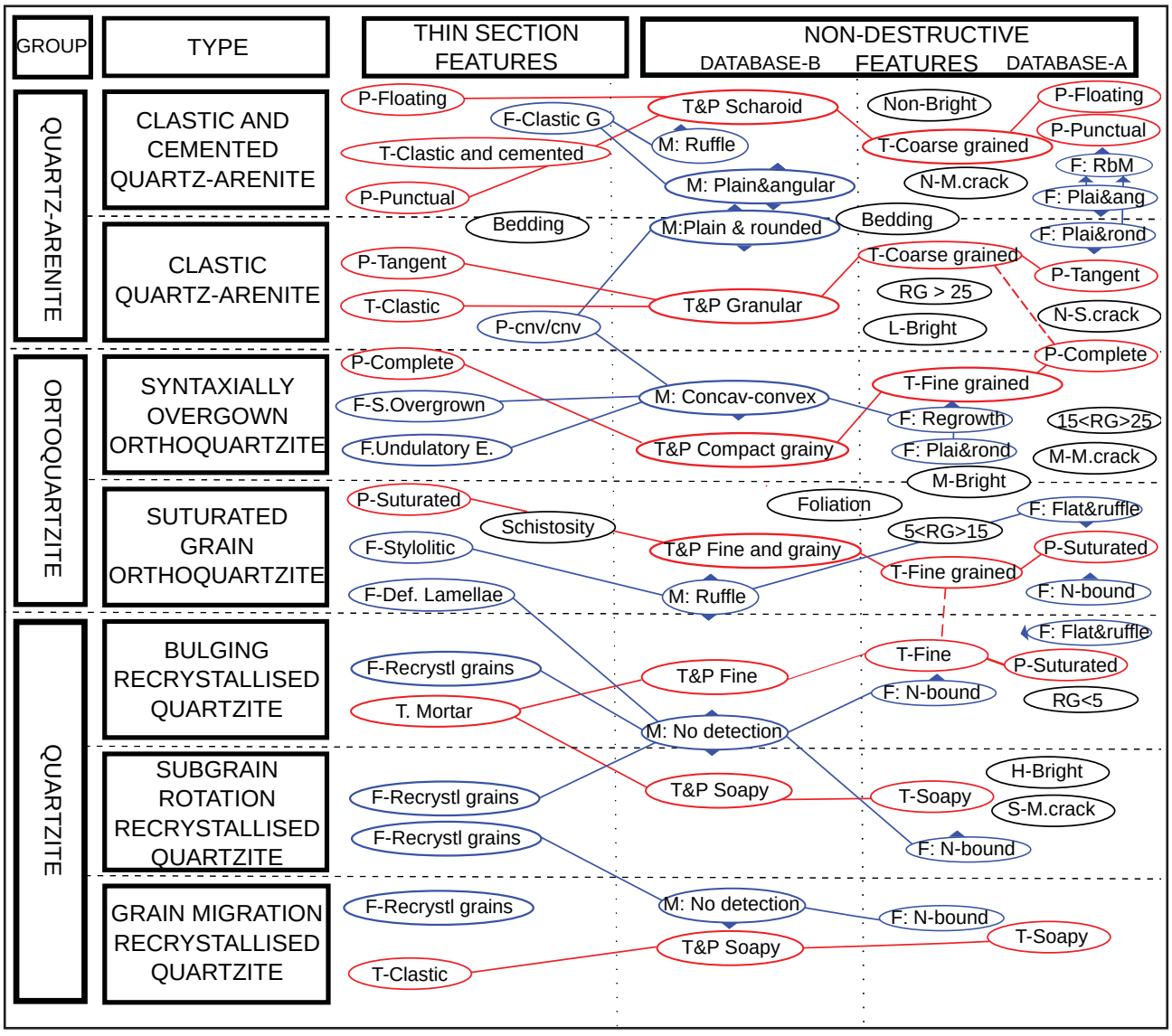

Figure-5.26: Schematic representation of the features that define the groups and types of "archaeological quartzites", showing the relationship between the petrographic characterisation and the non-destructive petrological characterisation (using databases A and B). In red textural, packing or T&P characterisation. In blue the features of quartz grain. In black unclear diagnostic features. The solid lines that link different columns represent the association of similar characteristics. The dashed lines represent unclear or infrequent relationships. Blue triangles (sometimes linked to lines) represent relationships where the presence of a quartz grain feature conditions texture, packing, T&P or any other quartz grain feature. In order to avoid duplicated information, features of quartz grains present in previous phases do not appear in the following types. P: Packing; T: Texture; F: Quartz grain feature; M: Morphology of quartz grains

Textural and quartz grain through binocular non-destructive techniques shows analogous association of features and forces to those appreciated through petrographic characterisation. Nevertheless, the forces (diagenetic or metamorphic), understood through the petrographic analysis, are not so clearly appreciated on the present surface of the stone as on thin section. However, the correlation between destructive petrography and binocular characterisation, allow us to recognise the forces and, therefore, the types. In this way it lets us extrapolate the information from the petrographic characterisation of a representative sample to the complete collection.

In the group of quartz-arenite, grains are easy to recognise and the borders from the former clastic sediment are well defined. They are only modified by the presence of cement or matrix. In this group, compaction and cementation are the diagenetic forces that consolidated former sediments into sedimentary rocks. In the group of orthoquartzite, the grain borders are not so easy to observe, since they are modified by silica overgrowth (more evident in the type OO) and the deformation of quartz grains. For these reasons, and also because of the increase of undulate extinction on quartz grains, brightness is more intense. The presence of micro-crack is more frequent, due to the increase of compactness. In type SO, foliation or schistosity is also a consequence of the deformation. Overgrowth and deformation are the main forces that affect and create these features on stone surfaces. In the group of quartzite, grains could not be recognised due to high deformation, but also because of the presence of new small recrystallised grains creating a bright and crystalline surface. The successive increase of the metamorphic forces generates an increase of crystalline structures, resulting in very soft and flat surfaces that make it impossible to recognise former quartz grains.

Due to methodological limitations, grain size and morphology as observed with binocular microscopy do not show any correlation with thin section analysis. Only a general increase in size for the type OO is appreciated. Therefore, grain size determination is used as a cumulative feature to understand variability within types, as a possible consequence of the internal characteristics of the former sediment from which “archaeological quartzites” were created. This variability will be explored in the following chapters in order to understand its effect on raw material catchment and management strategies through the definition of varieties of petrogenetic groups and types of “archaeological quartzite”. Varieties are defined taking into account grain size and its distribution.

Neither non-quartz mineral characterisation through petrography nor geochemical FX-R characterisation show any clear relationship with petrogenetic types. The influence of the mineralogy of the former sediment and post-depositional weathering could explain the variability of non-quartz minerals. This will be analysed in the following chapters.

The petrogenetic groups and types, together with their grain size variety of “archaeological quartzite” and non-quartz mineral characterisation are included in the survey point database in the lithology section and in the database of geological samples and lithic artefacts too.

CHAPTER-6

RESULTS. "ARCHAEOLOGICAL QUARTZITE" IN THE DEVA, CARES, AND GÜEÑA VALLEYS: POTENTIAL CATCHMENT AREAS

6.1. Archaeological quartzite" outcrops

6.1.1. The Cambrian-Ordovician series: The Barrios Formation

6.1.2. The Devonian series: The Murcia Formation

6.1.3. The Carboniferous series: The Potes, Mongrovejo, Viorna, and Cavandi **formations**

6.2. "Archaeological quartzite" in the conglomerate outcrops

6.2.1. The Lower Pennsylvanian series: The Potes Group Conglomerates

6.2.2. The Middle Pennsylvanian series: The Curavacas Conglomerate

6.2.3. The Middle Pennsylvanian series: The Porrera, Bárcena, Cubo, and Pesaguero Conglomerates

6.2.4. The Middle Pennsylvanian series: The Lechada Conglomerate

6.2.5. The Middle Pennsylvanian series: The Viorna Conglomerate

6.2.6. The Upper Pennsylvanian series: The Pontón Group Conglomerates

6.2.7. The Upper Pennsylvanian series: The Maraña-Brañas Group

6.2.8. The Upper Pennsylvanian series: The Valdeón Group

6.2.9. The Upper Pennsylvanian series: The Campollo Group and the Narova Conglomerate

6.2.10. The Upper Pennsylvanian series: The Remoña Group

6.2.11. Other formations of conglomerates

6.3. Deposits with "archaeological quartzite"

6.3.1. Gravitational deposits

6.3.2. River beach deposits

6.4. The rock cycle and its consequences on human life: Potential raw material catchment strategies in the Deva, Cares, and Güeña Basins

Here we present the results from the geological surveys and the petrological characterisation of the samples analysed. The main objectives are to locate and characterise the presence of "archaeological quartzite" and understand the distribution of its petrogenetic types in the research area. This allow us to analyse the complex geology of the area and the forces that rule the formative and modification processes. Additionally, the characterisation of "archaeological quartzite" in its geological context allow us to propose potential acquisition areas and context where "archaeological quartzite" were caught, suggesting different raw material acquisition strategies.

There are three main context analysed here: massive outcrops, consolidate deposits (conglomerates), and secondary deposits; hereafter "deposits. These three context follow a chronological order from outcrops, generally the older strata and dated between the Cambrian to the Carboniferous, to the non-consolidate deposits, created during the Quaternary. The conglomerates are dated between the Pennsylvanian Carboniferous to the Cretaceous. Supplementary information-II for outcrops, Supplementary information-III for conglomerates, and Supplementary information-IV for deposits contain the detailed description of each survey point analysed. As it was previously exposed, each context have different features that must be taken into account to understand them and to infer different raw material acquisition strategies potentially carried out along the Palaeolithic.

In this chapter we will address the information obtained from the geological surveys and its systematization following first, the three different context previously explained. Second, and in each of these context, we will analysed the survey points grouped by the formations where "archaeological quartzites" are inserted and following the information derived from the GEODE project (Merino-Tomé et al., 2016). In order to understand all these contexts and formations, we summarise the information in Figure-6.1. In addition, in Supplementary information-V, we include the complete stratigraphic chart of the Cantabrian zone offered by the IGME, emphasising the formations here analysed.

CONTEXT	FORMATION	∑ SURVEY POINTS	∑ SAMPLES BINOCULAR	∑ SAMPLES THIN SECTION	Petrogenetic types CC	CA	OO	SO	BQ	RQ	PERIOD	EPOCH	AGE
DEPOSIT	Offset	4	-	-	?	?	?	?	?	?	QUATERNARY	HOLOCENE PLEISTOCENE	
	Flank deposit	5	-	-	?	?	?	?	?	?			
	Deva river beach	12	63	4	**CC**	CA	OO	SO	-	-			
	Cares River beach	13	52	1	**CC**	CA	OO	SO	BQ	-			
	Total	34	115	5									
CONGLOMERATE	Remoña	4	16	4	**CC**	-	**OO**	**SO**	**BQ**	-	CARBONIFEROUS	PENNSYLVANIAN	Gzhelian
	Campollo	3	13	4	**CC**	CA	OO	-	-	-			
	Valdeón	4	24	6	**CC**	CA	**OO**	SO	BQ	RQ			Kasimovian
	Maraña-Brañas	1	4	1	-	-	**OO**	**SO**	BQ	-			
	Pontón	8	21	4	**CC**	**CA**	**OO**	SO	BQ	RQ			
	Viorna	3	6	2	**CC**	CA	OO	-	-	-			
	Lechada	2	15	1	**CC**	CA	**OO**	SO	-	-			Moscovian
	Porrera, Bárcena, Cubo, and Pesaguero	5	18	1	**CC**	CA	OO	-	BQ	-			
	Curavacas	14	78	20	**CC**	**CA**	**OO**	SO	-	-			
	Potes	5 - 1	23	4	**CC**	**CA**	**OO**	SO	BQ	-			Bashkirian
	Total	48	218	47									
OUTCROP	Cavandi	4	13	1	**CC**	-	-	-	-	-	CARBONIFEROUS	PENNSYLVANIAN	Gzhelian
	Viorna	1			**CC**	-	-	-	-	-			Kasimovian
	Mogrovejo	2			**CC**	-	-	-	-	-			Moscovian
	Potes	1			**CC**	-	-	-	-	-			Bashkirian
	Murcia	3	8	1	**CC**	-	-	-	-	-	DEVONIAN	UPPER	Fammenian
	Barrios	15 + 2	58	2	**CC**	**CA**	OO	-	-	-	CAMBRIAN-SILUREAN / Guzhangian-Rhuddanian		
	Total	28	79	4									

Figure-6.1: Chart summarising the information obtained from the survey points grouped by context and formations. The quantity of survey points and the number of samples analysed (through binocular and petrography) are reported. The petrogenetic types represented in each formation is included. Cells in black are the types with major representation (≥ 50%). Cells in grey are the types well represented (≥10%). Cells in white and type code in dark are types with smaller representation than 10%. Cells in white and type code in light grey are types with smaller representation than 5%. Finally, a stratigraphic chart with formation analysed is included.

Finally, in order to understand the geographic display of each analysed formation Supplementary information-VI shows the resulting map using different 1:50,000 MAGNA map files. It shows the polygon of the geological formations analysed and the geographical dispersion of the survey points where formation were described. In addition, Supplementary information-VII shows the base map we used with the information offered by IGME (Merino-Tomé et al., 2016) to relate the formations from different MAGNA file maps. The information offered in this map allow to understand not only the interested strata, but also contextual strata and other strata not analysed in the text.

6.1. "ARCHAEOLOGICAL QUARTZITE" OUTCROPS

"Archaeological quartzite" outcrop is the first context we consider in this text due to geological and archaeological reasons. Starting with the geological ones, "archaeological quartzite" outcrops are the oldest formations here analysed. In addition, the analysis of these outcrop allow us to understand formative processes of "archaeological quartzites", especially the sedimentary ones. Finally, these strata have the broad extension in the research area. The archaeological reasons are related with the abundancy of determined rock in massive stratum which allow Prehistoric societies to catch big quantities of interesting rock. In addition, multiple studies have proven the use of massive outcrop for acquisition of lithic resources in the Iberian Peninsula, e.g. (Tarriño et al., 2014; Terradas, 2002; Terradas and Ortega, 2017).

The description of formations and the information obtained from them through the survey points certify these formations are the oldest one. Starting from the Barrios Formation, its base is dated in the Cambrian and the last accumulation of this formation is dated in the Middle Ordovician. Murcia Formation is dated in the Upper Devonian, reflecting a gap of siliciclastic deposits between the Ordovician and the Devonian. Finally, the last formations here analysed are dated in the Pennsylvanian Carboniferous, and they are part of a succession of strata generally formed by sandstone, conglomerates, shale, and limestone layer. Other siliciclastic massive outcrop formations from the Cantabrian Zone could not be analysed due to accessibility problems (Arroyacas and Carazo formations) or because they are not represented in the research area (Herrería Formation, Vidrieros, or Robledo formations). Figure-6.2 represents all outcrop strata and the most relevant features obtained on each survey point.

Figure-6.2: Map of the outcrop formations in the area of study. Each point marks a survey point and its main features. The rounded icons represent bedding categories: empty for no-bedding, dashed horizontal lines for unclear bedding, and horizontal lines for bedding. The first square icon represents the characteristics of joints based on two criteria: 1) quantity of joint directions using horizontal lines for single directional joints, horizontal and vertical lines for two directional joints, and horizontal, vertical, and diagonal lines for three or more directional joints, and 2) presence of mineral precipitates using different colours, red colour for Fe-oxides, black for silica, light blue for manganese, orange for carbonates, green for clay, and purple for sandy materials. The petrological characterisation is symbolised by one to three icons containing the initial of most interesting petrogenetic types. The external form of these symbols describes the morphology of clasts, where the squares represent tabular clasts, rounded squares represent tabular pebbles, oval forms represent flat pebbles, and circles represent spherical pebbles. Grain size distribution is represented by the main colour of the symbol. One mode homogenous distribution is represented by red, two modes heterogeneous distribution is represented by green, and heterogeneous distribution is represented by blue. Grain size characterisation is represented by the brightness of the previously commented colours, light red, green, or blue for coarse size grains; medium red, green, or blue for medium size grains and dark red, green, or blue for small size grains.

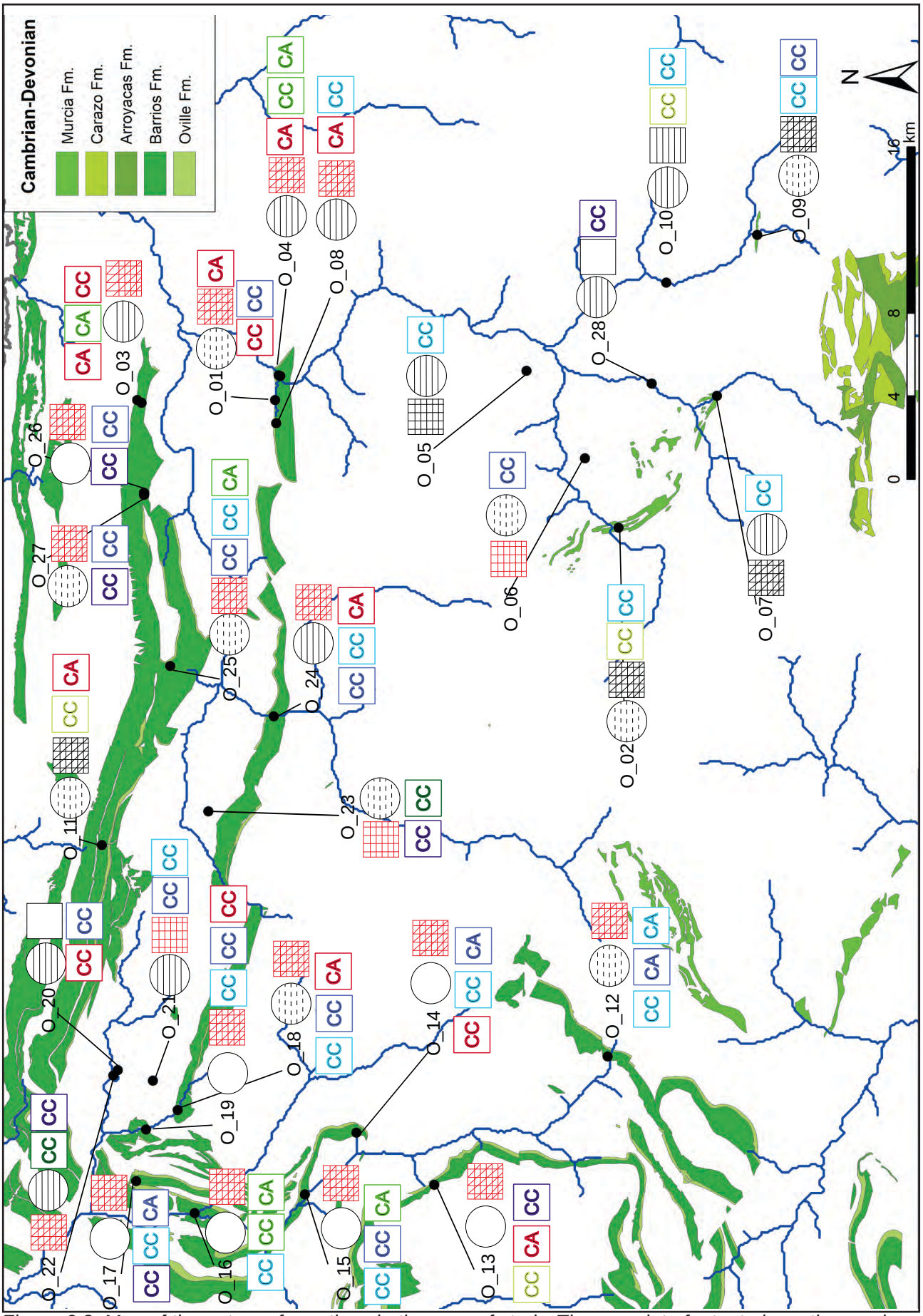

Figure-6.2: Map of the outcrop formations in the area of study. The complete footnote is on the previous page

6.1.1. THE CAMBRIAN-ORDOVICIAN SERIES: THE BARRIOS FORMATION

The Barrios Formation is the oldest siliciclastic formation we consider in this work. This formation lays on the top of the Oville Formation, a Middle Cambrian siliciclastic formation characterised by the succession of glauconitic shales and non-compacted sandstone layers. The Barrios Formation is chrono-stratigraphically dated between the Upper Cambrian and the Middle Ordovician, although the top of the Somiedo unit is dated to the Lower Silurian. The thickness is variable, ranging from some meters up to 1020 meters, due to distention tectonics movements and associated local volcanism. This formation crops out throughout the entire Cantabrian Zone, except for the Pisuerga-Carrión Province. A lateral increase on grain-size is appreciated on East-West direction due to the sedimentary conditions created by this formation, a cross-plain delta. The formation is clearly modified by the thin-skinned tectonism generated by the Variscan orogeny and its reactivation during Alpine orogenesis. Folds, faults, and joints in different directions appear along the formation (Aramburu et al., 2004; Aramburu et al., 1992).

In our research area the Barrios Formation crops out to the North and to the West. On the first one, the formation crops out on successive massive outcrops almost in parallel to the coastline. On the eastern area, it appears as a succession of outcrops in North-South direction due to the influence of Variscan orogeny.

We approach the formation through 15 survey points scattered in different areas in order to understand possible differences. In addition, we include two further points from the Oville Formation in order to make comparison between both formations visible. Except for the outcrops nearest to the coast, the entire area of study is well represented. Supplementary Information-II gathers the systematised information from the points surveyed. The coordinates of these points are the following:

- O_001/DC004: 30T 366401 4793238
- O_003/DC010: 30T 366402 4799882
- O_004/DC013: 30T 365291 4793181
- O_008/DC036: 30T 367599 4793067
- O_011/DC080: 30T 344962 4801578
- O_012/SE05: 30T 334786 4777208
- O_013/SE06: 30T 328602 4785562
- O_014/SE07: 30T 331112 4789315
- O_015/SE08: 30T 328138 4791804
- O_016/SE09: 30T 327234 4797110
- O_017/GU03: 30T 328777 4799929
- O_018/GU05: 30T 332198 4797928
- O_019/GU06: 30T 331265 4799454
- O_024/DC098: 30T 351168 4793300
- O_025/DC100: 30T 353596 4798291
- O_026/DC105: 30T 361940 4799551 (Oville Formation)
- O_027/DC106: 30T 361838 4799555 (Oville Formation)

Regarding the features analysed and systematised in the database, bedding can be clearly appreciated in four of the survey places (26.7%), unclearly appreciated in five (33.3%), and it is absent in six of the points surveyed (40%). According to the geographical distribution, bedding is related to the different areas where the Barrios crops out. In the zone parallel to the coastline and in northern areas bedding is clearly or unclearly appreciated. Meanwhile, in the western area and along the Sella river basin bedding is absent. In some cases it can be appreciated but it is not easily recognisable (Figure-6.2).

As for the joints of the Barrios Formation, in all the survey points joints follow at least three or more different directions. The intensity of joints to the material is high in 12 of the survey points (80%), while in the other three points intensity of joints is medium (20%). The previously commented influence of the thin-skinned tectonism caused by Variscan and Alpine orogenesis created multiples joints as consequence of the hardness and compactness of the material. Joints are always filled with iron oxide, as well as with quartz in 12 of the cases and manganese oxides in only three cases.

Mechanical weathering caused by water, ice, and plants erodes mainly the joints. In consequence, it creates orthogonal and angular fragments of rock in the areas surrounding the Barrios Formation outcrops (e.g. O_003 in S.I.-II). For example, in point O_016 (S.I.-II) it could be appreciated the effect of water, that eroded mainly the joints creating rounded and orthogonal fragments of rock.

The visibility of the Barrios Formation is variable due to differences in relief. Generally the formation is associated to soft or intermediate relief, where the formation usually underlies below a layer of soil or vegetation (e.g. O_025 in S.I.-II, where the outcrop is only visible in the cut generated by the road). In the cases where the relief is really steep the outcrop is visible and it appears in big cliffs, normally maintaining the direction of the most important joints, creating foliation surfaces (e.g. O_014 or O_011 in S.I.-II). The Barrios Formation can also be observed when it is cut by rivers or contemporary road systems.

Figure-6.3 summarises features commented above and shows the stratigraphic succession between Oville (shale rich in glauconite, coloured in green) and Barrios formations.

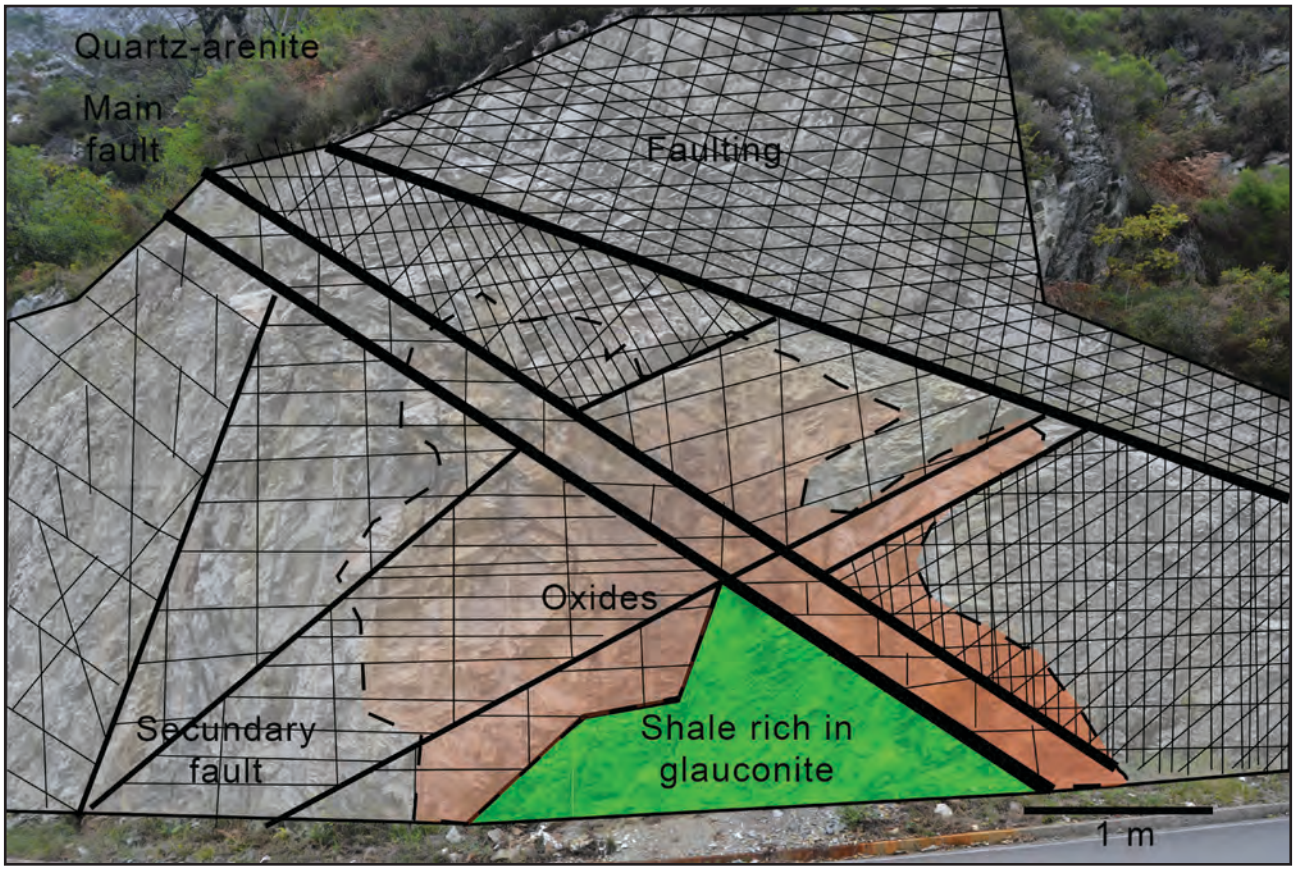

Figure-6.3: Geological cut of Barrios and Oville formations at point O_013. In green, the shaly Oville Formation, rich in glauconite. In white/grey, the clastic grained Barrios Formation. Different faults can be appreciated, as well as oxides areas around the main fault and the area closer to the Oville Formation.

Regarding the lithological characterisation of the formation, almost all the material is “archaeological quartzite”. We only found some small relicts of shale inside the formation. In general, characterisation under binocular microscope reveals that quartzarenite is the most frequently represented petrogenetic group and that the CC and CA types are widely extended. As for grain size and its distribution, there is high variability. The total number of samples obtained for detailed analysis is 58. Table-6.1 summarises the petrogenetic features and the characteristics of grain size obtained by non-destructive techniques. The results show clearly that the most represented types are CC and CA, both corresponding to the quartzarenite petrogenetic group. Only one sample, collected at point O_001, shows features related with the orthoquartzite group and the OO type according to characterisation under binocular microscope. Coming to grain size characterisation, heterogeneous distribution is verified, with higher quantities of medium and coarse grain sizes (Table-6.1). With regard to mineral characterisation, Fe-oxide, mica, and non-identified black and heavy minerals are the most represented non-quartz minerals. Manganese oxides, pyrite, and feldspar appear in a small portion of the sample (Table-6.2). The analysis of the colour of the quartzarenites reveals one of the most

important features of the outcrop: white as the primary colour. Other different colours, related with the influence of non-quartz minerals, are also observable. Red and orange, the most represented secondary colours, are caused by the major presence of Fe-oxides in the samples. As it was previously explained, this is related with the presence of iron oxides filling the multiples joints present in the outcrop (Table-6.3). Figure-6.4 displays the textures of two different petrogenetic types, showing the most of the features explained above.

Grain size characterisation		Petrogenetic type															
		CC		CA		OO		SO		BQ		RQ		MQ		Total	
		Σ	%	Σ	%	Σ	%	Σ	%	Σ	%	Σ	%	Σ	%	Σ	%
Homogeneous and one mode distribution	Fine grain	1	2			1	100									2	3
	Medium grain																
	Coarse grain																
Heterogeneous and two modes distribution	Fine grain																
	Medium grain	8	20	2	13											10	17
	Coarse grain	15	37	1	6											16	28
Heterogeneous distribution	Fine grain	4	10													4	7
	Medium grain	13	32	13	81											26	45
	Coarse grain																
	Total	41	71	16	28	1	2									58	100

Table-6.1: Frequency table of the petrological features of the Barrios Formation based on binocular characterisation. Columns are the petrogenetic types and rows contain the characteristics of grains according to size, classified first by distribution and second by size itself.

Non-quartz minerals	A		B		C		General	
	Σ	%	Σ	%	Σ	%	Σ	%
Absence			1	2	1	2	2	1
Fe-Oxides	56	97	1	2			57	33
Mn-Oxide			1	2	1	2	2	1
Calcite								
Mica	2	3	52	90	1	2	55	32
Black mineral			2	3	53	91	55	32
Pyrite					1	2	1	1
Feldspar			1	2	1	2	2	1
Total	58	100	58	100	58	100	174	100

Table-6.2: Frequency table of the features of non-quartz minerals of the Barrios Formation based on binocular characterisation. Columns are the three fields examined and rows are non-quartz minerals identified.

Colour	Primary		Secondary	
	Σ	%	Σ	%
Absence			33	57
White	51	88	1	2
Grey	5	9	2	3
Black				
Blue				
Green			1	2
Orange	1	2	14	24
Brown			4	7
Yellow			2	3
Red	1	2	1	2
Total	58	100	58	100

Table-6.3: Frequency table of the colour hue of the samples from the Barrios outcrop. Columns are the fields for primary and secondary colour hues and rows are the colours considered.

As for the external morphology of the samples from the outcrop or from the surrounding area, tabular clast is the most frequent category, followed by tabular pebble when fragments were eroded, usually by water (Table-6.4). Cortical joints are present in the fragments sampled, with patterns similar to those directly observed directly in the surface. The presence of internal joints is also clear and they follow similar patterns (three directional joints). Bedding is generally absent, although unclear bedding is observable in a small part of them. Finally, the samples selected show no schistosity.

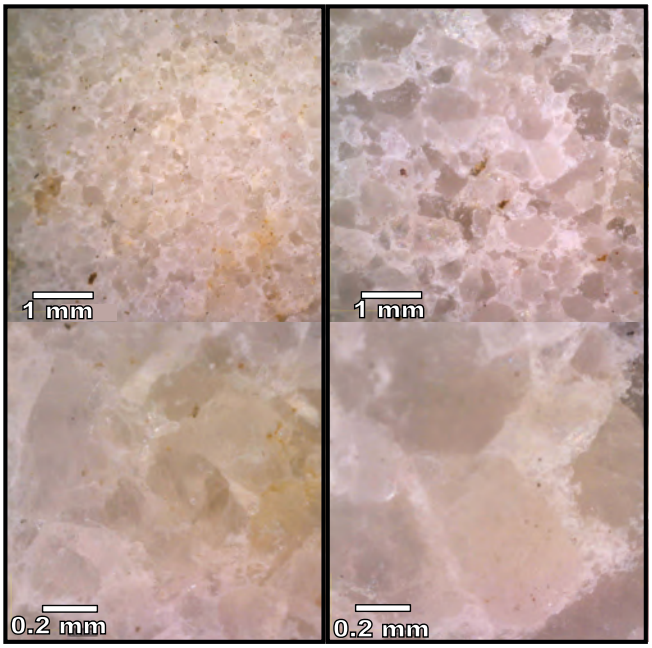

Figure-6.4: Binocular pictures of two samples from the Barrios Formation. Sample DC36_02 (on the left) is a CA petrogenetic type of quartz-arenite composed by medium size quartz grains heterogeneously distributed around two modes. Fe-Oxides can be appreciated at 50x magnification, together with some non-identified black minerals. Sample SE09_05 (on the right) is a CC petrogenetic type of quartz-arenite composed by coarse size quartz grains heterogeneously distributed. Fe-oxides can also be appreciated.

	Features	Σ	%
Morphology	Tabular clast	50	86
	Tabular pebble	7	12
	Flat pebble		
	Spherical pebble	1	2
	Total	58	100
Cortical joints	Not analysed	10	17
	Absence	4	7
	Unidirectional		
	Bidirectional	3	5
	Three-directional	41	71
	Total	58	100
Joints	Absence	7	12
	Unidirectional	5	9
	Bidirectional	1	2
	Three-directional	45	78
	Total	58	100
Bedding	Absence	49	84
	Unclear	7	12
	Clear	2	3
	Total	58	100
Schistosity	No	58	100
	Yes		
	Total	58	100

Table-6.4: Frequency table of the morphology, quantity of cortical joints, quantity of internal joints, bedding, and schistosity of the samples from the Barrios Formation.

We carried out the petrographic characterisation of sample DC04_05, the only one from the OO type, in order to better understand the features of this petrogenetic group. The clastic-grained texture and complete packing, the major presence of concavo-convex quartz limits, and the syntaxially overgrown quartz grains clearly classify the sample within the OO petrogenetic type. However, the absence of undulatory extinction and the presence (as minor elements) of clastic quartz grains, indicating the absence of clear deformation features, nuance this assignation (Figure-6.5). The distribution of grain size (see S.I.-I DC04_05) reveal that most of the grains are around the very fine sand Udden-Wentworth category. Matrix is also observable, but with small percentages around the fine silt Udden-Wentworth category. Morphological characterisation of quartz grains reveals they are not deformed. Circularity and roundness indexes show negative skewness and positive kurtosis, as a consequence of the presence of non-elongated and non-deformed grains. Then, former sediment is considered mature sediment deposited after long transport on a delta plain. There is no preferential orientation of quartz grains. The analysis of non-quartz minerals reveals the presence of mica, chlorite, and clay on the samples. XRF characterisation indicates major presence of silica (98%) and small representation of Al_2O_3 (1% of the sample). Other constituents, such as K_2O and TiO_2, are present in the sample in small percentages, related with the small presence of phyllosilicates.

In general, the Barrios outcrop is a massive formation composed mainly of quartzarenite with some shaly strata (probably linked to the underlying Oville Formation) and a few relicts of orthoquartzite, related to a slight increase of pressure caused by regional metamorphism affecting mainly to small quartz grains. We do not appreciate any clear geographical gradation along our research area, but great variability in quartz grain size (focused mostly on medium and coarse size categories) is observable. Local varieties can be explained by small differences in the sedimentation process. The multiplicity of directional joints and faults and their differential erosion generates many angular clasts scattered in the areas of Barrios outcrops close to cliffs, in zones of much steeped relief or where the river system cuts the formation. Despite the wide extension covered by this outcrop along the research area, intensive catchment activities and exploitation of quartzarenite must have been carried out in reduced areas where the formation is not covered by soil (Figure-6.6). In some of these areas, given the scarcity of orthoquartzite on the formation, intensive selection mechanisms could

have been employed for the exploitation of the OO type.

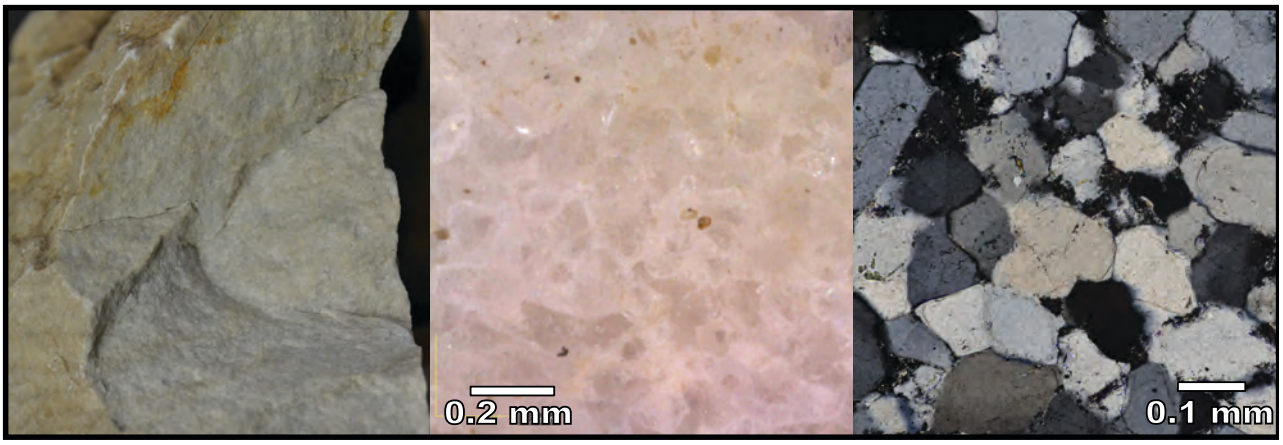

Figure-6.5: Pictures of sample DC04_05. On the left, a hand sample picture is shown to understand general features. External joints are easy to recognise, also oxides. In the middle, a microscopic picture of the surface of the samples is shown. Complete packing, easy quartz grain distinction, and appearance of regrowth are appreciated. Compact and grainy T&P with concavo-convex and rounded quartz grain limits are easy to recognise. On the thin section 200x picture on the right, quartz grains exhibit silica overgrowth on the outlines generating concavo-convex quartz grain limits. No evidence of undulate extinction is appreciated in any pictures.

Figure-6.6: The Barrios formation crops out around the village of San Esteban, between survey points O_01 and O_08. Due to differential sedimentary processes, the Barrios formation is covered by soil and vegetation and is only visible on cliffs or very steep terrain. Behind the Barrios formation, the Barcaliente limestone Formation exhibits rougher terrain and the grey and carbonate rock is easily recognisable.

6.1.2. THE DEVONIAN SERIES: THE MURCIA FORMATION

The Murcia Formation, also known as Camporredondo Formation, lays on the top of the Middle-Devonian Gustalapiedra, Cardaño, Portilla, and Candás formations, mainly composed by limestone and shale, and is covered by the Lower-Carboniferous Vidrieros and Alba formations, mainly composed by limestones, shales, and cherts. The Murcia Formation is chrono-stratigraphically dated between the Frasnian and the Famennian ages, in the Upper Devonian Epoch. The thickness of the formation ranges between 60 and 200 meters. The formation crops out in the Pisuerga-Carrión Province, to the south of our research area. This formation is mainly composed by siliciclastic material creating a sandstone/quartzite and shale alternation. There are microconglomerates in some parts of the sequence. The formation was created under marine sedimentary conditions, as a consequence of either turbidity currents or under platform conditions (Aramburu et al., 2004; Rodríguez Fernández et al., 2003). Folds, faults, and joints in different directions, caused by Variscan and Alpine orogenesis, are observed in the formation.

We describe the formation based on three points located in La Liébana area. Supplementary Information-II contains the systematised information on the points surveyed. The formation crops out in the area of La Liébana in Northwest-Southeast direction, while in the Cares River headwater it crops out in Southwest-Northeast direction, as a consequence of the deformation caused by the Variscan orogen. Due to problems related with accessibility to the outcrop, we could not survey the formation in the Cares headwater. In return, the lithology of the Murcia Formation in this latter area is analysed through a subsidiary survey point located in the foothills of a Murcia outcrop (D_028 in S.I.-IV). The points surveyed are the following:

- O_002/DC008: 30T 360266 4776695
- O_007/DC029: 30T 366608 4771945
- O_009/DC054: 30T 374361 4770002

Coming to the features analysed in the database of survey points, bedding is clearly recognised in one of these points, while it is unclearly observed in the other two. As to the joints of the Murcia Formation, all the three points exhibit at least three directional joints but they show heterogeneous intensity. The survey point O_009 clearly has a high concentration and intensity of joints, but intensity is smaller in the survey point O_007, probably as a consequence of the succession of sandy and shaly materials. In the survey point O_002 the intensity of joints is small too. Joints are always filled with quartz, as well as with Fe-oxides in two of the three cases. Given the smaller impact of the joint system and the presence of quartz in the cement filling the joints, these are not distinctly eroded. Instead they create orthogonal clasts, usually with sharp edges. In the area surrounding the outcrops it is easy to find this kind of clasts, broken not only due to the consequences of the differential erosion of joints.

The Murcia Formation is intensively folded in La Liébana province due to the effect of comprehensive forces during the Variscan and Alpine orogenesis. This, together with differential erosion, created good visibility conditions for the recognition of the formation, which crops out producing steeped relieves and cliffs easy to recognise in the landscape. Both in the main and the last picture of the survey point O_02, it is easy to recognise the folded formation creating a long mountain chain. As stated above, we were unable to find the formation in the Cares headwater partially due to visibility issues.

Figure-6.7 summarises the features exposed in the previous paragraph. It also shows the stratigraphic alternation between shaly and sandy layers that compose the formation.

Regarding the lithological characterisation of the formation, two main layer are clearly distinguishable. The first one, and the most interesting for this study, is predominantly formed by "archaeological quartzite". The second one, which creates the aforementioned alternation, is composed by shale. In the following lines we will focus on the first layer. In general, based on characterisation under binocular microscope, the CC type is the only one present in the entire formation. The distribution of grain size is mainly heterogeneous, but occasionally it is organised around two different modes. There are small differences in quartz grain size, but there is a tendency to middle-coarse quartz grain size. There is no a clear association between different lithology (neither in bedding nor in joint impact, direction, or mineral filling) and geographical distribution. Therefore, the small differences observable must be understood as a consequence of slight changes in the sedimentation process or the posterior conditions that create small local varieties.

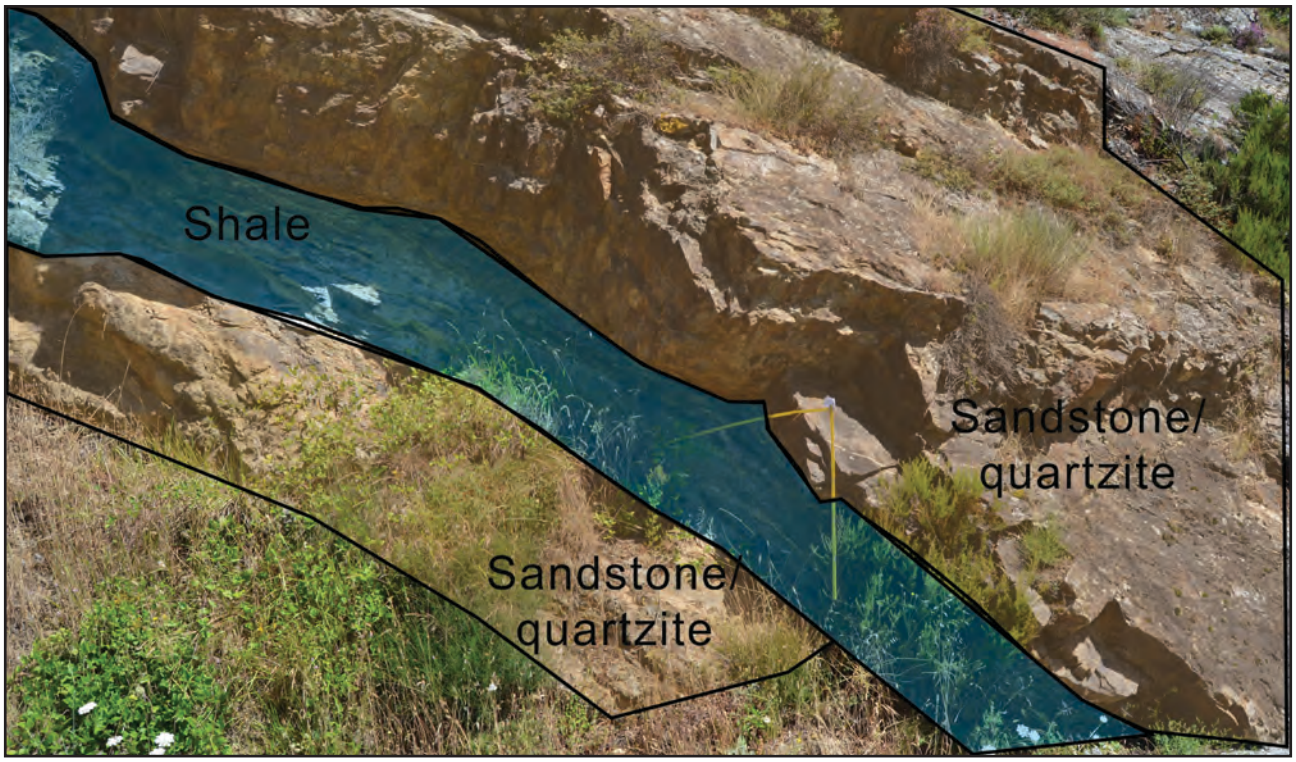

Figure-6.7: Geological cut of the Murcia Formation at point O_007. In blue, the shale layer, that exhibits clear bedding. In brown/grey, clastic grained layers folded on, at least, three different directions. The main plain of fault is observable.

The total of samples analysed in the laboratory through non-destructive techniques is eight. This analyses confirms that the formation is major composed by clastic and cemented quartzarenite and that grain size is heterogeneously distributed between middle and coarse grain sizes (Table-6.5). In regard to the mineral characterisation of the samples, most of them include iron oxides and non-identified black and heavy minerals. Feldspar and mica are present in some of the samples, while pyrite was identified in one quartzarenite (Table-6.6). The colour characterisation of the samples reveals that most of them are dark grey or dark brown as a consequence of the presence of non-identified black and heavy minerals and various iron oxides (Table-6.7). Colour shows clear differences between this outcrop and the one previously analysed. Figure-6.8 compares the textures of two samples: The first one is a CC type, heterogeneously classified and grey-black. The second one belongs to the same type, but is distributed around two modes and is brown-grey.

Grain size characterisation		Petrogenetic type															
		CC		CA		OO		SO		BQ		RQ		MQ		Total	
		Σ	%	Σ	%	Σ	%	Σ	%	Σ	%	Σ	%	Σ	%	Σ	%
Homogeneous and one mode distribution	Fine grain																
	Medium grain																
	Coarse grain																
Heterogeneous and two modes distribution	Fine grain																
	Medium grain	3	38													3	38
	Coarse grain	1	13													1	13
Heterogeneous distribution	Fine grain																
	Medium grain	4	50													4	50
	Coarse grain																
	Total	8	100													8	100

Table-6.5: Frequency table of the petrological features of the Murcia Formation based on binocular characterisation. Columns are petrogenetic types and rows contain the characteristics of grains according to size, classified first by distribution and second by size itself.

Non-quartz minerals	A		B		C		General	
	Σ	%	Σ	%	Σ	%	Σ	%
Absence					1	13	1	4
Fe-Oxides	4	50	1	13	2	25	7	29
Mn-Oxide								
Calcite								
Mica	1	13	3	38			4	17
Black mineral	3	38	2	25	2	25	7	29
Pyrite					1	13	1	4
Feldspar			2	25	2	25	4	17
Total	8	100	8	100	8	100	24	100

Table-6.6: Frequency table of the features of non-quartz minerals of the Murcia Formation based on binocular characterisation. Columns are the three fields considered and rows are the non-quartz minerals identified.

Colour	Primary		Secondary	
	Σ	%	Σ	%
Absence				
White				
Grey	5	63	3	38
Black	1	13	4	50
Blue			1	13
Green				
Orange				
Brown	2	25		
Yellow				
Red				
Total	8	100	8	100

Table-6.7: Frequency table of the colour hue of the samples from the Murcia outcrop. Colums are the fields for primary and secondary colour hues and rows are the colours considered.

	Features	Σ	%
Morphology	Tabular clast	8	100
	Tabular pebble		
	Flat pebble		
	Spherical pebble		
	Total	8	100
Cortical joints	Not analysed		
	Absence	1	13
	Unidirectional		
	Bidirectional	6	75
	Three-directional	1	13
	Total	8	100
Joints	Absence		
	Unidirectional	1	13
	Bidirectional	6	75
	Three-directional	1	13
	Total	8	100
Bedding	Absence	7	88
	Unclear	1	13
	Clear		
	Total	8	100
Schistosity	No	8	100
	Yes		
	Total	8	100

Table-6.8: Frequency table of the morphology, quantity of cortical joints, quantity of internal joints, bedding, and schistosity of the samples from the Murcia formation.

As for the external morphology of the samples taken from the outcrops or the fragments collected in the surrounding area, tabular clast is the most frequent category (Table-6.8). There are cortical joints in the samples, following patterns similar to those of internal joints. Two directional joints are the most common category. These facts prove that the disaggregation of clasts was not only caused by the joints. There is an almost completely absence of bedding and schistosity in the samples.

Next we will present the petrographic characterisation of sample DC29_06 (Figure-6.9). The analysis confirms the results of the non-destructive analyses set out above. The clastic-grained texture and floating packing, as well as the major presence of detrital quartz grains, confirm the classification of this quartzite within the clastic and cemented petrogenetic type. The existence of quartz grains with concavo-convex limits and the minor presence of undulatory extinction in some of them can be explained by the presence of older and more eroded quartzite grains in the former sediment. Analysis of grain size (see S.I.-I DC29_06) reveals that most of the quartz grains are around the very fine sand Udden-Wentworth category. The matrix is not easily recognisable due to the heterogeneity of quartz grain size, among which it is possible to identify some big quartz grains classified as medium sand and with measurements bigger than 0.34 mm. The morphology of quartz grains, characterised by negative circularity and roundness kurtosis indexes, is also variable as a consequence of the absence of modifications of quartz grains by pressure. Then, it can be concluded that the irregularity observed in the morphology of the quartz grains that compose the sample is a consequence of the forces that deposited the former sediment: coastal swell, occasionally increased by storms. These results agree the research by Rodríguez Fernández (1992) on the sedimentary conditions of this

formation. There is no preferential orientation in quartz mineral. The major presence of clayey matrix is also coherent with the proposal of this author, while the minor presence of carbonate cement could be related with the dissolution of limestone from upper formations and the subsequent precipitation on the incompletely packed quartzarenite. In regard to mineral characterisation, the only non-quartz minerals identified are mica and Fe-oxides. The latter is related with the clayey matrix and the former is probably associated with the mineral characterisation of the original sediment. Finally, XRF undoubtedly indicate that SiO_2 is the most represented constituent (97%). Alumina (2%), which is probably related to the composition of the matrix and phyllosilicates fraction, is the second most frequent element. Other components, such as Fe_2O_3, TiO_2, K_2O, or CaO, are present in the samples in residual percentages.

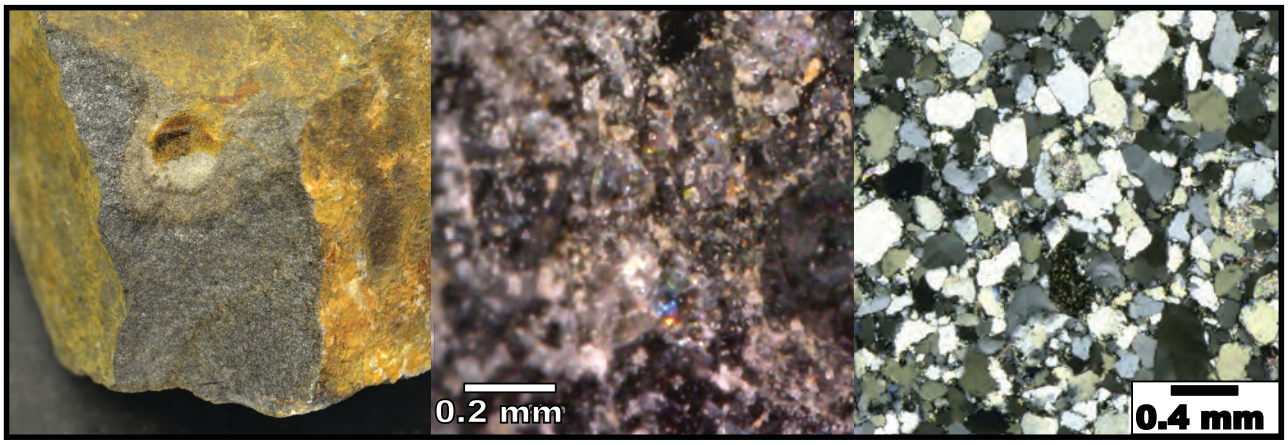

Figure-6.9: Pictures of sample DC29_06. On the left, a hand sample picture is shown to understand general features. External joints are easy to recognise, also oxides. In the middle, a microscopic picture of the surface of the sample is shown. Saccharoid T&P with ruffled quartz grains of irregular limits are recognisable. On the right, the thin section picture shows general clastic grained texture and floating-punctual packing, as well as clayey matrix and carbonated cement and other non-silica minerals. One of the grains shows undulate extinction as a relic of the former and eroded metamorphic rock.

In general, the Murcia or Camporredondo outcrop is a formation composed by an alternation of quartzarenite and shale. This quartzarenite (the interesting layer for the current study) shows no evidence of deformation or metamorphic processes. Therefore, according to its petrogenesis, it can classified as CC type, with presence of matrix and cemented by small portion of carbonates. Grain size and morphology reveal a general heterogeneity of the quartzarenite layer. There are no geographic differences in the formation, nor in petrological, mineral, or external features (Figure-6.2). Despite the multiple directional joints and faults, the filling quartz material does not permit differential erosion. For this reason the clasts derived from the outcrops are not determined by the joints of the formation. In the area of La Liébana the formation is easily recognisable, allowing the exploitation of the quartzarenite layers at the foothills of the cliffs generated by the folds of the formation and the differential erosion affecting the surrounding formations. In this formation the catchment activities would have been related with the intensive exploitation of the CC type and they could have been carried out by simply picking up the material. We do not exclude the possibility of the exploitation of other petrogenetic types or grain-size varieties not identified during this research. However, as in the case of the previous outcrop, they would have been conditioned by the major presence of the CC type.

6.1.3. THE CARBONIFEROUS SERIES: THE POTES, MOGROVEJO, VIORNA, AND CAVANDI FORMATIONS

In this section we analyse four sandstone massive formations dated to the Carboniferous and where literature does not provide any clear indication of the presence of “archaeological quartzite”. The objectives of this section are to analyse them in order to definitively discard them as possible sources of lithic raw material and to understand their relationship with the regional geology and its possible influence on Prehistoric catchment and procurement strategies. This analysis led us to reduce the initial outcrop of “archaeological quartzite” (see Figure-2.24 from Chapter-2) resulting into the final “archaeological quartzite” outcrop shown in Figure-6.2.

The oldest layer with siliciclastic massive outcrop from the Carboniferous series is the sandstone from the Potes Formation. It was analysed at the survey point O_05, in La Liébana area, 30T 367810 4781120 (for detailed information see S.I.-II). This formation is dated between the Bashkirian and the Moscovian ages, between the Lower and Middle Pennsylvanian epochs. This massive outcrop formation consists of a shale, sandstone and greywacke alternation with local presence of conglomerates (later analysed in detail) (Rodríguez Fernández et al., 2003). The point analysed shows the presence of two directional joints that affect the formation moderately. The joints are generally filled with quartz, although manganese oxides are also present. There is clear bedding, as well as folded areas. The colour of this formation is dark grey. Lithologically, the sandstone/greywacke layers consist of consolidated sandstone or CC petrogenetic type. The grain size of the samples analysed exhibits clearly heterogeneous distribution, with presence of coarse grains. The mineral characterisation shows major presence of oxides, feldspar, and non-identified black and heavy minerals. In order to get more detailed data, one of the samples (DC16_01) was analysed using destructive techniques. The results confirm the characterisation of the CC type based on non-destructive methods. The clastic texture with matrix or cement, the punctual packing and the abundant presence of clastic quartz grains led us to assign that sample to the CC type (Figure-6.10). The analysis of grain size shows great variability with values ranging from very fine silt to coarse sand (see DC16_01 in S.I.-I). The roundness and circularity indexes do also point to great variability in the irregularity of the particles. Regarding mineralogy, clayey matrix is major present. There is also a great presence of mica, clay, and Fe-oxides. X-Ray fluorescence reveals smaller importance of SiO_2 (still majority) when compared to the formations previously analysed. This quartzarenite CC type is clearly in the submature-inmature stages of Folk's sandstone classification (Folk, 1980) because of the non-static sedimentary conditions.

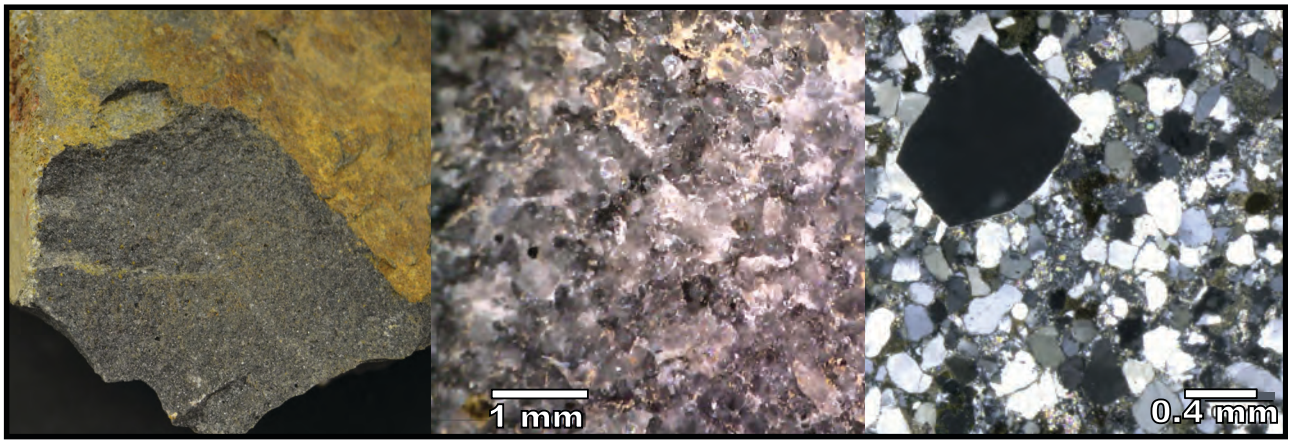

Figure-6.10: Pictures of sample DC16_01. On the left, a hand sample picture is shown to understand general features. In the middle, a microscopic picture of the surface of the sample is shown. Saccharoid T&P with ruffled quartz grains of irregular limits are easy to recognise. On the right, thin section picture shows general clastic grained texture, punctual packing, and major presence of clayey matrix and other non-silica minerals. A big quartz grain with angular outline can be appreciated.

The sandstones from the Mogrovejo Formation are dated to the Moscovian age, in the Middle Pennsylvanian epoch (Rodríguez Fernández et al., 2003). We analysed the outcrop at two different points in La Liébana area because some differences were previously appreciated in the bibliography. The first one is the point O_06 (30T 363604 4778284). It is a massive grey to brown sandstone/greywacke layer without clear bedding (for detailed information see O_06 in S.I.-II). A two directional system of joints affects the formation with low-medium intensity. The joints are filled with iron and manganese oxides. The second point is the O_10 (30T 372060 4774383). It consists of a massive grey to brown shale and sandstone/greywacke alternation (for detailed information see O_10 in S.I.-II). The point analysed demonstrates the presence of single directional joints affecting the formation moderately. The joints are usually filled with quartz, including iron oxides. Bedding is clear. Lithologically the sandstone/greywacke layer is made of consolidated sandstone or the CC petrogenetic type similar to the formation previously analysed. The distribution of grain size is also related with the previous formation, with clearly heterogeneous grain size distribution and predominance of coarse size grains. Regarding mineral characterisation, most of the samples contain iron and manganese oxides and non-identified black and heavy minerals. Non-destructive analyses were performed in this formation in order to understand the association with the lithology of the outcrops previously analysed.

The sandstone outcrop from the Viorna Formation are dated between the Moscovian and the Kasimovian ages, between the Middle and Upper Pennsylvanian epochs (Rodríguez Fernández et al., 2003). We analysed the outcrop in La Liébana area through the survey point O_28, 30T 367202 4775085. It is a thin shale and sandstone alternation exhibiting clear bedding surfaces without joints being affected. The formation is grey to brown. Lithologically the layers of sandstone are made of CC petrogenetic types, with heterogeneous grain size distributions around the fine grain size classes. Sandstone is not compact; therefore, this formation is not suitable for knapping, moreover due to the presence of this thin layer of sandstone.

The last outcrop analysed is the sandstone stratum from the Cavandi Formation, dated between the Kasimovian and the Gzelian ages, in the Upper Pennsylvanian epoch (Navarro, 2003). This formation was analysed at four points in the Güeña and Casaño valleys: O_20 (30T 334121 4800822), O_21 (30T 333617 4799126), O_22 (30T 333865 4801033), and O_23 (30T 346589 4796455). The formation shows clear bedding at three of the four points analysed (point O_23 exhibits unclear bedding). One point shows three directional joints, two bi-directional joints, and point O_20 shows no directional joints. When they were present, joints were filled with iron oxides. There is medium joint intensity. In regard to lithological properties, there are clear differences in the compaction of sandstones, showing an obvious progression from almost unconsolidated material in survey point O_23, to the clearly consolidated material in survey point O_22. Focusing on the consolidated material, all this “archaeological quartzite” belongs to the CC type. There is high variability in grain size, even within each survey point. Grain size too is heterogeneously distributed in most of the samples. As to the characterisation of non-quartz minerals, there is major presence of iron oxides, mica, and non-identified black and heavy minerals. The former are the responsible of the reddish, yellowish, or orange areas scattered within the original major white colour of the formation. No destructive analyses were carried out in this formation because its lithology is clearly correlated with that of previously analysed outcrops.

In general, all these formations were generated during the Pennsylvanian Carboniferous epoch, but they form a chronological gradation of ages within this period. In this way, these siliciclastic formations are representative of the heterogeneous conditions of the area during the Carboniferous as a result of the Variscan orogenesis. As it was explain in Materials section, during the Carboniferous this was a heterogeneous area with diverse and small sedimentary basins creating discontinuities in the stratigraphy. Respecting the lithological varieties, all the previously commented “archaeological quartzite” outcrops show similar characteristics, such as abundant presence of the CC type, heterogeneous distribution of the size of quartz grains (generally predominating medium-coarse grain size) and, as to minerals, presence of iron oxides, mica and non-identified black and heavy minerals: that is, they are submature-inmature sandstones created as a consequence of non-static sedimentary conditions. In the points analysed deformation or metamorphic processes are absent and intense diagenetic processes are also absent in some of them. Table-6.9 shows the types and distribution of grain size attending to non-destructive characterisation. Summing up, the raw material catchment activities on these strata were restricted to proposed CC type and grain size variety. Finally, it is important to remark, that these strata extend along a wide extension in the research area considered.

Grain size characterisation		Petrogenetic type															
		CC		CA		OO		SO		BQ		RQ		MQ		Total	
		Σ	%	Σ	%	Σ	%	Σ	%	Σ	%	Σ	%	Σ	%	Σ	%
Homogeneous and one mode distribution	Fine grain																
	Medium grain																
	Coarse grain																
Heterogeneous and two modes distribution	Fine grain																
	Medium grain	2	15													2	15
	Coarse grain	5	38													5	38
Heterogeneous distribution	Fine grain	3	23													3	23
	Medium grain	3	23													3	23
	Coarse grain																
	Total	13	100													13	100

Table-6.9: Frequency table of the petrological features of the Carboniferous formations based on binocular characterisation. Columns are petrogenetic types and rows contain the characteristics of grains according to size, classified first by distribution and second by size itself.

Therefore, the exploitation of this resource could be easily done in multiples areas without the need of any selective mechanisms.

Finally, we base ourselves on bibliography to describe two "archaeological quartzite" outcrops that could not be included in the present research due to time and accessibility issues: the Arroyacas and the Carazo formations. Both formations are situated to the South of our research area, along the administrative border between the provinces of Palencia and Cantabria (Figure-6.2). The first one is dated between the Wenlock and the Ludlow epochs in the upper stages of Silurian period. Two layers can be differentiated: the former is made by a locally ferruginous alternation of shale and dark quartzarenites. The latter is completely formed by shale. The quarzitic layer is one meter thick. It was created in marine sedimentary conditions in proximity to the shoreline. The second formation is dated in the Pridoli epoch, within the Silurian period and the Lower Devonian epoch. Once again, two layers can be distinguished. The first one consists of a massive locally ferruginous dark quartzarenite stratum of medium to coarse grain size and up to 100 meters of thickness. The second one is a sandstone, shale, and limestone alternation. Both formations have descriptions similar to those of previously presented Murcia or Camporredondo formations.

6.2. CONGLOMERATE OUTCROPS

In this section we will analyse the data obtained from the geological surveys in the conglomerate strata. Conglomerates are relatively frequent in research area, especially in the South, in Pisuerga-Carrión Province. Different studies have suggested catchment activities in consolidate deposits in the Cantabrian Region, e.g. (Carrión and Baena, 2005; Castanedo, 2001; Castanedo et al., 1993; Manzano et al., 2005; Santamaría, 2012). The presence of "archaeological quartzite" in these contexts is clear, and as we will detailed later, all types, except MQ quartzite are represented. All these reasons carried us to analyse in detail this conglomerates to understand first, the formative processes of conglomerates, and second, the potential catchment activities carried out in this context.

Conglomerate strata are mainly dated in the Pennsylvanian Carboniferous, although some formations, without interesting varieties or "archaeological quartzite" are dated in the Permian, Triassic, and Paleogene ages. Most of the conglomerate here analysed belong to formations composed by succession of strata composed by sandstone, limestone, shale and conglomerates. This is the consequence of changeable condition of the area during the carboniferous. The lithologically variability of rocks inserted in conglomerates also points at a high variability of rock source area.

6.2.1. THE LOWER PENNSYLVANIAN SERIES: THE POTES GROUP CONGLOMERATES

The Potes Group is the oldest formation with presence of conglomerates in the research area. In the previous section, we analysed the sandstone/"archaeological quartzite" massive outcrop. In this one, we will describe in detail the conglomerates from the Potes Group. In La Liébana area, the Potes Group lies as an unconformity on top of the Barcaliente Formation. It is covered by the Bárcena, Porrera, Cubo, and Pesaguero conglomerates. The Potes Group was created in similar ages and conditions as the Priorio Group, the other stratum with the same age within the Pisuerga-Carrion Unit. It is chrono-stratigraphically dated between the Lower Pennsylvanian and the Middle Pennsylvanian, although the conglomerates are situated in the Primkamsky (Bashkirian age) and the Kashirsky (Moscovian age). In general, the thickness of this formation ranges between 1000 and 2000 meters, although its entire thickness is unknown because the base has never been found. The Potes Group is mainly formed by siliciclastic material created in heterogeneous sedimentary conditions (from turbidity to delta-fan deposits) in different basins during the Variscan orogenesis (Fernández et al., 2004; Rodríguez Fernández et al., 2003).

From here on, we focus on the conglomerate outcrops of the Potes Group. In our research area the Potes Formation crops out as successive thin and discontinuous layers arranged in Northwest-Southeast direction. It crops out in different places in the South-eastern area, but it is only observable at road cuts, natural cliffs or steep flanks generated as a consequence of the folding caused by Variscan and (less importantly) Alpine orogenesis. Differential erosion of the mainly siliciclastic-shaly strata makes the conglomerates visible at certain points (i.e. C_009 or C_018 in S.I.-III). We approach the formation through five survey points distributed along different areas in order to better understand the possible differences. Supplementary Information-III contains the systemised information about these points. Note that on point C_15 the conglomerate was not found. The points

analysed are the following:

- C_009/DC025: 30T 360961 4772765
- C_015/DC042: 30T 366719 4782443 (conglomerate not found)
- C_018/DC046: 30T 384097 4771669
- C_023/DC053: 30T 374491 4769416
- C_029/DC062: 30T 361579 4772859

According to the features analysed and systematised in the database, bedding is clearly appreciated in three of the four survey points, while it is unclearly appreciated in the last one. The presence of joints is limited in the C_018 survey point, with single directional joints and low effect on the conglomerate. The survey point C_023 survey point presented two directional joints and more important (middle) impact. In the first case the joints are filled with argillaceous material, as the main component, while in the second case they were filled with iron-oxides. In the C_009 and C_029, joints are absent. With regards to the properties of cement, it is composed of clayey material with iron-oxides that confer the brown colour to the sediment (rock). In general, the compaction of cement is soft. For this reason the extraction of the pebbles contained in this formation is easy or easy-to-medium. The packing of these pebbles is tangential or isolated. In case the lower or upper strata are present, both are shale and sandstone alternations, in general the most extended rock-types of the Potes Group. A similar sandstone layer is found inside the conglomerate. All these conglomerates display similar features with small particularities and, although there are not many survey points, they are geographically homogeneous (Figure-6.11).

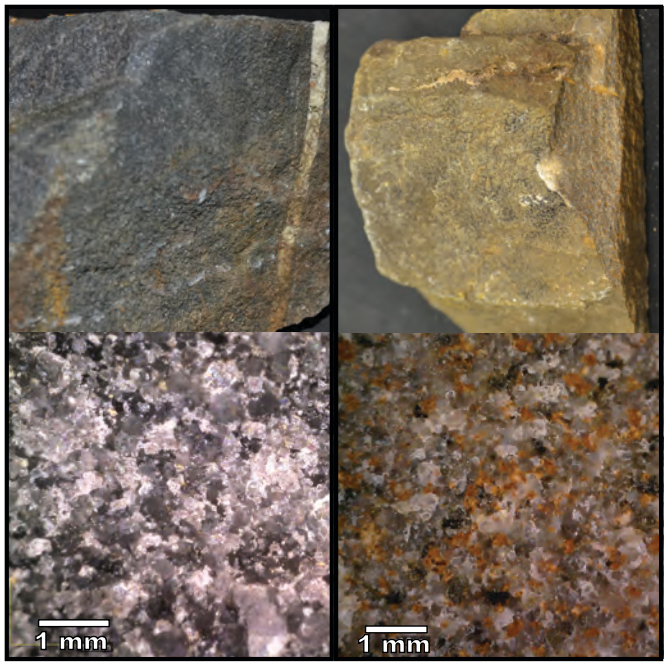

Figure-6.8: Hand sample picture and binocular pictures of two samples from the Murcia Formation. Sample DC54_01 is a CC petrogenetic type of quartz-arenite composed by coarse size quartz grains heterogeneously distributed. Mica can be appreciated at 50x magnification. Sample DC29_03 is a CC petrogenetic type of quartzarenite composed by medium size quartz grains distributed heterogeneously around two modes. Fe-oxides can also be appreciated, in addition to mica and small undetermined black/heavy minerals.

Figure-6.11: Map of the conglomerate formations from the Lower and Middle Pennsylvanian in the area of study. Each point marks a survey point and its main features. Rounded icons represents bedding categories: empty for no-bedding, dashed horizontal lines for unclear bedding, and horizontal lines for bedding. The first square icon represents the characteristics of joints according to two criteria: 1) quantity of joint directions, using horizontal lines for single directional joints, horizontal and vertical lines for two directional joints, and horizontal, vertical, and diagonal lines for three or more directional joints, and 2) presence of mineral inclusions, using different colours, red for Fe-oxides, black for silica, light blue for manganese, orange for carbonates, green for clay, and purple for sandy materials. The last rounded and coloured icon represents the properties of cement. The colour represents the composition of the cement, applying the same colour code as the one previously used for joint filling material. The first letter inside the circle simplifies the type of extraction (I for impossible to extract only pebbles; H for hard to extract pebbles; M for medium difficulty to extract clasts; and E for easy extraction of pebbles or clasts). The second letter synthetises the packing properties (F for floating, I for isolated, T for tangential, and C for complete packing).

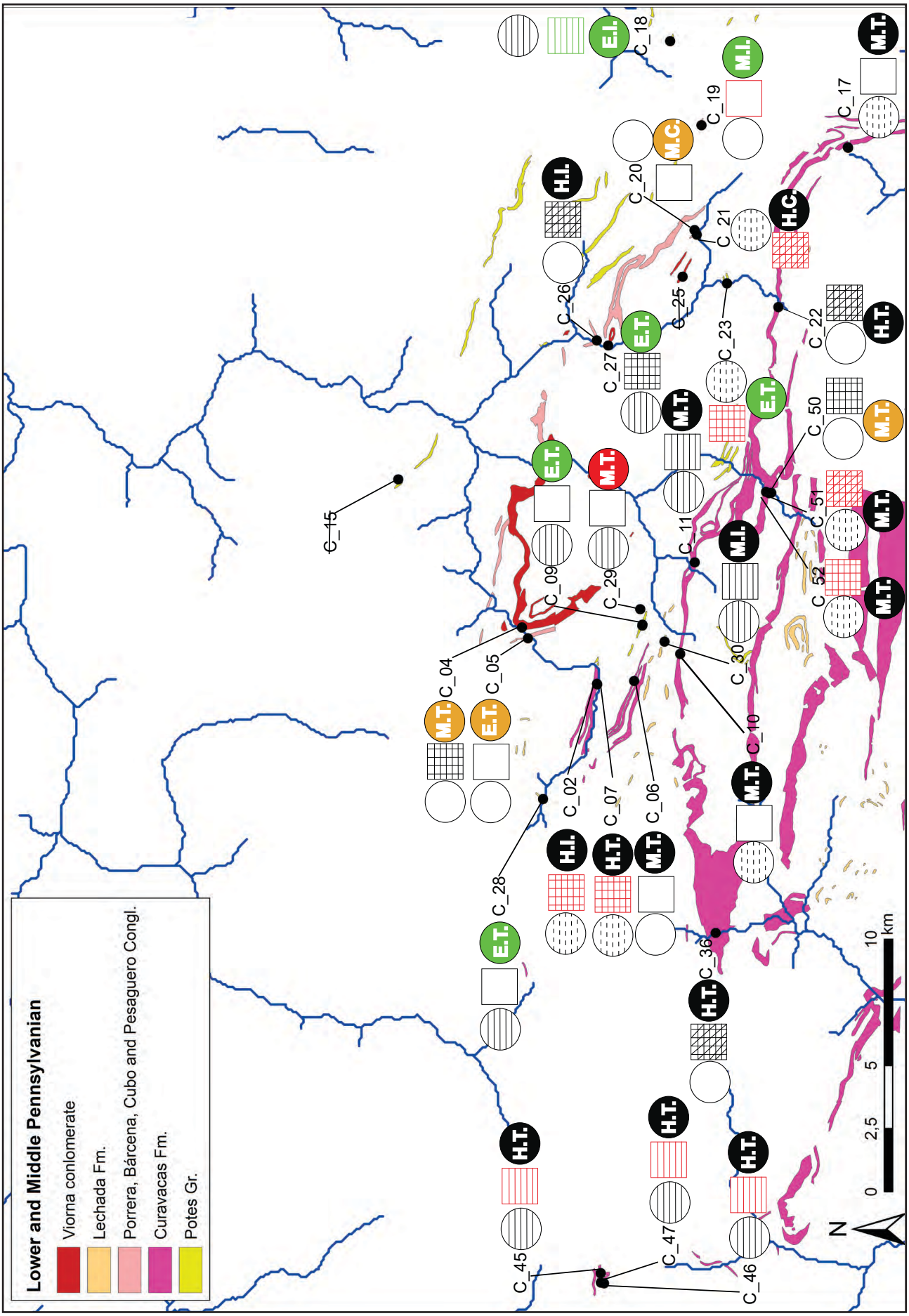

Figure-6.11: Map of the conglomerate formations from the Lower and Middle Pennsylvanian in the area of study. The complete footnote is on the previous page.

Grain size characterisation		Petrogenetic type															
		CC		CA		OO		SO		BQ		RQ		MQ		Total	
		Σ	%	Σ	%	Σ	%	Σ	%	Σ	%	Σ	%	Σ	%	Σ	%
Homogeneous and one mode distribution	Fine grain					2	40	2	50	1	50					5	22
	Medium grain			1	100											1	4
	Coarse grain															0	0
Heterogeneous and two modes distribution	Fine grain	2	18					2	50	1	50					5	22
	Medium grain	3	27													3	13
	Coarse grain	2	18													2	9
Heterogeneous distribution	Fine grain	2	18			2	40									4	17
	Medium grain	2	18			1	20									3	13
	Coarse grain															0	0
	Total	11	48	1	4	5	22	4	17	2	9					23	100

Table-6.10: Frequency table of the petrological features of the pebbles from the Potes group based on binocular characterisation. Columns are petrogenetic types and rows contain the characteristics of grains according to size, classified first by distribution and second by size itself.

There is a high variability among the class coming from the conglomerates based on the lithological varieties of “archaeological quartzites” identified. In general, lithological varieties such as lutites or limestone are also frequent. Focusing on “archaeological quartzite”, there is a high frequency of CC type, generally in percentages greater than 50%. The presence of CA type is also high, but with lower percentages, as well as that of the OO types. Finally, the presence of SO and BQ types are restricted to small or residual quantities, in case they are present. Eleven out of 23 samples are clastic and cemented quartzarenites, showing a generally heterogeneous grain size distribution. Only one of the samples presents homogeneous distribution and medium quartz grain size, demonstrating the presence of clastic quartzarenite (although its representation in survey field is higher). The orthoquartzite group, comprising OO and SO types, is also represented in low percentages. The former presents heterogeneous and homogeneous distribution, generally related with fine grain sizes. The latter is undoubtedly associated with fine grain size and more homogeneous distribution. Finally, the BQ type is represented by two samples with fine quartz grains distributed around one or two modes (Table-6.10). As to the mineral characterisation, Fe-oxides, mica, and non-identified black and heavy minerals are the most common minerals, while manganese oxides and feldspar are not so frequent (Table-6.11). The colour of the cortical areas of clasts selected is mainly grey and brown, but also orange, black, and white, while in fresh-cut orange is not so frequent. This last colour and, less importantly, brown are the result of the more intense impact of the pigments of cement on cortical areas than on inner zones (Table-6.12).

Non-quartz minerals	A		B		C		General	
	Σ	%	Σ	%	Σ	%	Σ	%
Absence								
Fe-Oxides	12	52	5	22	5	22	22	32
Mn-Oxide			1	4			1	1
Calcite								
Mica	9	39	9	39	4	17	22	32
Black mineral	2	9	6	26	14	61	22	32
Pyrite								
Feldspar			2	9			2	3
Total	23	100	23	100	23	100	69	100

Table-6.11: Frequency table of the features of non-quartz minerals of the pebbles from the Potes group based on binocular characterisation. Columns are the three fields considered and rows are the non-quartz minerals identified.

Colour	Cortical area				On fresh cut			
	Primary		Secondary		Primary		Secondary	
	Σ	%	Σ	%	Σ	%	Σ	%
Absence							1	4
White	1	4	1	4	1	4	4	17
Grey	13	57	4	17	15	65	5	22
Black			4	17	3	13	5	22
Blue							1	4
Green								
Orange	4	17	2	9	1	4		
Brown	5	22	11	48	3	13	6	26
Yellow			1	4				
Red							1	4
Total	23	100	23	100	23	100	23	100

Table-6.12: Frequency table of the colour hue of the samples from the pebbles from the Potes group. Columns are the fields for primary and secondary colour hues of cortical areas and in fresh cut respectively and rows are the colours considered.

	Features	Σ	%
Morphology	Tabular clast	1	4
	Tabular pebble	3	13
	Flat pebble	1	4
	Spherical pebble	18	78
	Total	23	100
Cortical texture	Coarse and grained	2	9
	Fine and grained	15	65
	Fine	6	26
	Really fine		
	Total	23	100
Mineral inclussion on cortical area	Absence		
	Fe-oxides	23	100
	Carbonated		
	Siliceaus		
	Total	23	100
Cortical joints	Not analysed		
	Absence	7	30
	Unidirectional	8	35
	Bidirectional	8	35
	Three-directional		
	Total	23	100
Joints	Absence	4	17
	Unidirectional	7	30
	Bidirectional	9	39
	Three-directional	3	13
	Total	23	100
Bedding	Absence	21	91
	Unclear	1	4
	Clear	1	4
	Total	23	100
Schistosity	No	23	100
	Yes		
	Total	23	100

Table-6.13: Frequency table of the morphology, cortical texture, mineral inclusions on the cortex, quantity of cortical joints, quantity of internal joints, bedding, and schistosity of the samples from the Potes group conglomerates.

In regard to the external morphology of the samples, most of them are spherical pebbles. However, tabular pebbles are also present, always related with the CC petrogenetic types, lutites or limestone (Table-6.13). As for cortical texture, most of the samples are fine and grained, followed in frequency by fine texture. Finally there are a few coarse and grained textures. The fine texture is associated with the more deformed petrogenetic types (SO and BQ types). Fe-oxides appear on most of the cortical areas due to the cement composition, as it was explained a few lines above. Respecting the presence of cortical joints, most of the samples show unidirectional or bidirectional joints on cortical areas, while seven of the 23 samples show no joints on cortical areas. There is a higher presence of joints in inner areas too, although four of the 23 samples show no influence of joints at all inside the pebbles. Then, it is possible to conclude that the joints in the pebbles were generated first in the former rock outcrops and secondarily by the joint system that affects these conglomerates at. In general bedding is absent in these samples and only two samples, both belonging to the CC petrogenetic type, show bedding surfaces. Schistosity is not present either, even though a small percentage of the samples are deformed.

Four samples from these conglomerates were selected for thin section analysis, three of them from the survey point C_009 (DC25_01, DC25_05, and DC25_06) and the last one (DC46_12) from the survey point C_018. The first two are OO types and they exhibit clastic grained texture with complete packing, abundant presence of syntaxial quartz grain overgrowth, concavo-convex quartz limits and undulatory extinction. The characterisation of grain size is developed in Supplementary information-I. The grain size of the first sample is coarser than that of the second sample. Being more specific, while in the first sample most of the grains are situated between the very fine and fine sand categories (similar to sample DC04_05), in

the second sample most of the grains are around the coarse silt and very fine sand categories. The morphological characterisation shows similar values for both samples. None of them present preferential orientation (Figure-6.12).

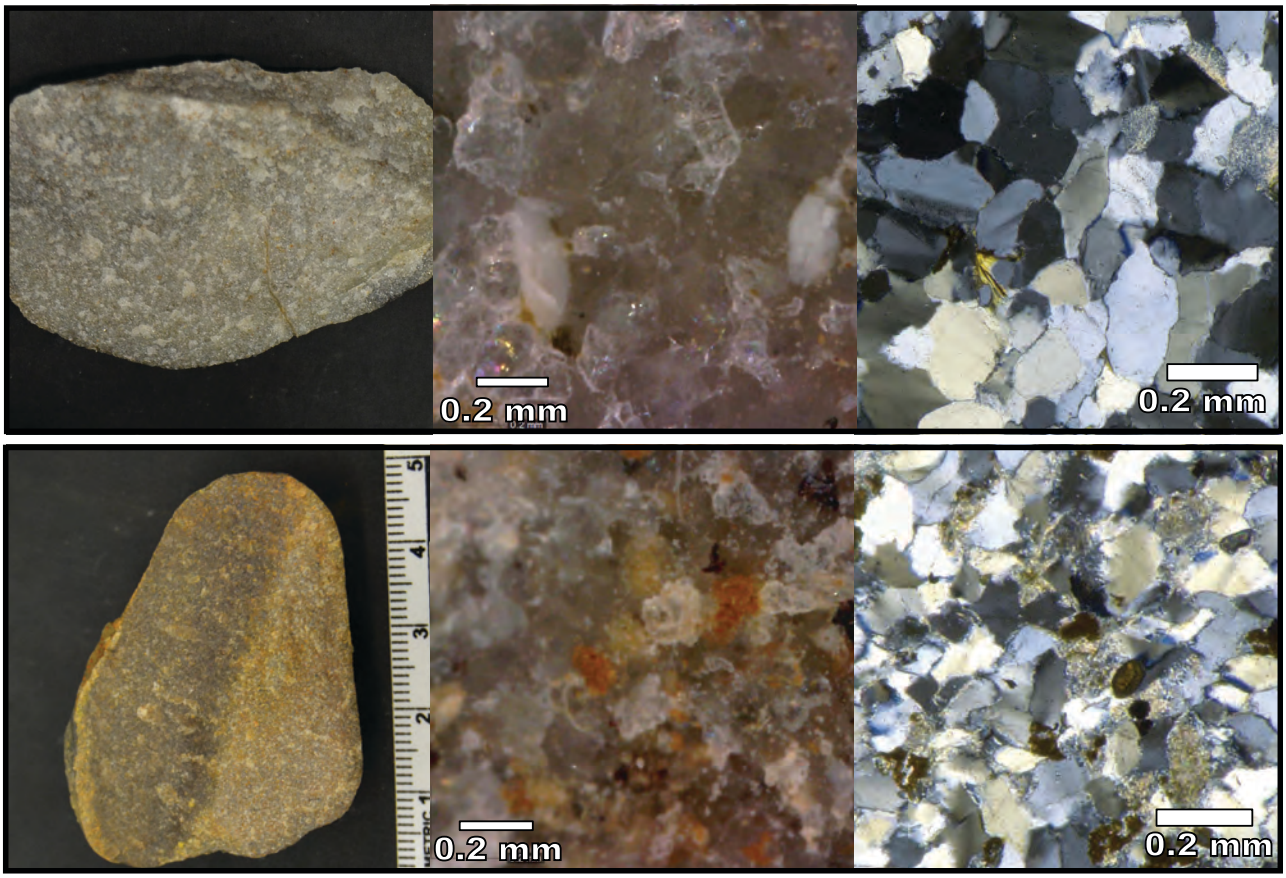

Figure-6.12: Pictures at different magnifications of the OO type samples from the Potes formation. The first one is the DC25_01. It has bigger quartz grain than the second one, the DC25_05 sample. The presence of clayey matrix on the latter sample is clear.

The samples from the SO petrogenetic type (DC25_06 and DC46_12) exhibit clastic grained texture with suturated packing, major presence of undulatory extinction, concavo-convex grain limits, and microstylolitic contacts. Grain sizes are clearly different. While the first sample shows smaller values (most of the grains around the coarse silt category), the second one has bigger quartz grains, within the fine sand category. Even though no schistosity was identified based on non-destructive characterisation, destructive analyses revealed that both types exhibit schistosity in thin section as a consequence of the low degree of deformation of the structures (Figure-6.13).

In regard to mineral characterisation, the DC25_05 and DC25_06 samples present small amounts of clayey matrix. At the same time, non-quartz mineral characterisation reveals that Fe-oxides and mica are present in every sample, while pyrite is present in three of the samples. Other minerals, such as rutile, zircon, and tourmaline appear only in the OO types. Conversely, chlorite is present in SO type. XR-F reveals the major presence of SiO_2 component (greater than 90% in every sample). Fe_2O_3 too is present in all the samples. Finally, Al_2O_3 and carbonate, probably derived from the cement of the conglomerate, is also well represented in every case.

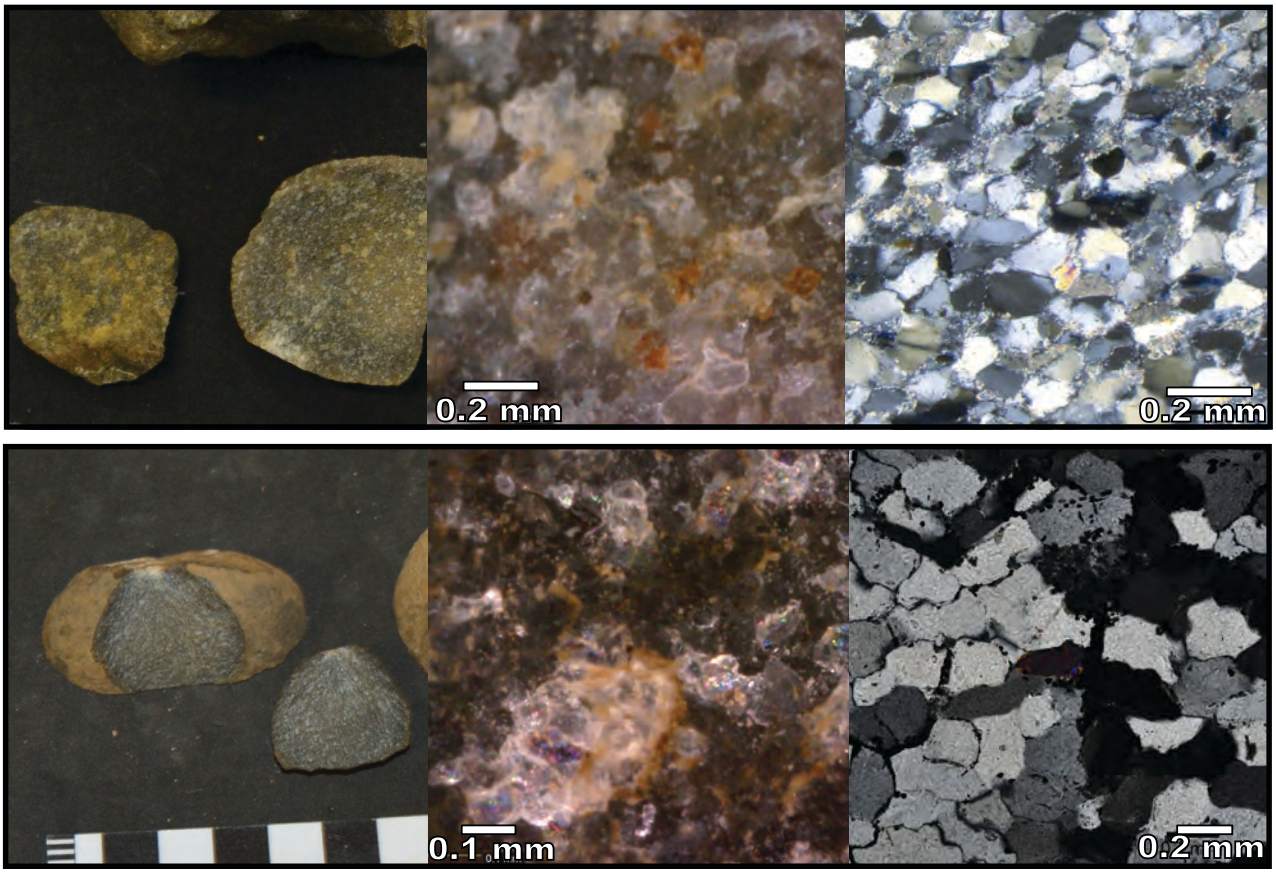

Figure-6.13: Pictures at different magnifications of the SO type samples from the Potes formation. The first one is the DC25_06, with smaller quartz grain size than the second one, the DC46_12, also characterised by the major presence of pyrite.

Summing up, the conglomerates from the Potes Group spread along the south of La Liébana area as small strata and are not easily recognisable in the field. According to the general features established for the characterisation of conglomerates (characterisation of cement, packing, bedding, presence of joints, bedding), they are relatively homogeneous. However, they are not uniform when it comes to the lithological varieties of the clasts of “archaeological quartzite”. Except for sample C_018, the only BQ type found, they do not show clear geography differences (Figure-6.14). The exploitation of different types of “archaeological quartzite” could have been done by directly collecting them in the surrounding areas or by direct hand-made pebble extraction from the conglomerates, facilitated by the softness of cement, which contributes Fe-oxides to the pebbles, conferring them their particular orange-brown colour. The intense exploitation of the CC petrogenetic type (similar in grain size and morphology to the previously commented Murcia or Potes outcrop formations) could have been easily done thanks to its frequent presence. The exploitation of the CA and OO petrogenetic types too could have been easy, without the need sophisticated selection mechanisms, once again thanks to their moderately frequent presence. It is important to mention that different grain size varieties with fine and medium grain size and homogeneous or heterogeneous varieties could be also found, especially among OO types. Finally, given the scarcity of the SO and the BQ types (the latter not having been confirmed by thin-section analysis), these would necessarily have been caught by means of strong selective mechanism. In general, all these clasts present spherical morphologies or shapes tending to spherical pebbles and they are bigger in size than the coarse pebbles (>32mm Ø) appropriated for knapping. To finish, figure-6.15 represents the non-shown petrogenetic types described above and the grain size varieties from the Potes Formation.

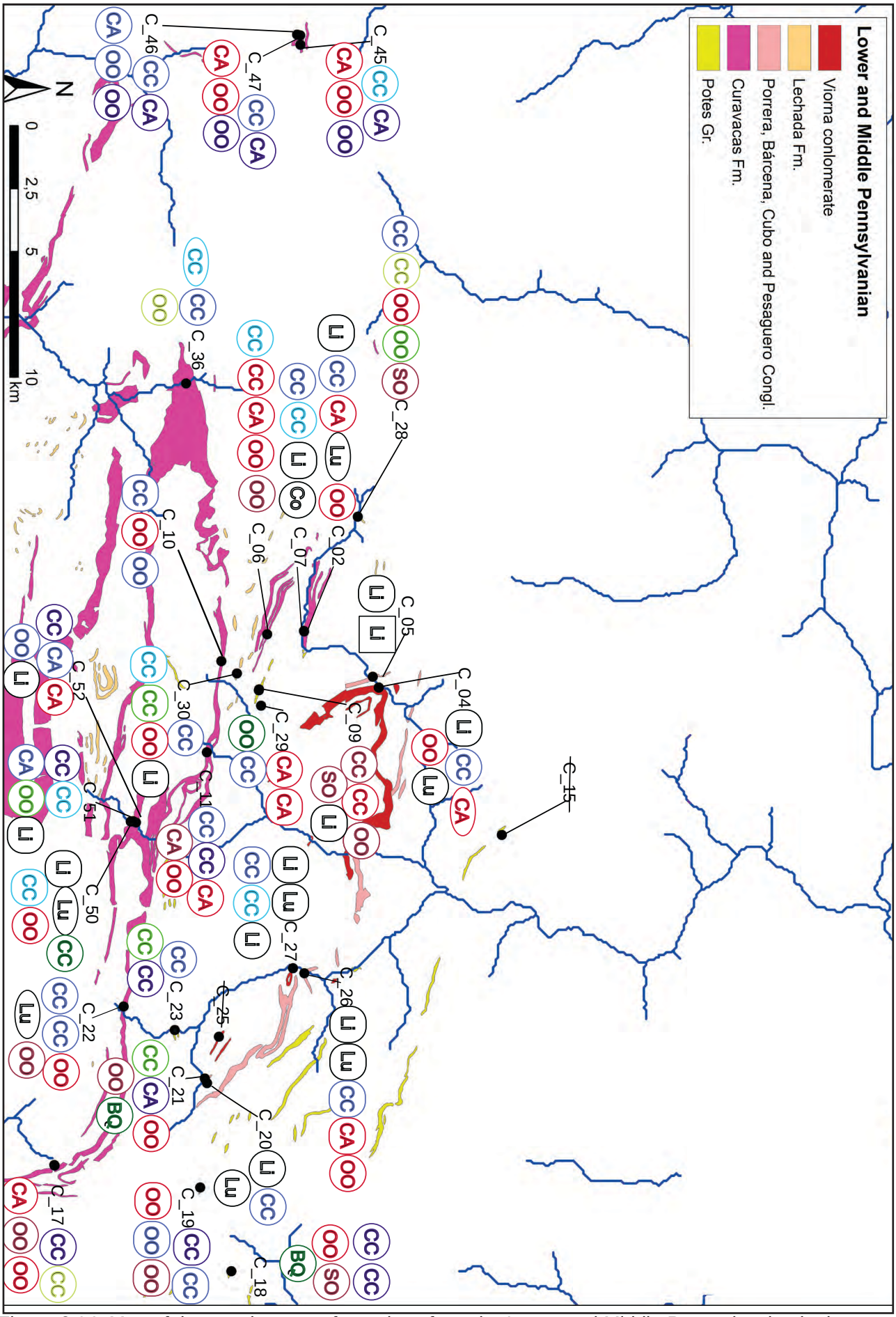

Figure-6.14: Map of the conglomerate formations from the Lower and Middle Pennsylvanian in the area of study. The complete footnote is on the next page.

Figure-6.14: Map of the conglomerate formations from the Lower and Middle Pennsylvanian in the area of study. Each point marks a survey point, whose main lithologies are defined through icons. The petrological characterisation is represented by one to five icons with the initial of the most interesting petrogenetic types, in the case of “archaeological quartzites”, or with those of the main lithology. The external form of the icons describes the morphology of clasts, where squares represent tabular clasts, rounded squares represent tabular pebbles, oval forms represent flat pebbles, and circles represent spherical pebbles. Grain size distribution is represented by the main colour. Homogenous distribution with single mode is represented in red, heterogeneous distribution with two modes is represented in green, and heterogeneous distribution is represented in blue. Grain size characterisation is represented by the brightness of colours previously presented: light red, green, or blue for coarse size grains; medium red, green, or blue for medium size grains, and dark red, green, or blue for small size grains.

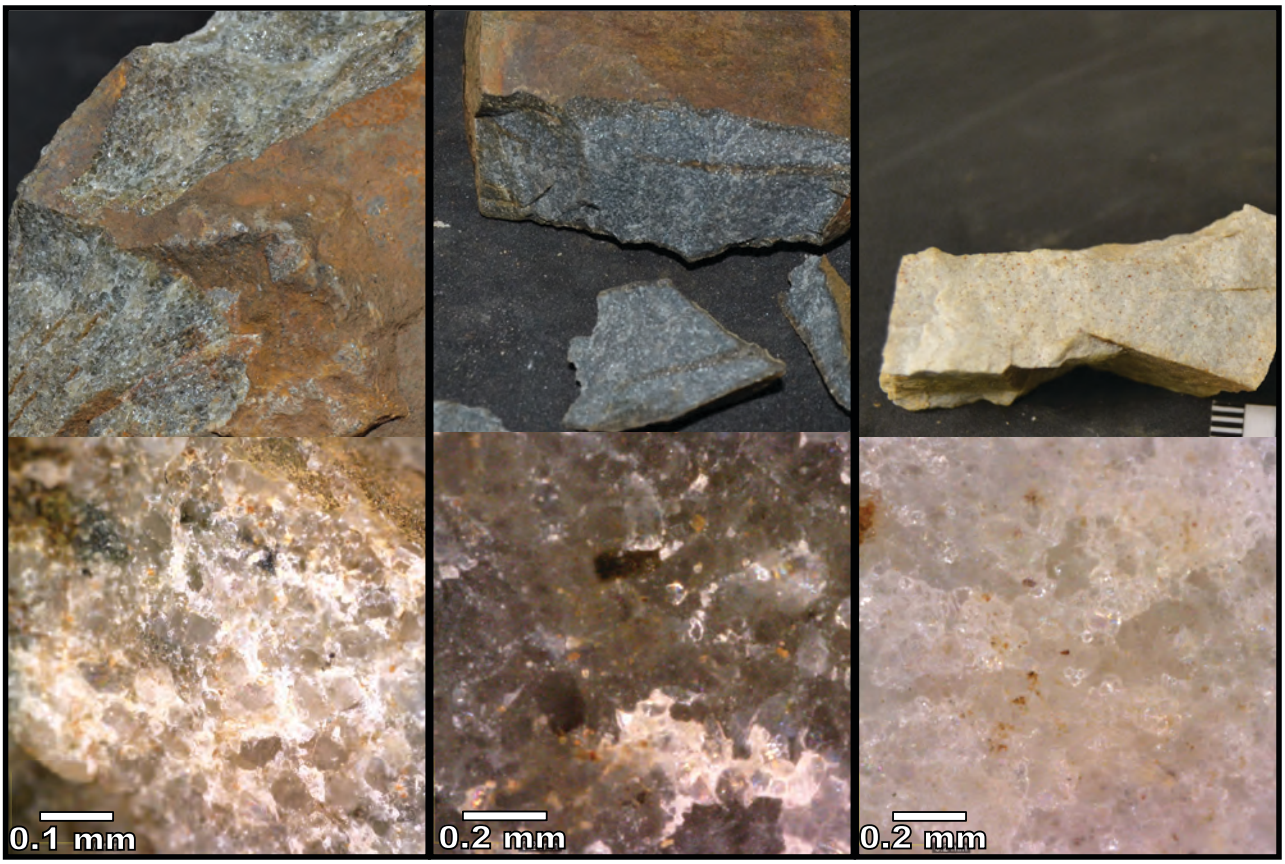

Figure-6.15: Pictures of the petrogenetic types from the Potes group conglomerates not represented previously. On the left, the CC type with coarse and heterogeneously distributed quartz grain size represented by sample DC46_03. In the middle, BQ type with fine and homogeneously distributed quartz grain size represented by sample DC46_09. On the right, the CA type represented by sample DC62_03.

6.2.2. THE MIDDLE PENNSYLVANIAN SERIES: THE CURAVACAS CONGLOMERATE

The Curavacas conglomerate, despite being coetaneous to the Porrera, Bárcena, del Cubo and Pesaguero conglomerates, is the first Middle Pennsylvanian conglomerate formation from the research area. This formation lies on the top of the Priorio Formation and was created on heterogeneous sedimentary conditions derived from the complex basin system generated by the Variscan Orogenesis. Different authors (Fernández et al., 2004; Heredia et al., 2003a; Heredia et al., 2003b; Rodríguez Fernández et al., 2003) proposed that the conglomerate was formed by four different subaerial facies of sea fan. The Curavacas conglomerate is chrono-stratigraphy dated to the Moscovian ages, in the Kashirsky sub-stage. Its thickness is greater than 1000 meters. It crops out to the South of the research area, but it is clearer in La Liébana area than in the Valdeón area. In general, this conglomerate follows a West-East direction. However, some of the strata are on a slight NW-SE or N-S direction (Supplementary Information-VI)

We will analyse the formation through 14 survey points distributed along different areas in order

to understand the possible geographic differences. Supplementary Information-III contains the systemised information about these points. The points are the following:

- C_002/DC007: 30T 358622 4774572
- C_006/DC021: 30T 358733 4773101
- C_007/DC022: 30T 358594 4774565
- C_010/DC026: 30T 359805 4771271
- C_011/DC027: 30T 363466 4770694
- C_017/DC045: 30T 379894 4764637
- C_022/DC052: 30T 373553 4767385
- C_036/DC077: 30T 348738 4769866
- C_045/SE02: 30T 335252 4774423
- C_046/SE03: 30T 334845 4774293
- C_047/SE04: 30T 334873 4774413
- C_050/DC114: 30T 366194 4767667
- C_051/DC115: 30T 366176 4767758
- C_052/DC116: 30T 366227 4767872

The features analysed in the database reveal that this conglomerate is very heterogeneous. The analysis of bedding indicates that the three categories appear in similar percentages: five out of 14 survey points show unclear bedding or absence of bedding, while in the other four points bedding is clear. The survey points where bedding is clear are located in the western areas, while the other two categories are scattered along the central and eastern areas (Figure-6.11). The presence of joints is also heterogeneously distributed and only three of the 14 survey points show no joint activity. Single directional joints are observed in four survey points, mainly in the western area. Two directional joints are present in another four points, but they are not associated with any specific area. This is also the case with three directional joints, which are present in three of the points. If joints are present, its intensity is generally medium (8 of 10), but low impact is also observed in two of the survey points. Joints use to be filled with iron oxides and quartz. Regarding the properties of cement, it is mainly composed of siliceous material, which confers to the Curavacas conglomerate a grey or brown colour. This component gives to the cement a medium or hard compaction, creating medium or hard conditions for the extraction of the blocks that contain the conglomerate. The quantity of the cement on the Curavacas conglomerate is high, ranging between 5 and 50% in most of the survey points. As a consequence, packing is isolated or tangential.

Grain size characterisation		Petrogenetic type															
		CC		CA		OO		SO		BQ		RQ		MQ		Total	
		Σ	%	Σ	%	Σ	%	Σ	%	Σ	%	Σ	%	Σ	%	Σ	%
Homogeneous and one mode distribution	Fine grain			2	12											2	3
	Medium grain	1	3	1	6	4	16									6	8
	Coarse grain																
Heterogeneous and two modes distribution	Fine grain	2	6	2	12	4	16									8	10
	Medium grain	13	36	6	35	3	12									22	28
	Coarse grain	7	19													7	9
Heterogeneous distribution	Fine grain	5	14	1	6	6	24									12	15
	Medium grain	6	17	5	29	7	28									18	23
	Coarse grain	2	6			1	4									3	4
	Total	36	46	17	22	25	32									78	100

Table-6.14: Frequency table of the petrological features of the pebbles from the Curavacas conglomerate based on binocular characterisation. Columns are petrogenetic types and rows contain the characteristics of grains according to size, classified first by distribution and second by size itself.

Attending to the lithology of the different clasts present in the conglomerates, there are some very frequent lithological varieties, such as lutites and limestones. The presence of "archaeological quartzite" is also high, generally represented by CC petrogenetic types. CA or OO types are less important quantitatively. The SO type and the quartzite groups are not present in the Curavacas conglomerates. The distribution of quartz grain size is variable, ranging from homogeneous distributions organised around one mode with fine grain size to heterogeneous quartz grain size distributions with coarse grain sizes. There are no geographical differences or zones based on the lithological features.

We selected a total of 78 samples for non-destructive characterisation in the laboratory. Table-6.14 shows the petrogenetic classification and grain size characterisation. Most of the samples can be classified as CC types. The presence of OO and CA types is smaller. The characterisation of grain size reveals that most of the samples are heterogeneously distributed. Regarding the identification of non-quartz minerals, most of the samples show a significant presence of iron oxides, mica and non-identified black and heavy minerals. There is a small presence of feldspar, generally in CC types, as well as of manganese oxides and pyrite, distributed among the different types of "archaeological quartzites". The colour of the cortical areas is related with the composition of cement. Grey and brown predominate, the latter being related with the presence of iron oxides (Table-6.15). The colour of the inner areas, more closely related with the colour of the original lithologies, is heterogeneously distributed. Grey, white, brown, and black are the most frequent colours (Table-6.16).

Non-quartz minerals	A		B		C		General	
	Σ	%	Σ	%	Σ	%	Σ	%
Absence					6	8	6	3
Fe-Oxides	57	73	4	5	11	14	72	31
Mn-Oxide	1	1	2	3	3	4	6	3
Calcite								
Mica	8	10	44	56	12	15	64	27
Black mineral	9	12	22	28	38	49	69	29
Pyrite					3	4	3	1
Feldspar	3	4	6	8	5	6	14	6
Total	78	100	78	100	78	100	234	100

Table-6.15: Frequency table of the features of non-quartz minerals of the pebbles from the Curavacas Formation based on binocular characterisation. Columns are the three fields considered and rows are the non-quartz minerals identified.

Colour	Cortical area				On fresh cut			
	Primary		Secondary		Primary		Secondary	
	Σ	%	Σ	%	Σ	%	Σ	%
Absence			7	9			11	14
White	2	3	4	5	15	19	22	28
Grey	46	59	16	21	55	71	13	17
Black			8	10	4	5	9	12
Blue			3	4			8	10
Green								
Orange	1	1	9	12				
Brown	29	37	30	38	4	5	12	15
Yellow								
Red			1	1			3	4
Total	78	100	78	100	78	100	78	100

Table-6.16: Frequency table of the colour hue of the samples from the pebbles from the Curavacas conglomerate. Columns are the fields for primary and secondary colour hues of cortical areas in in fresh cut respectively and rows are the colours considered.

As to the external morphology of the samples, most of them are spherical pebbles. Tabular and flat pebbles are also present in percentages slightly above 10%. These are mainly related with the CC petrogenetic type (Table-6.17). Cortical textures are grained, mainly fine. Some fine textures can also be identified. The presence of mineral inclusion is related to the mineral composition of the cement: siliceous with presence of iron oxides. Actually, iron oxide is the most frequent mineral inclusion because of its high visibility in the samples. Cortical and internal joints show similar number of directions, even though inner joints are slightly more numerous as a consequence of the

	Features	Σ	%
Morphology	Tabular clast	1	1
	Tabular pebble	12	15
	Flat pebble	9	12
	Spherical pebble	56	72
	Total	78	100
Cortical texture	Coarse and grained	7	9
	Fine and grained	46	59
	Fine	25	32
	Really fine		
	Total	78	100
Mineral inclussion on cortical area	Absence		
	Fe-oxides	54	69
	Carbonated	4	5
	Siliceaus	20	26
	Total	78	100
Cortical joints	Not analysed	2	3
	Absence	15	19
	Unidirectional	19	24
	Bidirectional	33	42
	Three-directional	9	12
	Total	78	100
Joints	Absence	15	19
	Unidirectional	20	26
	Bidirectional	29	37
	Three-directional	14	18
	Total	78	100
Bedding	Absence	69	88
	Unclear	7	9
	Clear	2	3
	Total	78	100
Schistosity	No	77	99
	Yes	1	1
	Total	78	100

Table-6.17: Frequency table of the morphology, cortical texture, mineral inclusions on the cortex, quantity of cortical joints, quantity of internal joints, bedding, and the schistosity of the samples from the Curavacas Formation.

joints created in the strata where clasts were originally located. In general, it is possible to observe a greater number of joints in the Curavacas conglomerate than in those previously analysed. This is due to the compaction of cement. There were no clear bedding structures in the samples (bedding structures were only present in nine of the 78 samples), nor schistosity, only present in one of the 78 samples.

We selected 20 samples for thin section and X-Ray Fluorescence analysis. Four samples came from the survey point C_002 (DC07_02, DC07_03, DC07_07, and DC07_08), four from the survey point C_006 (DC21_01, DC21_03, DC21_06, and DC21_07), two from the survey point C_007 (DC22_01 and DC22_04), two from the survey point C_010 (DC26_02 and DC26_03) six from the survey point C_011 (DC27_1, DC27_3, DC27_4, DC27_6, DC27_9, and DC27_12), one from the survey point C_017 (DC45_05), and one from the survey point C_036 (DC77_04). CC, CA, and OO types are well represented among the samples selected, with eight samples classified in the first petrogenetic type, six in the second one and four in the third one (Figures-6.16, Figure-6.17, and Figure-6.18). Textures, packing, and quartz grain features are synthesised in Table-5.1 from Chapter-5. In Figure-5.26 also from Chapter-5, each sample is classified on each petrogenetic type. The last two samples (DC45_05 and DC77_04) are classified as SO type even though the features of quartz grain size reveal incompletely deformed structures, without deformation lamellae but small amounts of recrystallized grains. The moderate presence of stylolite grain boundaries supports this explanation (Figure-6.19). The characterisation of quartz grain size and their morphological analysis is developed in Supplementary information-I. In general, it confirms the differences between the petrogenetic types previously proposed. The analysis of each sample, taking into account its petrogenetic type, reveals different varieties of quartz grain sizes (Figure-6.20). Regarding grain size distribution, in the CC and CA types there are samples with heterogeneous distributions, but there are other ones with more homogeneous distributions too. There is also great variability in size, which ranges from small to big quartz grain sizes. This high variability among the samples reflects the high diversity of clast source areas. The OO and SO types show high variability too. There are at least two different source areas for the clasts of the Curavacas conglomerate. The first one presents heterogeneous distribution and coarse quartz grains (samples DC26_03, DC27_01, and DC45_05). The second one has more homogeneous distribution but finer quartz grains (DC 27_01, DC21_06, and DC77_04). Sample DC21_03 probably came from another source area. The characterisation of non-quartz minerals is shown in Table-5.11 and the results of X-Ray Fluorescence can be found in the Table-5.17, both from chapter-5. These data do not outline any clear relationship between any parameter and the presence of specific non-quartz minerals or components. The high variability of the various non-quartz minerals and components could also be a consequence of the great number of source areas of the clasts forming the Curavacas conglomerate.

Figure-6.16: Pictures at different magnifications of the CC type samples from the Curavacas Formation. The first one is the DC21_07, with coarse and heterogeneous quartz grain variety. The second one is the sample DC21_01, with high presence of clay in the matrix, probably mixed with carbonated cement (not clearly appreciable in the sample).

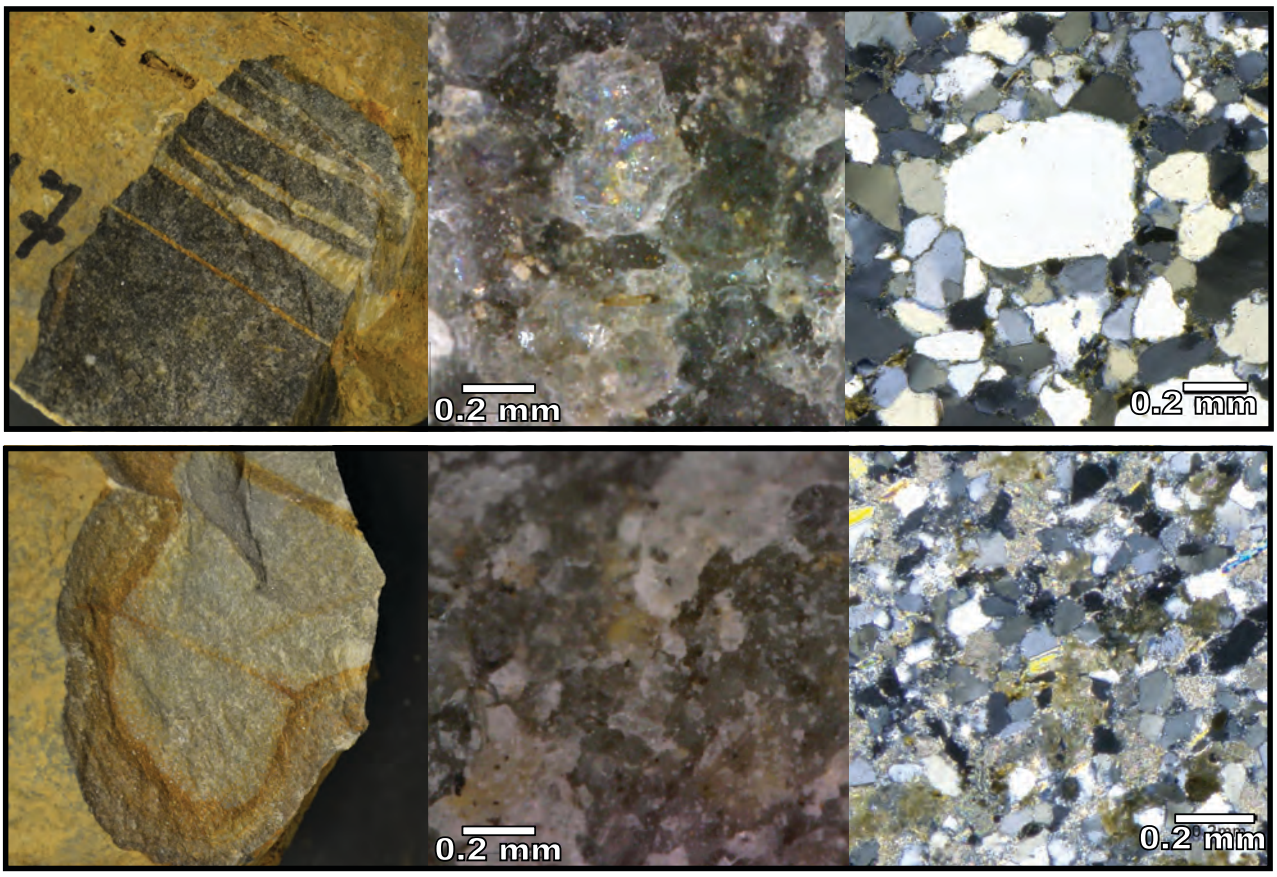

Figure-6.16: The complete footnote is on previous page

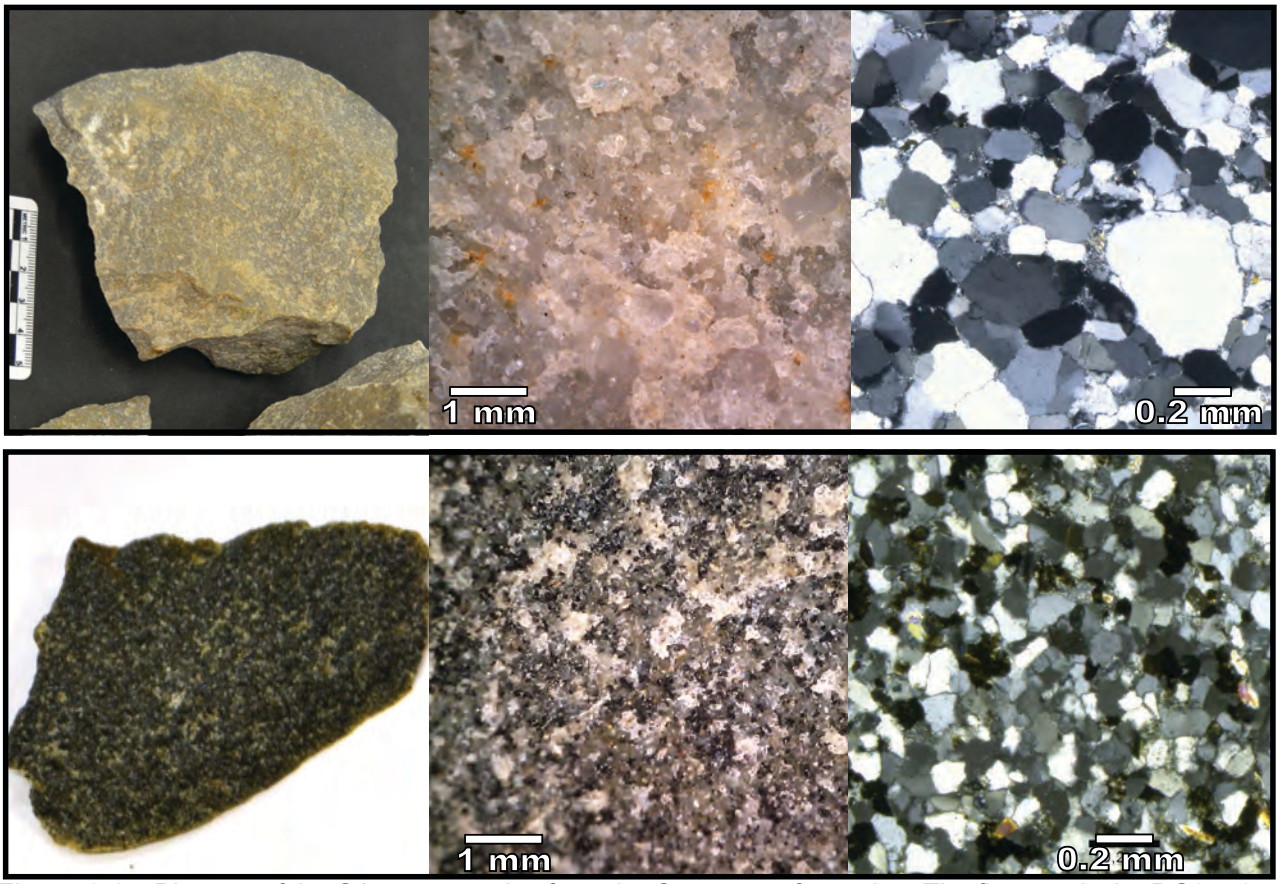

Figure-6.17: Pictures of the CA type samples from the Curavacas formation. The first one is the DC07_07, with coarse and heterogeneous quartz grain variety. The second one is the sample DC27_09, with small and homogeneous quartz grain size. Note the high presence of iron oxides and tourmalines in the last one. The binocular picture is made at 50x magnifications.

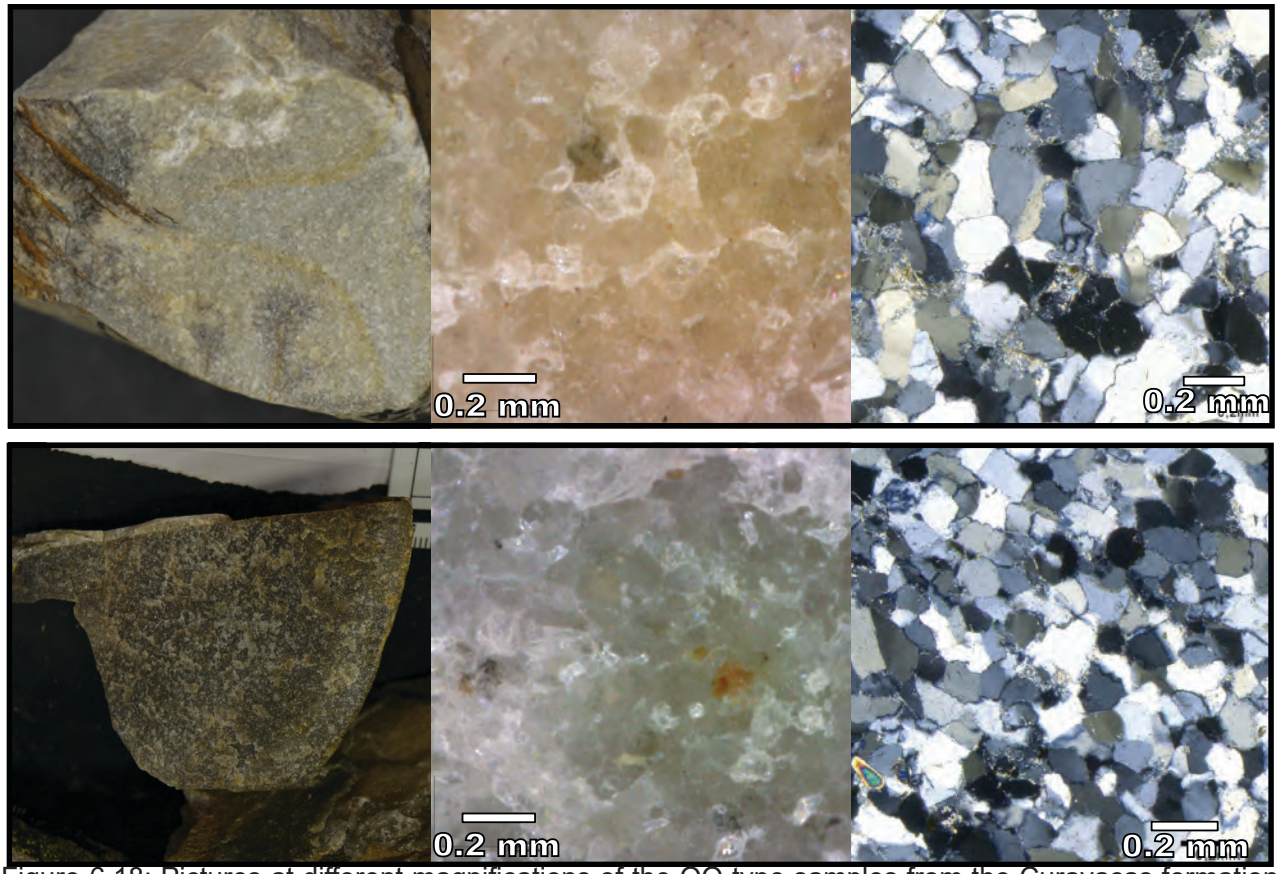

Figure-6.18: Pictures at different magnifications of the OO type samples from the Curavacas formation. The first one is the DC26_03, with coarse grain size. The second sample is the DC21_07, with finer quartz grain sizes, also more homogeneous.

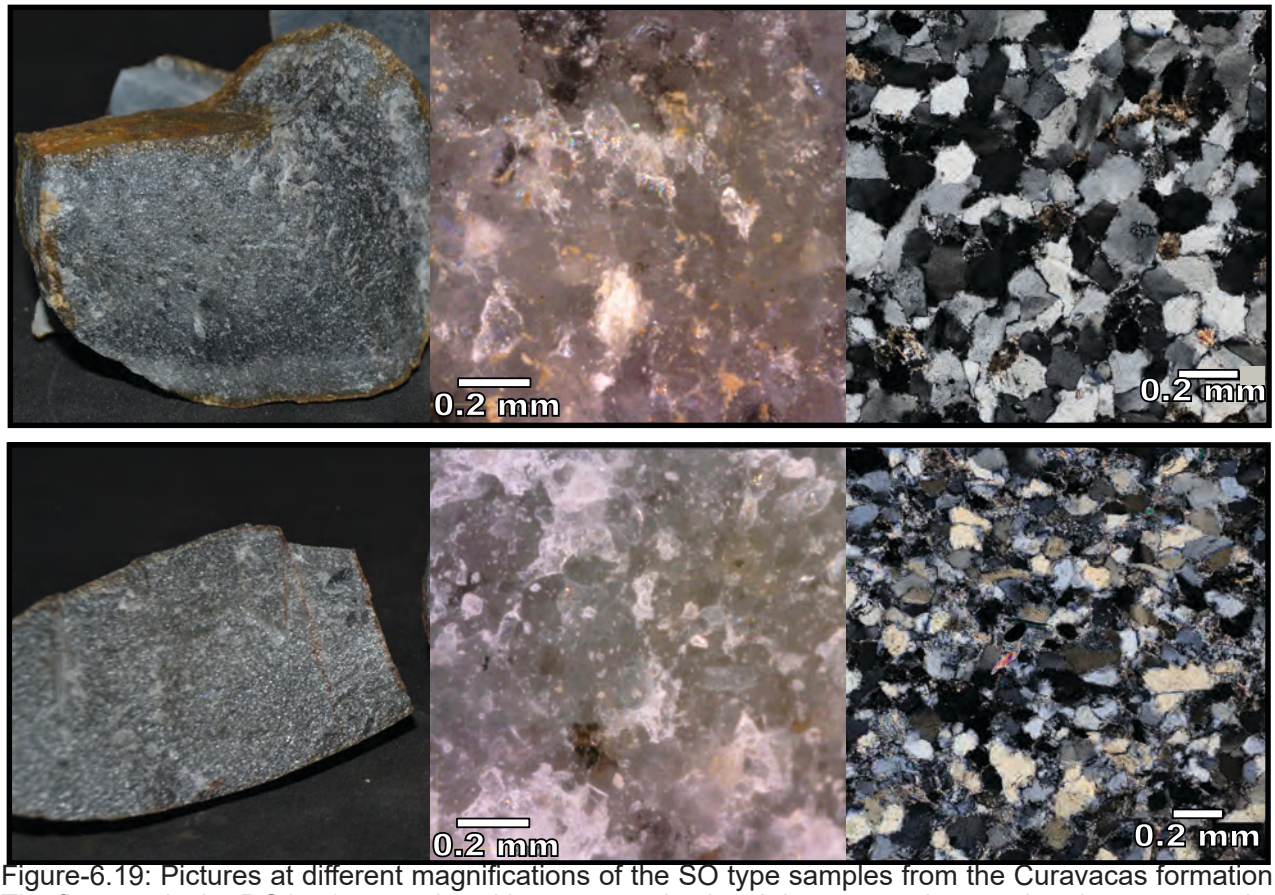

Figure-6.19: Pictures at different magnifications of the SO type samples from the Curavacas formation. The first one is the DC45_05 sample, with coarse grain size. It is easy to observe that the quartz grains show no clear stylolite borders. The second sample is the DC77_04, with clearly smaller quartz grain size and presence of clayey matrix.

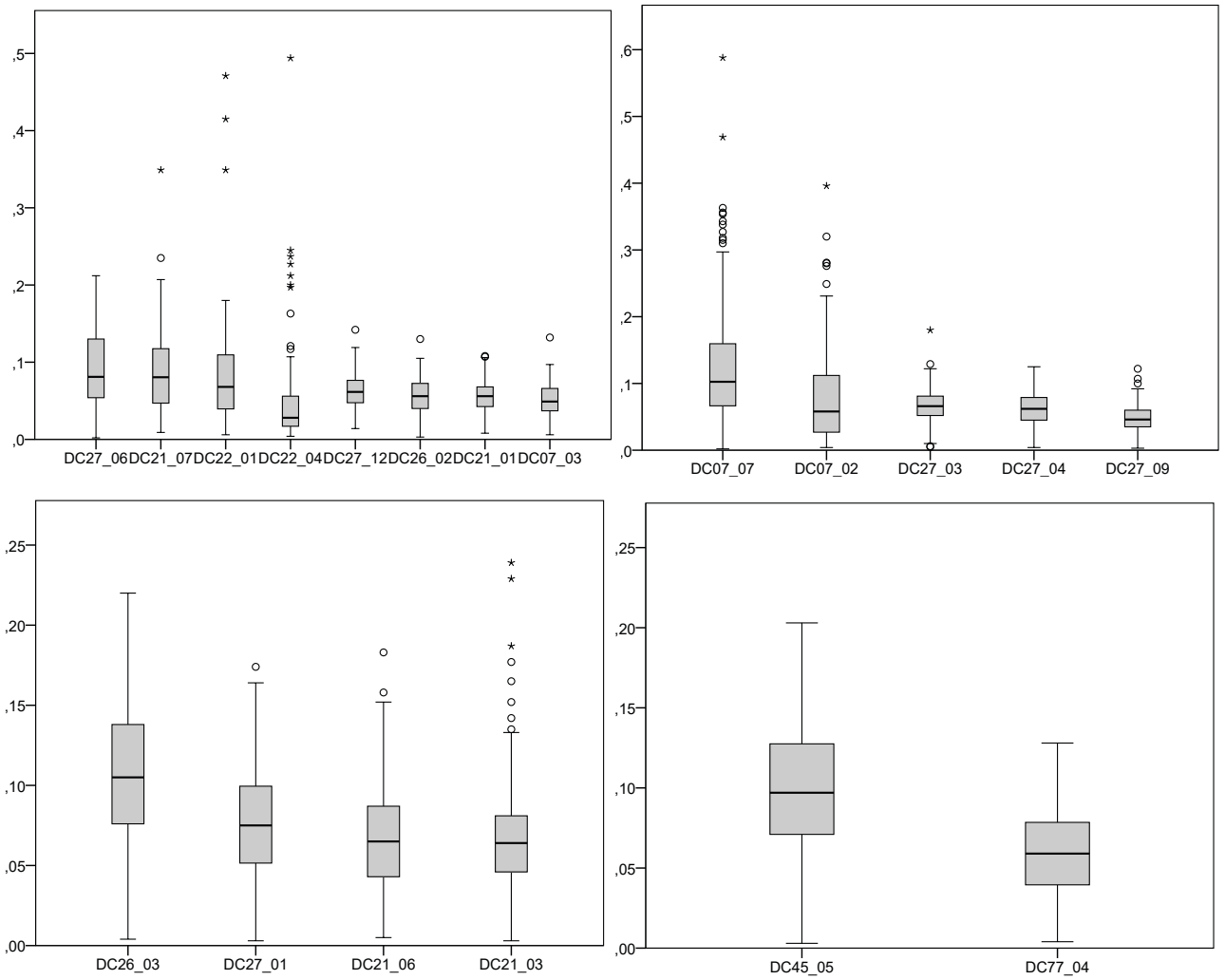

Figure-6.20: Four boxplot charts representing the analysis of grain size of the samples from the Curavacas conglomerates classified by petrogenetic type. From left to right and from top to bottom: CC, CA, OO, and SO types. In each chart samples are classified from heterogeneous and coarse quartz grains to homogeneous and fine quartz grains.

Summing up, the conglomerates of the Curavacas Formation spread along the south of the research area as big and massive strata, easily recognisable in the field (e.g. graphic information on C_011, C_022, C_036, or C_052 in Supplementary Information-III). According to the properties of joints and bedding they are clearly heterogeneous, but they are more homogeneous when it comes to cement colour and composition, cortical and inner colour, packing, and facility of rock extraction. Lithology is varied and it includes limestones, lutites, quartz-arenites, and orthoquartzites, the first three being predominant. Geographical patterns are only observed in the characterisation of bedding. The exploitation of different types of lithic resources in the Curavacas Formation could have been done by direct gathering in the areas surrounding the conglomerate. However, given the compaction conferred by cement, the extraction of the rocks directly from the conglomerate must have been carried out using hammers or other tools. The presence of silica on the cortical area of some of the samples is also a consequence of the compaction caused by cement. The intense catchment of different varieties of the CC petrogenetic type could have been easy thanks to its high presence. In the same way, the exploitation of different varieties of the CA and OO petrogenetic types would have been possible, but, given the smaller presence of these two types, selective mechanisms would have been necessary. Finally, the exploitation of the scarce unclearly deformed SO type would only have been possible by applying important selective mechanism. The clasts from the Curavacas conglomerate are within the Udden-Wentworth's category of cobbles.

6.2.3. THE MIDDLE PENNSYLVANIAN SERIES: THE PORRERA, BÁRCENA, CUBO, AND PESAGUERO CONGLOMERATES

In this section we describe the Porrera, Bárcena, Cubo and Pesaguero conglomerates. These polygenic or polymictic conglomerates are a series of different and heterogeneous conglomerates, contemporary to each other and to Curavacas conglomerate presented above. These formations lie on the top of the Priorio Formation and were generated under the same heterogeneous sedimentary conditions derived from the complex basin system present in the area during the Upper Carboniferous. They are chrono-stratigraphically situated in the Moscovian ages, in the Kashirsky sub-stage. They are located to the south of our research area, generally in northwest-southeast direction. We will describe the location of three out of these four contemporary conglomerates: The Bárcena conglomerate extends over the western zone of the La Liébana area and near the village of La Bárcena. The Porrera conglomerate is located in the central-eastern zone of La Liébana area, between the villages of Lerones and Cabezón. Finally, the Pesaguero conglomerate is situated in the south-eastern zone of La Liébana area, near the village of Pesaguero. Visibility and thickness are different in each conglomerate, ranging from more than 100 meters to 10 meters (Fernández et al., 2004; Heredia et al., 2003b; Rodríguez Fernández et al., 2003).

We analyse these formations through five survey points. Supplementary Information-III contains the systemised information about the points. The points are the following:

- C_005/DC019: 30T 360421 4777309 in the Bárcena conglomerate
- C_019/DC048: 30T 380763 4770430 probably in the Pesaguero conglomerate
- C_020/DC050: 30T 376611 4770704 in the Pesaguero conglomerate
- C_021/DC051: 30T 376427 4770617 in the Pesaguero conglomerate
- C_026/DC057: 30T 372231 4774580 in the Porrera conglomerate

The features analysed in the database reveal that this series of conglomerates is very heterogeneous, except for bedding. Four out of five points display no bedding structures and only one of the points shows unclear bedding. The joint systems affecting the conglomerates show clear differences between them and vary between some conglomerates with three-directional joint systems to others without any joints. Its impact is diverse too, as some of them are filled in with siliceous material and others with oxides. The composition of cement is also heterogeneous, with the possibilities of being carbonated, siliceous, or clayey. The Pesaguero conglomerate, the only one surveyed at two points, presents siliceous cement in one of them and carbonate cement in the other one. Rock extraction is variable too. It can be easy in the cases of calcareous cemented conglomerates or hard in siliceous cemented conglomerates. There are also differences in packing between different conglomerates, ranging from isolated packing of the clasts to (almost) complete packing. These differences do not follow a geographical pattern (Figure-6.11)

According to the lithological varieties of these conglomerates, most of the clasts are limestones and lutites, as well as “archaeological quartzites”. The latter belong mainly to the CC petrogenetic type, although other types, such as CA, OO, and BQ types are also present. The morphology for the first two lithologies is diverse. However, tabular pebbles are usually associated to limestones, lutites, and CC petrogenetic types. The other petrogenetic types tend to be more spherical. There are several quartz grain size varieties of “archaeological quartzite” in the conglomerate. We do not appreciate any geographic differences based on lithology.

We discarded to take samples from the survey points C_005 and C_020 because they are exclusively formed by limestones, lutites and CC type “archaeological quartzites”. We selected a total of 18 samples for laboratory characterisation from the other three survey points. Table-6.18 shows the petrogenetic characterisation of these samples, as well as the features of their grain size. There is a high frequency of CC, CA, and OO types. The samples from the quartz-arenite group are mainly related with heterogeneous distributions of quartz grain size. Meanwhile the OO type is more associated with homogeneous distributions of quartz grain size. One sample from the survey point C_021 was classified as BQ type (unconfirmed by petrographic characterisation). Regarding the mineral characterisation, the most frequent categories are iron-oxides, mica, and non-identified black and heavy minerals, present on most of the samples (Table-6.19). The manganese oxides are restricted to three OO type samples and feldspar to the CC type. Due to the high variability of cement, the colour of the cortical areas is heterogeneous too. In fresh cut the colours are also variable, although grey and white are predominant (Table-6.20). As to the external morphology of the stones, every

shape considered is present, but spherical pebbles are the most frequent one, as shown in the general characterisation of the clasts (Table-6.21). Cortical texture is also variable, with the identification of diverse types of textures from the very fine texture of type BQ to the coarse and grained texture of a CC type. Fine and grained, as well as fine texture, are the most frequent textures. The former is generally associated with CC or CA types and the latter to OO types. All the mineral inclusions on the cortical area are siliceous, the main component of the cement of two of three survey points sampled. Unidirectional joints were predominant on the cortical area, as well as in the inner part of the stones. In general, there is a greater number of directional joints in the inner part, as a consequence of the joints affecting the rocks on the former strata. Only one of the clasts, a CC type, exhibits bedding. No schistosity was found among the samples.

Grain size characterisation		Petrogenetic type															
		CC		CA		OO		SO		BQ		RQ		MQ		Total	
		Σ	%	Σ	%	Σ	%	Σ	%	Σ	%	Σ	%	Σ	%	Σ	%
Homogeneous and one mode distribution	Fine grain					3	33									3	17
	Medium grain					2	22									2	11
	Coarse grain																
Heterogeneous and two modes distribution	Fine grain	1	20			1	11			1	100					3	17
	Medium grain					1	11									1	6
	Coarse grain																
Heterogeneous distribution	Fine grain	2	40	2	67	1	11									5	28
	Medium grain	2	40	1	33	1	11									4	22
	Coarse grain																
	Total	5	28	3	17	9	50			1	6					18	100

Table-6.18: Frequency table of the petrological features of the pebbles from the Porrera, Bárcena, and Pesaguero conglomerates based on binocular characterisation. Columns are petrogenetic types and rows contain the characteristics of grains according to size, classified first by distribution and second by size itself.

Non-quartz minerals	A		B		C		General	
	Σ	%	Σ	%	Σ	%	Σ	%
Absence								
Fe-Oxides	9	50	3	17	2	11	14	26
Mn-Oxide			3	17			3	6
Calcite								
Mica	5	28	6	33	7	39	18	33
Black mineral	4	22	5	28	8	44	17	31
Pyrite								
Feldspar			1	6	1	6	2	4
Total	18	100	18	100	18	100	54	100

Table-6.19: Frequency table of the features of non-quartz minerals of the pebbles from the Porrera, Bárcena, and Pesaguero conglomerates based on binocular characterisation. Columns are the three fields considered and rows are the non-quartz minerals identified.

We selected sample DC51_01 for thin section and XRF. The analysis corroborated the OO petrogenetic type, with presence of syntaxial regrowth, undulatory extinction and concavo-convex and slightly suturated quartz grain limits. The characterisation of grain size reveals that most of the quartz grains are within the fine sand category. This type and grain size variety is very similar to the sample DC25_01 analysed for the Potes Group conglomerate, as well as to some samples from the Curavacas conglomerates, for example DC26_03 (Figure-6.21). The characterisation of non-quartz minerals reveals the presence of mica, rutile and tourmaline. Regarding X-Ray fluorescence, the sample is mainly composed by silica (98.3%), followed by alumina oxides (0.8%) and iron oxides (0.4%) The presence of other components is not significant.

Colour	Cortical area				On fresh cut			
	Primary		Secondary		Primary		Secondary	
	Σ	%	Σ	%	Σ	%	Σ	%
Absence			2	11			2	11
White	2	11	1	6	4	22	5	28
Grey	12	67	3	17	13	72	4	22
Black	1	6	2	11			1	6
Blue			2	11			4	22
Green								
Orange	1	6						
Brown	2	11	7	39			2	11
Yellow			1	6				
Red					1	6		
Total	18	100	18	100	18	100	18	100

Table-6.20: Frequency table of the colour hue of the samples from the pebbles from the Porrera, Bárcena, and Pesaguero conglomerates. Columns are the fields of primary and secondary colour hues of cortical areas and in fresh-cut respectively and rows are the colours considered.

	Features	Σ	%
Morphology	Tabular clast	1	1
	Tabular pebble	12	15
	Flat pebble	9	12
	Spherical pebble	56	72
	Total	78	100
Cortical texture	Coarse and grained	7	9
	Fine and grained	46	59
	Fine	25	32
	Really fine		
	Total	78	100
Mineral inclussion on cortical area	Absence		
	Fe-oxides	54	69
	Carbonated	4	5
	Siliceaus	20	26
	Total	78	100
Cortical joints	Not analysed	2	3
	Absence	15	19
	Unidirectional	19	24
	Bidirectional	33	42
	Three-directional	9	12
	Total	78	100
Joints	Absence	15	19
	Unidirectional	20	26
	Bidirectional	29	37
	Three-directional	14	18
	Total	78	100
Bedding	Absence	69	88
	Unclear	7	9
	Clear	2	3
	Total	78	100
Schistosity	No	77	99
	Yes	1	1
	Total	78	100

Table-6.17: Frequency table of the morphology, cortical texture, mineral inclusions on the cortex, quantity of cortical joints, quantity of internal joints, bedding, and the schistosity of the samples from the the Porrera, Bárcena, and Pesaguero conglomerates.

Summing up, the Porrera, Bárcenas, and Pesaguero conglomerates are very heterogeneous. Based on survey points C_005 and C_020, where there was high presence of limestones and lutites and a smaller representation of CC types, the exploitation of siliceous lithic raw material from these conglomerates would not have been possible. Both survey points are similar according to almost all the features analysed. In contrast the other three points shows similarities with other conglomerates in the region, such as the previously presented Potes Group or the Viorna conglomerate. These survey points raise the possibility of the presence in the region of conglomerates that were not correctly identified in the regional geology. At the survey points C_019 and C_026 the exploitation of siliceous raw material would have been easy if it was restricted to gathering at the foothills of the conglomerates but, because of the compaction of cement, it would have been more difficult to extract the rocks directly from the conglomerate. In this case the use of hammers or other tools would have been mandatory. Conversely, at the survey point C_021 the extraction of rocks from the conglomerate would have been possible thanks to the softer and argillaceous cement present here. In any case, the exploitation of CC types could have be easy done in any of the three conglomerates because of its major presence, but the exploitation of CA and OO types would have required selection strategies, more sophisticated if certain grain size varieties were to be selected. The presence of one sample belonging to the BQ reveals the existence of access to more deformed quartzites in these conglomerates, but its residuality indicates its exploitation is more casual than planned. Overall, the characterisation of these conglomerates reveals the importance of being as detailed as possible in the descriptions to define the features of each strata properly. In general, we should discard these formations as a source of raw material, excluding small areas related with other types of conglomerates.

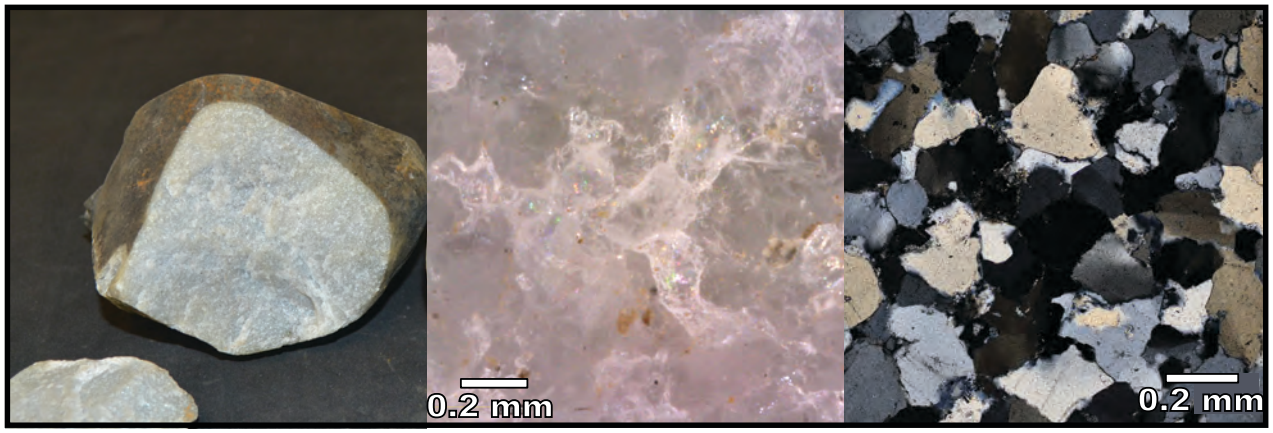

Figure-6.21: Pictures at different magnifications of the sample DC 51_01 from the Pesaguero Formation. The OO type is easily recognisable in thin section and binocular pictures, as well as the medium to coarse grain size.

6.2.4. THE MIDDLE PENNSYLVANIAN SERIES: THE LECHADA CONGLOMERATE

The Lechada Formation is also a sandstone, shale and conglomerate alternation generated by (mainly siliciclastic) sedimentary processes during the second part of the Carboniferous. These processes were caused by the Variscan orogenesis, which created multiple sedimentary basins reflected in this area of research on delta-fan transitions, preferentially in the Pisuerga-Carrión Unit. The conglomerates of the Lechada Formation are dated to the Moscovian age, in the Podolsky, and they are coetaneous to other similar strata, such as the aforementioned Curavacas deposit or the Mogrovejo sandstone Formation, in the Pisuerga-Carrión Unit. The stratum underlying the Lechada Formation is the Curavacas conglomerate and it is covered, after a hiatus, by the Kasimovian Remoña Formation. The conglomerates from the Lechada Formation extend along the south of our research area, but they are only visible in the southwestern part of La Liébana zone. Its visibility is restricted, except for the areas where the conglomerates are cut by any landform. They are arranged into small and discontinuous strata among the Curavacas conglomerates and generally with Northwest-Southeast orientation.

We analyse the formation based on only two survey points located in different areas in order to understand the possible differences between them. Supplementary information-II contains the systemised information about these points. The points are the following:

- C_028/DC061: 30T 354047 4776710
- C_030/DC063: 30T 360293 4771898

The observations carried out conclude that bedding is clear in both points while the presence of directional joins is unequal. The impact of joints in the survey point C_030 is medium and they are cemented and filled by silica. The properties of cement also differ between the two survey points. The cement of the survey point C_028 is argillaceous, brown, of soft compaction and easy to extract rocks from. The cement of the C_030 survey point is also brown, but its compaction is medium, hindering rock extraction in comparison with the first survey point. The presence in survey point C_028 of quartz inside the joints and the cement as a consequence of a post-depositional event could be the explanation what makes both survey points different. The packing of the pebbles, either isolated or tangential, is similar in both cases. In general, the clasts are abundant and could be easily extracted (although this is slightly harder when quartz is present). The upper and lower strata consists of either sandstone or sandstone and lutite. In conclusion, these two survey points show similar patterns and they are geographically homogeneous (Figure-6.11).

There is an abundant presence of “archaeological quartzite”, as it constitutes the main lithological variety. This is only disrupted by the presence of limestone in survey point C_030. The most represented types are CC and OO and there is a small representation of the SO type too. Regarding the grain size varieties, there are different ones are represented. They range between heterogeneous and homogeneous grain size distributions, with a tendency to medium to coarse grain sizes. Heterogeneous grain size distribution is generally associated to the CC petrogenetic type. We selected 15 samples from both conglomerates and, in general terms, the laboratory classification results into similar lithological distribution. There are five samples of CC type, which are characterised by hetero-

geneous grain size distribution and either medium or coarse grain size (Table-6.22). The OO type, with eight samples, is well represented and it is associated to medium-grained grain size variety with homogeneous or heterogeneous distributions. The only sample identified as SO type is fine-grained and presents a homogeneous distribution. Finally, we recognised one CA type with two modes and coarse grains. As to the mineral characterisation of the samples, the most represented non-quartz mineral are Fe-oxides, mica, and non-identified black and heavy minerals (Table-6.23). Feldspar also appears in some of CC type samples. Colour classification of the cortical area and in fresh cut is similar, although clearest colours are preferentially in the inner zones due to the cement of the conglomerate (Table-6.24). Respecting external morphology, most of the rocks are spherical pebbles, as a consequence of long sedimentary transport (Table-6.25). Other rocks, less relevant quantitatively, present tabular clast and pebble morphologies, evidence of shorter sedimentary transport. The most represented cortical texture is fine and grained texture, although coarse and grained texture are present too, generally in CC types. Fe-oxides is the only mineral inclusion identifiable in the cortical area and it is considered a consequence of the presence of oxides in the cement of the conglomerate. Joints are more frequent in the inner part of the clasts from the conglomerate than on the cortical area. This is because of the presence of more directional joints were generated in the original outcrops than in the conglomerates. Finally, bedding in fresh cut was identified in two “archaeological quartzites” of the CC type. No rock exhibits foliation.

Grain size characterisation		Petrogenetic type															
		CC		CA		OO		SO		BQ		RQ		MQ		Total	
		Σ	%	Σ	%	Σ	%	Σ	%	Σ	%	Σ	%	Σ	%	Σ	%
Homogeneous and one mode distribution	Fine grain							1	100							1	7
	Medium grain					4	50									4	27
	Coarse grain																
Heterogeneous and two modes distribution	Fine grain																
	Medium grain	2	40			1	13									3	20
	Coarse grain	1	20	1	100											2	13
Heterogeneous distribution	Fine grain																
	Medium grain	2	40			2	25									4	27
	Coarse grain					1	13									1	7
	Total	5	33	1	7	8	53	1	7							15	100

Table-6.22: Frequency table of the petrological features of the pebbles from the Lechada conglomerates based on binocular characterisation. Columns are petrogenetic types and rows contain the characteristics of grains according to size, classified first by distribution and second by size itself.

Non-quartz minerals	A		B		C		General	
	Σ	%	Σ	%	Σ	%	Σ	%
Absence								
Fe-Oxides	9	50	3	17	2	11	14	26
Mn-Oxide			3	17			3	6
Calcite								
Mica	5	28	6	33	7	39	18	33
Black mineral	4	22	5	28	8	44	17	31
Pyrite								
Feldspar			1	6	1	6	2	4
Total	18	100	18	100	18	100	54	100

Table-6.23: Frequency table of the features of non-quartz minerals of the pebbles from the Lechada conglomerates based on binocular characterisation. Columns are the three fields considered and rows are the non-quartz minerals identified.

Colour	Cortical area				On fresh cut			
	Primary		Secondary		Primary		Secondary	
	Σ	%	Σ	%	Σ	%	Σ	%
Absence								
White			3	20	2	13	6	40
Grey	12	80	3	20	11	73	4	27
Black			1	7				
Blue			2	13			4	27
Green								
Orange								
Brown	3	20	6	40	2	13	1	7
Yellow								
Red								
Total	15	100	15	100	15	100	15	100

Table-6.24: Frequency table of the colour hue of the samples from the pebbles from the Lechada conglomerates. Columns are the fields for primary and secondary colour hues of cortical areas and in fresh cut respectively and rows are the colours considered.

	Features	Σ	%
Morphology	Tabular clast	2	13
	Tabular pebble	1	7
	Flat pebble		
	Spherical pebble	12	80
	Total	15	100
Cortical texture	Coarse and grained	5	33
	Fine and grained	9	60
	Fine	1	7
	Really fine		
	Total	15	100
Mineral inclussion on cortical area	Absence		
	Fe-oxides	15	100
	Carbonated		
	Siliceaus		
	Total	15	100
Cortical joints	Not analysed		
	Absence	5	33
	Unidirectional	8	53
	Bidirectional	1	7
	Three-directional	1	7
	Total	15	100
Joints	Absence	2	13
	Unidirectional	9	60
	Bidirectional	3	20
	Three-directional	1	7
	Total	15	100
Bedding	Absence	13	87
	Unclear	1	7
	Clear	1	7
	Total	15	100
Schistosity	No	15	100
	Yes		
	Total	15	100

Table-6.25: Frequency table of the morphology, cortical texture, mineral inclusions on the cortex, quantity of cortical joints, quantity of internal joints, bedding, and schistosity of the samples from the Lechada conglomerates.

We selected one sample for thin section characterisation and XRF. This is sample DC61_04 from survey point C_028. The analysis of the thin section certifies its classification as OO type based on the abundant presence of syntaxial overgrowth, quartz grains with concavo-convex, and a smaller number of quartz grains with suturated limits. Most of the quartz grains are within the fine sand Udden-Wentworth category, although there is a small presence of matrix too. The morphological analysis reveals that most of the grains are well rounded, but their shapes are quite irregular, with mean circularity index around 0.41 (for detailed information see S.I.-I). In this sample there is no preferential orientation of the quartz grains. Characterisation of non-quartz minerals points out the scarce presence of zircon, mica and clay minerals, as well as small quantities of clayey matrix (Figure-6.22). XRF confirms the high presence of quartz in the composition of the sample with a percentage greater than 97%. The presence of Al_2O_3 is verified (1.5%) and a reduced quantity of iron oxides is identified, the latter possibly as a consequence of the composition of cement. The non-sampled types previously described as CC, CA, and SO petrogenetic types are represented in Figure-6.23.

Summing up, the Lechada conglomerates spread along the south east of La Liébana area as small strata, not easy to recognise in the field. Although we only surveyed two points, we did not identify any clear differences between them based on the general characterisation or the lithological varieties. The exploitation of the various grain size varieties of the CC type would have been easy thanks to its widespread presence. The exploitation of OO type, which must have been exploited looking for specific grain size varieties, would not have required important selection mechanisms either. Finally, the exploitation of CA and SO types would have certainly needed strong selection mechanisms due to their scarcity. The exploitation of these different types of "archaeological quartz-

ites" could have been done by simply picking them up in the area around the conglomerate and also directly at the conglomerates, a task facilitated thanks to the relatively softness of cement. The impact of joint is not relevant. Therefore, clast could be used for knapping. The sizes of the pebbles or clasts are variable, ranging between very coarse pebbles and small cobbles, but they are all of good size for knapping.

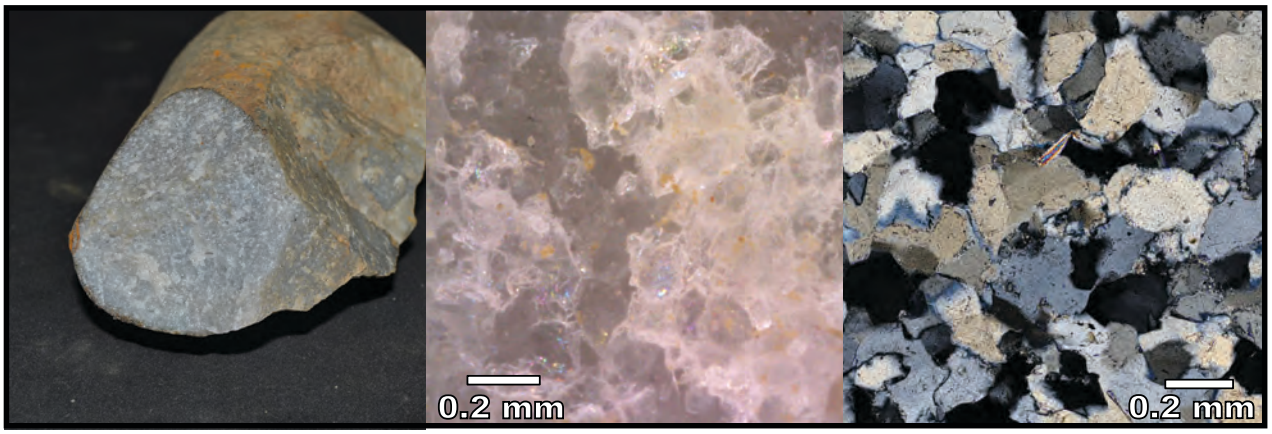

Figure-6.22: Pictures at different magnifications of the sample DC61_04 from the Lechada Formation. The OO type is easily recognisable in thin section and binocular pictures, as well as the medium grain size.

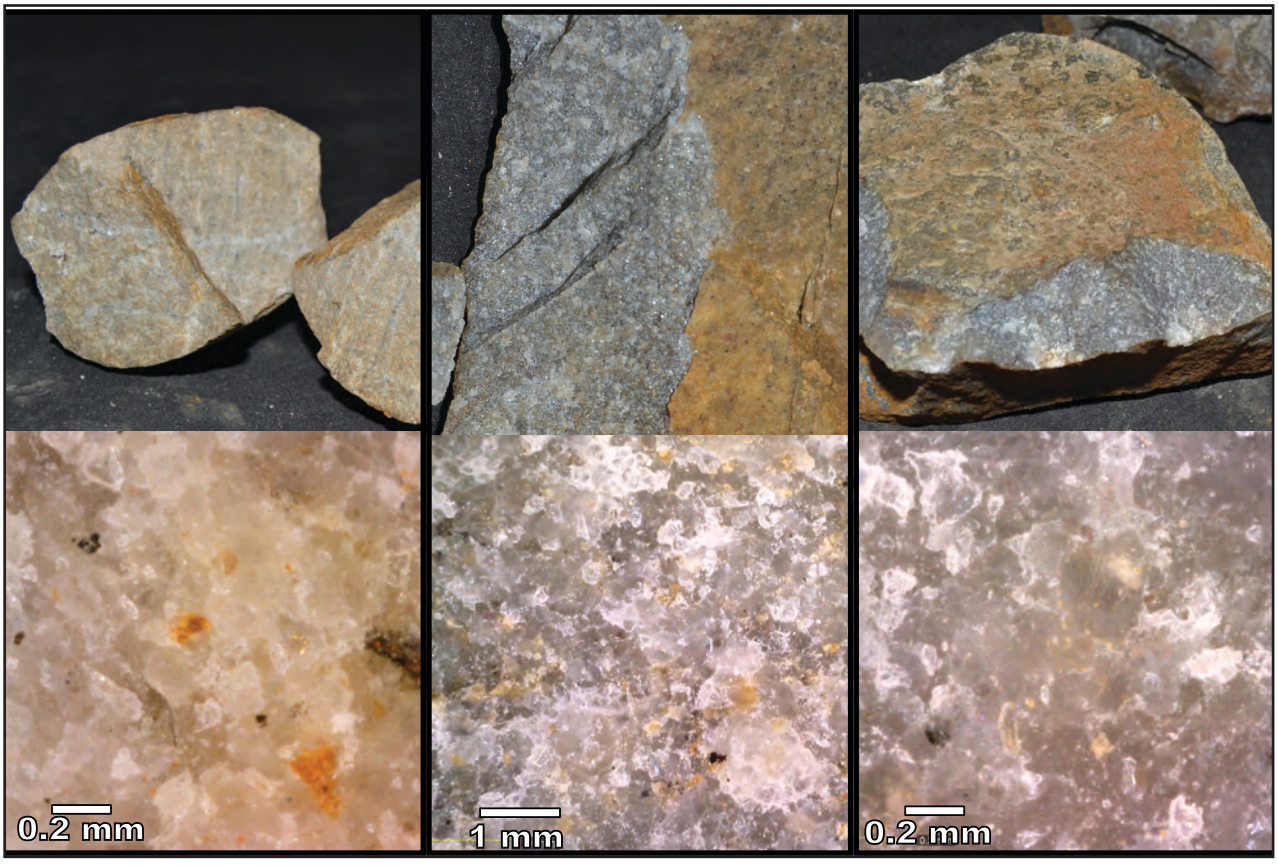

Figure-6.23: Pictures of petrogenetic types from the Lechada conglomerates not represented previously. On the left, CC type with medium quartz grain size heterogeneously distributed around two modes, represented the sample DC61_08. In the middle, CA type with coarse quartz grain size heterogeneously distributed around two modes, represented the sample DC63_05. On the right, SO type represented by sample DC61_09, with fine and homogeneous grain size distribution.

6.2.5. THE MIDDLE PENNSYLVANIAN SERIES: THE VIORNA CONGLOMERATE

The Viorna conglomerate is the last conglomerate from the Middle Pennsylvanian Carboniferous. It is dated between the Myachkovsky, last subage of the Moscovian stage, and the Kreviakinsky, first subage of the Kasimovian. The conglomerate is on the base of the Viorna Group, a formation of sandstone, shale, and calcareous olistostrome. It lies over an unconformity on the top of the Mogrovejo Formation and is covered by the Viorna Group. The Viorna conglomerate is a polymictic conglomerate. It was created in sedimentary submarine conditions in the sea talus as turbidity deposits of grain flowed (Rodríguez Fernández et al., 2003). The Viorna conglomerates are in the central area of La Liébana zone. In the western area the conglomerate crops out as a big and folded stratum, with a thickness of about 75 meters. In the eastern part there are some small strata scattered around the Bullón River in general in northwest-southeast direction. The western conglomerate is easily recognisable in the field in the cliffs close to the village of Los Llanos. However, it is not as visible in other parts (especially in the eastern zones), except for the zones cut by contemporary roads.

We analyse the formation based on three survey points, but in one of them we did not find the conglomerate. Supplementary Information-III contains the systemised information about these points. The points are the following:

- C_004/DC018: 30T 360851 4777542
- C_025/DC056: 30T 374760 4771176
- C_027/DC058: 30T 372030 4774132

The features analysed in the dataset reveal that the conglomerates examined are different. In the survey point C_004 point the conglomerate presents absence of bedding and bidirectional joints filled with quartz. Cement is mainly calcareous, grey and soft, which makes rock extraction easy. Instead, the survey point C_027 displays clear bedding and the same bidirectional joints, also filled with quartz. In this case cement is mainly composed of brown, soft and argillic material. This cement allows easy rock extraction too. In both points the quantity of cement is high, with percentages between 5 and 50% at the surface of the conglomerates, which creates tangential relationships between the clasts. The presence of the same amount of directional joints indicates similar impact of folding in the formations.

Grain size characterisation		Petrogenetic type															
		CC		CA		OO		SO		BQ		RQ		MQ		Total	
		Σ	%	Σ	%	Σ	%	Σ	%	Σ	%	Σ	%	Σ	%	Σ	%
Homogeneous and one mode distribution	Fine grain																
	Medium grain	1	25													1	17
	Coarse grain																
Heterogeneous and two modes distribution	Fine grain	1	25			1	100									2	33
	Medium grain	2	50													2	33
	Coarse grain																
Heterogeneous distribution	Fine grain																
	Medium grain			1	100											1	17
	Coarse grain																
	Total	4	67	1	17	1	17									6	100

Table-6.26: Frequency table of the petrological features of the pebbles from the Viorna conglomerates based on binocular characterisation. Columns are petrogenetic types are the columns and rows contain the characteristics of grains according to size, classified first by distribution and second by size itself.

The lithology of the clasts of both conglomerates are similar. Limestone is the most frequent material, with percentages greater than 50%. Generally, they are tabular pebbles. This is also the case of lutites, the second most frequent material in the formation. Conversely, "archaeological quartzite" is quantitatively less important in this conglomerate. In survey point C_004 the CC, CA, and OO types are present, while in survey point C_027 only CC type is represented. The morphology of the

pebbles is varied and it includes spherical, flat and tabular pebbles. We selected six samples from both survey points for laboratory characterisation. The results confirm the assignation of types and varieties of quartzite, the major presence of the CC petrogenetic type and a minor importance of CA and OO types (Table-6.26). The identification of non-quartz minerals reveals the high presence of Fe-oxides and non-identified black and heavy minerals. The presence of mica and pyrite are also important (Table-6.27). The colour of the cortical areas is different from the colour in fresh cut (Table-6.28). In the former predominance was for brown, yellow and orange, while in the latter colours were clearer. Then, it is possible to conclude that the abundant presence of iron oxides on the cortical surface affects the colour of the clast (Table-6.29). The external morphology of the pebbles is heterogeneously distributed, as it was reported in the general descriptions. Even though spherical pebble is the most frequent category, the presence of flat and tabular pebbles is abundant too. Cortical texture is generally grained and coarse. The impact of joints on cortical areas is smaller than in fresh cut as a consequence of the smaller impact of joints and the type of cement in the conglomerate. The joints are less frequent than in the conglomerates analysed previously, especially according to the direction in the cortical area. The rocks show no bedding, nor schistosity.

Non-quartz minerals	A		B		C		General	
	Σ	%	Σ	%	Σ	%	Σ	%
Absence								
Fe-Oxides	3	50	2	33	1	17	6	33
Mn-Oxide								
Calcite								
Mica	2	33	1	17			3	17
Black mineral			3	50	3	50	6	33
Pyrite	1	17			2	33	3	17
Feldspar								
Total	6	100	6	100	6	100	18	100

Table-6.27: Frequency table of the features of non-quartz minerals of the pebbles from the Viorna conglomerates based on binocular characterisation. Columns are the three fields considered and rows are the non-quartz minerals identified.

Colour	Cortical area				On fresh cut			
	Primary		Secondary		Primary		Secondary	
	Σ	%	Σ	%	Σ	%	Σ	%
Absence							4	67
White					2	33		
Grey	2	33	3	50	2	33	1	17
Black					1	17		
Blue							1	17
Green								
Orange			1	17				
Brown	4	67	1	17	1	17		
Yellow			1	17				
Red								
Total	6	100	6	100	6	100	6	100

Table-6.28: Frequency table of the colour hue of the samples from the pebbles from the Viorna conglomerates. Columns are the fields for primary and secondary colour hues of cortical areas and in fresh cut respectively and rows are the colours considered.

We selected two samples for thin section and X-Ray Fluorescence analysis. These are samples DC18_01 and DC18_02 from the survey point C_004. Both belong clearly to the CC type and are characterised by the high presence of matrix and cement, floating or tangential packing, and large amounts of clastic quartz grains (Figure-6.24). The first sample presents a heterogeneous distribution organised around two modes and medium size grains, while the second one has homogeneous distribution and fine size grains. The circularity index reveals that quartz grains from the first samples are more regular than those from the second sample and the roundness index confirms this pattern. Regarding mineral characterisation, there are clear differences in the composition of matrix and cement between the two samples: the cement of the first one is calcareous and the second one has a clayey matrix. Both samples contain great quantities of iron oxides as a consequence of the weathering of other minerals. Abundant non-quartz minerals were identified. However, clay mineral

	Features	Σ	%
Morphology	Tabular clast		
	Tabular pebble	1	17
	Flat pebble	2	33
	Spherical pebble	3	50
	Total	6	100
Cortical texture	Coarse and grained	4	67
	Fine and grained	1	17
	Fine	1	17
	Really fine		
	Total	6	100
Mineral inclussion on cortical area	Absence		
	Fe-oxides	5	83
	Carbonated	1	17
	Siliceaus		
	Total	6	100
Cortical joints	Not analysed		
	Absence		
	Unidirectional	5	83
	Bidirectional	1	17
	Three-directional		
	Total	6	100
Joints	Absence		
	Unidirectional		
	Bidirectional	4	67
	Three-directional	2	33
	Total	6	100
Bedding	Absence	6	100
	Unclear		
	Clear		
	Total	6	100
Schistosity	No	6	100
	Yes		
	Total	6	100

Table-6.29: Frequency table of the morphology, cortical texture, mineral inclusions on the cortex, quantity of cortical joints, quantity of internal joints, bedding, and schistosity of the samples from the Viorna conglomerates.

and pyrite are absent. XRF brings out clear differences between the samples. Sample DC18_01 has the smallest percentage of SiO_2 (64.45%) and the greatest percentage of CaO (35.09%) found in this research. In contrast, sample DC18_02 has 4.58% CaO, a similar percentage of Al_2O_3 and a smaller amount of Fe_2O_3 (1.89%). The first sample presents a comparable percentage of Fe_2O_3. The presence of carbonates and iron oxides in the cement of the conglomerates contributed to the results of XRF. Despite the high presence of CaO on the DC18_01 must be also explained by the former rock stratum.

Summing up, the Viorna conglomerate extends preferentially along the central area of La Liébana area, close to other formations of conglomerates. The visibility of the conglomerate varies between western and eastern areas depending on the thickness and the disposition of the formation, as well as on the erosion of surrounding material. According to bedding and the composition of cement, the formation is heterogeneous in both zones, but it is homogeneous when it comes to joints affecting the conglomerates, the lithologies present, and the ease of extraction of rocks. The exploitation of lithic resources could have been easily carried out in the areas surrounding the conglomerate and by direct rock extraction in the conglomerate themselves. The CC type could have been exploited without the need of any selective mechanism, but some kind of strategy would have been necessary for more compact types (CA and OO types) due to their scarcity (Figure-6.25). It is important to mention that the cement of the conglomerate clearly affects internal areas of the clasts, creating internal defects. Still, the size of the clasts is between coarse pebble and small cobbles, optimal for knapping.

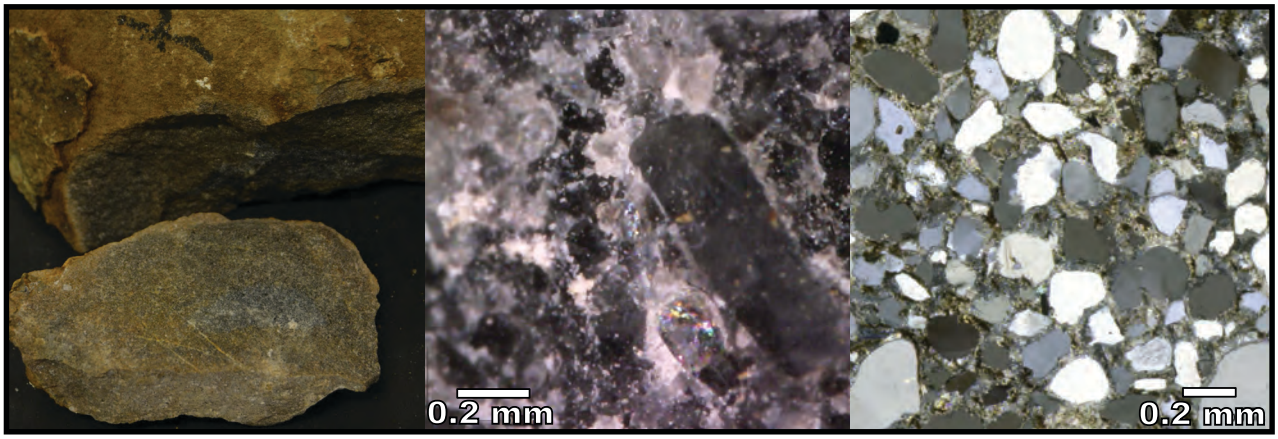

Figure-6.24: Pictures at different magnifications of the samples DC18_01 and DC18_02 from the Viorna conglomerate. Both samples belong to the CC type, but they have different varieties of grain size. The first one presents a heterogeneous distribution around two modes. The cement is carbonated. The DC18_02 is fine grained and it has a homogeneous quartz grain size distribution. The matrix composition is clayey. DC18_02 is in following page

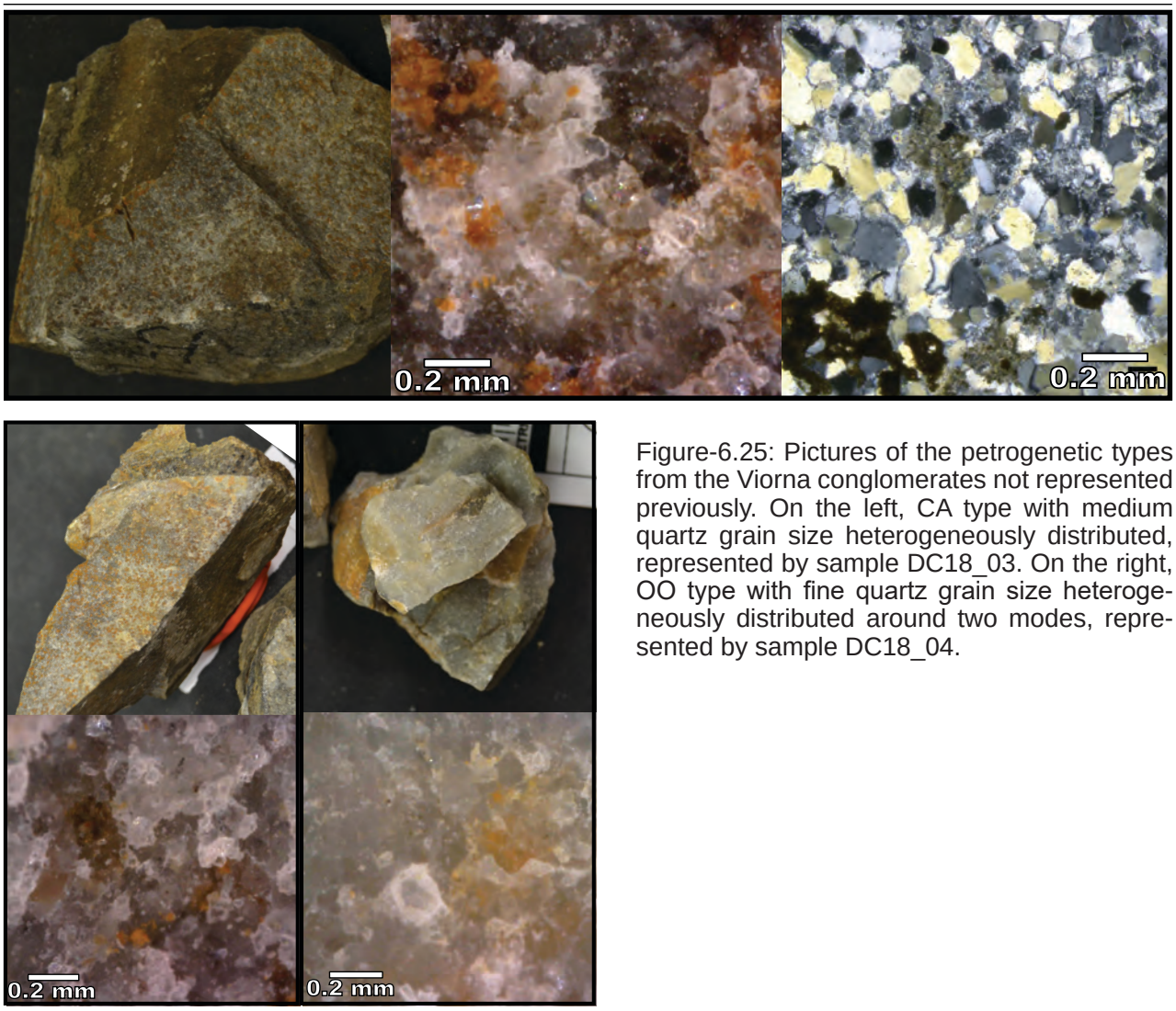

Figure-6.25: Pictures of the petrogenetic types from the Viorna conglomerates not represented previously. On the left, CA type with medium quartz grain size heterogeneously distributed, represented by sample DC18_03. On the right, OO type with fine quartz grain size heterogeneously distributed around two modes, represented by sample DC18_04.

6.2.6. THE UPPER PENNSYLVANIAN SERIES: THE PONTÓN GROUP CONGLOMERATES

The Pontón Group is the first formation generated during the Upper Pennsylvanian epoch, chronostratigraphically dated to the Kreviakinsky, the first sub-stage of the Kasimovian stage. This formation lies over an unconformity on the Maraña Formation and is covered by the Valdeón Group. The formation consists of a massive shale, siltstone, sandstone, and conglomerates succession with a polymictic conglomerate at the base. It is created in an intermediate sedimentary basin filled with massive clastic subaquatic and fan-delta sediments. This sedimentation process generated a sequence of more than 1000 meters of thickness, although the layers of the conglomerate are less than 10 meters thick (Heredia et al., 2003a). In this section we will describe in detail the conglomerates of this group. They appear as small, thin, discontinuous, and successive layers in southwest-northeast direction. They crop out in the Southwestern zone of our area of research, in the Valdeón area. These conglomerates are not easily recognisable in the field. They are only observable at road cuts, small natural cliffs, or steep flanks. The differential erosion of the mainly shaly strata does also contribute to the visibility of this conglomerate.

We analyse the formation based on eight survey points. Supplementary information-III contains the systemised information about these points. They are the following:

- C_035/DC075: 30T 342863 4778664
- C_038/DC088: 30T 341390 4778310
- C_039/DC089: 30T 341569 4778431
- C_040/DC090: 30T 341708 4778445
- C_041/DC091: 30T 341752 4778459

- C_042/DC092: 30T 339936 4776707
- C_043/DC093: 30T 339387 4777017
- C_044/SE01: 30T 337509 4774560

In general, these points do present bedding structures: six of them show clear bedding and another two unclear bedding. There are joints in almost all surveyed points. Only one of the points does not display any joints. In the other seven points, the intensity of the joint is medium and they show two or three directions. Regarding the filling material, most of them are filled with iron oxides, as well as with silica. The properties of cement are more heterogeneous and its composition is diverse. In five points the cement is mainly composed of argillaceous material, in another two points of quartz and in the last one of iron oxides. This diversity generates different colours, levels of cement compaction and proportions and ease of extraction of blocks. We do not appreciate any geographic differences in the properties of cement (Figure-6.26). In general, in the points with argillaceous material, the compaction is smaller and, therefore, extraction is easier. In the conglomerates where cement is composed of quartz or iron oxide the compaction is higher, hindering the extraction of rocks.

Grain size characterisation		Petrogenetic type															
		CC		CA		OO		SO		BQ		RQ		MQ		Total	
		Σ	%	Σ	%	Σ	%	Σ	%	Σ	%	Σ	%	Σ	%	Σ	%
Homogeneous and one mode distribution	Fine grain							1	33							1	5
	Medium grain																
	Coarse grain																
Heterogeneous and two modes distribution	Fine grain					1	10			2	67	1	100			4	19
	Medium grain					5	50	1	33							6	29
	Coarse grain																
Heterogeneous distribution	Fine grain			3	75	2	20									5	24
	Medium grain			1	25	2	20			1	33					4	19
	Coarse grain							1	33							1	5
	Total			4	19	10	48	3	14	3	14	1	5			21	100

Table-6.30: Frequency table of the petrological features of the pebbles from the Pontón group conglomerates based on binocular characterisation. Columns are petrogenetic types and rows contain the characteristics of grains according to size, classified first by distribution and second by size itself.

Non-quartz minerals	A		B		C		General	
	Σ	%	Σ	%	Σ	%	Σ	%
Absence								
Fe-Oxides	19	90	2	10			21	33
Manganese Oxides			2	10	2	10	4	6
Calcites								
Micas			10	48	5	24	15	24
Black mineral	2	10	7	33	12	57	21	33
Pyrites					2	10	2	3
Feldspars								
Total	21	100	21	100	21	100	63	100

Table-6.31: Frequency table of the features of non-quartz minerals of the pebbles from the Pontón group conglomerates based on binocular characterisation. Columns are the three fields considered and rows are the non-quartz minerals identified.

The main lithology on these conglomerates is "archaeological quartzite". Other lithologies such as limestone or lutites are difficult to find. There is a high variability of petrogenetic groups and types, as well as of grain size varieties. In general, there is a high presence of CC, CA and OO types with different grain size varieties. There are also important quantities of more deformed orthoquartzites (SO types) in the half of the surveyed points. Finally, metamorphic quartzites can be obtained in a few points. For example, type RQ can be found at survey point C_037 and type BQ at survey point C_035. Except for the quartzite group, restricted to the northern part of the conglomerates, there are

no clear geographic differences (Figure-6.27). We selected 21 samples for detailed non-destructive characterisation, which reveals patterns similar to those proposed during fieldwork. The samples confirm the presence of different petrogenetic types of “archaeological quartzite”. The most relevant conclusion is the absence of the CC petrogenetic type, discarded from the selection because of its abundance in other conglomerates previously analysed. The types CA, OO, SO, BQ, and RQ, with great variability of grain size, are clearly identified. The most frequent type, as it was in the characterisation made in the field, is the OO type, which presents a mostly heterogeneous distribution and fine-medium quartz grain sizes. The CA type is also well represented with four of the samples. All the samples are heterogeneously distributed and generally fine grained. The SO type is present in different grain size varieties too. Finally, there are two clearly metamorphic types: the BQ and the RQ types, more and less frequent respectively. The features of grain size too point at the existence of differences (Table-6.30). Meanwhile, the mineralogy of these samples, where it is possible to identify iron oxides, non-identified back and heavy minerals and mica, is similar to that of other “archaeological quartzites. There are also manganese oxides and pyrite (Table-6.31). Feldspar is absent due to the sampling strategy, focused on deformed or metamorphic samples. The colour of the samples differs between cortical and inner areas. On cortical areas colours associated to iron oxides, such as red, brown or orange, are more frequent; while in inner areas white, grey or black predominate (Table-6.32). All the mineral inclusions on the cortical area come from siliceous materials, sometimes crystallised (Table-6.33). The most frequent external morphology of the samples is spherical pebbles, which agrees with the data collected in the field. Cortical texture is generally fine and grained, and only two of the samples present coarse and grained texture. There are not clear differences in the impact of joints on pebbles between inner and cortical areas. Therefore, it can be deduced that the impact of joints on pebbles is mainly caused by the joints affecting the conglomerate. The joints clearly affect almost every sample in one, two, or three different directions. There is no evidence of bedding, nor schistosity in the cut fresh surface, even though deformed and metamorphic types are abundant.

Colour	Cortical area				On fresh cut			
	Primary		Secondary		Primary		Secondary	
	Σ	%	Σ	%	Σ	%	Σ	%
Absence	1	5	1	5			3	14
White			1	5	2	10	9	43
Grey	15	71	1	5	17	81	3	14
Black	1	5	3	14	2	10	1	5
Blue							1	5
Green								
Orange			7	33				
Brown	4	19	7	33			4	19
Yellow								
Red			1	5				
Total	21	100	21	100	21	100	21	100

Table-6.32: Frequency table of the colour hue of the samples from the pebbles from the Pontón group conglomerates. Columns are the fields for primary and secondary colour hues of cortical areas and in fresh cut respectively and rows are the colours considered.

Figure-6.26: Map of the conglomerate formations from the Upper Pennsylvanian in the area of study. Each point marks a survey point and its main features. The rounded icons represent bedding categories: empty for no-bedding, dashed horizontal lines for unclear bedding, and horizontal lines for bedding. The first square icon represents the characteristics of joints according to two criteria: 1) quantity of joint directions, using horizontal lines for single directional joints, horizontal and vertical lines for two directional joints, and horizontal, vertical, and diagonal lines for three or more directional joints, and 2) presence of mineral inclusions, using different colour, red colour for Fe-oxides, black for silica, light blue for manganese, orange for carbonates, green for clay, and purple for sandy materials. The last rounded and coloured icon represents the properties of cement. The colour represents the composition of the cement, using the same colour code as the one employed for the joint filling materials. The first letter inside the circle describes the type of extraction (I for impossible to extract only pebbles; H for hard to extract pebbles; M for medium difficulty to extract clasts; and E for easy extraction of pebbles or clasts). The second letter synthetises the packing properties (F for floating, I for isolated, T for tangential, and C for complete packing).

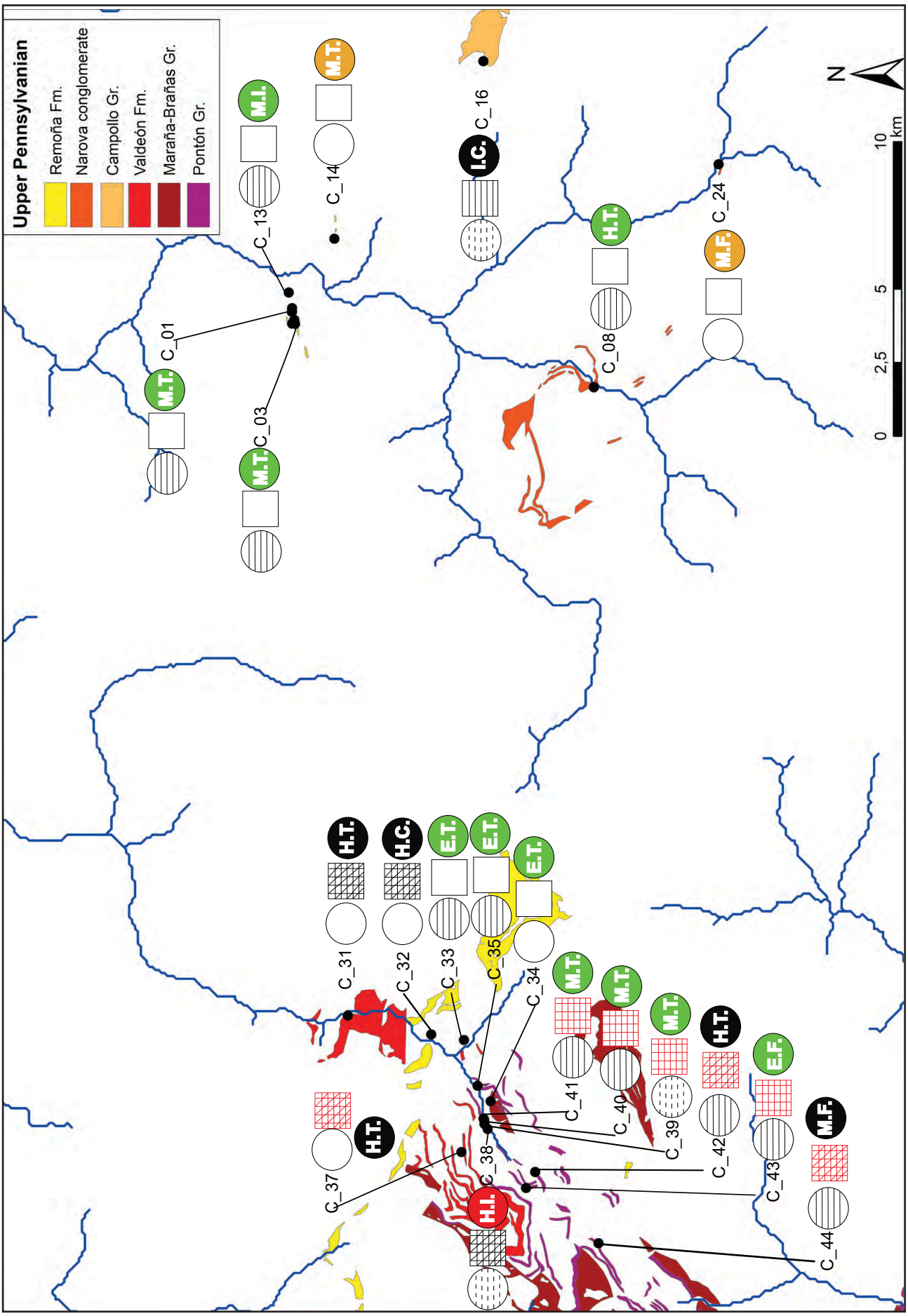

Figure-6.26: Map of the conglomerate formations from the Upper Pennsylvanian in the area of study. The complete footnote is on the previous page.

	Features	Σ	%
Morphology	Tabular clast		
	Tabular pebble	1	5
	Flat pebble	2	10
	Spherical pebble	17	85
	Total	20	100
Cortical texture	Coarse and grained	2	10
	Fine and grained	18	90
	Fine		
	Really fine		
	Total	20	100
Mineral inclussion on cortical area	Absence		
	Fe-oxides	20	100
	Carbonated		
	Siliceaus		
	Total	20	100
Cortical joints	Not analysed	1	5
	Absence	1	5
	Unidirectional	4	19
	Bidirectional	12	57
	Three-directional	3	14
	Total	21	100
Joints	Absence	1	5
	Unidirectional	4	19
	Bidirectional	10	48
	Three-directional	6	29
	Total	21	100
Bedding	Absence	21	100
	Unclear		
	Clear		
	Total	21	100
Schistosity	No	20	100
	Yes		
	Total	20	100

Table-6.33: Frequency table of the morphology, cortical texture, mineral inclusions on the cortex, quantity of cortical joints, quantity of internal joints, bedding, and schistosity of the samples from the Pontón group conglomerates.

We selected four samples from survey point C_035 for thin section and X-Ray Fluorescence analyses. Sample DC75_03 is clearly a SO type with an abundant presence of syntaxial overgrowth, undulate extinction, suturated quartz grain limits, and a small presence of deformation lamellae. The characterisation of grain size reveals a high presence of Udden-Wentworth's category of fine sand. Other size categories, mostly the finest ones, are also present as consequence of the abundance of matrix. Sample DC75_01 is a clear BQ type, with abundant presence of syntaxial overgrowth which creates suturated quartz grain limits and moderate presence of recrystallised quartz grains (Figure-6.28). The other two samples (samples DC75_02 and DC75_05) belong to the BQ type, with some features, such as the abundant presence of recrystallised grains that could be the result of an increase of metamorphic processes. There is high presence of stylolite borders and scarcity of deformation lamellae. The characterisation of grain size and morphology reveal differences between these two samples. Sample DC75_02 presents a big amount of grains within the fine silt category due to the increase of metamorphic process which involve the expansion in size and quantity of recrystallised quartz grains. Regarding circularity and roundness indexes, there are clearly two modes. Sample DC75_05 clearly presents two modes too. The first mode is made of recrystallised grains of very fine silt size. The second and clearest mode is composed of fine and very fine sand, which are the predominant sizes of deformed quartz grains in both samples (see S.I.-I). Then, we cannot discard sample DC75_02 to belong to the RQ type (Figure-6.29). Mineral characterisation underlines the important role of iron oxides coming from the cement of the conglomerate, which percolates in quartzites, probably through the joints, and is deposited in its inner parts. Pyrite is also homogeneously present in all the samples. X-Ray fluorescence does not emphasise any specific components for this conglomerate, but it indicates that in all the samples silica is abundant and iron oxides are present in variable quantities.

Figure-6.27: Map of the conglomerate formations from the Upper Pennsylvanian in the area of study. Each point marks a survey point and its main lithologies are defined through icons. The petrological characterisation is represented by one to five icons with the initial of most interesting petrogenetic types, in case of "archaeological quartzites", or that of the main lithology. The external form describes the morphology of clasts, where squares represent tabular clasts, rounded squares represent tabular pebbles, oval forms represent flat pebbles, and circles represent spherical pebbles. Grain size distribution is represented by the main colour. Single mode homogenous distribution is represented in red, two modes heterogeneous distribution is represented in green, and heterogeneous distribution is represented in blue. Grain size characterisation is represented by the brightness of colours just presented, light red, green, or blue for coarse size grains; medium red, green, or blue for medium size grains, and dark red, green, or blue for small size grains.

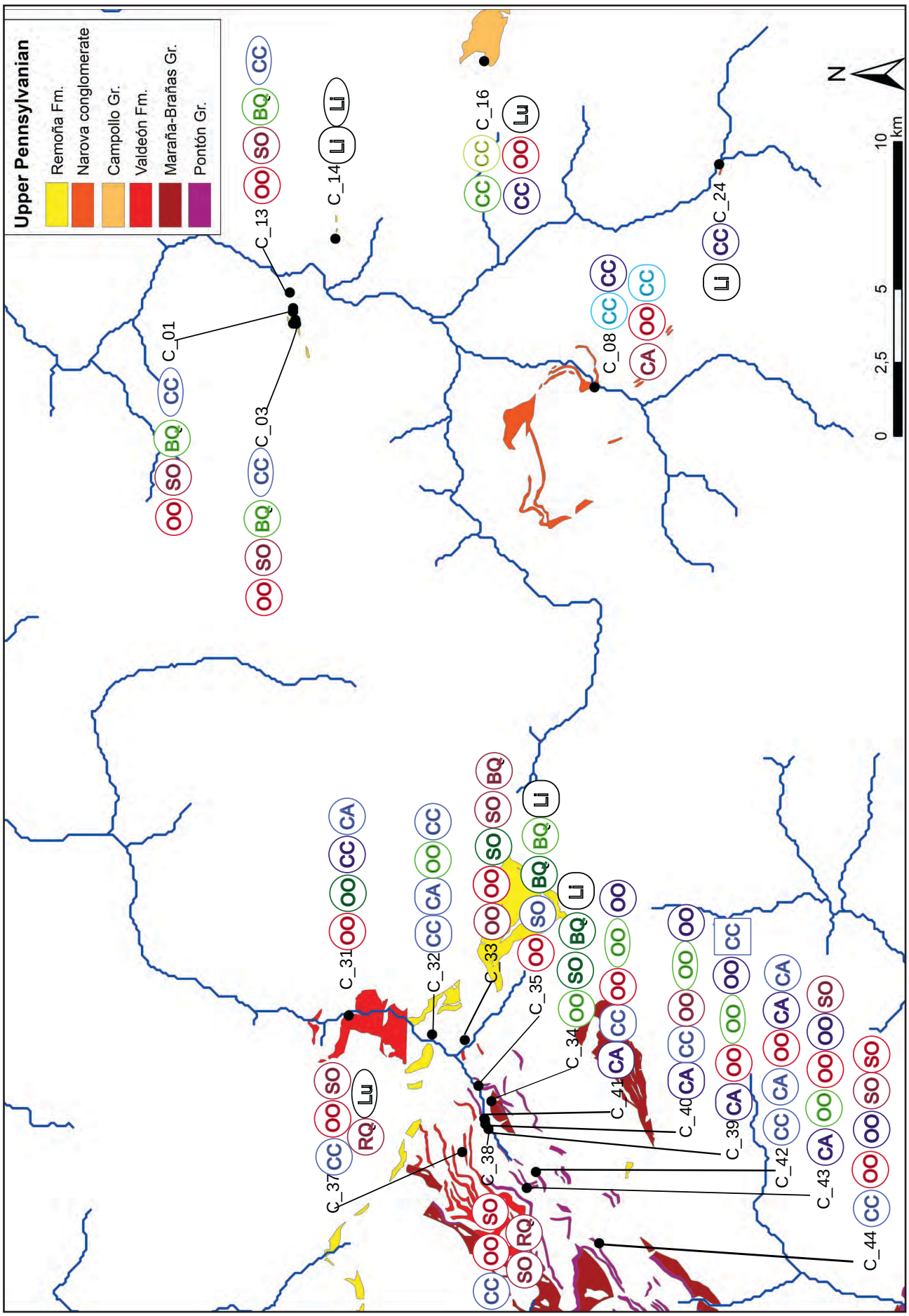

Figure-6.27: Map of the conglomerate formations from the Upper Pennsylvanian in the area of study. The complete footnote is on the previous page.

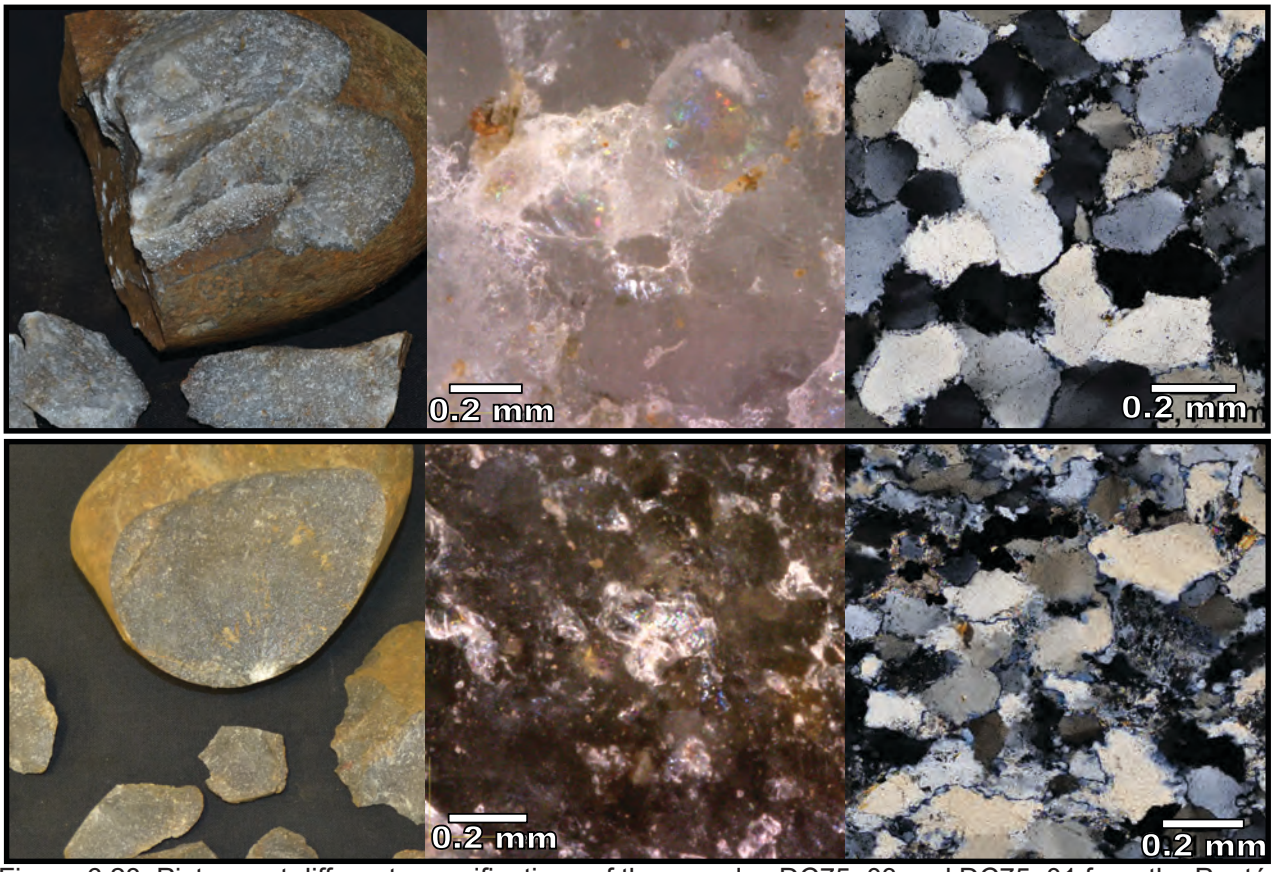

Figure-6.28: Pictures at different magnifications of the samples DC75_03 and DC75_01 from the Pontón conglomerate. The first sample is a SO type with medium size quartz grains heterogeneously distributed around two modes. The second sample is a BQ type with fine grain quartz sizes.

Figure-6.29: Pictures at different magnifications of the samples DC75_02 and DC75_05 from the Pontón conglomerate. The first sample is a BQ type (maybe RQ type) with fine quartz grain size heterogeneously distributed. The second sample is a BQ type with fine quartz grain sizes.

Considering all the features analysed, the conglomerate of the Pontón Formation extends along the southwestern zone of the research area, as a small and thin stratum, difficulty to recognise in the field. They are relatively homogeneous according to the bedding and the properties of joints. On the contrary, based on the properties of cement they are quite heterogeneous, even though the presence of iron oxides in the cement is a constant. The ease of rock extraction clearly differs from one conglomerate to another, but it is always between relatively easy and medium. Therefore, it is possible to obtain pebbles directly from the conglomerate, as well as from the surrounding area. Multiples varieties of "archaeological quartzites" could have been exploited, from non-deformed types, such as CC and CA types, to real quartzite of BQ and probably RQ types. The presence of this first type of quartzite is moderate and the latter is even more reduced. Ortoquartzite could have also been exploited thanks to the high frequency of the OO type and the moderate presence of the SO types. The size of all the clasts, ranging between very coarse pebbles and small cobbles, is optimal for knapping. Even though there is an important amount of joints on the conglomerate and in the clasts themselves, they are not completely affected by them.

6.2.7. THE UPPER PENNSYLVANIAN SERIES: THE MARAÑA-BRAÑAS GROUP

The Maraña-Brañas Group consists of two different formations created on marine basin sedimentary conditions. The Maraña group is dated to the Myachkovsky, the last stage of the Moscovian Carboniferous. The Brañas Group is dated to the Kreviankinsky, almost coetaneous to the previously analysed Pontón Group but in Riaño area. Both groups are made of a heterogeneous stratum of shale, sandstone, and calcareous breccia and olistoliths. Some of these conglomerates are also described in the regional geology (Heredia et al., 2003a). The strata analysed in the present research is probably linked to the Brañas Group, but the results of the analyses lead us to nuance this conclusion. This formation is situated on the southwestern zone of our research area. The conglomerates are not distinguished in the regional geology. Therefore, the stratum represented in the map is the massive formation. We analyse the conglomerate of this formation based on just one survey point, described in detail in Supplementary Information-I. The point is the following:

- C_034/DC074: 30T 342336 4778223

This conglomerate presence an absence of bedding structures and joints, showing clear differences with the conglomerates previously analysed. The cement of this conglomerate is composed of argillaceous and brown material, which makes rock extraction easy. In this conglomerate there is high presence of cement, leading to the tangential packing of the pebbles. Regarding the lithological varieties in the conglomerate, most of the clasts are archaeological quartzite. However, limestone (of tabular morphology) is also present. We found three different types of quartzites: OO, SO and BQ types. The first type is a quartzite of medium quartz grain size and with a heterogeneous distribution organised around two modes. The latter two types do also present heterogeneous distributions organised around two modes but they have fine quartz size. The laboratory analyses performed on four of these samples certify this assignation of types and varieties. Mineral characterisation indicates the presence of iron oxide, non-identified black and heavy minerals and mica in all the samples, resulting into quartzites of a wide variety of colours. The presence of iron oxides on cortical surfaces is high, but it does not modify the colour of the cortical fine and grainy surfaces. The external morphology of the samples is spherical pebbles. Joints are more frequent in the inner areas of quartzite than in cortical areas because of the impact of joints on the original strata, not on the current conglomerates. We selected the sample DC74_03 for petrography and XRF analysis. These tests certify the ascription to the SO type, characterised by the abundant presence of suturated quartz grain limits and the small percentages of recrystallised grains and deformation lamellae. Mineralogical analysis verifies the clayey nature of matrix and the presence of iron oxides and pyrite among non-quartz minerals. These results are in accordance with the previous non-destructive characterisation (Figure-6.30). X-Ray fluorescence reveals the major presence of silica and the existence of alumina and Fe_2O_3 in small proportions, possibly derived from the matrix or from the iron oxides on cortical areas.

In general, the conglomerate analysed in the Maraña-Brañas polygon is not easy to recognise in the field, probably due to the small dimensions of this thin layer packed between two massive shale strata of the Maraña or Brañas groups. Lithic resources could have been easily exploited directly extracting the rocks from the conglomerate, but catchment would have been more limited in the surrounding area due to its scarcity. The intensive exploitation of deformed types such as OO and SO types would have been possible, but not that of non-deformed types. Given the scarcity of the BQ type, it exploitation of would have only been likely through the application of strong selective mechanisms. The size for the clasts is small cobbles, optimal for knapping.

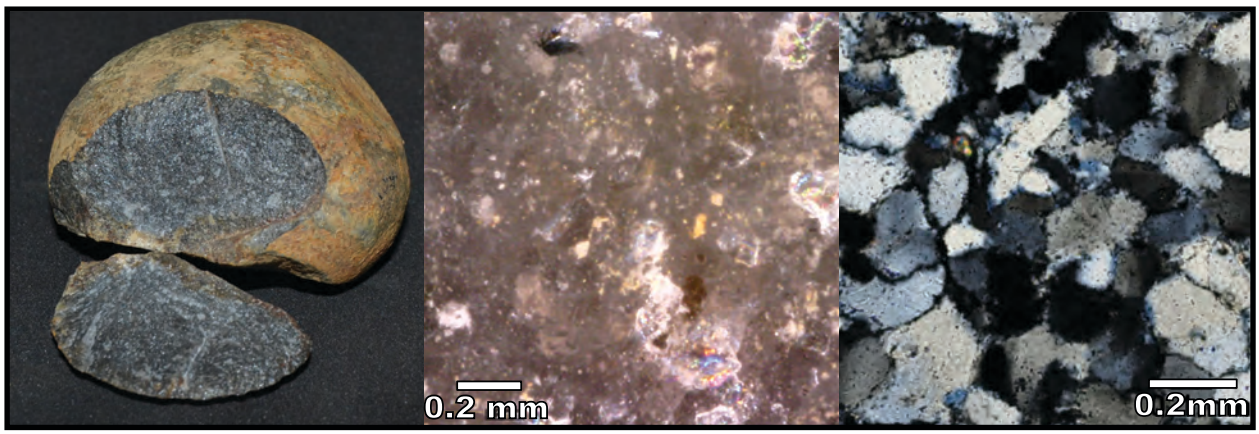

Figure-6.30: Pictures at different magnifications of the samples DC74_03 from the Maraña or Brañas group. The sample is a SO type with fine quartz grain size heterogeneously distributed around two modes and with major presence of pyrite and Fe-oxides.

6.2.8. THE UPPER PENNSYLVANIAN SERIES: THE VALDEÓN GROUP

The Valdeón Group consists of a sandstone, shale, lutite, conglomerate and coal strata more than 1200 meters thick extending along our area of research. It is chronostratigraphically dated to the Khamovnichesky substage, the second phase on the Kasimovian Carboniferous. It is situated on the top of the Pontón Formation and is covered by the Remoña Group through an unconformity. This group was generated under subaerial fan conditions in the final filling of a synorogenic basin (Heredia et al., 2003a; Julivert and Navarro, 2003). In this section, we will only describe in detail the conglomerate strata. This formation is manifested as thin and successive layers generally in southwest-northeast direction extending along the southwestern zone of our research area, close to the village of Posada de Valdeón. These conglomerates are recognisable in the field in contemporary roads cuts or in the relief generated by the differential erosion of the other strata mainly made of sandstone and shale.

We will describe the formation based on four survey points. Supplementary Information- III contains the systemised information about these points. The points are the following:

- C_031/DC068: 30T 345250 4783065
- C_032/DC070: 30T 344611 4780237
- C_033/DC073: 30T 344418 4779129
- C_037/DC087: 30T 340615 4779206

There is no bedding in three out of the four survey points, while this feature is clear in the remaining sample. The same survey point does not show any evidence of joints. Meanwhile, in the other three survey points the intensity of joints is high and they have at least three directions. The joints are filled with siliceous and ferruginous material. The composition of the cement of three survey points is predominantly siliceous, which generates high compaction and hinders rocks extraction. In the remaining survey point, cement is composed of argillaceous material, which results into softer compaction and easier rock extraction. The abundance of the cement is also variable and it can generate complete or tangential packing. When the superior and the inferior strata are visible, they are always shaly. There are no geographical differences between the four survey points analysed, but it is obvious that survey points C_031, C_032, and C_037 are closer from each other and different from survey point C_033 (Figure-6.27).

Regarding the field lithological characterisation, “archaeological quartzite” is the most frequent category. Besides this, there are some lutites and limestones, generally as tabular pebbles. “Archaeological quartzites” are spherical pebbles, with the exception of the clast from survey point C_032, which is a tabular pebble. Six petrogenetic types are present. There is an abundant presence of the CC type in every conglomerate. Conversely, the CA type is not represented in every conglomerate and, when it is presents, it is usually scarce. The OO type is well represented in every conglomerate more frequently than the CA type. The SO type is well represented in two of the conglomerate, while the BQ type only is present in a single one. Finally, the RQ type is identified in one conglomerate in small amounts. There are no clear geographic differences in the dispersion of the lithological varieties.

Grain size characterisation		Petrogenetic type															
		CC		CA		OO		SO		BQ		RQ		MQ		Total	
		Σ	%	Σ	%	Σ	%	Σ	%	Σ	%	Σ	%	Σ	%	Σ	%
Homogeneous and one mode distribution	Fine grain							1	17							1	4
	Medium grain					2	22									2	8
	Coarse grain					1	11									1	4
Heterogeneous and two modes distribution	Fine grain	2	40			2	22	3	50	1	100	1	100			9	38
	Medium grain	3	60	2	100											5	21
	Coarse grain																
Heterogeneous distribution	Fine grain							2	33							2	8
	Medium grain					3	33									3	13
	Coarse grain					1	11									1	4
	Total	5	21	2	8	9	38	6	25	1	4	1	4			24	100

Table-6.34: Frequency table of the petrological features of the pebbles from the Valdeón group conglomerates based on binocular characterisation. Columns are petrogenetic types and rows contain the characterisation of grains according to size characterisation, classified first by distribution and second by size itself.

We took 24 samples for non-destructive petrological characterisation. In general the results certify the previous field characterisation. The petrogenetic characterisation confirms the high presence of the CC type, distinguished by the heterogeneous distribution organised around two modes and fine and medium quartz grain sizes. The CA type is less frequent. It also presents a heterogeneous distribution organised around two modes and medium grain sizes. The OO type is the most frequent type. It is identified with different grain sizes and both homogeneous and heterogeneous grain size distributions. There is also an important representation of the SO type, with diverse grains size distributions always associated with fine grain sizes. Then, orthoquartzite is the most frequent group among "archaeological quartzites". Finally, the group of quartzites is the less frequent one with only one sample each from the BQ and RQ types, both presenting heterogeneous distributions organised around two modes and fine grain sizes (Table-6.34). The characterisation of non-quartz minerals points at the presence of iron oxides, mica and non-identified black and heavy minerals. The latter are the most represented non-quartz minerals in "archaeological quartzites". In addition, there is a small presence of manganese oxides in CC petrogenetic type (Table-6.35). Colour classification of the inner part is heterogeneous, due to the wide range of types and non-quartz minerals present (Table-6.36). On the cortical areas, colour is altered by the presence of iron oxides, creating red, orange, or brown hues. Clasts are predominantly spherical pebbles, except for a few coming from the survey point C_032, which are tabular. The texture of cortical areas of the samples is mostly granular and fine, although one of them are granular and coarse (CC type) and another one is fine (SO type). The presence of joints is slightly more frequent in the inner areas than on cortical areas. This is a consequence of joints or fractures previously generated in the original outcrops where the "archaeological quartzites" come from. However, the joints created in the conglomerate do also cause new joints in the rocks fragments. Therefore, they are intensively affected by multiple directional joints (Table-6.37). We do not observe any bedding on the inner areas of the quartzites, whereas schistosity is identified in two samples (SO and RQ types).

Non-quartz minerals	A		B		C		General	
	Σ	%	Σ	%	Σ	%	Σ	%
Absence								
Fe-Oxides	15	63	7	29	1	4	23	32
Mn-Oxide	0	0	1	4	1	4	2	3
Calcite								
Mica	6	25	6	25	11	46	23	32
Black mineral	3	13	10	42	11	46	24	33
Pyrite								
Feldspar								
Total	24	100	24	100	24	100	72	100

Table-6.35: Frequency table of the features of non-quartz minerals of the pebbles from Valdeón group conglomerates based on binocular characterisation. Columns are the three fields considered and rows are the non-quartz minerals identified.

Colour	Cortical area				On fresh cut			
	Primary		Secondary		Primary		Secondary	
	Σ	%	Σ	%	Σ	%	Σ	%
Absence			1	4			6	25
White			2	8	5	21	7	29
Grey	18	75	4	17	18	75	2	8
Black	2	8	6	25	1	4	6	25
Blue							2	8
Green								
Orange			1	4				
Brown	4	17	9	38			1	4
Yellow								
Red			1	4				
Total	24	100	24	100	24	100	24	100

Table-6.36: Frequency table of the colour hue of the samples from the pebbles from the Valdeón group conglomerates. Columns are the fields for primary and secondary colour hues of cortical areas and in fresh cut respectively and rows are the colours considered.

	Features	Σ	%
Morphology	Tabular clast	1	4
	Tabular pebble		
	Flat pebble	1	4
	Spherical pebble	22	92
	Total	24	100
Cortical texture	Coarse and grained	1	4
	Fine and grained	22	92
	Fine	1	4
	Really fine		
	Total	24	100
Mineral inclussion on cortical area	Absence		
	Fe-oxides	23	96
	Carbonated		
	Siliceaus	1	4
	Total	24	100
Cortical joints	Not analysed	1	4
	Absence	3	13
	Unidirectional	2	8
	Bidirectional	8	33
	Three-directional	10	42
	Total	24	100
Joints	Absence		
	Unidirectional	5	21
	Bidirectional	8	33
	Three-directional	11	46
	Total	24	100
Bedding	Absence	24	100
	Unclear		
	Clear		
	Total	24	100
Schistosity	No	22	92
	Yes	2	8
	Total	24	100

Table-6.37: Frequency table of the morphology, cortical texture, mineral inclusions on the cortex, quantity of cortical joints, quantity of internal joints, bedding, and schistosity of the samples from the Valdeón group conglomerates.

We selected six samples from these conglomerates for petrographic and X-Ray Fluorescence analysis. They are DC68_02, DC68_05, DC70_01, DC73_01, DC73_02 and DC73_06. Three of them belong to the OO type, two to the SO type and another one to the CA type. The OO type presents an abundant presence of syntaxial overgrowth, which generates concavo-convex quartz grain limits. In addition, in two of them it results into slightly suturated quartz grain limits. The characterisation of grain size reveals differences between the samples DC70_01 and DC73_01. While in the former most of the clasts range between coarse silt and very fine sand (small size and heterogeneous distribution), in the latter grain size is coarser (medium size and homogeneous distribution) (Figure-6.31). The identification of non-quartz minerals indicates similarities in the presence of clayey matrixes but differences based on the minerals identified, with presence of pyrite and iron oxides in the sample DC73_01. Sample DC68_02 presents the same mineral characterisation as DC73_01. The samples belonging to the SO type exhibit major presence of serrated quartz grain limits, and deformation lamellae in the sample DC73_02 and recrystallised grains in the sample DC73_06. Quartz grain characterisation is similar for both samples: fine grain size predominates, with most of grains with the very fine Udden-Wentworth category. Small amounts of recrystallised grains are identified in the sample DC73_02. This sample presents a homogeneous distribution organised around a single mode with predominantly fine silt grain size (see-S.I.-I). Both samples show similar amounts of clayey matrix, but in addition sample DC73_02 has important amounts of pyrite and iron oxides (Figure-6.32). The CA type is characterised by the major presence of detrital quartz grains, the moderate presence of undulate extinction quartz grains and a residual presence of deformed quartz grains derived from other quartzites (Figure-6.33). The results of X-Ray Fluorescence of the five samples conclude that the composition of the samples is not homogeneous.

Figure-6.31: Pictures at different magnifications of the samples DC70_01 and DC73_01 from the Valdeón group conglomerate. Both samples are OO type with different grain size varieties. The upper sample has fine quartz grain size heterogeneously distributed. The second sample has medium quartz grain sizes more homogeneously distributed. The presence of pyrite and ferruginous material gives its characteristic grey colour to the first sample. The second one is white and similar to other OO types and medium quartz grain size varieties.

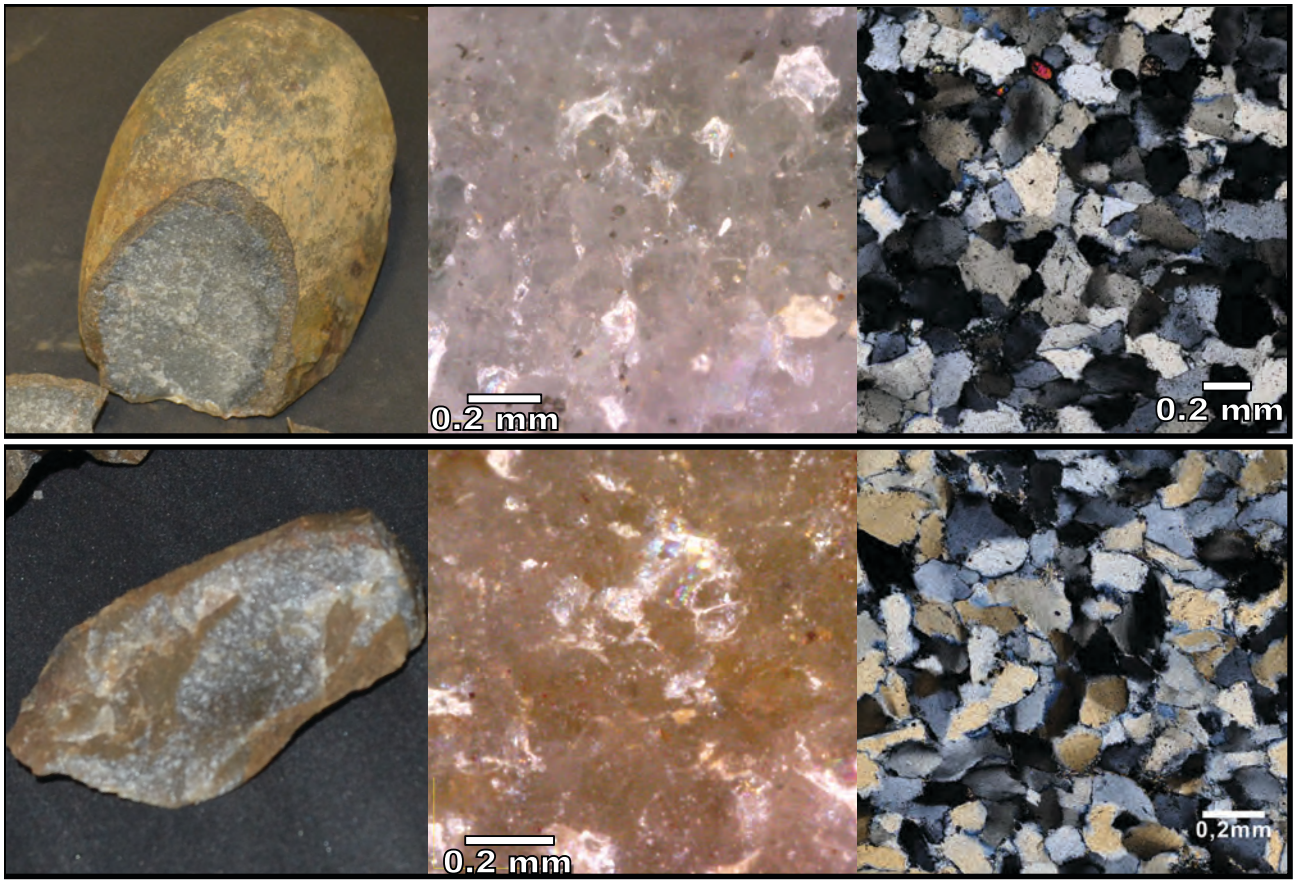

Figure-6.32 (Figure on previous page): Pictures at different magnifications of the samples DC73_02 and DC73_06 from the Valdeón group conglomerate. Both samples are SO type with similar quartz grain size varieties.

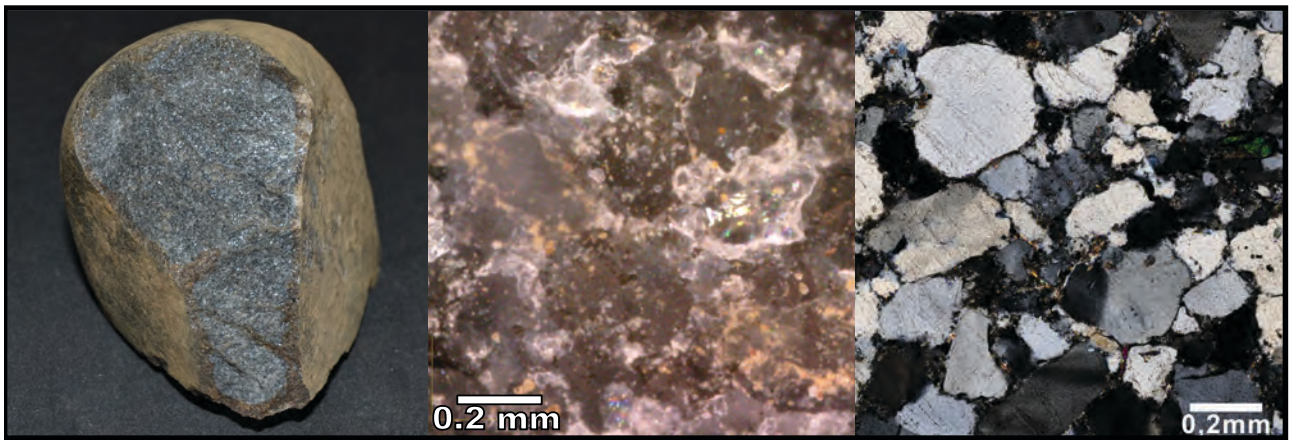

Figure-6.33: Pictures at different magnifications of the sample DC68_05, a CA type quartz-arenite with reduced presence of argillaceous matrix.

Summing up, the conglomerates from the Valdeón Group extend along the southwestern zone of the research area as small, thin, and successive strata. They are recognisable, but only in small areas where differential erosion wore away the shaly strata covering the conglomerates. In general, this group presents a high variability of “archaeological quartzites” potentially used during the Palaeolithic. In this conglomerate the exhaustive exploitation of quartz-arenite and orthoquartzite could have been easy thanks to its high proportion. Although the samples selected do not show any metamorphic features during petrographic analysis, the two samples from the metamorphic group of “archaeological quartzites” do present clear metamorphic features based on non-destructive analysis (Figure-6.34). The exploitation of these types of quartzite would have required strong selective mechanisms due to its reduced proportion. The exploitation of all these “archaeological quartzites” could have been done in areas surrounding the conglomerates just through collection. However, the direct exploitation of the conglomerate must have been necessarily implied the use of hammers or other tools because of the composition and compaction of cement. Despite the easiness to collect different petrogenetic types, the presence of joints makes knapping activities hard. Nevertheless, the high frequency of pebbles, the combined presence of deformed and metamorphic “archaeological quartzites” and the appropriate size of the rocks (between coarse pebble and big cobble) make this conglomerates an optimal choice for raw material catchment activities.

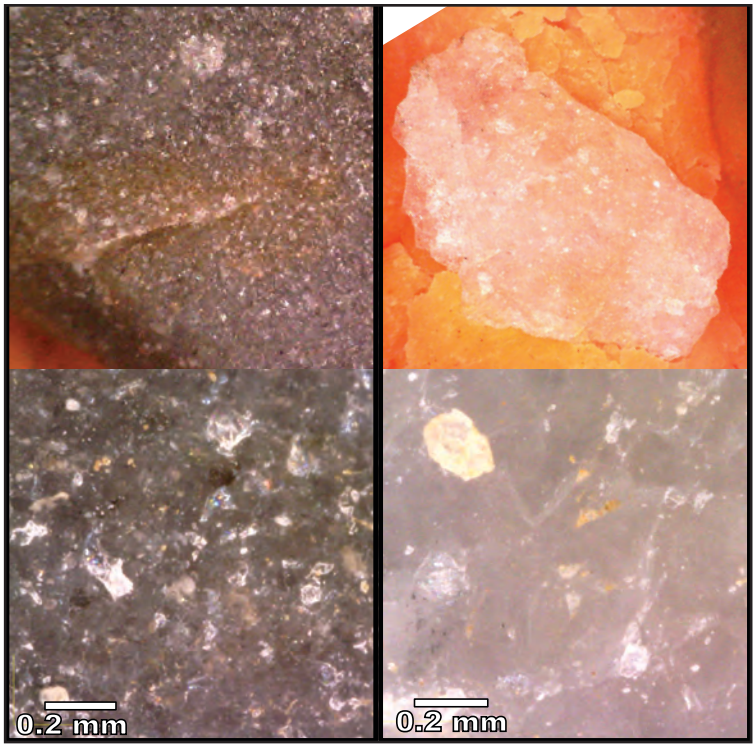

Figure-6.34: Picture at 20 x and 250 x magnifications of the petrogenetic types absent from destructive characterisation. On the left, sample DC73_05, from the BQ quartzite type. On the right, sample 87_03, from the RQ type.

6.2.9. THE UPPER PENNSYLVANIAN SERIES: THE CAMPOLLO GROUP AND THE NAROVA CONGLOMERATE

The Campollo Group is another shale, sandstone, conglomerate, and limestone succession from the Upper Pennsylvanian Carboniferous. It was created under sedimentary and synorogenic conditions related with underwater and high-density grains and mudflow. It is situated over an unconformity on the top of the Viorna Group and is covered by the Remoña by another unconformity. The chronostratigraphic position of the Campollo Group is between the Khamovnichesky and the Dorogmilovsky, the last two sub-stages of the Kasimovian age. The Campollo Formation crops out in La Liébana zone, in two different areas. The first one is in the eastern part, near the Peña Sagra mountain chain. The second one is in the central area, near the village of Naroba[1]. Geological text and maps difference the two strata assigning the name "Narova conglomerate" to the conglomerate layers of the Campollo Formation in the central area of La Liébana. In the eastern part there is no lithological differentiation. We decided to distinguish both formations in this research, maintaining the information generated by previous researchers (Heredia et al., 2003b; Rodríguez Fernández et al., 2003). From here on, we will focus on the conglomerates from the Campollo Group and the Narova conglomerate. The conglomerate extends along the central area as a belt around the Campollo sandstone and shale alternation, creating an incomplete circular shape (Figure-6.26). There are also some thin strata in northeast-southwest direction in the central-southern zones of La Liébana area. The conglomerates in the western zone are not represented in the geological maps. For this reason we could not examine its arrangement. The conglomerates are easily recognisable due to their thickness (at least 137 meters in the area around the village of Naroba) and the differential erosion of the surrounding strata.

We will analyse the Campollo Group based on three survey points: one in the central area, another one within the small conglomerates in the central-southern area, and the last one within the eastern conglomerates. Supplementary Information-III contains detailed information about these points. The points are the following:

- C_008/DC024: 30T 366610 4774716
- C_024/DC055: 30T 374189 4770478
- C_016/DC043: 30T 377695 4778467

The points analysed show clear differences between the concerning bedding. Each point presents a different bedding category. Regarding the presence of joints, in the two conglomerates from the central zone of la Liébana area there are no joints, while in the eastern point there is one directional joints filled with quartz and iron oxides. As to the characteristics of cement, all these points are different from each other. In the Narova conglomerate, cement is argillaceous, probably carbonated, with medium compaction, which causes hard rock extraction. As can be observed in the graphic representation of this conglomerate (S.I.-III C_008), there is a carbonate cement conglomerate under the main analysed stratum. Meanwhile, the eastern conglomerate is siliceous and very compact, making rock extraction impossible. Finally, the cement composition of the survey point C_024 is carbonated and, therefore, heterogeneous, probably due to different sedimentary conditions. Except for the last conglomerate, the cement percentage is smaller than 5% on the surface of the conglomerates, which creates complete or tangential packing.

Regarding the lithology of the clasts present in the conglomerates, there is a wide variety of "archaeological quartzites", lutites and limestones. Focusing on the first category, only quartz-arenites and OO type are present. The most frequent type is the CC one, present as spherical pebbles in every conglomerate in high quantities (except for survey point C_024, where limestone is highly represented). The CA type only appears in the survey point C_008, while the OO type is present in two points (in percentages smaller than 20%).

We selected 13 samples from the survey points C_008 and C_016 and they certify the characterisation made in the field. There is an abundant presence of CC types with diverse grain sizes, some of them related with the Murcia, Barrios, or Carboniferous outcrop formations. The samples of the CA type (less frequent) are related to fine grained size varieties, either with homogeneous distributions or with heterogeneous distributions arranged around two modes. There is also a moderate presence of OO type samples, with medium grain sizes and heterogeneous distributions (Table-6.38).

1 The name of the village is Naroba, but in geological text is referred as Narova. The discrepancy between both names (the conglomerate and the village) is probably due to a spelling mistake. In the present research, we maintain the name of the conglomerate, not the name of the village.

The mineral characterisation reveals the frequent presence of mica, iron oxides, and non-identified black and heavy minerals in “archaeological quartzites” (Table-6.39). Feldspar is present in three CC type samples (from survey point C_008) and in another one (from survey point C_016) manganese oxides were identified. The colour of the samples indicates differences between the inner and cortical areas of the samples. In the latter brown, orange, or yellow are the predominant colours, as a consequence of the presence of iron oxide in the cement of the conglomerate (Table-6.40). All the mineral inclusions in cortical areas of the samples are iron oxides. The most represented morphological category is spherical pebble, although tabular and flat pebbles are also present associated to the CC types. Cortical texture is fine or fine and grained, without any clear difference between petrogenetic types or geographical areas. There are similar numbers of directional joints in inner and cortical areas (Table-6.41).

Grain size characterisation		Petrogenetic type															
		CC		CA		OO		SO		BQ		RQ		MQ		Total	
		Σ	%	Σ	%	Σ	%	Σ	%	Σ	%	Σ	%	Σ	%	Σ	%
Homogeneous and one mode distribution	Fine grain	1	13	1	50											2	15
	Medium grain					2	67									2	15
	Coarse grain																
Heterogeneous and two modes distribution	Fine grain	1	13	1	50											2	15
	Medium grain	1	13													1	8
	Coarse grain	1	13													1	8
Heterogeneous distribution	Fine grain	2	25													2	15
	Medium grain	2	25			1	33									3	23
	Coarse grain																
	Total	8	62	2	15	3	23									13	100

Table-6.38: Frequency table of the petrological features of the pebbles from the Campollo group conglomerates based on binocular characterisation. Columns are petrogenetic types and rows contain the characteristics of grains according to size, classified first by distribution and second by size itself.

Non-quartz minerals	A		B		C		General	
	Σ	%	Σ	%	Σ	%	Σ	%
Absence					1	8	1	3
Fe-Oxides	9	69	2	15	1	8	12	31
Mn-Oxide			1	8			1	3
Mica	1	8	3	23	8	62	12	31
Black mineral	2	15	6	46	2	15	10	26
Feldspar	1	8	1	8	1	8	3	8
Total	13	100	13	100	13	100	39	100

Table-6.39: Frequency table of the features of non-quartz minerals of the pebbles from the Campollo group conglomerates based on binocular characterisation. Columns are the three fields considered and rows are the non-quartz minerals identified.

Colour	Cortical area				On fresh cut			
	Primary		Secondary		Primary		Secondary	
	Σ	%	Σ	%	Σ	%	Σ	%
White			2	15	4	31	2	15
Grey	6	46	2	15	6	46	4	31
Blue							4	31
Orange			4	31				
Brown	6	46	5	38	2	15	3	23
Yellow	1	8						
Red					1	8		
Total	13	100	13	100	13	100	13	100

Table-6.40: Frequency table of the colour hue of the samples from the pebbles from the Campollo group conglomerates. Columns are the fields for primary and secondary colour hues of cortical areas and in fresh cut respectively and rows are the colours considered.

	Features	Σ	%
Morphology	Tabular clast	1	4
	Tabular pebble		
	Flat pebble	1	4
	Spherical pebble	22	92
	Total	24	100
Cortical texture	Coarse and grained	1	4
	Fine and grained	22	92
	Fine	1	4
	Really fine		
	Total	24	100
Mineral inclussion on cortical area	Absence		
	Fe-oxides	23	96
	Carbonated		
	Siliceaus	1	4
	Total	24	100
Cortical joints	Not analysed	1	4
	Absence	3	13
	Unidirectional	2	8
	Bidirectional	8	33
	Three-directional	10	42
	Total	24	100
Joints	Absence		
	Unidirectional	5	21
	Bidirectional	8	33
	Three-directional	11	46
	Total	24	100
Bedding	Absence	24	100
	Unclear		
	Clear		
	Total	24	100
Schistosity	No	22	92
	Yes	2	8
	Total	24	100

Table-6.41: Frequency table of the morphology, cortical texture, mineral inclusions on the cortex, quantity of cortical joints, quantity of internal joints, bedding, and schistosity of the samples from the Campollo group conglomerates.

We selected four samples from survey point C_008 for thin section and X-Ray Fluorescence. The results agree with the non-destructive characterisation. Samples DC24_03 and DC24_05 are CC petrogenetic types with floating or tangential packing and major presence of clastic quartz grains. The matrix composition of the first one is clayey, while in the second one it is siliceous. In the first case the cement is composed of carbonated material, similar to the sample DC18_02 from the Viorna conglomerate. The analysis of grain size reveals similar patterns, but the morphology of the grains is more rounded and circular in the first sample than in the second one (Figure-6.35). Sample DC24_02 is a CA type with major presence of concavo-convex quartz grain limits and general undulate extinction. Sample DC24_09 is an OO type with an abundant presence of concavo-convex grain limits, general undulate extinction, and syntaxial overgrowths. The characteristics of grain size of these two samples are similar, as well as matrix, which is predominantly clayey (Figure-6.36). X-Ray Fluorescence reveals that all the samples have important presence of Al_2O_3, more abundant in the quartz-arenite group than in the other samples, probably as a consequence of the compaction of the material and the higher amount of matrix.

Summing up, the conglomerates of the Campollo Group (including the Narova conglomerate) extend along the centre and the eastern part of La Liébana zone and they are easily recognisable in the field. In these conglomerates it is easy to obtain CC petrogenetic types, but it is more difficult to find other types, such as CA or OO one, which are scarcer. In any case, selective mechanism must have been needed for obtaining the latter two types. There is no evidence of more deformed types. The catchment activities directly on the conglomerate would have been determined by the composition of cement. In cases where the cement is calcareous, it is easy to extract the rocks directly from the conglomerate or its finding in the surrounding area. In cases where the cement is argillaceous, it is possible to extract the rocks using hammers or similar tools, as well as to collect pebbles from the surrounding area. Finally, in case the cement is siliceous, it is not possible to extract the pebbles directly from the conglomerate and they are scarce in the surrounding areas. In the latter, pebbles can only be extracted using hammers or other tools, but it is almost impossible to extract only pebbles because of the hardness of cement. In some cases, cement is more compact than pebbles contained in the conglomerate.

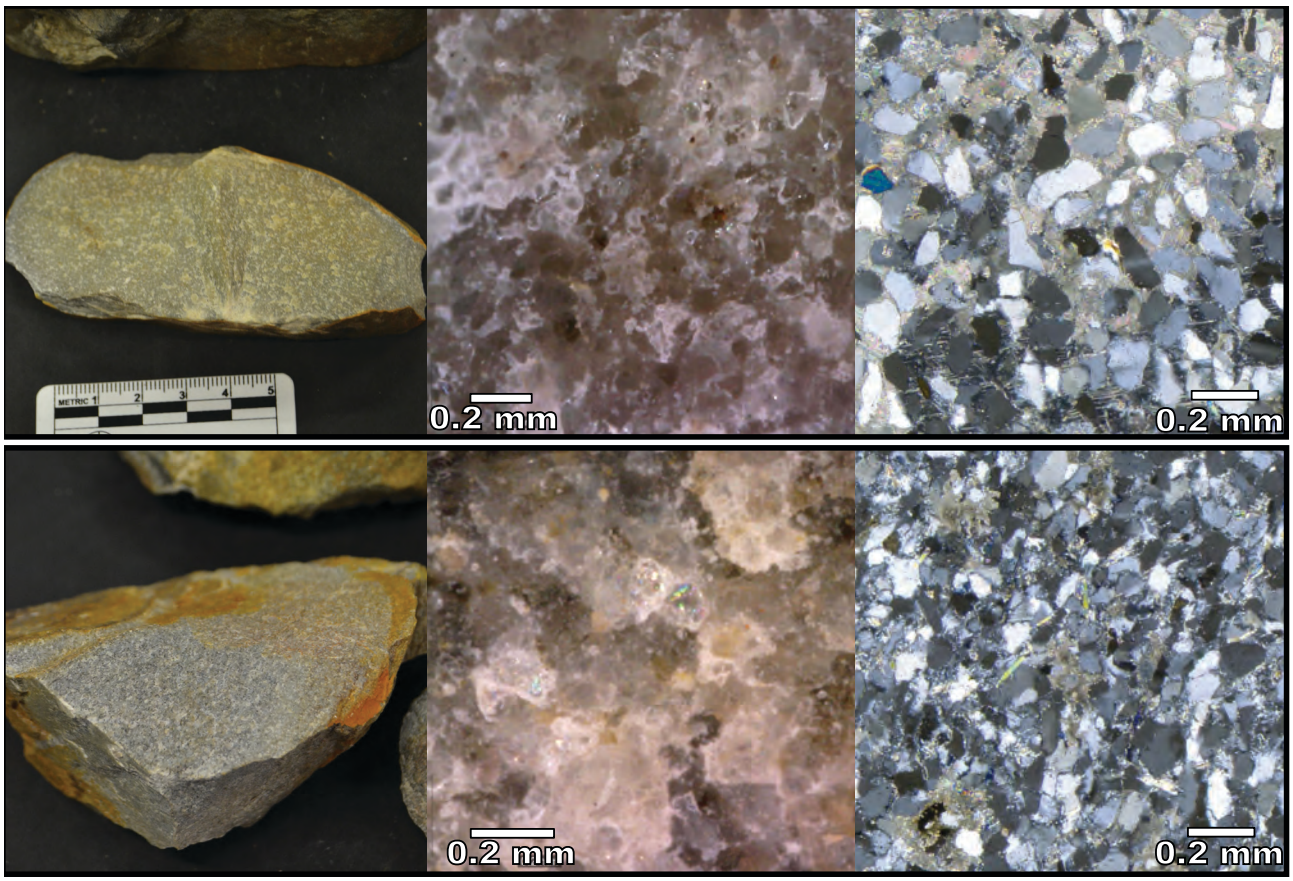

Figure-6.35: Pictures at different magnifications of the samples DC24_03 and DC24_05 from the Campollo-Narova group conglomerate. Both samples are from the CA type and have similar quartz grain size varieties. The samples DC24_03 exhibits clear carbonated cement, while in sample DC24_05 the matrix is siliceous.

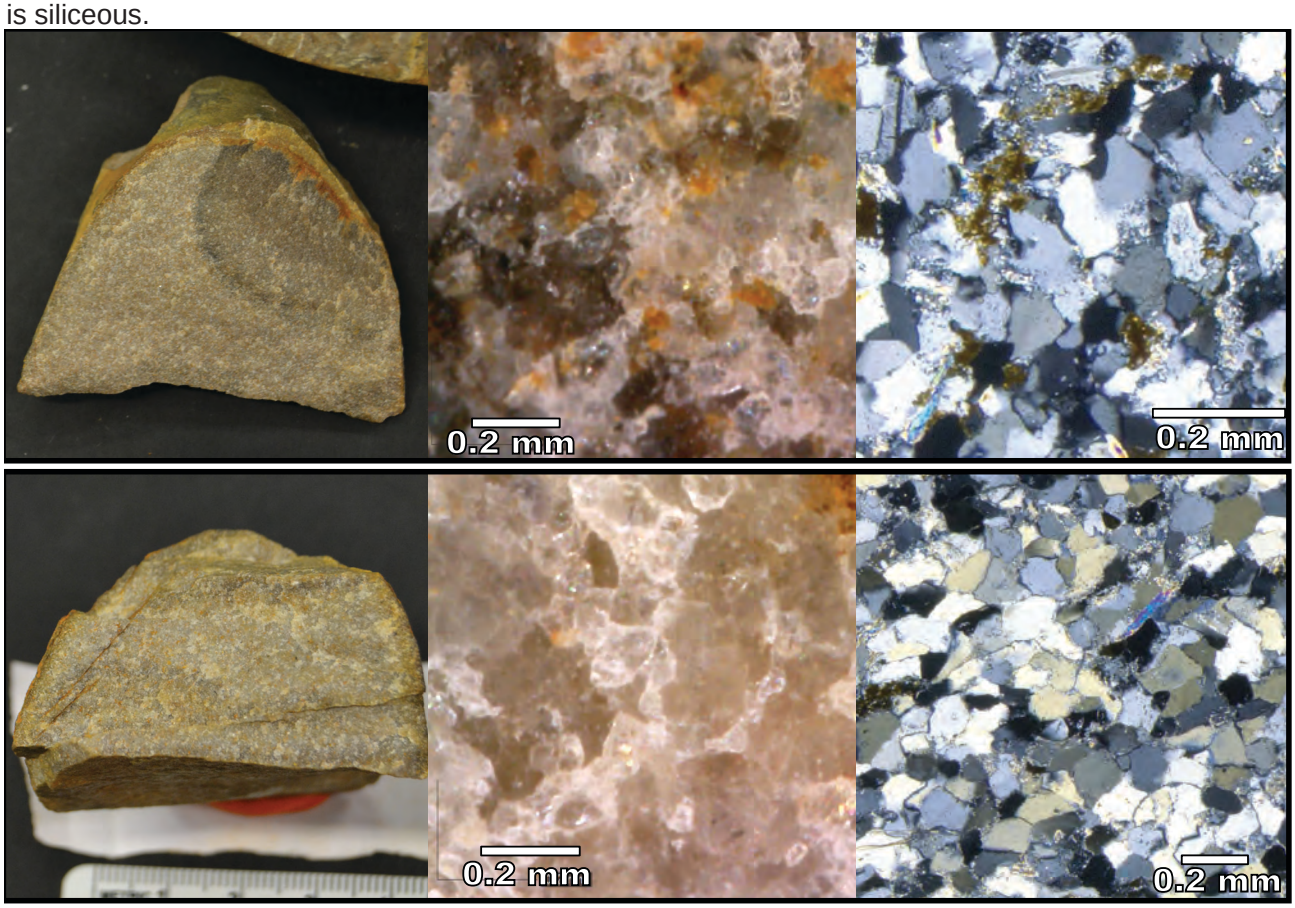

Figure-6.36: Pictures at different magnifications of the samples DC24_02 and DC24_09 from the Campollo-Narova group conglomerate. The first sample is a CA type, while the second is an OO type.

6.2.10. THE UPPER PENNSYLVANIAN SERIES: THE REMOÑA GROUP

The Remoña Group is the last group with presence of conglomerates analysed in this research. The group consists of another succession of shale, sandstone, and conglomerate with an approximate thickness of 900 meters. It was created in a foreland basin system, on the filling area of a basin created in the surroundings of the Picos de Europa orogen (the foredeep). The entire group is chronostratigraphically dated between the Dorogomilovsky (the last sub-stage of the Kasimovian) and the Pavlovoposadansky, in the Gzhelian (the last stage of the Carboniferous). The formation covers through an unconformity multiple groups or formations, from the Barrios Formation to the Valdeón, Campollo, or Lechada Carboniferous groups, and it is covered by Permian or recent materials (Heredia et al., 2003a; Rodríguez-Fernández, 1987; Rodríguez Fernández et al., 2003). The conglomerates from the Remoña formations extend around the village of Posada de Valdeón, in the southwest of our research area, as small conglomerates within the thick Remoña Group alternation in northwest-south east direction. The region marked in different maps shows the complete layer of the Remoña Group. The formation also appears in the centre of the area of study, surrounding the current limit of the Picos de Europa mountain chain in the eastern zone. The sheet 56 of the 1:50000 MAGNA series finished during the year 2003 differentiates some small and thin conglomerate layers between the villages of Pendes and Cabanes, as well as some small layers to the east of the village of Cobeña (Martínez García et al., 2003). In the present research, we drew these layers on the maps generated, but we did not draw the general layer. The most recent GEODE 1:50000 continuous map does not differentiate these strata, but it distinguishes a new one near the village of Espinama, not considered in the present research.

Due to visibility and accessibility issues, we only analysed the Remoña Group in the Liébana area. We examined three different conglomerates in the area between the villages of Pendes and Cabanes and another one to the east. The information about the survey points analysed is in the Supplementary Information-III. The points are the following:

- C_001/DC006: 30T 369181 4784956
- C_003/DC015: 30T 369303 4784968
- C_013/DC039: 30T 368777 4784957
- C_014/DC040: 30T 371655 4783520

Grain size characterisation		Petrogenetic type															
		CC		CA		OO		SO		BQ		RQ		MQ		Total	
		Σ	%	Σ	%	Σ	%	Σ	%	Σ	%	Σ	%	Σ	%	Σ	%
Homogeneous and one mode distribution	Fine grain					2	29			1	33					3	19
	Medium grain					4	57	1	25							5	31
	Coarse grain																
Heterogeneous and two modes distribution	Fine grain	1	50					2	50	1	33					4	25
	Medium grain																
	Coarse grain																
Heterogeneous distribution	Fine grain	1	50							1	33					2	13
	Medium grain					1	14	1	25							2	13
	Coarse grain																
	Total	2	13			7	44	4	25	3	19					16	100

Table-6.42: Frequency table of the petrological features of the pebbles from the Remoña group conglomerates based on binocular characterisation. Columns are petrogenetic types and rows contain the characteristics of grains according to size, classified first by distribution and second by size itself.

The data collected reveal clear differences between the first three survey points and the last one. The survey point C_014 is a calcareous cemented conglomerate without bedding or joints structures, composed by heterogeneous and angular clasts of limestone, not relevant for the present research. Therefore, we decided to discard this small conglomerate from further analysis. Coming back to the first three survey points, all of them exhibit clear bedding. Joints are absent in all of them.

The characterisation of cement indicates it is mainly composed of relatively compacted, orange and argillaceous material. The percentage of cement in the surface is between 5 and 50 %, which creates the isolated to tangential packing of rock fragments. Thin and plain sandstone layers are present below, above and inside the formation, creating a conglomerate and sandstone alternation. The presence of these layers allows the preservation of parts of these conglomerates at the top of the hills where they crop out.

Non-quartz minerals	A		B		C		General	
	Σ	%	Σ	%	Σ	%	Σ	%
Absence			1	6	2	13	3	6
Fe-Oxides	12	75	4	25			16	33
Mn-Oxide								
Calcite								
Mica	3	19	7	44	2	13	12	25
Black mineral			2	13	9	56	11	23
Pyrite	1	6	2	13	3	19	6	13
Feldspar								
Total	16	100	16	100	16	100	48	100

Table-6.43: Frequency table of the features of non-quartz minerals of the pebbles from the Remoña group conglomerates based on binocular characterisation. Columns are the three fields considered and rows are the non-quartz minerals identified.

Colour	Cortical area				On fresh cut			
	Primary		Secondary		Primary		Secondary	
	Σ	%	Σ	%	Σ	%	Σ	%
Absence			2	13			2	13
White	2	13	1	6	3	19	2	13
Grey	9	56	3	19	11	69	1	6
Black	3	19	5	31			7	44
Blue			1	6			2	13
Green								
Orange								
Brown	2	13	2	13	2	13	2	13
Yellow			1	6				
Red			1	6				
Total	16	100	16	100	16	100	16	100

Table-6.44: Frequency table of the colour hue of the samples from the pebbles from the Remoña group conglomerates. Columns are the fields for primary and secondary colour hues of cortical areas and in fresh-cut respectively and rows are the colours considered.

The lithological characterisation of these conglomerates at fieldpoints at the major presence of “archaeological quartzites” in the conglomerate. There is an abundant presence of orthoquartzite, including the two petrogenetic types. The presence of quartz-arenite, only represented by the CC type, and quartzites, represented by the BQ type, is smaller. We selected 16 samples for laboratory characterisation. The results certify the characterisation proposed in the field. The samples confirm the high presence of the OO type, with grain size up to medium, either homogeneous or heterogeneously distributed. The SO type is also well represented, with a high diversity of quartz grains. There is also an important quantity of BQ types, associated with fine grain sizes and various distributions. The CC type is also present and it is related with heterogeneous gran size distributions similar to those observed in the sandstone outcrop formation from the Carboniferous (Table-6.42). The characterisation non-quartz mineral characterisation reveals the major presence of iron oxides in every sample, as well as the presence of mica, non-identified black and heavy minerals, and pyrite. Latter is not clearly related with some CC petrogenetic types (Table-6.43). The analysis of colour reveals small differences between cortical and inner areas. Colours derived from the presence of iron oxides (represented as cortical inclusions), such as brown, red, or yellow, are more frequent on cortical surfaces (table-6.44). The external morphology of the samples is spherical and flat pebbles, the latter being exclusively related with CC petrogenetic types. The cortical texture is heterogeneous, with major presence of fine texture, followed by fine and grained and two samples with really fine cortical texture. The fine and really fine textures are related with metamorphic or SO types. There is a slightly higher presence of joints in the inner part than on the external area. However, joints are not really

frequent. The most represented categories are unidirectional and bidirectional joints. Only one sample presents bedding (unclear). Two samples do also show schistosity on their surfaces (Table-6.45).

	Features	Σ	%
Morphology	Tabular clast		
	Tabular pebble		
	Flat pebble	2	13
	Spherical pebble	14	88
	Total	16	100
Cortical texture	Coarse and grained		
	Fine and grained	6	38
	Fine	8	50
	Really fine	2	13
	Total	16	100
Mineral inclussion on cortical area	Absence		
	Fe-oxides	16	100
	Carbonated		
	Siliceaus		
	Total	16	100
Cortical joints	Not analysed		
	Absence	3	19
	Unidirectional	9	56
	Bidirectional	4	25
	Three-directional		
	Total	16	100
Joints	Absence	2	13
	Unidirectional	8	50
	Bidirectional	5	31
	Three-directional	1	6
	Total	16	100
Bedding	Absence	15	94
	Unclear	1	6
	Clear		
	Total	16	100
Schistosity	No	14	88
	Yes	2	13
	Total	16	100

Table-6.45: Frequency table of the morphology, cortical texture, mineral inclusions on the cortex, quantity of cortical joints, quantity of internal joints, bedding, and schistosity of the samples from the Remoña group conglomerates.

The petrographic characterisation of four samples certifies the presence of the OO, SO and BQ types. The OO type samples are the DC06_04 and the DC39_03. Both show similar features: high presence of concavo-convex quartz grain limits, syntaxial overgrowths and undulate extinction, as well as a small presence of suturated quartz grain limits. The characterisation of quartz grain size and morphology between both samples points at similar patterns. Both samples also show minor presence of clayey matrix and contain iron oxides, pyrite, mica, clays, chlorite and zircon (Figure-6.37). The quartz grains from the DC39_03 sample exhibit preferential orientation, but this feature is not clearly observed in sample DC06_04. The sample belonging to the SO type is DC06_05. It presents major presence of concavo-convex quartz grain limits, clearly suturated and residual presence of recrystallised quartz grains. The analysis of grain size and morphology reveals the prevalence quartz grains of small size and the presence of deformed quartz grains, together with some small non-deformed quartz grains. The sample DC06_06 is classified as BQ type based on the high presence of suturated quartz grains, deformation lamellae and the moderate presence of recrystallised quartz grains. The characterisation of quartz grain size and morphology clearly reveals a heterogeneous distribution organised around two modes (Figure-6.38). The last two samples clearly exhibit preferential orientation and mineral characterisation similar to that of the first two samples from the Remoña conglomerates. Regarding X-Ray fluorescence analysis of the four samples, all of them are mainly composed of SiO_2, with small presence of alumina and iron oxides.

In general, the conglomerates from the Remoña Group are small and thin conglomerate layers located inside the Remoña Group with small visibility. They extend to the south and south-east of the area surrounding the Picos de Europa mountain chain. The small portion of them analysed reveals similar features, including clear bedding structures, absence of joints and presence of argillaceous cement that would allow an easy to medium rock extraction. The lithologies found in these conglomerates indicate that catchment activities related with the exploitation of CC, OO, SO, and BQ petrogenetic types would have certainly been carried out here. The exploitation of orthoquartzites could have been easily done thanks to the abundancy of this group. The exploitation of the metamorphic BQ type could have been possible just applying weak selective mechanisms, because they are frequent in this conglomerate. Meanwhile, the exploitation of CC type could have been done by directly extracting the pebbles from the conglomerate. Summing up, the exploitation of lithic resources could have been easily carried out by direct extraction in the conglomerate or by gathering activities around the conglomerate. The exploitation of these conglomerates during the Middle Palaeolithic is certified at the El Habario, located in close proximity to these conglomerates.

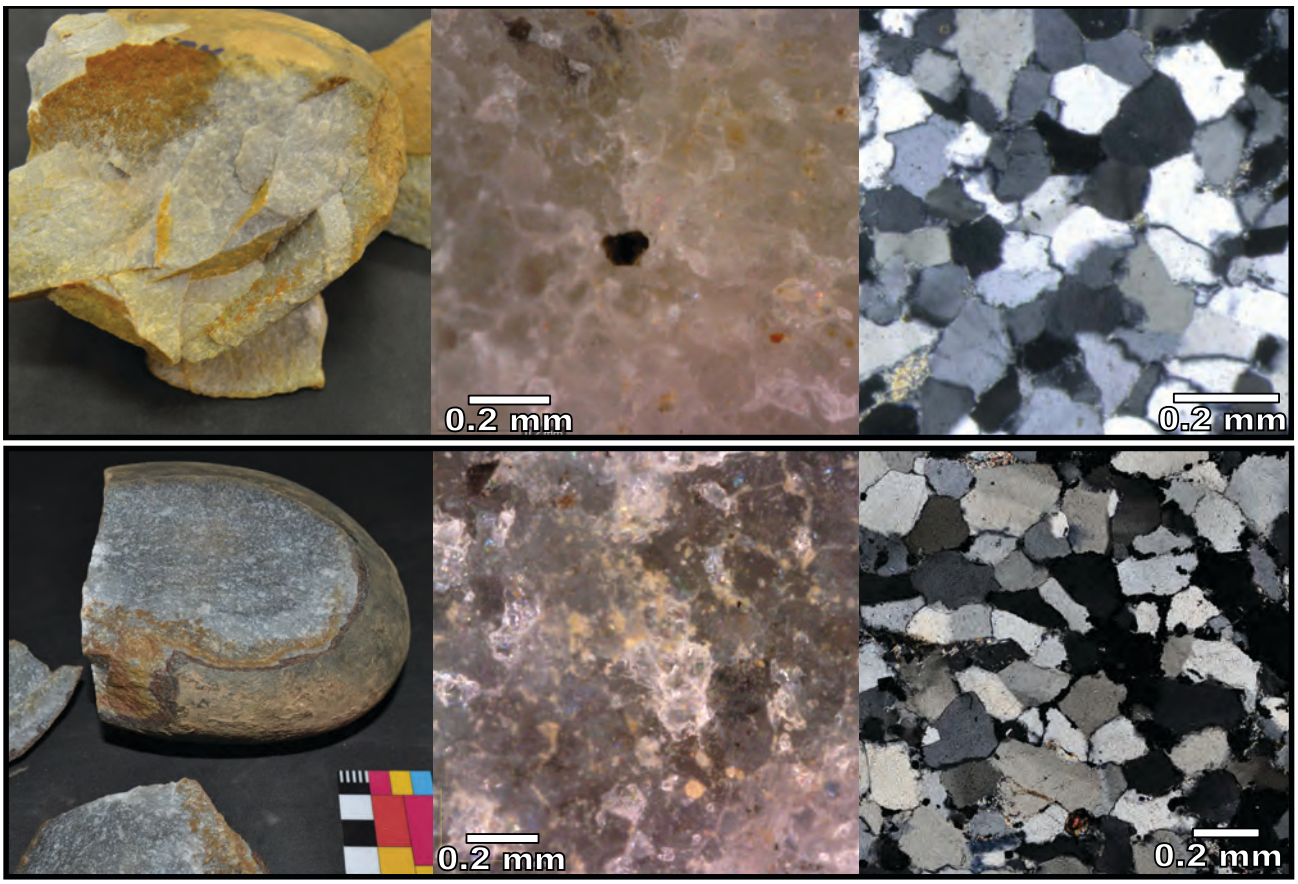

Figure-6.37: Pictures at different magnifications of the samples DC06_04 and DC39_03 from the Remoña group conglomerate. Both samples are from the OO type and have similar grain size varieties.

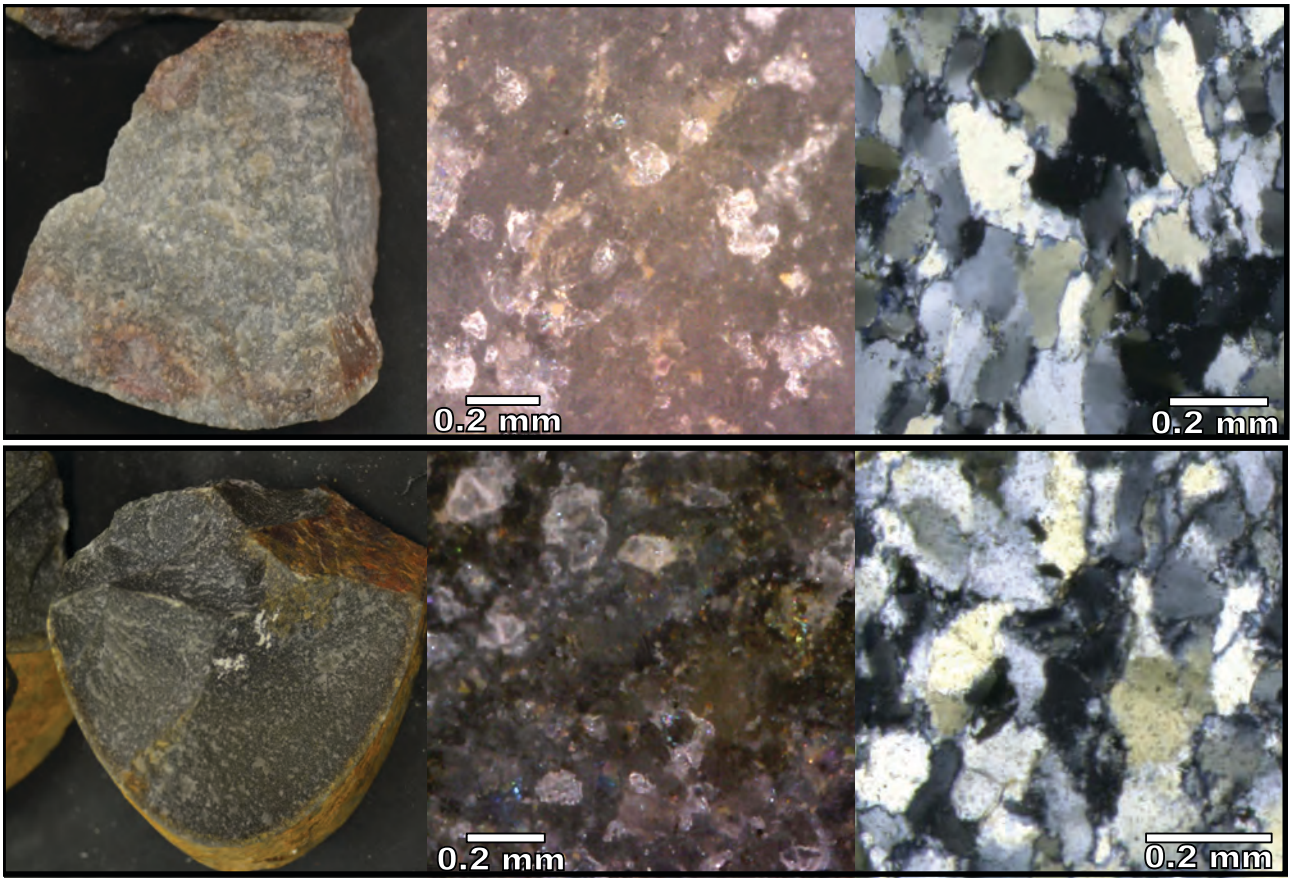

Figure-6.38: Pictures at different magnifications of the samples DC06_05 and DC06_06 from the Remoña group conglomerate. The first sample is a SO type and the second is a BQ type.

6.2.11. OTHER FORMATIONS OF CONGLOMERATES

In this section, we will describe other formations with conglomerates that are not interesting for the present research or that could not be surveyed due to accessibility and time issues. These conglomerates are the Cavandi Formation, the Peñacruz Formation, the Sotres, Cabranes, Caravia and Fuentes Formations and a conglomerate layer from the Paleogene. The Cavandi Formation is a succession of shale, sandstone, conglomerates and breccia dated to the end of the Carboniferous, between the Kasimovian and the Gzhelian stages. We sampled the formation in different points, and analysed the survey point C_048 (see S.I.-III) located in the conglomerate stratum of the formation. We do not find any "archaeological quartzite" among the pebbles. The Peñacruz, Cabranes, Carabia, and Fuentes Formations are mixed strata with presence of conglomerates situated in the southeaster part of the research area and dated between the Permian and the Triassic periods. Due to their difficult accessibility and time limitations, we could not sample them. The conglomerates of the Peñacruz Formation, also known as Saja conglomerates, are a conglomerate formation dated to the Upper Jurassic. We sampled the formation at the C_012 survey point (see S.I.-III) finding no evidence of "archaeological quartzite". Finally, we analysed a Paleogene conglomerate formation at the survey point C_049 (see S.I.-III). The main lithology is sandstone or CC type of "archaeological quartzite", not compact and with a wide variety of grain sizes.

6.3. SECONDARY DEPOSITS WITH "ARCHAEOLOGICAL QUARTZITES"

In this section we describe different types of secondary deposits (henceafter deposits) where "archaeological quartzite" appears. The acquisition of interesting rocks on these context is certified in the Iberian Peninsula, especially in river deposits e.g. (Arrizabalaga, 2010; Arrizabalaga and Tarriño, 2010; Manzano et al., 2005; Montes and Muñoz, 1992; Roy et al., 2017). The presence of "archaeological quartzite" in both context is clear, especially the CC petrogenetic type, the most frequent type in the research area. All these reasons carried us to analyse in detail both types of deposits to understand the potential catchment activities and strategies carried out in both analysed contexts during the Palaeolithic. These deposits are chrono-stratigraphically dated in the Quaternary. We identify two main types of deposits: gravitational deposits and river deposits.

6.3.1. GRAVITATIONAL DEPOSITS

The gravitational deposits consist of the accumulation of unconsolidated sediments or parts of outcrops derived from other unconsolidated deposits or outcrops as a consequence of weathering and erosion processes. Gravity is the main process of transport. We classify the gravitational deposit as offsets or flank deposits.

On one hand, the term **offset** characterises the fragments of massive or conglomeratic outcrops found on the current surface or in movement. The following offsets were part of conglomerate outcrops and we find them close to the areas where conglomerates crop out. During geological surveys we identified four offsets. We present the information on them in Supplementary Information-IV. The points where offsets were identified are the following:

- D_020/DC047: 30T 386023 4773385: Near the conglomerates of the Potes Group
- D_021/DC049: 30T 378837 4770303: Near the conglomerates of the Potes Group
- D_022/DC060: 30T 372227 4778410: Near the conglomerates of the Potes Group
- D_026/DC076: 30T 347433 4777447: Near the conglomerates of Curavacas and Remoña groups

The first three are fragments of conglomerates derived from the Potes Group. The properties of cement are similar to those of the Potes Group, with presence of iron oxides and low-medium degree of compaction. The clasts from these offsets show lithologies similar to those of the Potes Group, with prevalence of lutites, limestone, and "archaeological quartzites". The most represented petrogenetic type is the CC, followed by OO and CA types. The mineral and colour characterisation and the characterisation of external and internal features are similar to those observed in the Potes conglomerates. The last offset derived probably from the Curavacas Formation, since its cement composition, petrological characterisation, and external and internal features where similar to those of this latter formation.

In general, the presence and characterisation of these types of offsets in areas lower than those where conglomerates crop out demonstrates the existence of catchment zones beyond to the geological strata themselves. These offsets are potential catchment areas with features similar to those of the outcrop or conglomerate. In these cases catchment was practiced by direct exploitation of the conglomerate (in the last survey point necessarily using hammers due to cement compaction) or by collecting fragments in the surrounding offset area. In these cases the exploitation is limited to the CC, CA and OO types applying strong selective mechanisms for the last two types.

On the other hand, we used the term **flank deposit** to characterised stable or relatively stable deposits where "archaeological quartzite" is found in soil. The following points represent flank deposits. They are presented in detail in Supplementary Information-IV:

- D_019/DC041: 30T 370555 4782639: Near the Potes Formation
- D_024/DC071: 30T 344522 4780147: Near the Valdeón and Remoña conglomerate formations
- D_028/DC084: 30T 341267 4776053: Near the Murcia outcrop Formation
- D_029/DC085: 30T 341279 4776254: Near the Murcia outcrop Formation
- D_030/DC086: 30T 341189 4776424: Near the conglomerates of the Pontón Group

As in the case of offsets, these points were not systematically surveyed, but they were found when travelling between other planned survey points. However, these points suggest the presence of possible catchment areas in zones not indicated by outcrops. The last four points are situated in the Valdeón area, within gravitational deposits drawn in geological maps, but the first point is in the area of La Liébana and it is not drawn as deposit in the current map (Figure-6.39). Each point presents differences that help us to understand the features of each flank deposit. Moreover, they are also useful to understand erosion, transport, deposit, and weathering processes that modify our perception of the geographical dispersion of lithologies and, therefore, of source areas.

The survey point D_019 is a flank deposit located in a cut in the soil cause by a small road near the village of Trillayo. The slope of this flank deposit is soft, generating a relatively stable soil, covered by vegetation (except for the cut itself). The clasts of this deposit are mainly non-compacted sandstone (could be as assigned to the CC type) from the Potes Group, with tabular or rounded external morphologies and different sizes. There is also high frequency of lutites. The most interesting element of this flank deposit is the presence of a big fragment of conglomerate within the soil. Its presence, as well as the heterogeneous distribution of the clasts, is the reflection of a quick sedimentary event of slope formation that moved a big quantity of sediment to a previously flatten area as a consequence of a landslide. The presence in this flank deposit of a part of a conglomerate reinforces the existence of catchment areas outside the polygons drawn in the geological maps. In addition, it underlines the idea that rock acquisition processes were conditioned by the lithology of the outcrops (or conglomerates) that formed these flank deposits. In this case, the lithologies of the clasts in this conglomerate are similar to those of the Potes Group, with high percentages of lutites, limestone, CC type "archaeological quartzite", and more occasionally CA, and OO types. Therefore, the exploitation of raw materials in this type of flank deposit is determined by the presence or absence of interesting raw materials and its proportion. Finally, the small visibility of these flank deposits stops these areas from becoming optimal raw material catchment areas. We do not consider this type of areas interesting for intensive or planned raw material catchment activities, but accept the possibility of occasional finding and gathering of raw material.

Figure-6.39: Map of the different types of deposit in the area of study. Each point indicates a survey point. Icons define the main lithologies analysed. The colour of each point indicates the type of deposit: Blue marker for river beaches and brown marker for gravitational deposits. The petrological characteristics are represented by one to five icons with the initial of the most interesting petrogenetic types in the case of "archaeological quartzites" or those of the main lithology. The external form of the symbols represents the morphology of clasts where the squares are tabular clasts, rounded squares tabular pebbles, ovals flat pebbles and circles spherical pebbles. Finally, grain size distribution is represented by main colours. Homogenous distributions organised around one mode are represented in red, heterogeneous distribution organised around two modes in green and heterogeneous distributions in blue. Grain size characterisation is depicted through the brightness of colours just presented: light red, green, or blue for coarse size grains; medium red, green, or blue for medium size grains; dark red, green, or blue for small size grains.

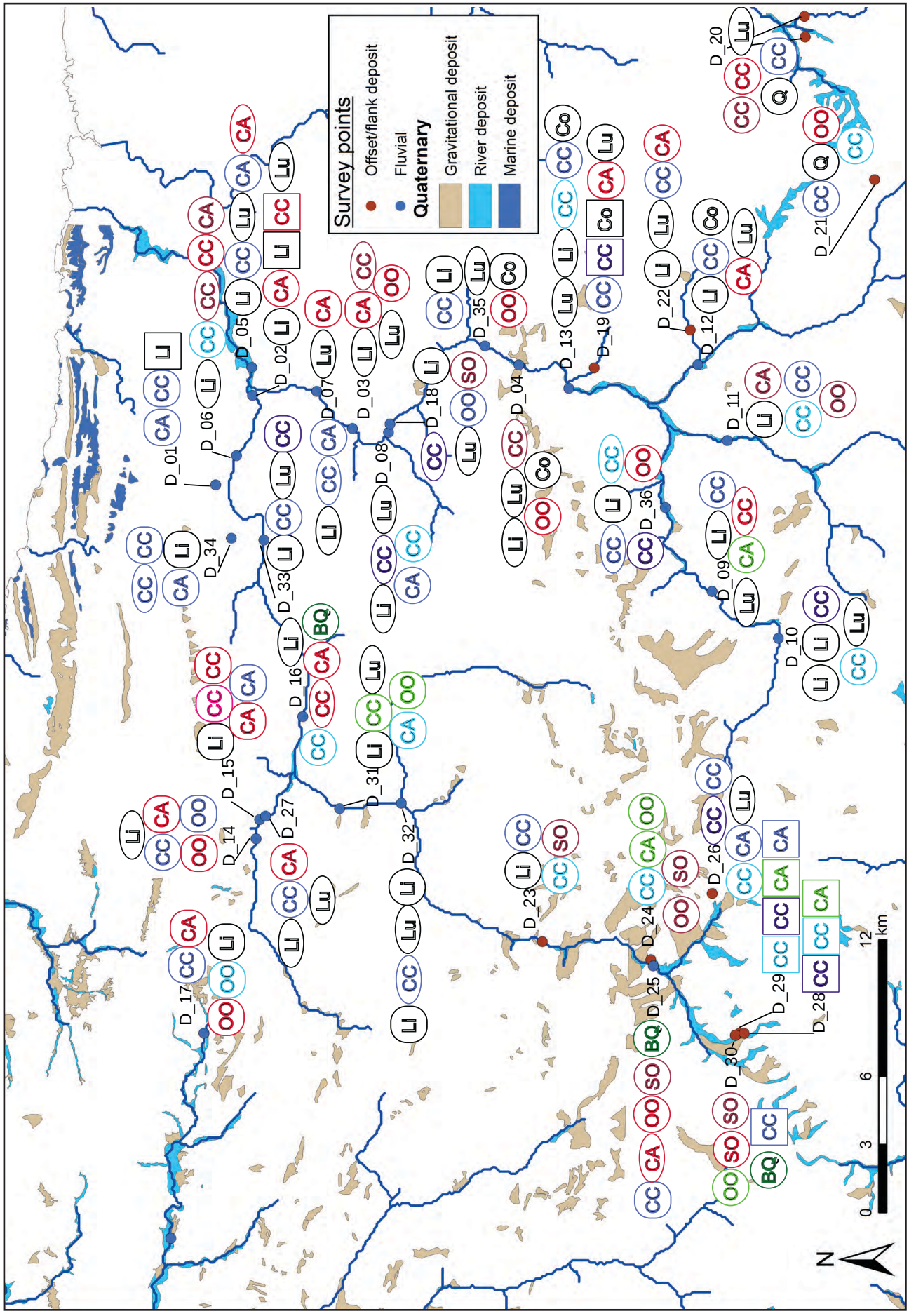

Figure-6.39: Map of the deposit (gravitational and fluvial) formations from the Upper Pennsylvanian in the area of study. The complete footnote is on the previous page.

The survey points D_024 and the D_030 are two flank deposits situated in the Valdeón area. The former is near the Cares River to the north of the village Posada de Valdeón, while the latter is to the south of Capdevilla de Valdeón, near the Cares River too. The first one is close to the Valdeón and Remoña formations. The second is associated to the Pontón Formation. Both flank deposits are slightly cut by current roads or paths, which make them visible (still visibility was hampered by vegetation, grass in the first case and forest in the second). In both cases the surveyed area consists of an accumulation of rounded and spherical pebbles of different types of "archaeological quartzites" with presence of iron oxides on the surfaces and variable presence of joints. These pebbles appear as accumulations, mixed with the current soil and extending over surfaces smaller than 20 square meters. We sampled "archaeological quartzites" from both survey points and they resulted into different petrogenetic types. In the survey point D_024 the most frequent clasts are classified as quartz-arenite, but the presence of orthoquartzites is relevant too, especially the OO type. In the survey point D_030 there is no presence of quartz-arenites and most of the samples are SO or BQ types. There is also a small percentage of OO type. Lithologies and external features of the flank deposits indicate the possible conglomerate of origin: the Remoña conglomerate in the first case and the Pontón conglomerates in the second. The cement of both formations is composed mainly of clayey material with presence of iron oxides, a soft element that could be easily weathered once in the soil. We propose that these soil accumulations of clasts are conglomerate outcrops or fragments of conglomerates covered by soil modified by underground weathering process. These processes make cement softer, dissolving it into the soil and releasing the clasts or pebbles into the soils. This process can also be appreciated in the figures of the survey point C_013, in the conglomerates of the Remoña Formation (see S.I.-III). As in the case of the survey point D_019 presented above, the visibility of this type of flank deposits flank is restricted. Then, the possibilities of having been used for intense and planned catchment activities are small, limited to occasional findings. However, both places, especially the second one, are interesting places for orthoquartzite and quartzite procurement, as the Remoña and Pontón conglomerates are.

The last two survey points, D_028 and D_030, are flank deposits situated close to each other in the Valdeón zone. Both points are near the Murcia sandstone formation, not analysed in this area because of visibility and accessibility issues. The survey point D_028 is a landslide mainly composed by fragments of sandstone with tabular morphologies from the Murcia Formation. There is no soil or matrix between the clasts. The second survey point is situated some meters below the first. It consists of a small accumulation of tabular clasts lithologically characterised as CC type from the Murcia Formation. These points illustrate the process of erosion and movement of clasts from a massive outcrop formation, revealing the successive quantitative loss of a specific lithology once the rock is detached from its original outcrop. The predominantly tabular clasts of heterogeneous sizes of the first point are replaced by more homogeneous and bigger clasts in their second point. The smaller clasts disappear in the latter point, probably due to its scattering in the soil or to the movement generated by water sources. Catchment would have been possible in both cases, but only for exhaustive exploitation of CA and CC petrogenetic types. These points also demonstrate the possible existence of secondary catchment areas near outcrops.

6.2.2. RIVER BEACH DEPOSITS

River beach deposits consist in the accumulation of unconsolidated sediment or fragments of outcrop derived from other unconsolidated deposits or outcrops as a consequence of weathering, erosion and, finally, transportation by water sources. In the present research we only take into account deposits generated by the action of rivers, not marine deposits. It is important to mention that we only analysed current river beaches. We divide the beach deposits analysed in two groups according to the river basins they belong to: the Cares and the Deva basins. Additionally, we also analysed a point at the intersection of both rivers and another two in the Güeña River basin.

The Deva River is a 64 kilometres long river with multiple tributary rivers, such as the Urdón, the Quiviesa and the Bullón rivers, that creates a sedimentary basin of more than 1195 km2. The Deva River springs at Fuente Dé, on the eastern part of the province of Cantabria and flows into the Cantabrian Sea at the Tina Mayor sea inlet between the provinces of Cantabria and Asturias after joining the Cares River. The Deva River and the Bullón and Quiviesa tributary rivers conduct the water from multiple and sloped water streams originating in the mountains situated on the southern part of the area of research (from the East to the West: the Sierra del Híjar, the Peña Sagra mountains, the Fuentes Carrionas mountains and the Urrieles and Ándara massifs from Picos de Europa). In the area of La Liébana these rivers do not create a stepped relief, neither important canyons nor defiles. In this area the small streams in the aforementioned mountain ranges are faster, creating

small river beach deposits. But the river system is less active in the central area of La Liébana, resulting into medium size river beaches and terraces. Once the Bullón and Quiviesa tributaries flow into the Deva River around the village of Potes, the main river travels until the Hermida defile. Here it crosses the Hermida defile, created by the erosion of the river on the eastern limestone formation of Picos de Europa, helped by its karstic systems. Many other small rivers, such as the Urdón, Covera or Cicera rivers, and the karstic system flow their waters into the Deva River, generating an increase of its volume. For this reason in this area the river passes faster and the river beaches are smaller. Once the Deva River crosses the Hermida defile, the softer relief allows the increase in size of the beaches. Later, the Cares River flows into the Deva River and, together and with the softer relief and the proximity of the Tina Mayor sea inlet, it creates huge river beaches and, further on, a big extension of fluvial sediment within a delta system.

We analysed 12 river beaches in the Deva basin. The systemised data about them is gathered in the S.I.-IV. The survey points are the following:

- D_003/DC003: 30T 367886 4793260
- D_004/DC005: 30T 370688 4785945
- D_007/DC012: 30T 373438 4798548
- D_008/DC014: 30T 367717 4791675
- D_009/DC020: 30T 360602 4777076
- D_010/DC023: 30T 358660 4774533
- D_011/DC030: 30T 367358 4776781
- D_012/DC031: 30T 370696 4778077: At the Bullón River
- D_013/DC032: 30T 369659 4783753: At the Quiviesa River
- D_018/DC037: 30T 368089 4791608
- D_035/DC107: 30T 371524 4787449
- D_036/DC109: 30T 364413 4779506

The data collected reflect a clearly heterogeneous distribution of lithologies, sizes, and morphologies of the rocks present in the river beaches. The most frequent lithology is limestone, followed by the CC petrogenetic type of quartzite and lutite. Conglomerates and other types of "archaeological quartzites", such as CA, OO, and SO types, are also present, the latter two in really small amounts. There are clear differences between the Liébana and the Hermida zones (Figure-6.39). The presence of limestone is more frequent in the northern area than to the south. Conversely, lutites are more frequent in the south. The presence of the CC petrogenetic type is slightly smaller in the northern area, especially in the survey points D_003, D_008 and D_018. This general geographic gradation of the main lithologies reflects the influence of the original lithological composition of outcrops on the formation of beach deposits. However, the identification of lithologies from distant outcrops in the beach deposits too points at the importance of stone transport by fluvial and active water sources (in smaller quantities). The size and morphological features of the rocks from the river beach deposits agree with this idea. Larger and more angular morphologies are related to closer source areas. Rounded and smaller morphologies are related to distant source areas. In addition, and as a second order relationship, each lithology is associated with a specific morphology. Lutites are related with flat pebbles, because of their origin in outcrops organised as alternations and exhibiting bedding surfaces. Instead, limestone is related with either tabular or flat pebbles. Finally, quartz-arenite is related to spherical or flat pebbles. Orthoquartzites are exclusively associated to spherical pebbles.

We selected 63 samples of "archaeological quartzite" from the different survey points for obtaining more detailed information. The petrological characterisation agrees with the major presence of the CC type and the smaller importance of CA and OO types. The presence of the SO type is negligible. Grain size characterisation reveals to the prevalence of heterogeneous distribution of quartz grains size (Table-6.46). Non-quartz mineral characterisation indicates the main presence of iron oxides and non-identified black minerals in the samples, very common in the "archaeological quartzites" analysed. The presence of mica and manganese oxides is also frequent. Feldspar, associated to CC types, is present on a few samples, as well as pyrite, which is not clearly related with any petrogenetic type (Table-6.47). The characterisation of colour of the rocks reveals differences between the cortical and the inner areas. However, these differences are moderate compared with most of the conglomerates due to the smaller influence of iron oxides on cortical areas, which are clearly washed. The most frequent colour is grey, followed by brown and white. Black coloured rocks

appear only in small numbers (Table-6.48). The morphology of the samples is heterogeneous, with clear predominance of flat pebbles. Tabular and spherical pebbles are also present, as well as tabular clasts, with only one sample. Spherical pebbles are associated with the rocks transported from afar, while tabular pebbles and flat pebbles are associated with moderate or small fluvial transport (Table-6.49). The texture of the cortical areas is heterogeneous, with presence of all the categories, except for the really fine category. The CC petrogenetic type is associated to grained and coarse-grained textures, the latter being related to coarse and heterogeneous grain size varieties. Fine tex-

Grain size characterisation		Petrogenetic type															
		CC		CA		OO		SO		BQ		RQ		MQ		Total	
		Σ	%	Σ	%	Σ	%	Σ	%	Σ	%	Σ	%	Σ	%	Σ	%
Homogeneous and one mode distribution	Fine grain																
	Medium grain					1	11									1	2
	Coarse grain																
Heterogeneous and two modes distribution	Fine grain	4	9													4	6
	Medium grain	13	28	1	17	1	11									15	24
	Coarse grain	17	36	2	33											19	30
Heterogeneous distribution	Fine grain	4	9	2	33	3	33	1	100							10	16
	Medium grain	8	17	1	17	2	22									11	17
	Coarse grain	1	2			2	22									3	5
Total		47	75	6	10	9	14	1	2							63	100

Table-6.46: Frequency table of the petrological characterisation of the pebbles from the river beach in the Deva basin based on binocular microscope observation. Columns are the petrogenetic types. Rows are grain size characterisation, classified first by distribution and then by size.

Non-quartz minerals	A		B		C		General	
	Σ	%	Σ	%	Σ	%	Σ	%
Absence			1	6	2	13	3	6
Fe-Oxides	12	75	4	25			16	33
Mn-Oxide								
Calcite								
Mica	3	19	7	44	2	13	12	25
Black mineral			2	13	9	56	11	23
Pyrite	1	6	2	13	3	19	6	13
Feldspar								
Total	16	100	16	100	16	100	48	100

Table-6.47: Frequency table of the non-quartz minerals identified in the pebbles from the river beach in the Deva basin based on binocular microscope observation. Columns are the three fields considered and rows are the non-quartz minerals identified.

Colour	Cortical area				On fresh cut			
	Primary		Secondary		Primary		Secondary	
	Σ	%	Σ	%	Σ	%	Σ	%
Absence			2	13			2	13
White	2	13	1	6	3	19	2	13
Grey	9	56	3	19	11	69	1	6
Black	3	19	5	31			7	44
Blue			1	6			2	13
Green								
Orange								
Brown	2	13	2	13	2	13	2	13
Yellow			1	6				
Red			1	6				
Total	16	100	16	100	16	100	16	100

Table-6.48: Frequency table of the colour hue of the samples from the pebbles from the river beach in the Deva basin. Columns are the primary and secondary colours of cortical areas and in fresh-cut. Rows are the colours considered.

tures are mainly associated to OO petrogenetic types. The mineral inclusions on the cortical areas are mostly iron oxides, despite having been washed by water sources. The quantification of directional joints on the cortical and inner areas of rocks shows patterns different to those of the contexts previously analysed. There is higher presence of multiple directional joints on cortical areas than in inner areas. In general, the presence of joints is smaller than in the conglomerates and outcrops previously analysed. This is a consequence of the transport of the rocks in water streams, which breaks rock into fragments at the joints. Bedding is present in some of the quartz-arenite samples, mainly of the CC type; but in general, samples do not exhibit bedding. Schistosity is completely absent as a consequence of the lack of clearly deformed or metamorphic types.

	Features	Σ	%
Morphology	Tabular clast	1	2
	Tabular pebble	17	27
	Flat pebble	29	46
	Spherical pebble	16	25
	Total	63	100
Cortical texture	Coarse and grained	4	6
	Fine and grained	41	65
	Fine	18	29
	Really fine		
	Total	63	100
Mineral inclussion on cortical area	Absence	1	2
	Fe-oxides	59	94
	Carbonated	2	3
	Siliceaus	1	2
	Total	63	100
Cortical joints	Not analysed		
	Absence	17	29
	Unidirectional	21	36
	Bidirectional	11	19
	Three-directional	10	17
	Total	59	100
Joints	Absence	25	40
	Unidirectional	17	27
	Bidirectional	12	19
	Three-directional	9	14
	Total	63	100
Bedding	Absence	53	84
	Unclear	5	8
	Clear	5	8
	Total	63	100
Schistosity	No		
	Yes	63	100
	Total	63	100

Table-6.49: Frequency table of morphology, cortical texture, mineral inclusions on cortical areas, quantity of cortical joints, quantity of internal joints, bedding and schistosity of the samples from the river beach in the Deva basin.

We selected four samples for petrographic and geochemical characterisation. Two come from the survey point D_003 and another two from the survey point D_004. Thin section reveals that three of the four samples belong to the most frequent type of "archaeological quartzite" in the Deva river beaches, the CC petrogenetic type (Figures-6.40 and Figure-6.41). All of them present an abundancy of detrital quartz grains. In addition, samples DC03_02 and DC05_02 have high presence of clayey matrix. Instead, the matrix of sample DC05_01 is siliceous. All these samples have an important quantity of non-quartz minerals, such as mica, chlorite, clay and iron oxides. The characteristics of grain size of the samples DC03_02 and DC05_01 are similar to each other. Most of the quartz grains are very fine sands. However, smaller grain sizes are also very frequent and some bigger quartz grains are observable too. Grain size of sample DC05_02 is slightly bigger. The morphology of quartz grains is heterogeneous in all the three samples, with predominance of angular and rounded quartz grains. These samples are clearly similar to the Murcia and Potes outcrop formations. Sample DC03_03 is a clear OO type of orthoquartzite, with presence of undulatory extinction, concavo-convex quartz grain limits and the abundant presence of syntaxial overgrowth (Figure-6.41). There is an occasional presence of clayey matrix. Regarding quartz grain size, very fine sands prevail, even though coarse silt and fine sand are well represented too. The analysis of the morphology of grains reveals a high degree or circularity and roundness, slightly deformed though. Among non-quartz minerals, there is a sporadic presence of mica, chlorite and clay. This sample is clearly similar to sample DC04_05, an OO type from the Barrios outcrop.

Figure-6.40 (on the following page): Pictures at different magnifications of samples DC03_02 and DC05_02 from the Deva river beach. Both samples are of the CC type with medium quartz grain size for the former and more heterogeneous and coarse quartz grain size variety for the latter. The presence of cement is frequent on both.

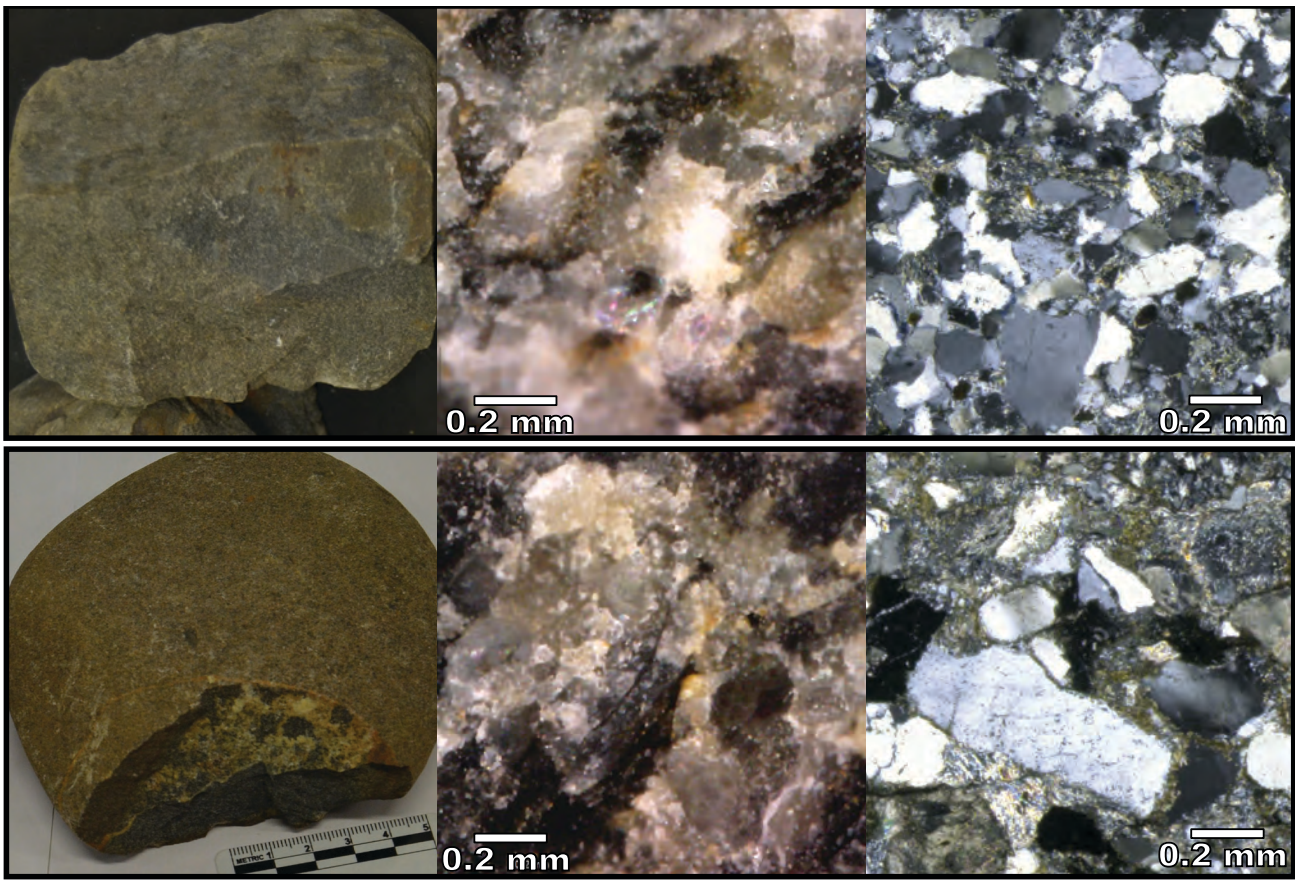

Figure-6.40: The complete caption is on the previous page

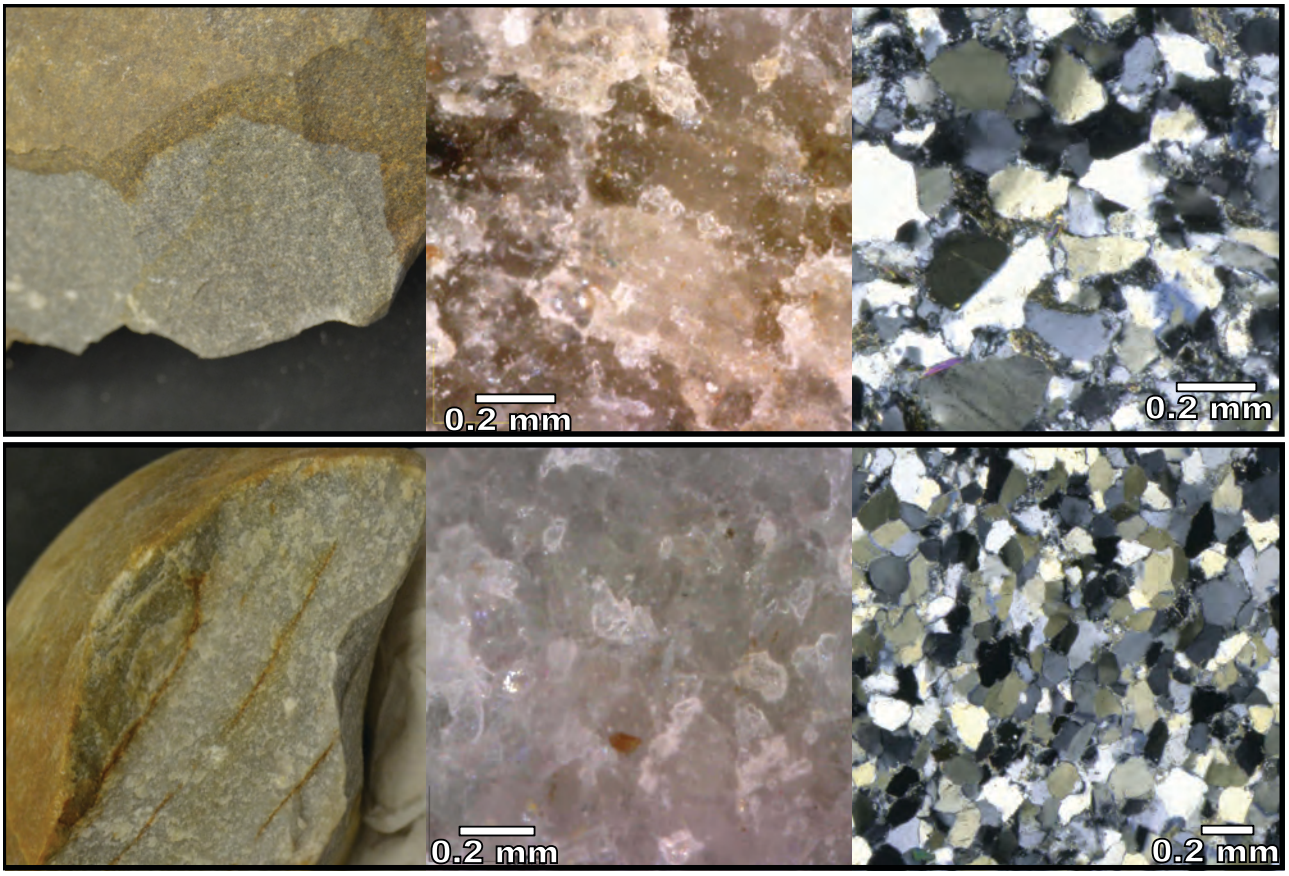

Figure-6.41: Pictures at different magnifications of the samples DC05_01 and DC03_03 from the Deva river beach. The first sample is of the CC type and the second is of the OO type.

All in all, the river beach deposits from the Deva basin form a changeable source of raw material thanks to the heterogeneous lithology of the basin and the transport carried out by this active river. The strata eroded by the rivers determine the lithologies present in each river beach, although distant lithologies also appear occasionally. The morphologies of the most frequent lithologies are tabular and conditioned by their arrangement in the original formation. Meanwhile, the morphology of the distant and less frequent lithologies is always rounded, as the original arrangement in the former formation is eroded. In general, the most frequent lithologies are limestone, lutite and "archaeological quartzites", with higher percentages of the first one. Regarding the diversity of later type of rock, the CC type is clearly predominant, with heterogeneous quartz grain size distribution and high presence of cement or matrix. The source area of this type extends widely along the Liébana zone comprising the outcrops of Potes, Mogrovejo, Viorna and, less importantly, Murcia, and Barrios formations. The presence of CA and OO types is small. When they are present, they always make less than 5% of the survey point. Their source areas are the slightly deformed zones of the Barrios outcrops or the rocks derived from conglomerates in the southern zone. Finally, the negligible presence of the SO type is related with the conglomerates just mentioned. The presence of small pieces of conglomerates in Deva River reinforces this hypothesis. Then, the catchment strategies in river beach deposits must have implied the application of some kind of selective mechanism in order to obtain the CC types, but selective mechanism must have been stronger for CA or OO types. The intensive exploitation of the former type would have been possible thanks to the big amounts of CC type. Conversely, the intensive exploitation of the latter two types would have not been possible, given its scarcity. The exploitation of SO type or other petrogenetic types not identified here would have been more casual than planned.

The Cares River is a 54 kilometres long river that springs in the Valdeón area, in the province of León, region of Castilla y León. The Cares River has many other small and active tributaries, such as the Bulnes, Duje and Casaño rivers. At the end the Cares River converges with the Deva River at the village of Panes, to finally flow into the Cantabria Sea. The river crosses the Picos de Europa mountain range, creating big slopes and defiles. In general, the Cares River is an active and fast river that passes through a general slope of around 1600 meters. The river starts creating river beachs around the area of Valdeón, as a consequence of the increase of water volume thanks to the contribution of small tributary rivers. These small rivers collect the water and sediments from the southern Urrieles and Ándara massifs of Picos de Europa. Once the Cares River passes by Cordiñales de Valdeón, it runs between the steep banks of the mountains creating big defiles, with almost complete absence of river beaches. The river becomes more active as a consequence of the increase of water volume coming from small tributaries rivers, the karstic system and melting snow. Once the river passes by the village of Poncebos and the Duje river flows into the Cares, small river beaches are more frequent. From this point up until the area around the village of Panes, other tributary rivers flow into the Cares River, such as the Casaño, Ribeles or Jano rivers. River beach are more developed in this area, despite being conditioned by the changeable morphology of relief. In the area around Panes, the river travels slowly through this flatter region, enabling the creation of big pebbles beaches.

We analysed 13 river beaches in the Cares basin. The systemised information about them is gathered in the S.I.-IV. The survey points are the following:

- D_001/DC001: 30T 365411 4799273. At La Candiliega River
- D_002/DC002: 30T 369348 4797656
- D_006/DC011: 30T 366695 4798360
- D_014/DC033: 30T 349841 4797500: At the Casaño River
- D_015/DC034: 30T 350679 4797349: At the Casaño River
- D_016/DC035: 30T 355212 4795448
- D_023/DC067: 30T 345311 4784918
- D_025/DC072: 30T 344251 4780037
- D_027/DC081: 30T 350833 4797081: At the Casaño River
- D_031/DC097: 30T 351168 4793827
- D_032/DC099: 30T 351403 4791115
- D_033/DC102: 30T 362975 4797156
- D_034/DC104: 30T 363059 4798585: At the Besnes River

Grain size characterisation		Petrogenetic type															
		CC		CA		OO		SO		BQ		RQ		MQ		Total	
		Σ	%	Σ	%	Σ	%	Σ	%	Σ	%	Σ	%	Σ	%	Σ	%
Homogeneous and one mode distribution	Fine grain			1	8			1	33							2	4
	Medium grain	1	4	3	23											4	8
	Coarse grain																
Heterogeneous and two modes distribution	Fine grain							2	67	3	75					5	10
	Medium grain	13	52	4	31	4	57									21	40
	Coarse grain	10	40	1	8											11	21
Heterogeneous distribution	Fine grain	1	4	1	8					1	25					3	6
	Medium grain			3	23	3	43									6	12
	Coarse grain																
	Total	25	48	13	25	7	13	3	6	4	8					52	100

Table-6.50: Frequency table of the petrological characterisation of the pebbles from the river beach in the Cares basin based on binocular microscope observation. Columns are petrogenetic types. Rows are grain size characterisation, classified first by distribution and then by size.

As it happened in the case of the Deva basin, the data collected show great heterogeneity in the lithologies, morphologies, and sizes of the rocks found in beach deposits. In general, the most frequent lithology is limestone, followed by “archaeological quartzite” and, less importantly, lutites. We did not identify any fragments of conglomerates. Regarding “archaeological quartzites”, the CC type is predominant, CA and OO type are moderately frequent and there is a very small presence of SO and BQ types. The latter four types are more frequent in this basin than in the Deva Valley. There are clear geographic differences between the southern (only two survey point analysed) and the northern areas, as well as between the Cares River and the smaller tributary rivers. In the northern zone, “archaeological quartzites” are highly presented, mainly represented by the CC type, although the presence of the CA type, orthoquartzites and the BQ type is important too. Limestone replaces “archaeological quartzites” as the main lithology once the Cares River pass by the massive limestone strata of Picos de Europa. Survey point D_023 is a small fossil beach attached to a limestone wall a few meters above the Cares River, once the river has passed by the steep banks. The lithology of this point incipiently reflects the increase of limestone and the decrease of “archaeological quartzite”, also appreciated at survey point D_032, before the river runs between the steep banks formed by the Valdeteja and Picos de Europa limestones. The CC type is more frequent once the Cares River passes through the first Barrios strata, immediately before survey point D_031. There is an increase of the CC type and a moderate presence of CA and OO types. Once the river crosses these strata, other Barrios strata (massively present in this area) are also eroded by the Cares River and its tributaries. This process increases the proportion of “archaeological quartzites” in river beaches, although its percentages are always smaller than limestone, the main lithology. Regarding survey points D_001 and D_006 (survey points at small tributary rivers), the CC type from the Barrios strata, just eroded by the river system, predominates massively in their lithologies. The presence of CA and OO types is scarce, usually in percentages smaller than 5%. The presence of SO or BQ types is negligible in this final part of the river. Morphologies are varied, with more frequent presence of tabular pebbles than in Deva valley. However, there is also an important presence of spherical pebbles. As in the case of the river previously analysed, the main lithology of the river beach depends on the strata just cut by the river. Nevertheless, the presence of farther lithologies is always present in residual percentages, exhibiting eroded morphologies and smaller sizes. The association between lithology and morphology is similar to the one verified on the Deva valley.

We selected 52 “archaeological quartzites” to performance detailed analysis. The results mostly confirm the results obtained during field survey: predominance of the CC type, moderate presence of CA and OO types and an occasional presence of SO and BQ types. The characterisation of grain size indicates the predominance of heterogeneous distribution in CC, CA, and OO types. The presence of medium or coarse quartz grain sizes is prevalent in these types. Among SO and BQ types, grains are finer, despite quartz grain size distribution being diverse (Table-6.50). The mineral characterisation of the samples is similar to other contexts analysed, with high presence of iron oxides, non-identified black minerals and mica. The presence of manganese oxides is also high. Pyrite is

present associated to BQ samples and feldspar was identified in a CC sample (Table-6.51). The characterisation of colour shows patterns similar to those appreciated in the beaches of the Deva basin. In general, the cortical areas are clearer than those derived from conglomerates, resulting into a reduction of the presence of reddish surfaces. Regarding inner areas, the most frequent colour is black, followed by brown, white and grey (Table-6.52). The morphology of the samples selected is heterogeneous, but the most frequent category is the spherical pebbles, followed by flat and tabular pebbles. There is a small presence of tabular clasts too. The presence of the last three categories is the consequence of the faster movement of water, which generates multiples fractures in rocks. The analysis of the texture of cortical areas revealed the high presence of fine and grained textures as a consequence the rock erosion in the river. The presence of iron oxides is abundant on cortical areas and they are washed, as it happened in the Deva basin beaches. In the beaches represented by survey points D_001 or D_034 the presence of iron oxides on cortical areas is abundant. In general, the presence of cortical joints is more frequent on cortical zones than in inner areas. As in the Deva basin beaches, the presence of joints is less frequent than in other kind of contexts. This is a consequence of rock transport, which deletes many joints due to rock fragmentation. Some of the samples show bedding in small proportions. Schistosity was identified in one BQ sample (Table-6.53).

Non-quartz minerals	A		B		C		General	
	Σ	%	Σ	%	Σ	%	Σ	%
Absence			1	6	2	13	3	6
Fe-Oxides	12	75	4	25			16	33
Mn-Oxide								
Calcite								
Mica	3	19	7	44	2	13	12	25
Black mineral			2	13	9	56	11	23
Pyrite	1	6	2	13	3	19	6	13
Feldspar								
Total	16	100	16	100	16	100	48	100

Table-6.51: Frequency table of the non-quartz minerals identified in the pebbles from the river beach in the Cares basin based on binocular microscope observation. Columns are the three fields considered and rows are the non-quartz minerals identified.

Colour	Cortical area				On fresh cut			
	Primary		Secondary		Primary		Secondary	
	Σ	%	Σ	%	Σ	%	Σ	%
Absence			2	13			2	13
White	2	13	1	6	3	19	2	13
Grey	9	56	3	19	11	69	1	6
Black	3	19	5	31			7	44
Blue			1	6			2	13
Green								
Orange								
Brown	2	13	2	13	2	13	2	13
Yellow			1	6				
Red			1	6				
Total	16	100	16	100	16	100	16	100

Table-6.52: Frequency table of the colour hue of the samples from the pebbles from the river beach in the Cares basin. Columns are the primary and secondary colours of cortical areas and in fresh-cut hue. Rows are the colours considered.

We only selected one sample for thin section and compositional analyses from the river beaches of the Cares basin, sample DC02_05. This rock is an OO petrogenetic type, still with some clastic quartz grains, high presence of syntaxial overgrowths and concavo-convex quartz grain limits. The characterisation of grain size points at the predominance of fine sand and medium sand quartz grains organised around a relatively well-defined mode. The circularity and roundness indexes reveal the high presence of well-rounded and regular quartz grain morphologies. Clayey matrix is present in small amounts filling the small holes of the clast framework. Only chlorite is identified among non-quartz minerals (Figure-6.42). The X-Ray fluorescence concludes that this sample is mainly composed of silica, although it contains small percentages of Al_2O_3 too. This sample is similar to sample DC04_05 belonging to the Barrios formation and some other samples from secondary

formations, such as sample DC25_05 from the Potes Group conglomerate or sample DC03_03 from fluvial beaches in the Deva valley. Because of time and economic issues, we could not make more thin sections in order to confirm the results of non-destructive analyses. Figure-6.43 shows each non-represented type of quartzite (except for the CC type).

	Features	Σ	%
Morphology	Tabular clast	4	8
	Tabular pebble	13	25
	Flat pebble	14	27
	Spherical pebble	21	40
	Total	52	100
Cortical texture	Coarse and grained	1	2
	Fine and grained	39	75
	Fine	12	23
	Really fine		
	Total	52	100
Mineral inclussion on cortical area	Absence	1	2
	Fe-oxides	46	88
	Carbonated	2	4
	Siliceaus	3	6
	Total	52	100
Cortical joints	Not analysed		
	Absence	10	19
	Unidirectional	17	33
	Bidirectional	17	33
	Three-directional	8	15
	Total	52	100
Joints	Absence	17	33
	Unidirectional	13	25
	Bidirectional	13	25
	Three-directional	9	17
	Total	52	100
Bedding	Absence	44	85
	Unclear	4	8
	Clear	4	8
	Total	52	100
Schistosity	No	51	98
	Yes	1	2
	Total	52	100

Table-6.53: Frequency table of morphology, cortical texture, mineral inclusions on cortical areas, quantity of cortical joints, quantity of internal joints, bedding, and schistosity of the samples derived from the river beach in the Cares basin.

In general, the river beach deposits of the Cares basin are variable accumulations of raw material heterogeneously distributed along the river. The previous and immediate subsequent eroded strata determine the main lithologies of each river beach. However, there is always a smaller presence of other lithologies that crop out farther away from the river beach. The morphologies of the most frequent lithologies are tabular and they are conditioned by their arrangement in the original formation. Conversely, the morphologies of the distant and less frequent lithologies are rounded. The most frequent lithologies are limestone, “archaeological quartzites” and lutites. Focusing on “archaeological quartzite”, the most frequent type is the CC one, from the predominant one in the Barrios, Murcia, Pontón and Valdeón outcrop formations. The latter three formations are well represented in the Valdeón area, while the first one is restricted to the norther area. The Barrios Formation can also be responsible of the introduction of small percentages of CA and OO types in the river system. The conglomerates from the Valdeón area, which contain the CA, OO, SO and BQ types, can also be the sources of these varieties in the Cares basin. The quantity of the CA and OO petrogenetic types in river beachs is moderate in the Valdeón area and the presence of SO and BQ types is residual. The quantity of these types gradually decreases once the river system starts eroding other strata, such as Valdeteja and Picos de Europa limestones. The absence of conglomerates in the Cares river beaches is a consequence of the composition of the cement of these conglomerates, which liberates the pebbles easily.

The catchment strategies at the Cares river beach deposits would have differed between southern and northern areas. To the north, during catchment selective mechanisms must have been applied for obtaining CC types. Stronger selective mechanism would have been necessary for getting CA or OO types. Thanks to its wide presence, intensive exploitation of the former type would have been possible. On the contrary, exhaustive exploitation of the latter two types would have not been possible, due to their scarce presence. However, moderate exploitation on these types would have certainly been possible. Finally, the exploitation of SO or BQ types in this area would have been negligible, but still more important than in the Deva basin. We do not discard its planned exploitation, but it would have been clearly residual. In the southern zones the potential catchment strategies would have been different because of the higher presence of “archaeological quartzites”. The extensive presence of outcrops of the CC type would have allowed its intense exploitation in river beaches without important the need of any selective mechanisms. Still, the exploitation of CA and OO types would have required moderated selective mechanisms. Finally, the exhaustive exploitation of SO and BQ types would have been possible by applying important selective mechanisms.

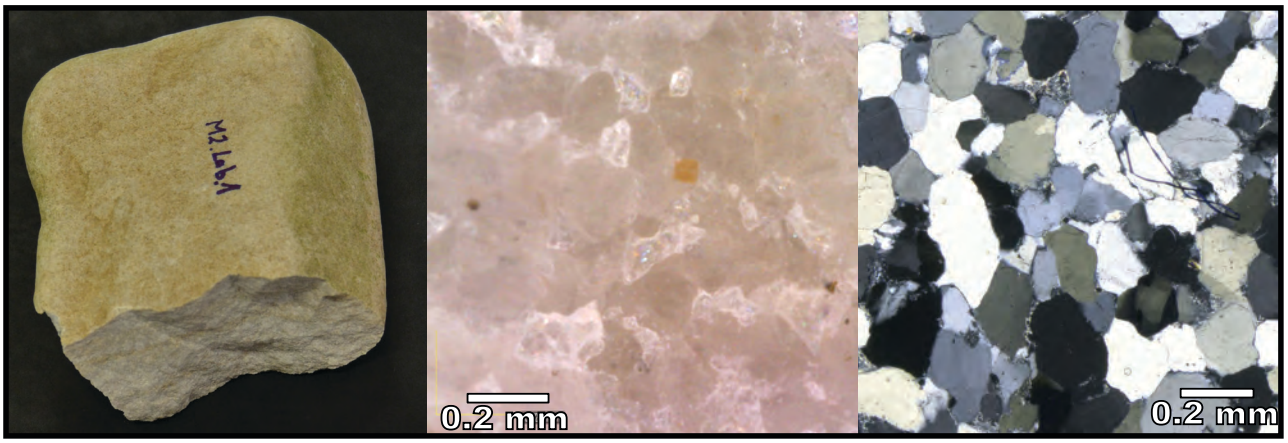

Figure-6.42: Picture at different magnifications of the sample DC02_05 from the Cares river beach. Clayey matrix is present and quartz grain size is big.

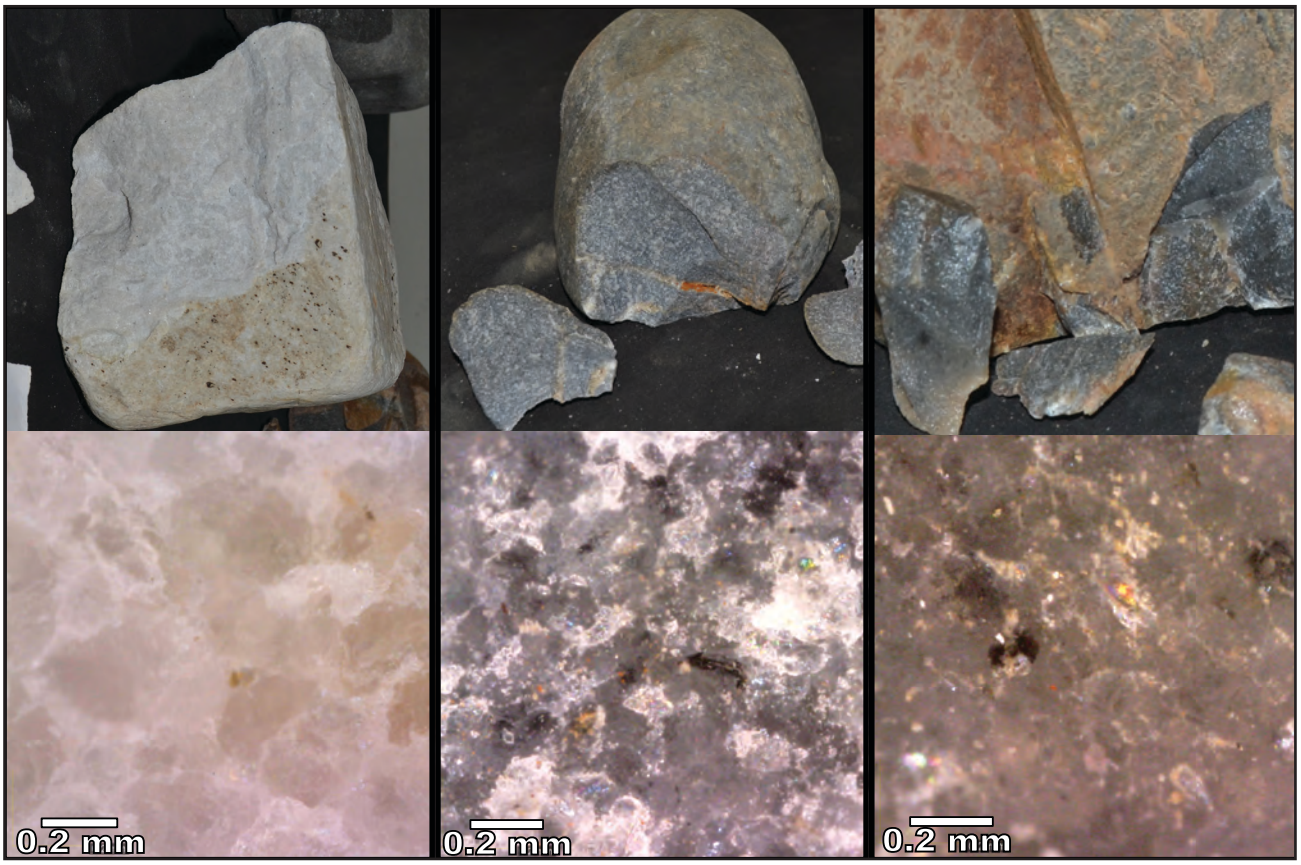

Figure-6.43: Picture at different magnifications of three samples from the Cares river basin. The first sample is the DC35_05, a CA type. The second is the DC72_08, a SO type. The last one is the DC75_05, clearly a BQ type.

To finish, we present the river beach deposits that were not within the two basins analysed above. One of them is at the junction between the Deva and the Cares Rivers and the other two are in the Güeña river basin. The first one is the survey poiny D_05 (see detailed information in S.I.-IV). This point is located immediately after the union of the Cares and Deva rivers. Its lithology is mainly composed of limestone, but other raw materials such as lutites and “archaeological quartzites” are present too. The prevalent petrogenetic types among “archaeological quartzites” are CC and CA, with clear similitudes to the Barrios CC and CA types. The most frequent morphology is spherical pebbles. Flatten pebbles, directly related to the CA type of “archaeological quartzite” and lutites, are present too and they are as a consequence of their arrangement in the original strata. The last two points are the survey point D_17 and a non-systematic point near the village of Corao (Asturias). Both points are within the Güeña River basin. The former, located at the headwater of the river, reflects the surrounding lithology, with predominance of tabular morphologies due to the scarce impact of fluvial erosion on the rocks. The main lithologies are limestone and “archaeological quartzite”.

The types and size varieties of the latter point are mainly related to the white Barrios outcrop, with predominance of the CC types, a smaller presence of the CA type, a negligible percentage of the OO type and medium grain size varieties. This point presents similar lithologies but different morphologies, mainly composed of spherical pebbles.

6.4. THE ROCK CYCLE AND ITS CONSEQUENCES ON HUMAN LIFE: POTENTIAL RAW MATERIAL CATCHMENT STRATEGIES IN THE DEVA, CARES AND GÜEÑA BASINS

All the information presented above reveals the variety of contexts where "archaeological quartzite" appears. Each context shows different features (the matter) that are determined by formative, erosive and transport processes (the forces). The analysis of the former allows us to understand the process: the rock cycle. Both together, matter and forces, are the basis to propose different raw material catchment strategies.

The outcrop formations analysed reflect, through the size and morphological features of grains, the dynamics of erosion and sedimentation of former quartz grains. The Barrios Formation is the result of a cross-plain delta sedimentation processes, observable in the moderately sorted ad well rounded sediment. Meanwhile, the Murcia Formation is the consequence of a marine and turbidity sedimentary process, evidenced by heterogeneous size and morphology of quartz grains and major presence of matrix in the samples. Similar heterogeneous distribution of quartz grains is observable in the four Carboniferous outcrop formations. These reflect the heterogeneous sedimentary conditions experienced during the second half of the Carboniferous. The scarcity of deformed or metamorphic petrogenetic types (only found in small amounts and geographically localised) in these formation is an evidence of the low degree of metamorphism which underwent this area of research (Bastida, 1982).

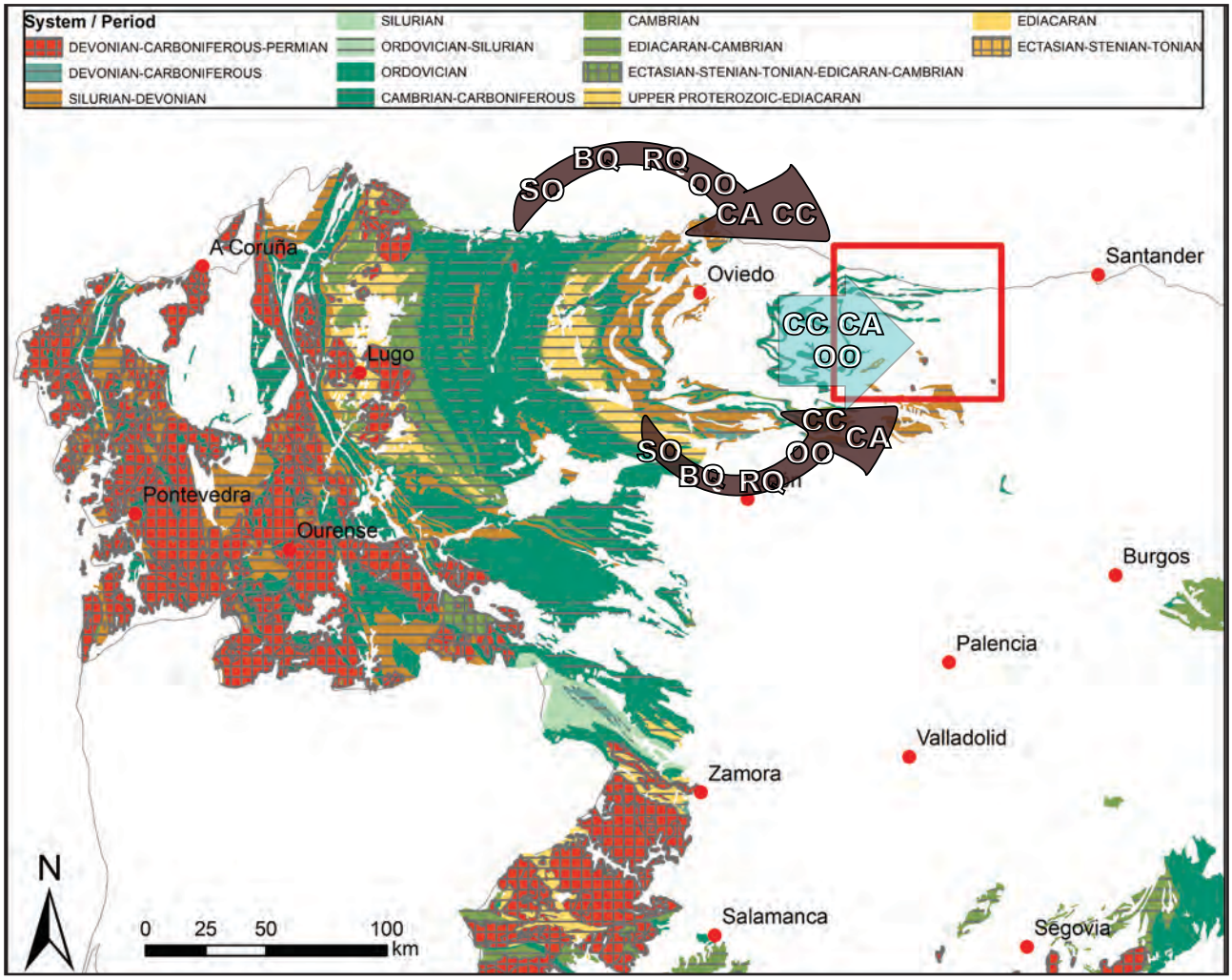

Figure-6.44: Schematic representation of the transport of petrogenetic types from Precambrian, Cambrian, Ordovician, Silurian, and Devonian outcrop during the Upper Carboniferous (Pennsylvanian).

The conglomerate formations analysed show greater complexity, determined by successive sedimentary, transport and sometimes deformation processes. Starting with the last sedimentary process, the formations where conglomerates got inserted are alternation of sandstone, shale and conglomerate. These heterogeneous successions reflect the variable sedimentary basin conditions experienced in this area of research during the Carboniferous, caused by the Variscan Orogen. The heterogeneity of the clasts (based on morphology and size) and cement (of the conglomerates) too point at the heterogeneity of the sedimentary conditions that created the conglomerates. Finally, the lithological characterisation of the clasts indicates the concurrence of multiple rock source areas. Some of them come from near strata, such as limestone, shale and CC, CA or OO types (generally from Barrios, Murcia or older Carboniferous formations), while others originate in more distant strata, as revealed by the presence of other petrogenetic types, such as SO, BQ or RQ. The latter three are related to the western Precambrian, Silurian, or Devonian formations in the Cantabrian and the western Astur-Leonesa zones in the Iberian Massif (Figure-6.44). Some conglomerate strata, such as Lechada, Pontón, Maraña-Brañas, Valdeón or Remoña formations, do also contain orthoquartzites and quartzites from distant source areas. Conversely, in other conglomerate formations, for example the Curavacas, Porrera, Bárcena, Cubo, Pesaguero, Viorna, Campollo or Narova conglomerates, only the nearest lithologies and types are present. The variable conditions of the Carboniferous in this area caused by the Variscan Orogeny, that creates a changeable geography too and the connection and enclosure of multiple basins. The general heterogeneity of petrogenetic types too indicates the scarce impact of deformation processes on the clasts composing conglomerates, despite the presence of joints in some conglomerates.

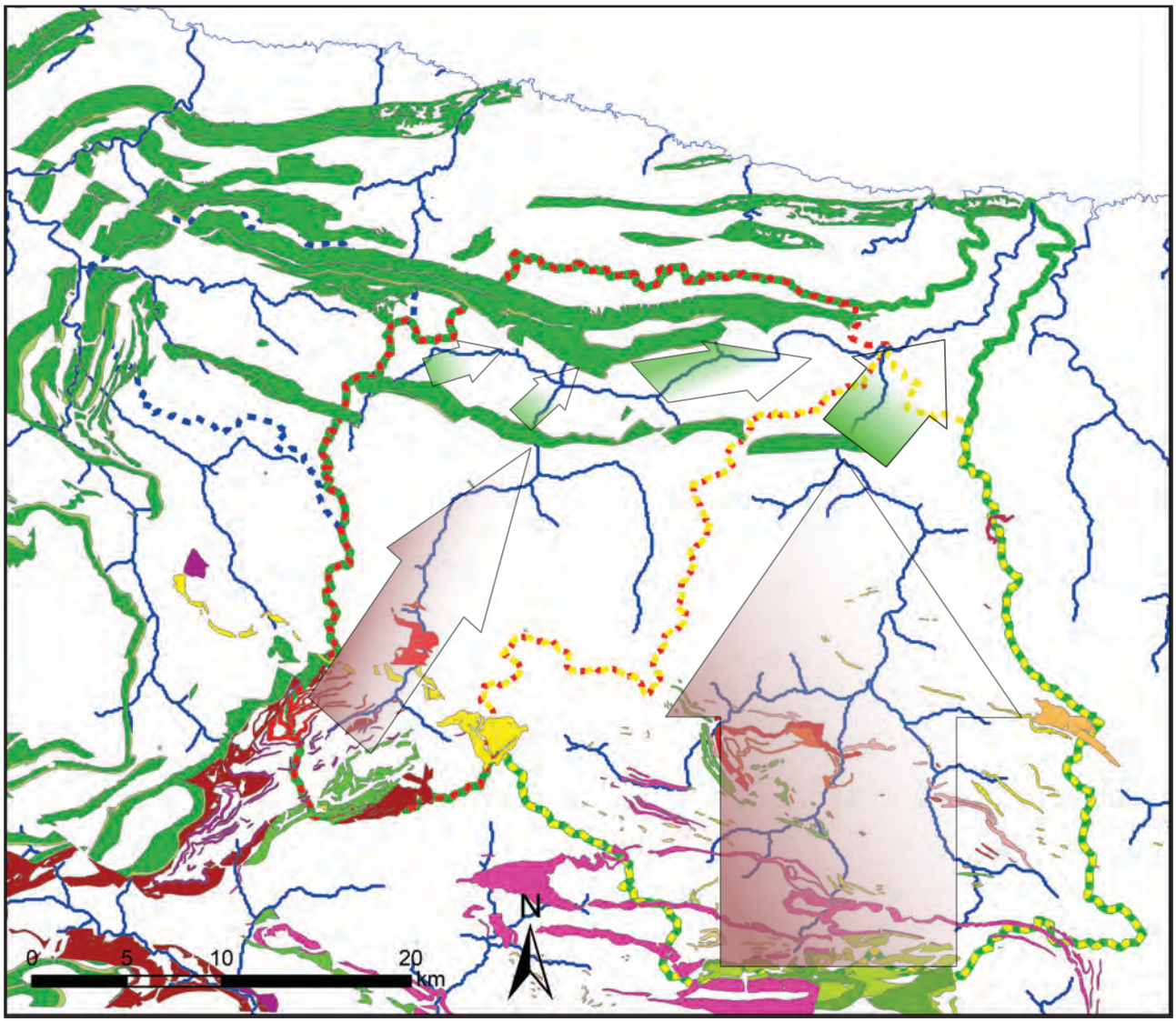

Figure-6.45: Schematic representation of transport of rock derived from “archaeological quartzite” massive outcrops (green polygons) and from conglomerates (red polygons) during the Quaternary.

Finally, the analyses performed on secondary deposits containing “archaeological quartzites” show active processes of weathering, erosion, transport and deposition. The weathering processes affecting siliciclastic massive outcrop formations, affect mainly the joint system. In cases where there is a siliceous filling material, the weathering processes affect all the surface evenly. The first situation creates tabular and angular rock fragments in the immediate surroundings of the outcrops. In conglomerate outcrop formations, the weathering processes affect mainly cement. In this way pebbles are easily freed forming the rock framework. Additionally, and affecting for both types of outcrops, tectonic movements can break big parts of the outcrops. Finally, fluvial and eolian forces do also eroded pre-existing elements, creating rounded morphologies. Gravitational, fluvial and probably glacial processes transport and deposit the rocks fragments, spreading them along the basins. Flank deposits and offsets are the results of gravitational and glacial transport, while river beach deposits are the outcome of fluvial transport. The lithologies of each strata analysed decrease gradually as a consequence of their geographic dispersion. Therefore, the quantity of material in the field is greater near the outcrop formation (Figure-6.45). In addition, the size of each rock fragment decreases as a consequence of erosion during the transport. Morphology varies too, from morphologies similar to those of the original outcrop arrangement to spherical ones.

The potential “archaeological quartzite” catchment strategies in these contexts were varied and they would have been determined mainly by the presence or absence of the petrogenetic types and their features, morphologies and abundance. Figure-6.46 shows a general picture of the most interesting types of “archaeological quartzite”.

In the massive outcrops of “archaeological quartzites”, the direct and intensive exploitation of visible strata would have been easy. The direct extraction of the rock fragments resulting from weathering of the joint system simply using the hands would have been the simplest option. The extraction of rock fragments using hammers or other proto-mining tools taking advantage of the same joint system would have eased collection too. A final alternative to get important quantities of “archaeological quartzite” would have been the gathering of rock fragments around the strata on areas not covered by soil. The resulting morphologies of the flanks or cores resulting from these catchment strategies would have been tabular and relatively angular. Regarding the lithologies potentially exploited, it would have been possible to perform an intensive exploitation of the CC type on all formations (present in almost all the area of research). Conversely, the exploitation of CA or OO types would have been restricted to the Barrios Formation. Its exploitation would have been geographically limited to specific outcrop areas and it would have required selective processes. The selection of specific petrogenetic types, prioritizing homogeneous and certain grain size varieties, could have been done by selectively knapping the rock fragments. There would also have been a selection of non-joined or non-weathered areas.

Therefore, the catchment strategies of massive outcrop strata would have been determined by 1) the geographic dispersion of interesting strata, 2) the characteristics of the joint system, 3) the presence of interesting lithologies and 4) weathering processes affecting the outcrop. Then, human adaptive mechanisms may have included 1) knowledge about the environment and human mobility, 2) extraction/mining strategies, 3) selective mechanism of massive outcrop, and 4) selective knapping.

In the mixed strata of Carboniferous conglomerates where “archaeological quartzites” are present, the direct and intensive exploitation would have been done using selective mechanisms. The direct extraction of the pebbles inserted in the conglomerate would have depended on the composition of cement. In the cases where cement is argillaceous, sandy or carbonated, extraction could have been carried out by direct hand collection. Instead, in the cases where cement is siliceous or composed of other type of compact material, the extraction must necessarily have been made using hammers or other proto-mining tools. In some cases, cement does not allow the extraction of pebbles. Direct collection of detached fragments would have also been possible in the areas surrounding the conglomerate crops out. In these cases, the resulting morphology of the cores or blanks would have been generally spherical. The exploitation of raw material from conglomerate strata would have been easier in the southern part of our area of research thanks to the greater presence of these materials here. In most of the conglomerates, the intense exploitation of the quartz-arenite group would have been possible without the need of important selective mechanisms (harder for the CA type). The exhaustive exploitation of OO type would have been geographically restricted and, it would have required selective mechanism. The exploitation of SO, BQ and RQ types would have been reduced to some small conglomerate outcrops concentrated in the Valdeón area. The intensive exploitation of these types would have been restricted to the latter area and the small Remoña conglomerate in the

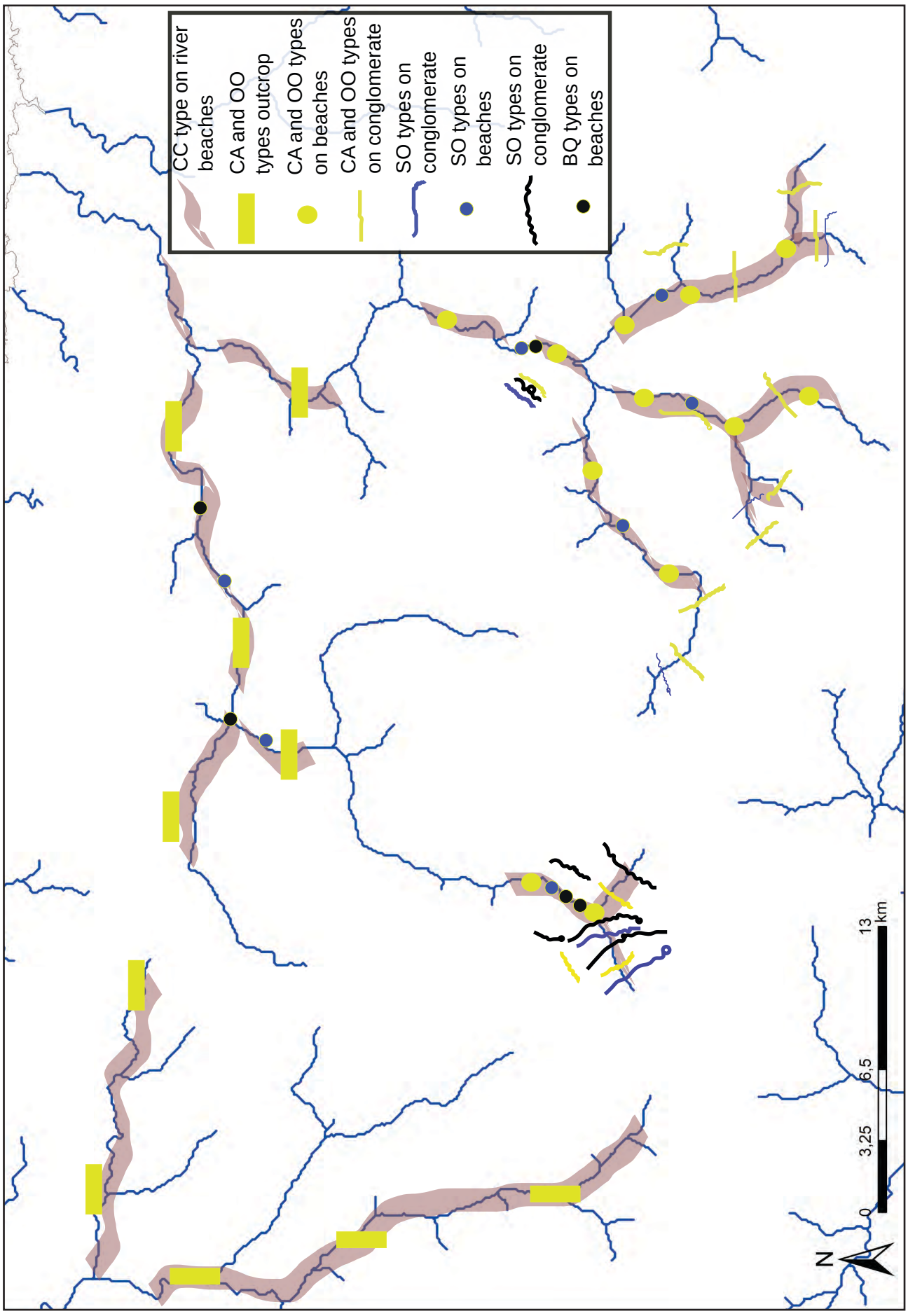

Figure-6.46: Schematic representation of the petrogenetic types of quartzites in the area of study.

Liébana area. Its exploitation would have required strong selective mechanism. In other conglomerates, its exploitation would have been restricted to occasional findings. The selection of these types and their grain size varieties would have required cobble testing. Selective mechanism would have been necessary for the obtention of non-weathered or joined pebbles.

Considering all the above, the catchment strategies in conglomerate formations would have been determined by 1) the geographical dispersion of interesting types and varieties, 2) the properties of cement conditioning rock extraction, 3) the proportion of interesting lithologies, and 4) the weathering process affecting the pebbles. Then, human adaptive mechanism may have included 1) knowledge about the environment and human mobility, 2) extraction/mining strategies, 3) selective mechanisms and 4) selective knapping.

In the quaternary deposits from the area of research where “archaeological quartzites” are present intensive exploitation would have not been possible due to the scarcity of this lithology. The direct gathering of interesting pebbles would have been easy, but strong selection mechanisms would have been necessary. In the river beach deposits, there are big amounts of pebbles, while in flank deposits its quantity is limited. The morphology of the cores or blanks resulting from collection here would have ranged from tabular clasts to spherical pebbles. The more deformed types of “archaeological quartzites” would have been directly associated to the latter morphology. The exploitation of raw material in these contexts would have been geographically restricted to the plain zones. Meanwhile on the defiles and steep areas the formation of deposits is limited. The intense exploitation of the CC type would have possible in this kind of deposit, while the exploitation of CA and OO types would have been limited due to their scarcity. Important selective mechanism must have been applied for the acquisition of the latter two types. The gathering of SO, BQ and RQ types is possible, but it would have been more related to occasional findings as a consequence of the exploitation of river areas than to planned catchment strategies. In the Valdeón area the exploitation of latter five types could have been planned, thanks to the greater presence of these materials in this area. However, as in all deposits, selective mechanisms would have been necessary.

Therefore, the catchment strategies in quaternary deposits would have been determined by 1) the type of transport, 2) relief, 3) the geographical dispersion of interesting types, and 4) the proportion of interesting lithologies. Then, potential human adaptive mechanisms may have included 1) mobility along zones with deposits (mainly river beaches) or river environment exploitation, 2) knowledge about the environment and human mobility and 3) selective mechanism.

CHAPTER-7

RESULTS. THE ARCHAEOLOGICAL SITE OF EL HABARIO

7.1. GENERAL ISSUES AND STATE OF PRESERVATION OF THE COLLECTION

The archaeological site of El Habario is an open-air site situated in the western part of the Cantabria Autonomous Community, within the municipality of Cillórigo de Liébana, between the villages of Pendes and Cabañes. The open-air site of El Habario is situated in a small Colluvium of unconsolidated sediments on the top of the Remoña Formation. The area where El Habario is situated is a small basin almost on the top and relatively flat surface between two small hill tops. The area was prospected in various campaigns: the first one by members of the C.A.E.A.P in the beginning of the 1990s (Castanedo et al., 1993), and later by Elena Carrión and Javier Baena (Carrión and Baena, 1999; Carrión et al., 1995). The first one was carried out by systematic surface material collection and later excavation of a secondary stratigraphy. The second one applied the same methodology, followed by four exploratory excavation pits in high findings concentration surfaces that led to the next excavation in the area around the pit where more and better preserved archaeological remains were found. The total excavated surface was around 14 square meters, where two archaeological layers were found after the three first layers clearly affected by vegetation. The first four layers had archaeological material clearly affected by erosion, and they were not assigned to any primary deposit. The last layer was composed by silty and yellow sediments formed as a consequence of weathering processes on shale bedrock. The total of pieces recovered from this archaeological layer was 517. No faunal remain was preserved.

The chronological attribution is hampered by lack of material susceptible of being dated. However, the last layer was assimilated to the Middle Palaeolithic, mainly based on typological and technological studies. The latter technological research, made by Elena Carrión and Javier Baena, points that dominant lithic reduction model was based on hierarchical centripetal reduction processes focused on flake production. Raw material characterisation of the assemblage points at a major presence of quartzite (“archaeological quartzite”), although other raw material were also characterised, such as flint or radioralite. All these reasons, also the proximity to the Remoña Conglomerates, make assimilate this site as a workshop of quartzite, probably related with a complex the El Arteu and El Esquilleu (Carrión and Baena, 2005).

The archaeological assemblage analysed here is the complete collection recovered in the excavation of the site described as El Habario-B. We analysed 473 lithics, although due to data acquisition mistakes, the results here exposed belong to 470. All of them are preserved in the MUPAC. The general state of preservation is medium. Most of the rocks are altered by weathering processes which modify the colour of them, especially in cases of lighter varieties. The colour of many pieces turn into red, orange or brown, the same colour from the soil. It is also noticeable that some lithics have slightly eroded edges and arrises. In addition, some lithics present evidences of chemical weathering processes altering specific areas such as cortical surfaces, non-deformed/metamorphic surfaces or jointed areas. Finally, the high alteration in some lithics have yielded a sandy touch apparent and their surfaces have become into sandy texture.

3.2. PETROLOGICAL STRUCTURE

Here we present the results of raw material characterisation. We were able to determine the main lithology of every piece. In general, the collection is mainly formed by “archaeological quartzites” with residual representation of radioralite and flint (Table-7.1).

Main Raw Material	Archaeological quartzite	Flint	Limestone	Limonite	Lutite	Quartz	Radioralite	Volcanic rock	Undeterminate
Σ	467	1	0	0	0	0	2	0	0
%	99,4	0,2	0	0	0	0	0,4	0	0

Table-7.1: Frequency table of lithologies identified in the archaeological site of El Habario.

Focussing on “archaeological quartzite”, we could identify the seven petrogenetic types proposed through binocular microscopy. Quartzite is the best represented group thanks to the high quantity of the BQ petrogenetic type, which represent more than 50% of the assemblage. Orthoquartzite is the second most represented group of “archaeological quartzite”, and both petrogenetic types (OO and SO types) are well represented. Finally, the group of quartzarenite is underrepresented, with less than 1% of the lithics (Table-7.2). We were unable to identify seven items, 2% of the collection. Coming to the distribution of grain size, the most frequent category is heterogeneous distribution with 47% of the cases, even though homogeneous distribution is also well represented, in 37% of them. Regarding grain size, the most frequent category is fine grain size, although medium size is also well represented. Coarse grain size variety is represented in small frequency. As to “archaeological quartzite” types and size varieties, we identify nine preferential varieties associated to OO, SO, and BQ types and fine and medium grain sizes.

			Petrogenetic type																	
			CC		CA		OO		SO		BQ		RQ		MQ		Unknow		Total	
			Σ	%	Σ	%	Σ	%	Σ	%	Σ	%	Σ	%	Σ	%	Σ	%	Σ	%
Grain size characterisation	Homogeneous and one mode distribution	Fine grain					12	11	19	24	**67**	**28**	4	21	1	25			103	22
		Medium grain					19	17	3	4	43	18	4	21					69	15
		Coarse grain																	0	0
	Heterogeneous and two modes distribution	Fine grain					11	10	7	9	12	5							30	6
		Medium grain			1	25	11	10	4	5	13	5	2	11					31	7
		Coarse grain					1	1			1								2	0
	Heterogeneous distribution	Fine grain					25	23	30	38	41	17	5	26	3	75	3	30	107	23
		Medium grain	1	100	2	50	30	27	15	19	**60**	**25**	4	21					112	24
		Coarse grain			1	25	2	2	2	3	1	0							6	1
	Unknown																7	70	7	1
	Total		1	0	4	1	111	24	80	17	238	51	19	4	4	1	10	2	467	100

Table-7.2: Frequency table of petrological features identified in El Habario based on binocular characterisation. Columns are petrogenetic types and rows contain the characteristics of grains according to size, classified first by distribution and second by size itself. Cells in black are the categories representing more than 10% of the total cases. Cells in dark grey are the categories representing between 5 and 10% of cases. Finally, cells in light grey are the categories representing between 1 and 5% of cases.

Non-quartz mineral	A		B		C		General	
	Σ	%	Σ	%	Σ	%	Σ	%
Absence	8	2	9	2	44	10	61	4
Fe-Oxide	196	43	70	15	94	21	360	26
Manganese Oxide	15	3	29	6	35	8	79	6
Mica	99	22	185	40	124	27	408	30
Black mineral	128	28	145	32	131	29	404	29
Pyrite	11	2	17	4	28	6	56	4
Feldspar	0	0	2	0	1	0	3	0
Total	457	100	457	100	457	100	1371	100

Table-7.3: Frequency table of non-quartz minerals identified in El Habario based on binocular characterisation. Columns are the three fields examined and rows are the non-quartz minerals identified.

We identified non-quartz minerals in 457 samples of “archaeological quartzite”, after having excluded the lithics assigned to unknown type (Table-7.3). Non-quartz mineral characterisation reveals the major presence of iron oxides, non-identified black and heavy minerals, and mica. Manganese oxides and pyrite are less represented, only in 5% of “archaeological quartzites”. Feldspar are lim-

Colour	On fresh cut			
	Primary		Secondary	
	Σ	%	Σ	%
Absence	5	1	74	16
White			7	2
Grey	82	18	105	23
Black	40	9	39	9
Blue			6	1
Green			16	4
Orange	86	19	96	21
Brown	236	52	68	15
Yellow	3	1	6	1
Red	5	1	40	9
Total	457	100	457	100

Table-7.4: Frequency table of colour hue of the samples from El Habario. Columns are primary and secondary colour hues and rows are the colours considered.

ited to three samples. All main minerals are associated to any petrogenetic type. The only exception is pyrite, which are mainly associated with BQ type. Moreover, the scarce feldspars are associated to CA petrogenetic type. Characterisation of colour indicates that most frequent colours are brown, grey, orange, and black (Table-7.4). The few white coloured "archaeological quartzites" and the brown ones are associated to OO type. Grey, blue and green colour varieties are associated to SO orthoquartzite. Finally, black and orange colours are mainly associated to BQ type. In spite of everything, there is a high variability of colour as a consequence of weathering processes in the clayey soil.

We carried out petrographic and geochemical characterisation of five lithic items, with the aim of recognising better represented petrogenetic types (Figure-7.1). The description of these samples helps us understand the differences between types, as well as define and establish one interesting variety. Still, we analysed the other three petrogenetic types using non-destructive characterisation[1].

7.2.1.THE OO PETROGENETIC TYPE AT EL HABARIO

One of the samples analysed is an OO orthoquartzite: HA-5855. It shows clastic grained texture and complete packing. It is characterised by syntaxial overgrown and concavo-convex grain boundary. Undulatory extinction is clear in the sample. Grain size characterisation points at the major presence of very fine and fine sand U-W categories on a relatively single mode. Nevertheless, there are other grains with small sizes. The grains are relatively rounded and circular with indexes around 0.60. Directional analysis shows that the grains of the sample are preferentially oriented at α = 0.05, not at α = 0.01. The features observed through binocular microscopy are in concordance with this characterisation: compact and grainy T&P and concave-convex limits even though regrowths are not easy to observe. Grain size characterisation of this sample points at medium grains with heterogeneous distribution. Under binocular microscope there is no preferential orientation of the grains.

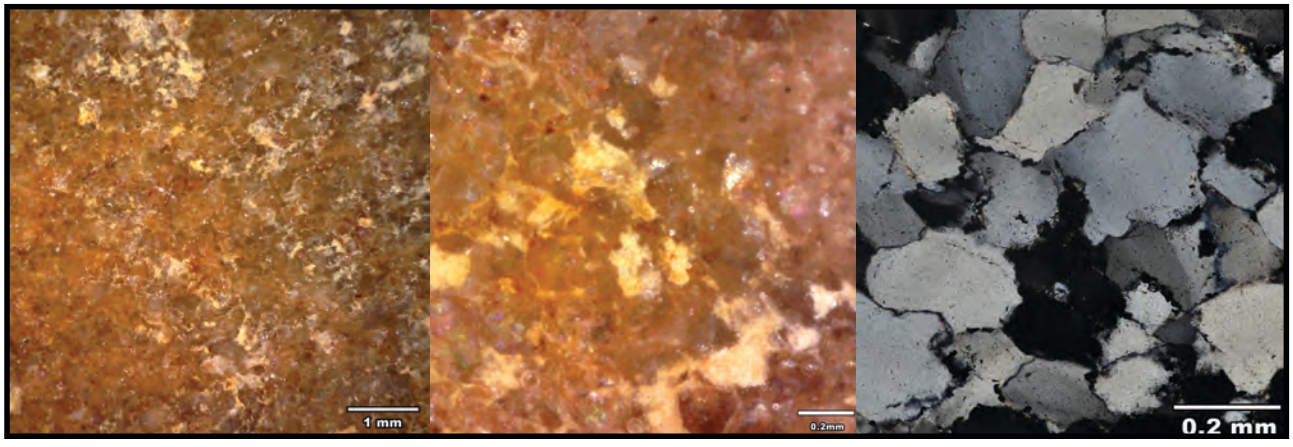

Figure-7.2: Pictures of the OO type sample from the archaeological site of El Habario: HA-5855. From left to right, microscopy binocular picture at 50x, microscopy binocular picture at 250x, and thin section microscopy picture.

The characterisation of matrix and cement in thin section reveals the presence of small quantities of clayey matrix, especially near the original lithic surface. There are also non-quartz minerals such as iron oxide and pyrite, again more abundant near cortex surfaces. Chlorites appears in inner areas of the thin section (Figure-7.2). The mineral non-destructive characterisation of the sample points at the presence of iron oxides, mica, and black and heavy non-identified minerals. The first, is repre-

1 The CC type is not analysed here because the only presence of one item.

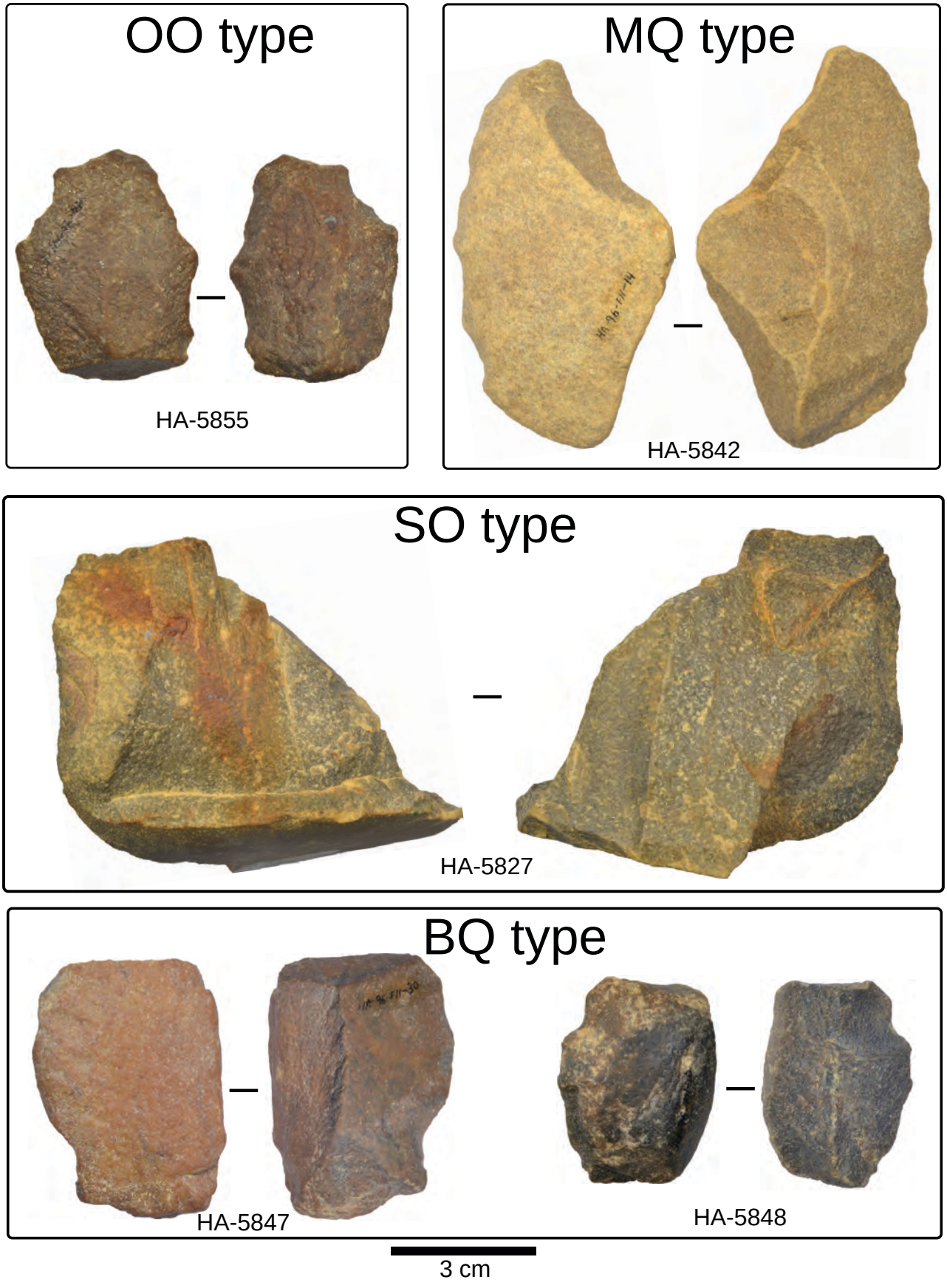

Figure-7.1: Pictures of the samples selected from the archaeological site of El Habario. Samples are grouped by petrogenetic type.

sented on all surface of the sample and it gives to the lithic surface its reddish colour. The result from the X-Ray fluorescence is consistent with the mineralogical characterisation. SiO_2 is highly represented in the sample with 95.8%. Nevertheless, there are other components such as SO_3, Fe_2O_3,

and Al2O3. The first explain the high presence of pyrite.

After having analysed the features of the OO petrogenetic type with the sample HA-5855, we can extrapolate these results to those of non-destructive techniques. This sample confirms and allows understanding the existence of OO type and the modification of some features and the colour. The first is especially relevant because it hinders the observation of regrowth structures on quartz grains. The heterogeneous distribution around medium grain size represents one of the grain sizes varieties observed in this lithic assemblage. There are another two clear varieties only described through binocular: the first one also has medium grains of quartz but has homogeneous distribution. The second one is characterised with fine grains and heterogeneous distribution. All these three varieties are well represented. Other grain-size varieties are also recognised in small frequency and they can be caused by, either methodological mistakes or specific varieties, less represented. Colour and mineral characterisation reveals most OO types are brown or orange coloured caused by the effect of rich in iron oxides soil in the white lithic surfaces and also by alteration of pyrite crystals. The mineral characterisation of this orthoquartzite is also homogeneous, and most of them have iron oxides, mica, and black and heavy non-identified minerals. Therefore, there are no different varieties detected using mineral/colour characterisation.

7.2.2. THE SO PETROGENETIC TYPE AT EL HABARIO

The sample HA-5827 belongs to the SO petrogenetic type. Under microscope, this the section shows clastic grained texture, suturated packing, major presence of undulatory quartz extinction, and suturated/microstylolitic quartz grain limits. There are also some recrystallised grains in small frequency. Under binoculars, the sample is described as grainy and fine T&P with suturated packing created by ruffle and irregular quartz grain limits (in case they are recognisable). Micro-cracks are frequent and the luster is high. In general, grain size characterisation of the thin section reveals the major presence of coarse silt and very fine sand, also smaller quartz grains (matrix and some recrystallised grains). The morphology of quartz grains points at the existence of two modes: the first one is the main grain framework and has irregular morphologies of grains. It is formed by the former grains and the matrix. The second grain framework is formed by more regular grains created as a consequence of recrystallization dynamics (Figure-7.3). Grains are not preferentially oriented. The characterisation of grain size using non-destructive techniques is consistent with petrography one. Quartz grains are fine in size and they display creating a heterogeneous distribution. Foliation fabric is not recognised in the lithic surface.

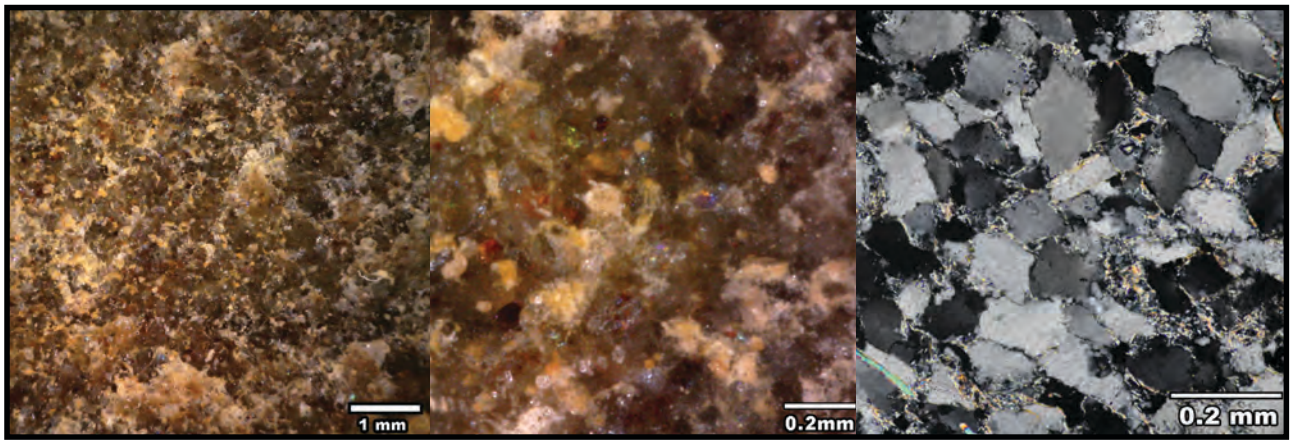

Figure-7.3: Pictures of the SO type sample from the archaeological site of El Habario: HA-5827. From left to right, microscopy binocular picture at 50x, microscopy binocular picture at 250x, and thin section microscopy picture at different magnifications.

Coming to non-quartz mineral characterisation, siliceous matrix appears in negligible percentages in the sample. The mineral identification reveals multiple non-quartz minerals: zircon, tourmaline, rutile, mica, clays, and pyrite. Compositional characterisation is in concordance with the high variability of non-quartz minerals. The quantity of SiO2 is reduced to 93% and there are many other components represented, especially Al_2O_3, Fe_2O_3, K2O, and TiO_2. The non-destructive mineral characterisation points at the presence of iron oxides, mica and non-identified blank and heavy minerals. The colour of the sample is grey to blue coloured. The latter colour is probably related with the high presence of Al_2O_3.

The data obtained through destructive characterisation allow us to extrapolate these results to the complete lithic assemblage, only analysed by non-destructive techniques. Most of the SO orthoquartzites are characterised with fine or fine to medium grained varieties. Different varieties based on grain distribution are difficult to propose due to the limitation of binocular scope in this type, which is also hampered by weathering processes. We do not observe clear differences in colour and most of the SO petrogenetic type are grey, sometimes modified by blue or green coloration as a consequence of weathering processes in lithic surfaces. There are also some reddish or yellow lithics surfaces.

7.2.3. THE BQ PETROGENETIC TYPE IN EL HABARIO

Two of the samples selected belong to the BQ quartzites: HA-5847 and HA-5848 (Figure-7.4). Under thin section, they are characterised by mortar texture and suturated packing, also by the major presence of microstylolitic limits of quartz grains and a moderate presence of recrystallised quartz grains and Böhm lamellae. The analysis of the size and morphology of the grains of both samples reveals two different modes: the first, formed by the main grain framework, is between coarse silt and fine sand. The second one is mainly created by new recrystallised quartz grains between very fine silt and medium silt categories. The first mode is more deformed than the second, as pointed by roundness and circularity indexes. There are differences in size in this mode between both samples. While on HA-5847 most grains are around very fine and fine sand, on HA-5848, these grains are around coarse silt and very fine sand categories. Moreover, grains are more heterogeneous in the second sample. Preferential orientation of quartz grains is also observable on both samples at σ = 0.05 and σ = 0.01. Non-destructive characterisation is in concordance with the features observed: fine texture and suturated packing (i.e. fine T&P). Nevertheless, it is easier to distinguish borders of quartz grains than BQ samples from other contexts, maybe due to the effect of soil. The luster is relatively high and micro cracks are abundant. The size characterisation of grains in the HA-5847 points at bigger and more homogeneous distribution than in the HA-5848, fine and heterogeneous. Foliation fabric is clear in both samples under binocular microscope. The weathering processes in these two samples are weaker than those observed in previous two samples.

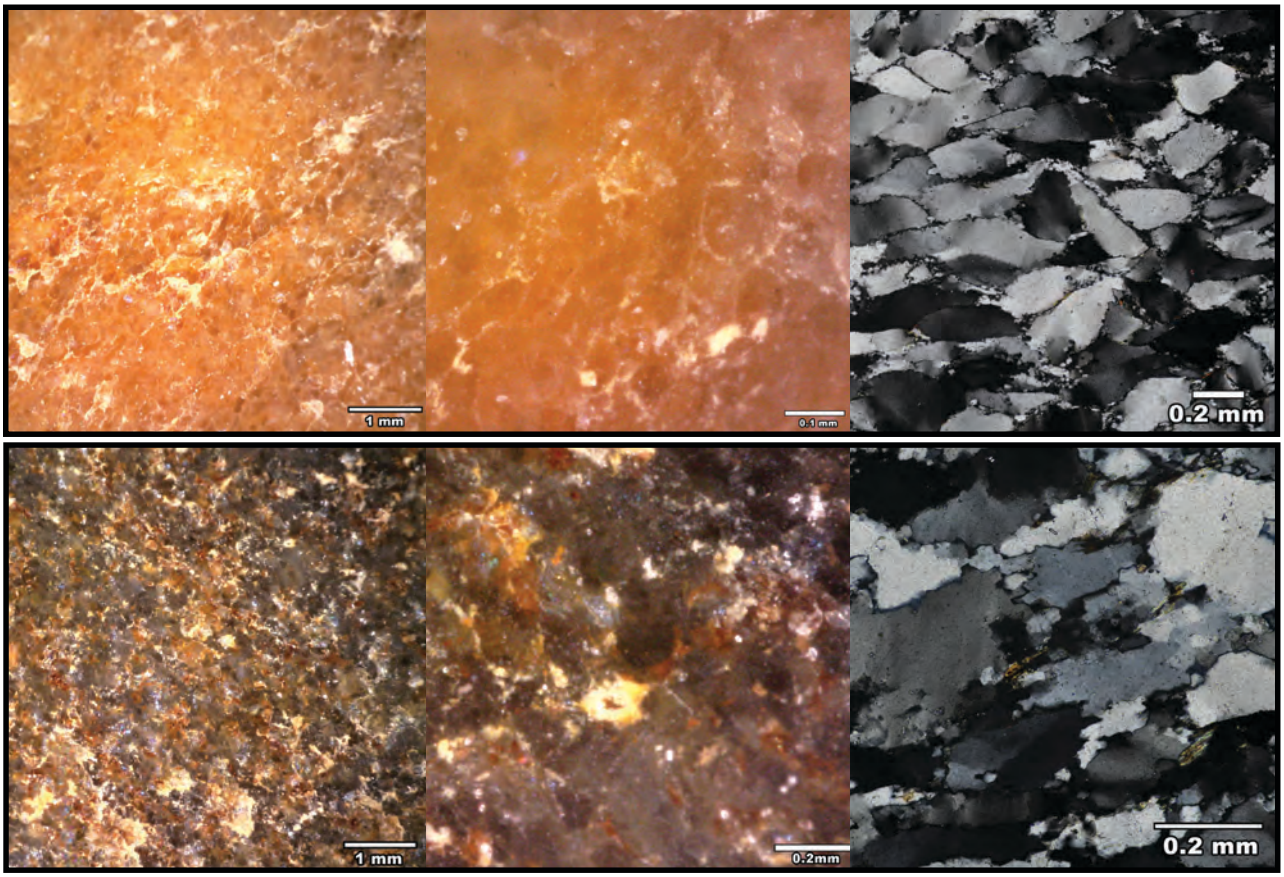

Figure-7.4: Pictures of the BQ type samples from the archaeological site of El Habario. From top to bottom, samples HA-5847 and HA-5848. From left to right, microscopy binocular picture at 50x, microscopy binocular picture at 250x, and thin section microscopy picture at different magnifications.

Coming to mineral characterisation, none of these samples have matrix, neither cement. Mineral identification reveals clear differences between both samples. The HA-5847 has zircon, mica, chlorite, and iron oxide, while HA-5848 has the latter two minerals and rutile, and pyrite. The latter two are probably related with the colour characterisation of this sample: black. Iron oxides, better represented in outer than inner areas in HA-5847 thin section, relates this mineral with its colour: orange, probably modified by the influence of soil minerals. The results of X-Ray characterisation support the differences observed between both samples due to the higher presence of SiO_2 in the sample HA-5847 (99.31%) than in the HA-5848 (96.95%). Other component, such as Al_2O_3, Fe_2O_3, CaO, and SO_3 are better represented in the latter sample according to the higher presence of non-quartz minerals, and they could create the black colour, which is homogeneous in inner and outer areas.

After having analysed the features and variability of the BQ quartzites, we can extrapolate these results to those of non-destructive techniques. We observe that fine and medium grain size varieties are similar distributed one each other, as heterogeneous or homogeneous varieties, both well represented in the assemblage. The two colour varieties, the black and the orange ones, do also have similar percentages in the assemblage.

7.2.4. THE MQ PETROGENETIC TYPE OF EL HABARIO

The only sample from this type is HA-5842 (Figure-7.5). It is characterised by a clastic grained texture and suturated packing. Recrystallised quartz grains are frequent, but sutured quartz grains are less frequent. Grains also show plain and angular limits. In general, it is impossible to distinguish between recrystallised and non-recrystallised quartz grains. Quartz grain size characterisation shows a single wide mode, with grains between very fine silt and very fine sand. The biggest peak is between fine silt and coarse silt. The analysis of grain morphology points at the general irregularity of particles, while roundness index reveals particles are not clearly elongated. Grains are not preferentially oriented. Non-destructive characterisation in inner area once has been cut for thin section, reveals soapy texture and no quartz grain limit detection. The luster is high. Foliation fabrics are absent, due to the extremely crystallinity of surface. Nevertheless, on the surface of the lithics, significantly altered by weathering processes, the texture is similar to quartzarenites, with sandy appearance and touch.

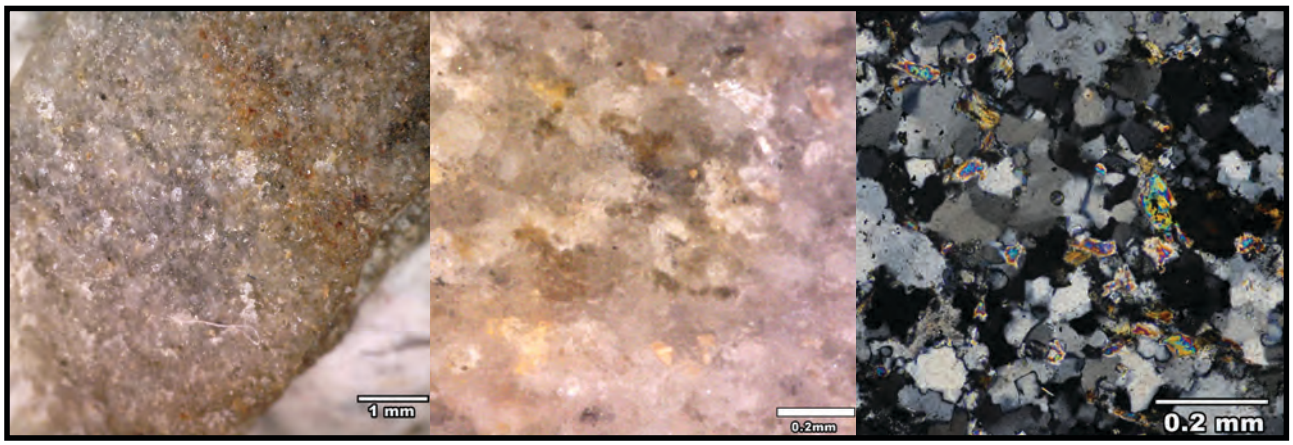

Figure-7.5: Pictures of the RQ type sample from the archaeological site of El Habario: HA-5842. From left to right, microscopy binocular picture at 50x, microscopy binocular picture at 250x, and thin section microscopy picture at different magnifications.

The mineral characterisation of this sample does not reveal matrix or cement. There are multiple non-quartz mineral distributed in all thin section: zircon, tourmaline, rutile and iron oxides. The results of X-Ray Fluorescence are in accordance with the minerals detected, especially due to its quantity. Although 90% of the sample is composed by SiO_2, there are many other well represented components, especially Al_2O_3 (5.82%). Other components such as Fe_2O_3 and Na_2O are well represented. The colour of the sample is white on inner areas, while on the surface is brown and orange. This is the consequence of weathering processes caused by the soil.

Coming back to the analysis of all the MQ petrogenetic type in El Habario, we do not observe different varieties, mainly because there are only another three implements characterised as MQ quartzite. In addition, weathering processes on lithic surfaces also hinder us to characterised features to stablish different varieties.

7.2.5. NON-DESTRUCTIVE CHARACTERISATION OF CA AND MQ PETROGENETIC TYPES AT EL HABARIO

The CA petrogenetic type is represented in this archaeological layer with only four items. Under binocular microscope most of the textures are coarse grained, although fine grained textures are observable. Packing is generally tangent or tangent-complete. Grains are easy to recognise, with rounded or angular borders. The presence of cement is small or non-existent. Granular T&P is clear in this petrogenetic type. The grain size of this type is heterogeneous, related with medium and coarse sizes (Figure-7.6). All represented minerals are iron oxides, mica, feldspar, and non-identified black minerals. The most frequent colours are brown, orange and grey. Due to the small quantity of this quartzarenite and the lack of thin section and X-Ray analysis, we do not stablish any variety.

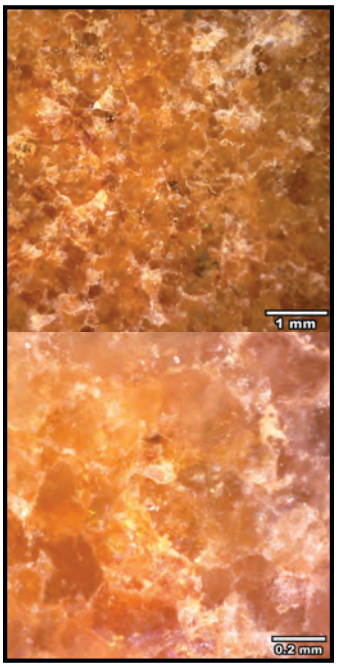

Figure-7.6: Pictures of a CA type from the archaeological site of El Habario: HA-5824 Upper row shows microscopy binocular picture at 50x. Lower row shows microscopy picture at 250x. Grains are classified as medium sizes with heterogeneous distribution.

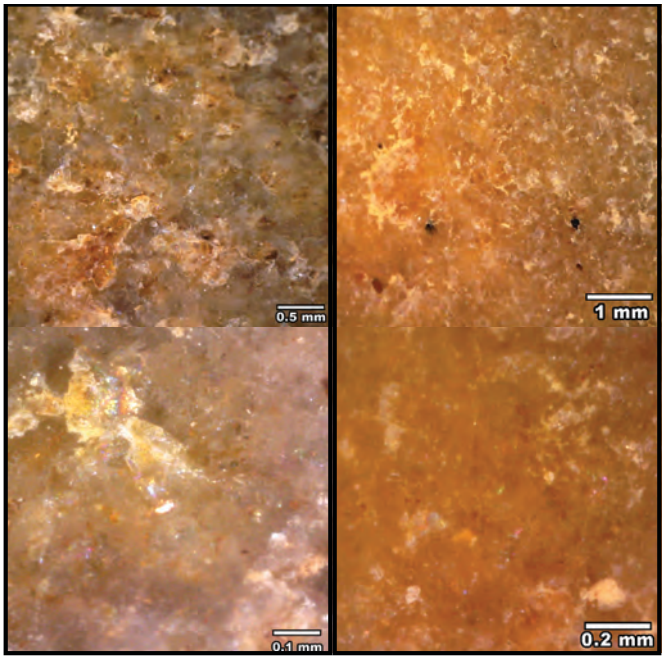

Figure-7.7: Pictures of the MQ type from the archaeological site of El Habario. From left to right, samples HA-5560 and HA-5592. The first sample has medium grain size with heterogeneous distribution. Its characteristic colour is white-orange. Grains from the second quartzite are fine in homogeneous distribution. Its colour is orange.

There are only 19 lithics made on the RQ petrogenetic type, 4% of the assemblage. Under binocular microscopy, these quartzites are characterised by soapy texture and suturated packing. Grain boundary detection is easier on medium sizes varieties than on finer ones, even though grain boundaries are not easily observed. The bright or luster is high and micro-cracks are limited (i.e. soapy T&P). Medium and fine grain size varieties are observed, with either homogenous or heterogeneous distribution. All of them have similar representation. Iron oxides, mica and non-identified heavy and dark minerals are the best represented non-quartz minerals detected on quartzite surfaces. Nevertheless, manganese oxides and pyrite are characterised on two quartzites. These two quartzites have darker colours than most of the collection, generally coloured as light orange. This dark variety has heterogeneous quartz grain size distribution around medium sizes and it is only represented by two lithics. (Figure-7.7). Nevertheless, due to the small quantity of this quartzite type and the absence of thin section samples, the conclusion obtained must be nuance.

7.2.6. CHARACTERISATION OF CORTICAL AREAS AT EL HABARIO

Here we present the result of the characterisation of cortical areas. All cortical surfaces are on “archaeological quartzites”, and they represent 57.2% of this raw material, 271 items. Coming to the types of cortex, 14% of the collection could not be characterised due to the absence of diagnostic features. None of the cortex identified could be interpret as evidence of direct extraction from the outcrop.

Conglomerate cortex is the most frequent type, representing 82% of the lithic implements with cortical areas. Conglomerate cortical areas are characterised by the presence of cements from the conglomerates, generally as red or dark iron oxides. In addition, voids are usually present, even though they are generally filled with conglomerate cement. Marks derived from the wing could be observed on some cortex, also isolated impacts derived from rock movements which display irregularity on cortical surfaces.

Cortical areas from fluvial sources is the less frequent category, representing 4% of the cortical areas analysed. Fluvial cortex is mainly characterised by the presence of impact cracks in the surface and fine or soapy textures. Voids are less frequent in this cortex type and cement is absence.

There are no different representation of cortical areas between the different petrogenetic types (Table-7.5). Nevertheless, fluvial cortex is only represented in the OO, SO, and BQ petrogenetic types in similar proportion.

Archaeological quartzite	Cortex type												∑ of each type
	Conglomerate			Fluvial			Unknown			Total			
	∑	%	% rel	∑	%	% rel	∑	%	% rel	∑	%	% rel	
CC							1	3	100	1	0	100	1
CA	3	1	75							3	1	75	4
OO	54	24	49	5	45	5	9	24	8	68	25	61	111
SO	37	17	46	2	18	3	7	18	9	46	17	58	80
BQ	116	52	49	3	27	1	16	42	7	135	50	57	238
RQ	9	4	45				2	5	10	11	4	55	20
MQ													3
Undetermined	3	1	30	1	9	10	3	8	30	7	3	70	10
Total	222	82	48	11	4	2	38	14	8	271	100	58	467

Table-7.5: Frequency table of types of cortex identified in El Habario grouped by petrogenetic type. Columns are the types of cortex, including the frequency of each cortex type for each petrogenetic type and the total of items with cortex of each petrogenetic type. The last column quantifies the total of items with and without cortex of each petrogenetic type. The columns % are the percentage of each petrogenetic type in relation to each cortex type, while the columns % rel. columns are the percentage of cortex type in relation to the total of each petrogenetic type (including items with and without cortex).

7.3. TECHNOLOGICAL STRUCTURE

Here we present the results of the technological analysis on the assemblage from El Habario, taking into account the results from the study of petrological structure. According to the methodology previously exposed, the most frequent category is knapping product (76%), followed by core (15%), and chunk (9%). The two radioralites and the flint implements are knapping products, both classified as blanks. Focusing the analysis on “archaeological quartzites”, the cores are restricted to orthoquartzites and quartzites groups (Table-7.6). Cores made on orthoquartzite and BQ type have similar representation, around 15%. Nevertheless, on RQ and MQ types cores are more frequent, conditioned by the small quantity of lithics made on these two types. Knapping product is the most frequent technological category in all petrogenetic types, except on CC quartzarenite. Nevertheless, there are differences in its representation when they are compared between petrogenetic types. On CA type, knapping product is the only technological category represented. In addition, there is a higher representation of knapping products in the OO, SO, BQ types than in RQ and MQ quartzites. Finally, chunks are only represented on CC, OO, SO, and BQ types. The only CC type implement is a chunk.

7.3.1. CORES

We identified 71 cores in the whole collection. The most frequent type of core is the irregular (polyhedral) one with 26 cores. Discoid core with 21, core on flake with 19, and levallois with only three cores are also well represented. In addition there is a prismatic shaped core. There is no clear correlation between type of core and petrogenetic types of “archaeological quartzites”, even though most of levallois cores are made on SO type (Table-7.7). In addition, the representation of core on flake is different between petrogenetic types, especially comparing the orthoquartzite and quartzite groups. Core on flakes are more frequent in the latter group than in the former.

	Technological order										
	Cores			Knapping prdct.			Chunk			Total	
	∑	%	% rel	∑	%	% rel	∑	%	% rel	∑	%
CC							1	2	100	1	0
CA				4	1	100				4	1
OO	14	20	13	**90**	**25**	**81**	7	17	6	111	24
SO	9	13	11	**63**	**18**	**79**	8	20	10	80	17
BQ	40	56	17	**180**	**51**	**76**	18	44	8	238	51
RQ	6	8	32	13	4	68				19	4
MQ	1	1	25	3	1	75				4	1
Undetermined	1	1	10	2	1	20	7	17	70	10	2
Total	71	15		355	76		41	9		467	100

Table-7.6: Frequency table of main technological categories identified in El Habario grouped by petrogenetic types of “archaeological quartzite”. Columns are the main technological categories and the total of items belonging to each petrogenetic type. The columns % are the percentage of each petrogenetic type in relation to each technological category, while the columns % rel. are the percentage of each technological category in relation to the each petrogenetic type of “archaeological quartzite”. Cells in black are the categories representing more than 10% of the total cases. Cells in dark grey are the categories representing between 5 and 10% of cases. Finally, cells in light grey are the categories representing between 1 and 5% of cases.

The irregular cores from this assemblage are diverse. Regarding its raw material, most of them are made on BQ type (twelve items). OO (eight items), SO (three items), and RQ (two items) petrogenetic types are represented too. Finally, the only core made on MQ quartzite belongs to this category. Except on BQ quartzite, irregular core is the most frequent type on every petrogenetic type of “archaeological quartzite”. Most of the cores (17) are complete and only nine are fractured. The number of percussion platforms and flacking surfaces in irregular cores are varied, even though most of them have at least two percussion platform and flacking surfaces. This is especially clear in the BQ petrogenetic type, in which only one core has one percussion platform and one flacking surface. Coming to the presence of cortical areas, most of them preserve small areas of cortex (16 cores), generally less than 33% of the total surface (ten). Other four have cortex covering between 33 and 66% and only two cores have cortex more extended than 66% of their surfaces. All except one characterised cortex derived from conglomerate cortex. The other core is made on OO orthoquartzite and it derived from fluvial deposits.

	Type of core					
	Irregular	Discoid	Levallois	Prismatic	On flake	Total
CC						
CA						
OO	8	4			2	14
SO	3	3	2		1	9
BQ	12	11	1	1	14	39
RQ	2	2			2	6
MQ	1					
Undetermined		1				1
Total	26	21	3	1	19	69

Table-7.7: Frequency table of types of cores identified in El Habario grouped by petrogenetic types of “archaeological quartzite”. Columns are the types of cores.

Discoidal cores are represented in this site by 21 complete pieces. BQ quartzite is the most frequent petrogenetic type in this type of core, followed by OO and SO orthoquartzites and the RQ quartzite. All except one have the same number of percussion platform (more than three) and flacking surfaces (two). It is clear the same technique, with alternative and consecutives extractions is clear. The only core with only one flacking surface is made on a BQ type. Most of the cores, 15 items, have cortical areas, and only three of them have extended cortex than 66%. The other two categories are equally represented, with six items on each case. All identified cortex derived from conglomerates.

Cores on flake is well represented type with 19 items. Thirteen of them are complete, while the other six are fractured. The most common petrogenetic type for this type of core is BQ quartzite, followed by OO and RQ types. Finally, there is another core made on SO orthoquartzite. It is remarkable the high presence of BQ cores, namely 14. The quantity of percussion platforms and flacking surfaces is varied. Some cores were not intensively exploited and they present just one percussion platform and one flacking surface. On the contrary, other cores, with three or more percussion platforms and flaking surfaces, are thoroughly exploited. The presence of cortical areas in this type of cores is restricted to the dorsal faces of the flakes. Fifteen of the cores preserved any cortex, generally covering less than 33% of dorsal surface. Eleven of them are characterised as derived from conglomerates, while the other two (one for OO and another for BQ type) derived from fluvial deposits. The only SO core has no cortical areas.

There are three levallois cores in this layer and all of them are complete. Two are made on SO orthoquartzite and another one on BQ quartzite. All three cores have at least three percussion platform. The quantity of flacking surface difference a SO levallois core, with two flacking surfaces, from the other two made on BQ quartzite, with only one flacking surface. The latter two have cortex extended than 66% of the lithics, while cortical surface in the former only covers between 33 and 66% of the surface. All these cortex derived from conglomerates.

Finally, there is a prismatic shaped core made on SO orthoquartzite. It is a complete core with three or more percussion platform and three or more flacking surfaces. Cortical surfaces is extended between 33 and 66% of its surface. This cortex derived from a conglomerate.

7.3.2. KNAPPING PRODUCTS

In the lithic assemblage from El Habario we identified 358 knapping products. The most frequent type is blank, making more than 98% of the items analysed. Core preparation/rejuvenations products are scarce, forming less than 2% of the assemblage. Finally, we do not identify any burin spall. Core preparation/rejuvenation products are only made on “archaeological quartzites”, more specifically on SO, BQ, and MQ petrogenetic types (Table-7.8).

	Knapping products							
	Blanks			Core preparation/rej			Total	
	∑	%	% rel	∑	%	% rel	∑	%
Other RM	3	1	100				3	1
CC								
CA	4	1	100				4	1
OO	**90**	**26**	**100**				90	25
SO	**62**	**18**	**98**	1	14	2	63	18
BQ	**175**	**50**	**97**	5	71	3	180	50
RQ	13	4	100				13	4
MQ	2	1	67	1	14	33	3	1
Unknown	2	1	100				2	1
Total	351	98		7	2		358	100

Table-7.8: Frequency table of the categories of knapping products identified in El Habario grouped by the petrogenetic types of “archaeological quartzite”. Columns are the categories of knapping products and the total of items belonging to each petrogenetic type. The columns % are the percentage of each petrogenetic type in relation to each category of knapping product, while the columns % rel. are the percentage of each category of knapping product in relation to each petrogenetic type of “archaeological quartzite. Cells in black are the categories representing more than 10% of the total cases. Cells in light grey are the categories representing between 1 and 5% of cases. Other raw material (RM) includes radioralite (2) and flint (1).

Blank is the most frequent technological category in this layer, with 351 pieces. Coming to their integrity, 77% of the pieces are complete and 23% are fragmented (Figure-7.8). The most frequent fragments are proximal ones, followed by longitudinal and distal. Medial fragments are scarcer (≈1%). Finally, 10% of the pieces could not be classified due to the absence of diagnostic features, mainly the bulb of percussion or the striking platform. Then, most of these undetermined fragments must be part of distal or medial fragments.

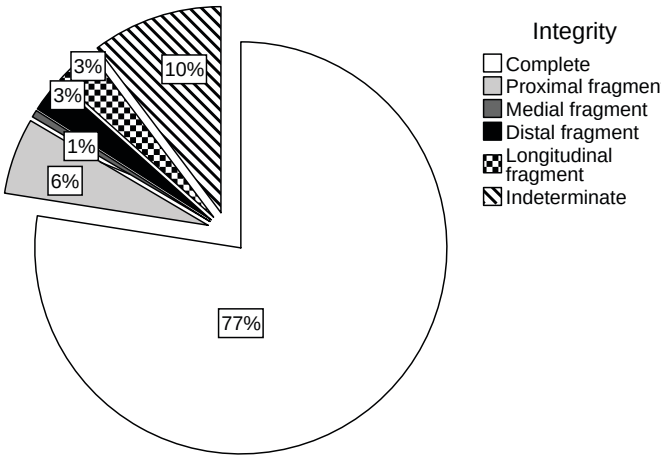

Figure-7.8: Pie chart showing percentage of each state of integrity of blanks.

There is a great variability in the number of negative scars depending on raw material. The blanks on radioralite and flint have at least three negative scars, while on "archaeological quartzites" are variable. Regarding "archaeological quartzite" we do not observe statically differences between the number of negative scars on blanks and different petrogenetic types, as supported by Chi-square test (χ^2 (15, N = 346) = 18.924, p = .217). Nevertheless, Table-7.9 points at some differences between types of "archaeological quartzite" and the number of negative scars on their blanks. The clearest difference arrises in the comparison between CA and MQ types with all other types. On the first two, all blanks have, at least two negative scars, while on the other four, all categories are represented. This is related with the small quantity of blanks in the CA and MQ types. In other four types, all four categories are similarly distributed. Nevertheless, there are more blanks with high quantity of negative scars made on SO and RQ types than on BQ and OO types. The latter type is the "archaeological quartzite" with greater frequency of blanks without negative scars.

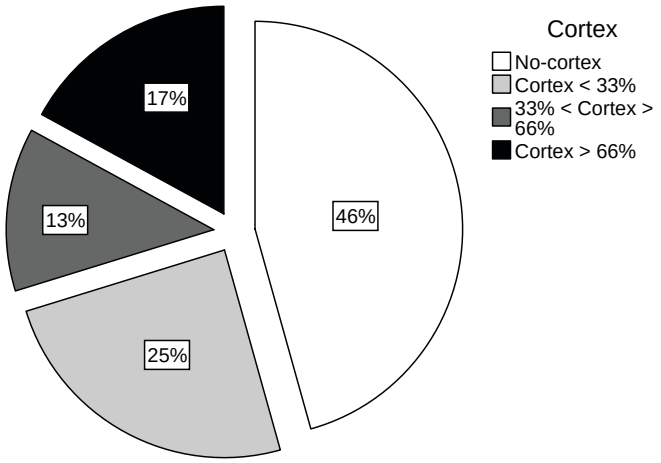

Figure-7.9: Pie chart showing percentage of absence, presence and extension of cortex on blanks.

The preservation of cortical areas on these blanks does also provide interesting data about raw material exploitation in this site (Figure-7.9). Cortical surfaces are observables in 54% of the blanks. Most of them cover less than 33% of the dorsal surface. Broad cortical areas are reduced to 30% of blanks. Finally, 17% of blanks have cortical areas covering more than 66% of their dorsal surfaces. There are no statistically significant differences between the extension of cortex in dorsal surfaces and the petrogenetic types proposed, as Chi-square test shows (χ^2 (15, N = 346) = 24.452, p = .058). Nevertheless, the test is near sigma confidence level α = 0.05, suggesting differences unveils on Table-7.10. These are caused by the absent of cortical surfaces on MQ blanks and the small extension of them in CA blanks. It is important to remark that the quantity of blanks on both petrogenetic types is reduced. There are also differences in the extension of cortical areas in blanks between the SO and RQ types with the OO and BQ. Blanks with cortex extended than 66% are more frequent on the former two types than on the latter two petrogenetic types.

Among the items which preserved any cortical area (191), it was possible to characterise 168 of them. The features that define cortex from fluvial sources (8) are underrepresented, and those from conglomerate cortex are overrepresented (160). The only represented petrogenetic types with fluvial cortex are OO orthoquartzite, with three, and SO and BQ types, with two.

Core preparation/rejuvenation products is the less frequent knapping product, represented by just ten pieces. Most of them are complete and only one is fractured. Regarding the petrogenetic type of "archaeological quartzite", the only represented raw material, BQ is the most frequent type with five core preparation/rejuvenation products, followed by SO and RQ type (Table-7.8). These data are in concordance with distribution of cores between petrogenetic types. Moreover, there is no core preparation/rejuvenation products made on OO orthoquartzite, a type with high quantity of cores. Only one of the core preparation/rejuvenation product made on BQ quartzite has cortical areas. It derived from a conglomerate and it cover less than 33% of its surface.

	Dorsal scars							
	None		One		Two		≥ Three	
	∑	**%**	∑	%	∑	%	∑	%
CA	0	0,0	0	0,0	1	25,0	3	75,0
OO	18	20,0	17	18,9	23	25,6	32	35,6
SO	6	9,7	7	11,3	19	30,6	30	48,4
BQ	15	8,6	35	20,0	60	34,3	65	37,1
RQ	2	15,4	1	7,7	5	38,5	5	38,5
MQ	0	0,0	0	0,0	0	0,0	2	100
Total	41	11,8	60	17,3	108	31,2	137	39,6

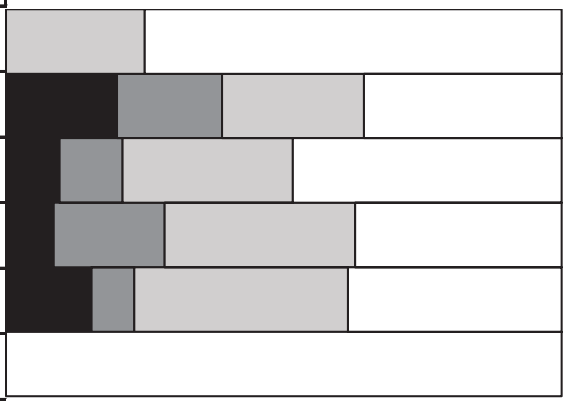

Table-7.9: Frequency table and its representation through a bar chart using the percentage of each blank category (determined by the quantity of scars on dorsal surface) according to each petrogenetic type of "archaeological quartzite".

7.3.3. CHUNK

Chunk is the less frequent technological order category in this site, only represented by 41 pieces. The integrity of the pieces is not analysable due to the absence of diagnostic features.

All of them are made on "archaeological quartzites", but they are not represented in all petrogenetic types and there are differences in their distribution, as Table-7.6 shows. The only CC quartzarenite is a chunk. Chunk are well represented in orthoquartzites and BQ type, with similar frequencies. Nevertheless, there is no chunk in CA, RQ, and MQ types, probably conditioned by the small quantity of lithic remains in these types.

Twenty-eight chunks have cortex. Cortex generally cover less than 33% of their surface. Only on four chunks, the cortex cover between 33% and 66% of the surface. Ten chunks have cortical surfaces more extended than 66%. All cortical areas of chunks derived from conglomerates, 19.

7.4. RETOUCH: MODAL AND MORPHOLOGICAL STRUCTURES

Here we present the analysis of the retouched artefacts and its relationship with the data previously exposed. According to the methodology defined above, there are 172 retouched artefacts, 37% of the lithic collection. Thirty-one blanks have two different primary types (6.5%) and 17 have three different primary types (5.3%). The number of primary types individualised is 253. Starting from orders (modes of retouch), we do not find evidence of Plain (P) mode of retouch. Simple (S) mode is the most frequent one (175 items), followed by Abrupt (A), Burin (B) and Splinter (E) (52, six and three items, respectively) (Figure-7.10 and the total from Table-7.12). Going down from order to typological group (or morphothema) of retouch, we start with the most frequent one, the Simple mode. The most frequent typological group is that of Sidescrapers (R) (46%), followed by Denticulates (D) (20%), Endscrapers (G) (6%), and Points (P) (4%). In the following order, the Abrupt (A) one, the most frequent morphological group is that of unspecific Abrupts (A) (21%). The Truncation (T) group is underrepresented with 1%. Finally, no typological groups are distinguished in the Burin and Splinter modes.

After having understood the general classification of the retouch, now we will deepen into the analysis of the pieces with multiple primary types. Starting from the blanks with two primary types, there are multiple combinations. The most frequent association of primary types in one blank is Sidescraper and Sidescraper, represented in ten artefacts. Blanks with Sidescraper and Denticulate, six, are also well represented, as blanks with Sidescraper and unspecific Abrupt, in four artefacts. Other blanks with two primary types are Abrupt and Denticulate, unspecific Abrupt and unspecific Abrupt, (three artefacts each association); Endscraper and Endscraper (two); and Sidescraper and

Endscraper, Burin and Burin (each combination of morphothema is only represented in one blank). The analysis of the blanks with three different primary types also agree with the importance of Sidescrapers.

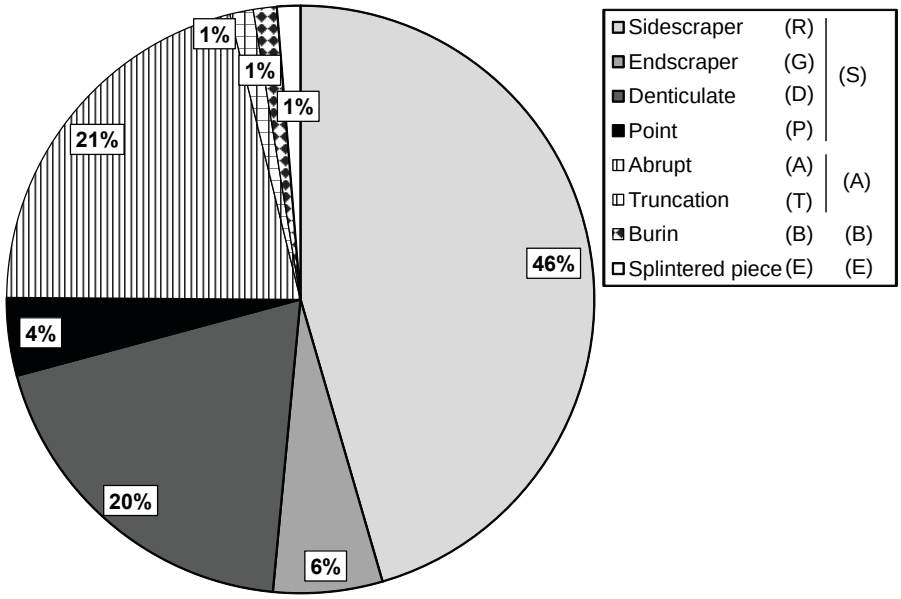

Figure-7.10: Pie chart showing the percentage of modes of retouch and morphological groups of the retouched material from El Habario.

Next, we will analyse the relationships between retouched artefacts and the technological structure. There is a statistically significant association between the presence of retouch and technological blanks they are configured (χ^2 (*2*, N = 470) = 55.115, $p < .001$). Forty-six percent of knapping products are retouched, while only 8% of cores and 4% of chunks are retouched. In addition, only two cores have multiples primary types and only one chunk has multiple primary types. Focussing on knapping products, the most frequent type of knapping product represented with primary types is the blank, even though there are two core preparation/rejuvenation products retouched. The representation of mode of retouch and typological group among blanks follows similar patters to those observed in the complete collection.

Finally, we will analyse the relationship between the retouched artefacts and the raw material of the blanks they are configured. The two lithics made on radioralite are retouched. On the contrary, the only flint artefact has no retouch. There is no statistically significant relationship in the presence of retouch in the different types of "archaeological quartzite", as proven by Chi-square test (χ^2 (5, *N* = 456) = 2.196, $p = .821$). Nevertheless, the CA and RQ types have higher incidence in retouched material than OO, SO, BQ, and MQ types (Table-7.11). Nevertheless, the number of lithics of the first two types and the latter one determine these frequencies. In addition, there is a moderate increase in the frequency of retouched artefacts in the increase of deformation/metamorphic processes throughout the OO, SO, and BQ types.

	Non-retouched		**Retouched**	
	Σ	%	**Σ**	**%**
CA	2	50,0	2	50,0
OO	74	66,7	37	33,3
SO	50	62,5	30	37,5
BQ	147	61,8	91	38,2
RQ	10	52,6	9	47,4
MQ	3	75,0	1	25,0

Table-7.11: Frequency table and its representation through a bar chart using the percentage of retouched material taking into account each petrogenetic type of "archaeological quartzite".

There is no clear association between the mode and group of retouch and petrogenetic types in which blanks are retouched. Nevertheless, there are tendencies that could explain some relationships between the types of "archaeological quartzite" in which retouch is configured (Table-7.12). The first remarkable tendency arises from the observation that most frequent morphological groups in orthoquartzites and BQ and RQ types are Sidescraper (R), followed by Denticulate (D) and unspecific Abrupt. The first one is more frequent than the two other morphological group. On the contrary, the retouch is differently distributed in the CA and MQ because the absence of Sidescraper group. In addition, Points (P) are only made on OO, BQ, and RQ types. Burins, slightly represented are only made on OO and BQ. On the contrary, artefacts configure using the Splinter mode are only made on SO type. Finally, it is also remarkable the absence of Endscraper (G) and Truncation (T) on OO orthoquartzite, a type with high representation of other morphological groups.

	Simple				Abrupt		Splinter	Burin	
Order	Sidescraper	Endscraper	Denticulate	Point	Abrupt	Truncation	Splintered	Burin	Total
Other RRMM	2								2
CA					1	1			2
OO	**24**		10	4	10			1	49
SO	22	4	3		6	1	3		39
BQ	**52**	9	**29**	5	**30**	1		2	128
RQ	6	1	2	1	2				12
MQ			1						1
Total	106	14	45	10	49	3	3	3	233

Table-7.12: Frequency table of mode of retouch and morphological groups grouped by petrogenetic type. In the cases of pieces with multiple primary types, each morphological group is quantified individually. Cells in black are the categories representing more than 10% of the total cases. Cells in dark grey are the categories representing between 5 and 10% of cases. Cells in light grey are the categories representing between 1 and 5% of cases.

Finally, we analyse the relationship between retouched artefacts and cortical areas. In general, they follow similar patterns to the general characterisation of cortex in the complete assemblage. Twenty-five percent of retouched blanks has cortex less preserved than 33% of their surfaces. Sixteen percent of retouched artefacts have cortex broad between 33 and 66%, and 15% of retouched artefacts have cortical areas extended than 66% of their surfaces. Similar pattern is also observable in blanks with multiple primary types. Regarding the characterisation of cortical areas of retouched artefacts, most of them derived from conglomerates (84%), and the presence of cortex from fluvial sources is smaller (3%). We are unable to identify the type of cortex for 13% of the pieces with cortex. These data also point at similar patterns to those observed in the characterisation of the complete assemblage.

7.5. TIPOMETRICAL STRUCTURE

In this section, we will describe the results of the analysis of the tipometrical structure and its relationship with structures studied above. We made the measurements using the technological axis (length, width and thickness) on 346 lithic pieces (74% of the assemblage). The remaining 123 pieces were measured using the longest axis (X, Y, Z), due to the absence of features signalling the technological axis[2]. All chunks, most of the cores (some cores on flake were measured using the technological axis) and some incomplete knapping products were measured using the latter criterion.

An overview of length, width, and thickness reveals that all three measurements have positive skewness and kurtosis, the highest values being those of thickness, followed by length (Figure-7.11). The mean length is 44 mm, the mean width 38.39 mm, and the mean thickness 15.21 mm. The measurements of the first two axes are similar between them. A general outlook of X, Y, and Z axes does also points at positive skewness and kurtosis. Nevertheless, all the means are significantly different between them: the mean of the X axis is 50.43 mm, the mean of the Y is 38.91 mm, and the mean of the Z axis is 22.25 mm (Figure-7.12). The relationship between the three measurements according to the Tarriño indexes (Tarriño, 2015) reveals different morphologies depending on the

2 Due to mistake in the data acquisition processes one piece was not analysed.

measurement method employed (Figure-7.13). All implements measured based on the X/Y/Z axes are between 0.5 and 0.7 of RBEI and between 0.2 and 0.5 of RFL, determining similar measurement between the three axes, in relatively cubic-bladed shapes. Regarding the material measured using L/W/T axes, the resulting forms are similar, but they also include an important presence of tabular elements. The range for RBEI axis is between 0.35 and 0.7, and for RFL is between 0.2 and 0.5.

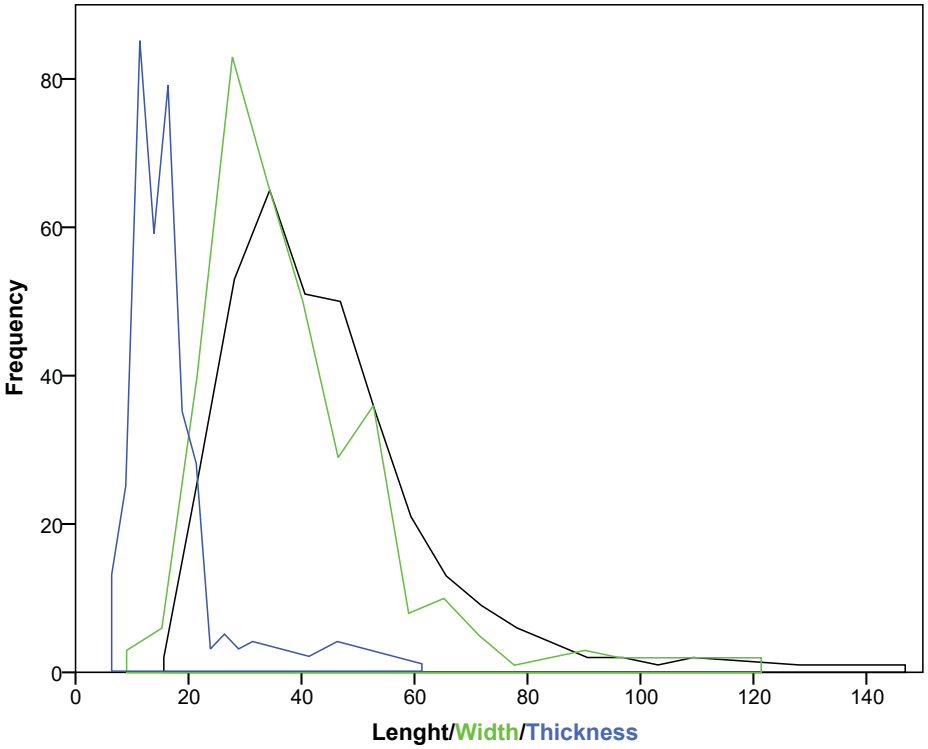

Figure-7.11: Frequency area chart showing the distribution of length, width and thickness of lithic remains from El Habario measured in relation to technological axis. Black line represents length, green line represents width, and blue line represents thickness. Horizontal axis is in millimetres.

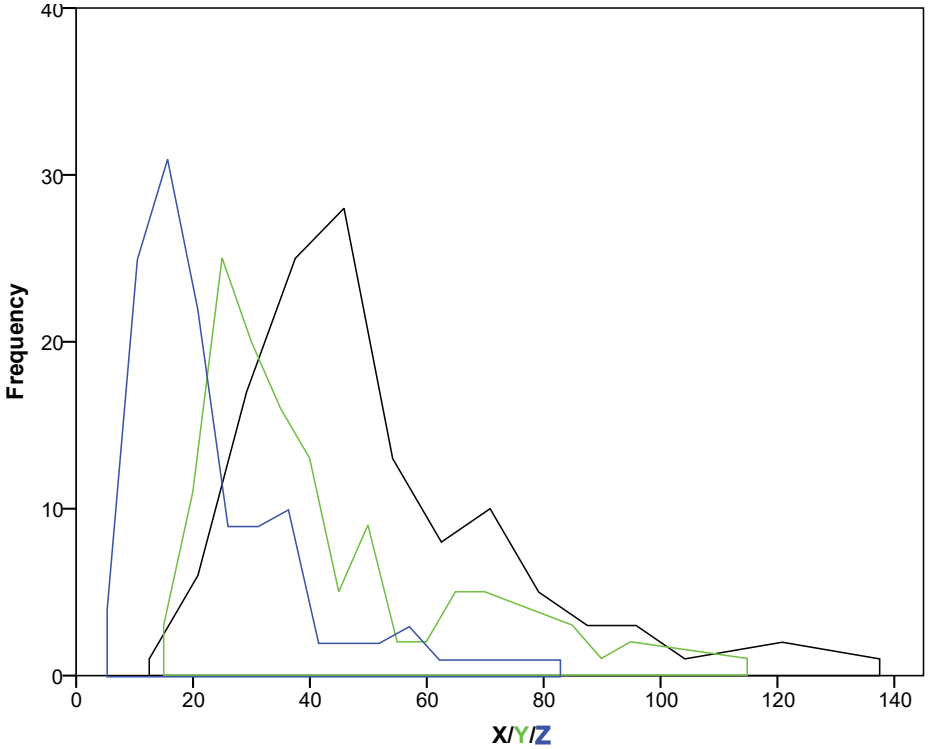

Figure-7.12: Frequency area chart showing the distribution of X, Y and Z axes of lithic remains from El Habario. Black line represents the X axis, green line represents the Y axis, and blue line represents the Z axis. Horizontal axis is in millimetres.

The last measurement used here is the weight of each lithic implement. The minimum weight recorder is 1.78 g, and the maximum 1124.7 g. The mean is 54 g. Weight represents high positive kurtosis (35) and positive skewness (5.39) as a consequence of the high percentage of lithic implements lighter than 50 g. The total of pieces weighted in this layer is 460 and the total weight of all them is 25,016 g[3].

None of the aforementioned measurements is normality distributed[4].

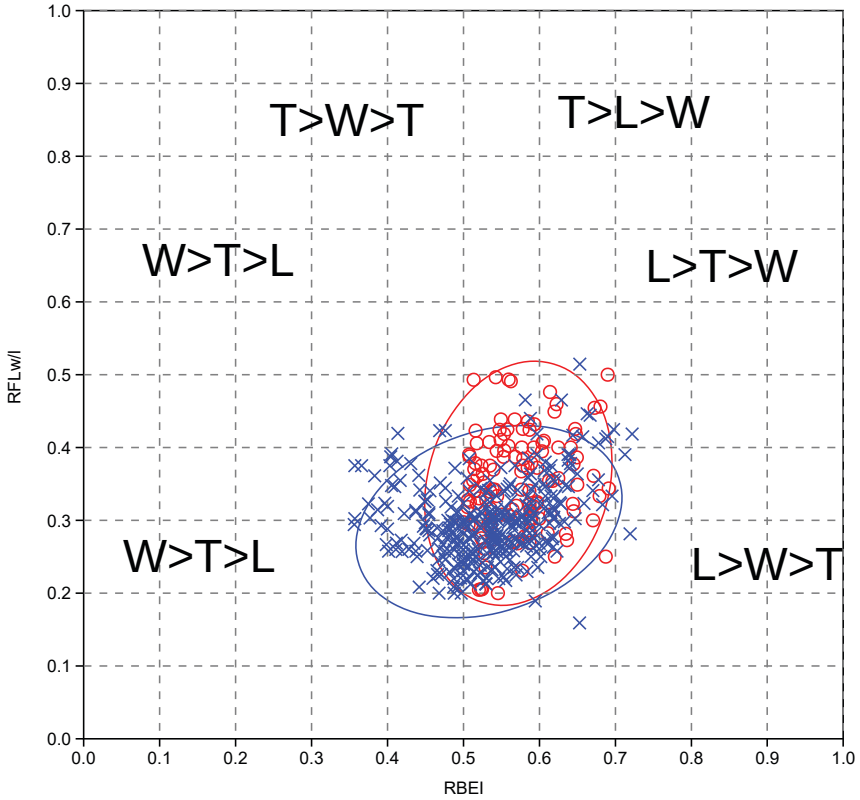

Figure-7.13: Scatter plot of RFLw or RFLl and RBEI indexes. Blue crosses and ellipse are the measurements made in relation to technological axis. Red circles and ellipse are the measurements made in relation to X/Y/Z axis. Ellipses enclose 95% of cases of each category.from El Habario measured in relation to technological axis. Black line represents length, green line represents width, and blue line represents thickness. Horizontal axis is in millimetres.

Once the general metric characteristics have been understood we will relate this data with the technological structure. The three technological orders proposed show similar morphologies. Figure-7.14 shows three overlapping but slightly different groups using 95% confidence ellipses. The ellipses of cores and chunks are the smallest, and they are situated in the central and upper part of the chart, showing positive elongation in the chart. The confidence ellipse of cores is more vertical than chunk ellipse. Therefore, core morphologies are more cubical. The ellipse of knapping products is located on the lower area and it presents horizontal elongation due to the high quantity of tabular morphologies and the small representation of thicker morphologies. The distribution of weight of each orders show clear differences in variance, as demonstrated by *H* Kruskal-Wallis test: $H\ \chi^2$ (2, N = 460) = 71.748, $p < 0.001$. The differences are clear, especially when comparing the distribution of the heavier lithics of the assemblage (Figure-7.14b). In general, cores are bigger than other orders, with weights around 171 g for each piece (Table-7.13). Knapping products and chunks have similar grams/piece ratios, significantly smaller in comparison with cores.

3 Due to mistake in the data acquisition processes ten pieces were not weighted.
4 KS = 0.118; df = 346; p < 0.01 for length
KS = 0.129; df = 346; p < 0.01 for width
KS = 0.149; df = 346; p < 0.01 for thickness
KS = 0.174; df = 123; p < 0.01 for X-axis
KS = 0.189; df = 123; p < 0.01 for Y-axis
KS = 0.183; df = 123; p < 0.01 for Z-axis
KS = 0.323; df = 460; p < 0.01 for weight

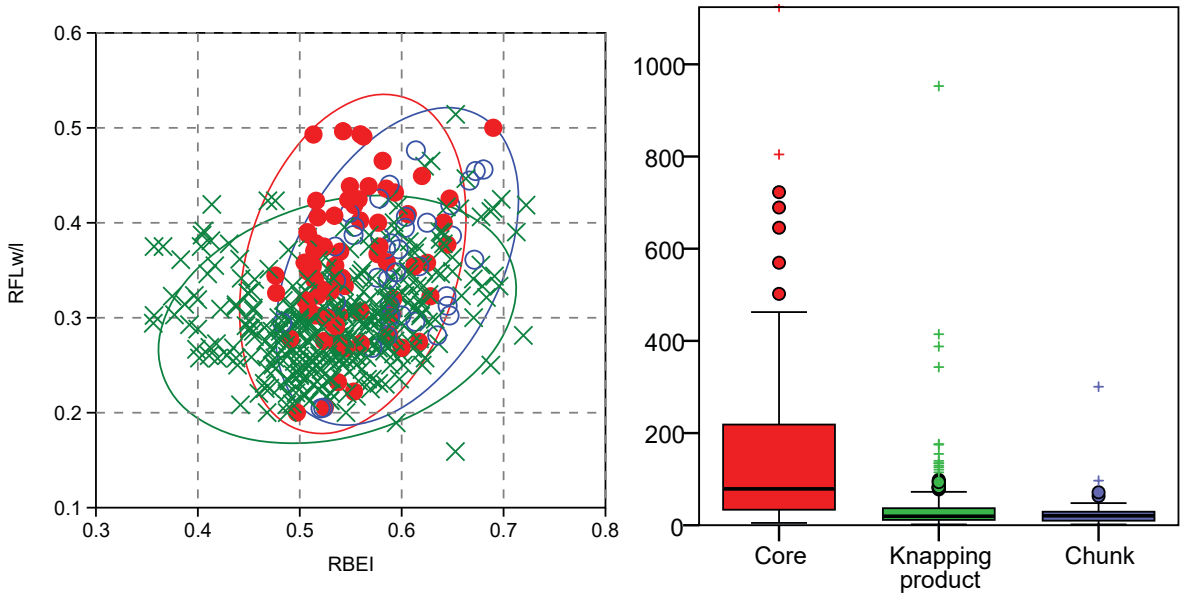

Figure-7.14: Double chart showing: a) Scatter plot of RFLw or RFLl and RBEI indexes. Green crosses and ellipse are knapping products. Red points and ellipse are cores. Blue circles and ellipse are chunks. Ellipses enclose 95% of cases of each category. b) Boxplot showing differences in weight between the technological orders.

Technological order	Weight		∑ of pieces		Ratio
	∑	%	∑	%	Grams/Piece
Core	11680,6	46,7	68	14,8	171,8
Knapping product	12167,7	48,6	353	76,7	34,5
Chunk	1168,4	4,7	39	8,5	30,0

Table-7.13: Frequencies and weight of main technological orders. The ratio grams/piece is reported. Weight is expressed in grams.

Coming to cores, there are differences in morphology between the types proposed, as displayed in Figure-7.15a through the relationship between RBEI and RFL indexes. Cores on flake morphologies are reduced to those related with cubic and tabular shapes. Discoid cores are more cubical than previous cores and they have less variability in width. Finally, confidence ellipse of irregular cores is more dispersed, showing a high variety of morphologies, generally related with cubic formats. Weight distribution also reveals differences between the cores, as demonstrated by *H* Kruskal-Wallis tests: $H\ \chi^2$ (4, N = 68) = 14.173, p = .007. Regarding the average weight of each category of cores, irregular cores and Levallois ones are above the average weight of all considered cores. Meanwhile, discoidal and cores on flake are under this average value and they are clearly differentiated from the first two. Finally, the only prismatic core is one of smallest cores in the assemblage (Table-7.14).

Core groups	Weight		∑ of pieces		Ratio
	∑	%	∑	%	Grams/Piece
Irregular core	5575,7	49,4	25	36,8	223,0
Discoid core	2360,0	20,2	20	29,4	118,0
Levallois core	856,4	7,3	3	4,4	285,5
Prismatic core	56,2	0,5	1	1,5	56,2
Core on flake	2632,3	22,5	19	27,9	138,5

Table-7.14: Frequencies and weight of different groups of cores. The ratio grams/piece is reported. Weight is expressed in grams.

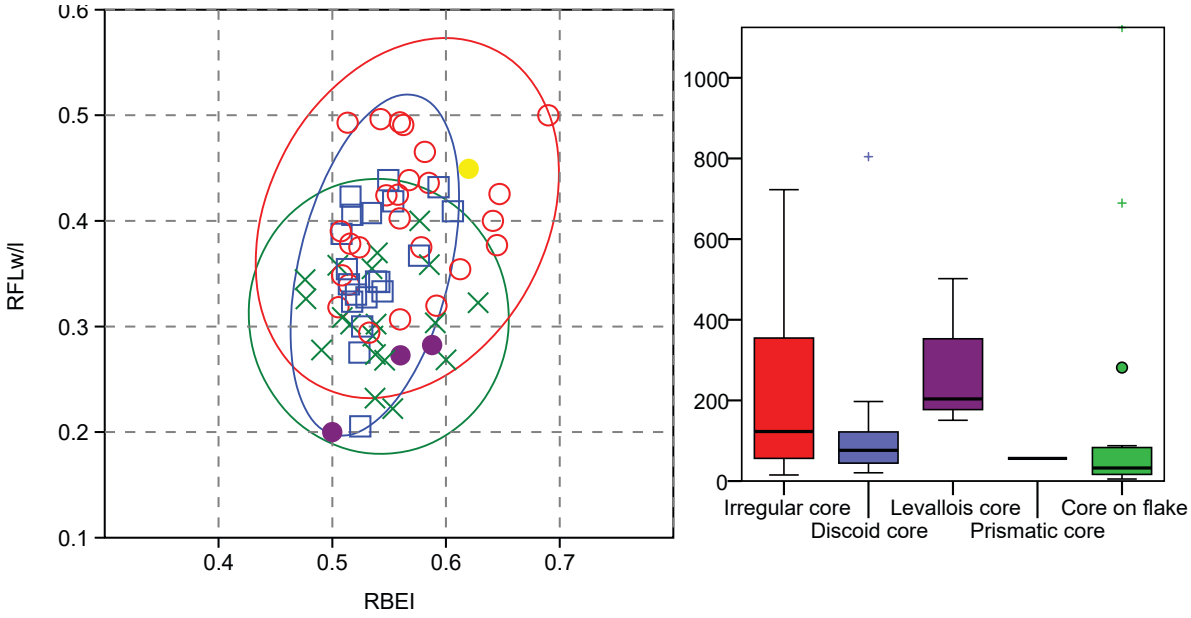

Figure-7.15: Double chart showing: a) Scatter plot of RFLw or RFLl and RBEI indexes. Green crosses and ellipse are cores on flakes. Red circles are irregular cores. Blue squares and ellipse are discoidal cores. Purple points are the Levallois cores. The yellow point is a prismatic core. Ellipses enclose 95% of cases of each category. b) Boxplot showing differences in weight between types of cores. The weight is expressed in grams.

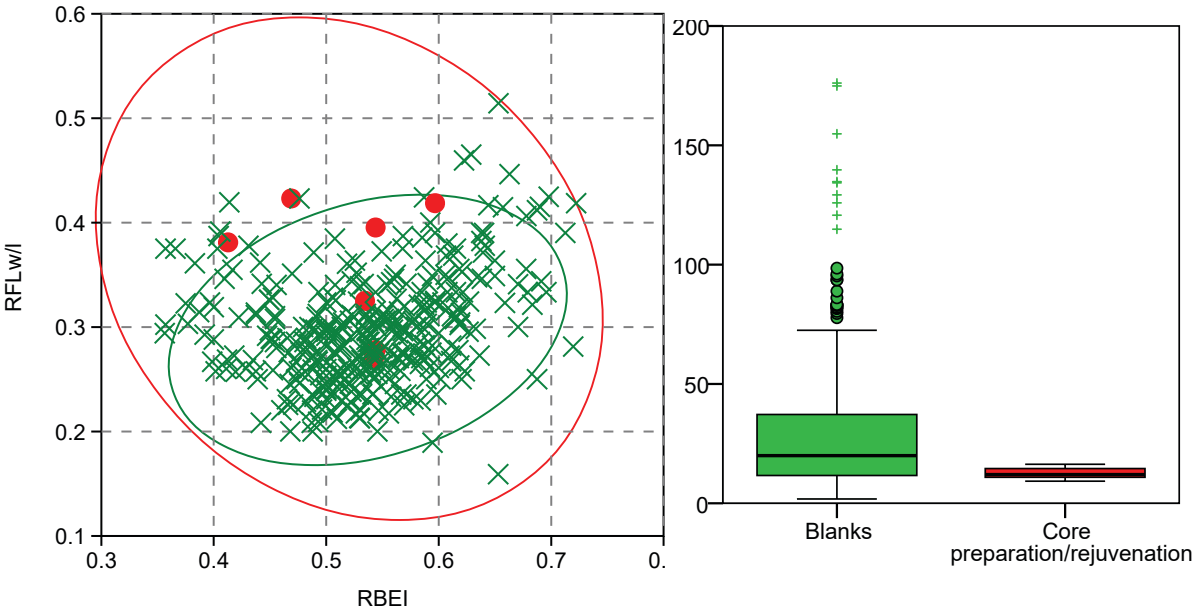

Figure-7.16: Double chart showing: a) Scatter plot of RFLw or RFLl and RBEI indexes. Green crosses and ellipse are blanks. Red points and ellipse are core preparation/rejuvenation products. Ellipses enclose 95% of cases of each category. b) Boxplot showing differences in weight between blanks and core preparation/rejuvenation products. There are four outliers outside the chart in the category of blanks with the following weights: 343.15, 387.96, 414.49, and 952.8 grams. The weight is expressed in grams.

Knapping product group	Weight		∑ of pieces		Ratio
	∑	%	∑	%	Grams/Piece
Blank	12079	99,3	346	98,0	34,9
Core prep./rejuv.	88,6	0,7	7	2,0	12,7

Table-7.15: Frequencies and weight of different groups of knapping products. The ratio grams/piece is reported. Weight is expressed in grams.

The knapping product shows clear differences in the form of lithic remains, as shown on Figure-7.16a. The areas defined by 95% confidence ellipses are different for blanks and core preparation/rejuvenation products. The former is arranged like a horizontal elongated ellipse in the region between the 0.2 ≤ RFL ≥ 0.5 and 0.3 ≤ RBEI ≥ 0.7. The second forms a rounded circle in a wider region where points scatter with high variability. Nevertheless, these differences are influenced by the different items on each category. Weight distribution does also differ from one category to another, as it can be observed in Figure-7.16b. Moreover, *U* Mann-Whitney test reveals differences in the distribution and the median between blanks (M = 19.96 g) and core preparation/rejuvenation products (M =12.04 g), $U = 682.00$, $p = 0.048$. The gram per piece ratio points at clear differences in the mean weight of the items from each group: blanks weight 34.9 g on average, while core preparation/rejuvenation products weight 12.7 g on average (Table-7.15).

Focussing on blanks there are no clear differences in their formats based on the number of negative scars on their dorsal surfaces (Figure-7.17a). All four categories are similarly distributed, represented by relatively rounded circles in the region between 0.1 ≤ RFL ≥ 0.5 and 0.35 ≤ RBEI ≥ 0.75. However, there are clear differences in weight based on the number of negative scars, as shown in Figure-7.17b and statistically demonstrated by *H* Kruskal-Wallis test: $H\ \chi^2\ (3, N = 346) = 26.727$, $p < 0.001$. The blanks without negative scars and those with at least three negative scars are heavier than the blanks with one and two negative scars. The comparison between grams per piece ratios of each category confirms this idea, especially in the comparison between the first three categories and blanks with at least three negative scars (Table-7.16).

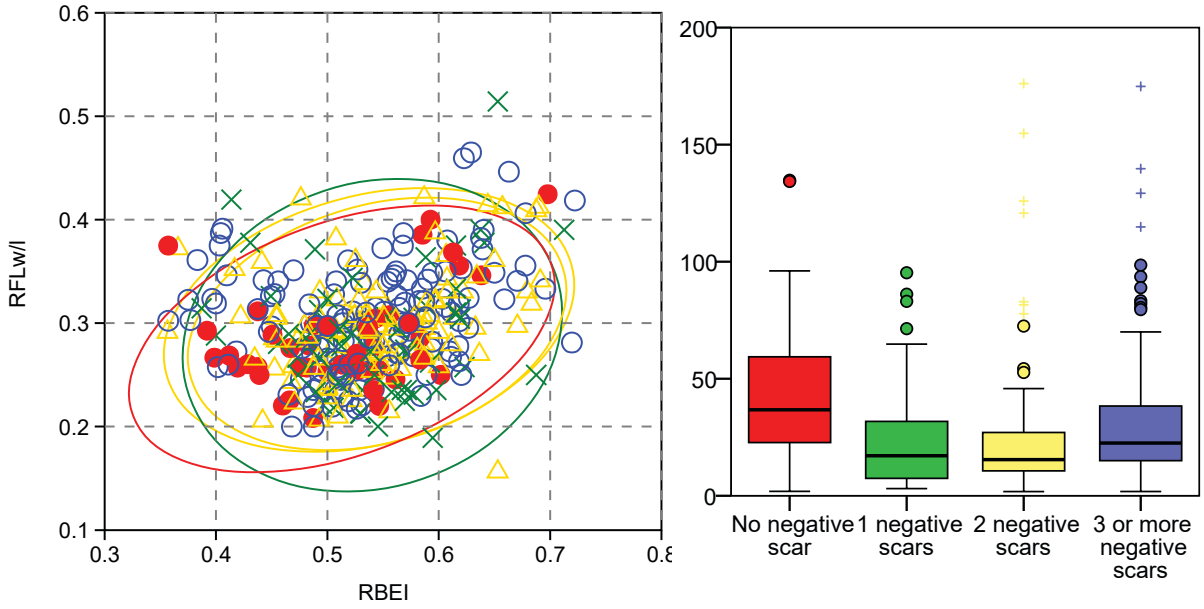

Figure-7.17: Double chart showing: a) Scatter plot of RFLw or RFLl and RBEI indexes. Red points and ellipse are blanks without negative scar. Green crosses and ellipse are blanks with one negative scar. Yellow triangles and ellipse are blanks with two negative scars. Blue circles are blanks with three or more negative scars. Ellipses enclose 95% of cases of each category. b) Boxplot showing differences in weight between blanks with different number of negative scars on dorsal surface. There are four outliers outside the chart: a 414.49 g blank in the one negative scar category, a 387.96 g blank in the two negative scars category, and another two blanks with, at least, three scars weighted on 952.8 and 343.15 grams. The weight is expressed in grams.

Number of negative scars	Weight		∑ of pieces		Ratio
	∑	%	∑	%	Grams/Piece
No-negative scars	1179,4	14,7	41	11,8	28,8
One negative scar	1861,8	15,4	61	17,6	30,5
Two negative scars	3002,3	24,9	108	31,2	27,8
Three or more negative scars	5435,6	45,0	136	39,3	40,0

Table-7.16: Frequencies and weight of blanks grouped by number of negative scars. The ratio grams/piece is reported. Weight is expressed in grams.

Regarding the integrity of the blanks, there are differences based on the form of the pieces (Figure-7.18). The ellipse of complete pieces is horizontally elongated and it is situated between 0.2 ≤ RFL ≥ 0.4 and 0.35 ≤ RBEI ≥ 0.7 (mainly tabular, cubic and bladed formats). Proximal fragments, forms an elongated ellipse in negative relation between the 0.15 ≤ RFL ≥ 0.45 and 0.3 ≤ RBEI ≥ 0.65 are more closely related with tabular and cubic forms. Longitudinal fragments make an elongated ellipse in positive relationship where more elongated shapes are present. Comparing the distribution of weight between these blanks, *H* Kruskal-Wallis test indicates differences between them: $H\ \chi^2$ (5, N = 346) = 35.266, p < 0.001. In Figure-7.18b it is possible to observe that complete lithic pieces are heavier than fragment items, even though medium weight of longitudinal fragments is similar to complete blanks. The weight distribution between the types of fragments is also different. Heavier fragments are longitudinal ones, followed by distal and medial fragments. Proximal and undetermined fragments are lighter than others. Grams per piece ratio of each category points at similar conclusions (Table-7.17).

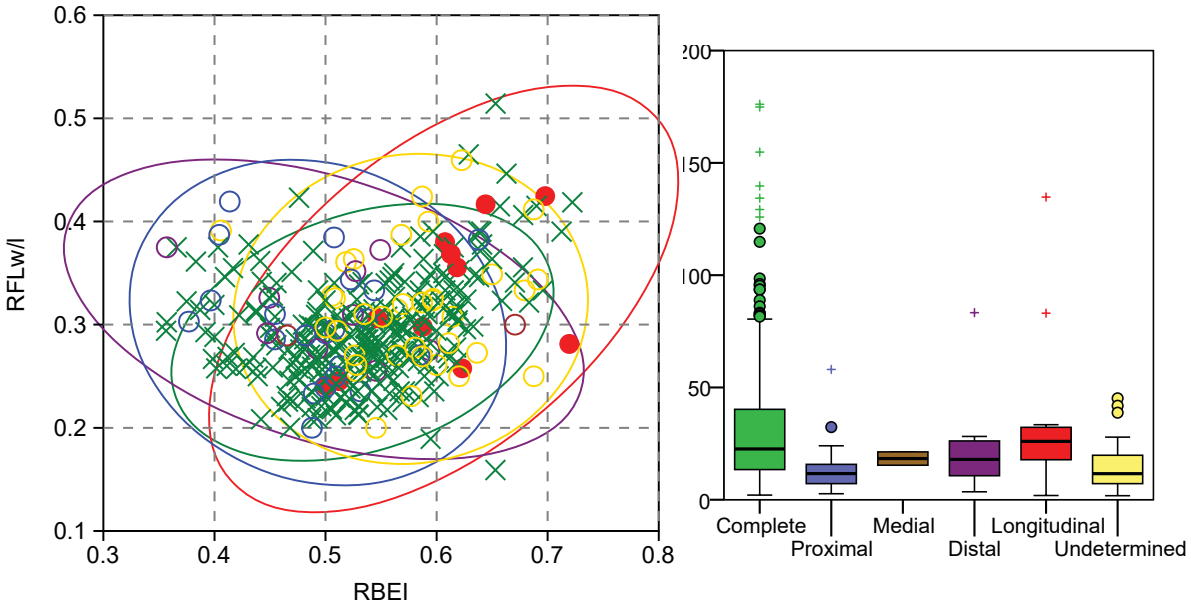

Figure-7.18: Double chart showing: a) Scatter plot of RFLw or RFLl and RBEI indexes. Green crosses and ellipse are complete blanks. Blue circles and ellipse are proximal blank fragments. Brown circles are medial fragments. Purple circles and ellipse are distal fragments. Red points and ellipse are longitudinal blank fragments. Yellow circles and ellipse are undetermined blank fragments. Ellipses enclose 95% of cases of each category. b) Boxplot showing differences in weight between blanks preserved in diverse states of integrity. There are four outliers outside the chart in the category of complete blank with following weights: 343.15, 387.96, 414.49, and 952.8 grams. The weight is expressed in grams.

Integrity of blanks	Weight		∑ of pieces		Ratio
	∑	%	∑	%	Grams/Piece
Complete	10597,2	87,6	267	77,2	39,7
Proximal fragment	304,9	2,5	21	6,1	14,5
Medial fragment	36,7	0,3	2	0,6	18,4
Distal fragment	219,7	1,8	9	2,6	24,4
Longitudinal fragment	415,1	3,4	11	3,2	37,7
Undetermined fragm	515,5	4,3	36	10,4	14,3

Table-7.17: Frequencies and weight of blanks grouped by integrity. The ratio grams/piece is reported. Weight is expressed in grams.

The classification of complete blanks reveals the predominance of flakes (82% of complete blanks), followed by a moderate quantity of elongated flakes (15% of complete blanks) and an occasional find of blades (4% of complete blanks) (Figure-7.19a). There is no difference in weight between these three categories, which show similar distributions, as depicted in Figure-7.19b and proven by *H* Kruskal-Wallis test: $H\ \chi^2$ (2, N = 307) = 1.246, p = .536. The comparison of gram/piece ratios between the three types of blanks proposed reveals differences in mean weight (Table-7.18). The gram/piece ratio of flakes is similar to the ratio of all blanks, while the ratio of elongated flakes is slightly. In contrary, blades are lighter.

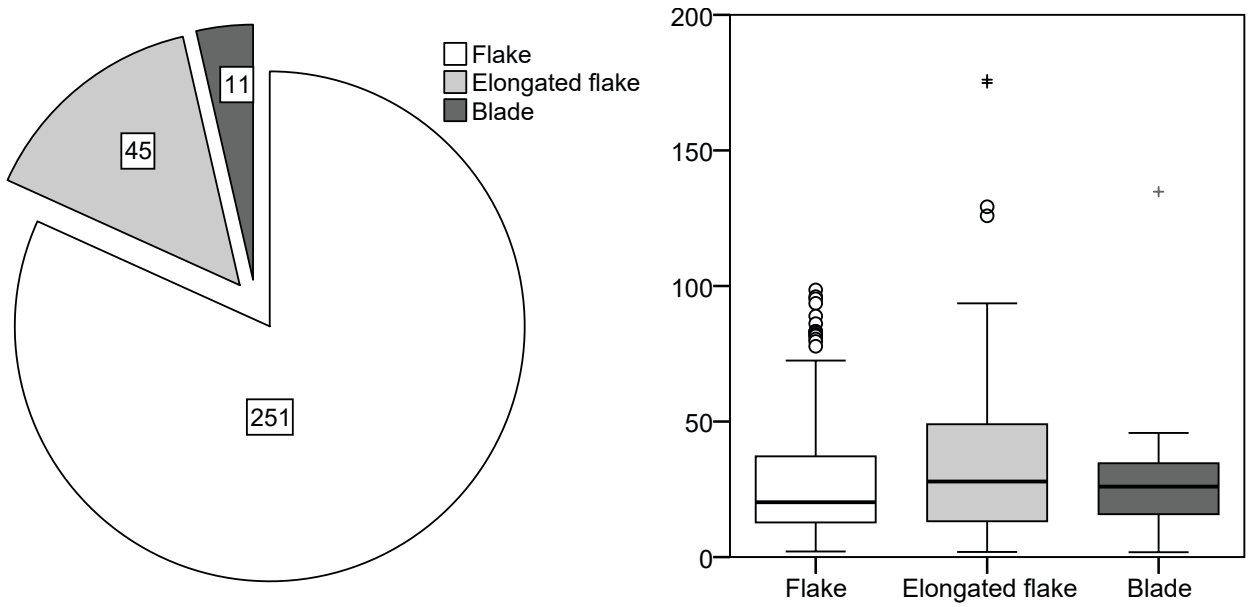

Figure-7.19: Double chart showing a) pie chart showing the distribution of complete blank products, and b) boxplot showing differences in weight between metrical categories. There are four outliers outside the chart in the category of flake with following weights: 343.15, 387.96, 414.49, and 952.8 grams. The weight is expressed in grams.

Complete blank characterisation	Weight		∑ of pieces		Ratio
	∑	%	∑	%	Grams/Piece
Flake	9205,0	81,0	251	81,8	36,7
Elongated flake	1789,8	15,7	45	14,7	39,8
Blade	371,0	3,3	11	3,6	33,7

Table-7.18: Frequencies and weight of different types of complete blanks (flakes, elongated flakes, blades). The ratio grams/piece is reported. Weight is expressed in grams.

Next, we will liken (typo)metrical structure with retouched artefacts. There are no differences in weight based on the presence (M = 24.63) or absence (M = 21.32) of retouch in the pieces, as corroborated by *U* Mann-Whitney test: $U = 26{,}442.5$, $p = 0.149$. Grams per piece ratio also points at similar weights (Table-7.19 and Figure-7.20b). The morphology between artefacts with and without retouch slightly differ between both categories due to the higher range of morphologies of non-retouched artefacts (Figure-7.20a). Nevertheless, there are no morphological differences between artefacts with one, two or three primary types on each blank (Figure-7.21a). The weight is also similar in the three categories, as certified by *H* Kruskal-Wallis: $H\ \chi^2\ (2, N = 167) = 0.165$, $p = 0.921$. Nevertheless, grams/piece ratio of artefacts with two modes of retouch is greater than artefacts with one or two different modes of retouch (Table-7.20).

Piece	Weight		∑ of pieces		Ratio
	∑	%	∑	%	Grams/Piece
Non-retouched	16496,8	65,9	293	63,7	56,3
Retouched	8519,9	34,1	167	36,3	51,0

Table-7.19: Frequencies and weight of retouched and non-retouched pieces. The ratio grams/piece is reported. Weight is expressed in grams.

Quantity of retouch in each piece	Weight		∑ of pieces		Ratio
	∑	%	∑	%	Grams/Piece
One primary type	5980,3	70,19	120	71,86	49,8
Two primary types	1903,9	22,35	30	17,96	63,5
Three primary types	635,7	7,46	17	10,18	37,4

Table-7.20: Frequencies and weight of the retouched pieces grouped by the quantity of primary types identified in each blank. The ratio grams/piece is reported. Weight is expressed in grams.

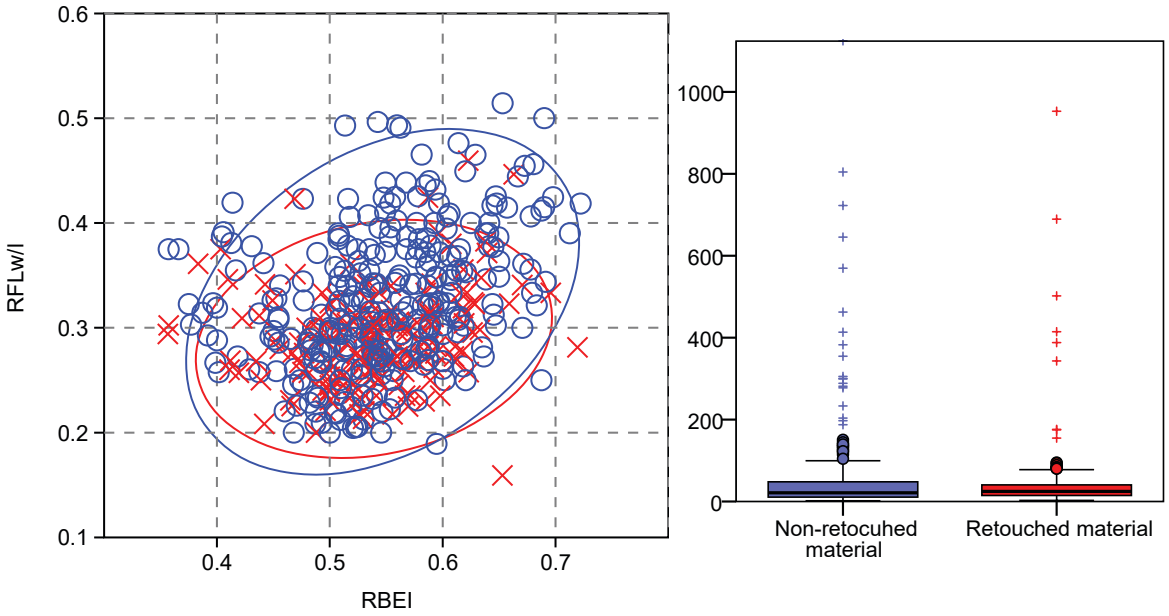

Figure-7.20: Double chart showing: a) Scatter plot of RFLw or RFLl and RBEI indexes. Red crosses and ellipse are retouched lithic material. Blue circles and ellipse are non-retouched lithic material. Ellipses enclose 95% of cases of each category. b) Boxplot showing differences in weight between retouched and non-retouched lithic artefacts. The weight is expressed in grams.

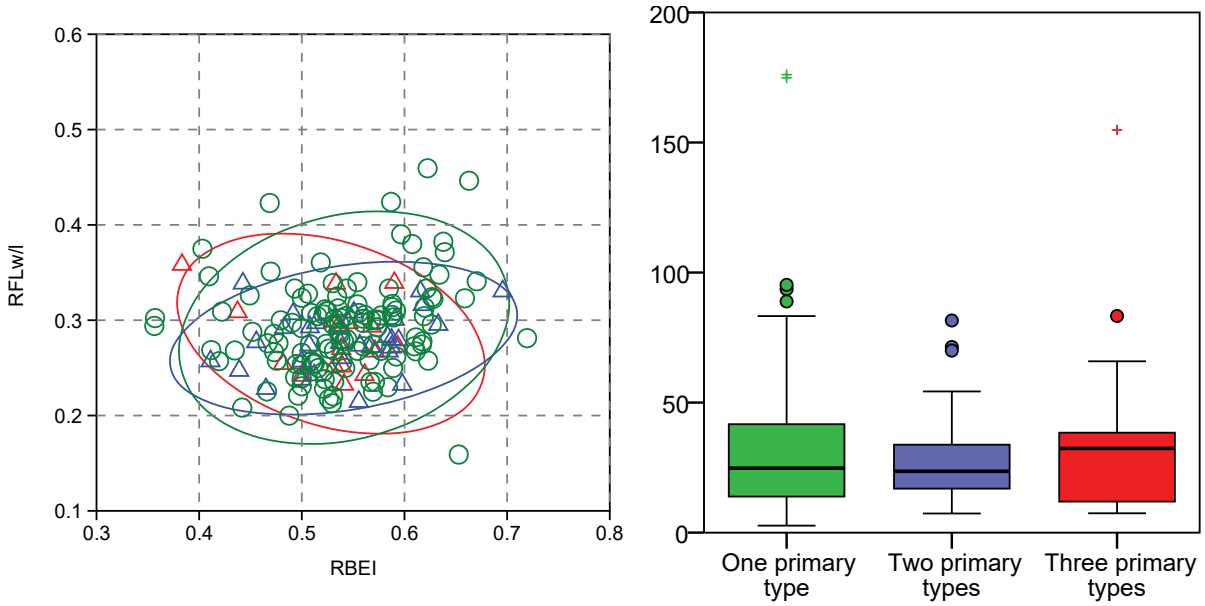

Figure-7.21: Double chart showing: a) Scatter plot of RFLw or RFLl and RBEI indexes. Green circles and ellipse are artefacts with one primary type. Blue triangles and ellipse are artefacts with two primary types. Red crosses and ellipse are artefacts with three primary types. Ellipses enclose 95% of cases of each category. b) Boxplot showing differences in weight between retouched artefacts by quantity of primary types. There are six outliers outside the chart: three artefacts with one primary type that weight 387.96, 502, and 952.8 grams, two artefacts with two primary types that weight 414.49 grams, and a 343.15 g artefact with three primary types. The weight is expressed in grams.

Then, we will confront metrical features of retouched artefacts with the features of retouch, categorised in orders (modal structure) and groups (morphological structure). Due to the methodology used to define retouch here, we only included in this analysis the pieces with one primary type of retouch. The comparison does not reveal differences in morphology between the blanks retouched using the three different modes described, as represented in Figure-7.22a. The Simple and Abrupt 95% confidence ellipses are similar one each other. There are neither differences in the weight of the retouched blanks between the first two categories categories, also proven by *H* Kruskal-Wallis test: $H\ \chi^2$ (2, N = 112) = 1.378, p = 0.502. Grams per piece ratio of three categories are also similar, even though Abrupt artefacts are lighter than other two modes (Table-7.21). There are neither weight nor morphological differences between morphological groups of retouch, even though truncations are the lightest artefacts.

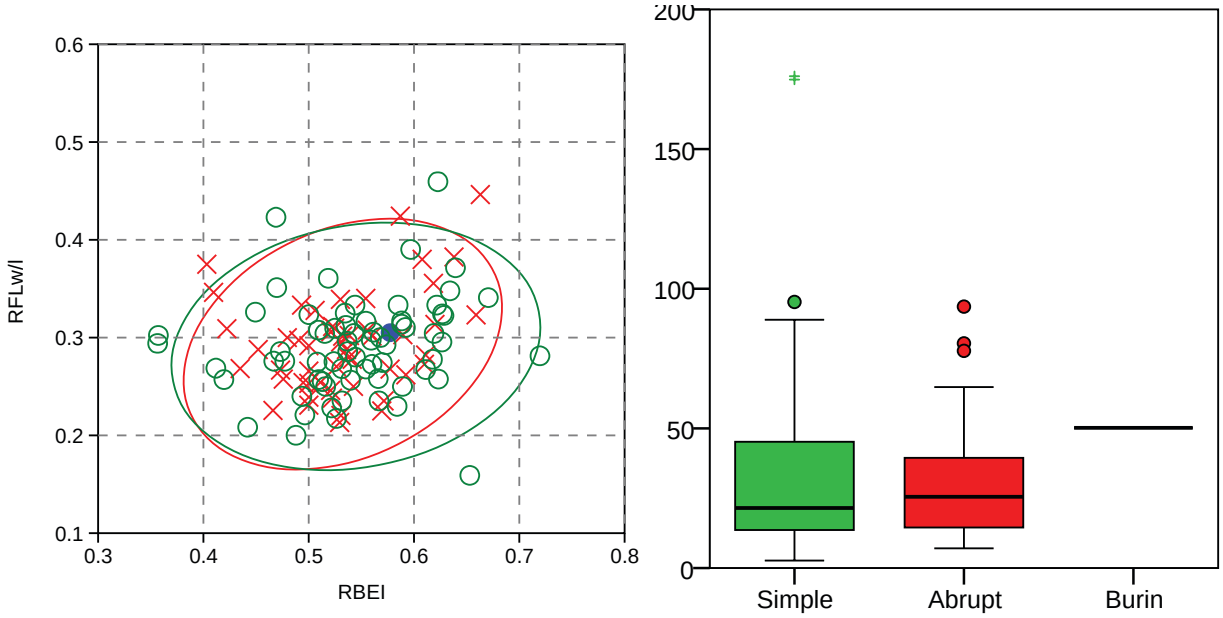

Figure-7.22: Double chart showing: a) Scatter plot of RFLw or RFLI and RBEI indexes. Red crosses and ellipse are pieces retouched with Abrupt mode of retouch. Green circles and ellipse are pieces configured with Simple mode of retouch. Blue point is the piece configured with a Burin mode of retouch. Ellipses enclose 95% of cases of each category. b) Boxplot showing differences in weight between different orders of retouch. There are six outliers outside the chart: five Simple mode retouched artefacts that weight 343.15, 414.49, 502, 689.34, and 952.8 grams and another Abrupt artefact that weight 387.96 grams. The weight is expressed in grams.

Order of retouch	Weight		∑ of pieces		Ratio
	∑	%	∑	%	Grams/Piece
Simple	4708,7	78,7	91	75,8	51,7
Abrupt	1221,4	20,4	28	23,3	43,6
Burin	50,2	0,8	1	0,8	50,2

Table-7.21: Frequencies and weight of retouched artefacts with one primary type grouped by the mode of retouch. Blanks with multiple primary types are not included. The ratio grams/piece is reported. Weight is expressed in grams.

The last structure to be tackled here is the petrological one. The weights of the two radioralite (16.16 and 2.68 g) and the flint (3.52 g) is smaller than “archaeological quartzite” weight (mean = 54.69 g). The morphology of three raw material is similar one each other. Focussing on “archaeological quartzite” there are no differences in the morphology between the petrogenetic types (Figure-7.23a). There are neither statistically significant differences in weight between types of “archaeological quartzite”, as demonstrate by *H* Kruskal-Wallis test: $H\ \chi^2$ (5, N = 447) = 7.602, p = 0.18. Nevertheless, the grams per piece ratio of OO implements is above the mean, while the ratio of MQ and RQ is below the mean. CA, SO and BQ grams per piece ratios are near the mean weight of “archaeological quartzite” (Table-7.22).

Petrogenetic type	Weight		∑ of pieces		Ratio
	∑	%	∑	%	Grams/Piece
CA	258,9	1,1	4	0,9	64,7
OO	8835,9	36,4	109	24,4	81,1
SO	4313,1	17,8	79	17,7	54,6
BQ	10379,2	42,7	235	52,6	44,2
RQ	441,3	1,8	18	4,0	24,5
MQ	64,2	0,3	2	0,4	32,1

Table-7.22: Frequencies and weight of different petrogenetic types of “archaeological quartzites”. The ratio grams/piece is reported. Weight is expressed in grams.

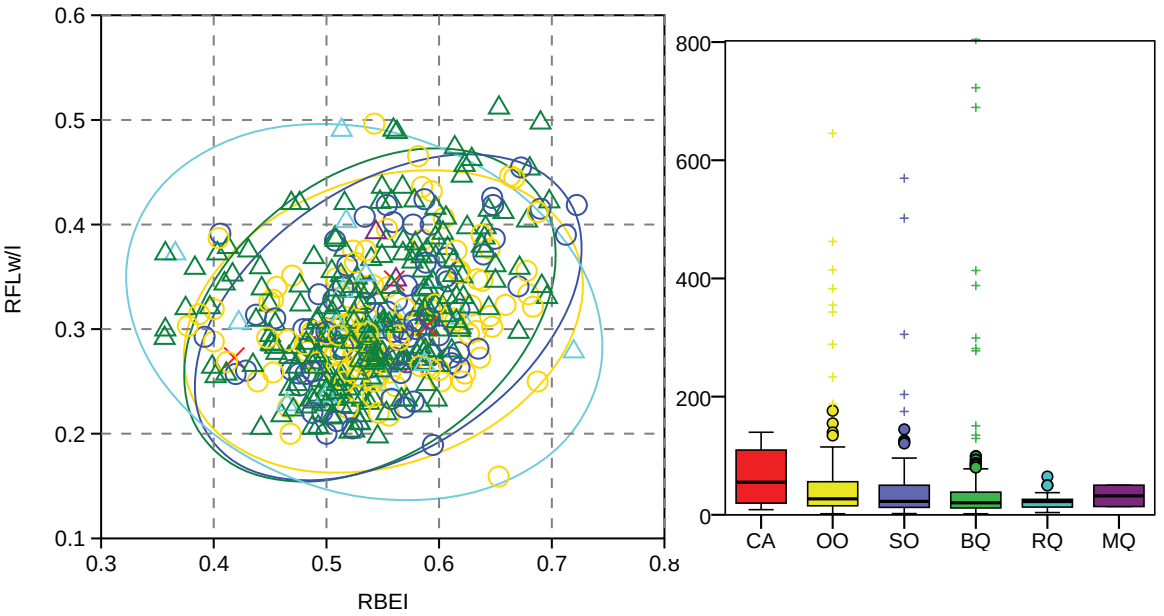

Figure-7.23: Double chart showing: a) Scatter plot of RFLw or RFLl and RBEI indexes. Red crosses are CA type pieces. Yellow circles and ellipse are OO type artefacts. Blue circles and ellipse are SO type pieces. Green triangles and ellipse are BQ type artefacts. Light blue triangles and ellipse are RQ type artefacts. Purple triangles are MQ type artefacts. Ellipses enclose the 95% of cases of each category. b) Boxplot showing differences in weight between different petrogenetic types of "archaeological quartzite". There are another six "archaeological quartzites" with higher weight than 800 g, outside the chart: three OO orthoquartzites that weight 1124.7, 952.8, and 645.5 grams and others three BQ quartzites that weight 804.45, 722.62 and 689.34 grams. The weight is expressed in grams.

Now we will delve into the relationship between raw material, technology, retouch and the metrical structure, focusing on size. Due to the small representation of flint and radioralite, we only compare types of "archaeological quartzite".

Starting with technology, there are clear differences in weight based on the technological order and petrogenetic types of "archaeological quartzite" (Figure-7.24). There are clear differences between petrogenetic types in core category, especially due to the absence of OO and SO cores lighter than 40 g. This is especially relevant when these cores are compared with those from RQ quartzite, all lighter than 40 g. In addition, heavier cores than 600 g are limited to those made on OO and BQ petrogenetic types. Moreover, the grams per piece ratio comparison points that heavier cores are made on OO and SO types, followed by BQ. Finally RQ cores are the lightest cores (Table-7.23). There are also differences in knapping product, even though they are smaller. In general there is a clear decrease of weight from CA quartzarenite to RQ quartzite. In addition, the weight of orthoquartzites and BQ type is more variable than RQ and MQ types. Finally, chunk weight also differs between the OO, SO, and BQ petrogenetic types due to the decrease in mean weigh and variability as long as deformation increase.

Raw material	Petrgen. type	Lithic collection											
		Core			Knapping			Chunks			Total		
		∑	W	g/p	∑	W	g/p	∑	W	g/p	∑	W	g/p
Archaeological quartzite	CC												
	CA				4	259	64,7				4	259	65
	OO	14	4209	300,6	88	4378	49,7	7	249	35,6	109	8836	81
	SO	9	2024	224,9	63	2156	34,2	7	133	19,0	79	4313	55
	BQ	39	5117	131,2	178	4884	27,4	18	378	21,0	235	10379	44
	RQ	5	133	26,6	13	308	23,7				18	441	25
	MQ				2	64	32,1				2	64	32
	Undet.	1	197	197,0	2	97	48,3	7	407	58,1	10	701	70
	Total	68	11680	171,8	350	12145	34,7	39	1168	29,9	457	24993	55

Table-7.23: Frequency table of different orders of lithic remains grouped by raw material, including frequencies, weight and the ratio grams/piece for each case. Weight is expressed in grams.

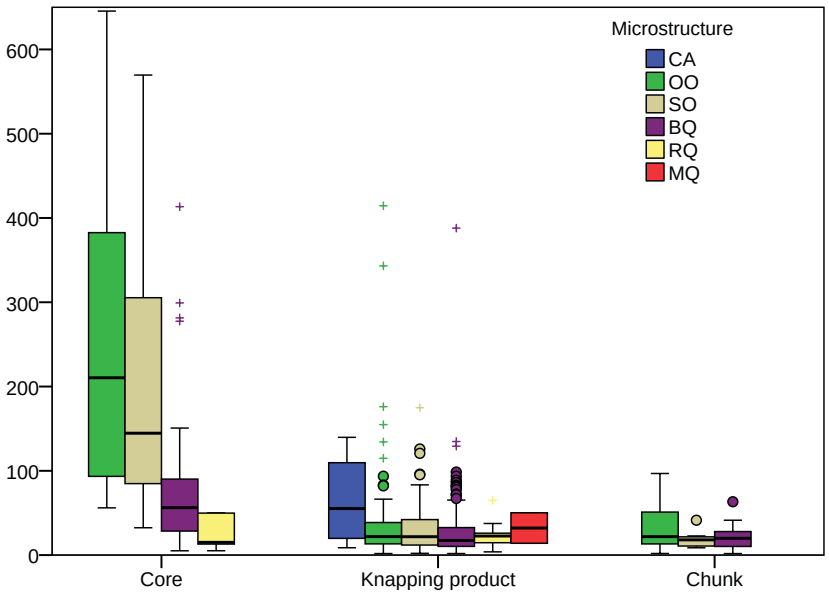

Figure-7.24: Boxplot showing the distribution of weight in grams of all lithic remains grouped first by technological order and second by petrogenetic type. There are another five “archaeological quartzites” with higher weight than 650 g not show on chart: one OO orthoquartzites core and another knapping product with weight of 1124.7 and 952.8 grams and other three BQ quartzites cores with weight of 804.45, 722.62 and 689.34 grams. The weight is expressed in grams.

Focussing on cores, weight distribution also differ between types proposed and petrogenetic types. In irregular cores, orthoquartzites cores are bigger than cores on BQ and RQ types, especially when they are compare with the second quartzite. In addition, the range of weight in the cores made on orthoquartzite and BQ type is higher than the range of RQ type (Figure-7.25 and Table-7.24). The weight of discoidal cores gradually decrease from those made on OO to cores made on RQ type. The same reduction of weight is observed in the core on flake category, from those made on OO type to the BQ type cores.

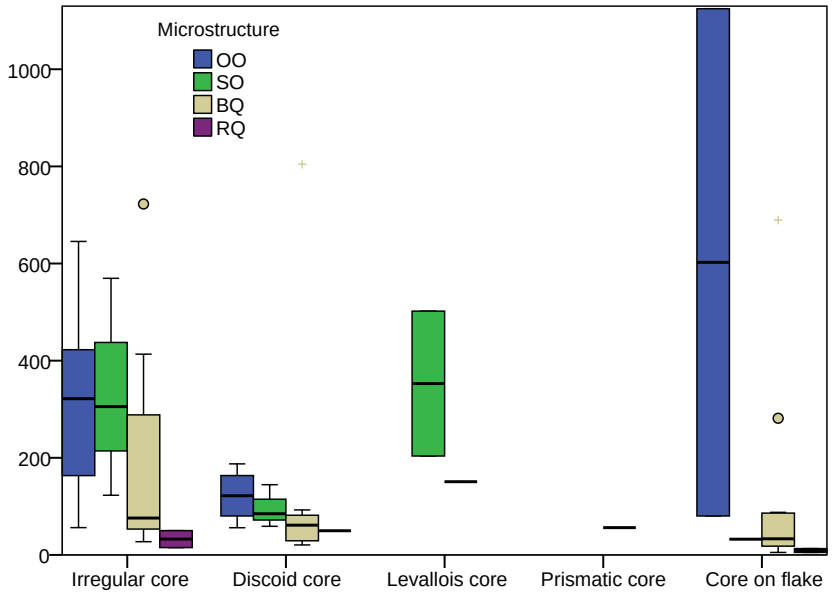

Figure-7.25: Boxplot showing the distribution of weight in grams of cores grouped first by type and second by petrogenetic type.

In regard to knapping products, Table-7.25 displays the differences between core preparation/rejuvenation products and blanks. The former are lighter than the latter. Focussing on core preparation/rejuvenation products, the heaviest are made on MQ and BQ types, although these differences are small. There are no differences in the weight of blanks depending the number of negative scars between various petrogenetic types. In general, the heavier blanks does not have negative scars

Raw material	Petr. type	Cores																	
		Irregular			Discoid			Levallois			Prismatic			Core on flake			Total		
		∑	W	g/p	∑	W	g/p	∑	W	g/p	∑	W	g/p	∑	W	g/p	∑	W	g/p
Archaeological quartzite	CC																		
	CA																		
	OO	8	2517	315	4	487	122							2	1205	4	14	4209	301
	SO	3	998	333	3	288	96	2	706	353				1	32	32	9	2024	225
	BQ	12	2196	183	11	1337	122	1	151	151	1	56	56	14	1377	98	39	5117	131
	RQ	2	65	33	1	50	50							2	18				
	MQ																		
	Undet				1	197	197										1	197	197,0
	Total	25	5776	231	20	2360	118	3	856	285				19	2632	139	67	11624	173

Table-7.24: Frequency table of different core types grouped by raw material, including frequencies, weight and the ratio grams/piece for each case. Weight is expressed in grams.

and there is an enlargement of weight with the increase of extractions from the blanks with one negative scar (Figure-7.26). Nevertheless, blanks without negative scars made on SO type, are heavier than other types.

Raw material	Petrgen. type	Knapping products																	
		Core preparation			Blanks														
					No neg.scar			1 neg.scar			2 neg.scar			3 or more			Blank total		
		∑	W	g/p	∑	W	g/p	∑	W	g/p	∑	W	g/p	∑	W	g/p	∑	W	g/p
Archaeological quartzite	CC																		
	CA										1	9	8,7	3	250	83	4	259	65
	OO				18	726	40	17	770	45	23	808	35	30	2074	69	88	4378	50
	SO	1	11	11	6	348	58	7	179	26	19	499	26	30	1119	37	62	2144	35
	BQ	5	63	13	14	589	42	35	816	23	60	1597	27	64	1819	28	173	4821	28
	RQ				2	52	26	1	65	65	5	90	18	5	101	20	13	308	24
	MQ	1	14	14										1	50	50	1	50	50
	Undet				1	64	64	1	32	32	2	16	7,9				4	112	28
	Total	7	89	13	41	1779	43	61	1862	31	110	3018	27	133	5413	41	345	12073	35

Table-7.25: Frequency table of different knapping products grouped by raw material, including frequencies, weights and the ratio grams/piece for each case. The knapping products considered are core preparations/rejuvenations and blanks sorted by the number of negative scars present. Weight is expressed in grams.

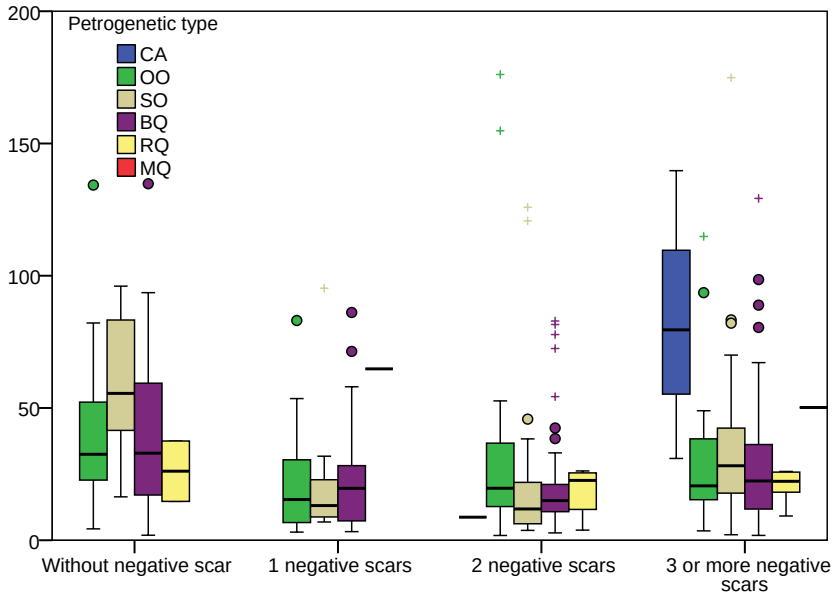

Figure-7.26: Boxplot showing the distribution of weight in grams of blanks grouped first by the number of negative scars on dorsal surface and second by petrogenetic type. There are another four “archaeological quartzites” with higher weight than 200g, not shown on chart: three OO orthoquartzites blanks that weight 952.8, 414.49, and 343.1 grams and another BQ quartzite that weight 387.9 grams. The quantity of negative scars are at least three for the first and third blanks, one for the second, and two for the latter. The weight is expressed in grams.

Finally, differences in the weight of chunks based on petrogenetic types are verifiable in Figure-7.24 and Table-7.23. Chunks made on OO type are heavier and they are more variable than those made on BQ and SO types. In addition, there is an absence of lighter than eight grams made on SO orthoquartzite.

The analysis of the relationship between raw material and retouch concludes that the heaviest retouched artefacts configured with the Simple mode are made on orthoquartzite blanks and they are lighter in the quartzite group (Figure-7.27). This relation changes in the blanks configured using the Abrupt mode. In this case, artefacts configured on quartzite are generally heavier than those made on orthoquartzite. Deeping into the morphological structure of retouch, the weight of different morphological groups maintain the differences observed in the mode of retouch (Table-7.26).

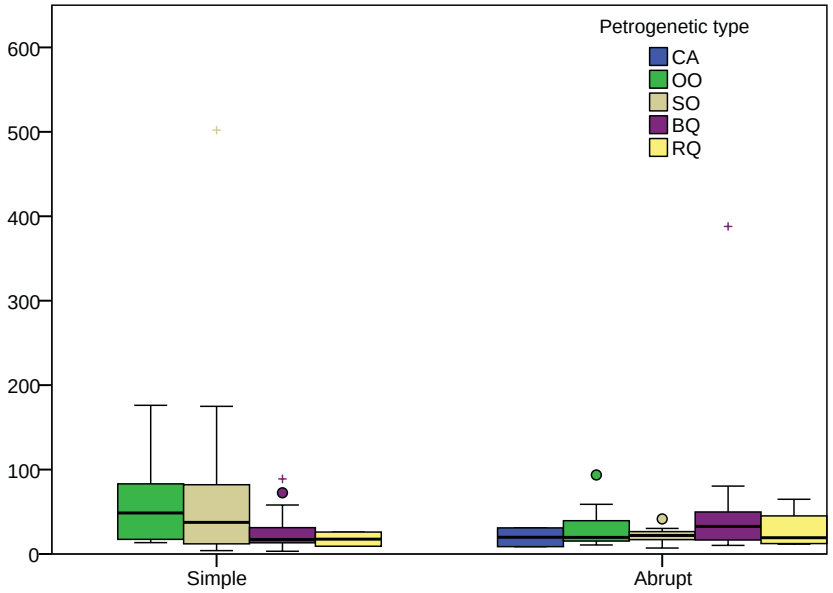

Figure-7.27: Boxplot showing the distribution of weight in grams of retouched material grouped first by order of retouch and second by petrogenetic type. There is another “archaeological quartzite” with higher weight than 600g, not shown on chart: a simple retouched OO orthoquartzites blanks that weight 952.8 grams.

		Single-retouched pieces																				
	Petrgen. type	Simple												Abrupt						Burin		
		Sidescraper			Endscraper			Denticulate			Point			Abrupt			Truncation			Burin		
		∑	W	g/p	∑	W	g/p	∑	W	g/p	∑	W	g/p	∑	W	g/p	∑	W	g/p	∑	W	g/p
Archaeological quartzite	CC																					
	CA													1	31	31	1	9	9			
	OO	12	1556	130				4	73	18	4	464	116	7	241	34				1	50	50
	SO	13	948	73	4	271	68	3	92	31				3	52	17	1	14	14			
	BQ	27	666	25	1	16	16	13	451	35	3	64	21	12	789	66	1	10	10			
	RQ	2	35	18				2	39	15	1	15	15	2	76	38						
	MQ																					
	Undet.																					
	Total	54	3206	59	5	287	57	22	654	30	8	543	68	25	1189	48	3	33	11	4	6	2

Table-7.26: Frequency table of retouched artefacts with one primary type sorted by mode of retouch and morphological group and grouped by raw material, including frequencies, weight and the ratio grams/piece for each case. Weight is expressed in grams.

7.6. RAW MATERIAL ACQUISITION AND MANAGEMENT PROCESSES IN EL HABARIO

Once the raw data from this layer have been presented, in this section we bring face to face geographical, geological, and archaeological data (the matter) to understand the forces that got these materials deposited here, that is, the human raw material acquisition and management strategies.

The main acquisition process verified in this layer is the extraction of big quantities of orthoquartzites and BQ quartzites for human activities, as demonstrated by the quantity of them found in this layer both in number and in weight. The adjacent strata of Remoña conglomerate, with abundancy of these three types, clearly determines major lithologies and most of the features of this lithic assemblage. Main lithologies and its technological features clearly define this site as a quarry/workshop. Moreover, the (small) representation of other raw materials, types of quartzites, and quartzarenite indicates they had different roles in human activities.

The management of raw material has been analysed including the raw data of all raw materials in a general reduction process model based on a simple “chaîne opératoire” (Figure-7.28). The primary technological product of lithic reduction we find in this layer are cores (irregular, discoid, levallois, or prismatic). From here on, we expose and analyse the different processes that generate other lithic products based on the understanding of their features.

1. Blanks, as well as smaller blanks (sometimes fragmented) and chunks, were obtained as a results of the reduction process of some cores. Blanks and chunks are secondary products generated as a consequence of knapping procedures.

    a. Using retouching procedures, some of these primary blanks were modified, creating retouched artefacts as primary products and more blanks and chunks as secondary products. The latter are lighter than five grams and sometimes are fragmented. In addition, new primary types can be made in the blanks to obtain retouched artefacts with multiples primary types, generating more blanks and chunks as secondary products.

    b. Some other blanks were reconfigured by percussion to obtain new flakes. The resulting products are a core on flake and blanks as primary products and other blanks and chunks, derived from the reconfiguration processes, as secondary products.

        i. Some cores on flakes were retouched, creating a retouched core on flake. Small chunks and blanks derived from the retouching process are again secondary products.

        ii. As a consequence of the reduction processes of the cores on flakes, blanks were obtained, also secondary products classified as chunks and blanks (smaller than previous blanks).

            • The latter blanks could also be retouched, creating new retouched artefact and secondary products: chunks and blanks.

2. Going back to cores, these can be retouched to obtain retouched cores. Moreover, small chunks and blanks were generated as secondary products as a consequence of the retouching process.

3. Following with cores, some of them were reconfigured to obtain new flaking surfaces, or new striking platforms. This process generated new forms or types of cores and three different secondary products: chunks, blanks (generally lighter than five grams and sometimes fragmented), and a core preparation/rejuvenation product.

    a. Some core preparation/rejuvenation products were retouched, creating retouched core preparation/rejuvenation products. As a consequence, small chunks and blanks were produced as secondary products.

    b. Some of these new cores were retouched, creating retouched cores. As a consequence, small chunks and blanks were produced as secondary products.

Some of the chunks were also retouched. They are always heavier than five grams. Blanks and chunks were generated as secondary products of retouch techniques, and they are generally lighter than five grams.

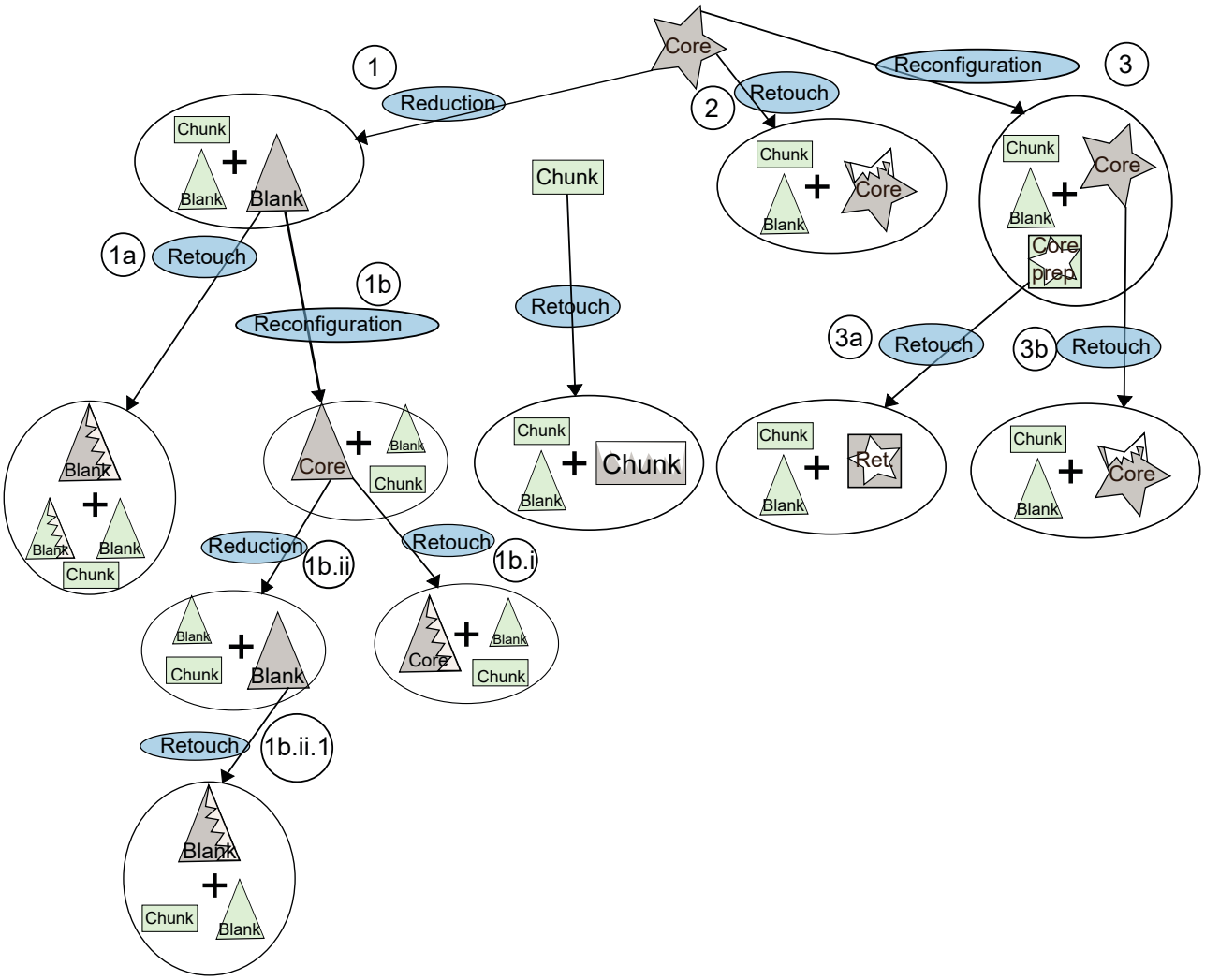

Figure-7.28: Schematic “chaîne opératoire” derived from the analysis of the lithic assemblage from El Habario. Stars represent cores, rectangles chunks, squares with stars core preparation/rejuvenation products and triangles blanks. Zig-zag lines added to any of these icons represent retouched artefacts. Grey icons are primary products and green ones secondary products. The blue ellipses indicate human activities. Alphanumeric codes inside circles are references to the text.

We start explaining the conclusion related with the acquisition and management of “archaeological quartzites” by petrogenetic types, and later, other raw material. Figure-7.29 and Figure-7.31 schematically represent the acquisition process of “archaeological quartzites” and other raw materials. Figure-7.30 displays the relationship between acquisition and management strategies. Finally, Figure-7.32 shows the Cost map from El Habario with the geological formations where raw material could have been caught.

As has been previously mentioned, “archaeological quartzite” is the most relevant raw material, both in number and weight, present in El Habario. Next, we will explain the raw material catchment and management strategies of this raw material by petrogenetic types.

The CC type is the less frequent type of “archaeological quartzite”. There is only one chunk and it is almost completely cortical. This quartzarenite has a heterogeneous grain size distribution around medium sizes and it is brown-red. This chunk has pebble morphology. Cortex is undetermined due to the influence of weathering processes on this quartzarenite. Due to the high representation of this type of “archaeological quartzite” in the adjacent Remoña conglomerate, we proposed this chunk is related with it. We propose two different hypothesis to understand its features on its context: it could be a testing rock or a hammer. The first hypothesis proposes this chunk was a wasted product derived from block testing to obtain other types of “archaeological quartzites”. The second one suggests the versatility and adaptation of human behaviour in raw material catchment strategies.

The CA type, only constitutes a small portion of the total of “archaeological quartzites”, but it is

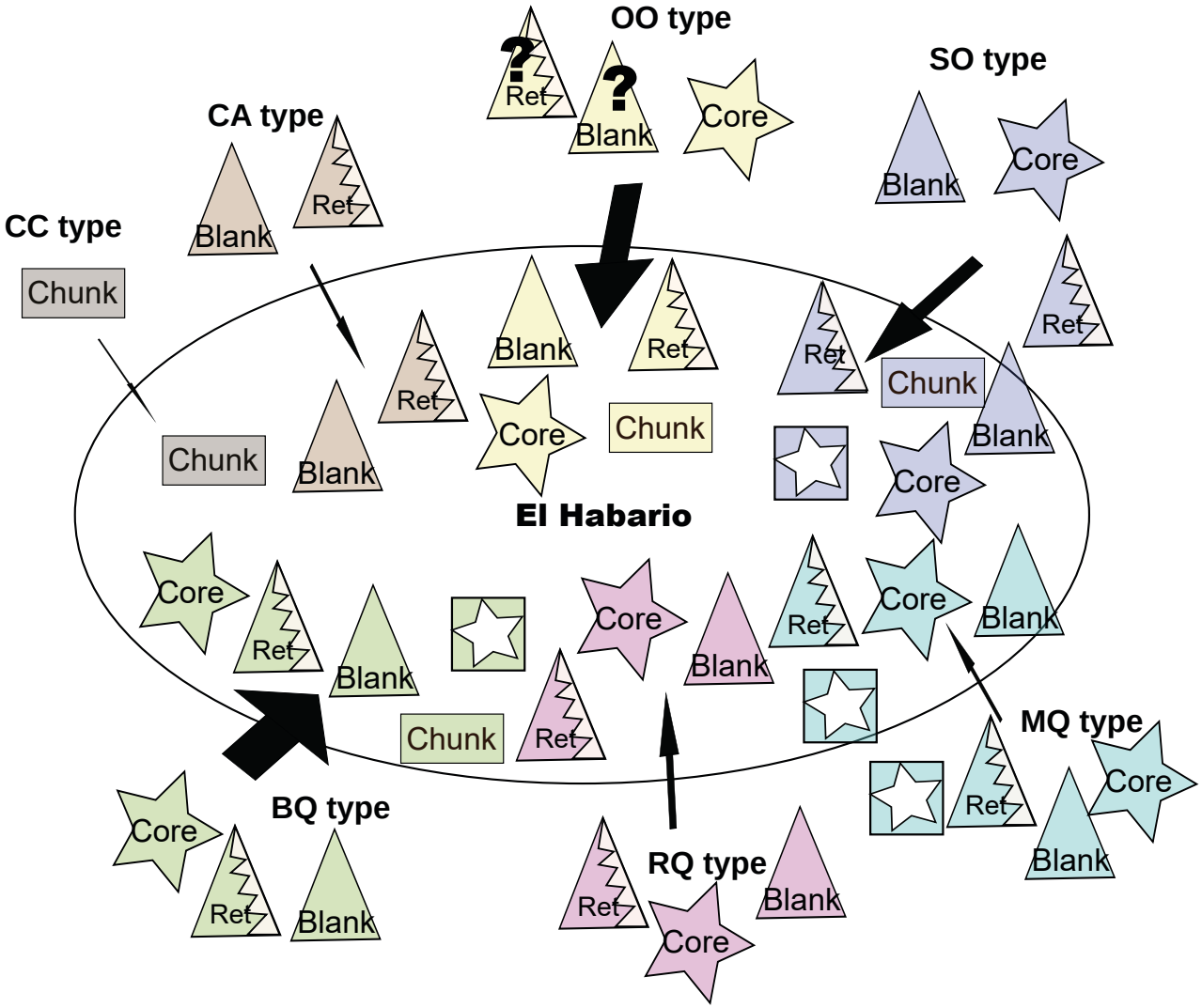

Figure-7.29: Schematic representation of the input of the different petrogenetic types of “archaeological quartzite”, taking into account the different technological products present. Stars represent cores, triangles blanks, triangles with zig-zag retouched material, ellipses fully cortical chunks and rectangles chunks. Question marks indicate products whose presence is not certain.

better represented than the CC type with four items. All four are blanks and, even though three have cortex, it is always less extended than 33% of their dorsal surfaces. The quantity of negative scars is high, with at least two negative scars on all blanks. Two of them were retouched with two abrupt retouches. Weight distribution and categories identified does not points that knapping or resharpening processes were carried out in the site. In addition, weight distribution suggests this material was not intensively exploited. All these features allow us to propose this quartzarenite was medium intensity exploited, probably used for specific activities.

The characterisation of this petrogenetic type reveals grain size is heterogeneously distributed across the lithics. Colour is more homogeneous, and there is no differences in mineral characterisation between different implements. The input in the site of CA quartzarenite probably derived from only one pebble. The colour variety links this quartzarenite with Carboniferous conglomerate formations. The characterisation of cortical areas points that all cortex derived from conglomerates. In the adjacent Remoña Formation conglomerate, we do not characterised this CA. Therefore, CA petrogenetic were carried into the site from other carboniferous formations. These conglomerates could be the Curavacas conglomerate to the south, nine Cost Units away; Valdeón (25 CU) or Pontón (26 CU) conglomerates to the south-west, in the Valdeón area; or Pesaguero (nine CU) or Porrera (seven CU) conglomerates, to the south or south-east. All of them are located at middle-altitudes. In these conglomerate there is an important presence of this petrogenetic types. Therefore, strong selective mechanism are not necessaries. We propose catchment of CA quartzarenites was based on sporadic activities. These activities would have been complementary to other tasks, such as catchment of other petrogenetic quartzite types or exploitation of the landscape where these conglomerates

display. The input to the site could have been made in form of blanks or retouched material, showing distant catchment and movement of raw material as a material, probably stored for specific purposed and maybe related with its size.

The OO petrogenetic type of orthoquartzite shows clear differences in management and

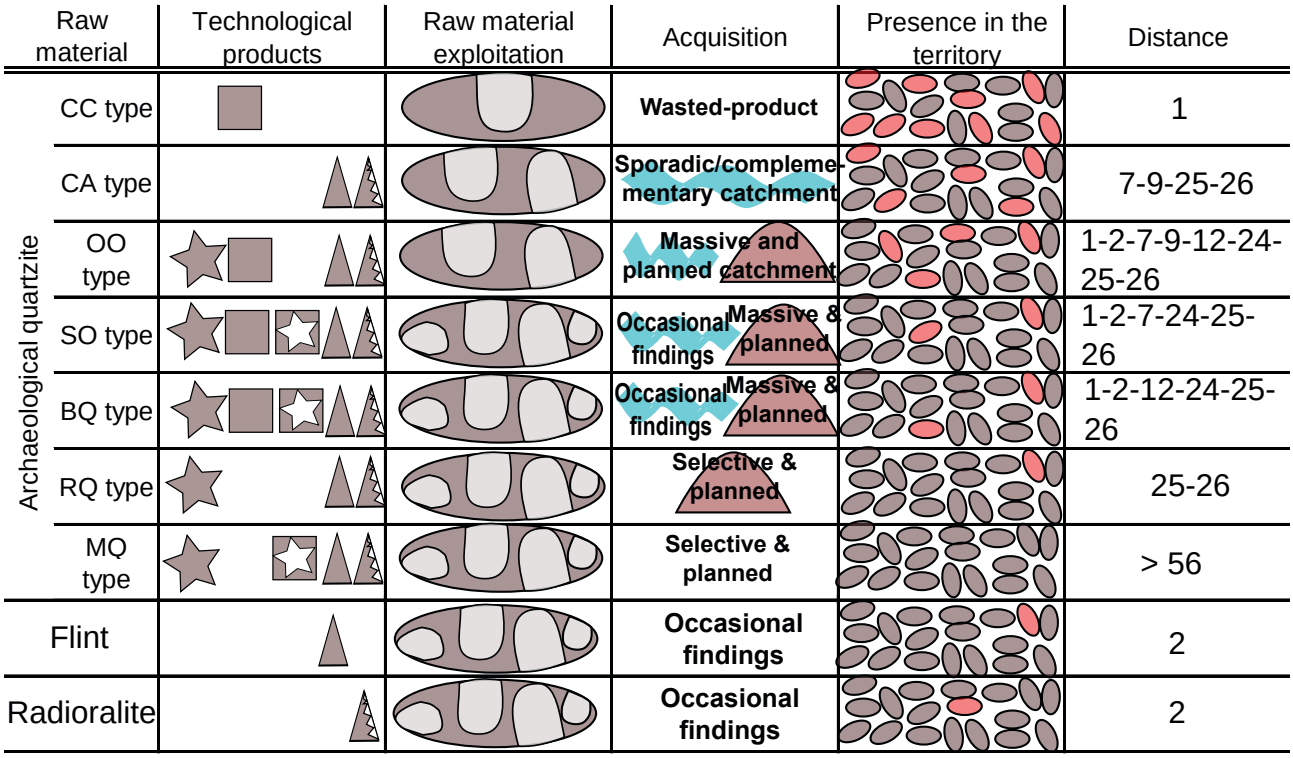

Figure-7.30: Schematic representation simplifying raw material acquisition and management evidences from El Habario. In the column “Technological products” stars represent cores, squares chunks, squares with starts core preparation/rejuvenation products, and triangles blanks. Zig-zag lines added to any of these icons represent retouched artefacts. In the column “Raw material exploitation”, circles represent unexploited raw material, ovals with one scar represent low intensity raw material exploitation, ovals with two scars represent medium intensity raw material exploitation, and ovals with four scars represent high-intensity raw material exploitation. In the column “Acquisition” waving blue lines represent river acquisition and brown semicircles represent conglomerate acquisition. In column “Presence in territory”, the complete set of ovals represents all the raw materials available in the territory. The ones highlighted in red represent the proportional presence of each specific raw material in the territory. Higher presence of the latter means weaker selection degree.

catchment in comparison with the raw material and types of “archaeological quartzite” tackle above. It represents 24% of the lithic assemblage in number and 36% of weight. These data mean there was an intensive and planned input of this type. The three technological categories considered are present in the layer, although there are no core preparation/rejuvenation products. It is obvious knapping and reshaping activities were practised in the site. This is also certified by the presence of blanks and chunks with weight between one and 700 g. There is a high quantity of cores and almost all types of them are represented. Nevertheless, cores on flake are less frequent than on other types. In addition, cores are generally heavier than on other petrogenetic types, and none of them is lighter than 50 g. The quantity of negative scars on dorsal surfaces is variable and the categories proposed have similar frequencies to those observed in SO and BQ types. Nevertheless, the quantity of knapping products without negative scars is the highest of all “archaeological quartzite” types. The frequency and extension of cortical areas on dorsal surfaces is higher than SO and BQ types. The frequency of retouched artefacts is slightly smaller than on other petrogenetic types and no chunk is retouched. Nevertheless, artefacts with multiples primary types are well represented. In addition all order of retouch and morphological group are defined (except the Truncation and Endscraper). This evidence reveals medium intensity exploitation. The grams/piece ratio of the lithics from this layer, generally heavier than on other types, agrees with this hypothesis.

The characterisation of this raw material based on grain size and colour indicates it is a more heterogeneous type, with at least three different varieties represented. Due to the impact of weathering processes and the sediment composition, we could not determine colour or mineral varieties.

The original source strata of three grain sizes varieties is in the more deformed bands of Barrios outcrops Formation, as well as in the pebbles of carboniferous conglomerates from older layers. The characterisation of cortical area reveals that most of them come from conglomerates. Still, there is a presence of fluvial cortex in five implements (two of them are cores). There is no evidence of outcrop cortex. Therefore, although the most-likely source strata is the Barrios Formation, catchment was probably made in conglomerates and deposits. Most of the conglomerates in the area have OO orthoquartzites, as in the adjacent conglomerates from Remoña Formation. In this conglomerate it is possible to find them without the need to apply any selective mechanism. Other conglomerates, such as the Curavacas series, the Lechada (eleven CU), Campollo (twelve CU), Maraña-Brañas (24 CU), Narova (seven CU), Pesaguero, Pontón, Potes (twelve CU), and Valdeón conglomerates have important amounts of this type. However, at least low intensity of selective mechanisms are necessary to choose specific varieties, forms and sizes. Except the adjacent Remoña conglomerate, all these conglomerates are to the south, in medium altitude plateaus. In fluvial deposits the presence of this petrogenetic type is scarcer. Therefore, the selective mechanisms required pick special varieties, forms and sizes would have been more intensive. The acquisition in the site, then, is mixture in fluvial and conglomerate areas, with a clear predominance of the latter.

Taking into account the management of this orthoquartzite and the information of OO type in the area, we proposed two different human raw material behaviours: The first is characterised by a primary access and acquisition of an abundance material in the adjacent Remoña conglomerate. The second points at more complex acquisition processes in distant areas in river deposits and in conglomerates. The first is related with primary acquisition and selection of interesting blocks and forms of raw material for activities in the site and its output for future uses. The abandonment of this material in non-completely exploited stages could reveal this orthoquartzite was a secondary but used product. The second raw material behaviour is more related with the discard of raw material storage in abundance of lithic resources. This raw material were acquire in distant conglomerates or in fluvial deposits. In the latter, the selective mechanism require are more intensive than in the former context.

The SO petrogenetic type shows different management strategies, but similar catchment process to previous type. Eighteen percent of items and weight of “archaeological quartzite” are made on SO type. It shows a higher exploitation of this orthoquartzite type than previous one, even though the smaller quantity of items. The three technological orders, as well as core preparation/rejuvenation products are represented in this site. It is clear knapping and reshaping activities were carried out in the site, as demonstrated by the presence of blanks and chunks with smaller weights than three grams. Core types and their weights reveal this raw material is the most intensively exploited orthoquartzite, even though all cores are heavier than 30 g. Despite there are small differences between petrogenetic types in the distribution of negative scars on blanks, the SO type is the most exploited “archaeological quartzite”. In addition, cortex on dorsal surfaces is worst represented and extended than on other “petrogenetic types”. The proportion of retouched artefacts is greater than in previous orthoquartzite. There is an important presence of artefacts with multiple primary types. These evidences indicate this material is very intensively exploited. The grams per piece ratio of the items, is smaller than in previous one, even it is still heavier than quartzite types.

The petrological characterisation of this petrogenetic type does not allow us to stablish different grain size or mineral/colour varieties. The original outcrop strata of this orthoquartzite is not located in the research area, but they can be found in conglomerate strata and deposits. The conglomerates with the SO petrogenetic type are the adjacent Remoña Formation, the Lechada, Maraña-Brañas, Pontón, Potes, and Valdeón conglomerates. In all of them its presence is between 5 and 50%, except for the Lechada and Potes conglomerates, where they represent less than 5% of the pebbles. The presence of SO orthoquartzite in fluvial deposits is negligible. Despite only two recognised cortical surfaces derive from fluvial deposits, both types of cortex are represented. Conglomerate cortex is majority.

Taking into account the management of this orthoquartzite and the information of the type in the area, we proposed two different human raw material behaviours: The first is characterised by a primary access and acquisition of an abundance raw material in the adjacent Remoña conglomerate. The second one shows a more complex acquisition process in distant areas in fluvial deposits or conglomerates. The first is related with primary acquisition and selection of interesting blocks and forms of raw material for activities in the site and its export for future uses. The abandonment of this material in more exploited stages than on previous type points that this orthoquartzite was a primary or main product acquire in Remoña conglomerate. The second raw material behaviour is related with the discard of raw material storage or specific toolkit in abundance of lithic resources . This

raw material were acquire in distant conglomerates or in fluvial deposits. In the latter, the selective mechanism require are more intense than in the former context. The acquisition in river deposits is more related with occasional findings than planned strategies.

The management and catchment strategies observed in the previous type are clearer in the BQ quartzite type, especially due to the higher quantity. The quantity of lithics, 53% of "archaeological quartzite" and its weight, 43% of the complete assemblage, points at exhaustive, planned and intensive catchment strategies. All the technological products are defined, all of them are retouched. Therefore, it can be concluded that knapping and reshaping activities were performance in the site are clear. The presence of chunks and blanks smaller than three grams supports this statement. The grams per piece ratio, especially that of blanks, indicates lithic implements in this type tend to be lighter than on previous group. Core types (with high quantity of cores on flake), and its weight reveal this petrogenetic type is intensively exploited. Nevertheless, there is a high variability of weight in cores, from smaller values than ten grams to heavier than 800. Despite there are small differences between petrogenetic types in the distribution of negative scars on blanks, the quantity of scars in dorsal surfaces (generally with more than two) point at this "archaeological quartzite" was intensely exploited. Nevertheless, the frequency of cortical surfaces in blanks is similar to OO petrogenetic type. The frequency of retouch in this petrogenetic type is high, also the frequency of artefacts with multiples primary types. In addition, all morphological groups defined in the site are made on BQ type. All in all, the data gathered demonstrate this quartzite is an intensively exploited raw material and all phases of lithic reduction were performed in the site.

The petrological characterisation of BQ type allows us to propose two different grain size varieties, as well as another two mineral/colour varieties. Therefore, four different varieties of BQ type coexists in the site. All of them have similar frequencies. We did not find the original outcrop strata for this type of quartzite in the field survey. However, it was clearly identified in some small conglomerates. The presence in fluvial deposits is negligible. There are important quantities (between 5 and 50%) of BQ quartzite in the Remoña, Valdeón, and Pontón (nearest location at 26 CU) conglomerates. In other conglomerates, such as Maraña-Brañas, Pesaguero, and Potes, it is scarcer. Coarser grain size varieties of BQ are restricted to the Pontón conglomerate, although we do not discard its presence in Remoña conglomerates. Most of the cortical surfaces identified derived from conglomerates. Therefore, most of the BQ quartzite type were acquire in these contexts. Fluvial cortex presence is only identified in three implements. Fluvial cortex is not associated to any specific variety.

As it happened in the previous two orthoquartzites catchment activities were done based on two mechanisms. The main acquisition activity is related with the extraction of big quantities of BQ type in the adjacent Remoña conglomerate applying medium intensity selective mechanisms. This mechanism is characterised by a primary selection and acquisition of interesting blocks and forms of raw material for activities in the site and its later export to other sites for future uses. The abandonment of this material in more exploited stages than on previous two orthoquartzite reveals this quartzite was the main raw material here exploited. This is also reinforced by a more complex management of raw material here described, especially due to the quantity of core preparation/rejuvenation products identified, the quantity of core on flakes, and the weight distribution of cores. The second raw material acquisition mechanism points at more complex acquisition in distant areas and the abandon of raw material storages. This mechanism is based in occasional finding in river deposits in relation with other activities, such as movement along river or the acquisition of other resources. Nevertheless, we do not discard acquisition of BQ quartzites in other conglomerates distant to the site of El Habario in medium-scale mobility and in South and South-west direction.

The RQ quartzite type presents different patterns of catchment and management. The quantity of this type of raw material found in this context is reduced to 4% of total of items and 2% of assemblage weight. Despite cores and knapping products are frequent in the assemblage, chunks and core preparation rejuvenation products are not represented. Cores are overrepresented, especially in the comparison with other petrogenetic types. Retouched material is also overrepresented. The presence of lighter than ten grams blanks is reduced, then, even though knapping and resharpening processes were carried in the site, they were reduced in number. Most of blanks have at least two negative scars, despite blanks without and with one negative scars are also represented. The presence of cortex on blanks and cores is scarce. All these data suggest this resource was intensively exploited. The gram per piece ratio is the smallest of all "archaeological quartzites" types, especially in the core category. The latter reinforces the idea that this resource was intensively exploited. We propose the input of this type was occasional and it was brought as cores, blanks or retouched artefacts that could be used, reduced or reshaped for specific activities. The lack of chunks (derived

from knapping and reshaping) and core preparation/rejuvenation products support this hypothesis.

The petrological characterisation of this raw material does also agree with the previous hypothesis. The analysis of grain size reveals two different varieties: the medium-grained and the fine grained one. Both varieties are similarly represented. There are also another two mineral/colour varieties: the dark and the orange one. The first is reduced to only two items. Therefore, there are, at least, three different blocks of rocks input into the site. We were unable to find any evidence of this quartzite in the massive outcrops of the surveyed area. Its presence is reduced to two conglomerate formations: the Pontón and the Valdeón conglomerates, both in the south-west of the research area. Still, the presence of this type is scarce in both conglomerate formations. Taking into account the recognisable cortical areas, all of them derive from conglomerates. These data indicate that catchment activities of this type necessarily implied medium or long distance movement even outside the Deva basin. In addition, the evidence above supports the existence of strong selective mechanisms, not only in deposits (probably related with occasional findings), but in conglomerates. The presence of this type in the site does also reveal a conscious mechanism of selective and conservative exploitation of raw material. The intense exploitation of this material and its appreciation as singular, valuable, and exiguous is clear. Nevertheless, and probably due to the abundancy of other interesting raw material, the small quantity of RQ quartzites carried as a toolkit or as storage of lithic mass were abandoned in El Habario.

The MQ quartzite type shows catchment and management patterns similar to the previous type. The quantity of this type of quartzite is even smaller than previous type. As a consequence of this small number of lithics, conclusion must be nuance. There are only four implements, 0.3% of the lithic assemblage. The representation of technological products is not complete due to the absence of chunks. There is neither cores made on flakes. The quantity of retouched material is the smallest of all “archaeological quartzites” types. Retouch is only observable in a core. The gram/piece ratio is greater than previous RQ quartzite, but smaller than ratio of other types. There is no obvious evidence of knapping processes in the site, chunks are absent and none of blanks weight less than ten grams. The quantity of negative scars on dorsal surfaces is always higher than two. In addition, none of the implements have cortex. All this data suggest an even more intensively exploitation of this raw material than on previous type. Even the existence of a core preparation/rejuvenation product and a core, we consider knapping or reshaping activities were not carried out in the site.

We do not identify different colour or grain size varieties among the MQ quartzites in this layer, conditioned by the small quantity of this type and the preservation of surfaces. We did not found any evidence of this quartzite in the research area surveyed. Then, the only possibilities are a) in non-surveyed strata, b) outside of the research area, or c) hidden in deposits or conglomerates in small percentages. The absence of cortical surfaces in these quartzites does not allow to stablish its possible source area. Nevertheless, the MQ quartzite points at conscious mechanism of selective and conservative exploitation of raw material. It is clear this quartzite was intensively exploited as a singular, valuable, and exiguous raw material, maybe related with mobile tool-kit or storage of raw material that travel along long distance dynamics, as proposed in by other authors on other regions (Turq et al., 2013).

Next we will explain the raw material catchment and management strategies of other raw material. These material are not frequent in El Habario assemblage, although they reveal different roles of raw material and interesting catchment and management behaviour.

Starting with the small representation of radioralite, it is the second less represented raw material with two only items. Both are blanks with at least three negative scars. They are retouched with Simple Sidescraper. None of them have cortex. The weight of one is reduced to 2.7 g, while the other is bigger, 16.16 g. This features points at this raw material was intensively exploited. Nevertheless, there is no evidence of knapping or resharpening activities. The input of radioralite is probably related with mobile tool-kit for specialised actions. Regarding the physical features of radioralites, both are red to brown and are characterised by the presence of Radiolaria fossils. We only find evidence of radioralite in the area surrounding the fluvial deposits of Cares and Deva rivers, in negligible proportions and small sizes. Therefore, catchment activities would have necessarily implied strong and intensive selection mechanisms. This means that the acquisition of radioralite would have been related with occasional findings, rather than with planned raw material selection strategies in river beaches.

Flint is the less represented raw material with only one piece. It is a blank with at least three negative scars, it has no cortex and it weights 3.52 g. This blanks is not retouched. Therefore, flint is

intensively exploited, but as on radioralite, there is no evidence of knapping or retouching processes in the site. The flint is black and it can give a hint on its origin, probably related with Palaeozoic Black chert such as Vegamián Formation (Herrero-Alonso et al., 2016). Due to the absence of cortex, we could not determine the area where flint were caught. The input of this intensively exploited blank was probably related with its physical properties and its scarcity in the area, carried into the site as a mobile toolkit, as proposed by other authors (Bustos-Pérez et al., 2017).

All in all, we observe different catchment and management strategies for each raw material. This

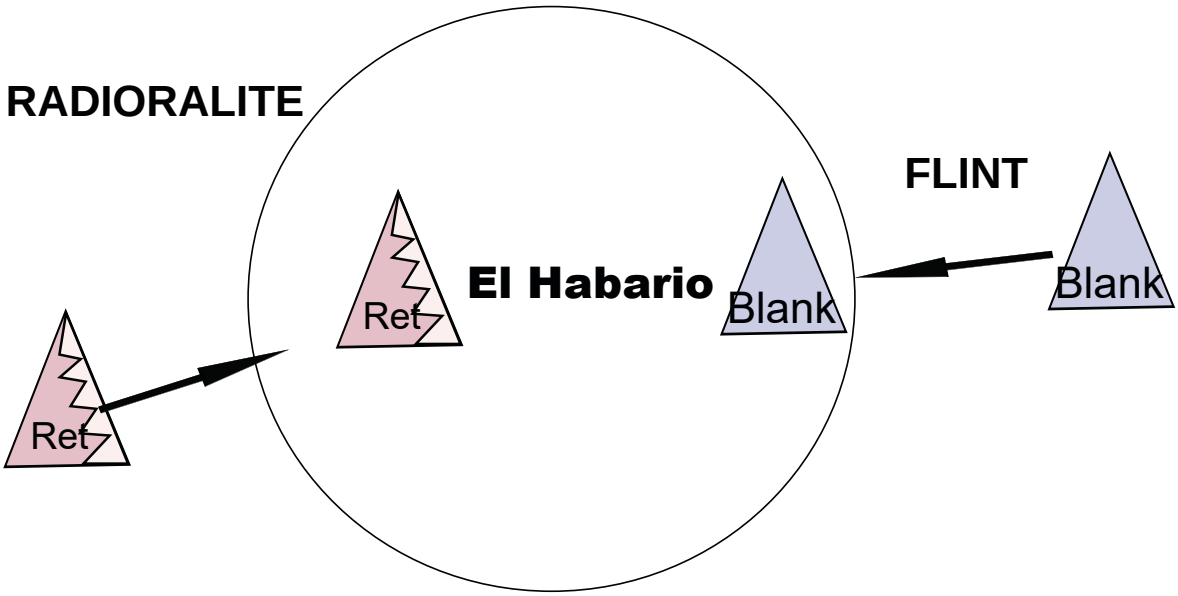

Figure-7.31: Schematic representation of the input of non-“archaeological quartzite” raw material, taking into account the different technological products present. Triangles represent blanks and triangles with zig-zag retouched material.

allows us to propose the following human mobility, landscape use and selective and exploitation mechanisms.

- Low, medium and high scale mobility to the South and South-west of the research area, as well as outside it.
- Exploitation of diverse landscapes, from fluvial courses in low altitudes areas to plateaus in medium altitudes zones.Selective and non-selective mechanisms for obtaining specific raw materials or petrogenetic types in deposits and conglomerates.
- Diversity of raw materials exploited, selected based on their physical properties and their availability in the landscape.
- Direct exploitation and management of lithic resources in conglomerate surrounding areas. This points at a) technological and selective behaviours to take advantage of specific raw materials, b) technological and selective behaviours to take advantage of other resources as secondary products, c) dismissal of non-interesting type.
- Management of raw material through the abandonment of storages in abundancy of raw material, that is, the substitution of storages and tool-kits.

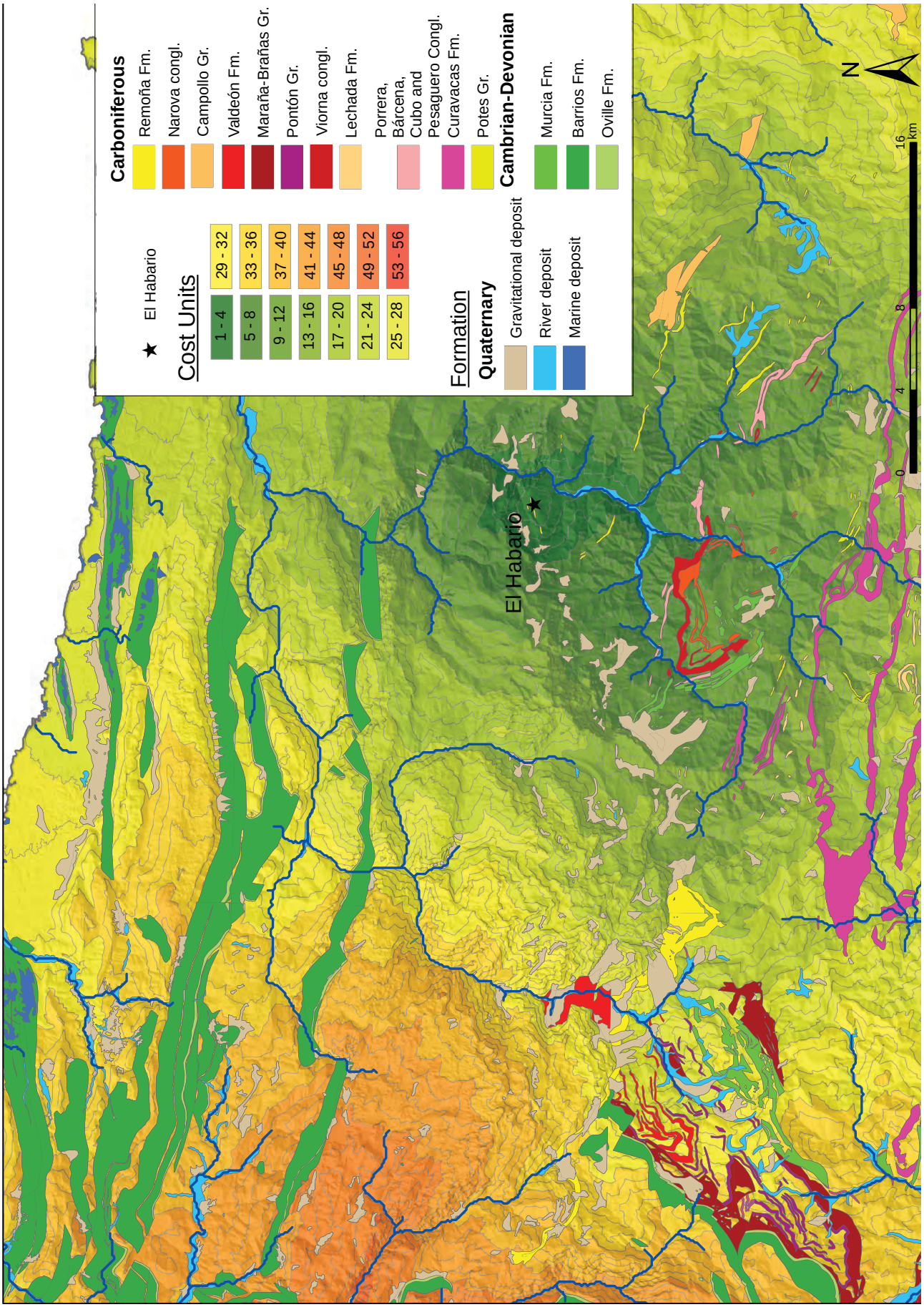

Figure-7.32: Cost map from the site of El Habario to polygons with presence of “archaeological quartzites” and other raw materials.

CHAPTER-8

RESULTS. THE LAYER-XXII-R FROM THE ARCHAEOLOGICAL SITE OF EL ESQUILLEU

8.1. GENERAL ISSUES AND STATE OF PRESERVATION OF THE COLLECTION

In the next three chapter, we present the results obtained at the archaeological site of El Esquilleu. The description of the three archaeological layer analysed will follow the stratigraphy sequence from the bottom to the top of the sequence. The archaeological site of El Esquilleu is a small cave situated in the Cantabria Autonomous Community near the villages of Lebeña and Allende. It is situated 100 meters away from the left margin of the Deva River and 70 meters above it. The cave is within the Valdeteja Formation, mainly composed of massive limestone. Cliffs, defiles, talus slopes, moraines, caves and deep gorges are the most important geomorphological features in the area surrounding El Esquilleu Cave. The area is crossed by the Deva River valley that creates a deep and narrow gorge in North-South direction called The Hermida Defile, where the cave is located. The excavation of the site was directed by Dr. Javier Baena Preysler between 1997 and 2006 trying to understand the Middle Palaeolithic societies of the area through a diachronic perspective. The sequence was entirely excavated, at leas in a four meters pit. The stratigraphic depth was 4.20 meters and it was divided into 41 layers (29 with anthropic evidences). Although the research processes in El Esquilleu Cave is still in progress, several studies have already been carried out by different specialist.

In general, the information provided by all perspectives, previously commented in chapter-2, offered interesting perspectives about the human groups who inhabited this cave in Prehistoric times, especially during the late Middle Palaeolithic. In general terms, the sequence of El Esquilleu Cave showed sophisticated strategies of habitat and land use by Neanderthals groups, which were modified through time according to environmental conditions and cultural, social and economic circumstances (Baena et al., 2012). Summing up, we can say that El Esquilleu is one of the most important archaeological sites in the Cantabrian Region for understanding the last Neanderthal groups in the Iberian Peninsula.

The layer-XXII-R is the first and the oldest analysed layer in this research. Sedimentological, this layer is in the third part of the sequence, ESQ-C, and it is mainly composed of thin and dark layers created as consequence of widespread flooding and intensive human activities, represented as fireplaces and other dispersed burned findings. The presence of siliceous material was massive in the sandy and silty matrix. This layer had been diagenetically altered by a source of dissolved phosphate, which triggered the partial dissolution of bone and ash in the sediments of this anthropogenic-rich layers (Jordá et al., 2008; Mallol et al., 2010). Numerical data obtained from Layer-XXII-R (OxA-20321 > 59600BP, Mad3299 = 51034 ± 5114BP, and Mad3300 = 53491 ± 5114BP) point that this Layer must be older than 50 kyrs Cal BP (Baena et al., 2012; Cuartero et al., 2015; Maroto et al., 2012). During the formation of Layer-XXII-R, paleoenvironmental conditions are related with cold conditions in open landscape mainly represented by *Pinus*, *Betula*, and *Cupressaceae*. The first specie was used as fuel in the numerous fireplaces documented in the ESQ-C sequence in which Layer-XXII-R is situated (Uzquiano et al., 2012). Faunal analysis point at the consumption of *Capra pyrenaica*, although other species, such as chamois or deer were also introduced in the site. The bones have no marks from carnivores, therefore, humans is the main agent who introduced fauna in the site during the formation of this layer. In addition, most of the bones are burned and extremely fractured, probably used as fuel for fires or because sanitary purposes (Yravedra and Gómez-Castanedo, 2014; Yravedra and Uzquiano, 2013). Concerning to lithic raw material, previous studies point that “archaeological quartzite” is the better represented raw material in the layer (Manzano et al., 2005). Nevertheless, flint, quartz, or radioralites are also represented. The techno-typological characterisation of the layer concludes that main reduction sequence used is the discoid method (Baena et al., 2005; Carrión et al., 2008; Carrión et al., 2013).

The archaeological assemblage analysed is a sample of the complete collection. We analysed the complete lithic assemblage from the square J-10 for current study. The analysed set is composed by 791 lithic objects. The general state of preservation is medium because many pieces have carbonates and clayey minerals in surfaces. In addition there are chemical weathering and other processes in part of them altering parts or complete surfaces, especially in cortical areas, non-deformed/metamorphic surfaces or jointed areas. Patinas also appear in some lithics. Nevertheless, the preservation of others are good, as previously pointed by Jordá et al. 2008. As on other layers from El Esquilleu Cave, most of the pieces were not previously washed to preserve possible residues or use/hafting-wear marks to be analysed in the future. In the cases where no part of the surface was not clean enough, I washed a small portion of it to obtain a clear analysis surface.

8.2. PETROLOGICAL STRUCTURE

Here we present the data of raw material characterisation. We were able to determine all main lithologies except in one piece. In general, the collection is mainly formed by “archaeological quartzites” with small representation of quartz and flint. The presence of radioralite and lutites is residual (Table-8.1).

Main Raw Material	Archaeological quartzite	Flint	Limestone	Limonite	Lutite	Quartz	Radioralite	Volcanic rock	Undetermined
Σ	684	39	0	0	8	40	19	0	1
%	86,5	4,9	0,0	0,0	1,0	5,1	2,4	0,0	0,1

Table-8.1: Frequency table of lithologies identified in layer-XXII from the archaeological site of El Esquilleu.

Focussing on “archaeological quartzites”, the seven proposed petrogenetic types are represented in this layer. Orthoquartzite is the best represented group, with higher representation than 71% of “archaeological quartzites”. Quartzarenite and quartzite groups are underrepresented with 14% and 11%, respectively (Table-8.2). We were unable to identify 22 pieces, 3% of the collection. Coming to the distribution of grain size, the majority of “archaeological quartzites” is distributed on a single mode (51%), followed by general heterogeneous distribution (33%), and bimodal distribution (13%). Regarding grain size, the most frequent category is medium size even though small size category is also well represented. Coarse grain size varieties are scarce. As to “archaeological quartzites” types and sizes varieties, we identify some preferential varieties: OO type characterised by medium grain size in, both homogeneous or heterogeneous distribution, and SO petrogenetic type with fine grain size varieties. These association is reinforced by the Chi-square test (χ^2 (48, N = 662) = 414.987, p < .001).

			Petrogenetic type																	
			CC		CA		OO		SO		BQ		RQ		MQ		Unknow		Total	
			Σ	%	Σ	%	Σ	%	Σ	%	Σ	%	Σ	%	Σ	%	Σ	%	Σ	%
Grain size characterisation	Homogeneous and one mode distribution	Fine grain	3	6	4	9	29	9	55	30	22	42	13	76	4	67			130	19
		Medium grain			7	16	**166**	**54**	30	17	11	21	2	12	1	17	2	9	219	32
		Coarse grain							4	2									4	1
	Heterogeneous and two modes distribution	Fine grain			4	9	8	3	44	24	13	25	1	6			2	9	72	11
		Medium grain	4	8			1	0	4	2					1	17	3	14	13	2
		Coarse grain									1	2					2	9	3	0
	Heterogeneous distribution	Fine grain	3	6	3	7	1	0	6	3	1	2							14	2
		Medium grain	24	45	14	32	**97**	**31**	27	15	2	4	1	6					165	24
		Coarse grain	19	36	12	27	7	2	11	6	2	4							51	7
	Unknown																13	59	13	2
		Total	53	8	44	6	309	45	181	26	52	8	17	2	6	1	22	3	684	100

Table-8.2: Frequency table of petrological features identified in layer-XXII from El Esquilleu based on binocular characterisation. Columns are petrogenetic types and rows contain the characteristics of grains according to size, classified first by distribution and second by size itself. Cells in black are the categories representing more than 10% of the total of cases. Cells in dark grey are the categories representing between 5 to 10% of the cases. Finally, cells in light grey are the categories representing between 1 and 5% of cases.

Non-quartz mineral	A		B		C		General	
	Σ	%	Σ	%	Σ	%	Σ	%
Absence	26	4	26	4	27	4	79	4
Fe-Oxides	643	94	8	1	4	1	655	32
Manganese Oxides	8	1	81	12	127	19	216	11
Calcites					1	0	1	0
Micas	5	1	302	44	116	17	423	21
Black mineral	1	0	258	38	376	55	635	31
Pyrites	1	0	4	1	21	3	26	1
Feldspars			5	1	12	2	17	1
Total	684	100	684	100	684	100	2052	100

Table-8.3: Frequency table of non-quartz minerals identified in layer-XXII from El Esquilleu based on binocular characterisation. Columns are the three fields examined and rows are the non-quartz minerals identified.

Colour	On fresh cut			
	Primary		Secondary	
	Σ	%	Σ	%
Absence	5	1	74	16
White			7	2
Grey	82	18	105	23
Black	40	9	39	9
Blue			6	1
Green			16	4
Orange	86	19	96	21
Brown	236	52	68	15
Yellow	3	1	6	1
Red	5	1	40	9
Total	457	100	457	100

Table-8.4: Frequency table of colour hue of the samples from layer-XXII from El Esquilleu. Columns are primary and secondary colour hues and rows are the colours considered.

We identified non-quartz minerals in 684 pieces of “archaeological quartzite”, after having excluded the lithics assigned to unknown type (Table-8.3). The most represented mineral is the iron oxide, followed by non-identified black mineral, mica and manganese oxide. All these minerals are present in any petrogenetic type. The only exception are manganese oxides, which are mainly associated with SO and BQ types. Pyrite and feldspar are worse represented than previous minerals. They are related with specific petrogenetic types: pyrite with RQ and MQ quartzites, and feldspar with the quartzarenite group. The characterisation of colour indicates that most of the frequent colours are grey, white, black, and brown (Table-8.4). There is an association between the light-white colour with OO and MQ petrogenetic types. Black colour is associated with SO and BQ types. Finally, brown coloured lithics are associated with quartzarenites. Most of lithic objects described with blue tonality are associated with SO petrogenetic type.

We have carried out petrographic and geochemical characterisation of nine items, with the aim of better recognising the variability on OO and SO types (Figure-8.1). The description of these samples helps us understand the differences between types, as well as define and establish some interesting varieties. Finally, we analysed in detailed other petrogenetic types using non-destructive techniques.

8.2.1. THE CA PETROGENETIC TYPE IN EL ESQUILLEU, LAYER XXII

ES-263 is the only CA type sample. The thin section shows clastic grained texture and tangential packing. The qualitative characterisation of grain features points out the major presence of clastic quartz grains, concavo-convex quartz limits and a limited quantity of syntaxial quartz overgrown. Some isolated grains show evidence of old metamorphic processes such as undulatory extinction and deformation bands. Regarding quartz grain size, we observe a clear heterogeneous distribution with grains from medium sand to medium silt sizes. The circularity and roundness indexes also certify a heterogeneous distribution of quartz, with rounded and irregular quartz grains. There is no preferential orientation of quartz grains in the sample. The features observed through binocular microscopy are in concordance with this characterisation: coarse grained texture and tangent packing, granular T&P. The size characterisation of grains under binoculars also shows a heterogeneous distribution and coarse grain size (Figure-8.2).

Petrographic characterisation of this sample points at the small presence of siliceous matrix and carbonated cement. Non-quartz minerals are well represented in the sample, mainly as iron oxides, zircon and mica. The X-Ray fluorescence reveals multiple components in addition to SiO_2 such as Al_2O_3, Fe_2O_3, or K_2O. The characterisation of non-quartz minerals under binoculars is consistent with previous data due to the presence of mica, non-identified heavy and black minerals, and iron oxides. The colour of sample is mainly white. Nevertheless, orange or reddish oxides are visible on the surface due to the presence of iron oxides.

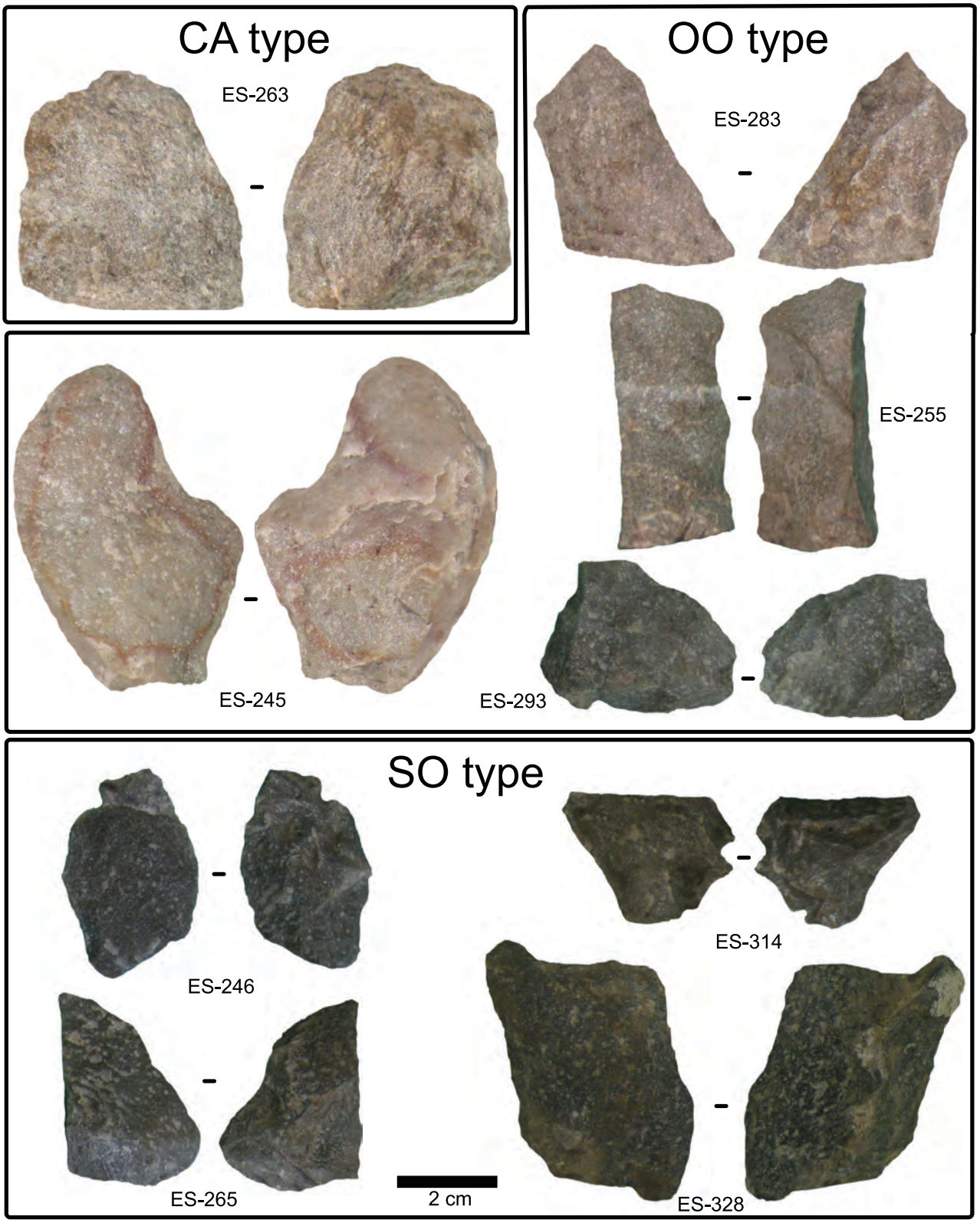

Figure-8.1: Pictures of the samples selected from Layer-XXII of the archaeological site of El Esquilleu. Samples are grouped by petrogenetic type.

The characterisation of this sample allows us to certify the presence of quartzarenites in Middle-Palaeolithic contexts and certifying its role as raw material on knapping activities. This sample also proves that non-destructive characterisation of quartzarenites in archaeological contexts is consistent and it is not the consequence of weathering processes on lithic surfaces. Regarding the characterisation of the complete lithic assemblage of this type, this sample is one of the multiple input of different grain-size and colour varieties in the layer. Despite quantitatively this sample belongs to the most common variety there is also a smaller grain size variety. There are other two colour and

mineral varieties, the brown one with iron-oxides, non-identified heavy and black minerals, and mica or feldspar; and the black variety, minority, with the latter first two minerals and manganese oxides or pyrite.

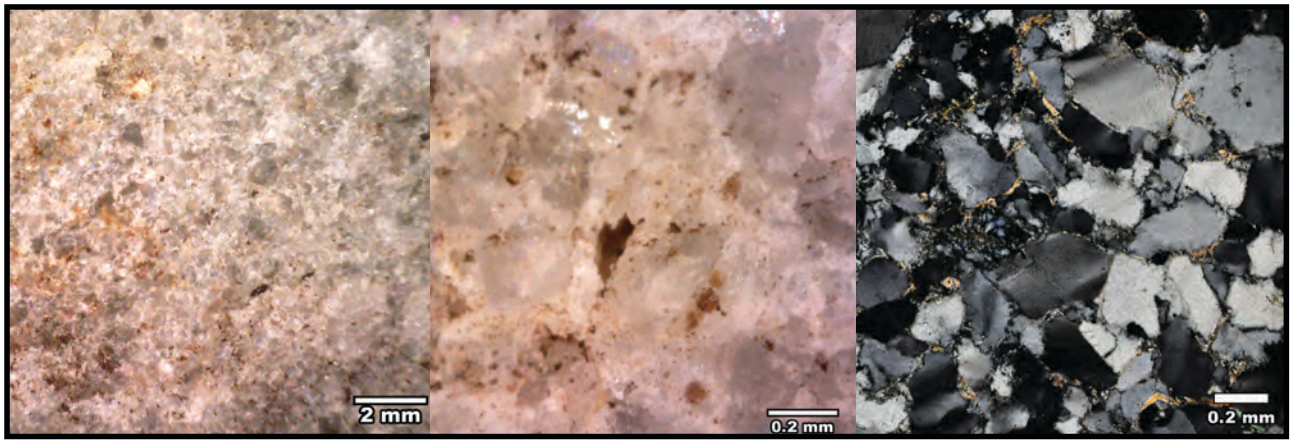

Figure-8.2: Pictures of the CA type sample, ES-263, from Layer-XXII of the archaeological site of El Esquilleu. From left to right, microscopy binocular picture at 20x, microscopy binocular picture at 250x, and thin section microscopy picture at different magnifications.

8.2.2.THE OO PETROGENETIC TYPE IN EL ESQUILLEU, LAYER-XXII

Four of the samples analysed are OO orthoquartzites: ES-245, ES-255, ES-283, and ES-293. Under microscope, all four show similar characterisation, grained texture and complete packing. The most relevant quartz grain features are syntaxial overgrown, undulatory extinction and concave-convex grain boundaries. In few cases, small bulges and suturated contacts arise. There are two grain size varieties: a homogeneous distribution one, with grains between fine and medium grain sizes and represented by the samples ES-255 and ES-283 (Figure-8.3). The second group is more heterogeneous and it is related with coarser grain sizes and it is represented by the samples ES-245 and ES-293 (Figure-8.4). The quartz matrix is around fine silt and the grain framework range from very fine sand to medium sand. Morphology of quartz grains is similar in all samples except in ES-255, more irregular than others due to the presence of some bulges in quartz grains. In all four samples the quartz grains are preferentially oriented. The characterisation through binoculars is consistent with previous information, fine grained texture and complete packing: Compact grainy T&P. Nevertheless, regarding grain features, we differentiate the ES-255 from the other three samples due to the presence of flat & ruffle borders instead of concave-convex quartz grains. We also distinguish the two grain size varieties. The samples ES-255 and ES-283 have fine grains and homogeneous distribution, while other two samples have medium or coarse grain sizes and a general heterogeneous distribution. Under the binocular microscope there is no preferential orientation of the grains. Regarding the mineral characterisation of thin section, we observe clayey matrix in all four samples, also iron oxides as non-quartz mineral. Other minerals, such as rutile and zircon, are described in all except one sample. We only observed mica in two of them. There is a higher presence of clayey matrix in the sample ES-255, the only sample with feldspar. The X-Ray Fluorescence, not performance on ES-283, reveals the high presence of SiO_2 (around 97%), also small quantities of TiO_2, Al_2O_3, and Fe_2O_3. The two latter components are better represented in sample ES-255. The non-destructive description of the samples is consistent with petrographic characterisation, allowing us to understand the connections between mineral and colour. All samples, except the ES-293, have the same mineral characterisation: iron oxides, non-identified black and heavy minerals, and mica. The colour is in general grey-white, although there are reddish zones influenced by iron-oxides. ES-293 sample is dark-grey coloured due to the presence of manganese oxides instead mica. These data reveals two different mineral-colour varieties: The white-grey variety, and the grey-dark ones.

After having analysed the features and the variability of the OO type, we can extrapolate these results to those of non-destructive techniques in the complete assemblage. Firstly, the samples confirm the major presence of OO type. Secondly, these data reveals two different grain size varieties: the homogeneous and medium-fine one, well represented, and the medium-coarser and heterogeneous ones less important. Nevertheless, both are well represented with the highest proportion of these varieties than other petrogenetic types. The colour and mineral characterisation allow us to stablish two different varieties: the grey-white, highly represented; and the grey-dark, with smaller representation.

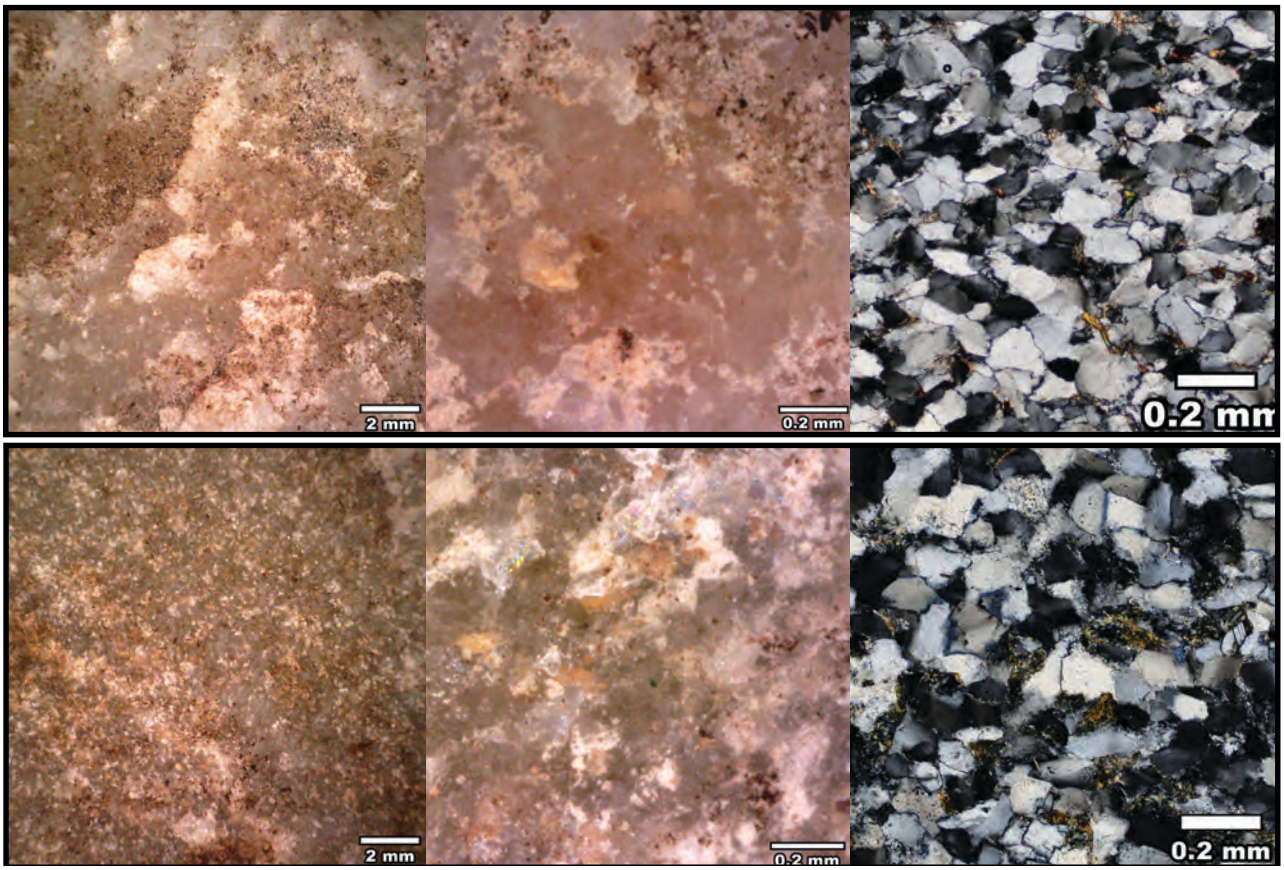

Figure-8.3: Pictures of the OO type samples from Layer-XXII of the archaeological site of El Esquilleu. From top to bottom, samples ES-283 and ES-255. From left to right, microscopy binocular picture at 20x, microscopy binocular picture at 250x, and thin section microscopy picture at different magnifications.

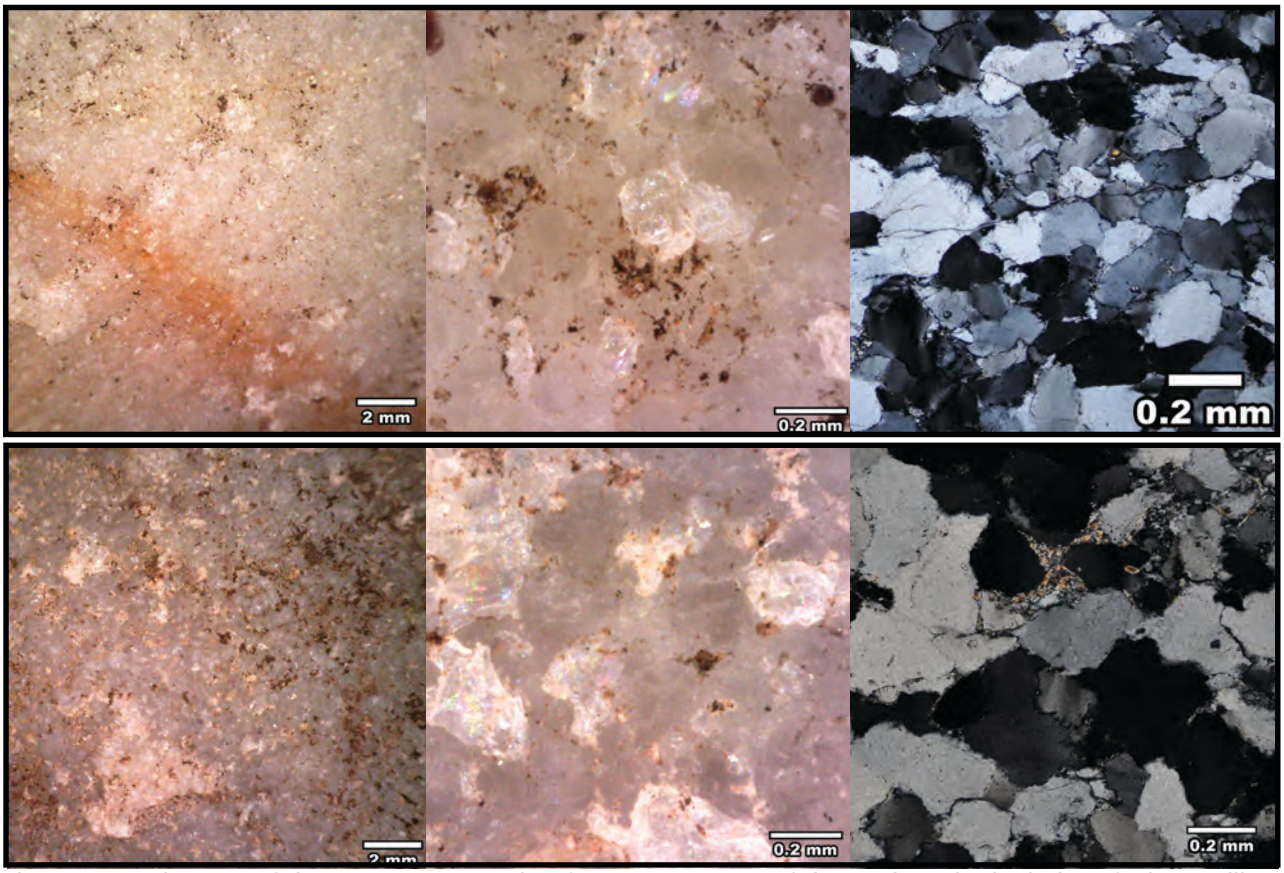

Figure-8.4: Pictures of the OO type samples from Layer-XXII of the archaeological site of El Esquilleu. From top to bottom, samples ES-245 and ES-293. From left to right, microscopy binocular picture at 20x, microscopy binocular picture at 250x, and thin section microscopy picture at different magnifications.

8.2.3. THE SO PETROGENETIC TYPE IN EL ESQUILLEU, LAYER-XXII

Four of the samples analysed belong to the SO petrogenetic type: ES-246, ES-265, ES-314, and ES-328. All of them show clastic grained texture, suturated packing, major presence of undulatory extinction, and suturated/microstylolitic quartz grain limits. Nevertheless, there are differences in the presence of some features. Samples ES-265 and ES-328 have features resulting by the increase of deformation processes such as deformation lamellae or recrystallised quartz grains (in small quantity) (Figure-8.5). These features are absent in ES-246 and ES-314 (Figure-8.6). The grain size characterisation through petrography points at differences between samples, especially by comparing ES-246 with the other three. The first reveals a more heterogeneous and coarse grain sizes around fine sand, while the other three are distributed around very fine sand. Moreover, in the sample ES-328, due to the presence of quartz grains as matrix and the small presence of recrystallised quartz grains, there are two modes. Preferential orientation of quartz grains is clear in all samples except on the ES-246. Non-destructive characterisation of samples is consistent with features previously exposed. Texture is characterised as fine grained with suturated packing and flat and ruffle quartz grain limits: Fine and grainy T&P and general ruffle borders. Except in the quartz grain limits detection, we do not observed differences between the less/more deformed types. The non-destructive grain size characterisation shows the high presence of fine grained varieties, generally with homogeneous distribution around one mode. Nevertheless, medium size and heterogeneous distribution is also represented, as the size characterisation of the ES-246 reveals. The only foliated sample is the ES-314, revealing, again, the limitation of non-destructive characterisation to observe preferential orientation structures in these highly compact samples. All in all, we proposed two different types according to grain size characterisation, the fine grained variety, and the medium grained one.

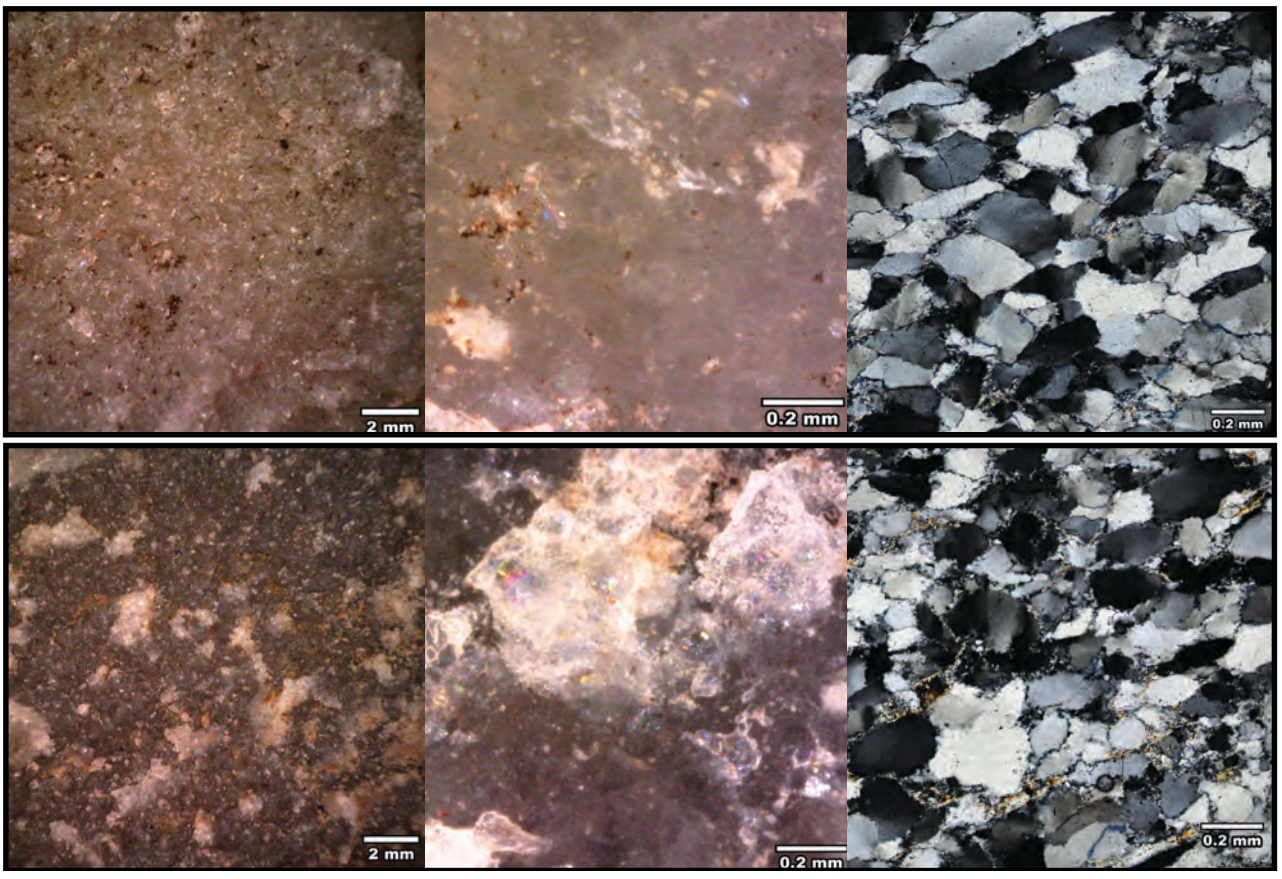

Figure-8.5: Pictures of the SO type samples from the Layer-XXII of the archaeological site of El Esquilleu. From top to bottom, samples ES-265 and ES-328. From left to right, microscopy binocular picture at 20x, microscopy binocular picture at 250x, and thin section microscopy picture at different magnifications.

According to the mineral characterisation of samples, all except the ES-246 have clayey matrix. There is no cement in the samples. We observe small differences, due to the absence of rutile and iron oxides in the sample ES-265, main non-quartz minerals detected on other three samples. The XRF data of ES-265 and ES-328, reveals differences in the presence of SiO_2, Fe_2O_3, and Al_2O_3. The first element is better represented in the ES-265 with 98% of chemical signature, while on ES-328 its presence is reduced to 95% due to the increase of iron and alumina oxides. Under binoculars, we observe pyrite and manganese oxides in all samples, except in ES-265. Colour characterisation

points out this small difference with a relatively lighter colour of the sample ES-265. Nevertheless, all are classified as grey or dark-grey. Therefore, we could not propose mineral/colour varieties on this petrogenetic type.

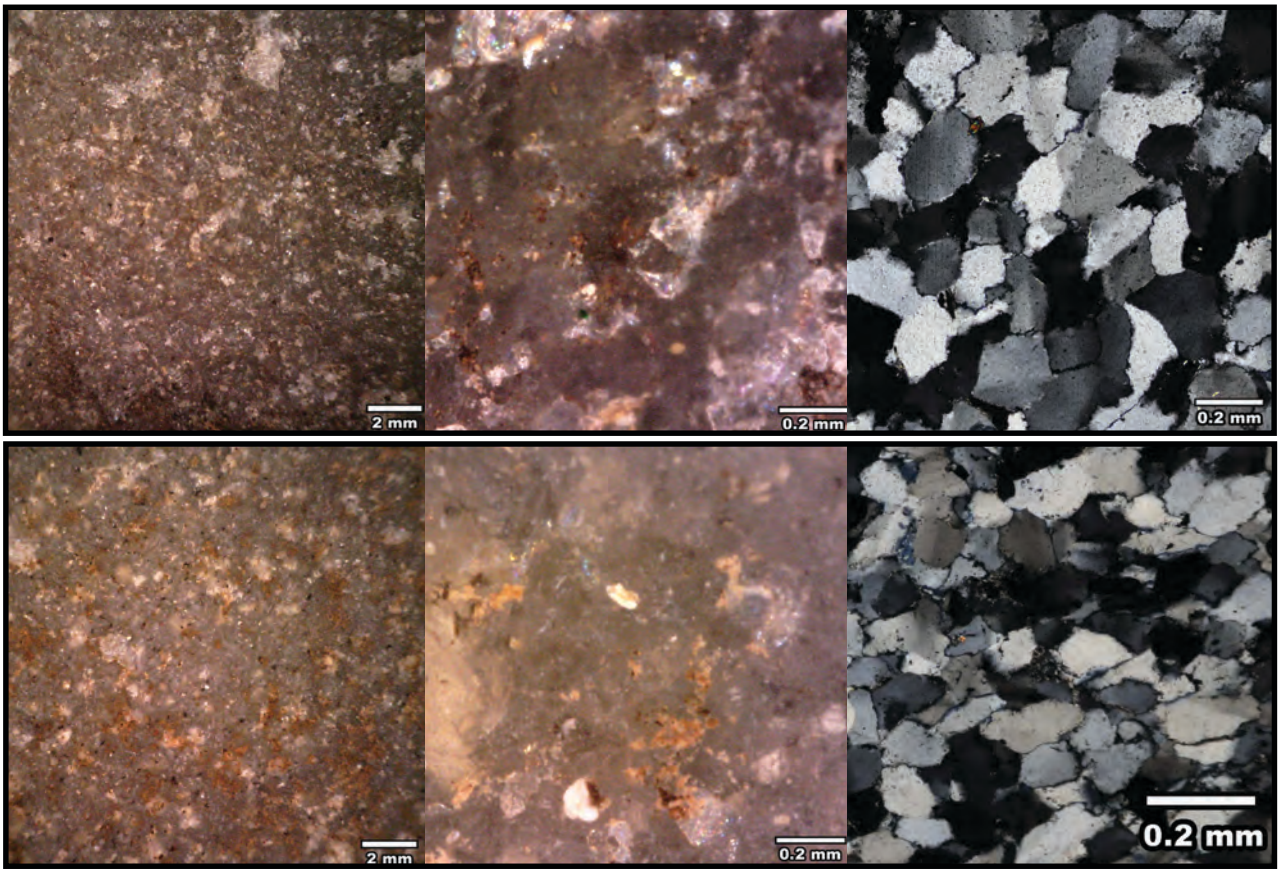

Figure-8.6: Pictures of the SO type samples from the Layer-XXII of the archaeological site of El Esquilleu. From top to bottom, samples ES-246 and ES-314. From left to right, microscopy binocular picture at 20x, microscopy binocular picture at 250x, and thin section microscopy picture at different magnifications.

Coming back to the characterisation of the entire SO collection from this layer, we observe that most of the SO orthoquartzites are related with fine grained variety. Nevertheless, there is also presence of coarse grain size variety. The input of rock of the latter is reduced to few pieces, while the former require higher quantities.

8.2.4. NON-DESTRUCTIVE CHARACTERISATION OF CC, BQ, RQ, AND MQ PETROGENETIC TYPES IN EL ESQUILLEU, LAYER-XXII

The CC petrogenetic type is well represented in this layer with 8% of “archaeological quartzites”. Under binocular microscopy, most of them have coarse grained texture with floating or punctual packing: saccharoid T&P. Quartz grain features vary from plain and angular to plain and rounded ones. There are ruffled limits between grains arise as a consequence of the cement (Figure-8.7). In general, and due to post-depositional processes most of the cements appear as fluids. Quartz grain size characterisation reveals a major presence of medium and coarse grain sizes generally with heterogeneous distribution. Nevertheless, there are also homogeneous and fine grain CC varieties. The mineral characterisation puts this type as the most variable on, also non-common mineral in other petrogenetic types, such as feldspar and calcite, well represented in this type. Other minerals, such as manganese and iron oxides, mica, and non-identified black and heavy minerals are well represented. The colour characterisation also points out this type as highly variable attending to the complete collection and inside each sample. Brown, white, and red colour varieties are better colours, also other secondary tones.

The BQ petrogenetic type is the fourth better frequent type. It is characterised under binocular by the presence of a fine texture and suturated packing. The bright is high. In general, quartz grain limits are not detected, although if they are recognisable, they have flat and ruffle borders: Fine T&P (Figure-8.8). The grain size characterisation is relatively homogeneous and most of the quartz-

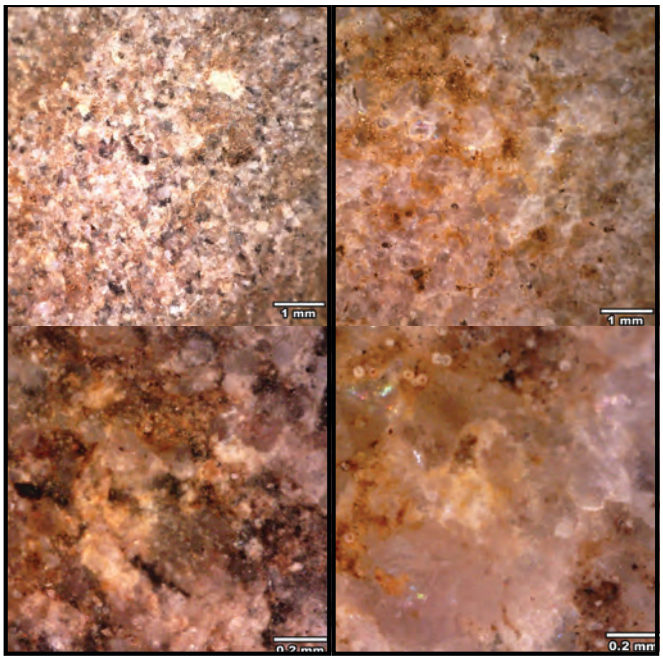

Figure-8.7: Pictures of the CC type from layer-XXII of the archaeological site of El Esquilleu. From left to right ES-318, a CC type with small quartz grain size and heterogeneous distribution and ES-226, a CC type with coarse grain size and heterogeneous distribution. Upper rows show microscopy binocular pictures at 50x. Lower rows show microscopy pictures at 250x.

ites have fine grains organised around one or two modes. Nevertheless, there is a small presence of quartzites with coarser grains. There are foliation structures in most of the BQ quartzites. Mineral and colour characterisation reveals a higher variability. Fe-oxides and non-identified black and heavy minerals are the better represented minerals, followed by manganese oxides, mica and pyrite. The colour characterisation reveals that most of the quartzites are grey coloured and black and brown quartzites are less represented. Finally white varieties are minority. Grey and brown quartzites are related with Fe-oxides and non-identified black and heavy minerals, also pyrite. Black quartzites are also associated with manganese oxides. Finally, we only detect mica on white varieties. Hampered by the lack of BQ samples for petrography and the low quantity of quartzites we do not stablish colour neither grain size varieties.

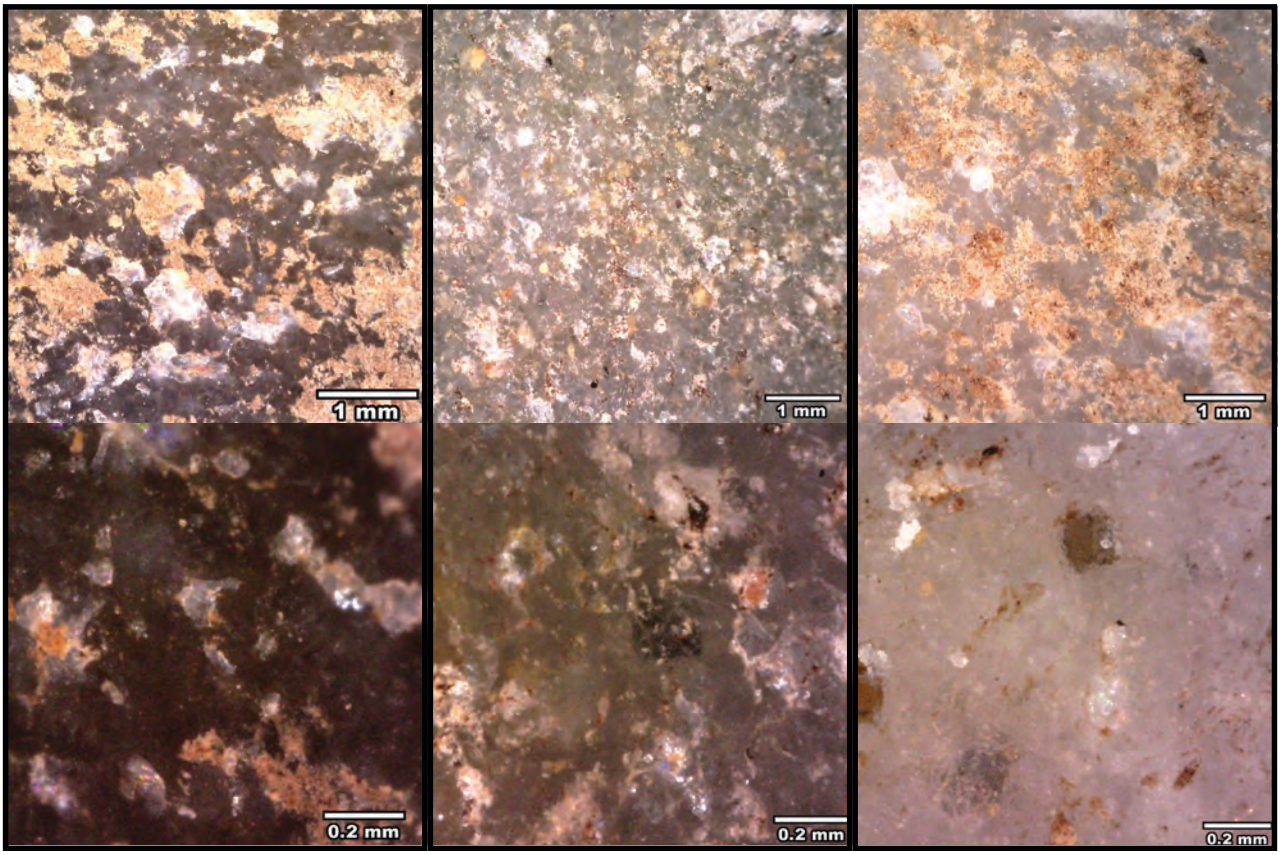

Figure-8.8: Pictures of the BQ type from layer-XXII of the archaeological site of El Esquilleu. From left to right, ES-321, a BQ type with medium quartz grain size and homogeneous distribution, it is a grey-dark colour with pyrites, manganese and iron oxides. ES-331 is a BQ type with fine grain size and homogeneous distribution in grey colour. ES-322 is a BQ quartzite with medium grain size and homogeneous distribution in white colour and with iron oxides, micas, pyrites, and black and heavy dark minerals.

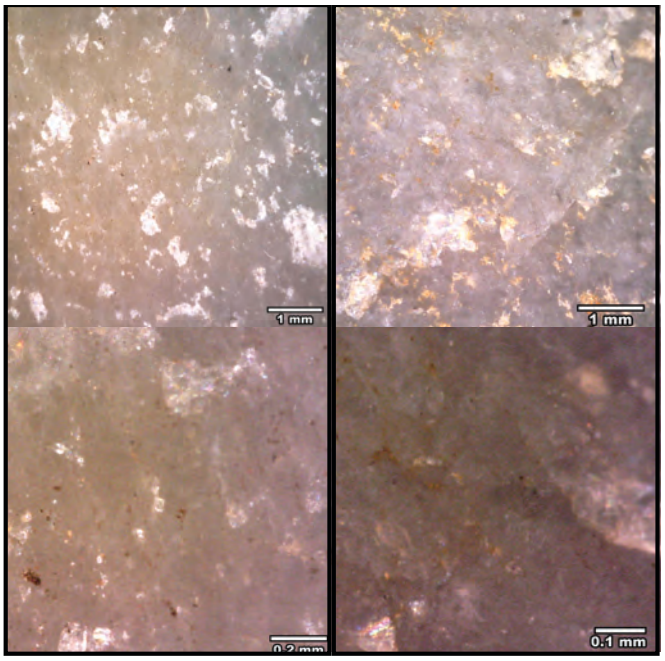

Figure-8.9: Pictures of the RQ quartzite type from layer-XXII of the archaeological site of El Esquilleu. From left to right, ES-R242 is a RQ type, grey-clear coloured with fine quartz grain size and homogeneous distribution. ES-R344 is a grey-dark coloured RQ type with fine grain size and homogeneous distribution. Upper rows show microscopy binocular pictures at 50x. Lower rows show microscopy pictures at 250x.

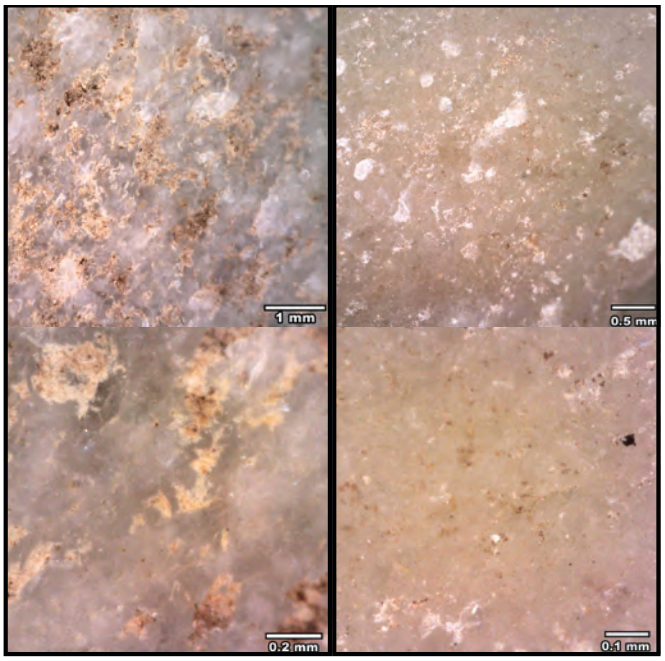

Figure-8.10: Pictures of the MQ quartzite type from layer-XXII of the archaeological site of El Esquilleu. From left to right, ES-R039 is a MQ type, white coloured, with fine quartz grain size and homogeneous distribution. ES-R093 is a grey-clear MQ type with fine grain size and homogeneous distribution. Foliation structures are on both samples. Upper rows show microscopy binocular pictures at 50x. Lower rows show microscopy pictures at 250x.

The presence of RQ petrogenetic type is limited in this collection to 17 lithics. Then, conclusion must be nuance. Under binoculars, these quartzites are characterised by soapy texture without clear grain boundary detection. The bright is high and micro-cracks are limited: Soapy T&P (Figure-8.9). Even though the size of the grains is almost impossible to detect, they are related with small sizes and apparently homogeneous distribution. According to the colour characterisation, most of them are grey, although white, brown, and black varieties are also represented. Mineral characterisation reveals the high presence of iron oxides, mica, and non-identified black and heavy minerals. Manganese oxides and pyrite also appear, associated to grey and dark varieties. Due to the reduced number of RQ quartzites in the layer, also due to the limitation of binocular scope, we could not identified clear varieties.

The last petrogenetic type here analysed is the MQ quartzite type. It is the less represented “archaeological quartzite”, with only six lithics. They are characterised by soapy texture and no grain detection. Nevertheless, it is possible to recognise some and partial grains, especially at 50x magnifications (Figure-8.10). The luster is high and the presence of micro-cracks is variable. Attending to grain size, most of them are fine grained with homogeneous variety, although medium sizes are also appreciated. The limitation in number of the collection and the lack of samples for petrography characterisation do not allow us to proposed different varieties. Attending to the colour characterisation, all of them are white or clear grey. The mineral characterisation is consistent with this homogeneity, and most of them have iron oxides, mica, and non-identified black and heavy minerals. Two of the samples have pyrite.

8.2.5. CHARACTERISATION OF CORTICAL AREAS FROM EL ESQUILLEU, LAYER-XXII

Here we present the result of the characterisation of cortical areas (Table-8.5). “Archaeological quartzite” is the most frequent raw material with cortical areas, which is in accordance with predominance in the whole assemblage. Attending to the relative presence, it is the second most represented material after the lutite, with 25%. Other raw materials have smaller relative presence, such as flint, quartz or radioralite.

Raw material	Cortex type												∑ of each type
	Conglomerate			Fluvial			Undetermined			Total			
	∑	%	% rel	∑	%	% rel	∑	%	% rel	∑	%	% rel	
Archaeological quartzite	22	100	3	110	96	16	12	92	2	144	96	21	684
Flint							1	8	3	1	1	3	39
Limestone													
Limonite													
Lutite				2	2	25				2	1	25	8
Quartz				2	2	5				2	1	5	40
Radioralite				1	1	5				1	1	5	19
Unknown													1
Total	22	15	3	115	77	15	13	9	2	150	100	19	791

Table-8.5: Frequency table of types of cortex identified in layer-XXII from El Esquilleu grouped by main raw material. Columns are types of cortex, including the frequency of each cortex type for each raw material and the total of items with cortex of each raw material. The last column quantifies the total of items with and without cortex of each raw material. The columns % are the percentage of each raw material in relation to each cortex type, while the columns % rel. are the percentage of cortex type in relation to the total of each raw material (including items with and without cortex).

Concerning the types of cortex, 9% of the collection could not be characterised due to the absence of diagnostic features. None of the cortex types identified could be interpreted as evidence of direct extraction from the outcrop.

Conglomerate cortex is underrepresented, representing 15% of the lithic implements with cortical areas. All 22 are on “archaeological quartzites”. No conglomerate cortex was identified among flint, lutite, quartz, or radioralite. Conglomerate cortical areas are characterised by the presence of cements from the conglomerate itself, which are generally recognisable as red iron oxides or dark silica precipitates. In addition, voids are usually present, even though they are generally filled with conglomerate cement. No clear impact cracks are observable on cortical areas.

Archaeological quartzite	Cortex type												∑ of each type
	Conglomerate			Fluvial			Undetermined			Total			
	∑	%	% rel	∑	%	% rel	∑	%	% rel	∑	%	% rel	
CC				13	12	25				13	9	25	53
CA				11	10	25	1	8	2	12	8	27	44
OO	1	5	0	61	55	20	2	17	1	64	44	21	309
SO	13	59	7	17	15	9	6	50	3	36	25	20	181
BQ	4	18	8	4	4	8	1	8	2	9	6	17	52
RQ	2	9	12	3	3	18	1	8	6	6	4	35	17
MQ	1	5	17							1	1	17	6
Undetermined	1	5	5	1	1	5	1	8	5	3	2	14	22
Total	22	15	3	110	76	16	12	8	2	144	100	21	684

Table-8.6: Frequency table of types of cortex identified in layer-XXII from El Esquilleu grouped by petrogenetic type. Columns are the types of cortex, including the frequency of each cortex type for each petrogenetic type and the total of items with cortex of each petrogenetic type. The last column quantifies the total of items with and without cortex of each petrogenetic type. The columns % are the percentage of each petrogenetic type in relation to each cortex type, while the columns % rel. columns are the percentage of cortex type in relation to the total of each petrogenetic type (including items with and without cortex).

Cortical areas from fluvial deposits is the most frequent cortex type, representing 77% of the cortical areas analysed. “Archaeological quartzite” is again the most frequent raw material with fluvial cortex. However, there are lithic implements with fluvial cortex among quartz, radioralite, and lutites too. Fluvial cortex is mainly characterised by the presence of impact cracks in the surface and fine or soapy textures. Voids are less frequent in this cortex type and cement is absent (except for the carbonated clay stuck on the whole surface due to post-depositional processes).

Focussing on the distribution of cortex among “archaeological quartzites” and their different petrogenetic types, there is a clear overrepresentation of cortical areas among the RQ, CA, and CC petrogenetic types. Conversely, lithics with cortex are underrepresented among the MQ and BQ types (Table-8.6).The remaining petrogenetic types have similar distribution of “archaeological quartzites” as a whole, around 20%.

Cortical areas from conglomerate and fluvial contexts are present in different percentages when considering all “archaeological quartzites” (3% against 15%). There are also differences when sorting them by petrogenetic types. Chi-square test (χ^2 (6, N = 130) = 44.721, p < .001) statistically confirms these differences and standardised residues, in Figure-8.11, graphically shows them. The fluvial cortex type is overrepresented in the quartzarenite (without cortical areas derives from conglomerate) and in the OO petrogenetic type (with only one cortical area derived from conglomerate). In the SO orthoquartzite type, the relationship changes and the cortex from conglomerates is overrepresented, as in the quartzite group, even though fluvial cortex is also represented.

	Fluvial	**Conglm**
CC	0,6	-1,4
CA	0,6	-1,3
OO	1,3	-2,8
SO	-1,6	3,7
BQ	-1	2,4
RQ	-0,6	1,3
MQ	-0,9	2,1

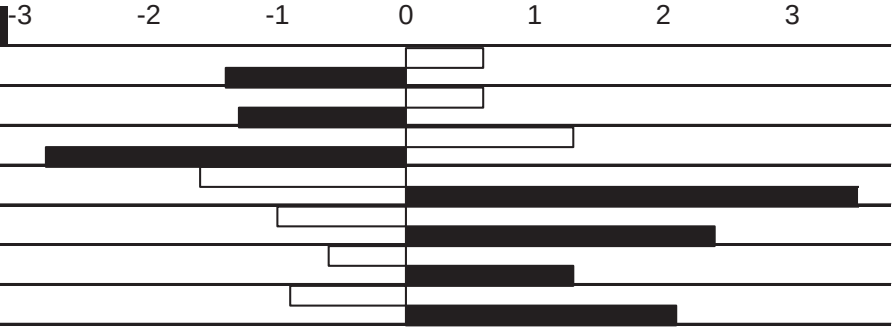

Figure-8.11: Standardised residues of χ^2 test of “archaeological quartzites” with cortex, showing the weight of each type of cortex in different petrogenetic types.

8.3.TECHNOLOGICAL STRUCTURE

Here we present the results of the technological analysis of the material from layer XXII of El Esquilleu, taking into account the results from the study of the petrological structure. The most frequent category is that of the knapping product (86%), followed by chunk (10%), and core (3%). The distribution of technological products sorted by main lithologies is shown in Table-8.7. Cores are restricted to “archaeological quartzite”, quartz, and flint. Flint and quartz cores are abundant, especially considering the importance of these raw material in the complete lithic collection. Knapping products of all raw material are well represented. There is only knapping products made on lutites. The representation of knapping products is different according to each raw material and its relative percentages, following an inverse relationship with chunks. The highest representation of knapping products is on “archaeological quartzites”, while on flint, quartz, and radioralite, the representation of this technological products is smaller, and replaces by higher percentages of chunks.

Focusing the analysis on “archaeological quartzites”, the cores are restricted to CC, CA, OO, SO, and BQ types (Table-8.8). Most of them are on the SO orthoquartzites. On other petrogenetic types except for BQ quartzite, cores are scarce. Knapping products are more frequent among all types, even though there are differences between them: They are less frequent (<82%) among CC type and the undetermined type and more frequent among other types (>88%). On the contrary, chunks are very frequent among the CC quartzarenite and the undetermined type. In any other of the petrogenetic types, the quantity of chunk is reduced, with smaller percentages than 8%. Nevertheless, chunks are overrepresented on the MQ type while knapping products are underrepresented, determined by the small number items of this petrogenetic type.

	Technological order										
	Cores			Knapping prdct.			Chunk			Total	
	∑	%	% rel	∑	%	% rel	∑	%	% rel	∑	%
Arch. Quartzite	21	81	3	**609**	**89**	**89**	54	67	8	684	87
Flint	2	8	5	28	4	72	9	11	23	39	5
Limestone											
Limonite											
Lutite				8	1	100				8	1
Quartz	3	12	8	25	4	63	12	15	30	40	5
Radioralite				13	2	68	6	7	32	19	2
Volcanic rock											
Total	26	3	3	683	86	86	81	10	10	790	100

Table-8.7: Frequency table of main technological categories identified in layer-XXII from El Esquilleu grouped by raw material. Columns are the main technological categories and the total of items of each raw material. The columns % are the percentage of each raw material in relation to each technological category, while the columns % rel. are the percentage of each technological category in relation to each raw material. Cells in black are the categories representing more than 10% of the total cases. Cells in dark grey are the categories representing between 5 to 10% of cases. Finally, cells in light grey are the categories representing between 1 to 5% of cases.

	Technological order										
	Cores			Knapping prdct.			Chunk			Total	
	∑	%	% rel	∑	%	% rel	∑	%	% rel	∑	%
CC	1	5	2	43	7	81	9	17	17	53	8
CA	2	10	5	39	6	89	3	6	7	44	6
OO	2	10	1	**287**	**47**	**93**	20	37	6	309	45
SO	10	48	6	**158**	**26**	**87**	13	24	7	181	26
BQ	4	19	8	48	8	92	0	0	0	52	8
RQ	0	0	0	16	3	94	1	2	6	17	2
MQ	0	0	0	5	1	83	1	2	17	6	1
Undetermined	2	10	9	13	2	59	7	13	32	22	3
Total	21	3		609	89		54	8		684	100

Table-8.8: Frequency table of main technological categories identified in layer layer-XXII from El Esquilleu grouped by petrogenetic types of “archaeological quartzites”. Columns are the main categories and the total of items belonging to each petrogenetic type. The columns % are the percentage of each petrogenetic type in relation to each technological category, while the columns % rel. are the percentage of each technological category in relation to each petrogenetic type of “archaeological quartzite”. Cells in black are the categories representing more than 10% of the total cases. Cells in dark grey are the categories representing between 5 to 10% of cases. Cells in light grey are the categories representing between 1 and 5% of cases.

8.3.1.CORES

We identified 26 cores in the whole collection. The most frequent types of core are core on flake, irregular, and discoid cores, followed by the Levallois ones. There is only a prismatic core analysed and there is no pyramidal shape core. There is no clear correlation between type of core and raw material, neither with petrogenetic types of “archaeological quartzites” (Table-8.9).

The cores on flake is the best represented type in this assemblage with ten examples. Five of the cores are complete, while the others five incomplete. The most common raw material for is “archaeological quartzites”, with seven items. The other two cores on flake are made on flint and the last one is made on quartz. The most frequent petrogenetic type of “archaeological quartzites” are SO and BQ types, with two cores, followed by the OO type with another one. The quantity of percussion platforms and flacking surfaces is small and they generally present just one percussion platform and one flacking surface. We do only observed one cortical area in a core made on BQ type. This cortex is characterised as fluvial derived.

The irregular core is the second better represented type, with seven items. Regarding raw material, most of them are made on SO type with four. CA, BQ and an undetermined “archaeological quartzite” are represented with one core each. Most of the cores (5) are completes, and only two

are fractured. The number of percussion platforms and flacking surfaces in this type are varied and the three categories proposed are similarly represented. No clear standardisation is observed in this type of cores. Coming to the presence of cortical areas, most of them preserve small areas of cortex, generally less than 33% of the total surface. The features of these cortical areas vary between fluvial (4) and conglomerate (1). Only two of the irregular cores are not cortical.

	Type of core						
	Irregular	Discoid	Levallois	Prismatic	Pyramid	On flake	Total
Other RM		1		1		3	5
CC		1					1
CA	1	1					2
OO			1			1	2
SO	4	2	1			3	10
BQ	1					3	4
RQ							
MQ							
Undetermined	1		1				2
Total	7	5	3	1		10	26

Table-8.9: Frequency table of types of cores identified in layer-XXII from El Esquilleu grouped by petrogenetic types of “archaeological quartzite”. Columns are the types of cores. In this case the only other RM (raw material) is flint.

Discoidal cores are represented in this layer by five pieces. Three are complete and the other two are fractured. Four of the cores are made on “archaeological quartzites” and the remaining one on quartz. Among the former, SO (two items), CC (one item), and CA (another item) are the three present petrogenetic types. All four discoidal cores have more than three percussion platform and two flacking surfaces. It is clear the same technique, with alternative and consecutive extractions was used. The presence of cortical zones is restricted to the CA and SO petrogenetic types. The first is characterised as fluvial cortex. The latter cortex could not be identified. Its extension vary from less than 33% to more than 66%.

There are three levallois cores in this layer. All three are made on “archaeological quartzites”. One is made on OO type, another one on SO. We could not identify the petrogenetic type on the remaining core. All, except one are complete. All three levallois cores have more than three percussion platforms and two flaking surfaces. The preserve of cortical zones is restricted to smaller surface than 33% in the SO petrogenetic type core. It is characterised as fluvial derived cortex.

There is one prismatic shaped core made on quartz. This core is complete and it has two percussion platform and another two flacking surfaces. There is an absence of cortical areas.

8.3.2. KNAPPING PRODUCTS

We identified 683 knapping products in the lithic assemblage from the Layer-XXII. The most frequent type is blank, making more than 98% of the items analysed. Core preparation/rejuvenation products are scarce, forming less than 1% of the assemblage. Finally, we do not identify any burin spall. Core preparation/rejuvenation products are on “archaeological quartzites”, more specifically orthoquartzites group, and on flint and quartz (Table-8.10).

Blanks is the technological category better represented in this layer. Coming to their integrity, 56% of the pieces are complete and 44% are fragmented (Figure-8.12). The most frequent fragments are longitudinal ones, followed by the proximal ones. Distal and medial pieces are scarce (≈2%). Finally, 19% of the pieces could not be classified due to the absence of diagnostic features, mainly the bulb of percussion or the striking platform. Then, most of these undetermined fragments must be part of distal or medial fragments.

The characterisation of dorsal surfaces using the number of negative scars shows a high quantity of more than two negative extractions and an underrepresentation in the category of absence of negative scars. We do not observe statistically differences between quantity of negative scars and raw material, as Chi-square test shows (χ^2 (12, N = 679) = 14.302, p = .282). Nevertheless, as Table-8.11 suggest a higher presence of negative scars in flint, quartz and radioralite than lutites and “archaeological quartzites”. We do neither observe statistic differences when the number of negative scars

	Knapping products							
	Blaks			Core preparation/rej			Total	
	∑	%	% rel	∑	%	% rel	∑	%
Other RM	73	11	97	2	22	3	75	11
CC	43	6	100				43	6
CA	39	6	100				39	6
OO	**285**	**42**	**99**	3	33	1	288	42
SO	**155**	**23**	**97**	4	44	3	159	23
BQ	50	7	100				50	7
RQ	16	2	100				16	2
MQ	5	1	100				5	1
Unknown	13	2	100				13	2
Total	679	99		9	1		688	100

Table-8.10: Frequency table of the categories of knapping products identified in layer-XXII from El Esquilleu grouped by the petrogenetic types of “archaeological quartzite”. Columns are the categories of knapping products and the total of items belonging to each petrogenetic type. The columns % are the percentage of each petrogenetic type in relation to each category of knapping product, while the column % rel. are the percentage of each category of knapping product in relation to each petrogenetic type of “archaeological quartzite”. Cells in black are the categories representing more than 10% of the total cases. Cells in dark grey are the categories representing between 5 and 10% of cases. Cells in light grey are the categories representing between 1 and 5% of cases. Other RM (raw materials) includes flint (27 blanks and one core preparation product), lutite (eight blanks), quartz (24 blanks and one core preparation), and radioralite (13 blanks).

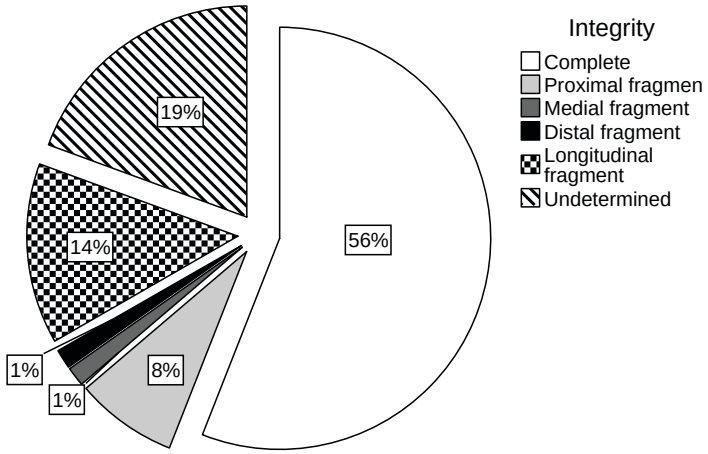

Figure-8.12: Pie chart showing percentage of each state of integrity of blanks.

	Dorsal scars							
	None		One		Two		≥ Three	
	∑	**%**	∑	%	∑	%	∑	%
Arch. Qzt.	30	5,0	178	29,4	233	38,4	165	27,2
Flint	0	0,0	4	14,8	12	44,4	11	40,7
Lutite	1	12,5	3	37,5	3	37,5	1	12,5
Quartz	0	0,0	7	28,0	13	52,0	5	20,0
Radioralite	0	0,0	1	7,7	8	61,5	4	30,8
Total	31	5	193	28	269	40	186	27

Table-8.11: Frequency table and its representation through a bar chart using the percentage of each blank category (determined by the quantity of dorsal scar) taking into account each raw material.

Dorsal scars

	None		One		Two		≥ Three	
	∑	%	∑	%	∑	%	∑	%
CC	3	7,0	10	23,3	18	41,9	12	27,9
CA	2	5,1	10	25,6	16	41,0	11	28,2
OO	13	4,6	93	32,6	110	38,6	69	24,2
SO	9	5,8	44	28,4	55	35,5	47	30,3
BQ	2	4,0	14	28,0	20	40,0	14	28,0
RQ	0	0,0	5	31,3	7	43,8	4	25,0
MQ	0	0,0	1	20,0	2	40,0	2	40,0
Total	29	5	177	30	228	38	159	27

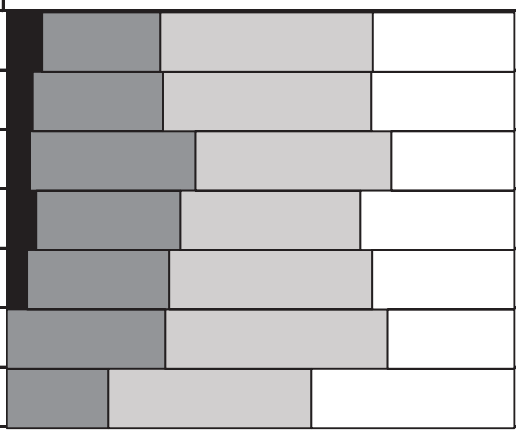

Table-8.12: Frequency table and its representation through a bar chart using the percentage of each blank category (determined by the quantity of dorsal scar) taking into account each petrogenetic type of "archaeological quartzite".

and petrogenetic types are compared, as the Chi-square test shows (χ^2 (18, N = 593) = 6.317, p = .995). Table-8.12 shows negligible differences between each type and the number of negative scars.

The preservation of cortical areas on these blanks does also provide interesting data about raw material exploitation in this collection (Figure-8.13). Cortex is observable in the 20% of the blanks from this assemblage. Most of them cover less than 33% of the dorsal surface. Broad cortical areas on dorsal surfaces are only present in 9%, and only 6% of items analysed have cortical areas covering more than 66% of the surface. There is no statistic differences regarding the representation of cortical area in different raw material, as Chi-square test shows (χ^2 (12, N = 679) = 17.87, p = .119). Nevertheless, quartz, radioralite and flint show similitudes due to the higher presence blanks without cortical surfaces. There is a higher presence of them in the "archaeological quartzites" and lutites (Table-8.13). There is neither statistically significance differences between the presence of cortical surfaces and the petrogenetic types of "Archaeological quartzites", as the Chi-square test shows (χ^2 (18, N = 693) = 18.38, p = .43). Nevertheless, Table-8.14 shows quartzarenite group has higher proportion and extension of cortical surfaces, also observed in RQ blanks.

Presence of cortex on dorsal surfaces

	Absence		X < 33%		33<X>66		X > 66%	
	∑	%	∑	%	∑	%	∑	%
Arch. Qzt.	485	80,0	65	10,7	19	3,1	37	6,1
Flint	26	96,3	1	3,7	0	0,0	0	0,0
Lutite	6	75,0	0	0,0	0	0,0	2	25,0
Quartz	24	96,0	1	4,0	0	0,0	0	0,0
Radioralite	13	100,0	0	0,0	0	0,0	0	0,0
Total	554	82	67	9,9	19	3	39	6

Table-8.13: Frequency table and its representation through a bar chart using the percentage of each blank category (determined by the quantity of cortex on dorsal surfaces) taking into account each raw material.

Among the items which preserved any cortical area (119), it was possible to characterised 110 of them. Only two lutites and one quartz have cortex, all derived from fluvial deposits. Focussing on "archaeological quartzites", the features that define cortex from fluvial sources (90) and from conglomerates (17), are differently distributed. There are another nine items with cortical surfaces which do not have enough features to define them. Clear differences between petrogenetic types were

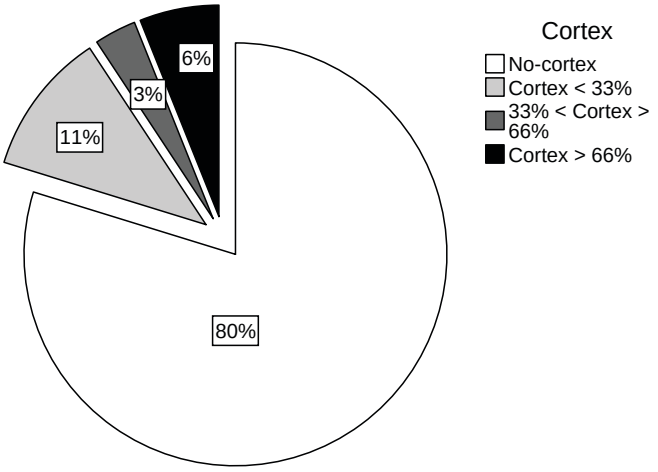

Figure-8.13: Pie chart showing percentage of absence, presence and extension of cortex on blanks.

pointed out by chi-square test (χ^2 (12, N = 116) = 49.925, p < .001) (Table-8.15). Cortex from rivers are more frequent among quartzarenites and in the OO type, while cortex from conglomerate are more common in the SO, BQ, RQ, and MQ types.

Core preparation/rejuvenation products are the less frequent knapping products, represented by just nine pieces. Most of them are complete and three are undetermined fragments. Most of the core preparation/rejuvenation products are made on "archaeological quartzite", one on flint, and another one on quartz. Among the first raw material, all of them are made on orthoquartzites, three on OO and four on SO type (Table-8.10). Two core preparation/rejuvenation products have cortical areas, covering less than 33% of the surface. All of them derive from fluvial deposits. One belongs to SO type and another to OO one.

Presence of cortex on dorsal surfaces

	Absence		X < 33%		33<X>66		X > 66%	
	∑	%	∑	%	∑	%	∑	%
CC	31	72,1	6	14,0	3	7,0	3	7,0
CA	29	74,4	4	10,3	3	7,7	3	7,7
OO	228	80,0	32	11,2	6	2,1	19	6,7
SO	129	83,2	13	8,4	4	2,6	9	5,8
BQ	42	84,0	5	10,0	1	2,0	2	4,0
RQ	10	62,5	4	25,0	2	12,5	0	0,0
MQ	4	80,0	1	20,0	0	0,0	0	0,0
Total	473	80	65	11	19	3	36	6

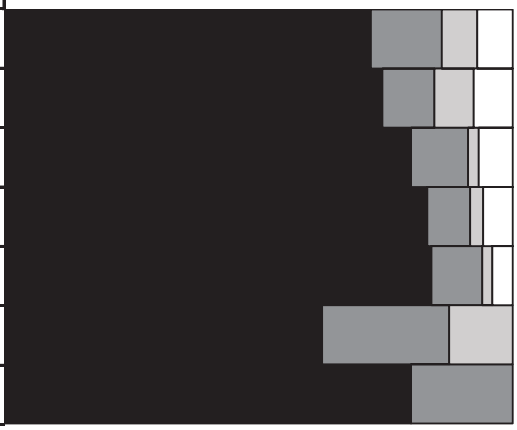

Table-8.14: Frequency table and its representation through a bar chart using the percentage of each blank category (determined by the quantity of cortex on dorsal surfaces) taking into account each petrogenetic type of "archaeological quartzite".

8.3.3. CHUNK

Chunk is the second most important technological category in this collection, represented by 81 items. The integrity of this pieces is not analysable due to the absence of diagnostic features.

The raw materials presents in this category are "archaeological quartzite", flint, radioralite, and quartz (Table-8.7). Concerning to the relative weight of chunks in each raw material, these are clearly overrepresented in radioralite and quartz, with 32% and 30% of their items respectively. Chunks in "archaeological quartzite" are less frequent, with 8% of its pieces. Focussing on specific petrogenetic types, chunks are more frequent in CC and MQ petrogenetic types (17%) than in the others (7%). There is no BQ type chunk.

Twenty chunks have cortex. Among the 18 on "archaeological quartzites", one in quartz, and remaining one in radioralite. The extension of cortex in in all these chunks, is reduced than the 66% of the surface, generally reduced to 33%. Fifteen cortical areas derived from fluvial beaches, four from conglomerates and the remaining is undetermined.

8.4. RETOUCH: MODAL AND MORPHOLOGICAL STRUCTURES

Here we present the analysis of the retouched artefacts and its relationship with the data previously exposed. According to the methodology defined above, there are 53 lithics retouched, the 6.7% of the assemblage. Six lithic artefacts have two different primary types, 0.6%. The number of primary types individualised is 59. Starting from the orders (mode of retouch), we do not find evidence of Plain (P) or Burin (B) modes of retouch. The most frequent one is the Simple mode (44 items), followed by Abrupt (eleven), and Splinter (four) (Figure-8.14 and Table-8.18). Going down from order to typological group (or morphothema), we start with the Simple mode. The most frequent typological group is that of Sidescraper (R) (34), followed by Denticulate (D) (seven), Endscraper (G) (2), and Point (P) (1). In the Abrupt mode, there is only one group, the unspecific Abrupt (A) (15 items). No typological groups are distinguished within the Splinter mode, therefore, all of them are Splinter (E).

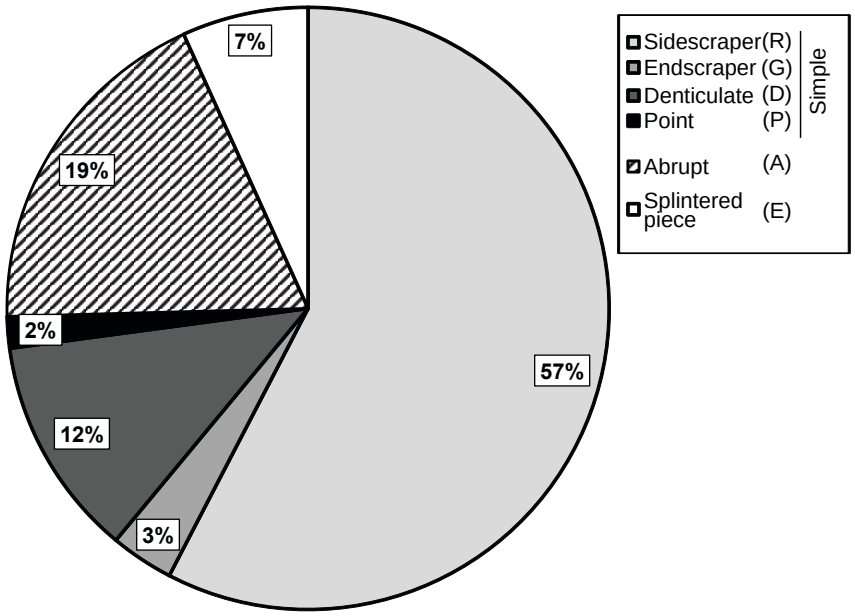

Figure-8.14: Pie chart showing percentage of modes of retouch and morphological groups of retouched artefacts from layer XXII of El Esquilleu rockshelter.

After having understood the general characterisation of the retouch using the modes and morphological groups of retouch, now we will deepen into analysis of the pieces with two primary types. There are only four associations. The most frequent association is Sidescraper and Sidescraper, represented in three pieces. There are also one blank with a Sidescraper and an Endscraper, another blank with a Sidescraper and an unspecific Abrupt, and another blank with two unspecific Abrupt.

Next, we will analyse the relationships between retouched artefacts and the technological structure. There is no statistically significant association between the presence of retouch and the technological order of blanks they are configured, as chi-square shows χ^2 (2, N = 791) = 2.891, p = .236. Nevertheless, the presence of primary types on knapping products (7.3%) is more frequent than on cores (5%) and chunks (2.4%). In addition, all pieces with two primary types are configured on knapping products (all of them on blanks). The only retouched core is a Sidescraper, and the retouched chunks are an unspecific Abrupt and a Sidescraper. The distribution of morphological group of retouch on knapping products follows similar distribution than those observed in the complete assemblage.

Finally, we will analyse the relationships between the retouched artefacts and the raw material of the blanks they are configured. The quantity of retouched artefacts is differently distributed depending on the raw material of the blanks, as demonstrated by Chi-square test (χ^2 (4, N = 791) = 25.030, p < .001). Quartz is the raw material with the greatest percentage of retouched blanks (25%), followed by flint, radioralite (both with 10%), and finally, “archaeological quartzite” (5%). There is no evidence of retouch on lutite blanks (Table-8.16). “Archaeological quartzites”, with four pieces, and quartz with two are the only raw material with artefacts with multiple primary types. There is no statistically significant relationship in the presence of retouch in the blanks with different types of “archaeological quartzite”, as proven by Chi-square test (χ^2 (6, N = 662) = 2.102, p = .91). Nevertheless, there

are small differences according to the percentage of retouched blanks on each petrogenetic type, as shown on Table-8.17. There are higher percentages of retouched artefacts on SO and BQ types than on the others, especially CA, MQ, and OO petrogenetic types. The retouched artefacts with more than one primary types are made on CC, BQ, and SO (two different artefacts on each type).

	Non-retouched		**Retouched**		-2	0	2	4
	Σ	Std. Res	**Σ**	**Std. Res**				
Qzt.	647	0,4	37	-1,3				
Flint	35	-0,2	4	0,9				
Lutite	8	0,2	0	-0,7				
Quartz	30	-1,2	10	4,5				
Radio.	17	-0,2	2	0,6				

Table-8.16: Frequency table and standardised residues of χ^2 test of retouched and non-retouched artefacts grouped by raw material.

	Non-retouched		**Retouched**	
	Σ	%	**Σ**	**%**
CC	50	94,3	3	5,7
CA	43	97,7	1	2,3
OO	294	95,1	15	4,9
SO	170	93,9	11	6,1
BQ	48	92,3	4	7,7
RQ	16	94,1	1	5,9
MQ	6	100,0	0	0,0

Table-8.17: Frequency table and its representation through a bar chart using the percentage of retouched and non-retouched artefacts grouped by petrogenetic types of “archaeological quartzite”.

	Simple				Abrupt	Splinter	
Order	Sidescraper	Endscraper	Denticulate	Point	Abrupt	Splintered piece	Total
Arch. Qzt	**23**		5	1	**8**	4	41
Flint	1		2		1		4
Lutite							
Quartz	**9**	1			2		12
Radioralite	1	1					2
Total	34	2	7	1	11	4	59

Table-8.18: Frequency table of order of retouch and morphological groups grouped by raw material. In the cases of pieces with multiple primary types, each retouch is quantified individually. Cells in black are the categories representing more than 10% of the total cases. Cells in dark grey are the categories representing between 5 and 10% of cases.

In order to better understanding the relationship between the morphological group and the raw material of the blanks they are configured, we simplified the data through the Table-8.18. Sidescraper morphothema, the best represented group, is the only one configured in every raw material. It is also noteworthy the absence of Endscraper morphothema in “archaeological quartzite” despite there is one Endscraper configured on a quartz blank and another on a radioralite. It is also recognisable the absence of Splinter morphothema in blanks made on the latter two raw materials, also on flint. Going into a deeper detail of “archaeological quartzites”, there are interesting association between the morphological group and the petrogenetic types they are configured (Table-8.19). Except in the MQ quartzite (without retouched artefacts), Sidescrapers are configured in every petrogenetic type and they are the most common morphothema. Moreover, the Sidescraper group is the only morphothema defined in quartzarenites. Denticulate morphothema is only configured in orthoquartzite blanks, with similar distribution than unspecific Abrupts. The latter morphotema is also configured in BQ type blanks. Finally, there is a clear association between the Splinter morphothema and the petrogenetic type of the blanks, always made on OO orthoquartzite.

	Simple				Abrupt	Splinter	
Order	Sidescraper	Endscraper	Denticulate	Point	Abrupt	Splintered piece	Total
CC	4						4
CA	1						1
OO	6		3		2	4	15
SO	**9**		2		2		13
BQ	2				3		5
RQ				1			1
MQ							
Total	22	0	5	1	7	4	39

Table-8.19: Frequency table of order and group of retouches grouped by petrogenetic type. In the cases of pieces with multiple primary types, each retouch is quantified individually. Cells in black are the categories representing more than 10% of the total cases. Cells in dark grey are the categories representing between 5 and 10% of cases.

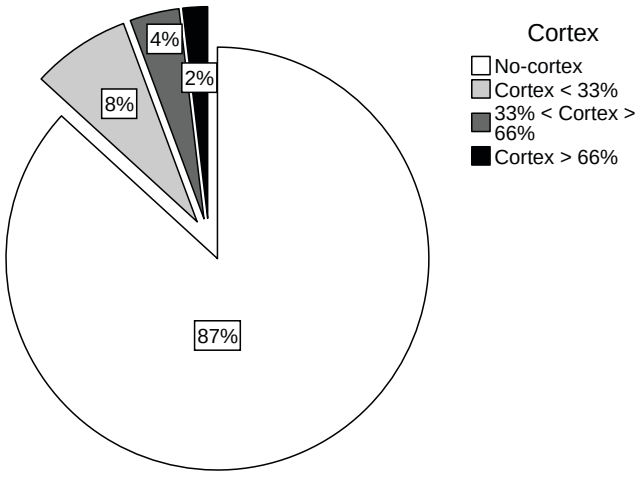

Figure-8.15: Pie chart showing percentage of absence, presence and extension of cortex on retouched artefacts from layer-XXII of El Esquilleu rockshelter.

Finally, we analyse the relation between retouched blanks and its cortex preservation Figure-8.15. Eight per cent of the retouched blanks has cortex covering less than 33% of the surface. Only 6% of retouched blanks have cortex covering more than 33% of the surface and only one retouched blank has cortex covering more than 66%. Two of the six blanks with multiple primary types have cortex. Regarding the characterisation of cortical areas on retouched blanks, three of them derived from fluvial deposits and other two from conglomerates. We were unable to identify the type of cortex on two artefacts.

8.5. TIPOMETRICAL STRUCTURE

In this section we will describe the results of the analysis of the tipometrical structure and its relationship with the structures studied previously. We made the measurement using the technological axis (length, width and thickness) on 562 lithic pieces (71% of the assemblage). The remaining 227 items were measured using the longest axis (X, Y and Z), due to the absence of features signalling the technological axis[1]. All chunks, most of the cores (some cores on flakes were measured using the technological axis) and some incomplete knapping products were measured using the latter criterion.

An overview of length, width and thickness reveals that all three measurement have positive skewness and kurtosis, the highest values being those of length, followed by width (Figure-8.16). The mean length is 21.18 mm, the mean width 18.87 mm, and the mean thickness 6.04. The measurements of the first two axes are similar between them. A general outlook of X, Y, and Z axes does also point at positive skewness and kurtosis. Nevertheless, all the means are clearly different between them: the means of the X is 21.33 mm, the mean of Y axis is 14.15mm, and the mean of the Z is 7.37 mm (Figure-8.17). The relationship between the three measurements with according to the Tarriñini indexes (Tarriño, 2015) reveals different morphologies depending on the measurement method employed (Figure-8.18). All pieces measured based on the X/Y/Z axes are between 0.5 and 0.8 of RBEI and between 0 and 0.5 of RFL, determining similar measurement between the three axes, in relatively cubic-bladed shapes. Material measured in relation to the technological axis follows similar pattern, also with tabular morphologies.

The last measurement used here is the weight of each lithic implement. The minimum weight is 0.06 g, and the maximum 90.6 g. The mean is 3.25 g. Weight presents high positive kurtosis (79.68) and positive skewness (6.75) as a consequence of the high percentage of lithic implements lighter than 5 g. The total of pieces weighted in this layer is 786 and the total weight of all of them is 2,560.64 g.

None of the aforementioned measurements is normally distributed[2].

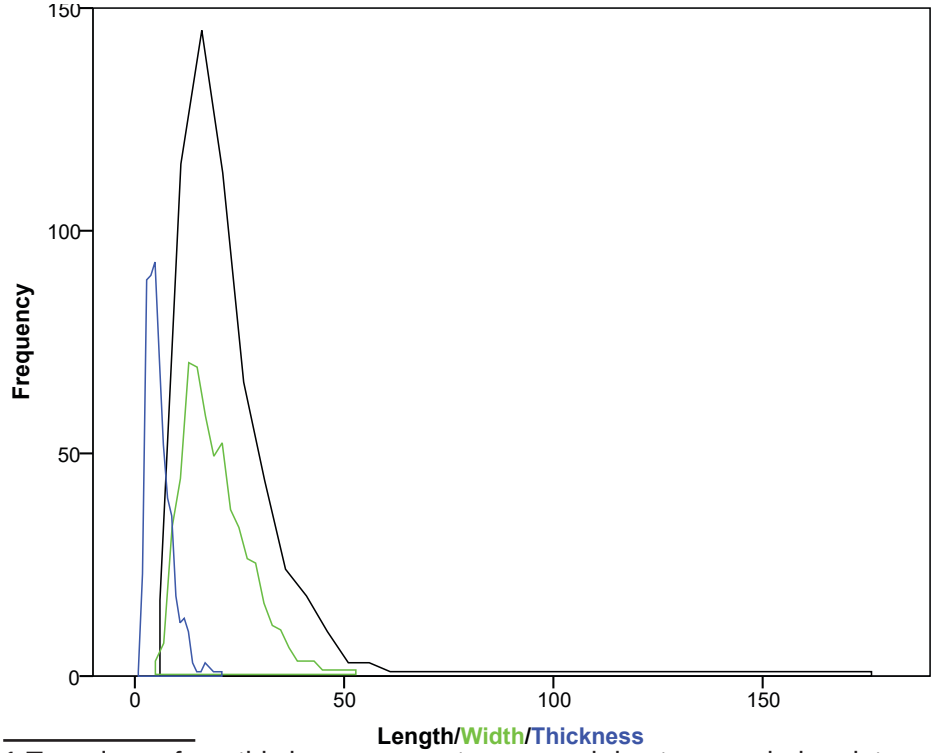

Figure-8.16: Frequency area chart showing the distribution of length, width and thickness of lithic remains from layer-XXII of El Esquilleu measured in relation to technological axis. Black line represents length, green line represents width, and blue line represents thickness.

1 Two pieces from this layer were not measured due to error during data acquisition.
2 *KS* = 0.135; *df* = 563; *p* < 0.01 for length
KS = 0.105; *df* = 563; *p* < 0.01 for width
KS = 0.160; *df* = 563; *p* < 0.01 for thickness
KS = 0.161; *df* = 226; *p* < 0.01 for X-axis
KS = 0.147; *df* = 226; *p* < 0.01 for Y-axis
KS = 0.179; *df* = 226; *p* < 0.01 for Z-axis
KS = 0.286; df = 786; *p* < 0.01 for weight

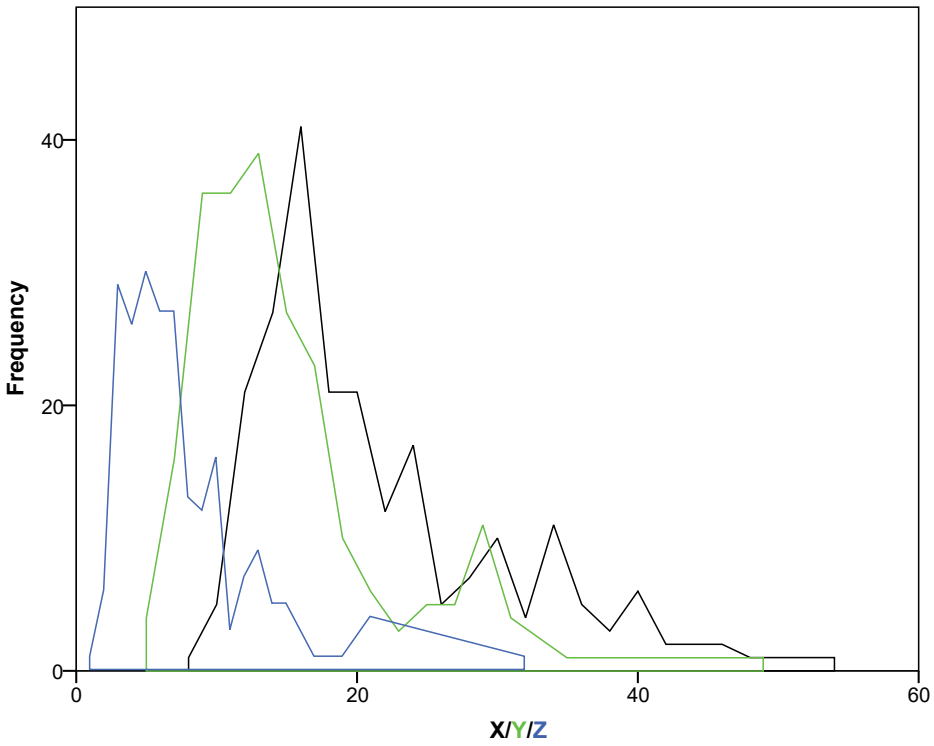

Figure-8.17: Frequency area chart showing the distribution of X, Y and Z axes of lithic remains from layer-XXII of El Esquilleu measured in relation to technological axis. Black line represents the X axis, green line represents the Y axis, and blue line represents the Z axis.

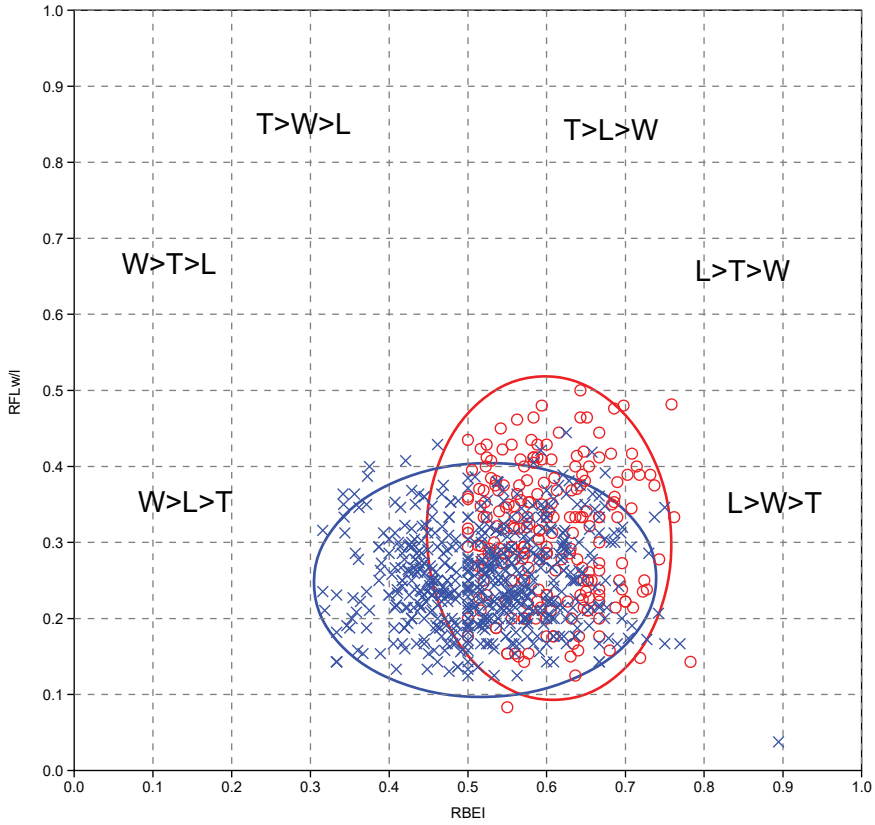

Figure-8.18: Scatter plot of RFLw or RFLl and RBEI indexes. Blue crosses and ellipse are measurements made in relation to technological axis. Red circles and ellipse are the measurements made in relation to X/Y/Z axis. Ellipses enclose 95% of cases of each category.

Once the general metric characteristics have been understood, we will relate this data with the technological structure. The three technological orders proposed show differences in shape between. Figure-8.19a shows three different but overlapping groups using 95% confidence ellipses. The ellipse of cores ellipse is the smallest one and it is situated in the central and upper part of the

chart, describing vertical elongation. The ellipse of knapping products is located on the lower area and it describes a horizontal elongation. Finally, the ellipse of chunks is positioned in the central area, displaying a circular shape. The distribution of weight of each order does also show clear differences in variance, as demonstrated by *H* Kruskal-Wallis test: $H\ \chi^2\ (2, N = 786) = 46.960, p < 0.001$ (Figure-8.19b). In general, cores are bigger than other orders, with weight around 15 g for each piece (Table-8.20). Knapping products and chunks have similar ratios (2.9 g), significantly smaller in comparison with cores.

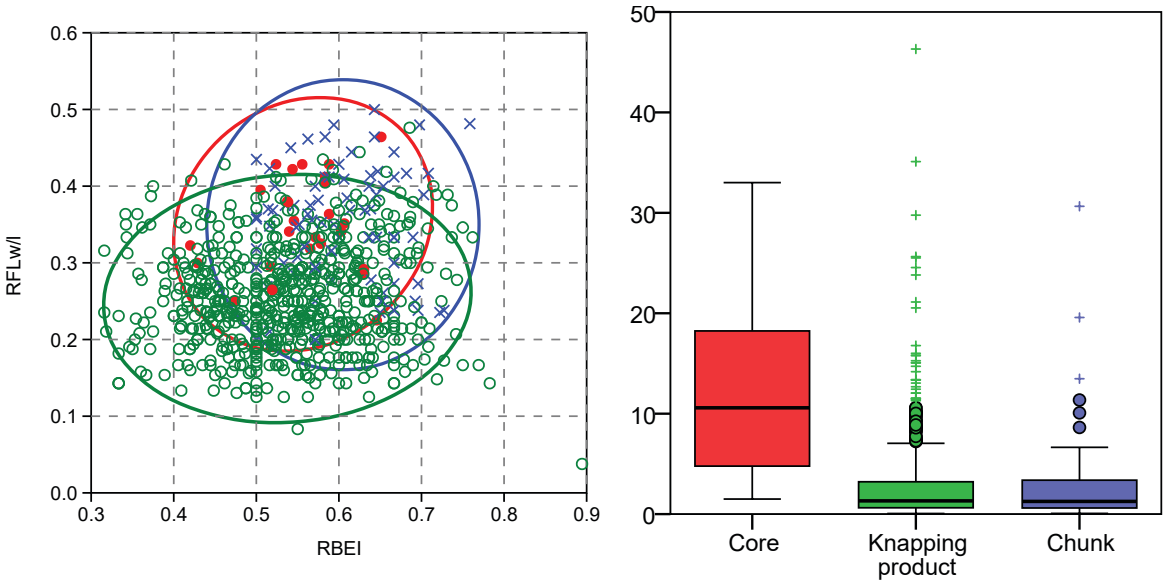

Figure-8.19: Double chart showing: a) Scatter plot of RFLw or RFLl and RBEI indexes. Green circles and ellipse are knapping products. Red points and ellipse are cores. Blue crosses and ellipse are chunks. Ellipses enclose 95% of cases of each category. b) Boxplot showing differences in weight between various technological orders. There is another core with weight of 90.6g.

Technological order	Weight		∑ of pieces		Ratio
	∑	%	∑	%	Grams/Piece
Core	377,0	12,9	26	2,5	14,5
Knapping product	1955,7	87,2	680	77,8	2,9
Chunk	228,0	10,3	80	9,3	2,8

Table-8.20: Frequencies and weight of main technological orders. The ratio grams/piece is reported. Weight is expressed in grams.

Coming to cores, there are no differences regarding in morphology between the types proposed, as displayed in Figure-8.20a through the relationship between RBEI and RFL even though discoid, levallois and irregular cores 95% confidence ellipses displays different than cores on flake one. Weight is different distributed within each category as indicated by the analysis of variance based on *H* Kruskal-Wallis test: $H\ \chi^2\ (4, N = 26) = 15.126, p < 0.05$. Bigger differences are visible by comparing means between each type of core as (Figure-8.20b). Regarding the average weight of each category of cores, discoidal cores are the biggest ones. Prismatic, irregular, and levallois cores are lighter than the first. Finally, cores on flake are the smallest, with a 5.4 g/p average (Table-8.21).

Core groups	Weight		∑ of pieces		Ratio
	∑	%	∑	%	Grams/Piece
Irregular core	95,6	25,8	7	30,0	13,7
Discoid core	171,5	51,7	5	25,0	34,3
Levallois core	33,9	10,2	3	15,0	11,3
Prismatic core	21,7	6,6	1	5,0	21,7
Core on flake	54,2	5,6	10	25,0	5,4

Table-8.21: Frequencies and weight of different groups of cores. The ratio grams/piece is reported. Weight is expressed in grams.

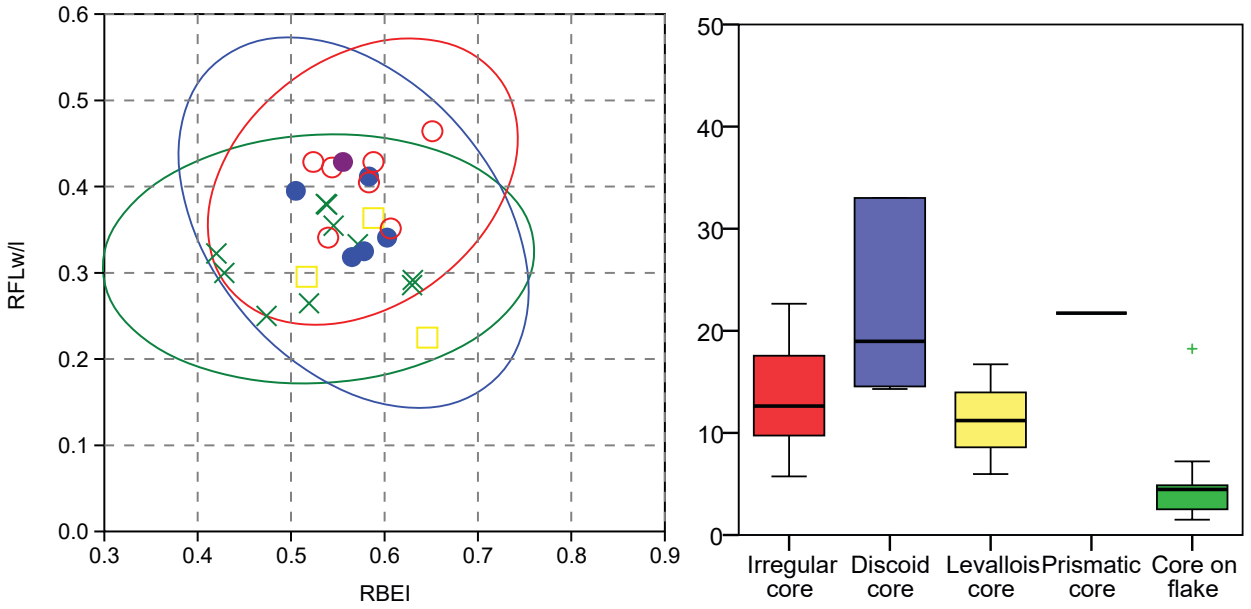

Figure-8.20: Double chart showing: a) Scatter plot of RFLw or RFLl and RBEI indexes. Green crosses and ellipse are cores on flakes. Red circles and ellipse are irregular cores. Blue points and ellipse are discoidal cores. The yellow squares are Levallois cores and the purple point is a prismatic shape core. Ellipses enclose 95% of cases of each category. b) Boxplot showing differences in weight between types of cores.

The two groups of knapping products do not reveal differences in the form of lithic remains, as shown on Figure-8.21a. The areas defined by the 95% confidence ellipses are similar for blanks and core preparation/rejuvenation products with small differences due to the small quantity of the latter. Nevertheless, there are differences in weight distribution, as it can be observed in Figure-8.21b. Moreover, *U* Mann-Whitney test reveals differences in the distribution, $U = 4{,}806$, $p < 0.05$. The gram per piece ratio points out clear differences in the mean weight of the items from each group: blanks weight 2.9 g on average while the core preparation/rejuvenation products weight 6.9 g on average (Table-8.22).

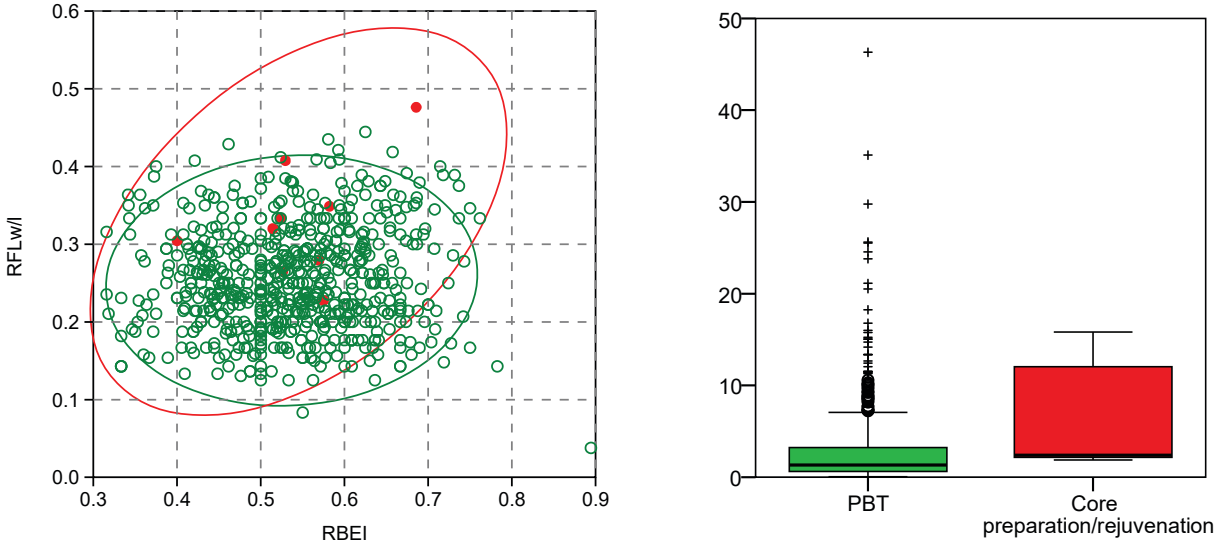

Figure-8.21: Double chart showing: a) Scatter plot of RFLw or RFLl and RBEI indexes. Green circles and ellipse are blanks. Red points and ellipse are core preparation/rejuvenation products. Ellipses enclose the 95% of cases of each category. b) Boxplot showing differences in weight between blanks and core preparation/rejuvenation products.

Knapping product group	Weight		∑ of pieces		Ratio
	∑	%	∑	%	Grams/Piece
Blank	1929,5	96,9	676	98,7	2,9
Core prep./rejuv.	61,8	3,1	9	1,3	6,9

Table-8.22: Frequencies and weight of different groups of knapping products. The ratio grams/piece is reported. Weight is expressed in grams.

Focusing on, there are differences in their formats based on the number of negative scars on their dorsal surfaces (Figure-8.22a). Blanks without negative scars are different to others. The 95% confidence ellipse of the first is smaller than other ellipses, and it has clearer horizontal elongation. Three other 95% confidence ellipses are wider and the elongation is less pronounced, situated in the area of tabular, bladed and more cubic morphologies. It could reveals decortication of lithic mass in the site. The thickness for the last three categories is more variable and could be higher. Moreover, there are clear differences weight based on the number of negative scars observable, as shown in Figure-8.22b and statistically demonstrated by *H* Kruskal-Wallis test: $H\ \chi^2$ (3, N = 676) = 87.863, p < 0.001. The weight of the pieces with three or more negative scars is higher than on the other three categories and the distribution is also wider. The comparison of the grams per piece ratio of each category confirms this idea (Table-8.23).

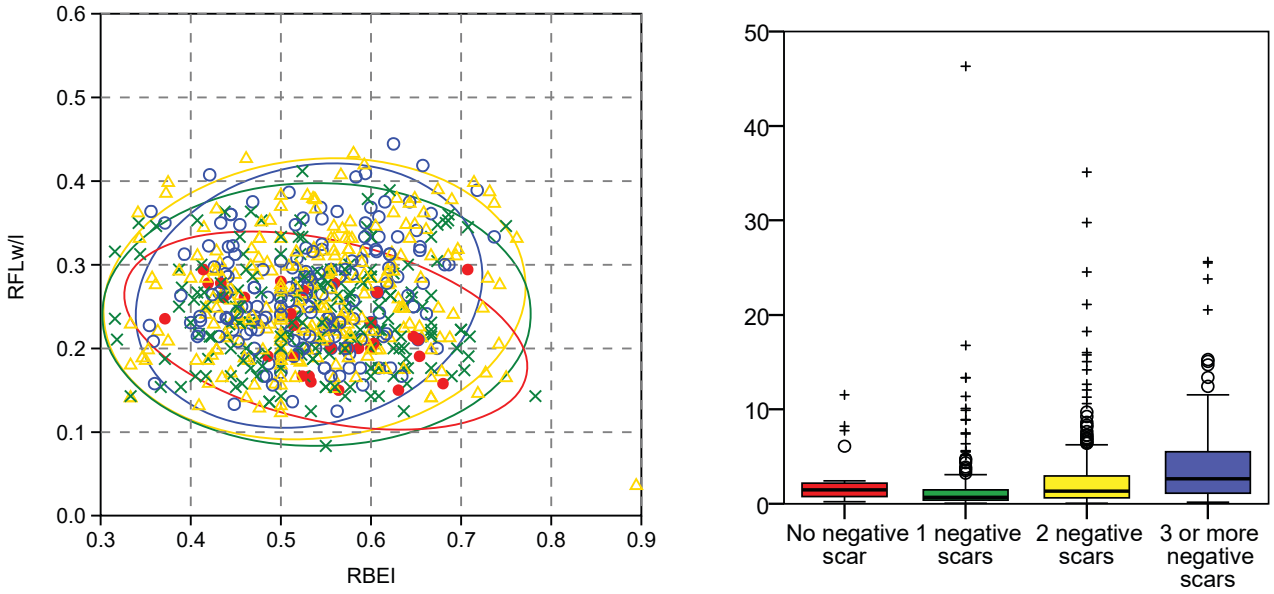

Figure-8.22: Double chart showing: a) Scatter plot of RFLw or RFLl and RBEI indexes. Red points and ellipse are blanks without negative scar. Green crosses and ellipse are blanks with one negative scar. Yellow triangles and ellipse are blanks with two negative scars. Blue circles and ellipse are blanks with three or more negative scars. Ellipses enclosure the 95% of the points from each category. b) Boxplot showing differences in weight between blanks with different number of negative scars on dorsal surface.

Number of negative scars	Weight		∑ of pieces		Ratio
	∑	%	∑	%	Grams/Piece
No-negative scars	69,2	3,6	31	4,6	2,2
One negative scar	352,4	18,3	191	28,3	1,8
Two negative scars	736,9	38,2	268	39,6	2,7
Three or more negative scars	771,0	40,0	186	27,5	4,1

Table-8.23: Frequencies and weight of blanks grouped by number of negative scars. The ratio grams/piece is reported. Weight is expressed in grams.

Regarding the integrity of the blanks, there are differences based on the form of the pieces (Figure-8.23a). The ellipse of complete pieces is horizontally elongated and it is situated between 0.1 ≤ RFL ≥ 0.4 and 0.3 ≤ RBEI ≥ 0.7 (mainly tabular, cubic and bladed formats). Proximal fragments forming an elongated ellipse too are more closely related with the tabular and cubic forms between 0.1 ≤ RFL ≥ 0.45 and 0.2 ≤ RBEI ≥ 0.7. Instead, medial fragments creates a more elongated ellipse in

negative elongation due to the smaller presence of thicker morphologies. Distal fragments describes a positive and elongated 95% confidence ellipse in relation with the tabular and prismatic shapes and in similar region where medial fragments embodied. Longitudinal fragments 95% confidence ellipse describes a relatively rounded ellipse in the region where more elongated and thicker shapes are present in between 0.1 ≤ RFL ≥ 0.45 and 0.4 ≤ RBEI ≥ 0.75. Finally indeterminate fragments outline a circular ellipse located in the RBEI values higher than 0.1 and RFL values below the 0.5. This is because of the use of X/Y/Z axes for the measurement of every fragment, and the relatively homogeneity of the three measurements. Comparing the distribution of weight between various types of blanks *H* Kruskal-Wallis test indicates there are statistically differences between them: $H\ \chi^2$ (5, N = 676) = 15.431, $p < 0.01$. In Figure-8.23b it is possible to observe that complete lithic assemblages are different from the others, even though there are some similitudes in the distribution with the proximal and longitudinal fragments. The grams/piece ratio leads to the same conclusions (Table-8.24).

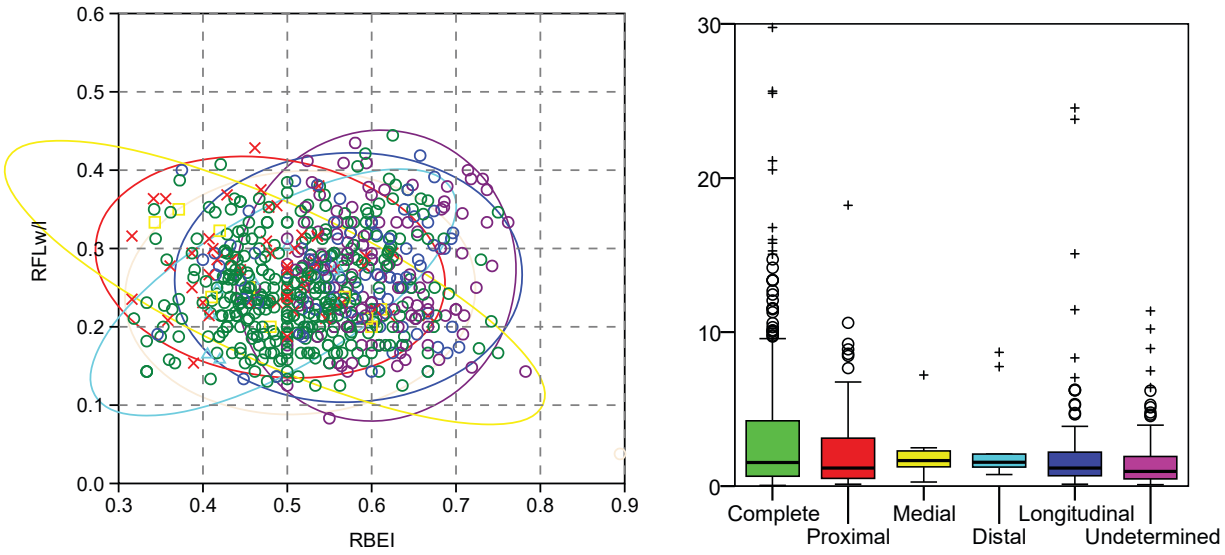

Figure-8.23: Double chart showing a) Scatter plot RFLw or RFLl and RBEI indexes. Green circles and ellipse are complete blanks. Red crosses and ellipse are proximal blank fragments. Yellow squares and ellipse are medial blank fragments. Light blue triangles and ellipse are distal blank fragments. Blue circles and ellipse are longitudinal blank fragments. Purple circles and ellipse are undetermined blank fragments. Ellipses enclosure the 95% of the points from each category. b) Boxplot showing differences in weight between blanks preserved in diverse states of integrity.

Integrity of blanks	Weight		∑ of pieces		Ratio
	∑	%	∑	%	Grams/Piece
Complete	1298,8	67,3	379	56,1	3,4
Proximal fragment	145,6	7,5	53	7,8	2,7
Medial fragment	21,0	1,1	10	1,5	2,1
Distal fragment	27,8	1,4	10	1,5	2,8
Longitudinal fragment	231,4	12,0	94	13,9	2,5
Undetermined fragm	205,0	10,6	130	19,2	1,6

Table-8.24: Frequencies and weight of blanks grouped by integrity. The ratio grams/piece is reported. Weight is expressed in grams.

The classification of complete blanks products as flakes (Figure-8.24a) reveals the major predominance of flakes (83% of complete blanks), followed by a moderate presence of elongated flakes (13% of complete blanks) and a really occasional of blades (4% of complete collection). There is no difference in weight between these three categories, which show similar distributions, as depicted in Figure-8.24b and proven by *H* Kruskal-Wallis: $H\ \chi^2$ (2, N = 379) = 2.901, p = .234. The gram/piece ratio of three proposed types only reveals small differences in the weight between the elongated flakes and the other two categories (Table-8.25).

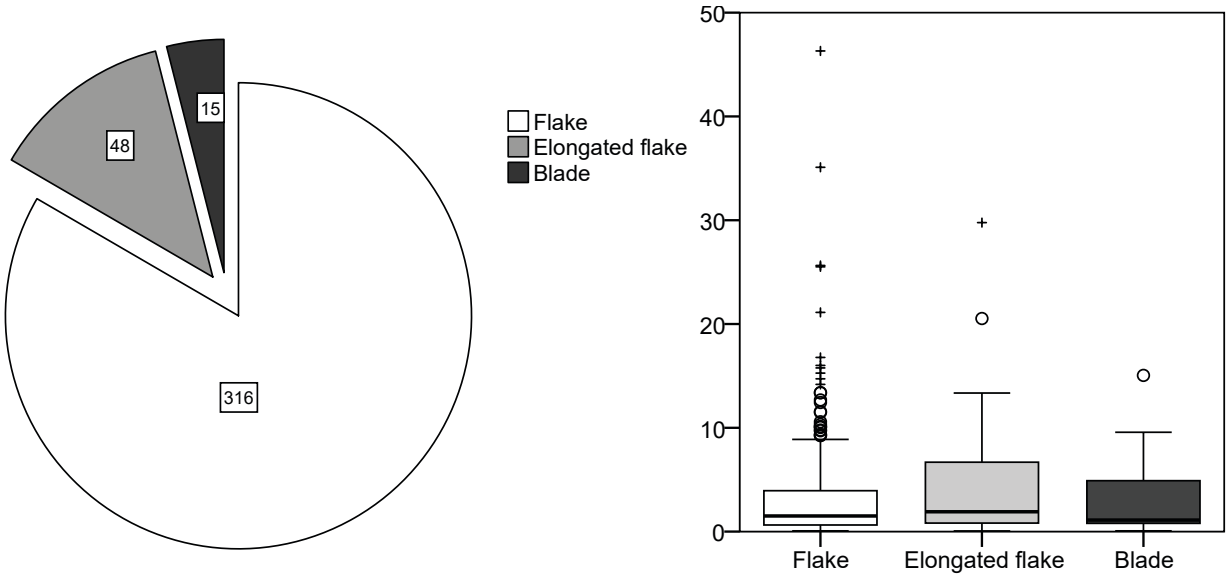

Figure-8.24: Double chart showing a) pie chart showing the distribution of complete blank products, and b) boxplot showing differences in weight between metrical categories.

Complete blank characterisation	Weight		∑ of pieces		Ratio
	∑	%	∑	%	Grams/Piece
Flake	1031,7	79,4	316	83,4	3,3
Elongated flake	215,5	16,6	48	12,7	4,5
Blade	51,5	4,0	15	4,0	3,4

Table-8.25: Frequencies and weight of different types of complete blanks (flakes, elongated flakes, blades). The ratio grams/piece is reported. Weight is expressed in grams.

Next, we will analysed the (typo)metrical structure of retouched artefacts. First, we observe weight differences based on the presence (M = 6.64) or absence (M = 1.3) of retouch in the pieces, as corroborated by *U* Mann-Whitney test: $U = 27{,}538.5$, $p < 0.001$. Retouched artefacts are heavier than artefacts than unretouched ones (Figure-8.25b). The mean weight of unretouched lithics is similar to the mean ratio of the whole assemblage, while the grams/piece ratio of retouched blanks is noticeably bigger (Table-8.26). There are no differences in morphology between retouched artefacts and non-retouched blanks (Figure-8.25a). There are neither differences in morphology or weight of blanks depending on the quantity of primary types on them (Figure-8.26 and Table-8.27).

Piece	Weight		∑ of pieces		Ratio
	∑	%	∑	%	Grams/Piece
Non-retouched	2256,4	88,1	735	93,5	3,1
Retouched	304,3	11,9	51	6,5	6,0

Table-8.26: Frequencies and weight of the retouched and non-retouched pieces. The ratio grams/piece is reported. Weight is expressed in grams.

Quantity of retouch in each piece	Weight		∑ of pieces		Ratio
	∑	%	∑	%	Grams/Piece
One primary type	266,6	87,7	46	90,2	5,8
Two primary types	37,7	12,3	5	9,8	7,5

Table-8.27: Frequencies and weight of retouched pieces grouped by the quantity of primary types identified in each blank. The ratio grams/piece is reported. Weight is expressed in grams.

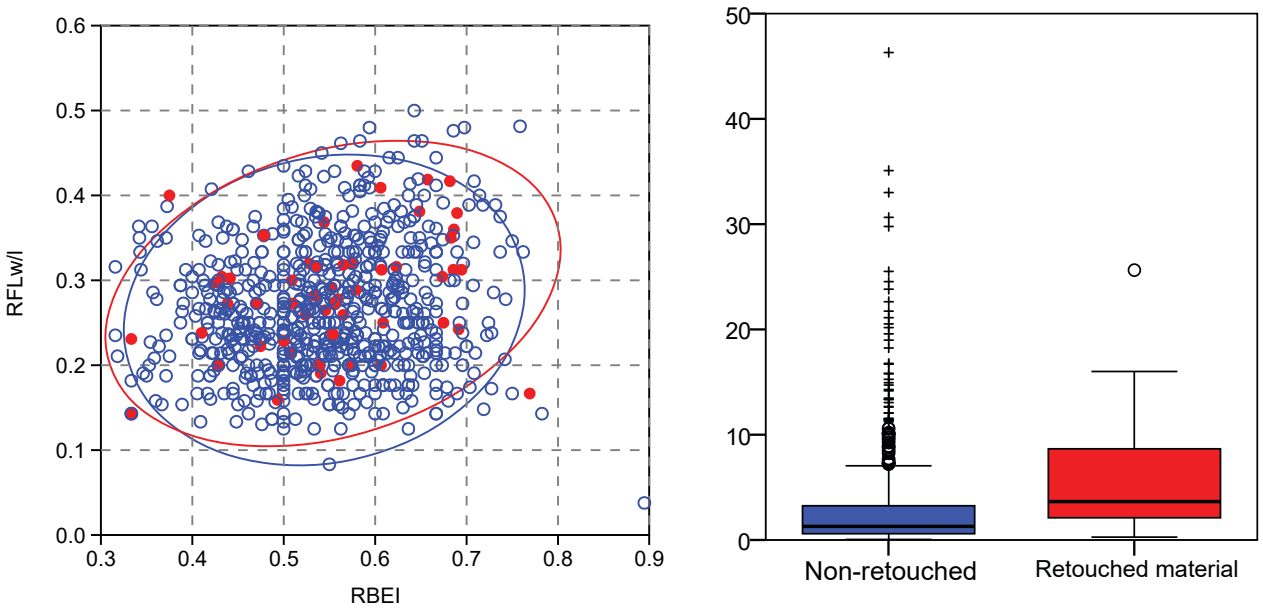

Figure-8.25: Double chart showing: a) Scatter plot of RFLw or RFLl and RBEI indexes. Red points and ellipse are retouched artefacts. Blue circles and ellipse are non-retouched lithic material. Ellipses enclose 95% of cases of each category. b) Boxplot showing differences in weight between retouched and non-retouched lithic material.

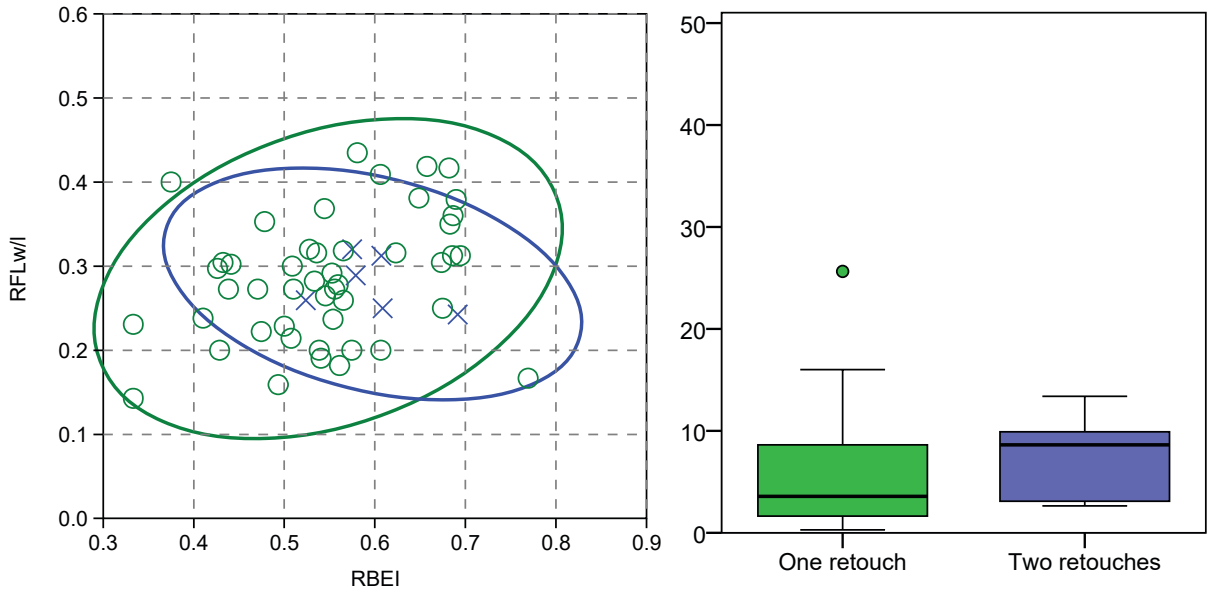

Figure-8.26: Double chart showing: a) Scatter plot of RFLw or RFLl and RBEI indexes. Green circles and ellipse are retouched artefacts with one primary type on each blank. Blue crosses and ellipse are retouched artefacts with two primary types on each blank. Red point is the retouched artefact with three primary types on each blank. Ellipses enclose 95% of cases of each category. b) Boxplot showing differences in weight between retouched artefacts with different quantity of primary types configured on each blank.

Then, we will confront metrical features of retouched artefacts with the features of retouch, categorised in orders (modal) and groups (morphological). Due to the methodology used to define retouch here, we only includes in this analysis the pieces with one primary type. The comparison reveals similitudes in the morphologies and weights between blanks retouched with the three orders of retouch identified (Figure-8.27). Nevertheless, the grams/piece ratio of blanks configured with the splinter mode is smaller than other two orders of retouch (Table-8.28).

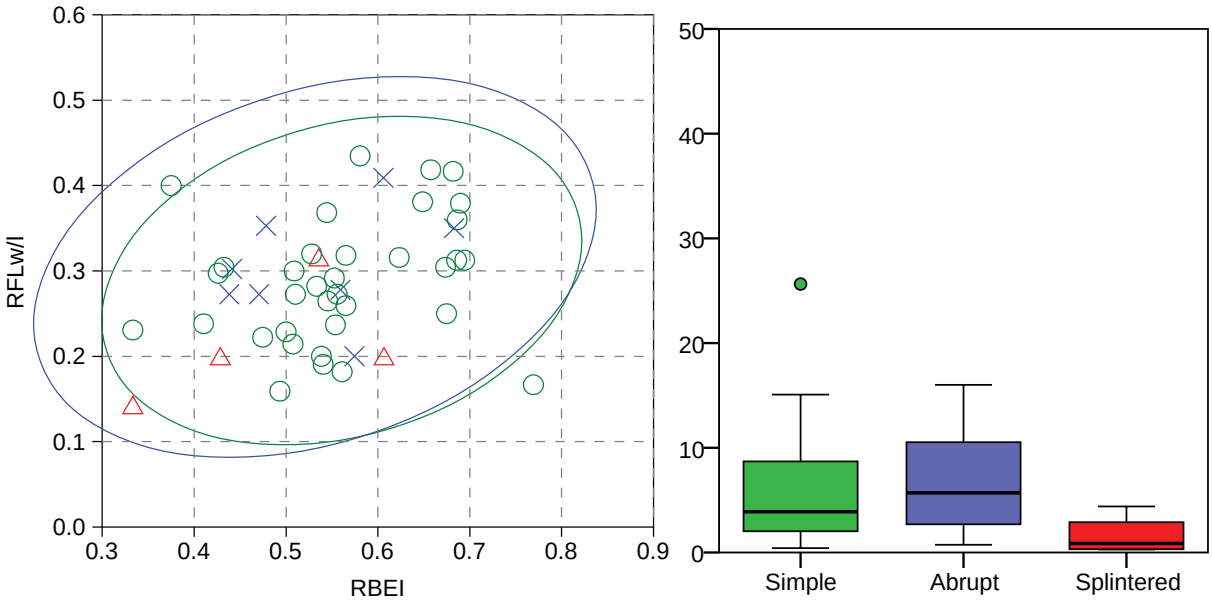

Figure-8.27: Double chart showing: a) Scatter plot of RFLw or RFLl and RBEI indexes. Green circles and ellipse are Simple mode of retouch. Blue crosses and ellipse are Abrupt mode of retouch. Red triangles are Splinter mode of retouch. b) Boxplot showing differences in weight between different orders of retouch.

Order of retouch	Weight		∑ of pieces		Ratio
	∑	%	∑	%	Grams/Piece
Simple	205,6	77,3	34	73,9	6,0
Abrupt	54,6	20,5	8	17,4	6,8
Splinter	6,4	2,4	4	8,7	1,6

Table-8.28: Frequencies and weight of artefacts with one primary type grouped by the mode of retouch. The ratio grams/piece is reported. Weight is expressed in grams.

The last structure to be tackled here is the petrological one. There are differences in the morphology of the lithics depending on each raw material (Figure-8.28a). “Archaeological quartzites” are situated in the centre of the chart and they are represented by a rounded but slightly elongated ellipse, in the area of thinner than thicker forms. Flint shows thicker forms, as quartz. The morphology of radioralite is variable without clear tendencies. Finally, lutites morphologies embodied by 95%confidence ellipse reveals not elongated, neither tabular forms with a high variability in thickness. Regarding weight distribution of raw material, there are no statistically differences between them, as *H* Kruskal-Wallis test proves: $H\ \chi^2\ (4, N = 785) = 8.477$, $p = 0.076$. Moreover, the comparison of grams/piece ratio between raw material points out that radioralite and flint are lighter than others (Table-8.29).

Raw material	Weight		∑ of pieces		Ratio
	∑	%	∑	%	Grams/Piece
"Arch. quartzite"	2282,0	89,2	681	86,8	3,4
Flint	86,2	3,4	39	5,0	2,2
Lutite	23,2	0,9	8	1,0	2,9
Quartz	140,0	5,5	38	4,8	3,7
Radioralite	28,1	1,1	19	2,4	1,5

Table-8.29: Frequencies and weight of different types of raw material. The ratio grams/piece is reported. Weight is expressed in grams.

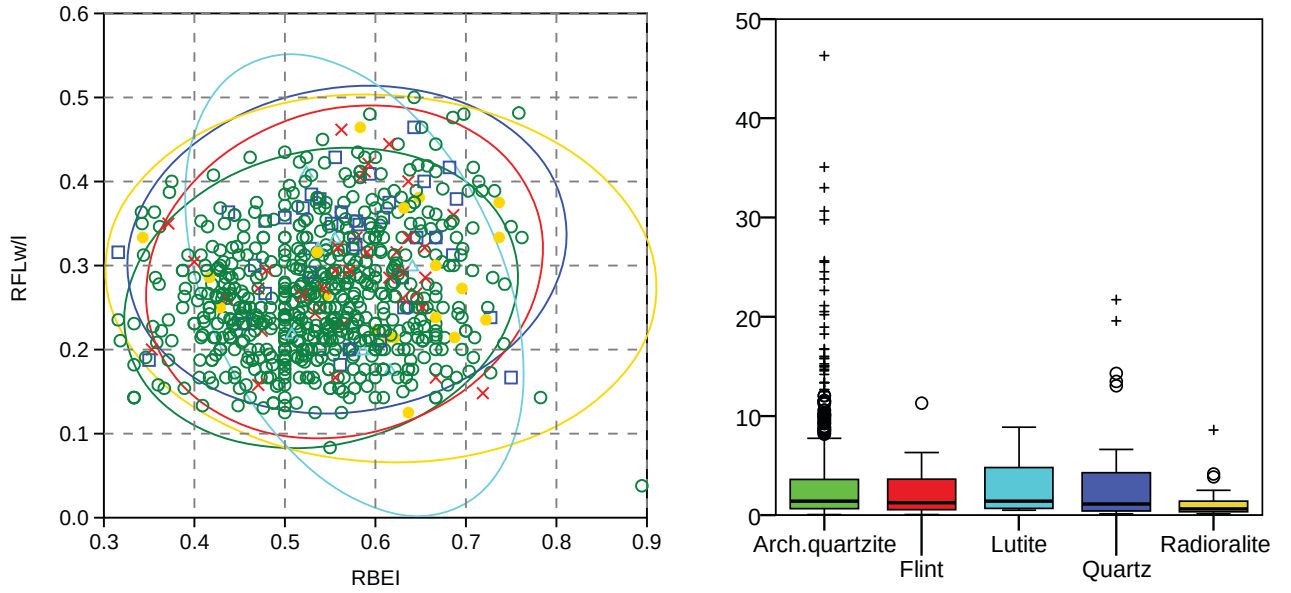

Figure-8.28: Double chart showing: a) Scatter plot of RFLw or RFLI and RBEI indexes. Green circles and ellipse are “archaeological quartzites”. Red crosses and ellipse are flint. Light blue triangles and ellipse are lutites. Blue squares and ellipse are quartz. Yellow points and ellipse are radioralite. Ellipses enclose 95% of cases of each category. b) Boxplot showing differences in weight between different raw materials.

There are small differences in the morphology between the BQ quartzite and other petrogenetic types due to the higher presence of thinner forms in this type (Figure-8.29a). The different morphology of the ellipse of RQ pieces is conditioned by its small presence. There are also small differences when analysing the weight distribution between petrogenetic types, even they are not statistically significant: *H* Kruskal-Wallis shows: $H\ \chi^2$ (6, N = 659) = 11.906, p = 0.064. The grams/piece ratio suggest that heavier lithics are on quartzarenite group (Table-8.30).

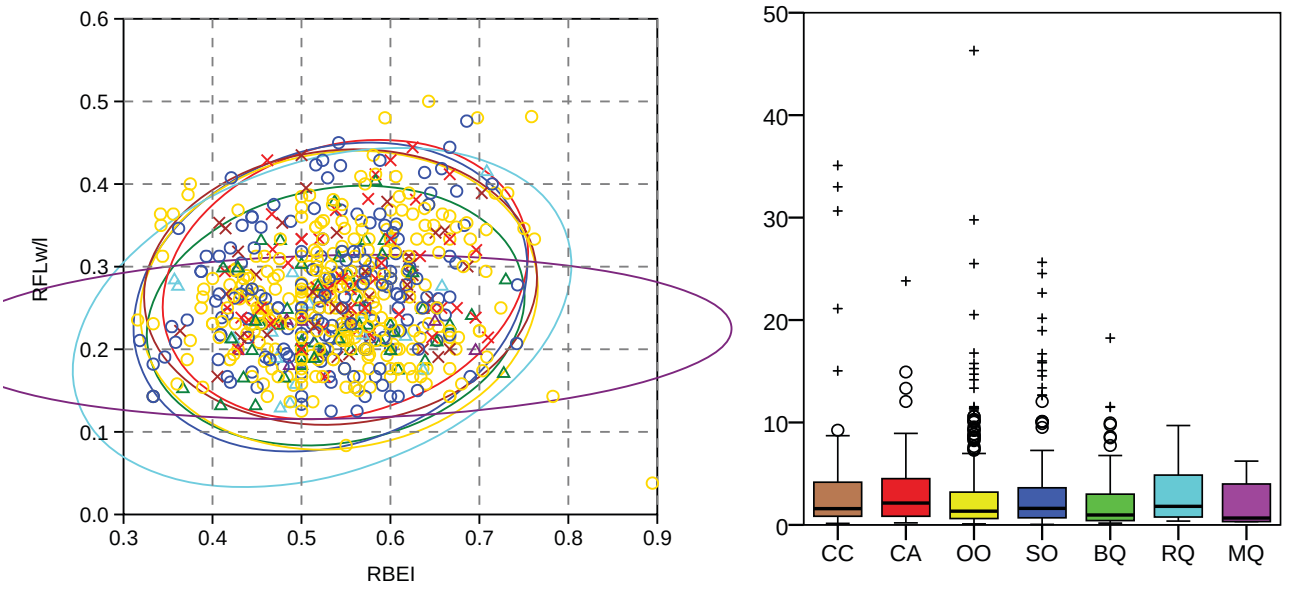

Figure-8.29: Double chart showing: a) Scatter plot of RFLw or RFLI and RBEI indexes. Brown crosses and ellipse are CC type pieces. Red crosses and ellipse are CA type pieces. Yellow circles and ellipse are OO type pieces. Blue circles and ellipse are SO type pieces. Green triangles and ellipse are BQ type pieces. Light blue triangles and ellipse are RQ type pieces. Purple triangles and ellipse are MQ types. Ellipses enclose the 95% of cases of each category. b) Boxplot showing differences in weight between different petrogenetic types of “archaeological quartzites”.

Petrogenetic type	Weight		∑ of pieces		Ratio
	∑	%	∑	%	Grams/Piece
CC	246,8	11,1	53	8,0	4,7
CA	253,8	11,4	44	6,7	5,8
OO	913,7	41,2	309	46,9	3,0
SO	600,4	27,1	179	27,2	3,4
BQ	142,4	6,4	51	7,7	2,8
RQ	50,3	2,3	17	2,6	3,0
MQ	12,2	0,5	6	0,9	2,0

Table-8.30: Frequencies and weight of different petrogenetic types of “archaeological quartzites”. The ratio grams/piece is reported. Weight is expressed in grams.

Now, we will delve into the relationship between raw material, technology, retouch and the metrical structure, focusing on size and weight. Starting with technology, there are clear differences in weight based on the technological order and raw material (Figure-8.30 and Table-8.31). Cores on “archaeological quartzites” and quartz are bigger than flint ones. There are differences between petrogenetic types too. For example, cores on quartzarenites are heavier than orthoquartzite and quartzite cores. Despite the small number of cores, there are differences in weight based on the type of core and raw material (Figure-8.31 and Table-8.32). These differences are especially relevant in the case of core on flake between flint cores and quartz and quartzite ones. These differences increase in the comparison between petrogenetic types of “archaeological quartzites” in the cores on flake, higher and more variable in the BQ than others. Moreover, the heaviest cores are the discoidal ones, influenced by quartzarenite group with cores heavier than 30 grams (there is a non-represented core in Figure-8.30 neither in Figure-8.31, which belongs to CA type and weight 90.7 g). Nevertheless, irregular, Levallois and prismatic cores are similar distributed in ranges between 5 and 23 grams.

Raw material	Petrgen. type	Lithic collection											
		Core			Knapping			Chunks			Total		
		∑	W	g/p	∑	W	g/p	∑	W	g/p	∑	W	g/p
Archaeological quartzite	CC	1	33	33,0	43	170	3,9	9	44	4,9	53	247	4,7
	CA	2	106	52,8	39	142	3,6	3	7	2,2	44	254	5,8
	OO	2	15	7,5	287	837	2,9	20	61	3,1	309	914	3
	SO	10	129	12,9	158	444	2,8	11	27	2,5	179	600	3,4
	BQ	4	34	8,6	47	108	2,3				51	142	2,8
	RQ				16	47	2,9	1	3	3,4	17	50	3
	MQ				5	12	2,4	1	0	0,3	6	12	2
	Undet.	2	12	5,9	13	35	2,7	7	16	2,3	22	63	2,8
	Total	21	329	15,7	608	1794	3,0	52	159	3,1	681	2282	3,4
Flint		2	7	3,6	28	72	2,6	9	7	0,8	39	86	2,2
Lutite					8	23	2,9				8	23	2,9
Quartz		3	41	13,6	23	44	1,9	12	55	4,6	38	140	3,7
Radioralite					13	22	1,7	6	6	1,0	19	28	1,5

Table-8.31: Frequency table of different orders of lithic remains grouped by raw material, including frequencies, weight and the ratio grams/piece for each case. Weight is expressed in grams.

Raw material	Petr. type	Cores																	
		Irregular			Discoid			Levallois			Prismatic			Core on flake			Total		
		∑	W	g/p	∑	W	g/p	∑	W	g/p	∑	W	g/p	∑	W	g/p	∑	W	g/p
Archaeological quartzite	CC				1	33	33,0										1	33	33,0
	CA	1	15	14,9	1	91	90,7										2	106	52,8
	OO							1	11	11,2				1	4	3,8	2	15	7,5
	SO	4	65	16,2	2	34	16,8	1	17	16,7				3	14	4,6	10	129	12,9
	BQ	1	10	9,7										3	25	8,2	4	34	8,6
	RQ																		
	MQ																		
	Undet.	1	6	5,7				1	6	6,0							2	12	5,9
	Total	7	95	13,6	4	157	39,3	3	34	11,3				7	42	6,0	21	329	15,6
Flint														2	7	3,6	2	7	3,6
Limestone																			
Lutite																			
Quartz					1	14	14,3				1	22	21,7	1	5	4,9	19	41	2,2
Radioralite																1,0	1,3	0	0,0

Table-8.32: Frequency table of different core types grouped by raw material, including frequencies, weight and ratio grams/piece for each case. Weight is expressed in grams.

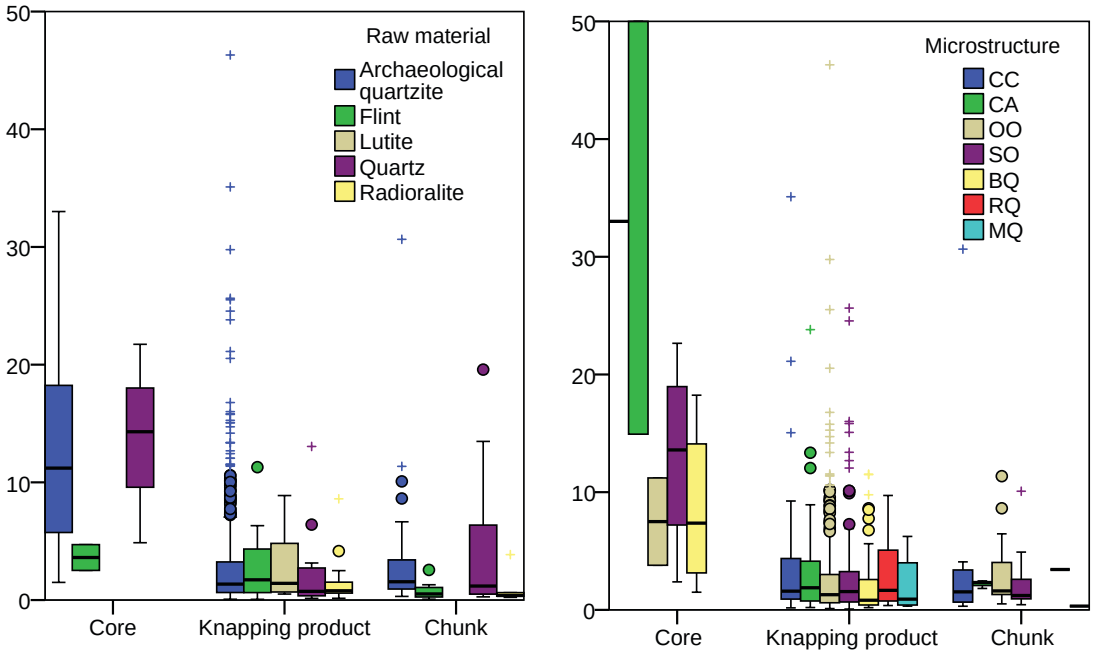

Figure-8.30: Double box-plot showing the distribution of weight in grams of all lithic remains grouped first by technological order and second by raw material in the chart on the left and by petrogenetic type in the chart on the right.

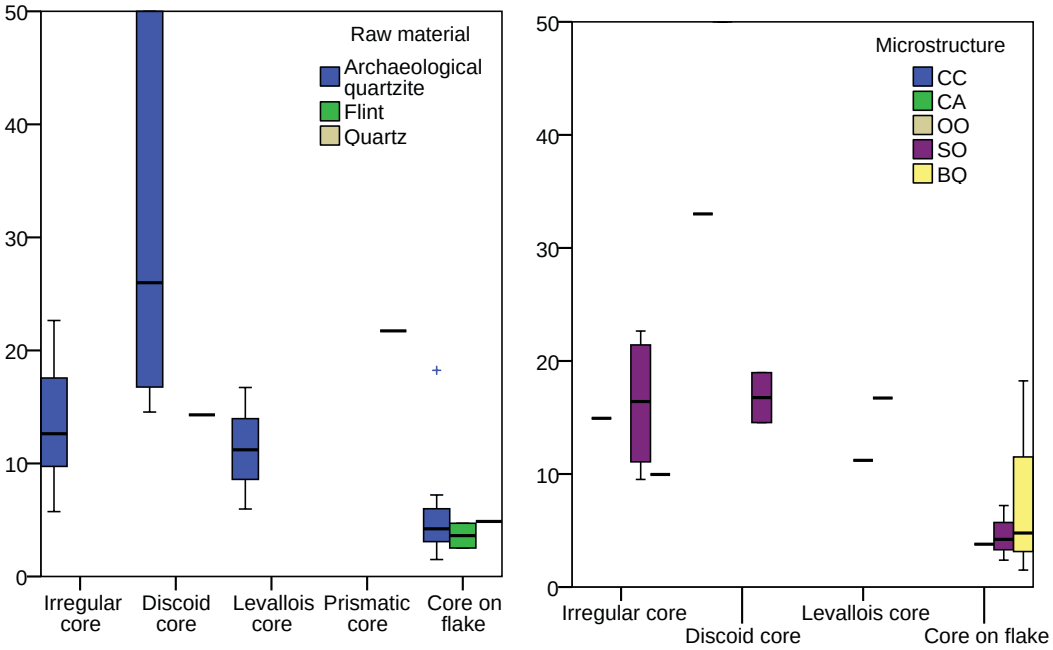

Figure-8.31: Double box-plot showing the distribution of weight in grams of cores grouped first by type and second by raw material in the chart on the left and by petrogenetic type in the chart on the right.

In regard to knapping products, Table-8.33 displays the differences between core preparation/rejuvenation products and blanks. The first are bigger than the second, except in the flint. Focusing on specific petrogenetic types of “archaeological quartzite”, the biggest core preparation/rejuvenation products are made on OO type. There are also differences in weight of blanks based on the number of negative scars between raw materials (Figure-8.32). “Archaeological quartzite”, radioralite, and flint enlarge with the increase in number of negative scars. On the contrary, quartz and specially lutite follow the opposite process. The orthoquartzite group and the BQ and MQ follow similar enlargement of weight in the intensification in number of negative scars, while on the quartzarenite and RQ type, this association is not evidenced. The weight distribution of blanks without negative scars is also interesting due to a) the absence of flint, quartz, radioralite, and RQ and MQ quartzites, and b) the weight differences between the BQ and any other types or raw material. It is also interesting to note the lack of blanks on the lutites, quartzarenites and MQ and RQ types lighter than one gram.

Raw material	Petrgen. type	Knapping products																	
		Core preparation			Blanks														
					No neg.scar			1 neg.scar			2 neg.scar			3 or more			Blank total		
		∑	W	g/p	∑	W	g/p	∑	W	g/p	∑	W	g/p	∑	W	g/p	∑	W	g/p
Archaeological quartzite	CC				3	3	0,9	10	11	1,1	18	103	5,7	12	53	4,4	43	170	3,9
	CA				2	3	1,3	10	39	3,9	16	40	2,5	11	60	5,5	39	142	3,6
	OO	3	15	4,9	13	38	2,9	93	190	2	110	289	2,6	69	310	4,5	285	826	2,9
	SO	4	32	8	9	16	1,7	44	72	1,6	55	155	2,8	47	177	3,8	155	419	2,7
	BQ				2	8	4,1	13	12	0,9	20	47	2,3	14	61	4,4	49	128	2,6
	RQ							5	5	0,9	7	32	4,6	4	10	2,6	16	47	2,9
	MQ							1	0	0,4	2	4	2,2	2	7	3,6	5	12	2,4
	Undet.				1	1	1,3	1	0	0,2	5	4	0,9	6	29	4,9	13	35	2,7
	Total	7	47	6,7	30	69	2,3	177	328	1,9	233	673	2,9	165	708	4,3	605	1778	2,9
Flint		1	2	2,2				4	9	2,3	12	23	1,9	11	38	3,5	27	70	2,6
Lutite					1	1	0,5	3	11	3,7	3	11	3,6	1	1	0,8	8	23	2,9
Quartz		1	13	13				6	4	0,6	12	23	1,9	5	10	2	23	36	1,6
Radioralite								1	0	0,2	8	8	1	4	14	3,6	13	22	1,7

Table-8.33: Frequency table of different knapping products grouped by raw material, including frequencies, weights and the ratio grams/piece for each case. The knapping products considered are core preparations/rejuvenations and blanks sorted by the number of negative scars present. Weight is expressed in grams.

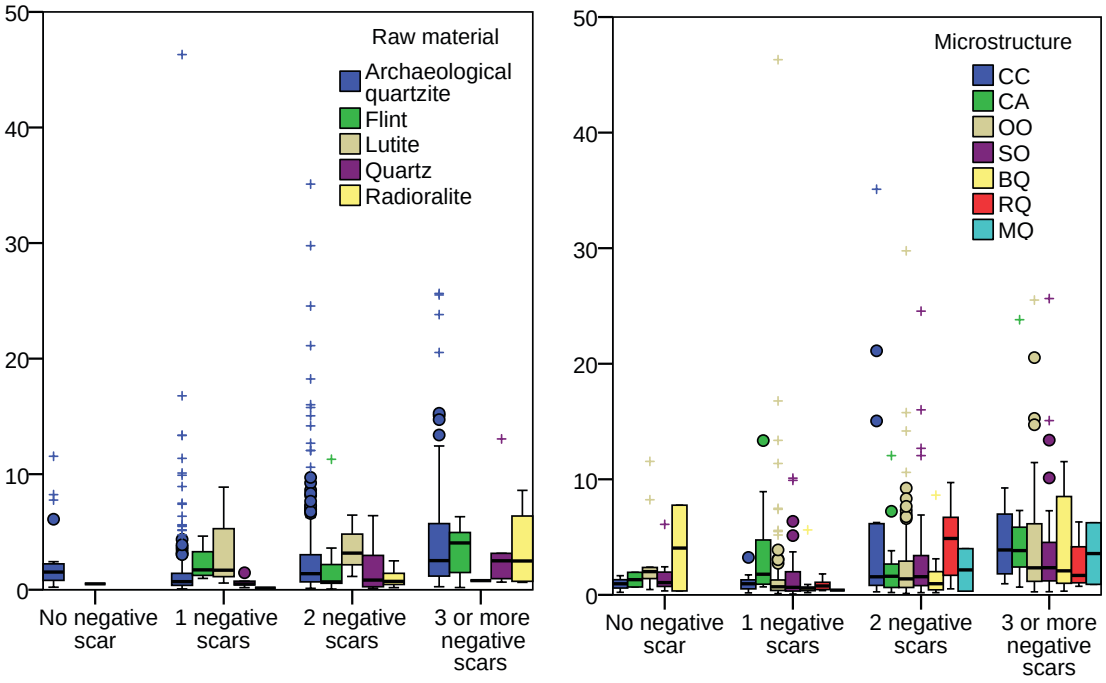

Figure-8.32: Double box-plot showing the distribution of weight in grams of blanks grouped first by the number of negative scars on dorsal surface and second by raw material in the left chart and by petrogenetic type in the chart on the right.

Finally, differences in weight of chunks based on raw material are verifiable in Figure-8.30 and Table-8.31. While chunks on “archaeological quartzite” and quartz are heavier, chunks on radioralite and flint are lighter. Due to the small quantity of chunks in “archaeological quartzites”, especially in CA and the quartzite group, we could not observed differences in weight distribution. Nevertheless, its absence evidence different management of these types.

The analysis of the relationship between raw material and the retouch concludes that the heaviest retouched artefacts are made on “archaeological quartzite” and radioralite. Meanwhile retouched artefacts configured on flint and quartz blanks are lighter (Figure-8.33 and Table-8.35). The same analysis based on petrogenetic types reveals that the heaviest retouched artefacts configured using the Simple and Abrupt modes are made on the SO type blanks.

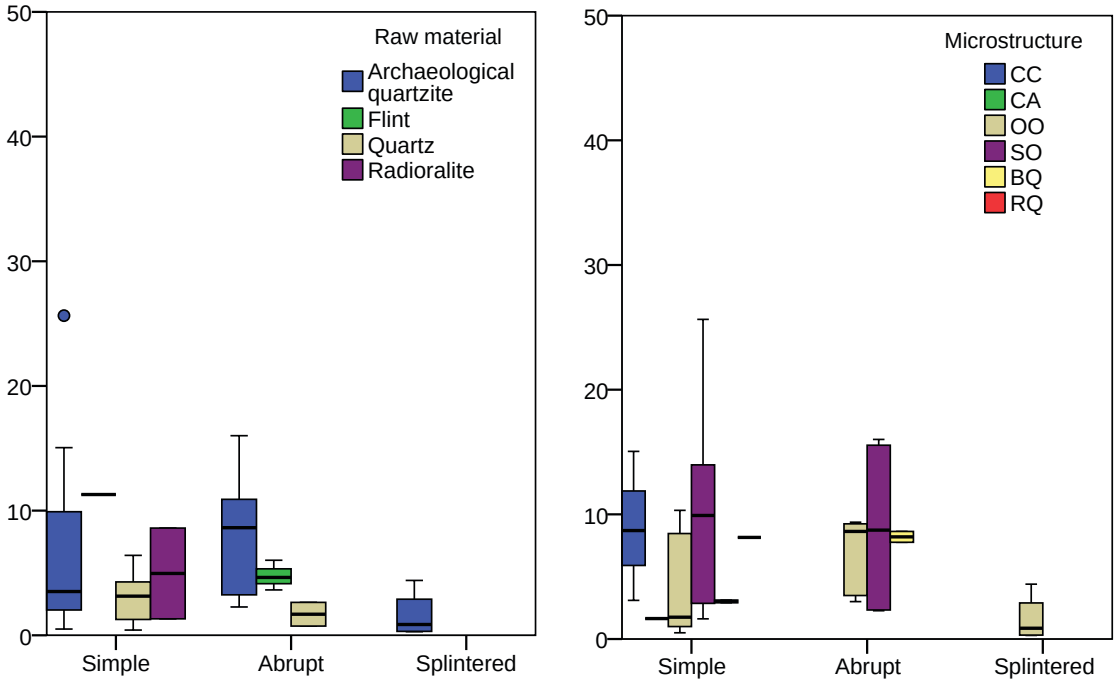

Figure-8.33: Double box-plot showing the distribution of weight in grams of retouched material grouped first by mode of retouch and second by raw material in the chart on the left and by petrogenetic in the chart on the right.

Raw material	Petrgen. type	Single-retouched pieces																	
		Simple												Abrupt			Splinter		
		Sidescraper			Endscraper			Denticulate			Point			Abrupt			Splintered		
		∑	W	g/p	∑	W	g/p	∑	W	g/p	∑	W	g/p	∑	W	g/p	∑	W	g/p
Archaeological quartzite	CC	2	24	11,9															
	CA	1	2	1,6															
	OO	6	24	4,0				3	22	7,4				2	12	5,8	4	6	1,6
	SO	5	48	9,5				2	17	8,7				2	18	9,2			
	BQ	2	6	3,0										1	8	7,8			
	RQ										1,0	8,2	8,2						
	MQ																		
	Undet.	1	5	4,7										1	12	12,4			
	Total	17	107	6,3				5	39	7,9				6	50	8,4	4	6	1,6
Flint		1	11	11,3				2	11	5,3				1	4	3,6			
Quartz		6	19	3,1										1	1	0,7			
Radioralite		1	1	1,3	1	9	8,6												

Table-8.34: Frequency table of retouched pieces with one primary type sorted by order of retouch and morphological group and grouped by raw material, including frequencies, weight and the ratio grams/piece for each case. Weight is expressed in grams.

8.6. RAW MATERIAL ACQUISITION AND MANAGEMENT PROCESSES IN THE LAYER XXII FROM EL ESQUILLEU

Once the raw data from this layer have been presented, in this section we bring face to face geographical, geological, and archaeological data to understand the forces that got these materials deposited here, that is, human raw material acquisition and management strategies.

The main acquisition process verified in this layer is the extraction of big quantities of orthoquartzites for human activities, as demonstrated by the great quantity of them found in this layer both in number and in weight. The small representation of other petrogenetic types and raw materials indicates they had different roles in human activities.

The management of raw material has been analysed including the raw data on all raw materials in a general reduction process model based on a simple "chaîne opératoire" (Figure-8.34). The primary technological product of lithic reduction we find in this layer are cores (irregular, discoid, levallois, or prismatic). From here on, we expose and analyse the different processes that generate other lithic products based the understanding of their features.

1. Blanks, as well as smaller blanks (sometimes fragmented) and chunks, were obtained as a results of the reduction process of some cores. Smaller blanks and chunks are secondary products generated as a consequence of knapping procedures.

    a. Using retouching procedures, some of these primary blanks were modified, creating retouched artefact as primary products and more blanks and chunks as secondary products. The latter are lighter than 5 g and sometimes fragmented. In addition, new primary types can be made in the blanks to obtain artefacts with multiple primary types, generating more blanks and chunks as secondary products.

    b. Some other blanks were reconfigured by percussion to obtain new flakes. The resulting products are a core on flake and blanks as primary products and other blanks and chunks, derived from the reconfiguration processes, as secondary products.

        i. As a consequence of the reduction processes of the cores on flakes, further blanks were obtained, also secondary products classified as chunks and blanks (smaller than the previous blanks).

            • The latter blanks can also be retouched, creating new retouched artefacts and secondary products (chunks and blanks).

2. Going back to cores, these can be retouched to obtain a retouched cores. Moreover, small chunks and blanks were generated as secondary products as a consequence of the retouching process.

3. Following with cores, some of them were reconfigured to obtain new flaking surfaces, or new striking platforms. This process generated new forms or types of cores and three different secondary products: chunks, blanks (generally lighter than 5 g and sometimes fragmented), and core preparation/rejuvenation products.

    a. Some of these new cores were retouched, creating retouched cores. As a consequence, small chunks and blanks were produced as secondary products.

Some of the chunks were also retouched. They are always heavier than 4 g. Blanks and chunks were generated as secondary products of retouching techniques, and they are generally lighter than 5 g.

Next, we present the conclusions reached about the acquisition and management of, first, "archaeological quartzites" by petrogenetic types, and later, other raw material. Figure-8.35 and Figure-8.37 schematically represent the acquisition process of "archaeological quartzites" and other raw materials. Figure-8.36 displays the relationship between acquisition and management strategies. Finally, Figure-8.38 shows the Esquilleu Cost map with the formation where raw material could be caught.

As has been previously mentioned, "archaeological quartzite" is the most relevant raw material, both in number and weight, present in the layer-XXIIR of El Esquilleu. Next, we will explain the raw material catchment and management strategies of this raw material by petrogenetic types.

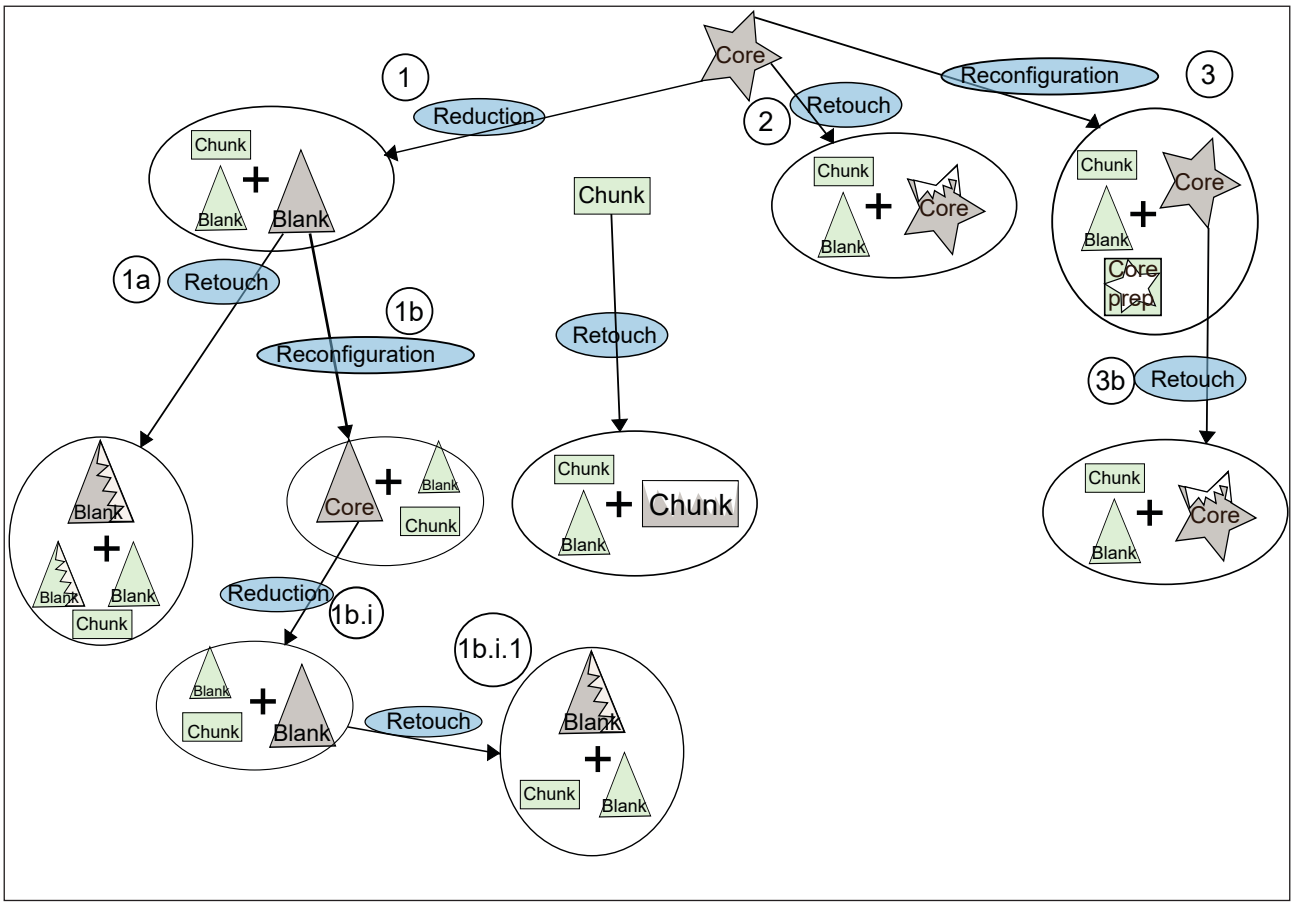

Figure-8.34: Schematic “chaîne opératoire” derived from the analysis of the lithic assemblage from layer XXII of El Esquilleu. Stars represent cores, rectangles chunks, squares with stars core preparation/rejuvenation products, and triangles blanks. Zig-zag lines added to any of these icons represent retouched artefacts. Grey icons are primary products and green ones secondary products. The blue ellipses indicate human activities. Alpha-numeric codes inside circles are references to the text.

The CC type is one of the less frequent type of “archaeological quartzite” with 53 pieces. All technological categories, except core preparation/rejuvenation products, are represented in the site. Therefore, except core maintenance managed by latter products, knapping reduction process is completely represented. There is a clear overrepresentation of chunks and an underrepresentation of knapping products. The weight of chunks and knapping products, which range from less than one grams to remains heavier than 30 grams, supports the idea of knapping and reshaping activities were practiced in the site. There are only three retouched artefacts (one has two primary types), a small number in comparison with those of other petrogenetic types or raw material. There is a high variability in the presence of dorsal negative scars, although their quantity is generally less than on other raw material such as flint or quartz, or on orthoquartzites. Cortical surfaces on knapping products and chunks made of the CC petrogenetic type are abundant. All these reasons carried us to propose this quartzarenite as a low intensity exploited material.

This petrogenetic type is characterised by multiple grain size varieties, generally with heterogeneously distributed grain sizes. Colour is also greatly heterogeneous, due to the impact of many different non-quartz mineral on these rocks. The presence of bedding on these quartzarenites is uneven. All these elements lead us to conclude: a) the CC petrogenetic type is heterogeneous, and b) the input in the site of CC quartzarenites comes from different pebbles from diverse origins. White varieties are related with the CC type from Barrios or Cavandi formations, while dark and brown varieties with Murcia Formation or with carboniferous sandstone strata such as the Potes, Mogrovejo or Viorna formations. Nevertheless, the analysis of cortical areas reveals the fluvial origin of all the cortical surfaces identified. All in all, we proposed that the CC petrogenetic type is a raw material caught in fluvial beach deposits, probably near the site of El Esquilleu. We observe an important presence of this petrogenetic type in these beaches. Different pebbles with diverse colours and grain size varieties were also found during geological surveys. The general size and morphological features of CC pebbles is also heterogeneous: multiple sizes (from medium pebbles to big cobbles) and

both spherical and elongated morphologies are present. Then, strong selection mechanisms would not have been required for the acquisition of this type. In addition, it can be said there is no selection based on colour or on grain size. Putting all this information together, it is possible to conclude that the input of the CC type is made as cores and probably as knapping products, as reveals the multiple varieties and the only presence of one core. The scale of this type in this site reveals its use as raw material was sporadic, maybe related with the scarcity of other petrogenetic types or raw material more suitable. We also propose this petrogenetic type was preferentially selected based on the size of the pebbles. Therefore, in the deposits there must have been a selection of the CC pebbles based on size.

The CA type only constitutes a small portion of the assemblage, with 44 lithic implements. All three technological orders are present, although there are no core preparation/rejuvenation products. The distribution of the three technological is similar to the frequent of all "archaeological quartzite" assemblage. There is only one retouched blank configured with a primary type. Weight of blanks and chunks range from less than one gram to more than 20 grams. This proves that knapping and reshaping processes were carried out in the site. The average weight of blanks is lower than for the previous type, but still higher than the median of all "archaeological quartzites". One of the cores is the heaviest of this assemblage. The frequent presence of cortical areas, generally covering more than the 33% of the dorsal surface, and the occasional presence of blanks with more than two negative scars, indicates this type of quartzarenite is weakly exploited, similarly to the CC type.

The characterisation of this petrogenetic type reveals different grain size and colour-mineral varieties. Nevertheless, most frequent varieties are related with medium-coarse grain sizes. Bedding is significantly reduced. These features point out in a) the CA type is variable, b) the input of CA quartzarenite to the site got supplied with pebbles from different origins. Colour links this quartzarenite with the Barrios or Cavandi outcrop and with clasts from Carboniferous conglomerate formations in the case of white or brown/clear varieties. We do not discard the origin of black or brown varieties in non-identified CA strata from Murcia Formation. However, the characterisation of cortical areas indicates all identified cortex are from fluvial sources. Therefore, we proposed that CA type of quartzarenite were brought to the site from fluvial deposits, probably close to the El Esquilleu. The existent of multiple varieties in the site, could reveal the absence of selective mechanism in these fluvial deposits for select specific varieties. Nevertheless, at least, medium selection mechanism are necessary to obtain CA quartzarenite in fluvial courses near El Esquilleu. They are more important than those necessaries to obtain CC type. We propose sporadic catchment activities to obtain CA type, complementary to others, such as catchment activities of other petrogenetic types or raw material, or biotic resources. The input to the site could be made as core or blanks.

The OO petrogenetic type of orthoquartzite shows clear differences in management and catchment in comparison with the raw materials and types of "archaeological quartzite". It represents 47% of the lithic assemblage in number and 41% in weight. These data mean there was an intense and planned exploitation of this type, making this type as the most important input in the layer assemblage. The three technological categories considered, as well as core preparation/rejuvenation products, are present in this layer. It is obvious knapping and reshaping activities were practised in the site. This is also certified by the presence of blanks and chunks between less than 1 g to more than 40 g. The relationship between chunks and knapping products is positive for the latter. The quantity of negative scars on these blanks is varied, even though the number of them is higher than in the former quartzarenite but is scarcer than in more deformed types of "archaeological quartzite". The presence of cortical surfaces is also varied with, even though they are less extended than on quartzarenites and more extended than on more deformed orthoquartzites. In general, weight distribution is smaller than on other petrogenetic types. The weight of the non-core-on-flake shows that it the smallest one. Retouched artefacts are less represented than in other orthoquartzites and quartzites, although it is more frequent than in two preceding types. This evidence reveals medium intensity exploitation.

The characterisation of this raw material based on grain size and colour indicates it is a more homogeneous type. Nevertheless, there are two well represented grain size varieties: a fine-medium and homogeneous variety and a medium-coarse and heterogeneous one. According to mineral-colour characterisation, there are two different varieties, the better represented is the grey-white one while the grey-dark one is less frequent. Therefore, the input of the first is made with multiples lithic block, while the latter is restricted to few. The original source strata of the lighter colour variety are in the more deformed bands of the Barrios outcrop Formations, as well as in the carboniferous conglomerates from older layers. The darker variety originates exclusively in the latter. The charac-

terisation of cortical areas reveals that most of them come from fluvial deposits, and only one come from conglomerates. There is no evidence of outcrop cortex. Therefore, although the most likely source strata are in the Barrios Formation, catchment was probably made in fluvial deposits and secondarily in conglomerates. Most of the conglomerates have OO orthoquartzite, more frequently the white varieties. In the nearby conglomerate of the Remoña Formation, 5 CU away, it is possible to find them without the need to apply any selective mechanism. Other conglomerates, such as the Curavacas series, Lechada (13 CU), Campollo (16 CU), Maraña-Brañas (27 CU), Narova (10 CU), Pesaguero (12 CU), Pontón (26 CU), Potes (12 CU), and Valdeón (32 CU) conglomerates have important amounts of this type. However, at least low intensity selective mechanisms are necessary to choose specific varieties, forms and sizes. All these conglomerates are to the south, in medium-altitude plateaus. In fluvial deposits, the main catchment area, the presence of this petrogenetic type is scarcer. Therefore, the selective mechanisms required to pick special varieties, forms and sizes would have been more intensive. The black variety does also derive from conglomerate or fluvial deposits. In conglomerates this variety is restricted to the south-west conglomerates. The only conglomerate cortex in the layer is on a dark-grey variety, therefore this variety probably was obtained in conglomerates. In fluvial deposits, their presence is negligible All in all, catchment of this type would have included both fluvial and conglomerate areas. Nevertheless, main acquisition of this type was done in fluvial deposit, obtaining big amounts of this material through intensive strategies. The latter require conscious planned catchment strategies based on strong selective mechanism. In addition, the presence of fine blanks without negative scars points out in a primary transformation of the pebbles into a core. The acquisition on conglomerates also point out on sporadic catchment on distant zones. The arrival of the pieces to the site could have been, either as core, blanks or retouched material. The overrepresentation of knapping products reinforces the input of this type as blanks. Nevertheless, it also suggests a possible primary exploitation of cores, and a later transportation to other sites of non-completely exploited cores.

The SO petrogenetic type shows different management and catchment strategies in comparison with the previous types, mainly due to the smaller representation of this type in the assemblage. Twenty-seven percent of “archaeological quartzites” are SO type. Planned and intense exploitation of this orthoquartzite is observable. As in the previous type, the three technological orders, as well as core preparation/rejuvenation products are represented in the site. It was clear knapping and reshaping activities were carried out in the site as demonstrated by the presence of blanks and chunks with weights between less than 1 g and more than 20 g. Core types (with cores on flake), their weight and flacking and knapping surfaces reveal this raw material is the most intensively exploited orthoquartzite. The presence of negative scars is more frequent than in the previous type, with greatest rate of three or more extraction on negative scars. Presence of cortex is rare and it generally covers less than 33% of the pieces. The proportion of retouched artefacts is the highest, in similar rates than BQ petrogenetic type and the retouch is configured in all technological products, excluding chunks. These evidences indicate this material is very intensively exploited. The gram/piece ratio of this petrogenetic type is slightly greater than in previous one, due to the heavier weight of blanks and the higher presence of cores. There is an important presence of irregular cores, maybe due to the non-systematic exploitation of cores in final reductions.

The characterisation of this raw material reveals there are two different grain size varieties of the SO type: the coarse and heterogeneous one (present in small percentages) and the fine and homogeneous one (the clear majority). The presence of the former is limited to a few pieces, while many lithics of the latter variety type were input into the site. There is no different colour/mineral varieties stablished. The original outcrop strata of the two varieties defined is not located in the research area, but they can be found in conglomerate strata and deposits. The conglomerates with the SO petrogenetic type are the Lechada, Maraña-Brañas, Pontón, Potes, Remoña, and Valdeón conglomerates. In all of them the presence of the fine grained variety range between 5 and 50%, except for the Lechada and Potes conglomerates, where they represent less than 5% of the pebbles. The presence of coarse variety is restricted to the Pontón conglomerates (26CU). The analysis of cortical surfaces reveals a clear change in acquisition dynamics in their provenance even fluvial cortical surfaces is more frequent than fluvial. The SO type is the best represented type with conglomerate cortex. The presence of SO orthoquartzites in beach deposits is negligible, especially near fluvial deposits. We propose the input of this type to the site is mixed: on one hand, there is a intensive and planned catchment strategies based on intensive selective protocols in river beach deposits. The presence of fine blanks without negative scars points out in the primary transformation of the pebbles into core. On the other, there is an acquisition based on medium distant movement to conglomerate areas in south/south-west direction. The latter strategy does not require important selective strategies for intensive catchment. The input in the site could be made as core, blanks or retouched material.

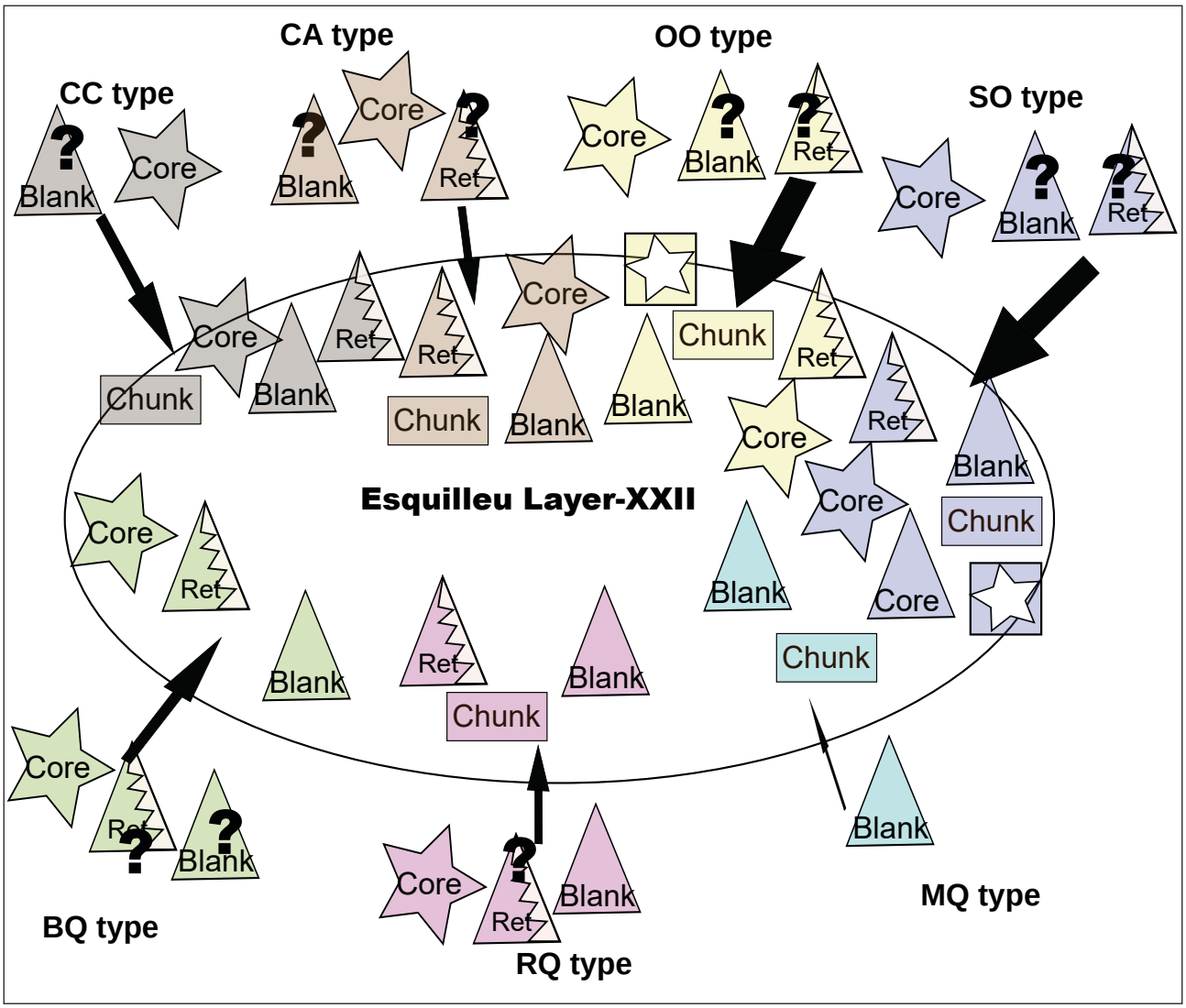

Figure-8.35: Schematic representation of the input of the different petrogenetic types of “archaeological quartzite”, taking into account the different technological products present. Stars represent cores, squares with star core preparation/rejuvenation products, triangles blanks, triangles with zig-zag retouched artefacts, and rectangles non-complete cortical chunks. Question marks indicate products whose presence is not certain.

The management and catchment strategies observed in the previous type clearly change in **the BQ quartzite type**. The number of items and their weight points at non-intensive catchment strategies to acquire this material. The representation of technological products is uncomplete due to the absence of chunks and core preparation/rejuvenation products. Core are overrepresented, especially the cores on flake (3). The size distribution of blanks, between less than one gram and more than ten indicates that knapping and reshaping processes were carried out. Nevertheless, they were probably reduced. The small gram/ratio also point at the reduced weight of this type in this lithic assemblage. The number of negative scars in dorsal surfaces is elevated and the occasional presence of cortical surfaces suggest an intensively exploitation of this quartzite. Retouched artefacts are frequent and all of them are made on blanks. All in all, the data gathered demonstrate this quartzite is an intensively exploited material, and all phases of lithic reduction were carried out in the site, although they were probably not frequent. Blanks and retouched material have been brought as final product, as the indicated by the absence of chunks and the high quantity of knapping products.

The petrological characterisation of this type is hampered by the lack of destructive characterisation that certify the varieties of the BQ type proposed. In general, there is great homogeneity in grain size and most of pieces are fine grained quartzites. Coarser or more heterogeneous varieties could be, either zones from the same block of rock, more or probably, distinct few original lithic blocks. Colour does also distinguish several varieties: a major grey variety, and another two minor varieties, a black-grey one and a brown one. Finally, some lithics implements are white. Therefore, and due to small quantity of lithic implements made on BQ, we consider the input into the site of varied former

blocks, probably as blanks products. We did not find the original outcrop strata for this type of quartzite in the field survey. However, it was clearly identified in some small conglomerates. The presence in fluvial or gravitational deposits is negligible. There are important quantities (between the 5 and 50%) of BQ quartzite in the Remoña, Valdeón, and Pontón (nearest location at 26 CU) conglomerates. In other conglomerates, such as Maraña-Brañas, Pesaguero, and Potes conglomerates, it is scarcer. Coarser grain varieties of the BQ quartzite are restricted to the Pontón conglomerate. The characterisation of cortex in lithic implements shows the same presence of lithics from conglomerates and fluvial deposits. Fluvial cortical surfaces are only characterised on dark and brown varieties, while conglomerate cortex is in the coarse grained variety and in the black variety, also the white ones. Therefore, it can be deduced that catchment of the BQ type is based on the extraction of small quantities of this material in conglomerates applying medium-intensity selective mechanisms. For this purpose mobility could have been either low scale to the near conglomerates of the Remoña Formation or medium scale to the Southern and South-western conglomerates. The latter hypothesis is reinforced due to the small frequent of this type, the overrepresentation of blanks, and its size. As it happened in the previous case of SO orthoquartzite, there is a mixture of catchment strategies: the first one would consist of procurement in conglomerate (probably exhaustive) inserted in medium distance mobility routes. The second one would be based in occasional findings in river deposits in relation with other activities, such as journeys along the river or conscious acquisition of other lithic or biotic resources. The latter strategy would require strong selective mechanisms and accurate identification of raw material.

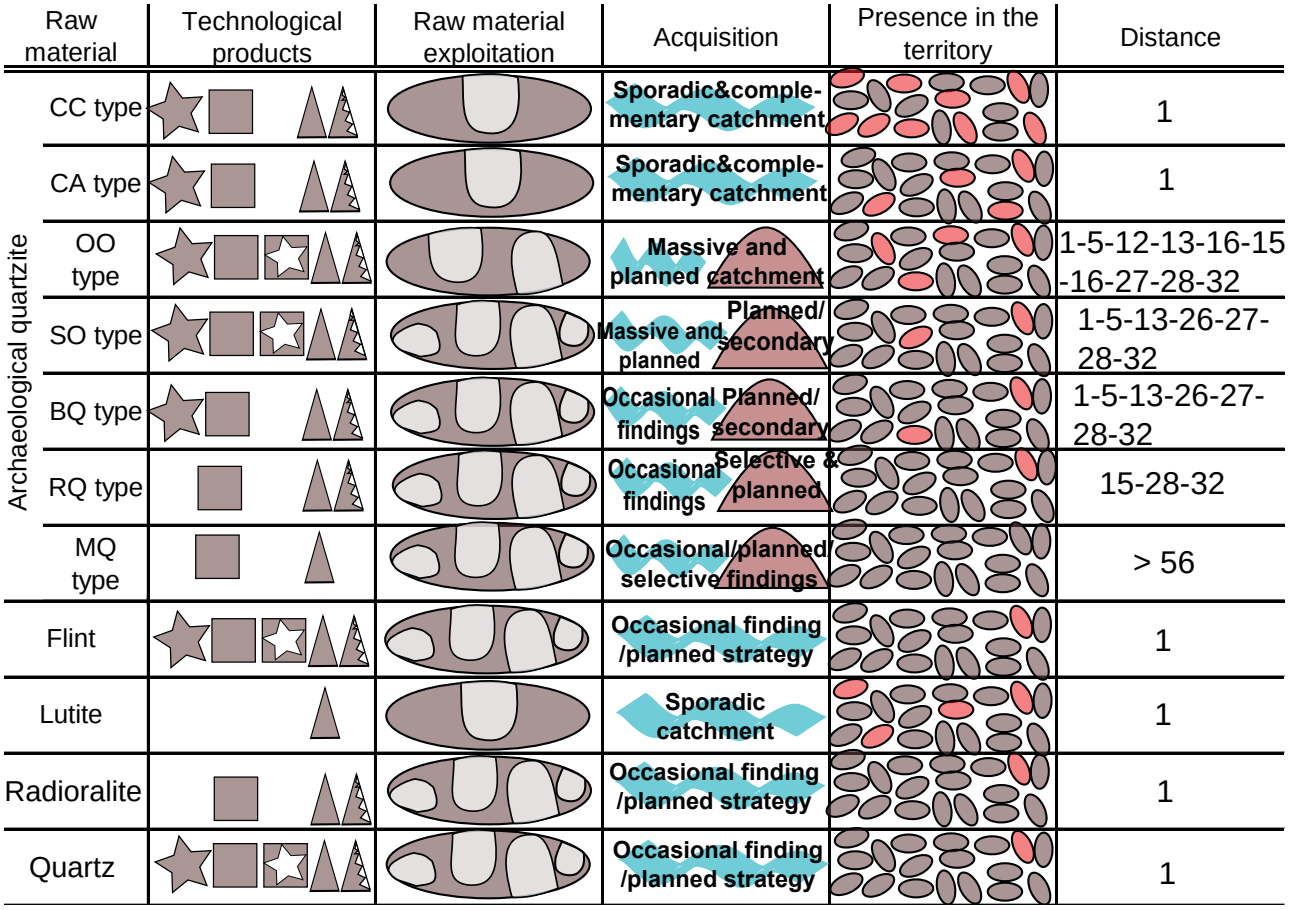

Figure-8.36: Schematic representation simplifying raw material acquisition and management evidences from layer XXII of El Esquilleu. In the column “technological products” stars represent cores, squares chunks, squares with stars core preparation/rejuvenation products, triangles blanks, and triangles with zig-zag retouched artefacts. In the column “Raw material exploitation”, oval with one scar represent low intensity raw material exploitation, ovals with two scars represent medium intensity raw material exploitation, and oval with four scars represent high-intensity raw material exploitation. In the column “Acquisition” waving blue lines represent river acquisition and brown semicircles represent conglomerate acquisition. In column “Selection degree”, the complete set of ovals represents all the raw materials available in the territory. The ones highlighted in red represent the proportional presence of each specific raw material in the territory. Higher presence of the latter means weaker selection degree.

The RQ quartzite type reinforces the catchment and management previously commented that connect an appreciated raw material highly exploited with its scarcity in the area through a medium mobility, intensive selection and fragmented exploitation, as other authors argue (Meignen et al., 2009; Turq et al., 2013). The quantity of this type of raw material is reduced. Cores and core preparation/rejuvenation products are absent, the quantity of chunks is small, and the most frequent technological products are blanks. Although there is only one retouched artefact, it is the only configured point in the assemblage. The presence of blanks and also chunks ranging from less than one grams to more than ten grams indicates knapping and reshaping activities were performance in the site, but probably reduced to small or specific actions. The scarce presence of negative scars on dorsal surfaces indicates low intensity exploitation of this type, despite the occasional preservation of cortex, the low gram/piece ratio and the high integrity of blanks. All these data point at a complex management of this material, related with its scarcity. We propose the input of this type was occasional and it was brought as cores, blanks or retouched elements that could be used, reduced or reshaped for specific activities. The underrepresentation of chunks (derived from knapping and reshaping) and lack of cores support the input into the site of this type as blanks or retouched artefact.

The petrological characterisation of this raw material does also agree with the previous hypothesis. The analysis of grain size reveals a great homogeneity. No clear differences are appreciated by colour-mineral varieties. We were unable to find evidence of this petrogenetic type in the massive outcrops of the surveyed area. Its presence is reduced to two conglomerate formations: The Pontón and the Valdeón conglomerates, both in the South-west of the research area. Still, the presence of this type is scarce in both conglomerate formations. Taking into account the cortical areas, two derives from conglomerates and three from fluvial deposits. We did not find evidence of this petrogenetic type in fluvial deposits during our surveys. However, its presence cannot be completely discarded, at least in the Cares River, which creates the erosive basin where conglomerates surface. These data indicate that catchment of this type necessarily implied medium or long distance movement outside the Deva Basin, only suggested with the previously types. In addition, the evidence above reinforces that the application of strong selective mechanisms, are not restrained in deposit areas (probably related with occasional findings), but in conglomerate ones. The presence of this type in the site does also reveal a conscious mechanism of selective and conservative exploitation of a particular raw material. The intensive exploitation of this material, as singular, valuable, and exiguous is clear. It could be related with a mobile tool-kit, as other authors proposed in different regions (Bustos-Pérez et al., 2017).

Finally, **the MQ quartzite type** shows catchment and management patterns similar to the previous type, mainly motivated by its scarce presence. It is important to emphasise the small quantity of this type of quartzite: six items. The representation of technological products is not complete: cores and core preparation/rejuvenation products are absence. Chunks are significantly underrepresented with only one piece and blanks are overrepresented. None of the MQ were retouched. The grams/piece ratio is the smallest all petrogenetic types. The quantity of negative scars is the highest regarding all raw material and the cortical areas are restricted. The presence of blanks and one chunk lighter than one gram could reveals knapping or reshaping activities, even though, due to the number of lithic implements, they must be reduced,. All these features point at the importance of this raw material as a highly exploited one. Nevertheless, the absence of retouched artefacts force us to nuance the latter conclusions.

We do not identify different colour, or grain size varieties in the MQ quartzites in this layer. Almost all material represents homogenous grain sizes between fine and medium sizes. Colour characterisation shows that all samples are white or white-grey. We do not find any evidence of this quartzite in the research area surveyed. Then, the only possibilities are: a) in non-surveyed strata, b) outside of the research area, or c) hidden in deposits or conglomerates in small percentages. The analysis of the cortical surfaces reveals that all of them derived from conglomerates. Therefore, the catchment strategies are related with high mobility and/or strong selective mechanism in conglomerates. As it was verified in the previous type, MQ quartzite involves a conscious mechanism of selective and conservative exploitation of raw material. It is clear this quartzite is intensively exploited as a singular, valuable, and exiguous raw material, maybe related with a mobile tool-kit as proposed by other authors in different regions (Bustos-Pérez et al., 2017). Nevertheless, the conclusion must be nuance due to the small quantity of this type and the lack of destructive characterisation to confirm its presence.

Next we will explain the raw material catchment and management strategies of other raw material. These material are not frequent in the layer XXII-R of El Esquilleu, although they reveal different

roles of raw material and interesting catchment and management behaviour.

We start to understand management and catchment strategies in this assemblage with the **Quartz**, the most frequent non-"archaeological quartzite" material. The analysis of the technological products reveals it is present in all phases of lithic reduction process. The quantity of cores is elevated, especially when compared to their relative presence, also the chunks. The quantity of knapping products is small, as consequence of the overrepresentation of chunks. The occasional presence of cortical areas in surfaces reveals and the high presence of negative scars, generally with more than two, points at the intense exploitation of this raw material. The high frequency of retouched artefacts (the highest compared with all raw material or petrogenetic types of "archaeological quartzites"), as well as the existence of two blanks with two primary types reinforce the idea of the intense exploitation of quartz, also its used for specific activities. The distribution of weight in blanks and chunks, from lighter than one to heavier than 15 grams, points out that knapping and reshaping activities were carried out in the site. The medium weight is 3.7 grams.

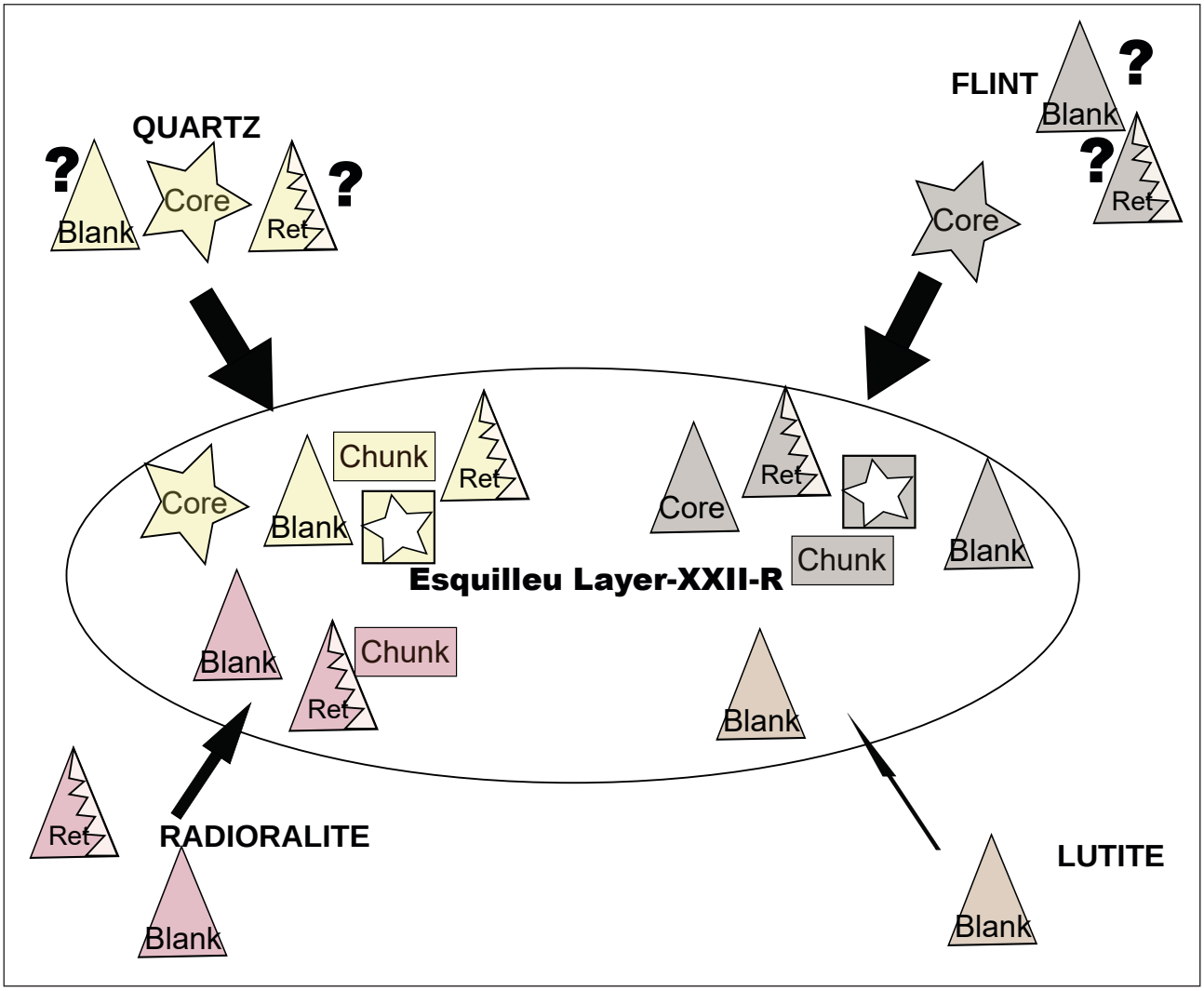

Figure-8.37: Schematic representation of the input of other raw material, than "archaeological quartzite" taking into account the different technological products represent. Stars icons represent cores, triangles blanks, triangles with zig-zag lines retouched material and rectangles non-complete cortical chunks. Question marks indicate products whose presence is not certain.

Regarding the properties of quartz, we observed a high variability. Some are part of a single crystal quartz, others are quartz aggregates, the remaining are a succession of quartz lamellae. The colour also differs from white/yellow and opaque varieties to transparent ones. In the research area defined for this study we only identified quartz on fluvial deposits, mainly in the headwaters of Deva and Cares rivers. The characterisation of two cortex from fluvial sources point out that catchment was done on fluvial deposits. The presence of quartz in these deposits is scarce. Then, the catchment of this material would have required strong selective mechanism. Still, this acquisition could be related with either occasional finding or with intensive and planned raw material strategies in rivers.

The latter is reinforced due to the presence of quartz in the assemblage and multiple varieties characterised. The intensive exploitation of the material reveals its importance for prehistoric societies. Due to the presence of all types of technological products, we consider that all phases of lithic reduction were carried out in the site. Nevertheless, due to the overrepresentation of retouched artefacts, we do not discard the direct input of retouched pieces.

The third better represented raw material is **flint**. The analysis of the technological products made on this material reveals it is present in all phases of the lithic reduction process. The three technological categories considered, as well as core preparation/rejuvenation products. The quantity of flint cores is elevated, especially when compared to their relative weight in the assemblage. In addition, the frequent presence of cores on flake, despite presenting a small number of extractions, points at the intense exploitation of this lithic resource. The occasional presence of cortical areas and the high presence of negative scars on this raw material do also support the idea of intense exploitation. The distribution of weight is coherent with this hypothesis too. This is based on the frequent presence of small flakes and chunks, probably as derived products from knapping, retouching and resharpening processes. However, the majority of material is around the 2.2 g. The overrepresentation of retouched artefacts made on flint reinforces this intense exploitation.

The colour of flint pieces, mainly on black, can give a hint on their origin, probably related with Palaeozoic Black cherts such as the Vegamián Formation (Herrero-Alonso et al., 2016). Moreover, there are other flint implements with orange or brown colour. The only piece with cortex could not characterised. Therefore, we could not properly determine the potential catchment area of flint. The information derived from the geological surveys conducted out during this research and from other studies in the surrounding area (Álvarez et al., 2013; Manzano et al., 2005) reveals a negligible presence of flint in fluvial rock beaches or other secondary deposits, reduced to small sizes and relatively tabular forms. Due to the scarcity of diagnostic elements to characterise the source area, we only suggest its input throughout deposits. Then, catchment activities must have necessarily implied intensive selection in deposits. These would have not been planned or based on systematic intense raw material exploitation strategies. Flint catchment would have been based on occasional findings in deposits as a results of casual transit or other activities. This high intensity exploitation of flint founded on the analysis of technological and metrical features suggests the qualitative importance of this raw material. The interaction between qualitative and quantitative information unveils the importance of this raw material for human activities that maybe could have been related with knapping and use properties, but also with its scarcity. In addition, considering the presence of all types of technological products, we conclude that all phases of lithic reduction were carried out in the site. That is, flint knapping was probably performed in the site and it involved a first core intensively knapped to obtain blanks and artefacts for human activities, perhaps specialised. The only presence of cores on flakes, the presence of one core preparation/rejuvenation product and flakes and chunks derived from knapping and resharpening processes could be the consequence of core transportation, as suggested by other authors (Bustos-Pérez et al., 2017; Meignen et al., 2009; Turq et al., 2013). Still, we do not discard the input of some blanks or retouched artefacts already prepared from outside.

The catchment and management of **radioralite** clearly differ from the other two analysed raw materials, especially hampered by the small quantity of the items, reduced to 19 items. There are no cores, neither core preparation/rejuvenation products. Nevertheless, the proportion between knapping products and chunks is similar to other two raw materials. There is an overrepresentation of retouched artefacts even though all of them are configured using the Simple order. In addition, there is a retouched chunk. These elements point at intensive exploitation of this raw material. Latter hypothesis is also supported by the high quantity of dorsal scars in knapping products and the occasional presence of cortical areas on them. The distribution of weight do also point the idea of intensive exploitation of quartz. The distribution of weight (with smaller pieces than one gram), also suggest that knapping and reshaping activities were carried out in the site. All these data suggest that radioralite probably inputs as blanks or as retouched blanks.

Coming to the physical features of radioralites, most of them are red to brown, even though a small quantity of them are black-grey coloured. All of them are characterised by the presence of Radiolaria fossils. The characterisation of cortical areas in a radioralite reveals its possible catchment context: fluvial deposits. We only find evidence of radioralite in the area surrounding in fluvial deposits, of Cares and Deva rivers, in negligible proportions and small sizes. In the first river is more frequent than in the second. Therefore, catchment activities would have implied strong and intensive selection mechanisms, similar to those observed for flint or quartz. This means that the acquisition of radioralite would have been related with occasional findings, rather than with intensive and planned

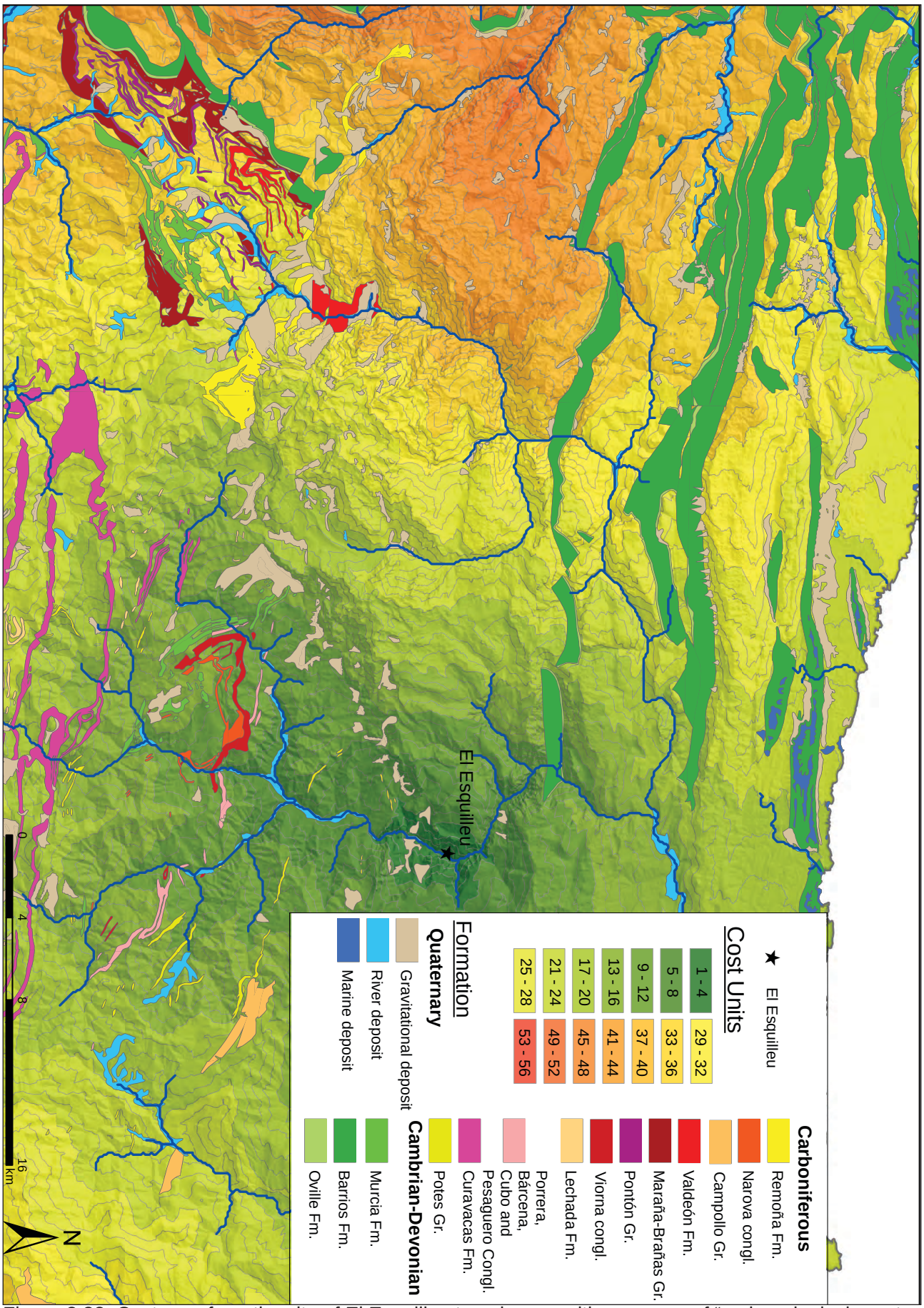

Figure-8.38: Cost map from the site of El Esquilleu to polygons with presence of “archaeological quartzites” and other raw materials.

raw material selection strategies in river beaches.

Finally, **lutite** is the raw material with smaller representation in this layer only represented with eight pieces. The conclusion, then, must be nuance. The only technological product represented in the collection are blanks. None of them is retouched. The reduced quantity of negative scars and the extension of cortical areas point that lutites were a weakly exploited material. The distribution of weight probably denotes that knapping activities were not performance in the site. Therefore the input in the site probably was made as blanks. The absence of small chunks also point out in this idea.

Regarding the properties of this raw material, most lutites are grey to black coloured and are similar to the siliceous cemented varieties found in the area around the site, in outcrops (associated to limestone, sandstone and conglomerate alternations from the Carboniferous), conglomerates (Carboniferous), and river deposits. Their presence in the latter two was analysed in this research, revealing changeable percentages generally higher than 10% of the rocks present in both types of contexts. This raw material has also been analysed in archaeological contexts from other regions, such as the Basque Country (Fernández-Eraso et al., 2017). Two lutites from the assemblage have cortex derived from fluvial deposits. Then, the catchment probably was carried out in fluvial deposits, obtained as a secondary product on these areas without applying important selective mechanism. Summing up, this raw material was only used sporadically, probably when other raw materials were scarce or as expedient behaviour technology. Therefore, the material was not exploited intensively.

All in all, we observe different catchment and management strategies each raw material. This allows us to propose the following human mobility, landscape use, selection, and exploitation mechanism. These are:

- A low, medium and high scale mobility strategies to the South, South-west, and North of the research area, as well as outside it.
- The use of low altitudes areas through the exploitation of river resources near El Esquilleu, which include primary preparation for later exploitation in other areas. The use of medium altitudes areas through the exploitation of conglomerates in plateaus. The latter, reflects previous human mobility routes and the successive exploitation of valuable lithic resources.
- Selective and non-selective mechanisms for obtaining specific raw materials or petrogenetic types in deposits and conglomerates.
- Diversity of raw materials exploited, selected and managed based on their physical properties and their availability in the landscape.

CHAPTER-9

RESULTS. THE LAYER-XIII FROM THE ARCHAEOLOGICAL SITE OF EL ESQUILLEU

9.1. GENERAL ISSUES AND STATE OF PRESERVATION OF THE COLLECTION

The archaeological site of El Esquilleu is a small cave situated in the Cantabria Autonomous Community near the villages of Lebeña and Allende. It is situated 100 meters away from the left margin of the Deva River and 70 meters above it. The cave is within the Valdeteja Formation, mainly composed of massive limestone. Cliffs, defiles, talus slopes, moraines, caves and deep gorges are the most important geomorphological features in the area surrounding El Esquilleu Cave. The area is crossed by the Deva River valley that creates a deep and narrow gorge in North-South direction called The Hermida Defile, where the cave is located. The excavation of the site was directed by Dr. Javier Baena Preysler between 1997 and 2006 trying to understand the Middle Palaeolithic societies of the area through a diachronic perspective. The sequence was entirely excavated, at leas in a four meters pit. The stratigraphic depth was 4.20 meters and it was divided into 41 layers (29 with anthropic evidences). Although the research processes in El Esquilleu Cave is still in progress, several studies have already been carried out by different specialist.

In general, the information provided by all perspectives, previously commented in chapter-2, offered interesting perspectives about the human groups who inhabited this cave in Prehistoric times, especially during the late Middle Palaeolithic. In general terms, the sequence of El Esquilleu Cave showed sophisticated strategies of habitat and land use by Neanderthals groups, which were modified through time according to environmental conditions and cultural, social and economic circumstances (Baena et al., 2012). Summing up, we can say that El Esquilleu is one of the most important archaeological sites in the Cantabrian Region for understanding the last Neanderthal groups in the Iberian Peninsula.

The layer-XIII is the second analysed layer and it is in the middle of the long sequence of El Esquilleu. Sedimentology, this layer is in the third part of the sequence, ESQ-C, and it is mainly composed of thin and dark layers created as consequence of widespread flooding and intensive human activities, represented as fireplaces and other dispersed burned findings. The presence of siliceous material was massive in the sandy and silty matrix. This layer had been diagenetically altered by a source of dissolved phosphate, which triggered the partial dissolution of bone and ash in the sediments of this anthropogenic-rich layers (Jordá et al., 2008; Mallol et al., 2010). There is a numerical data obtained from the Layer-XIII (Beta149320 = 39000 BP ± 300), which agrees with the general sequence of El Esquilleu and date this layer around the 40.000 BP. During the formation of Layer-XIII, paleoenvironmental conditions are related with mesophilic taxa and a more closed landscape, even *Pinus* is still represented. *Pinus*, also other species, such as *Juniperous*, *Betula*, *Sorbus* or shrubs were used as fuel in the numerous fireplaces documented in the ESQ-C sequence in which Layer-XIII is situated (Uzquiano et al., 2012). Faunal analysis point at the consumption of *Capra pyrenaica*, deer and chamois. *Bison*/*Bos* is also consumed, although in small quantity. The bones have no marks from carnivores, therefore, humans is the main agent who introduced fauna in the site during the formation of this layer. In addition, most of the bones are burned and extremely fractured, probably used as fuel for fires or because sanitary purposes (Yravedra and Gómez-Castanedo, 2014; Yravedra and Uzquiano, 2013). Concerning to lithic raw material, previous studies point that “archaeological quartzite” is the better represented raw material in the layer. Nevertheless, flint, quartz, or radioralites are also represented (Manzano et al., 2005). The techno-typological characterisation of the layer concludes that main reduction sequence used is the Quina reduction method (Baena et al., 2005; Carrión et al., 2008; Carrión et al., 2013).

The archaeological assemblage analysed here is a sample of the complete collection. The complete set from this layer is formed by 9,855 lithics. We analysed the complete lithic assemblage from the square J-11, with a total of 2,444 lithic fragments, 25% of the whole collection. After having filtered all the data collected, the total of lithic items considered here is 2,419. The general state of preservation is good. Most of the pieces were not previously washed to preserve possible residues or use/hafting-wear marks to be analysed in the future. In the cases where no part of the surface was clean enough, I washed a small portion of it in order to obtain a clear analysis surface. We did not find important presence of carbonates in the surface of lithics, as previously pointed out by Jordá et al. 2008. Nevertheless, on a small portion of them, carbonate precipitates did not allow to observe the surface of the stones. We also found clayey minerals in surfaces of some of the lithics analysed. Finally, a negligible part of them presented evidence of chemical weathering processes altering any type of surface, but especially on cortical areas, non-deformed/metamorphic surfaces or jointed areas.

9.2. PETROLOGICAL STRUCTURE

Here we present the results of raw material characterisation. We were able to determine the main lithology of every piece. In general, the collection is mainly formed by “archaeological quartzites” with residual representation of flint, limestone, lutite, quartz and radioralite (Table-9.1).

Main Raw Material	Archaeological quartzite	Flint	Limestone	Limonite	Lutite	Quartz	Radioralite	Volcanic rock	Undetermined
Σ	2324	35	21	0	27	7	5	0	0
%	96.1	1.4	0.9	0	1.1	0.3	0.2	0	0

Table-9.1: Frequency table of lithologies identified in layer-XIII from the archaeological site of El Esquilleu.

Focusing on “archaeological quartzite”, through binocular microscopy we could identify the seven petrogenetic types proposed. Orthoquartzites have major representation in more than 50% of the lithic implements. Thanks to the high quantity of the BQ petrogenetic type, quartzite is the second most important group. Finally, the group of quartzarenites is underrepresented, with less than 5% of the “archaeological quartzites” (Table-9.2). We were unable to identify 160 pieces, 6% of the collection. Coming to the distribution of grain size, the most frequent category is homogeneous distribution around one mode, with the 59% of the cases; even though heterogeneous distribution is also well represented, with 26% of the cases. Regarding grain size, the most frequent categories are fine and medium grain sizes. As to “archaeological quartzite” types and size varieties, we identify five preferential varieties: SO and BQ types, characterised by homogeneous distribution of fine grains; the OO type, characterised by homogeneous distribution of medium grains around one mode, and OO and SO types, characterised by medium grains heterogeneously distributed. Chi-square test (χ^2 (48, N = 2126) = 1054.692, p < .001) reinforces the idea of a preferential acquisition of these varieties.

			Petrogenetic type																	
			CC		CA		OO		SO		BQ		RQ		MQ		Undet.		Total	
			Σ	%	Σ	%	Σ	%	Σ	%	Σ	%	Σ	%	Σ	%	Σ	%	Σ	%
Grain size characterisation	Homogeneous and one mode distribution	Fine grain	5	5	18	16	25	4	414	55	240	56	45	49	21	28	6	3	774	33
		Medium grain	4	4	13	12	238	42	113	15	87	20	30	33	49	65	5	3	539	23
		Coarse grain	3	3	7	6	56	10	5	1	6	1	2	2	2	3			81	3
	Heterogeneous and two modes distribution	Fine grain	5	5	23	20			36	5	32	7	2	2	1	1	4	2	103	4
		Medium grain	13	14	2	2	2	0	20	3	15	3					6	3	58	2
		Coarse grain	1	1	4	4	1	0											6	0
	Heterogeneous distribution	Fine grain	19	21	6	5	24	4	23	3	16	4					3	2	91	4
		Medium grain	28	30	29	26	136	24	119	16	33	8	2	2	1	1	13	7	361	16
		Coarse grain	14	15	11	10	88	15	23	3	2	0	11	12	1	1	1	1	151	6
	Undetermined																160	81	160	7
		Total	92	4	113	5	570	25	753	32	431	19	92	4	75	3	198	9	2324	100

Table-9.2: Frequency table of petrological features identified in layer-XIII from El Esquilleu based on binocular characterisation. Columns are petrogenetic types and rows contain the characteristics of grains according to size, classified first by distribution and second by size itself. Cells in black are the categories representing more than 10% of the total cases. Cells in dark grey are the categories representing between 5 and 10% of cases. Finally, cells in light grey are the categories representing between 1 and 5% of cases.

Non-quartz mineral	A		B		C		General	
	Σ	%	Σ	%	Σ	%	Σ	%
Absence	26	4	26	4	27	4	79	4
Fe-Oxides	643	94	8	1	4	1	655	32
Manganese Oxides	8	1	81	12	127	19	216	11
Calcites					1	0	1	0
Micas	5	1	302	44	116	17	423	21
Black mineral	1	0	258	38	376	55	635	31
Pyrites	1	0	4	1	21	3	26	1
Feldspars			5	1	12	2	17	1
Total	684	100	684	100	684	100	2052	100

Table-9.3: Frequency table of non-quartz minerals identified in layer-XIII from El Esquilleu based on binocular characterisation. Columns are the three fields examined and rows are the non-quartz minerals identified.

Colour	On fresh cut			
	Primary		Secondary	
	Σ	%	Σ	%
Absence	5	1	74	16
White			7	2
Grey	82	18	105	23
Black	40	9	39	9
Blue			6	1
Green			16	4
Orange	86	19	96	21
Brown	236	52	68	15
Yellow	3	1	6	1
Red	5	1	40	9
Total	457	100	457	100

Table-9.4: Frequency table of colour hue of the samples from layer-XIII from El Esquilleu. Columns are primary and secondary colour hues and rows are the colours considered.

We identified non-quartz minerals in 2,126 samples of “archaeological quartzite”, after having excluded the items assigned to unknown type (Table-9.3). Non-quartz mineral characterisation reveals the high presence of iron oxides, non-identified black minerals, manganese oxides, and micas. All these minerals are present in any petrogenetic type. The only exception are manganese oxides, which are mainly associated with SO, BQ and RQ types. The scarce feldspars identified are clearly associated to CC and CA petrogenetic types. Characterisation of colour indicates that most frequent hues are grey, white, black, and brown (Table-9.4). The first one is not associated to any petrogenetic type. Most of the white coloured “archaeological quartzites” are associated with OO, RQ and MQ types. Dark colours are associated with SO and BQ petrogenetic types. Finally, brown coloured samples are associated with quartzarenites. The presence of other colours, such as blue, red or yellow is restricted to small areas or to surfaces of quartzites. Then, they are not so frequent.

We carried out petrographic and geochemical characterisation of twelve lithic items, with the aim of better recognising more deformed and metamorphic types (Figure-9.1). The description of these samples helps us understand the differences between types, as well as define and establish some interesting varieties. Due to problems related with the sampling process, we could not analyse any sample of the BQ petrogenetic type. Still, we analysed this and the other two petrogenetic types using non-destructive techniques.

9.2.1. THE OO PETROGENETIC TYPE AT EL ESQUILLEU, LAYER-XIII

Three of the samples analysed are OO orthoquartzites: ES-315, ES-419, and ES-435 (Figure-9.2). All three samples show clastic grained texture and complete packing. They are characterised by syntaxial overgrown and concavo-convex grain boundaries that in a few cases generate suturated relationship between grains. Undulatory extinction is clear on the three samples. Grain size characterisation reveals the major presence of very fine and fine U-W categories on a relatively single mode (some grains from the ES-419 and ES-435 are bigger, showing more heterogeneous distribution). The grains are relatively rounded, with indexes around 0.60, while the regularity of quartz grains is smaller, due to the small increase of deformation. Directional analysis shows that the grains of samples ES-419 and ES-435 are preferentially oriented at $\alpha = 0.05$ and $\alpha = 0.01$, but sample ES-315 is not oriented at $\alpha = 0.01$. The features observed through binocular microscopy are in concordance with this characterisation: compact and grainy T&P, concave-convex limits, as well as some regrowth. Grain size characterisation of these samples points at medium grains with either homogeneous distributions around one mode or heterogeneous distributions. Under the binocular microscope there is no preferential orientation of the grain.

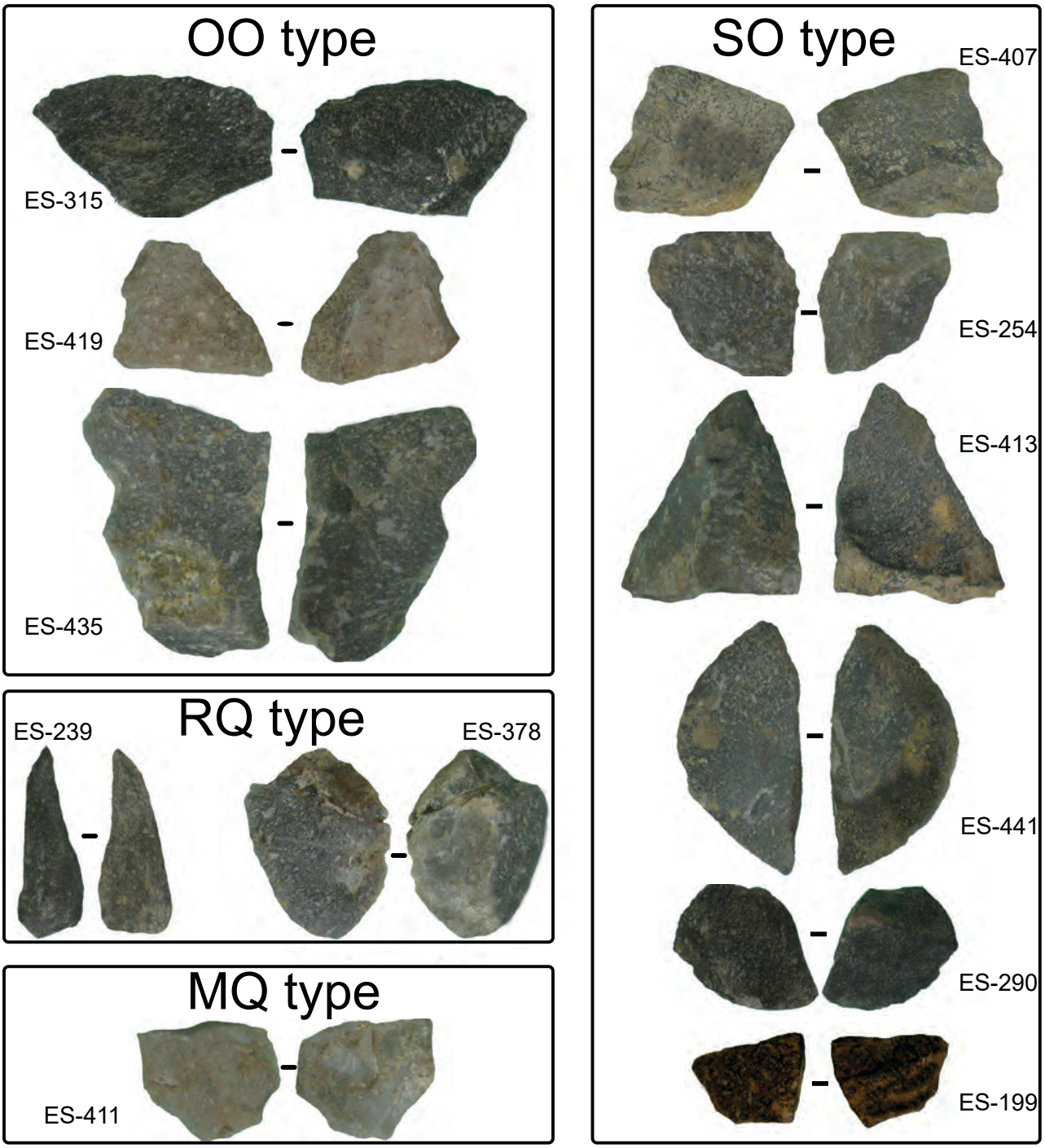

Figure-9.1: Pictures of the samples selected from Layer-XIII of the archaeological site of El Esquilleu. Samples are grouped by petrogenetic type.

The characterisation of matrix, cement and non-quartz minerals reveals differences between the orthoquartzites analysed, which create different colours (See Table-5.11). The high presence of iron oxide, rutile, pyrite and other non-identified opaque minerals is what confers sample ES-315 its grey to black colour. The smaller presence of these minerals in ES-419 prevents the appearance of different colours. The clayey matrix of ES-435 is probably what transforms white colour into grey. Regarding the non-destructive characterisation of the material, in sample ES-315 there is a combination of iron and manganese oxides and black and heavy non-identified minerals. Moreover, the non-quartz minerals detected in ES-435 and ES-419 include iron oxides, micas, and black and heavy non-identified minerals. The results of X-ray fluorescence are consistent with mineralogical characterisation. The quantity of SiO_2 is smaller in sample ES-315 (95.83%) due to the increase of TiO_2 (1.95%) and Al_2O_3 (1.17%). In samples ES-435 and ES-419 the SiO_2 is slightly more abundant (≈97%) with similar concentration of some other compounds, except for the peak of Al_2O_3 (1.53%) in the former.

After having analysed the features and variability of the OO petrogenetic type, we can extrapolate these results to those of non-destructive techniques. The samples destructed confirm and allow understanding the major presence of OO type “archaeological quartzites” with medium grain sizes, probably as consequence of syntaxial quartz regrowth. The homogeneous grain size distribution organised around one mode is the most frequent grain size category. This is followed by heterogeneous distribution, due to the presence of some bigger grains, as observable in samples ES-419 and ES-435. Clear bimodal distributions are negligible (Table-9.2). Colour and mineral characterisation reveals white and grey varieties, together with non-identified black minerals, micas, and iron oxides are the most frequent varieties. Black or dark-grey varieties are scarcer. Finally, preferential orientation is only appreciable in 6.1% of the samples, although in thin section it is clear in two of the three samples. This last conclusion is an example of the limitations of non-destructive characterisation.

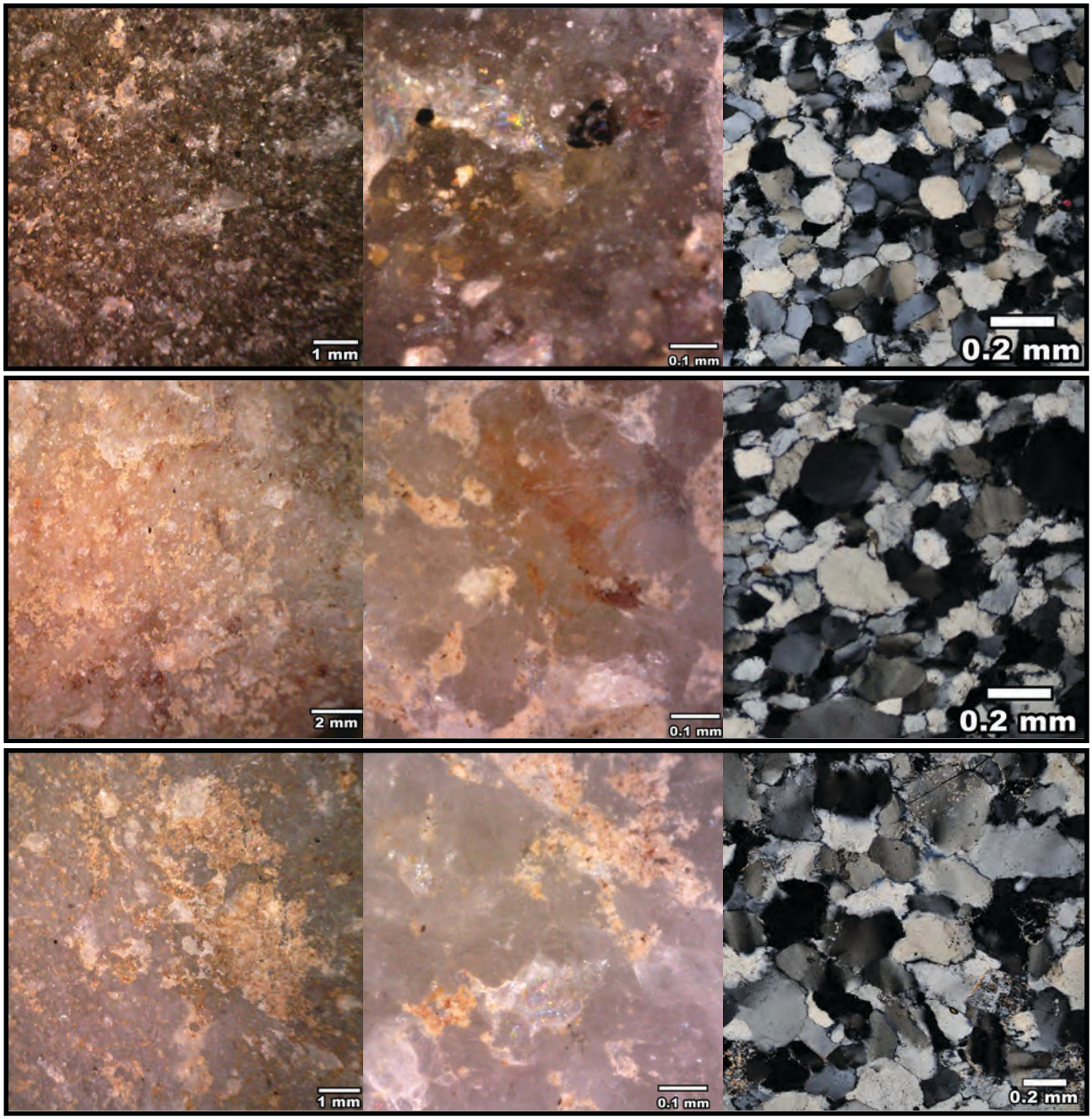

Figure-9.2: Pictures of the OO type samples from Layer-XIII of the archaeological site of El Esquilleu. From top to bottom, samples ES-315, ES-419 and ES-435. From left to right, microscopy binocular picture at 20x, microscopy binocular picture at 250x, and thin section microscopy picture at different magnifications.

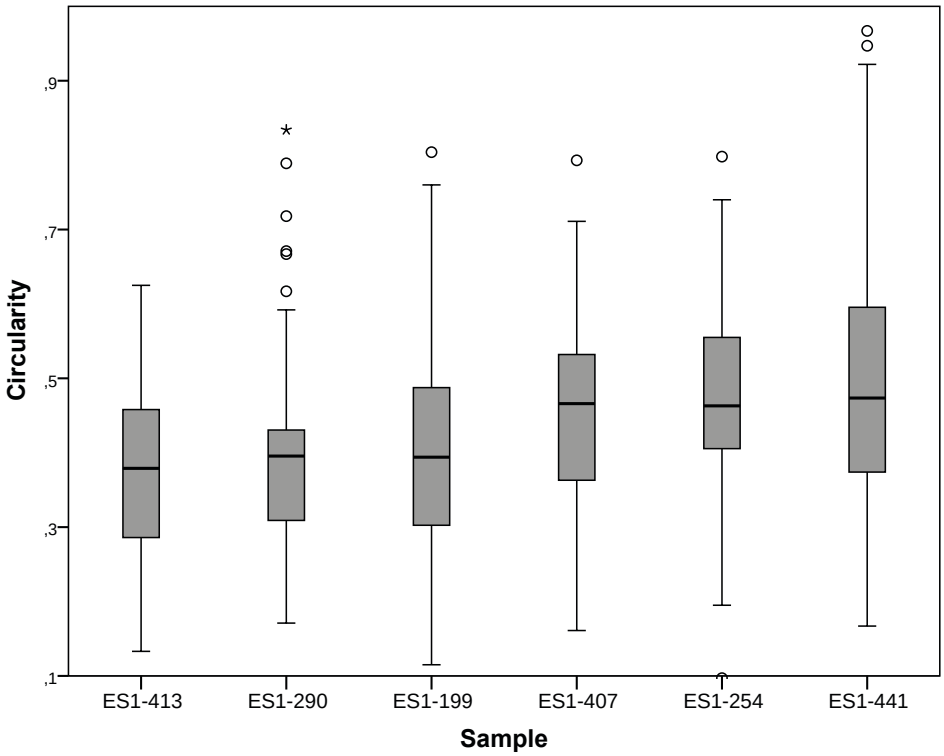

Figure-9.3: Boxplot representing morphology of quartz grains of SO samples from layer-XIII of El Esquilleu based on circularity index.

9.2.2. THE SO PETROGENETIC TYPE AT EL ESQUILLEU, LAYER-XIII

Six of the samples analysed belong to the SO petrogenetic type: ES-407, ES-254, ES-413, ES-441, ES-199, and ES-290. All of them show clastic grained texture, suturated packing, high presence of undulatory quartz extinction, and suturated/microstylolitic quartz grain limits. Böhm lamellae are restricted to ES-254 and ES-290 samples. There is also small presence of recrystallised quartz grains in two samples: ES-199 and ES-413. Finally, concavo-convex quartz grain limits are clear in samples ES-407 and ES-441, together with syntaxial quartz overgrowth. In general, the characterisation of grain size points at the major presence of very fine sand (as well as coarse silt and fine sand) and smaller quartz grains (matrix and some recrystallised grains). Grain size of sample ES-254 is bigger than that of other samples. The morphology of quartz grains reveals differences in circularity indexes and similarities in the roundness one. According to the first one, there are two groups. The first one is formed by samples ES-254, ES-407, and ES-441 and is characterised by the highest circularity indexes of the SO type. Instead, samples ES-413, ES-290 and ES-199 have the lowest circularity indexes (Figure-9.3). Only one of the six samples does not exhibit preferential orientation.

Regarding non-destructive characterisation of the samples, the majority shows moderate to high bright, micro-cracks on surface, suturated packing, difficult grain distinction, and ruffle quartz grain limits, i.e. grainy and fine T&P with ruffle and irregular grains limits. Nevertheless, fine T&P, associated with concave-convex quartz grain limits is observed in sample ES-254. This is explained by the differential affection of deformation processes in bigger quartz grains (Figure-9.4). It is also possible to identify fine T&P in association with the impossibility to detect grain boundaries, as in sample ES-441 (due to smaller grain size). Foliation structures are only appreciable in samples ES-290, ES-254, and ES-199. Differences in grain size and its association with recognisable features, allow us to propose two main varieties: a) a homogeneous fine grained variety with clear fine and grained T&P and b) a heterogeneous medium-coarse grained variety with foliation structures, represented only by sample ES-254.

Coming to non-quartz mineral characterisation, clayey matrix appears in negligible percentages in every sample. None of the samples exhibits cement. As in the previous type, the minerals detected create different colours. Pyrite and manganese oxides observed under non-destructive techniques determine the black colour of samples ES-199 and ES-290 (Figure-9.5). Mineral characterisation using petrography is consistent with these mineral associations, as indicated by the detection of pyrite,

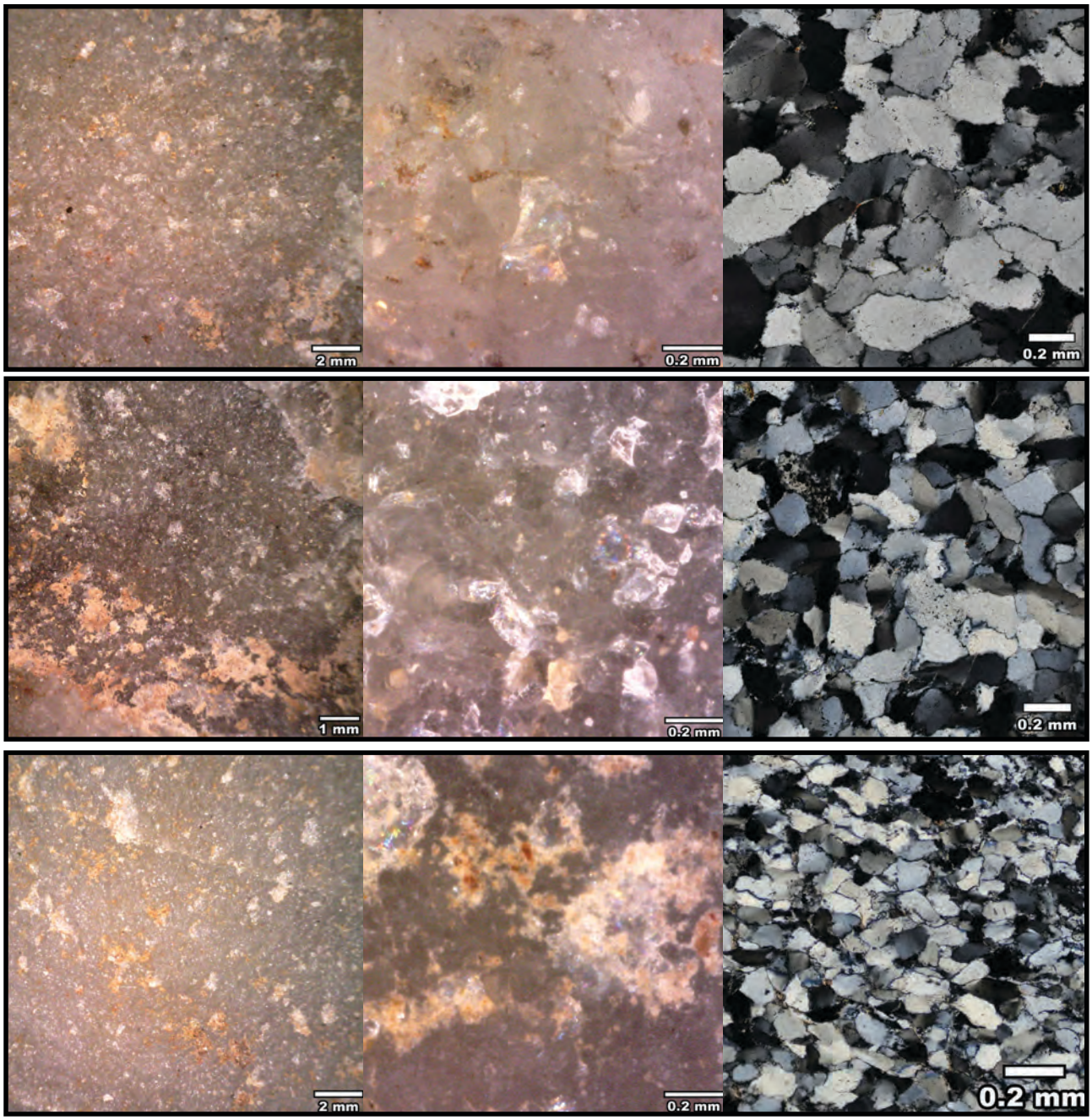

Figure-9.4: Pictures of the SO type samples from Layer-XIII of the archaeological site of El Esquilleu. From top to bottom, samples ES-254, ES-407, and ES-441. From left to right, microscopy binocular picture at 20x, microscopy binocular picture at 250x, and thin section microscopy picture at different magnifications.

tourmaline and other non-identified black minerals. The other samples analysed by non-destructive techniques do not show these minerals. It is important to mention that other minerals, such as zircon, Fe-oxides, chlorite, and clays are common in all thin sections in association with non-identified black and heavy minerals, iron oxides, and micas. These non-quartz minerals are probably the ones generating the grey colour. The results of X-ray fluorescence are in concordance with these differences. SiO_2 is slightly smaller in sample ES-290 than in other samples (note this analysis was not performed for sample ES-199). In addition, Al_2O_3 and Fe_2O_3 present the highest values among all the samples analysed. Then, there are two mineral/colour varieties: black or dark-grey and grey or clear-grey one.

The data obtained through destructive characterisation allow us to extrapolate these results to the complete lithic collection, only analysed by non-destructive techniques. Most of the SO type quartzites from this layer are related with the homogeneously distributed and fine or fine to medium grain size varieties (≈70%). The coarse or medium to coarse SO variety is only present in small percent-

ages (≈15%). Regarding the two varieties defined by mineral characterisation, dark and clear varieties are found in similar proportions. It is important to mention, that the first mineral variety is also related with foliation structures, observable on most of the samples of the dark SO variety.

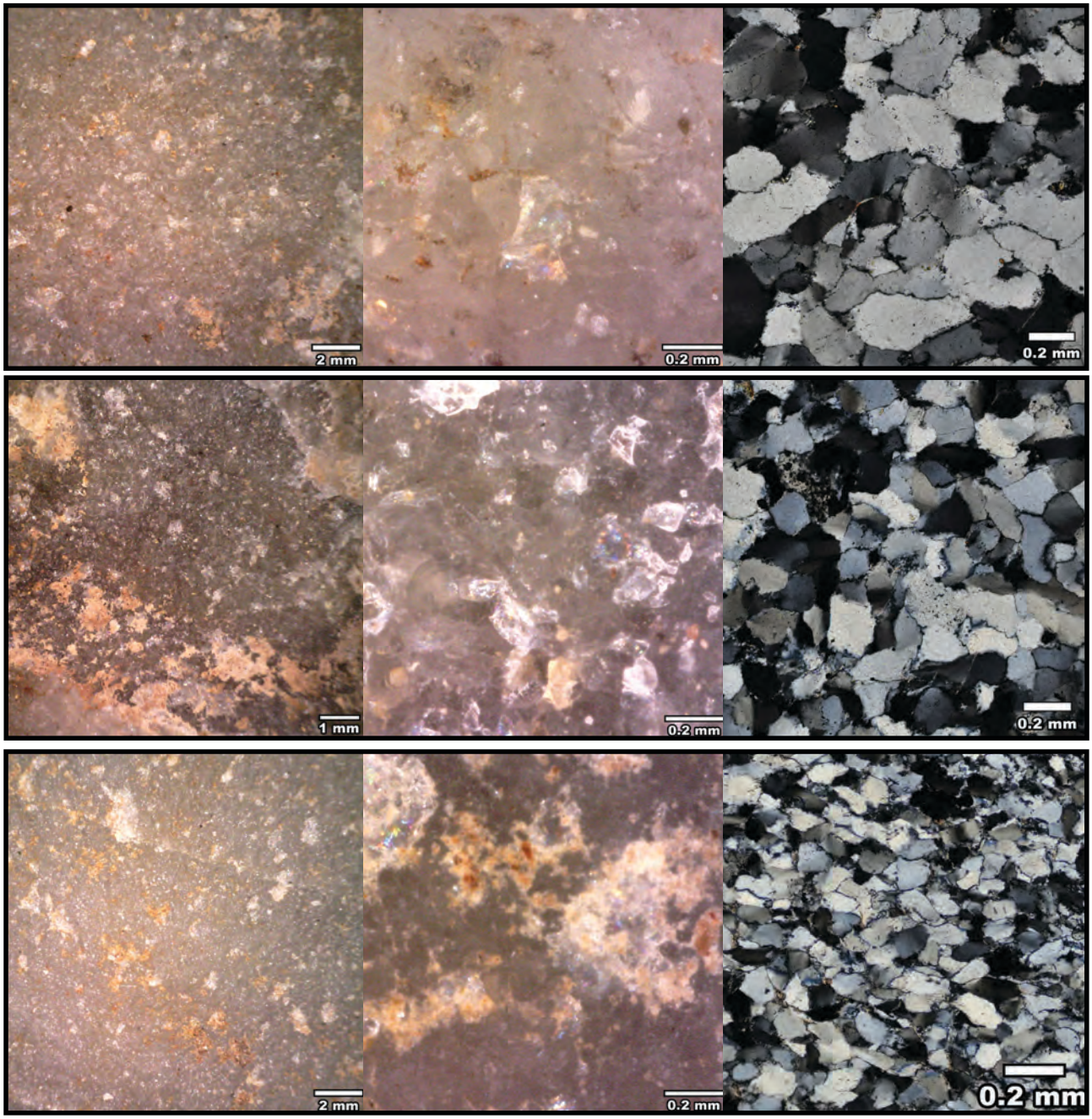

Figure-9.5: Pictures of the SO type samples from Layer-XIII of the archaeological site of El Esquilleu. From top to bottom, samples ES-199, ES-290, and ES-413. From left to right, microscopy binocular picture at 20x, microscopy binocular picture at 250x, and thin section microscopy picture at different magnifications.

9.2.3. THE RQ PETROGENETIC TYPE AT EL ESQUILLEU, LAYER-XIII

Two of the samples selected belong to the RQ petrogenetic type. These are samples ES-239 and ES-378 (Figure-9.6). They are characterised by a mortar texture and suturated packing. Quartz grains are featured by are recrystallised quartz grains and suturated limits in non-recrystallised grains. In some of the latter, Böhm lamellae are clear. The analysis of the size and morphology of the grains of both samples reveals two modes: the main one situated around medium silt and a secondary and smaller one around fine sand. Fine sand is coarser in sample ES-378 than in ES-239 due to the features of the original sand sediment or to abnormal enlargement of quartz grains as a consequence of the metamorphic process. The morphology of the grains, expressed by circularity index, emphasises the bimodal distribution. On both samples (non-recrystallised) grains are preferentially oriented. Non-destructive characterisation points at soapy texture without detectable grain boundaries (except for the 50x magnification, where some big grains from the ES-378 sample are appreciated), high bright and limited micro-cracks (i.e. soapy T&P). Even though the size of the grains in sample ES-239 are classified as fine grain, they are almost impossible to detect. As a consequence of metamorphic processes, foliation structures are clear under binocular microscope. Summing up, in this type, two grain size varieties are recognisable: a fine variety and a coarse-medium variety.

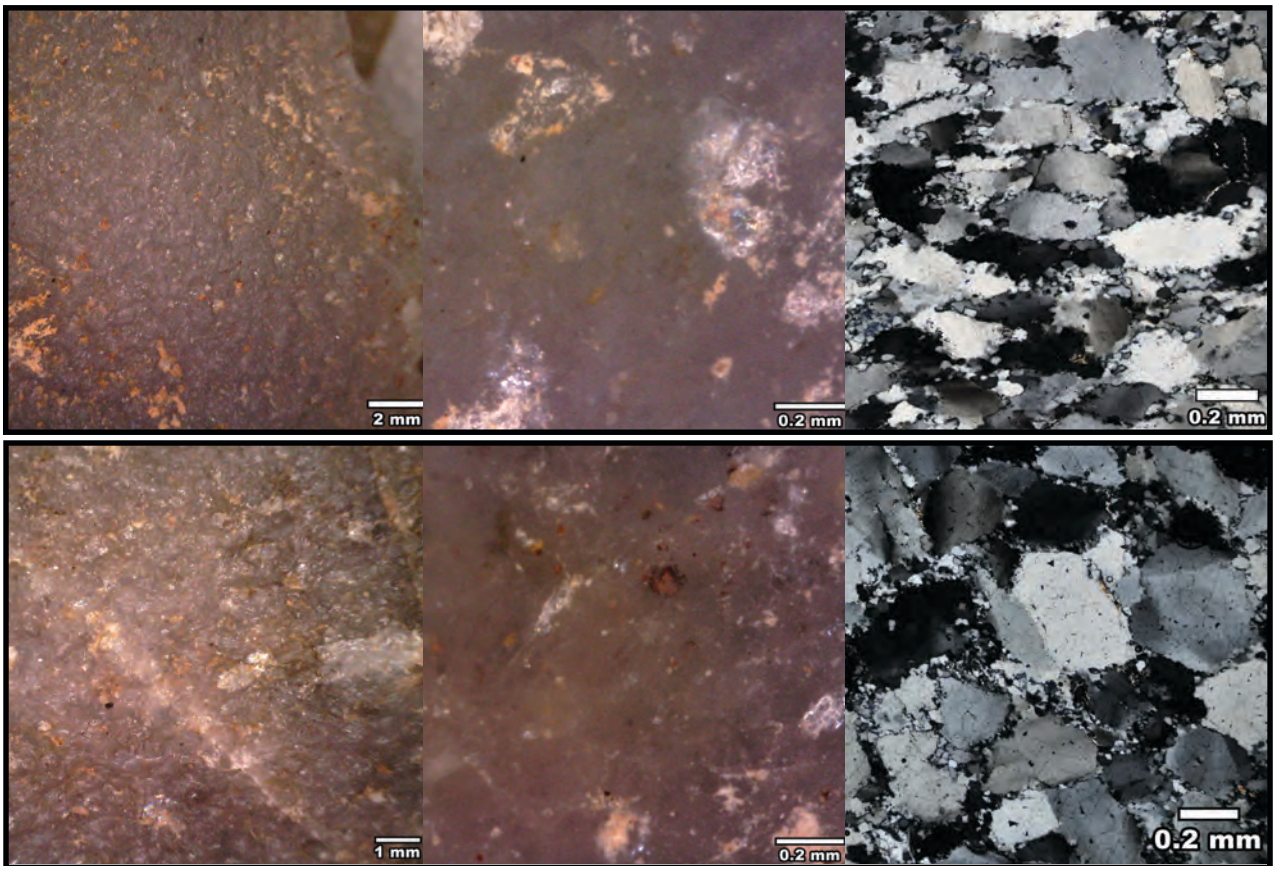

Figure-9.6: Pictures of the RQ type samples from Layer-XIII of the archaeological site of El Esquilleu. From top to bottom, samples ES-239 and ES-378. From left to right, microscopy binocular picture at 20x, microscopy binocular picture at 250x, and thin section microscopy picture at different magnifications.

Regarding to mineral characterisation, none of the samples show neither matrix nor cement. Iron oxides and pyrite are present in both samples, in reduced quantities, though. In sample ES-378 it is also possible to observe zircon and elongated mica flakes. There is no clear difference in colour between the samples, classified as grey, as almost all the RQ type quartzites from this layer. X-ray fluoresce was only performed on sample ES-378. It revealed a major presence of SiO_2 (>97%) and small percentages of Al_2O_3 and CaO. Then, differences were not enough for establishing distinct mineralogical varieties.

Coming back to the complete collection and comparing it with the data obtained from the thin section characterisation of these two samples, it can be said that the two grain size varieties defined are well represented. However, the small grain size variety is slightly more frequent. It is important to mention that this type is only represented by 92 lithic implements.

9.2.4. THE MQ PETROGENETIC TYPE AT EL ESQUILLEU, LAYER-XIII

The only sample selected from this type is sample ES-411 (Figure-9.7). It is characterised by a clastic grained texture and suturated packing. Recrystallised quartz grains appear mainly, but sutured quartz grains are less frequent. Grains also show plain and angular limits. In general, it is impossible to distinguish between recrystallised and non-recrystallised quartz grains. Quartz grain size characterisation shows a single wide mode, with grains between medium silt and fine sand, the biggest peak being at the very fine sand category. The analysis of grain morphology points at the general irregularity of particles, while roundness index reveals particles are not clearly elongated. Preferential orientation of quartz grains is clear, due to the increase of pressure during metamorphic processes. Non-destructive characterisation indicates soapy texture and no quartz grain limit detection. Bright is high. Foliation structures are absent, due to the extremely crystallinity of surface.

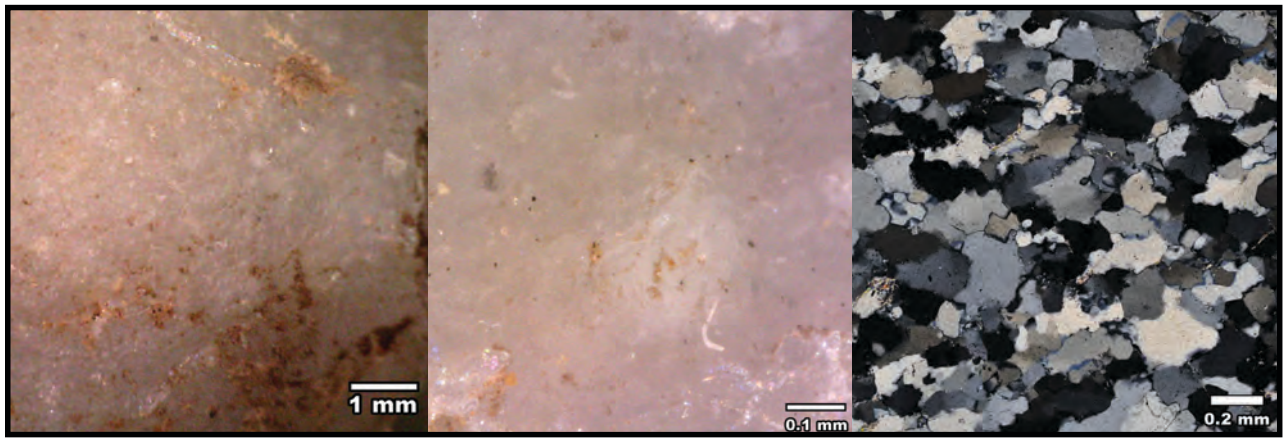

Figure-9.7: Pictures of the MQ type sample, ES-411, from Layer-XIII of the archaeological site of El Esquilleu. From left to right, microscopy binocular picture at 20x, microscopy binocular picture at 250x, and thin section microscopy picture at 50x magnification.

The mineral characterisation of this sample shows a negligible quantity of clayey matrix and absence of cement. There are micas (flake shaped) and clays in small quantities. The results of X-Ray Fluorescence are in accordance with the minerals detected in thin section. The sample is mainly composed of SiO_2 (>98%). The only component with a representation greater than 0.5% is Al_2O_3. The colour of the sample is white. Still, within the complete assemblage of MQ quartzites there are some grey-clear ones. Iron oxides and non-identified black and heavy minerals are common in the surface of these quartzites due to post-depositional processes.

Coming back to the analysis of all the MQ type quartzites from layer XIII, we do not observe different varieties. Most of the samples are within a homogeneous mode, between fine and medium quartz grain sizes. As on the petrogenetic type analysed previously, the inability to define clearly different varieties could be due to the small quantity of items analysed (n=75).

9.2.5. NON-DESTRUCTIVE CHARACTERISATION OF CC, CA AND BQ PETROGENETIC TYPES AT EL ESQUILLEU, LAYER-XIII

The CC petrogenetic type is the less frequent type in this layer. Under binocular microscopy, most of these quartzarenites exhibit coarse grained textures with floating or punctual packing (i.e. saccharoid T&P). Quartz grain features vary from plain and angular quartz limits to plain and rounded ones. There are ruffled limits between grains as a consequence of cement (Figure-9.8). A small quantity of samples presents bedding. As shown in Table-9.2, there is high variability in grain size. Therefore, the most common type of grain size distribution is heterogeneous. The analysis of non-quartz minerals puts this type as the most variable on, with all non-quartz minerals considered present. The most common ones are iron and manganese oxides, micas, non-identified black and heavy minerals, and feldspar. Colour is also variable in this type. Brown and grey are the most frequent ones, followed by white, black, and orange.

The CA petrogenetic type is also present in this archaeological layer, but only in small proportions. Under binocular microscope most of the textures are coarse grained, although fine grained textures are also observable. Packing is generally tangent or tangent-complete. Grains are easy to recognise,

with rounded or angular borders. The presence of cement is small or non-existent. Granular T&P is clear in this petrogenetic type. The grain size of this type is heterogeneous, although the presence of homogeneous and fine-medium sizes is significant (Figure-9.8). The distribution of non-quartz minerals is more homogeneous distribution than in the previous type. The most frequent minerals are iron and manganese oxides, micas, and non-identified black minerals. Feldspar presence is scarce, as pyrite. The most frequent colour is grey, followed by brown, and less importantly, white and black.

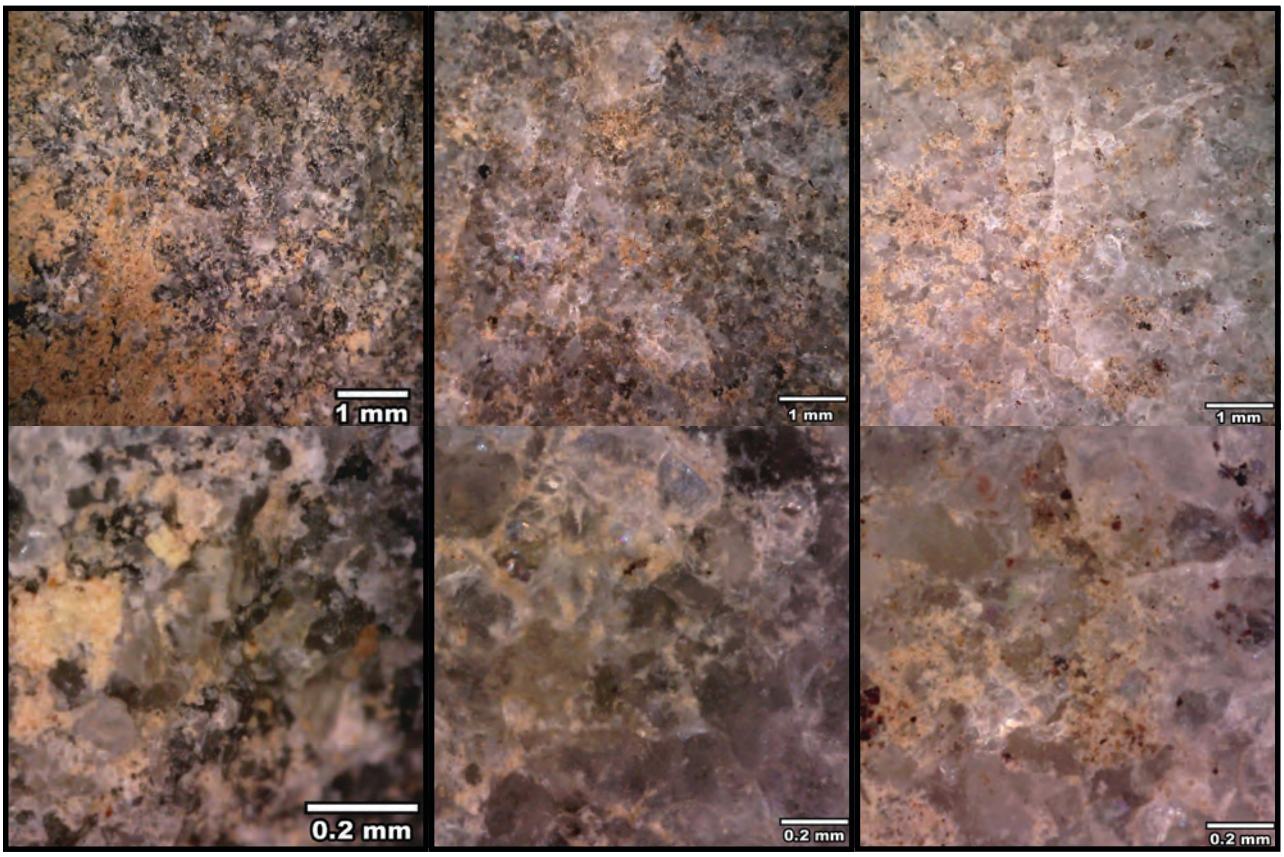

Figure-9.8: Pictures of the CC and CA types from layer-XIII of the archaeological site of El Esquilleu. From left to right, ES-140 (CC type), ES-135 and ES-168 (CA type). Upper rows show microscopy binocular pictures at 50x. Lower rows show microscopy pictures at 250x. The presence of carbonated clays is clear in all surfaces.

The BQ petrogenetic type is the third most frequent type. Although the sampling process did not detect this type correctly, the determination under binocular microscopy clearly points at the importance of this type in the layer analysed. The two samples selected for characterising this BQ type were ES-199 and ES-290. Under binocular microscope these two samples are similar to the BQ petrogenetic type, also in some of the features observed under petrographic microscope: clastic grained texture, suturated packing and high presence of undulatory extinction and suturated quartz grain limits. Additionally, sample ES-290 contained recrystallised grains. They were present in minor proportions, while they were a major element in the BQ type.

Regarding binocular characterisation, this type is mainly predominated by fine texture with suturated packing (i.e. fine T&P). In some cases grains cannot be clearly detected, but in others it is possible to observe ruffled borders. Coming to grain size characterisation, most of the pieces analysed are within the fine grain categories. Medium grain sizes could form a variety, but the limits of non-destructive characterisation prevent us from doing so. The distribution of quartz grain size is generally homogeneous and organised around one mode, although some pieces are more heterogeneous. The non-quartz mineral distribution of this type is varied, due to the presence of manganese oxides (≈21%) and pyrite (≈5%) instead of micas (≈9%) commonly present in other types. Nevertheless, the most frequent non-quartz minerals recognised are non-identified dark and heavy minerals (≈32%) and iron oxides (≈33%). Colour characterisation points at the main presence of grey and dark quartzites. Others colours, such as brown (≈7%) and white or clear grey (≈4%) are also present (Figure-9.9). Once again, no clearly distinguished varieties could be defined due to a) the scarce presence of brown and clear grey varieties and b) the lack of samples for thin section characterisation.

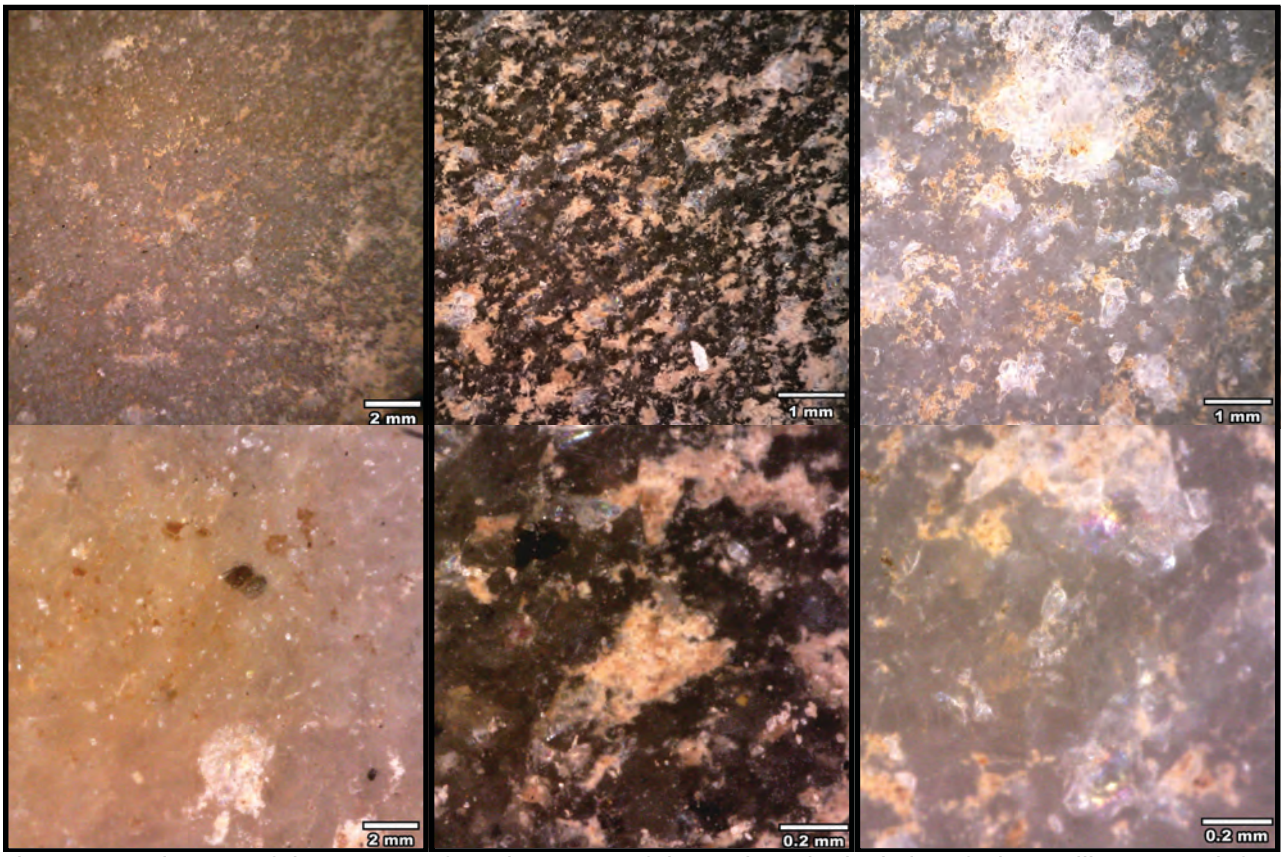

Figure-9.9: Pictures of the BQ type from layer-XIII of the archaeological site of El Esquilleu. From left to right, samples ES-207, ES-325, and ES-186. The first sample presents fine grains size with homogeneous distribution. Its characteristic colour is grey-brown. Grains from the second quartzite are also fine and homogeneous. Its colour is black or grey-black. The last sample is grey-white coloured. Quartz grains size is medium with heterogeneous distribution.

9.2.6. CHARACTERISATION OF CORTICAL AREAS AT EL ESQUILLEU, LAYER-XIII

Here we present the result of the characterisation of cortical areas. The distribution of cortex in the lithics analysed between different types of raw material is shown in Table-9.5. “Archaeological quartzite” is the most frequent raw material with cortical areas, which is in accordance with its predominance in the whole assemblage. Others raw materials do not present this correlation. For example, cortical areas were underrepresented among flint (4%), while they were overrepresented among limestone or lutites. For example, almost 50% of the lutites analysed preserved cortex. The relative presence of cortical areas among archaeological quartzites, quartz, and radioralites is around the 20%.

Regarding the types of cortex, 11% of the collection could not be characterised due to the absence of diagnostic features. None of the cortex types identified could be interpreted as evidence of direct extraction from the outcrop.

Conglomerate cortex is quite frequent, representing 38% of the lithic implements with cortical areas. One of them is a lutite, while the remaining 199 pieces are “archaeological quartzites”. No conglomerate cortex was identified among flint, limestone, quartz, or radioralite. Conglomerate cortical areas are characterised by the presence of cements from the conglomerate itself, which are generally recognisable as red iron oxides or dark silica precipitates. In addition, voids are usually present, even though they are generally filled with conglomerate cement. No clear impact cracks are observable on cortical areas.

Cortical areas from fluvial sources is the most frequent cortex type, representing 50% of the cortical areas analysed. “Archaeological quartzite” is again the most frequent raw material areas among the lithics with this type of cortex. However, there are lithic implements with fluvial cortex among flint, limestone, quartz, radioralite, and lutite too. Actually, this is overrepresented among lutites and limestones. Fluvial cortex is mainly characterised by the presence of impact cracks in the surface and fine or soapy textures. Voids are less frequent in this cortex type and cement is absent (except for the carbonated clay stuck on the whole surface due to post-depositional processes).

Raw material	Cortex type												∑ of each type
	Conglomerate			Fluvial			Undetermined			Total			
	∑	%	% rel	∑	%	% rel	∑	%	% rel	∑	%	% rel	
Archaeological quartzite	199	100	9	242	92	10	59	98	3	500	96	22	2324
Flint				1	0	3				1	0	3	35
Limestone				7	3	33				7	1	33	21
Limonite													0
Lutite	1	1	4	10	4	37	1	2	4	12	2	44	27
Quartz				1	0	14				1	0	14	7
Radioralite				1	0	20				1	0	20	5
Undetermined													0
Total	200	38	8	262	50	11	60	11	2	522	100	22	2419

Table-9.5: Frequency table of types of cortex identified in layer-XIII from El Esquilleu grouped by main raw material. Columns are the types of cortex, including the frequency of each cortex type for each raw material and the total of items with cortex of each raw material. The last column quantifies the total of items with and without cortex of each raw material. The columns % are the percentage of each raw material in relation to each cortex type, while the columns % rel. are the percentage of cortex type in relation to the total of each raw material (including items with and without cortex).

Focusing on the distribution of cortex among “archaeological quartzites” and their different petrogenetic types, there is a clear overrepresentation of cortical areas among the CC petrogenetic type. They are less frequent among the CA petrogenetic type. Conversely, lithics with cortex are underrepresented among the MQ type and just slightly more frequent among the OO type (Table-9.6). The remaining petrogenetic types show percentages of items with cortex around 22%, similar to those of “archaeological quartzites” as a whole.

Archaeological quartzite	Cortex type												∑ of each type
	Conglomerate			Fluvial			Undetermined			Total			
	∑	%	% rel	∑	%	% rel	∑	%	% rel	∑	%	% rel	
CC				55	23	60	3	5	3	58	12	63	92
CA	2	1	2	24	10	21	7	12	6	33	7	29	113
OO	37	19	6	59	24	10	7	12	1	103	21	18	570
SO	73	37	10	65	27	9	20	34	3	158	32	21	753
BQ	61	31	14	18	7	4	14	24	3	93	19	22	431
RQ	17	9	18	7	3	8				24	5	26	92
MQ	4	2	5	2	1	3	3	5	4	9	2	12	75
Undetermined	5	3	3	12	5	6	5	8	3	22	4	11	198
Total	199	40	9	242	48	10	59	12	3	500	100	22	2324

Table-9.6: Frequency table of types of cortex identified in layer-XIII from El Esquilleu grouped by petrogenetic type. Columns are the types of cortex, including the frequency of each cortex type for each petrogenetic type and the total of items with cortex of each petrogenetic type. The last column quantifies the total of items with and without cortex of each petrogenetic type. The columns % are the percentage of each petrogenetic type in relation to each cortex type, while the columns % rel. columns are the percentage of cortex type in relation to the total of each petrogenetic type (including items with and without cortex).

Cortical areas from conglomerate and fluvial contexts are present in similar percentages when considering all “archaeological quartzites” as a whole (cortex from conglomerates account for 9% of “archaeological quartzites” and cortex from rivers for 10%). Still, they are clear differences when sorting them by petrogenetic types. Chi-square test (χ^2 (7, N = 441) = 107.067, p < .001) statistically confirms these differences and standardised residues, represented in Figure-9.10, graphically shows them. The fluvial cortex type is overrepresented in the quartzarenite group, mainly because of the contribution of the CC type. In this group, the presence of conglomerate cortex is clearly underrepresented, with only two examples of this cortex in the CA type. Conversely in the orthoquartzite group cortex from both conglomerates and fluvial deposits are present in similar proportions. Nevertheless, fluvial cortex is predominant in the OO type, while conglomerate cortex is the main one in the SO type. In the quartzite group conglomerate cortex is overrepresented. This type of cortex was proportionally more important in the BQ type than in RQ and MQ types.

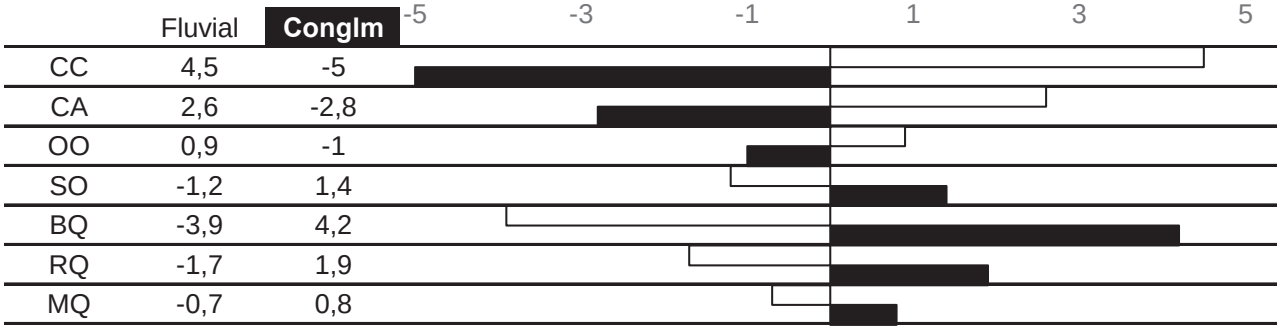

Figure-9.10: Standardised residues of χ^2 test of "archaeological quartzites" with cortex, showing the weight of each type of cortex in different petrogenetic types.

9.3. TECHNOLOGICAL STRUCTURE

Here we present the results of the technological analysis of the material from layer-XIII of El Esquilleu, taking into account the results from the study of the petrological structure. According to the methodology previously exposed, the most frequent category are the knapping products (84%), followed by chunks (15%), and cores (1%). The distribution of technological products sorted by lithologies is shown in Table-9.7. Cores are restricted to quartzite and flint. Flint core abundance is remarkable, especially considering the low presence of this raw material in the complete lithic collection. Knapping products of all raw materials are well represented. They are the predominant technological product for every raw material, except for limestone. This is because there is a clear overrepresentation of chunks among limestones because a single piece of this raw material was classified as knapping product. In contrast, chunks are scarce among "archaeological quartzites" (the raw material with the smallest proportion of chunks), flint, quartz, and lutite. There is no chunk in radioralite.

	Technological order										
	Cores			Knapping prdct.			Chunk			Total	
	∑	%	% rel	∑	%	% rel	∑	%	% rel	∑	%
Archaeological Quartzite	28	82	1	1979	97	85	317	89	14	2324	96
Flint	6	18	17	22	1	63	7	2	20	35	1
Limestone				1	0	5	20	6	95	21	1
Limonite											
Lutite				18	1	67	9	3	33	27	1
Quartz				5	0	71	2	1	29	7	0
Radioralite				5	0	100				5	0
Volcanic rock											
Total	34		1	2030		84	355		15	2419	100

Table-9.7: Frequency table of main technological categories identified in layer-XIII from El Esquilleu grouped by raw material. Columns are the main technological categories and the total of items of each raw material. The columns % are the percentage of each raw material in relation to each technological category, while the columns % rel. are the percentage of each technological category in relation to the each raw material. Cells in black are the categories representing more than 10% of the total cases.

Focusing the analysis on "archaeological quartzites", the cores are restricted to CA, OO, SO, BQ, and MQ types (Table-9.8). However, they are scarce in all of them (1% of the total lithics for each of these petrogenetic types), except for the BQ type, whose proportion of cores is higher. Knapping products are more frequent among all types, even though there are differences between them: They are less frequent (<73%) among quartzarenites and the undetermined group and more frequent among others groups (>89%). This situation is clearer when comparing CC and MQ types, which have 39% and 97% of knapping products respectively. On the contrary, chunks are very frequent among quartzarenites (as well as among undetermined material). Regarding orthoquartzites and quartzites, the amount of chunks is reduced, with percentages smaller than 11%. The proportion of chunks in the MQ type is really small (1%).

	Technological order										
	Cores			Knapping prdct.			Chunk			Total	
	∑	%	% rel	∑	%	% rel	∑	%	% rel	∑	%
CC				36	2	39	56	18	61	92	4
CA	2	7	2	82	4	72	30	9	26	114	5
OO	3	11	1	505	25	89	62	19	11	570	24
SO	7	25	1	689	35	91	60	19	8	756	32
BQ	15	54	3	390	20	90	30	9	7	435	19
RQ				86	4	93	6	2	7	92	4
MQ	1			74	4	97	1	0	1	76	3
Undetermined				123	6	62	75	23	38	198	8
Total	28		1	1985		85	320		14	2333	100

Table-9.8: Frequency table of main technological categories identified in layer-XIII from El Esquilleu grouped by petrogenetic types of “archaeological quartzite”. Columns are the main technological categories and the total of items belonging to each petrogenetic type. The columns % are the percentage of each petrogenetic type in relation to each technological category, while the columns % rel. are the percentage of each technological category in relation to the each petrogenetic type of “archaeological quartzite”. Cells in black are the categories representing more than 10% of the total cases. Cells in light grey are the categories representing between 1 and 5% of cases.

9.3.1. CORES

We identified 34 cores in the whole collection. The most frequent type of core are irregular or polyhedral cores and cores on flakes, with 14 items each, followed by discoid cores, represented by four examples. There is only a prismatic core and a pyramid shaped core. There is no clear correlation between type of core and neither raw material, nor petrogenetic types of “archaeological quartzites” (Table-9.9).

	Type of core						
	Irregular	Discoid	Levallois	Prismatic	Pyramid	On flake	Total
Other RM	1	1				4	6
CC							
CA	2						2
OO	1	1				1	3
SO	4				1	2	7
BQ	6	2		1		6	15
RQ							
MQ						1	1
Undetermined							
Total	14	4		1	1	14	34

Table-9.9: Frequency table of types of cores identified in layer-XIII from El Esquilleu grouped by petrogenetic types of “archaeological quartzite”. Columns are the types of cores. In this case the only other raw material (RM) is flint.

The irregular cores from this assemblage are diverse. Regarding raw material, most of them are made on BQ “archaeological quartzites” (six items). SO (four items), CA (two items) and OO (one item) petrogenetic types are represented too. An irregular core made of flint is also present. Most of the cores (8) are complete and six fractured. The number of percussion platforms and flacking surfaces in irregular cores is varied and the three groups of “archaeological quartzites” are similarly represented. No clear standardisation is appreciated in this type of core. Coming to the presence of cortical areas, most of them preserve small areas of cortex, generally less than 33% of the total surface. Three of these cores present wider areas of cortex on the surface (between 33% and 66%). The features of these cortical areas vary between fluvial (7) and conglomerate (5). Two of the irregular cores are not cortical.

Cores on flake are a well-represented type too. Four of them are complete, while the other five are incomplete. The most common raw material for this type of cores is “archaeological quartzites”, with ten items. Nevertheless, flint is pretty well represented too, with four pieces. Regarding the type of “archaeological quartzites” present, the most frequent type is the BQ one, with six cores, followed

by the SO type, with two. Finally, there is a single core made on the OO type and another one on the MQ type. The quantity of percussion platforms and flacking surfaces is varied. Some cores were not intensively exploited and present just one percussion platform and one flacking surface. On the contrary, other cores, with three or more percussion platforms and flaking surfaces, are thoroughly exploited. The presence of cortical areas in this type of cores is restricted to the dorsal faces of the flakes. Seven of the cores made on "archaeological quartzites" preserved any cortex covering variable parts of the dorsal zones. Conversely, flint cores on flakes kept no cortical zones. Fluvial and conglomerate cortex types appear in similar proportions.

Discoidal cores are represented in this layer by four complete pieces. Three of them are made on "archaeological quartzites" and the remaining one on flint. Among the former, BQ (two items) and OO (one item) are the two petrogenetic types present. All four discoidal cores have more than three percussion platforms and two flacking surfaces. It is clear the same technique, with alternative and consecutive extractions, was used. The presence of cortical zones is restricted to the BQ petrogenetic type and it corresponds to the conglomerate type. Its extension of cortex on surface varies from one item with less than 33 to another one with more than 66%.

Finally, there is a prismatic and a pyramid shaped core. The former is made on a BQ type quartzite. Despite being incomplete, it is characterised by the presence of one percussion platform with three or more flacking surfaces associated to it. Cortex from conglomerate covered less than 33% of the surface. Meanwhile, the pyramidal shaped core is made a SO type orthoquartzite. It has two percussion platforms and three or more flacking surfaces. The presence of cortex is scarce, but it is enough to classify it as conglomerate.

9.3.2. KNAPPING PRODUCTS

In the lithic assemblage from Layer-XIII of El Esquilleu we identified 2030 knapping products. The most frequent type are blanks, making more than 99% of the elements analysed. Core preparation/rejuvenations elements are scarce, forming less than 1% of the assemblage. Finally, we do not identify any burin spall. Core preparation/rejuvenation elements are only found on "archaeological quartzites", more specifically orthoquartzites and quartzites (Table-9.10).

	Knapping products							
	Blanks			Core preparation/rej			Total	
	∑	%	% rel	∑	%	% rel	∑	%
Other RM	51	3	100				51	3
CC	36	2	100				36	2
CA	82	4	100				82	4
OO	503	25	100	2	20	0	505	25
SO	686	34	100	3	30	0	689	34
BQ	386	19	99	4	40	1	390	19
RQ	85	4	99	1	10	1	86	4
MQ	74	4	100				74	4
Unknown	123	6	100				123	6
Total	2026	100		10	0		2036	100

Table-9.10: Frequency table of the categories of knapping products identified in layer-XIII from El Esquilleu grouped by the petrogenetic types of "archaeological quartzite". Columns are the categories of knapping products and the total of items belonging to each petrogenetic type. The columns % are the percentage of each petrogenetic type in relation to each category of knapping product, while the columns % rel. are the percentage of each category of knapping product in relation to each petrogenetic type of "archaeological quartzite. Cells in black are the categories representing more than 10% of the total cases. Cells in dark grey are the categories representing between 5 and 10% of cases. Cells in light grey are the categories representing between 1 and 5% of cases. Other raw material (RM) includes flint (22), lutite (18), quartz (5), radioralite (5), and limestone (1).

Blanks is the technological category better represented in this layer, with 2,020 pieces. Coming to their integrity, 60% of the pieces are complete and 40% are fragmented (Figure-9.11). The most frequent fragments are longitudinal ones, followed by proximal ones. Distal and medial pieces are scarce (≈2%). Finally, 14% of the pieces could not be classified due to the absence of diagnostic features, mainly the bulb of percussion or the striking platform. Then, most of these undetermined fragments must be part of distal or medial fragments.

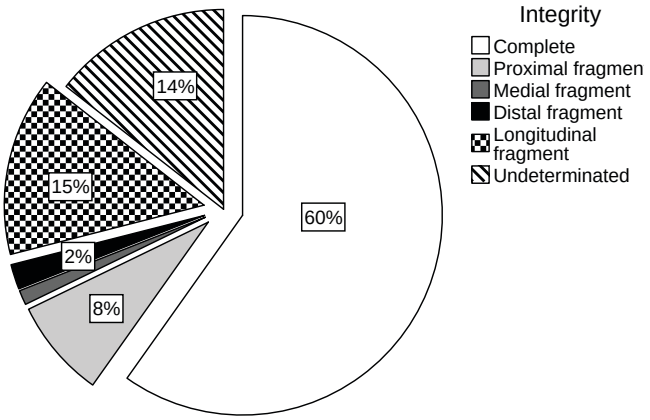

Figure-9.11: Pie chart showing percentage of each state of integrity of blanks.

There is great variability in the number of negative scars depending on raw material. All flint pieces have, at least, one negative scar (nine items with one negative scar, seven items with two negative scars, and six items with three or more negative scars). Quartz presents a similar distribution. On the contrary, four lutites have dorsal faces without any negative scar. Still, seven lutites present two negative scars and six three or more negative scars. Radioralite follows patterns similar to those of lutite. Finally, "archaeological quartzites" include a small number of items with dorsal faces without negative scars, a high presence of pieces one and two negative scars and, again, a reduced amount of blanks with three or more negative scars.

Regarding "archaeological quartzite" we also observe clear differences in the number of negative scars on dorsal surfaces between different petrogenetic types, as supported by Chi-square test (χ^2 (18, N = 1852) = 184.844, p < .001). Table-9.11 shows the total number of items in each category and the representation of standardised residues. In the CC petrogenetic type the absence of negative scars is especially relevant. The CA type is distributed similarly to the previous type, with high an overrepresentation of dorsal faces without negative scars, but an important presence of blanks with a single negative scar. The presence of two or more negative scars is small. In the OO type the quantity of blanks with negative scars increases, as a result of the reduction of the number of blanks without negative scars and the increase of blanks with one and two negative scars. Still, the number of blanks with three or more scars is scarce. Blanks with three or more scars clearly increase in the SO and BQ petrogenetic types. In these two groups, dorsal surfaces without negative scars, as well as dorsal surfaces with one negative scar, are scarce. There is a high presence of blanks with one and two extractions in RQ and MQ types. Blanks with three or more negative scars are not so abundant and blanks without negative scars on their dorsal surfaces are almost completely absent.

	Dorsal scars							
	None		One		Two		≥ Three	
	∑	**res**	∑	res	∑	res	∑	res
CC	14	11,5	10	-1,0	9	-1,3	3	-1,5
CA	7	2,5	38	1,2	26	-1,0	11	-1,3
OO	17	0,0	210	1,4	201	0,4	75	-2,4
SO	15	-1,7	238	-1,4	269	0,1	164	2,4
BQ	7	-1,7	134	-1,0	159	0,7	86	1,1
RQ	3	0,1	31	-2,0	35	0,3	16	-0,2
MQ	0	-1,6	41	2,4	22	-1,3	11	-0,9
Total	63	3	702	38	721	39	366	20

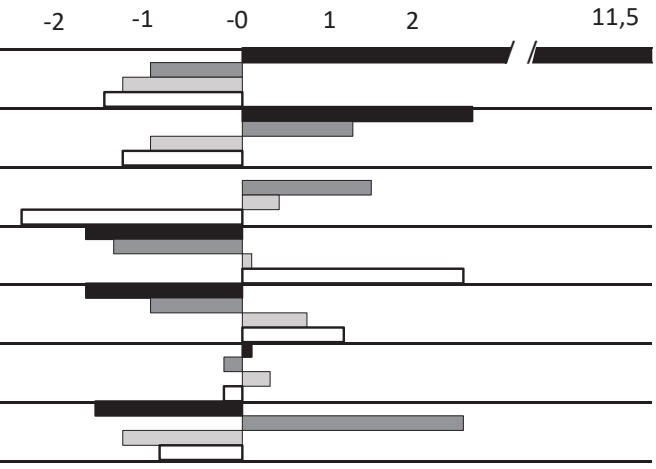

Table-9.11: Frequency table and standardised residues of χ^2 test of the quantification of dorsal scars grouped by petrogenetic types. The last row shows totals, and the second column for each category is its percentage in relation to the total of items analysed.

The preservation of cortical areas on these blanks does also provide interesting data about raw material exploitation in this context (Figure-9.12). Cortex is observable in 19% of the blanks from this collection. Most of them cover less than 33% of the dorsal surface. Broad cortical areas on dorsal surfaces (covering between 33% and 66% of it) are only present in 7% of the blanks and only 4% of the items analysed have cortical areas covering more than 66% of the surface. Their distribution according to raw materials reveals most lithics with cortical areas are on "archaeologi-

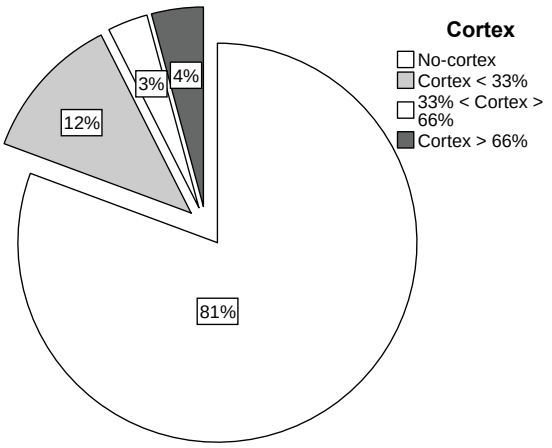

Figure-9.12: Pie chart showing percentage of absence, presence and extension of cortex on blanks.

cal quartzites". Still, lutites with cortical areas (one with cortex covering between 33% and 66% of the surface and six with cortex covering more than 66% of the surface) were also identified. There was also one radiolarite with cortex covering more than 66% of the surface. Focusing on "archaeological quartzites", there are clear differences between petrogenetic types, as supported by Chi-square test (χ^2 (18, N = 1852) = 171.59, p < .001). In general, the presence of cortex is more frequent in the quartzarenite group than in others. However, it is also important in the blanks from the RQ petrogenetic type (Table-9.12). Regarding the extent of cortex, pieces with more than 66% of the surface covered by cortex are, again, more frequent in the quartzarenite group than in other groups of quartzites. Nevertheless, this feature can also be found in the MQ and the OO petrogenetic types. Lithics with between 33% and 66% of the dorsal surface covered by cortex are common in the quartzarenite group too; as well as in the OO petrogenetic type, which has the highest standardised residue. Finally, the presence of cortical areas covering less than 33% of the dorsal surfaces is frequent in the SO, BQ, and RQ petrogenetic types, and scarcer in the quartzarenite group. The importance of this category in the OO type is very small.

Presence of cortex on dorsal surfaces

	Absence		X < 33%		33<X>66		X > 66%	
	∑	res	∑	res	∑	res	∑	res
CC	13	-2,9	5	0,2	3	1,6	15	11,1
CA	60	-0,7	11	0,2	4	0,7	7	2,0
OO	413	0,6	43	-2,6	25	1,9	22	0,3
SO	554	0,3	96	1,0	17	-1,3	19	-1,7
BQ	312	0,2	54	0,7	12	-0,3	8	-2,0
RQ	61	-0,8	18	2,2	2	-0,5	4	0,3
MQ	65	0,8	8	-0,5	0	-1,6	1	-1,2
Total	1478	80	235	13	63	3	76	4

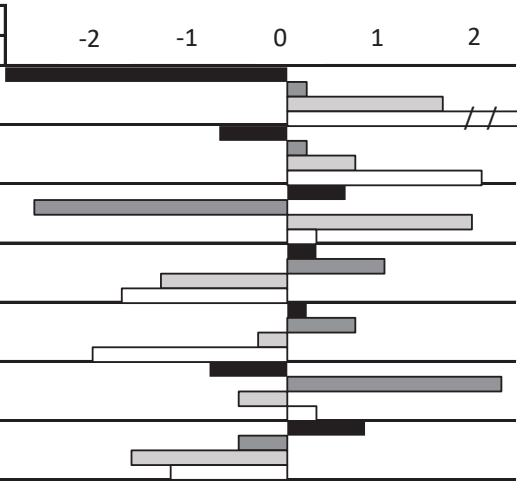

Table-9.12: Frequency table and standardised residues of χ2 test of the quantification of the presence of cortex on dorsal surfaces grouped by petrogenetic types. The last row shows totals, and the second column for each category is its percentage in relation to the total of items analysed.

Among the items which preserved any cortical area (392), it was possible to characterise 341 of them. Among the six lutites with cortex, four of them were defined as coming from rivers and another one from conglomerates. The remaining one could not be defined. The only blank on radioralite with cortex is of fluvial origin. Focusing on "archaeological quartzites", the features that define cortex from fluvial sources (167) and from conglomerates (168) are similarly distributed. There are another 50 pieces with cortical surfaces which do not have enough features to define them. Clear differences between petrogenetic types were pointed out by chi-square test (χ^2 (12, N = 374) = 84.975, p < .001) (Table-9.13). Cortex from rivers are more frequent among quartzarenites and in the OO type, while cortex from conglomerate are more common in the SO, BQ and RQ types. The MQ type is no clearly associated with any type of cortex, probably due to its scarcity.

	Type of cortex					
	Unknown		Fluvial		Conglom.	
	∑	res	∑	res	∑	res
CC	1	-1,1	22	3,8	0	-3,2
CA	1	-1,0	20	3,4	1	-2,8
OO	7	-1,2	50	1,7	33	-1,1
SO	20	1,0	48	-1,3	64	0,7
BQ	13	1,4	14	-3,2	47	2,5
RQ	0	-1,7	7	-1,1	17	1,9
MQ	3	1,8	2	-1,0	4	0,0
Total	45	12	163	44	166	44

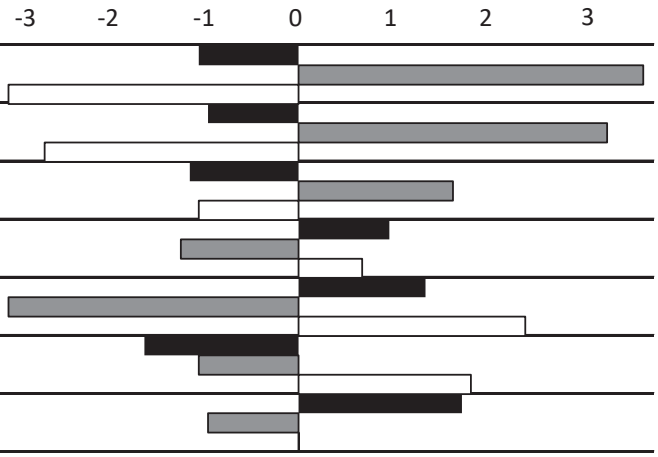

Table-9.13: Frequency table and standardised residues of χ^2 test of the type of cortex on dorsal surfaces grouped by petrogenetic types. The last row shows totals, and the second column for each category is its percentage in relation to the total of items analysed.

Core preparation/rejuvenation products are the less frequent knapping product, represented by just ten pieces. Most of them are incomplete, all of them as undetermined fragments (6). The others four are completes. “Archaeological quartzites” is the only represented raw material identified for core preparation/rejuvenation products. Among them BQ is the most frequent type, followed by SO, OO and RQ types (Table-9.10). These data are in concordance with the distribution of cores between petrogenetic groups, with the exception of the RQ type. Three core preparation/rejuvenation products have cortical areas, all of them covering less than 33% of the surface and coming from conglomerates. Two of them belong to the BQ petrogenetic type and another one to SO one.

9.3.3. CHUNK

Chunks, represented by 355 pieces, is the second most important type of technological product in this collection. The integrity of the pieces is not analysable due to the absence of diagnostic features.

The raw materials present in this category are “archaeological quartzite”, flint, limestone, lutite and (Table-9.7). Regarding the relative weight of chunks in each raw material, these are clearly overrepresented in limestone, making 95% of the pieces. Chunks form an important portion of lutite, quartz and, less importantly, flint. Chunks in “archaeological quartzites” are present in a percentage similar to that of this technological product in the whole assemblage. Focusing on specific petrogenetic types, chunks are more frequent in the quartzarenite group than in other types and their number gradually decreases as deformation and metamorphic processes increase.

One hundred and ten chunks have cortex. Among them 96 are “archaeological quartzites” and the remaining 14 limestones (7 items), lutites (6 items) and quartz (1 item). The extent of cortex in “archaeological quartzites” is heterogeneous. They can be classified in two groups: on one hand, chunks formed by orthoquartzites and quartzites with cortex covering between 1% and 66% of the surface and, on the other, chunks made of quartzarenites with cortex covering more than 66% of the surface. In the other raw materials cortical areas cover more than 66 % of the surface of the stones in every case. (Note that some of them are clasts completely covered by cortex.) All cortical areas of chunks are of fluvial origin.

9.4. RETOUCH: MODAL AND MORPHOLOGICAL STRUCTURES

Here we present the results of retouched artefacts and its relationship with the data previously exposed. According to the methodology defined above, there are 414 pieces retouched, 17.7% of the assemblage. Thirty-four lithics have different primary types (1.4%) and five at least three (0.2%).

The number of primary types individualised is 458. Starting from orders (mode of retouch), we do not find evidence of Plain (P) or Burin (B) modes of retouch. Splinter (E) mode is the most frequent one (245 items), followed by Simple (S) and Abrupt (A) modes (207 and seven retouches respectively) (Figure-9.13). Going down from order to typological group (or morphothema), we start with Splinter mode, the most frequent one. No morphological groups are distinguished within this order. Within the Simple mode the most frequent typological group is that of Sidescrapers (R) (172 items), followed by Point (P) (13 items), Denticulate (D) (twelve) and Endscraper (G) (ten). In the Abrupt mode, the least frequent one, there are two groups: unspecific Abrupt (A) (five items) and Truncation (one).

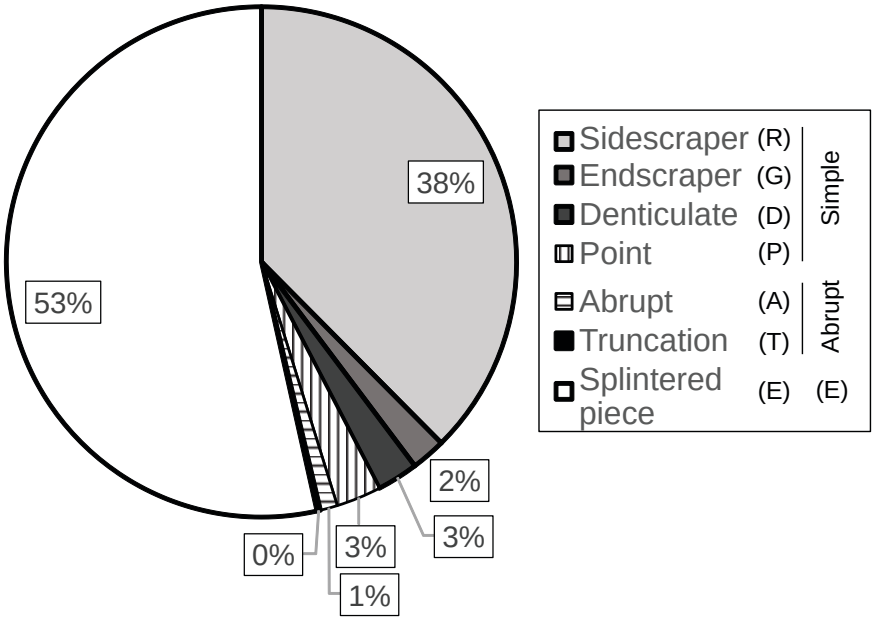

Figure-9.13: Pie chart showing the percentage of modes of retouch and morphological groups of the retouched material from layer-XIII of El Esquilleu.

After having understood the general characterisation of the retouch using the modes and morphological groups, now we will deepen into the analysis of the pieces with multiple primary types (Table-9.14). Starting from the blanks with two primary types, there are multiple associations. The most frequent association of primary types in one blank is Sidescraper and Sidescraper, represented in 16 blanks. The association Sidescraper and Splinter, in seven blanks, is also well represented. Other association of two primary types in one blank are: Sidescraper and Denticulate (in two blanks), Sidescraper and unspecific Abrupt (in one blank), Endscraper and Endscraper (in two blanks), Endscraper and Denticulate (in two blanks), Denticulate and Denticulate (in one blank), and Splinter and Splinter (in three blanks). The analysis of the blanks with three different primary types brings out the following combinations of morphothema: Sidescraper, Sidescraper, and Sidescraper (in one blank) and Sidescraper, Sidescraper, and Endscraper (in four different blanks).

		Simple				Abrupt		Splinter
Order	Group	Sidescraper	Endscraper	Denticulate	Point	Abrupt	Truncation	Splintered piece
Simple	Sidescraper	16		2		1		7
	Endscraper		2	2				
	Denticulate			1				
	Point							
Abrupt	Abrupt							
	Truncation							
Splinter	Splintered piece							3
Total	Total							34

Table-9.14: Frequency table including mode of retouch and morphological groups of pieces with two primary types.

Next, we will analyse the relationships between retouched artefacts and the technological structure. There is a statistically significant association between the presence of retouch and technological blanks they are configured (χ^2 (2, N = 2419) = 68.026, p < 0.001). Twenty percent of knapping products are retouched, while only 8% of cores and 2% of chunks are. In addition, every pieces with multiple primary types are made on knapping products (all of them on blanks). Focusing on knapping products, the most frequently retouched technological group are blanks (401 pieces), followed by core preparation/rejuvenation products (three pieces). Among the latter, two are configured as Sidescrapers and the other one as a Splintered morphothema. The representation of mode of retouch and typological group among knapping products follows similar patterns to those observed for the complete collection, due to the great weight of this technological group in the assemblage. That is, a great quantity of Splinter and Simple modes and a smaller presence of Abrupt mode. Coming to the type of cores retouched, one is an irregular core and the other is a core on flake. The morphothema configured on both cores is the Sidescraper one.

	Non-retouched		**Retouched**	
	Σ	Std. Res	Σ	**Std. Res**
CC	89	1,6	3	-3,4
CA	105	1,3	8	-2,8
OO	490	1,1	80	-2,4
SO	600	-0,6	153	1,3
BQ	319	-1,8	112	3,7
RQ	68	-0,8	24	1,7
MQ	65	0,5	10	-1

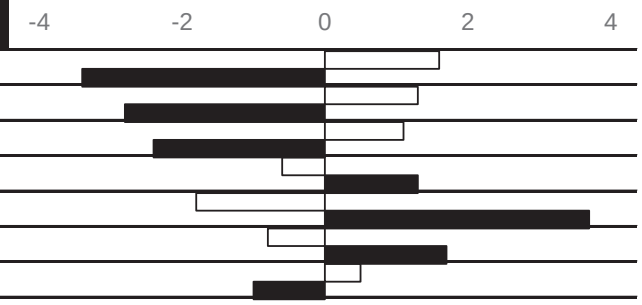

Table-9.15: Frequency table and standardised residues of χ^2 test of retouched and non-retouched "archaeological quartzites" grouped by petrogenetic types.

Finally, we will analyse the relationships between the retouched artefacts and the raw material of the blanks they are configured. The quantity of retouched artefacts is differently distributed depending on the raw material of the blanks, as demonstrated by Chi-square test (χ^2 (5, N = 2419) = 12.351, p = 0.03). Quartz is the raw material with the greatest percentage of retouched artefacts (42%), followed by flint (20%), "archaeological quartzite" (17%), and lutite (2%). Radioralites and limestones blanks are not retouched. All blanks with multiple primary types are made on "archaeological quartzite" (38 pieces) and lutite (one piece). There are also statistically significant differences in the distribution of retouch between the types of "archaeological quartzite", as proven by Chi-square test (χ^2 (6, N = 2126) = 54.915, p < 0.001). Table-9.15 shows that retouched pieces are positively associated with SO, BQ and RQ petrogenetic types. Meanwhile, retouched artefacts are less frequent in the CC, CA, OO, and MQ types, mentioned in descending order of importance. The petrogenetic type with higher presence of artefacts with multiple primary types are BQ SO, OO, RQ, and MQ types.

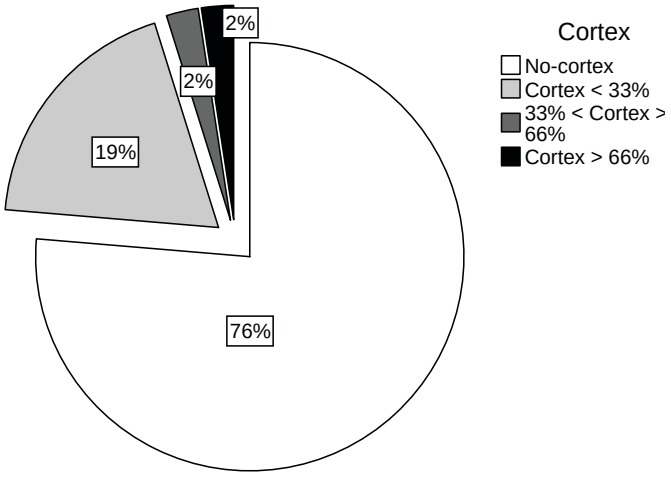

Figure-9.14: Pie chart showing percentage of absence, presence and extension of cortex on retouched material from layer-XIII of El Esquilleu.

There is no clear association between the morphological group of retouch and raw material. Nevertheless, there are tendencies that could explain differences between the types of quartzite and their relationship with the order and mode of retouch (Table-9.16). The first remarkable tendency arises from the observation of the categories which represent more than 10% of the assemblage. It is clearly observable the association between OO, SO, and BQ petrogenetic types and the group of Sidescrapers (R). In addition, Splinter (E) morphothema is also highly represented in SO and BQ types and, less importantly, OO, RQ, and MQ types too. Finally, it is interesting to note that most Endscrapers (G), Denticulates (D), Points (P), and unspecific Abrupt (A) morphothemas are made on orthoquartzites

and quartzites. Finally, most of the Points are made on BQ petrogenetic type.

Finally, we analyse the relation between retouched blanks and the cortical areas. Figure-9.14 shows the preservation of cortex on retouched artefacts. Nineteen per cent of the retouched material has cortex covering less than 33% of the surface. Only 4% of the retouched pieces have cortex covering more than 33% of the surface. The blanks with cortex preserved and multiple primary types are also important in the collection, although in smaller proportions than the artefacts with one primary type. Thirty-two per cent of the pieces with two primary types and 20% of the blanks with three primary types have cortex. Regarding the characterisation of cortical areas, most of them derived from conglomerates (50%), while the presence of cortex from fluvial sources is smaller (38%). We are unable to identify the type of cortex for 12% of the pieces with cortex.

	Simple				Abrupt		Splinter	
Order	Sidescraper	Endscraper	Denticulate	Point	Abrupt	Truncation	Splintered piece	Total
CC		1					2	3
CA	5						4	9
OO	**39**	3	2	3	1		44	92
SO	**55**	1		2	1		**106**	165
BQ	**53**	3	2	6	3	1	**58**	126
RQ	8		2	1			14	25
MQ	5						6	11
Total	165	7	6	12	5	1	234	431

Table-9.16: Frequency table of order and group of retouches grouped by petrogenetic type. In the cases of pieces with multiple retouches, each retouch is quantified individually. Cells in black are the categories representing more than 10% of the total cases. Cells in dark grey are the categories representing between 5 and 10% of cases. Cells in light grey are the categories representing between 1 and 5% of cases.

9.5. TIPOMETRICAL STRUCTURE

In this section we will describe the results of the analysis of the tipometrical structure and its relationship with the structures studied previously. We made the measurements using the technological axis (length, width and thickness) on 1,793 lithic pieces (74.9% of the assemblage). The remaining 601 pieces were measured using the longest axis (X, Y and Z), due to the absence of features signalling the technological axis[1]. All chunks, most of the cores (some cores on flakes were measured using the technological axis) and some incomplete knapping products were measured using the latter criterion.

An overview of length, width and thickness reveals that all three measurements have positive skewness and kurtosis, the highest values being those of thickness, followed by width (Figure-9.15). The mean length is 19.86 mm, the mean width 18.58 mm and the mean thickness 5.75 mm. The measurements of the first two axes are similar between them. A general outlook of X, Y, and Z axes does also point at positive skewness and kurtosis. Nevertheless, all the means are clearly different between them: the mean of the X axis is 20.29 mm, the mean of the Y axis is 13.27 mm and the mean of the Z axis is 4.73 (Figure-9.16). The relationship between the three measurements according to the Tarriño indexes (Tarriño, 2015) reveals different morphologies depending on the measurement method employed (Figure-9.17). All lithics measured based on the X/Y/Z axes are between 0.5 and 0.9 of RBEI and between 0 and 0.5 of RFL. Instead, most of the pieces measured in relation to the technological axis are between 0.5 and 0.7 RBEI and between 0.1 and 0.5 of RFL, meaning similar measurement between the three axes and relatively cubic-bladed shapes. Regarding the material measured using L/W/T axes, the resulting forms are similar, but they also include an important presence of tabular elements.

The last measurement used here is the weight of each lithic implement. The minimum weight recorded is 0.02 g and the maximum 113.17 g. The mean is 3.73 g. Weight presents high positive kurtosis (46.18) and positive skewness (5.59) as a consequence of the high percentage of lithic implements smaller than 5 g. The total of pieces weighted in this layer is 2,394 and the total weight of all of them is 8,935 g.

1 Fifty pieces from this layer were not measured due to error during data acquisition.

None of the aforementioned measurements is normally distributed[2].

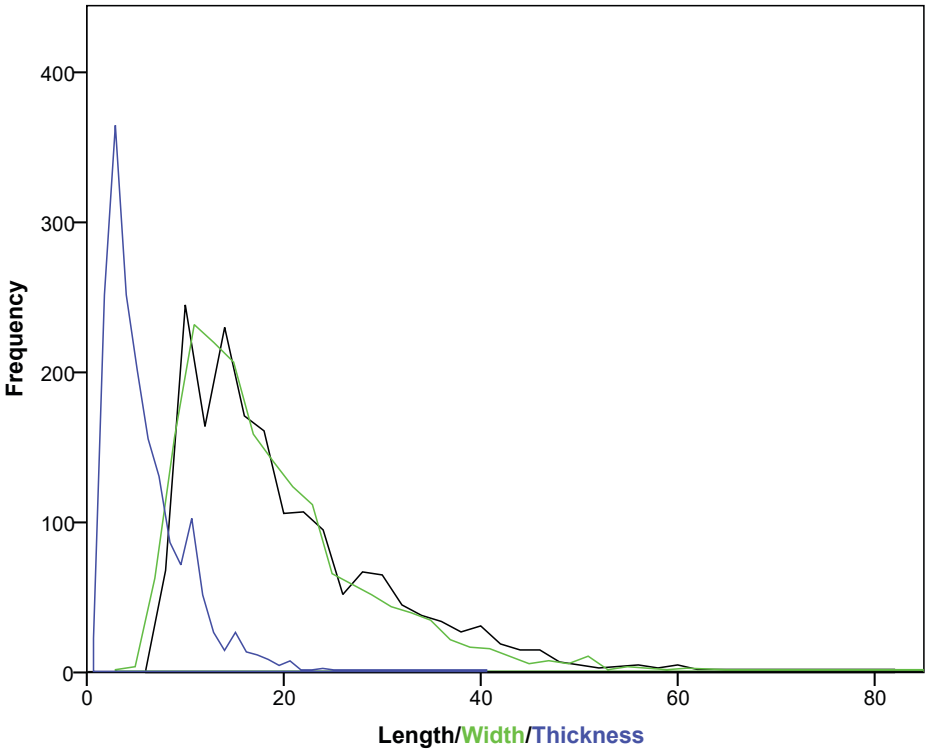

Figure-9.15: Frequency area chart showing the distribution of length, width and thickness of lithic remains from layer-XIII of El Esquilleu measured in relation to technological axis. Black line represents length, green line represents width, and blue line represents thickness. Horizontal axis measurement are in millimetres.

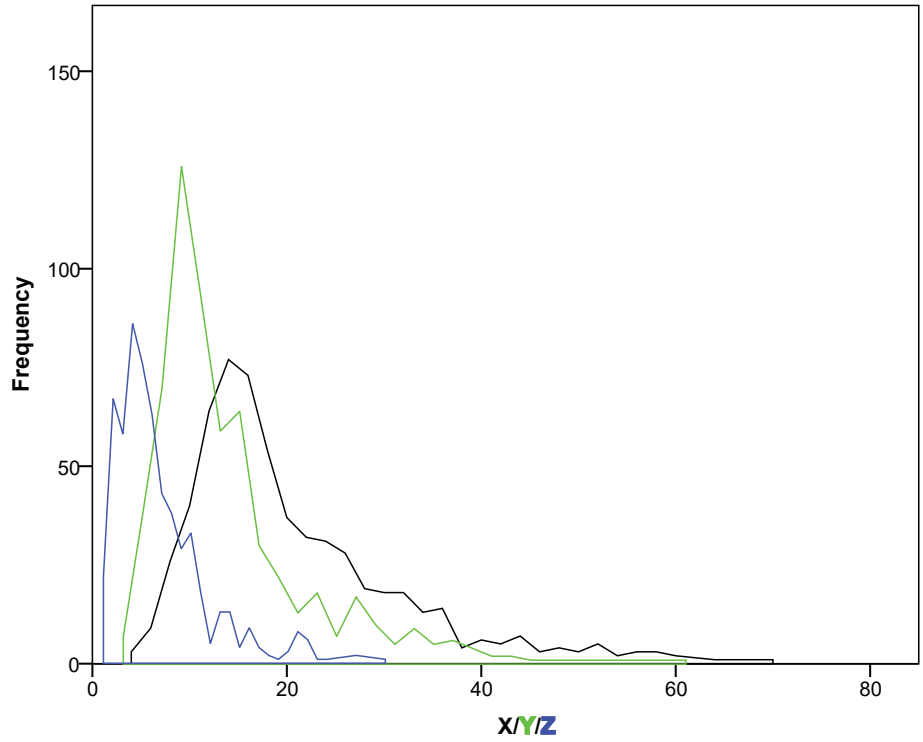

Figure-9.16: Frequency area chart showing the distribution of X, Y and Z axes of lithic remains from layer-XIII of El Esquilleu. Black line represents the X axis, green line represents the Y axis, and blue line represents the Z axis. Horizontal axis measurement are in millimetres.

2 *KS* = 0.147; *df* = 1793; *p* < 0.01 for length
KS = 0.132; *df* = 1793; *p* < 0.01 for width
KS = 0.180; *df* = 1793; *p* < 0.01 for thickness
KS = 0.152; *df* = 601; *p* < 0.01 for X-axis
KS = 0.178; *df* = 601; p < 0.01 for Y-axis
KS = 0.172; *df* = 601; p < 0.01 for Z-axis
KS = 0.324; *df* = 2394; *p* < 0.01 for weight

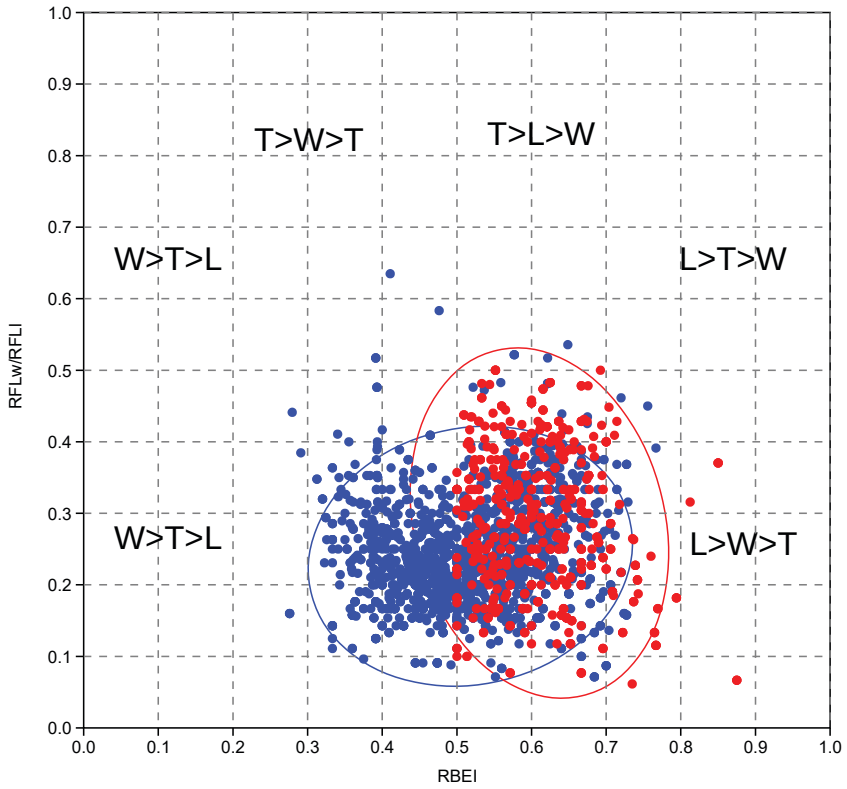

Figure-9.17: Scatter plot of RFLw or RFLI and RBEI indexes. Blue points and ellipse are the measurements made in relation to technological axis. Red points and ellipse are the measurements made in relation to X/Y/Z axis. Ellipses enclose 95% of cases of each category.

Once the general metric characteristics have been understood, we will relate this data with the technological structure. The three technological orders proposed show differences in shape between them. Figure-9.18 shows three different but overlapping groups using 95% confidence ellipses. The ellipse of cores is the smallest one and it is situated in the central and upper part of the chart, showing positive elongation. The ellipse of knapping products is located on the lower area and it presents horizontal elongation. Finally, the ellipse of chunks is positioned in the central area, displaying negative elongation. The distribution of weight of each order does also show clear differences in variance, as demonstrated by *H* Kruskal-Wallis test: $H\ \chi^2$ (2, N = 2,394) = 50.393, $p < 0.001$ (Figure-9.19). In general cores are bigger than other orders, with weights around 28 g for each piece (Table-9.17). Knapping products and chunks have similar grams/piece ratios, significantly smaller in comparison with cores.

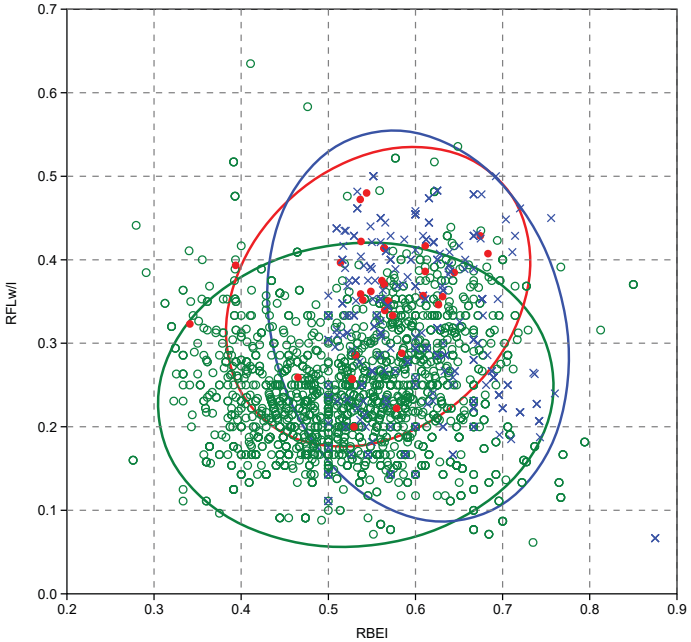

Coming to cores, there are no differences in morphology between the types proposed, as displayed in Figure-9.20 through the relationship between RBEI and RFL. Weight is similarly distributed within each category, as indicated by the analysis of variance based on H Kruskal-Wallis test: H χ2 (4, N = 33) = 4.789, p = 0.310). Regarding the average weight of each category of cores, irregular and pyramidal ones are above the average of all the cores considered. Meanwhile, discoid cores, cores on flake and prismatic cores are under this average value (Table-9.18).

Figure-9.18: Scatter plot of RFLw or RFLI and RBEI indexes. Green circles and ellipse are knapping products. Red points and ellipse are cores. Blue crosses and ellipse are chunks. Ellipses enclose 95% of cases of each category.

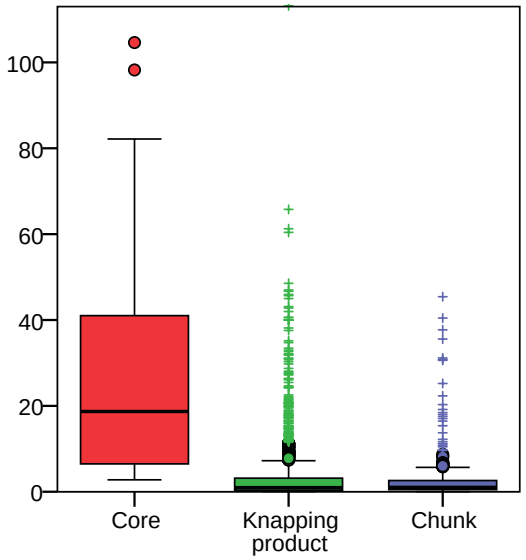

Figure-9.19: Boxplot showing differences in weight between various technological orders. The weight is expressed in grams.

The knapping products exhibit clear differences in the form of lithic remains, as shown in Figure-9.21a. The areas defined by the 95% confidence ellipses are very different for blanks and core preparation/rejuvenation products. The former is arranged in a circle between $0.05 \leq RFL \geq 0.65$ and $0.3 \leq RBEI \geq 0.7$. The latter forms an elongated form overlapped to the upper half of the blank ellipse between the $0.2 \leq RFL \geq 0.45$ and $0.3 \leq RBEI \geq 0.65$, covering the regions of cubic, tabular and prismatic shapes. In the first ellipse the presence of blade forms is also important. In addition, a great number of blank points stick out of these ellipses, probably due to the different number of implements in each category. Weight distribution does also differ from one category to another, as it can be observed in Figure-9.21b. Moreover, *U* Mann-Whitney test reveals differences in the distribution and the median between blanks (M = 0.96 g) and core preparation/rejuvenation products (M = 12.63), $U = 17{,}661.5$, $p < 0.001$. The gram per piece ratio points at clear differences in the mean weight of the items from each group: blanks weight 3.5 g on average, while core preparation/rejuvenation products weight 13.1 g on average (Table-9.19).

Technological order	Weight		∑ of pieces		Ratio
	∑	%	∑	%	Grams/Piece
Core	929,3	7,60	33	0,01	28,2
Knapping product	6943,5	79,70	2017	0,85	3,4
Chunk	1063,2	12,80	344	0,15	3,1

Table-9.17: Frequencies and weight of main technological orders. The ratio grams/piece is reported. Weight is expressed in grams.

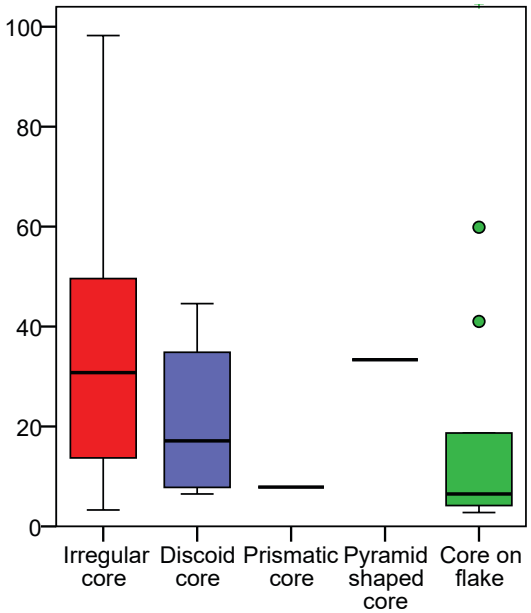

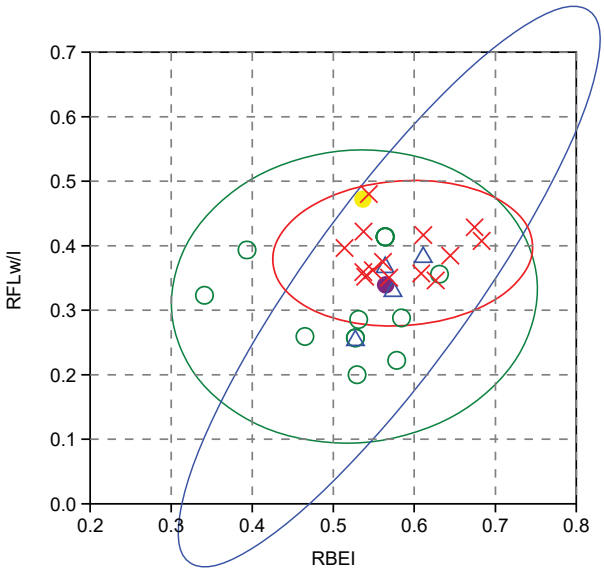

Figure-9.20: Double chart showing: a) Scatter plot of RFLw or RFLl and RBEI indexes. Green circles and ellipse are cores on flakes. Red crosses and ellipse are irregular cores. Blue triangles and ellipse are discoidal cores. The yellow point is a prismatic core and the purple point is a pyramid shape core. Ellipses enclose 95% of cases of each category. b) Boxplot showing differences in weight between types of cores. The weight is expressed in grams.

Core groups	Weight		∑ of pieces		Ratio
	∑	%	∑	%	Grams/Piece
Irregular core	517,0	55,6	14	42,42	36,9
Discoid core	85,3	9,2	4	12,12	21,3
Levallois core					
Prismatic core	7,9	0,8	1	3,03	7,9
Pyramid shaped core	33,4	3,6	1	3,03	33,4
Core on flake	285,7	30,7	13	39,39	22,0

Table-9.18: Frequencies and weight of different groups of cores. The ratio grams/piece is reported. Weight is expressed in grams.

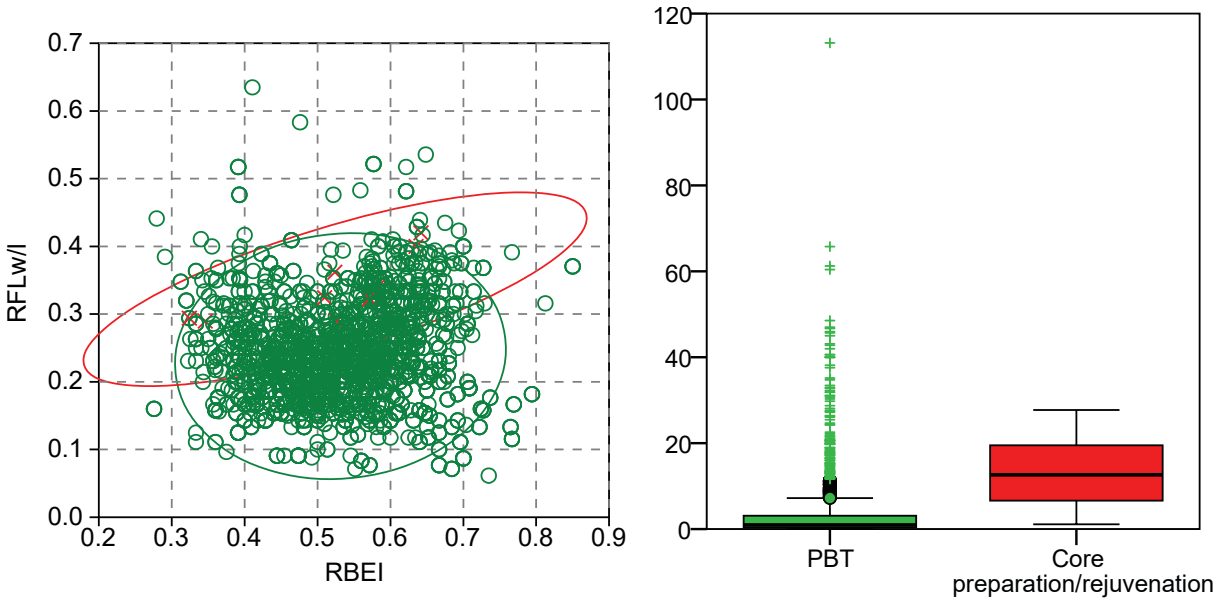

Figure-9.21: Double chart showing: a) Scatter plot of RFLw or RFLl and RBEI indexes. Green circles and ellipse are blanks. Red crosses and ellipse are core preparation/rejuvenation products. Ellipses enclose 95% of cases of each category. b) Boxplot showing differences in weight between blanks and core preparation/rejuvenation products. The weight is expressed in grams.

Knapping product group	Weight		∑ of pieces		Ratio
	∑	%	∑	%	Grams/Piece
Blank	12079	99,3	346	98,0	34,9
Core prep./rejuv.	88,6	0,7	7	2,0	12,7

Table-9.19: Frequencies and weight of different groups of knapping products. The ratio grams/piece is reported. Weight is expressed in grams.

Focusing on, there are no clear differences in their formats based on the number of negative scars on their dorsal surfaces (Figure-9.22a). All four categories are similarly distributed, represented by relatively rounded circles in the region between $0.05 \leq RFL \geq 0.45$ and $0.3 \leq RBEI \geq 0.75$. However, there are clear differences in weight based on the number of negative scars observable, as shown in Figure-9.22b statistically demonstrated by *H* Kruskal-Wallis test: $H\ \chi^2\ (3, N = 2{,}013) = 312.376$, $p < 0.001$. The pieces without negative scars and those with three or more negative scars are heavier than the blanks with one and two negative scars. The comparison of the grams per piece ratio of each category confirms this idea (Table-9.20).

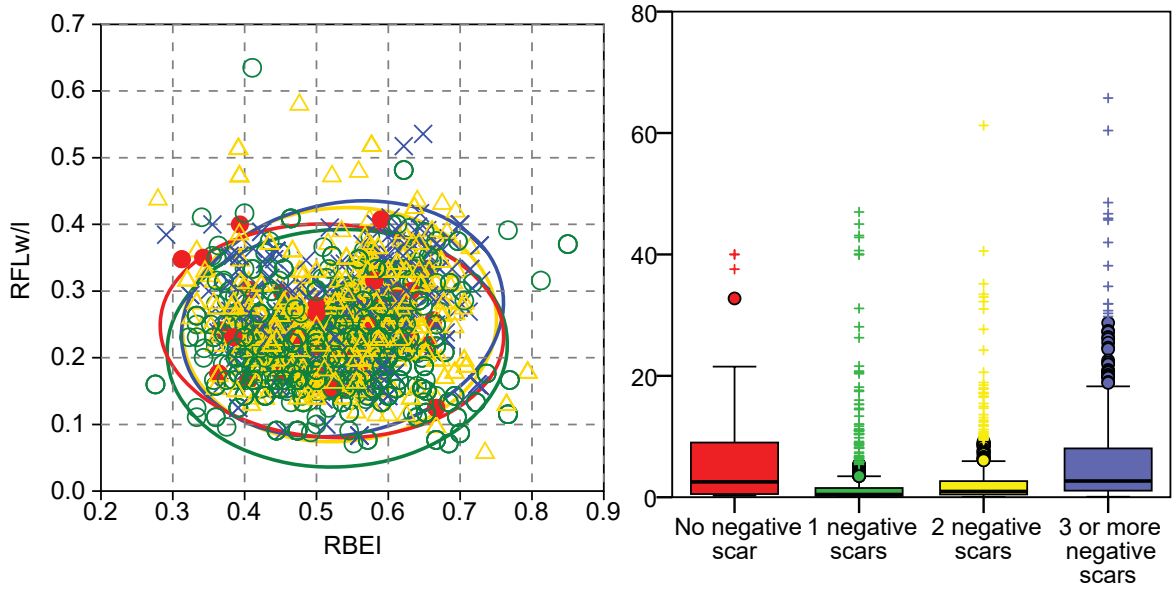

Figure-9.22: Double chart showing: a) Scatter plot of RFLw or RFLl and RBEI indexes. Red points and ellipse are blanks without negative scar. Green circles and ellipse are blanks with one negative scar. Yellow triangles and ellipse are blanks with two negative scars. Blue crosses are blanks with three or more negative scars. Ellipses enclose 95% of cases of each category. b) Boxplot showing differences in weight between blanks with different number of negative scars on dorsal surface. There is an outlier outside the chart (113.17 g) in the category of blanks with two negative scars. The weight is expressed in grams.

Number of negative scars	Weight		∑ of pieces		Ratio
	∑	%	∑	%	Grams/Piece
No-negative scars	500,0	7,2	69	3,4	7,2
One negative scar	1618,4	23,2	759	37,7	2,1
Two negative scars	2229,7	31,9	773	38,4	2,9
Three or more negative scars	2639,3	37,8	412	20,5	6,4

Table-9.20: Frequencies and weight of blanks grouped by number of negative scars. The ratio grams/piece is reported. Weight is expressed in grams.

Regarding the integrity of the blanks, there are differences based on the form of the pieces (Figure-9.23a). The ellipse of complete pieces is rounded and it is situated between 0.05 ≤ RFL ≥ 0.4 and 0.3 ≤ RBEI ≥ 0.7 (mainly tabular, cubic and bladed formats). Proximal fragments, forming a rounded ellipse too between 0.05 ≤ RFL ≥ 0.45 and 0.2 ≤ RBEI ≥ 0.6, are more closely related with tabular and cubic forms. Instead, medial and distal fragments create more elongated ellipses (in the RBEI axis). This is probably due to the smaller presence of tabular and cubic forms, as a consequence of the use of X/Y/Z axes rather than L/W/T axes for the measurement these elements, which generally lack the features to determine the technological axis. Meanwhile, longitudinal fragments make a relatively rounded ellipse between 0.05 ≤ RFL ≥ 0.45 and 0.4 ≤ RBEI ≥ 0.85, the region where more elongated shapes are present. Finally, indeterminate fragments outline a circular ellipse located in the RBEI values higher than 0.5 and RFL values below 0.5. This is because of the use of X/Y/Z axes for the measurement of every fragment and the relative homogeneity of the three measurements. Comparing the distribution of weight between the various types of blanks, *H* Kruskal-Wallis test indicates there are statistically significant differences between them: $H\ \chi^2$ (5, N = 2,013) = 56.698, p < 0.001. In Figure-9.23b it is possible to observe that complete lithic pieces and longitudinal fragments have similar weights. At the same time, they are clearly different from other types of lithic fragments. The grams/piece ratio leads to the same conclusions: The smallest lithic fragments are medial ones, followed by proximal, distal and undetermined fragments. Complete blanks and longitudinal fragments present similar grams/piece ratios, distinctly greater than those of the rest of the categories (Table-9.21).

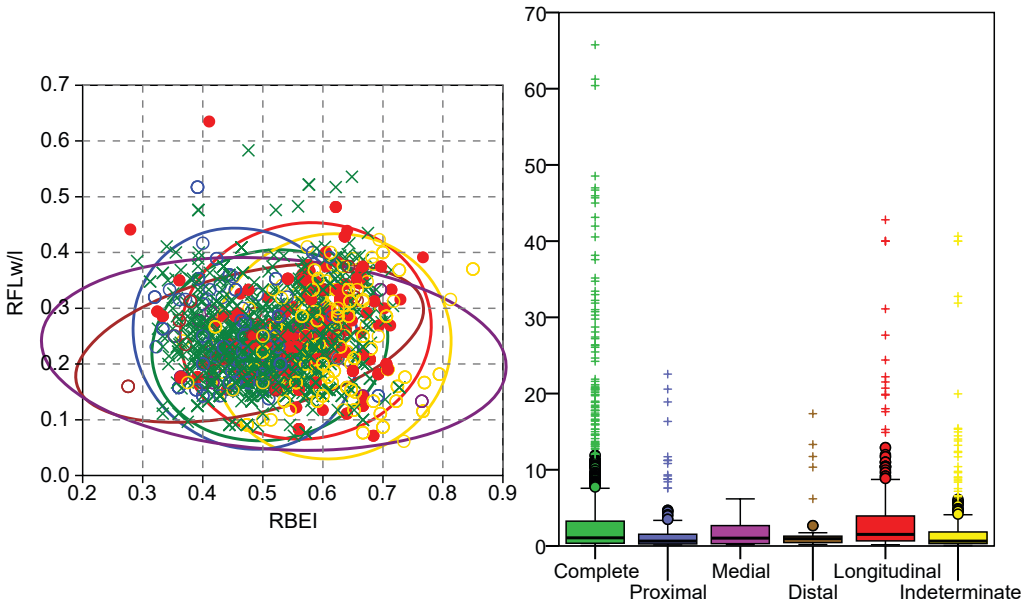

Figure-9.23: Double chart showing: a) Scatter plot of RFLw or RFLl and RBEI indexes. Green crosses and ellipse are complete blanks. Blue circles and ellipse are proximal blank fragments. Purple circles and ellipse are medial blank fragments. Brown circles and ellipse are distal blank fragments. Red points and ellipse are longitudinal blank fragments. Yellow circles and ellipse are undetermined blank fragments. Ellipses enclose 95% of cases of each category. b) Boxplot showing differences in weight between blanks preserved in diverse states of integrity. There is an outlier outside the chart (113.17 g) in the category of complete blanks. The weight is expressed in grams.

Integrity of blanks	Weight		∑ of pieces		Ratio
	∑	%	∑	%	Grams/Piece
Complete	4628,2	66,2	1203	59,8	3,8
Proximal fragment	340,3	4,9	162	8,0	2,1
Medial fragment	39,2	0,6	24	1,2	1,6
Distal fragment	92,4	1,3	41	2,0	2,3
Longitudinal fragment	1160,8	16,6	294	14,6	3,9
Undetermined fragm	726,6	10,4	289	14,4	2,5

Table-9.21: Frequencies and weight of blanks grouped by integrity. The ratio grams/piece is reported. Weight is expressed in grams.

The classification of complete blanks (Figure-9.24a) reveals the major predominance of flakes (86% of complete blanks), followed by a moderate presence of elongated flakes (10% of complete blanks) and really occasional find of blades (4% of complete blanks). There is no difference in weight between these three categories, which show similar distributions, as depicted in Figure-9.24b and proven by *H* Kruskal-Wallis: $H\ \chi^2$ (2, N = 2,157) = 2.513, p = 0.285. The comparison of gram/piece ratios between the three types of blanks proposed reveals differences in mean weight (Table-9.22). The grams/piece ratio of flakes (most frequent category) is similar to the ratio of all blanks, while the ratios of elongated flakes and blades are higher.

Complete blank characterisation	Weight		∑ of pieces		Ratio
	∑	%	∑	%	Grams/Piece
Flake	3653,5	80,2	1000	86,4	3,7
Elongated flake	725,4	15,9	116	10,0	6,3
Blade	177,2	3,9	41	3,5	4,3

Table-9.22: Frequencies and weight of different types of complete blanks (flakes, elongated flakes, blades). The ratio grams/piece is reported. Weight is expressed in grams.

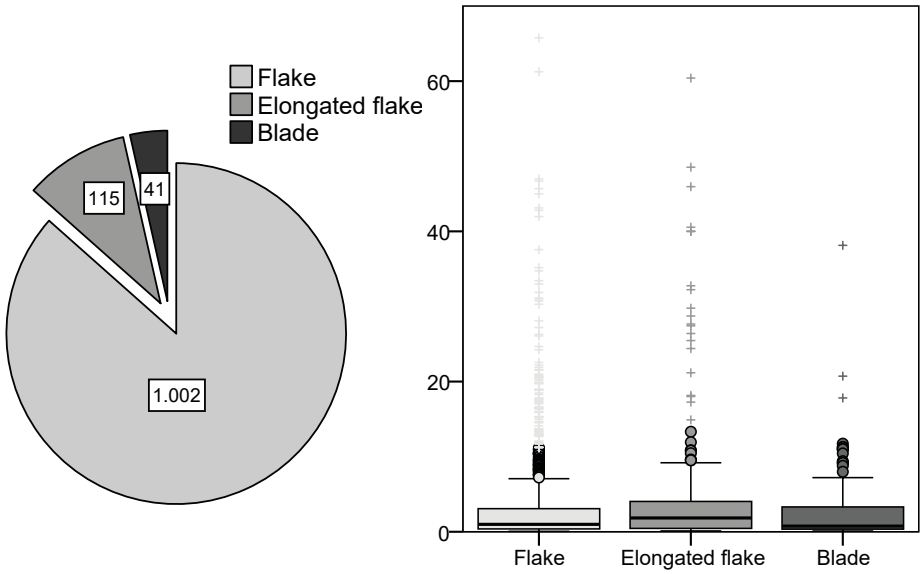

Figure-9.24: Double chart showing a) pie chart showing the distribution of complete blank products, and b) boxplot showing differences in weight between metrical categories. There is an outlier outside the chart (113.17 g) in the category of flakes. The weight is expressed in grams.

Next, we will liken the (typo)metrical structure with retouched material. There are clear weight differences based on the presence (M = 2.03) or absence (M = 0.91) of retouch in the pieces, as corroborated by *U* Mann-Whitney test: $U = 523{,}371$, $p < 0.001$. In general, retouched artefacts are heavier than unretouched blanks (Figure-9.25b). The mean weight of non-retouched material is similar to the mean grams/piece ratio of the whole assemblage, while the grams/piece ratio of retouched artefacts is noticeably bigger (Table-9.23). There are no differences in forms between retouched and non-retouched lithics, as shown in figure25a. There are neither differences in the morphology of the artefacts depending on the quantity of primary types individualised in each blank (Figure-9.26a). Nevertheless, the weight changes significantly based on the quantity of primary types individualised. The difference is especially obvious when comparing single-retouched pieces and other two categories. H Kruskal-Wallis test supports this statement: $H\ \chi^2\ (2, N = 412) = 57.58$, $p < 0.001$. This can be explained by the main presence of single-retouched pieces with low weight (Figure-9.26b). The grams/piece ratio of each category does also reflect this difference (Table-9.24).

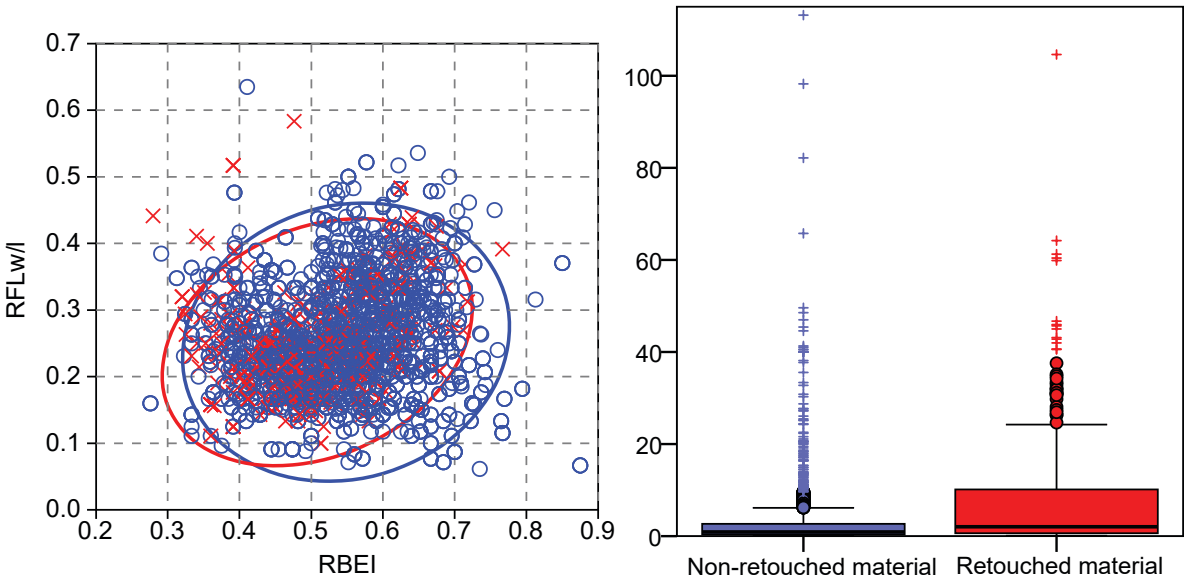

Figure-9.25: Double chart showing: a) Scatter plot of RFLw or RFLl and RBEI indexes. Red crosses and ellipse are retouched lithic material. Blue circles and ellipse are non-retouched lithic material. Ellipses enclose 95% of cases of each category. b) Boxplot showing differences in weight between retouched and non-retouched lithic material. The weight is expressed in grams.

Piece	Weight		∑ of pieces		Ratio
	∑	%	∑	%	Grams/Piece
Non-retouched	5812,4	65,0	1982	82,8	2,9
Retouched	3123,5	35,0	412	17,2	7,6

Table-9.23: Frequencies and weight of retouched and non-retouched pieces. The ratio grams/piece is reported. Weight is expressed in grams.

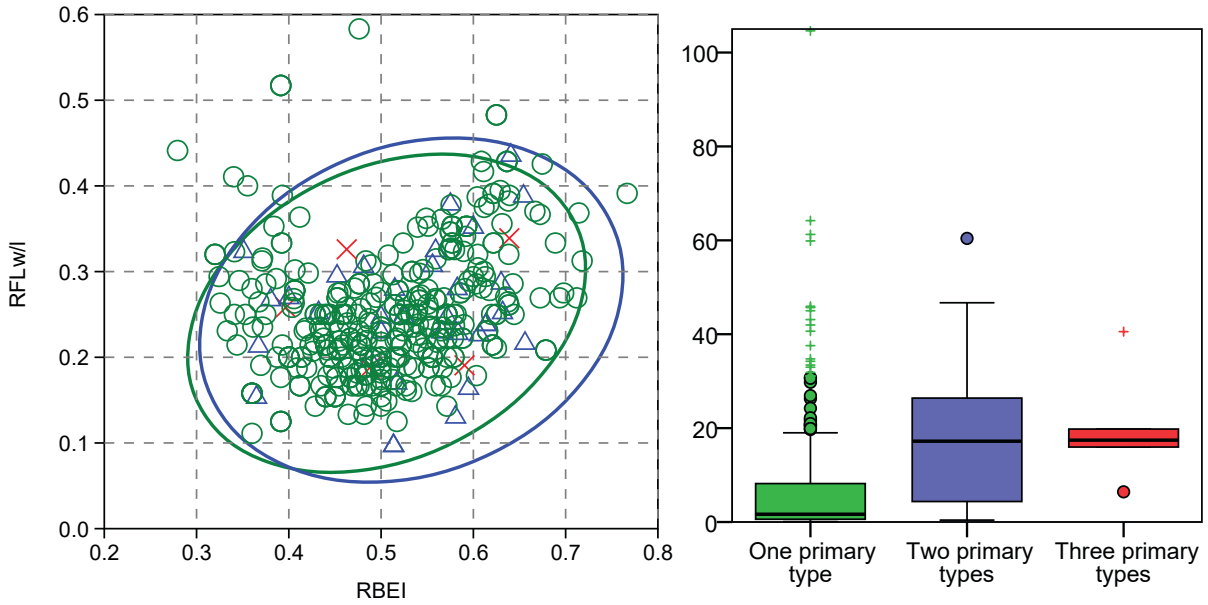

Figure-9.26: Double chart showing: a) Scatter plot of RFKw or RFLl and RBEI indexes. Green circles and ellipse are artefacts with one primary type. Blue triangles and ellipse are artefacts with two primary types. Red crosses and ellipse are artefacts with three primary types. Ellipses enclose 95% of cases of each category. b) Boxplot showing differences in weight between retouched artefacts by quantity of primary types. The weight is expressed in grams.

Blank with	Weight		∑ of pieces		Ratio
	∑	%	∑	%	Grams/Piece
One primary type	2431,8	77,9	373	90,5	6,5
Two primary types	591,5	18,9	34	8,2	17,4
Three primary types	100,2	3,2	5	1,2	20,0

Table-9.24: Frequencies and weight of the retouched pieces grouped by the quantity of primary types. The ratio grams/piece is reported. Weight is expressed in grams.

Then, we will confront metrical features of retouched artefacts with the features of retouch, categorised in orders (modal) and groups (morphological). Due to the methodology used to define retouch here, we only included in this analysis the pieces with one primary type on each blank. The comparison reveals clear in morphologies between the Simple and Splinter modes, as represented in Figure-9.27a. The Splinter (E) order differs evidently from the Simple (S) one. The ellipse of the former is round, and even though it is the most numerous order, it has the smallest ellipse. Most of the points are between $0.1 \leq RFL \geq 0.4$ and $0.3 \leq RBEI \geq 0.7$, in the region of thick and tabular forms. The ellipse of the Simple mode is more elongated. Although an important part of the measurements are located in the same area as the Splinter mode, the blanks configured with the Simple mode tend to have more elongated shapes. Weight is also different between the artefacts with different modes, as proven by *H* Kruskal-Wallis test: $H\ \chi^2\ (2, N = 373) = 185.081$, $p < 0.001$. This is especially obvious when comparing, on one hand, the Splinter mode and, on the other, Simple and Abrupt modes retouched blanks. Artefacts configured with the Splinter mode are lighter, as pointed out by the grams/piece ratio (Table-9.25). These differences in weight are also applicable when going down to morphological groups. This is because splintered pieces are all homogeneously light, while all the groups within Simple and Abrupt retouch modes are heavier.

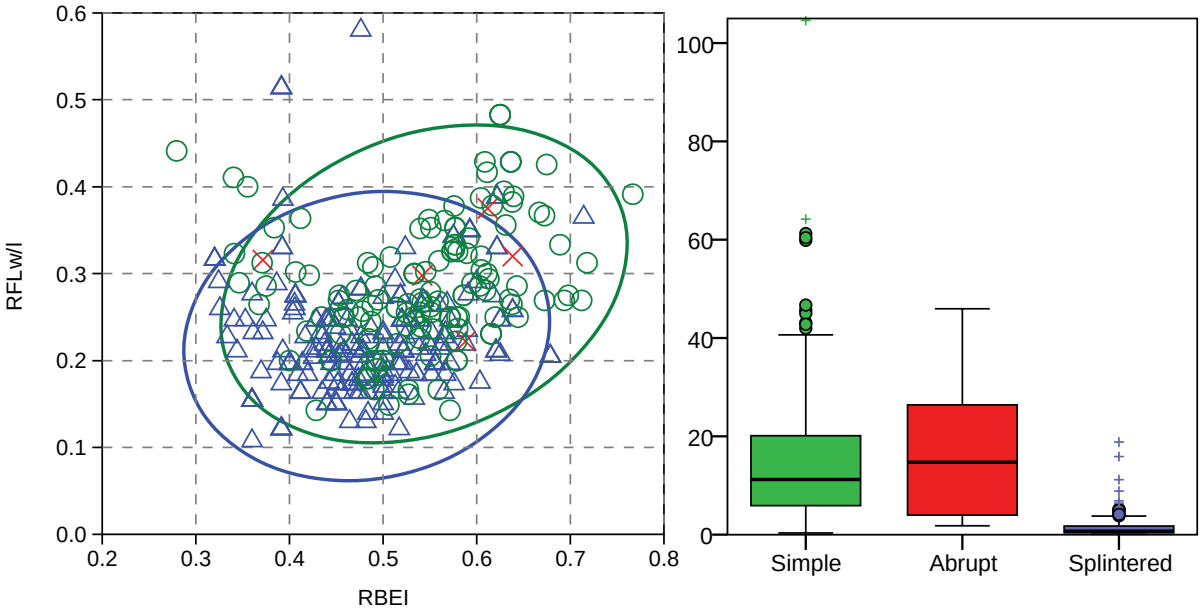

Figure-9.27: Double chart showing: a) Scatter plot of RFLw or RFLI and RBEI indexes. Green circles and ellipse are pieces retouched with the Simple mode of retouch. Red crosses and ellipse are pieces retouched with Abrupt mode of retouch. Blue triangles and ellipse are pieces retouched with a Splinter mode of retouch. Ellipses enclose 95% of cases of each category. b) Boxplot showing differences in weight between different modes of retouch. There is an outlier outside the chart (106.2 g) in category of abrupt retouch. The weight is expressed in grams.

Order of retouch	Weight		∑ of pieces		Ratio
	∑	%	∑	%	Grams/Piece
Simple	2064,0	66,1	138	29,4	15,0
Abrupt	62,3	20,0	4	6,4	15,6
Splinter	305,5	13,9	231	64,2	1,3

Table-9.25: Frequencies and weight of retouched artefacts with one primary type grouped by the order of retouch. The ratio grams/piece is reported. Weight is expressed in grams.

The last structure to be tackled here is the petrological one. There are differences in the morphology of the lithics depending on their raw material (Figure-9.28a). “Archaeological quartzites” are situated in the centre of the chart and are represented by a rounded ellipse which includes all forms. Flint is embodied by an ellipse similar in morphology and width to that of “archaeological quartzites” and covers approximately the same forms. The ellipse of lutites does not include elongated or tabular forms. The ellipses of radioralite and quartz are alike. In both raw materials shapes are not elongated but tabular. Last, the distribution of limestone attends to more elongated and thicker forms, far away from tabular morphologies. As to the distribution of weight, *H* Kruskal-Wallis test demonstrates there are statistically significative differences in the distribution of weight based on the type of raw material: $H\ \chi^2$ (5, N = 2,394) = 26.069, $p < 0.001$. The gram/piece ratio is the same for “archaeological quartzites” as for flint. The gram/piece ratio of other raw materials is smaller, the smallest one being that of limestone (Table-9.26).

Raw material	Weight		∑ of pieces		Ratio
	∑	%	∑	%	Grams/Piece
"Arch. quartzite"	8703,9	97,4	2302	96,2	3,8
Flint	127,9	1,4	34	1,4	3,8
Limestone	16,8	0,2	20	0,8	0,8
Limonite					
Lutite	56,7	0,6	26	1,1	2,2
Quartz	21,2	0,2	7	0,3	3,0
Radioralite	9,5	0,1	5	0,2	1,9

Table-9.26: Frequencies and weight of different types of raw material. The ratio grams/piece is reported. Weight is expressed in grams.

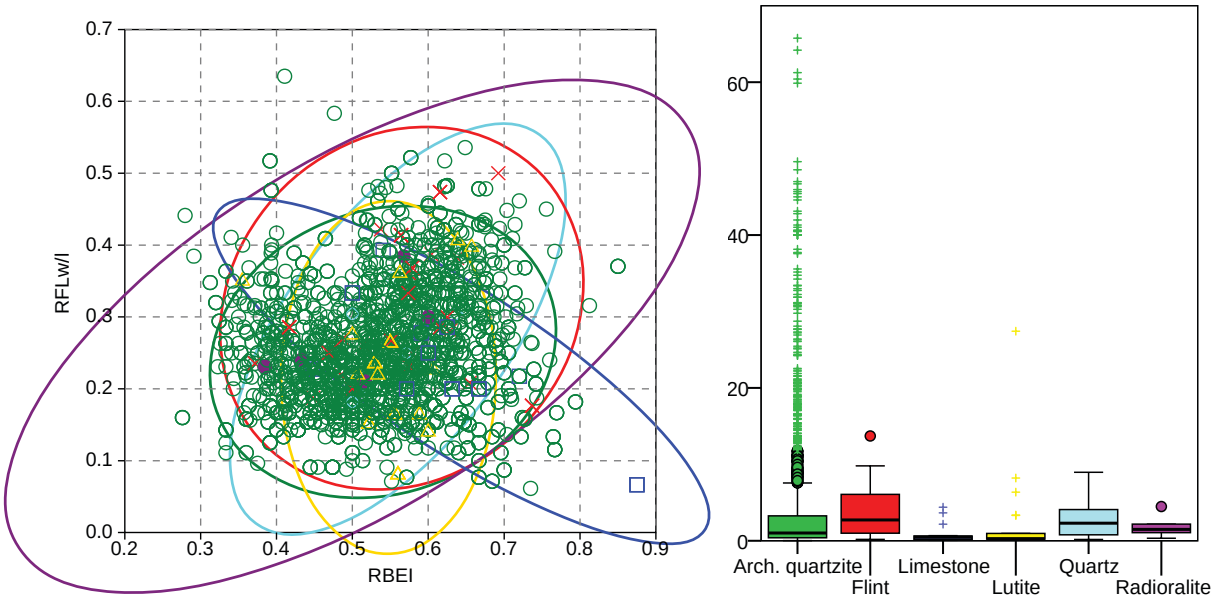

Figure-9.28: Double chart showing: a) Scatter plot of RFLw or RFLl and RBEI indexes. Green circles and ellipse are “archaeological quartzites”. Red crosses and ellipse are flint. Blue squares and ellipse are limestone. Yellow triangles and ellipse are lutites. Light blue circles and ellipse are quartz. Purple points and ellipse are radioralite. Ellipses enclose 95% of cases of each category. b) Boxplot showing differences in weight between different raw materials. There are another four “archaeological quartzites” with higher weight than 70g, not show on chart. The weight is expressed in grams.

There are no clear differences in morphology between different petrogenetic types (Figure-9.29a). Nevertheless, differences arise when analysing weight by petrogenetic types. This is proven by *H* Kruskal-Wallis test: $H\ \chi^2$ (6, N = 2,110) = 70.607, $p < 0.001$. The grams/piece ratio is coherent with this statement. Differences in weight are especially remarkable between the group formed by quartzarenite and the BQ type, and other petrogenetic types (Table-9.27).

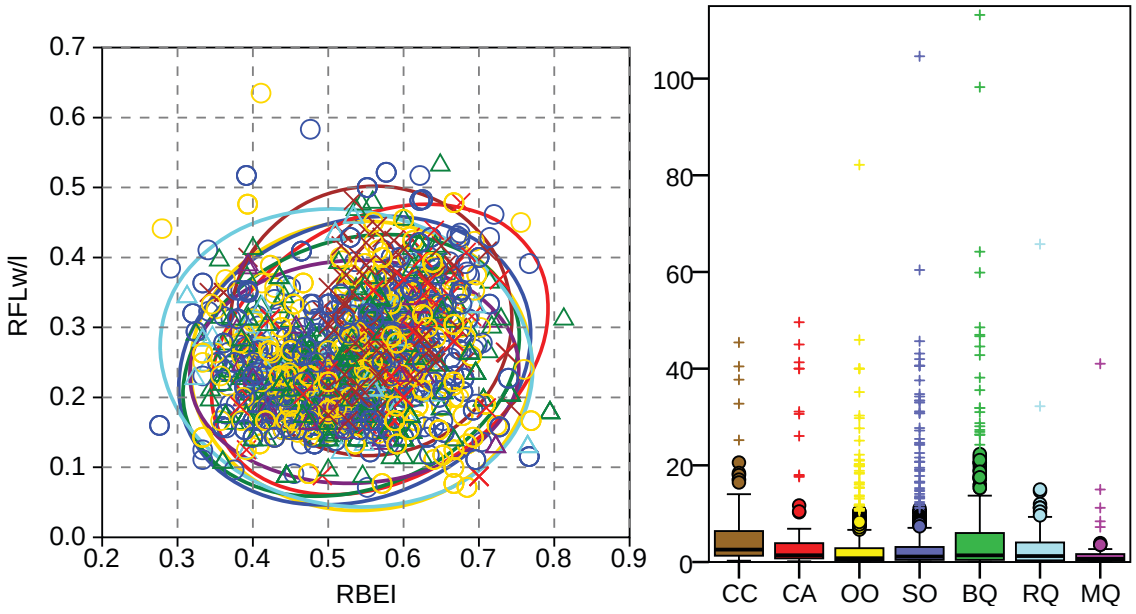

Figure-9.29: Double chart showing: a) Scatter plot of RFLw or RFLl and RBEI indexes. Brown crosses and ellipse are CC type pieces. Red crosses and ellipse are CA type pieces. Yellow circles and ellipse are OO type pieces. Blue circles and ellipse are SO type pieces. Green triangles and ellipse are BQ types. Light blue triangles and ellipse are RQ type pieces. Purple circles and ellipse are MQ types. Ellipses enclose the 95% of cases of each category. b) Boxplot showing differences in weight between different petrogenetic types of “archaeological quartzite”. The weight is expressed in grams.

Petrogenetic type	Weight		∑ of pieces		Ratio
	∑	%	∑	%	Grams/Piece
CC	566,5	6,8	91	4,3	6,2
CA	561,0	6,7	109	5,2	5,1
OO	1767,1	21,2	565	26,8	3,1
SO	2615,8	31,3	752	35,6	3,5
BQ	2344,1	28,1	428	20,3	5,5
RQ	346,4	4,1	92	4,4	3,8
MQ	152,9	1,8	73	3,5	2,1

Table-9.27: Frequencies and weight of different petrogenetic types of “archaeological quartzites”. The ratio grams/piece is reported. Weight is expressed in grams.

Now we will delve into the relationship between raw material, technology, retouch and the metrical structure, focusing on size and weight. Starting with technology, there are clear differences in weight based on the technological order and raw material (Figure-9.30 and Table-9.28). Cores on “archaeological quartzites” are bigger than flint cores. There are differences between petrogenetic types too. For example, there are no cores on the CA or OO petrogenetic types lighter than 20 grams. Despite the small number of cores, there are notable differences in weight based on technological group and petrogenetic type. These differences are especially relevant in the case of irregular cores (Figure-9.31 and Table-9.29). There are also some differences in weight among cores on flake between those made on the SO type and those made on the BQ type. Considering the small number of cores available, we were unable to observe further differences.

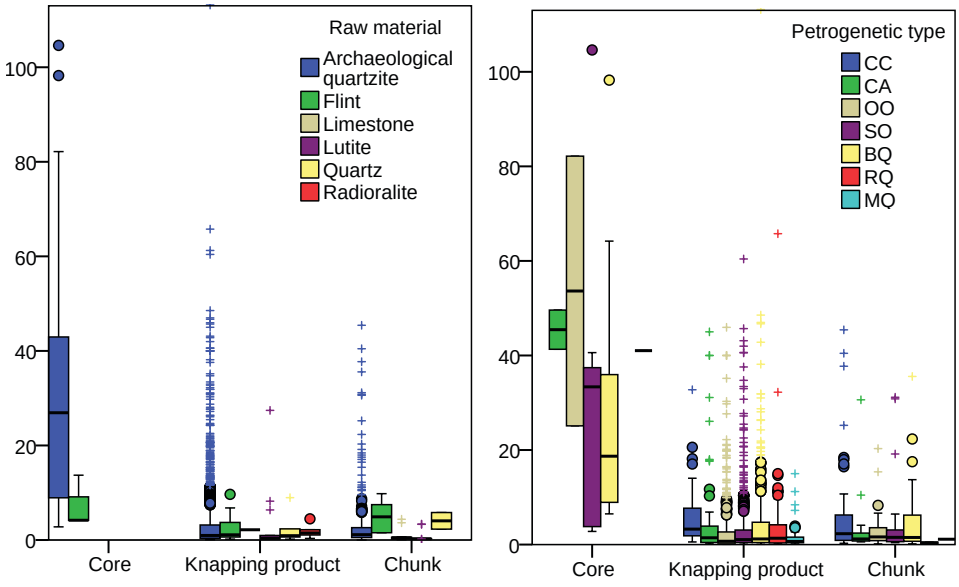

Figure-9.30: Double boxplot showing the distribution of weight in grams of all lithic remains grouped first by technological order and second by raw material in the chart on the left and by petrogenetic type in the chart on the right.

In regard to knapping products, Table-9.30 displays the differences between core preparation/rejuvenation products and blanks. The former are bigger than the latter. Focusing on specific petrogenetic types of “archaeological quartzites”, the biggest core preparation/rejuvenation products are made on SO and RQ petrogenetic types. There is no difference in the weight of blanks based on the number of negative scars between raw materials, except for quartz blanks, which are always lighter (Figure-9.32). Conversely, there are differences in the weight of blanks depending on the number of negative scars between various petrogenetic types. This is especially true for blanks without any negative extraction. In addition, the absence of pieces lighter than one gram among blanks without negative scars and blanks with three or more scars made on RQ and MQ petrogenetic types is noteworthy. It is also interesting to note the lack of blanks on the CC petrogenetic type with one or more negative scars lighter than one gram. Other petrogenetic types of “archaeological quartzite” are diversely distributed, even in regards to the grams per piece ratio (Table-9.30). Figure-9.33 represents graphically the distribution of weight based on raw material and integrity of the blanks. As shown on Table-9.31, differences in weight between blanks made on different types of “archaeological quartzite” and classified according to their integrity are observable.

Raw material	Petrgen. type	Lithic collection											
		Core			Knapping			Chunks			Total		
		∑	W	g/p	∑	W	g/p	∑	W	g/p	∑	W	g/p
Archaeological quartzite	CC				36	224	6,22	55	343	6,23	91	566	6,22
	CA	2	41	20,7	82	391	4,77	25	79	3,15	109	511	4,69
	OO	2	107	53,6	501	1496	2,99	62	164	2,65	565	1767	3,13
	SO	7	183	26,1	687	2205	3,21	58	188	3,24	752	2575	3,42
	BQ	15	304	20,3	384	1768	4,6	29	149	5,12	428	2221	5,19
	RQ				86	344	4	6	2	0,38	92	346	3,77
	MQ	1	41	41	71	111	1,56	1	1	1,13	73	153	2,09
	Undet.				121	277	2,29	71	73	1,02	192	350	1,82
	Total	27	676	25,1	1968	6816	3,46	307	998	3,25	2302	8491	3,69
Flint		6	40	6,59	21	54	2,58	7	34	4,9	34	128	3,76
Limestone					1	2	2,17	19	15	0,77	20	17	0,84
Lutite					17	48	2,84	9	8	0,93	26	57	2,18
Quartz					5	13	2,61	2	8	4,06	7	21	3,02
Radioralite					5	10	1,91				5	10	1,91

Table-9.28: Frequency table of different orders of lithic remains grouped by raw material, including frequencies, weight and the ratio grams/piece for each case. Weight is expressed in grams.

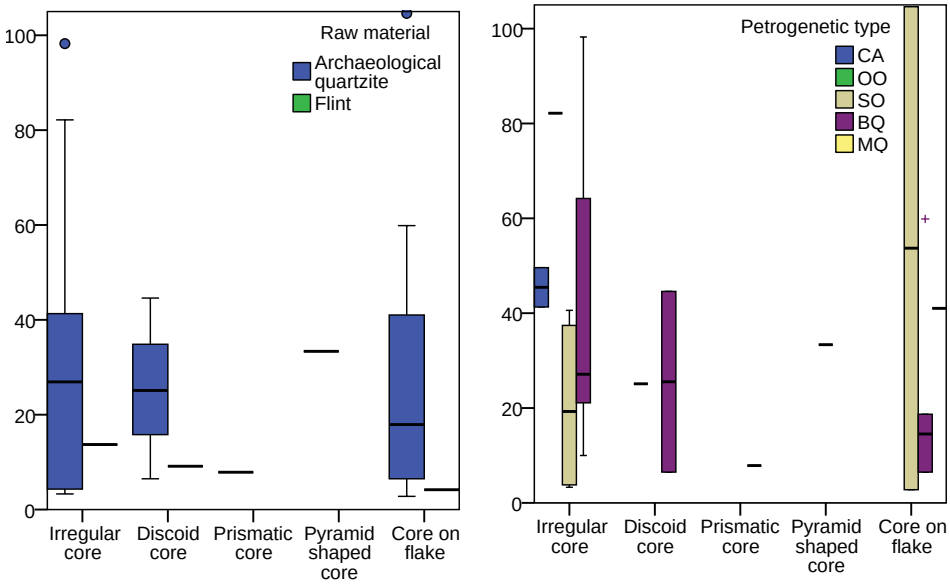

Figure-9.31: Double boxplot showing the distribution of weight in grams of cores grouped first by type and second by raw material in the chart on the left and by petrogenetic type in the chart on the right.

Raw material	Petrgen. type	Cores																	
		Irregular			Discoid			Prismatic			Pyramidal			Core on flake			Total		
		∑	W	g/p	∑	W	g/p	∑	W	g/p	∑	W	g/p	∑	W	g/p	∑	W	g/p
Archaeological quartzite	CC																		
	CA	2	91	45,5													2	91	45,5
	OO	2	94	46,9	1	25	25,1										3	119	39,6
	SO	7	92	13,2							1	33	33,4	2	107	53,7	10	233	23,3
	BQ	6	248	41,3	2	51	25,5	1	7,9	7,9				6	121	20,1	15	427	28,5
	RQ																		
	MQ													1	41	41,0	1	41	41,0
	Undet.																		
	Total	17	525	30,9	3	76	25,4	1	7,9	7,9	1	33	33,4	9	269	29,9	31	911	29,4
Flint		1	14	13,7	1	9,1	9,1							4	17	4,2	6	40	6,6
Limestone																			
Lutite																			
Quartz																			
Radioralite																			

Table-9.29: Frequency table of different core types grouped by raw material, including frequencies, weight and the ratio grams/piece for each case. Weight is expressed in grams.

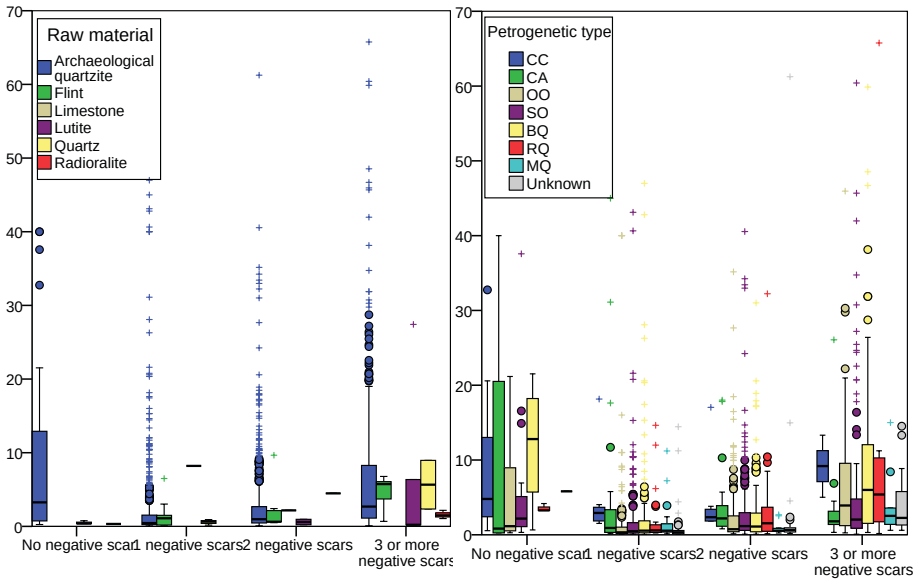

Figure-9.32: Double boxplot showing the distribution of weight in grams of blanks grouped first by the number of negative scars on dorsal surface and second by raw material in the chart on the left and by petrogenetic type in the chart on the right.

Raw material	Petrgen type	Knapping products																	
		Core preparation			Blanks														
					No neg.scar			1 neg.scar			2 neg.scar			3 or more			Blank total		
		∑	W	g/p	∑	W	g/p	∑	W	g/p	∑	W	g/p	∑	W	g/p	∑	W	g/p
Archaeological quartzite	CC				14	117	8,4	10	42	4,2	9	37	4,2	3	27,5	9,2	36	224	6,2
	CA				7	83	12	38	162	4,3	26	98	3,8	11	48,4	4,4	82	391	4,8
	OO	2	19	9,7	17	106	6,3	207	356	1,7	200	481	2,4	75	533	7,1	499	1496	3
	SO	3	54	17,9	15	92	6,2	238	485	2	269	762	2,8	164	848	5,2	686	2242	3,3
	BQ	4	42	10,6	7	83	12	134	387	2,9	156	545	3,5	86	808	9,4	383	1865	4,9
	RQ	1	15	15,0	3	11	3,6	31	59	1,9	35	113	3,2	16	146	9,2	85	344	4
	MQ							41	53	1,3	20	56	2,8	11	42	3,8	72	152	2,1
	Undet.				1	6	5,8	47	50	1,1	43	109	2,5	30	112	3,7	121	277	2,3
	Total	10	131	13,1	64	498	7,8	746	1594	2,1	758	2203	2,9	396	2566	6,5	1964	6860	3,5
Flint								9	15	1,6	7	16	2,3	5	23	4,6	21	54	2,6
Limestone											1	2	2,2				1	2	2,2
Lutite					4	1,9	0,5	1	8	8,2	6	4	0,6	6	35	5,8	17	48	2,8
Quartz								3	2	0,6				2	11	5,7	5	13	2,6
Radioralite					1	0,3	0,3				1	4	4,5	3	5	1,6	5	10	1,9

Table-9.30: Frequency table of different knapping products grouped by raw material, including frequencies, weights and the ratio grams/piece for each case. The knapping products considered are core preparations/rejuvenations and blanks sorted by the number of negative scars present. Weight is expressed in grams.

Finally, differences in the weight of chunks based on raw material are verifiable in Figure-9.30 and Table-9.28. While chunks on “archaeological quartzite”, flint and quartz are heavier, chunks on lutite and limestone are lighter. The differences are more evident when comparing the weight of chunks between different petrogenetic types. Chunks made on CC and BQ petrogenetic types are heavier than those made on the other types, especially in comparison with those made on RQ and MQ petrogenetic types.

The analysis of the relationship between raw material and retouch concludes that the heaviest artefacts (in the three represented modes) are made on archaeological quartzites. Meanwhile retouched pieces on flint and quartz are lighter (Figure-9.34 and Table-9.32). The same analysis based on petrogenetic types reveals that the heaviest blanks configured with the Simple mode are made most frequently on the CA petrogenetic type, followed by SO, BQ, and OO petrogenetic types. The pieces configured with Splinter mode are smaller, although there are some bigger ones on CA and SO petrogenetic types.

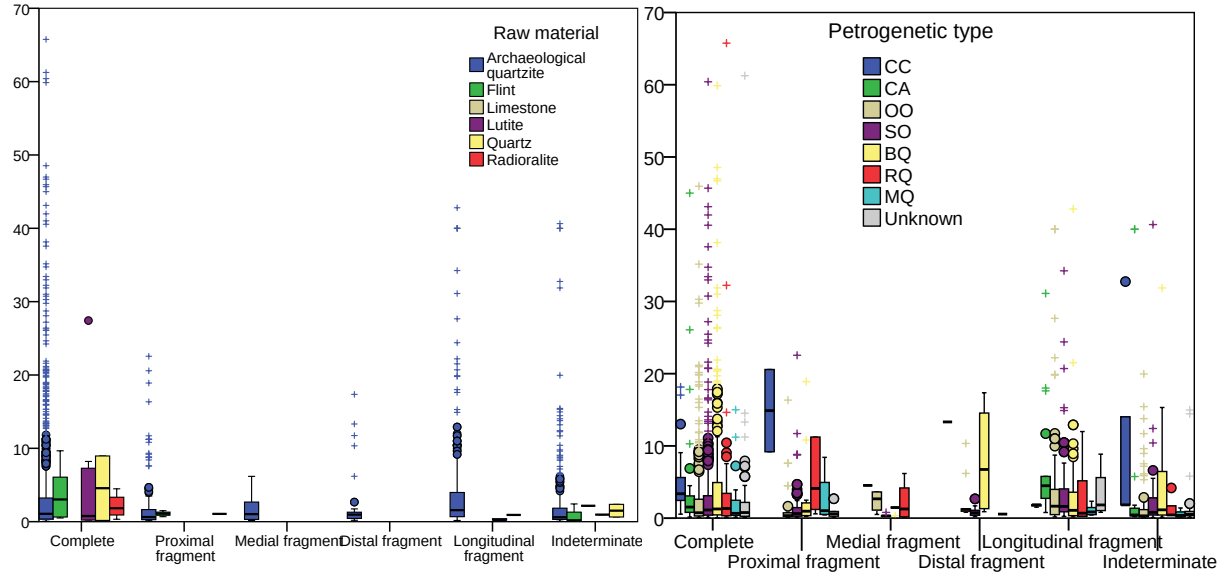

Figure-9.33: Double boxplot showing the distribution of weight in grams of blanks grouped first by their integrity and second by raw material in the chart on the left and by petrogenetic type in the chart on the right.

Raw material	Petrgen type	Knapping products: Blanks																	
		Complete			Proximal f.			Medial f.			Distal f.			Longitudinal f.			Unknown F.		
		∑	W	g/p	∑	W	g/p	∑	W	g/p	∑	W	g/p	∑	W	g/p	∑	W	g/p
Archaeological quartzite	CC	24	121	5,1	2	30	15				1	13	13	3	5	1,7	6	54	9
	CA	38	159	4,2				1	5	4,5				18	127	7	25	102	4,1
	OO	292	855	2,9	42	56	1,3	4	9	2,4	9	24	2,7	80	385	4,8	72	147	2
	SO	387	1448	3,7	73	130	1,8	7	3	0,4	25	22	0,9	109	399	3,7	85	187	2,2
	BQ	266	1390	5,2	18	46	2,6	5	6	1,2	4	32	7,9	52	191	3,7	38	157	4,1
	RQ	56	229	4,1	9	53	5,8	7	16	2,3				8	25	3,1	5	7	1,4
	MQ	44	121	2,8	4	11	2,7				2	1	0,6	12	13	1,1	10	5	0,5
	Undet.	70	198	2,8	9	9	1							4	13	3,3	38	57	1,5
	Total	1177	4520	3,8	157	335	2,1	24	39	1,6	41	92	2,3	286	1158	4	508	1373	2,7
Flint		13	47	3,6	4	4	1,1										4	3	0,7
Limestone																	1	2	2,2
Lutite		7	43	6,2										7	2	0,3	3	3	1
Quartz		2	9	4,6										1	1	0,9	2	3	1,5
Radioralite		4	8	2,1	1	1	1,1												

Table-9.31: Frequency table blanks sorted by integrity and grouped by raw material, including frequencies, weight and the ratio grams/piece for each case. Weight is expressed in grams.

Raw material	Petrgen. type	Single-retouched pieces																	
		Simple												Abrupt			Splinter		
		Sidescraper			Endscraper			Denticulate			Point			Abrupt			Splintered		
		∑	W	g/p	∑	W	g/p	∑	W	g/p	∑	W	g/p	∑	W	g/p	∑	W	g/p
Archaeological quartzite	CC				1	18	18										2	6	3,2
	CA	4	124	31,1													3	12	4,1
	OO	24	230	9,6							3	47	6,3	1	46	46,0	43	42	1,0
	SO	42	752	17,9							2	54	3,7	1	4	4,0	97	127	1,3
	BQ	32	436	13,6				2	68	34,2	6	106	5,6	1	11	10,6	56	84	1,5
	RQ	6	56	9,4				2	23	11,6	1	15	15,0				14	20	1,4
	MQ	3	18	5,9													6	6	1,0
	Undet.	2	70	35,1													9	7	0,7
	Total	113	1686	14,9	1	18	18	4	91	22,9	12	222	5,4	3	61	20,2	230	304	1,3
Flint		3	22	7,4				2	2	1,1	1	7	7,0				1	1	0,5
Limestone																			
Lutite																			
Quartz		2	15	7,4													1	1	0,6
Radioralite																			

Table-9.32: Frequency table of retouched artefacts sorted by typological mode and morphological group and grouped by raw material, including frequencies, weight and the ratio grams/piece for each case. Pieces with more than one primary types are not included. Weight is expressed in grams.

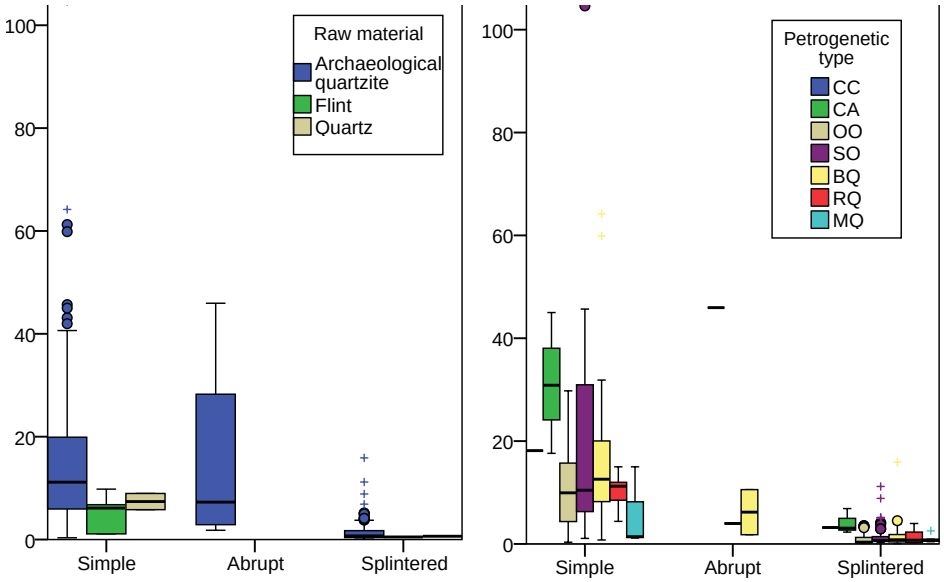

Figure-9.34: Double boxplot showing the distribution of weight in grams of retouched material with one primary type grouped first by mode of retouch and second by raw material in the chart on the left and by petrogenetic type in the chart on the right.

9.6. RAW MATERIAL ACQUISITION AND MANAGEMENT PROCESSES AT LAYER-XIII OF EL ESQUILLEU

Once the raw data from this layer have been presented, in this section we bring face to face geographical, geological, and archaeological data to understand the forces that got these materials deposited here, that is, the human raw material acquisition and management strategies.

The main acquisition process verified in this layer is the extraction of big quantities of orthoquartzites and quartzites for human activities, as demonstrated by the great quantity of them found in this layer both in number and in weight. The small representation of other raw materials and quartzarenite indicates they had different roles in human activities.

The management of raw material has been analysed including the raw data on all raw materials in a general reduction process model based on a simple "chaîne opératoire" (Figure-9.35). The primary technological product of lithic reduction we find in this layer are cores (irregular, discoid, pyramidal, or prismatic). From here on, we expose and analyse the different processes that generate other lithic products based on the understanding of their features.

1. Blanks, as well as smaller blanks (sometimes fragmented) and chunks, were obtained as a result of the reduction process of some cores. Blanks and chunks are secondary products generated as a consequence of knapping procedures.

    a. Using retouching procedures, some of these primary blanks were modified, creating retouched artefacts as primary products and more blanks and chunks as secondary products. The latter are lighter than 5 g and sometimes fragmented. Due to the impact of successive simple retouches (the most frequent retouch on blanks heavier than 5 g), some of these blanks lighter than 5 g only have a single splinter retouch. The production of Quina sidescrapers, characterised by the succession of multiple simple retouches on the same edge, is what mainly creates these derived products (Baena and Carrión, 2010; Carrión, 2002; Carrión and Baena, 2003; Cuartero et al., 2015). In addition, new retouches can be made in the blanks to obtain artefacts with multiple primary types, generating more blanks and chunks as secondary products.

    b. Some other blanks were reconfigured by percussion to obtain new flakes. The resulting products are a core on flake and blanks as primary products and other blanks and chunks, derived from the reconfiguration processes, as secondary products.

        i. Some cores on flakes were retouched, creating a retouched core on flake. Small chunks and blanks derived from the retouching process are again secondary products.

        ii. As a consequence of the reduction processes of the cores on flakes, further blanks were obtained, also secondary products classified as chunks and blanks (smaller than the previous blanks).

            • The latter blanks can also be retouched, creating new retouched artefacts and secondary products (chunks and blanks).

2. Going back to cores, these can be retouched to obtain retouched cores. Moreover, small chunks and blanks were generated as secondary products as a consequence of the retouching process.

3. Following with cores, some of them were reconfigured to obtain new flaking surfaces or new striking platforms. This process generated new forms or types of cores and three different secondary products: chunks, blanks (generally lighter than 5 g and sometimes fragmented) and core preparation/rejuvenation products.

    a. Some core preparation/rejuvenation products were retouched, creating retouched preparation/rejuvenation products. As a consequence, small chunks and blanks were produced as secondary products.

    b. Some of these new cores were retouched, creating retouched cores. As a consequence, small chunks and blanks were produced as secondary products.

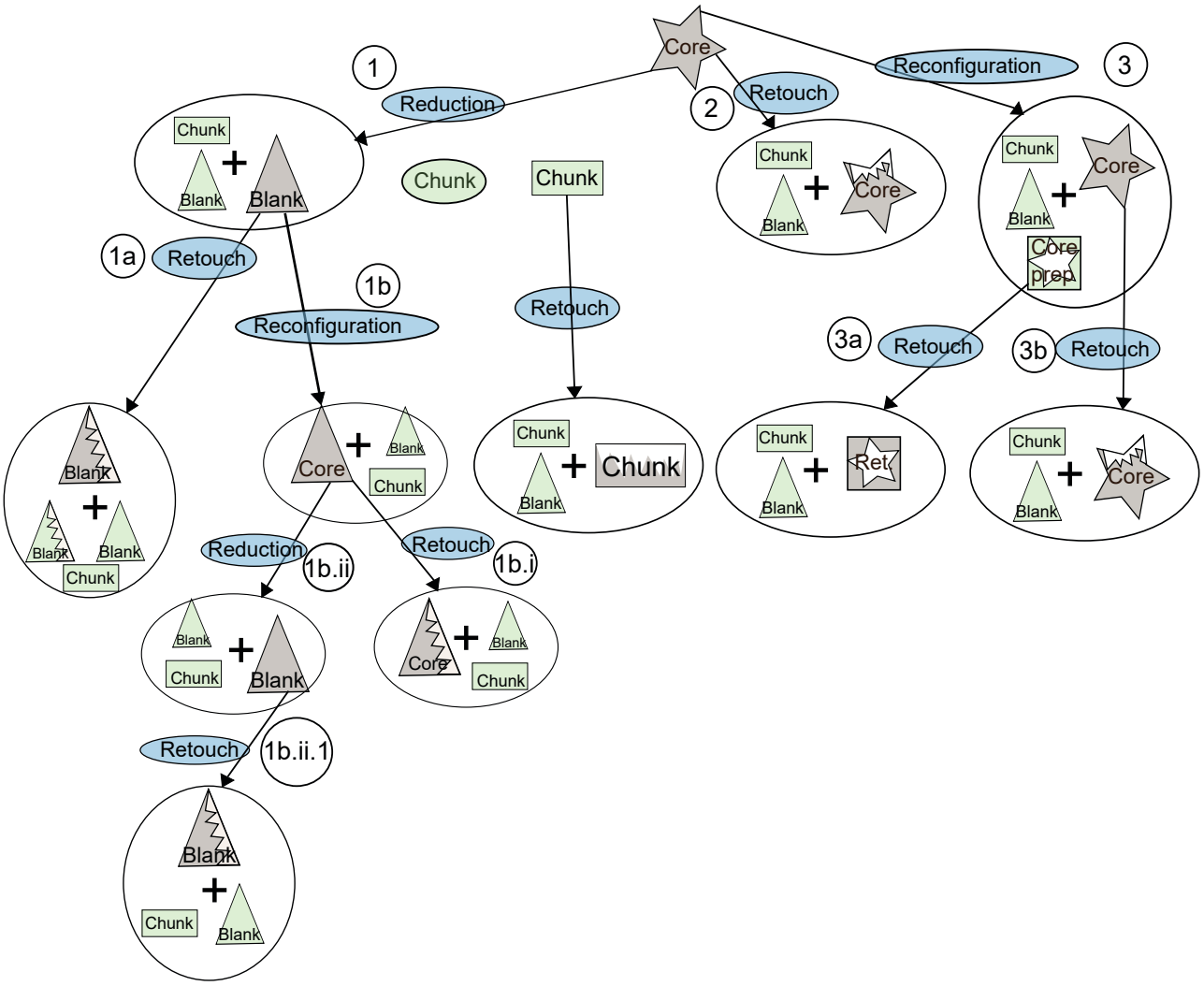

Figure-9.35: Schematic “chaîne opératoire” derived from the analysis of the lithic assemblage from layer-XIII of El Esquilleu. Stars represent cores, rectangles chunks, elongated circles completely cortical chunks, squares with stars core preparation/rejuvenation products and triangles blanks. Zig-zag lines added to any of these icons represent retouched artefacts. Grey icons are primary products and green ones secondary products. The blue ellipses indicate human activities. Alphanumeric codes inside circles are references to the text.

Some of the chunks were also retouched. They are always heavier than 5 g. Blanks and chunks were generated as secondary products of retouch techniques and they are generally lighter than 5 g.

In addition to these products inserted in the “chaîne opératoire”, we identified multiple smalls chunk completely cortical and without evidences of having been used in knapping activities.

Next, we present the conclusion related with the acquisition and management of “archaeological quartzites” by petrogenetic types, and later, other raw material. Figure-9.36 and Figure-9.38 schematically represent the acquisition process of “archaeological quartzites” and other raw materials, respectively. Figure-9.37 displays the relationship between acquisition and management strategies. Finally, Figure-9.39 shows the Cost map from El Esquilleu with the geological formations where raw material could have been caught.

As it has been previously mentioned, “archaeological quartzite” is the most relevant raw material, both in number and weight, present in the layer-XIII of El Esquilleu. Next, we will explain the raw material catchment and management strategies of this raw material by petrogenetic types.

The CC type is one of the less frequent type of “archaeological quartzite”. Not all technological categories are represented. Cores, as well as core preparation/rejuvenation products, are absent. There is a clear overrepresentation of chunks and an underrepresentation of knapping products. Despite the presence of significant quantities of lithic remains, the knapping reduction process is not completely represented. However, the weight of chunks and knapping products, which range

from less than 1 g to more than 40 g, supports the idea of knapping and reshaping activities were practiced in the site. The grams/piece ratio makes it clear that the chunks made of this type of "archaeological quartzite" are heavier than those produced in other raw materials and other types of "archaeological quartzites". There are only three retouched artefacts, a small number in comparison with those of other petrogenetic types. Negative scars on dorsal surfaces are scarce and they are generally less than two on each lithic. Cortical surfaces on knapping products and chunks made of the CC petrogenetic type are abundant. Some of the chunks, low in weight and completely covered by cortex fluvial deposits, are similar to the matrix of river beaches. Conversely other chunks and blanks point at the use of this material for low intensity knapping activities.

This petrogenetic type is characterised by multiple grain size varieties, generally with heterogeneously distributed grain sizes. Colour is also greatly heterogeneous, due to the impact of many different non-quartz minerals on these rocks. The presence of bedding on these quartzarenites is uneven. All these elements lead us to conclude: a) the CC petrogenetic type is heterogeneous, and b) the input in the site of CC quartzarenites comes from different pebbles from diverse origins. White varieties are related with the CC type from Barrios or Cavandi formations, while dark and brown varieties are linked with the Murcia Formation or with carboniferous sandstone strata such as the Potes, Mogrovejo or Viorna formations. The analysis of cortical areas reveals the fluvial origin of all the cortical surfaces identified. This is true not only for light chunks completely covered by cortex, but also for other technological categories. All in all, we proposed that the CC petrogenetic type is a raw material caught in fluvial beach deposits, probably near the site of El Esquilleu. We observe an important presence of this petrogenetic type in these beaches. Different pebbles with diverse colours and grain size varieties were also found during geological survey. The general size and morphological features of CC pebbles in these beaches is also heterogeneous: multiples sizes (from medium pebbles to big cobbles) and both spherical and elongated morphologies are present. Then, strong selection mechanisms would not have been required for the acquisition of this type. In addition, it can be said there is no selection based on colour or on grain size. Putting all this information together, it is possible to conclude the following on the management of the CC type: a) there is an unconscious transport of small round chunks completely covered by cortex; and b) the remaining assemblage is consciously input, not as cores, but probably as knapping products. The scale of this type in this site reveals its use as raw material was sporadic, maybe related with the scarcity of other petrogenetic types or raw materials more suitable. We also propose this petrogenetic type was preferentially selected based on the size of the pebbles. Therefore, in the deposits there must have been a further selection of CC pebbles based on size.

The CA type only constitutes a small portion of the total of "archaeological quartzites", but it is better represented than the CC type. In this case, all three technological orders are present, although there are no core preparation/rejuvenation products. The distribution of the three technological orders points at a smaller presence of knapping products and a greater frequency of chunks. There are no chunks completely covered by cortex. Then, it can be concluded that the overrepresentation of chunks is due to conscious knapping activities. Retouched artefacts are frequent, but in smaller proportions than in other petrogenetic types. There is only one retouched artefact with two primary types. The most frequent mode of retouch is the Simple one (all of them are Sidescrapers). Splinter retouch is also well represented. Three of the four artefacts with Splinter mode on small blanks, probably derived from retouching processes for obtaining Sidescrapers. Weight of blanks and chunks ranges from less than 1 g to more than 40 g. This proves that knapping and reshaping processes were carried out in the site. The average weight of blanks is lower than for the previous type, but still higher than the median of all "archaeological quartzites". The frequent presence of cortical areas, generally covering more than the 33% of the dorsal surface, and the occasional presence of blanks with more than two negative scars, indicates this type of quartzarenite is weakly exploited, similarly to the CC type.

The characterisation of this petrogenetic type reveals grain size is more homogeneously distributed, with the predominance of fine-medium sizes. Colour is more heterogeneous due to the variability of non-quartz minerals. The presence of bedding is significantly smaller. These features suggest a) the CA type is very variable, b) the input of CA quartzarenites to the site got supplied with pebbles from different origins, and c) there was a preferential selection of homogeneous grain size varieties. Colour links this quartzarenite with the Barrios or Cavandi outcrop formations and with clasts from Carboniferous conglomerate formations in the case of white or brown/clear varieties. However, the characterisation of cortical areas points at a major presence of cortex from fluvial sources. Nevertheless, acquisition from conglomerates is evident in two of these quartzarenites. All in all, we proposed that CA petrogenetic type quartzarenites were brought to the site from two different source areas: a)

fluvial deposits, probably close to the site the El Esquilleu and b) from conglomerates. Focusing on the later, this type of quartzarenite is present in most of the conglomerates in different proportions. According to the siliceous and black-grey cement of one of the two pieces (a core) with cortex from a conglomerate, we propose five possible origins: a) the Curavacas conglomerate, to the south, 12 Cost Units (CU) away; b) Valdeón (32 CU) or Pontón (26 CU) conglomerates, to the south-west, in the Valdeón area; or c) Pesaguero (12 CU) or Porrera (9 CU) conglomerates, to the south. All of them are located at middle-altitudes. Obtaining homogeneous (but coarse) grain size varieties from these conglomerates requires medium intensity selection mechanisms. Taking into account the selection mechanisms needed to obtain CC quartzarenites from fluvial courses near El Esquilleu, stronger selection mechanisms would have been necessary for getting the CA type from river beaches. These selection mechanisms would have been stronger in fluvial deposits than in conglomerates. Moreover, preferential choosing of specific grain sizes and homogeneous varieties would have required further selective mechanisms in these fluvial courses. We propose catchment of CA quartzarenites was based on sporadic activities, both in fluvial and conglomerate contexts. These sporadic catchment activities would have been complementary to other tasks, such as acquisition of different

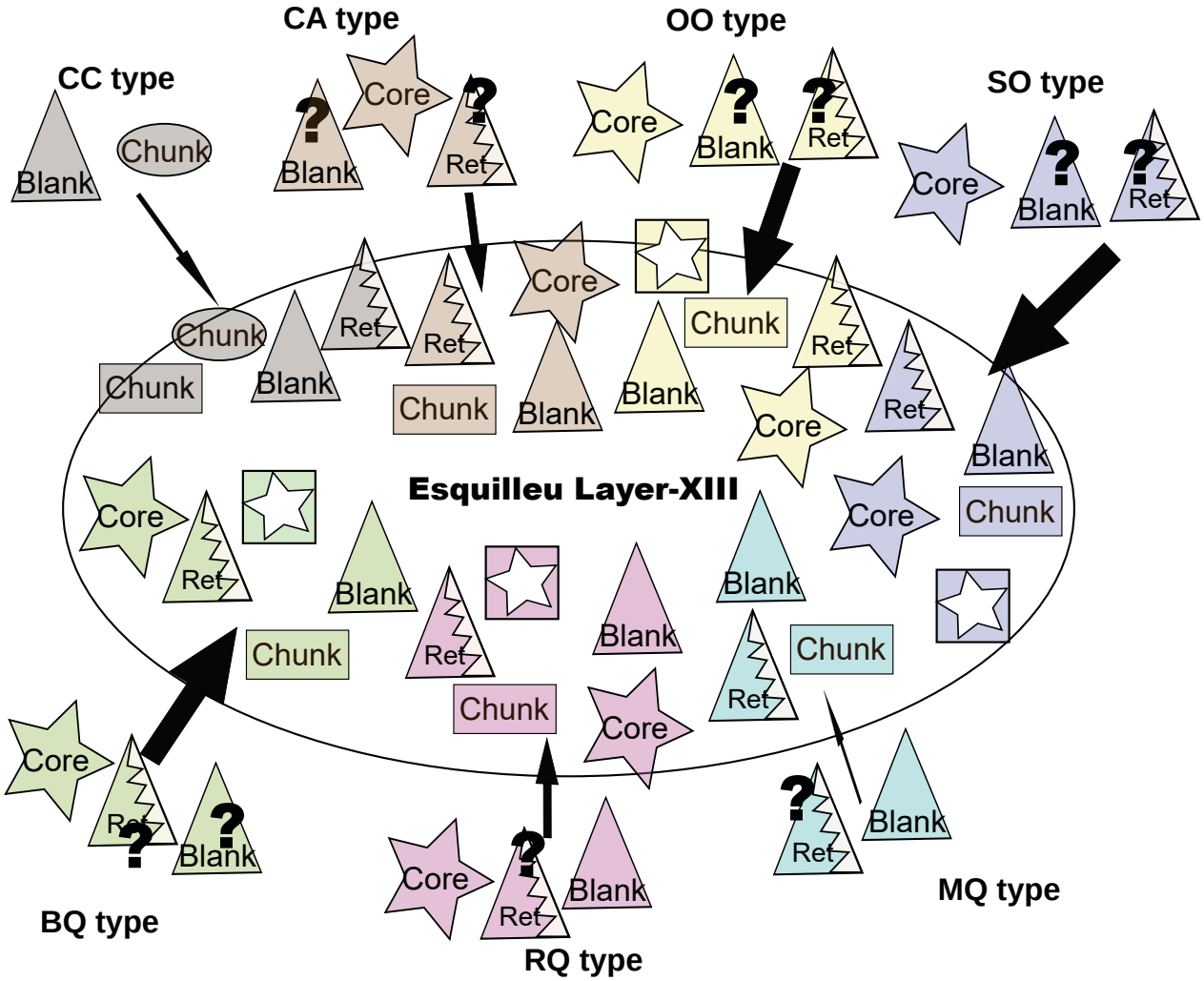

Figure-9.36: Schematic representation of the input of the different petrogenetic types of “archaeological quartzite”, taking into account the different technological products present. Stars represent cores, triangles blanks, triangles with zig-zag retouched material, ellipses fully cortical chunks and rectangles chunks. Question marks indicate products whose presence is not certain.

resources in river beaches or catchment of other petrogenetic quartzite types in conglomerates. The input to the site could have been made in form of cores, blanks or retouched material.

The OO petrogenetic type of orthoquartzite shows clear differences in management and catchment in comparison with the raw materials and types of “archaeological quartzite” tackled above. It represents 25% of the lithic assemblage in number and 21% in weight. These data mean there was a planned and intensive exploitation of this type. The three technological categories considered, as

well as core preparation/rejuvenation products, are present in this layer. It is obvious knapping and reshaping activities were practised in the site. This is also certified by the presence of blanks and chunks between less than 1 g to more than 40 g. Cores types, weight and flacking and knapping surfaces reveal this raw material is more intensively exploited than the quartzarenite group exposed in the previous paragraphs. The presence of negative scars is more frequent than in the former two types, but is scarcer than in more deformed types of "archaeological quartzite" or flint. The presence of cortical areas shows a pattern similar to SO orthoquartzite, quartzites and flint. Retouched material is less frequent than in other orthoquartzites and quartzites, although it is more frequent than in the two preceding types. The absence of retouched chunks and cores does also points at the smaller importance of retouching activities in this petrogenetic type. Conversely, artefacts with two and three primary types are common and all modes of retouch and morphological groups (except for Truncation) are present in this petrogenetic type. The quantity of Points is also elevated. This evidence reveals medium intensity exploitation. The grams/piece ratio of the lithic pieces from this layer, smaller than that of quartzarenites, agrees with this hypothesis.

The characterisation of this raw material based on grain size and colour indicates it is a more homogeneous type. Most of the grains are medium size and homogeneously distributed. According to colour, the more important varieties are white and grey. These are associated to stable presence of non-quartz minerals, probably as a result of the intensive input of this variety in the site. The dark varieties are rarer. They may be the consequence of the transportation of a few blocks of this variety to the site. The original source strata of the lighter colour variety are in the more deformed bands of the Barrios outcrop formations, as well as in the carboniferous conglomerates from older layers. The darker variety originates exclusively in the latter. The characterisation of cortical areas reveals that most of them come from fluvial deposits. Still, there is an important presence of conglomerate cortex too. There is no evidence of outcrop cortex. Therefore, although the most likely source strata are in the Barrios Formation, catchment was probably made in deposits and conglomerates. Most of the conglomerates have OO type orthoquartzites, more frequently the white varieties. In the nearby conglomerate of the Remoña Formation, 5 CU away, it is possible to find them without the need to apply any selective mechanism. Other conglomerates, such as the Curavacas series, which include Lechada (13 CU), Campollo (16 CU), Maraña-Brañas (27 CU), Narova (10 CU), Pesaguero, Pontón, Potes (12 CU), and Valdeón conglomerates have important amounts of this type. However, at least low intensity selective mechanisms are necessary to choose specific varieties, forms and sizes. All these conglomerates are to the south, in medium altitude plateaus. In fluvial deposits the presence of this petrogenetic type is scarcer. Therefore, the selective mechanisms required to pick special varieties, forms and sizes would have been more intensive. The black variety does also derive from conglomerates and fluvial deposits. In conglomerates this variety is only present in south-western conglomerates. All in all, catchment of this type would have included both fluvial and conglomerate areas, which would have provided big amounts of material as a result of planned raw material procurement strategies. The arrival of the pieces to the site could have been as either cores, blanks or retouched material.

The SO petrogenetic type shows different management and catchment strategies in comparison with the previous types, despite its representation in the site being similar in quantity. Thirty-two per cent of the implements in "archaeological quartzites" and 31% of the total weight of this raw material belong to the SO type. Planned and exhaustive exploitation of this orthoquartzite is observable, which makes it the most intensively exploited type of this group. As in the previous type, the three technological orders, as well as core preparation/rejuvenation products, are represented in this layer. It is clear knapping and reshaping activities were carried out in the site, as demonstrated by the presence of blanks and chunks with weights between less than 1 g and more than 60 g. Core types, their weight and flacking and knapping surfaces reveal this raw material is the most intensively exploited orthoquartzite. The presence of negative scars is more frequent than in the previous type, with the greatest rate of three or more extractions on dorsal surfaces. Presence of cortex is rare and it generally covers less than 33% of the pieces. The proportion of retouched material is greater than in previous types. Still, it is smaller in comparison with the first type of quartzite. There is an important presence of artefacts with two and three primary types on them. The only non-retouched technological category is the core preparation/rejuvenation product. This evidence indicates this material is very intensively exploited. The grams/piece ratio of this petrogenetic type is slightly greater than in the previous one, probably due to the heavier weight of blanks (and some cores too).

The characterisation of this raw material reveals there are two different grain size varieties of the SO type: the coarse and heterogeneous one (present in small percentages) and the fine and homogeneous one (the clear majority). The presence of the former is limited to a few pieces, while

many pieces of the latter variety were input into the site. At the same time, two different classes can be distinguished within the fine and homogenous grain size variety based on colour and non-quartz minerals: a darker one and a grey one. Both are identified in similar numbers. The original outcrop strata of the three varieties defined is not located in the research area, but they can be found in conglomerate strata and deposits. The conglomerates with the SO petrogenetic type are the Lechada, Maraña-Brañas, Pontón, Potes, Remoña, and Valdeón conglomerates. In all of them the presence of the fine grained variety range between 5 and 50%, except for the Lechada and Potes conglomerates, where they represent less than 5% of the pebbles. The presence of coarse variety is restricted to the Pontón conglomerates (26 CU). The analysis of cortical surfaces reveals a clear change in acquisition dynamics with an inversion in their provenance. The presence of conglomerate cortical surfaces is more frequent than fluvial ones. Although both origins are present among the three varieties, the majority of pieces made in the coarse grained variety come from fluvial deposits. The presence of SO orthoquartzites in beach deposits is negligible, especially near fluvial deposits. We propose the input of this type to the site is mixed: on one hand, there is an intense and planned catchment strategy carried out in conglomerates; on the other, there are occasional findings in river deposits in relation with other activities, such as journey along rivers or acquisition of other resources. The latter strategy requires strong selection and identification mechanisms of raw material. The input of this type to the site could have been made as cores, blanks or retouched material.

The management and catchment strategies observed in the previous type are clearer in the **BQ quartzite type**. The number of items of this type and their weight points at intensive and planned catchment strategies. All the technological products are identified and all of them are retouched. Therefore, it can be concluded that knapping and reshaping activities were performed in the site. The presence of chunks and blanks between less than 1 g and more than 60 g supports this statement. The grams/piece ratio, especially that of blanks, indicates lithic implements in this type tend to be bigger. This is certainly related to the smaller presence of fractured lithic pieces in comparison with any other types. Core types, weight and flacking and knapping surfaces reveal this raw material is intensively exploited. The frequent presence of cores on flake, the number of extractions on dorsal surfaces (generally more than two) and the occasional presence of cortical areas on dorsal surfaces do also agree with the idea that this resource is an intensively exploited material. Finally, this petrogenetic type is the most frequently retouched type of “archaeological quartzite”, as well as the one with higher quantity of artefacts with two and three primary types on them. All morphological groups defined are present in this BQ type. The high quantity of Points configured on blanks of this material, evidences an especial and important role of this petrogenetic type (Arrizabalaga et al., 2014). All in all, the data gathered demonstrate this quartzite is an intensively exploited material and all phases of lithic reduction are performed in the site. Blanks and retouched material could have been brought as final products, but also created in the site through a reduction sequence from a core form.

The petrological characterisation of this type is hampered by the lack of destructive/thin section samples that certify the varieties of the BQ type proposed. In general, there is great homogeneity in grain size and most of the pieces are fine grained quartzites. Coarser or more heterogeneous varieties could be either different zones from the same block of rock or, more probably, distinct lithic blocks. Colour does also distinguish several varieties: a major dark-grey variety and another two minor varieties, a light-grey one and a brown one. The major dark and fine varieties are significantly more abundant than minor brown, white-grey, or coarser varieties, which are only represented by a few blocks each. We did not find the original outcrop strata for this type of quartzite in the field survey. However, it was clearly identified in some small conglomerates. The presence in fluvial deposits is negligible. There are important quantities (between 5 and 50%) of BQ quartzite in the Remoña, Valdeón, and Pontón (nearest location at 26 CU) conglomerates. In other conglomerates, such as Maraña-Brañas, Pesaguero, and Potes conglomerates, it is scarcer. Coarser grain varieties of the BQ quartzite are restricted to the Pontón conglomerate. Most of the cortical surfaces identified this type was mainly acquired in conglomerates. Fluvial cortex is only identified in a few pieces of the dark varieties. Therefore, it can be deduced that catchment of the BQ type is based on the extraction of big quantities of this material in conglomerates applying medium intensity selective mechanisms. For this purpose mobility could have been either low scale to the near conglomerates of the Remoña Formation or low or medium -scale to Southern and South-western conglomerates. As it happened in the previous case of SO orthoquartzite, there is a mixture of catchment strategies: The first one would consist of exhaustive and planned procurement in conglomerates. The second one would be based in occasional findings in river deposits in relation with other activities, such as journeys along the river or acquisition of other resources. The latter would require strong selective mechanisms and accurate identification of raw materials.

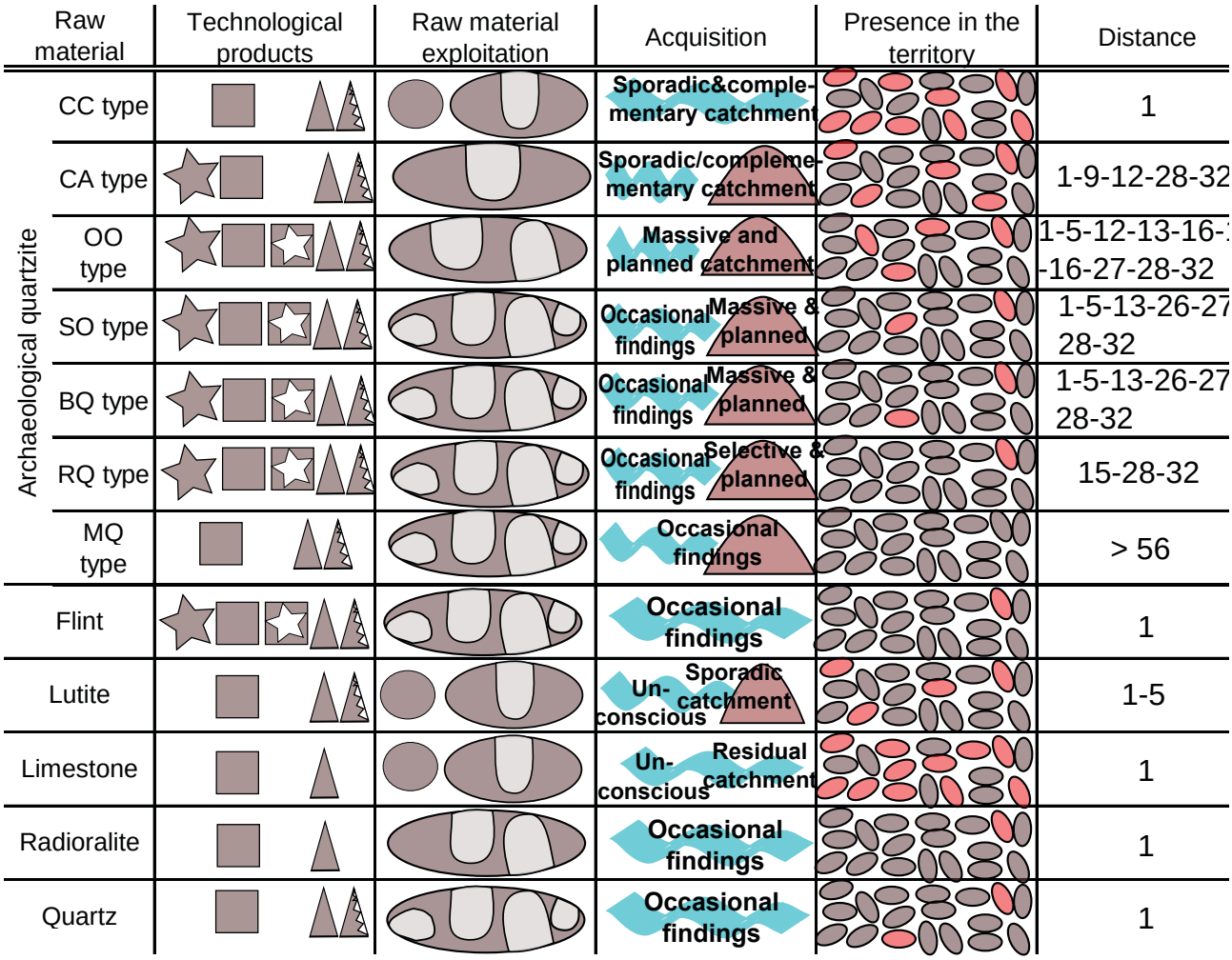

Figure-9.37: Schematic representation simplifying raw material acquisition and management evidences from layer-XIII of el Esquilleu. In the column “Technological products” stars represent cores, squares chunks, squares with starts core preparation/rejuvenation products, and triangles blanks. Zig-zag lines added to any of these icons represent retouched artefacts. In the column “Raw material exploitation”, circles represent unexploited raw material, ovals with one scar represent low intensity raw material exploitation, ovals with two scars represent medium intensity raw material exploitation, and ovals with four scars represent high-intensity raw material exploitation. In the column “Acquisition” waving blue lines represent river acquisition and brown semicircles represent conglomerate acquisition. In column “Presence in territory”, the complete set of ovals represents all the raw materials available in the territory. The ones highlighted in red represent the proportional presence of each specific raw material in the territory. Higher presence of the latter means weaker selection degree.

The RQ quartzite type presents different patterns of catchment and management. The quantity of this type of raw material found in this context is reduced. There is no cores, although a core preparation/rejuvenation product is represented. The quantity of chunks is small and the most frequent technological products are blanks. Retouched material is clearly overrepresented. The presence of blanks (and chunks) ranging from less than 1 g to more than 10 g indicates knapping and reshaping activities were performed in the site. The scarce presence of negative scars on dorsal surfaces indicates a low intensity exploitation of this raw material, despite the occasional preservation of cortex, the low grams/piece ratio and the high integrity of blanks. All these data point at a complex management of this material, related with the scarcity of the RQ type. We propose the input of this type was occasional and it was brought as cores, blanks or retouched artefacts that could be used, reduced or reshaped for specific activities. The underrepresentation of chunks (derived from knapping and reshaping) and incomplete blanks support this hypothesis.

The petrographic characterisation of this raw material does also agree with the previous hypothesis. The analysis of grain size reveals great homogeneity with only two clear varieties: the coarse one and the fine one. No clear colour or non-quartz mineral differences are observed. At least two

different blocks of rock were brought to the site. We were unable to find any evidence of this petrogenetic type in the massive outcrops of the surveyed area. Its presence is reduced to two conglomerate formations: the Pontón and the Valdeón conglomerates, both in the South-west of the research area. Still, the presence of this type is scarce in both conglomerate formations. Taking into account the cortical areas, most of them derive from conglomerates, even though fluvial cortex is also present. We did not find any evidence of this petrogenetic type in fluvial deposits during our surveys. However, its presence cannot be completely discarded, at least in the Cares river, which creates the erosive basin where conglomerates surface. These data indicate that catchment of this type necessarily implied medium or long distance movement, even outside the Deva basin, only suggested with the previous types. In addition, the evidence above supports the existence of strong selective mechanisms, not only in deposits (probably related with occasional findings), but in conglomerates. The only core preparation/rejuvenation product could shows that a core (not found in the site) was probably input and reduced in the site and, afterwards, it was carried to another place (other site?). The presence of this type in the site does also reveal a conscious mechanism of selective and conservative exploitation of raw material. The intense exploitation of this material and its appreciation as singular, valuable and exiguous is clear.

The MQ quartzite type shows catchment and management patterns similar to the previous type. The quantity of this type of quartzite is the smallest in the layer and it is mainly limited to blanks. The representation of technological products is not complete due to the absence of core preparation/rejuvenation, also non-core on flake cores. Chunks are significantly underrepresented (only one piece) and blanks are overrepresented. The amount of retouched material is clearly smaller than in the previous type: Only nine pieces are retouched. Three present Simple modes and the other ones Splinter. The latter are a consequence of successive retouches due to reshaping. The grams/piece ratio is the smallest in the site, even though the integrity of blanks is similar to the previous two types. There is no obvious evidence of knapping processes in the site, since chunks are restricted to a 1 g item. Only a few lithic lithics, most of them retouched, are heavier than 5 g. The quantity of extractions on dorsal surfaces is variable. Still, of the most frequent situation is to find only one dorsal negative scar. The remaining three options are rarer. The presence of cortical surfaces on blanks is the smallest in the site. All this data suggest a less intense exploitation of this raw material in comparison with the previous type, even though it would still be quite intense. We propose reshaping activities and maybe extraction of small flakes through knapping were carried out in the site.

We do not identify different colour or grain size varieties among the MQ quartzites in this layer. Almost all material presents homogenous grain sizes between fine and medium. Regarding colour, most of the samples are white or white-grey. We do not find any evidence of this quartzite in the research area surveyed. Then, the only possibilities are: a) in non-surveyed strata, b) outside of the research area, or c) hidden in deposits or conglomerates in small percentages. The analysis of the cortical surfaces of these quartzites reveals that most of them derived from conglomerates, although fluvial cortex is well represented too. Therefore, the input of MQ quartzites would also be mixed. Catchment strategies would imply high mobility and/or strong selective mechanism in conglomerates and fluvial deposits. As it was verified in the previous type, MQ quartzite involves a conscious mechanism of selective and conservative exploitation. It is clear this quartzite is intensively exploited as a singular, valuable, and exiguous raw material, maybe related with a mobile tool-kit, as proposed by other authors in different regions (Bustos-Pérez et al., 2017; Meignen et al., 2009; Turq et al., 2013).

Next we will explain the raw material catchment and management strategies of other raw material. These material are not frequent in El Arteu assemblage, although they reveal different roles of raw material and interesting catchment and management behaviour.

Starting with **flint**, the analysis of the technological products made on this material reveals it is present in all phases of the lithic reduction process. Nevertheless, there is no core preparation/rejuvenation product in flint. The quantity of flint cores is elevated, especially when compared to their relative weight. In addition, the frequent presence of cores on flake, despite presenting a small number of extractions, points at the intense exploitation of this lithic resource. The occasional presence of cortical areas and the high presence of negative scars on this raw material do also support the idea of intense exploitation. The distribution of weight is coherent with this hypothesis too. This is based on the frequent presence of small flakes and chunks, probably secondary products derived from knapping, retouching and reshaping processes. However, the majority of lithics is around 3.8 g. The presence of retouch on 20% of the pieces also reinforces the idea of an intense exploitation of flint.

The colour of flint pieces, mainly black, can give a hint on their origin, probably related with Palaeozoic Black cherts such as the Vegamián Formation (Herrero-Alonso et al., 2016). The only piece

where cortex could be characterised points at its possible fluvial origin. This indicates the context where catchment activities were carried out, secondary deposits. The information derived from the geological surveys conducted during this research and from other studies in the surrounding area (Álvarez et al., 2013; Manzano et al., 2005) reveals a negligible presence of flint in river beaches, reduced to small sizes and relatively tabular forms. Then, catchment activities must have necessarily implied intensive selection in fluvial deposits. These would have not been planned or based on systematic intense raw material exploitation strategies. Flint catchment would have been based on occasional findings in river courses as a result of casual transit or other activities. This high intensity exploitation of flint founded on the analysis of technological and metrical features suggests the qualitative importance of this raw material. Furthermore, quantitative information reveals the scarcity of this material. The interaction between qualitative and quantitative information unveils the importance of this raw material for human activities that maybe could have been related with knapping and use properties, but also with its scarcity. In addition, considering the presence of all types of technological products, we conclude that all phases of lithic reduction were carried out in the site. That is, flint knapping was probably performed in the site and it involved a first core intensively knapped to obtain blanks and artefacts for human activities, perhaps specialised. Still, we do not discard the input of some blanks or retouched artefacts already prepared from outside.

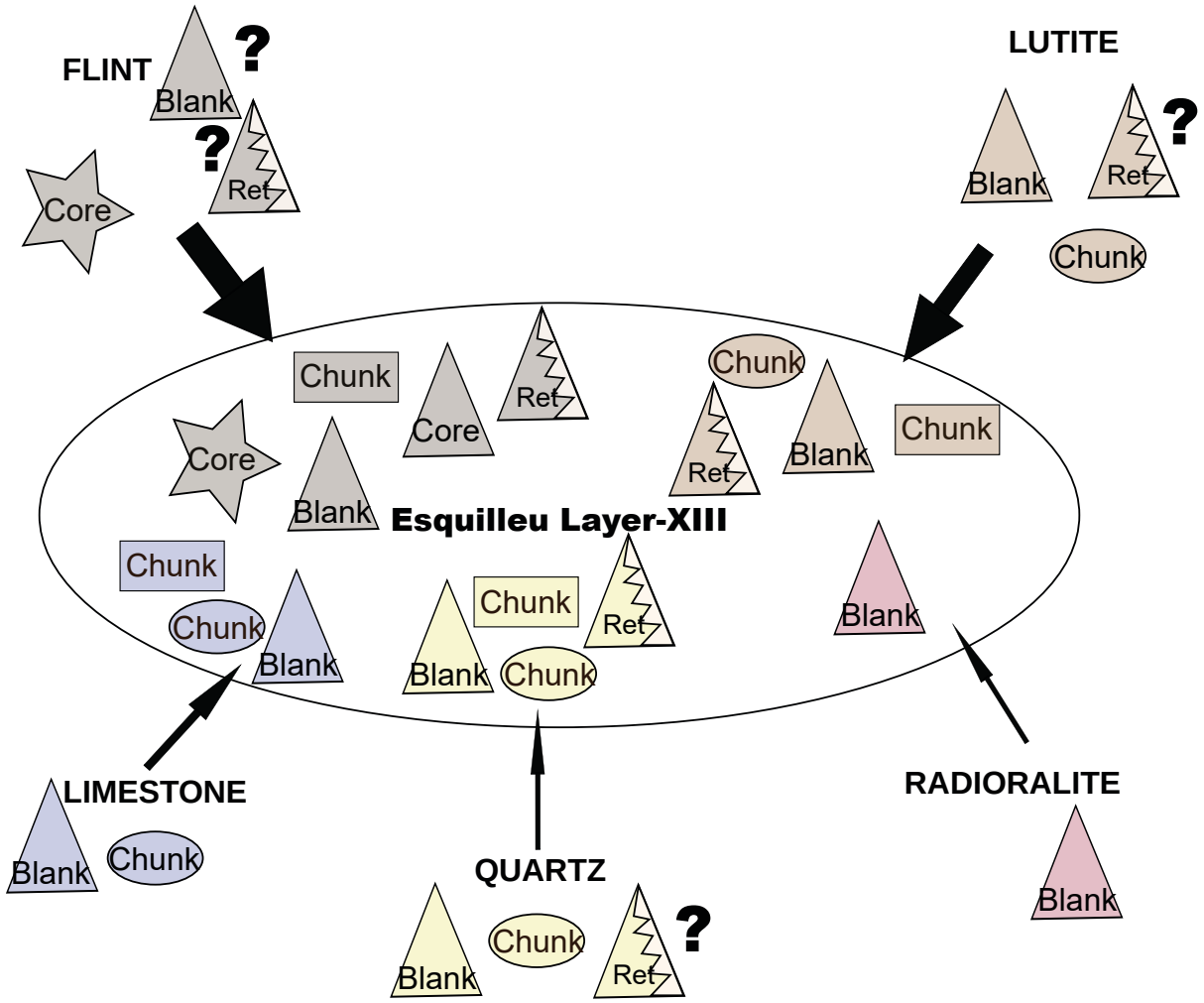

Figure-9.38: Schematic representation of the input of non-“archaeological quartzite” raw material, taking into account the different technological products present. Stars represent cores, triangles blanks, triangles with zig-zag retouched material, ellipses fully cortical chunks and rectangles chunks. Question marks indicate products whose presence is not certain.

The scarce presence of **lutites** reveals different patterns of acquisition and management. Not all technological products are present. Cores are absent, while knapping products are overrepresented. Chunks do also appear. The presence of cortical surfaces on lutite lithic remains is the highest of all types of raw material. All except one of the cortical areas come from fluvial beaches and most of them cover all stone surface. The association of this feature with weight classifies lutites in two

groups: The first one is formed by low weight chunks completely covered by cortex. Considering the absence of knapping traits, these lutites probably had no importance in lithic technology. Conversely, the second group of lutites, formed by knapping products and some chunks, would have certainly been related with knapping activities. Lutite blanks have weights around 2.84 g, similar to those of flint blanks, although three of them are significantly bigger. The presence of negative scars on dorsal surfaces is variable, but most of them have at least two or more. The majority of blanks are complete and their average weight is 6.2 g. There are also complete cortical dorsal surfaces and others with only one negative scar, generally lighter. We only found one retouched lutite, which presents two Denticulate retouches. The small and sometimes fragmented blanks could be part of the reshaping processes carried out for obtaining the denticulate. All these arguments lead us to propose a residual and non-intensive exploitation of lutites. The absence of cores and core preparation/rejuvenation products clearly indicates that some phases of knapping are absent in the site. Therefore, it can be concluded that lutites were carried as blanks.

Regarding the properties of this raw material, most lutites are grey to black and are similar to the siliceous cemented varieties found in the area around the site, in outcrops (associated to limestone, sandstone and conglomerate alternations from the Carboniferous), conglomerates (Carboniferous), and river deposits. Their presence in the latter two was analysed in this research, revealing changeable percentages generally higher than 10% of the rocks present in both types of contexts. This raw material has also been analysed in archaeological contexts from others regions, such as the Basque Country (Fernández-Eraso et al., 2017). The knapped lutites do usually present cortical areas and, although they mainly come from fluvial beaches, one of them derives from a conglomerate. All this information allow us to propose two different inputs of lutites to the site: a) the first one was probably casual and unconscious. It would be characterised by the transportation of small and completely cortical chunks from river beaches. Not coincidentally, these are similar in size and form to the matrix of river deposits. b) The second input would have been conscious and it would have been related with the use of lutites for knapping and other activities in the site. Its catchment is mainly carried out in river beaches, but it could have also taken place in other locations, such as conglomerates. Due to the absence of some technological products, it can be stated that this raw material was brought as blanks, probably obtained as secondary products of the exploitation of primary products in river beaches and conglomerates. The selection of siliceous cemented varieties is clear. Summing up, this raw material was only used sporadically, probably when other raw materials were scarce, and, therefore, it was not exploited intensively.

Limestone shows distinct patterns of acquisition and management. The technological characterisation reveals it is mainly represented by chunks and there is only one knapping product. The weight of the former (0.7 g/p) indicates they are small elements, generally completely covered by cortex. Then, as it happened with lutites, a first group of limestones has no importance in lithic knapping activities and it comes from casual and unconscious inputs. Chunks without cortical areas are also light in weight and they could derive from the wall of the cavity. However, the presence of a single blank in limestone may relate these chunks with secondary knapping products. This blank has two dorsal negative scars and no cortical surface. Therefore, we could not determine the source area of this unique blank. Still, the only other chunk of limestone with cortex (not covering the entire rock surface) points to its origin in fluvial deposits. The colour of all limestones is grey with different secondary colours. Nevertheless, we were unable to identify different varieties. Regarding their source area, we conclude the first group of limestones, constituted by small chunks completely covered by cortex, was probably carried unconsciously from river beaches. Actually, these pieces present sizes and forms similar to those of matrix from river deposits. The second group, formed by other small chunks and the blank, comes from fluvial deposits. However, it is not possible to discard some chunks (without fluvial cortical surface) to be rock fragments detached from the structure of the shelter. The exploitation of this second group is clearly residual and of low intensity. Others studies have previously proved the use of limestone as raw material in Middle Palaeolithic archaeological sites from Iberia (Eixea et al., 2016).

Quartz shows mixed acquisition and management strategies between those of limestone and flint. First of all, it is important to mention the scarcity of quartz in this layer, with only seven pieces identified. Not all types of technological products are present. Therefore, it was not possible to analyse the complete sequence of lithic reduction. More specifically, cores are absent, knapping products are underrepresented and chunks are overrepresented. Only one of the chunks presents any cortical surface, which reveals it fluvial origin. However, cortex covers completely the surface and weight is low. These two features allow us to propose this quartz to come from the matrix of a fluvial beach. The average weight of quartz implements is 2.2 g/p, without any clear difference between

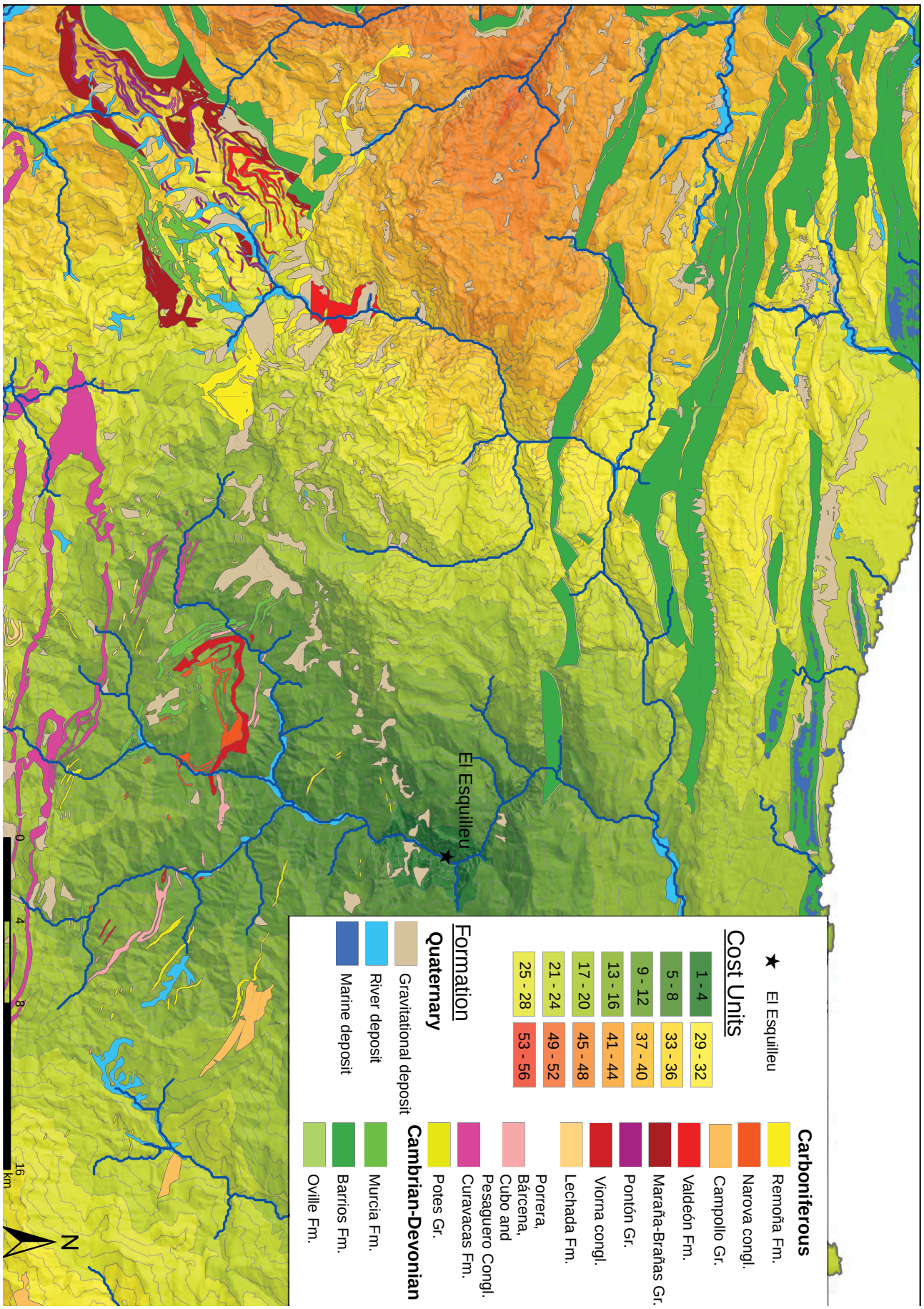

Figure-9.39: Cost map from the site of El Esquilleu to polygons with presence of “archaeological quartzites” and other raw materials.

chunks and knapping products. Still, two blanks, with 7.4 g of mean weight, are clearly heavier. These two pieces are retouched, creating two Sidescraper. There is another retouched small blank, which is a splintered piece. The remaining blanks, as well as the rest of the knapping products, are lighter than 1 g. Although we were unable to identify the complete lithic reduction sequence (due to the absence of cores and core preparation/rejuvenation products), small blanks and chunks derived from knapping and reshaping activities were recognised. In addition to the high percentage of retouched material, the great number of negative scars on the dorsal surfaces of blanks supports the idea of an intense exploitation of this material.

Regarding the properties of quartz, all of them are transparent, slightly white and none of them is an aggregate of different quartz crystals (except for the one completely covered by cortex). In the research area defined for this study we only identified quartz on fluvial deposits in negligible proportions, mainly in the headwaters of Deva and Cares rivers. Due to the scarcity of diagnostic elements to characterise the source area, we can only affirm they were caught in fluvial deposits. As it happened in the case of flint, the presence of quartz in these deposits is scarce. Then, the catchment of this material would have required strong selective mechanism. Still, the acquisition of quartz would have probably been more related with occasional findings rather than with intensive and planned raw material catchment strategies. The intensive exploitation of the material reveals its importance for prehistoric societies. However, considering the absence of cores, quartz was probably brought to the site as flakes and only reshaping processes were carried out in the site. We do not discard direct input of retouched pieces later reshaped in the site either. The presence of a small and fully cortical chunk points at its casual origin from river beach matrix and reflects similarities between quartz and the first group of limestones and lutites respectively.

The catchment and management strategies of **radioralite** are similar to of flint. Only five radioralites were found in the site. Therefore, the conclusions obtained, must be taken with caution. All the radioralites were classified as knapping products. All of them were low in weight, but one of them was clearly heavier. Only one blank has cortex covering entirely its dorsal surface. Its origin can be traced back to fluvial deposits. Regarding its exploitation, except for the blank with cortex, all blanks have at least two negative scars, revealing that this material was intensively exploited. However, we do not identify any retouched artefact. The full knapping process was carried out in the cave, as demonstrated by the presence of small blanks. Regarding the physical features of radioralites, all of them are red to brown and are characterised by the presence of Radiolaria fossils. We only find evidence of radioralite in the area surrounding the fluvial deposits of Cares and Deva rivers, in negligible proportions and small sizes. Therefore, catchment activities would have necessarily implied strong and intensive selection mechanisms, similar to those observed for flint. This means that the acquisition of radioralite would have been related with occasional findings, rather than with intensive and planned raw material selection strategies in river beaches.

All in all, we observe different catchment and management strategies for each raw material. This allows us to propose the following human mobility, landscape use, and selection and exploitation mechanisms:

- Low, medium and high-scale mobility strategies South and South-west of the research area, as well as outside it.
- Exploitation of diverse landscapes, from river courses in low altitudes areas to plateaus in medium altitudes zones.
- Selective and non-selective mechanisms for obtaining specific raw materials or petrogenetic types in deposits and conglomerates.
- Diversity of raw materials exploited, selected based on their physical properties and their availability in the landscape.

CHAPTER-10

RESULTS. THE LAYER-VI FROM THE ARCHAEOLOGICAL SITE OF EL ESQUILLEU

10.1. GENERAL ISSUES AND STATE OF PRESERVATION OF THE COLLECTION

The archaeological site of El Esquilleu is a small cave situated in the Cantabria Autonomous Community near the villages of Lebeña and Allende. It is situated 100 meters away from the left margin of the Deva River and 70 meters above it. The cave is within the Valdeteja Formation, mainly composed of massive limestone. Cliffs, defiles, talus slopes, moraines, caves and deep gorges are the most important geomorphological features in the area surrounding El Esquilleu Cave. The area is crossed by the Deva River valley that creates a deep and narrow gorge in North-South direction called The Hermida Defile, where the cave is located. The excavation of the site was directed by Dr. Javier Baena Preysler between 1997 and 2006 trying to understand the Middle Palaeolithic societies of the area through a diachronic perspective. The sequence was entirely excavated, at leas in a four meters pit. The stratigraphic depth was 4.20 meters and it was divided into 41 layers (29 with anthropic evidences). Although the research processes in El Esquilleu Cave is still in progress, several studies have already been carried out by different specialist.

In general, the information provided by all perspectives, previously commented in chapter-2, offered interesting perspectives about the human groups who inhabited this cave in Prehistoric times, especially during the late Middle Palaeolithic. In general terms, the sequence of El Esquilleu Cave showed sophisticated strategies of habitat and land use by Neanderthals groups, which were modified through time according to environmental conditions and cultural, social and economic circumstances (Baena et al., 2012). Summing up, we can say that El Esquilleu is one of the most important archaeological sites in the Cantabrian Region for understanding the last Neanderthal groups in the Iberian Peninsula.

The layer-VI-F is the first and the earliest analysed layer in this research. Sedimentological, this layer is in the second part of the sequence, ESQ-B, and it is mainly composed of clastic (gravel) autochthonous materials and small percentages of sandy and calcareous matrix. The sedimentary process that created this unit was related to frost weathering and widespread flooding activities which affected this open cave. This unit showed good preservation but its internal structure had been affected by cryoturbation, as a consequence of the frost weathering (Jordá et al., 2008; Mallol et al., 2010). There is one numerical date obtained from Layer-VI-F (AA37883 = 34380 ± 670 BP) which agree with the general sequence of El Esquilleu Cave, making this layer as one of the earliest Middle Palaeolithic in Cantabrian Region (Baena et al., 2012; Cuartero et al., 2015; Maroto et al., 2012). During the formation of Layer-VI-F, paleoenvironmental conditions are related with mesophilic taxa and a more closed landscape, even *Pinus* is still represented. Faunal analysis point at the main consumption of *Capra* and *Capra rupicabra*. The bones have no marks from carnivores, therefore, humans is the main agent who introduced fauna in the site during the formation of this layer. In addition, most of the bones are burned and extremely fractured, probably used as fuel for fires or because sanitary purposes (Yravedra and Gómez-Castanedo, 2014; Yravedra and Uzquiano, 2013). Concerning to lithic raw material, previous studies point that “archaeological quartzite” is the better represented raw material in the layer. Nevertheless, ferruginous rocks, flint, or limestone are also represented. The techno-typological characterisation of the layer concludes that main reduction sequence used is the discoid reduction method (Baena et al., 2005; Carrión et al., 2008; Carrión et al., 2013).

The archaeological assemblage analysed here is a sample of the complete collection. The complete set from this layer is formed by 1,123 lithics. We analysed the complete lithic assemblage from the square J-11, with a total of 301 items, 27% of the whole collection. Most of the pieces were not previously washed to preserve possible residues or use/hafting-wear marks to be analysed in the future. In the cases where no part of the surface was clean enough, I washed a small portion of it in order to obtain a clear analysis surface. We did not find important presence of carbonates in the surface of lithics, as previously pointed out by Jordá et al. 2008. Nevertheless, on some of them, carbonate precipitates did not allow to observe the surfaces of the stones. We also find clayey minerals in some of the lithic surfaces, creating dirt surfaces. Finally, a negligible part of the lithic materials presented evidence of chemical weathering altering cortical areas, non-deformed/metamorphic surfaces or jointed areas. Therefore, the general state of preservation is medium.

10.2. PETROLOGICAL STRUCTURE

Here we present the results of raw material characterisation. We were able to determine the main lithology of every piece except on one. In general, the collection is massively formed by “archaeological quartzites” although lutite is well represented as the second most important raw material. Finally, there is a residual representation of flint, limonite, limestone, and quartz (Table-10.1).

Main Raw Material	Archaeological quartzite	Flint	Limestone	Limonite	Lutite	Quartz	Radioralite	Volcanic rock	Undeterminate
Σ	213	3	2	3	78	1	0	0	1
%	70,8	1,0	0,7	1,0	25,9	0,3	0,0	0,0	1,0

Table-10.1: Frequency table of lithologies in layer-VI from the archaeological site of El Esquilleu.

Focussing on “archaeological quartzite”, we could identify through binocular microscopy the seven petrogenetic types proposed. Orthoquartzites are massively represented in more than 50% of the lithic implements. The quartzites are the second most important group especially to the great frequent of BQ petrogenetic type. Finally, the group of quartzarenite group is underrepresented, with 13% of the lithics (Table-10.2). We were unable to identify five items, 4% of the collection. Coming to the distribution of grain size, the most frequent category is heterogeneous distribution mode with 52% of the cases, even though homogeneous distribution around one mode is also well represented with 37% of the cases. Regarding grain size, the most frequent categories are fine and medium grain sizes. As to “archaeological quartzite” types and quartz grain size varieties, we identify two preferential varieties: The OO, characterised by heterogeneous distribution of medium grains, and the SO type characterised by homogeneous distribution around fine grain size. Moreover, OO type with one mode distribution around medium grain size, SO type with heterogeneous distribution around fine and medium grain sizes, and BQ type with homogeneous distribution are also well represented. Chi-square test (χ^2 (30, N = 205) = 152.446, p < .001) reinforces the idea of a preferential acquisition of these varieties.

			Petrogenetic type																	
			CC		CA		OO		SO		BQ		RQ		MQ		Unknow		Total	
			Σ	%	Σ	%	Σ	%	Σ	%	Σ	%	Σ	%	Σ	%	Σ	%	Σ	%
Grain size characterisation	Homogeneous and one mode distribution	Fine grain			2	10			**23**	**36**	17	52	7	64	1	10	1	13	51	24
		Medium grain					19	33	1	2					7	70			27	13
		Coarse grain																		
	Heterogeneous and two modes distribution	Fine grain			1	5			8	13	8	24					1	13	18	8
		Medium grain																		
		Coarse grain																		
	Heterogeneous distribution	Fine grain	3	33	5	25	7	12	14	22	3	9	3	27	1	10	1	13	37	17
		Medium grain	4	44	10	50	**29**	**50**	18	28	5	15	1	9	1	10			68	32
		Coarse grain	2	22	2	10	3	5											7	3
	Unknown																5	63	5	2
		Total	9	4	20	9	58	27	64	30	33	15	11	5	10	5	8	4	213	100

Table-10.2: Frequency table of petrological features identified in layer-VI from El Esquilleu based on binocular characterisation. Columns are petrogenetic types and rows contain the characteristics of grains according to size, classified first by distribution and second by size itself. Cells in black are the categories representing more than 10% of total cases. Cells in dark grey are the categories representing between 5 and 10% of cases. Finally, cells in light grey are the categories representing between 1 and 5% of cases.

Non-quartz mineral	A		B		C		General	
	Σ	%	Σ	%	Σ	%	Σ	%
Absence	7	3	7	3	8	4	22	3
Fe-Oxides	202	95	2	1			204	32
Manganese Oxides	1	0	25	12	64	30	90	14
Calcites								
Micas	1	0	85	40	30	14	116	18
Black mineral			94	44	109	51	203	32
Pyrites	2	1			1	0	3	0
Feldspars					1	0	1	0
Total	213	100	213	100	213	100	639	100

Table-10.3: Frequency table of non-quartz minerals identified in layer-VI from El Esquilleu based on binocular characterisation. Columns are the three fields examined and rows are the non-quartz minerals identified.

Colour	On fresh cut			
	Primary		Secondary	
	Σ	%	Σ	%
Absence	5	2	82	38
White	8	4	25	12
Grey	177	83	14	7
Black	18	8	59	28
Blue			9	4
Green			1	0
Orange			3	1
Brown	5	2	17	8
Yellow			1	0
Red			2	1
Total	213	100	213	100

Table-10.4: Frequency table of colour hue of the artefacts from layer-VI from El Esquilleu. Columns are primary and secondary colour hues and rows are the colours considered.

We identified non-quartz minerals in 213 samples of “archaeological quartzite”, after having excluded the lithics assigned to unknown type (Table-10.3). Non-quartz mineral characterisation reveals the massive presence of iron oxides, non-identified black minerals, micas, and manganese oxides. The first two minerals are not associated to any petrogenetic type, even though micas are associated to OO type and manganese oxides to SO and BQ types. There are no other associations between minerals and petrogenetic types. The characterisation of colour indicates that most frequent colours are grey, white, black, and brown (Table-10.4). The first one is not associated to any petrogenetic type. Most of the white coloured “archaeological quartzites” are associated with OO, RQ, and MQ types. Dark colours are associated with SO and BQ petrogenetic types. Finally, brown coloured lithics are associated with quartzarenites and BQ quartzite. The presence of other colours, such as blue, red, green or yellow is restricted to small areas or to surfaces of quartzites. Therefore, they are not so frequent.

10.2.1. NON-DESTRUCTIVE CHARACTERISATION OF CC, CA, OO, SO, BQ, RQ AND MQ PETROGENETIC TYPES AT EL ESQUILLEU, LAYER-VI

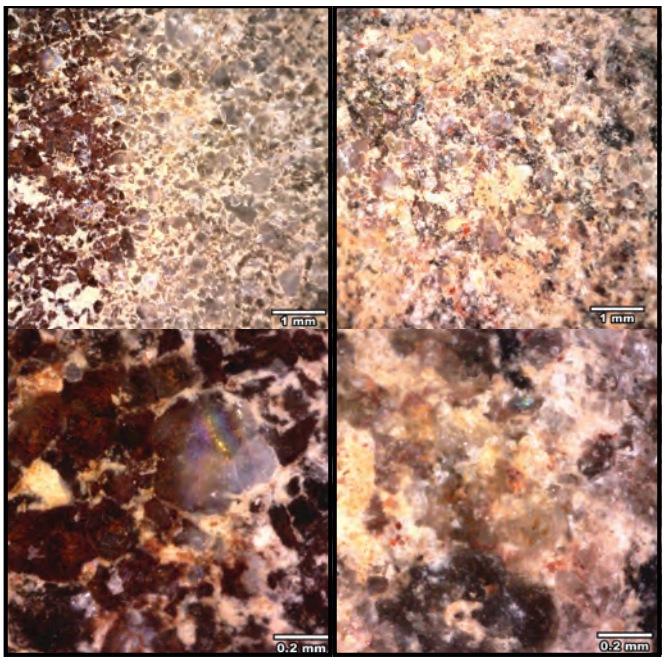

We did not select lithics for destructive characterisation due to the small quantity of lithic remains in the layer and the presence of petrographic samples from El Esquilleu rockshelter to define and characterise “archaeological quartzites”. Therefore, in this section we defined each petrogenetic type according to non-destructive characterisation.

The CC petrogenetic type is slightly represented in the layer with 4% of “archaeological quartzites”. Under binocular microscopy,

Figure-10.1: Pictures of the CC type from layer-VI of the archaeological site of El Esquilleu. From left to right, ES-021, is a CC type with coarse grain size and heterogeneous distribution, and ES-116, has fine grain size and heterogeneous distribution. Carbonated clays are observables in the surface of the second sample. Upper rows show microscopy binocular pictures at 50x. Lower rows show microscopy pictures at 250x.

most of them have coarse grained texture with floating or punctual packing (i.e. saccharoid T&P). Quartz grain features vary from plain and angular to plain and rounded ones. There are ruffled limits between grains that arise as consequence of the cement (Figure-10.1). A portion of the lithics has bedding structures. Quartz grain size characterisation points at the high frequency of heterogeneous distribution ranging between fine and coarse grain sizes. Mineral characterisation point at the massive presence of manganese and iron oxides, micas, and non-identified black and heavy minerals in most of the materials. Colour characterisation shows multiple colour varieties attending to the complete assemblage. In addition, most of the samples have different colours. Nevertheless, most of the lithics are black, brown, white, or grey. The first two are major.

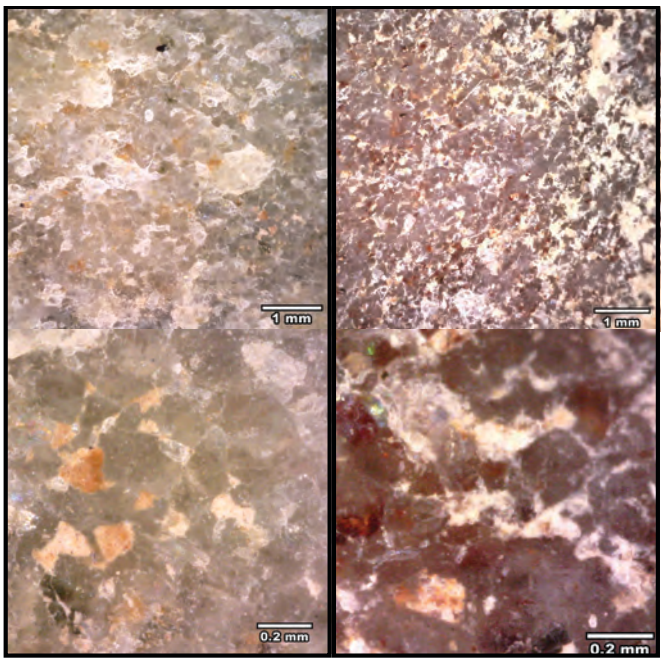

Figure-10.2: Pictures of the CA type from layer-VI of the archaeological site of El Esquilleu. From left to right, ES-126, is composed by medium sized grains, heterogeneously distributed, and it is light-grey; and ES-116 which has fine quartz grain sizes in heterogeneous distribution and it is grey-brown coloured. Upper rows show microscopy binocular pictures at 50x. Lower rows are microscopy pictures at 250x.

The CA petrogenetic type is better represented in this assemblage than previous type with 9% of “archaeological quartzites”. Under binocular microscope most of the textures are coarse grained, although fine grained textures are also observable. Packing is generally tangent or tangent-complete. Grains are easy to recognise, with rounded or angular borders. The presence of cement is small or absent. Granular T&P is clear in this petrogenetic type. The grain size of this type is heterogeneous, although there are also some lithics with homogeneous distributions. All grain sizes are represented, but more frequent one is the medium size (Figure-10.2). The distribution of non-quartz minerals reveals is more homogeneous than on the previous type. The most frequent minerals are iron and manganese oxides, micas, and non-identified heavy and black minerals. Feldspar presence is scarce, as pyrite. The most frequent colour is dark-grey, followed by brown, and less importantly, white. The first is associated with manganese oxides, while the white quartzarenite with micas.

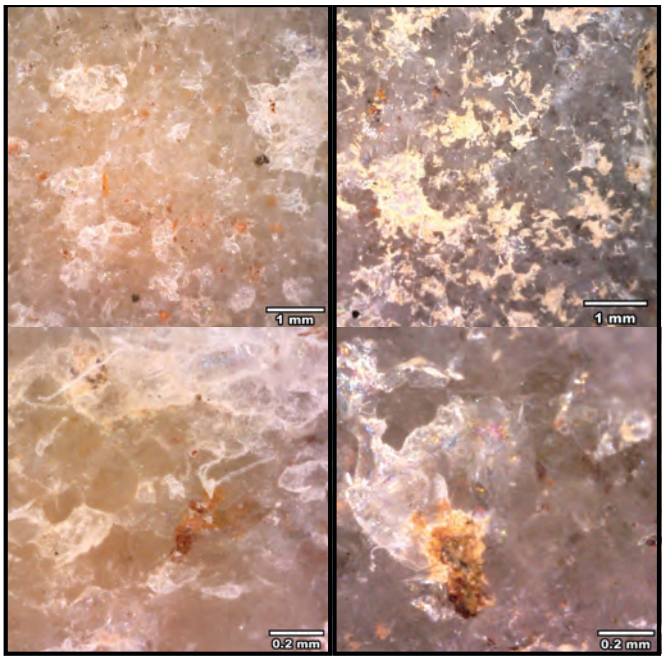

Figure-10.3: Pictures of the OO orthoquartzite from layer-VI of the archaeological site of El Esquilleu. From left to right, ES-004, is an OO type with medium grain size and homogeneous distribution and white colour. ES-231 is another OO type with coarse grain size, heterogeneous distribution and grey colour. Upper rows show microscopy binocular pictures at 50x. Lower rows show microscopy pictures at 250x.

The OO petrogenetic type is the second better represented “archaeological quartzite” in the lithic collection, 27%. Under binoculars, packing is complete and the most frequent texture is fine grained one, even though some are classified as coarse grained textures. Best represented quartz grain features are concavo-convex grain boundaries, generally with regrowth structures. Cement is absent in these orthoquartzites. Therefore, compact grainy T&P is recognise in all samples. The grain size of this type is massively represented by medium size quartz grains in either heterogeneous or homogeneous distribution. In addition fine and coarse grain sizes are described in heterogeneous distribution (Figure-10.3). Mineral characterisation of samples point at most of OO lithics have iron oxides,

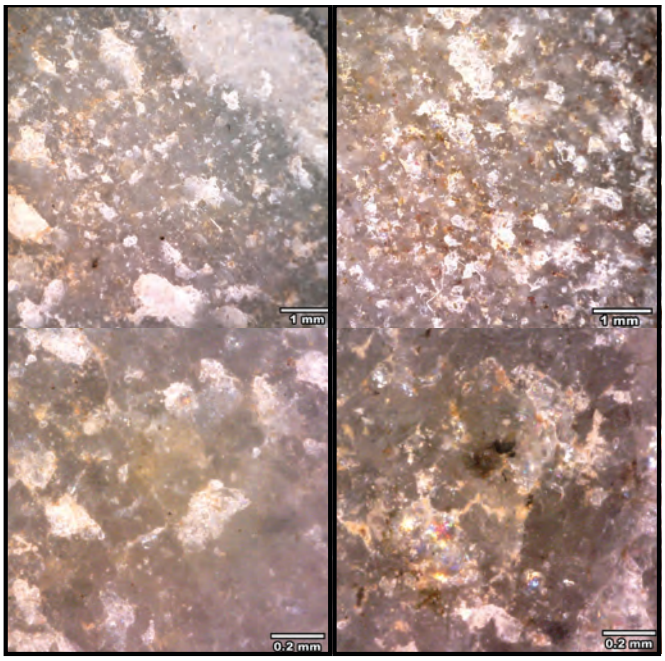

Figure-10.4: Pictures of the SO orthoquartzite from layer-VI of the archaeological site of El Esquilleu. From left to right, ES-005 is a SO type with medium grain size, homogeneous distribution and grey-white coloured. ES-006 is another SO type with fine grain size, heterogeneous distribution and grey coloured. Upper rows show microscopy binocular pictures at 50x. Lower rows show microscopy pictures at 250x.

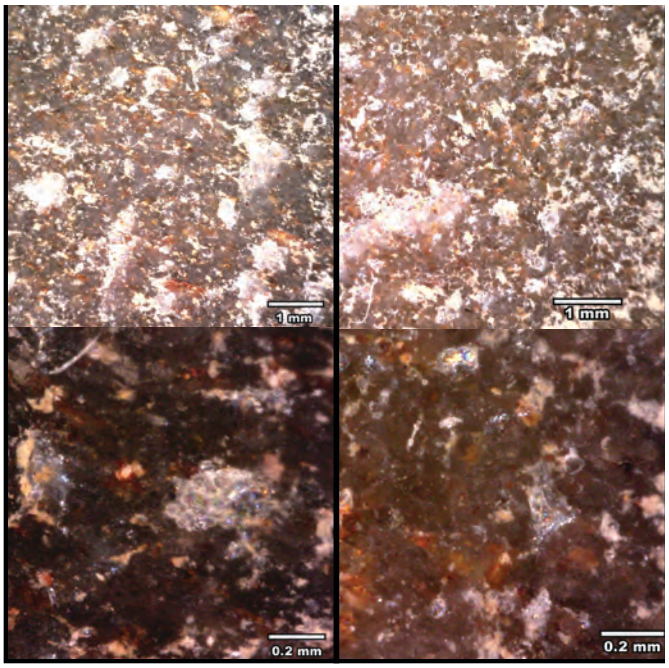

Figure-10.5: Pictures of the BQ quartzite from layer-VI of the archaeological site of El Esquilleu. From left to right, sample ES-127 is a BQ type composed by fine size quartz grains with homogeneous distribution and black coloured (also some red oxides). The sample ES-092 is a BQ type composed by fine size quartz grains with homogeneous distribution and brown coloured. Upper rows show microscopy binocular pictures at 50x and lower rows are microscopic pictures at 250x.

non-identified black and heavy minerals, and micas. The latter is clearly associated to this petrogenetic type. In addition, there are some OO orthoquartzites with manganese oxides, associated with iron oxides. The colour characterisation points at the massive presence of white or grey-clear varieties, in association with micas. The black or grey-black lithics are associated with manganese oxides, although their presence is scarce.

The SO petrogenetic type is the best represented type with 33% of the lithic assemblage. Under binoculars we recognised suturated packing and fine grained textures, also some fines ones. Quartz grains are not easy recognise than on previous orthoquartzite, even it is possible to observe some borders. In case they are observables they are fine, and generally create ruffle borders. Foliation structures are recognisable in some lithics. All SO orthoquartzites are classified as fine and grainy T&P. The grain size of these orthoquartzites evidences points that most of them have fine grains, even some lithics have medium grain sizes. Most SO orthoquartzites have homogeneous distribution of quartz grains, although heterogeneous distribution is also represented. Therefore, there are different grain size varieties. The non-quartz mineral characterisation shows that most frequent minerals are iron and manganese oxides, micas, and non-identified dark and heavy minerals. The association of them with the colour of lithics reveals that manganese oxides are related with dark or grey-dark varieties representing 33% of the SO assemblage. Grey or light-grey orthoquartzites are associated with micas, and they have a major representation in the layer. Therefore, two different colour-mineral varieties of SO type coexists in the layer (Figure-10.4).

The BQ petrogenetic type is well represented in the layer with 15% of lithics. Most of them are described under binoculars with fine texture and suturated packing, generally with high brightness or luster. Grains cannot be clearly detected but in others, it is possible to observe ruffled borders: fine T&P. The quantity of surface micro-cracks is smaller than on previous orthoquartzite. Coming to grain size characterisation, most of the pieces analysed are within the fine grain category, generally with homogeneous distribution. There are also some BQ quartzites with heterogeneous distribution of quartz grains in small incidence (Figure-10.5). The non-quartz mineral distribution points at the massive presence of manganese and iron oxides, and non-identified black and heavy minerals. The presence of micas is more reduced than on other types.

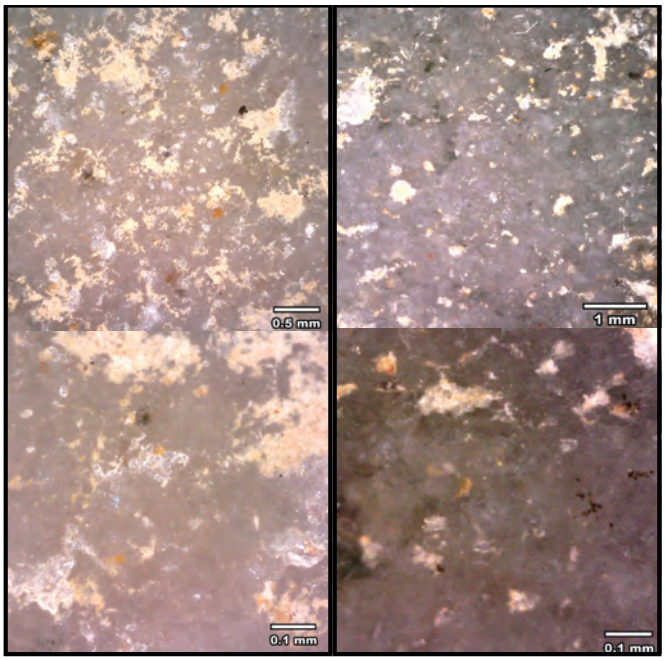

Figure-10.6: Pictures of the RQ quartzite from layer-VI of the archaeological site of El Esquilleu. From left to right, ES-125 is a RQ type composed by quartz grains with medium size heterogeneously distributed and grey-white coloured. ES-193 is a RQ type with fine size quartz grains heterogeneously distributed and dark-grey coloured. Upper rows show microscopy binocular picture at 50x. Lower rows are microscopy pictures at 250x.

Colour characterisation reveals that most of them are dark-grey or black, although there are also some brown quartzites. We do not observe clear differences in colour/mineral varieties, neither in grain size characterisation.

There are only eleven lithics characterised as RQ petrogenetic type, 5% of the assemblage. Under binoculars, these quartzites are characterised by soapy texture without clear grain boundary detection. The luster is high and micro-cracks are limited: Soapy T&P. All except one RQ quartzites are fine grained, generally with homogeneous distribution of quartz grains. Iron oxides, micas and non-identified heavy and dark minerals are the most frequent non-quartz minerals detected on quartzite surfaces. Nevertheless, there are also manganese oxides and pyrite in two quartzites. These quartzites have darker colours than others, generally in grey or light-grey. Therefore, there are two varieties, even though the small quantity of this quartzite type and the lack of other analysis. Therefore, conclusion obtained must be nuance (Figure-10.6).

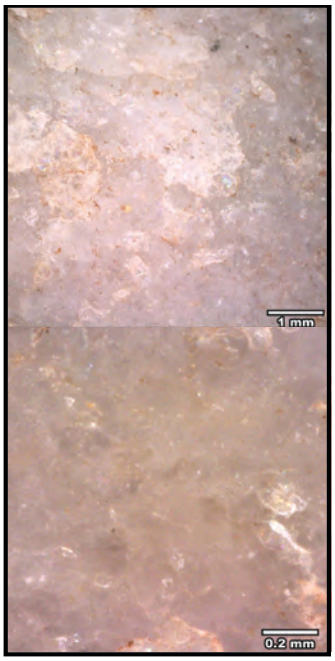

The last petrogenetic type here analysed is the MQ quartzite type, the second worst represented type in the assemblage with ten items. They are characterised by soapy texture and no grain detection. Nevertheless, it is possible to recognise some and partial grains, especially at 50x magnifications. The luster is high and the presence of micro-cracks is variable. Attending to grain size, most of them are classified as medium sizes and they are homogeneously distributed. Non-quartz mineral detection shows the same association in all MQ quartzite: micas, non-identified, heavy and black minerals and iron oxides, all of them in small proportion. The colour of these quartzites is light-grey or white, even small orange areas are appreciated around iron oxides (Figure-10.7).

Figure-10.7: Pictures of the MQ quartzite from layer-VI of the archaeological site of El Esquilleu. ES-219 is a MQ type composed by medium size quartz grains homogeneously distributed and white coloured. Upper row shows microscopy binocular picture at 50x and the lower row is a microscopic picture at 250x.

10.2.2.CHARACTERISATION OF CORTICAL AREAS FROM EL ESQUILLEU, LAYER-VI

Here we present the result of the characterisation of cortical areas. The distribution of cortex in the lithics analysed between different types of raw material is shown in Table-10.5. “Archaeological quartzite” is the most frequent raw material with cortical areas (30%), which is in accordance with its predominance in the whole assemblage. The quantity of lutites with cortex is reduced to 20%. There is only one flint with cortex. Due to the small quantity of the latter raw material the relative percentage is the highest (33%). Other identified raw material have no cortical areas.

Raw material	Cortex type												∑ of each type
	Conglomerate			Fluvial			Unknown			Total			
	∑	%	% rel	∑	%	% rel	∑	%	% rel	∑	%	% rel	
Archaeological quartzite	15	100	7	39	72	18	10	83	5	64	79	30	213
Flint				1	2	33				1	1	33	3
Limestone													2
Limonite													3
Lutite				14	26	18	2	17	3	16	20	21	78
Quartz													1
Unknown													1
Total	15	19	5	54	67	18	12	15	4	81	100	27	301

Table-10.5: Frequency table of types of cortex identified in layer-VI from El Esquilleu grouped by main raw material. Columns are types of cortex, including the frequency of each cortex type for each raw material and the total of items with cortex of each raw material. The last column quantifies the total of items with and without cortex of each raw material. The columns % are the percentage of each raw material in relation to each cortex type, while the columns % rel. are the percentage of cortex type in relation to the total of each raw material (including items with and without cortex).

Regarding the types of cortex, 15% of the cortical areas could not be characterised due to the absence of diagnostic features. None of the cortex types identified could be interpreted as evidence of direct extraction from the outcrop.

Conglomerate cortex is underrepresented, representing 19% of the lithic implements with cortical areas. All 15 pieces are on “archaeological quartzite”. Conglomerate cortical areas are characterised by the presence of cements from the conglomerate itself, which are generally recognisable as red iron oxides or dark silica precipitates. In addition, voids are usually present, even though they are generally filled with conglomerate cement, generally in black colour. No clear impact cracks are observable on cortical areas.

Cortical areas from fluvial sources is the most frequent cortex type, representing 67% of the cortical areas analysed. “Archaeological quartzite” is again the most frequent raw material among the lithics with this type of cortex. There are also cortical areas derived from fluvial deposits in flint and lutites. Fluvial cortex areas is mainly characterised by the presence of impact cracks in the surface and fine or soapy textures. Voids are less frequent in this cortex type and cement is absence (except for the carbonated clay stuck on the whole surface due to post-depositional processes).

Archaeological quartzite	Cortex type												∑ of each type
	Conglomerate			Fluvial			Unknown			Total			
	∑	%	% rel	∑	%	% rel	∑	%	% rel	∑	%	% rel	
CC				5	13	56				5	8	56	9
CA				7	18	35				7	11	35	20
OO	2	13	3	13	33	22	3	30	5	18	28	31	58
SO	7	47	11	8	21	13	4	40	6	19	30	30	64
BQ	5	33	15	1	3	3	1	10	3	7	11	21	33
RQ				3	8	27	1	10	9	4	6	36	11
MQ													10
Unknown	1	7	13	2	5	25	1	10	13	4	6	50	8
Total	15	23	7	39	61	18	10	16	5	64	100	30	213

Table-10.6: Frequency table of types of cortex identified in layer-VI from El Esquilleu grouped by petrogenetic types. Columns are types of cortex, including the frequency of each cortex type for each petrogenetic type and the total of items with cortex of petrogenetic type of material. The last column quantifies the total of items with and without cortex of each petrogenetic type. The columns % are the percentage of each type in relation to each cortex type, while the columns % rel. are the percentage of cortex type in relation to the total of each petrogenetic type (including items with and without cortex).

Focussing on the distribution of cortex among “archaeological quartzites” and their different petrogenetic types, there is a clear overrepresentation of cortical areas among the CC petrogenetic type. They are less frequent among CA and RQ petrogenetic types. Conversely, material with cortex are underrepresented among the BQ type (Table-10.6). The remaining petrogenetic types show percentages of items with cortex around 30%, similar to those of “archaeological quartzites” as a whole.

Cortical areas from conglomerates are underrepresented in “archaeological quartzites”, while fluvial contexts are overrepresented. There are differences when sorting them by petrogenetic types. Chi-square test (χ^2 (5, N = 51) = 19.366, p = .002) statistically confirms these differences and standardised residues, in Figure-10.8, graphically shows them. The fluvial cortex type is overrepresented in the quartzarenite group, the OO type and the RQ type (conglomerate cortex in these types is only represented in the OO type). In the SO type, both types of cortex are similarly distributed, and in the BQ quartzite there is only one lithic derived from fluvial deposits.

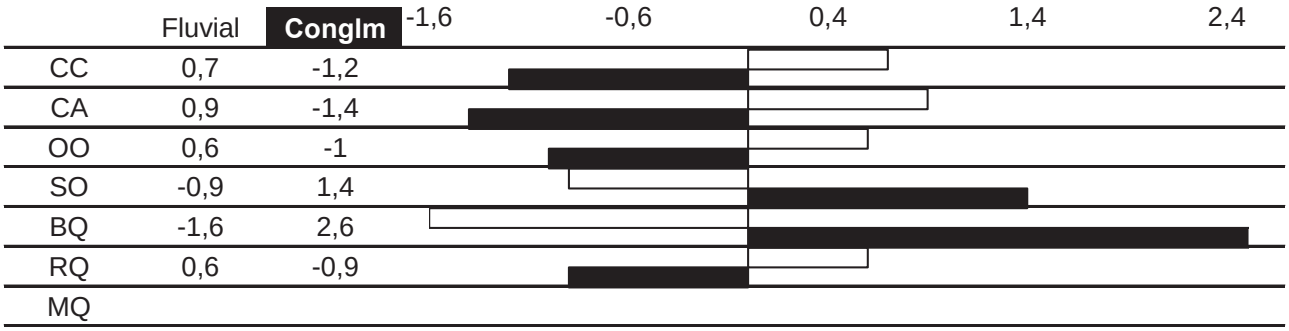

Figure-10.8: Standardised residues of χ^2 test of “archaeological quartzites” with cortex, showing the weight of each type of cortex in different petrogenetic types.

10.3. TECHNOLOGICAL STRUCTURE

Here we present the results of the technological analysis of the material from layer-VI taking into account the results from the petrological structure. The most frequent category is the knapping product (87%), followed by core (8%), and chunk (6%). The distribution of technological products shorted by main lithologies is shown in Table-10.7. Cores are restricted to “archaeological quartzite” and lutite. Knapping products are well represented in all raw material, except on quartz and limestone. The only quartz is a chunk. In limestone, one item is a knapping product and another is a chunk. In contrast, chunks are not represented on flint and limonite, and they are underrepresented on “archaeological quartzites” and lutite.

	Technological order										
	Cores			Knapping prdct.			Chunk			Total	
	∑	%	% rel	∑	%	% rel	∑	%	% rel	∑	%
Arch. Quartzite	17	74	8	**186**	**71**	**87**	10	59	5	213	71
Flint				3	1	100				3	1
Limestone				1	0	50	1	6	50	2	1
Limonite				3	1	100				3	1
Lutite	6	26	8	**67**	**26**	**86**	5	29	6	78	26
Quartz							1	6	100	1	0
Unknown				1	0	100				1	0
Total	23	8	8	261	87	87	17	6	6	301	100

Table-10.7: Frequency table of main technological categories identified in layer-VI from El Esquilleu grouping by raw material. Columns are the main technological categories and the total of items of each raw material. The columns % are the percentage of each raw material in relation to each technological category, while the columns % rel. are the percentage of each technological category in relation to each raw material. Cells in black are the categories representing more than 10% of the total cases. Cells in dark grey are the categories representing between 5 and 10% of cases. Finally, cells in light grey are the categories representing between 1 and 5% of cases.

Focusing the analysis on “archaeological quartzites”, the cores are restricted to CA, OO, SO, BQ, and RQ types (Table-10.8). However, they are reduced to 5% in all of them, except for the BQ, and RQ types with greater representation. Note that on latter type there are only eleven lithics. Knapping products are well represented on every type, although on RQ and quartzarenite group, its percentages are smaller to the mean (<87%). Finally, chunks are better represented on quartzarenite group than on more deformed or metamorphic types.

	Technological order										
	Cores			Knapping prdct.			Chunk			Total	
	∑	%	% rel	∑	%	% rel	∑	%	% rel	∑	%
CC				7	4	78	2	20	22	9	4
CA	1	6	5	17	9	85	2	20	10	20	9
OO	2	12	3	**55**	**30**	**95**	1	10	2	58	27
SO	5	29	8	**56**	**30**	**88**	3	30	5	64	30
BQ	6	35	18	**26**	**14**	**79**	1	10	3	33	15
RQ	3	18	27	8	4	73				11	5
MQ				10	5	100				10	5
Undetermined				7	4	88	1	10	13	8	4
Total	17	8		186	87		10	5		213	100

Table-10.8: Frequency table of main technological categories identified in layer-VI from El Esquilleu grouped by petrogenetic types of “archaeological quartzites”. Columns are the main categories and the total of items belonging to each petrogenetic type. The columns % are the percentage of each petrogenetic type in relation to each technological category, while the columns % rel. are the percentage of each technological category in relation to each petrogenetic type of “archaeological quartzite”. Cells in black are the categories representing more than 10% of the total cases. Cells in dark grey are the categories representing between 5 and 10% of cases. Finally, cells in light grey are the categories representing between 1 and 5% of cases.

10.3.1. CORES

We have identified 23 cores in the whole collection. The most frequent type of core is discoid ones with eleven, followed by irregular cores, with seven, and core on flakes with four items. There is only a levallois core. There is no clear correlation between type of core and the raw material, neither with petrogenetic “archaeological quartzites” types (Table-10.9).

	Type of core				
	Irregular	Discoid	Levallois	On flake	Total
Other RM	1	3	1	1	6
CC					
CA				1	1
OO	1	1			2
SO	2	2		1	5
BQ	1	4		1	6
RQ	2	1			3
MQ					
Undetermined					
Total	7	11	1	4	23

Table-10.9: Frequency table of types of cores identified in layer-VI from El Esquilleu grouped by petrogenetic types of “archaeological quartzite”. Columns are the types of cores. In this case the only other RM (raw material) is lutite.

The discoidal cores are represented in this layer by ten complete items and one other fragmented core. Three are made on lutite, and the others on “archaeological quartzites”. Among the latter, BQ quartzite (four items) is the best represented type, even there are cores made on orthoquartzites and RQ quartzite. All ten discoidal cores have more than three percussion platform and two flacking surfaces. It is clear the same technique, with alternative and consecutive extractions, was used. In some cases, especially in lutite cores it is observe elongated scars in one of the flacking surface

creating slightly pyramidal shapes. The presence of cortical zones is restricted to six cores (orthoquartzites, quartzites, and lutites), always in smaller extension than 33%. Two of them derived from river deposits (lutite and OO orthoquartzite) and other three from conglomerates.

The irregular cores from this assemblage are diverse. Lutites and "archaeological quartzites" are well represented. In the latter, they are similar distributed between both orthoquartzites and quartzites. Most of the cores (6) are fractured while only one is complete (the core on lutite). The number of percussion platforms and flacking surfaces is varied and the three categories are similarly represented. No clear standardisation is appreciated in this type of cores. Coming to the presence of cortical areas, only two preserve cortex: the core on lutite, in smaller proportion than 33% and one of the RQ quartzite core, between 33 and 66% of its surface. Both cortex derived from fluvial deposits.

Cores on flake is the third better represented type of core with four items. Three are fragmented and only one is complete. The most common raw material for this type of cores is, again "archaeological quartzites" with three items, although there is also a lutite one. Regarding the type of "archaeological quartzites" present, there is one on CA quartzarenite, one on SO orthoquartzite, and another one is made on a BQ quartzite. All of them have only one percussion platform and another flacking surface. Only the CA core has cortical area, covering high extension than 66% of its dorsal surface. This zone reveals the origin of the quartzarenite in a fluvial deposit.

Finally, there is one levallois core made on lutite. This core is complete and it has more than three percussion platform and two flacking surfaces. The extension of cortex is reduced than 33% of its surface, and it derives from fluvial deposits.

10.3.2. KNAPPING PRODUCTS

In the lithic assemblage from Layer-VI we identified 261 knapping products. The most frequent type is blank, with more than 98% of the items analysed. Core preparation/rejuvenations elements are scarce forming less than 2% of knapping products. Finally, we do not identify any burin spall. The core preparation/rejuvenation elements are only found on "archaeological quartzites" (Table-10.10).

	Knapping products							
	Blanks			Core preparation/rej			Total	
	∑	%	% rel	∑	%	% rel	∑	%
Other RM	**75**	**29**	**100**				75	29
CC	6	2	86	1	25	14	7	3
CA	17	7	100				17	7
OO	**54**	**21**	**98**	1	25	2	55	21
SO	**55**	**21**	**98**	1	25	2	56	21
BQ	**25**	**10**	**96**	1	25	4	26	10
RQ	8	3	100				8	3
MQ	10	4	100				10	4
Unknown	7	3	100				7	3
Total	257	98		4	2		261	100

Table-10.10: Frequency table of the categories of knapping products identified in layer-VI from El Esquilleu grouped by the petrogenetic types of "archaeological quartzite". Columns are the categories of knapping products and the total of items belonging to each petrogenetic type. The columns % are the percentage of each petrogenetic type in relation to each category of knapping product, while the column % rel. are the percentage of each category of knapping product in relation to each petrogenetic type of "archaeological quartzite". Cells in black are the categories representing more than 10% of the total cases. Cells in dark grey are the categories representing between 5 and 10% of cases. Cells in light grey are the categories representing between 1 and 5% of cases. Other RM (raw materials) includes flint (3), lutite (67), limestone (1), limonite (3), and one undetermined raw material.

Blank is the technological category better represented in this layer, with 257 pieces. Coming to their integrity, 64% of the pieces are complete and 36% are fragmented (Figure-10.9). The most frequent fragments are longitudinal ones, followed by the proximal ones. We do not determined distal or medial fragments. Finally, 13% of the pieces could not be classified due to the absence of diagnostic features, mainly the bulb of percussion or the striking platform. Then, most of these undetermined fragments must be part of distal or medial fragments.

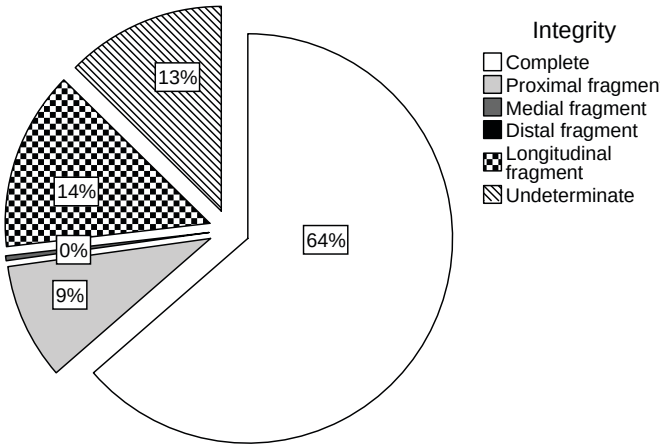

Figure-10.9: Pie chart showing percentages of each state of integrity of blanks.

The characterisation of dorsal surfaces using the number of negative scars shows a high quantity of blanks with three of them and an underrepresentation of the category without them. We do not observe statistically differences between the quantity of negative scars and raw material, as Pearson Chi-square test shows (χ^2 (15, N = 257) = 18.222, p = .251). Nevertheless, as Table-10.11 suggests, there is a high variability in the number of negative scars influenced by raw material. This is clear in the comparison between "archaeological quartzites" and lutites, especially due to the absence of blanks without negative scars in the latter. In addition, the representation of blanks with at least three negative scars is greater in lutites than in "archaeological quartzites". Finally, in flint, all blanks have at least three scars.

	Dorsal scars							
	None		One		Two		≥ Three	
	∑	**%**	∑	%	∑	%	∑	%
Arch. Qzt.	7	3,8	32	17,6	58	31,9	85	46,7
Flint	0	0,0	0	0,0	0	0,0	3	100,0
Limonite	0	0,0	2	66,7	0	0,0	1	33,3
Lutite	0	0,0	10	14,9	19	28,4	38	56,7
Total	7	2,7	44	17,3	77	30,2	127	49,8

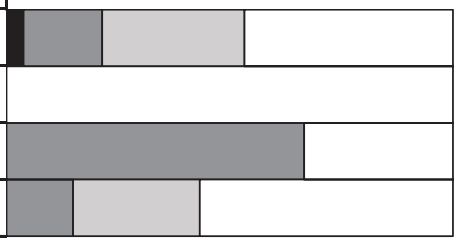

Table-10.11: Frequency table and its representation through a bar chart using the percentage of each blank category (determined by the quantity of dorsal scar) taking into account each raw material.

Regarding the petrogenetic types of "archaeological quartzite" we neither observe statistically significance differences, as Chi-square test shows (χ^2 (18, N = 126) = 24.957, p = .126). Nevertheless, Table-10.12 point at some differences between types of "archaeological quartzites" and the presence of negative scars on their blanks. CC type is the "archaeological quartzite" with greater frequency of blanks without negative scars. In addition, there is an absence of latter category in the group of quartzites. Finally, on the latter group there is high quantity of negative scars, especially in RQ type. CA type and the orthoquartzites have similar distribution of negative scars categories between them.

	Dorsal scars							
	None		One		Two		≥ Three	
	∑	**%**	∑	%	∑	%	∑	%
CA	0	0,0	0	0,0	1	25,0	3	75,0
OO	18	20,0	17	18,9	23	25,6	32	35,6
SO	6	9,7	7	11,3	19	30,6	30	48,4
BQ	15	8,6	35	20,0	60	34,3	65	37,1
RQ	2	15,4	1	7,7	5	38,5	5	38,5
MQ	0	0,0	0	0,0	0	0,0	2	100
Total	41	11,8	60	17,3	108	31,2	137	39,6

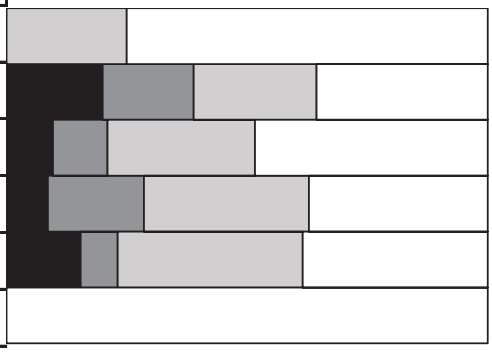

Table-10.12: Frequency table and its representation through a bar chart using the percentage of each blank category (determined by the quantity of dorsal scar) taking into account each petrogenetic type of "archaeological quartzite".

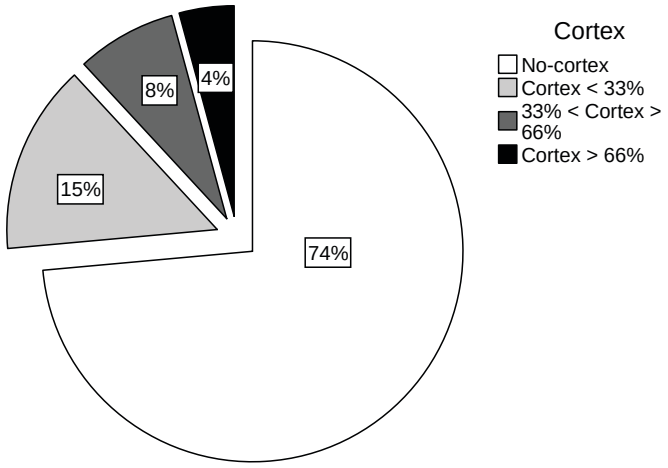

Figure-10.10: Pie chart showing percentages of absence, presence and extension of cortex on blanks.

The preservation of cortex on dorsal surfaces on these blanks also provide interesting data about raw material exploitation in this context (Figure-10.10). Cortex in blacks is observable in 27% of the collection. Most of them cover less than 33% of the surface of the dorsal surface. Broad cortical areas on dorsal surfaces are reduced to 12% of the blanks, and only 4% of items analysed have cortical areas covering more than 66% of the surfaces. Their distribution according to raw materials, reveals most blanks with cortical areas are on "archaeological quartzites". Still, lutite is the only raw material with cortex covering more than 33% of their dorsal surfaces. Limonite and flint have smaller cortex on dorsal surfaces, limited to small extension (Table-10.13). Focusing on "archaeological quartzite" there are no statistically significant differences between the extension of cortex in dorsal surfaces and the petrogenetic types, as chi-square test shows: (χ^2 (18, N = 175) = 28.046, p = .061). However, the extension of cortex is higher in the CC quartzarenite than in other petrogenetic types, especially when compared with MQ quartzite, without cortical surfaces (Table-10.14). Higher cortex extension than 66% is better represented in the CC quartzarenite, although it is also represented in CA type and the orthoquartzite group. Moreover, in quartzite group there is no blanks with cortex extended than 66% of dorsal surfaces. Finally, it is also mentionable the general and gradually decrease of cortex invasiveness in blanks as deformation and metamorphic processes in "archaeological quartzites" increase.

Presence of cortex on dorsal surfaces

	Absence		X < 33%		33<X>66		X > 66%	
	∑	**%**	∑	%	∑	%	∑	%
Arch. Qzt.	132	71,0	30	16,1	16	8,6	8	4,3
Flint	2	66,7	1	33,3	0	0,0	0	0,0
Limonite	3	100	0	0,0	0	0,0	0	0,0
Lutite	53	79,1	7	10,4	4	6,0	3	4,5
Total	190	73,4	38	14,7	20	73,4	11	4,2

Table-10.13: Frequency table and its representation through a bar chart using the percentage of each blank category (determined by the quantity of cortex on dorsal surfaces) taking into account each raw material.

Among the items which preserved any cortical areas (69), it was possible to characterise 56 of them. Among the 14 lutites with cortex, eleven of them were defined as coming from rivers. The remaining three could not be defined. The only blank on flint with cortex is from fluvial deposits. Focussing on archaeological quartzites with cortex the features that define cortex from fluvial sources (22) and from conglomerates (11) are different distributed. There are another ten "archaeological quartzites" with cortical surfaces which do not have enough features to define them. The cortical areas from conglomerates are restrained to orthoquartzite group and BQ type. In the OO type they are only represented in a small proportion (14%), while on SO (42%), and the BQ type (75%) are better represented.

Core preparation/rejuvenation product is the less frequent knapping product, only with four items. Two of them are complete, and other two fragmented. All of them are made on "archaeological quartzites" and only CC, OO, SO and BQ types are represented (Table-10.10). There are cores on all these petrogenetic types, except on the CC one. Only one of the core preparation/rejuvenation product has cortex, in smaller extension than 33% of its dorsal surface. It is on a SO orthoquartzite and it came from fluvial deposits.

	Presence of cortex on dorsal surfaces							
	Absence		X < 33%		33<X>66		X > 66%	
	∑	%	∑	%	∑	%	∑	%
CC	2	33,3	0	0,0	2	33,3	2	33,3
CA	11	64,7	4	23,5	1	5,9	1	5,9
OO	37	68,5	8	14,8	6	11,1	3	5,6
SO	40	72,7	8	14,5	5	9,1	2	3,6
BQ	20	80,0	5	20,0	0	0,0	0	0,0
RQ	5	62,5	2	25,0	1	12,5	0	0,0
MQ	10	100,0	0	0,0	0	0,0	0	0,0
Total	125	80	27	11	15	3	8	6

Table-10.14: Frequency table and its representation through a bar chart using the percentage of each blank category (determined by the quantity of cortex on dorsal surfaces) taking into account each petrogenetic type of “archaeological quartzite”.

10.3.3. CHUNK

Chunk, represented by 17 pieces, is the less important technological order product in the assemblage. The integrity of the pieces is not analysable due to the absence of diagnostic features.

The raw materials present in this category are “archaeological quartzite”, limestone, lutite, and quartz (Table-10.7). The only lithic made on quartz is a chunk and one of the two limestones is also a chunk. The representation of chunks made on lutites and “archaeological quartzites” is similar, around 5%. Focussing on specific petrogenetic types, chunks are more frequent in the quartzarenite group (especially in the CC type) than in others (Table-10.8). In orthoquartzite group and BQ type the quantity of chunks is limited to five items. There is no chunks in the other two petrogenetic types.

Only four chunks have cortex, all of them in “archaeological quartzite”. The extension of cortex covers more than 33% of the stone surface but none of them is completely cortical. Three cortex derived from fluvial deposits (one from a CC type, another one from a SO orthoquartzite, and the latter is unknown). The remaining chunk cortex derived from conglomerates.

10.4. RETOUCH: MODAL AND MORPHOLOGICAL STRUCTURES

Here we present the results of retouched artefacts and its relationship with the data previously exposed. According to the methodology defined above, there are 53 retouched pieces, 17.6% of the lithic assemblage. Eleven have two different primary types. The total number of retouches identified is 64. Starting from orders (mode of retouch), we do not find evidence of Plain (P), Splinter (E), or Burin (B) modes of retouch. Simple (S) mode is the most frequent one (58 items), followed by Abrupt mode (twelve items) (Figure-10.11 and Table-10.16). Going down from order of retouch to morphological group (or morphothema), we start with Simple mode, the most frequent one. The most frequent morphological group is that of Sidescraper (R) (64% of the Simple mode), followed by Denticulate (D) (22%), Endscraper (G) (9%), and finally Point (P) (5%). In the Abrupt mode, the least represented order, there are only unspecific Abrupts (A).

After having understood the general characterisation of the retouch using the modes and morphological groups, now we will deepen into the analysis of the pieces with two primary types. There are multiple associations. The most frequent association of morphological groups are Sidescraper and Sidescraper (in five blanks), followed by unspecific Abrupt and Denticulate (in two blanks). The association between unspecific Abrupt and unspecific Abrupt, unspecific Abrupt and Endscraper, Denticulate and Denticulate, Denticulate and unspecific Abrupt, and Denticulate and Sidescraper in one blank are also represented.

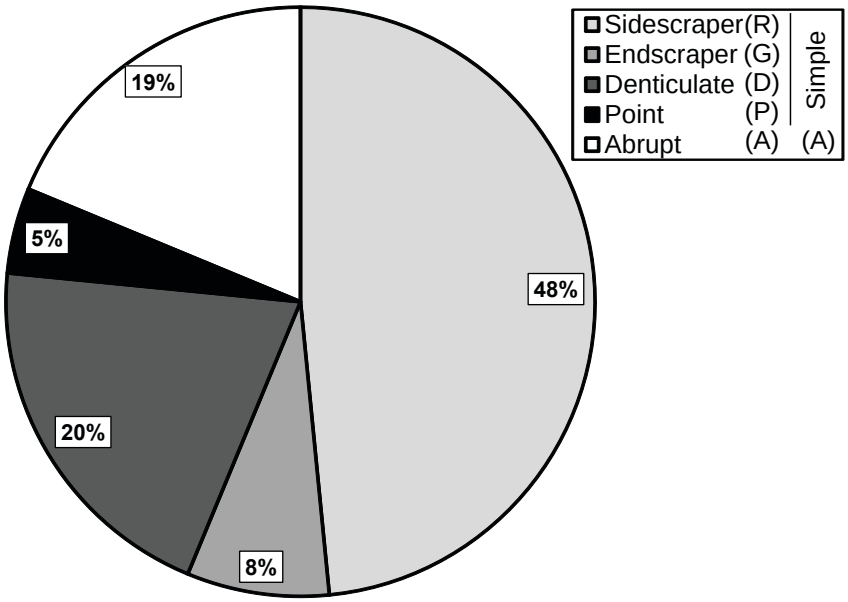

Figure-10.11: Pie chart showing percentages of orders (modes) and groups (morphological) of retouch on retouched artefacts from layer-VI of El Esquilleu rockshelter.

Next, we will analyse the relationship between retouched artefacts and the technological structure. There is no statistically significant association between the presence of retouch artefacts and the technological blanks they are configured (χ^2 (2, N = 301) = 2.186, p = .335). Nevertheless, there is greater representation of retouch on knapping products, 19%, than on cores, 13%, or chunks, with only a retouched chunk. In addition, all artefacts with two primary types except one, a core, are on configured on knapping products. Core preparation/rejuvenation products are not retouched.

Finally, we will analyse the relationships between the retouched artefacts and the raw material of the blanks they are configured. The quantity of retouched artefacts is not differently distributed depending on raw material of the blanks, as demonstrated by Chi-square test (χ^2 (6, N = 301) = 4.142, p = .657). Moreover, limonite and flint are the raw material with higher representation of retouch, 33%. Nevertheless, due to the small number of each raw material, only three, we should nuance the importance of this rate. Eighteen percent of the lutite blanks are retouched and only the 15% of the "archaeological quartzite" blanks are. Seven of the eleven artefacts with two primary types are made on "archaeological quartzite", three are configured on lutite, and the last one on limonite. There are statistically significant differences in the distribution of retouch between the types of "archaeological quartzites", as proven by Chi-square test ($\chi 2$ (6, N = 205) = 15.813, p = .015). Table-10.15 shows that retouched pieces are positively associated with the quartzite group. Meanwhile, retouched artefacts are less frequent in the orthoquartzite and quartzarenite groups, especially on CC type.

	Non-retouched		**Retouched**	
	Σ	Std. Res	Σ	**Std. Res**
CC	9	0,5	0	-1,2
CA	18	0,3	2	-0,7
OO	52	0,5	6	-1,1
SO	56	0,3	8	-0,7
BQ	24	-0,7	9	1,6
RQ	6	-1,1	5	2,4
MQ	7	-0,5	3	1,1

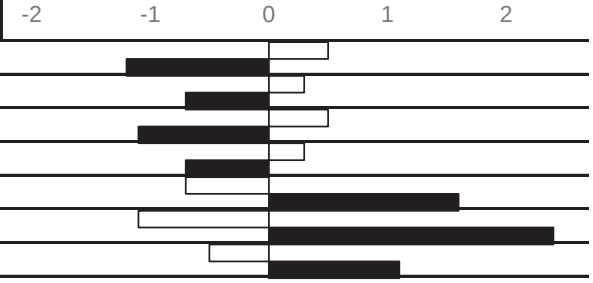

Table-10.15: Frequency table and standardised residues of χ^2 test of retouched and non-retouched artefacts grouped by raw material.

Order	Simple				Abrupt	Total
	Sidescraper	Endscraper	Denticulate	Point	Abrupt	
Arch. Qzt	**16**	5	**9**	1	**9**	40
Flint	1					1
Lutite	**12**		4	2	3	21
Limonite	2					2
Total	31	5	13	3	12	64

Table-10.16: Frequency table of order and group of retouches grouped by raw material. In the cases of pieces with different primary types, each type is quantified individually. Cells in black are the categories representing more than 10% of the total cases. Cells in dark grey are the categories representing between 5 and 10% of the cases. Finally, light grey are the categories representing between 1 and 5% of the cases.

There is no clear association between the morphological group and raw material. All well represented raw material have similar distribution of morphological groups: a high quantity of Sidescrapers, a secondary presence of Denticulate and Abrupt, and a small representation of Points. The group of Endscraper is the only one associated to one raw material: “archaeological quartzite”. The only retouched artefact on flint is a Sidescraper, the better represented group of retouch (Table-10.16). There are neither statistic association between the morphological group and petrogenetic type of “archaeological quartzites” they are configured. Nevertheless, some tendencies could be appreciated in Table-10.17. In general, Sidescraper is the better represented group. Other morphological groups, such as Endscraper, Denticulate, and unspecific Abrupt are secondary. The only configured morphological group on CA blank is that of Sidescrapers. On OO type, the group of Denticulates is better represented than Sidescraper one. Sidescraper is also secondary in retouched pieces made on MQ type blank. In this case, the group of unspecific Abrupt is the better represented group. Finally, the only configured Point in “archaeological quartzite” is made in a MQ type blank.

Order	Simple				Abrupt	Total
	Sidescraper	Endscraper	Denticulate	Point	Abrupt	
CC						
CA	2					2
OO	2	1	3		2	8
SO	4	1	2		2	9
BQ	**7**	1	3			11
RQ	1	1	1	1	2	6
MQ		1			3	4
Total	16	5	9	1	9	40

Table-10.17: Frequency table of order and group of retouches grouped by petrogenetic type. In the cases of pieces with different primary types, each type is quantified individually. Cells in black are the categories representing more than 10% of the total cases. Cells in dark grey are the categories representing between 5 and 10% of the cases. Cells in light grey are the categories representing between 1 and 5% of cases.

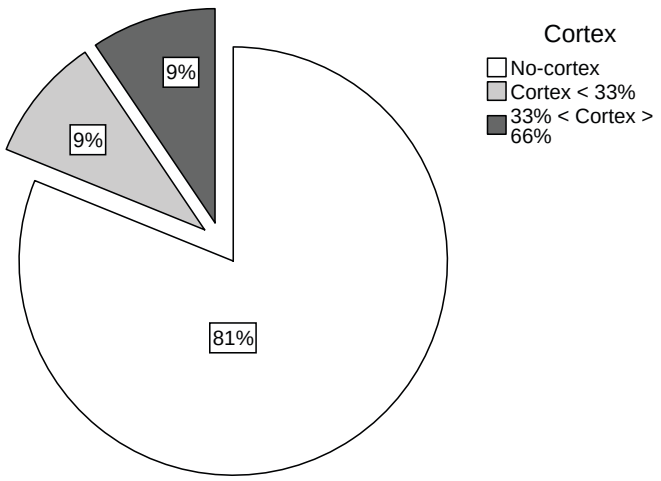

Figure-10.12: Pie chart showing percentages of absence, presence and extension of cortex on retouched artefacts from layer-VI of El Esquilleu rockshelter.

Finally, we analyse the relation between retouched artefacts and the preservation of cortex in the blanks they are configured (Figure-10.12). Nine per cent of the retouched material has cortex covering less than 33% of the surface. Nine per cent of the retouched artefacts have cortical areas extended between 33 and 66%. There is no retouch in blanks in which cortex is more extended than 66%. Three of the eleven pieces with two primary types have cortex. Regarding the characterisation of cortical areas, only one came from a conglomerate, the other nine artefacts came from fluvial deposits.

10.5. TIPOMETRICAL STRUCTURE

In this section we will describe the results of the analysis of the tipometrical structure and its relationship with the structures studied previously. We made the measurement using the technological axis (length, width and thickness) on 232 lithic pieces (77% of the assemblage). The remaining 69 pieces, were measured using the longest axis (X, Y and Z), due to the absence of features signalling the technological axis. All chunks, most of the cores (some cores on flakes were measured using the technological axis) and some incomplete knapping products were measured using the latter criterion.

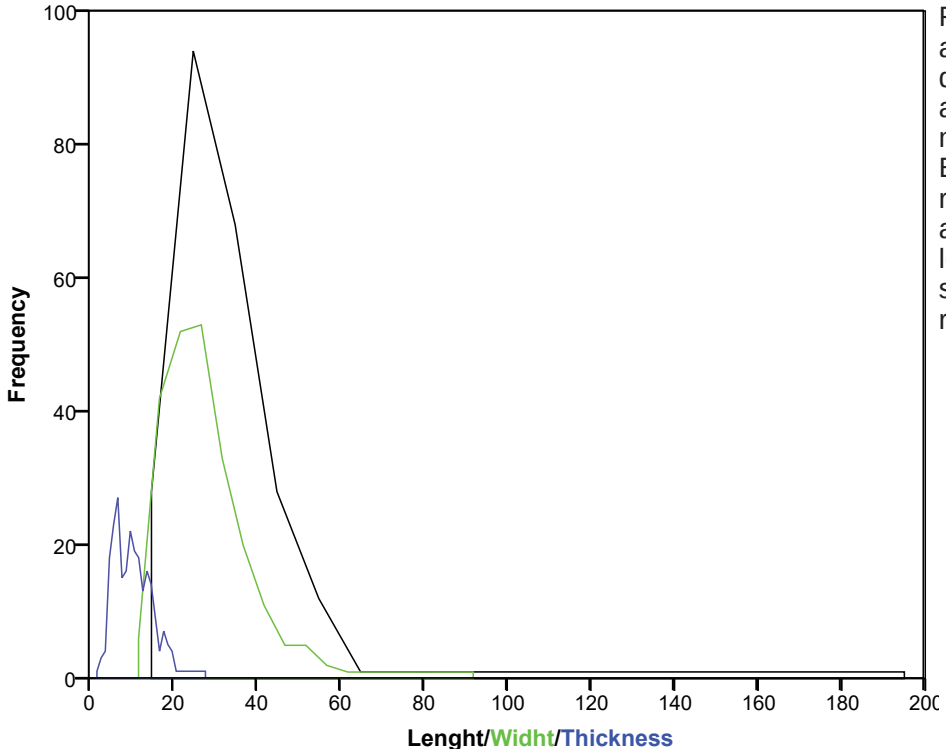

Figure-10.13: Frequency area chart showing the distribution of length, width and thickness of lithic remains from layer-VI of El Esquilleu measured in relation to technological axis. Black line represents length, green line represents width, and blue one represents thickness.

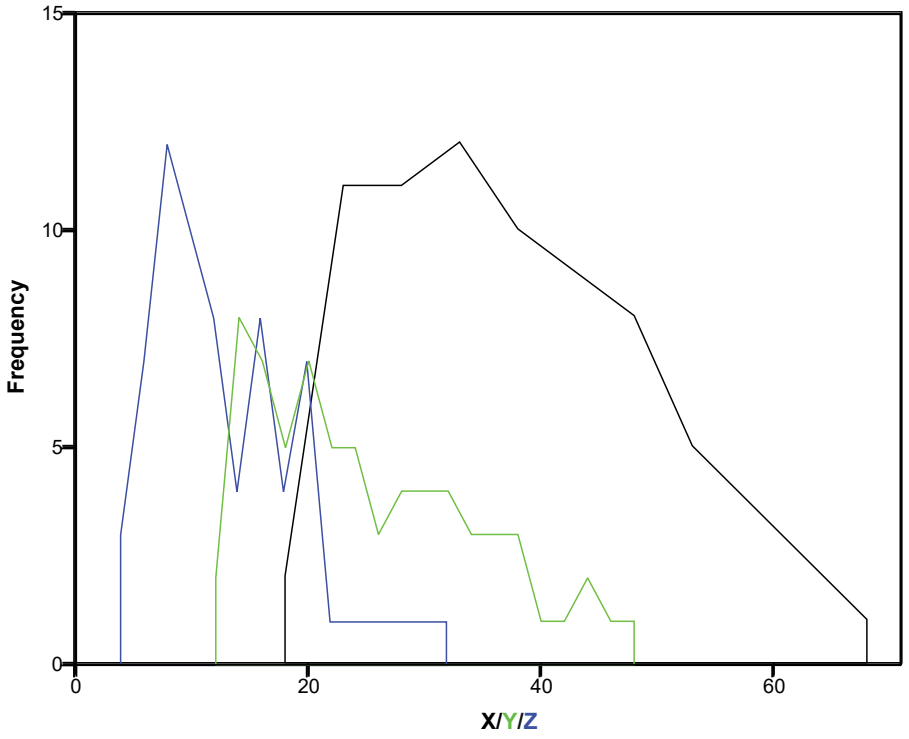

Figure-10.14: Frequency area chart showing the distribution of X, Y and Z axes of lithic remains from layer-VI of El Esquilleu rockshelter. Black line represents the X-axis, green line represents the Y-axis, and the blue line represents the Z-axis.

An overview of length, width, and thickness reveals that all three measurements have positive skewness and kurtosis, the highest values being those of length, followed by the width (Figure-10.13). The mean for length is 31.14 mm, the mean for width is 27.65 mm, and the mean thickness 10.33 mm. The measurements for the first two axes are similar between them. A general outlook of X, Y, and Z axes points at different kurtosis of three axes, ranging between -1 and +1 values. The first two axes have negative rates and the kurtosis for the latter axis is positive. The skewness is similar one each other with positive values smaller than +1. Nevertheless, all the means are clearly different between them: the means of the X is 35.87 mm, the mean of the Y is 24.62 mm, and the mean of the Z axis is 12.65 (Figure-10.14). The relationship between the three measurements according to the Tarriño indexes (Tarriño, 2015) reveals different morphologies depending on the measurement method employed (Figure-10.15). All lithics measured based on the X/Y/Z axes are between 0.5 and 0.8 RBEI and between 0 and 0.5 of RFL, meaning similar measurement between the three axes, and in relatively cubic-bladed shapes. Confidence ellipse shape which embodied these points describe a positive elongation in RBEI and RFL axes. Regarding the material measured using L/W/T axes, the resulting forms are similar, but they also include an important presence of tabular elements. Ninety-five percent confidence ellipse shape is different due to its elongation in horizontal display.

The last measurement used here is the weight of each lithic implement[1]. The minimum weight recorder is 0.64 g, and the maximum 300.00 g. The mean is 11.92 g. Weight presents high positive kurtosis (140.18), and positive skewness (10.18) as a consequence of the high percentage of lithic implements lighter than 5 g. The total of pieces weighted in this layer is 300 and the total weight of all of them is 3,578 g.

Length, width, thickness, Y axis, Z axis, and weight are not normally distributed, but X axis is normality distributed[2].

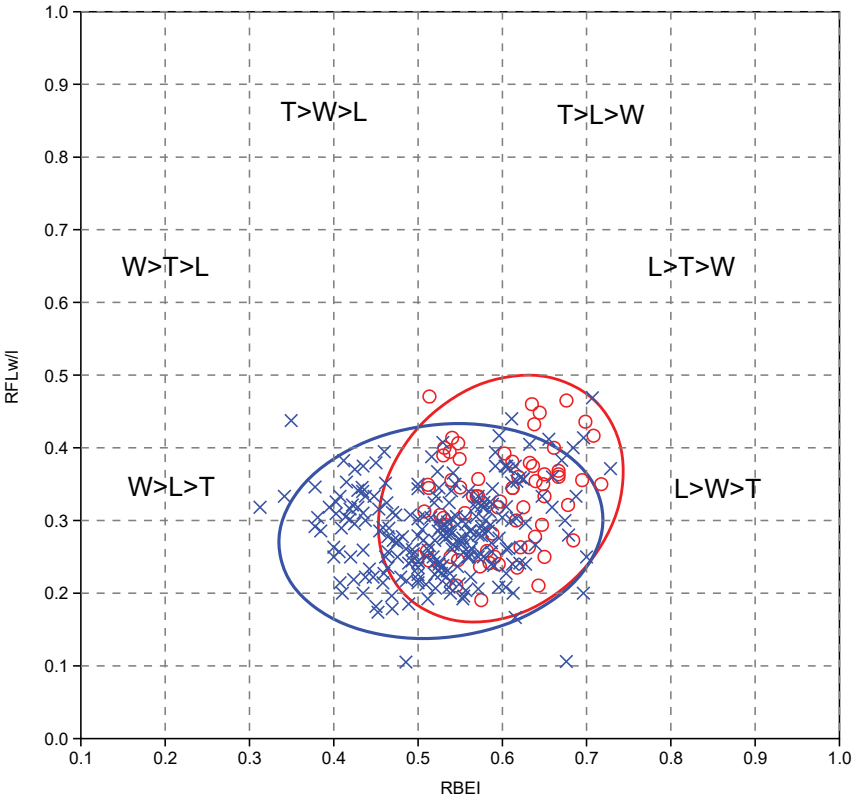

Figure-10.15: Scatter plot of RFLw or RFLl and RBEI indexes. Blue crosses and ellipse are the material measured using the technological axis. Red circles and ellipse are the measurements made in relation to X/Y/Z axis. Ellipses enclosure 95% of cases of each category. The weight is expressed in grams.

1 One lithic was not weighted due to error during data acquisition.
2 *KS* = 0.137; *df* = 232; *p* < 0.01 for length
KS = 0.120; *df* = 232; *p* < 0.01 for width
KS = 0.106; *df* = 232; *p* < 0.01 for thickness
KS = 0.091; *df* = 69; *p* < 0.01 for X-axis
KS = 0.116; *df* = 69; *p* = 0.02 for Y-axis
KS = 0.123; *df* = 69; *p* = 0.01 for Z-axis
KS = 0.288; *df* = 300; *p* < 0.01 for weight

Once the general metric characteristics have been understood, we will relate this data with the technological structure. The three technological orders proposed, show differences in shape between them. Figure-10.16a shows three different but overlapping groups using 95% confidence ellipses. The confidence ellipse of cores is the smallest one and it is situated in the central and upper part of the chart, showing positive elongation in both axes. The ellipse of knapping product is also located in the central area, but displaying horizontal elongation. Finally, the confidence ellipse of chunks is positioned in the central area, displaying vertical elongation. The distribution of weight of each category does also shows clear differences in variance, as demonstrated by *H* Kruskal-Wallis test: $H\ \chi^2$ (2, N = 200) = 36.907, $p < 0.001$ (Figure-10.16b). In general cores are bigger than other orders, with weights around 28 g for each piece, (Table-10.18). Chunks have similar, but smaller grams/piece ratio, around 25.3, specially influenced by the weight of one chunk, 300g. The median, 5.44 g, is similar with the knapping product one. The latter is the lighter category.

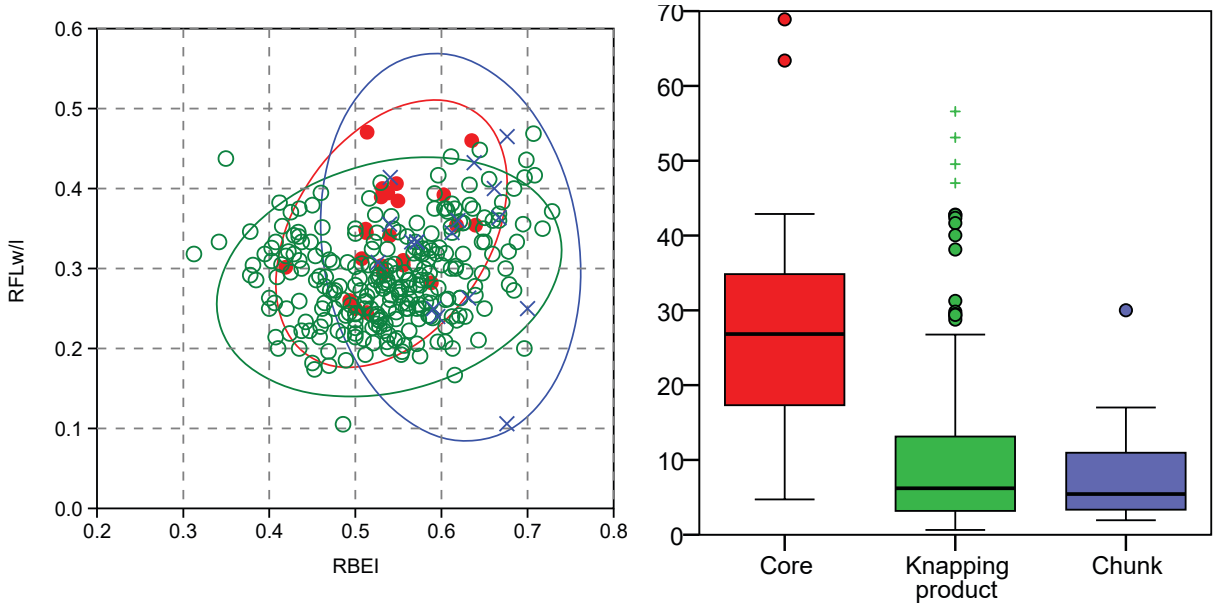

Figure-10.16: Double chart showing a) a scatter plot of RFLw or RFLl and RBEI indexes. Green colour circles and ellipse are knapping products. Red points and ellipse are cores. Blue crosses and ellipse are chunks. Ellipses enclose 95% of cases of each category. b) Boxplot showing differences in weight between various technological orders. There is another chunk with weight of 300.00g. The weight is expressed in grams.

Technological order	Weight		∑ of pieces		Ratio
	∑	%	∑	%	Grams/Piece
Core	642,9	18,00	23	7,70	28,0
Knapping product	2505,1	70,00	260	86,70	9,6
Chunk	430,3	12,00	17	5,70	25,3

Table-10.18: Frequencies and weight of main technological orders. The ratio grams/piece is reported. Weight is expressed in grams.

Coming to cores, there are differences in morphology between irregular and discoidal cores with core on flakes. The latter core morphologies embody in a positive elongated 95% confidence ellipse, the points of first two types of cores are similar one each other and both 95% confidence ellipses describe a vertical elongation (Figure-10.17). Weight is similarly distributed within each category, as indicated by the analysis in variance based on *H* Kruskal-Wallis test: $H\ \chi^2$ (4, N = 23) = 3.731, p = 0.292. Regarding the average weight of each category of cores, irregular and discoidal ones are above the average weight of all the cores considered. Meanwhile, levallois cores and, especially cores on flake are under this average value (Table-10.19).

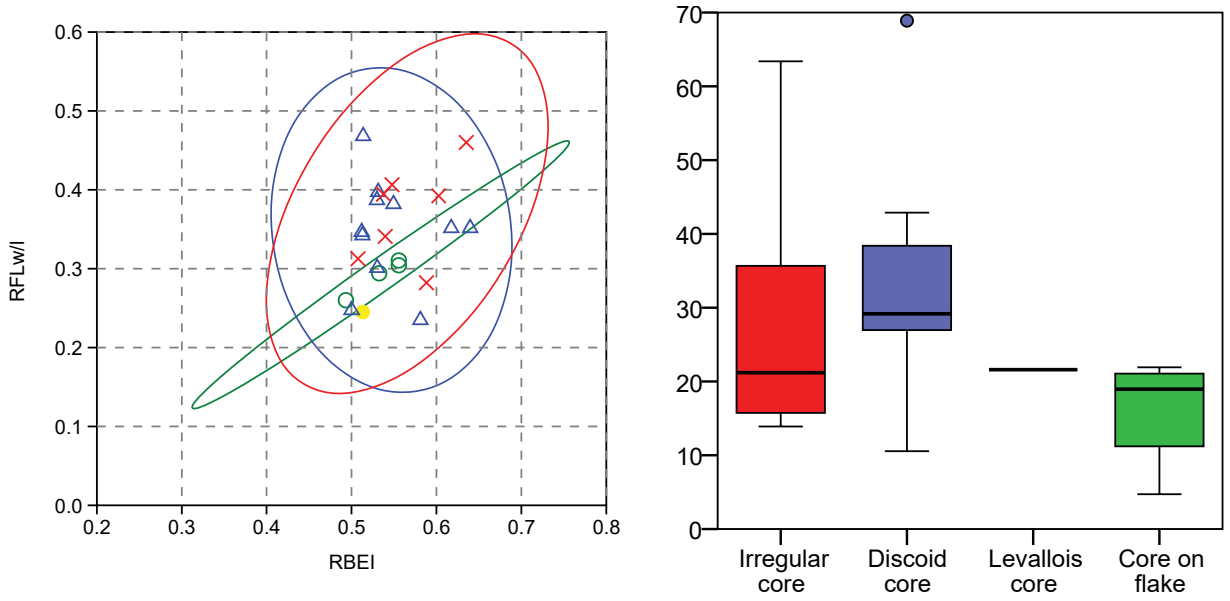

Figure-10.17: Double chart showing: a) Scatter plot of RFLw or RFLl and RBEI indexes. Green circles and ellipse are cores on flakes. Red crosses and ellipse are irregular cores. Blue triangles and ellipse are discoidal cores. The yellow point is a levallois core. Ellipses enclose 95% of cases of each category. b) Boxplot showing differences in weight between types of cores. The weight is expressed in grams.

Core groups	Weight		∑ of pieces		Ratio
	∑	%	∑	%	Grams/Piece
Irregular core	201,3	31,3	7	30,4	28,8
Discoid core	335,5	55,3	11	47,8	30,5
Levallois core	21,6	3,4	1	4,3	21,6
Core on flake	64,6	10,0	4	17,4	16,1

Table-10.19: Frequencies and weight of different groups of cores. The ratio grams/piece is reported. Weight is expressed in grams.

We could not evaluate differences between different groups of knapping products due to the small quantity of core preparation/rejuvenation products. Therefore, we will start by understanding the characterization of blanks using the number of negative scars on dorsal surfaces. There are differences in the form of blanks even all four 95% confidence ellipse of each blanks categories overlaps once each other (Figure-10.18a). Confidence ellipse of blanks without negative scars is situated in the central part of the chart describing horizontal elongation where tabular and bladed morphologies are represented without modification in its thickness. Other three 95% confidence ellipses describe similar shapes: with small positive elongation. Nevertheless, there is an increase of morphology variability in categories with small number of negative scars than those categories with higher quantity of extractions. There are also differences in weight based on the number of negative scars, as shown in Figure-10.18b and statistically demonstrated by *H* Kruskal-Wallis test: $H\ \chi^2\ (3, N = 256) = 34.898$, $p < 0.001$. Weight of blanks without negative scars is higher than other blanks. The grams/piece ratio of blanks with three or more negative extractions is higher than other two categories, both around six grams, and following a general increase of weight with the increase of negative scars (Table-10.20).

Number of negative scars	Weight		∑ of pieces		Ratio
	∑	%	∑	%	Grams/Piece
No-negative scars	129,3	5,3	7	2,7	18,5
One negative scar	246,0	10,1	45	17,6	5,5
Two negative scars	556,5	22,8	77	30,1	7,2
Three or more negative scars	1513,3	61,9	127	49,6	11,9

Table-10.20: Frequencies and weight of blanks grouped by number of negative scars. The ratio grams/piece is reported. Weight is expressed in grams.

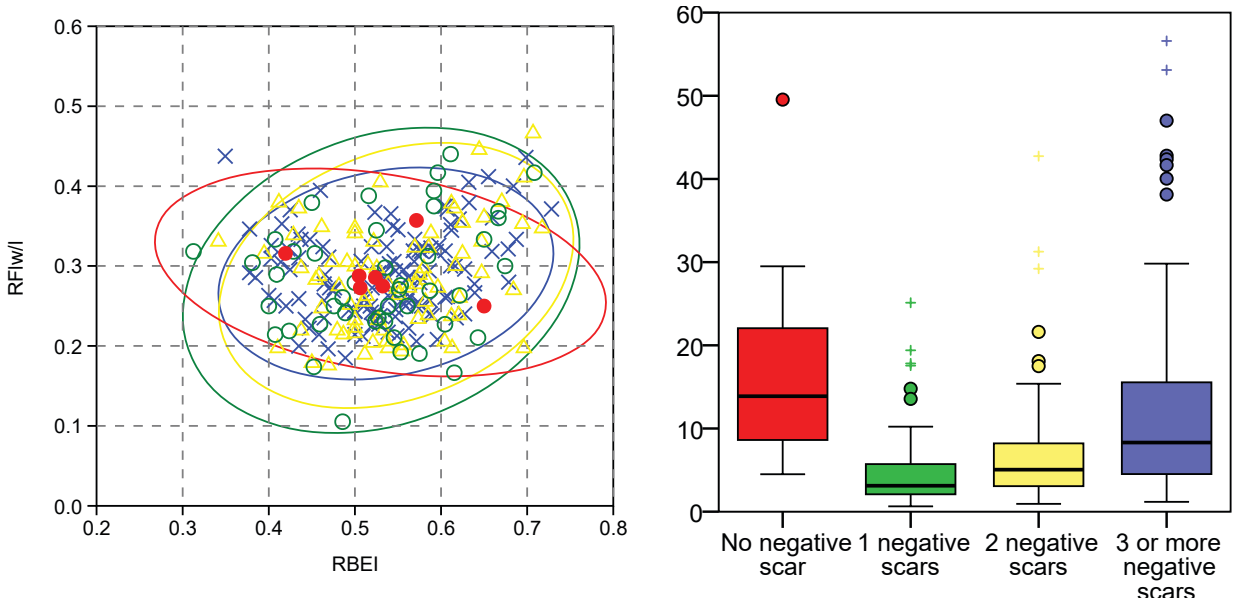

Figure-10.18: Double chart showing: a) Scatter plot of RFLw or RFLl and RBEI indexes. Red points and ellipse are blanks without negative scar. Green circles and ellipse are blanks with one negative scar. Yellow triangles and ellipse are blanks with two negative scars. Blue crosses are blanks with three or more negative scars. Ellipses enclose 95% of cases of each category. b) Boxplot showing differences in weight between blanks with different number of negative scars on dorsal surface. The weight is expressed in grams.

Regarding the integrity of the blanks, there are differences based on the form of the lithics (Figure-10.19a). The confidence ellipse of complete and proximal materials are similar. They arrange in a rounded and slightly elongated confidence ellipse in horizontal position and they are situated between 0.1 ≤ RFL ≥ 0.4 and 0.3 ≤ RBEI ≥ 0.7 (mainly tabular, cubic and bladed formats). Longitudinal and undetermined fragments morphologies embodied in a positive elongated 95% confidence ellipses in the region of thick and elongated forms (note that ellipse of former fragments is wider). Confidence ellipse for longitudinal fragments range between 0.4 ≤ RBEI ≥ 0.8 and between 0.1 ≤ RFL ≥ 0.5. Comparing the distribution of weight between the various types of blanks, *H* Kruskal-Wallis test indicates there are no statistically significant differences between them: $H\ \chi^2$ (4, N = 256) = 5.089, p = 0.278. In Figure-10.19b there are small differences observables in the smaller weight of the longitudinal fragments when compared with other three categories. The latter are heavier than the former. The grams/piece ratio of these categories also points at this small differences even though undetermined fragments are lighter, especially due to the absence of fragmented lithics heavier than 30 grams (Table-10.21).

Integrity of blanks	Weight		∑ of pieces		Ratio
	∑	%	∑	%	Grams/Piece
Complete	1702,5	69,6	164	64,1	10,4
Proximal fragment	235,5	9,6	23	9,0	10,2
Longitudinal fragment	238,7	9,8	37	14,5	6,5
Undetermined fragm	268,4	11,0	32,0	12,5	8,4

Table-10.21: Frequencies and weight of blanks grouped by integrity. The ratio grams/piece is reported. Weight is expressed in grams.

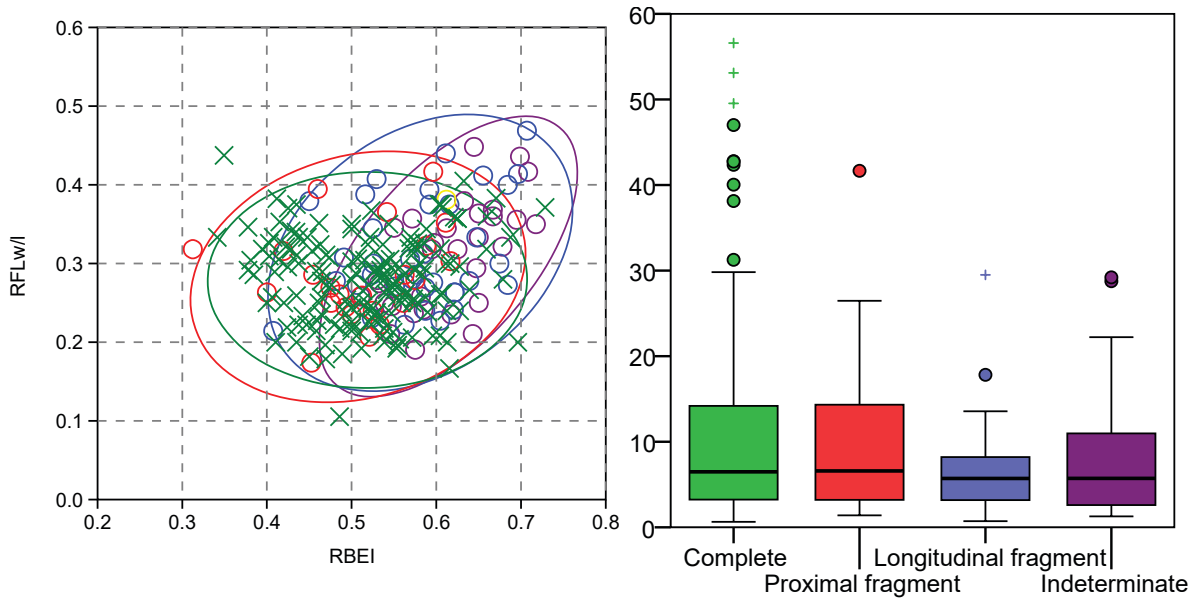

Figure-10.19: Double chart showing: a) Scatter plot of RFLw or RFLl and RBEI indexes. Green crosses and ellipse are complete blanks. Red circles and ellipse are proximal blank fragments. Blue circles and ellipse are longitudinal blank fragments. Purple circles and ellipse are undetermined blank fragments. Ellipses enclose 95% of cases of each category. b) Boxplot showing differences in weight between blanks preserved in diverse states of integrity. The weight is expressed in grams.

The classification of complete blanks products (Figure-10.20a) reveals the massive predominance of flakes (83% of complete blanks), followed by a moderate presence of elongated flakes (13% of complete blanks), and really occasional find of blades (4% of complete blanks). There is no difference in weight between these three categories, which show similar distributions, as depicted in Figure-10.20b and proven by H Kruskal-Wallis test: H χ2 (2, N = 223) = 2.268, p = .322. The comparison of gram/piece ratios between the three types of blanks proposed reveals differences in mean weight (Table-10.22). The grams/piece ratio of flake and blade are similar to the general ones, while the grams/piece ratio of elongated flakes is slightly smaller.

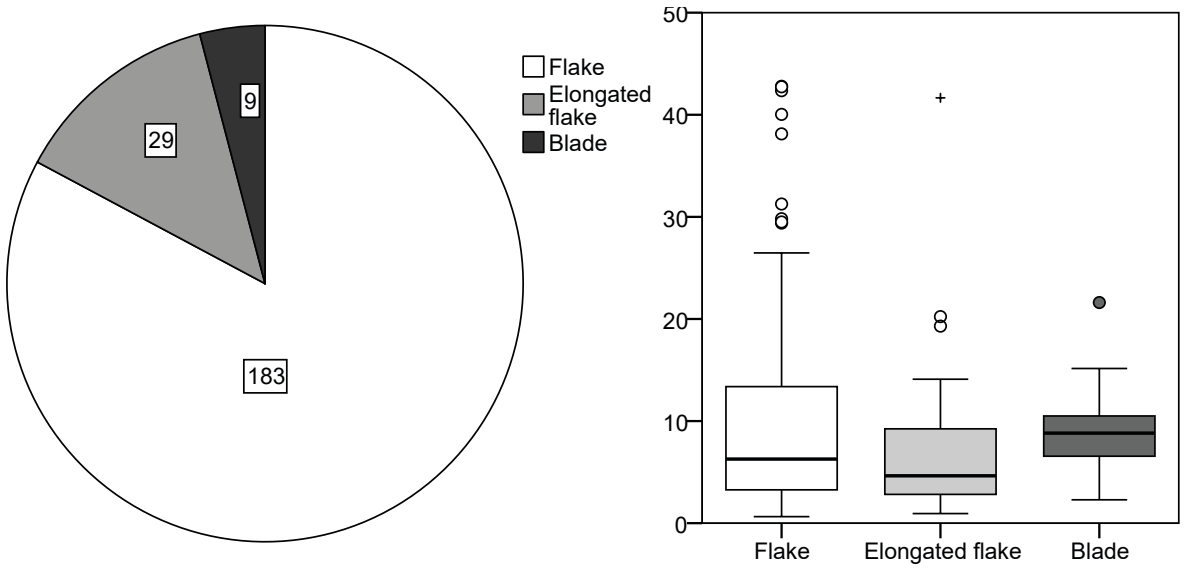

Figure-10.20: Double chart showing a) pie chart showing the distribution of complete blank products, and b) boxplot showing differences in weight between metrical categories. The weight is expressed in grams.

Complete blank characterisation	Weight		∑ of pieces		Ratio
	∑	%	∑	%	Grams/Piece
Flake	1872,8	85,5	186	83,0	10,1
Elongated flake	230,8	10,5	29	12,9	8,0
Blade	86,9	4,0	9	4,0	9,7

Table-10.22: Frequencies and weight of different types of complete blanks (flakes, elongated flakes, blades). The ratio grams/piece is reported. Weight is expressed in grams.

Next, we will liken the metrical structure with retouched material. There are clear weight differences based on the presence (M = 9.16) or absence (M = 6.4) of retouch in the pieces, as corroborated by *U* Mann-Whitney test: $U = 7{,}671$, $p = 0.031$. In general, retouched artefacts are heavier (Figure-10.21b). Medium weigh of non-retouched material is similar to general mean, while retouched artefact mean is slightly higher (Table-10.23). There are no differences in morphology between retouched and non-retouched blanks, as shown in Figure-10.21a. There are neither differences in morphology in artefacts attending to the quantity of primary types identified in each blank, as shown in Figure-10.22a. There are neither weight differences between the artefacts with one or two primary types on each blank, as pointed by H Kruskal-Wallis: $H\,\chi^2\,(2, N = 52) = 0.907$, $p = 0.635$. (Table-10.24 and Figure-10.22b).

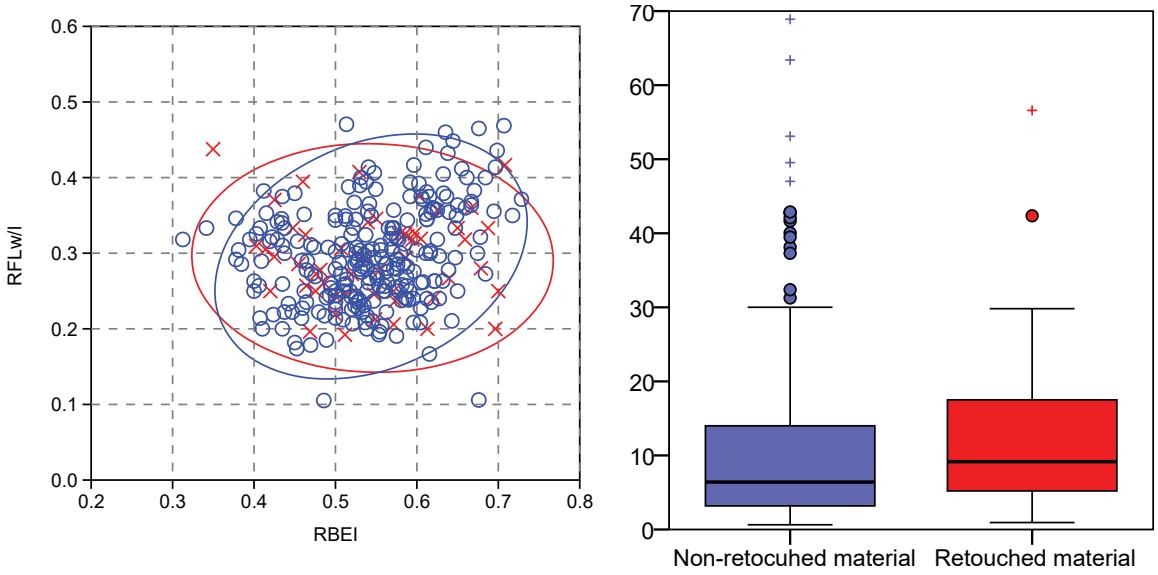

Figure-10.21: Double chart showing: a) Scatter plot of RFLw or RFLl and RBEI indexes. Red crosses and ellipse are retouched lithic material. Blue circles and ellipse are non-retouched lithic material. Ellipses enclose 95% of cases of each category. b) Boxplot showing differences in weight between retouched and non-retouched lithic material. The weight is expressed in grams.

Piece	Weight		∑ of pieces		Ratio
	∑	%	∑	%	Grams/Piece
Non-retouched	2934,5	82,0	248	82,7	11,8
Retouched	643,9	18,0	52	17,3	12,4

Table-10.23: Frequencies and weight of retouched and non-retouched pieces. The ratio grams/piece is reported. Weight is expressed in grams.

	Weight		∑ of pieces		Ratio
	∑	%	∑	%	Grams/Piece
One primary type	498,3	77,3	41	78,8	12,2
Two primary types	145,6	22,6	11	21,2	13,2

Table-10.24: Frequencies and weight of the retouched pieces grouped by quantity of primary types on each blank. The ratio grams/piece is reported. Weight is expressed in grams.

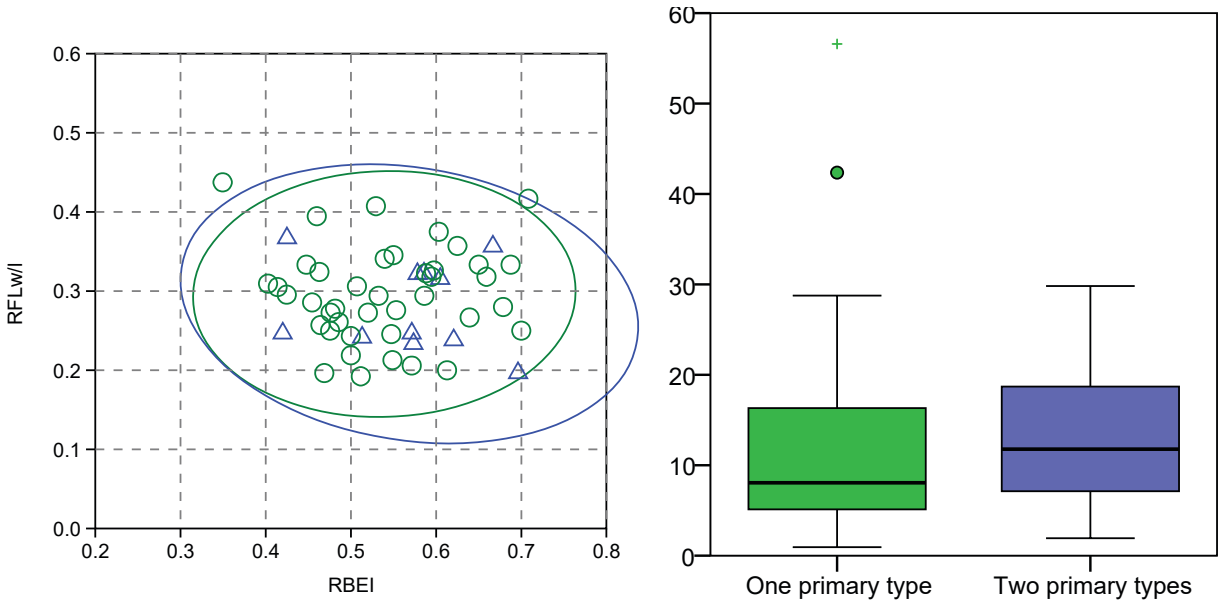

Figure-10.22: Double chart showing: a) Scatter plot of RFLw or RFLI and RBEI indexes. Green circles and ellipse are artefacts with one primary type. Blue triangles and ellipse are artefacts with two primary types. Ellipses enclose 95% of cases of each category. b) Boxplot showing differences in weight between artefacts grouped by the quantity of primary types identified on each blank. The weight is expressed in grams.

Then, we will confront metrical features of retouched artefacts with the features of retouch, categorised in orders (modal) and groups (morphological). Due to the methodology used to define retouch here, we only included in this analysis the pieces with one primary type on each blank. The comparison reveals no differences in morphologies between those blanks configured using the Simple or the Abrupt modes, represented by Figure-10.23a. Weight distribution of blanks configured with Abrupt and Simple modes are similar weight, as proven by *U* Mann-Whitney: $U = 115.00$, $p = 0.064$. Nevertheless, the significance level is near the two sigma, then, this conclusion must be nuance (Figure-10.23b). The median for the weight of Simple mode is 9.5 g, while for Abrupt one is 5.69 g. The grams/piece ratio of two order represented reinforces this idea (Table-10.25).

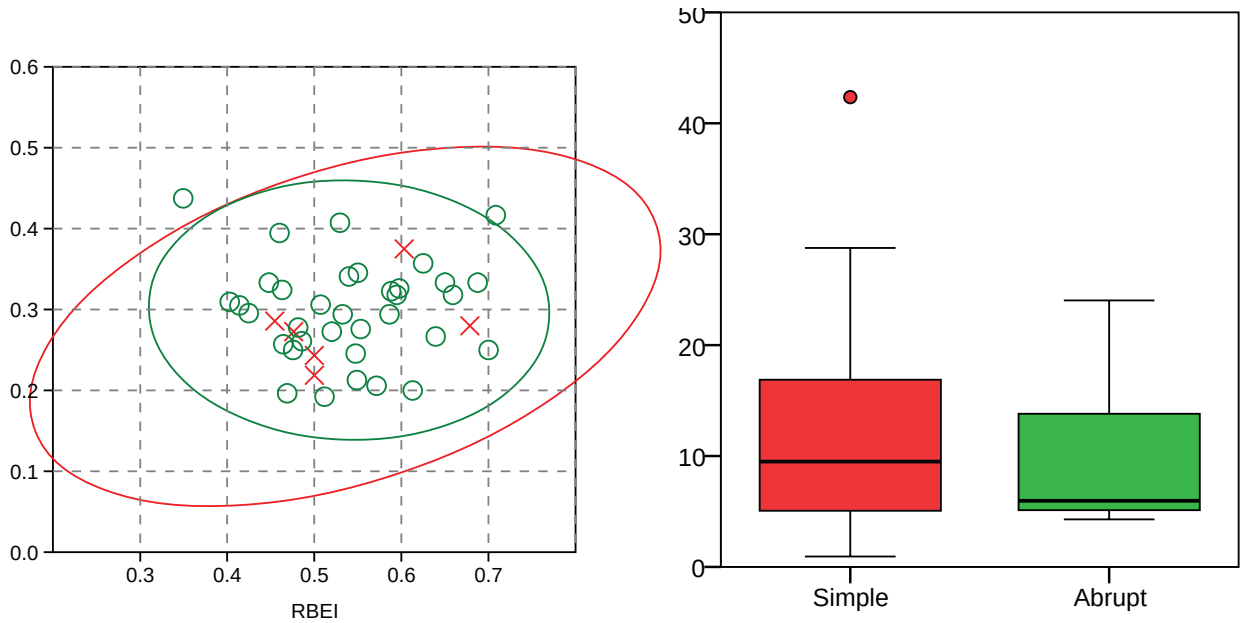

Figure-10.23: Double chart showing: a) Scatter plot of RFLw or RFLI and RBEI indexes. Red crosses and ellipse are artefacts configured with the Simple mode of retouch. Green circles and ellipse are artefacts configured with the Abrupt mode of retouch. Ellipses enclose 95% of cases of each category. b) Boxplot showing differences in weight between different orders of retouch. The weight is expressed in grams.

Order of retouch	Weight		∑ of pieces		Ratio
	∑	%	∑	%	Grams/Piece
Simple	439,2	88,1	35	85,3	12,5
Abrupt	59,2	11,9	6	14,7	9,9

Table-10.25: Frequencies and weight of retouched artefacts grouped by the mode of retouch. The ratio grams/piece is reported. Weight is expressed in grams.

The last structure to be tackle here is the petrological one. We do not observe differences in the morphology of the lithics depending on their raw material (Figure-10.24a). The morphologies of "archaeological quartzites" and lutites, the only raw materials with higher representation than three items, embodied in two overlapping 95% confidence ellipses which describe two slightly elongated areas. The morphology of lithics of other raw materials are in the region of previous "archaeological quartzite" and lutite ellipses. Weight distribution neither point at statistically significant differences between each raw material, as proven by *H* Kruskal-Wallis test: $H\ \chi^2$ (6, N = 300) = 9.622, p = 0.141. The gram/piece ratios of "archaeological quartzite", limestone, and lutite are similar. However, flint, quartz, and especially limonite have smaller ratios (Figure-10.24b and Table-10.26).

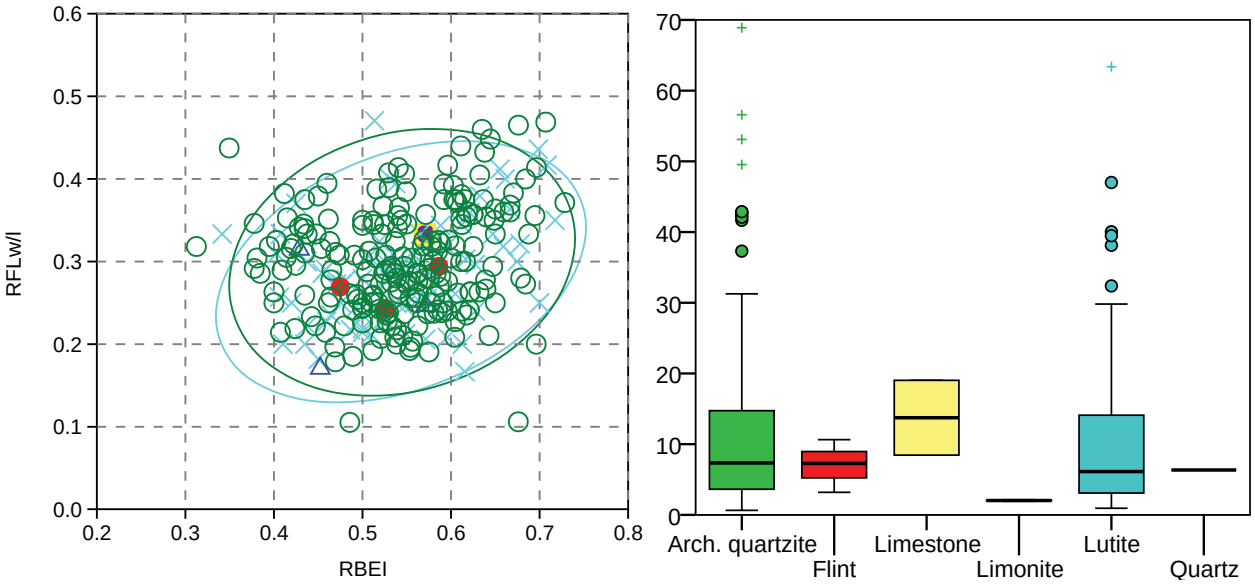

Figure-10.24: Double chart showing: a) Scatter plot of RFLw or RFLI and RBEI indexes. Green circles and ellipse are "archaeological quartzites". Red points are flint. Yellow squares are limestone. Blue triangles are limonites. Light blue crosses and ellipse are lutites. Purple point is quartz. Ellipses enclose 95% of cases of each category. b) Boxplot showing differences in weight between different raw materials. The weight is expressed in grams.

Raw material	Weight		∑ of pieces		Ratio
	∑	%	∑	%	Grams/Piece
"Arch. quartzite"	2678,3	74,8	212	70,7	12,6
Flint	21,1	0,6	3	1,0	7,0
Limestone	27,5	0,8	2	0,7	13,7
Limonite	6,1	0,2	3	1,0	2,0
Lutite	836,9	23,4	78	26,0	10,7
Quartz	6,4	0,2	1	0,3	6,4

Table-10.26: Frequencies and weight of different types of raw material. The ratio grams/piece is reported. Weight is expressed in grams.

There are no clear differences in morphology between different petrogenetic types, and most of them are in the region between 0.4 < RBEI > 0.7 and 0.2 < RFLw/RFLl > 0.4. However, the range of 95% confidence ellipse is wider in the RQ, MQ and the CC types, as can be observed in Figure-10.25a. There are no statistically significant differences in distribution of weight, as proven by *H* Kruskal-Wallis test: $H\ \chi^2$ (6, N = 204) = 8.874, p = 0.174. Nevertheless, the grams/piece ratio points at differences in the comparison between CC and RQ type with other petrogenetic types. The first two are heavier than other (Table-10.27 and Figure-10.25b). The MQ ratio is the lightest one.

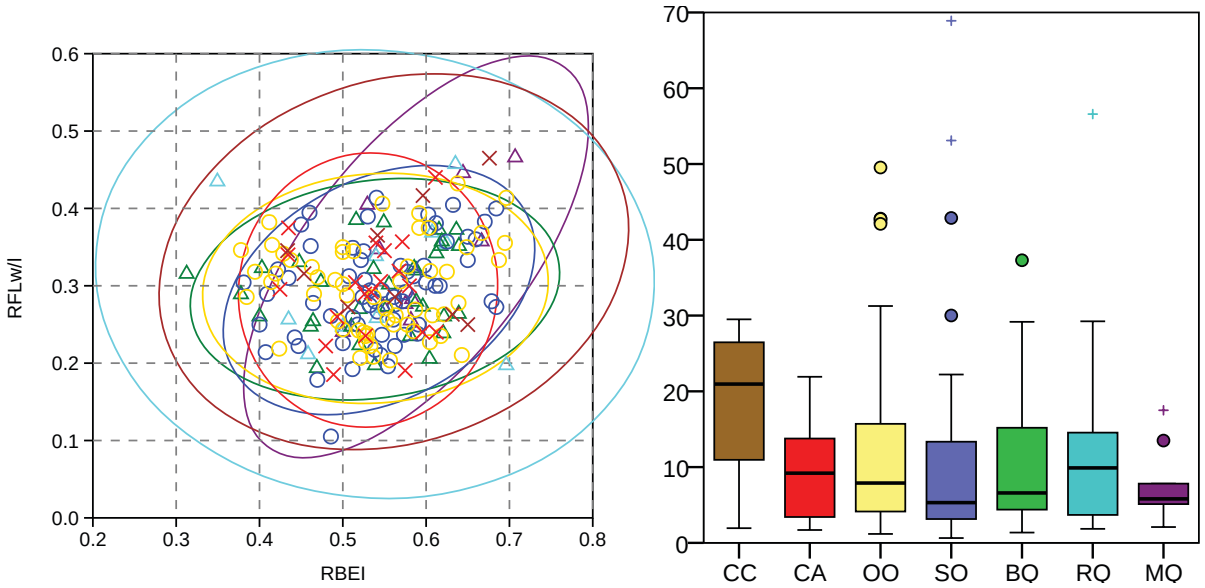

Figure-10.25: Double chart showing: a) Scatter plot of RFLw or RFLl and RBEI indexes. Brown crosses and ellipse are CC type pieces. Red crosses and ellipse are CA type pieces. Yellow circles and ellipse are OO type pieces. Blue circles and ellipse are SO type pieces. Green triangles and ellipse are BQ types. Light blue triangles and ellipse are RQ type pieces. Purple triangles and ellipse are MQ types. Ellipses enclose the 95% of cases of each category. b) Boxplot showing differences in weight between different petrogenetic types of "archaeological quartzite". The weight is expressed in grams.

Petrogenetic type	Weight		∑ of pieces		Ratio
	∑	%	∑	%	Grams/Piece
CC	162,7	7,1	9	4,4	18,1
CA	189,2	8,3	20	9,8	9,5
OO	731,4	31,9	58	28,4	12,6
SO	639,5	27,9	64	31,4	10,0
BQ	344,5	15,0	33	16,2	10,4
RQ	149,3	6,5	10	4,9	14,9
MQ	75,6	3,3	10	4,9	7,6

Table-10.27: Frequencies and weight of different petrogenetic types of "archaeological quartzites". The ratio grams/piece is reported. Weight is expressed in grams.

Now, we will delve into the relationship between raw material, technology, retouch, and the metrical structure, focusing on size through its weights. Starting with technology, there are clear differences in weight based on the technological order and raw material (Figure-10.26 and Table-10.28). There are no clear differences in medium weight between "archaeological quartzites" and lutites. However, lutite cores are more variable, and there are lighter cores than ten grams. The weight of cores in each petrogenetic types of "archaeological quartzites" differ one each other and they follow a general decrease of weight from the OO orthoquartzite to the RQ quartzite. In addition, SO cores, the most frequent, are also the most variable ones. Despite the small number of cores, there are also differences in weight based on the types of cores and raw material. The most representative differences are in the irregular cores, in which, "archaeological quartzite" cores are lighter than those made on lutite. On the contrary, in core on flake type, the lutite core is lighter than "archaeological quartzite" cores (Figure-10.27 and Table-10.29). There are some differences in the weight of each type of "archaeological quartzite" when they are compared by core type, especially in irregular and discoidal ones.

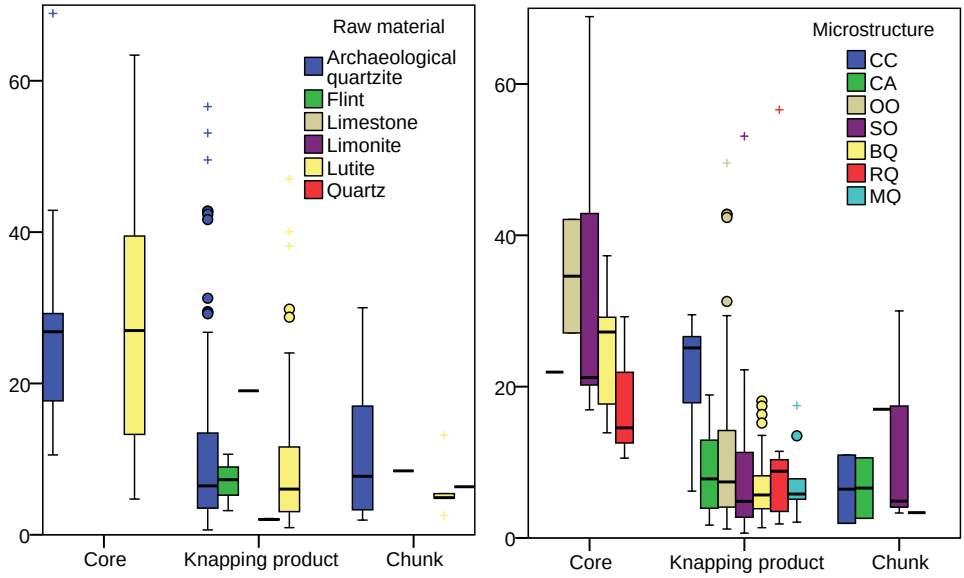

Figure-10.26: Double boxplot showing the distribution of weight in grams of all lithic remains grouped first by technological order and second by raw material in the chart on the left and by petrogenetic type in the chart on the right. There is another undetermined "archaeological quartzite" chunk with weight of 300.00g not represented on chart. The weight is expressed in grams.

Table-10.28: Frequency table of different orders of lithic remains grouped by raw material, including frequencies, weight and the ratio grams/piece for each case. Weight is expressed in grams.

Raw material	Petrgen. type	Lithic collection											
		Core			Knapping			Chunks			Total		
		∑	W	g/p	∑	W	g/p	∑	W	g/p	∑	W	g/p
Archaeological quartzite	CC				7	150	21	2	13	6,5	9	163	18
	CA	1	22	22	17	154	9,1	2	13	6,6	20	189	9,5
	OO	2	69	35	55	645	12	1	17	17	58	731	13
	SO	5	170	34	56	431	7,7	3	38	13	64	639	10
	BQ	6	153	25	26	189	7,3	1	3	3,4	33	345	10
	RQ	3	54	18	7	95	14				10	149	15
	MQ				10	76	7,6				10	76	7,6
	Undet.				7	86	12	1	300	300	8	386	48
	Total	17	468	28	185	1826	9,9	10	385	38	212	2678	13
Flint					3	21	7				3	21	7
Limestone					1	19	19	1	8	8,4	2	27	14
Lutite		6	175	29	67	631	9,4	5	31	6,2	78	837	11
Quartz								1	6	6,3	1	6	6,3
Limonite					3	6	2				3	6	2

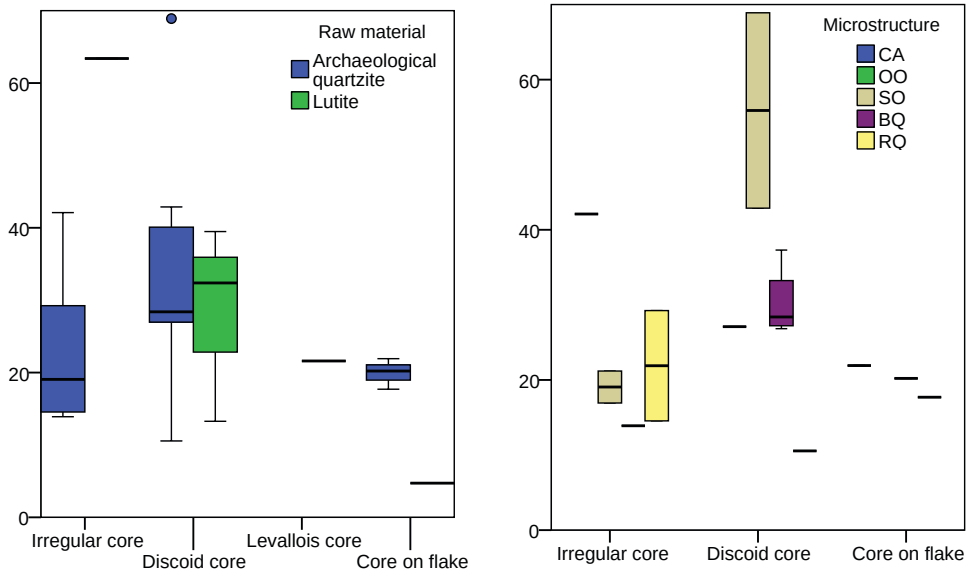

Figure-10.27: Double boxplot showing the distribution of weight in grams of cores grouped first by type and second by raw material in the chart on the left and by petrogenetic type in the chart on the right. The weight is expressed in grams.

Raw material	Petrgen. type	Cores														
		Irregular			Discoid			Levallois			Core on flake			Total		
		∑	W	g/p	∑	W	g/p	∑	W	g/p	∑	W	g/p	∑	W	g/p
Archaeological quartzite	CC															
	CA										1	22	22	1	22	22
	OO	1	42	42	1	27	27							2	69	35
	SO	2	38	19	2	112	56				1	20	20	5	170	34
	BQ	1	14	14	4	121	30				1	18	18	6	153	25
	RQ	2	44	22	1	11	11							3	54	18
	MQ															
	Undet.															
	Total	6	138	23	8	270	34				3	60	20	17	468	28
Flint																
Limestone																
Lutite		1	63	63	3	85	28	1	22	22	1	5	5	6	175	29
Quartz																

Table-10.29: Frequency table of different core types grouped by raw material, including frequencies, weight and the ratio grams/piece for each case. Weight is expressed in grams.

In regard to knapping products, Table-10.30 displays the differences in weight between core preparation/rejuvenation products and blanks. The former are bigger than the latter. Focussing on specific petrogenetic types of “archaeological quartzites”, the biggest core preparation/rejuvenation product is made on CC type, 27 grams. OO core preparation/rejuvenation product is slightly lighter and it is clearly differentiated from the SO and BQ core preparation/rejuvenation products, due to the heavier weight of the first. There are no differences in weight of blanks depending on the number of negative scars between “archaeological quartzites” and lutites. Nevertheless, there are weight differences in the comparison between latter two raw materials and flint and limonite, due to the smaller weight of the latter two raw materials (Figure-10.28 and Table-10.30). Differences expand taking into account the weight of each petrogenetic type, especially in the comparison between CC type and the others. It is also remarkable the general increase in weight of the quartzarenite and orthoquartzites groups in the increase of negative scars, in comparison with quartzite group. Finally, there is an almost absence of lighter than three grams materials in the MQ and RQ types.

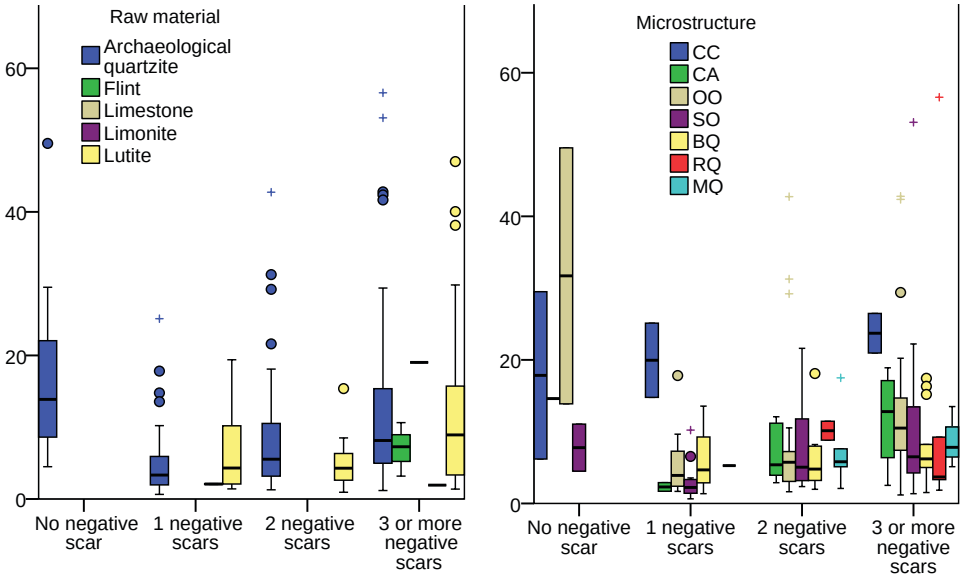

Figure-10.28: Double boxplot showing the distribution of weight in grams of blanks grouped first by the number of negative scars on dorsal surface and second by raw material in the chart on the left and by petrogenetic in the chart on the right. The weight is expressed in grams.

Finally, differences in the weight of chunks based on raw material are verifiable in Figure-10.26 and Table-10.28. “Archaeological quartzites” are generally heavier and more variable than other raw materials chunks. These differences are not so evident taking into account each petrogenetic type, due to the small presence of chunks in each type and the similar variability in weight between the CC, CA, and SO types.

Raw material	Petrgen. type	Knapping products: Core preparation ∑	Core preparation W	Core preparation g/p	Blanks: No neg.scar ∑	No neg.scar W	No neg.scar g/p	1 neg.scar ∑	1 neg.scar W	1 neg.scar g/p	2 neg.scar ∑	2 neg.scar W	2 neg.scar g/p	3 or more ∑	3 or more W	3 or more g/p	Blank total ∑	Blank total W	Blank total g/p
Archaeological quartzite	CC	1	27	27	2	36	18	2	40	20				2	47	24	6	150	25
	CA				1	15	15	2	5	2,3	6	41	6,8	8	94	12	17	154	9,1
	OO	1	21	21	2	63	32	10	56	5,6	17	171	10	25	333	13	54	645	12
	SO	1	3	3,4	2	16	7,8	11	35	3,2	17	129	7,6	25	249	10	55	431	7,8
	BQ	1	7	6,6				4	24	6,1	8	52	6,5	13	104	8	25	187	7,5
	RQ										2	20	10	5	75	15	7	95	14
	MQ							1	5	5,3	6	44	7,3	3	26	8,8	10	76	7,6
	Undet.							2	6	2,9	2	6	3,1	3	74	25	7	86	12
	Total	4	58	15	7	129	18	32	171	5,3	58	463	8	84	1002	12	181	1824	10
Flint														3	21	7	3	21	7
Limestone														1	19	19	1	19	19
Lutite								10	69	6,9	19	93	4,9	38	469	12	67	631	9,4
Quartz																			
Limonite								2	4	2,1							2	4	2,1

Table-10.30: Frequency table of different knapping products grouped by raw material, including frequencies, weights and the ratio grams/piece for each case. The knapping products considered are core preparations/rejuvenations and blanks sorted by the number of negative scars present. Weight is expressed in grams.

The analysis of the relationship between raw material and retouch through its weight points at clear similitudes between different raw materials (Figure-10.29 and Table-10.31). Nevertheless, there are differences in weight between artefacts configured with the Simple mode. The heaviest retouched blanks with the Simple mode are made on RQ and OO types. The weight is lower in other petrogenetic types. In contrary, the weight of blanks retouched using the Abrupt mode is similar in the different petrogenetic types represented. Nevertheless, these conclusion must be nuance due to the small quantity of retouched artefacts.

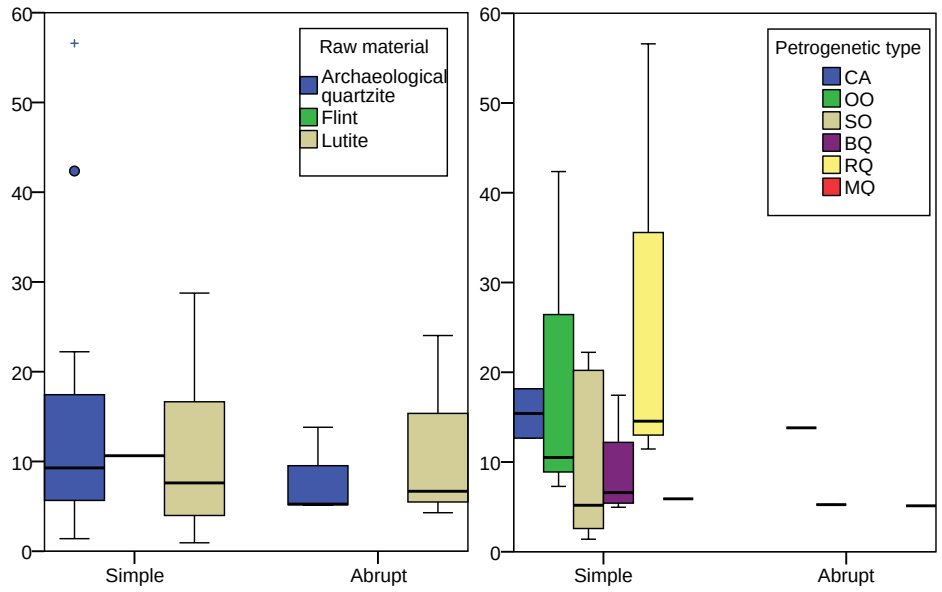

Figure-10.29: Double boxplot showing the distribution of weight in grams of retouched material grouped first by mode of retouch and second by raw material in the chart on the left and by petrogenetic in the chart on the right. The weight is expressed in grams.

Raw material	Petrgen. type	Single-retouched pieces: Simple, Sidescraper ∑	Sidescraper W	Sidescraper g/p	Endscraper ∑	Endscraper W	Endscraper g/p	Point ∑	Point W	Point g/p	Denticulate ∑	Denticulate W	Denticulate g/p	Abrupt ∑	Abrupt W	Abrupt g/p
Archaeological quartzite	CC															
	CA	2	31	15												
	OO	1	42	42							2	18	8,9	1	14	14
	SO	4	32	8	1	22	22				1	3	2,6	1	5	5,3
	BQ	3	17	5,8	1	16	16				3	30	10			
	RQ	1	15	15	1	57	57	1	11	11						
	MQ				1	6	5,9							1	5	5,1
	Undet.															
	Total	11	137	12	4	101	25	1	11	11	6	51	8,5	3	24	8,1
Flint		1	11	11												
Limestone																
Lutite		8	99	12				2	21	11	2	8	4	3	35	12
Quartz																
Radioralite																

Table-10.31: Frequency table of artefacts sorted by mode of retouch and grouped by raw material, including frequencies, weight and the ratio grams/piece for each case. Pieces with different primary types are not included. Weight is expressed in grams.

10.6. RAW MATERIAL ACQUISITION AND MANAGEMENT PROCESSES AT LAYER-VI OF EL ESQUILLEU

Once the raw data from this layer have been presented, in this section we bring face to face geographical, geological, and archaeological data (the matter) to understand the forces that got these materials deposits here, that is the human behaviour focusses on raw material acquisition and management strategies.

The main acquisition process verified in this layer is the supply of big quantities of orthoquartzites and lutites for human activities, as demonstrated by the great quantity of them found in this layer both in number and in weight. BQ quartzite has also input to the site as a secondary raw material. Other raw material such as quartzarenite, RQ, MQ, flint, limestone, quartz and limonite were also input in the site in small percentages. The latter group indicates different roles as raw material in human activities.

The management of raw material has been analysed including the raw data on all raw materials in a general reduction process model based on a simple “chaîne opératoire” (Figure-10.30). The primary technological product of lithic reduction we find in this layer are cores (irregular, discoid, or levallois). From here on, we expose and analyse the different processes that generate other lithic products based on the understanding of their features.

1. Blanks, as well as smaller blanks (sometimes fragmented) and chunks were obtained as a results of the reduction process of some cores. Smaller blanks and chunks are secondary products generated as a consequence of knapping procedures.

    a. Using retouching procedures, some of these primary blanks were modified, creating retouched artefacts as primary products and more blanks and chunks as secondary products. The latter are lighter than five grams and sometimes fragmented. In addition, new retouches can be made in the blanks to obtain artefacts with multiple primary types, generating more blanks and chunks as secondary products.

    b. Some other blanks were reconfigured by percussion to obtain new flakes. The resulting products are a core on flake and blanks as primary products and other blanks and chunks, derived from the reconfiguration processes, as secondary products.

        i. Some cores on flakes were retouched, creating a retouched core on flake. Small chunks and blanks derived from the retouching process are, again, secondary products.

        ii. As a consequence of the reduction processes of the cores on flakes, further blanks were obtained, also secondary products classified as chunks and blanks (smaller than the previous blanks).

            • The latter blanks can also be retouched, creating new retouched artefacts and secondary products (chunks and blanks).

2. Going back to cores, these can be retouched to obtain retouched cores. Moreover, small chunks and blanks were generated as secondary products as a consequence of the retouching process.

3. Following with cores, some of them were reconfigured to obtain new flaking surfaces or new striking platforms. This process generated new forms or types of cores and three different secondary products: chunks, blanks (generally lighter than five grams and sometimes fragmented) and core preparation/rejuvenation products.

    a. Some of these new cores were retouched, creating retouched cores. As a consequence, small chunks and blanks were produced as secondary products.

Some of the chunks were also retouched. They are always heavier than five grams. Blanks and chunks were generated as secondary products derived of retouch techniques, and they are generally lighter than 5g.

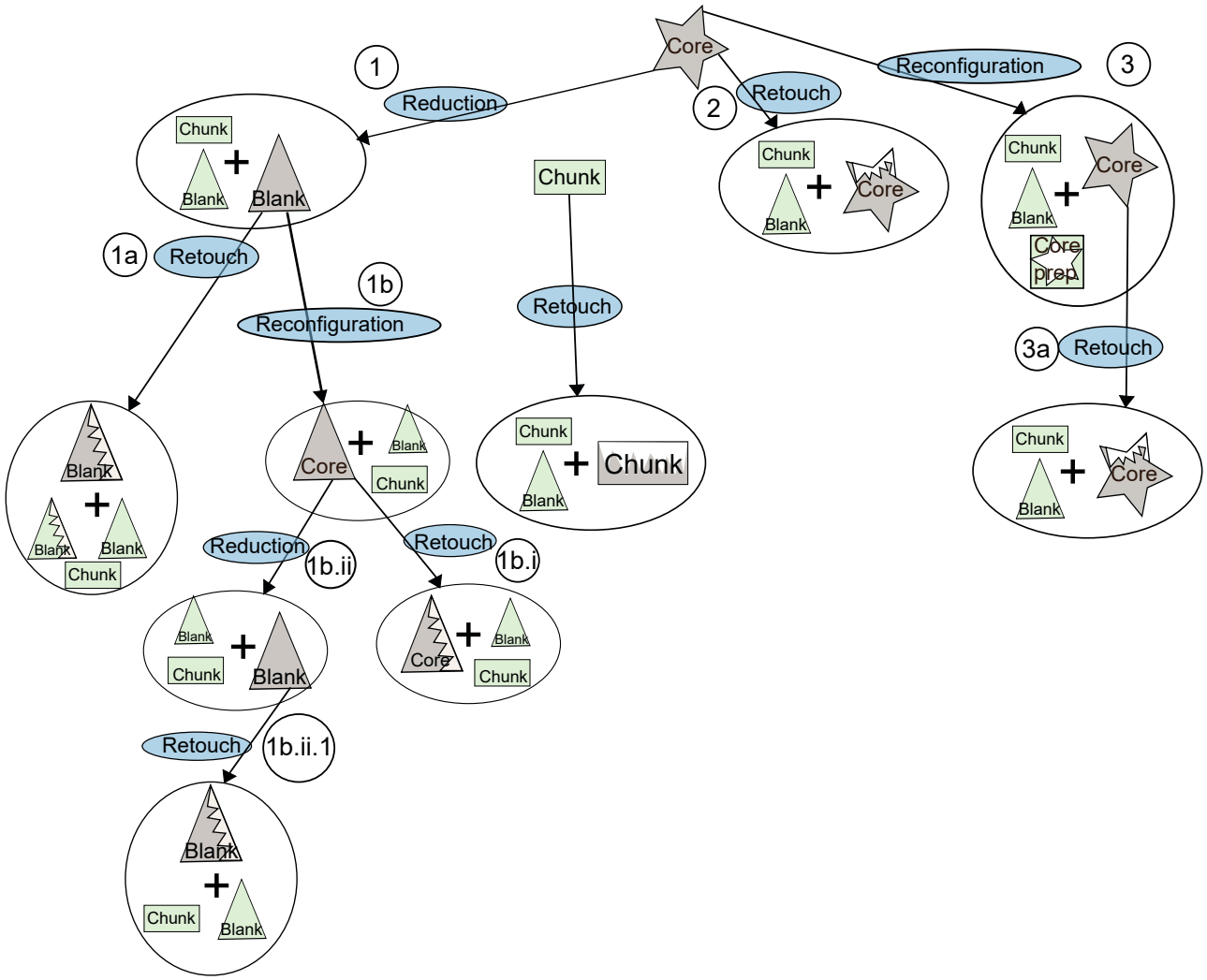

Figure-10.30: Schematic “chaîne opératoire” derived from the analysis of the lithic assemblage from layer-VI of El Esquilleu. Stars represent cores, rectangles chunks, elongated circles completely cortical chunks, squares with stars core preparation/rejuvenation products and triangles blanks. Zig-zag lines added to any of these icons represent retouched artefacts. Grey icons are primary products and green ones secondary products. The blue ellipses indicate human activities. Alphanumeric codes inside circles are references to the text.

Next, we present the conclusions reached about the acquisition and management of, “archaeological quartzites” by petrogenetic types, and later, other raw material. Figure-10.31 and Figure-10.33 schematically represent the acquisition process of “archaeological quartzites” and other raw materials. Figure-10.32 displays the relationship between acquisition and management strategies. Finally, Figure-10.34 shows the Cost map from El Esquilleu with the geological formations where raw material could have been caught.

As has been previously mentioned, “archaeological quartzite” is the most relevant raw material, both in number and weight, present in the layer-VI. Next, we will explain the raw material catchment and management strategies of this raw material taking by petrogenetic types.

The CC type is one of the less frequent type of “archaeological quartzite”. Not all technological categories are represented due to the absence of cores, even though there is a core preparation/rejuvenation product. There is an overrepresentation of chunks and an underrepresentation of knapping products. The weight of chunks and knapping products, which range from one gram to more than 20 grams, supports the idea of knapping and reshaping activities were practiced in the site. The grams/piece ratio of knapping products make it clear that this type is heavier than those produced in other raw materials and other types of “archaeological quartzites”. There are no retouched artefacts. Negative scars on dorsal surfaces are scarce, and they are generally less than one. This petrogenetic type has the higher presence of cortical surfaces on knapping products. All these reason carried

us to consider this material was knapped in the site with low intensity exploitation mechanism. The CC type probably was introduced as cores (absent, although evidenced by one core preparation/ rejuvenation product) or as blanks.

This petrogenetic type is characterised by multiple grain size varieties, generally with heterogeneously distribution of grain sizes. Colour is also greatly heterogeneous, due to the effect of many different non-quartz minerals on these rock. All these elements lead us to conclude: a) the CC petrogenetic type is heterogeneous, and b) the input in the site of CC quartzarenites comes from different pebbles from diverse origins. White varieties could be related with the CC type from Barrios or Cavandi formations, while dark and brown varieties are linked with Murcia Formation or with carboniferous sandstone strata such as the Potes, Mogrovejo or Viorna formations. The analysis of cortical areas reveals the fluvial origin of all the cortical surfaces identified. All in all, we proposed that the CC petrogenetic type is a raw material caught in fluvial beach deposits, probably near the site of El Esquilleu. We observe an important presence of this petrogenetic type in these beaches. Different pebbles with diverse colours and grain size varieties were also found during geological surveys. The general size and morphological features of CC pebbles in these beaches is also heterogeneous: multiple sizes (from medium pebbles to big cobbles) and both spherical and elongated morphologies are present. Then, strong selection mechanisms are would not have been required for the acquisition of this type. In addition, it can be said there is no selection based on colour or on grain size. Putting all this information together, it is possible to conclude that the input of CC type is made as cores or knapping products. The scale of this type in this assemblage reveals its use as raw material was sporadic, maybe related with the scarcity of other raw materials petrogenetic types more suitable.

The CA type, only constitutes a small portion of the total of “archaeological quartzites”, but it is better represented than the CC type. In this case, all three technological orders are present, although there are no core preparation/rejuvenation products. The distribution of the three technological orders points at a smaller presence of knapping products and greater frequency of chunks, especially when this type is compare with orthoquartzites and quartzites. The only represented core made on this quartzarenite is a core on flake. There are two retouched artefacts and both create Sidescraper morphological group, the most frequent morphothema. Weight of blanks and chunks ranges from one gram to more than 15 grams. This proves that knapping and reshaping processes were carried out in the site. The average weight of blanks is lower than for the previous type, but still higher than other petrogenetic types, such as SO or BQ types. The frequency and extension of cortical areas on knapping products is smaller than on previous quartzarenite, but slightly higher than on deformed petrogenetic types. The extension of cortex on dorsal surfaces on blanks, is generally reduced to smaller areas than 33%. The quantity of negative scars on the dorsal surfaces is also higher than on previous type, with similar values observed in orthoquartzites. All these reason carried us to propose this type of quartzarenite was medium intensity exploited. Nevertheless, the small quantity of retouched artefacts make us to nuance this conclusion.

The characterisation of this petrogenetic type based on grain size indicates a general heterogeneous distribution, generally represented by medium grain sizes, even though fine sizes are also well represented. The characterisation based on mineral and colour is more homogeneous than previous type, due to the smaller variability in non-quartz minerals. Nevertheless, there are three different varieties. Then, at least three different former rocks were input in the layer. These features point at a) the CA type is very variable, and b) the input of CA quartzarenites to the site got supplied with pebbles from different source strata. Colour links this quartzarenite with the Barrios or Cavandi outcrop formations, and with clast from Carboniferous conglomerate formations in the case of white or light brown varieties. However, the characterisation of cortical areas points at the only presence of cortex derived from fluvial sources. Therefore, even the former strata could be on the area, they were brought to the site from secondary fluvial deposits. Taking into account the selection mechanisms needed to obtain CA quartzarenites from fluvial courses near El Esquilleu, stronger selection mechanisms would have been necessary for getting this type than for obtain CC type. Although this petrogenetic type is not massively represented in the assemblage, it is well represented showing its importance for the Palaeolithic societies who inhabit this rockshelter during the time-frame this layer were created. Therefore, we propose planned catchment of the type in fluvial deposits that could be, either complementary to the catchment of other raw material; or related with massive catchment of the type, maybe in scarcity of more suitable types. The input in the site could be made as core or blanks. Nevertheless, due to the scarcity of cores (only represented by a core on flake) and the existence of at least three different former blocks of rock, we consider that the massive input was done as blanks.

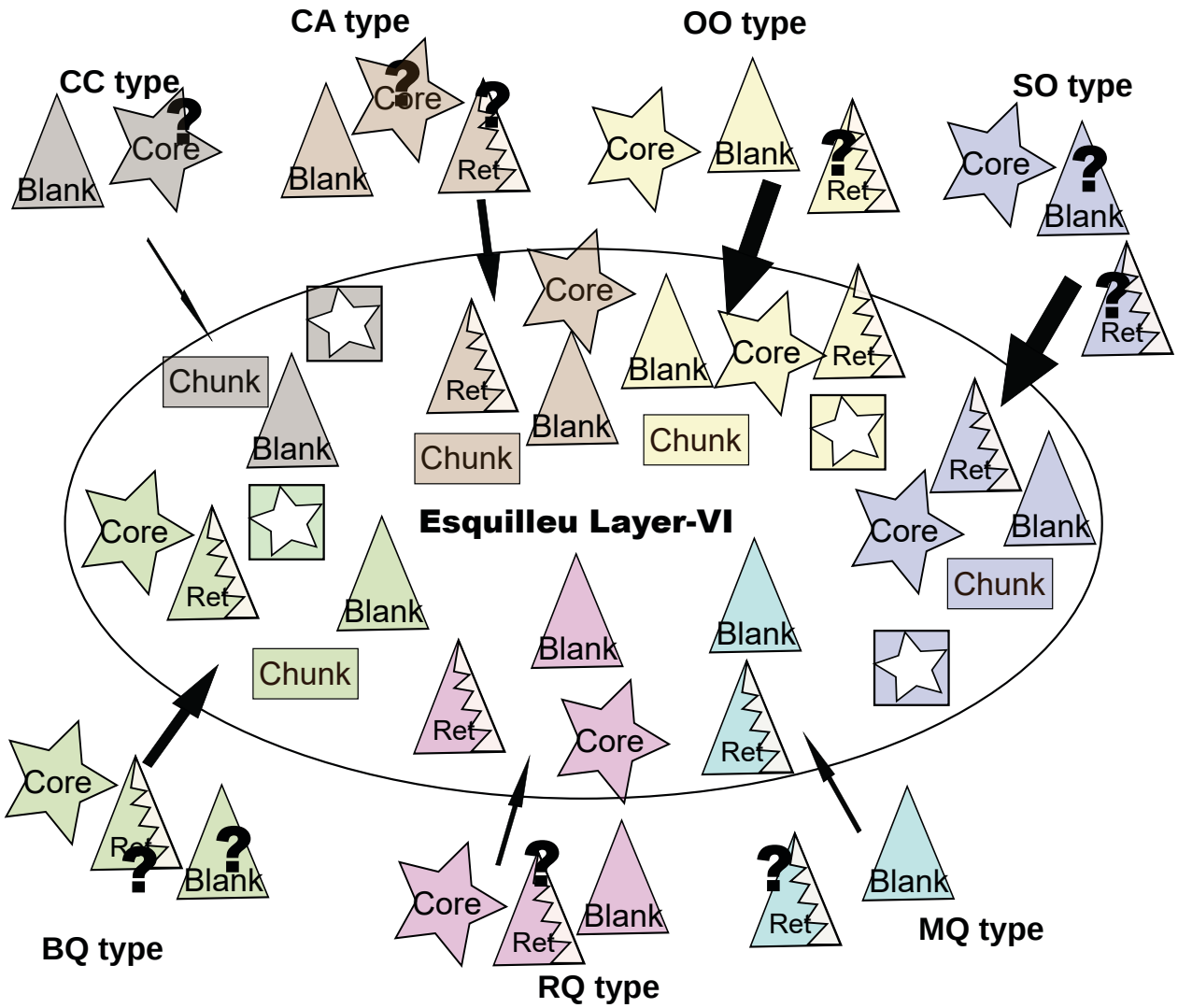

Figure-10.31: Schematic representation of the input of the different petrogenetic types of “archaeological quartzite”, taking into account the different technological products present. Stars represent cores, triangles blanks, triangles with zig-zag retouched material, ellipses fully cortical chunks and rectangles chunks. Question marks indicate products whose presence is not certain.

The OO petrogenetic type of orthoquartzite shows clear differences in management and catchment in comparison with the raw material and types of “archaeological quartzite” tackle above. It represents 27% of the lithic assemblage, a massive input of this type. These data mean there was a planned and massive exploitation of this type. The three technological categories considered are represented in the layer, as well as core preparation/rejuvenation products. It is obvious knapping and reshaping activities were practised in the site. This is also certified by the presence of blanks and chunks between one gram to more than 40 g. Cores types and flacking and knapping surfaces reveal this raw material is more intensively exploited than the quartzarenite group exposed in previous paragraphs. The grams/piece ratio of cores is the highest by comparing with other “archaeological quartzites”, probably due to the abandonment of cores in non-exhausted condition. There is no core on flake. The presence of negative scars is slightly more frequent than in the former two types, revealing similar proportion than the SO type, both with residual percentages of blanks without negative scars. The presence and extension of cortex in blanks is smaller than on quartzarenites, but higher than on more deformed types. This evidence reveals a medium intensity exploitation of this type. The latter idea is also supported by the frequency of retouched material, higher than on quartzarenite, although smaller than on other orthoquartzite and quartzite. The grams/piece ratio of the knapping products is also the highest of all “archaeological quartzites” and the retouched blanks are heavier than 10 grams. Latter two arguments could be related with the used of this orthoquartzite for specific knapping processes or future uses.

The characterisation of this raw material based on grain size and colour, indicates it is a more homogeneous type. Most of the grains are medium size, either on homogeneous or heterogeneous

distribution. According to colour, the most important variety is white-grey one. This variety is associated to stable mineral characterisation, probably as a result of the massive input of this variety in the site. The dark variety is rarer. It may be the consequence of the transportation of a few or only one block of this variety to the site. The original source strata of the lighter colour variety are in the more deformed bands of the Barrios outcrop Formations, as well as in the carboniferous conglomerates from older layers. The darker variety, is inserted exclusively in the latter. The characterisation of cortical areas reveals that most of them come from fluvial deposits. Still, conglomerate cortex is also represented in two dorsal surfaces of blanks. Both cortex are located in the black-grey colour variety. There is no evidence of cortex from outcrop. Therefore, although the most likely source strata are in the Barrios Formation, catchment was probably made in deposits and conglomerates. Most of the conglomerates analysed in the research area have OO orthoquartzites, more frequently the white varieties. In the nearby conglomerates of the Remoña Formation, 5 CU away, it is possible to find them without the need to apply any selective mechanism. Other conglomerates, such as the Curavacas series (12 CU), the Lechada (13 CU), Campollo (16 CU), Maraña-Brañas (27 CU), Narova (10 CU), Pesaguero (12CU), Pontón (28 CU), Potes (12 CU), and Valdeón (32 CU) conglomerates have important amounts of this type. However, at least low intensity selective mechanisms are necessary to choose specific varieties, forms and sizes. All these conglomerates are to the south, in medium altitude plateaus. In this assemblage, the black variety only derives from conglomerates. In research area, this variety is restricted in the south-west conglomerates, therefore, its catchment must be done in these conglomerate formations. In fluvial deposits the presence of this petrogenetic type is scarcer. Therefore, the selective mechanisms required, pick special varieties, forms and sizes would have been more intensive. All in all, catchment of this type was mainly done on fluvial deposits, which would have provided big amounts of material as a results of planned raw material procurement strategies. In addition, a secondary acquisition, related with the dark-grey variety was also done, especially in conglomerates in middle altitudes plateaus. The small frequent of the latter variety points at the use of area where conglomerates are located and the catchment of resources in these areas. Furthermore, this also evidence long-term life of some lithics, probably storage as blanks. Finally, the small frequency of cores in the site, and the relatively abundance of white variety with fluvial cortex, could reveals the acquisition of this material, not as core, but as blanks. Nevertheless, the input to the site, could be made as core, blanks or retouched material.

The SO petrogenetic type shows different management and catchment in comparison with the previous type, despite its representation in the site being similar in quantity. Thirty per cent of the "archaeological quartzites" belong to the SO type. Planned and massive exploitation of this orthoquartzite is observable, which makes it the most intensively exploited type. As in the previous type, the three technological orders, as well as core preparation/rejuvenation products, are represented in this assemblage. It is clear knapping and reshaping activities were carried out in the site, as demonstrated by the presence of blanks and chunks with weights between one gram and more than 50. Core types, their weight and flacking and knapping surfaces reveal this raw material is the most intensively exploited orthoquartzite even though the weight of one of the core is similar to OO type cores. The presence of negative scars is similar to previous type. Nevertheless, cortical areas are less extended than previous OO type and they generally covers less than 33% of their dorsal surfaces. The proportion of retouched artefacts is greater than in the OO type. Still it is under the mean, influenced by the quartzite group. This evidence indicates this material was very intensively exploited. Latter hypothesis is reinforced by the grams/piece ratio of the blanks, lighter than on previous type.

The characterisation of this petrogenetic type reveals there are different grain size varieties, mainly related with fine and middle varieties. There are also differences in grain size distribution, from homogeneous to heterogeneous patterns. At same time, two different colour/mineral varieties can be distinguished: The dark variety and the light-grey one. The first is better represented in this layer. The input in the site of multiple lithic mass is clear. The original outcrop strata of all these varieties defined is not located in the research area, but they can be found in conglomerate strata and deposits. The conglomerates with the SO petrogenetic type are in the Lechada, Maraña-Brañas, Pontón, Potes, Remoña, and Valdeón formations. In all of them the presence of the fine grained varieties range between 5 and 50%, except for the Lechada and Potes conglomerates, where they represent less than 5% of the pebbles. The analysis of cortical surfaces reveals a clear change in acquisition dynamics with an inversion in their provenance. The presence of conglomerate cortical surfaces is more frequent than fluvial ones. The presence of SO orthoquartzites in beach deposits is negligible, especially near fluvial deposits. We propose the input of this type to the site is mixed: on one hand, there is a massive and planned catchment strategy carried out in conglomerates; on the other, there are occasional findings in river deposits in relation with the extraction of other raw materials (previously exposed) throughout massive and planned catchment strategies. The latter strategy requires

strong selection and identification mechanism of raw material, while the first input demand, at least medium-term mobility. The input in the site, could have been made as cores, blanks or retouched material.

The management and catchment strategies observed in previous type show similitudes and differences with the **BQ quartzite type**. The clearest differences are in the quantity of this type, worse represented than previous orthoquartzites. Nevertheless, its presence (also the quantity, as the third better represented "archaeological quartzite" type) points at its importance as raw material, also its availability in the research area. All technological products are identified in this type, also core preparation/rejuvenation products. Cores are overrepresented and chunks are underrepresented. In addition, the presence of chunks and blanks between one gram and more than 15 g, help us to conclude that knapping and reshaping activities where performance in the site. The grams/piece ratio especially that of blanks is one of the smaller ones. Core types, weight and flacking and knapping surfaces reveal this raw material was intensively exploited, also supported by the presence of a really small core on flake. The number of extractions on dorsal surfaces (generally more than two) and the occasional presence of cortical areas in dorsal surfaces agree with the idea that this resource as intensively exploited material. Finally, the frequency of retouched artefacts is higher than most other "archaeological quartzites". It is also the petrogenetic type with higher incident of artefacts with multiple primary types on them. All in all, the data gathered demonstrate this quartzite was an intensively exploited material and all phases of lithic reduction were performance in the site. Due to the overrepresentation of cores, especially by compare with OO and the quartzarenite, this raw material probably inputs as cores. Nevertheless blanks and retouched material could have been brought as final product, used and afterwards abandoned in the site.

The BQ type in this layer is relatively homogeneous with small differences in grain size characterisation (in size and distribution). The mineral characterisation does neither reveal clear varieties. Nevertheless, there are two different varieties attending to colour: the black-grey variety and the brown one. Therefore, there are, at least, two different mass of rock in the layer. The first correspond with the dark variety, massively represented, and the second is limited to one lithic block from the brown variety (one of the brown BQ variety is a core). Regarding the former, and due to the presence of four cores, at least four different blocks were introduced in the site. We did not find the original outcrop strata for this type of quartzite in the field survey. However, it was identified in some small conglomerates. Its presence in fluvial deposits is negligible. There are important quantities (between 5 and 50%) of BQ quartzite in the Remoña, Valdeón, and Pontón (nearest location at 26 CU) conglomerates. In other conglomerates, such as Maraña-Brañas, Pesaguero, and Potes conglomerates, the BQ type is less frequent. All except one cortical surfaces identified derive from conglomerates. Therefore, it can be deduced that its acquisition is based on massive exploitation of these contexts. Therefore, catchment activities were based on the extraction of big quantities of this material in conglomerates applying medium intensity selective mechanisms. For this purpose mobility could have been either low scale to the near conglomerates of the Remoña Formation or medium or long scale mobility to the Southern and South-western conglomerates. The only fluvial cortex identified is on a brown variety BQ quartzite, therefore, the acquisition of this block of rock was done on a river deposit. The scarcity of this material in this context require important selective and identification strategies. The catchment of this lithic block is associated to a casual finding, probably associated with massive catchment of others petrogenetic types. The scarcity of this petrogenetic type in the layer and the high representation of cores (also their weight and features) could be the consequence of long transportation of an appreciated raw material derived from at least, low mobility. The overrepresentation of cores made on this BQ quartzite reveals clear differences with previous orthoquartzites, especially when compare with the OO type. This points at different storage mechanism of lithic raw material, in this case as cores made on a more interesting and versatile raw material.

The RQ quartzite type presents similar patterns of catchment and management even though the quantity of this type is reduced to 5% of the lithic assemblage. There is no chunk, neither core preparation/rejuvenation products. Nevertheless, there are three cores and knapping products are frequent. Retouched material is overrepresented, and its frequency is the highest of all petrogenetic types. In addition, all morphological groups are represented in blanks made on RQ type. It is especially interesting that the only Point configured on "archaeological quartzite" is made on this type. One of the cores is also retouched. The presence of blanks ranging from one gram to more than 50 g indicates knapping and reshaping activities were performed in the site. Nevertheless, these activities were limited, as the quantity of small lithic fragments reveals. The quantity of negative scars on dorsal surfaces points at an intensive exploitation of this material despite the increase and the extension of cortex on dorsal surfaces (in comparison with previous orthoquartzites and quartzite

types). The grams/piece ratio of blanks is high, similar than core one. The latter one is the lightest ratio when it is compared with other raw materials and petrogenetic types of this assemblage. All these data points at a complex management of this material, related with the scarcity of the RQ type. We propose the input of this type was occasional and it was brought as cores, blanks or retouched artefacts that could be used, reduced or reshaped for specific activities. It is also noticeable that all blanks were complete and maybe configured outside the site. The latter hypothesis is reinforced by the similar weight between blanks and cores.

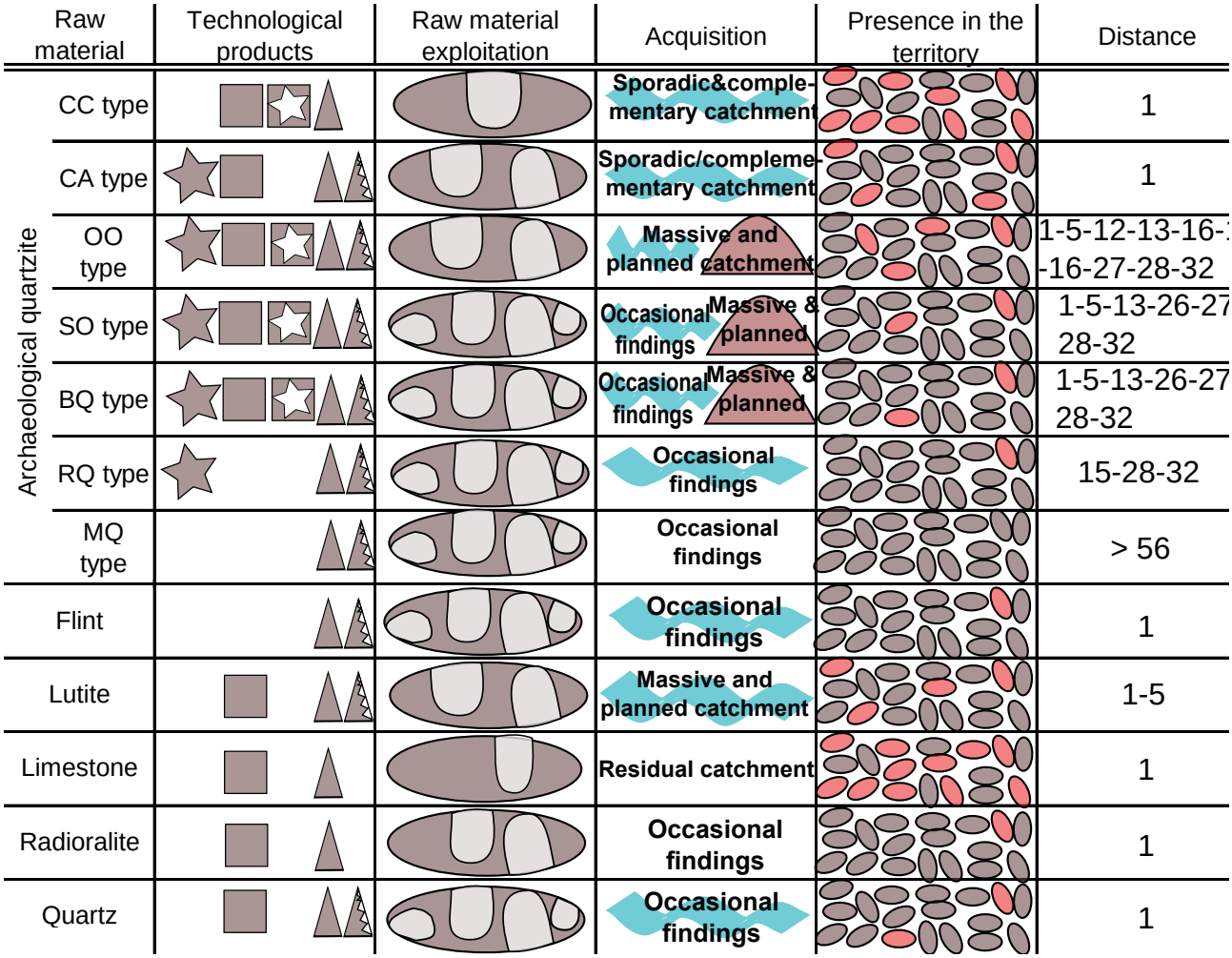

Figure-10.32: Schematic representation simplifying raw material acquisition and management evidences from layer-XIII of el Esquilleu. In the column “Technological products” stars represent cores, squares chunks, squares with starts core preparation/rejuvenation products, and triangles blanks. Zig-zag lines added to any of these icons represent retouched artefacts. In the column “Raw material exploitation”, circles represent unexploited raw material, ovals with one scar represent low intensity raw material exploitation, ovals with two scars represent medium intensity raw material exploitation, and ovals with four scars represent high-intensity raw material exploitation. In the column “Acquisition” waving blue lines represent river acquisition and brown semicircles represent conglomerate acquisition. In column “Presence in territory”, the complete set of ovals represents all the raw materials available in the territory. The ones highlighted in red represent the proportional presence of each specific raw material in the territory. Higher presence of the latter means weaker selection degree.

The petrological characterisation of this type also agree with the previous hypothesis. There are no clear differences in grain size to stablish different varieties of this material. Clearest differences arise using the colour-mineral features, creating two different varieties: the dark and the light ones. Therefore, at least two different blocks of rock were brought to the site. We were unable to find any evidence of this petrogenetic type in massive outcrops of the surveyed area. Its presence is reduced to two conglomerate formations: the Pontón and the Valdeón conglomerates, both in the South-west of the research area. Still, the presence of this type is scarce in both conglomerate formations. Nevertheless, the characterisation of cortical areas of the RQ quartzite lithics only show fluvial cortex. We did not find any evidence of this petrogenetic type in fluvial deposits during our survey. However,

its presence cannot be completely discarded, at least in the Cares River, which creates the erosive basin where conglomerates surface. These data indicate that catchment of this type necessarily implied medium distance movement outside the Deva Basin. In addition, the evidence above supports the existence of strong selective mechanisms in deposits. The presence of this type in the site does also reveal a conscious mechanism of selective and conservative exploitation of raw material. The intensive exploitation of this material, and its appreciation as singular, valuable, and exiguous is clear. The scarce presence of this petrogenetic type in the layer and the high representation of cores (also their weight and features), could be the consequence of long-term core transportation. These cores evidenced the later use of an appreciated raw material derived from long scale-mobility. Therefore, these evidences reinforce the hypothesis suggested in previous BQ type. In addition, the abundance and weight of retouched artefacts, also point at long-term use of blanks and retouched artefacts. In these cases they were mobilised as final product, as a tool-kit. The catchment of RQ quartzite is related with long-term mobility and it is based on the storage of cores and probably retouched artefacts. This strategy is probably based on sporadic catchment in deposits and long-term mobility.

The MQ quartzite type shows catchment and management patterns similar to the previous type. The quantity of this type of quartzite is the smallest in the layer and it is limited to blanks. The amount of retouched material is smaller than in previous quartzites, but higher than on quartzarenites and orthoquartzites. Abrupt morphothema are abundant. The grams/piece ratio is slightly smaller than the mean of “archaeological quartzites” blanks. There is no obvious evidence of knapping processes in the site since chunks are not represented and the small quantity of blanks between one and five grams. The quantity of extraction on dorsal surfaces is high, even though most blanks have two extraction. We do not observe cortical surfaces on the ten blanks, revealing the smallest rate of cortex in the lithic collection. All these data suggest this type was intensively exploited. We propose reshaping activities and maybe extraction of small flakes through knapping were carried out in the site.

We do not identity different in mineral-colour characterisation or grain size among the MQ quartzites in this assemblage. All material represents a homogenous grain size between fine and medium classes. Regarding colour, most of the samples are white or white-grey. We do not find any evidence of this quartzite in the research area surveyed. Then, the only possibilities are a) in non-surveyed strata, b) outside of the research area, or c) hidden in deposits or conglomerates in negligible quantity. Catchment strategies would imply high mobility and/or really strong selective mechanism in conglomerates or fluvial deposits. As it was verified in the previous type, MQ quartzite involves a conscious mechanism of selective and conservative exploitation of raw material. The only presence of blanks could be again related with storage products in blanks form (also retouched products). It is clear this quartzite is intensively exploited as a singular, valuable, and exiguous raw material maybe related with a mobile tool-kit, as proposed by other authors in different regions (Bustos-Pérez et al., 2017; Meignen et al., 2009; Turq et al., 2013).

Next we will explain the raw material catchment and management strategies of other raw material. These material are not frequent in the layer VI-F of El Esquilleu, although they reveal different roles of raw material and interesting catchment and management behaviour.

Starting with the scarce presence of **flint**, it is only represented by blanks. All these blanks have at least three negative scars on their dorsal surfaces. It point at the intensive exploitation of this raw material. Cortex extension does also agree with latter hypothesis, due to its reduced representation in only one blank, covering less than 33% of its dorsal surface. One blank is retouched, reinforcing the intensive exploitation of this rock. Due to the lack of blanks lighter than three grams, also chunks, and the small quantity of lithic materials, we consider that knapping or reshaping were not carried out in the site.

The colour of all flint pieces is black and can give a hint on their origin, probably related with Palaeozoic Black cherts such as the Vegamián Formation (Herrero-Alonso et al., 2016). The only piece where cortex could be characterised points at its possible fluvial origin. This indicates the context where catchment activities were carried out, secondary deposits. The information derived from the geological surveys conducted during this research and from other studies in the surrounding area (Álvarez et al., 2013; Manzano et al., 2005) reveals a negligible presence of flint in river beaches, reduced to small sizes and relatively tabular forms. Then, catchment activities must have necessarily implied intensive selection in fluvial deposits. These would have not been planned or based on systematic intense raw material exploitation strategies. Flint catchment would have been based on occasional findings in river courses as a result of casual transit or other activities. This high intensity exploitation of flint founded on the analysis of technological and metrical features suggests the

qualitative importance of this raw material. Furthermore, quantitative information reveals the scarcity of this material. The interaction between qualitative and quantitative information unveils the importance of this raw material for human activities that maybe could have been related with knapping and use properties, but also its scarcity. The absence of all types of technological products, also lighter blanks than 3 grams could indicate these three pieces were input in the site as end product, as part of a tool-kit, as proposed by other authors (Bustos-Pérez and Baena Preysler, 2016; Turq et al., 2013; Vaquero and Romagnoli, 2017).

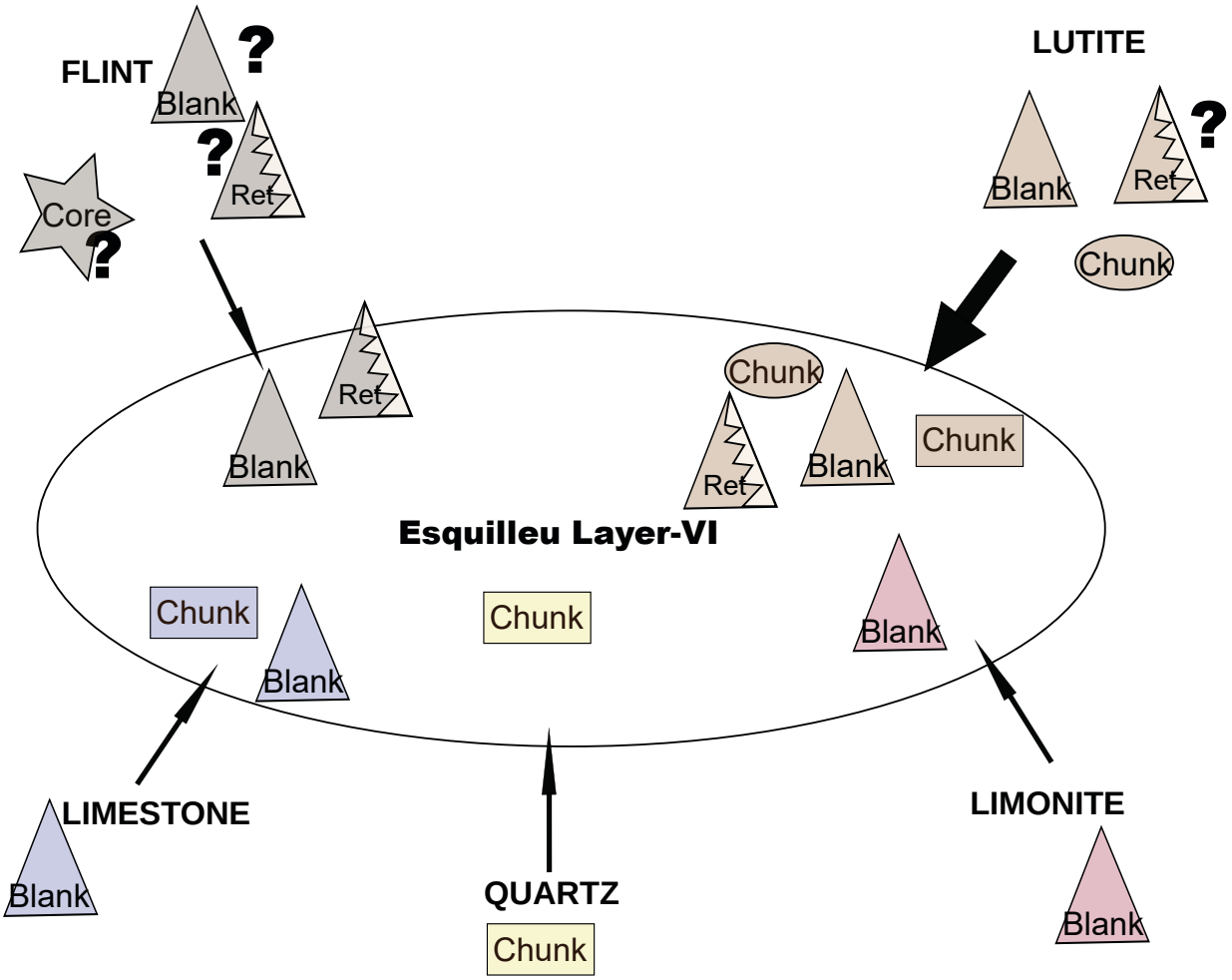

Figure-10.33: Schematic representation of the input of non-“archaeological quartzite” raw material, taking into account the different technological products present. Stars represent cores, triangles blanks, triangles with zig-zag retouched material, ellipses fully cortical chunks and rectangles chunks. Question marks indicate products whose presence is not certain.

Lutite is the second better represented raw material in the assemblage and it shows different pattern of acquisition and management of raw material than flint. There are all technological products in the site except core preparation/rejuvenation products. The three main technological products are distributed in similar proportion than the general characterisation of the complete assemblage. The distribution of weight on knapping products and chunks, ranging from less than one gram to others heavier than 60 grams points at knapping and resharpening activities in the site. All represented types of cores in the layer are made on this raw material, also the unique Levallois core. Cortical surfaces are less frequent than on “archaeological quartzite” and their extension is smaller than 66% of dorsal surfaces. The quantity of negative scars on blanks is variable, but there are no blanks without negative extraction and the majority of blanks have, at least, the three negative scars. The gram/piece ratio is lighter than “archaeological quartzites” one but similar to flint one. The frequency of retouched artefacts is similar than its incidence in the complete assemblage, even it is the raw material with higher quantity of points (2). All these arguments lead us to propose that this material was medium-intensity exploited. The presence of all technological main categories and the weight of knapping products, also points that knapping and reshaping activities were carried out in the site. Lutites were carried as either blanks, cores, or retouched artefacts.

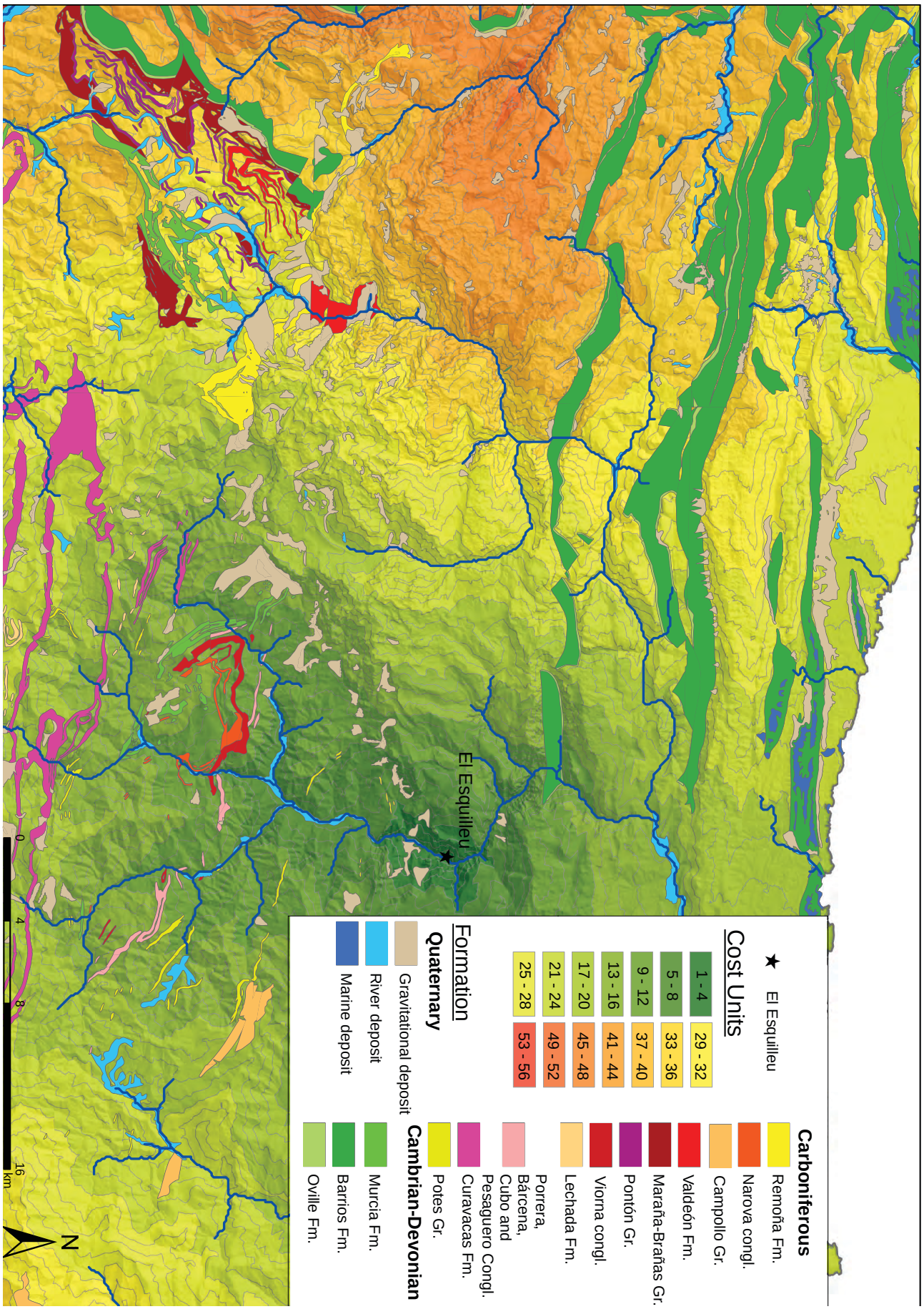

Figure-11.34: Cost map from the site of El Esquilleu to polygons with presence of “archaeological quartzites” and other raw materials.

Regarding the properties of this raw material, most lutites are grey to black, even though there are some reddish or brownish varieties, probably due to the impact of weathering process. All these lutites are similar to the siliceous cemented varieties found in the area around the site, in outcrops (associated to limestone, sandstone and conglomerate alternations from the Carboniferous), conglomerates (Carboniferous), and river deposits. Their presence in the latter two was analysed in this research, revealing changeable percentages generally higher than 10% of the rocks present in both types of contexts. This raw material has also been analysed in archaeological contexts from other regions, such as the Basque Country (Fernández-Eraso et al., 2017). All represented cortex is characterised with features coming from fluvial deposits. All this information allow us to propose an input of lutites to the site through conscious and massive acquisition mechanism for its use for knapping and other activities in the site. Its catchment was carried out in river beaches, probably in planned strategies to obtain big amounts of this material. In addition, considering the presence of all technological products, we conclude that the input was made as blanks, cores, or retouched material, obtained as primary product in the river beaches in the surrounding area. The selection of siliceous cemented varieties in this assemblage is obvious. Therefore, at least medium degree of selection mechanism must be applied in fluvial beaches to obtain this variety.

The limestone is one of the raw material with small quantitative importance in this assemblage, only represented by two items. This raw material suggests, again, different catchment and management strategies than the previous two. One is a blank and the other, a chunk. The first weight 20 g and has, at least, three negative scars. The chunk weight eight grams and does not show clear evidences of being knapped. None of them were retouched. Both limestones are compact have shaped edges, and are grey to blue. There are no cortical surfaces, then, we could not propose the area where limestone were caught. Multiple source strata are available for obtain limestone in the area. It is not possible to discard that at least the chunk to be rock fragments detached from the structure of the shelter. We do not have evidences of knapping, neither reshaping processes in the site, then, the rocks were directly input as finished object. Due to the small presence of this rock in the layer and its characterisation, its exploitation is clearly residual and of low intensity, related with its sporadic use in absence of other material.

The limonite is, again, one of the raw material with smaller quantitative importance in the assemblage, only represented by three blanks. The quantity of negative scars is small and there are no cortex on dorsal surfaces. Their weights are similar one each other and it is reduced around two grams. One of the blanks was retouched with two Sidescraper. All these reason carried us to consider this material was medium intensively exploited, maybe related with isolated and specific events of use. Due to the absence of lighter knapping products and chunk, we consider that knapping activities have not been taking place in the site. Regarding the physical features of limonites, all three are brown to red and they have really fine grains. We do not find cortical surfaces, then, we could determine its catchment areas. We do not find evidences of this type of material in the research area, but formative process of limonites allow its formation in wet and iron-oxides clay soils. Therefore, the caption could be made directly in the rockshelter.

The catchment and management of **quartz** could not be easily determinable due to the only presence of one item, which is classified as chunk. It weights six grams. This quartz is opaque and white. In the research area defined for this study we only identified quartz on fluvial deposits in negligible proportions, mainly in the headwaters of Deva and Cares rivers. Due to the scarcity of diagnostic elements to characterise the source area, we can only affirm they were caught in fluvial deposits.

All in all, we observe different catchment and management strategies for each raw material. This allows us to propose the following human mobility, landscape use, selective and exploitation mechanism. These are:

- Low, medium and high-scale mobility strategies to the South and South-west of the research area, as well as outside it.
- Exploitation of diverse landscapes, from river courses in low altitudes areas to plateaus in medium altitudes zones.
- Selective and non-selective mechanisms for obtaining specific raw materials or petrogenetic types in deposits and conglomerates.
- Diversity of raw materials exploited, selected based on their physical properties and their availability in the landscape. This includes storage of different raw material as blanks, cores, and retouched artefacts.

CHAPTER-11

RESULTS. THE ARCHAEOLOGICAL SITE OF EL ARTEU

11.1. GENERAL ISSUES AND STATE OF PRESERVATION OF THE COLLECTION

The rockshelter of El Arteu is small. No excavation has been carried out in this site and the material was collected in sediments derived from the fallen profiles in the 1990s by Gonzalo Gómez Casares. The sedimentary sequence was about 80 cm deep, and very rich archaeological layers seemed to be present. The collection recovered was small, 247 lithic fragments. Previous research certify this lithic collection was related within the Mousterian, with a main discoid reduction method focused on obtaining pointed flakes. The main raw material recovered in the site was quartzite, although other material are represented, such as ferruginous rocks, flint, sandstone and limestone. El Arteu site seemed to be related to a complex network between the previously described sites of El Habario and El Esquilleu due to similarities in technology and raw material procurement strategies. The prior interpretation of El Arteu for hunting activities inside a complex residential model in the area inside a single phase of Middle Palaeolithic was suggested.

The archaeological assemblage analysed here is the complete collection recovered from the fallen profile from original sedimentary sequence at El Arteu. Therefore, the analysed material are biased and results here exposed must be taken with caution. We have analysed all 255 lithics preserved in the MUPAC. The general state of preservation is medium. Some pieces have recent fractures. Carbonates, also clays stuck in lithic surfaces are frequent. In addition, some of them have altered surfaces due to the erosion of water. Finally, some lithics presented evidence of chemical weathering processes altering cortical areas, non-deformed/metamorphic surfaces or jointed areas.

11.2. PETROLOGICAL STRUCTURE

Here we present the results of raw material characterisation. We were able to determine the main lithology of every piece except for two. In general, the collection is mainly formed by “archaeological quartzite” with residual representation of radioralite, limestone, lutite, and quartz (Table-11.1).

Main Raw Material	Archaeological quartzite	Flint	Limestone	Limonite	Lutite	Quartz	Radioralite	Volcanic rock	Undeterminate
Σ	237	0	3	0	1	1	11	0	2
%	92,9	0	1,2	0	0,4	0,4	4,3	0	0,8

Table-11.1: Frequency table of lithologies identified in el Arteu.

Focussing on “archaeological quartzite”, through binocular microscopy we could identify six of the seven proposed petrogenetic types. Orthoquartzites are highly represented in more than 50% of the lithic implements, especially due to the high quantity of the OO petrogenetic type. Quartzarenite is the second most important group and both types are similarly represented. Finally, the group of quartzite is the less frequent one, with similar frequency than quartzarenite. MQ quartzite type is not recognised in the assemblage (Table-11.2). We were unable to identify six pieces, 3% of the collection. Coming to the distribution of grain size, the most frequent category is homogeneous distribution around one mode with 46% of cases, even though general heterogeneous distribution is also well represented with 37% of the cases. Regarding grain size, the most frequent categories are fine and medium grain sizes. As to “archaeological quartzite” types and size varieties, we identify six preferential varieties: three belongs to OO type, the first with fine size and homogeneous distribution, the second with medium size and homogeneous distribution, and the third with medium size and heterogeneous distribution. Other two varieties are BQ and SO types with fine grain size and homogeneous distribution. The last variety is a CA type with heterogeneous distribution and medium quartz grain sizes. Chi-square test (χ^2 (35, N =230) = 137.030, p < .001) reinforces the idea of a preferential acquisition of these varieties.

Grain size characterisation			Petrogenetic type															
			CC		CA		OO		SO		BQ		RQ		MQ		Unknow		Total	
			Σ	%	Σ	%	Σ	%	Σ	%	Σ	%	Σ	%	Σ	%	Σ	%	Σ	%
	Homogeneous and one mode distribution	Fine grain			3	10	**41**	**37**	13	59	20	51	2	29					79	33
		Medium grain			1	3	**25**	**22**	1	5	3	8					1	17	31	13
		Coarse grain																		
	Heterogeneous and two modes distribution	Fine grain	1	5	1	3	6	5			1	3	1	14					10	4
		Medium grain	5	23	2	7	3	3	1	5	1	3							12	5
		Coarse grain	8	36	2	7							1	14			1	17	12	5
	Heterogeneous distribution	Fine grain	1	5	2	7	10	9	2	9	7	18	2	29					24	10
		Medium grain	5	23	16	55	22	20	5	23	6	15					1	17	55	23
		Coarse grain	2	9	2	7	5	4					1	14					10	4
	Unknown										1	3					3	50	4	2
		Total	22	9	29	12	112	47	22	9	39	16	7	3			6	3	237	100

Table-11.2: Frequency table of petrological features identified in El Arteu based on binocular characterisation. Columns are petrogenetic types and rows contain the characteristics of grains according to size, classified first by distribution and second by size itself. Cells in black are the categories representing more than 10% of the total cases. Cells in dark grey are the categories representing between 5 and 10% of cases. Finally, cells in light grey are the categories representing between 1 and 5% of cases.

Table-11.3: Frequency table of non-quartz minerals identified in El Arteu based on binocular characterisation. Columns are the three fields examined and rows are the non-quartz minerals identified.

Non-quartz mineral	A		B		C		General	
	Σ	%	Σ	%	Σ	%	Σ	%
Absence	9	4	20	8	88	37	117	16
Fe-Oxide	78	33	34	14	29	12	141	20
Manganese Oxide	17	7	30	13	31	13	78	11
Mica	61	26	56	24	35	15	152	21
Black mineral	67	28	83	35	38	16	188	26
Pyrite	1	0	8	3	9	4	18	3
Feldspar	4	2	6	3	7	3	17	2
Total	237	100	237	100	237	100	711	100

Table-11.4: Frequency table of colour hue of the samples from El Arteu. Columns are primary and secondary colour hues and rows are the colours considered.

Colour	On fresh cut			
	Primary		Secondary	
	Σ	%	Σ	%
Absence	5	2	53	22
White	82	35	49	21
Grey	129	54	46	19
Black	13	5	19	8
Blue	2	1	44	19
Green			2	1
Orange			3	1
Brown	5	2	16	7
Red	1	0	5	2
Total	237	100	237	100

We identified non-quartz minerals in 225 samples of “archaeological quartzite”, after having excluded the implements assigned to unknown type (Table-11.3). Non-quartz mineral characterisation reveals the major presence of micas, non-identified black and heavy minerals, iron oxides, and manganese oxides. All these minerals are present in any petrogenetic type. Nevertheless, the scarce feldspars identified are mainly associated with CC type. Characterisation of colour indicates that most frequent colours are grey, white, black, and blue (Table-11.4). The first and the latter colours are not related associated to any petrogenetic type. Nevertheless, most of the white “archaeological quartzites” are associated with the OO type. In addition, dark colours are associated with BQ and CC petrogenetic types. Finally, brown coloured lithics are associated with quartzarenites.

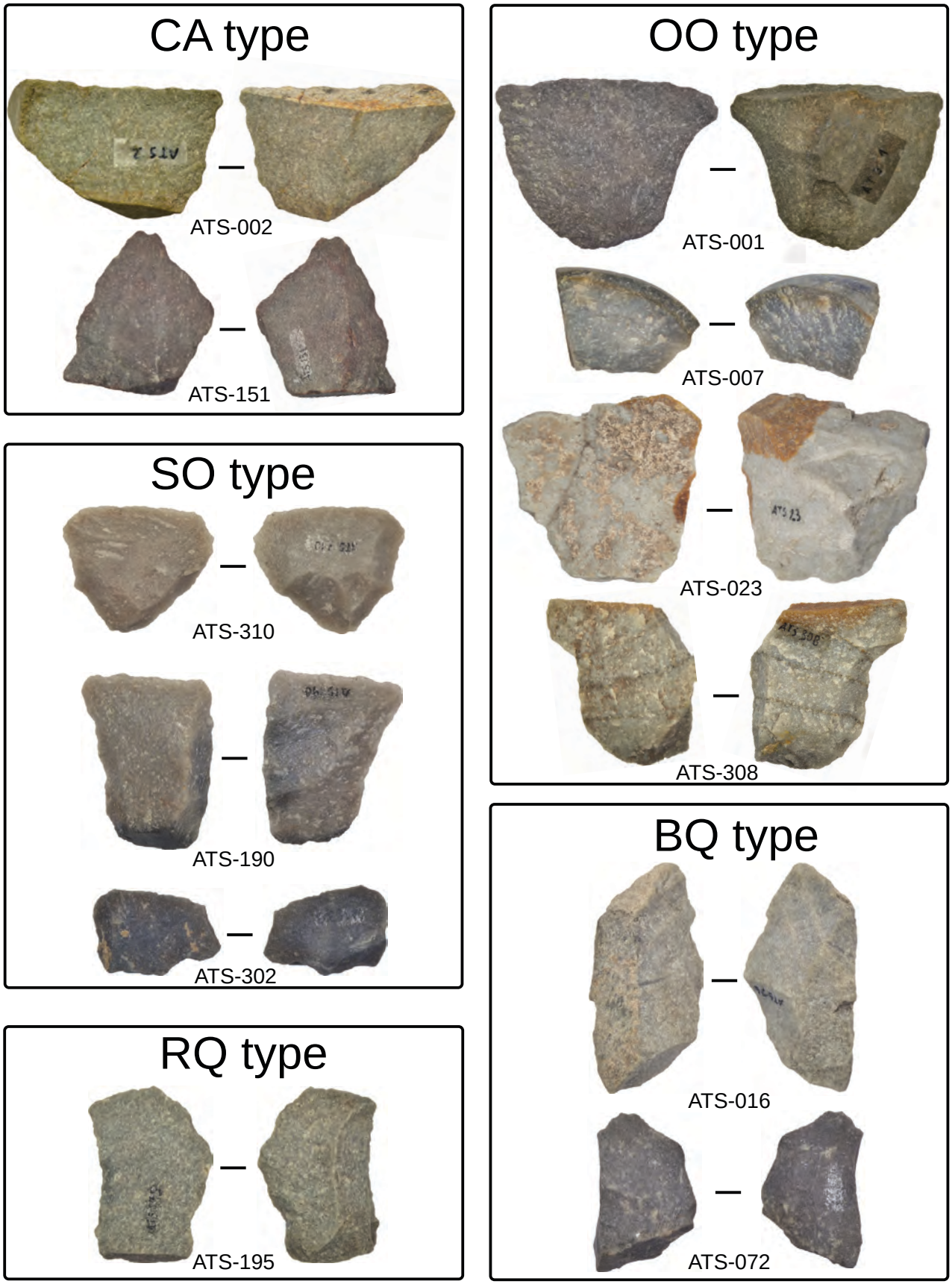

Figure-11.1: Pictures of the samples selected from El Arteu, grouped by petrogenetic type.

We carried out petrographic and geochemical characterisation of twelve items, with the aim of recognise all represented types and varieties of “archaeological quartzites” (Figure-11.1). The description of these samples helps us understand the differences between types, as well as define and establish some interesting varieties. CC type was not sampled due to the ease to describe features under binocular characterisation. We analyse this type using non-destructive techniques.

11.2.1. THE CA PETROGENETIC TYPE AT EL ARTEU

Two of the samples selected belong to the CA petrogenetic type. These are samples ATS-002 and ATS-151. Both thin sections are characterised by clastic grained texture and tangential packing. On both samples, there are zones with clastic quartz grains and other with undulatory extinction, even though the latter zones are more frequent in the first sample than in the second. There are also some regrowth around the former quartz grain limits in both samples. Regarding quartz grain sizes, we observe similitudes in the range of quartz grain framework, from medium silt to fine sand sizes. Nevertheless, most of grains are between coarse silt and very fine sand categories. The roundness index are similar in both samples, but the irregularity of the particles differs. The morphology of grains from ATS-151 is more regular than grains from ATS-002. The grains from the latter samples have ruffled quartz limits.

Preferential orientation at σ = 0.05 of quartz grains is observed in both samples, although they are only preferentially oriented at σ = 0.01 on sample ATS-002. The preferential orientation of quartz grains on both samples is related to sedimentation processes, not to metamorphic foliation. The features observed through binocular microscopy are in concordance with this characterisation, that is, coarse grained texture and tangent packing (i.e. granular T&P). The size characterisation of grains under binoculars also points at heterogeneous distribution of grains around medium size quartz grains (Figure-11.2).

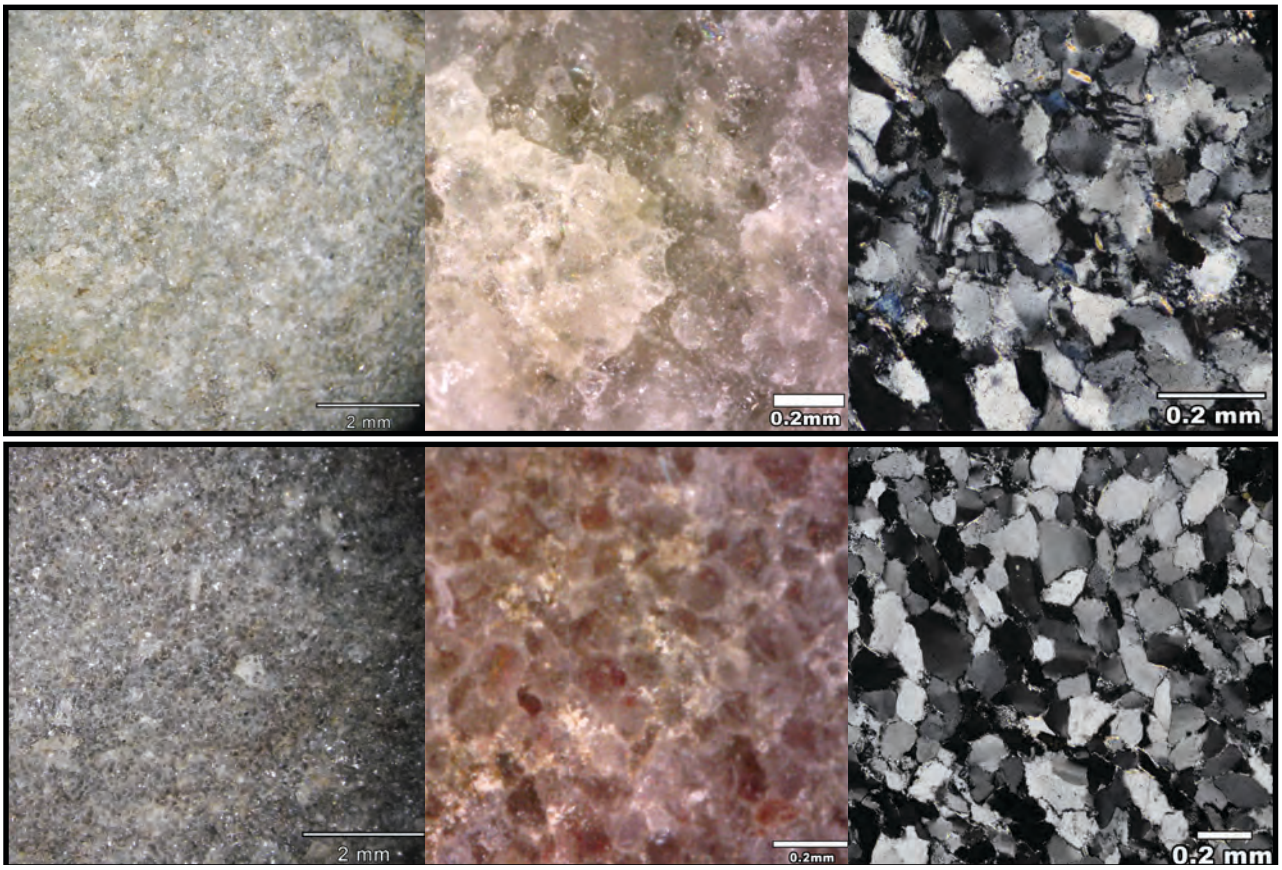

Figure-11.2: Pictures of the CA type samples from El Arteu. From top to bottom, samples ATS-002 and ATS-151. From left to right, microscopy binocular picture at 20x, microscopy binocular picture at 250x, and thin section microscopy picture at different magnifications.

Petrographic characterisation of these samples points at the small presence of siliceous matrix in the ATS-002 and clayey matrix in the ATS-151. Non-quartz minerals are well represented in both samples, mainly as iron oxides and tourmaline. There are also micas and feldspar on ATS-001 and clay, chlorite, and zircon in the ATS-151. X-Ray fluorescence reveals the major presence of SiO_2 in both samples, around 90%. Other components such as Al_2O_3 and Fe_2O_3 are frequent in both samples. The first one is better represented in ATS-002 and the second in ATS-151. In the first sample, the presence of Na_2O is also relevant and it is probably related with the feldspar characterised. The characterisation of non-quartz minerals under binoculars is consistent with previous data due to the presence of non-identified heavy and black minerals, oxides and micas for the ATS-151 and feldspar, iron oxides and micas for the ATS-002. The latter sample is white, with orange or red areas in the surface as a consequence of iron oxides. ATS-151, is brown-red, due to the higher presence of iron oxides and the clayey matrix extended in all the sample.

The characterisation of these samples allows us to certify the presence of quartzarenites in Middle-Palaeolithic contexts, also to prove its role as raw material used for knapping activities. These samples also prove non-destructive characterisation of quartzarenites in archaeological contexts is consistent and its characterisation is not the consequence of weathering processes on external lithic surfaces. Regarding the characterisation of the complete lithic assemblage from this site, both samples are representative of the most frequent size variety: the medium size one. Nevertheless, they are different in the mineral and colour characterisation. ATS-002 is associated to feldspar, mica and iron oxides. The latter mineral is represented in cortical zones and joints. Nevertheless, the extension of iron oxides in all lithic surface (as a consequence of the clayey matrix) and the major presence of non-identified heavy and black minerals, make the brown-red colour of the ATS-151 sample. There is also mineral/colour variety characterised with manganese oxides and coloured in black.

11.2.2. THE OO PETROGENETIC TYPE AT EL ARTEU

Four of the samples analysed are OO orthoquartzite: ATS-001, ATS-007, ATS-023, and ATS-308. All four have clastic grained texture, but they differ in the packing. While the first has tangential packing, the other three have complete packing. The characterisation of grain features slightly differs between four samples due to the small quantity of syntaxial quartz overgrowths in ATS-001. In the other three samples, this feature is more frequent. Moreover, undulatory extinction and concave-convex quartz grain limits are observable in all four samples. The grain size characterisation points at two different varieties: The first one is characterised by ATS-001 and ATS-007 samples. The most frequent quartz grain sizes are coarse silt and very fine sand (Figure-11.3). The second group of samples is formed by ATS-023 and ATS-308 and quartz grains size are around the very fine sand and fine sand categories (Figure-11.4). Regarding grain size distribution, the ATS-007 sample is more homogeneous than other three. The quartz grain morphology is similar in all four samples. Roundness indexes in all four samples are around 0.6 and circularity indexes around 0.53. These measurement points at non-elongated and regular shapes. The only sample with grains preferentially oriented is the ATS-007, only at $\sigma = 0.05$. The features observed through binocular microscopy are in concordance with this characterisation: compact and grainy T&P, concave-convex limits, as well as some regrowth. It is easy to observe quartz grains, generally surrounded by overgrowths. Grain size characterisation of the samples also points at two different varieties. The first has medium quartz grains. The second has fine quartz grains. Grain size distribution of ATS-007 is homogeneous, while other three are more heterogeneous. None of the samples have preferential orientation grains under binoculars.

The characterisation of matrix, cement and non-quartz minerals reveals differences between the orthoquartzites analysed, which create different colours (see Table-5.11).

All four samples have clayey matrix, always in smaller proportion than 5%. Iron oxides are also characterised in all four samples. The major presence of clay, rutile, pyrite, and zircon is what confers sample ATS-001 its brown colour. The smaller presence of these minerals on the ATS-023 and ATS-308 prevents the appearance of different colours, therefore, both samples are white. ATS-007 sample is grey and slightly blue coloured. It is not associated to specific minerals. The results of X-Ray fluorescence are consistent with mineralogical characterisation. The quantity of SiO_2 is smaller in sample ATS-001 (92.94%) due to the increase of Al_2O_3 (3.60%), Fe_2O_3 (1.34), and Na_2O (0.91%). In other three samples SiO_2 is more abundant (≈98%) with similar concentration of some other compounds, except for the peak of Al_2O_3 (≈1.3%) in all the samples.

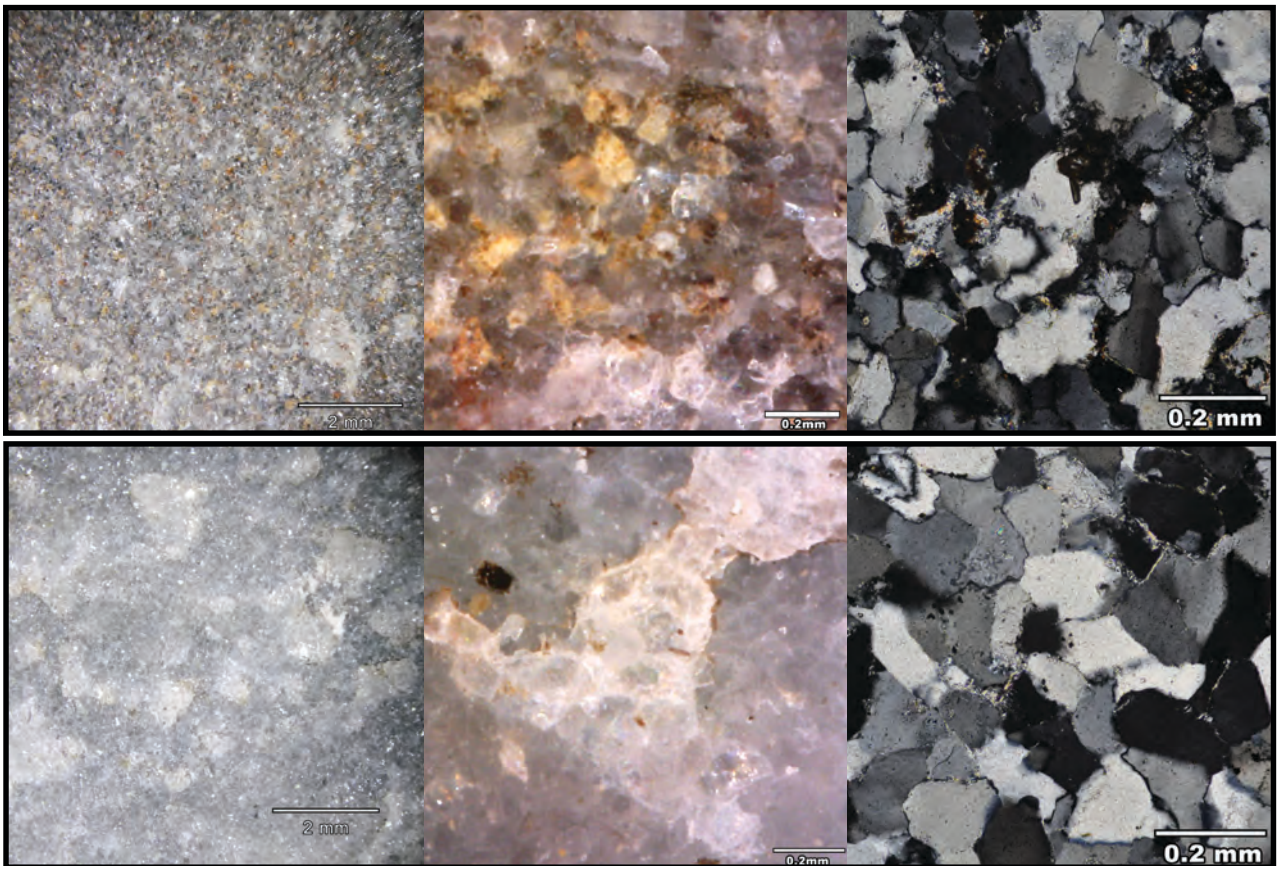

Figure-11.3: Pictures of the OO type samples from El Arteu. From top to bottom, samples ATS-001 and ATS-007. From left to right, microscopy binocular picture at 20x, microscopy binocular picture at 250x, and thin section microscopy picture at different magnifications.

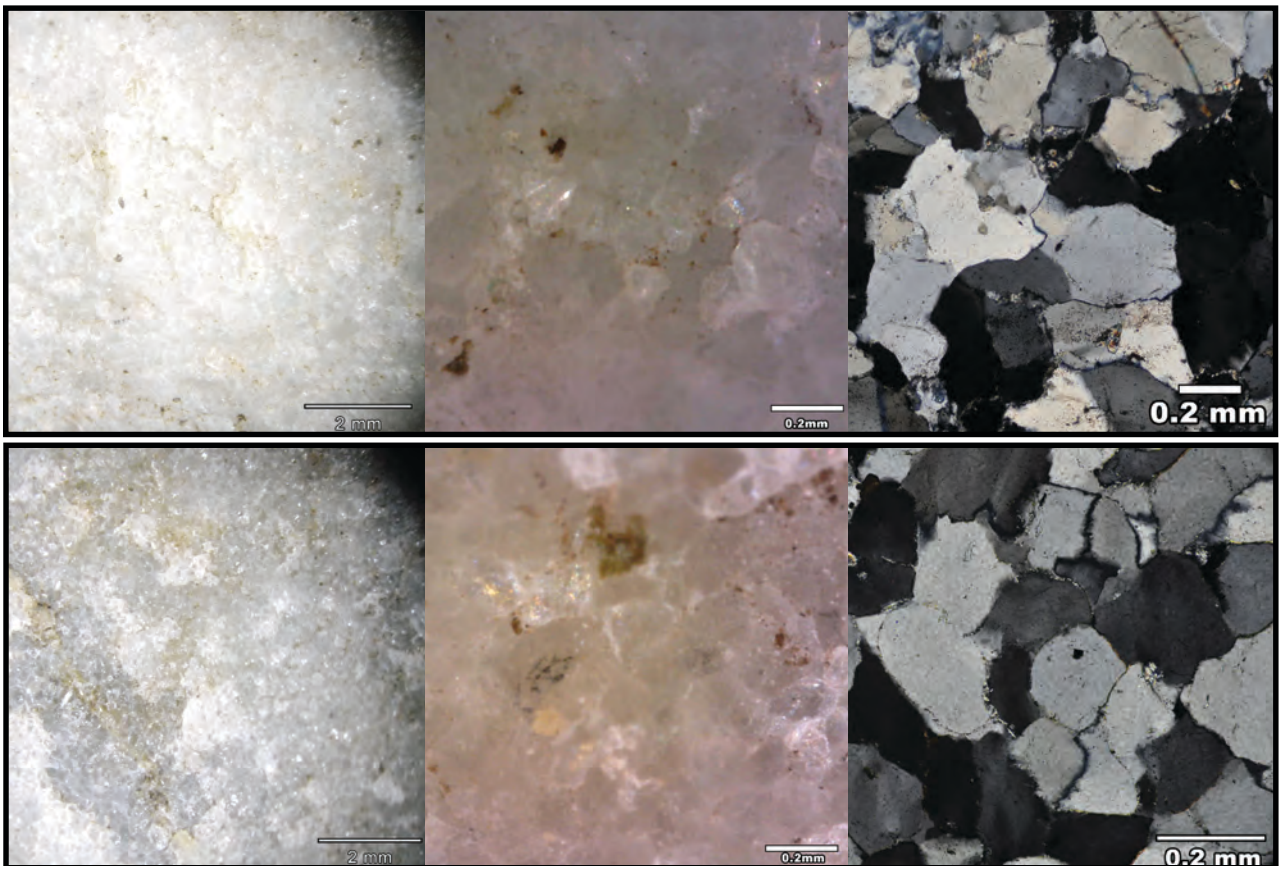

Figure-11.4: Pictures of the OO type samples from El Arteu. From top to bottom, samples ATS-023 and ATS-308. From left to right, microscopy binocular picture at 20x, microscopy binocular picture at 250x, and thin section microscopy picture at different magnifications.

After having analysed the features and variability of the OO petrogenetic type, we can extrapolate these results to those of non-destructive techniques. Thin sections confirm two different varieties: the first one with sizes around fine grain size with homogeneous or heterogeneous distribution, and the second one with heterogeneous distribution around medium quartz grain size. The better represented varieties are the fine grained one with homogeneous distribution and another non-sampled variety characterised by medium size quartz grains. Heterogeneous quartz grain sizes distribution are also well represented, as Table-11.2 shows. The colour and mineral characterisation points that white or grey varieties in association with non-identified black and heavy mineral, mica, and iron oxides are the most important varieties. In addition, the brown-red variety is represented in less frequency.

11.2.3. THE SO PETROGENETIC TYPE AT EL ARTEU

Three of the samples analysed belong to the SO petrogenetic type: ATS-190, ATS-302, and ATS-310. All of them show clastic grained texture, suturated packing, high presence of undulatory quartz extinction, and suturated/microstylolitic quartz grain limits. Böhm lamellae are restricted to ATS-190 and ATS-310 samples. There is also small presence of recrystallised quartz grains in ATS-302 sample. There are two different varieties according to grain size characterisation. The first one is related with two modes distribution. The main grain framework is between the coarse silt and the very fine sand categories and the second grain framework is a mixture of grains derived from matrix and other grains created as a consequence of recrystallization processes, all of them between very fine silt and medium silt. The sample ATS-302 belongs to this variety. The second variety is represented by ATS-190 and ATS-310 samples. Quartz grains are bigger and they are more homogeneous creating one mode between very fine sand and fine sand U-W categories. Morphology of quartz grains is similar in the three samples, with smaller indexes than those observed in previous type. All three samples have grains with preferential orientation at $\sigma = 0.05$, even though at $\sigma = 0.01$ grains from ATS-302 are not oriented.

Regarding non-destructive characterisation of the samples, the majority shows moderate to high luster, micro-cracks on surface, suturated packing, difficult grain distinction, and ruffled quartz grain limits, i.e. grainy and fine T&P with ruffled and irregular grains limits. Nevertheless, it is possible to identify fine T&P associated with the impossibility to detect grain boundaries, in sample ATS-310 (Figure-11.5). Foliation structures are not appreciable in all the samples. Differences in grain size and its association with recognisable features, allow us to propose two main varieties: a) a homogeneous fine grained variety with fine and grained T&P; and b) the medium grained variety without quartz grains detection in the sample ATS-310.

Coming to non-quartz mineral characterisation, clayey matrix appears in negligible percentages in the ATS-190 and the ATS-310 samples. In the ATS-302, there is higher presence of clay. None of the samples exhibits cement. As in the previous type, mineral detected create different colours. Pyrite and manganese oxides observed under non-destructive techniques determine the black colour of the sample ATS-302. Mineral characterisation using petrography is consistent with this mineral association, as indicated by the detection of a more abundant matrix, rutile, pyrite, and other non-identified black minerals. The other samples analysed by non-destructive techniques do not show these minerals. It is important to mention that other minerals, such as zircon, Fe-oxides, chlorite, and clays are common in all thin sections in association with non-identified black and heavy minerals, iron oxides, and micas. These non-quartz minerals, probably the ones generating the (light) grey colour. The results of X-Ray fluorescence are in concordance with these differences. SiO_2 is lower in the ATS-302 sample (95.26%) than in the other two (98%). We proposed, then, two different colour/mineral varieties: the light grey one and the blank one.

The data obtained through destructive characterisation allow us to extrapolate these results to the complete lithic assemblage. Most of the SO type from this layer are related with the homogeneously distributed and fine grained varieties (≈59%). The medium variety of SO is reduced to smaller percentages (≈20%). Other quartz grain sizes varieties SO orthoquartzites could be related with specific intra-variability of the type. Regarding the two varieties defined by mineral characterisation, dark and light grey varieties are found in similar proportions.

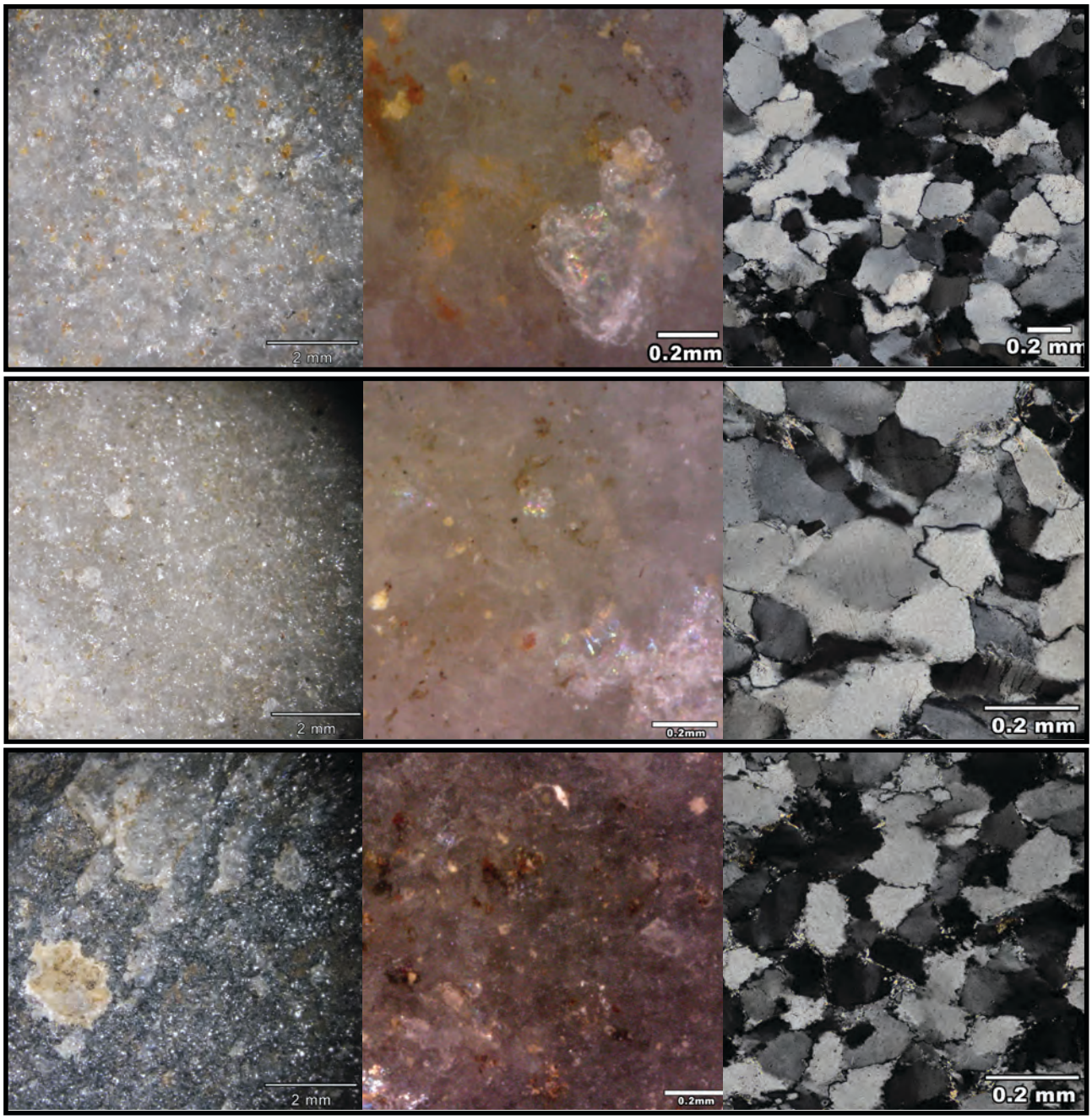

Figure-11.5: Pictures of the SO type samples from El Arteu. From top to bottom, samples ATS-190, ATS-310 and ATS-302. From left to right, microscopy binocular picture at 20x, microscopy binocular picture at 250x, and thin section microscopy picture at different magnifications.

11.2.4. THE BQ PETROGENETIC TYPE AT EL ARTEU

Two of the samples selected belong to the BQ petrogenetic type: ATS-016 and ATS-072 (Figure-11.6). Under thin section, they are characterised by mortar texture and suturated packing, also by the major presence of microstylolitic limits of quartz grains and recrystallised quartz grains, also a small presence of Böhm lamellae. The analysis of size and morphology of quartz grains of both samples reveals two different modes. The first one is composed by the main grain framework with quartz grain sizes between coarse silt and fine sand. The second mode is mainly created by the new recrystallised quartz grains and the grain sizes are between very fine silt and medium silt categories. The first mode is more deformed than the second, as pointed by the roundness and circularity indexes. There are differences in size in the main grain framework between both samples. While on ATS-016 sample, most of grains are around very fine sand, on ATS-072, these grains are around coarse silt. In addition, the grains are more heterogeneous in the first sample. Preferential orientation of quartz grains is only observable on the ATS-072 sample at $\sigma = 0.05$ and $\sigma = 0.01$. Non-destructive characterisation is in accordance with the features characterised: fine texture and suturated packing

(i.e. fine T&P). Nevertheless, it is not easy to distinguish quartz grain boundaries, but it is possible to observe small speck of quartz grains that generates ruffled boundaries. The bright is relatively high and micro cracks are abundant. In cases where grains are recognisable, especially in ATS-016 sample, they are medium with heterogeneous distribution. In ATS-072 grain size determination is harder. Nevertheless, they are smaller and more homogeneous than on previous sample. We do not observe foliation structures in none of the samples using non-destructive characterisation. Finally, we would like to emphasise that all these features must be observed in ATS-016 in small and specific areas where weathering processes do not alter the surface, highly modified.

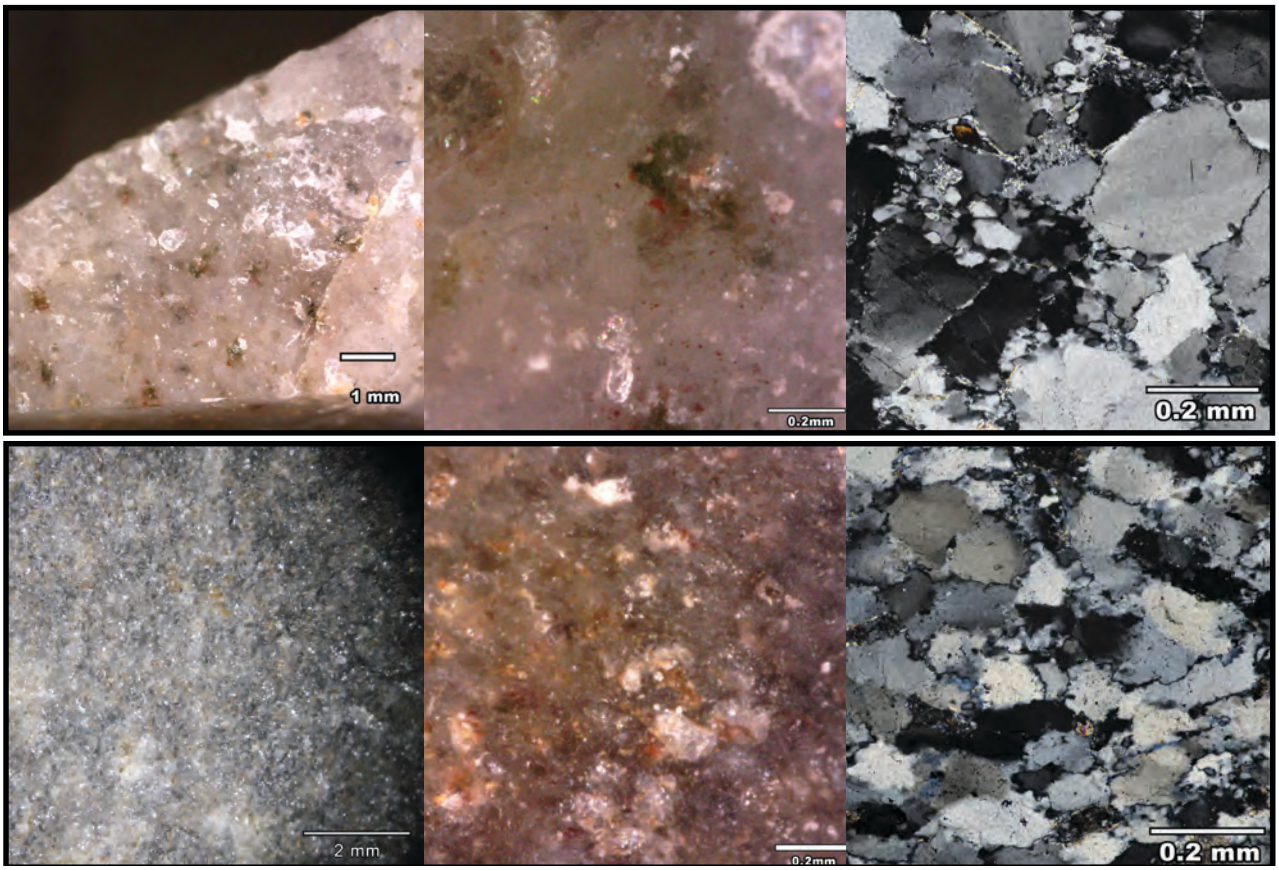

Figure-11.6: Pictures of the BQ type samples from El Arteu. From top to bottom, samples ATS-016 and ATS-072. From left to right, microscopy binocular picture at 50x for ATS-016 and 20x for ATS-072, microscopy binocular picture at 250x, and thin section microscopy picture at different magnifications.

Coming to mineral characterisation, both samples have clayey matrix in reduced extension than 5% of thin section surface. Cement is absent in both samples. Mineral identification reveals clear differences between both samples. The ATS-016 has pyrite, chlorite, clay minerals, mica, and iron oxides. The ATS-072 sample has the latter three minerals and zircon, tourmaline and rutile. The latter two are probably related with the colour characterisation of this sample: black. It is important to mention that although most of the surface of the first sample is white, non-alter areas are grey, with black speck, as a consequence of clays and iron oxides. The results of X-Ray characterisation support the differences observed between both samples in the higher presence of Fe_2O_3, CaO, and SO_3 are higher in the ATS-072 than in the ATS-016.

After having analysed the features and variability of the BQ quartzites, we can extrapolate these results to those of non-destructive techniques. We observe that fine grain size variety (≈72%) is more frequent than medium grained and heterogeneous distribution variety (≈20%). Similar distribution of varieties is also observed when compare colour varieties. The most frequent variety is the grey-black or black, while grey or light grey variety is less frequent.

11.2.5. THE RQ PETROGENETIC TYPE AT EL ARTEU

The last sample selected is a RQ petrogenetic type: ATS-195 (Figure-11.7). This sample is characterised by a mortar texture and suturated packing. Most of quartz grains are characterised as recrystallised, while other are characterised by suturated limits of quartz grain. The latter are less represented. The size and morphological characterisation of grains emphasised the two types of grains: a first group around fine silt and rounded quartz limits, and a less frequent second group of grains between coarse silt and very fine sand categories. The morphology of the second type of grains is more irregular and elongated than the former group. Grains are preferentially oriented at $\sigma = 0.05$ and $\sigma = 0.01$. Non-destructive characterisation is not easy to achieve due to the alteration of the lithic surfaces. In weathered areas, the sample is defined as granular T&P. Even grains are not easy to detect and they have ruffled borders. In non-altered areas or in the surface cut for thin section, texture is soapy without grain boundary detection. The luster is high and micro-cracks are limited (i.e. soapy T&P). Even though the size of grains in the sample are classified as fine grains, they are almost impossible to detect. As a consequence of metamorphic processes, foliation is clear under binocular microscope.

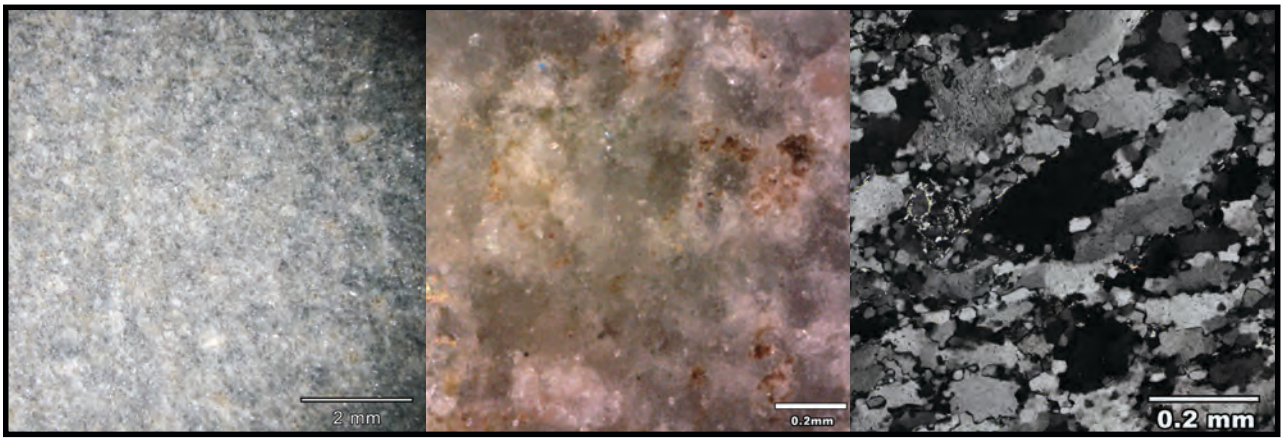

Figure-11.7: Pictures of the MQ type sample, ATS-195, from El Arteu. From left to right, microscopy binocular picture at 10x, microscopy binocular picture at 250x, and thin section microscopy.

Regarding mineral characterisation, the ATS-195 sample has clayey matrix. Mineral detection points at the presence of iron oxides, mica, zircon, rutile, and tourmaline. X-Ray fluoresce reveals major presence of SiO_2 (96%) and small percentages of Al_2O3, Fe_2O_3, and CaO. This sample is light grey to brown coloured, due to the affection of weathering on the surface. In non-altered areas, the colour is light grey.

Coming back to the complete assemblage and comparing it with the data obtained from the thin section and X-Ray fluorescence, we observed there is another variety based on grain size characterisation. The sample selected belongs to the first grain size variety, characterised by small quartz grains. The second variety, non-sampled, has coarser quartz grains. The first is more frequent than the second. We do not observe different varieties according to colour/mineral characterisation and all lithics are light grey, at least, in non-altered areas. Nevertheless, most of them are also modified by weathering processes on their surfaces, colouring in brown the stone surfaces. It is important to mention that this type is only represented by seven lithic implements, then, conclusion must be nuance.

11.2.6. NON-DESTRUCTIVE CHARACTERISATION OF CC PETROGENETIC TYPE AT EL ARTEU

The CC petrogenetic type is a non-frequent type in this layer, only represented in 9% of the assemblage. Under binocular microscopy, most of these quartzarenite exhibits coarse grained textures with floating or punctual packing (i.e. saccharoid T&P). Quartz grain features are vary, from plain and angular quartz limits to plain and rounded ones. There are ruffled limits between grains as a consequence of cement (Figure-11.8). One third part of the implements present bedding. As shown in Table-12.2, most lithics has heterogeneous quartz grain distribution. The analysis of non-quartz minerals puts this petrogenetic type as the most variable on. The most common ones are iron oxides, micas, non-identified black and heavy minerals. Colour is also variable in this type. Brown and grey are the frequent ones, followed by white and black.

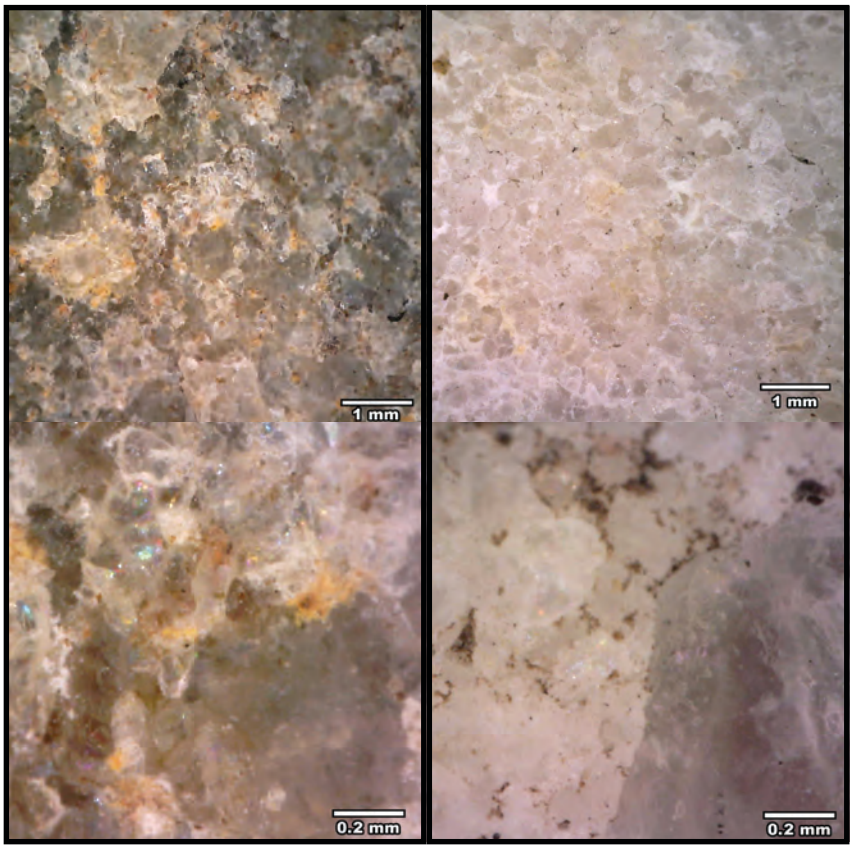

Figure-11.8: Pictures of the CC type from El Arteu. From left to right, ATS-282 (grey-brown coloured with heterogeneous and medium grain size) and ATS-276 (white coloured with heterogeneous coarse grain size). Upper rows show microscopy binocular pictures at 50x. Lower rows show microscopy pictures at 250x.

11.2.7. CHARACTERISATION OF CORTICAL AREAS AT EL ARTEU

Here we present the result of the characterisation of cortical areas. The distribution of cortex in the lithics analysed between different types of raw material is shown in Table-11.5. “Archaeological quartzite” is the most frequent raw material with cortical areas, which is in accordance with its predominance in the whole assemblage (35% of them have cortex). Nevertheless, the representation of cortical areas in other raw materials attending to its quantities is higher. All limestones and lutites have cortex, and 55% of radioralites also have cortex.

Raw material	Cortex type												∑ of each type
	Conglomerate			Fluvial			Unknown			Total			
	∑	%	% rel	∑	%	% rel	∑	%	% rel	∑	%	% rel	
Archaeological quartzite	11	100	5	55	89	23	18	86	8	84	89	35	237
Limestone							3	14	100	3	3	100	3
Lutite				1	2	100				1	1	100	1
Quartz													1
Radioralite				6	10	55				6	6	55	11
Unknown													2
Total	11	12	4	62	66	24	21	22	8	94	100	37	255

Table-11.5: Frequency table of types of cortex identified in El Arteu grouped by main raw material. Columns are the types of cortex, including the frequency of each cortex type for each raw material and the total of items with cortex of each raw material. The last column quantifies the total of items with and without cortex of each raw material. The columns % are the percentage of each raw material in relation to each cortex type, while the columns % rel. are the percentage of cortex type in relation to the total of each raw material (including items with and without cortex).

Regarding the types of cortex, 21% of the collection could not be characterised due to the absence of diagnostic features. None of the cortex types identified could be interpreted as evidence of direct extraction from the outcrop.

Conglomerate cortex is only represented in 4% of the assemblage, and it is only defined in "archaeological quartzite". Conglomerate cortical areas are characterised by the presence of cements from the conglomerate itself, which are generally recognised as red iron oxides or dark silica fluids. In addition, voids are usually present, even though they are generally filled with conglomerate cement. No clear impact cracks are observable on cortical areas.

Cortical areas from fluvial sources is the most frequent cortex type, representing 62% of the cortical areas. "Archaeological quartzite" is again the most frequent raw material areas among the lithic implements with this type of cortex. However the only lutite has cortex from fluvial deposits and all radioralite cortical areas derive from these contexts. Fluvial cortex is mainly characterised by the presence of impact cracks in the surface and fine or soapy textures. Voids are less frequent in this cortex type and cement is absent.

Focussing on the distribution of cortex among "archaeological quartzites" and their petrogenetic types, there is a clear overrepresentation of cortical areas among the quartzarenite group and BQ type. Conversely, lithics with cortex are underrepresented among the SO type (Table-11.6). The remaining petrogenetic types show percentages of items with cortex around 35%, similar to those of "archaeological quartzite" as whole. There are also differences in the representation of cortex type in the petrogenetic types characterised. While fluvial cortex is in all of them, conglomerate cortex is only represented in orthoquartzites and the BQ petrogenetic type. In the latter type cortex from conglomerate is more frequent than on orthoquartzite group.

Archaeological quartzite	Cortex type												∑ of each type
	Conglomerate			Fluvial			Unknown			Total			
	∑	%	% rel	∑	%	% rel	∑	%	% rel	∑	%	% rel	
CC				8	15	36	1	6	5	9	11	41	22
CA				9	16	31	5	28	17	14	17	48	29
OO	4	36	4	23	42	21	8	44	7	35	42	31	112
SO	1	9	5	3	5	14				4	5	18	22
BQ	6	55	15	9	16	23	2	11	5	17	20	44	39
RQ				2	4	29				2	2	29	7
Unknown				1	2	17	2	11	33	3	4	50	6
Total	11	13	5	55	65	23	18	21	8	84	100	35	237

Table-11.6: Frequency table of types of cortex identified in El Arteu grouped by petrogenetic types of "archaeological quartzites". Columns are the types of cortex, including the frequency of each cortex type for each raw material and the total of items with cortex of each raw material. The last column quantifies the total of items with and without cortex of each raw material. The columns % are the percentage of each raw material in relation to each cortex type, while the columns % rel. are the percentage of cortex type in relation to the total of each raw material (including items with and without cortex).

11.3.TECHNOLOGICAL STRUCTURE

Here we present the results of the technological analysis of the material of El Arteu, taking into account the results from the study of the petrological structure. According to the methodology previously exposed, the most frequent category is knapping product (73%), followed by chunk (19%), and core (8%). The distribution of technological products sorted by main lithologies is shown on Table-11.7. Cores are restricted to quartzite and radioralite. On both raw material, they follow similar representation even though the quantity of radioralite is limited. Knapping products are well represented in all raw material. They are predominant technological product for every raw material. Moreover, there is a clear overrepresentation of chunk among limestones. In contrast, chunks are less frequent in radioralite and "archaeological quartzites". There is no chunk in lutite and quartz.

Focusing the analysis on "archaeological quartzites", cores are represented in all petrogenetic types, except for RQ quartzite (Table-11.8). However, they have less frequency than 10% in all of them, except for the CC type, whose proportion of cores is higher. Knapping products are more frequent among all types, even though on CC type are underrepresented due to the quantity of chunks and cores. Chunks are also well represented in RQ and OO type. Nevertheless, they are underrepresented in the SO and CA petrogenetic types.

	Technological order										
	Cores			Knapping prdct.			Chunk			Total	
	∑	%	% rel	∑	%	% rel	∑	%	% rel	∑	%
Arch. Quartzite	17	94	7	**174**	**93**	**73**	**46**	**92**	**19**	237	93
Limestone				2	1	67	1	2	33	3	1
Radioralite	1	6	9	9	5	82	1	2	9	11	4
Lutite				1	1	100				1	0
Quartz				1	1	100				1	0
Unknown							2	4	100	2	1
Total	18	7		187	73		50	20		255	100

Table-11.7: Frequency table of main technological categories identified in El Arteu grouped by raw material. Columns are the main technological categories and the total of items of each raw material. The columns % are the percentage of each raw material in relation to each technological category, while the columns % rel. are the percentage of each technological category in relation to the each raw material. Cells in black are the categories representing more than 10% of the total cases.

	Technological order										
	Cores			Knapping prdct.			Chunk			Total	
	∑	%	% rel	∑	%	% rel	∑	%	% rel	∑	%
CC	4	24	18	11	6	50	7	15	32	22	9
CA	1	6	3	**25**	**14**	**86**	3	7	10	29	12
OO	6	35	5	**80**	**46**	**71**	**26**	**57**	**23**	112	47
SO	2	12	9	19	11	86	1	2	5	22	9
BQ	2	12	5	**30**	**17**	**77**	7	15	18	39	16
RQ				5	3	71	2	4	29	7	3
Undetermined	2	12	33	4	2	67				6	3
Total	17	7		174	73		46	19		237	100

Table-11.8: Frequency table of main technological categories identified in El Arteu grouped by petrogenetic types of “archaeological quartzite”. Columns are the main technological categories and the total of items of each raw material. The columns % are the percentage of each raw material in relation to each technological category, while the columns % rel. are the percentage of each technological category in relation to the each raw material. Cells in black are the categories representing more than 10% of the total cases.

11.3.1.CORES

We identified 18 cores in the whole collection. The most frequent type of core is core on flake, with eight cores, followed by discoid and irregular cores, represented by five and four items, respectively. There is only a prismatic shaped core. There is no clear correlation between type of core and neither raw material, nor petrogenetic types of “archaeological quartzite” (Table-11.9).

Core on flake is the most frequent type of core in the layer, represented by eight items. Five of them are complete, while the other three are fractured. The most common raw material for this type of cores is “archaeological quartzites”, with seven. Nevertheless, the only core made on another raw material, radioralite, is a core on flake. Regarding the types of “archaeological quartzite” present, the most frequent type is the OO, with three cores, followed by the BQ, with two. Finally, there is one core made on CC type and another on SO type. The quantity of percussion platforms and flacking surfaces is similar in all cores and most of them just have one percussion platform and one flacking surface. Moreover, there is a core with two percussion platform and another core with three. On both cores there are more than one flacking surface. The first core is made on OO orthoquartzite and the second on BQ quartzite. The presence of cortical areas in this type of cores is restricted to the dorsal faces of the flakes. Five of the cores made on “archaeological quartzite” and the other core, made on radioralite, have cortex. All recognisable cortex derive from fluvial deposits.

Discoidal cores are represented in this layer by five complete pieces. All of them are made on “archaeological quartzite”. Focussing on petrogenetic types of “archaeological quartzite” OO (two items) and CA and SO (one item of each petrogenetic type) are the petrogenetic types present. Except for the OO core, just with one flacking surface, all discoidal cores have two flacking surfaces

and more than three percussion platform. It is clear the same technique, with alternative and consecutive extractions was used. On the first core, the technique was not based on alternative percussion and only one side was exploited. Three cores have cortical areas with less than 33% of their surfaces. The only core in which cortex was identified is one made on CA type and it derives from a fluvial deposit.

	Type of core				
	Irregular	Discoid	Prismatic	On flake	Total
Other RM				1	1
CC	3			1	4
CA		1			1
OO		2	1	3	6
SO		1		1	2
BQ				2	2
RQ					
Undetermined	1	1			2
Total	4	5	1	8	18

Table-11.9: Frequency table of types of cores identified in El Arteu grouped by petrogenetic types of “archaeological quartzite”. Columns are the types of cores. In this case the only other raw material (RM) is radioralite.

The irregular cores from this collection are made on CC petrogenetic type. The other core was made on an unknown “archaeological quartzite”. Three are complete and the other one is fragmented. The quantity of percussion platform and flacking surfaces is small and almost all cores have two percussion platform and two flacking surfaces. Three of them have cortical areas, generally broader than 66% of their surfaces, pointing at low exploitation of cores. Two of the three cortical zones were identified from fluvial deposits. The other one is unknown.

Finally, there is a prismatic shaped core made on OO petrogenetic type. It has two percussion platform and other two flacking surfaces. Cortex is not represented in this core.

11.3.2. KNAPPING PRODUCTS

In the lithic assemblage from El Arteu, we identified 187 knapping products. The most frequent type is blank, making more than 97% of the elements analysed. Core preparation/rejuvenations products are scarce, forming less than 3% of the assemblage. Finally, we do not identify any burin spall. Core preparation/rejuvenation products are only found on “archaeological quartzites”, more specifically on CA type and orthoquartzite group (Table-11.10).

	Knapping products							
	Blanks			Core preparation/rej			Total	
	∑	%	% rel	∑	%	% rel	∑	%
Other RM	13	7	100				13	7
CC	11	6	100				11	6
CA	**24**	**13**	**96**	1	20	4	25	13
OO	**77**	**42**	**96**	3	60	4	80	43
SO	18	10	95	1	20	5	19	10
BQ	**30**	**16**	**100**				30	16
RQ	5	3	100				5	3
Unknown	4	2	100				4	2
Total	182	97		5	3		187	100

Table-11.10: Frequency table of the categories of knapping products identified in El Arteu grouped by the petrogenetic types of “archaeological quartzite”. Columns are the categories of knapping products and the total of items belonging to each petrogenetic type. The columns % are the percentage of each petrogenetic type in relation to each category of knapping product, while the columns % rel. are the percentage of each category of knapping product in relation to each petrogenetic type of “archaeological quartzite. Cells in black are the categories representing more than 10% of the total cases. Cells in dark grey are the categories representing between 5 and 10% of cases. Cells in light grey are the categories representing between 1 and 5% of cases. Other raw material (RM) includes, one lutite, one quartz, nine radioralites, and two limestones.

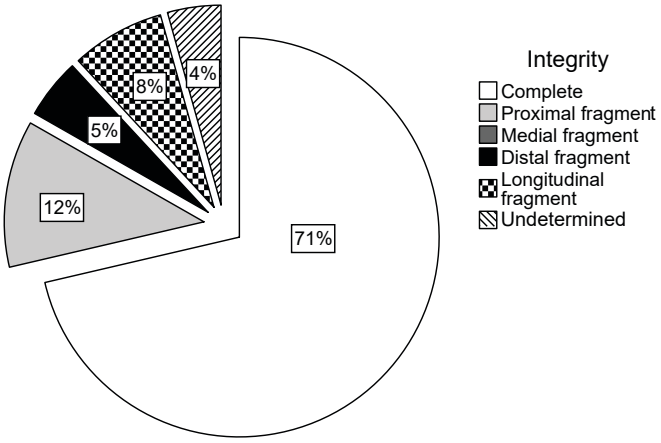

Figure-11.9: Pie chart showing percentage of each state of integrity of blanks.

Blank is the technological category better represented in the assemblage with 182 items. Coming to their integrity, 71% of the blanks are complete and 29% are fragmented (Figure-11.9). The most frequent fragments are proximal ones, followed by the longitudinal fragments. Distal blanks are scarce (≈5%). Finally, 4% of the pieces could not be classified due to the absence of diagnostic features, mainly the bulb of percussion or the striking platform. Then, most of these undetermined fragments must be part of distal or medial fragments.

There is a great variability in the number of negative scars depending on raw material. The only quartz blank has at least three scars, and all radioralite blanks have at least two negative scars. On the contrary, the only lutite has one negative scar. Limestone is more variable and one blank has two negative scars and the other one has no negative scars on its dorsal surface. On "archaeological quartzites" all types of blanks are presented, although most of them have at least two negative scars on dorsal surfaces. Regarding the latter raw material, there is no statistically association between the number of negative scars on blanks and different petrogenetic type of "archaeological quartzite", as demonstrated by Chi-square test (χ^2 (15, N = 165) = 16.789, p = .332). Nevertheless, Table-11.11 points at some differences in the distribution of blanks (characterised by the quantity of dorsal scars) between petrogenetic types. In general, small number of negative scars blanks are associated with the quartzarenite group, while the in orthoquartzites, especially in SO type, the quantity of blanks with at least two scars is more frequent. In BQ petrogenetic type, all categories except blanks without negative scars are similarly distributed.

	Dorsal scars							
	None		One		Two		≥ Three	
	∑	**%**	∑	%	∑	%	∑	%
CC	1	9,1	0	0,0	6	54,5	4	36,4
CA	2	8,3	4	16,7	12	50,0	6	25,0
OO	1	1,3	15	19,5	31	40,3	30	39,0
SO	0	0,0	4	22,2	5	27,8	9	50,0
BQ	1	3,3	9	30,0	12	40,0	8	26,7
RQ	1	20,0	1	20,0	1	20,0	2	40,0
Total	6	3,6	33	20,0	67	40,6	59	35,8

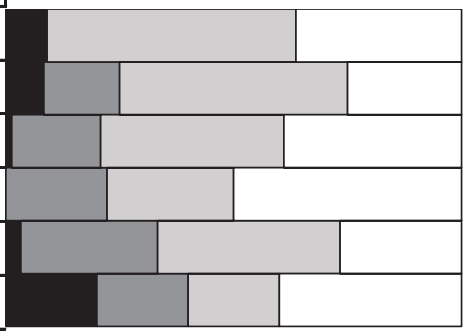

Table-11.11: Frequency table and its representation through a bar chart using the percentage of each blank category (determined by the quantity of dorsal scar) according to each petrogenetic type of "archaeological quartzite".

The preservation of cortical areas on these blanks does also provide some interesting data about raw material exploitation in this context (Figure-11.10). Cortex is observable in 35% of the blanks. Most of them cover less than 33% of the dorsal surfaces. Broad cortical areas on dorsal surfaces (covering between 33% and 66% of it) are only present in 8% of blanks, and only 6% of items analysed have cortical areas covering more than 66%. Their distribution according to raw materials reveals most cortical areas are on "archaeological quartzites". Still, lutites, limestone and radioralite with cortical area were also identified. The only lutite preserves the cortex in smaller extension than 33% of its dorsal surface. One limestone blank is completely cortical, while on the other, cortex extension is reduced to less than 33% of its surface. Finally, four radioralites preserve cortical surfaces in less extension than 33% of their surfaces. Focusing on "archaeological quartzite", there are no statistically differences between the petrogenetic types and the preservation of cortex, as supported by

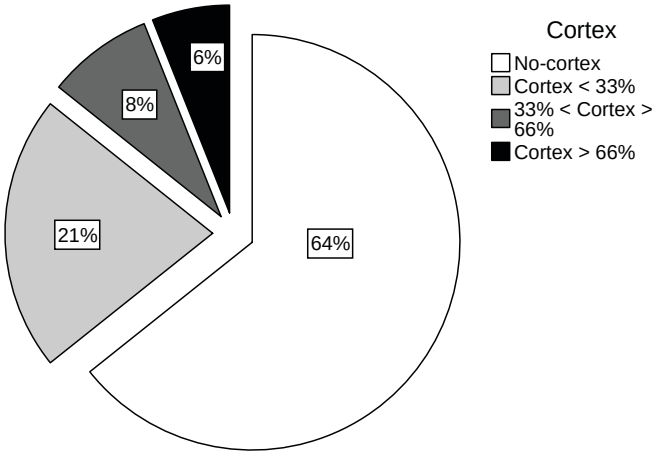

Figure-11.10: Pie chart showing percentage of absence, presence and extension of cortex on blanks.

Chi-square test (χ^2 (15, N = 165) = 14.523, p = .523). Nevertheless, cortical areas are more frequent in the CA type, while they are less frequent in the SO (Table-11.12). In general, other petrogenetic types follow similar patterns than general characterisation and the small differences are related with differences in the quantity of blanks of each petrogenetic type.

Among the items which preserved any cortical area (65), it was possible to characterise 49 of them. The four radioralites and the only lutite with cortex derive from fluvial deposits. The cortical area of the limestone could not be defined. Focussing on "archaeological quartzite", fluvial cortex (40) is more frequent than conglomerate cortex (nine). There are another 16 pieces with cortical surfaces which do not have enough features to be defined. There is no relationship between petrogenetic types and the type of cortex as point out by Chi-square test (χ^2 (10, N = 57) = 14.043, p = .171). All petrogenetic types have blanks with cortex from fluvial deposits but only OO and BQ types (22% and 45% of recognisable cortex) have cortex from conglomerates.

Presence of cortex on dorsal surfaces

	Absence		X < 33%		33<X>66		X > 66%	
	∑	%	∑	%	∑	%	∑	%
CC	8	72,7	2	18,2	0	0,0	1	9,1
CA	12	50,0	7	29,2	3	12,5	2	8,3
OO	52	67,5	17	22,1	6	7,8	2	2,6
SO	15	83,3	0	0,0	2	11,1	1	5,6
BQ	18	60,0	7	23,3	3	10,0	2	6,7
RQ	3	60,0	0	0,0	1	20,0	1	20,0
Total	108	80	33	11	15	3	9	6

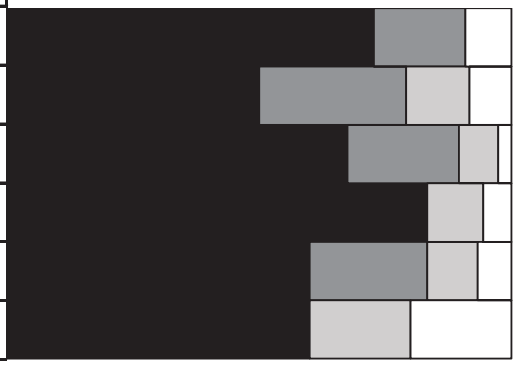

Table-11.12: Frequency table and its representation through a bar chart using the percentage of each blank category (determined by the quantity of cortex on dorsal surfaces) taking into account each petrogenetic type of "archaeological quartzite".

Core preparation/rejuvenation product is the less frequent knapping product, just represented by five pieces. All except one are complete and all are made on "archaeological quartzite". Two are made on OO orthoquartzite and one is made on CA type and another one on SO type (Table-11.10). Cores are also made on these three petrogenetic types. Two core preparation/rejuvenation products have cortical areas, all of them with smaller extension than 33% of their surfaces. One derives from a conglomerate (the SO type) and the other from fluvial deposits (the OO type).

11.3.3. CHUNK

Chunk, represented by 50 pieces, is the second most important technological product in this assemblage. The integrity of the pieces is not analysable due to the absence of diagnostic features.

The raw material represented in this category are "archaeological quartzites", limestone and radioralite, also another two undetermined stones (Table-11.7). Regarding the relative weight of chunks in each raw material, they are significantly overrepresented in limestone making 33% of the pieces. One chunk is made on radioralite. Chunks in "archaeological quartzites" present in a percentage similar to that of this product in the whole assemblage. Focussing on specific petrogenetic types,

chunks are more frequent in the OO orthoquartzite, and in the BQ and RQ quartzites. The latter frequency is hampered by the small quantity of RQ quartzite in the assemblage.

Sixteen chunks have cortex. Among them 14 are made on “archaeological quartzite”, one on limestone and another one on radioralite. The latter derived from fluvial deposits but the limestone cortex is undetermined. Only one of the cortical area from “archaeological quartzites” derived from conglomerates. The other twelve cortex derive from fluvial deposits. Cortical areas are generally less extended than 33% of their surfaces. Nevertheless, four of them have broad cortex than 66%. From them, one is completely cortical.

11.4. THE RETOUCH: MODAL AND MORPHOLOGICAL STRUCTURES

Here we present the analysis of retouched artefacts and its relationship with the data previously exposed. According to the methodology defined above, there are 97 lithics retouched, 38% of the collection. Twenty lithics have two different primary types and other four blanks have three different primary types.

The number of primary types individualised is 125. Starting from the orders (mode of retouch), we do not find evidence of Plain (P) or Splinter (E) modes of retouch. Simple (S) mode is the most frequent one (102 items), followed by Abrupt (A) and Burin (B) (17 and six items respectively) modes (Figure-11.11 and the total from Table-11.14). Going down from order to typological group (or morphothema) of retouch, we start with the Simple mode, the most frequent one. The most frequent typological group is that of Sidescrapers (R) (77 items), followed by Denticulates (D) (twelve), Points (P) (seven), and Endscrapers (G) (six). In the Abrupt mode, there are two typological groups represented, unspecific Abrupt (A) (15) and Truncation (T) (two). No typological groups are distinguished within the Burin mode.

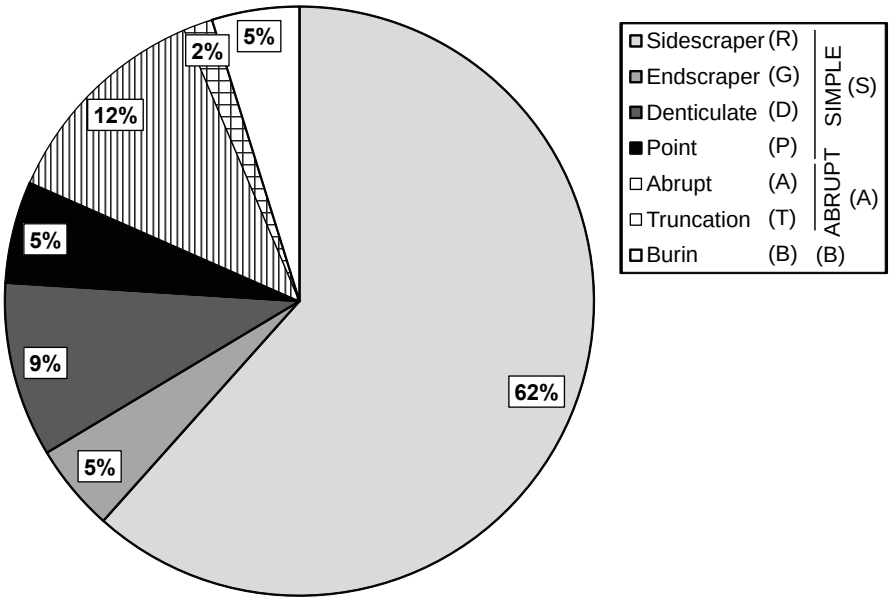

Figure-11.11: Pie chart showing the percentage of orders (modes) and groups (morphological) of retouch of the artefacts from El Arteu.

After having understood the general characterisation of the retouch using the modes and morphological groups of retouch, now we will deepen into the analysis of the pieces with multiple primary types. Starting from the blanks with two primary types, there are multiple associations. The most frequent association of primary types in one blank is Sidescraper and Sidescraper, represented in nine lithics. Blanks with Sidescraper and unspecific Abrupt, with three pieces, are also well represented. Endscraper and Sidescraper, Denticulate and Sidescraper, and Denticulate and unspecific Abrupt are represented in two blanks for each combination of morphothemas. Other blanks with two primary types are unspecific Abrupt and unspecific Abrupt and unspecific Abrupt and Burin. Each combination of morphothemas is only represented in one blank. The analysis of the blanks with three different primary types brings out the following combinations of morphothemas: one blank with three Sidescrapers, one blank with two Sidescrapers and a Truncation, one blank with two Endscrapers and a Sidescraper, and another blank with Sidescraper, Denticulate and Endscraper morphothemas.

Next, we will analyse the relationships between the retouched artefacts and the technological structure. There is a statistically significant association between the presence of retouch and technological blanks they are configured χ^2 (2, N = 255) = 21.46, p < .001. Forty-six percent of knapping products are retouched, while only 16% of cores and 14% of chunks are retouched. In addition, every pieces with multiple primary types are made on knapping products. The representation of mode of retouch and typological group among knapping products follows similar patterns to those observed for the complete collection, due to the great weight of this technological group in the assemblage. That is, a great quantity of Simple mode and a smaller presence of Abrupt and Burin modes. Coming to the retouched cores, all of them are made on core on flake. Two have Sidescraper and the other one has an Endscraper. There are seven chunks retouched, five configure Sidescrapers and the other two Burins.

	Non-retouched		**Retouched**	
	∑	%	**∑**	**%**
CC	16	72,7	6	27,3
CA	22	75,9	7	24,1
OO	73	65,2	39	34,8
SO	9	40,9	13	59,1
BQ	21	53,8	18	46,2
RQ	4	57,1	3	42,9

Table-11.13: Frequency table and its representation through a bar chart using the percentage of retouched material taking into account each petrogenetic type of “archaeological quartzite”.

Finally, we will analyse the relationships between the retouched artefacts and the raw material of the blanks they are configured. The quantity of retouched artefacts is differently distributed depending on the raw material of the blanks, as demonstrated by Chi-square test (χ^2 (5, N = 2419) = 14.435, p = .013). The only quartz in the site is retouched and nine of the eleven radioralites are retouched. Retouch is also frequent in “archaeological quartzite” blanks and 37% of them are retouched. In contrary, lutites and limestone blanks are not retouched. All blanks with three primary types are made on “archaeological quartzite”. Most of the blanks with two primary types configured on it are made on “archaeological quartzite”. Moreover, there are three blanks with two primary types made on radioralite. There is no statistically significant relationship in the presence of retouch in the different types of “archaeological quartzite”, as pointed out by Chi-square test (χ^2 (5, N = 231) = 9.261, p = .099). Nevertheless, Table-11.13 points at small differences in the representation of retouch in the blanks according to their petrogenetic types they are configured. The percentage of retouched blanks made on SO and quartzite types is higher than on other types of “archaeological quartzite”. Moreover, the percentage of retouched blanks is higher in OO orthoquartzite than in quartzarenite group. There is no statistically association between the presence of blanks with multiple primary types and “petrogenetic type”, even OO type, followed by SO and BQ are the petrogenetic types with the highest representation of blanks with multiple primary types. In addition, blanks with three primary types are only represented in these three petrogenetic types.

	Simple				Abrupt		Burin	
Order	Sidescraper	Endscraper	Denticulate	Point	Abrupt	Truncation	Burin	Total
Arch. Qzt	**67**	6	11	7	**14**	2	5	112
Limestone								
Lutite								
Quartz	1							1
Radioralite	9		1		1		1	12
Total	77	6	12	7	15		6	125

Table-11.14: Frequency table of order and group of retouches grouped by raw material. In the cases of pieces with different primary types, each type is quantified individually. Cells in black are the categories representing more than 10% of the total cases. Cells in dark grey are the categories representing between 5 and 10% of cases. Cells in light grey are the categories representing between 1 and 5% of cases.

There is no clear association between the morphological group of retouch and raw material they are configured. Nevertheless, it is easy to observe in Table-11.14 that “archaeological quartzite” is the only raw material with Endscrapers, Points, and Truncations groups. In addition, Sidescraper group is overrepresented in retouched radioralites. There are also some associations between morphological groups of retouch and petrogenetic types (Table-11.15). Burin and Point morphological groups are only represented in the OO, SO, and BQ types, while Truncations are only made on CC and OO types. Finally, it is also interesting to remark that most of unspecific Abrupt group are made on OO orthoquartzite blanks.

	Simple				Abrupt		Burin	
Order	Sidescraper	Endscraper	Denticulate	Point	Abrupt	Truncation	Burin	Total
CC	4		2			1		7
CA	6	1	2		1			10
OO	**30**	1	1	3	8	1	3	47
SO	**11**	3	3	1	2		1	21
BQ	**14**	1	1	3	2		1	22
RQ	1		2		1			4
MQ								
Total	66	6	11	7	14		5	111

Table-11.15: Frequency table of mode of retouch and morphological group grouped by petrogenetic type. In the cases of pieces with different primary types, each type is quantified individually. Cells in black are the categories representing more than 10% of the total cases. Cells in dark grey are the categories representing between 5 and 10% of cases. Cells in light grey are the categories representing between 1 and 5% of cases.

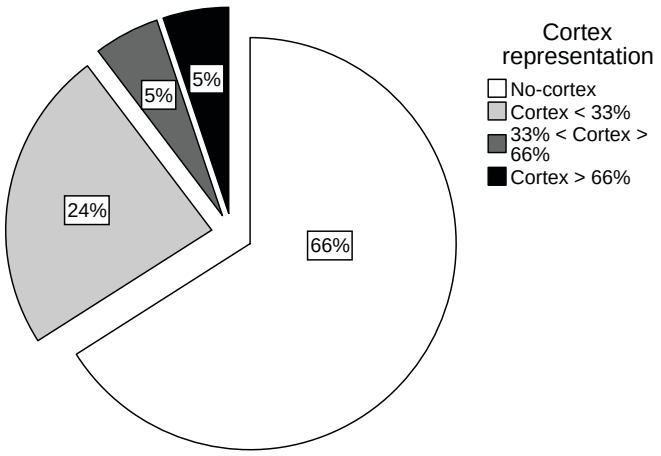

Figure-11.12: Pie chart showing percentage of absence, presence and extension of cortex on retouched material from El Arteu.

Finally, we analyse the relationship between retouched blanks and cortical areas. Figure-11.12 shows the preservation of cortex on retouched artefacts. Twenty-four percent of the retouched blanks has cortex covering less than 33% of the surface. Cortical surface broad between 33 and 66% is reduced to 5%. This frequency is the same for retouched blanks with greater cortex preservation than 66% of their surfaces. The pieces with cortex and multiple primary types have similar representation than retouched artefacts with only one primary type. Regarding the characterisation of cortical areas from retouched blanks, most of them derived from fluvial deposits (61%), while the presence of cortex from conglomerates is smaller (15%). We are unable to identify the type of cortex on 24% of artefacts. These percentages differs to those observed in the general characterisation of cortical zones as a consequence of the increase of cortex derived from conglomerate on retouched artefacts.

11.5. TIPOMETRICAL STRUCTURE

In this section we will describe the results of the analysis of the tipometrical structure and its relationship with the structures studied above. We made the measurements using the technological axis (Length, width and thickness) on 195 items (76.5% of the assemblage). The remaining 60 pieces were measured using the longest axis (X, Y and Z), due to the absence of features signalling the technological axis. All chunks, most of the cores (some cores on flake were measured using the technological axis) and some incomplete knapping products were measured using the latter criterion.

An overview of length, width and thickness reveals that all three measurements have positive skewness and kurtosis but the highest values being those of width, followed by length (Figure-11.13). The mean length is 30.58 mm, the mean width 27.13 mm, and the mean thickness 10.21 mm. The measurements of the first two axes are similar between them. A general outlook of X, Y, and Z axes does also points at positive skewness and kurtosis. Nevertheless, all the means are significantly different: the mean of the X is 34.04 mm, the mean of the Y axis is 22.33 mm, and the mean of the

Z axis is 11.83mm (Figure-11.14). The relationship between the three measurements according to the Tarriño indexes (Tarriño, 2015) reveals different morphologies depending on the measurement method employed (Figure-11.15). Most items measured based on the X/Y/Z axes are between 0.5 and 0.7 of RBEI and between 0.2 and 0.4 of RFL, meaning similar measurement between the three axes and relatively cubic-bladed shapes. Regarding the material measured using L/W/T axes, the resulting forms are alike, but they include an important quantity of tabular elements. In addition there are clear outliers in the latter category.

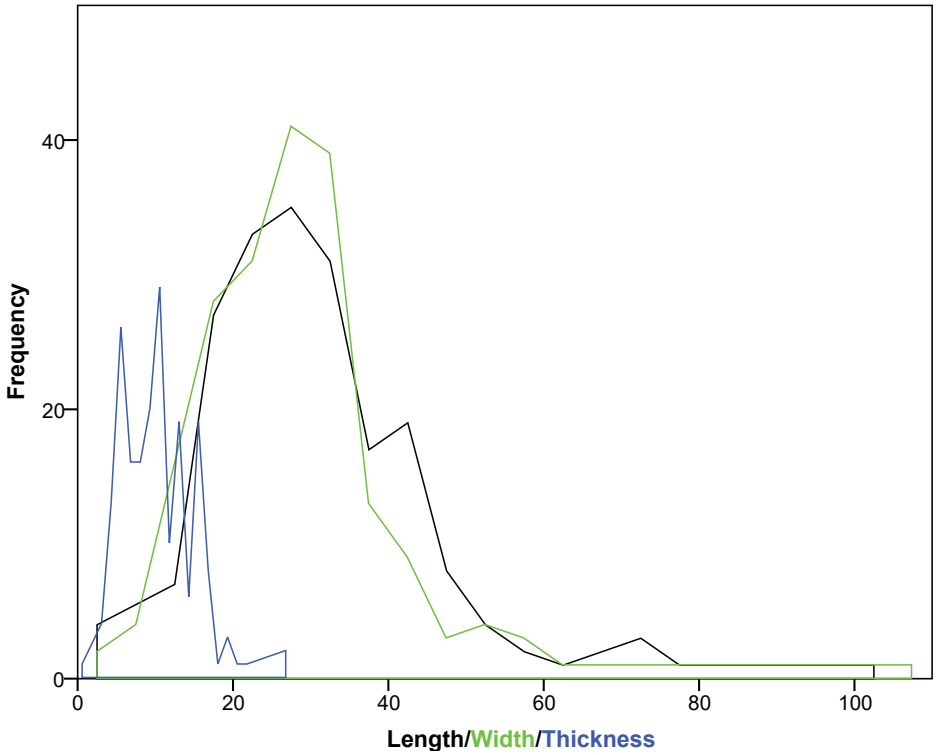

Figure-11.13: Frequency area chart showing the distribution of length, width and thickness of lithic remains from El Arteu measured in relation to technological axis. Black line represents length, green line represents width, and blue line represents thickness. Horizontal axis measurement are in millimetres.

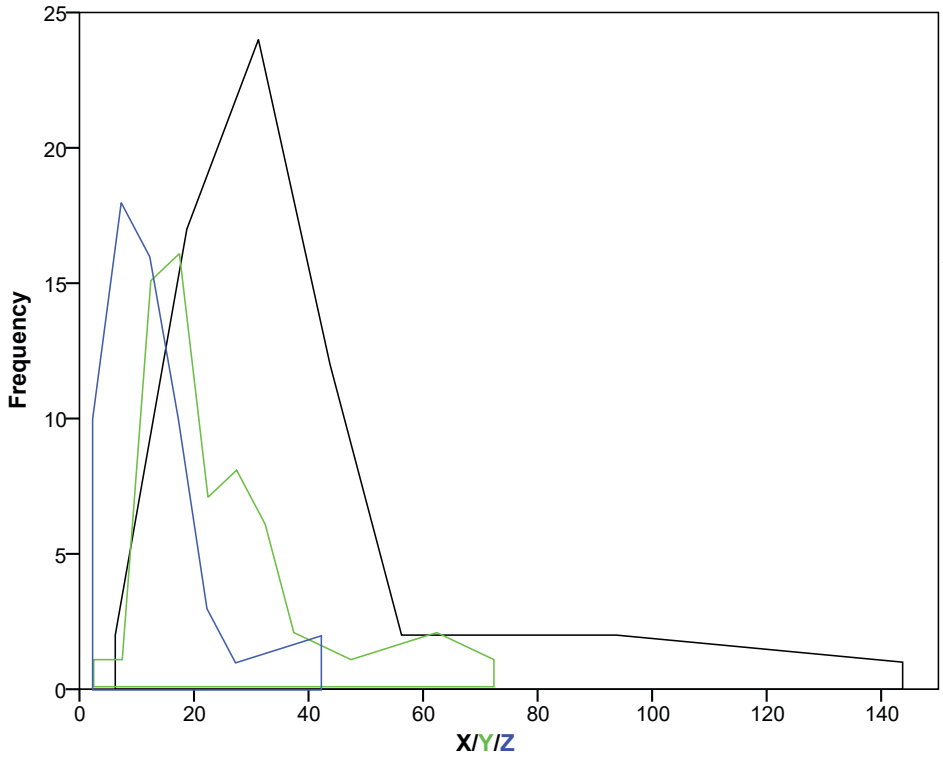

Figure-11.14: Frequency area chart showing the distribution of X, Y and Z axes of lithic remains from El Arteu. Black line represents the X axis, green line represents the Y axis, and blue line represents the Z axis. Horizontal axis measurement are in millimetres.

The last measurement used here is the weight of each lithic implement. Thirteen pieces from this layer were not measured due to error during data acquisition. The minimum weight recorder is 0.29 g and the maximum 722 g. The mean is 15.79 g. Weight presents high positive kurtosis (119.93) and positive skewness (10.13). The total of pieces weighted in this layer is 242 and the total weight is 3,822 g.

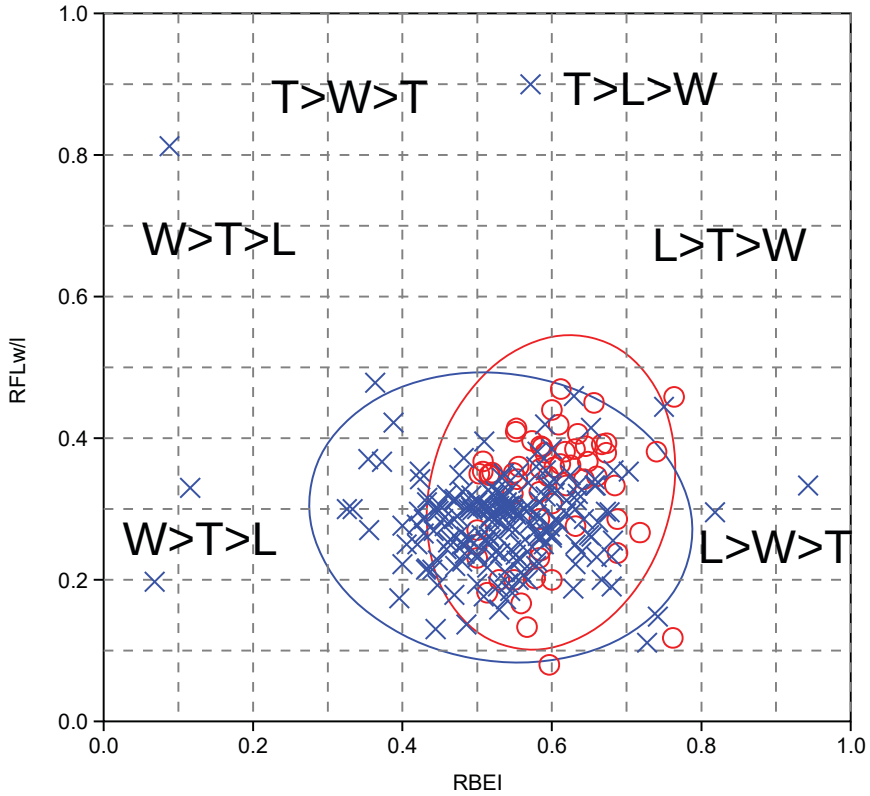

Figure-11.15: Scatter plot of RFLw or RFLl and RBEI indexes. Blue points and ellipse are the measurements made in relation to technological axis. Red points and ellipse are the measurements made in relation to X/Y/Z axis. Ellipses enclose 95% of cases of each category.

None of the aforementioned measurements is normally distributed[1].

Once the general metric characteristics have been understood, we will relate this data with the technological structure. The three technological orders proposed, shows differences in shape between them. Figure-11.16 shows three different but overlapping groups using the 95% confidence ellipses. The ellipse of cores is the smallest one and it is situated in the central part of the chart, showing a rounded morphology. The ellipse of knapping products is located on the lower area and it presents horizontal elongation. Finally, the ellipse of chunks is positioned in the central and upper area, displaying positive elongation. The distribution of weight between each category does also shows clear differences in variance, as demonstrated by *H* Kruskal-Wallis test: $H\ \chi^2$ (2, N = 242) = 27.265, $p < 0.001$ (Figure-11.16b). In general, cores are bigger than other two technological orders with weights around 56 g for each piece (Table-11.16). Chunk is the following category of medium weight, especially conditioned by a 722 g rock. The median weight is 3.98 g, a more representative weight of chunks. Finally, knapping product mean is 21.2 g, smaller than mean of previous categories. Nevertheless, and taking into consideration the chunk median, knapping products median is heavier than chunk one. The median of knapping product and core orders are 7 g and 26 g respectively.

Technological order	Weight		∑ of pieces		Ratio
	∑	%	∑	%	Grams/Piece
Core	898,5	23,5	16	6,6	56,2
Knapping product	1884,7	49,3	177	73,1	10,6
Chunk	1039,6	27,2	49	20,2	21,2

Table-11.16: Frequencies and weight of main technological orders. The ratio grams/piece is reported. Weight is expressed in grams.

1 *KS* = 0.103; *df* = 194; $p < 0.01$ for length
KS = 0.110; *df* = 194; $p < 0.01$ for width
KS = 0.094; *df* = 194; $p < 0.01$ for thickness
KS = 0.176; *df* = 59; $p < 0.01$ for X-axis
KS = 0.160; *df* = 59; $p < 0.01$ for Y-axis
KS = 0.149; *df* = 59; $p < 0.01$ for Z-axis
KS = 0.207; *df* = 241; $p < 0.01$ for weight

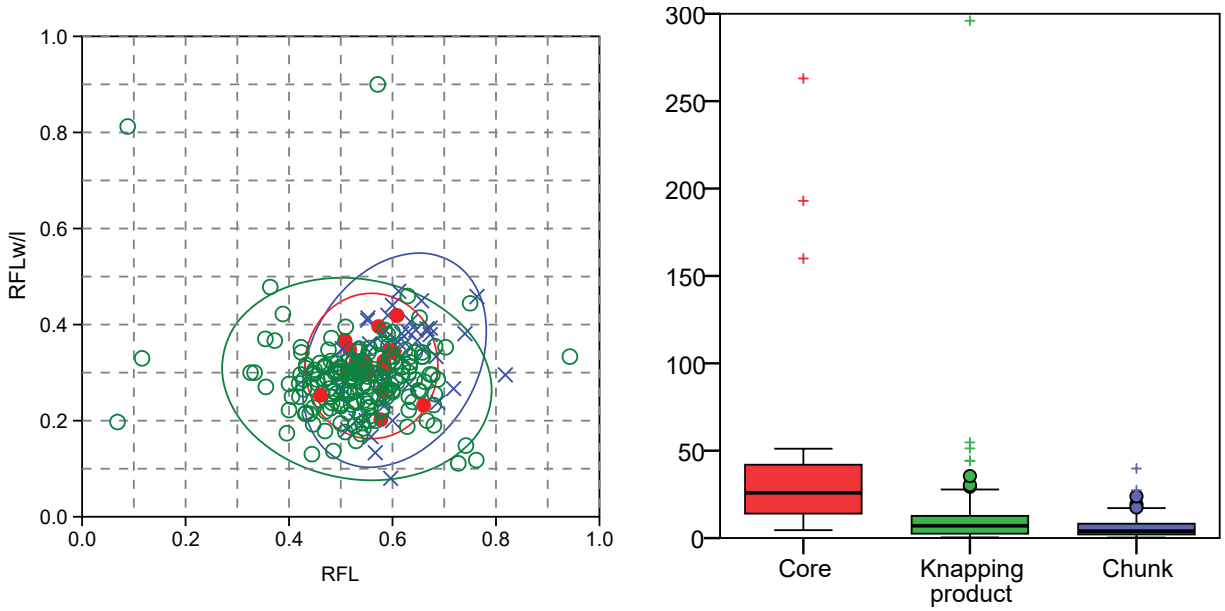

Figure-11.16: Double chart showing: a) Scatter plot of RFLw or RFLI and RBEI indexes. Green circles and ellipse are knapping products. Red points and ellipse are cores. Blue crosses and ellipse are chunks. Ellipses enclose 95% of cases of each category. b) Boxplot showing differences in weight between the technological orders. There is an outlier outside the chart (722.17 g) in the category of chunk. The weight is expressed in grams.

Coming to cores, there are no differences in morphology between the types proposed, as displayed in Figure-11.17 through the relationship between RBEI and RFL. Weight is similar distributed within each category, as indicated by the analysis of variance based on *H* Kruskal-Wallis test: $H\,\chi^2$ (3, N = 16) = 4.169, p = 0.244. Regarding the gram per piece ratio of each category of cores, irregular cores are above the average of all cores considered. Meanwhile core on flake and prismatic ones are under the average of cores. Finally, discoid cores have similar weight than average value of all cores considered (Table-11.17).

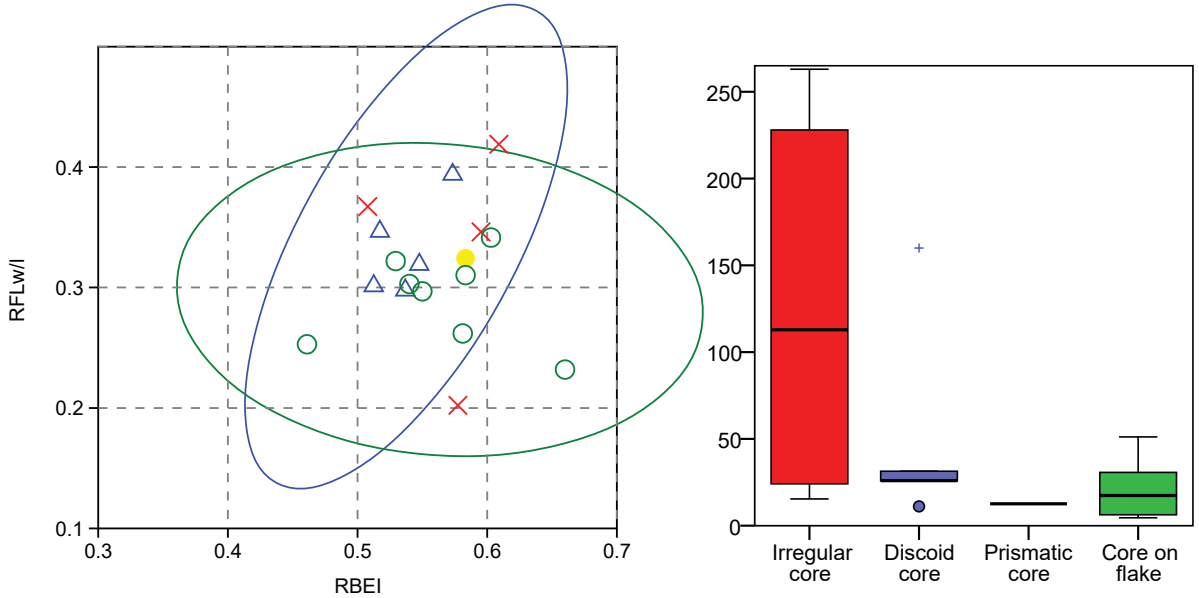

Figure-11.17: Double chart showing: a) Scatter plot of RFLw or RFLI and RBEI indexes. Green circles and ellipse are cores on flakes. Red crosses are irregular cores. Blue triangles and ellipse are discoidal cores. The yellow point is a prismatic core. Ellipses enclose 95% of cases of each category. b) Boxplot showing differences in weight between types of cores. The weight is expressed in grams.

Core groups	Weight		∑ of pieces		Ratio
	∑	%	∑	%	Grams/Piece
Irregular core	504,2	56,1	4	25,0	126,0
Discoid core	254,3	28,3	5	31,3	50,9
Prismatic core	12,6	1,4	1	6,3	12,6
Core on flake	127,4	14,2	6	37,5	21,2

Table-11.17: Frequencies and weight of different groups of cores. The ratio grams/piece is reported. Weight is expressed in grams.

Knapping products exhibit clear differences in the form of lithic remains, as shown in Figure-11.18a. The areas defined by 95% confidence ellipses are very different for blanks and core preparation/rejuvenation products. The former is arranged in a circle between 0.1 ≤ RFL ≥ 0.5 and 0.3 ≤ RBEI ≥ 0.8. The latter forms an ellipse overlapped to the upper half part of the blank ellipse between the 0.25 ≤ RFL ≥ 0.45 and 0.3 ≤ RBEI ≥ 0.65, covering the regions of cubic, tabular and prismatic shapes. Nevertheless, weight distribution is alike in both categories, certified by *U* Mann-Whitney test $U = 501.00$, $p < 0.126$. The differences observed in Figure-11.18b and Table-11.18 are a consequence of the small quantity of core preparation/rejuvenation products.

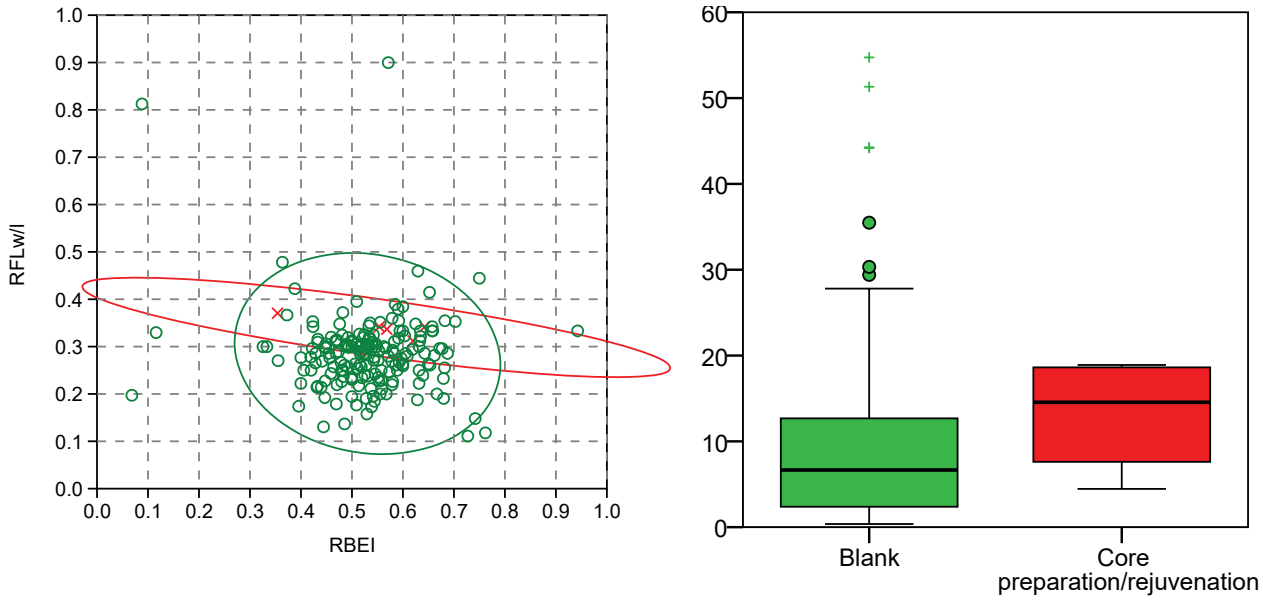

Figure-11.18: Double chart showing: a) Scatter plot of RFLw or RFLI and RBEI indexes. Green circles and ellipse are blanks. Red crosses and ellipse are core preparation/rejuvenation products. Ellipses enclose 95% of cases of each category. b) Boxplot showing differences in weight between blanks and core preparation/rejuvenation products. There is an outlier outside the chart (296 g) in the category of blanks. The weight is expressed in grams.

Knapping product group	Weight		∑ of pieces		Ratio
	∑	%	∑	%	Grams/Piece
Blank	1832,2	97,2	173	97,7	10,6
Core prep./rejuv.	52,5	2,8	4	2,3	13,1

Table-11.18: Frequencies and weight of different groups of knapping products. The ratio grams/piece is reported. Weight is expressed in grams.

Focussing on blanks, there are no clear differences in their formats based on the number of negative scars on their dorsal surfaces (Figure-11.19a). All four categories are similarly distributed, represented by relatively rounded circles in the region between 0.1 ≤ RFL ≥ 0.5 and 0.3 ≤ RBEI ≥ 0.75. However points are less dispersed in blanks with two negative scars than in other categories. Nevertheless, there are clear differences in weight based on the number of negative scars, as shown in Figure-11.19b and statistically demonstrated by *H* Kruskal-Wallis test: $H\ \chi^2\ (3, N = 173) = 10.826$, $p = 0.013$. The pieces without negative scars are the most variable category and they have the presence of the biggest blanks. The medium weight and its variability increase in the other three categories with the increment of negative scars. This relationship is also observable when grams per piece ratio of each category is compared (Table-11.19).

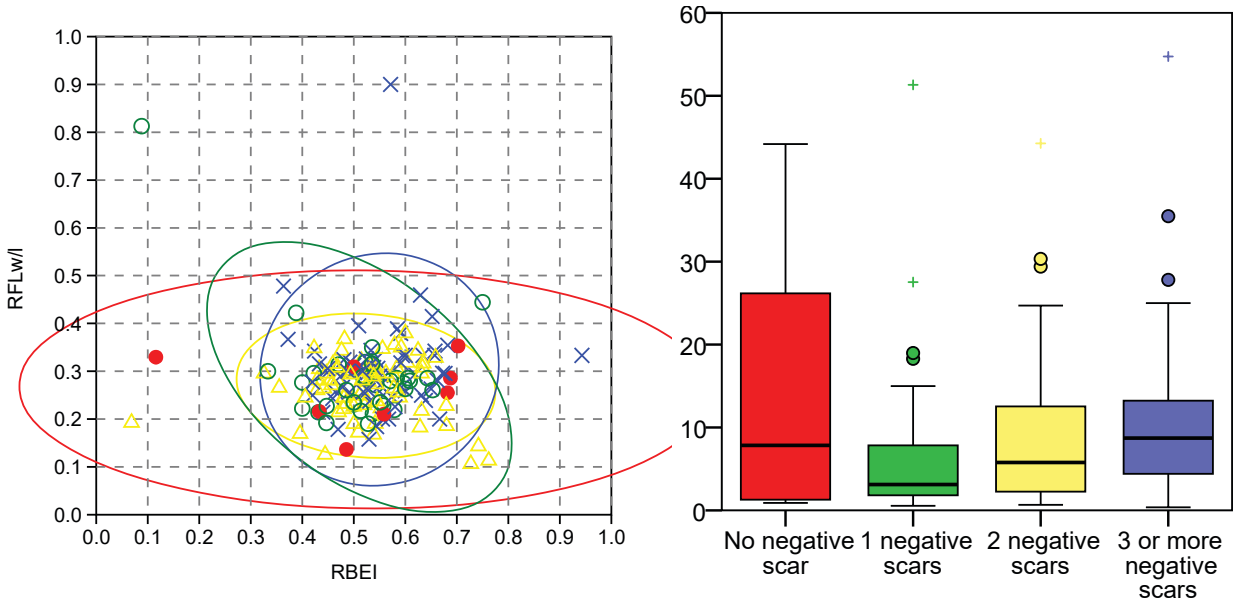

Figure-11.19: Double chart showing: a) Scatter plot of RFLw or RFLI and RBEI indexes. Red points and ellipse are blanks without negative scar. Green circles and ellipse are blanks with one negative scar. Yellow triangles and ellipse are blanks with two negative scars. Blue crosses are blanks with three or more negative scars. Ellipses enclose 95% of cases of each category. b) Boxplot showing differences in weight between blanks with different number of negative scars on dorsal surface. There is an outlier outside the chart (296g) in the category of blanks with without negative scar. The weight is expressed in grams.

Number of negative scars	Weight		∑ of pieces		Ratio
	∑	%	∑	%	Grams/Piece
No-negative scars	359,7	19,6	7	4,0	51,4
One negative scar	238,5	13,0	33	19,1	7,2
Two negative scars	574,5	31,4	71	41,0	8,1
Three or more negative scars	659,6	36,0	62	35,8	10,6

Table-11.19: Frequencies and weight of blanks grouped by number of negative scars. The ratio grams/piece is reported. Weight is expressed in grams.

Regarding the integrity of the blanks, there are no clear differences based on the form of the pieces (Figure-11.20a). All five 95% confidence ellipses are similarly distributed creating circles in the region between 0.1 ≤ RFL ≥ 0.5 and 0.3 ≤ RBEI ≥ 0.8. Nevertheless, there are two tendencies. The first associate proximal fragments with the lower part of the chart, in the region most closely related with tabular morphologies. The second tendency points at the association between longitudinal fragments and the right part of the chart, in the region most closely related to bladed morphologies. Comparing the distribution of weight between the various types of blank, *H* Kruskal-Wallis test indicates there are not statistically significant differences between them $H\ \chi^2$ (4, N = 173) = 5.812, p = 0.214. Figure-11.20b and Table-11.20 also point at similar conclusion. Moreover, longitudinal fragments and undetermined ones are slightly lighter than other three categories.

Integrity of blanks	Weight		∑ of pieces		Ratio
	∑	%	∑	%	Grams/Piece
Complete	1175,9	64,2	122	70,5	9,6
Proximal fragment	454,0	24,8	22	12,7	20,6
Distal fragment	90,5	4,9	9	5,2	10,1
Longitudinal fragment	66,1	3,6	14	8,1	4,7
Undetermined fragm	45,9	2,5	6	3,5	7,6

Table-11.20: Frequencies and weight of blanks grouped by integrity. The ratio grams/piece is reported. Weight is expressed in grams.

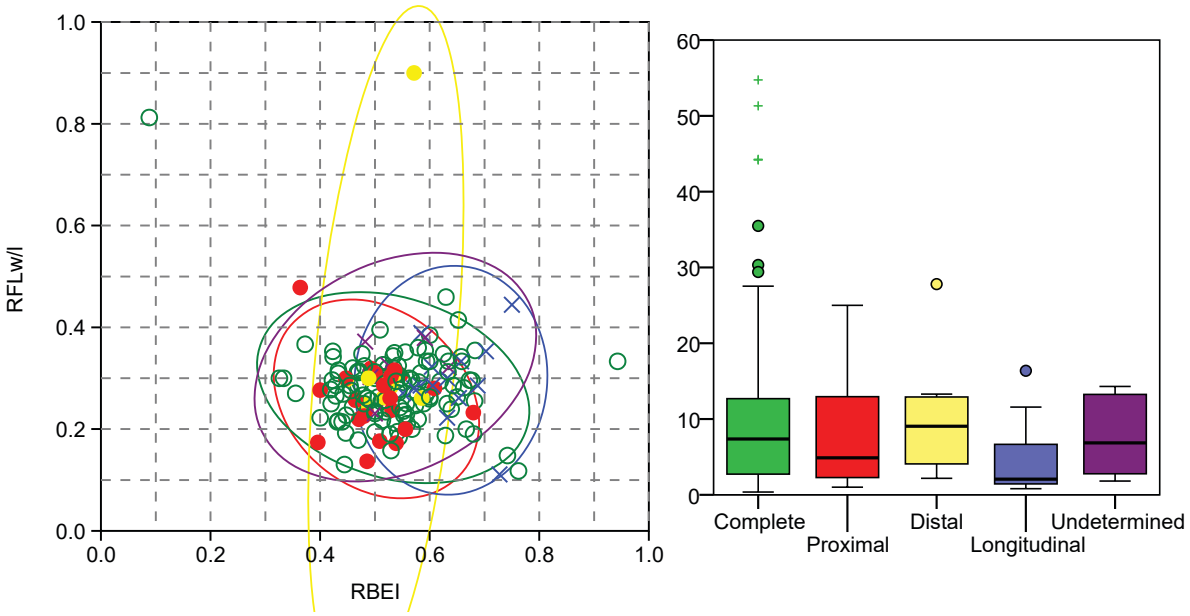

Figure-11.20: Double chart showing: a) Scatter plot of RFLw or RFLl and RBEI indexes. Green circles and ellipse are complete blanks. Red points and ellipse are proximal blank fragments. Yellow points and ellipse are distal fragments. Blue crosses and ellipse are longitudinal blank fragments. Purple points and ellipse are undetermined blank fragments. Ellipses enclose 95% of cases of each category. b) Boxplot showing differences in weight between blanks preserved in diverse states of integrity. There is an outlier outside the chart (296g) in the category of proximal blank fragment. The weight is expressed in grams.

The classification of complete blanks (Figure-11.21a) reveals the predominance of flakes (79% of complete blanks), followed by a moderate presence of elongated flakes (15% of complete blanks) and a really occasional find of blades (7% of complete blanks). There is no difference in weight between these three categories, which show similar distributions, as depicted by Figure-11.21b and proven by *H* Kruskal-Wallis test: $H\ \chi 2\ (2, N = 120) = 0.504$, $p = .504$. The comparison of gram/piece ratios between the three types of blanks proposed reveals differences in mean weight (Table-11.21). The grams per piece ratio of flakes (most frequent category) is similar to elongated flake one, while grams per piece ratio of blades is heavier than previous two types.

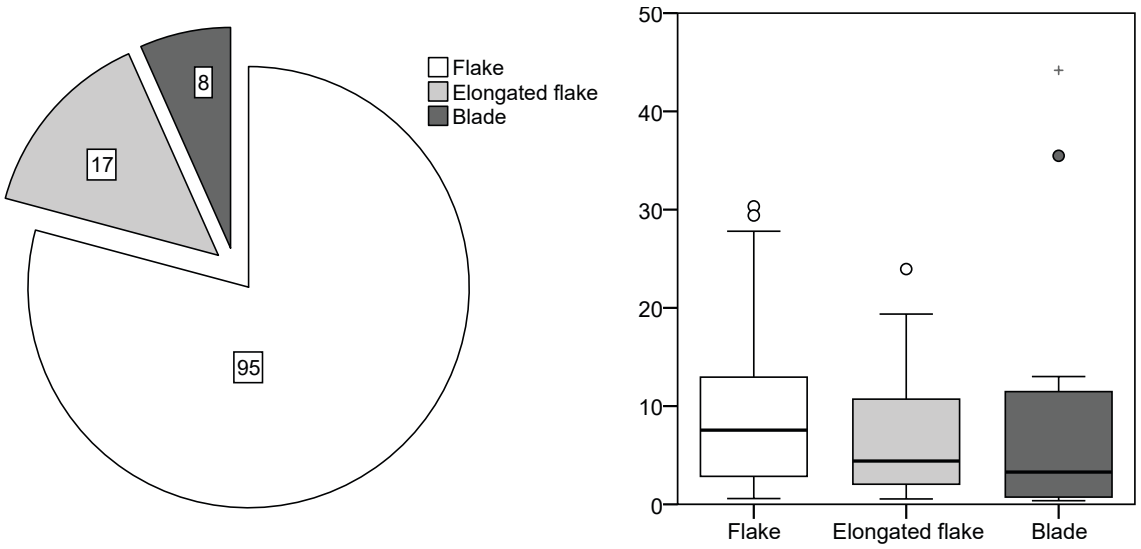

Figure-11.21: Double chart showing a) pie chart showing the distribution of complete blank products, and b) boxplot showing differences in weight between metrical categories. The weight is expressed in grams.

Complete blank characterisation	Weight ∑	Weight %	∑ of pieces ∑	∑ of pieces %	Ratio Grams/Piece
Flake	910,6	79,1	95	79,2	9,6
Elongated flake	136,3	11,8	17	14,2	8,0
Blade	104,3	9,1	8	6,7	13,0

Table-11.21: Frequencies and weight of different types of complete blanks (flakes, elongated flakes, blades). The ratio grams/piece is reported. Weight is expressed in grams.

Next, we will compare the (typo)metrical structure with retouched material. There are clear weight differences based on to the presence (M = 8.26 g) or absence (M = 5.13 g) of retouch in the pieces, as corroborated by *U* Mann-Whitney test: *U* = 8,265.5, *p* = 0.01. In general, retouched artefacts are heavier than unretouched ones, even though grams/piece ratio points at inversion of weights (Figure-11.22b and Table-11.22). There are also some differences according to morphology, especially due to different dispersal of points, as depicted in Figure-11.22a. The morphology of retouched artefacts is more standardised than the morphology of non-retouched material. Nevertheless, there are no differences in form of the artefacts according to the quantity of primary types on each blank (Figure-11.23a). There are neither weight distribution differences, as tested by H Kruskal-Wallis test: H χ2 (2, N = 92) = 1.836, p = 0.399 and displayed in Table-11.23.

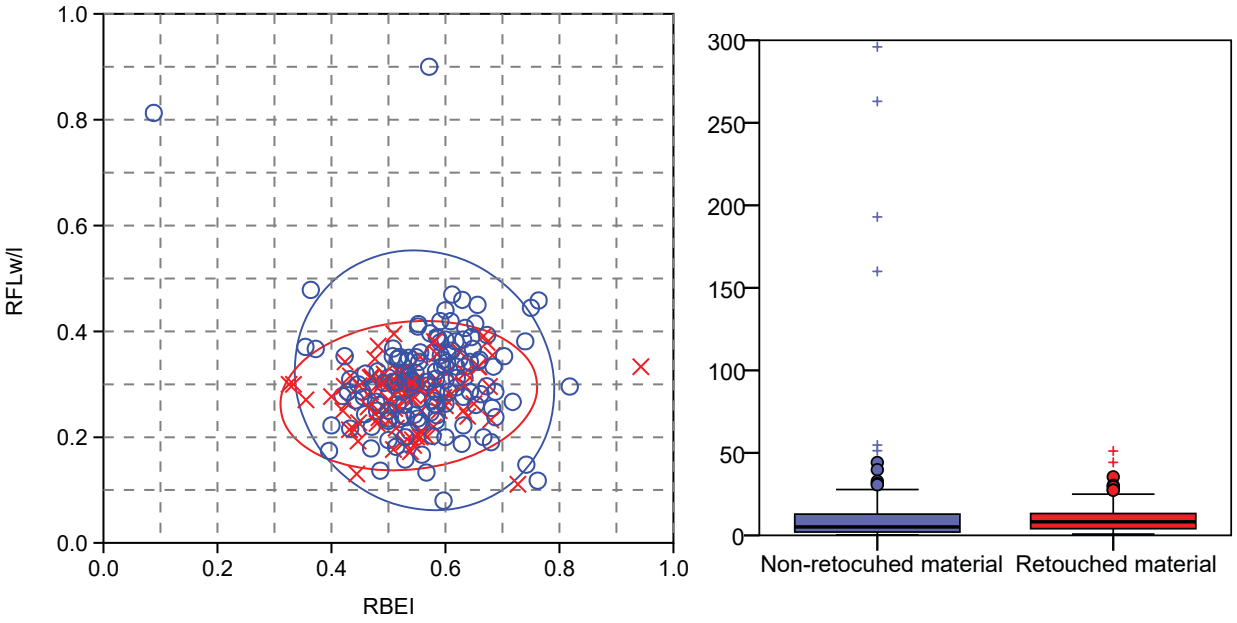

Figure-11.22: Double chart showing: a) Scatter plot of RFLw or RFLl and RBEI indexes. Red crosses and ellipse are retouched lithic material. Blue circles and ellipse are non-retouched lithic material. Ellipses enclose 95% of cases of each category. b) Boxplot showing differences in weight between retouched and non-retouched lithic material. The weight is expressed in grams.

Piece	Weight ∑	Weight %	∑ of pieces ∑	∑ of pieces %	Ratio Grams/Piece
Non-retouched	2850,8	74,6	150	62,0	19,0
Retouched	972,0	25,4	92	38,0	10,6

Table-11.22: Frequencies and weight of retouched and non-retouched pieces. The ratio grams/piece is reported. Weight is expressed in grams.

Quantity of retouch in each piece	Weight ∑	Weight %	∑ of pieces ∑	∑ of pieces %	Ratio Grams/Piece
One primary type	710,5	64,4	73	68,5	9,7
Two primary types	212,9	21,9	20	20,7	10,6
Three primary types	48,5	13,7	4	10,9	12,1

Table-11.23: Frequencies and weight of the retouched pieces grouped by the quantity of primary types. The ratio grams/piece is reported. Weight is expressed in grams.

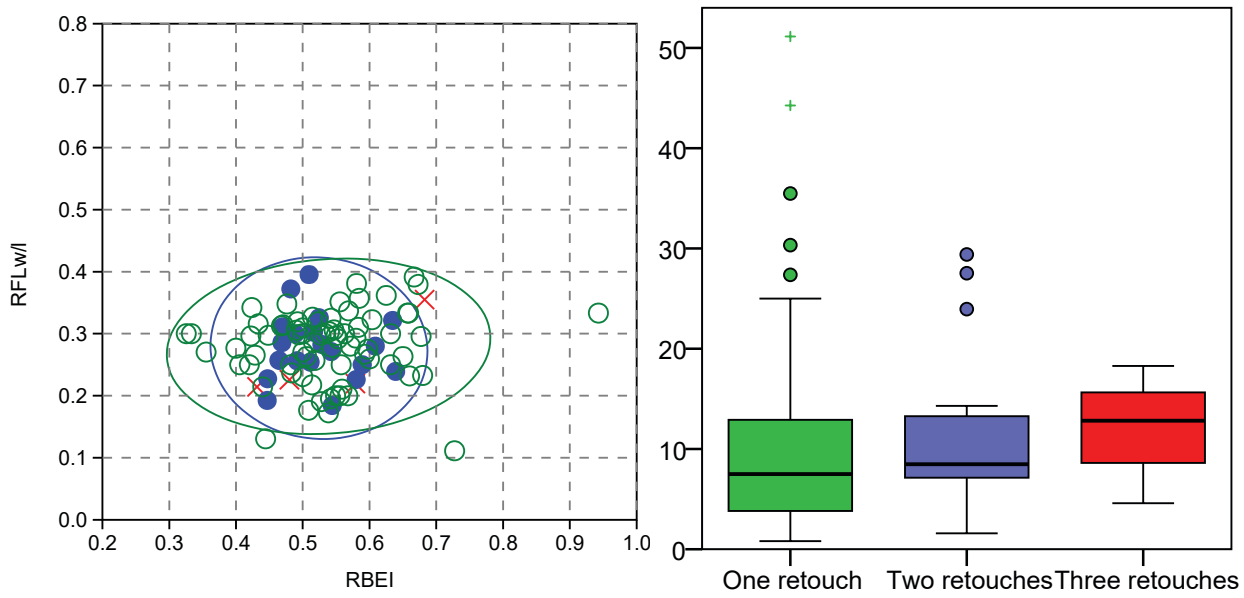

Figure-11.23: Double chart showing: a) Scatter plot of RFKw or RFLI and RBEI indexes. Green points and ellipse are artefacts with one primary type. Blue triangles and ellipse are artefacts with two primary types. Red crosses are artefacts with three primary types. Ellipses enclose 95% of cases of each category. b) Boxplot showing differences in weight between artefacts grouped by the quantity of primary types identified on each blank. The weight is expressed in grams.

Then, we will confront metrical features of retouched artefacts with the features of retouch, categorised in orders (modal) and groups (morphological). Due to the methodology used to define the retouch here, we only included in this analysis the pieces with one primary type. The comparison reveals similitudes between the lithics with Simple (S) and Abrupt (A) modes and differences between the latter two and the blanks of Burin (B) mode, as represented in Figure-11.24a. The lithics retouched with Burin mode (less in number) have a more specific distribution area than the area of Simple and Abrupt mode artefacts. Weight distribution also points at similar conclusion: alike weight distribution for artefacts with Simple and Abrupt modes, clearly differentiated from the artefacts retouched by Burin order. *H* Kruskal-Wallis test statistically reinforce these differences: χ^2 (2, *N* = 92) = 8.005, *p* = .018. Mean weight of artefacts retouched with Burin mode are lighter than mean weight of artefacts retouched by other two modes (Table-11.24).

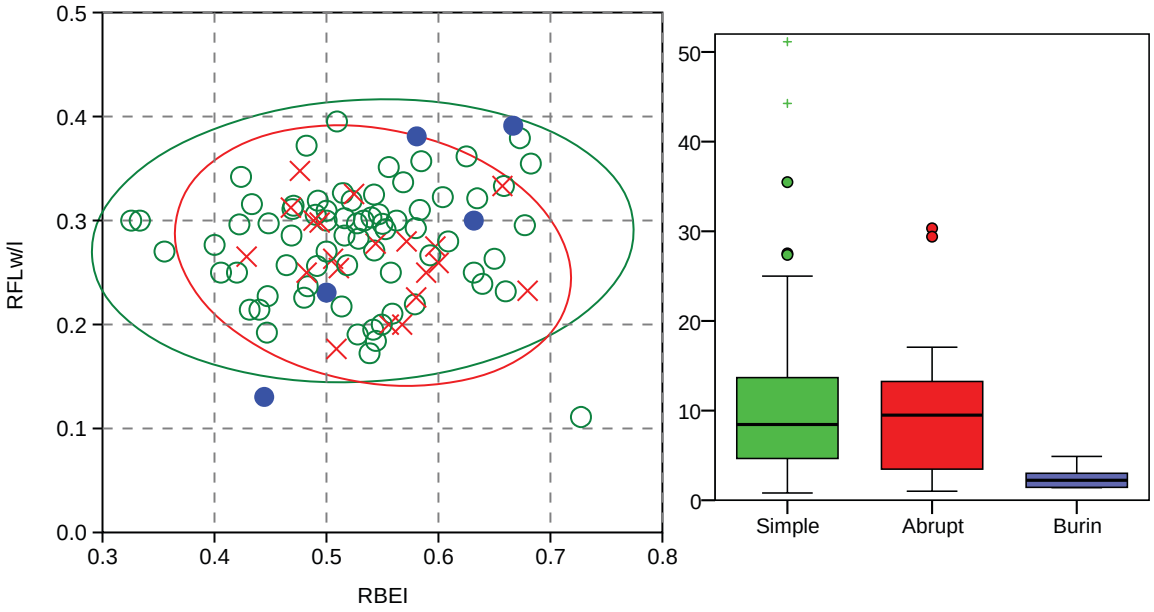

Figure-11.24: Double chart showing: a) Scatter plot of RFLw or RFLI and RBEI indexes. Red crosses are pieces configured with the Abrupt mode of retouch. Green circles and ellipse are artefacts configured with the Simple mode of retouch. Blue points and ellipse are artefacts configured with the Burin mode of retouch. Ellipses enclose 95% of cases of each category. b) Boxplot showing differences in weight between different orders of retouch.

Order of retouch	Weight		∑ of pieces		Ratio
	∑	%	∑	%	Grams/Piece
Simple	596,6	79,1	53	60,4	11,3
Abrupt	101,0	19,5	15	32,1	6,7
Burin	13,0	1,3	5	7,5	2,6

Table-11.24: Frequencies and weight of retouched artefacts grouped by the mode of retouch. The ratio grams/piece is reported. We only include artefacts with one primary type. Weight is expressed in grams.

The last structure to be tackled here is the petrological one. There are small differences in the variability of the morphology of the lithics depending their raw material. The morphology of "archaeological quartzites" is more variable than the morphology of radioralites, as could be observed in Figure-11.25. The small quantity of other raw material does not allow us to observe more differences. There are no statistically differences in weight distribution between different raw material, as proven by $H\ \chi^2$ (2, N = 238) = 3.900, p = 0.142. Nevertheless, only "archaeological quartzites" are heavier than 50 g. In addition, gram/piece ratio of limestone is slightly greater than "archaeological quartzite" and radioralite ratios (Table-11.25).

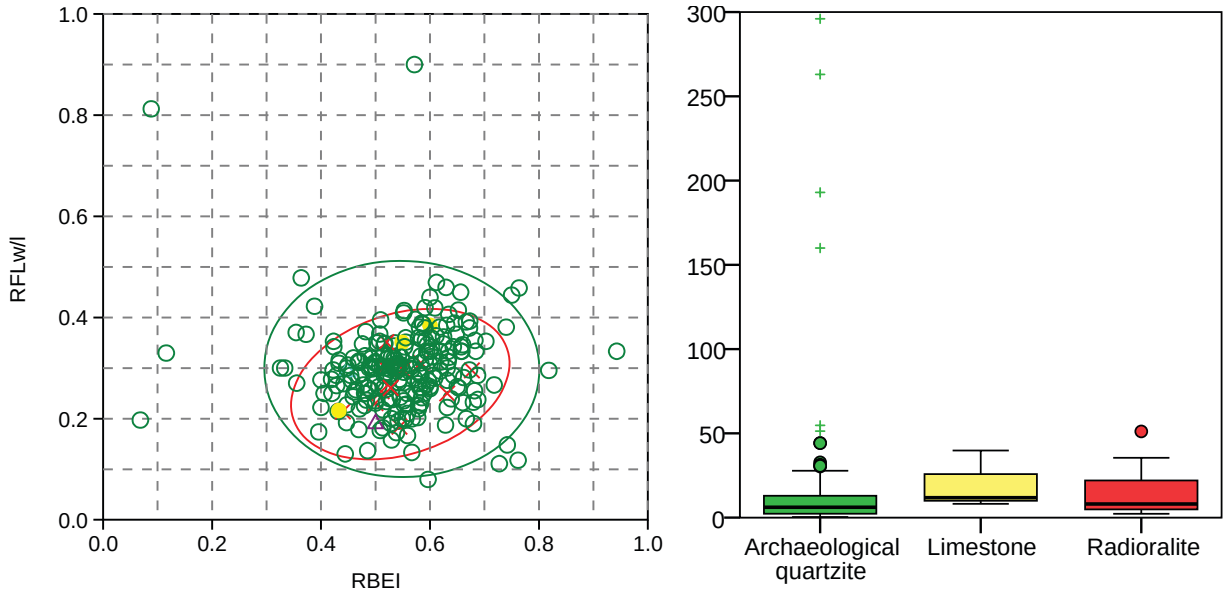

Figure-11.25: Double chart showing: a) Scatter plot of RFLw or RFLl and RBEI indexes. Green circles and ellipse are "archaeological quartzites". Red crosses and ellipse are radioralites. Yellow points and ellipse are limestones. Ellipses enclose 95% of cases of each category. b) Boxplot showing differences in weight between different raw materials. There is an outlier outside the chart (722 g) in the category of "archaeological quartzite". The weight is expressed in grams. The weight is expressed in grams.

Raw material	Weight		∑ of pieces		Ratio
	∑	%	∑	%	Grams/Piece
"Arch. quartzite"	3578,2	94,0	224	94,1	16,0
Limestone	59,8	1,6	3	3,0	19,9
Radioralite	169,2	4,4	11	11,0	15,4

Table-11.25: Frequencies and weight of different types of raw material. The ratio grams/piece is reported. Weight is expressed in grams.

There are no clear differences in morphology between different petrogenetic types. Moreover, small differences arises in the comparison of morphology variability between the SO orthoquartzite (less variable) and the other petrogenetic types (more variable) (Figure-11.26a). Nevertheless, statistical differences arise when weight distribution is compare between petrogenetic types, as demonstrated by H Kruskal-Wallis: $H\ \chi^2$ (5, N = 218) = 12.122, $p < 0.01$ and depicted in Figure-11.26b. The CC petrogenetic type is the most variable and the heaviest type. Other petrogenetic types have similar distribution between them, although different medians. Grams per piece ratio of each petrogenetic type reveals the differences (Table-11.26).

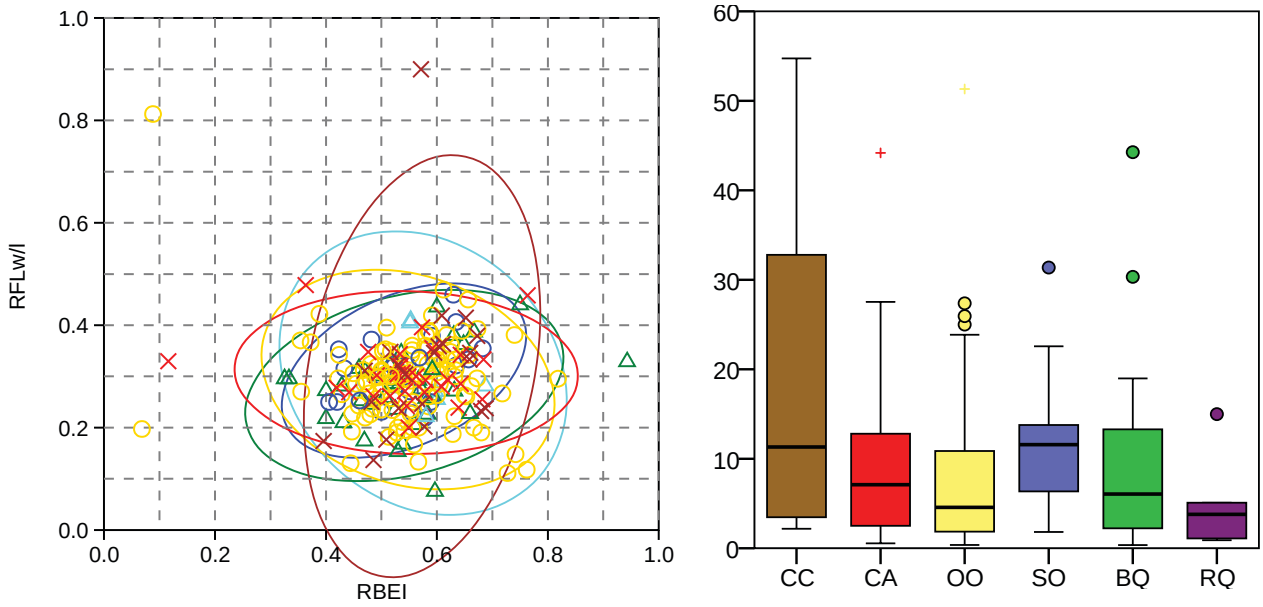

Figure-11.26: Double chart showing: a) Scatter plot of RFLw or RFLl and RBEI indexes. Brown crosses and ellipse are CC type pieces. Red crosses and ellipse are CA type pieces. Yellow circles and ellipse are OO type pieces. Blue circles and ellipse are SO type pieces. Green triangles and ellipse are BQ types. Light blue triangles and ellipse are RQ type pieces. Ellipses enclose the 95% of cases of each category. There are another four CC type with higher weight than 60g, not show on chart (192, 263, 296, and 722 g). b) Boxplot showing differences in weight between different petrogenetic types of "archaeological quartzite". The weight is expressed in grams.

Petrogenetic type	Weight		∑ of pieces		Ratio
	∑	%	∑	%	Grams/Piece
CC	1719,6	50,8	22	9,5	78,2
CA	282,3	8,3	29	12,6	9,7
OO	794,1	23,5	112	48,5	7,1
SO	218,9	6,5	22	9,5	10,0
BQ	338,8	10,0	39	16,9	8,7
RQ	29,7	0,9	7	3,0	4,2

Table-11.26: Frequencies and weight of different petrogenetic types of "archaeological quartzites". The ratio grams/piece is reported. Weight is expressed in grams.

Now, we will delve into the relationship between raw material, technology, retouch, and the metrical characterisation, focusing on weight. Starting with technology, there are clear differences in weight based on the technological order and raw material (Figure-11.27 and Table-11.27). Cores made on "archaeological quartzite" are heavier than radioralite core. There are differences between petrogenetic types too, especially in the comparison between cores made on CC type and other petrogenetic types. The former are bigger than other types. Due to the small quantity of cores, we could not compare their weight between different types of cores and raw material.

Raw material	Petrgen. type	Lithic collection											
		Core			Knapping			Chunks			Total		
		∑	W	g/p	∑	W	g/p	∑	W	g/p	∑	W	g/p
Archaeological quartzite	CC	4	519	129,9	11	443	40,3	7	757	108,1	22	1720	78
	CA	1	26	25,9	24	239	9,9	3	18	6,0	28	282	10
	OO	6	78	12,9	75	561	7,5	25	156	6,2	106	794	7,5
	SO	1	31	31,4	17	182	10,7	1	6	5,7	19	219	12
	BQ	1	18	17,6	29	272	9,4	7	50	7,1	37	339	9,2
	RQ				4	23	5,9	2	6	3,1	6	30	4,9
	MQ												
	Undet.												
	Total	13	672	51,7	160	1719	10,7	45	992	22,0	218	3383	16
Limestone					3	20	6,7	1	40	39,8	4	60	15
Lutite					1	6	6,1				1	6	6,1
Quartz					1	9	8,7				1	9	8,7
Radioralite		1	51	51,1	9	111	12,3	1	7	7,0	11	169	15

Table-11.27: Frequency table of main technological orders of lithic remains grouped by raw material, including frequencies, weight and the ratio grams/piece for each case. Weight is expressed in grams.

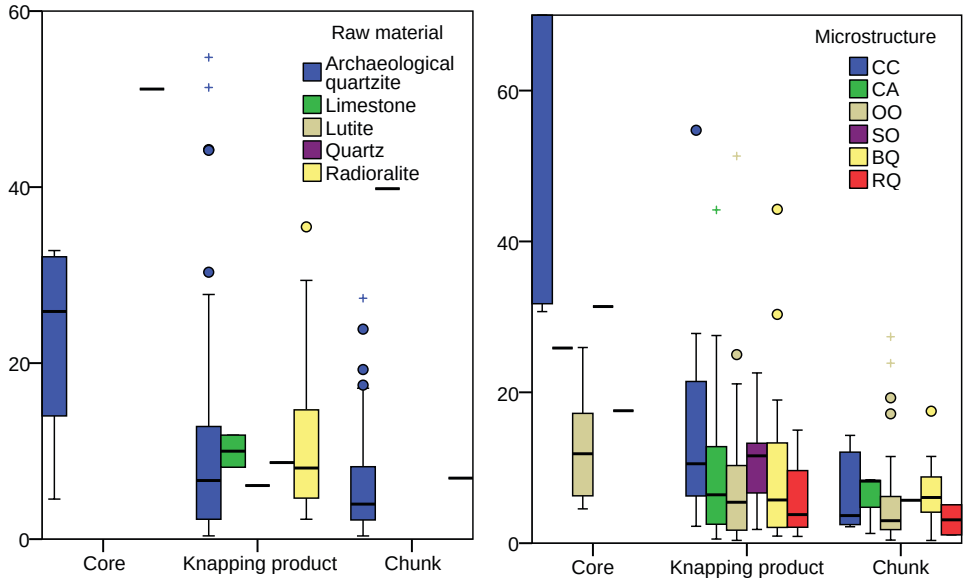

Figure-11.27: Double boxplot showing the distribution of weight in grams of all lithic remains grouped first by technological order and second by raw material in the chart on the left and by petrogenetic type in the chart on the right. There are another four CC petrogenetic type of "archaeological quartzites" with higher weight than 60 g, not show on chart (a 722 g chunk, a 296 g blank, and two cores with 192 and 263 g of weight). The weight is expressed in grams.

In regard to knapping products, Table-11.28 displays the differences between core preparation/rejuvenation products and blanks. The former are bigger than the latter in the two petrogenetic types with weighted core preparation/rejuvenation products. It is also interesting to observe that core preparation/rejuvenation products are bigger in CA type than in OO orthoquartzite. There is no difference between raw materials in the weight of blanks based on the number of negative scars (Figure-11.28). Nevertheless, there are differences in the weight of blanks depending on the number of negative scars between petrogenetic types. The most relevant are: a) blanks without negative extraction are heavier on quartzarenite group than on other groups; b) CA quartzarenite follows a reduction of weight with the increase of dorsal scars; c) weight of blanks made on OO orthoquartzite increase with the intensification of dorsal scars; d) the stable weight distribution for blanks made on SO orthoquartzite, around 15 g; e) the absence of clear tendencies in quartzite group (Table-11.28). There are no weight differences between the integrity of blanks and raw material.

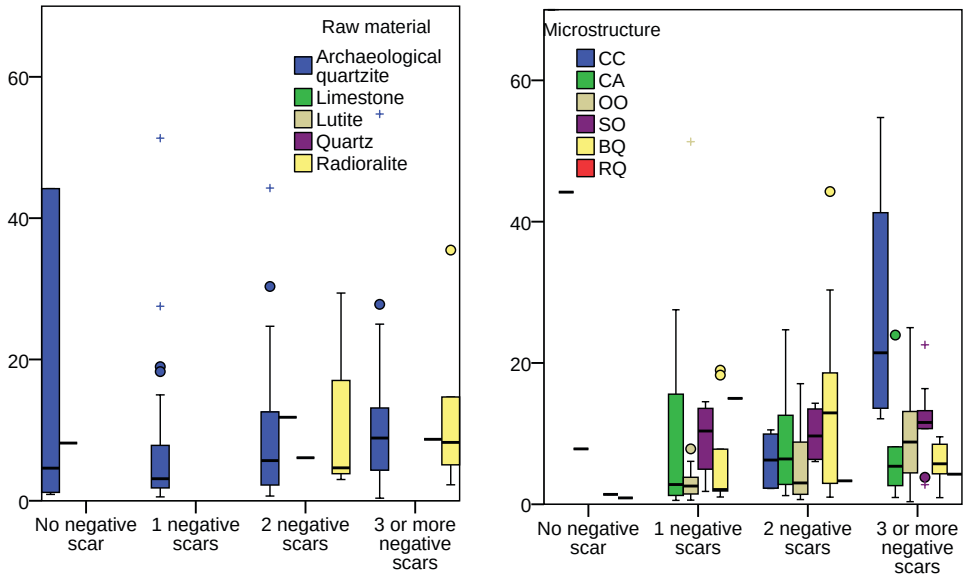

Figure-11.28: Double boxplot showing the distribution of weight in grams of blanks grouped first by the number of negative scars on dorsal surface and second by raw material in the chart on the left and by petrogenetic in the chart on the right. There is another CC petrogenetic type of "archaeological quartzites" with 296 g does not show on chart. The weight is expressed in grams.

Finally, differences in weight of chunks based on petrogenetic types are verifiable in Figure-11.27 and Table-11.27. Chunks made on CC quartzarenite are heavier than those made on the other petrogenetic types. In addition, there is no chunks made on SO orthoquartzite lighter than seven grams.

Raw material	Petrgen. type	Knapping products: Core preparation ∑	W	g/p	Blanks: No neg.scar ∑	W	g/p	1 neg.scar ∑	W	g/p	2 neg.scar ∑	W	g/p	3 or more ∑	W	g/p	Blank total ∑	W	g/p
Archaeological quartzite	CC				1	296	296				6	38	6,3	4	110	27	11	443	40
	CA	1	18	18	1	44	44	4	34	8,4	12	96	8	6	46	7,7	23	220	9,6
	OO	3	34	11	1	8	7,8	14	89	6,4	30	165	5,5	30	299	10	75	561	7,5
	SO							4	37	9,3	4	40	9,9	9	105	12	17	182	11
	BQ				1	1	1,4	9	61	6,8	12	167	14	7	42	6	29	272	9,4
	RQ				1	1	0,9	1	15	15	1	3	3,3	1	4	4,3	4	23	5,9
	MQ																		
	Undet.				1	1	1,2	1	3	2,5	2	16	7,9				4	19	4,9
	Total	4	52	13	6	352	59	33	239	7,2	67	524	7,8	57	606	11	163	1720	11
Limestone					1	8	8,2			12	1	12	12				2	20	10
Lutite										6,1	1	6	6,1				1	6	6,1
Quartz														1	9	8,7	1	9	8,7
Radioralite											3	37	12				3	37	12

Table-11.28: Frequency table of different knapping products grouped by raw material, including frequencies, weights and the ratio grams/piece for each case. The knapping products considered are core preparations/rejuvenations and blanks sorted by the number of negative scars present. Weight is expressed in grams.

The analysis of the relationship between raw material and retouch concludes that the heaviest retouched artefacts are made on radioralite (Figure-11.29 and Table-11.29). The same analysis based on petrogenetic types reveals that the heaviest pieces with Simple (S) retouch are made on CA type, followed by BQ, SO, and OO types. The blanks with Abrupt (A) mode are generally smaller than previous blanks retouched with Simple mode, and there are not clear differences between petrogenetic types. Finally, blanks with Burin (B) mode are the lightest retouched artefacts.

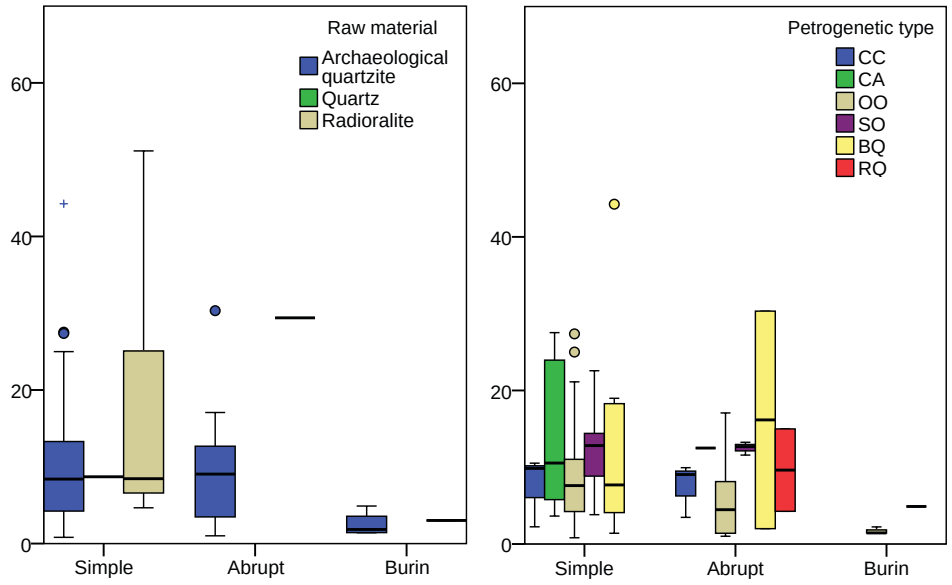

Figure-11.29: Double boxplot showing the distribution of weight in grams of retouched material grouped first by mode of retouch and second by raw material in the chart on the left and by petrogenetic in the chart on the right. The weight is expressed in grams.

Raw material	Petrgen. type	Single-retouched pieces: Simple — Sidescraper ∑	W	g/p	Endscraper ∑	W	g/p	Denticulate ∑	W	g/p	Point ∑	W	g/p	Abrupt — Abrupt ∑	W	g/p	Burin — Burin ∑	W	g/p
Archaeological quartzite	CC	2	12	6,0				2	19	9,5									
	CA	3	27	9,0				1	13	13,0									
	OO	19	195	10,2	1	8	8,0	1	6	6,0	3	31,2	10,4	4	28	6,9	3	5	1,7
	SO	3	48	16,0				1	12	12,0	1	3,8	3,8						
	BQ	9	92	10,3							3	57,5	19,2	1	2	2,0	1	5	4,9
	RQ							1	15	15,0				1	4	4,0			
	MQ																		
	Undet.	1	5	4,7										1	12	12,0			
	Total	37	379	10,2				6	64	10,6	7,0	92,5	13,2	7	46	6,6	4	6	1,6
Quartz		1	9	8,7															
Radior.		5	111	22,2													1	3	3,0

Table-11.29: Frequency table of artefacts sorted by mode of retouch and grouped by raw material, including frequencies, weight and the ratio grams/piece for each case. Pieces with different primary types are not included. Weight is expressed in grams.

11.6. RAW MATERIAL ACQUISITION AND MANAGEMENT PROCESSES AT EL ARTEU

Once the raw data from this collection have been presented, in this section we bring face to face geographical, geological, and archaeological data (the matter) to understand the forces that got these materials deposits here, that is, the human raw material acquisition and management strategies, the human behaviour. It is important to remark the material here analysed were recovered around the sedimentary sequence of the site, therefore, conclusion here exposed must be nuance.

The main acquisition process verified in this site is the extraction of big quantities of OO petrogenetic type for human activities, as demonstrated by the great quantity of them found in number and in weight. Moreover, the use of quartzarenite and SO and BQ petrogenetic types is clear. The small representation of other raw materials and RQ type indicates they had different roles in human activities.

The management of raw material has been analysed including the raw data of all raw materials in a general reduction process model based on a simple “chaîne opératoire” (Figure-11.30). The primary technological product of lithic reduction we find in this layer are cores (irregular, discoid, or prismatic). From here on, we expose and analyse the different processes that generate other lithic products based on the understanding of their features.

1. Blanks, as well as smaller blanks (sometimes fragmented) and chunks, were obtained as a result of the reduction process of some cores. Blanks and chunks are secondary products generated as a consequence of knapping procedures.

    a. Using retouching procedures, some of these primary blanks were modified, creating retouched artefacts as primary products and more blanks and chunks as secondary products. The latter are lighter than five grams and sometimes fragmented. In addition, new retouches can be made in the blanks, creating artefacts with different primary types, generating more blanks and chunks as secondary products.

    b. Some other blanks were reconfigured by percussion to obtain new flakes. The resulting products are a core on flake and blanks as primary products and other blanks and chunks, derived from the reconfiguration processes, as secondary products.

        i. Some cores on flakes were retouched, creating a retouched core on flake. Small chunks and blanks derived from the retouching process are again secondary products.

        ii. As a consequence of the reduction processes of the cores on flakes, further blanks were obtained, also secondary products classified as chunks and blanks (smaller than the previous blanks).

            • The latter blanks can also be retouched, creating new retouched artefacts and secondary products (chunks and blanks).

2. Following with cores, some of them were reconfigured to obtain new flaking surfaces or new striking platforms. This process generated a new form or type of core and three different secondary products: chunks, blanks (generally lighter than five grams and sometimes fragmented) and core preparation/rejuvenation products.

    a. One core preparation/rejuvenation product was retouched, creating a retouched preparation/rejuvenation product. As a consequence, small chunks and blanks were produced as secondary products.

Some of the chunks were also retouched. They are always heavier than two grams. Blanks and chunks were generated as secondary products derived of retouch techniques and they are generally lighter than two grams.

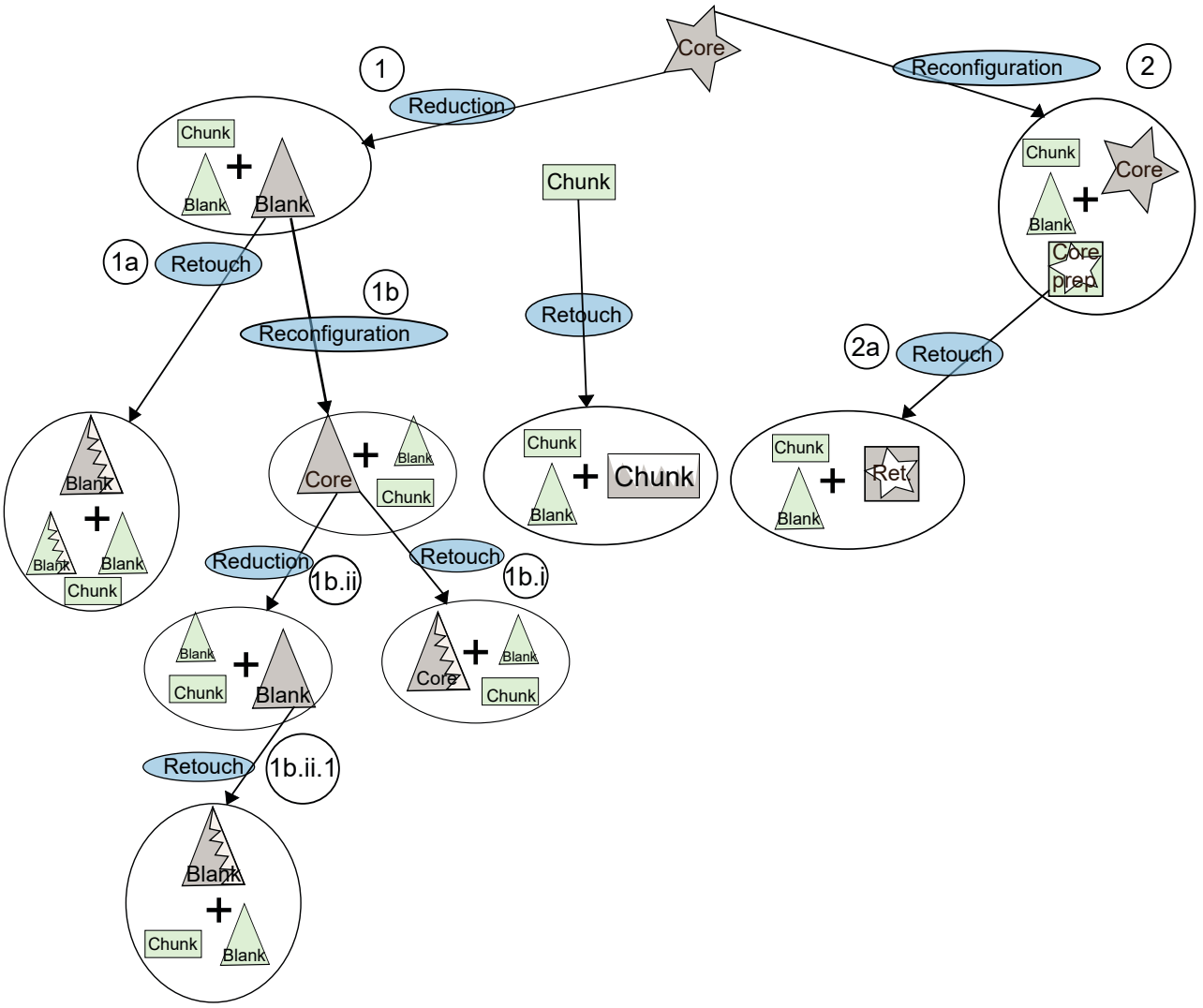

Figure-11.30: Schematic “chaîne opératoire” derived from the analysis of the lithic assemblage from El Arteu. Stars represent cores, rectangles chunks, elongated circles completely cortical chunks, squares with stars core preparation/rejuvenation products and triangles blanks. Zig-zag lines added to any of these icons represent retouched artefacts. Grey icons are primary products and green ones secondary products. The blue ellipses indicate human activities. Alphanumeric codes inside circles are references to the text.

Finally, there are some relevant features in this layer related with the nature of the recovery of the assemblage. This was not acquire from a proper archaeological excavation, but from a survey around the sedimentary profile. These features are:

1. the overrepresentation of retouched artefacts
2. the overrepresentation of cores instead of knapping products, even though chunks are frequent
3. the overrepresentation of large material instead the smaller lithics
4. the overrepresentation of blanks with high quantity of negative scars

We start explaining the conclusion related with the acquisition and management of “archaeological quartzites” by petrogenetic types, and later, other raw material. Figure-11.31 and Figure-11.33 schematically represent the acquisition process of “archaeological quartzites” and other raw materials. Figure-11.32 displays the relationship between acquisition and management strategies. Finally, Figure-11.34 shows the Cost map from El Arteu with the geological formations where raw material could have been caught.

As has been previously mentioned, “archaeological quartzite” is the most relevant raw material, both in number and weight, present in El Arteu. Next, we will explain the raw material catchment and management strategies of this raw material by petrogenetic types.

The CC type is one of the less frequent type of "archaeological quartzite". All main technological orders are represented in this layer, but core preparation/rejuvenation product is not represented. There is a clear overrepresentation of chunks and cores and an underrepresentation of knapping products. However, the weight distribution of chunk and knapping products which range from two grams to greater than 200 g, points that knapping activities were practiced in the site. The grams per piece ratio in all technological products, but especially on cores, makes clear this type is heavier than other raw materials or other types of "archaeological quartzite". There are six retouched artefacts, a small number in comparison with those of other petrogenetic types. These data suggest a low intensity exploitation. Nevertheless, the weight distribution of retouched artefacts (smaller than in other types) and the representation of cortex and negative scars on dorsal surfaces, suggest higher intensity of exploitation. The recovery condition of the collection probably determines the latter three reasoning due to the selection of stones with clearest human traces in a relatively common raw material in surrounding area. The different representation of cortical surfaces on knapping products (similar to other petrogenetic types) than on cores (greater than other petrogenetic types) confirms previous reasoning.

This petrogenetic type is characterised by multiple grain size varieties, generally with heterogeneous distribution of grain sizes. Colour is also greatly heterogeneous, due to the effect of many different non-quartz mineral on these rocks. The presence of bedding on these quartzarenites is uneven. All these elements lead us to conclude: a) the CC petrogenetic type is heterogeneous itself, and b) the input in the site of CC quartzarenites comes from different pebbles from diverse origins. White varieties are related with the CC type from Barrios or Cavandi formations, while dark and brown varieties are linked with the Murcia Formation or with carboniferous sandstone strata such as the Potes, Mogrovejo or Viorna formations. The analysis of cortical areas reveals the fluvial origin of all the cortical surfaces identified. All in all, we proposed that the CC petrogenetic type is a raw material caught in fluvial beach deposits, probably near the site of El Arteu. We observed an important presence of this petrogenetic type in these beaches. Different pebbles with diverse colours and grain size varieties were also found during geological survey. The general size and morphological features of CC pebbles in these beaches is also heterogeneous: multiple sizes (from medium pebbles to big cobbles) and both spherical and elongated morphologies are present. Then, strong selection mechanisms would not have been required for the acquisition of this type. In addition, it can be said there is no selection based on colour or on grain size. Putting all this information together, it is possible to conclude the input of the CC type is made through a conscious input, probably as cores directly knapped in the site. The scale of this type in this site reveals its use as raw material was sporadic, maybe related with the scarcity of other petrogenetic types or raw materials more suitable. We also propose this petrogenetic type was preferentially selected based on the size of the pebbles. Therefore, in the deposits there must have been a selection of CC pebbles based on size. Latter hypothesis is reinforced by the weight of CC quartzarenite in El Arteu.

The CA type, only constitutes a small portion of the total of "archaeological quartzites", but it is more frequent than the CC type. As on previous type all three technological orders are represented, also core preparation/rejuvenation products. Nevertheless, there is no core on flake and the only core is a discoid one. The distribution of the three technological orders points at an overrepresentation of knapping products and an underrepresentation of chunks and, especially, cores. Weight distribution is similar to other petrogenetic types, lighter than previous quartzarenite type. Knapping and resharpening activities are clear due to the weight range of blanks and chunks between one gram to other bigger than 40 g. Retouch material is frequent, but in smaller proportion than in more deformed petrogenetic types. Nevertheless, there are seven retouched artefacts and three of them have two different primary types. The most frequent mode of retouch is the Simple one, following similar dynamics than retouch characterisation of other types. All these elements reveals a medium intensive exploitation of this material. Nevertheless, the high presence of cortical areas on dorsal surfaces and the distribution of negative scars on dorsal surfaces, reveal this type of quartzarenite as a low intensive exploited material.

The characterisation of this petrogenetic type reveals grain size is heterogeneously distributed, as previous quartzarenite. Colour is also heterogeneous due to the variability of non-quartz minerals and the influence of matrix on some lithics. The presence of bedding is significantly smaller than previous types. These features suggest a) the CA type is very variable, and b) the input of CA quartzarenite to the site got supplied with pebbles from different origins. Colour varieties links this quartzarenite with the Barrios or Cavandi outcrop formations and with clast from Carboniferous conglomerate formations, especially in the case of brown or reddish varieties. However, the characterisation of cortical areas demonstrates all cortex identified derive from fluvial deposits. All in all, we proposed

that CA petrogenetic were brought to the site from fluvial deposits, probably close to the El Arteu site. Taking into account the selection mechanisms needed to obtain CA quartzarenite varieties from fluvial courses near El Arteu, stronger selection mechanisms would have been necessary for getting this one than previous CC type. We propose catchment of CA quartzarenites was based on sporadic activities, complementary to other task, such as catchment activities of other petrogenetic types or the acquisition of other resources in river beaches. The input to the site could have been made in form of cores, blanks or retouched material. Nevertheless, due to the grain size and mineral/colour varieties of CA we consider that most of this material input as blanks. Finally, it is important to stress that the core and the core preparation/rejuvenation product are on the same variety. It reinforces the input of other varieties as blanks.

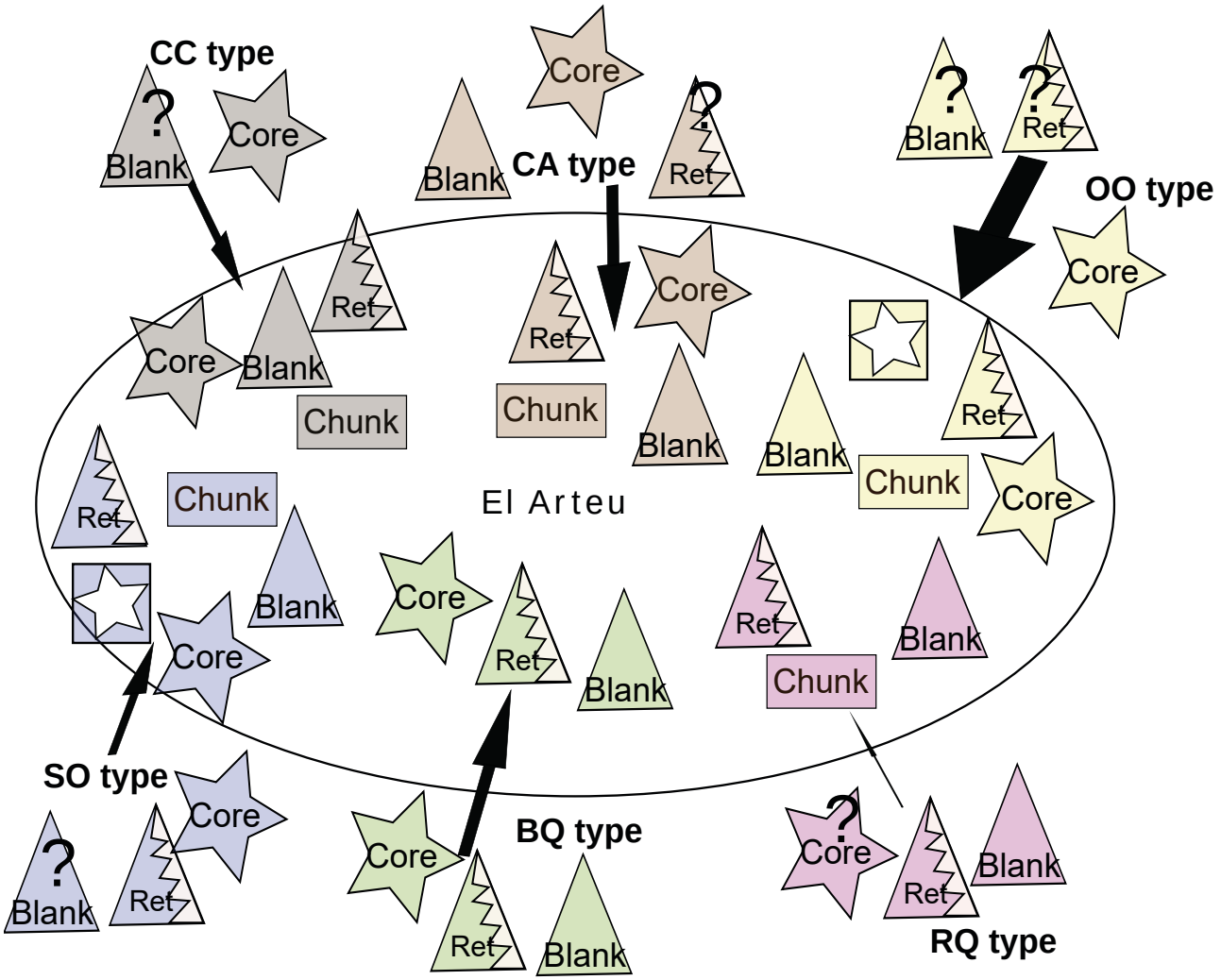

Figure-11.31: Schematic representation of the input of the different petrogenetic types of “archaeological quartzite”, taking into account the different technological products present. Stars represent cores, triangles blanks, triangles with zig-zag retouched material, ellipses fully cortical chunks and rectangles chunks. Question marks indicate products whose presence is not certain.

The OO petrogenetic type of orthoquartzite shows clear differences in management and catchment in comparison with “archaeological quartzite” types tacked above. It represents 47% of the lithic assemblage in number and 23% in weight. These data mean there was a planned and intensive exploitation of this type. The three technological categories, as well as core preparation/rejuvenation products, are present in this layer. It is obvious knapping and reshaping activities were practised in the site. This is also certified by the presence of blanks and chunks between less than one gram to more than 40 g. Cores types, weight and flacking and knapping surfaces reveal this raw material is more intensively exploited the previous quartzarenite group. The presence of negative scars is more frequent than in the former two types, but it is smaller than on SO type. Cortical areas are less ex-

tended than on previous type, especially the CA type. Retouched artefacts are less frequent than on more deformed types, but they are more frequent than previous quartzarenites. In addition, artefacts with two or three different primary types on them are frequent and all orders and groups of retouch are defined in this petrogenetic type. In addition, Abrupt and Burin modes are well represented. This evidence reveals a high intensity exploitation, reinforced by the gram per piece ratio of the lithics, smaller than previous quartzarenites and more deformed types.

The characterisation of this raw material based on grain size and colour indicates it is a more homogeneous type. Three main grain size varieties here stablished are represented, even though fine grained with homogeneous distribution variety is more frequent. According to colour, the most important varieties are the white or light grey. These are associated to stable presence of non-quartz minerals, probably as a result of the high input of this variety in the site. The brown-red variety is rarer. They may be the consequence of the transportation of few blocks of this variety to the site. The original source strata of the white-grey varieties are in the more deformed bands of the Barrios outcrop Formations, as well as in the pebbles from the carboniferous conglomerates from older layer. The brown variety only from the latter. The characterisation of cortical areas reveals that most of them come from fluvial deposits. Still, there is an important presence of conglomerate cortex too. There is no evidence of outcrop cortex. Therefore, although the most likely source strata are in the Barrios Formation, catchment was probably made in deposits and conglomerates. The conglomerate cortex is reduced to the white and light grey varieties, especially the second. Most of the conglomerates in the research area have OO orthoquartzite, more frequently the white variety, even though brown and light-grey varieties are also represented, in smaller proportion. In the conglomerates of the Remoña Formation, 14 CU away, it is possible to find them without the need to apply any selective mechanism. Other conglomerates, such as the Curavacas series (21 CU), the Lechada (23 CU), Campollo (25 CU), Maraña-Brañas (36 CU), Narova (19 CU), Pesaguero (21 CU), Pontón (38CU), Potes (22 CU), and Valdeón (37CU) conglomerates have important amounts of this type. However, at least low intensity selective mechanisms are necessary to choose specific varieties, forms and sizes. All these conglomerates are to the south, in medium altitude plateaus. In fluvial deposits the presence of this petrogenetic type is scarcer. Therefore, the selective mechanisms required pick special varieties, forms and sizes would have been more intensive.

All in all, catchment of this type would have included both fluvial and conglomerate areas. The acquisition on the first environment would have provided big amounts of material as a results of intensive and planned strategies. The acquisition in the second environment would have provided a reduced quantity into the El Arteu, as a consequence of the loss of material in the distance between the conglomerates and the site.

Most of OO type was probably input into the site as core forms in early stages of reduction, obtained from near fluvial deposits and maybe slightly modified there. This hypothesis is supported by the high presence of chunks in the site, also because most of them, also non-cores on flake are made on the white variety, better represented in fluvial deposit. Nevertheless, we also consider the input of this OO type into the site as blanks or retouched material, especially for the grey and brown varieties. This evidence distant and more complex raw material supply to the site.

The SO petrogenetic type shows different management and catchment strategies in comparison with the previous types. This is especially clear by the quantity in number, 9%, and weight, 6% of this type in El Arteu. As in the previous type, the three technological orders, as well as core preparation/rejuvenation products and a core on flake, are represented in the site. It is clear knapping and resharpening activities were carried in the site, although they were reduced to some action, as the quantity of blanks and chunks with less weight than five grams unveils. Except for this small quantity of small flakes and chunks, weight distribution of SO lithics follow similar pattern to previous orthoquartzite. The presence of negative scars in dorsal surfaces is more frequent than in the previous type, with the greatest rate of at least three negative scars. Presence of cortex is rare and it generally covers less than 33% of the pieces. The proportion of retouched artefacts is the highest of all petrogenetic types, even though only knapping products were retouched (also the only retouched core preparation/product). There is an important presence of artefacts with two or three primary types. This evidence indicates this material was very intensively exploited. Nevertheless, the grams per piece ratio of this petrogenetic type is greater than previous type ratio.

The characterisation of this raw material reveals there are two different grain size varieties of the SO type: the medium-coarse grain size with heterogeneous distribution (present in small percentages) and the fine and homogeneous one (the majority). The presence of the first is limited to a few pieces, while many lithics of the latter variety were input into the site. At same time, two different

varieties can be distinguished based on colour and non-quartz minerals: a dark one and a grey one. Both are identified in similar frequency. The original outcrop strata of these varieties is not located in the research area, but they can be found in conglomerate strata and deposits. The conglomerates with the SO petrogenetic type are the Lechada, Maraña-Brañas, Pontón, Potes, Remoña, and Valdeón conglomerates. In all of them the presence of the fine grained variety range between 5 and 50%, except for the Lechada and Potes conglomerates, where they represent less than 5% of the pebbles. Despite only four cortical surfaces were identified, one derived from conglomerates and another three from fluvial deposits. Therefore, catchment activities were carried out in both environment. The presence of SO orthoquartzites in beach deposits is negligible, especially near fluvial deposits. We propose the input this type to the site is mixed: on one hand, there is complex and planned catchment strategies in medium to distant conglomerates circuits; on the other, there are occasional findings in river deposits in relation with other activities, such as journey along rivers or acquisition of other resources or raw materials. The latter strategy requires strong selection and identification mechanism of raw material. The input of this type to the site could have been made as cores, blanks or retouched artefacts. Nevertheless, the high frequency of retouched artefacts and the small quantity of small blanks and chunks reinforce the latter option.

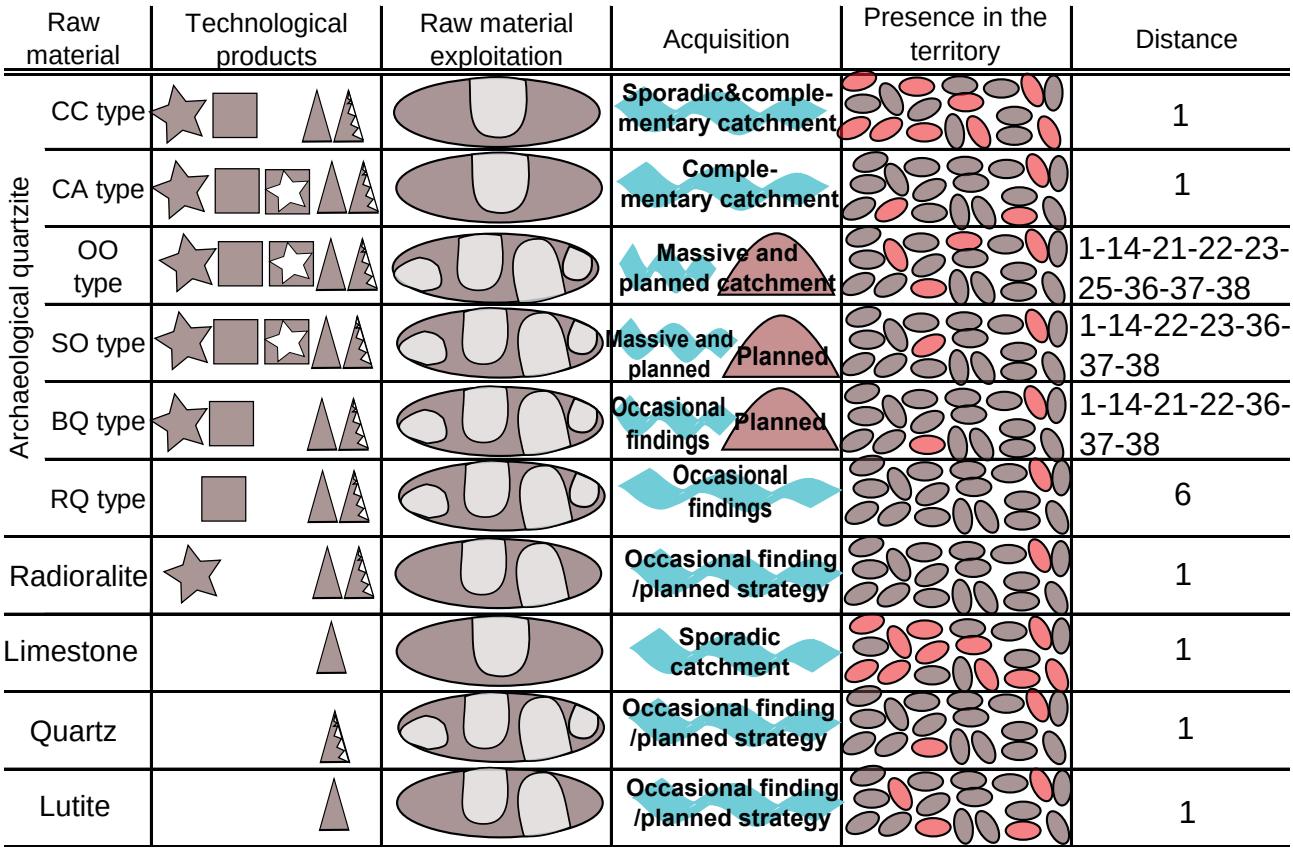

Figure-11.32: Schematic representation simplifying raw material acquisition and management evidences from El Arteu. In the column “Technological products” stars represent cores, squares chunks, squares with starts core preparation/rejuvenation products, and triangles blanks. Zig-zag lines added to any of these icons represent retouched artefacts. In the column “Raw material exploitation”, circles represent unexploited raw material, ovals with one scar represent low intensity raw material exploitation, ovals with two scars represent medium intensity raw material exploitation, and ovals with four scars represent high-intensity raw material exploitation. In the column “Acquisition” waving blue lines represent river acquisition and brown semicircles represent conglomerate acquisition. In column “Presence in territory”, the complete set of ovals represents all the raw materials available in the territory. The ones highlighted in red represent the proportional presence of each specific raw material in the territory. Higher presence of the latter means weaker selection degree.

The management and catchment strategies observed in the previous type are different in the **BQ quartzite type** especially because this quartzite type is better represented in quantity (17%) and weight (10%). All the technological products are identified, although core preparation/rejuvenation products and non-core on flake were not identified. Nevertheless, knapping and reshaping activities were performed in the site as pointed by the presence of chunks and blanks between four grams and 40 g. The gram per piece ratio is similar to the ratio of other orthoquartzites and quartzite. The only presence of core on flake, the quantity of percussion platform and flacking surface, the quantity of negative scars in dorsal surfaces, and the small extension of cortical areas in dorsal surfaces, point at this resource was intensively exploited. This hypothesis is also supported by the overrepresentation of retouched artefacts, which make this type as the second most retouched one. In addition there is an important quantity of artefacts with multiple primary types and points. All in all, the data gathered demonstrate this quartzite was an intensively exploited material and all phases of lithic reduction were performed in the site. Blanks and retouched material could have been brought as final products. They could have been used and afterwards abandoned in the site as indicated by the absence of non-core on flake. Nevertheless, we do not discard that BQ quartzite cores were carried outside the site, following their reduction as a valuable stock product in different locations. Latter hypothesis is reinforced by the high frequency of low weighted chunks and blanks, probably derived from knapping processes.

The input of different varieties of BQ type coexists in the site, based on quartz grain size and colour/mineral characterisation. There are two different grain size varieties, even more frequent is the fine grained one. Coarser or more heterogeneous variety is less frequent in the site. Colour does also distinguish two varieties: the most frequent one is dark-grey, and the less frequent is the white-grey one. The major dark and fine varieties are significantly more abundant than minor white-grey or dark and coarse varieties. We did not find the original outcrop strata for this type of quartzite in the field survey. However, it was clearly identified in some small conglomerates. The presence in fluvial deposits is negligible. There are important quantities (between 5 and 50%) of BQ quartzite in the Remoña, Valdeón, and Pontón conglomerates. In other conglomerates, such as Maraña-Brañas, Pesaguero, and Potes conglomerates, it is scarcer. Coarser grain varieties of the BQ quartzite are restricted to the Pontón conglomerate. Cortical surfaces identified in the assemblage reveals similar presence of cortex derived from fluvial deposits and from conglomerates. Therefore, it can be deduced that catchment is mixed. On conglomerates, the catchment was done by exhaustive and planned strategies in, at least medium mobility circuits, and applying medium intensity selective mechanism. The distant to the conglomerates probably determines the quantity of this material. The catchment on river deposits would be based in occasional findings in river deposits in relation with other activities, such as journeys along the river or acquisition of other resources, as the previous analysed OO type. This strategy would require strong selective mechanisms and accurate identification of raw materials.

The RQ quartzite type presents different patterns of catchment and management. The quantity of this type of raw material found in this context is reduced to 3% of “archaeological quartzites”. Therefore, conclusion must be nuance. There are no cores, neither core preparation/rejuvenation products because there are only five blanks and two chunks. The presence of blanks (also chunks) ranging from less than one gram to more than ten grams indicates knapping and specially retouching activities were performed in the site. The number of negative scars on dorsal surfaces is varied, as the cortex invasiveness representation. Nevertheless, weight distribution is the smallest of all petrogenetic types of “archaeological quartzite”. Retouched material is clearly overrepresented, with similar percentages of quartzite type tackled above. All these data points at a complex management of this material, related with the scarcity of the RQ type in the area. We propose the input of this type was occasional and it was brought in few rocks as cores, blanks or retouched artefacts that could be used or reshaped for specific activities. Nevertheless, previous arguments point at the input into the site as blanks or retouched artefacts as the more reliable formats.

The petrologic characterisation of this raw material does also agree with the previous hypothesis. The analysis of grain size reveals great homogeneity with only two clear varieties: the coarse one and the fine one. No clear colour or non-quartz mineral differences are observed. Therefore, at least two different blocks of rock were brought to the site. We were unable to find any evidence of this petrogenetic type in the massive outcrops of the surveyed area. Its presence is reduced to two conglomerate formations: the Pontón and the Valdeón conglomerates, both in the South-west of the research area. Still, the presence of this type is scarce in both conglomerate formations. Taking into account the two cortical areas in the assemblage made on RQ quartzite, both derive from fluvial deposits. We did not find any evidence of this petrogenetic type in fluvial deposits during our surveys.

However, its presence cannot be completely discarded, at least in the Cares river, which creates the erosive basin where conglomerates surface. These data indicate that catchment of this type necessarily implied medium or long distance movement even outside the Deva Basin, only suggested with the previous types. In addition, the evidence above supports the existence of strong selective mechanisms. The presence of this type in the site does also reveal a conscious mechanism of selective and conservative exploitation of raw material. The intense exploitation of this material and its appreciation as singular, valuable, and exiguous is clear.

Next we will explain the raw material catchment and management strategies of other raw material. These material are not frequent in El Arteu assemblage, although they reveal different roles of raw material and interesting catchment and management behaviour.

Now, we describe **the radioralite**, the second most frequent raw material in the assemblage. All main technological products, except core preparation/rejuvenation products and core on flakes, are represented in this site. Regarding its exploitation, all blanks have at least two negative scars, indicating this material was intensively exploited. Retouched artefacts are overrepresented and there are some artefacts with two primary types. Nevertheless, cortex on blanks is more extended than in other raw material. Weight distribution reveals all radioralites weight is, at least, of 19 g. The nonappearance of smaller blanks could be the consequence of the absence of knapping, retouching or resharpening processes in the site (it could be also due to recovery condition of this assemblage or as a consequence of water flooding processes which erode the lighter lithic implements). Finally, retouched artefacts with Simple mode are heavier than on other raw material. All these reasons point at medium exploitation of this raw material, related with specific activities. The most reliable input of radioralite into the site was made as blanks or retouched blanks rather than core.

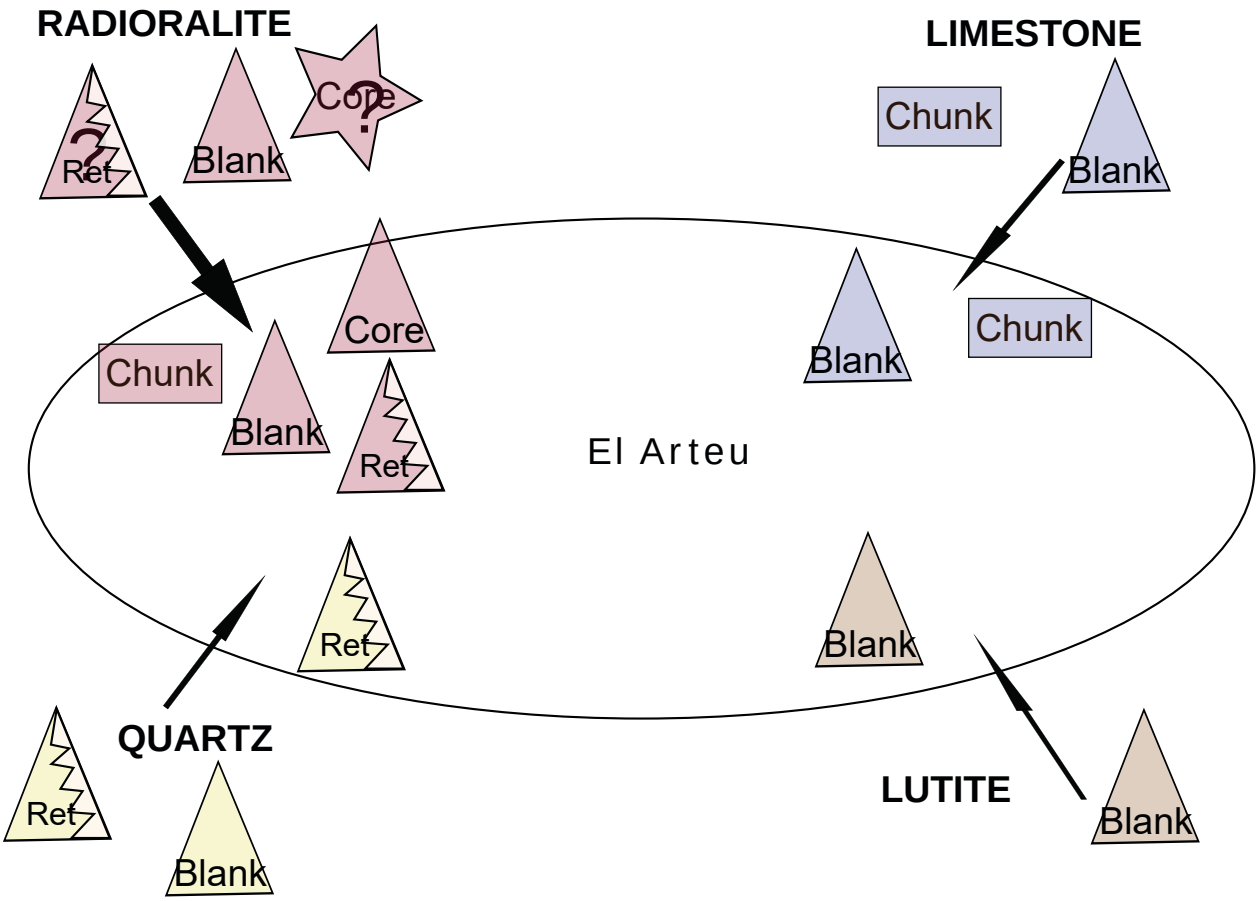

Figure-11.33: Schematic representation of the input of other raw material than “archaeological quartzite”, taking into account the different technological products present. Stars represent cores, triangles blanks, triangles with zig-zag retouched material, ellipses fully cortical chunks and rectangles chunks. Question marks indicate products whose presence is not certain.

Regarding the physical features of radioralites, most of them are red, red to brown, or grey. They are characterised by the presence of Radiolaria fossils. We only find evidence of radioralite in the

area surrounded in fluvial deposits of Cares and Deva rivers, in negligible proportions. Other researchers have also find them in this type of context in both rivers (Álvarez et al., 2013; Manzano et al., 2005). The characterisation of all six cortex determines that this material came from fluvial deposits. Therefore, catchment activities would have necessarily implied strong and intensive selective mechanisms. Due to the quantity of radioralite in the site and its features, we consider acquisition of radioralite was carried out in intensive and planned raw material strategies in river beaches.

Limestone is only represented by three lithics. Therefore, conclusion must be nuance. There are only two technological categories: chunk and knapping product. All three items have cortical presence in variable extension. The quantity of negative scars in the blanks is small and none of them is retouched. Evidence of knapping activities on the lithics are scarce. Weight distribution of blanks is around ten grams, while the chunk is heavier. All these reason carried us to propose this material was residually exploited. In addition, the absence of lithics smaller than nine grams suggest that knapping activities were not performance in the site (it could be also due to recovery condition of this assemblage or as a consequence of water flooding processes which erode the small lithic implements). The colour of all three limestones is grey and blue. The cortical zones were not described, then, we could not propose the environment where catchment was carried out. This raw material is overrepresented in surrounded area of the site, then, this material could be caught everywhere, and catchment do not require complex strategies. All these elements carried us to propose that catchment of limestone is related with sporadic and non-specific activities, maybe in scarcity of more suitable raw material in non-specialised activities.

Quartz is only represented by one piece. It is a retouched blank with a Sidescraper, the most represented retouch. It has at least three dorsal scars, indicating a high intensity exploitation. The weight of this blanks is similar to retouched artefacts of other raw material. Lithologically, this quartz is a quartz-aggregate and coloured as translucent to white. We could not identify cortical surfaces and due to the scarcity of diagnostic elements to characterise the source, we can only suggest it was caught in fluvial deposits. In the research area we have only identified quartz on fluvial deposits in negligible proportion, mainly in the headwaters of the Deva and Cares rivers. Therefore, the catchment of this material would have require strong selective mechanism. Still, the acquisition of quartz would have been more related with occasional findings rather than with intensive and planned raw material catchment strategies. The intensive exploitation of the material reveals its importance for prehistoric societies. Due to the absence of more evidence of quartz, we consider it was input in the site as it was recovered: as a retouched artefact. Nevertheless, we do not reject other hypothesis biases by the nature of this lithic collection.

The last raw material here analyse is the **lutite**, which it is only represented by one piece. It is a blank with two negative scars in its dorsal surface. It has cortex, derived from a fluvial deposit. The exploitation of this lutite seems to be reduced. The lutite is fine grained and brown coloured, showing similarities with those characterised in the surveyed deposits of Deva basin, especially near El Arteu. The abundance of this material in river deposits, generally with presence greater than 10%, makes an easy catchment and intensive selection mechanism are not require. The input of this lutite is related with non-selective catchment on river deposits and it is probably introduced as blank, due to the absence of other technological products. The catchment of this raw material is limited, and maybe as a consequence of the scarcity of other raw materials.

All in all, we observe different catchment and management strategies for each raw material. This allows us to propose the following human mobility, landscape use, selection and exploitation mechanisms. These are:

- Low, medium and high-scale mobilities to the South and South-west of the research area, as well as outside it.
- Exploitation of diverse landscapes, from river courses in low altitudes areas to plateaus in medium altitudes zones.
- Selective, and non-selective mechanisms for obtaining specific raw materials or petrogenetic types in deposits and conglomerates.
- Diversity of raw material exploited, selected based on their physical properties and their availability in the landscape.
- Versatility in technical and catchment procedures to take advantage of surrounded area around the site.

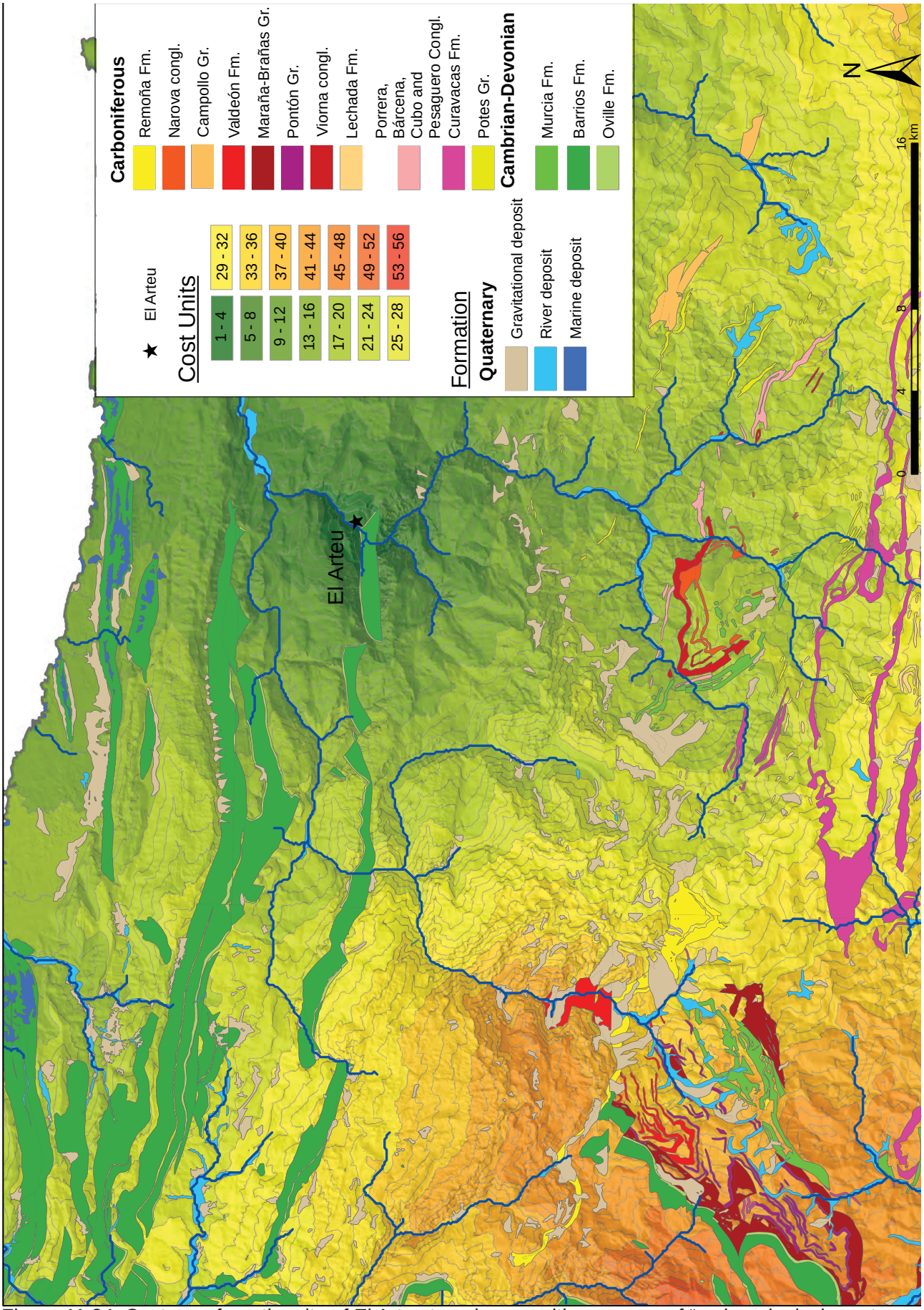

Figure-11.34: Cost map from the site of El Arteu to polygons with presence of “archaeological quartzites” and others raw materials.

CHAPTER-12

RESULTS. THE LAYER CO.B.6 FROM THE ARCHAEOLOGICAL SITE OF LA CUEVA DE COIMBRE

12.1. GENERAL ISSUES AND STATE OF PRESERVATION OF THE COLLECTION

Here we present the results obtained in the archaeological site of La Cueva de Coimbre. The Coimbre Cave is a big cave longer than 3.100 meters, with a complete slope of 73 meters. The entrance to the cave is eight meters wide and six to two meters high and opens to the main hall of the cave. Despite the cave has been studied under archaeological perspectives since the 1970 decade (focusses on Rock-Art engravings), the sediment of the cave was not excavated until the 2000 and 2010 decades. In successive excavation campaign, five archaeological layer was found. The first part of these layer (Co.B.1, Co.B.2, Co.B.4 and Co.B.5) correspond with a long Magdalenian sequence between 20070 cal. BP and 14071 cal. BP. The layer Co.B.6 is dated between 29660 and 28560 Cal. BP and it is chrono-culturally assigned to the Gravettian. We only present the results of the Co.B.6 layer. Previous research have already characterised this layer from multiples perspectives (Álvarez-Alonso et al., 2011; Álvarez-Alonso et al., 2013a; Álvarez-Alonso et al., 2009; Álvarez-Alonso et al., 2014; Álvarez-Alonso et al., 2013b). Paleoenvironmental analyses point that climatic condition was related with open areas of vegetation and cold condition. Faunal analysis point that most represented taxa are *Bos*/*Bison*, *Equus ferus*, and *Capra pyrenaica* highly fragmented and burned (Yravedra et al., 2016). This layer is not related with the rock art evidences, but three small shell pendant was found on it (Álvarez-Alonso et al., 2017). Previous analysis of lithic remains point that most represented raw material is quartzite, even though flint or radioralite are also represented. Technological characterisation of the assemblage point at a small representation of cortical surfaces, high frequency of flakes instead blades and a low standardisation of cores inserted in fragmented *chaîne opératoire*. The representation of retouched artefacts is small (Álvarez-Alonso et al., 2017). All these data suggest this layer represent a short occupation of the cave during this period, probably related with a functionality of the site as a hunting post.

The archaeological assemblage analysed here is the complete collection recovered during the excavation processes, but not still the material recovered by water-screening process, classified as debris, due to time restriction. The complete assemblage for this layer is 3,060 lithic pieces (considering also the debris) and we analysed 932 items. The general state of preservation is good, resulting this lithic assemblage as the better preserved one of all analysed assemblages. The pieces were previously washed in laboratory and most of them have clean surfaces, allowing an easy characterisation of raw material. Weathering processes do not alter most of the lithics, even though some of them have carbonate precipitations or clayey minerals stuck in some lithic surfaces.

12.2. PETROLOGICAL STRUCTURE

Here we present the results of raw material characterisation. We were able to determine the main lithology of every piece. In general, the collection is mainly formed by “archaeological quartzites” with small representation of flint and residual quantities of radioralite, quartz, limestone, and lutite (Table-12.1).

Main Raw Material	Archaeological quartzite	Flint	Limestone	Limonite	Lutite	Quartz	Radioralite	Volcanic rock	Undeterminate
Σ	761	141	1	0	1	13	15	0	0
%	81,7	15,1	0,1	0	0,1	1,4	1,6	0	0

Table-12.1: Frequency table of lithologies identified in layer Co.B.6 from the archaeological site of La Cueva de Coimbre.

Focusing on “archaeological quartzite”, through binocular microscopy we could identify six of the seven petrogenetic types proposed. Orthoquartzites are the most frequent group with more than 70% of the lithic implements, thanks to the high quantity of OO type. Quartzarenite is the second most frequent group of “archaeological quartzite” with 27% of the pieces. Finally, the group of quartzite is underrepresented, with 10% of the lithics (Table-12.2). We were unable to identify nine pieces,

1% of the collection. Coming to the distribution of grain size, the most frequent category is heterogeneous distribution with 50% of the cases, although one mode homogeneous distribution is also well represented with 39% of the items. Regarding grain size, the most frequent category is the medium grain size, followed by fine one. Only few “archaeological quartzites” have coarse grain size. As to “archaeological quartzite” types and size varieties, we identify two preferential varieties: OO type with homogeneous distribution of medium grains and the OO type with heterogeneous distribution of medium grains. Other varieties do not represent more than 5% of the “archaeological quartzite” assemblage. Chi-square test (χ^2 (30, N = 752) = 715.944, p < .001) reinforces the idea of a preferential acquisition of these two varieties.

Grain size characterisation			Petrogenetic type																	
			CC		CA		OO		SO		BQ		RQ		MQ		Unknow		Total	
			Σ	%	Σ	%	Σ	%	Σ	%	Σ	%	Σ	%	Σ	%	Σ	%	Σ	%
	Homogeneous and one mode distribution	Fine grain	2	3	4	8	15	3	23	23	22	29							66	9
		Medium grain	1	1	6	12	**194**	**44**	11	11	19	25					1	11	232	30
		Coarse grain																		
	Heterogeneous and two modes distribution	Fine grain	21	26					31	31	4	5							56	7
		Medium grain	2	3			7	2	7	7					2	100			18	2
		Coarse grain																		
	Heterogeneous distribution	Fine grain	29	36	4	8	1	0	4	4	23	30							61	8
		Medium grain	9	11	10	20	**219**	**49**	22	22	8	11					2	22	270	35
		Coarse grain	16	20	25	51	9	2	2	2									52	7
	Unknown																6	67	6	1
		Total	80	11	49	6	445	58	100	13	76	10			2	0	9	1	761	100

Table-12.2: Frequency table of petrological features identified in layer Co.B.6 from La Cueva de Coimbre based on binocular characterisation. Columns are petrogenetic types and rows contain the characteristics of grains according to size, classified first by distribution and second by size itself. Cells in black are the categories representing more than 10% of the total cases. Cells in light grey are the categories representing between 1 and 5% of cases.

Non-quartz mineral	A		B		C		General	
	Σ	%	Σ	%	Σ	%	Σ	%
Absence	10	1	10	1	25	3	45	2
Fe-Oxide	742	98	5	1	1	0	748	33
Manganese Oxide	4	1	185	24	53	7	242	11
Mica	2	0	485	64	36	5	523	23
Black mineral	2	0	74	10	633	83	709	31
Pyrite	1	0	2	0	11	1	14	1
Feldspar					2	0	2	0
Total	761	100	761	100	761	100	2283	100

Table-12.3: Frequency table of non-quartz minerals identified in layer Co.B.6 from La Cueva de Coimbre based on binocular characterisation. Columns are the three fields examined and rows are the non-quartz minerals identified.

Colour	On fresh cut			
	Primary		Secondary	
	Σ	%	Σ	%
Absence	11	1	98	13
White	127	17	295	39
Grey	609	80	133	17
Black	10	1	108	14
Blue			22	3
Green				
Orange				
Brown	4	1	103	14
Yellow				
Red			2	0
Total	761	100	761	100

Table-12.4: Frequency table of colour hue of the samples from layer Co.B.6 from La Cueva de Coimbre. Columns are primary and secondary colour hues and rows are the colours considered.

We identified non-quartz minerals in 751 "archaeological quartzite", after having excluded the lithics assigned to unknown type (Table-12.3). Non-quartz mineral characterisation reveals the high presence of iron oxides, non-identified black minerals, micas, and manganese oxides. The first two are not associated with any specific type, but micas are associated to OO and MQ types and manganese oxides to all other petrogenetic types. There are other non-quartz minerals defined, pyrite and feldspar. The first are associated to SO and CA types, and the second mineral to CA type. Characterisation of colour indicates that most frequent colours are grey, white, black, and brown (Table-12.4). The first one is not associated to any petrogenetic type. Most of the white coloured "archaeological quartzites" are associated with OO and MQ. Black colour is associated with SO, BQ, and CA petrogenetic types. Finally, brown coloured "archaeological quartzites" are associated with quartzarenites. The presence of other colours, such as blue or red is restricted to small areas or to surfaces of quartzites. Then, they are not so frequent.

We carried out the petrographic and geochemical characterisation of eleven lithics, with the aim of better recognising the types represented (Figure-12.1). The description of these samples helps us understand the differences between types, as well as define and establish some interesting varieties. Due to the small surface of the two RQ quartzites, we could not sample this petrogenetic type. Finally, we analysed this petrogenetic type using non-destructive techniques.

12.2.1. THE CC PETROGENETIC TYPE AT LA CUEVA DE COIMBRE, LAYER CO.B.6

CoB.K26.37.9 and CoB.J26.38.46 are the two samples characterised as CC type of quartzarenite. Both have clastic grained texture with matrix or cement and while the first has tangential packing, the second sample has floating packing. Quartz grains on the latter sample are clastic, but on the former there are some zones with undulatory extinction and some syntaxial overgrowth. Grain size characterisation is different in each sample. CoB.K26.37.9 is more homogeneous and quartz grains are generally smaller than those of COB.J26.38.46 (Figure-12.2). The morphology of grains is also different. The grains of the first sample are more irregular than grains from the second, especially by the comparison of Circularity index. Both samples have preferential orientation of quartz grains at $\sigma = 0.05$, although only CoB.K26.37.9 has preferential orientation at $\sigma = 0.01$. The preferential orientation on both samples is related with sedimentation processes, not from schistosity. The features observed through the binocular microscopy are similar in both cases: coarse grained texture and punctual packing, i.e. saccharoid T&P. Nevertheless, the quartz grains limits of CoB.K26.37.9 are ruffled, while for CoB.J26.38.46 are plain and rounded. The first boundaries makes more difficult grain recognition. The size characterisation of grains under binoculars points at heterogeneous distribution on both samples, and different size: fine size for CoB.K26.37.9 sample and medium size for CoB.J26.38.46 sample. Then, two different grain size classes are detected. None of them have metamorphic foliation fabric under binocular microscope.

The characterisation of matrix, cement and non-quartz mineral under on thin section points at the presence of clayey matrix in the CoB.K26.37.9 and siliceous matrix in the CoB.J26.38.46. Matrix is more frequent in the second sample than in the first one. Non-quartz minerals are frequent in both samples. Zircon, rutile, pyrite, and iron oxides are detected in both samples. Feldspar and tourmaline are also represented in the CoB.K26.37.9; chlorite and clay are represented in the CoB.J26.38.46. X-Ray fluorescence characterisation reveals the major presence of SiO_2 in both samples, although it is more abundant in CoB.J26.38.46 than in CoB.K26.37.9. Other components are represented in both samples but Al_2O_3, Na_2O, and K_2O have higher proportion in CoB.K26.37.9 than in CoB.J26.38.46. The characterisation of non-quartz minerals under binocular indicates the presence of non-identified heavy and black minerals, oxides and pyrite in both samples. The colour of CoB.J26.38.46 is grey and black and the colour of CoB.K26.37.9 is grown and grey. These two colour varieties are not correlated with its mineralogy.

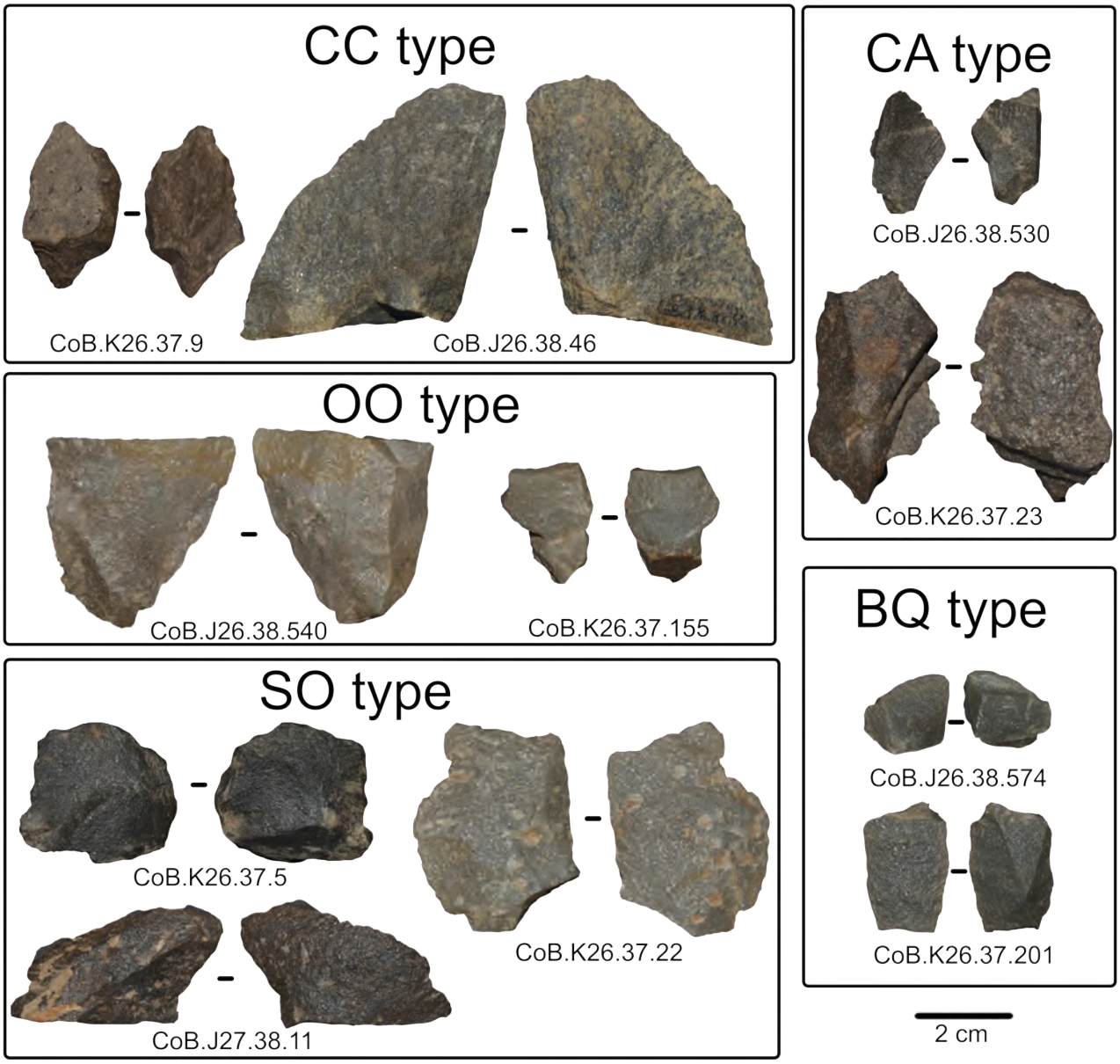

Figure-12.1: Pictures of the samples selected from Layer Co.B.6 of the archaeological site of La Cueva de Coimbre. Samples are grouped by petrogenetic type.

Regarding the characterisation of the complete lithic assemblage of this layer, each sample is a good example of the two most frequent grain size varieties: the CC type with fine quartz grains and CC type with medium/coarse quartz grains. Grains on both varieties are heterogeneously distributed. The colour characterisation does not allow us to stablish different varieties due to the lack of solid mineral criteria. Moreover, brown CC type is more frequent than grey-black CC type. There are also some white CC quartzarenites, represented in small frequency.

12.2.2. THE CA PETROGENETIC TYPE AT LA CUEVA DE COIMBRE, LAYER CO.B.6

Two of the samples selected belong to the CA petrogenetic type. These are the samples CoB.J26.38.530 and CoB.K26.37.23. Both are characterised by clastic grained texture and tangential packing. On both samples, there are facies with clastic quartz grains (majority) and other with undulatory extinction (minority). CoB.K26.37.23 has a residual quantity of grains with overgrowths and CoB.K26.37.23 has a moderate presence of concave-convex quartz grain limits in some facies (Figure-12.3). Regarding quartz grain size, CoB.K26.37.23 have bigger grains than CoB.J26.38.530. Grain size of the first sample is around very fine sand category and they are homogeneously distributed. Grains from CoB.J26.38.530 are bigger and they range in a more heterogeneous distribution around fine sand. Grains from both samples have similar circularity and roundness indexes. None of these two samples have preferential orientation. The features observed through the binocular

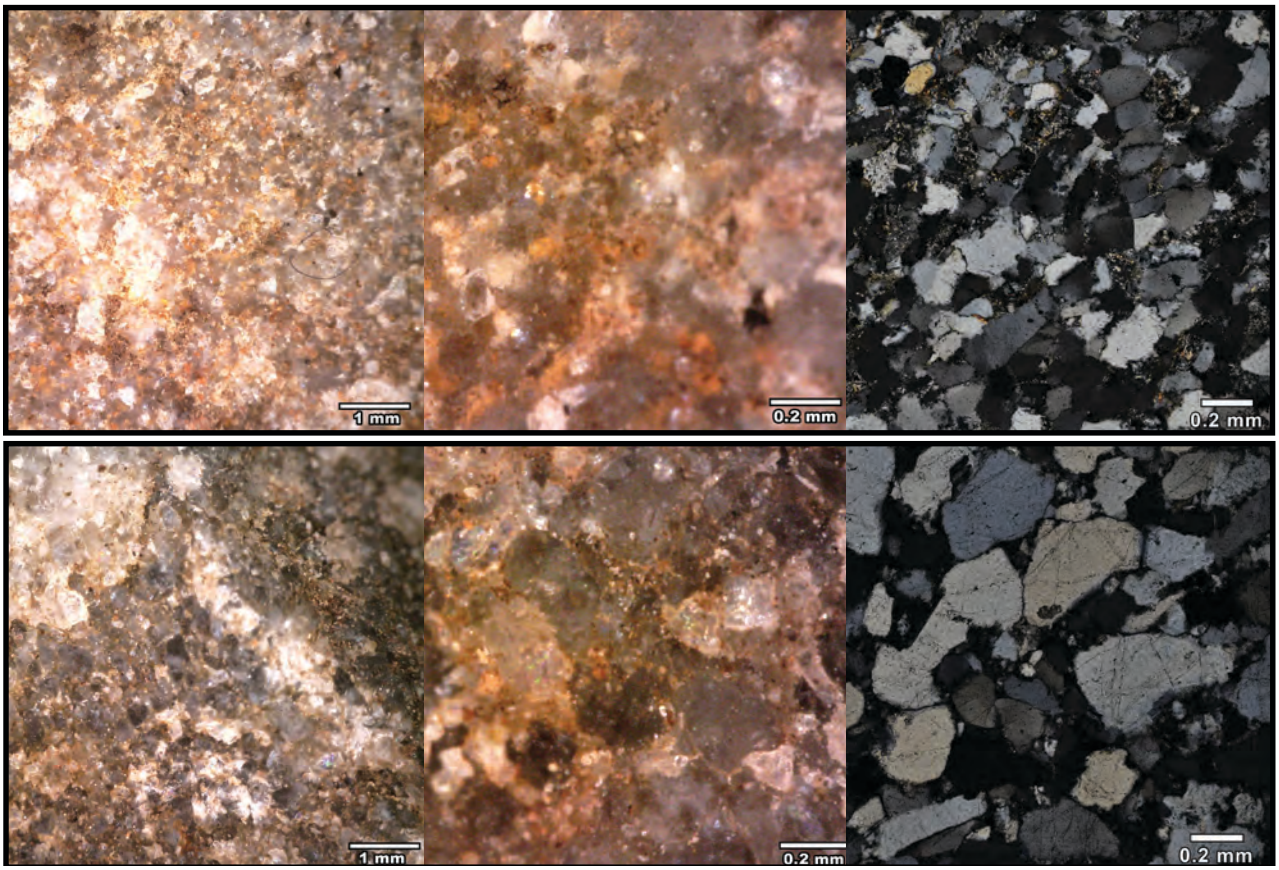

Figure-12.2: Pictures of the CC type samples from Layer Co.B.6 of the archaeological site of La Cueva de Coimbre. From top to bottom, samples CoB.K26.37.9 and CoB.J26.38.46. From left to right, microscopy binocular picture at 20x, microscopy binocular picture at 250x, and thin section microscopy picture at different magnifications.

microscopy are in concordance with characterisation proposed: coarse grained texture and tangent packing, i.e. granular T&P. The size of the quartz grains under binocular microscope in CoB.J26.38.530 points at homogeneous distribution of grains around fine category. Grains from CoB.K26.37.23 are coarser and they have a heterogeneous distribution. Grain morphology of the latter sample have rounded and angular quartz grain limits, while most of the grains from CoB.J26.38.530 are rounded. None of the sample have foliation structures or schistosity.

Petrographic characterisation of these samples points at the small presence of siliceous matrix in the CoB.J26.38.530 sample and clayey matrix in the CoB.K26.37.23 sample. Non-quartz minerals are well represented in both samples, mainly as iron oxides, pyrite, clays, and rutile. Feldspars and tourmaline are also represented in the CoB.J26.38.530, while micas are represented in the CoB.K26.37.23 sample. X-Ray fluorescence reveals the major presence of SiO_2 on both samples around 93% in CoB.K26.37.23 and 87% in CoB.J26.38.530. Other components such as Al_2O_3, Fe_2O_3, P_2O_5 are well represented in both samples. The characterisation of non-quartz minerals under binocular microscope points at the same combination in both samples: non-identified heavy and black mineral, oxides and pyrite, even though colour characterisation of CoB.K26.37.23 is brown and colour of CoB.J26.38.530 is black.

Regarding the characterisation of the complete assemblage of this type, both samples are representative of the two most frequent grain size varieties: the fine one with homogeneous distribution and the medium sized with heterogeneous distribution. The latter is more frequent than the first. Due to the absence of features to relate mineral and colour characterisation, we were unable to stablish specific varieties. Moreover, brown and grey-black CA quartzarenites are similarly distributed. There are also some white coloured CA quartzarenite.

12.2.3. THE OO PETROGENETIC TYPE AT LA CUEVA DE COIMBRE, LAYER CO.B.6

Two of the samples are OO orthoquartzite: CoB.J26.38.540 and CoB.K26.37.155. Both samples have clastic grained texture and complete packing. They are characterised by the presence of

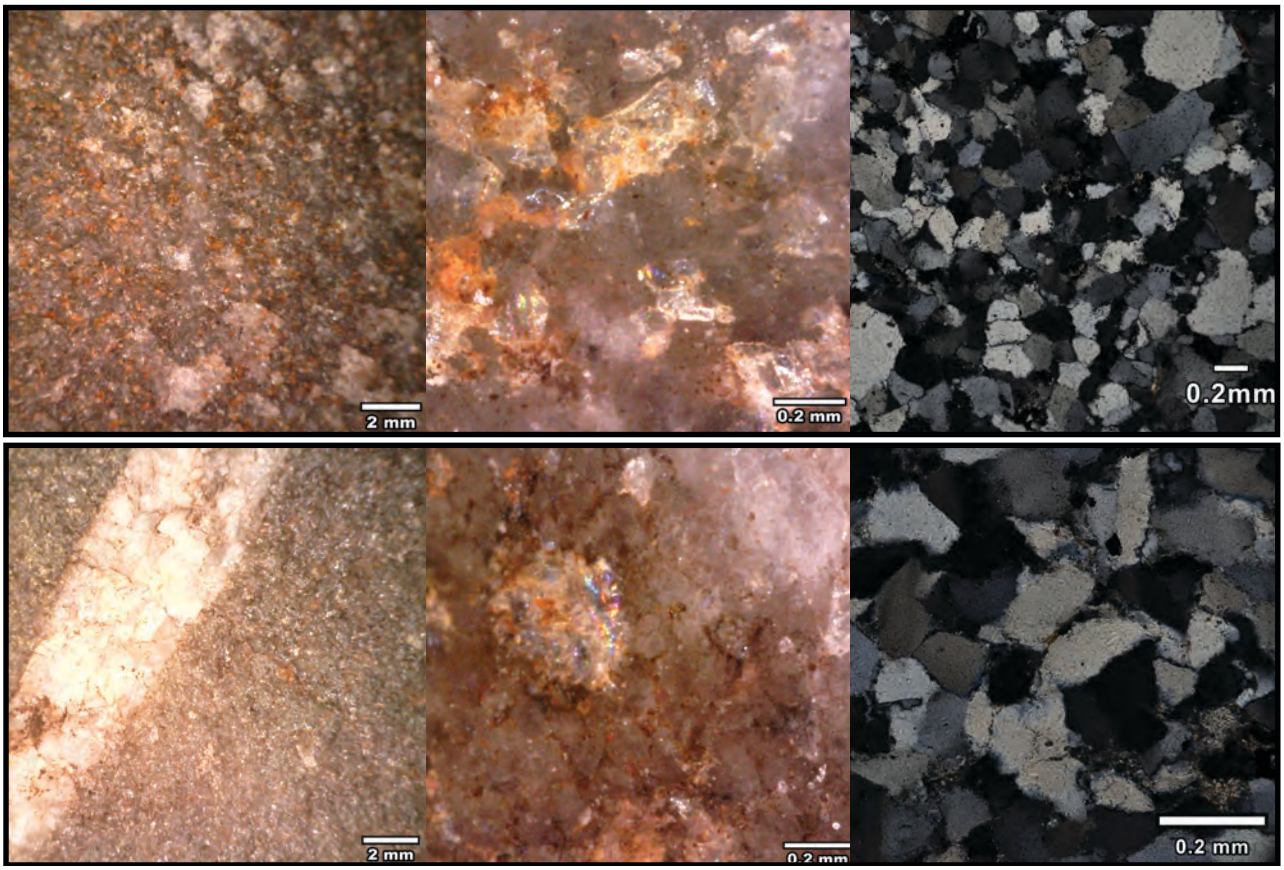

Figure-12.3: Pictures of the CA type samples from Layer Co.B.6 of the archaeological site of La Cueva de Coimbre. From top to bottom, samples CoB.K26.37.23 and CoB.J26.38.530. From left to right, microscopy binocular picture at 20x, microscopy binocular picture at 250x, and thin section microscopy picture at different magnifications.

syntaxial overgrowth around quartz grains and concavo-convex boundaries between grains that in few cases generates suturated quartz grain limits. Undulatory extinction is clear on both samples. Grain size characterisation points at the major presence of very fine and fine sand U-W categories on a relatively single mode in both samples. Quartz grains are relatively rounded, with indexes around 0.60, while the regularity of quartz grains is smaller, due to the small increase of deformation processes. The directional analysis shows that the grains of CoB.J26.38.540 are preferentially oriented at $\alpha = 0.05$ and $\alpha = 0.01$ while on CoB.K26.37.155 are not oriented. The feature observed through binocular microscopy are in concordance with these characterisation, compact and grainy T&P, concave-convex quartz limits, and some regrowth structures. The grain size characterisation of both samples points at medium sizes in one mode distribution. There is no preferential orientation of grains under binocular microscope (Figure-12.4).

The characterisation of matrix, cement and non-quartz minerals reinforces the similitudes between both analysed samples. The colour characterisation is also similar. None of the two samples have matrix or cement and both samples have zircon, mica, chlorite, and iron oxides. CoB.J26.38.540 also has clay minerals. X-Ray fluorescence shows clear differences between both samples, especially in the quantity of SiO_2. This component is more frequent in the CoB.J26.38.540 (>98%) than in CoB.K26.37.155 (90%). In the latter, the presence of other components, especially Al_2O_3 and Na_2O, is higher. Binocular characterisation of non-quartz minerals in both samples is the same, with mica, iron oxides and non-identified black and heavy mineral. Colour is also similar and both samples are light grey or white, with orange areas around iron oxides.

After having analysed the features of the OO petrogenetic type, we can extrapolate these results to those of non-destructive techniques. The samples destructed confirm and allow understanding the high presence of OO orthoquartzite with medium grain sizes, probably as a consequence of syntaxial quartz regrowth. The homogeneous grain size distribution organised around one mode is represented in both samples. Nevertheless, taking into account the complete assemblage, most frequent variety follows a heterogeneous distribution around medium grain size. Therefore, two main grain size varieties are represented. Colour and mineral characterisation reveals white and light grey

varieties together with non-identified black minerals, micas, and iron oxides are the most frequent variety. Moreover, there are also few black or dark-grey OO lithics together with non-identified black minerals, iron and manganese oxides. Therefore, there are also two different colour varieties.

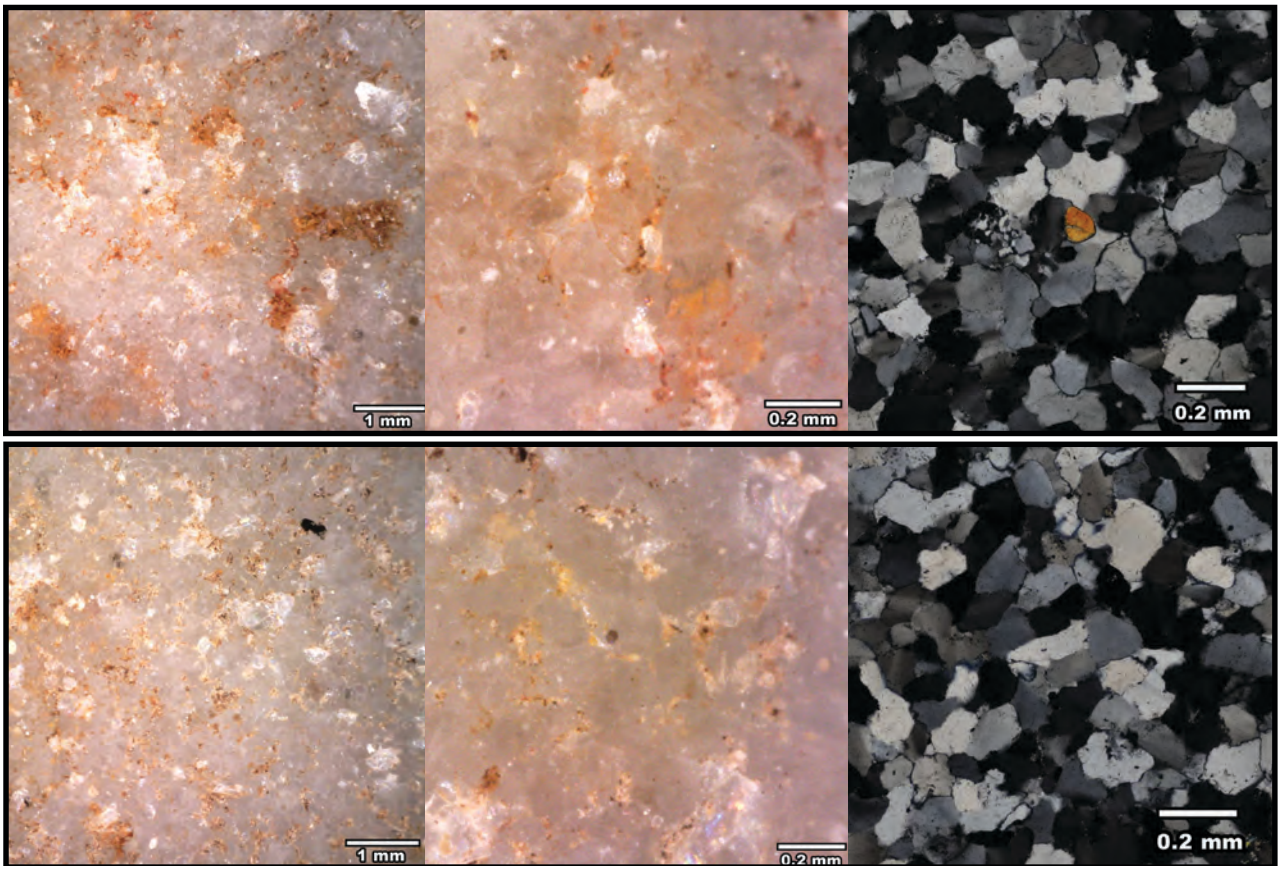

Figure-12.4: Pictures of the OO type samples from Layer Co.B.6 of the archaeological site of La Cueva de Coimbre. From top to bottom, samples CoB.K26.37.155 and CoB.J26.38.540. From left to right, microscopy binocular picture at 50x, microscopy binocular picture at 250x, and thin section microscopy picture at different magnifications.

12.2.4. THE SO PETROGENETIC TYPE AT LA CUEVA DE COIMBRE, LAYER CO.B.6

Three of the samples analysed belong to the SO petrogenetic type: CoB.K26.37.5, CoB.J27.38.11, and CoB.K26.37.22. All three show clastic grained texture, suturated packing, great presence of undulatory quartz extinction, and suturated/microstylolitic quartz grain limits. Syntaxially overgrowths are also represented in the CoB.K26.37.5 and the CoB.K26.37.22 samples, as recrystallised quartz grains in smaller appearance than 5%. Grain size characterisation shows two different varieties, the first is represented by the CoB.K26.37.5 and CoB.J27.38.11 and it is characterised by one homogeneous mode between coarse silt and very fine sand categories. The second variety is around fine sand and very fine sand in a more heterogeneous distribution (Figure-12.5). The morphology of quartz grains look alike in all three samples. All three samples have preferential orientation of quartz grains at $\sigma = 0.05$ but at $\sigma = 0.01$ quartz grains from the sample CoB.J27.38.11 are not preferentially oriented.

Regarding non-destructive characterisation of the samples, the majority shows moderate to high bright, micro-cracks on surface, suturated packing, difficult grain distinction, and ruffled quartz grain limits, i.e. grainy and fine T&P with ruffled and irregular grains limits. Nevertheless, fine T&P, associated with concave-convex quartz grain limits is observed in sample CoB.K26.37.22 probably due to the differential effects of deformation processes in bigger quartz grains (Figure-12.5). Foliation is not appreciable in the samples. Differences in grain size and its association with recognisable features, allow us to propose two main varieties: a) a homogeneous fine grained variety with clear fine and grained T&P and b) a heterogeneous medium-coarse grained variety, represented by the sample CoB.K26.37.22.

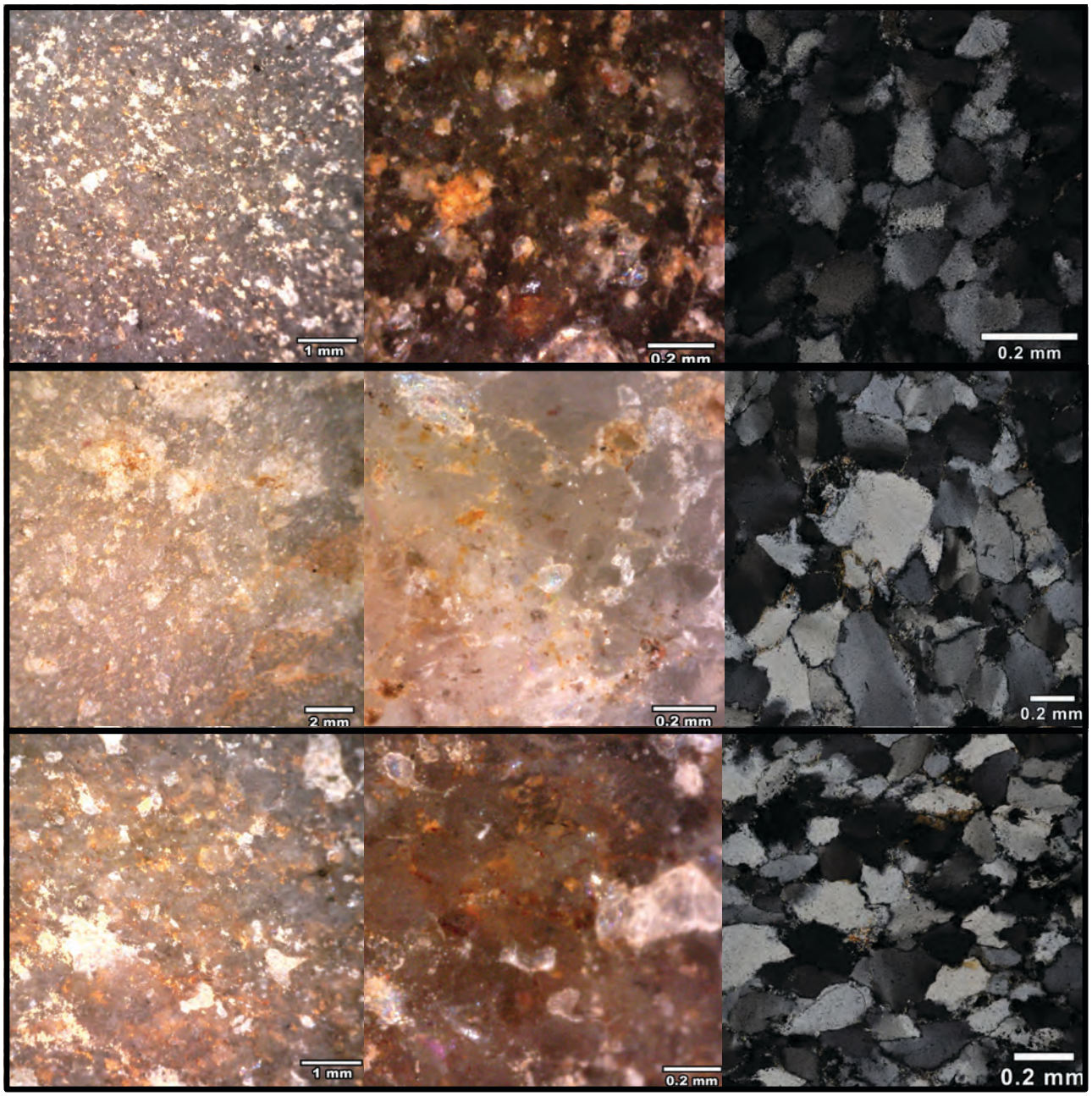

Figure-12.5: Pictures of the SO type samples from Layer Co.B.6 of the archaeological site of La Cueva de Coimbre. From top to bottom, samples CoB.K26.37.5, CoB.K26.37.22, and CoB.J27.38.11. From left to right, microscopy binocular picture at 50x, microscopy binocular picture at 250x, and thin section microscopy picture at different magnifications.

Coming to non-quartz mineral characterisation, clayey matrix appears in negligible percentages in every sample. None of the samples exhibits cement. Nevertheless, non-quartz mineral detection reveals differences that create changes of colour. Pyrite and manganese oxides, observed under non-destructive techniques determine the black colour of the samples CoB.K26.37.5 and CoB.J27.38.11. Mineral characterisation using petrography is consistent with these mineral associations, as indicated by the detection of pyrite, iron oxides, and rutile (also tourmaline and chlorite for the CoB.K26.37.5 and mica the clays for the CoB.J27.38.11). On the sample CoB.K26.37.22 there are less minerals detected under microscope, reduced to clays and iron oxides. Under binocular microscope this sample has mica, non-identified black and heavy minerals, and iron oxides. The latter two are not extended in all lithic surface. The results of X-Ray fluorescence are in concordance with these differences. SiO_2 is well represented in all three samples but it is slightly higher in CoB.K26.37.22 than in CoB.K26.37.5 and CoB.J27.38.11. Al_2O_3, Fe_2O_3, Na_2O, and K_2O are also present in all three samples. Therefore, there are two mineral/colour varieties: black or dark-grey and grey or light-grey one.

The data obtained through destructive characterisation allow us to extrapolate these results to the complete lithic collection, only analysed by non-destructive techniques. Most of the SO type from this layer are related with the fine or fine to medium grained variety, generally associated with dark or dark-grey colour (≈60%). The coarse or medium to coarse SO variety, mainly associated to white colour is reduced to smaller percentages (≈40%).

12.2.5. THE BQ PETROGENETIC TYPE AT LA CUEVA DE COIMBRE, LAYER CO.B.6

Two of the samples selected belong to the BQ petrogenetic type: CoB.J26.38.574 and CoB.K26.37.201. Under thin section, they are characterised by mortar texture and suturated packing. There is a major presence of microstylolitic limits of quartz grains and recrystallised quartz grains, also a small quantity of syntaxial overgrowth of quartz grains. The analysis of size and morphology of quartz grains on both samples reveals two different modes. The first one is composed by the main grain framework with quartz grain sizes between coarse silt and fine sand. The second mode is mainly created by the new recrystallised quartz grains with grain sizes between very fine silt and medium silt categories. The first mode is more deformed than the second, as pointed by the roundness and circularity indexes. The main framework is bigger in the CoB.J26.38.574 than in the CoB.K26.37.201. Preferential orientation of quartz grains at σ = 0.05 and σ = 0.01 is recognised in both

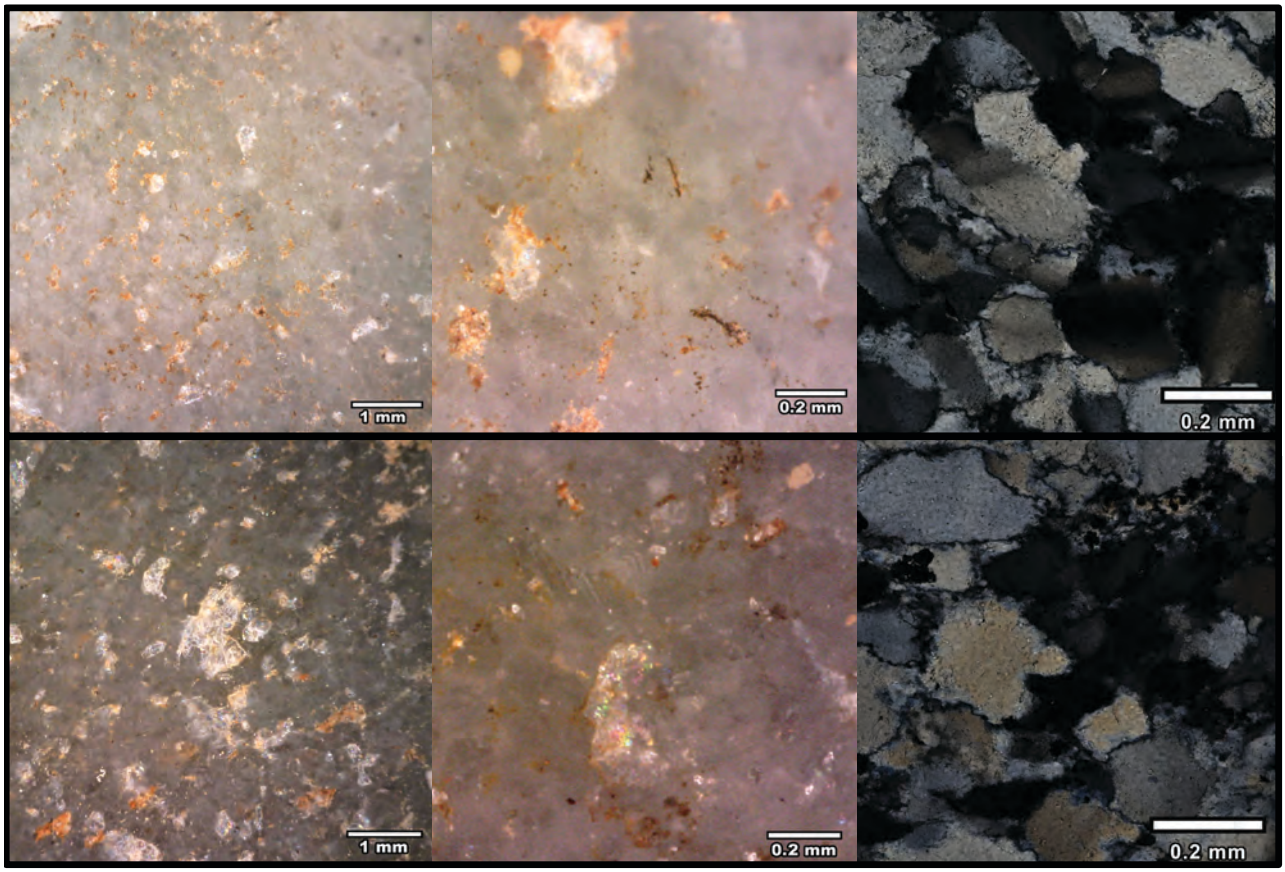

Figure-12.6: Pictures of the BQ type samples from Layer Co.B.6 of the archaeological site of La Cueva de Coimbre. From top to bottom, samples CoB.J26.38.574 and CoB.K26.37.201. From left to right, microscopy binocular picture at 50x, microscopy binocular picture at 250x, and thin section microscopy picture at 50x magnification.

samples as a consequence of schistosity. Non-destructive characterisation is in accordance with the features characterised: fine texture and suturated packing (i.e. Fine T&P). It is not easy to distinguish quartz grains boundaries, but it is possible to observe small speck of quartz grains that generates ruffled quartz limits. The luster is relatively high and micro cracks are abundant. In cases where grains are recognisable, they are fine with heterogeneous distribution in the CoB.K26.37.201 sample and medium with homogeneous distribution in the CoB.J26.38.574 sample (Figure-12.6). Nevertheless, we do not observe foliation in the samples using non-destructive characterisation.

Coming to mineral characterisation, both samples have matrix in reduced proportion than 5%. The matrix is clayey in the CoB.K26.37.201 sample and siliceous in the CoB.J26.38.574 sample.

Mineral identification reveals clear differences between both samples. The CoB.K26.37.201 has pyrite, feldspar, clay, rutile, zircon, tourmaline, and iron oxide. Meanwhile, in the CoB.J26.38.574 sample, only the latter mineral is represented, together with micas and chlorite. The higher presence of minerals identified and specially iron oxide, rutile and pyrite makes the black colour to the first, while the absence of these minerals prevent colour change in the sample CoB.J26.38.574, maintaining the grey colour of the rock. Non-destructive characterisation of the samples relates colour and mineral characterisation through the presence of manganese oxides in the CoB.J26.38.574 instead micas, represented in the CoB.K26.37.201. The other non-quartz minerals identified in both samples are iron oxides and pyrite. The results of X-Ray do not support the differences between both samples. The presence of SiO_2 in both samples is high, but it is smaller in the sample COB.J26.38.574 (86 %) than in the CoB.K26.37.201 sample (93.03%). Al_2O_3 and Na_2O are better represented in the latter.

After having analysed the features and variability of the BQ quartzites, we can extrapolate these results to those of non-destructive techniques. We observe that finer grain size variety (≈64%) is more frequent than medium grained one (≈36%). Black quartzites are associated with the fine size variety and grey one with the medium size variety. Therefore, similar proportion of colour/minerals varieties is also observed.

12.2.6. NON-DESTRUCTIVE CHARACTERISATION OF MQ PETROGENETIC TYPE AT LA CUEVA DE COIMBRE, LAYER CO.B.6

The MQ petrogenetic type is the less frequent petrogenetic type analysed in this layer. Under binocular microscopy, the two identified quartzites have soapy texture and no detection of quartz grains. The bright is high and foliation is not represented. Both quartzites are extremely crystalline. Grain size characterisation of both quartzites is the same: medium grain sizes in two modes distribution. Oxides, micas and non-identified heavy and black minerals were identified in both samples and the colour is classified as white (Figure-12.7).

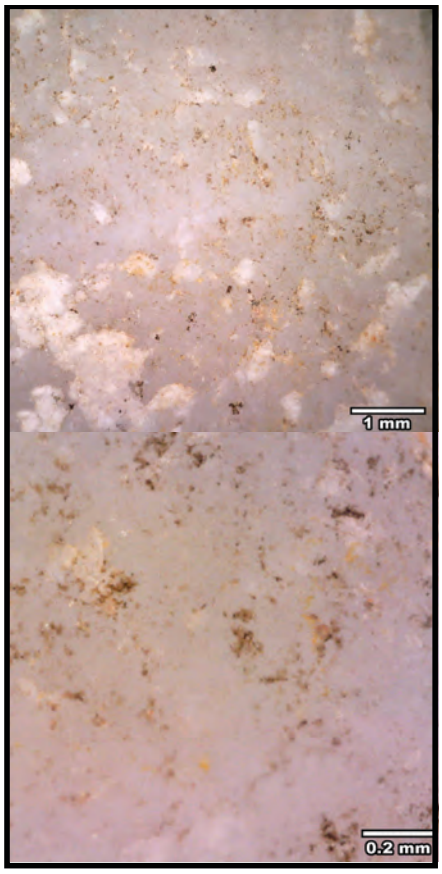

Figure-12.7: Pictures of the MQ type from layer 6 of the archaeological site of La Cueva de Coimbre. CoB.K26.37.198. Upper row shows microscopy binocular pictures at 50x. Lower row shows microscopy pictures at 250x.

12.2.7. CHARACTERISATION OF CORTICAL AREAS AT LA CUEVA DE COIMBRE, LAYER CO.B.6

Here we present the result of the characterisation of cortical areas. The distribution of cortex in the lithics analysed between different types of raw material is shown in Table-12.5. Cortex is represented in 14% of the pieces, and almost all of them have features related with fluvial deposits. “Archaeological quartzite” and radioralites have alike relative percentage of cortical areas, with similar percentage than the whole collection. The only lithic made on limestone has cortical surface. In contrast, quartz and the only lutite in the site have no cortical areas. Finally, although some flint pieces have cortex, the rate of cortical presence is under the average of the complete assemblage.

Regarding the types of cortex, 29% of the collection could not be characterised due to the absence of diagnostic features. None of the cortex type identified could be interpreted as evidence of direct extraction from the outcrop. Conglomerate cortex is poorly represented, and the only raw material with cortex from this place is the “archaeological quartzite” with six items. Conglomerate cortical areas are characterised by the presence of cements from the conglomerate itself, which are generally recognisable as red iron oxides or dark silica fluids. In addition, voids are usually present, even though they are generally filled with conglomerate cement. No clear impact cracks are observable on cortical areas.

Cortical area from fluvial sources is the most frequent cortex type. Fluvial cortex is mainly characterised by the presence of impact cracks in the surface and fine or soapy textures. Voids are less frequent in this cortex type and cement is absent. Every type of raw material input into the site with cortical have fluvial cortex.

Raw material	Cortex type												∑ of each type
	Conglomerate			Fluvial			Unknown			Total			
	∑	%	% rel	∑	%	% rel	∑	%	% rel	∑	%	% rel	
Archaeological quartzite	6	100	1	84	92	11	22	76	3	112	89	15	761
Flint				4	4	3	7	24	5	11	9	8	141
Limestone				1	1	100				1	1	100	1
Lutite													1
Quartz													13
Radioralite				2	2	13				2	2	13	15
Total	6	5	1	91	72	10	29	23	3	126	100	14	932

Table-12.5: Frequency table of types of cortex identified in layer Co.B.6 from La Cueva de Coimbre grouped by main raw material. Columns are the types of cortex, including the frequency of each cortex type for each raw material and the total of items with cortex of each raw material. The last column quantifies the total of items with and without cortex of each raw material. The columns % are the percentage of each raw material in relation to each cortex type, while the columns % rel. are the percentage of cortex type in relation to the total of each raw material (including items with and without cortex).

Focussing on the distribution of cortex among “archaeological quartzites” and their petrogenetic types, there is a clear overrepresentation of cortical areas among the quartzarenite group and an underrepresentation of them in among the MQ type (Table-12.6). The remaining petrogenetic types show percentages of items with cortex around 15%, similar to those of “archaeological quartzite” as a whole. Cortical areas from conglomerates are only represented on the OO and SO types, with small frequency.

Archaeological quartzite	Cortex type												∑ of each type
	Conglomerate			Fluvial			Unknown			Total			
	∑	%	% rel	∑	%	% rel	∑	%	% rel	∑	%	% rel	
CC				16	19	20	3	14	4	19	17	24	80
CA				9	11	18	3	14	6	12	11	24	49
OO	2	33	0	41	49	9	7	32	2	50	45	11	447
SO	4	67	4	11	13	11	4	18	4	19	17	19	98
BQ				6	7	8	4	18	5	10	9	13	76
MQ													2
Undetermined				1	1	11	1	5	11	2	2	22	9
Total	6	5	1	84	75	11	22	20	3	112	100	15	761

Table-12.6: Frequency table of types of cortex identified in layer Co.B.6 from La Cueva de Coimbre grouped by petrogenetic type. Columns are the types of cortex, including the frequency of each cortex type for each petrogenetic type and the total of items with cortex of each petrogenetic type. The last column quantifies the total of items with and without cortex of each petrogenetic type. The columns % are the percentage of each petrogenetic type in relation to each cortex type, while the columns % rel. columns are the percentage of cortex type in relation to the total of each petrogenetic type (including items with and without cortex).

12.3. TECHNOLOGICAL STRUCTURE

Here we present the results of the technological analysis of the material from layer Co.B.6 of La Cueva de Coimbre, taking into account the results from the study of the petrological structure. According to the methodology previously exposed, the most frequent category is the knapping product (88%), followed by chunk (11%), and core (1%). The distribution of technological products sorted by main lithologies is shown in Table-12.7. Cores are restricted to “archaeological quartzite” and quartz. Nevertheless, there is only one core made on quartz. Knapping products of all raw materials are well represented. In quartz, there is also an important quantity of chunks. The latter technological category is not represented in limestone and in lutite.

	Technological order										
	Cores			Knapping prdct.			Chunk			Total	
	∑	%	% rel	∑	%	% rel	∑	%	% rel	∑	%
Arch. Quartzite	10	91	1	**667**	**81**	**88**	84	83	11	761	82
Flint				**128**	**16**	**91**	13	13	9	141	15
Limestone				1	0	100				1	0
Radioralite				14	2	93	1	1	7	15	2
Lutite				1	0	100				1	0
Quartz	1	9	8	9	1	69	3	3	23	13	1
Total	11	1		820	88		101	11		932	100

Table-12.7: Frequency table of main technological categories identified in layer Co.B.6 from La Cueva de Coimbre grouped by raw material. Columns are the main technological categories and the total of items of each raw material. The columns % are the percentage of each raw material in relation to each technological category, while the columns % rel. are the percentage of each technological category in relation to the each raw material. Cells in black are the categories representing more than 10% of the total cases. Cells in dark grey are the categories representing between 5 and 10% of cases. Cells in light grey are the categories representing between 1 and 5% of cases.

Focusing the analysis on “archaeological quartzite”, the cores are restricted to CA, OO, SO, and BQ types (Table-12.8). Most of them are made on OO type, the most frequent petrogenetic type. Knapping product are more frequent among all types, even though on the CC type, knapping products are slightly underrepresented (84%). On the contrary, chunks are overrepresented in the latter type (also in undetermined material). In other types of “archaeological quartzite”, chunk is represented in smaller frequency than 11%.

	Technological order										
	Cores			Knapping prdct.			Chunk			Total	
	∑	%	% rel	∑	%	% rel	∑	%	% rel	∑	%
CC				67	10	84	13	15	16	80	11
CA	1	10	2	44	7	88	5	6	10	50	7
OO	5	50	1	**393**	**59**	**89**	46	55	10	444	58
SO	2	20	2	**89**	**13**	**89**	9	11	9	100	13
BQ	2	20	3	66	10	87	8	10	11	76	10
MQ				2	0	100				2	0
Undetermined				6	1	67	3	4	33	9	1
Total	10	1		667	88		84	11		761	100

Table-12.8: Frequency table of main technological categories identified in layer Co.B.6 from La Cueva de Coimbre grouped by petrogenetic types of “archaeological quartzite”. Columns are the main technological categories and the total of items belonging to each petrogenetic type. The columns % are the percentage of each petrogenetic type in relation to each technological category, while the columns % rel. are the percentage of each technological category in relation to the each petrogenetic type of “archaeological quartzite”. Cells in black are the categories representing more than 10% of the total cases. Cells in light grey are the categories representing between 1 and 5% of cases.

12.3.1. CORES

We identified ten cores in the whole collection. The most frequent type of core are irregular or polyhedral cores, with six, followed by cores on flake, represented by three cores. There is only one discoid core. There is no clear correlation between type of core and neither raw material, nor petrogenetic types of “archaeological quartzites” (Table-12.9).

The irregular cores from this assemblage are diverse. All of them are made on “archaeological quartzite”. Regarding raw material most of them are made on OO orthoquartzite (three items), followed by CA, SO, and BQ with one core made on each petrogenetic type. The half of the cores are complete and the other are fractured. The number of percussion platforms and flacking surfaces in irregular cores is high, generally with three or more, pointing at a high exploitation of cores. Most of them have a relatively prismatic morphologies, although due to the lack of clear standardisation, they were classified as irregular. Coming to the presence of cortical areas, four have cortex in smaller extension than 33%. Two derived from fluvial deposits and the other two are not determinable.

There are four cores on flake, the second most frequent type of core. They are made on quartz (one) and on “archaeological quartzites” (the other three). In the latter raw material, one is made on OO, another on SO, and the latter on BQ quartzite. The quantity of percussion platform and flacking surfaces is reduced to one of each category, then, these cores were not highly exploited. None of them has cortex.

Finally, there is a discoid core made on OO petrogenetic type. It has two flacking surfaces and at least three percussion platforms. This core has cortex broad between 33 and 66% of its surface. The cortical area derived from fluvial deposits.

	Type of core					
	Irregular	Discoid	Levallois	Prismatic	On flake	Total
Other RRMM					1	1
CC						
CA	1					1
OO	3	1			1	5
SO	1				1	2
BQ	1				1	2
MQ						
Undetermined						
Total	6	1	0	0	4	11

Table-12.9: Frequency table of types of cores identified in layer Co.B.6 from La Cueva de Coimbre grouped by petrogenetic types of “archaeological quartzite”. Columns are the types of cores. In this case the only other raw material (RRMM) is quartz.

12.3.2. KNAPPING PRODUCTS

In the lithic assemblage from layer Co.B.6 of La Cueva de Coimbre we identified 820 knapping products. The most frequent category is the blank, making more than 96% of the elements analysed. Core preparation/rejuvenations products and burin spall are scarcer, forming each category around 2% of knapping products. The latter two were only made on “archaeological quartzites” and flint (Table-12.10). The distribution of knapping products in “archaeological quartzites” shows that there are no core preparation/rejuvenation products made on CC and MQ types. Burin spalls are only made on orthoquartzites and BQ type (Table-12.11).

	Knapping products										
	Blanks			Core preparation/rej			Burin spall			Total	
	∑	%	% rel	∑	%	% rel	∑	%		∑	%
Archaeological quartzite	**644**	**82**	**97**	12	92	2	11	65	2	667	81
Flint	**121**	**15**	**95**	1	8	1	6	35	5	128	16
Limestone	1	0	100							1	0
Lutite	1	0	100							1	0
Quartz	9	1	100							9	1
Radioralite	14	2	100							14	2
Total	790	96		13	2		17	2		820	100

Table-12.10: Frequency table of the categories of knapping products identified in layer Co.B.6 from La Cueva de Coimbre grouped by raw material. Columns are the categories of knapping products and the total of items belonging to each petrogenetic type. The columns % are the percentage of each petrogenetic type in relation to each category of knapping product, while the columns % rel. are the percentage of each category of knapping product in relation to each petrogenetic type of “archaeological quartzite. Cells in black are the categories representing more than 10% of the total cases. Cells in light grey are the categories representing between 1 and 5% of cases.

	Knapping products										
	Blanks			Core preparation/rej			Burin spall			Total	
	∑	%	% rel	∑	%	% rel	∑	%		∑	%
CC	**67**	**10**	**100**							67	10
CA	42	7	95	2	20	5				44	7
OO	**379**	**59**	**96**	5	50	1	9	82	2	393	59
SO	**86**	**13**	**97**	2	20	2	1	9	1	89	13
BQ	64	10	97	1	10	2	1	9	2	66	10
MQ	2	0	100							2	0
Total	640	97		10	2		11	2		661	100

Table-12.11: Frequency table of the categories of knapping products identified in layer Co.B.6 from La Cueva de Coimbre grouped by the petrogenetic types of "archaeological quartzite". Columns are the categories of knapping products and the total of items belonging to each petrogenetic type. The columns % are the percentage of each petrogenetic type in relation to each category of knapping product, while the columns % rel. are the percentage of each category of knapping product in relation to each petrogenetic type of "archaeological quartzite. Cells in black are the categories representing more than 10% of the total cases. Cells in dark grey are the categories representing between 5 and 10% of cases. Cells in light grey are the categories representing between 1 and 5% of cases.

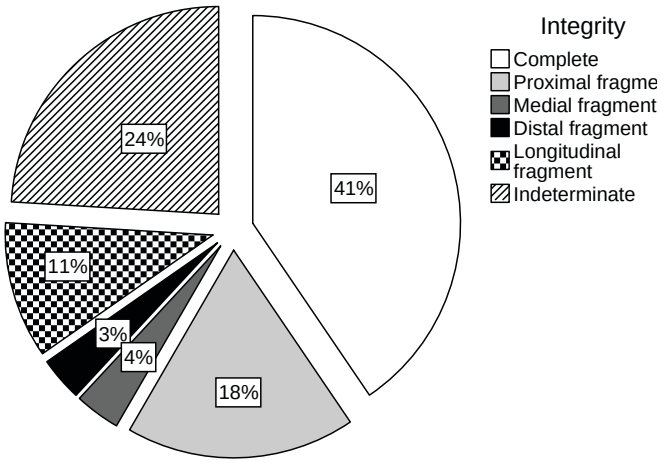

Figure-12.8: Pie chart showing percentage of each state of integrity of blanks.

Blank is the most frequent technological category in this layer, with 790 pieces. Coming to their integrity, 41% of the pieces are complete and 59% are fragmented (Figure-12.8). The most frequent fragments are proximal ones, followed by longitudinal ones. Distal and medial pieces are scarce (≈7%). Finally, 24% of the pieces could not be classified due to the absence of diagnostic features, mainly the bulb of percussion or the striking platform. Then, most of these undetermined fragments must be part of distal or medial fragments.

There is a great variability in the number of negative scars, depending on raw material, corroborated by Chi-square test (χ^2 (9, N = 788) = 26.982, p < .001) and displayed in Table-12.12. Flint is the raw material in which blanks with high quantity of negative scars are better represented. Conversely, "archaeological quartzite" is the raw material with smaller representation of blanks with high quantity of negative scars. The quantity of negative scars in blanks made on quartz is diverse. Radioralite follows similar pattern, even though there is an increase of blanks with at least three negative scars. Lutite and limestone are excluded in previous Chi-square test due to the small quantity of blanks. Even though, lutite blank has, at least, three negative scars and limestone blank only has one.

	None		One		Two		≥ Three	
	∑	res	∑	res	∑	res	∑	res
Arch Quartzite	9	0,3	213	1,4	260	-0,2	162	-1,2
Flint	0	-1,2	20	-2,7	55	0,8	46	2,2
Quartz	0	-0,3	3	0,2	3	-0,4	3	0,3
Radioralit	1	2,0	1	-1,6	5	-0,3	7	1,6
Total	10	1	237	30	323	41	218	28

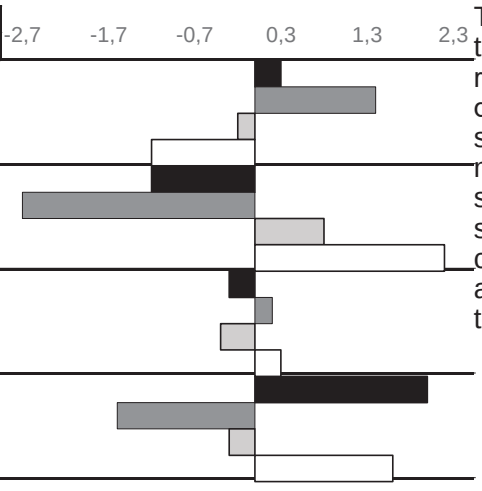

Table-12.12: Frequency table and standardised residues of χ^2 test of the quantification of dorsal scars grouped by raw material. The last row shows totals, and the second column for each category is its percentage in relation to the total of items analysed.

Regarding “archaeological quartzite” we also observe clear differences in the distribution of blanks according to the number of negative scars on their dorsal surfaces between different petrogenetic types, as supported by Chi-square test (χ^2 (15, N = 640) = 30.448, p = .01) and displayed in Table-12.13. In quartzarenite group the quantity of negative scars is relatively homogeneous, except in blanks without negative scars, overrepresented in CC type and underrepresented in CA type. In the orthoquartzite group, the distribution of negative scars clearly change. In OO type, the most frequent categories are those with one or two negative scars, in contrast with the absence of negative scars and three or more negative scars. Conversely, in SO orthoquartzite the relationship is inverse with an underrepresentation of blanks with one or two negative scars and an overrepresentation of blanks with three or more negative scars. Finally, in the quartzite group, the quantity of negative scars are homogeneously distributed, but blanks with at least three or more negative scars are slightly overrepresented.

	Dorsal scars							
	None		One		Two		≥ Three	
	∑	**res**	∑	res	∑	res	∑	res
CC	2	1,1	19	-0,7	28	0,2	18	0,3
CA	0	-0,8	15	0,3	17	0,0	10	-0,2
OO	3	-1,0	133	0,7	167	1,2	76	-2,0
SO	3	1,6	23	-1,0	23	-2,0	37	3,3
BQ	1	0,1	20	-0,2	23	-0,6	20	0,9
MQ	0	-0,2	1	0,4	0	-0,9	1	0,7
Total	9	1	211	33	258	40	162	25

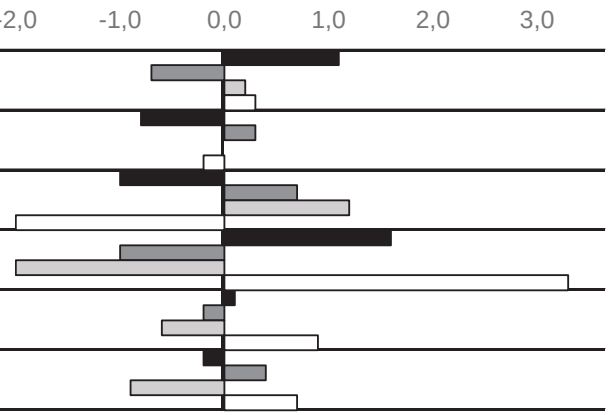

Table-12.13: Frequency table and standardised residues of χ^2 test of the quantification of dorsal scars grouped by petrogenetic type. The last row shows totals, and the second column for each category is its percentage in relation to the total of items analysed.

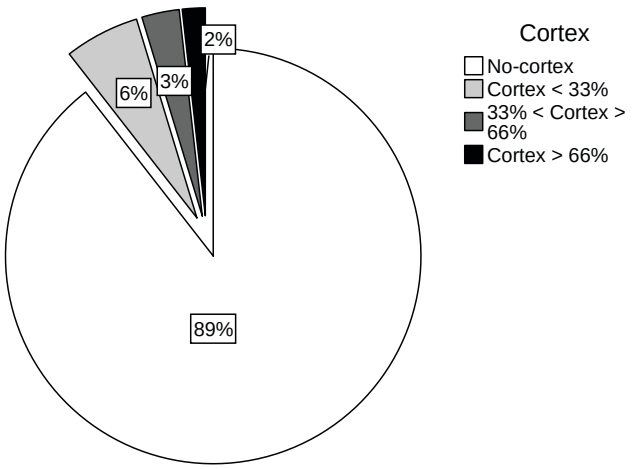

Figure-12.9: Pie chart showing percentage of absence, presence and extension of cortex on blanks.

The preservation of cortical areas on these blanks does also provide interesting data about raw material exploitation in this context (Figure-12.9). Cortex is observable in 11% of the blanks. Most of them cover less than 33% of the dorsal surface. Broad cortical areas on dorsal surfaces (covering between 33% and 66% of it) are only present in 3% of the blanks, and only 2% of the items analysed have cortical areas covering more than 66% of the surface. Their distribution according to raw materials does not reveal statistically significant differences as tested by Chi-square test χ^2 (9, N = 788) = 6.29, p = .711. Nevertheless, cortical surfaces are more frequent in “archaeological quartzites” than in other raw materials (Table-12.14). There are no statistically significant differences between petrogenetic types and the broad of cortex in blanks, as Chi-square test demonstrate χ^2 (15, N = 640) = 24.608, p = .055. Nevertheless, Table-12.15 points at some differences. The maintaining of cortex on blanks is higher in the quartzarenite group. Cortex is worst represented in OO, BQ and SO types. Cortex in not represented in the two RQ type blanks.

Among the items which preserved any cortical area (84), it was possible to characterise 60 of them. Among the “archaeological quartzite”, only four blanks have conglomerate cortex and all other cortical surfaces derived from fluvial deposits. The conglomerate cortex is preserved in three SO orthoquartzites and one OO type.

	Presence of cortex on dorsal surfaces							
	Absence		X < 33%		33<X>66		X > 66%	
	∑	**%**	∑	%	∑	%	∑	%
Arch. Qzt.	572	88,8	39	6,1	21	3,3	12	1,9
Flint	111	91,7	7	5,8	2	1,7	1	0,8
Quartz	9	100	0	0,0	0	0,0	0	0,0
Radiorali te	13	92,9	0	0,0	0	0,0	1	7,1
Total	705	89,5	46	5,8	23	89,5	14	1,8

Table-12.14: Frequency table and its representation through a bar chart using the percentage of each blank category (determined by the quantity of cortex on dorsal surfaces) taking into account each raw material.

	Presence of cortex on dorsal surfaces							
	Absence		X < 33%		33<X>66		X > 66%	
	∑	**%**	∑	%	∑	%	∑	%
CC	54	80,6	6	9,0	4	6,0	3	4,5
CA	34	81,0	6	14,3	2	4,8	0	0,0
OO	349	92,1	18	4,7	8	2,1	4	1,1
SO	72	83,7	7	8,1	3	3,5	4	4,7
BQ	58	90,6	1	1,6	4	6,3	1	1,6
RQ	2	100,0	0	0,0	0	0,0	0	0,0
Total	569	88,9	38	5,9	21	3,3	12	1,9

Table-12.15: Frequency table and its representation through a bar chart using the percentage of each blank category (determined by the quantity of cortex on dorsal surfaces) taking into account each petrogenetic type of “archaeological quartzite”.

Burin spall is the second most frequent group of knapping product, although its representation is reduced in the assemblage, with only 17 pieces. Fifty-nine percent of them are complete, and the other are fragmented. Eleven were made on “archaeological quartzite” and the other six on flint (Table-12.10). Coming to the first raw material, the most frequent type is the OO, with nine items, followed by SO and BQ types, with one respectively (Table-12.11). None of the burin spall has cortex.

Core preparation/rejuvenation product is the less frequent knapping product, only represented by 13 pieces (Table-12.10). Sixty-nine percent of them are fragmented. The only represented raw materials are “archaeological quartzite” and flint, although in the latter there is only one piece. Among “archaeological quartzites” CA, OO, SO, and BQ types are represented (Table-12.11). Five core preparation/rejuvenation products have cortical areas, three cover smaller extension than 33% of dorsal surface and other two have cortex broad between 33% and 66%. All of them derived from fluvial deposits. Two are made on SO type, other two on CA, and the other one on OO type.

12.3.3. CHUNK

Chunk is the second better represented technological order in the assemblage, with 101 pieces. The integrity of the pieces is not analysable due to the absence of diagnostic features.

The raw materials present in this category are “archaeological quartzites”, flint, radioralite, and quartz (Table-12.7). Except quartz, all other raw material have similar representation, between seven and eleven percent of the lithic assemblage. On quartz, the rate is higher. Regarding the representation of chunk in each petrogenetic type, except on the CC quartzarenite, they are similarly represented (Table-12.8).

Thirty-nine percent of chunks have cortex. Among them 34 are in “archaeological quartzite”, four in flint and the other one is on the only chunk made on radioralite. Twenty one of these cortical areas are less wide than 33% of lithic surface, on 14 items cortex range between 33% and 66%, and only four chunks have cortex broad than 66%. All recognisable cortex except two derived from river beaches.

12.4. RETOUCH: MODAL AND MORPHOLOGICAL STRUCTURES

Here we present the results of the analysis of retouched artefacts and their relationship with the data previously exposed. According to the methodology defined above, there are 46 lithics retouched, 4.9% of the assemblage. Five have two different primary types, 11% of retouched artefacts, and only one has three different primary types.

The total number of primary types individualised is 53. Starting from the orders, we do not find evidence of Plain (P) mode. Simple (S) mode is the most frequent one (34 items), followed by Abrupt (A), Splinter (E), and Burin (B) mode (32, ten, and eight respectively) (Figure-12.10 and Table-12.17). Going down from order to typological group (or morphotema), we start with the Simple mode, the most frequent one. The most frequent typological group is that of Sidescraper (R) (15 items). Other Simple groups are Endscraper (E) and Denticulate (D) (two and one morphothemas). In the Abrupt mode, the most frequent group is that of unspecific Abrupt (A) (nine), followed by Truncation (T) (4), Backed Blade (LD) (3), and backed point (PD) (1). No groups are distinguished within the Burin (B) and Splinter mode (E).

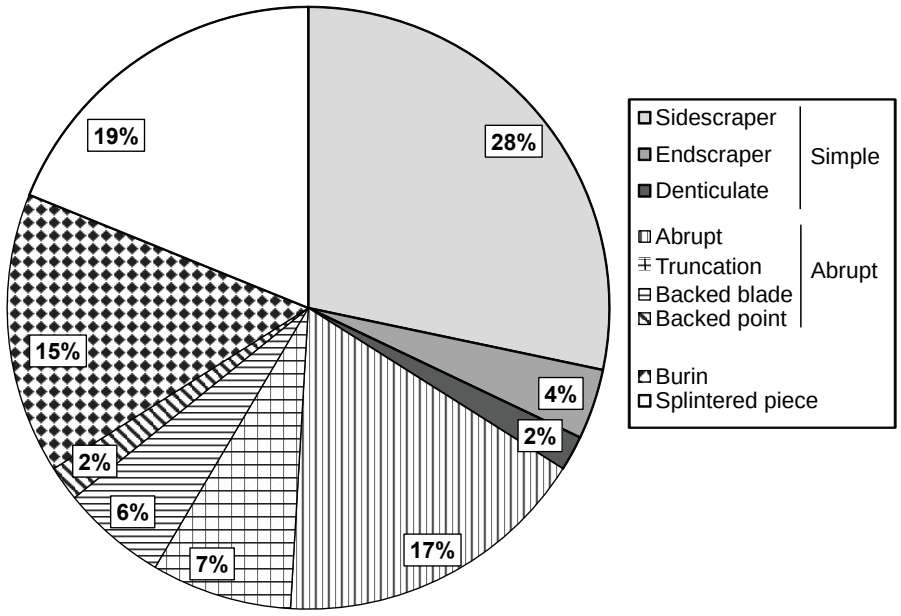

Figure-12.10: Pie chart showing the percentage of modes of retouch and morphological groups of the retouched material from layer Co.B.6 of La Cueva de Coimbre.

After having understood the general characterisation of the retouch using the modes and morphological groups of retouch, now we will deepen into the analysis of the pieces with multiple primary types. Starting from the blanks with two primary types, there are three association: Burin and unspecific Abrupt (in three blanks), two Splinter morphothema (in one blank), and unspecific Abrupt and Sidescraper (in one blank). There is only one blank with three different primary types: a blank with two Sidescraper and one Splinter morphothemas.

Next, we will analyse the relationship between the retouched artefacts and the technological structure. There is no statistically significant relationship between the presence of retouch and technological blanks they are configured χ^2 (2, N = 932) = 4.455, p = .11. Nevertheless, except one retouched artefact made on a chunk, all other are made on knapping products. The retouched chunk is Sidescraper. Regarding the technological groups of knapping products, most artefacts are made on blanks, 42 pieces, although two core preparation/rejuvenation products and one burin spall are also retouched. The morphothemas created on the core preparation/rejuvenation products are a Burin and an unspecific Abrupt, while the morphothema created on the burin spall is a Blacked Blade.

Finally, we will analyse the relationships between the retouched artefacts and the raw material of the blanks they are configured. The quantity of retouched artefacts is differently distributed depending on raw material of the blanks they are configured, as demonstrated by Chi-square test (only using raw material with retouched pieces) χ^2 (2, N = 915) = 9.090, p = .01. Quartz is the raw material with higher frequency of retouched pieces (23%), followed by "archaeological quartzite" (5%), and flint (4%). In contrary, radiolarite, lutite and limestone are not retouched. Blanks with two or three primary types are made on "archaeological quartzite" (four), flint (one) and quartz (one). There is no statistically significant relationship in the presence of retouch in the different types of "archaeological quartzite", as pointed out by Chi-square test (χ^2 (5, N = 752) = 8.501, p = .131). Nevertheless, Table-12.16 points at differences in the representation of retouch in the blanks according to their petrogenetic types they are configured. The percentage of retouched blanks is higher in CA and SO types than other types of "archaeological quartzite". There is no statistically association between the presence of blanks with multiple primary types and petrogenetic type: one in made on quartz, another on flint, and other four on "archaeological quartzite" (one on CA and other two on OO type).

	Non-retouched		**Retouched**	
	∑	%	**∑**	**%**
CC	78	97,5	2	2,5
CA	46	92,0	4	8,0
OO	425	95,7	19	4,3
SO	91	91,0	9	9,0
BQ	75	98,7	1	1,3
MQ	2	100,0	0	0,0

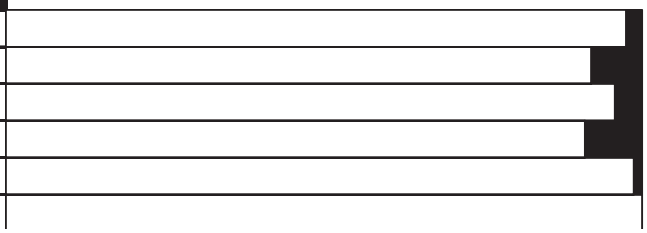

Table-12.16: Frequency table and its representation through a bar chart using the percentage of retouched material taking into account each petrogenetic type of "archaeological quartzite".

There is no clear association between the morphological group of retouch and raw material they are configured, as Table-12.17 shows. All raw material have similar representation of modes and morphological groups of retouch. Nevertheless, there are associations between morphological groups and the petrogenetic types they are configured, as Table-12.18 shows. The first association relates Sidescraper and Splinter groups with CA quartzarenite. The second points at the lack of association between Sidescraper and the SO type, even it is the most frequent morphothema. Finally, it is also interesting to observe that the only petrogenetic type with all defined retouches is the OO orthoquartzite.

	Simple			Abrupt				Burin	Spli	
Order	Sidescraper	Endscraper	Denticulate	Abrupt	Truncation	Backed blade	Backed point	Burin	Splintered	Total
Arch. Qzt	**12**	1	1	**7**	2	2	1	**7**	**9**	42
Flint	2	1		1	2				1	7
Quartz	1			1		1		1		4
Total	15	2	1	9	4	3	1	8		53

Table-12.17: Frequency table of order and group of retouches grouped by raw material. In the cases of pieces with multiple primary types, each retouch is quantified individually. Cells in black are the categories representing more than 10% of the total cases. Cells in light grey are the categories representing between 1 and 5% of cases.

	Simple			Abrupt				Splinter	Burin	
Order	Sidescraper	Endscraper	Denticulate	Abrupt	Truncation	Backed blade	Backed point	Splintered	Burin	Total
CC	2									2
CA	2							3		5
OO	**5**	1	1	4	1	2	1	2	4	21
SO	1			2	1			3	2	9
BQ				1						1
MQ										
Unknown	2							1	1	4
Total	12	1	1	7	2	2		9	7	42

Table-12.18: Frequency table of order and group of retouches grouped by petrogenetic type. In the cases of pieces with multiple primary types, each retouch is quantified individually. Cells in black are the categories representing more than 10% of the total cases. Cells in dark grey are the categories representing between 5 and 10% of cases. Cells in light grey are the categories representing between 1 and 5% of cases.

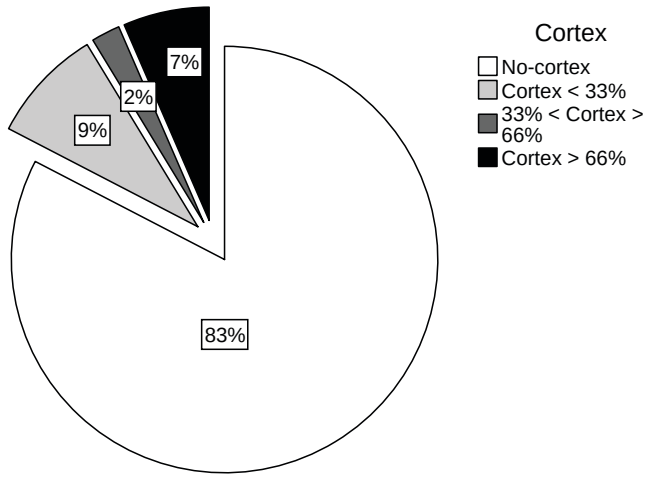

Finally, we analyse the relationship between retouched blanks and the preservation of cortex on them (Figure-12.11). Nine percent of them has cortex covering less than 33% of the surface. Only 2% of the artefacts have cortex between 33% and 66%. Seven percent of them have cortex broad than 66%. In general, cortex is more frequent in retouched artefacts than in non-retouched lithics. All identified cortical areas on artefacts derived from fluvial deposits.

Figure-12.11: Pie chart showing percentage of absence, presence and extension of cortex on retouched material from layer Co.B.6 of La Cueva de Coimbre.

12.5. TIPOMETRICAL STRUCTURE

In this section we will describe the results of the analysis of the tipometrical structure and its relationship with the structures studied previously. We made the measurement using the technological axis (length, width and thickness) on 624 lithics (67% of the assemblage). The remaining 308 pieces were measured using the longest axis (X, Y and Z) due to the absence of features signalling the technological axis. All chunks, most of the cores (some cores on flakes were measured using the technological axis) and some incomplete knapping products were measured using the latter criterion.

An overview of length, width and thickness reveals that all three measurement have positive skewness and kurtosis, the highest values being those of thickness, followed by length (Figure-12.12). The mean length is 16.32 mm, the mean width is 14.57 mm, and the mean thickness is 4.42 mm. The measurements of the first two axes are similar between them. A general outlook of X, Y, and Z axes does also points at positive skewness and kurtosis. Nevertheless, all the means are different between them: the mean of the X axis is 18.34 mm, the mean of the Y axis is 11.74 mm, and the mean of the Z axis is 5.43 mm (Figure-12.13). The relationship between the three measurements according to the Tarriño indexes (Tarriño, 2015) reveals different morphologies depending on the measurement method employed (Figure-12.14). Most of the pieces measured using the X/Y/Z axes are between 0.1 and 0.5 RFL index and between 0.5 and 0.8 of the RBEI, meaning similar measurement between the three axes and in relatively cubic-bladed shapes. Regarding the material measured with the technological axis, the resulting forms are similar, but they also include an important presence of tabular and bladed elements. Conversely, there is a decrease of cubic and carinated forms.

The last measurement used here is the weight of each lithic implement. The minimum weight recorded is 0.01 g and the maximum 133.34 g. The mean is 2.84 g. Weight presents high positive

kurtosis (80.45), and positive skewness (8.1) as a consequence of the high percentage of lithic implements lighter than five grams. The total of pieces weighted in this layer is 932 and the total weight of all of them is 2,652 g.

None of the aforementioned measurements is normally distributed[1]

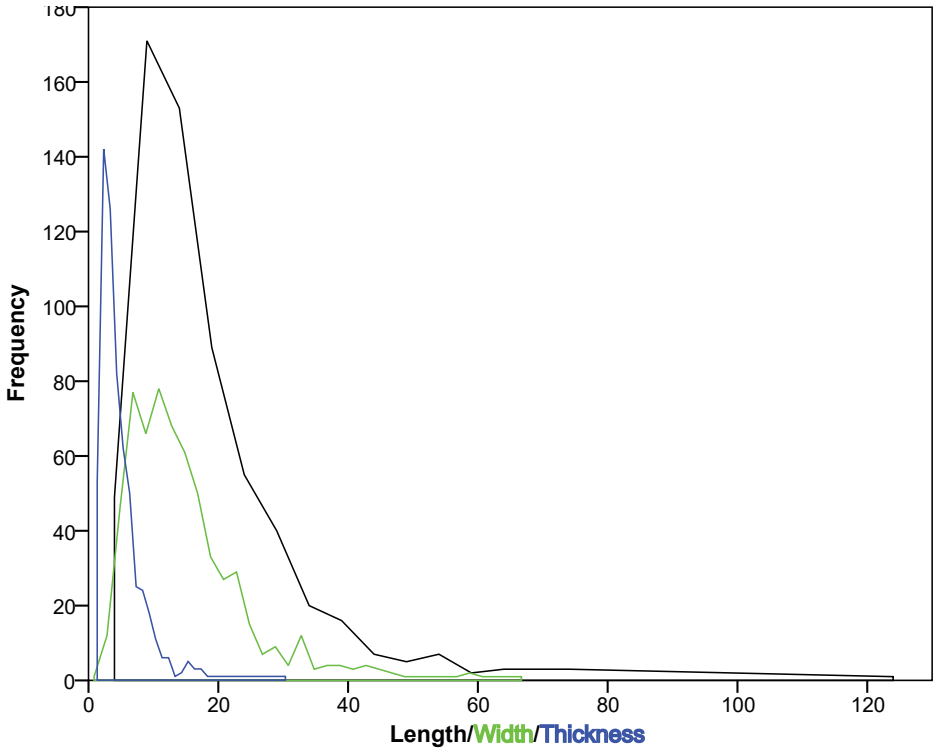

Figure-12.12: Frequency area chart showing the distribution of length, width and thickness of lithic remains from layer Co.B.6 of La Cueva de Coimbre measured in relation to technological axis. Black line represents length, green line represents width, and blue line represents thickness. Horizontal axis measurement are in millimetres.

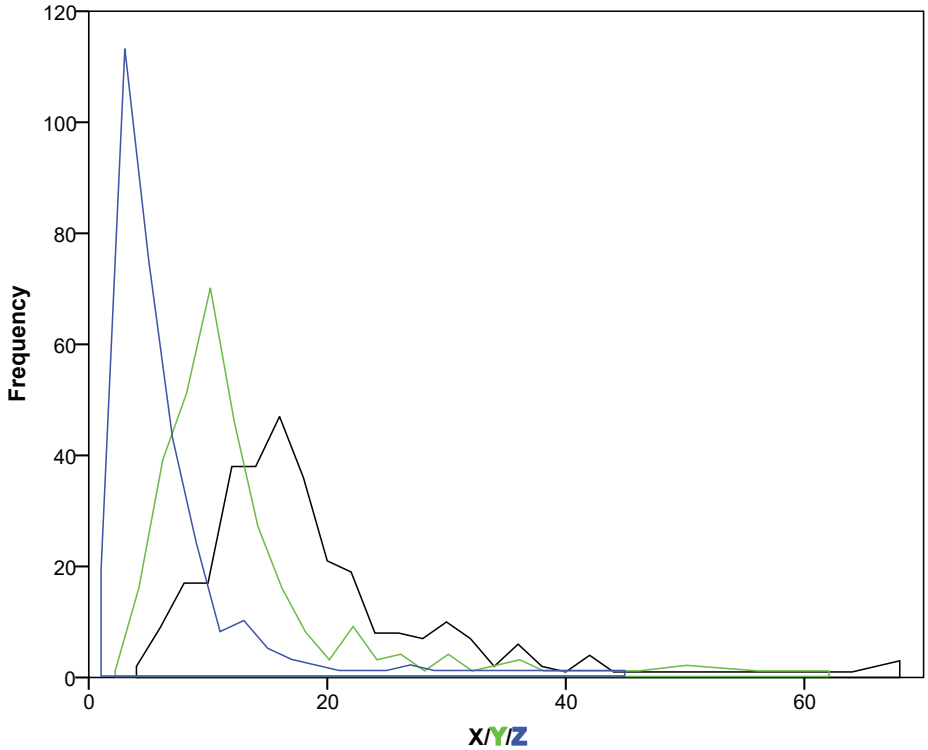

Figure-12.13: Frequency area chart showing the distribution of X, Y and Z axes of lithic remains from layer Co.B.6 of La Cueva de Coimbre. Black line represents the X axis, green line represents the Y axis, and blue line represents the Z axis. Horizontal axis measurement are in millimetres.

1 KS = 0.164; df = 624; p < 0.01 for length
KS = 0.137; df = 624; p < 0.01 for width
KS = 0.196; df = 624; p < 0.01 for thickness
KS = 0.176; df = 308; p < 0.01 for X-axis
KS = 0.213; df = 308; p < 0.01 for Y-axis
KS = 0.206; df = 308; p < 0.01 for Z-axis
KS = 0.387; df = 932; p < 0.01 for weight

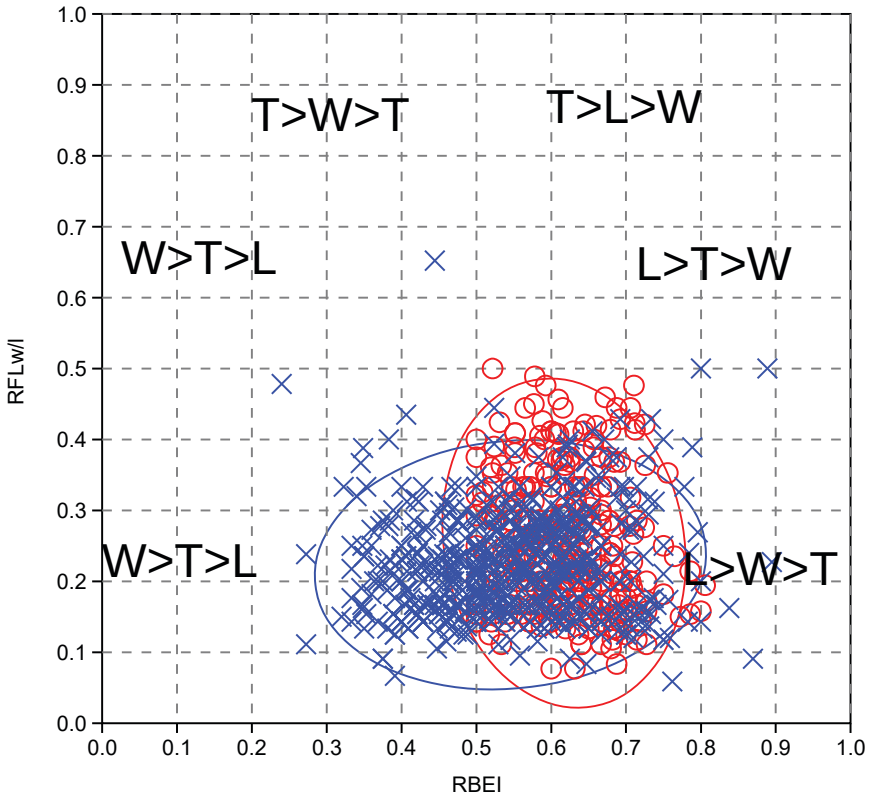

Figure-12.14: Scatter plot of RFLw or RFLl and RBEI indexes. Blue crosses and ellipse are the measurements made in relation to technological axis. Red circles and ellipse are the measurements made in relation to X/Y/Z axis. Ellipses enclose 95% of cases of each category.

Once the general metric characteristics have been understood, we will relate this data with the technological structure. The three technological orders proposed show differences in shape between them. Figure-12.15a shows three different but overlapping groups using 95% confidence ellipses. The ellipse of cores describes an uprising elongated form and it is situated in the central and upper part of the chart in the region of tabular and carinated morphologies. The ellipse of knapping product is located on the lower area, and it presents horizontal elongation. Finally, the ellipse of chunks is positioned in the central area, displaying negative elongation. The distribution of weight of each order does also show clear differences in variance, as demonstrated by *H* Kruskal-Wallis test: $H\ \chi^2$ (2, N = 932) = 45.022, $p < 0.001$ (Figure-12.15b). In general, cores are bigger than other orders, with weights around 30.3 g of each piece (Table-12.19). Knapping products and chunks have similar grams/piece ratios, significantly smaller in comparison with cores.

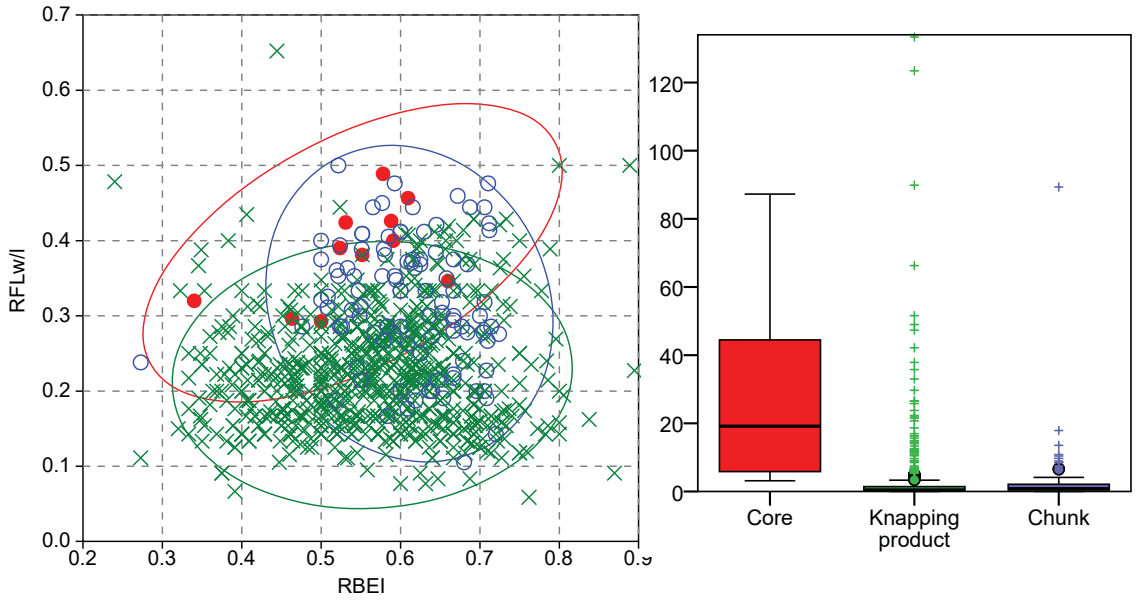

Figure-12.15: Scatter plot of RFLw or RFLl and RBEI indexes. Green crosses and ellipse are knapping products. Red points and ellipse are cores. Blue circles and ellipse are chunks. Ellipses enclose 95% of cases of each category. b) Boxplot showing differences in weight between technological orders. The weight is expressed in grams.

Technological order	Weight		∑ of pieces		Ratio
	∑	%	∑	%	Grams/Piece
Core	333,0	12,6	11	1,2	30,3
Knapping product	2019,5	76,1	820	88,0	2,5
Chunk	299,7	11,3	101	10,8	3,0

Table-12.19: Frequencies and weight of main technological orders. The ratio grams/piece is reported. Weight is expressed in grams.

Coming to cores, there are differences in morphology between the types proposed, especially comparing irregular cores and cores on flake, as displayed in Figure-12.16a. The former are concentred in the region between 0.4 and 0.5 of RFLw/l and 0.5 and 0.6 of RBEI, while the latter are more dispersed, especially in the RBEI axis. The distribution of weight of each category is also different, as demonstrated by *H* Kruskal-Wallis test: $H\ \chi^2$ (2, N = 11) = 7.614, p = 0.022 (Figure-12.16b). The grams per piece ratio shows that the discoid core and cores on flake have similar weight, lighter than irregular cores (Table-12.20).

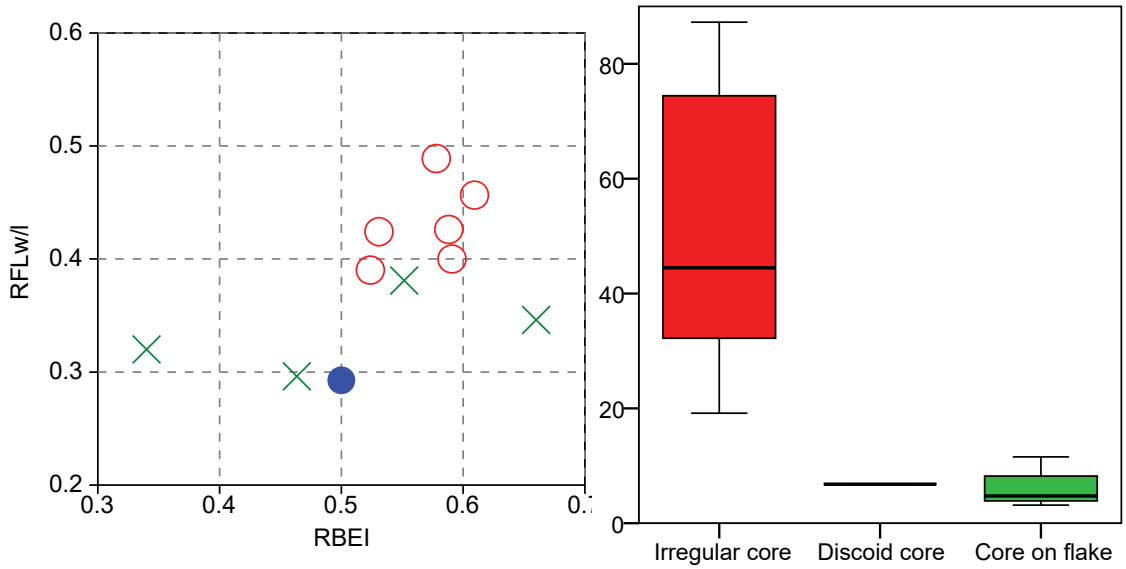

Figure-12.16: Double chart showing: a) Scatter plot of RFLw or RFLl and RBEI indexes. Green crosses are cores on flakes. Red circles are irregular cores. Blue point is the discoidal core. b) Boxplot showing differences in weight between types of cores. The weight is expressed in grams.

Core groups	Weight		∑ of pieces		Ratio
	∑	%	∑	%	Grams/Piece
Irregular core	302,0	90,7	6	54,5	50,3
Discoid core	6,8	2,0	1	9,1	6,8
Core on flake	24,2	7,3	4	36,4	6,0

Table-12.20: Frequencies and weight of different groups of cores. The ratio grams/piece is reported. Weight is expressed in grams.

The knapping products exhibit clear differences in form of lithic remains, as shown in Figure-12.17a. The areas defined by 95% confidence ellipses are very different for the three categories proposed. Burin spall ellipse is in the right part of the chart displaying a vertical elongation, in the area of bladed and carinated products. Core preparation product ellipse slightly overlaps the upper part of previous ellipse, but this ellipse extend into the prismatic and cubic zones, creating an elongated in horizontal position ellipse. Finally, 95% confidence ellipse of blanks is rounded and it is situated in the central-lower part of the chart. The latter overlaps with previous ellipses, but blanks are the only products in the region between 0.3-0.6 of RBEI and 0.05-0.2 of RFLw/l. Weight distribution between three categories is also different from one to other category, as could be graphically observed in Figure-12.17b and corroborated by *H* Kruskal-Wallis test $H\ \chi^2$ (2, N = 820) = 40.707, p < 0.001. Grams per piece ratio reveals clear differences according to the mean weight of each group: the highest value is for the core preparation/rejuvenation products, 13.1 g, while the smallest is for burin spalls, reduced to 0.2 g. Mean weight of blanks is similar to the general mean, 2.3 g (Table-12.21).

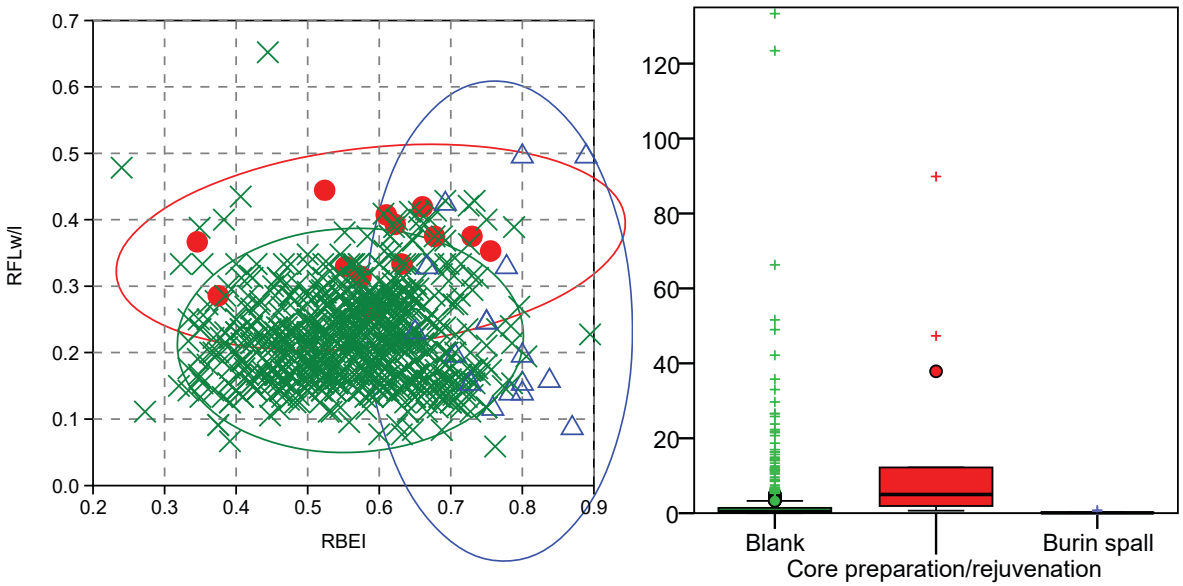

Figure-12.17: Double chart showing: a) Scatter plot of RFLw or RFLl and RBEI indexes. Green crosses and ellipse are blanks. Red points and ellipse are core preparation/rejuvenation products. Blue triangles and ellipse are burin spalls. Ellipses enclose 95% of cases of each category. b) Boxplot showing differences in weight between the groups of knapping products. The weight is expressed in grams.

Knapping product group	Weight		∑ of pieces		Ratio
	∑	%	∑	%	Grams/Piece
Blank	1797	89,0	790	96,3	2,3
Core prep./rejuv.	219,8	10,9	13	1,6	16,9
Burin spall	2,6	0,1	17	2,1	0,2

Table-12.21: Frequencies and weight of different groups of knapping products. The ratio grams/piece is reported. Weight is expressed in grams.

Focussing on blanks, there are no clear differences in their formats based on the number of negative scars on their dorsal surfaces (Figure-12.18a). All four categories are similarly distributed represented by relatively rounded circles in the region between 0.1 ≤ RFL ≥ 0.4 and 0.3 ≤ RBEI ≥ 0.8. Nevertheless, there are clear differences in weight based on the number of negative scars, as shown in Figure-12.18b and statistically demonstrated by *H* Kruskal-Wallis test: $H\ \chi^2$ (3, N = 790) = 91.873, p < 0.001. The pieces without negative scars and the blanks with three or more negative scars are heavier than blanks with one and two negative scars. The grams per piece ratio also points at the same idea (Table-12.22).

Number of negative scars	Weight		∑ of pieces		Ratio
	∑	%	∑	%	Grams/Piece
No-negative scars	54,1	3,0	10	1,3	5,4
One negative scar	368,3	20,5	238	30,1	1,5
Two negative scars	406,7	22,6	323	40,9	1,3
Three or more negative scars	967,9	53,9	219	27,7	4,4

Table-12.22: Frequencies and weight of blanks grouped by number of negative scars. The ratio grams/piece is reported. Weight is expressed in grams.

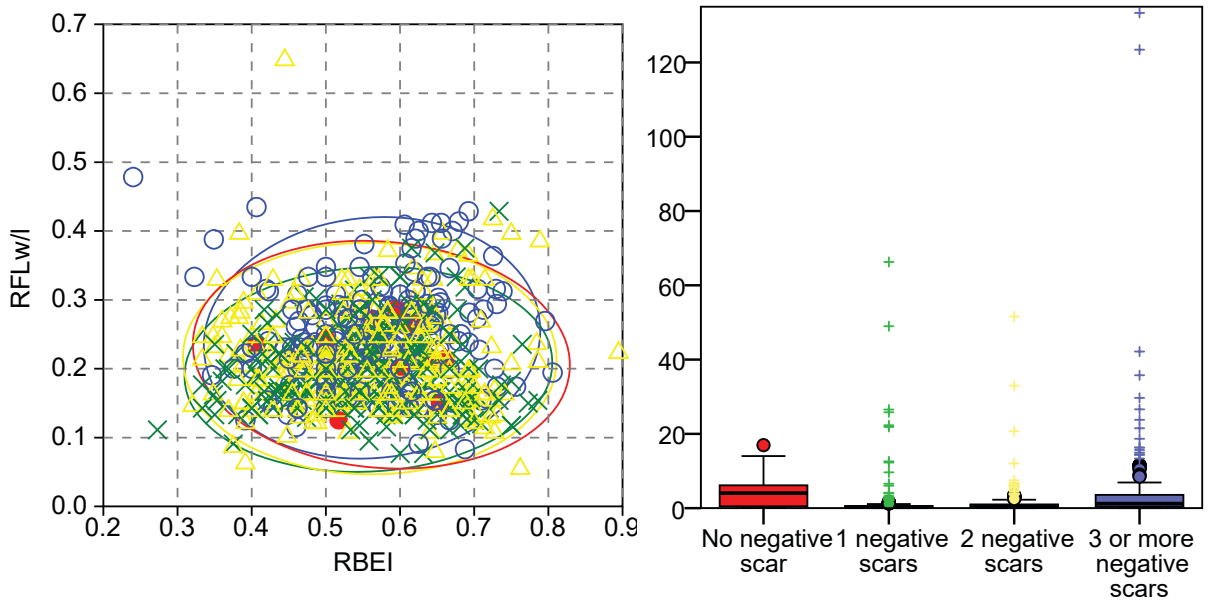

Figure-12.18: Double chart showing: a) Scatter plot of RFLw or RFLl and RBEI indexes. Red points and ellipse are blanks without negative scar. Green crosses and ellipse are blanks with one negative scar. Yellow triangles and ellipse are blanks with two negative scars. Blue circles are blanks with three or more negative scars. Ellipses enclose 95% of cases of each category. b) Boxplot showing differences in weight between blanks with different number of negative scars on dorsal surface. The weight is expressed in grams.

Regarding the integrity of the blanks, there are no differences based on the forms of the pieces (Figure-12.19a). All six 95% confidence ellipses are similarly distributed. Nevertheless, there are differences in weight distribution, as demonstrated by *H* Kruskal-Wallis test $H\ \chi^2$ (5, N = 790) = 14.109, p = 0.015. Figure-12.19b and Table-12.23 point that complete blanks are the most variable and heavier pieces. Proximal, longitudinal, and undetermined products are less variable and they are lighter. Finally, medial and distal fragments are even less variable and lighter.

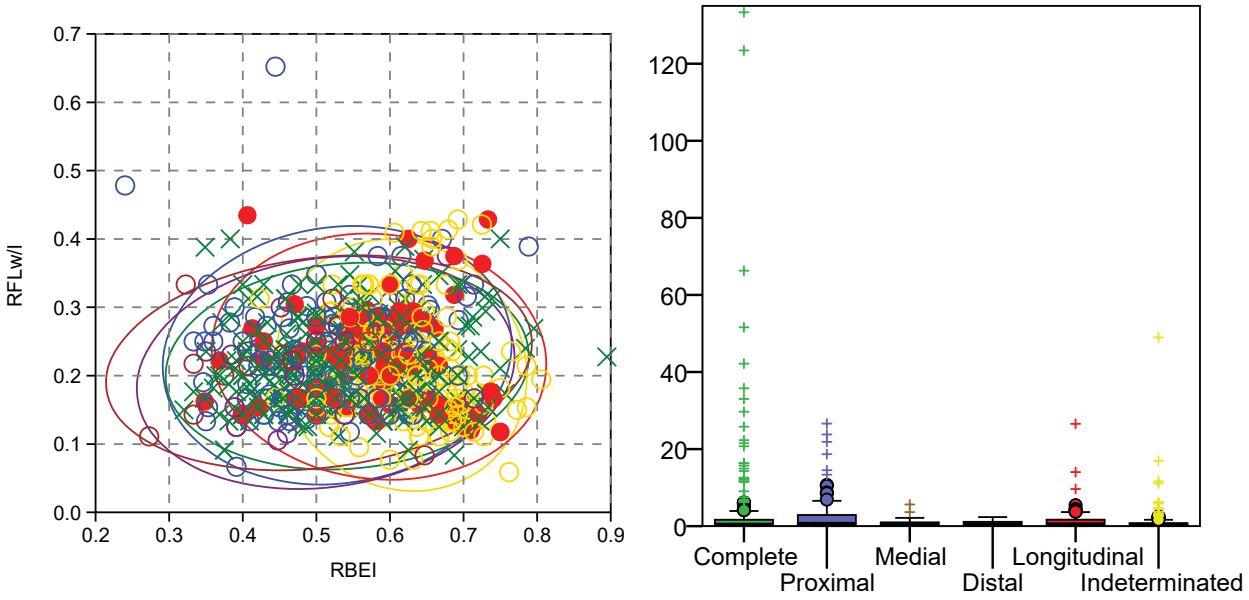

Figure-12.19: Double chart showing: a) Scatter plot of RFLw or RFLl and RBEI indexes. Green crosses and ellipse are complete blanks. Blue circles and ellipse are proximal blank fragments. Brown circles and ellipse are medial blank fragments. Purple circles and ellipse are distal blank fragments. Red points and ellipse are longitudinal blank fragments. Yellow circles and ellipse are undetermined blank fragments. Ellipses enclose 95% of cases of each category. b) Boxplot showing differences in weight between blanks preserved in diverse states of integrity. The weight is expressed in grams.

Integrity of blanks	Weight		∑ of pieces		Ratio
	∑	%	∑	%	Grams/Piece
Complete	1060,7	59,0	320	40,5	3,3
Proximal fragment	330,5	18,4	141	17,8	2,3
Medial fragment	22,8	1,3	28	3,5	0,8
Distal fragment	18,7	1,0	27	3,4	0,7
Longitudinal fragment	137,2	7,6	84	10,6	1,6
Undetermined fragm	227,3	12,6	190	24,1	1,2

Table-12.23: Frequencies and weight of blanks grouped by integrity. The ratio grams/piece is reported. Weight is expressed in grams.

The classification of complete blanks products (Figure-12.20a) reveals the predominance of flakes (69% of complete blanks), followed by a moderate presence of elongated flakes (19% of complete blanks) and a smaller presence of blades (12% of complete blanks). There is no differences in weight between the three categories, showing similar distribution, as *H* Kruskal-Wallis test and Figure-12.20b show: $H\ \chi^2$ (3, N = 594) = 4.78, p = .092. The comparison of gram/piece ratio between the three types of blanks proposed reveals small differences (Table-12.24). The flake and elongated flake ratios are similar, also to the overall ratio. Nevertheless, the gram per piece ratio of blades is higher.

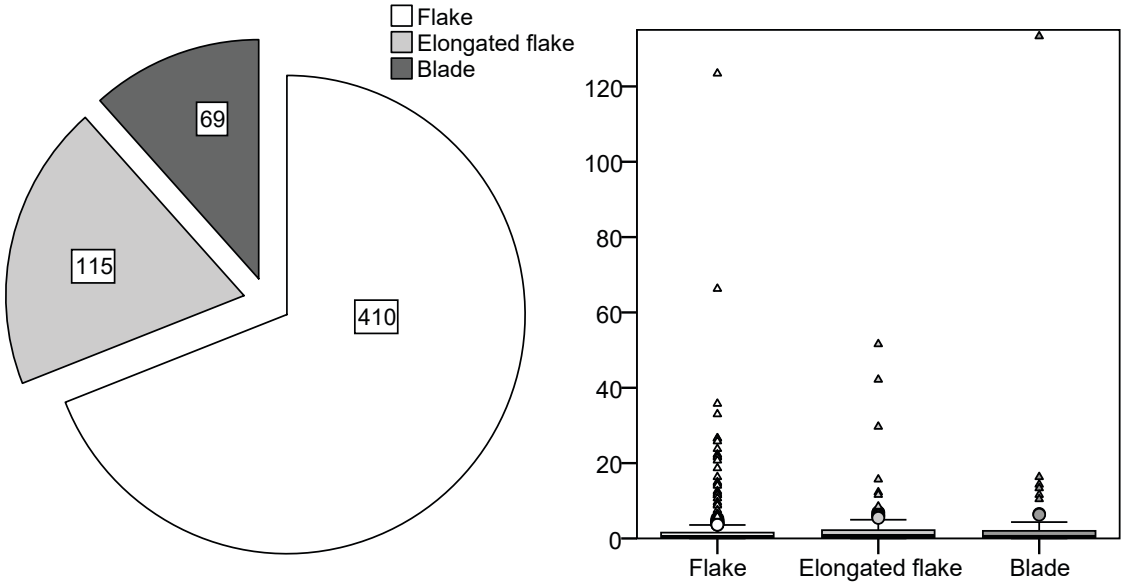

Figure-12.20: Double chart showing a) pie chart showing the distribution of complete blank products, and b) boxplot showing differences in weight between metrical categories. The weight is expressed in grams.

Complete blank characterisation	Weight		∑ of pieces		Ratio
	∑	%	∑	%	Grams/Piece
Flake	988,8	62,9	410	69,0	2,4
Elongated flake	320,9	20,4	115	19,4	2,8
Blade	262,3	16,7	69	11,6	3,8

Table-12.24: Frequencies and weight of different types of complete blanks (flakes, elongated flakes, blades). The ratio grams/piece is reported. Weight is expressed in grams.

Next, we will like the typo(metrical) structure with retouched artefacts. There are clear weight differences based on the presence (M = 4.92) or absence (M = 0.47) of retouch in the blanks, as corroborated by *U* Mann-Whitney test: U = 33,425.00, p < 0.001. In general, retouched blanks are heavier than other lithics (Figure-12.21b). The mean weight of non-retouched material is similar to the grams/piece ratio of the whole assemblage, while the ratio of retouched artefacts is noticeable bigger (Table-12.25). There are no differences in forms between artefacts and non-retouched mate-

rial, as shown in Figure-12.21a. There are neither differences in morphology of artefacts according to the quantity of primary types identified on each blank (Figure-22a). Weight between three categories is also similar, as pointed out by *H* Kruskal-Wallis test: $H\ \chi^2$ (2, N = 46) = 0.859, p = 0.651. Table-12.26 points at some small differences in grams per piece ratio, created as a consequence of some outliers, especially in blanks with one primary type.

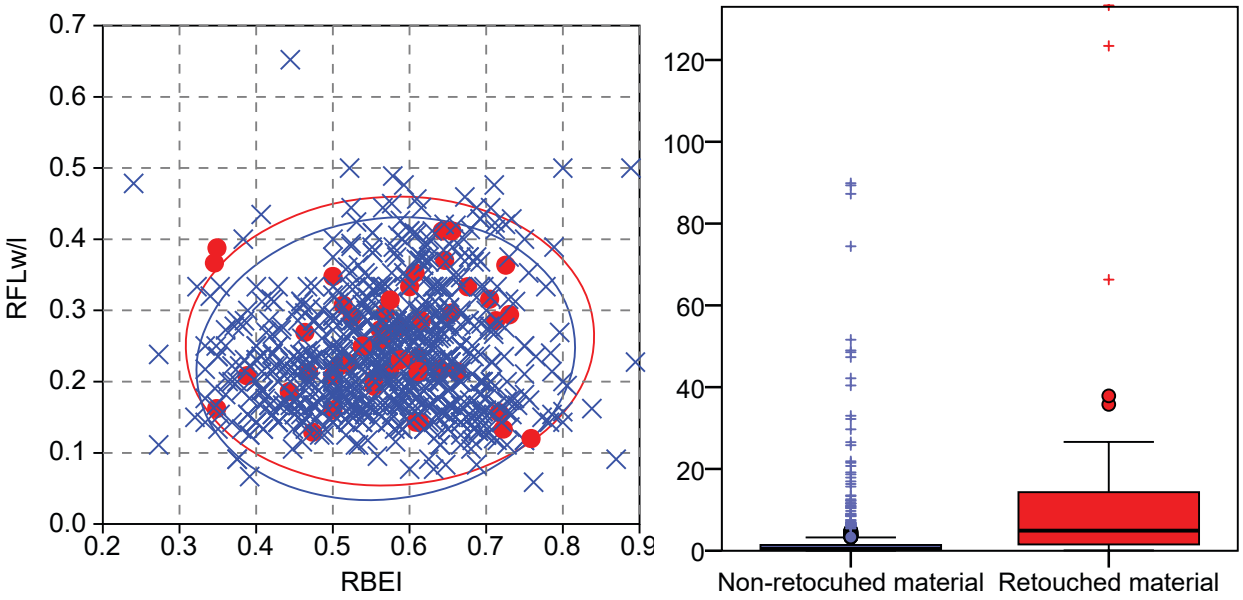

Figure-12.21: Double chart showing: a) Scatter plot of RFLw or RFLl and RBEI indexes. Red points and ellipse are retouched lithic material. Blue crosses and ellipse are non-retouched lithic material. Ellipses enclose 95% of cases of each category. b) Boxplot showing differences in weight between retouched and non-retouched lithic material. The weight is expressed in grams.

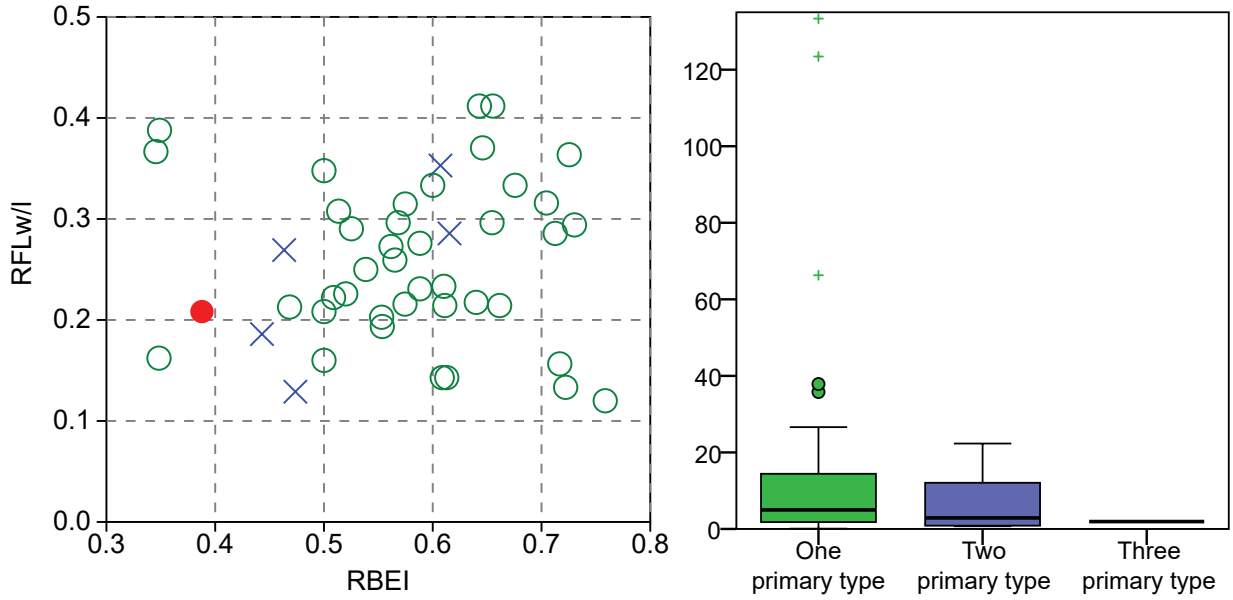

Figure-12.22: Double chart showing: a) Scatter plot of RFKw or RFLl and RBEI indexes. Green circles and ellipse are artefacts with one primary type. Blue crosses and ellipse are artefacts with two primary types. Red point is the artefact with three primary types. b) Boxplot showing differences in weight between retouched artefacts grouped by the quantity of primary types. The weight is expressed in grams.

Piece	Weight		∑ of pieces		Ratio
	∑	%	∑	%	Grams/Piece
Non-retouched	1990,7	75,1	886	95,1	2,2
Retouched	661,5	24,9	46	4,9	14,4

Table-12.25: Frequencies and weight of retouched and non-retouched pieces. The ratio grams/piece is reported. Weight is expressed in grams.

Quantity of retouch in each piece	Weight		∑ of pieces		Ratio
	∑	%	∑	%	Grams/Piece
One primary type	620,7	93,8	40	87,0	15,5
Two primary types	38,8	5,9	5	10,9	7,8
Three primary types	1,9	0,3	1	2,2	1,9

Table-12.26: Frequencies and weight of the retouched pieces grouped by the quantity of primary types. The ratio grams/piece is reported. Weight is expressed in grams.

Then, we will confront metrical features of artefacts with the characterisation of retouch, categorised in orders (modal structure) and groups (morphological). Due to the methodology used to define retouch here, we only included in this analysis the pieces with one primary type of retouch. The comparison does not reveal differences in artefact morphologies between the different modes of retouch (Figure-12.23). There are neither weight differences between artefacts according to the order of retouch, as proven by *H* Kruskal-Wallis $H\ \chi^2$ (2, N = 40) = 3.464, p = 0.325. Weight differences observed in Table-12.27 are the consequence of the small quantity of artefacts on each category and the existence of heavy outliers.

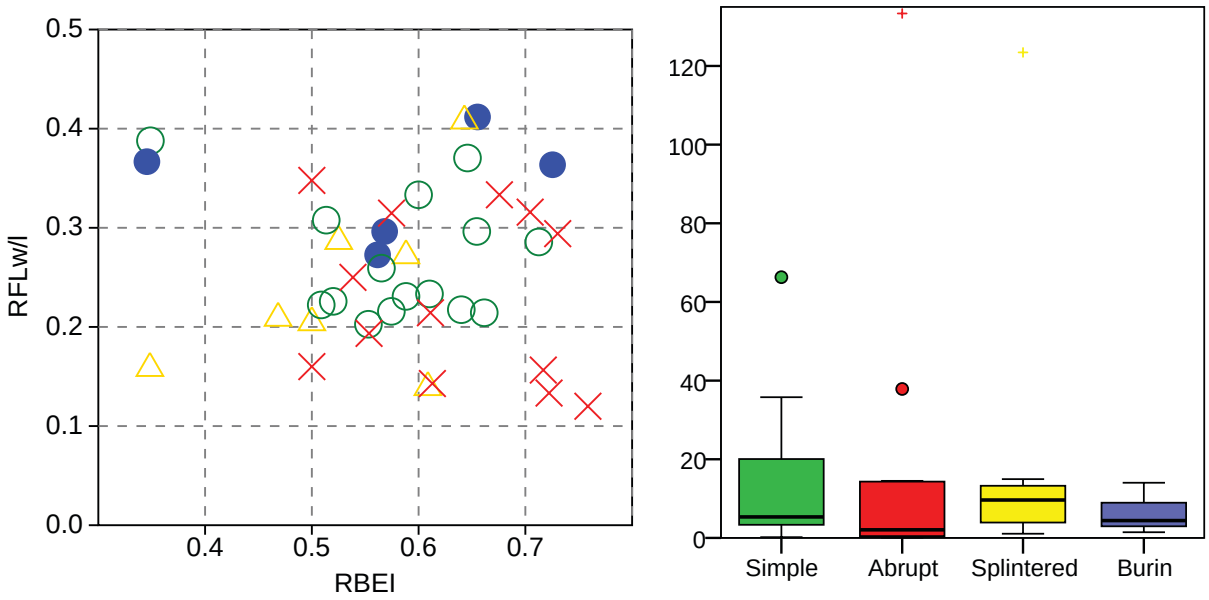

Figure-12.23: Double chart showing: a) Scatter plot of RFLw or RFLI and RBEI indexes. Red crosses are artefacts configured with the Abrupt mode of retouch. Green circles are artefacts with the Simple mode of retouch. Blue points are artefacts configured with the Burin mode of retouch. Yellow triangles are the artefacts configured with the Splinter mode. b) Boxplot showing differences in weight between different modes of retouch. The weight is expressed in grams.

Order of retouch	Weight		∑ of pieces		Ratio
	∑	%	∑	%	Grams/Piece
Simple	207,9	33,5	15	37,5	13,9
Abrupt	212,6	34,2	13	32,5	16,4
Splinter	168,5	27,1	7	17,5	24,1
Burin	31,8	5,1	5	12,5	6,4

Table-12.27: Frequencies and weight of retouched artefacts with one primary type grouped by the modes of retouch. The ratio grams/piece is reported. Weight is expressed in grams.

The last structure to be tackle here is the petrological one. There are no clear differences in the morphology of lithics between different raw materials (Figure-12.24a). All 95% confidence ellipses overlap one each other in similar position. Only quartz ellipse, with a vertical elongation, is different to others, as consequence of the small quantity of quartz items. The other ellipses display in horizontal elongation in the lower part of the chart. On the contrary, there are weight distribution differences between different raw materials, as demonstrated by *H* Kruskal-Wallis test: $H\ \chi^2$ (3, N = 930) = 77.842, $p < 0.001$. The grams per piece ratio of each raw material is also different (Table-12.28). Heavier lithics are made on "archaeological quartzites" and there is a clear gap of weight with radioralite, quartz and flint. The latter two are lighter than radioralite.

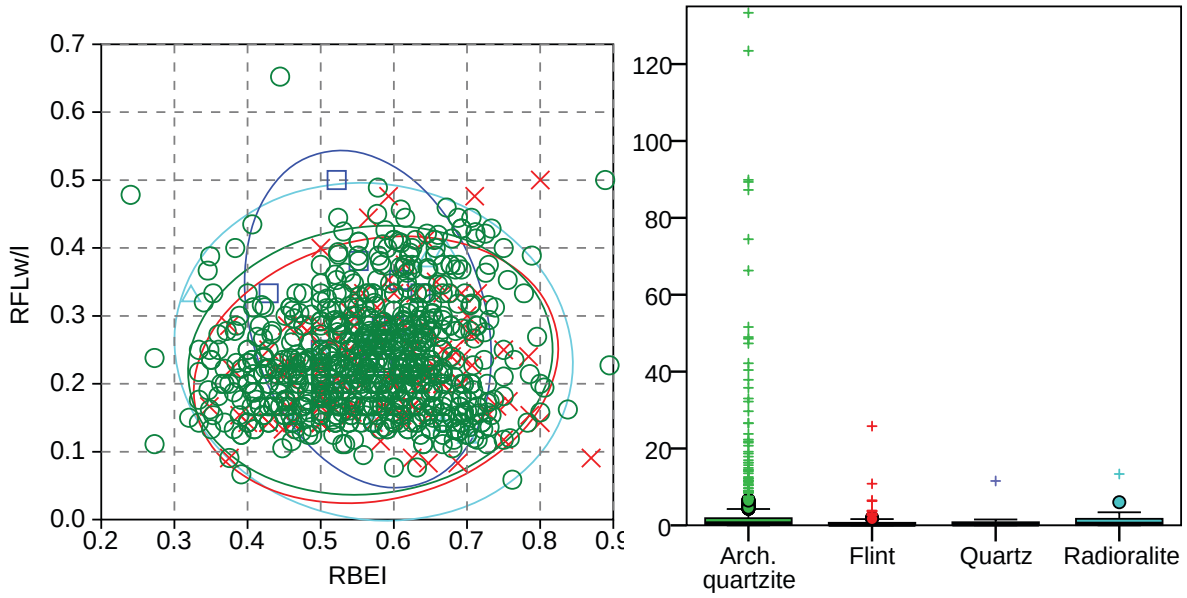

Figure-12.24: Double chart showing: a) Scatter plot of RFLw or RFLI and RBEI indexes. Green circles and ellipse are "archaeological quartzites". Red crosses and ellipse are flint. Blue squares and ellipse are quartz. Light blue triangles and ellipse are radioralite. Ellipses enclose 95% of cases of each category. b) Boxplot showing differences in weight between different raw materials. The weight is expressed in grams.

Raw material	Weight		∑ of pieces		Ratio
	∑	%	∑	%	Grams/Piece
"Arch. quartzite"	2490,2	93,9	761	761,0	3,3
Flint	115,9	4,4	141	141,0	0,8
Limestone	0,1	0,0	1	1,0	0,1
Lutite	0,3	0,0	1	1,0	0,3
Quartz	16,2	0,6	13	13,0	1,2
Radioralite	29,5	1,1	15	15,0	2,0

Table-12.28: Frequencies and weight of different types of raw material. The ratio grams/piece is reported. Weight is expressed in grams.

There are no clear differences in the morphology between different petrogenetic types (Figure-12.25a). Nevertheless, differences arise when analysing weight distribution by petrogenetic types, as proven by *H* Kruskal-Wallis test: $H\ \chi^2$ (4, N = 750) = 13.235, p = 0.01. The grams per piece ratio points that heavier lithics are made on CA type, and the lighter are made on OO, BQ, and MQ types (Table-12.29).

Petrogenetic type	Weight		∑ of pieces		Ratio
	∑	%	∑	%	Grams/Piece
CC	315,5	12,8	80	10,6	3,9
CA	372,4	15,1	50	6,6	7,4
OO	1156,4	46,8	444	59,0	2,6
SO	512,2	20,7	100	13,3	5,1
BQ	114,2	4,6	76	10,1	1,5
MQ	0,4	0,0	2	0,3	0,2

Table-11.26: Frequencies and weight of different petrogenetic types of "archaeological quartzites". The ratio grams/piece is reported. Weight is expressed in grams.

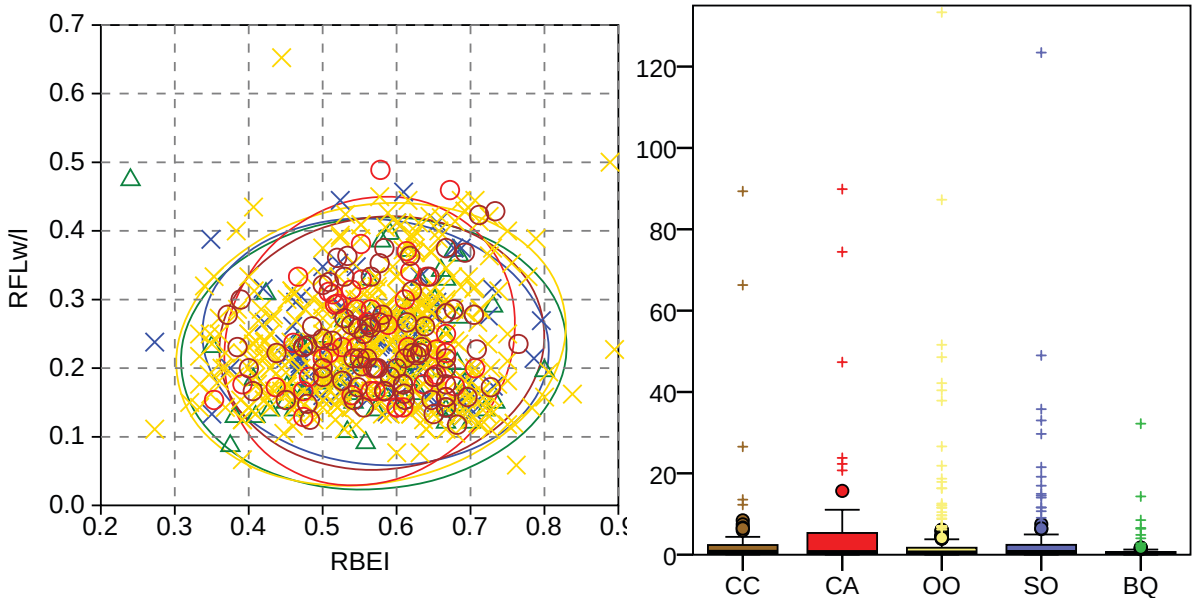

Figure-12.25: Double chart showing: a) Scatter plot of RFLw or RFLl and RBEI indexes. Brown circles and ellipse are CC type pieces. Red circles and ellipse are CA type pieces. Yellow crosses and ellipse are OO type pieces. Blue crosses and ellipse are SO type pieces. Green triangles and ellipse are BQ types. Ellipses enclose the 95% of cases of each category. b) Boxplot showing differences in weight between different petrogenetic types of "archaeological quartzite". The weight is expressed in grams.

Now, we will delve into the relationship between raw material, technology, retouch and the metrical structure, focusing on size. Starting with technology, there are clear differences in weight based on the technological order and raw material (Figure-12.26 and Table-12.30). Cores made on "archaeological quartzites" are bigger than the core made on quartz. There are differences between petrogenetic types too. Heavier cores are made on OO and CA types, and SO and BQ cores are lighter, especially the latter. The heaviest knapping products and chunks are also made on "archaeological quartzite". Deeping into the petrogenetic types of "archaeological quartzite", weight distribution is similar in knapping products. However, chunks are different, especially due to the heavier weight of those made on quartzarenite. Due to the small number of cores, comparison between types is not possible.

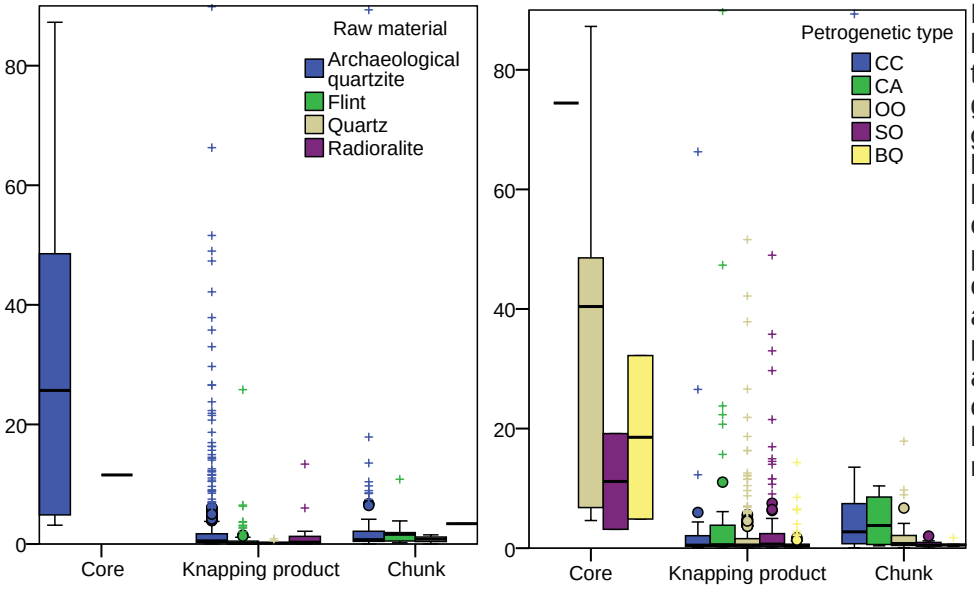

Figure-12.26: Double boxplot showing the distribution of weight in grams of all lithic remains grouped first by technological order and second by raw material in the chart on the left and by petrogenetic type in the chart on the right. There are another two knapping products made on OO and SO types of "archaeological quartzites" with higher weight than 90g, not show on chart.

Raw material	Petrgen. type	Lithic collection											
		Core			Knapping			Chunks			Total		
		∑	W	g/p	∑	W	g/p	∑	W	g/p	∑	W	g/p
Archaeological quartzite	CC				67	177	2,6	13	138	11	80	315	3,9
	CA	1	74	74	44	274	6,2	5	24	4,8	50	372	7,4
	OO	5	188	38	393	878	2,2	46	90	2	444	1156	2,6
	SO	2	22	11	89	483	5,4	9	7	0,7	100	512	5,1
	BQ	2	37	19	67	78	1,2	8	5	0,7	77	121	1,6
	MQ				2	0	0,2				2	0	0,2
	Undet.				6	17	2,8	3	2	0,7	9	19	2,1
	Total	10	321	32	668	1909	2,9	84	267	3,2	762	2497	3,3
Flint					127	82	0,6	13	27	2,1	140	109	0,8
Limestone					1	0	0,1				1	0	0,1
Lutite					1	0	0,3				1	0	0,3
Quartz		1	12	12	9	2	0,3	3	2	0,8	13	16	1,2
Radioralite					14	26	1,9	1	3	3,4	15	30	2

Figure-12.30: Double boxplot showing the distribution of weight in grams of retouched artefacts grouped first by mode of retouch and second by raw material in the chart on the left and by petrogenetic type in the chart on the right. There is another Abrupt mode artefact made on OO type of “archaeological quartzites” with higher weight than 90g, not show on chart.

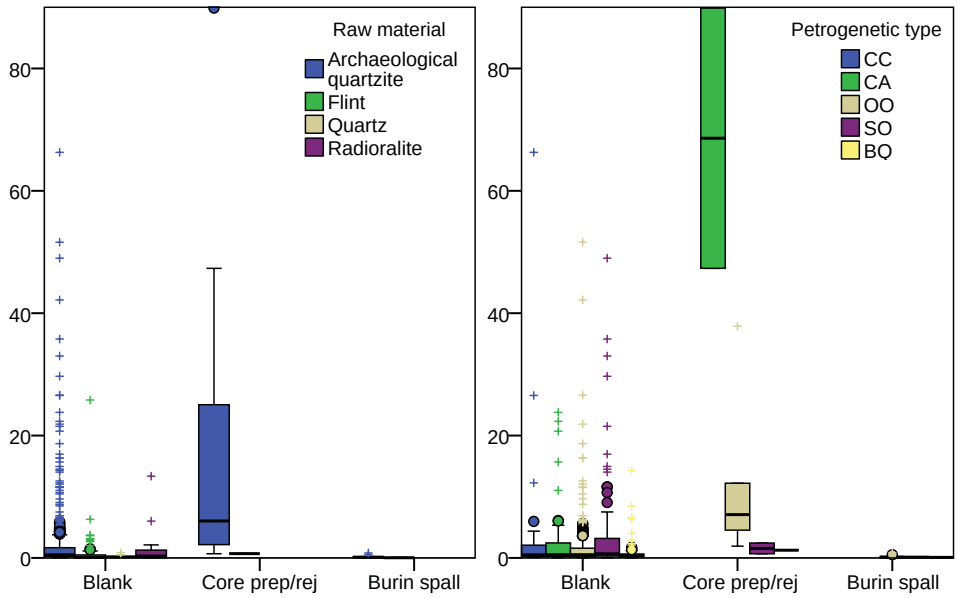

Figure-12.27: Double boxplot showing the distribution of weight in grams of all lithic remains grouped first by technological group and second by raw material in the chart on the left and by petrogenetic type in the chart on the right. There are another two blanks made on OO and SO types of “archaeological quartzites” with higher weight than 90g, not show on chart.

Raw material	Petrgen. type	Knapping products								
		Blanks			Core preparation			Burin spall		
		∑	W	g/p	∑	W	g/p	∑	W	g/p
Archaeological quartzite	CC	67	177	0,4						
	CA	42	137	0,3	2	137	69			
	OO	379	813	0,5	5	64	13	9	2	0,24
	SO	86	480	0,2	2	3	1,6	1	0	0,13
	BQ	65	77	0,8	1	1	1,3	1	0	0,09
	MQ	2	0	4,8						
	Undet.	4	3	1,3	2	14	7			
	Total	645	1687	0,4	12	219	18	11	2	0,21
Flint		120	81	1,5	1	1	0,7	6	0	0,04
Limestone		1	0	7,1						
Lutite		1	0	3,6						
Quartz		9	2	4						
Radioralite		14	26	0,5						

Table-12.31: Frequency table of different groups of knapping products grouped by raw material, including frequencies, weight and the ratio grams/piece for each case. Weight is expressed in grams.

In regard to knapping products, Table-12.31 and Figure-12.27 display the differences between the three technological groups (core preparation/rejuvenation products, burin spalls and blanks). “Archaeological quartzite” is the heaviest raw material in all three group. Focussing on specific petrogenetic types, blanks have similar weight between them, but core preparation/rejuvenation products made on CA type are heavier than others, especially SO and BQ types. Finally, weight distribution of burin spalls is similar in different petrogenetic types.

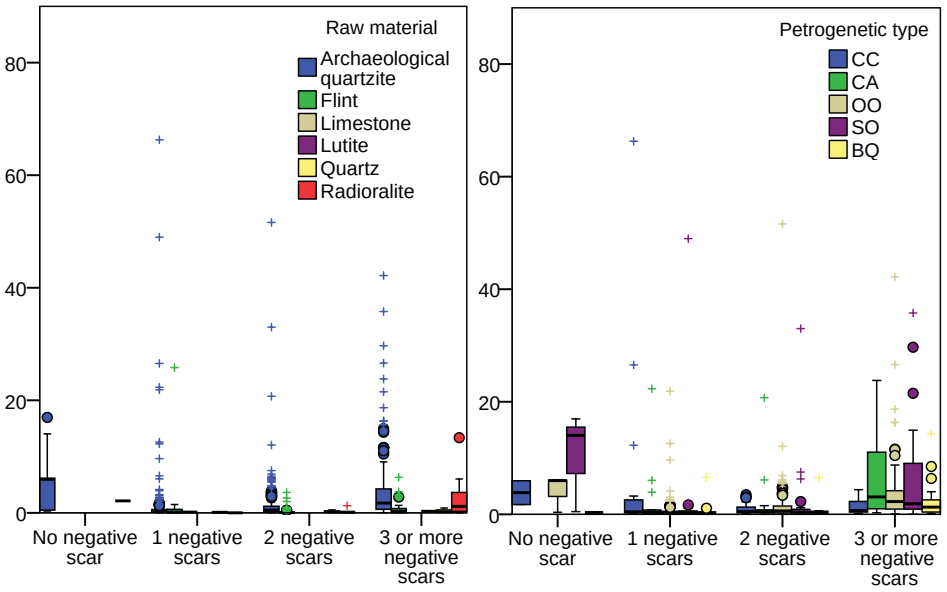

Figure-11.28: Double boxplot showing the distribution of weight in grams of blanks grouped first by the number of negative scars on dorsal surface and second by raw material in the chart on the left and by petrogenetic in the chart on the right. There is another CC petrogenetic type of “archaeological quartzites” with 296 g does not show on chart. The weight is expressed in grams.

Raw material	Petrgen. type	Blanks											
		No neg.scar			1 neg.scar			2 neg.scar			3 or more		
		∑	W	g/p	∑	W	g/p	∑	W	g/p	∑	W	g/p
Archaeological quartzite	CC	2	8	3,9	19	119	6,2	28	27	1	18	24	1,3
	CA				16	84	5,2	17	35	2	10	66	6,6
	OO	3	13	4,2	134	112	0,8	172	256	1,5	77	477	6,2
	SO	3	31	10	25	63	2,5	24	57	2,4	37	332	9
	BQ	1	0	0,3	20	13	0,6	25	14	0,6	20	50	2,5
	MQ				1	0	0,1				1	0	0,3
	Undet.				2	1	0,4	3	11	3,7			
	Total	9	52	5,8	217	391	1,8	269	400	1,5	163	948	5,8
Flint					20	32	1,6	55	15	0,3	48	34	0,7
Limestone					1	0	0,1						
Lutite											1	0	0,3
Quartz					3	0	0,1	3	1	0,3	3	1	0,4
Radioralite		1	2	0,5	1	0	0	5	2	0,3	7	22	3,2

Table-12.32: Frequency table of the quantity of negative scars in blanks grouped by raw material, including frequencies, weight and the ratio grams/piece for each case. Weight is expressed in grams.

There is no difference in the weight of blanks based on the number of negative scars between raw materials, following a general gradual increase of weight in all well represented raw material, excluding blanks without negative scars, the heaviest blanks (Table-12.32 and Figure-12.28). Conversely, there are differences in the weight of blanks depending on the number of negative scars between various petrogenetic types. There is a general decrease of CC type weight, instead the general increase of weight of other types in the increment of negative scars. Again, blanks without negative scars do not follow the same increase/decrease of weight. In addition, blanks without negative scars are heavier in the SO orthoquartzites than in other types. Furthermore, SO type, together with CC quartzarenite are the petrogenetic types in which blanks without negative scars are heavier than blanks with at least three extractions. The comparison between raw material and blanks integrity does not reveals clear differences and all of them follow the general tendency in which complete blanks are heavier than fragmented material. In the latter, proximal and longitudinal fragments are the heaviest fragments. All petrogenetic types, except the BQ quartzite follow this tendency. Moreover, it is also observable that on SO and especially on CC type, there is an increase of weight in longitudinal fragments, making similar weight to proximal fragments (Figure-12.29 and Table-12.33).

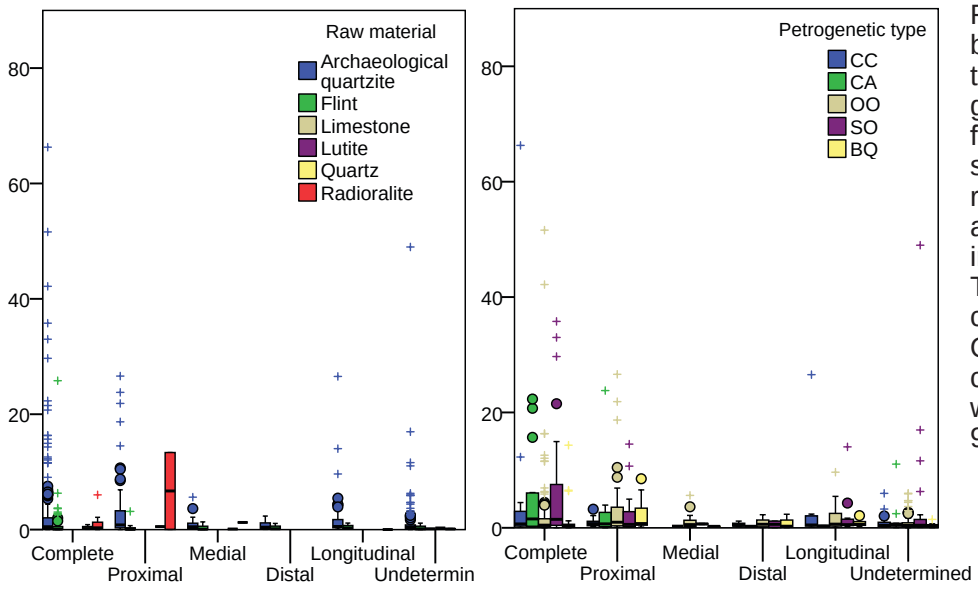

Figure-12.29: Double boxplot showing the distribution of weight in grams of blanks grouped first by their integrity and second by raw material in the chart on the left and by petrogenetic type in the chart on the right. There are another two complete blanks made on OO and SO types of "archaeological quartzites" with higher weight than 90g, not show on chart.

Raw material	Petrgen. type	Knapping products: Blanks: Complete ∑	Complete W	Complete g/p	Proximal f. ∑	Proximal f. W	Proximal f. g/p	Medial f. ∑	Medial f. W	Medial f. g/p	Distal f. ∑	Distal f. W	Distal f. g/p	Longitudinal f. ∑	Longitudinal f. W	Longitudinal f. g/p	Unknown F. ∑	Unknown F. W	Unknown F. g/p
Archaeological quartzite	CC	28	114	4,1	11	11	1				3	2	0,6	8	32	4	17	18	1,1
	CA	17	86	5,1	8	31	3,9	1	0	0,3	1	0	0,3	2	1	0,3	13	19	1,4
	OO	140	432	3,1	70	202	2,9	13	17	1,3	14	11	0,8	45	68	1,5	97	83	0,9
	SO	33	319	9,7	16	41	2,6	2	1	0,7	2	1	0,6	11	25	2,2	22	93	4,2
	BQ	22	33	1,5	11	26	2,4	2	1	0,3	4	3	0,7	9	8	0,8	17	7	0,4
	MQ	1	0	0,3													1	0	0,1
	Undet.	2	2	1,1													2	1	0,4
	Total	243	986	4,1	116	310	2,7	18	19	1	24	17	0,7	75	134	1,8	169	221	1,3
Flint		63	62	1	22	7	0,3	8	3	0,3	3	1	0,4	8	3	0,4	16	5	0,3
Limestone																	1	0	0,1
Lutite																	1	0	0,3
Quartz		4	1	0,3	1	1	0,5	1	0	0,1							3	0	0,1
Radioralite		10	11	1,1	2	13	6,7	1	1	1,2				1	0	0			

Table-12.32: Frequency table of the quantity of negative scars in blanks grouped by raw material, including frequencies, weight and the ratio grams/piece for each case. Weight is expressed in grams.

Finally, we do not observe differences in weight of chunk when they are filtered by raw material (Figure-12.26 and Table-12.30). Nevertheless, chunks have different weight distribution according to each "archaeological quartzites" type. Chunks made on quartzarenite are heavier than those made on orthoquartzite and quartzite.

Raw material	Petrgen. type	Single-retouched pieces: Simple: Sidescraper ∑	Sidescraper W	Sidescraper g/p	Endscraper ∑	Endscraper W	Endscraper g/p	Denticulate ∑	Denticulate W	Denticulate g/p	Abrupt: Abrupt ∑	Abrupt W	Abrupt g/p	Abrupt: Truncation ∑	Truncation W	Truncation g/p	Backed b/p ∑	Backed b/p W	Backed b/p g/p
Archaeological quartzite	CC	2	70	35															
	CA	2	29	15															
	OO	5	47	9,3	1	16	16	1	133	133	4	45	11				3	6	1,8
	SO	1	5	5							2	50	25	1	2	2,1			
	BQ										1	14	14						
	Undet.																		
	Total	10	150	15	1	16	16	1	133	133	7	110	16	1	2	2,1	3	6	1,8
Flint		1	3	2,6	1	3	2,7				1	0	0,5	2	1	0,4			
Quartz		1	0	0,2													1	0	0,2

Table-12.34: Frequency table of retouched pieces with one primary type sorted by mode of retouch and morphological group and grouped by raw material, including frequencies, weight and the ratio grams/piece for each case. Weight is expressed in grams.

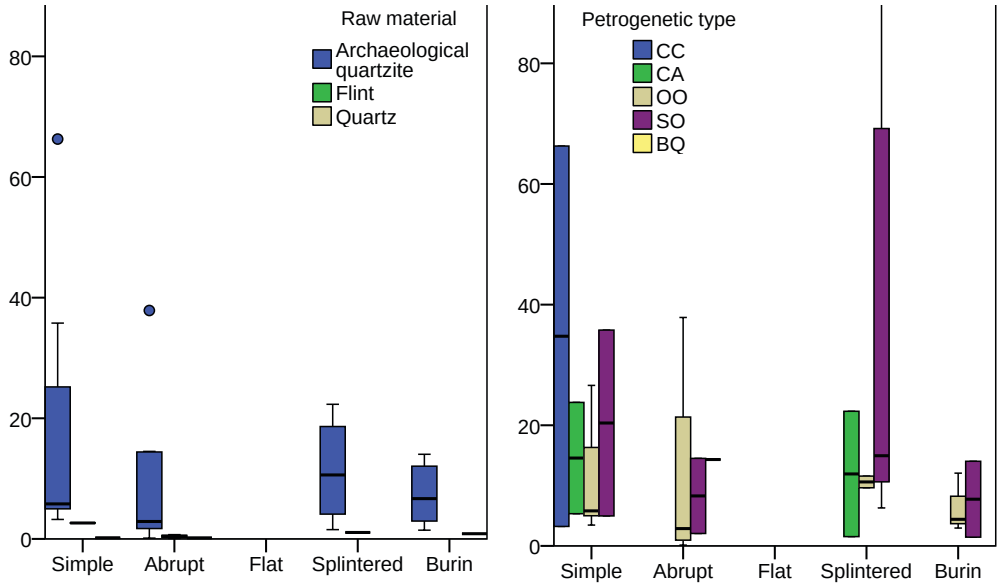

Figure-12.30: Double boxplot showing the distribution of weight in grams of retouched artefacts grouped first by mode of retouch and second by raw material in the chart on the left and by petrogenetic type in the chart on the right. There is another Abrupt mode artefact made on OO type of "archaeological quartzites" with higher weight than 90g, not show on chart.

The analysis of the relationship between raw material and retouch concludes that the biggest artefacts are made on archaeological quartzite. Meanwhile, flint and quartz artefacts are lighter (Figure-12.30 and Table-12.34). There are also differences between artefacts according to each petrogenetic type. The heaviest and more variable blanks are those retouched using the Simple mode and made on CC type. Blanks retouched with Abrupt and Burin modes, have similar weight distribution. Moreover, the heaviest artefacts retouched using the Splinter mode are heaviest on SO type.

12.6. RAW MATERIAL ACQUISITION AND MANAGEMENT PROCESSES AT LAYER CO.B.6 OF LA CUEVA DE COIMBRE

Once the raw data from this layer have been presented, in this section we bring face to face geographical, geological, and archaeological data (the matter) to understand the forces that got these materials deposited here, that is, the human raw material acquisition and management strategies.

The main acquisition process verified in this layer is the extraction of big quantities of OO orthoquartzite for human activities, as demonstrated by the great quantity of them found in this layer, both in number and in weight. Flint and SO petrogenetic types have also an important role in this lithic assemblage. The small representation of other raw materials, quartzites, and quartzarenite indicates they had different roles in the human activities carried out in La Cueva de Coimbre.

The management of raw material has been analysed including the raw data on all materials in a general reduction process model based on a simple "chaîne opératoire" (Figure-12.31). The primary technological product of lithic reduction we find in this layer are cores (irregular or discoid). From here on, we expose and analyse the different processes that generate other lithic products based on the understanding of their features.

1. Blanks as well as smaller blanks (sometimes fragmented) and chunks, were obtained as a result of the reduction process of some cores. Blanks and chunks are secondary products generated as a consequence of knapping procedures.

    a. Using retouching procedures, some of these primary blanks were modified, creating retouched artefacts as primary products and more blanks and chunks as secondary products. The latter are lighter than five grams and sometimes fragmented. In case a burin was created, there is another secondary product: a burin spall. In addition, new retouches can be made in the blanks, creating artefacts with different primary types, generating more blanks and chunks as secondary products.

        i. In one case the burin spall were later retouched, creating a retouched burin spall and some chunks and blanks as secondary products.

    b. Some other blanks were reconfigured by percussion to obtain new flakes. The resulting products are a core on flake and blanks as primary products and other blanks and chunks, derived by the reconfiguration processes, as secondary products.

i. Some cores on flakes were retouched, creating a retouched core on flake. Small chunks and blanks derived from the retouching process are, again, secondary products.

ii. As a consequence of the reduction processes of the cores on flakes, further blanks were obtained, also secondary products classified as chunks and blanks (smaller than the previous blanks).

- The latter blanks can also be retouched, creating new retouched artefacts and secondary products (chunks and blanks).

2. Going back to cores, some of them were reconfigured to obtain new flaking surfaces or new striking platforms. This process generated new forms or types of cores and three different secondary products: chunks, blanks (generally lighter than five grams and sometimes fragmented), and core preparation/rejuvenation products.

a. Some core preparation/rejuvenation products were retouched, creating retouched preparation/rejuvenation products. As a consequence, small chunks, blanks or burin spall were produced as secondary products.

Some of the chunks were also retouched. They are always heavier than five grams. Blanks and chunks were generated as secondary products of retouch techniques and they are generally lighter than five grams.

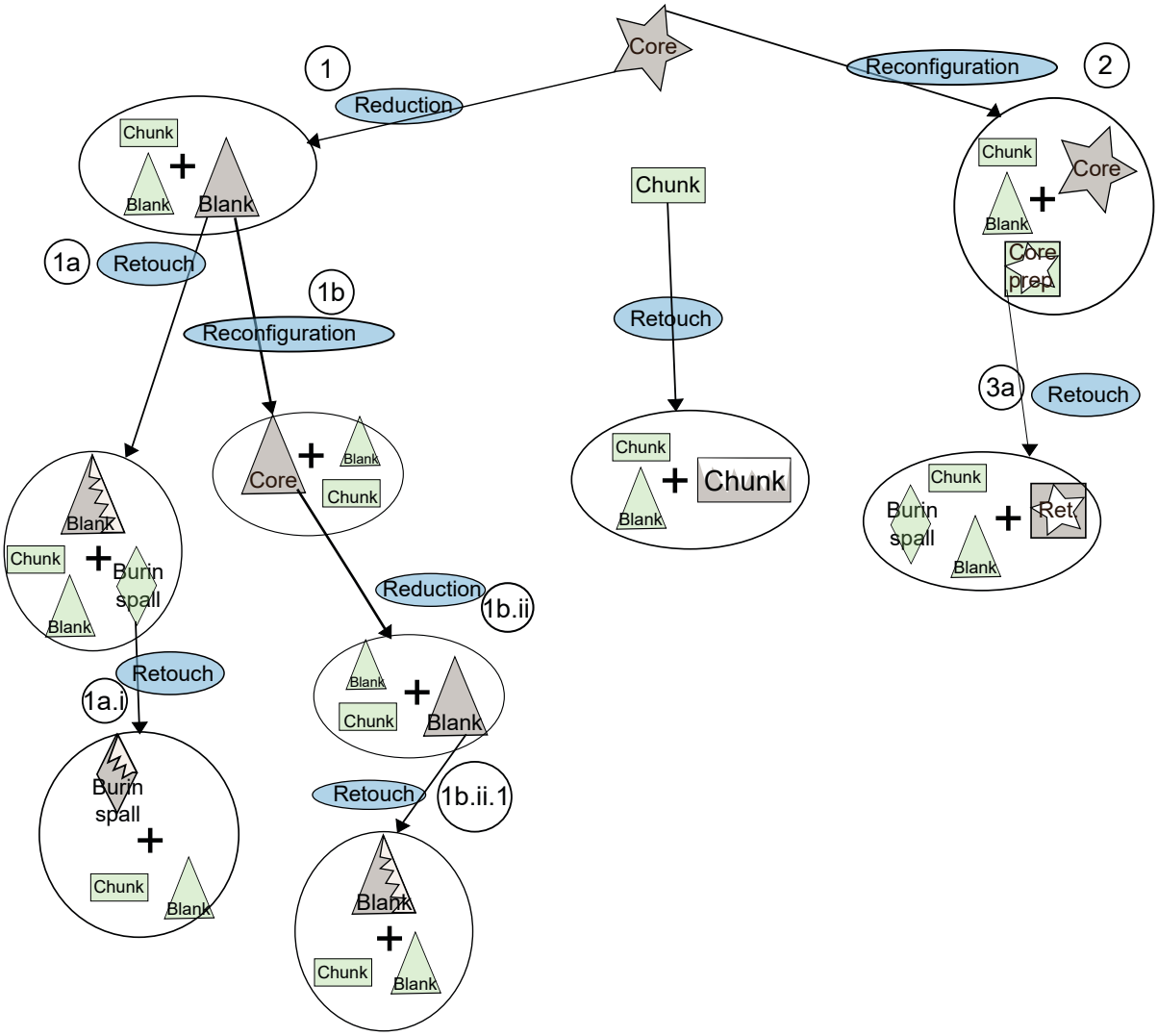

Figure-12.31: Schematic “chaîne opératoire” derived from the analysis of the lithic assemblage from layer Co.B.6 of La Cueva de Coimbre. Stars represent cores, rectangles chunks, diamonds burin spall, squares with stars core preparation/rejuvenation products and, triangles blanks. Zig-zag lines added to any of these icons represent retouched artefacts. Grey icons are primary products and green ones secondary products. The blue ellipses indicate human activities. Alphanumeric codes inside circles are references to the text.

Next, we present the conclusions reached about the acquisition and management of, first, "archaeological quartzites", and latter other raw materials. Figure-12.32 and Figure-12.34 schematically represent the acquisition process of "archaeological quartzite" and other raw material, respectively. Figure-12.33 displays the relationship between acquisition and management strategies. Finally, Figure-12.35 shows the cost map from La Cueva de Coimbre with the geological formations where raw material could have been caught.

As it has been previously mentioned, "archaeological quartzite" is the most relevant raw material, both in number and weight, present in the layer Co.B.6 in La Cueva de Coimbre. Here we will explain the raw material catchment and management strategies of this raw material by petrogenetic type.

The CC type is a frequent type of "archaeological quartzite" in weight and number. Not all technological categories are represented: Cores, core preparation/rejuvenation products, and burin spall are absent. There is an overrepresentation of chunks and an underrepresentation of knapping products. Despite the presence of significant quantities of lithic remains, the complete knapping reduction process is not completely represented. However, the weight of chunks and knapping products, which range from less than one gram to more than 80 g, supports the idea of knapping and reshaping activities were practiced in the site. The grams/piece ratio makes it clear that CC type materials are heavier than other raw material, but they are lighter than other petrogenetic types of "archaeological quartzites" such as SO and CA types. There are only two retouched artefacts, a small number in comparison with those of other petrogenetic types. In addition, both retouches are the most frequent morphothema in the assemblage: Sidescraper. Negative dorsal scars on dorsal surfaces are diverse, even most of blanks have two scars. Cortical surfaces on knapping products and chunks made on CC petrogenetic type are more abundant than in other petrogenetic types, showing similar percentages than CA type. All these reason carried us to propose this material was low intensity exploited.

This petrogenetic type is characterised by multiple grain size varieties, generally with heterogeneously grain sizes. Colour is also greatly heterogeneous, due to the impact of many different non-quartz minerals on these rocks. Nevertheless, we could not properly define colour varieties due to the absent of correlation between colour and non-quartz minerals. The presence of bedding on these quartzarenites is uneven. All these elements lead us to conclude: a) the CC petrogenetic type is heterogeneous, and b) the input in the site of CC quartzarenites comes from different pebbles from diverse origins. Dark and brown quartzarenite, the most frequent, are linked with the Murcia Formation or with carboniferous sandstone strata such as the Potes, Mogrovejo or Viorna formations, while white CC type are related with the CC type from Barrios or Cavandi formations. Nevertheless, the analysis of cortical areas reveals the fluvial origin of all the cortical surfaces. Therefore, we proposed that the CC petrogenetic type is a raw material caught in fluvial beach deposits, probably near the site of La Cueva de Coimbre. In nearest tributary to Cares river beaches, there is an important presence of this petrogenetic type with tabular or plain morphologies and different grain size varieties. These CC quartzarenites derive from the Barrios Formation that massively crops out in the Cuera Mountain Range. They are generally white or brown coloured. In the Cares River, the quantity of this petrogenetic type decrease, but there are more colour/mineral and grain sizes varieties. In addition, the general size and morphological features of CC pebbles in these beaches is also heterogeneous: multiple sizes (from medium pebbles to big cobbles) and both spherical and elongated morphologies are present. Then, strong selection mechanisms would not have been required for the acquisition of this type. In addition, it can be said there is no selection based on colour or on grain size. The relationship of this information with the management ones reveals that the input of CC type is made through a consciously input, not as cores, but as knapping products. The scale of this type in this site and the small quantity of retouched artefacts reveals its use as raw material in non-specific activities, maybe related with the scarcity of other petrogenetic types or raw materials more suitable.

The CA type only constitutes a small portion of the total of "archaeological quartzites" and it is worst represented than the CC type, with 50 items. In this case, all three technological orders are present, although there are no burin spalls, neither core on flakes. The distribution of the three technological orders is similar than the general frequency of all "archaeological quartzite". There are four retouched artefacts, but due to the small quantity of CA implements, its proportion is greater than other petrogenetic types. In addition, one of the retouched blank has two different primary types. The most frequent mode of retouch is the Splinter one, pointing at an intentional selection of this material for specific activities. Moreover, Sidescraper, the most frequent artefact in the assemblage, is also characterised. Weight of blanks and chunks ranges from less than one gram to more than 80 g. This proves that knapping and reshaping processes were carried out in the site. The average weight of this type reveals this CA type as the heaviest raw material of the assemblage. Nevertheless, this is

the consequence of the weight of the core and the two core preparation/rejuvenation products, heavier than the average of all "archaeological quartzite". Together with previous quartzarenite, this type has the greater presence of cortex on blanks. Nevertheless, cortical areas generally cover less than 33% of dorsal surfaces. The quantity of dorsal scars is diverse, but most of blanks have less than three negative extractions. These features indicates this type of quartzarenite as weakly exploited raw material, similarly to the CC type. Nevertheless, and due to the characteristics of retouch, we consider this quartzite have a special role in the activities carried out in this occupation of La Cueva de Coimbre.

The characterisation of this petrogenetic type reveals the presence of two varieties: the most frequent one is characterised by heterogeneous grain size distribution around medium or coarse quartz sizes. The other variety is less frequent and it is characterised by homogeneous grain size distribution around fine and medium sizes. Colour change is not supported by mineral differences. Moreover, brown and grey-dark CA quartzarenite are well represented. In addition, there are also some white lithics. These features suggest a) the CA type is very variable, b) the input of CA quartzarenites to the site got supplied with pebbles from different origins, and c) there was a preferential selection of homogeneous grain size variety. Colour links this quartzarenite with the Barrios or Cavandi outcrop formations in the case of white or brown/clear varieties and with clasts from Carboniferous conglomerate formations, especially for the brown or dark-grey CA type. However, the characterisation of cortical areas points at the only presence of cortex from fluvial sources. Therefore, we proposed that CA petrogenetic type were brought to the site from fluvial deposits, probably near the La Cueva de Coimbre. The presence of this type in the tributary rivers which erode the Cuera Mountain range (where Barrios Formation crops out) is small. Therefore, stronger selection mechanism are require to acquire this type than previous CC one. These mechanism would have been stronger for getting specific varieties. In the Cares beaches near the site, the average of CA quartzarenite is similar. Nevertheless, dark-grey or dark-brown varieties are rarer in Cares River and they are not represented in tributary to Cares River. We propose catchment of CA quartzarenites was based on sporadic activities, complementary to other tasks, such as acquisition of different resources in river beaches or catchment of other raw material. The input to the site could have been made in form of core. The latter was reduced in the site to obtain systematically blanks, using corrective mechanism in the management of the core. The latter, was probably discarded in non-exhausted stage of exploitation. The core and the two preparation/rejuvenation products have similar colour and grain size (grey-black and heterogeneous grain size distribution), supporting the input and reduction of, at least, one core. In addition, other varieties were input in the site, probably as blanks or retouched artefacts.

The OO petrogenetic type of orthoquartzite shows clear differences in management and catchment in comparison with the types of "archaeological quartzite" tackled above. It represents 58% of "archaeological quartzite" assemblage in number and 47% in weight. These data mean there was a planned and intensive exploitation of this type. The three technological categories considered, as well as all knapping products groups, are present in this layer. In addition burin spall are frequent. It is obvious knapping and reshaping activities were practised in the site. This is also certified by the presence of blanks and chunks between less than one gram to more than 130 g. Core types, weight, and flacking and knapping surfaces reveal this raw material is more intensively exploited than the quartzarenite group exposed in the previous paragraphs. The presence of negative scars is more frequent than in the former two types, but is scarcer than more deformed types of "archaeological quartzites" or flint, especially in the category of at least three negative scars. The presence of cortical areas in dorsal surfaces is smaller than in previous types, showing similar rates than BQ type. Retouched artefacts are less frequent than previous type, although they are more frequent than on CC, BQ or MQ types. In addition, artefacts with multiples primary types on them are frequent and all morphothemas are defined in this petrogenetic type. It is noticeable that the only Backed Blades and Points, Endscraper, and Denticulate are made on OO type blanks. This evidence reveals medium intensity exploitation. The grams per piece ratio of the lithics, smaller than that of quartzarenites and SO type agree with this hypothesis.

The characterisation of this raw material based on size and colour indicates it is a more homogeneous type. Most of the OO type are medium size varieties, with two different grain distribution: the homogeneous one and the heterogeneous one. Both varieties are frequent. According to colour, the most frequent variety is the white or light-grey associated to stable presence of non-quartz minerals, probably as a result of the intensive input of this variety in the site. The dark variety is rarer, probably as a consequence of the transportation of a few blocks of this variety. The original source strata of lighter colour variety is in the more deformed bands of the Barrios outcrop formations, as well as in the pebbles from older strata in the carboniferous conglomerates. The darker variety originates

exclusively in the latter. The characterisation of cortical areas reveals that most of them come from fluvial deposits. Still, the cortex of two lithics derive from conglomerates. There is no evidence of outcrop cortex. Therefore, although the most likely source strata are the Barrios Formation, catchment was probably made in deposits and conglomerates. Due to the small number of pieces with cortex from conglomerates, the latter catchment area must be nuance. Most of the conglomerates have OO orthoquartzites, more frequently the lighter varieties. Remoña (24 CU), Campollo (27), Lechada (28), Narova (29CU), the Curavacas series (31 CU), Potes (31 CU), Pesaguero (34 CU), Valdeón (38 CU), Maraña-Brañas (39 CU), and Pontón (41 CU) conglomerates have important amounts of this type. However, at least low intensity selective mechanisms are necessary to choose specific varieties, forms and sizes. All these conglomerates are to the south, in medium altitude plateaus, in Deva and Cares basins. In fluvial deposits the presence of this petrogenetic type is scarcer. Therefore, the selective mechanisms required picking up special varieties, forms and sizes would have been more intensive. We do not find this type in tributaries to Cares River in La Cuera Mountain Range during our fieldwork surveys. In the lower part of Cares River deposits, the presence of this type is scarce. The cortex of black variety only derives from fluvial deposits. The quantity of this variety is scarcer than previous one in these fluvial deposits.

All in all, catchment of this type would have been in fluvial deposits areas, which would have

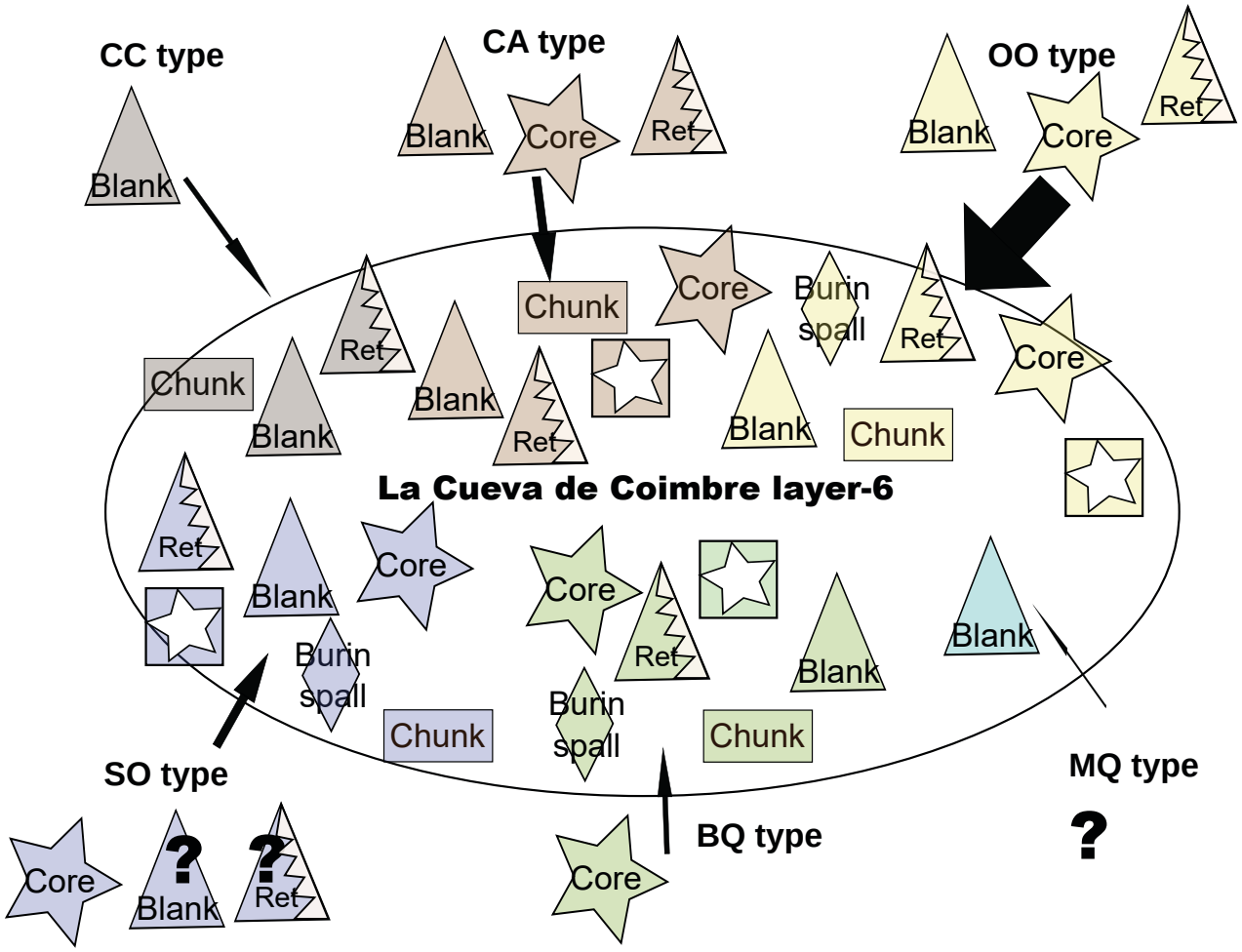

Figure-12.32: Schematic representation of the input of the different petrogenetic types of “archaeological quartzite”, taking into account the different technological products present. Stars represent cores, triangles blanks, diamonds burin spall, triangles with zig-zag retouched material, ellipses fully cortical chunks and rectangles chunks. Question marks indicate products whose presence is not certain.

provided big amounts of material as a results of planned raw material procurement strategies. In addition, we also observe traces of procurement of stone in conglomerate areas in the headwaters of Deva and Cares basins, or outside of research area. The arrival of the lithics to the site was made as core, reduced through knapping activities to obtain blanks for human activities. These cores were maintained to obtain new flacking surfaces and new percussion platform, and they were discarded

in different stages of reduction. In addition, there is an input of this OO orthoquartzite as blank or retouched material.

The SO petrogenetic type shows different management and catchment strategies in comparison with the previous types. Thirteen percent of the implements in "archaeological quartzites" and 21% of the total weight of this raw material belongs to the SO type. As in the previous type, the three technological orders, as well as core preparation/rejuvenation products and burin spall are represented in this layer. It is clear knapping and reshaping activities were carried out in the site, as demonstrated by the presence of blanks and chunks with weight between less than one gram and more than 120 g. Moreover, most frequent lithics are between 0.1 and 50 grams. Core types, weight and flacking and knapping surfaces reveal this raw material was intensively exploited. The presence of negative scars on dorsal surfaces is more frequent than in the previous type, especially due to the great rate of blanks with at least three extractions. Nevertheless, cortex invasiveness in blanks is broader than on previous type. The proportion of retouched artefacts is the highest of all "archaeological quartzite". Splinter, Abrupt, and Burin modes are the most abundant retouches. It probably evidences this petrogenetic type devoted a special role on the assemblage. This evidence indicates this material was intensive exploited, even though the grams per piece ratio of lithics, is heavier than on previous type.

The characterisation of this raw material reveals there are two different grain size varieties of the SO type, which are also associated with colour/mineral features: the most frequent is the dark-grey variety with fine grain size. The less frequent variety is grey or light-grey and it is associated with medium grain size. The original outcrop strata of the two varieties defined is not located in the research area, but they can be found in conglomerate strata and deposits. The conglomerates with the SO petrogenetic type are the Lechada, Maraña-Brañas, Pontón, Potes, Remoña, and Valdeón conglomerates. In all of them the presence of the fine grained variety range between 5 and 50%, except for the Lechada and Potes conglomerates, where they represent less than 5% of the pebbles. The presence of coarse variety is restricted to the Pontón conglomerates. The analysis of cortical surfaces reveals the acquisition was mixture between conglomerate and river deposits, even though cortex from river deposits is more frequent than from conglomerates. All four lithics with cortex from conglomerates are part of the fine grained and dark-grey SO variety. The presence of SO orthoquartzites in beach deposits is negligible, especially near fluvial deposits. We propose the input of this type to the site is mixed: on one hand, there are occasional findings in river deposits in relation with other activities, such as journeys along rivers or in planned acquisition of other abiotic and biotic resources. This strategy requires strong selection and identification mechanism of raw materials. On the other, there is a planned catchment strategy carried out in conglomerates. This strategy require medium or long distance movement in north-south direction or in East-West direction (in case the acquisition was made outside of our research area). The two only cores made on this type are from coarser and light-grey variety, while the two core preparation/products are made on the fine and dark variety. Then, the input of this type is made, at least from two different lithic mass, reduced through knapping activities to obtain blanks. The two cores where abandoned with low weight, indicating they were almost exhausted or exhausted. The two core preparation/rejuvenation products points at the movement of cores outside the site for subsequent exploitation. Therefore, the input in the site was made as core. Moreover, we consider the input of this type into the site could have been made as blank or retouched artefacts.

The management and catchment strategies observed in the previous types are different in this **BQ quartzite type**. The small frequency of lithics made on this type and their weight reveal its smaller quantitative importance in the assemblage. All the technological products, as well as core preparation/rejuvenation products and burin spall are identified in this assemblage. Therefore, it can be concluded that knapping and reshaping activities were performance in the site. The presence of chunks and blanks between less than one gram and more than 30 grams supports this statement. The gram/piece ratio, especially that of blanks, indicates lithic implements in this type tend to be lighter to other types (except the MQ quartzites). Core types, weight and flacking and knapping surfaces reveal this raw material was intensively exploited. The small frequency of cortical areas in dorsal surfaces and the high frequency of blanks with more than three dorsal scars also point out this resource was intensively exploited. Nevertheless, retouched artefacts are less frequent than in other types, and the only artefact made on this type is an unspecific Abrupt. All in all, the data gathered demonstrate the management of this quartzite was intensively exploited and all phases of lithic reduction were performed in the site.

The petrographic characterisation of this type certified the presence of two different varieties

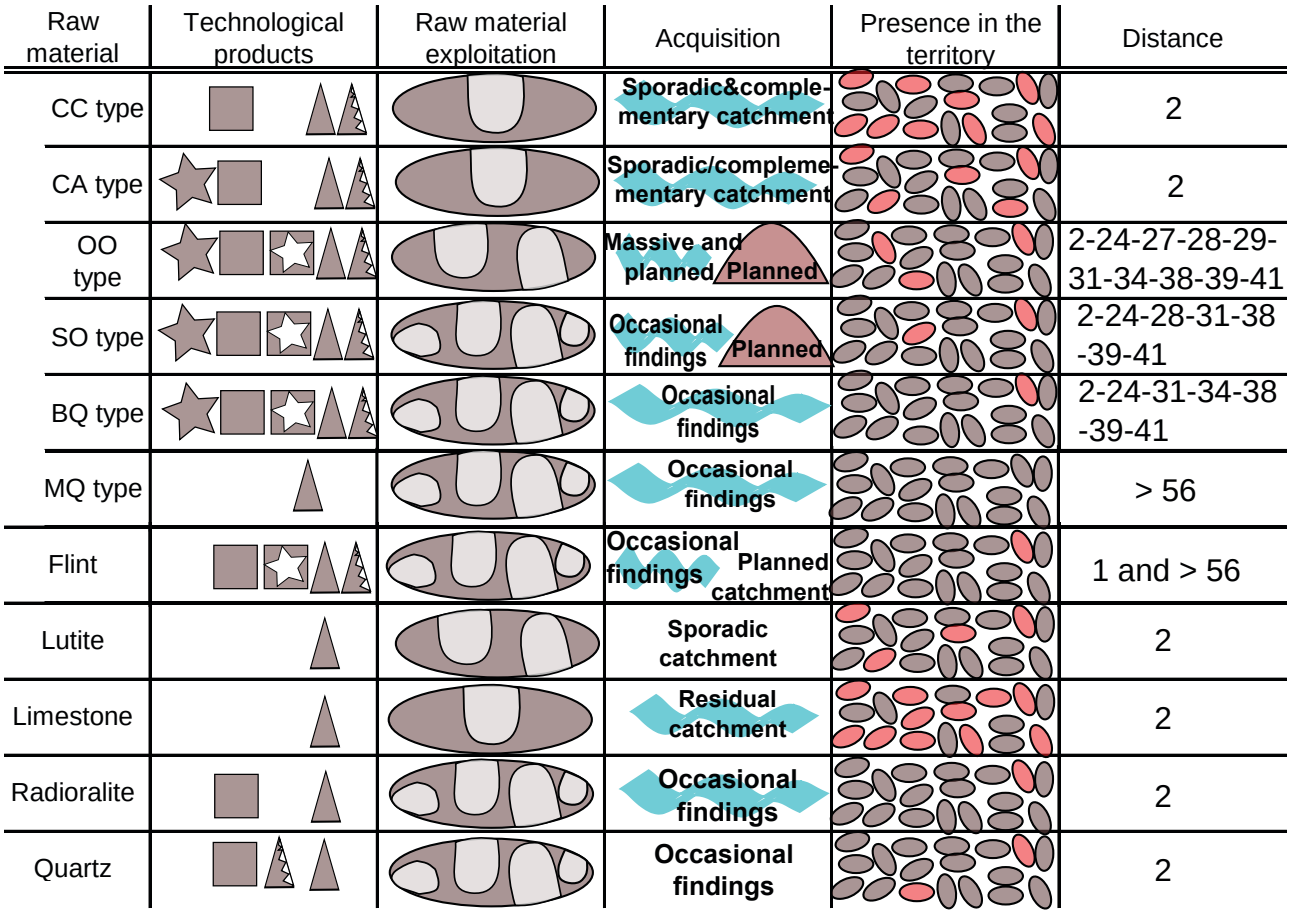

Figure-12.33: Schematic representation simplifying raw material acquisition and management evidences from layer Co.B.6 of La Cueva de Coimbre. In the column “Technological products” stars represent cores, squares chunks, squares with starts core preparation/rejuvenation products, and triangles blanks. Zig-zag lines added to any of these icons represent retouched artefacts. In the column “Raw material exploitation”, circles represent unexploited raw material, ovals with one scar represent low intensity raw material exploitation, ovals with two scars represent medium intensity raw material exploitation, and ovals with four scars represent high-intensity raw material exploitation. In the column “Acquisition” waving blue lines represent river acquisition and brown semicircles represent conglomerate acquisition. In column “Presence in territory”, the complete set of ovals represents all the raw materials available in the territory. The ones highlighted in red represent the proportional presence of each specific raw material in the territory. Higher presence of the latter means weaker selection degree.

of BQ type: the fine grained and black or dark-grey variety, which it is the most frequent one, and the medium grained and light-grey variety, which is less represented. We did not find the original outcrop strata for this type of quartzite in the field survey. However, it was clearly identified in some small conglomerates. There are important quantities (between 5 and 50%) of BQ quartzite in the Remoña, Valdeón, and Pontón conglomerates. In other conglomerates, such as Maraña-Brañas, Pesaguero, and Potes conglomerates, it is scarcer. The presence in fluvial deposits is negligible, with smaller frequency than 1% in Cares River beaches, but without representation in fluvial deposits in the tributaries to Cares River. In Deva River, its frequency is even smaller than in Cares River. All identified cortical surfaces in the lithics reveals that all BQ quartzite were acquired in fluvial deposits. Therefore, it can be deduced catchment activities of the BQ type is based on the extraction of small quantities of this material in river deposits, probably derived from occasional finding in river deposits in relation to other activities, such as journeys along rivers or the acquisition of other resources. This activities require low range of mobility and intensive identification and selection mechanisms. The irregular core is in the medium grained variety, while the core on flake, in the fine one. The core preparation/rejuvenation product is made on the first variety. Therefore, at least two different cores were introduced in the site. Probably a core was latter brought into other locations, revealing the role devoted to this raw material by Upper Palaeolithic societies and the existence of stock in core forms. In addition, the presence of a burin spall without correlation with any burin, support the existence of fragmented sequence of knapping and resharpening “chaîne opératoire”. Therefore, the input of the material probably was made as cores, reduced for obtain blanks for human activities. We do not

consider the input of other technological products due to the absence of more varieties and the small quantity of this BQ quartzite in the complete assemblage.

There are only two pieces made on **MQ quartzite type**, therefore, the conclusion here shown must be nuance. Both quartzites are blanks, one with one negative scars and another with, at least three. There is no cortex on dorsal surfaces. None of the blanks have retouch. The grams per piece ratio is the smallest regarding every raw material. All these reason carried us to propose this two blanks were secondary products derived from knapping or resharpening processes. We do not find the primary product obtained from these actions. The absence of petrological differences between both blanks, makes us to consider that both derived from the same lithic mass. We do not find any evidence of this quartzite in the research area surveyed. Then, the only possibilities are it is a) in non-surveyed strata, b) outside of the research area, or c) hidden in deposits or conglomerates in small frequency. We were unable to propose possible catchment strategies due to the absence of cortical surfaces.

Next we will explain the raw material catchment and management strategies of other raw material than “archaeological quartzites”. These material are not frequent at layer Co.B.6 of La Cueva de Coimbre assemblage. Nevertheless, they reveal different roles as raw material and interesting catchment and management behaviours.

Starting with **the flint**, the analysis of the technological products made on this material points at the absence of cores. Nevertheless, the presence of core preparation/rejuvenation products could show a hidden presence of cores. Burin spall is more frequent than in other raw material, probably related with a high intensity exploitation of this material, also suggested by previous studies (Álvarez-Alonso et al., 2017). The occasional presence of cortical areas and the high presence of negative scars on this raw material do also support the idea of intense exploitation. Grams per piece ratio of lithics made on flint is the smaller one, supporting previous hypothesis. In addition, the representation of chunks and blanks with weight smaller than five grams reveals that knapping and retouching activities were carried out in the site. The frequency of artefacts with retouch on flint is similar to those made on “archaeological quartzite” blanks but is less frequent than on quartz.

The colour of flint pieces is diverse: black, brown/orange, grey, or white, suggesting different source area. The presence of Palaeozoic Black cherts, such as the Vegamián Formation is clear (Herrero-Alonso et al., 2016), also other types of flint such as Piloña, Flysch, Monte Picota/Piedramuelle, Urbasa, or Chalosse, as it was suggested by previous studies (Álvarez-Alonso et al., 2017). All nine identified pieces where cortex could be characterised points at its possible fluvial origin. This indicates the context where catchment activities were carried out, secondary deposits. The information derived from the geological surveys conducted during this research and from other studies in the surrounding area reveals a negligible presence of flint in river beaches, reduced to small sizes and relatively tabular forms (Álvarez et al., 2013). These findings correspond with Vegamián flint. Other types of flint, then, must be caught outside of research area (Tarriño et al., 2015). Therefore, catchment activities are mixed: the first one correspond to local flint, and it must have necessarily implied intensive selection of raw material in fluvial deposits. These would have not been planned or based on systematic exploitation strategies. Flint catchment would have been based on occasional findings in river courses as a result of casual transit or other activities. The second catchment strategy correspond to non-local flint, and it must have necessarily implied distance movement strategies of acquisition of raw material or maybe based on raw material exchange. This high intensity exploitation of flint deduced on the analysis of technological and metrical features suggests the qualitative importance of this raw material. Furthermore, quantitative information reveals the scarcity of this material in surrounding area. The interaction between qualitative and quantitative information unveils the importance of this raw material for human activities that maybe could have been related with knapping and use properties, but also with its scarcity. In addition, considering presence of all types of technological products (or at least sings of them), we conclude that all phases of lithic reduction were carried out in the site. Due to the high quantity of different flint types, we consider this raw material was brought into the site as core, blanks and retouched artefacts.

The third most frequent raw material in quantity is **the radioralite**. There are only 15 lithics made on this raw material. There is no core made on this raw material, neither core preparation/rejuvenation products, or burin spall. There is neither retouched artefacts. There is only one chunk. The quantity of negative scars on blanks is diverse, although most frequent blanks have, at least three negative scars. Cortical representation on blanks is small, and only one has cortex broad than 66% of the surface. Previous features suggest this material was intensively exploited one. Nevertheless, the absence of retouched artefacts make us to nuance the latter conclusion. Weight distribution

reveals this material is lighter than the overall distribution, reinforcing this material was intensively exploited, also that knapping activities were carried out in the site (in small occurrences).

Regarding the physical features of radioralites, all of them are red to brown or black and are characterised by the presence of Radiolaria fossils. We only find evidence of radioralite in the area surrounding the fluvial deposits of Cares and Deva rivers, in negligible proportions and small sizes. Therefore, catchment activities would have necessarily implied strong and intensive selection mechanisms, similar to those observed for local flints. This means that the acquisition of radioralite would have been related with occasional findings, rather than with intensive and planned raw material selection strategies in river beaches.

Quartz has similar pattern of acquisition and exploitation than two previous raw material. The

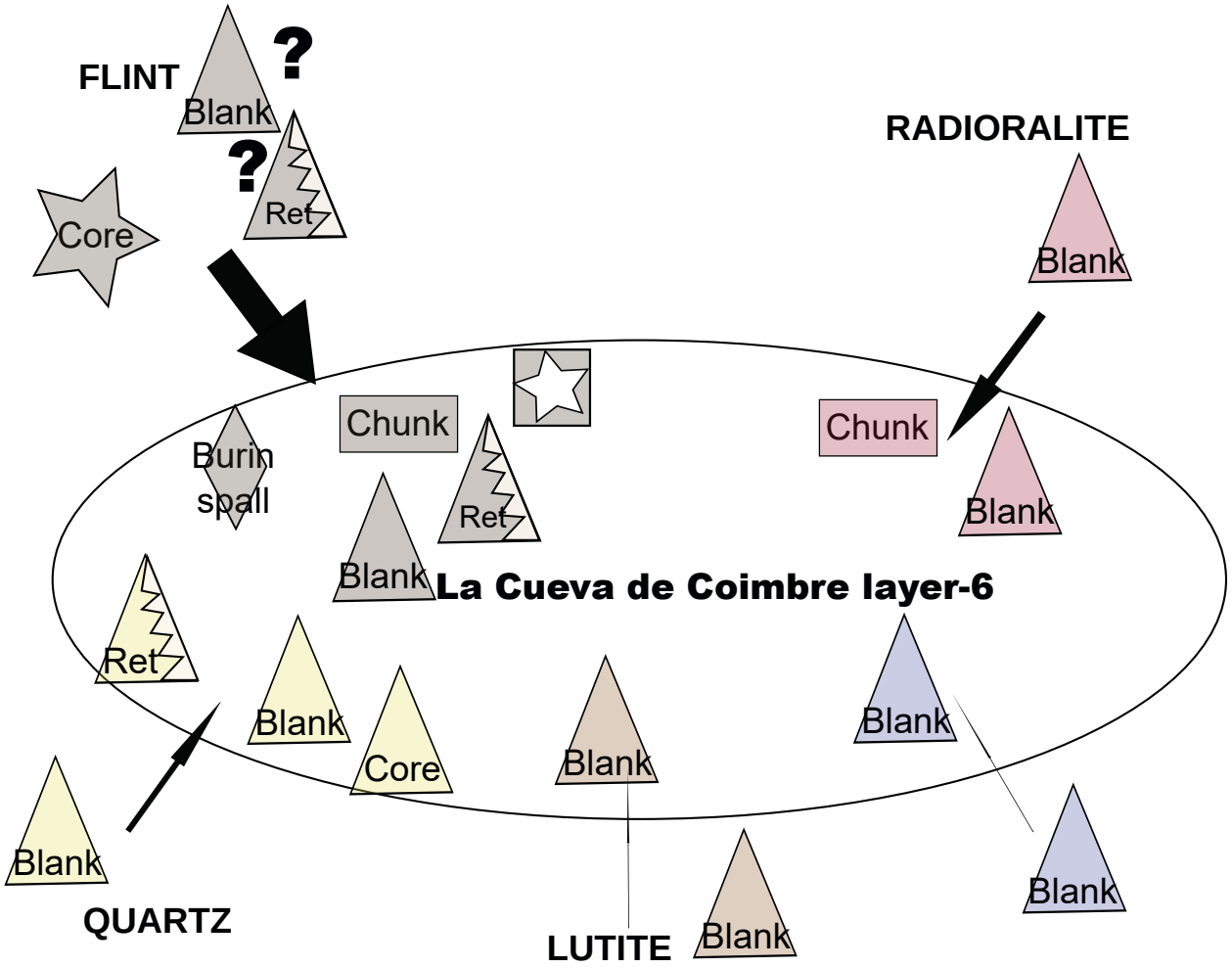

Figure-12.34: Schematic representation of the input of non-“archaeological quartzite” raw material, taking into account the different technological products present. Stars represent cores, diamonds burin spall, triangles blanks, triangles with zig-zag retouched material, ellipses fully cortical chunks and rectangles chunks. Question marks indicate products whose presence is not certain.

quantity of this material is, again, reduced (13 items). Therefore, the conclusion must be nuance. Not all types of technological products are present, due to the absence of burin spall and core preparation/rejuvenation products. In addition, the only core is a core on flake. Knapping products are underrepresented due to the presence of chunk and core, also hampered the small number of items made on quartz. The quantity of negative scars on blanks is varied, and cortical areas on dorsal surfaces are not represented. The frequency of retouched artefact is the highest of all analysed raw material. These data suggest an intensive exploitation of this raw material. The grams per piece ratio also point out in this hypothesis. In addition, weight distribution points that knapping or resharpening activities were carried out in the site. Finally, it is also noteworthy that one of the only three backed blade is made on this material, reinforcing the idea of a specialised role of quartz.

Regarding the properties of quartz, all of them are transparent, slightly white and none of them is

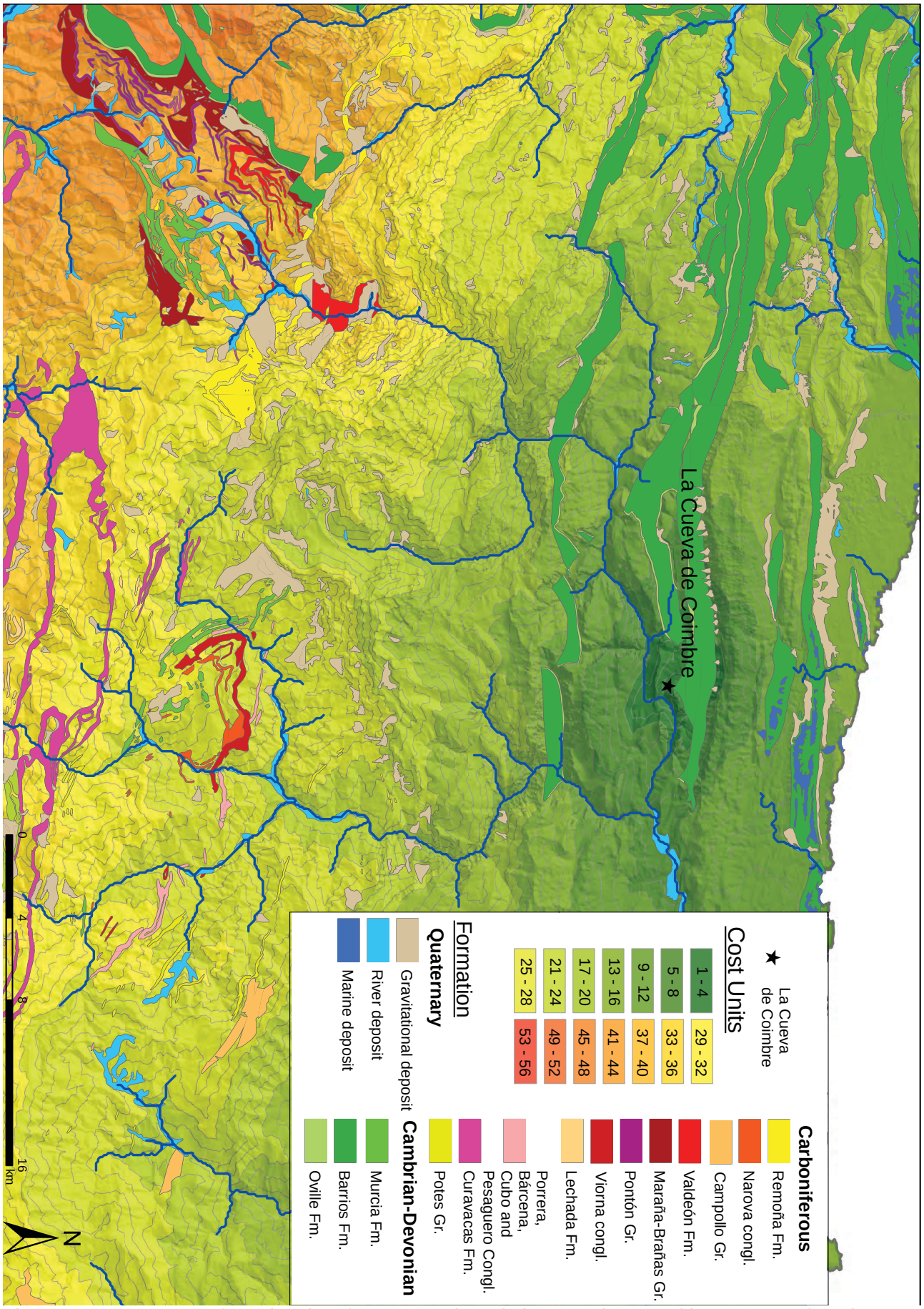

Figure-12.35: Cost map from the site of La Cueva de Coimbre to polygons with presence of “archaeological quartzites” and others raw materials.

an aggregate of different quartz crystals. In the research area defined for this study we only identified quartz on fluvial deposits in negligible proportions, mainly in the headwaters of Deva and Cares rivers. Due to the scarcity of diagnostic elements to characterise the source area, we can only affirm they were caught in fluvial deposits. As it happened in the case of flint and radioralite, its presence is scarce. Then, the catchment of this material would have required strong selective mechanism. Still, the acquisition of quartz would have probably been more related with occasional findings rather than with intensive and planned raw material catchment strategies. The intensive exploitation of the material reveals its importance for prehistoric societies. However, considering the absence of cores (not core on flake), quartz was probably brought to the site as blanks, and only reshaping processes were carried out in the site. We do not discard direct input of retouched pieces later reshaped in the site either.

The lutite is only represented by one lithic. The conclusion here exposed, then, must be nuance. It is a blank with at least three negative scars and without cortical area. It is a low weighted blank. There is no retouch on the blank. Then, the input of the lutite must be made in the present form. We consider there is no knapping or retouching activities of this raw material in the site. The lutite is grey to black and it is similar to the siliceous cemented varieties found in the area around the site, in outcrops (associated to limestone, sandstone and conglomerate alternations from the Carboniferous), conglomerates (Carboniferous), and river deposits. Their presence in the latter two was analysed in this research, revealing changeable percentages generally greater than 10% of the rocks present in both types of contexts. This raw material has also been analysed in archaeological contexts from other regions, such as the Basque Country (Fernández-Eraso et al., 2017). Due to the absence of cortex, we could not determine the context where this lutite were caught. Nevertheless, the selection of siliceous cemented variety is clear.

There is only one lithic made on **limestone**. Then, the conclusion are limited. It is a blank with one negative scar, cortex and it has no retouch. This features carried us to consider this raw material was weakly exploited, maybe used sporadically. Its weight is 0.14 grams. There is no knapping or resharpening processes in the site made on this raw material. This limestone is grey to blue and the cortical area derived from fluvial deposits. Limestone is the most frequent raw material in the surrounding area of La Cueva de Coimbre. We consider this material was caught in the absence of more suitable raw material.

All in all, we observe different catchment and management strategies for each raw material. This allows us to propose the following human mobility, landscape use, selection and exploitation mechanisms:

- A low, medium and high-scale mobility strategies to South of the research area, as well as outside. Movement in East-West direction are also certified, probably using natural coastal corridors.
- Intensive exploitation of local resources, especially those related from fluvial courses in low altitudes areas. The exploitation of plateaus in medium altitudes zones is not clear, as the exploitation of high altitudes.
- Selective, also non-selective mechanism for obtaining specific raw material or petrogenetic types in deposits.
- A diversity of exploitation of raw material according to its physical properties and presence in the landscape.
- Preferential exploitation of raw material and “archaeological quartzite” types for specific modes of retouch.

CHAPTER-13

RESULTS. QUALITATIVE CHARACTERISATION OF "ARCHAEOLOGICAL QUARTZITES" FROM LA COVACIELLA AND RAVENSBERG-TROISDORF

13.1. The lithic evidences in the palaeolithic cave art of la Covaciella

13.1.1. Description of the lithics

13.1.2. Connecting the features: a dialectic relationship between use-wear analysis and raw material characterisation.

13.1.3. Understanding and creating the artistic, geographical and (pre-)historical context.

13.2. The "archaeological quartzites" from the archaeological site of Ravensberg-Troisdorf

13.2.1. Petrographic, binocular, and geochemical characterisation of the material from Ravensberg-Troisdorf

13.2.1.1. The CC type with clayey matrix

13.2.1.2. The CC type with microcrystalline quartz cement

13.2.1.3. The OO type

13.2.1.4. Geochemical characterisation

13.2.2. Connecting the features: Stratigraphic relationships between types and varieties

13.2.3. Understanding the forces: Outcrop formation and human adaptation

In this chapter we describe the analysis performance in two different archaeological context based on a qualitative approach: The Cave Art of La Covaciella and the open air site of Ravensberg-Troisdorf (Germany).

The first archaeological context is the Palaeolithic Cave Art of La Covaciella. The archaeological site is a cave situated in the eastern part of the Asturias Autonomous Community, within the municipality of Cabrales. The cave is within the Valdeteja and Picos de Europa Formations, mainly composed of fossiliferous limestone, massive limestone with algal and microbial bioconstructions, and calcareous breccia. This archaeological site is mainly known due to its impressive cave paintings and was discovered shortly after the serendipitous opening of the cave (previously closed due to geological processes affecting the site) during the construction works derived from the road expansion that is adjacent to the present and artificial entrance of the cave in 1994 (Ochoa et al., 2015). Present study was inserted in the second archaeological project developed in the cave which was led by Marcos García-Díez and Blanca Ochoa (García-Díez et al., 2015). The project focused on cave art, but other studies were done to understand the context of the cave and other archaeological evidence. The result of the investigation was published in 2015 in a monography about the cave (García-Díez et al., 2015).

The second archaeological context here analysed is the open air site of Ravensberg-Troisdorf. This archaeological site is situated in the Lower zone of Rhine valley, in the village of Troisdorf, between the cities of Cologne and Bonn, in the North Rhine-Westphalia. The site was excavated by two different archaeologist team. The first one was made on 1967, and it was conducted by Gerhard Bosinski. The second archaeological campaign was made during the summer of 2015 and it is planned to be excavated in the next years. The latter campaign was made by Dr. Andreas Pastoors, from the Neanderthal Museum. In this campaign, nine square meters was opened showing an archaeological layer. The quantity of stones on this layer is elevated, with more than 5,000 pieces. Nevertheless, those with clear human traces are scarcer (around 400). The site is situated in the Köln Formation, a Tertiary (Late Oligocene-Early Miocene) cyclic fun/deposits composed by marine sand, lacustrine clay and brown coal horizons. Highly cemented siliciclastic sediments very rich in quartz (Quartzite of Ravensberg-Troisdorf) were probably exploited by Middle-Palaeolithic humans to manufacture diverse tools (Winterscheid and Kvaček, 2016).

13.1. THE LITHIC EVIDENCES IN THE PALAEOLITHIC CAVE ART OF LA COVACIELLA

Here we present the results obtained from the analysis performed on three lithics found in the Cave Art of La Covaciella. We are aware of the small number of lithic implements considered, so the conclusions must be taken cautiously. These results helped to understand the paintings and the relationship between both objects of study. This study was carried out together with Unai Perales, in collaboration with Marcos García-Díez and Blanca Ochoa. The results were already published in (Perales and Prieto, 2015).

The analysis presented here is mainly descriptive due to the small number of lithic remains found in the Cave Art of La Covaciella. We carried out petrological, technological, typological (through modal and morphological structures) and (typo)metrical analyses and use-wear characterisation of the material. The latter was based on the methodological approaches proposed by (Gibaja, 2007; González and Ibañez, 1994) for flint and by (Clemente and Gibaja, 2011; Sussanman, 1985) for quartzite. The macroscopic and microscopic observation of the material was done using a Nikon SMZ 800 binocular loupe and the dark-field microscope Nikon D1200. The pictures were processed using the software Helicon Focus v. 4.62. Petrological characterisation was performed using the non-destructive techniques exposed in the methodological section.

13.1.1. DESCRIPTION OF THE LITHICS

The lithics found during the survey carried out in La Covaciella are shown in Figure-13.1. They are the following:

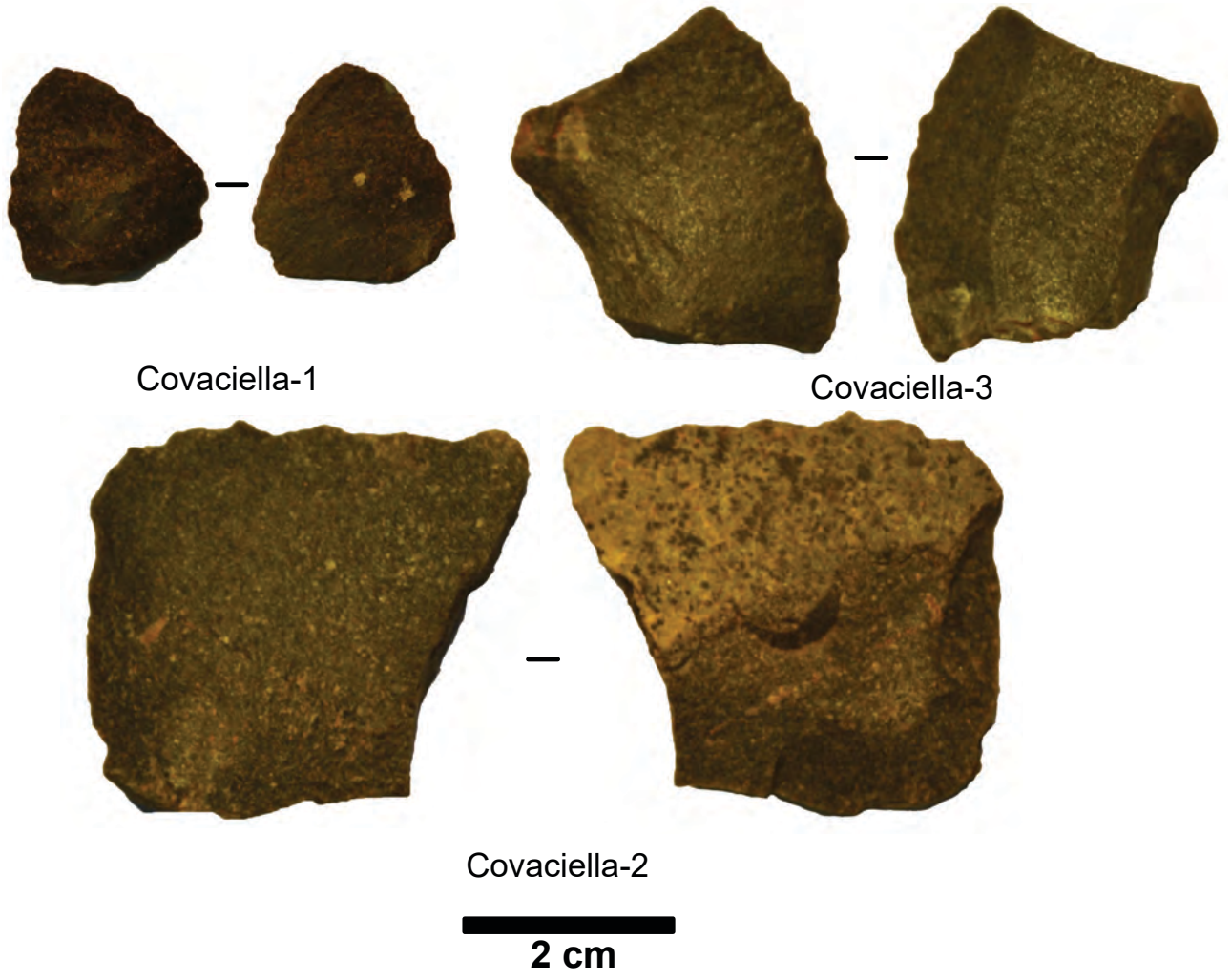

Figure-13.1: Pictures of the artefacts found in the Cave Art of La Covaciella.

Covaciella-1: It is a proximal blank fragment (almost complete) without negative scars made on flint, probably of the Flysch type (Tarriño, 2006). There are a few retouches on the distal-lateral area, creating a small Sidescraper. The use-wear characterisation evidenced: a) a micro-polished transversal work (scraping) in the ventral surface carried out against a an undeterminable medial-hard material (Figure-13.2b), and b) lineal and abrasive work concentred on the distal retouched part, maybe generated as a consequence of engraving against another rock (Figure-13.2a). The measurements of the artefact are: L = 21 mm, W = 19 mm, and W = 4 mm.

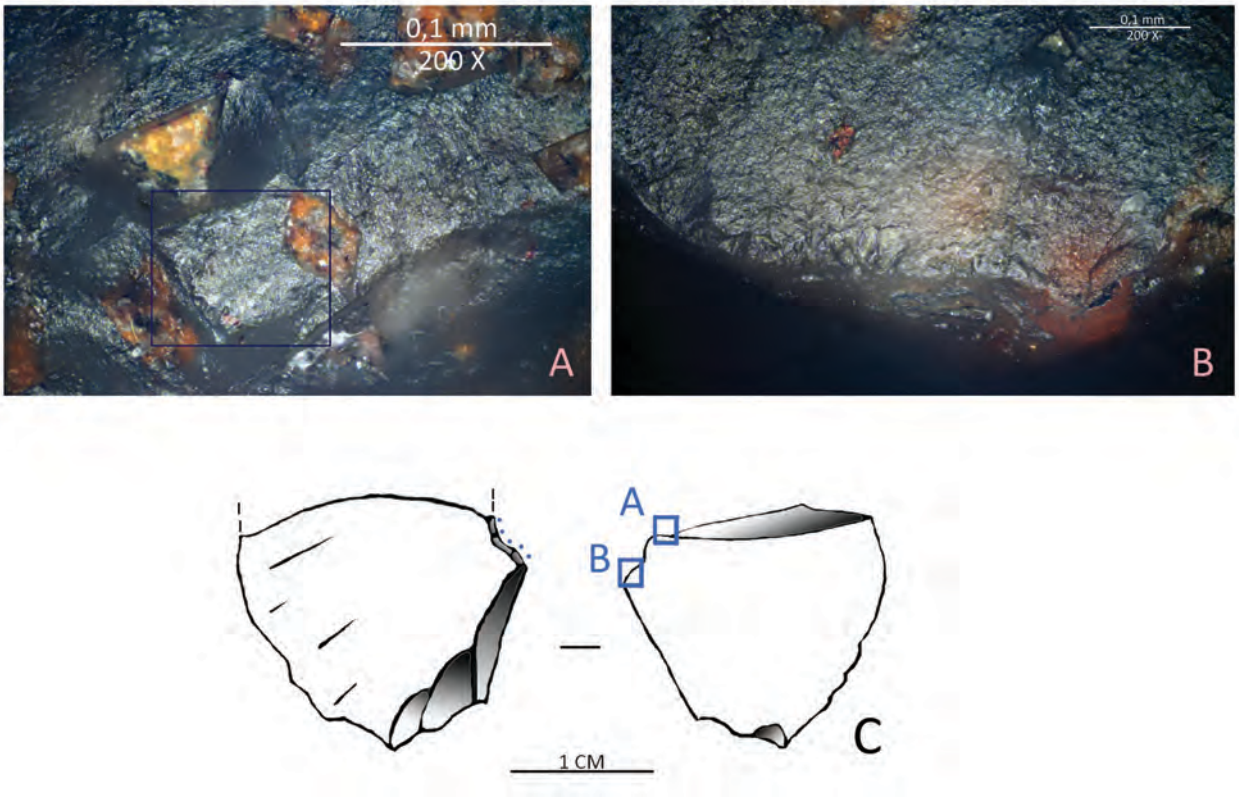

Figure-13.2: Detailed pictures taken with binocular microscope of the microscopic use-wear marks on the artefact Covaciella-1. A) Detailed picture of the lineal and abrasive work focused on the distal retouched part. B) Detailed picture of the micro-polished transversal work (scraping) on the ventral surface. C) Schematic representation of the location of use-wear marks.

Covaciella-2: It is a complete blank with at least three negative scars made on “archaeological quartzite”. There is no retouch. There are some macro-traces on the distal part of the flake without microscopic traces associated (Figure-13.3a). Texture, as characterised by binocular microscopy, is fine with suturated packing (fine T&P). Grains were not clearly detected, although it is possible to observe ruffled borders (Figure-13.4). The luster is intense and there are micro-cracks on the surface. We classified this lithic as a BQ quartzite. The size of quartz grains is small and they are relatively homogeneously distributed. The minerals detected are micas, manganese oxides and iron oxides. The colour of this orthoquartzite is dark-grey. Foliation is well defined. Cortex covers between 33 and 66% of the dorsal surface and comes from fluvial contexts. The measurements of the blank are: L = 33 mm, W = 25 mm, and W = 4 mm.

Covaciella-3: It is a proximal blank fragment with three negative scars made on “archaeological quartzite”. There is no retouch, although there are some macro-traces on the longitudinal part of the flake without microscopic traces associated (Figure-13.3b). Texture, as characterised by binocular microscopy, is fine with suturated packing (fine T&P). Grains could be detected at low magnifications but they cannot be clearly detected at higher magnifications. In the latter, it is possible to observe ruffled borders. Luster is high and there are micro-cracks on the surface (Figure-13.4). As the previous blank, this one is also classified as a BQ petrogenetic type. The size of quartz grains is small and they are relatively homogeneously distributed. The mineral detected are micas, manganese oxides and iron oxides. The colour of this orthoquartzite is dark-grey. Foliation is not clearly observed. The measurements of the lithic are: L = 33 mm, W = 25 mm, and W = 9 mm.

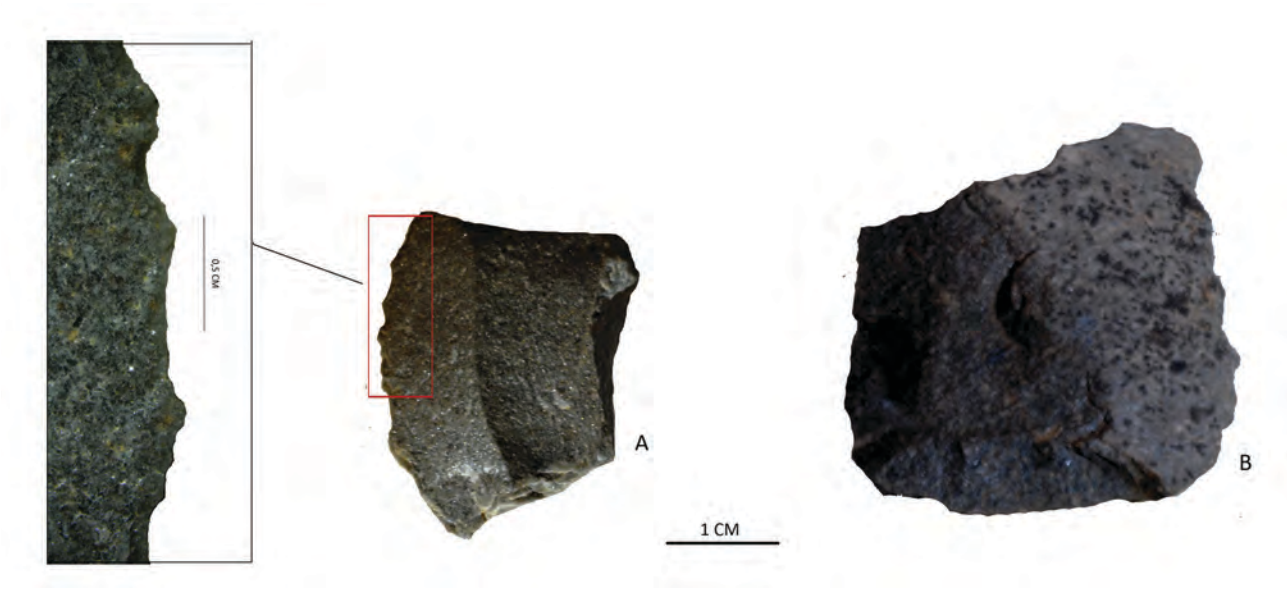

Figure-13.3: Detailed pictures taken with binocular microscope of the macro-traces observed on the edges of both BQ quartzites.

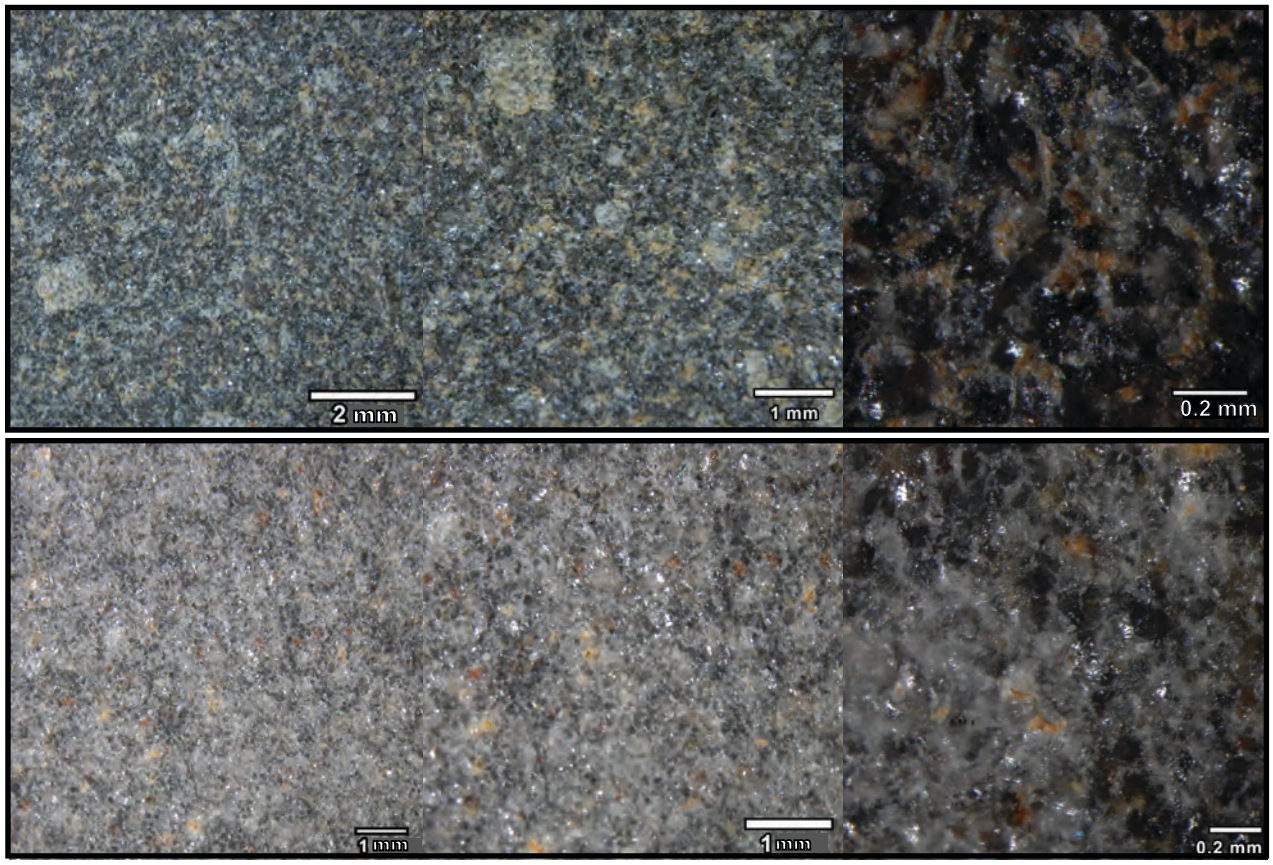

Figure-13.4: Pictures of the BQ artefacts from La Covaciella. Covaciella-2 above and Covaciella-3 below. From left to right, picture taken with binocular microscope at 10x magnification, picture taken with binocular microscope at 20x magnification, and picture taken with binocular microscope at 100x magnification.

13.1.2. CONNECTING THE FEATURES: A DIALECTIC RELATIONSHIP BETWEEN USE-WEAR ANALYSIS AND RAW MATERIAL CHARACTERISATION.

In this section we will describe the methodological relationship created for this investigation in order to understand the lithic evidences in their context: a rock art Upper-Palaeolithic sanctuary in the Cares basin.

In order to understand the use-wear traces detected by U. Perales, we created an experimental program. The aim was to test if such use-wear traces could have been formed by the engravings on rock found in the cave, as previously suggested by other studies (Plisson, 2007). According to specialists, Engraving on rock is one of the artistic techniques used to create the rock art panels of La Covaciella (García et al., 2015). For this purpose, we selected a block of Flysch flint from the Olistostrome of Barrika (Tarriño, 2006) and a pebble of BQ quartzite from the lower part of the Cares River (survey point D_016). In addition, we also used a piece of limestone from the same rock formation where the cave is located. Thanks to the devastation caused by the "discovery" of the galleries, it was possible to use a stone that originally was part of the wall of the cave (Ochoa et al., 2015).

The results obtained by this experimental program demonstrate that engravings on limestone could be produced in a relatively short period of time (less than one minute). Therefore, it can be concluded that these actions were not repetitive or prolonged. This may be one of the causes why the use-wear marks generated were not clear. The posterior analysis of the use-wear marks produced during the experimentation on both raw materials certifies that alteration of edges is minimal. The only observable traces were on flint, which exhibited minimal abrasive and lineal marks (Figure-13.5). On the blank of BQ quartzite, there were no marks derived from the experimental engravings.

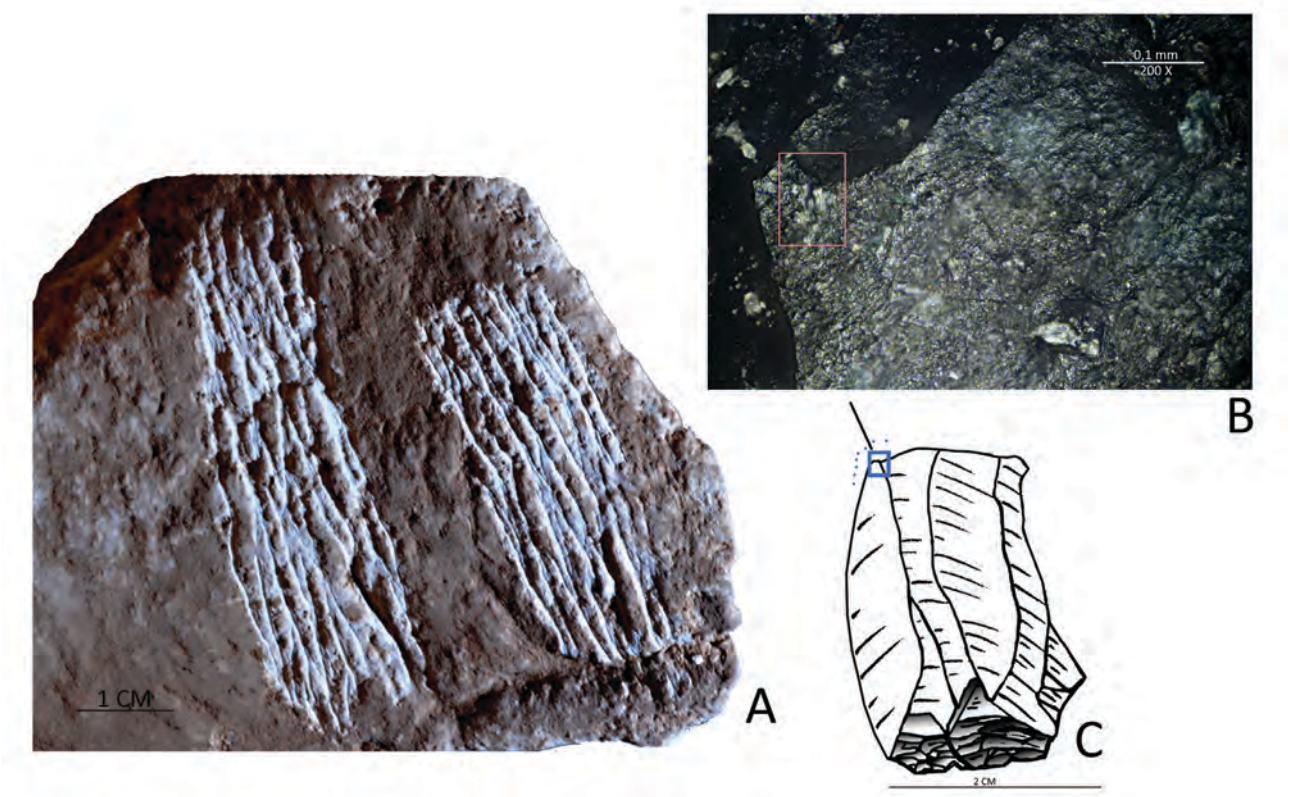

Figure-13.5: Summary of the experimental methodology: A) Detail of the engravings made on limestone with flint and BQ quartzite. B) Detail of the microscopic groove created as a consequence of use in the flint flake employed in experimental work. C) Drawing of the Flysch flint artefact used for experimentation.

This experimental program allowed us to certify that the formation of use-wear traces does not only depend on the material worked, but also on the raw material of the tool. In this case, the only identifiable traces were found on the flint. Use-wear marks were not developed enough in the BQ quartzite, probably due to its physical properties. This was also recently proposed by Pedergnana (2017), that is, that use-wear traces vary according to different petrogenetic types of "archaeological quartzites". Later studies reinforce the importance of proper selection of raw material for experimental programs as the one presented here.

13.1.3. UNDERSTANDING AND CREATING THE ARTISTIC, GEOGRAPHICAL AND (PRE-)HISTORICAL CONTEXT.

In this final section we will try to understand the human forces and the context which explain the material analysed based on the two main hypothesis proposed in this research:

- Understanding the relationship and the links between the lithicss and the paintings
- Understanding the cave art in the Regional and supra-Regional context

The first one cannot be clearly answered due to the lack of use-wear marks that link the lithics with rock art. During the experimental program we observed that formation of use-wear marks on lithics as a consequence of engraving on limestone requires using them during long periods of time. Still, the micro-traces identified in the flint artefact could be the result of engraving activities, which would mean an unconfirmed hypothesis for the use of this artefact for the creation of rock-art. In contrast, we did not observe any micro-wear marks on any of the quartzites. Then, it cannot be proposed they were used for the creation rock art, unless engravings were made in short period of time with other tools.

There is a more complex and robust response for the second hypothesis. Starting from the perspective of the management of raw materials, we observed that all the three lithics belong to intensively exploited raw materials. All of them have small dimensions. While the flint item presents a single small retouch, the other two blanks have at least three negative scars, even though the cortex on Covaciella-2 is quite extensive. In addition, it is possible to observe that the negative scars in Covaciella-3 are well structured perpendicularly to the technological axis. Finally, grain size, non-quartz minerals present and colour of both BQ quartzite lithics reveal that both derive from the same lithic mass.

The characterisation of raw materials shows the ones present at the site are not frequent in the research area. The BQ quartzites were probably brought from one of the near fluvial deposits in the Cares River, not from the Casaño one, as revealed by the presence of cortex from fluvial deposits on them. The nearest deposit with evidence of this petrogenetic type is four Cost Units away, although the quantity of this material in this deposit is smaller proportion than 1% (Figure-13.6). Then, important selective mechanisms would have been necessary to obtain this type. This points at the exploitation of the surrounding area through local or low mobility mechanisms.

The only flint artefact recovered is identified as flint of Flysh type, due to the presence of sponge spicules. The nearest source area of this type of flint is in Biscay, in the olistostrome of Barrika (Tarriño et al., 2015). Then, important long-distance movements must have been taken place in order to obtain it. This type of flint has also been identified in other archaeological sites with Upper Palaeolithic occupation such as Las Caldas (Corchón et al., 2007) or Coimbre (Álvarez-Alonso et al., 2017). This fact reinforces the hypothesis of cultural contacts within the Pyrenees/Cantabrian Region, previously proposed based on the artistic analysis of the Middle Magdalenian paintings of La Covaciella (Barandiarán, 2015; García-Diez et al., 2015). In addition, it provides another perspective, more material than cultural: the existence of long-distance mobility of people or long-distance mobility of materials during the Upper Palaeolithic.

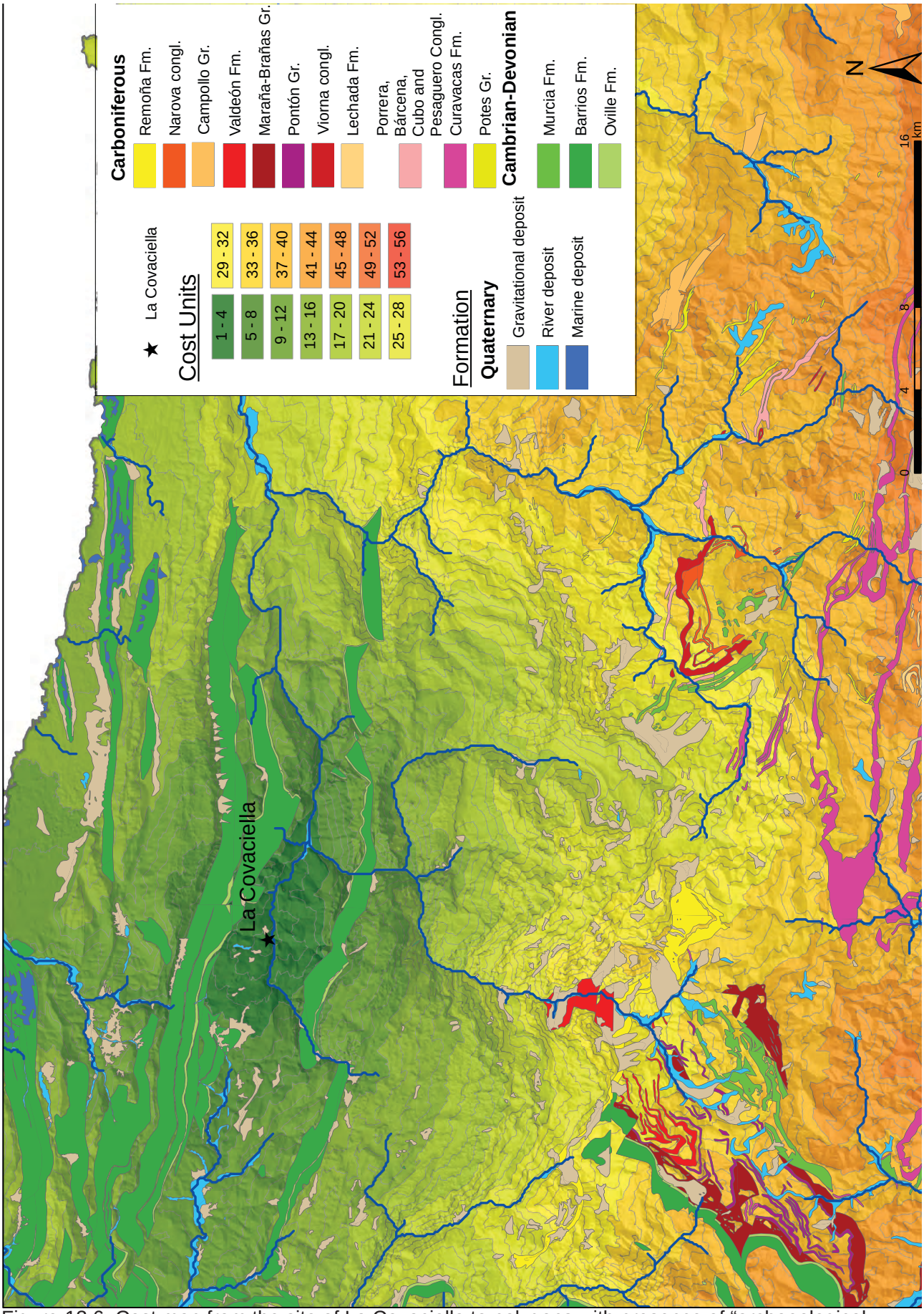

Figure-13.6: Cost map from the site of La Covaciella to polygons with presence of "archaeological quartzites" and other raw materials.

13.2. THE "ARCHAEOLOGICAL QUARTZITES" FROM THE ARCHAEOLOGICAL SITE OF RAVENSBERG-TROISDORF, GERMANY

Here we present the results from the archaeological site of Ravensberg-Troisdorf. It is an open-air site situated in the village of Troisdorf, between the cities of Cologne and Bonn, in the North Rhine-Westphalia (Figure-13.7). The Köln Formation, between the Cologne and Bonn cities, is a Tertiary (Late Oligocene-Early Miocene) cyclic fun/deposit composed by marine sand, lacustrine clay and brown coal horizons. Highly cemented siliciclastic sediments very rich in quartz (Quartzite of Ravensberg-Troisdorf) were exploited by Middle-Palaeolithic humans to manufacture diverse tools (Winterscheid and Kvaček, 2016).

The analysis performed here only includes the first step of the complete protocol applied to the previously discussed archaeological sites. This analysis constitutes a descriptive analysis of the 11 lithics sampled from the complete collection. These items of rocks were prepared for thin section analysis and X-Ray Fluorescence to understand the different types of "archaeological quartzites" potentially exploited at the site. Additionally, these lithics and another 49 items were described under binocular microscopy in order to guide the procedures of the following research, focused on the understanding of the management strategies of raw material in the site. Due to time constraints, we could not performance the in-situ analysis of the regional geology and geography, but relevant geological data is available in Dill, H. et al 2008, Schäfer, A. et al 2005, Winterscheid and Kvaček, 2016.

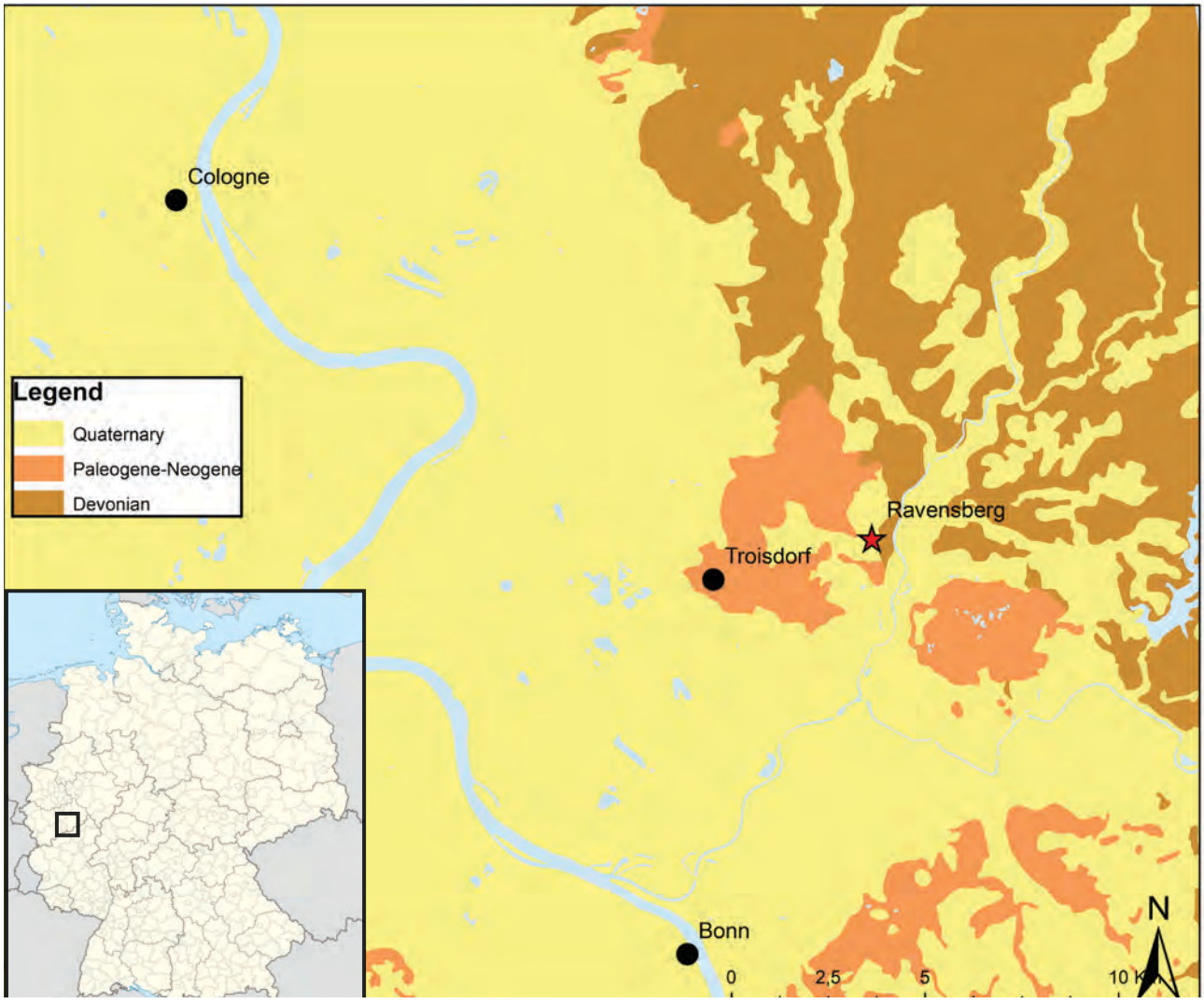

Figure-13.7: Geological map on 1:200.000 scale of the area surrounding Ravensberg (modified from Zitzmann et al. 2002)

13.2.1. PETROGRAPHIC, BINOCULAR, AND GEOCHEMICAL CHARACTERISATION OF THE MATERIAL FROM RAVENSBERG-TROISDORF

We selected 60 lithic fragments from the complete collection for binocular. The selection was made with naked eyes, helped by a hand loupe of up to 20x magnifications. We were aware of different types of post depositional processes affecting the material, such as mineral inclusions (generally iron or manganese oxides) or patinated surfaces, which could bias the sampling process. The main lithological characterisation reveals that all fragments are “archaeological quartzites”. Three main different types was recognised. Some of the selected samples exhibit different types or varieties of quartzite in the same item. Two samples show two facies and another two, three.

The petrographic characterisation reveals the presence of two different petrogenetic types. The clastic and cemented quartzarenite (CC type) is the most frequent type, while the syntaxially overgrown orthoquartzite (OO type) is the less common. Based on the presence of cement and its features, there are two different varieties within the first type: The first and most important cement is composed of microcrystalline quartz. Meanwhile, in the other one cement is almost completely absent and the matrix is composed of clayey minerals. Next we will show each type, its characteristics, and the possible differences between them.

13.2.1.1. CC TYPE WITH CLAYEY MATRIX

The first type analysed is the CC petrogenetic type with absence or residual presence of microcrystalline quartz and presence of small quantities of clayey matrix (CC_CM). Samples Tr-161-2b-2_Z1, Tr-222-12_Z3, and Tr-254-2_Z1 clearly belong to this type and variety (Figure-13.8). The petrographic characterisation of the texture of all the three samples is clastic with matrix or cement texture. Their packing varies from completely-tangential in the first sample to clearly tangential in the other two. The characterisation of grain reveals the high presence of clastic quartz grains and the presence of syntaxial overgrowth in most quartz grains, while concave-convex quartz grain boundaries are limited to small complete packing areas. There is a medium presence of undulatory extinction in some areas of sample Tr-222-12_Z3. The features of quartz grain size are similar in the three samples with heterogeneous distribution. However, most of the grains are between the very fine and fine categories. The former is more frequent in sample Tr-222-12_Z3, while the latter is more represented in the other two samples. The presence of smaller grains is frequent. There are also small quantities of bigger grains of up to 0.568mm (in sample Tr-222-12). The morphology of quartz grains is generally regular, with great circularity indexes. The roundness index of the particles indicates that most of the grains are not elongated. Still some elongated particles are present (for detailed information see S.I.-I). The samples Tr-222-12_Z3 and Tr-254-2_Z1 show preferential orientation at $\alpha = 0.05$, not at $\alpha = 0.01$. Regarding the mineral characterisation of the samples, the type of matrix is clayey. In the cases where cement is present, it is composed by microcrystalline quartz (in negligible proportions). There is presence of iron oxides among non-quartz minerals, probably related with the presence of clayey matrix.

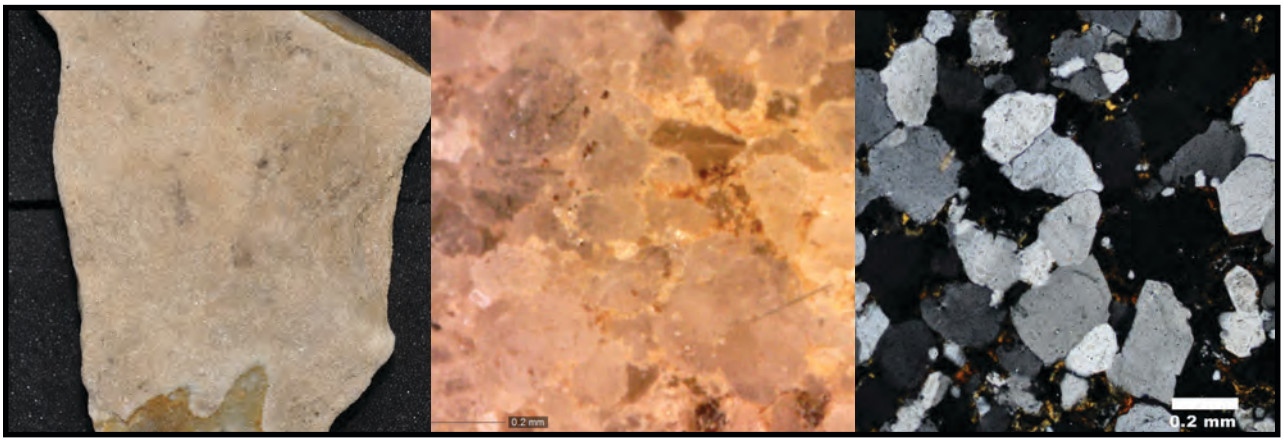

Figure-13.8: Pictures at different magnifications of sample Tr-254-2_Z1: an example of the CC petrogenetic type with presence of clayey matrix.

Regarding the characterisation of this type and variety under binocular microscopy, it is easy to recognise floating or punctual packing surfaces and coarse grained texture, which form saccharoid T&P. The clayey matrix appears as small specks in the surfaces of the samples and between quartz grains. The latter are easily recognisable and their borders are well defined. Generally they are rounded, although in some occasion it is also possible to find straight quartz grains limits and angular surfaces. The presence of iron oxides on surfaces is recurrent, as it can be appreciated in Figure-13.8.

13.2.1.2. CC TYPE WITH MICROCRYSTALLINE QUARTZ CEMENT

The second “archaeological quartzite” analysed is the CC petrogenetic type with presence of microcrystalline quartz cement (CC_MQC). Samples Tr-1-33, Tr-128-5, Tr-161-2-3, Tr-161-2b-2_Z2, Tr-161-2b-6, Tr-222-12_Z2, Tr-223-3-2_Z1/Z2, and Tr-254-2_Z2 belong to this type (Figure-13.9). The petrographic characterisation of the texture of all these samples is clastic with matrix or cement and packing varies from isolated to tangential packing. The most frequent features of quartz grains are clastic quartz grains, occasionally surrounded by syntaxial overgrowth. In some areas of the samples it is possible to recognise concavo-convex quartz grain limits. The grain characterisation reveals parameters similar to those appreciated in the previous variety of the CC type. The most represented quartz grain size categories are very fine and fine sand, generally with a prevalence of very fine sand category. There is also an important presence of smaller quartz grain sizes and some other bigger than fine sand quartz grains. The biggest quartz grain is 0.327mm, identified in sample Tr-161-2b-6 (detailed information in S.I.-I). Regarding the morphology of the particles, the data are similar to those previously commented: prevalence of regular shapes with high circularity indexes (C>0.57) and general tendency to non-elongated shapes with residual presence of elongated particles (roundness indexes around 0.62). No preferential orientation was detected in this type. Regarding the composition of cement, it is mainlly formed of microcrystalline quartz. The presence of microcrystalline quartz is generally between 5% and 20% of the samples and it tends to surround quartz grains (although syntaxial overgrowth is present). In the cases where packing is less compact, the quantity of cement is higher. Regarding the identification of non-quartz minerals, iron oxides is the most frequent material, followed by zircon and clays. Iron oxides appear as small crystals inside microcrystalline quartz too. Mica, pyrite, chlorite, and rutile, are present in some samples.

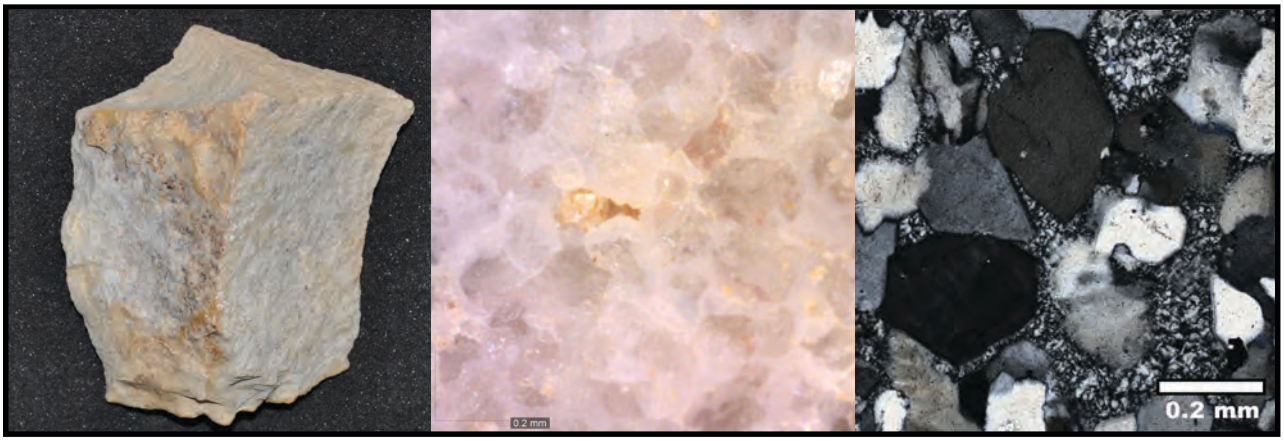

Figure-13.9: Pictures at different magnifications of sample Tr-161-2b-6, an example of the CC petrogenetic type with presence of microcrystalline quartz. The central picture, taken with a Dino-lite at x250, shows cement (crystalline) covering and enclosing quartz grains. These are rounded but sometimes they present slightly plain limits. The thin section picture at 200x on the left shows the microcrystalline cement around almost undeformed quartz grains.

The non-destructive characterisation of these quartzites shows similarities with the thin section characterisation. It is relatively easy to recognise the quartz grains, which present rounded and sometimes plain quartz limits. The grains generate punctual or tangent packing, while the textures are more related with fine grained textures than with coarse grained texture due to the presence of microcrystalline quartz cement. The latter is easy to recognise as a bright lustre (sometimes coloured by red oxides) which covers and encloses the quartz grains. Due to the characteristics of the cement, the saccharoid T&P texture is not observable. Then, granular T&P better defines this group.

In the cases where microcrystalline quartz is really abundant, fine texture is identified, even though grains are still visible. Iron oxides appear in some zones of the samples, generally together with small quartz grains or inside fractures.

13.2.1.3. OO TYPE

The last "archaeological quartzite" analysed is the OO petrogenetic type. Samples Tr-1-18, Tr-129-2-4, Tr-161-2b-2_Z3, and Tr-222-12_Z1 are classified within this type (Figure-13.10). The petrographic characterisation of the texture of these samples is clastic grained. Packing characterisation reveals that all the samples are within the complete category, although small porosity could be also observed in some of them. The characterisation of grains reveals the coexistence of clastic grains with others with clear undulatory extinction (in different areas of the thin section). Most of the grains exhibit syntaxial overgrowths that generate concave-convex quartz grain limits. The size characterisation of quartz grains in these samples shows parameters similar to those observed in the former type and varieties. Most of the grains are classified within the fine sand and very fine sand categories. The exception is sample Tr-222-12_Z1, where coarse silt is the most frequent category (note that in other parts of sample Tr-222-12, grain size characterisation is also smaller). The presence of smaller grains is clear and big quartz grains are less frequent than in previous type (the biggest quartz grain is 0.299mm). The morphology of the grains does not differ either from the types previously analysed, with regular and generally non-elongated shapes. No preferential orientation was detected in this type. The mineral characterisation of the small portion of matrix present in samples

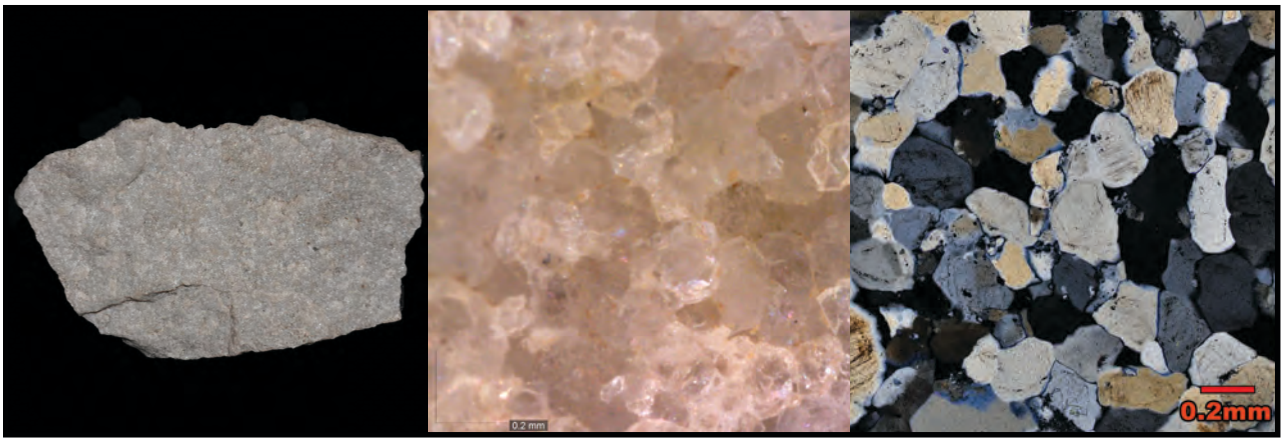

Figure-13.10: Picture at different magnifications of sample Tr-1-18: an example of the OO petrogenetic type from Ravensberg. In the binocular picture at 250x magnification complete packing and apparent regrowth of quartz grains are clearly observable. Generally rounded grains are identified. Thin section shows clearly the clastic grained texture, complete packing, massive presence of quartz syntaxial overgrowth, and concave-convex quartz grains limits.

Tr-1-18 and Tr-129-2-4 is siliceous. The mineral characterisation of the residual cement of the samples Tr-161-2b-2_Z3 and Tr-222-12_Z1 reveals the negligible presence of microcrystalline quartz. The mineral characterisation of the non-quartz elements shows the presence of iron oxides in three of the samples and rutile, clay, and pyrite in several ones.

Regarding characterisation under the binocular microscope, it is possible to recognise relatively fine grained (sometimes coarse grained) textures and complete packing. The compact and grainy T&P category is clearly recognised, as well as the concave-convex quartz limits with syntaxial overgrowth. In most of the grains it is easy to recognise rounded and discontinuous limits. There is presence of iron oxides in almost every sample, as well as some non-identified black and heavy minerals.

13.2.1.4. GEOCHEMICAL CHARACTERISATION

Finally, we include the geochemical characterisation of the "archaeological quartzites" from Ravensberg-Troisdorf (Table-5.17). X-Ray fluorescence was performed on every sample without facies distinction. The results show the major presence of SiO_2 in every sample, in percentages higher than 98%. Other components such as Al_2O_3, Fe_2O_3, or TiO_2 are represented in proportions smaller than 0.3%. The presence of the remaining components considered is residual. No clear differences are observed between the types and varieties proposed according to the geochemical characterisation.

13.2.2. CONNECTING THE FEATURES: STRATIGRAPHIC RELATIONSHIPS BETWEEN TYPES AND VARIETIES.

In this section we will describe the relationship found between the types and varieties defined using samples with different facies. Samples Tr-161-2b-2 (_Z1, _Z2, and Z3) and Tr-222-12 (_Z1, _Z2, and _Z3) have three facies and samples Tr-223-3-2 (Z_1 and Z_2) and Tr-254-2 (_Z1 and _Z2) have two. Here we will use binocular and petrographic characterisation to describe the first two, which are the most representative examples of the relationship between the three types and varieties described. Additionally, we will describe the features observed in sample Tr-223-3-2.

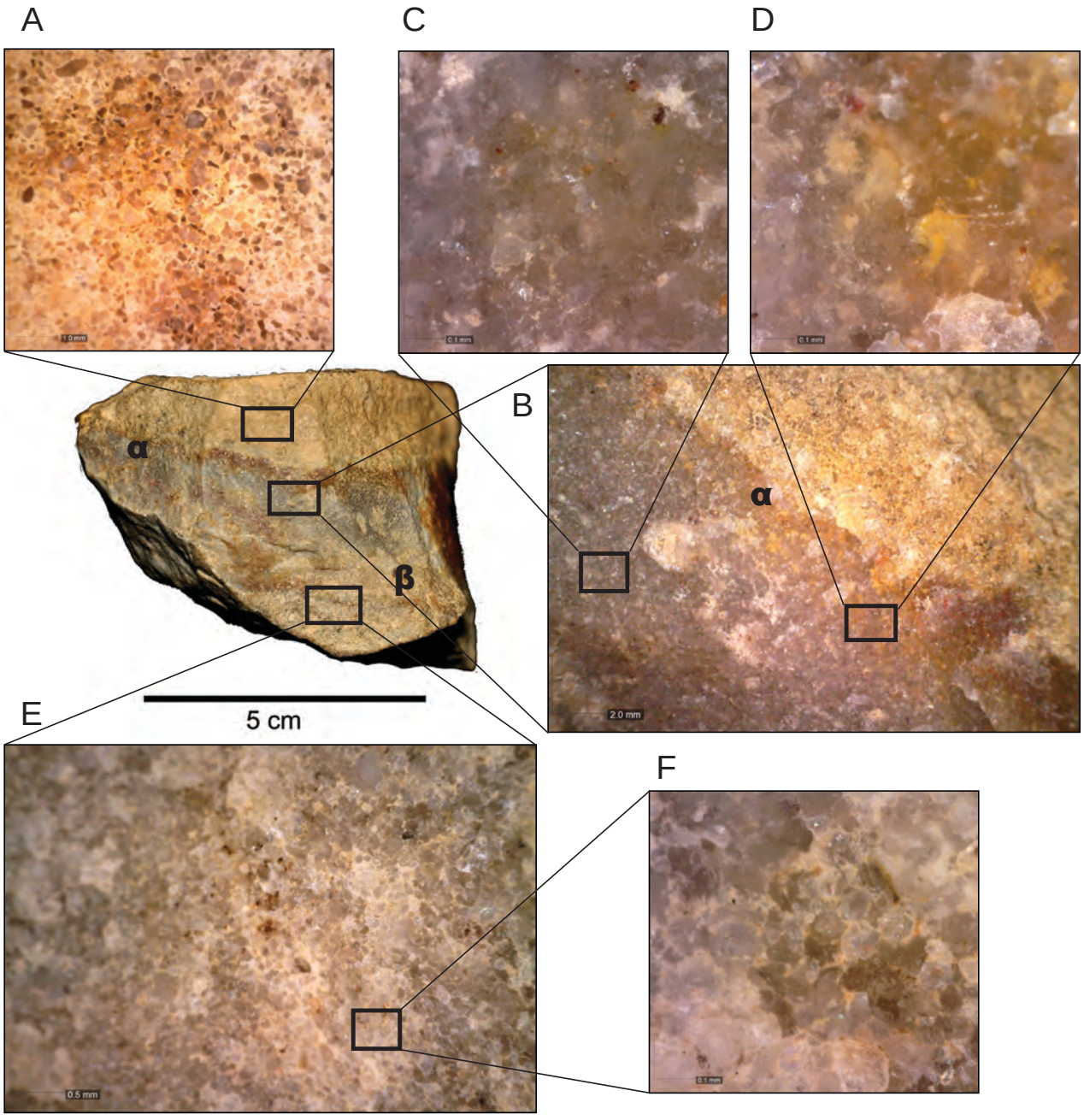

Figure-13.11: Picture of sample Tr-161-2b-2 and its surfaces photographed with Dino-lite at diverse magnifications. The source area of each microscopic photograph is indicated in the general picture. A: Detail picture of the CC_CM at 50x magnification. B: CC_MQC and transition with the CC_CM zones at 20x magnification. C: CC_MQC area without oxides at 250x magnification. D: CC_MQC area with oxides at 250x magnification. E and F: OO type layer at 20x and 250x magnification. α: Limit between CC_CM and CC_MQC areas. β: Limit between CC_MQC and OO areas.

Regarding non-destructive characterisation, the facies are easily recognisable based on texture, packing, and other features. In Figure-13.11 the three facies are displayed as a stratigraphy sequence of three facies. The CC_CM type is situated (Figure-13.11A) on top of the CC_MQC type (Figure-13.11B and C). Both facies are separated by an abrupt thin layer of iron oxides (Figure-13.11α), slightly dissolved in the CC_MQC type (Figure-13.11D). The change between both facies is clear and abrupt. Finally, the OO type (in this case with residual or negligible presence of microcrystalline quartz) is situated under the previous facie (Figure-13.11E and F). The relationship between the latter two facies is not as obvious as the former due to the progressive removal of microcrystalline quartz as a consequence of the increase of grain compactness in the OO type (Figure-13.11β). The presence of small quantities of iron oxides in almost all the sample surfaces is clear. There is a small presence of black and heavy non-identified minerals.

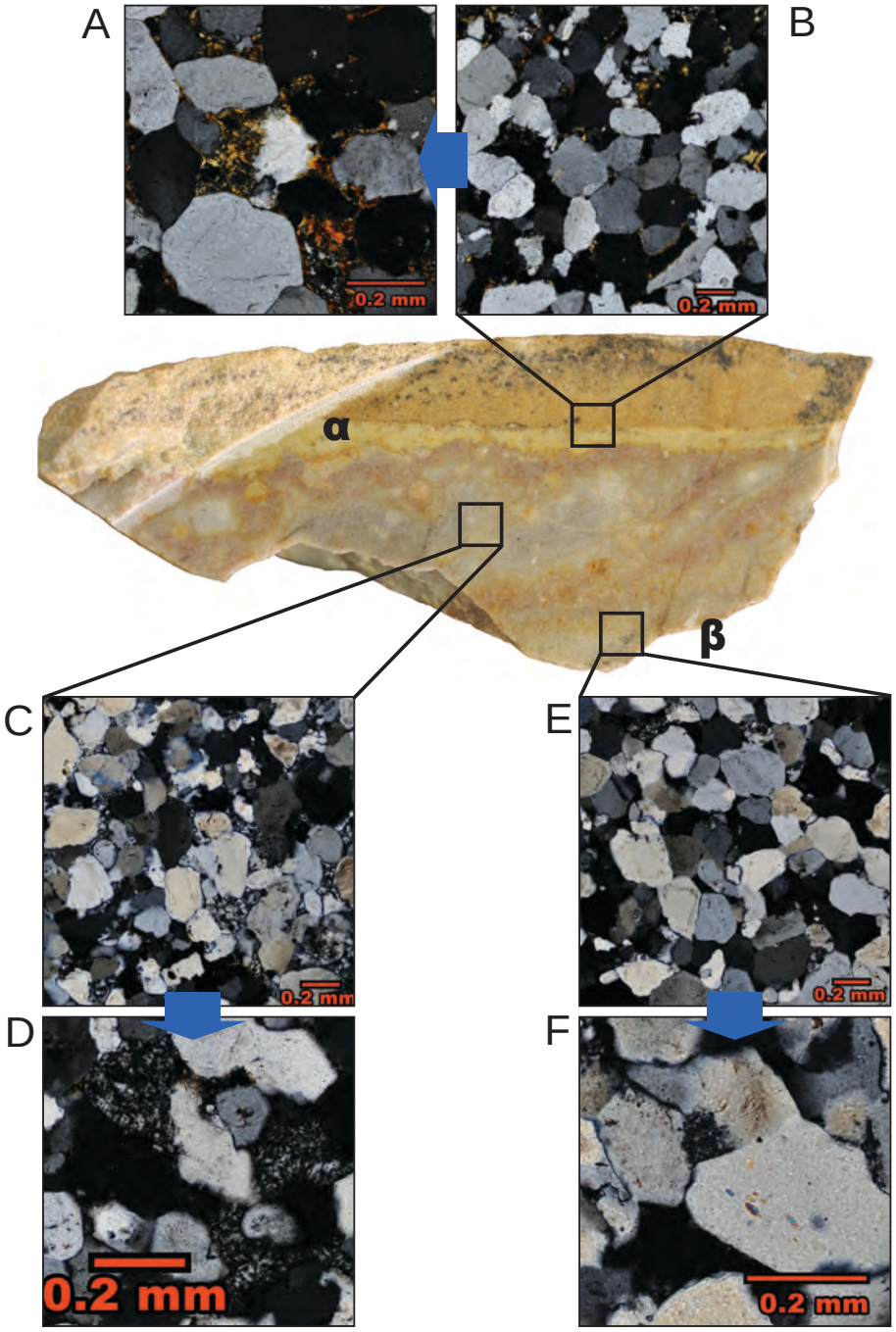

Figure-13.12: Picture of sample Tr-222-12 after being cut for thin section. Thin sections at diverse magnifications are also shown. The source area of each microscopic photograph is indicated in the general picture. A: Detail picture of the thin section at the limit between CC_CM and CC_MQC areas. Note that clay is the main component of the matrix. A small part of microcrystalline quartz can be observed. B: Thin section of the CC_CM area. C: Thin section picture from the CC_MQC area. D: Detail of the thin section of the microcrystalline quartz cement and the relationship with grain framework. E: Thin section picture of the OO area. F: Detail picture of the thin section of the OO area, exhibiting concavo-convex quartz grain limits and presence of syntaxial regrowth. α: Limit between CC_CM and CC_MQC areas. β: Limit between CC_MQC and OO areas.

The petrographic characterisation of the samples emphasised the existing relationship between the CC_CM, CC_MQC, and the OO types. On the cutting surface of sample Tr-222-12 the three layers are clearly defined and indicate the same relationship between the facies (Figure-13.12). The upper one is composed by the CC_CM type, the central is the CC_MQC type, and the lower facie is the OO type (in this case, the surface is smaller than in previous sample). Regarding the first, thin section shows the main presence of clayey matrix with many oxides that fill the space between quartz grains in the CC_CM part (Figure-13.12B). In the outer areas it is possible to observe black and undefined minerals (probably manganese oxides) as a consequence of the weathering process. The inner areas are relatively homogeneous, except for grain size. The abrupt change between this and the CC_MQC layer is exacerbated in fresh cut. It exhibits a lighter and thin area that clearly separates both layer (Figure-13.12α). In thin section, microcrystalline quartz progressively disappears in the transition from CC_MQC type to CC_CM (Figure-13.12A). Focusing on the CC_MQC layer, colour is generally heterogeneous, ranging from grey and lighter areas to orange zones in the fresh-cut. The presence of round and curved zones are clearly appreciated thanks to colour changes. Petrographic characterisation shows the major presence of microcrystalline quartz filling the pores or spaces between quartz grains (Figure-13.12C and D). These spaces have no matrix, but a small proportion of iron oxides in specific zones (probably the orange areas on the cutting surface). The OO type facie is not clearly distinguished from the layer above it (also observable without destructive characterisation). There is no differenced stratum, nor neat change between both facies. The change between CC_CMQ and OO types is gradual and determined by progressive change in packing, from tangential to complete categories (Figure-13.12E and F). This gradation progressively blocks the entrance of microcrystalline quartz from the CC_CMQ area to the OO type area, generating areas with absence of microcrystalline quartz cement, as those appreciated on Tr-1-18 o Tr-129-2-4. This process is probably related with the increase of quartz grains with syntaxial overgrowth in the OO type.

The last sample analysed to understand the relationship between the three types and varieties is Tr-223-3-2. This sample corresponds to the CC_CMQ variety and it is the only sample with clear presence of pores or chimneys filled with microcrystalline quartz cement (Figure-7). This sample evidences the bursting of microcrystalline quartz into the forming sandstone through chimneys or fluid insertions. Finally, the microcrystalline quartz flows through the space between quartz grains adapting to its shapes.

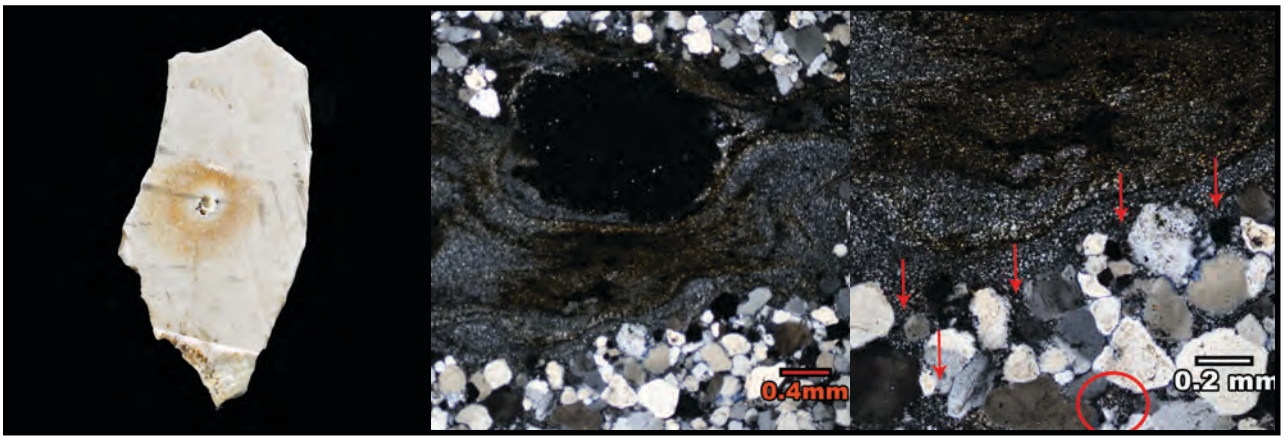

Figure-13.13: Pictures at different magnification of sample Tr-223-3-2. The first picture shows the sample after being cut for thin section preparation. The porosity where microcrystalline quartz is massively trapped, as well as the concentric oxides around it are easily observable. The following two thin sections display the microcrystalline quartz grains in the big pore and the filling process of the general CC type porosity. Oxides colouring areas of the microcrystalline quartz grains are also identified.

13.2.3. UNDERSTANDING THE FORCES: OUTCROP FORMATION AND HUMAN ADAPTATION

In this section we will hypothesise about the petrogenesis of the "archaeological quartzite" formation exploited by Palaeolithic societies at the site of Ravensberg-Troisdorf and describe the potential mechanisms put into action by humans for the exploitation of this raw material. The most relevant feature of the "archaeological quartzites" found at this site is the cementation through microcrystalline quartz in, at least, one defined type. The definition of the other variety of the CC type and the OO petrogenetic type help us to understand the formation of the first material, the CC_MQC variety.

Microcrystalline quartz cement in sandstone formation is described in other studies (e.g. (Block Vagle et al., 1994; Fischer et al., 2013; French et al., 2012; French and Worden, 2013; Lima and De Ros, 2002; Vagle et al., 1994; Weibel et al., 2010; Worden et al., 2012). These authors concluded that microcrystalline quartz forms by various diagenetic processes as circulation of groundwater enriched in dissolved silica or in-situ dissolution of sponge spicules or volcanic rock fragments. Here the latter two are discarded because the absence of both elements in the analysed material. In addition, in the CC_MQC variety from Ravensberg-Troisdorf the presence of chimneys filled in with microcrystalline quartz is clear, as shown in sample Tr-223-3-2 (Figure-13.13). Furthermore, the heterogeneous and curved distribution of zones in sample Tr-222-12_Z2 (Figure-13.12) also points at the presence of silica-fluid in this area. Then, we conclude that the passage of groundwater with elevated silica concentration through fluid insertions is the most convincing hypothesis for the origin of microcrystalline quartz cement.

Heterogeneously distributed microcrystalline quartz cement fills in the sandstone adjacent areas in those cases where packing is not complete and it expands from the cemented zones until a) packing is complete or b) the porous areas are filled in by matrix (in this case by clayey material) or c) by tectonically irregular deformed band zones (zones that expulse silica-rich water) (Fischer et al., 2013). Therefore, we could argue the following: a) the OO petrogenetic type does not allow the expansion of microcrystalline quartz due to the compactness generated by quartz syntaxial overgrowth. The reduced presence of microcrystalline quartz in samples Tr-222-12_Z1 and Tr-161-2b-2_Z3 can only be explained by the proximity to the fluid flow from the contiguous CC_MQC facies and the presence of small pores in the grain framework. b) The CC_CM stops or impedes the expansion of microcrystalline quartz due to the presence of clayey sediments in its matrix. The small presence of microcrystalline cement in the clayey matrix between CC_CM and the CC_MQC is probably what creates the neat layer differentiation. c) The only variety analysed with quartz grain preferentially orientated is the CC_CM variety. Then, the possible existence of tectonic deformation or irregular replacement/filling could expel the silica-rich water to the adjacent stratum, creating two clearly differenced facies.

The first hypothesis would solve the existing relationship between the CC_MQC variety and the OO type. The second and the third hypotheses propose two different explanations for the relationship between CC_MQC and CC_CM varieties. The latter hypothesis also proposes a source area for microcrystalline quartz, in accordance to Fischer et al., 2013. The geographic location of the site, in a small hill, and the geological strata around the site are consistent with this hypothesis (Figure-13.7). The geological strata around the site are mainly composed by siliciclastic (consolidate or unconsolidated sediments/rocks). The Devonian series could be the source strata for the siliciclastic material. The source area could also be the consolidated material from the Paleogene-Neogene or even Quaternary, modified by the microcrystalline quartz fluid-influx, following a model similar to the proposal by Fischer et al 2013 (in figure-7, p.56). Nevertheless, further analyses would be necessary for better understanding the relationship between the three different facies of this "archaeological quartzite".

Regarding human exploitation of "archaeological quartzites" in the site of Ravensberg-Troisdorf, we propose a selective and intensive exploitation focused on the CC_MQC quartz arenite, a probably casual exploitation of the OO type, and the dismissal of the CC_CM quartz arenite. This hypothesis is based on two factors: a) the physical properties of the material and b) selective knapping procedures observed in the archaeological material derived from the "archaeological quartzite" outcrop.

Coming to physical properties, the three types have similar quartz grain size features, with a distribution between the very fine sand and the fine sand categories. Nevertheless, the presence of smaller and clearly bigger quartz grains creates non-homogeneous surfaces that hampers knapping activities. The previous compactness degree of the grain framework for the two varieties of CC type also creates non-homogeneous surfaces. However, the major presence of microcrystalline cement in the CC_MQC variety creates homogeneous and compact rocks that prevent the creation of

pores and grain irregularities, easing knapping activities. In addition, the presence of microcrystalline quartz also creates sharp edges in flacking products. The compactness degree of the OO type prevents the porosity that hinders knapping activities, but it does not prevent the irregularities generated by the differences in size of quartz grains. Only in the cases where microcrystalline cement fills in the small spaces between quartz grains, the OO type, more homogeneous, becomes into an optimal knapping product.

The analysis performed in the site of Ravensberg-Troisdorf concludes that the properties of the CC_MQC variety make it optimal for knapping and use. Then, its intensive exploitation could be the main reason for human activity in this site. We propose that use and acquisition the OO type would be secondary and derived from the main product, the CC_MQC type. The CC_CM variety could not be used for knapping due to its friable properties. Then, its usefulness is reduced and it was probably considered a waste product.

CHAPTER-14

DISCUSIÓN

14.1. De micras a kilómetros: evaluación crítica de la metodología utilizada

14.2. Las cuarcitas arqueológicas: procesos formativos, el ciclo de las rocas y la acción humana

14.3. La adquisición y gestión de la cuarcita arqueológica por las sociedades prehistóricas en los valles del Deva, Cares y Güeña durante el Paleolítico medio y el Paleolítico superior

El trabajo que hemos expuesto en las páginas anteriores ha sintetizado el trabajo de varios años. Éste, nos ha permitido definir y caracterizar la cuarcita desde perspectivas geo-arqueológicas en los valles del Deva, Cares y Güeña y de una selección de los yacimientos paleolíticos de la zona. Para ello, hemos desarrollado una metodología específica que analiza la materialidad pétrea en tres niveles de profundidad, el análisis microscópico y composicional, la observación macroscópica y el estudio espacial a gran escala. Todo ello nos ha permitido, no solo entender el material, sino también inferir el conocimiento acerca de las estrategias de captación y transformación de la cuarcita por las sociedades paleolíticas.

En este capítulo plantearemos tres apartados que nos permitirán articular conceptos e ideas transversales tratadas a lo largo del texto. Debido al carácter experimental y metodológico de esta tesis, el primero de estos planteará una evaluación de la metodología empleada. El segundo tratará de entender y describir la cuarcita como roca, desde su génesis hasta su abandono final por parte de las sociedades paleolíticas. La tercera idea que desarrollaremos evidenciará la variabilidad de los mecanismos de adquisición, gestión y distribución de la cuarcita en la zona de estudio. Para ello, analizaremos los datos obtenidos a partir de un eje diacrónico y otro sincrónico, contextualizando la información obtenida en esta tesis con otros trabajos. Este apartado del capítulo tratará de entender la relación entre los seres humanos y el medio ambiente que habitaron a lo largo del Paleolítico, teniendo en cuenta la variabilidad temporal, geográfica y funcional de los conjuntos analizados.

14.1. DE MICRAS A KILÓMETROS: EVALUACIÓN CRÍTICA DE LA METODOLOGÍA UTILIZADA

"…el cambio de escala. No es cierto que si construimos un aparato a una escala y otro exactamente igual, con los mismos materiales, pero el doble de grande, ambos funcionarán exactamente de la misma manera."

"…Si me permiten usar una metáfora religiosa, ¿qué extremo está más cerca de Dios? ¿Belleza y esperanza o leyes fundamentales? Creo que la respuesta adecuada es, sin duda, que tenemos que fijarnos en la interconexión de las estructuras, y que todas las ciencias (y no sólo las ciencias, sino los esfuerzos intelectuales de toda clase) son un intento de entender las conexiones entre los niveles jerárquicos, de conectar la belleza con la historia, la historia con la psicología humana, la psicología humana con el funcionamiento del cerebro, el cerebro con el impulso nervioso, y así sucesivamente, arriba y abajo, en ambos sentidos. Hoy por hoy no podemos trazar, y es absurdo intentar convencernos de lo contrario, el camino exacto que va de un extremo a otro, porque sólo recientemente hemos empezado a darnos cuenta de que existe esta jerarquía relativa."

Richard Feynman. El carácter de la ley física, página 107 y página 139

Como hemos comentado previamente, esta tesis tiene un fuerte componente metodológico y experimental que creemos debe ser evaluada como parte de la crítica que debe imperar en cualquier trabajo científico. En esta sección abordaremos desde la metodología utilizada para el establecimiento de tipos cuarcíticos hasta las propuestas realizadas para entender el amplio espacio geográfico en el que se circunscribe este trabajo. Esto nos permitirá entender las limitaciones de esta tesis y de la metodología utilizada, planteando, también, sus potencialidades.

La caracterización de las cuarcitas en contextos arqueológicos y el establecimiento de tipos mediante la petrografía planteado en este trabajo suponen una aproximación novedosa y de carácter universal para entender el material cuarcítico en contextos arqueológicos. La caracterización del material nos ha permitido observar la variabilidad del mismo, que está determinado por 1) el aporte sedimentario que formará la roca 2) los procesos formativos de la cuarcita (diagenéticos y metamórficos), 3) los procesos que modifican esta roca en los contextos geológicos y 4) los procesos post-deposicionales de la cuarcita en yacimientos arqueológicos. Los siete tipos propuestos se asocian a su vez en los tres grandes órdenes, principalmente determinados por la textura y el empaquetamiento de las "cuarcitas arqueológicas". Los dos primeros tipos cuarcíticos, se crean en procesos estrictamente diagenéticos (cementación y/o compactación), generando

cuarzoarenitas, rocas sedimentarias ricas en sílice. Los dos tipos siguientes, aun produciéndose por procesos diagenéticos, están claramente diferenciados de los primeros debido al incremento paulatino de la presión y deformación que generan estructuras cada vez más compactas. Estos dos tipos se insertan dentro del grupo de las ortocuarcitas. Finalmente, los tres últimos tipos se agrupan dentro del grupo de la cuarcita o cuarcita *s.s.* En este caso, los procesos petrogenéticos son metamórficos y se basan en diferentes procesos de recristalización que cambian la estructura de la roca con el aumento de la temperatura y la presión. El aumento gradual de las condiciones diagenéticas (cementación-compactación-recrecimiento de cementos sintaxiales, límites de grano serrados y lamelas de deformación) que producen las cuarzoarenitas y las ortocuarcitas, así como el incremento de presión paulatino en las cuarcitas, generan estigmas o caracteres observables a través del microscopio petrográfico. La asociación de estos a las texturas y el empaquetamiento de las cuarcitas, nos ha permitido entender y caracterizar los tipos propuestos. A pesar de ello, la presencia de caracteres no asimilables al tipo de cuarcita, generalmente con frecuencia residual y no coherentes con el resto de granos, pueden modificar su caracterización, aunque el estudio de la totalidad de caracteres a través de la metodología aportada, evita la asignación incorrecta. Este tipo de procesos son comunes entre las cuarzoarenitas, donde existen zonas con extinción ondulante, límites cóncavo-convexos o presencia de clastos de rocas con texturas metamórficas, claramente relacionadas con la roca fuente del sedimento original.

Para conocer las propiedades métricas de los granos que componen las cuarcitas, hemos desarrollado una metodología basada en el calco de los límites de los granos observados en el microscopio petrográfico. A partir de este calco, hemos implementado la medición automatizada del mismo mediante una aplicación informática (*plugin del software Imagej)*, obteniendo una alta fiabilidad de las medidas y sobretodo un rápido procesado de la información. Somos conscientes de la posibilidad de automatización del calco de los límites de los granos, como han demostrado otros autores (Cross et al., 2017; Ghiasi-Freez et al., 2012; Heilbronner, 2000; Heilbronner and Tullis, 2006), pero debido a la cantidad de muestra utilizada y los intentos realizados, hemos preferido la realización manual de los calcos.

La caracterización previamente realizada a partir del tamaño de grano o la detección de minerales traza (Álvarez-Alonso et al., 2013a; Manzano et al., 2005; Sarabia, 2000) obviaba la complejidad del término cuarcita y los efectos que los procesos genéticos producen en la estructura de la roca. La determinación de los tamaños de los granos de cuarzo que componen cada cuarcita, aportan datos interesantes que deben ser valorados una vez el tipo está establecido. El tamaño de grano de las cuarcitas arqueológicas es el resultado de dos procesos formativos. El primero está determinado por las condiciones de sedimentación que conforman la roca original original y su área fuente. El segundo está relacionado con los procesos diagenéticos y metamórficos previamente mencionados y que producen modificaciones sustanciales en los tamaños de grano, la distribución de los mismos y sus morfologías. Por todo ello, la caracterización de las cuarcitas a través de su tamaño y morfología de grano está condicionado por el establecimiento de tipo, articulándose a él como variedad específica. Los diferentes minerales identificados a través de técnicas petrográficas está condicionada, no sólo por los dos procesos formativos previos, también por las modificaciones en procesos post-deposicionales en los contextos arqueológicos (principalmente) y en los diferentes contextos geológicos en los que hemos encontrado cuarcitas arqueológicas. Esto, sumado a la variabilidad de ambientes geológicos en la zona de estudio condiciona la trazabilidad de las mismas mediante técnicas relacionadas con la detección mineral. Adicionalmente, la durabilidad de las cuarcitas, genera que el aporte mineralógico sea grande y variado. El análisis composicional, también se ve afectado por la composición mineralógica y por los distintos ambientes en los que la cuarcita ha estado presente. Por todo ello, la caracterización mineral de las cuarcitas no articula tipos específicos sino variedades, en este caso altamente condicionadas por las condiciones de enterramiento de las cuarcitas, generalmente en contextos arqueológicos.

El reflejo de los tipos petrogenéticos mediante la observación macroscópica y microscópica no-destructiva nos ha permitido caracterizar no sólo una muestra reducida de las cuarcitas, también grandes conjuntos en ambientes geológicos y arqueológicos. Por un lado, la descripción de las cuarcitas (ya caracterizadas mediante técnicas petrográficas destructivas) a través de los siete campos de análisis de la “Database-A”, nos ha permitido entender las cuarcitas desde perspectivas no-destructivas, posibilitando la relación de caracteres observados a través de la petrografía y los observados en la superficie de las cuarcitas mediante lupas de gran aumento. Las descripciones aportadas por esta base de datos, nos ha permitido entender y ordenar los caracteres más importantes, agrupándolos a través del juego de T&P (texture & packing; texturas y empaquetamiento) y de caracteres específicos de los granos de cuarzo recogidas en la “Database-B”. Este proceso permite

el establecimiento final de cada tipo petrogenético cuarcítico. Somos conscientes que la utilización de técnicas no destructivas está limitado por la capacidad de observación mediante lupa, el análisis de superficies (en muchas ocasiones alteradas), la menor cantidad de caracteres que nos permiten establecer los tipos y la variación de algunos de los caracteres seleccionados en función del estado de conservación de las superficies líticas. Es por ello que consideramos imprescindible la realización de láminas delgadas previas a la determinación de los tipos y las litotecas. A pesar de que la cantidad de muestra utilizada en esta tesis ha sido amplia (hemos analizado más de 6.000 fragmentos de cuarcitas a través de técnicas no-destructivas, con más de 15.000 fotografías microscópicas a 20, 50 y 250x aumentos), no hemos podido implementar un *software* de reconocimiento textural de las fotografías microscópicas realizas, como hubiéramos deseado. La consecución de este objetivo, queda pendiente para desarrollar en trabajos venideros, aunque hemos dado en esta tesis los primeros pasos: la creación de una base de datos fotográfica, un primer análisis de las imágenes digitales y su relación con el juego de T&P y la exploración de softwares que nos permitan alcanzar el objetivo: *Imagej* y *weka*.

Por su parte, la caracterización métrica de los granos de cuarzo a través de técnicas no-destructivas ha sido positiva. La cantidad de granos de cuarzo observados en cada una de las muestras ha sido siempre superior a las cinco unidades, si bien, mayoritariamente hemos podido interpretar en la mayor parte de las muestras al menos 25 granos de cuarzo. A pesar de que la metodología utilizada no nos ha permitido obtener medidas numéricas exactas y de precisión similar a la obtenida mediante técnicas petrográficas, hemos podido caracterizar la mayor parte de las muestras a partir de a) el tamaño medio, aplicando la clasificación de fino, medio y grueso; y b) la distribución de las medidas utilizando las categorías de homogéneo, heterogéneo con dos modas y heterogéneo. A pesar de ello, no hemos podido correlacionar, de forma general, las distribuciones bimodales de los tipos petrogenéticos BQ y RQ (debido al pequeño tamaño de los granos de cuarzo recristalizados por el metamorfismo).

Respecto a la caracterización mineralógica no-destructiva, hemos podido describir diferentes minerales que adicionalmente al cuarzo, componen las cuarcitas arqueológicas. A pesar de ello, la mayoría de las cuarcitas descritas presentan únicamente cinco minerales además del cuarzo: óxidos de hierro, micas, minerales pesados negros no identificados, óxidos de manganeso y pirita. La presencia de feldespatos, generalmente asociados al grupo de las cuarzoarenitas ha sido el único mineral caracterizado claramente relacionado con un grupo de cuarcitas específico. La relación entre la coloración de las rocas y la presencia de minerales específicos observados mediante técnicas no-destructivas y la petrografía y la caracterización geoquímica, ha permitido identificar rocas y variaciones específicas de muchos ambientes geológicos y arqueológicos donde se encuentran las cuarcitas. Además, nos ha permitido identificar en algunos de los niveles arqueológicos el número mínimo de masas líticas en conjuntos industriales específicos, especialmente en aquellos en los que el número de evidencias líticas es bajo.

La caracterización de las cuarcitas y el establecimiento de tipos a partir de las técnicas previamente descritas han supuesto el cumplimiento del primer objetivo de esta tesis. Sobre éste, se asienta el resto de objetivos que se han marcado a través de metodologías específicas y que a través de una ampliación del zoom, nos permiten entender la disposición de las cuarcitas en los afloramientos, conglomerados y depósitos y los mecanismos de adquisición y gestión de materias primas de las colecciones líticas analizadas.

La aplicación de los principios dialécticos de la Tipología Analítica nos ha permitido caracterizar, a partir de sus cinco estructuras de análisis, cada uno de los implementos líticos. Por otra parte, el carácter estructural de esta metodología sumada al análisis integral de los conjuntos líticos, nos ha permitido entender, dentro de secuencias de talla complejas, las estrategias de adquisición y gestión de las materias primas líticas, así como los roles que pudieron asignarse a cada materia prima.

La estructura petrológica ha permitido caracterizar el tipo de roca dentro de categorías generales: cuarcita, sílex, lutita, cuarzo… La asignación de grupo y tipo petrogenético a cada una de las cuarcitas ha posibilitado observar la cantidad de cada tipo introducido en los yacimientos y en algunos casos, valorar la cantidad de masas líticas diferentes introducidas en el yacimiento. En determinados contextos, y a través de la caracterización granulométrica y mineralógica hemos podido precisar aún más en la cantidad de masas líticas adquiridas. Finalmente, a partir de la caracterización de las zonas corticales de las rocas analizadas, hemos podido inferir el contexto en el que las materias primas líticas fueron captadas. Somos consciente del alto número de materias primas que, a pesar de conservar córtex, no hemos podido caracterizar. La ausencia de marcadores

que indiquen el contexto de captación es grande y creemos necesario generar una metodología más precisa que nos permita caracterizar las zonas corticales.

La estructura tecnológica ha permitido entender los mecanismos de gestión del material lítico, especialmente los relacionados con su explotación. Adicionalmente, y junto al resto de estructuras, ésta nos ha permitido entender procesos de talla y caracterizar la presencia o ausencia de determinadas acciones como los testeos, la obtención de soportes, la configuración o reconfiguración o los procesos de retoque o los avivados de filos. Somos conscientes que la metodología no ha incidido en los procesos complejos de talla que realizaron los grupos paleolíticos, pero éste no es un objetivo de este trabajo.

Las estructuras modal y morfológica nos han permitido incidir en los roles que determinadas materias primas jugaron dentro de cada colección lítica y en la explotación de las mismas. Por un lado, la presencia de retoque en determinadas materias primas o tipos cuarcíticos ha determinado una mayor explotación de las mismas. Por otro, la presencia de determinados grupos tipológicos, como las puntas (P), los dorsos (PD y LD), los buriles (B) o los ecaillés (E) en materias primas y tipos cuarcíticos ha permitido observar roles específicos y ampliar el conocimiento de las complejas secuencias de talla, incidiendo de nuevo en la explotación de las masas líticas. Somos conscientes que no hemos utilizado toda la profundidad metodológica que aporta la Tipología Analítica en estas dos estructuras, y que lleva a la comprensión de pautas culturales o roles más específicos de cada materia prima, pero estos no eran los objetivos de este trabajo.

Finalmente, **la estructura tipométrica** nos ha permitido entender los mecanismos de adquisición y gestión de la materia prima, entendiendo las masas líticas a partir de su tamaño, determinado por el peso, y su morfología. A partir del tamaño y la información proporcionada por otras estructuras, hemos valorado la cantidad de masa lítica introducida en cada yacimiento, así como la determinación de procesos de talla o retoque y el rol de algunas materias primas. Por su parte, la información derivada de la caracterización morfológica ha aportado información acerca de las formas específicas de determinados soportes. La información derivada del tamaño ha resultado más interesante para evaluar los mecanismos de adquisición y gestión de la materia prima que la aportada por la morfología. La información que hemos obtenido de ésta no ha resultado especialmente interesante, lo que sumado al esfuerzo que requiere la obtención, análisis y visualización de datos, nos planteemos no utilizarla en próximos trabajos.

A pesar del escaso trabajo reflejado de **la estructura traceológica** en esta tesis doctoral, observamos que tiene un alto potencial para entender los mecanismos de gestión de la materia prima, como se ha observado en otros trabajos (Perales, 2015). Esto es especialmente relevante para conocer qué piezas de los conjuntos han sido efectivamente utilizadas como herramientas. Por otro lado, como se ha demostrado en este y otros trabajos (Pedergnana et al., 2017; Pedergnana and Ollé, 2017; Pedergnana et al., 2016), la materia prima y los tipos petrogenéticos condicionan la generación de huellas y la forma de las mismas.

Como previamente hemos comentamos, **el análisis macroscópico de las potenciales fuentes de aprovisionamiento de las cuarcitas** es otro de los objetivos de esta tesis. La metodología utilizada para entenderlas parte de la diferenciación de tres grandes ambientes donde aparece la cuarcita en la zona de estudio. Estos son los afloramientos masivos de rocas, los conglomerados compuestos por diferentes tipos de roca (conglomerados poligénicos) y los depósitos cuaternarios de diferente naturaleza. A pesar de la existencia de los mismos criterios para definir los tres ambientes, cada uno de ellos se ha analizado a partir de sus características específicas.

En los afloramientos masivos hemos valorado la presencia de las formaciones analizadas a partir de tres posibles litologías (incluyendo los grupos y tipos cuarcíticos y las variedades determinadas por la granulometría), de los estratos infra y supra yacentes, y de las posible presencia de nievles/ intercalaciones de otras rocas en cada afloramiento. Además, hemos valorado la presencia en cada una de las litologías de minerales que alteran los estratos. Dentro de los afloramientos hemos tenido presente los posibles sistemas de diaclasas que afectan a los estratos, así como las inclusiones minerales asociados. Finalmente, hemos tenido en cuenta las estratificaciones visibles en cada afloramiento. Para analizar los conglomerados, además de tener presente las diferentes litologías (hasta un máximo de cinco), hemos valorado su frecuencia, el tamaño medio de los nódulos y su morfología. En dichos contextos, hemos caracterizado igualmente las propiedades del cemento, teniendo en cuenta su composición, coloración, compactación, y la facilidad de extracción de los bloques que están en él insertos. Al igual que en los afloramientos, hemos caracterizado el sistema de diaclasas, los minerales precipitados en ellas y la estratificación de los estratos. Finalmente,

para los depósitos cuaternarios hemos tenido en cuenta las cinco variedades litológicas más representadas, sobrerrepresentando la presencia de cuarcitas. Además, hemos tenido en cuenta la presencia de matrices secundaras dentro de los mismos, y finalmente el empaquetamiento que se observa de las rocas.

Los datos recogidos e interpretados nos han sugerido potenciales contextos de captación de cuarcitas y otras materias primas líticas. Además, nos han permitido exponer los mecanismos potenciales de adquisición de la cuarcita como el grado de selección necesario para seleccionar materiales específicos en contextos heterogéneos o los procesos de cantería necesarios para obtener tipos y variedades cuarcíticas específicas. Finalmente, nos han proporcionado datos interesantes para interpretar los procesos de transformación de la materia prima, la potencialidad de determinados tamaños y formatos para ser explotados o las posibilidades de explotación de cada uno de estos contextos. A pesar de ello, somos conscientes de ciertas limitaciones que plantea esta metodología. La primera y más importante, es la del principio de actualismo que hemos utilizado, pues las descripciones de estos contextos se han realizado en las condiciones presentes en la actualidad. Si bien las características de los afloramientos y conglomerados no ha variado de forma brusca en el tiempo, si los hemos interpretado en zonas hoy visibles que pudieron no serlo en determinados momentos del Paleolítico. En los depósitos, creados a lo largo del Cuaternario, estas modificaciones son mayores, modificando la percepción que hoy tenemos de estos potenciales contextos de captación. La segunda limitación se basa en la percepción propia de los datos aportados, que aun tratados desde la mayor objetividad y rigor posibles, no son los propios de las sociedades que potencialmente utilizaron estas zonas para la captación de materias primas.

Finalmente, y desde **un enfoque regional a gran escala**, hemos aplicado una metodología específica que nos posibilita, a través de los **Sistemas de Información Geográfica**, entender los el conjunto de datos analizados en el espacio geográfico. Esta metodología tiene dos vertientes diferentes: la geológica y la histórica.

La primera nos ha servido para **optimizar el proceso de prospección geológica**. Para ello, hemos definido y acotado el área de estudio mediante diferentes geo-procesos con el fin de establecer las cuencas de drenaje completas de los valles analizados: El Valle del Deva, el del Cares y el del Güeña. Una vez delimitada la zona de trabajo, hemos analizado la información geológica disponible, los mapas de la Serie MAGNA del IGME, y hemos seleccionado las capas de afloramientos que contengan areniscas y cuarcitas así como las de conglomerados y depósitos cuaternarios. El siguiente paso ha consistido en la superposición de capas de información con los accidentes de terreno, pueblos y carreteras y otras vías de comunicación actuales sobre las capas previamente delimitadas. Finalmente, y a través de la prospección *in situ*, hemos explorado todos los estratos analizados en diferentes puntos con el fin de observar las variaciones horizontales que en estos pudieran desarrollarse. Esta metodología nos ha permitido la optimización del proceso de prospección, así como de la visibilización y análisis de afloramientos completos, extendiendo las características de los mismos obtenidas en diferentes puntos prospectados a toda la formación. A pesar de ello, somos conscientes de múltiples limitaciones de esta metodología.

La primera está relacionada con la información geológica aportada por las descripciones y mapas de la segunda serie MAGNA. El carácter fraccionado de dicha serie ha generado problemas de continuación espacial de las formaciones geológicas en los límites de las hojas y de descripción de los mismos (diferente composición de los estratos, asimilaciones a edades diferentes, o la diferente precisión utilizada en cada caso). Además, muchas de las descripciones, realizadas a gran escala y aplicando descripciones de campo, no son muy precisas. Muchos de estos problemas han sido corregidos a partir de la información aportada por los nuevos mapas de la serie SIGECO, que con una precisión similar, aportan una caracterización continua de los estratos. La utilización del primer tipo de mapas y no de los segundos se debe a dos factores. El primero es la ausencia del mapa para la Zona Cantábrica en los momentos iniciales de esta tesis doctoral, que nos obligaba, por tanto, a utilizar la información de la serie 2 del MAGNA. El segundo es la menor y peor descripción de las capas, así como la sobrerrepresentación de capas cuaternarios en la serie SIGECO. En futuros trabajos, mantendremos la utilización de las dos series. La Serie 2 del MAGNA para marcar las capas geológicas de interés y analizarlas, mientras que la información de la serie SIGECO, será utilizada para la correlación de las diferentes hojas que componen la Serie 2 del MAGNA. Respecto a la precisión y la descripción de estratos aportados por los diferentes mapas geológicos, consideramos que los mapas son una herramienta para delimitar zonas, para realizar un primer análisis exploratorio de los datos, pero en ningún caso, evitarán la realización de las prospecciones, básicas para cualquier trabajo que quiera profundizar en el conocimiento de las potenciales fuentes

de captación de materia prima lítica.

La segunda de las limitaciones se debe al reconocimiento de los puntos de prospección en zonas hoy cortadas por accidentes orográficos, carreteras y otras vías de comunicación. En el proceso de preparación de las prospecciones, hemos primado estas zonas por su accesibilidad y con el objetivo de entender la mayor cantidad de caracteres de campo de cada uno de los puntos. La visibilidad de estos estratos en la Prehistoria, no tuvo que ser, por tanto, la misma. Esto nos obliga a matizar muchas de nuestras afirmaciones y a buscar el estrato donde aflora también de forma natural.

La metodología utilizada para entender la movilidad en el Paleolítico a partir de los Sistemas de Información Geográfica es la segunda metodología que hemos utilizado en este trabajo para entender los datos a escala regional. Para ello, hemos aplicado la metodología ya planteada en trabajo anteriores (García-Rojas et al., 2017; Prieto et al., 2016; Sánchez et al., 2016) a la zona de estudio. La metodología está basada en los "*Least Cost Analysis*" o análisis de coste o fricción y nos permite entender el espacio, no sólo como el resultado de la distancia euclidiana entre diferentes puntos, también el desnivel o pendiente de las zonas atravesadas. Esto nos ha permitido, por un lado determinar el esfuerzo mínimo (*Cost Units, CU*), requerido para llegar desde un sitio arqueológico a un contexto potencial de captación de materia prima, pero también nos ha permitido delimitar las zonas de mayor accesibilidad y por las que el movimiento humano es más sencillo. A pesar de la amplia difusión del cálculo de rutas óptimas, no las hemos realizado debido al sesgo que generan en el conocimiento, especialmente determinado por la relación exclusivamente lineal y simple de la movilidad paleolítica. Somos conscientes de que la movilidad humana no sólo depende de las dos variables analizadas por esta metodología, pero nos acerca más a la realidad paleolítica a partir de dos variables importantes y que no han sufrido grandes modificaciones a lo largo del Cuaternario. Otras variables no han podido ser analizadas o no se han introducido en el análisis debido al desconocimiento de cómo influyeron durante el Paleolítico. Estas son, la masa vegetal, la presencia de accidentes orográficos como ríos o lagos que determinarán pasos específicos o la presencia de determinados estratos geológicos que dificultasen el paso, como lapiaces o derrubios de ladera accidentados. Finalmente, nos gustaría señalar que existen otras variables relacionadas con los comportamientos económicos, sociales y simbólicos y que hoy no podemos valorar.

A modo de resumen de la evaluación realizada, consideramos que la metodología establecida para la consecución de los objetivos de esta tesis doctoral ha sido correcta y ambiciosa. Esta tesis ha planteado la aplicación de diferentes metodologías que van desde la medición de objetos de tamaño micrométrico, como los granos de cuarzo, hasta otros de carácter kilométrico, como los valles analizados, aplicando un enfoque holístico a la caracterización de las materias primas líticas. Además, la metodología realizada ha permitido entender y articular los diferentes niveles de profundidad utilizados para entender los mecanismos de adquisición de la cuarcita, desde los motivos por los que se seleccionan determinados tipos en detrimento de otros, hasta la movilidad paleolítica.

14.2. LAS CUARCITAS ARQUEOLÓGICAS: PROCESOS FORMATIVOS, EL CICLO DE LAS ROCAS Y LA ACCIÓN HUMANA

"Tenemos que encontrar una nueva visión del mundo que coincida con todo lo que se sabe, pero que en algún aspecto haga previsiones distintas, de otro modo carecerá de interés. En estas previsiones tiene que coincidir con la naturaleza. Si ustedes construyen una nueva visión del mundo que coincida con la totalidad de las cosas ya observadas, pero que se distinga en algo aún por oberservar, habrán hecho un gran descubrimiento."

Richard Feynman. El carácter de la ley física, página 188.

Como previamente hemos mencionado, la segunda parte de esta discusión está dedicada a la cuarcita, entendiendo este material desde su formación hasta su extracción en los contextos arqueológicos por parte de las investigadoras.

La propia definición y caracterización formal de la cuarcita desde perspectivas geológicas y arqueológicas resulta compleja. En numerosos textos el término cuarcita hace referencia a las características composicionales de la roca con un contenido en cuarzo superior al 80% (Howard,

2005; Skolnick, 1965). Estos autores hacen referencia a características como el granulado, más o menos marcado, la fractura concoidea y la tenacidad del material. Atendiendo a la génesis del mismo, aceptan que ésta pueda ser sedimentaria o metamórfica. El término cuarcita, es también utilizada por estudios geológicos de campo para denominar afloramientos rocosos de génesis desconocida pero con un alto contenido en sílice de aspecto granular y con un grado de compacidad alto. Estos elementos le diferencian de las areniscas, utilizadas para denominar los afloramientos de areniscas con grado de compacidad más bajo o con presencia de cemento. A lo largo de los últimos años se han realizado diversos estudios acerca de la cuarcita proveniente de contextos arqueológicos donde también se pone de relieve la ambigüedad del término cuarcita, en los que se utiliza el término cuarcita para definir rocas con alto contenido en sílice incluso derivadas de ambientes volcánicos (Blomme et al., 2012; Cnudde et al., 2013; Dalpra and Pitblado, 2016; Pitblado et al., 2008; Pitblado et al., 2012; Prieto et al., 2018; Roy et al., 2017). Como ya hemos comentado, en este trabajo denominaremos cuarcita, o de forma más concreta, cuarcita arqueológica a las rocas que, independientemente de su origen (sedimentario o metamórfico), tengan un contenido en sílice superior al 80%, con gran tenacidad, fractura concoidea y una alta fragilidad e incluyendo, por tanto, todos los materiales que historiográficamente (a partir de la Geología y la Arqueología) se han definido como la cuarcita.

La génesis de este material es por tanto diversa, pero siempre comienza por la deposición de sedimento de tamaño fino (tamaño arena, principalmente), **cuyo origen está en función de la roca de partida (petrolito)**. Las características de este sedimento, como ya hemos comentado, determinarán la composición de la cuarcita y muchos procesos que modifican el material. Este sedimento puede tener una única procedencia, aunque de forma general hemos observado en las cuarzoarenitas diferentes aportes sedimentarios, desde granos de cuarzo monocristalinos a los policristalinos y otros fragmentos de otras rocas o matrices de diferentes composiciones. El tamaño de grano que componen los afloramientos de cuarzoarenitas caracterizados en este estudio ha permitido observar diferentes modelos deposicionales que conforman las rocas originales. Así, la mayor parte de las cuarzoarenitas muestreadas de la formación de Barrios reflejan condiciones de sedimentación lenta, de llanura deltaica, con distribuciones homogéneas de los granos de cuarzo que las componen. Por otro lado, la formación Murcia refleja condiciones sedimentarias heterogéneas, relacionadas con ambientes marinos de corrientes turbidíticas. Por su parte, las formaciones masivas de cuarzoarenitas carboníferas, además de reflejar condiciones heterogéneas de formación a través de sus heterogéneas tramas, muestran la presencia de matrices silíceas y arcillosas.

Una vez el aporte sedimentario ha finalizado, comienza **el proceso de litificación** (consolidación y endurecimiento) **del material a través de procesos diagenéticos**. Esta litificación se puede producir por dos mecanismos no excluyentes, bien por cementación, o bien por compactación por la presión de las capas suprayacentes. En este trabajo hemos expuesto distintos ejemplos de ambos tipos. Por un lado, hemos observado procesos de cementación en la formación Murcia, como se puede observar en las muestras del tipo CC (cuarzoarenita con granulado detríticos cementados o con matriz), por ejemplo la DC16_01 (Figure-6.9) con cemento calcáreo, o bien por cemento de cuarzo microcristalino, como el observado en el tipo CC_MQC del yacimiento de Ravensberg-Troisdorf (Figure-13.9, Figure-13.12 y Figure-13.13). Por el otro, hemos observado procesos de litificación por compactación en afloramientos masivos en partes de la formación de Barrios y que generan el tipo CA (cuarzoarenita con granulado detríticos sin cemento ni matriz) (DC36_02, en Figure-6.4).

El incremento de presión generado por las capas suprayacentes y el metamorfismo regional genera una modificación en el proceso de compactación que, sumado a la imbricación de los granos de cuarzo que componen las cuarzoarenitas, provoca la expansión de cementos sintaxiales de cuarzo. Este proceso de compactación es el que determina el cambio de textura, de las estrictamente sedimentarias, representadas por el grupo de las cuarzoarenitas, a las mixtas, representadas por el grupo de las ortocuarcitas. Este, es el último de los procesos documentados en afloramientos masivos de la zona de estudio, y únicamente en algunos puntos de la formación de Barrios (D04_05 en la Figure-6.5) con presencia del tipo OO (ortocuarcita con recremiento sintaxial de granos de cuarzo). Somos conscientes que no hemos podido documentar los tránsitos entre los dos grupos, aunque esperamos poder desarrollarlo en investigaciones futuras. Éstas requerirán de la aplicación de criterios no evaluados en este trabajo, como la delimitación de zonas de afección de procesos metamórficos de escala regional.

El paulatino aumento de la presión va generando una textura cada vez más compacta y en

la que la extinción ondulante se hace extensible de forma generalizada en todas las muestras seleccionadas. La sucesiva compactación del material crea igualmente una estructura con una mayor imbricación entre los granos de cuarzo, generando bordes aserrados y estilolíticos. Asimismo, la aparición de lamelas de deformación en algunos granos de cuarzo, evidencia este incremento de presión. La génesis, por tanto del tipo SO (ortocuarcita con bordes de granos suturados) hay que buscarla en este incremento de los mecanismos de deformación, incluso en procesos de iniciales de recristalización, como se observa en algunas de las muestras con presencia residual de granos de cuarzo recristalizados en los bordes aserrados. Este tipo de ortocuarcitas no están representadas en la zona de estudio en afloramiento masivo, lo que nos ha impedido evaluar estos procesos *in-situ*. A pesar de ello, su presencia en conglomerados, depósitos y también en yacimientos arqueológicos, nos ha permitido diferenciar el tipo y asociar la información petrogenética aportada por la literatura geológica (Bastida, 1982; Gapaist and White, 1982; Howard, 2000, 2005; Skolnick, 1965; Wilson, 1973). El área fuente de este tipo de ortocuarcita, así como de los que describiremos posteriormente, hay que buscarla en la zona más occidental de la Región Cantábrica, en estratos geológicos más antiguos y afectados por metamorfismo de mayor grado.

El incremento de presión generado por el metamorfismo regional sobre las cuarzoarenitas o las ortocuarcitas previamente comentadas, genera procesos de recristalización, que nos obligan a hablar, ahora sí, de una génesis del material puramente metamórfica. El grupo de las cuarcitas *s.s.* o cuarcitas, está caracterizado por la recristalización (evidencia de procesos metamórficos) y sus tres tipos reflejan ese aumento paulatino de presión y temperatura. El tipo BQ (cuarcita de recristalización por abultamiento de límites y fractura), el tipo RQ (cuarcita de recristalización por abultamiento de límites y fractura por rotación) y el tipo MQ (cuarcita de recristalización por migración de límites) muestran la afección de estos procesos metamórficos y los cambios que en la estructura de las cuarcitas y de los granos de cuarzo se producen. Estos tres tipos metamórficos no han sido descritos en afloramientos masivos, apareciendo en conglomerados y depósitos específicos los tipos BQ y RQ. El tipo MQ únicamente ha sido caracterizado en los yacimientos arqueológicos.

La presencia en el territorio de estudio de seis de los siete tipos comentados evidencia igualmente procesos geológicos complejos, la dureza del material y la presencia del mismo en diferentes contextos. Por un lado, hay una amplia presencia en el territorio del grupo de las cuarzo-arenitas, especialmente las del tipo CC, en afloramientos masivos, conglomerados y depósitos. En los dos últimos contextos, el porcentaje de este grupo (especialmente el tipo CC) es alto teniendo en cuenta otros grupos cuarcíticos, si bien, la cantidad de calizas o lutitas es mayor. La presencia de las ortocuarcitas en el territorio es limitada. El tipo OO aparece tanto en afloramiento masivo como en conglomerados y en depósitos. En afloramientos masivos únicamente está representado en algunas zonas de la formación de Barrios. La presencia en los dos últimos contextos suele ser inferior al 5% de las litologías presentes. El tipo SO únicamente aparece en conglomerados y en depósitos, en porcentajes claramente inferiores a los que aparece el tipo OO. Finalmente, la presencia del grupo de las cuarcitas en el territorio es limitada, apareciendo únicamente en conglomerados y depósitos y en porcentajes mínimos. El tipo BQ únicamente aparece en las formaciones Remoña, Valdeón, Maraña-Brañas, Pontón, Pesaguero y Potes. Por su parte, el tipo RQ sólo aparece en las formaciones de Valdeón y Pontón. La cantidad de estos dos tipos en depósitos es insignificante.

La presencia de los tipos CC, CA y OO en afloramientos masivos en la zona de estudio determina su mayor presencia en conglomerados y depósitos (especialmente del tipo CC). Por el contrario, la baja proporción de tipos petrogenéticos altamente deformados o recristalizados en contextos secundarios se debe a la ausencia de afloramientos masivos de estos tipos en el área de estudio. La presencia de estos tipos en el área se debe a procesos erosivos en zonas distantes (oeste de la Cornisa Cantábrica) y el transporte, depósito y encapsulamiento de clastos de ortocuarcitas y cuarcitas en los conglomerados.

De forma general, el análisis de las industrias líticas desarrollado en los últimos siete capítulos de los resultados nos ha permitido observar **una selección principal hacia los tipos cuarcíticos deformados o recristalizados por parte de las sociedades prehistóricas que habitaron la zona** en detrimento del grupo de las cuarzoarenitas (principalmente). A pesar de no haber desarrollado en profundidad un estudio para conocer las capacidades de talla y uso de cada uno de los tipos a través de un estudio experimental, son varios los criterios observados en las cuarcitas arqueológicas los que determinan la selección de unos tipos frente a otros. El primero está determinado por el aumento de deformación y los procesos de recristalización, que provocan en las cuarcitas arqueológicas una mejora de las propiedades de la talla, relacionadas con su mayor isotropía, el aumento de la fragilidad y la mayor uniformidad del material (independientemente del tamaño y homogeneidad

de los granos de cuarzo que conforman la trama principal) (Kocks et al., 1998). Estos mismos factores mejoran y aumentan las posibilidades de uso de estos tipos frente a otros, generando bordes más cortantes y duraderos, como se pudo demostrar en el estudio experimental expuesto en el Capítulo-13 y en recientes publicaciones (Pedergnana et al., 2017; Pedergnana and Ollé, 2017; Pedergnana et al., 2016).

Por otro lado, hemos observado una selección preferencial de cuarcitas arqueológicas debido a su granulometría, especialmente dentro del grupo de las cuarzoarenitas y en el tipo OO, con una selección preferencial hacia 1) tramas con granos homogéneos y 2) tramas con granos de tamaño fino y medio. Tanto la homogeneidad, como el tamaño de grano, determinan de forma secundaria las propiedades de talla y de uso. Así, una trama de grano fina y homogénea, determina una mayor fragilidad de las mismas y una talla más controlada. Además, estas tramas favorecen el desgaste homogéneo de los filos y una mayor durabilidad de los mismos. En cambio, en los tipos más deformados y recristalizados, especialmente en los tipos RQ y MQ, o en el yacimiento de *Ravensberg-Troisdorf*, hemos observado la escasa importancia del tamaño y distribución de grano.

Finalmente, y como quedó comprobado en el segundo apartado del capítulo cinco, se observa la selección preferente de cuarcitas arqueológicas de mayor contenido en sílice por parte de las sociedades paleolíticas. Esto se hace especialmente relevante en el yacimiento de *Ravensberg-Troisdorf*, en el que el que la selección de cuarcitas arqueológicas está determinada por la mayor presencia de cemento microcristalino y no por los tipos petrogenéticos (donde únicamente están presentes dos, el tipo CC y el tipo OO) o las características métricas de la trama principal. En este caso, la presencia de cuarzo microcristalino en los espacios no rellenos por la trama principal o la matriz, ha creado una estructura uniforme, isotrópa y frágil similar a la generada por los granos de cuarzo recristalizados del grupo de las cuarcitas *s.s.* y que permite mayores posibilidades de talla y posiblemente una mejora en las propiedades relacionadas con el uso.

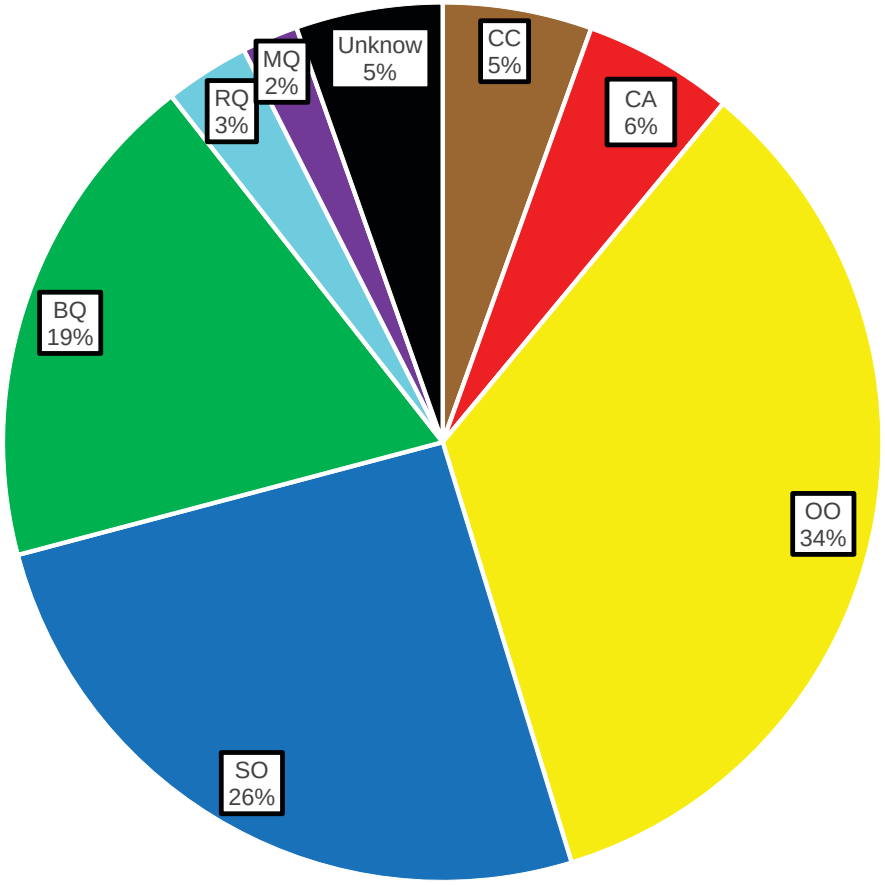

Figura-14.1: Gráfico circular mostrando los porcentajes de cada tipo cuarcítico en todas las colecciones líticas analizadas.

De forma general, la captación de cuarcita arqueológica a lo largo del Paleolítico en la zona de estudio se ha realizado teniendo en cuenta las propiedades de talla y uso, determinadas por los factores previamente discutidos, así como por la presencia y cantidad en el territorio, determinadas por la distribución y la presentación de los tipos existentes. La Figura-14.1, muestra la presencia masiva de los tipos cuarcíticos OO, SO, y BQ en los yacimientos. A pesar de las mejores características de talla y uso de los dos últimos tipos frente al primero, su mayor presencia en el

territorio determina la mayor captación del tipo OO frente a los tipos SO y BQ. La existencia de los tipos CA y CC está motivada por la presencia generalizada de estas rocas en la zona de estudio. A pesar de ello, sus propiedades físicas, hacen que la cantidad de cuarzoarenitas en los yacimientos sea minoritaria y su explotación sea poco intensiva. Por otro lado, la presencia de los tipos MQ y RQ en las colecciones líticas y su alta explotación evidencian su utilización y captación a pesar que estén infrarrepresentación en el territorio y su accesibilidad sea muy baja.

Respecto a **los contextos de captación de la cuarcita arqueológica,** hemos observado que la cuarcita ha sido adquirida preferentemente en depósitos secundarios, si bien, la adquisición en afloramientos de conglomerados también ha sido importante. Por el contrario, no tenemos ninguna evidencia que nos haga pensar en captación primaria en afloramientos masivos. Como ya hemos comentado, los mecanismos utilizados para la captación de los diferentes tipos cuarcíticos pasan por la selección del material y los procesos de movilidad que llevan a zonas con presencia de tipos específicos.

Finalmente, hemos observado algunas **características de los procesos post-deposicionales** que ha sufrido la cuarcita arqueológica una vez ha sido enterrada. Estos, han sido importantes en contextos al aire libre, como en El Habario, y posiblemente también en *Ravensberg-Troisdorf*, y más moderados en yacimientos en cueva o abrigo. Estos procesos alteran, de forma general, zonas superficiales de la cuarcita arqueológica o en zonas concretas de la misma, sin profundizar en la estructura interna por más zonas que las diaclasas o fisuras de las cuarcitas. Las alteraciones observadas consisten, por un lado, en la modificación de las superficies de las cuarcitas a través de su meteorización superficial. Esta modifica sus colores y en ocasiones, como en El Habario, modifican la textura y el tacto de la roca haciéndola más arenosa. Asimismo esto procesos generan una menor afección sobre las cuarcitas arqueológicas más deformadas o metamorfizadas. Por otro lado, las superficies de las cuarcitas se han visto igualmente alteradas por la precipitación de diferentes minerales como óxidos de hierro, calcita o fosfatos. Los últimos son muy evidentes en el yacimiento de La Cueva de Coimbre a causa del uso de la misma como redil para animales.

14.3. LA ADQUISICIÓN Y LA GESTIÓN DE LA CUARCITA ARQUEOLÓGICA EN LOS VALLES DEL DEVA, CARES Y GÜEÑA DURANTE EL PALEOLÍTICO MEDIO Y EL PALEOLÍTICO SUPERIOR

"This shift in prehistoric archaeology, as I see it, is from talk of artifacts to talk of societies, and from objects to relationships among different classes of data…

…it is to talk about meaningfully of societies of which these artefacts are the relict. To discuss their environment and subsistence, their technology, their social organization, their population density and so forth, and from these parameters to construct a picture and an explanation of these changes taking place."

Colin Renfrew: Before Civilization. The Radiocarbon Revolution and Prehistoric Europe. Página 277

Una vez hemos valorado desde una perspectiva general la metodología utilizada en esta tesis doctoral y hemos establecido y definido el objeto de estudio, nos centraremos en el sujeto de estudio de esta tesis, las sociedades humanas paleolíticas, focalizado en las pautas económicas y sociales que éstas generan en torno a la captación, gestión y distribución de la materia prima lítica. Para ello, articularemos este apartado en dos bloques diferenciados. Por un lado, y a través de una visión diacrónica, discutiremos acerca del rol que la cuarcita tuvo en cada una de las colecciones arqueológicas analizadas. Por otro lado, trataremos de entender las modificaciones temporales en la captación, distribución y gestión de las materias primas líticas.

En los siete últimos capítulos de los resultados (capítulos 7 a 13), hemos observado multitud de procesos que nos han llevado a plantear **la funcionalidad de cada sitio teniendo en cuenta los diferentes roles existentes y derivados de la adquisición y gestión de las materias primas**. De forma general, la figura-14.2 muestra esta variedad de comportamientos y las similitudes y diferencias entre las colecciones líticas analizadas, teniendo en cuenta la información de estudios

previos. A pesar de la simplicidad del esquema, cada nivel analizado plantea peculiaridades que analizaremos más detalladamente.

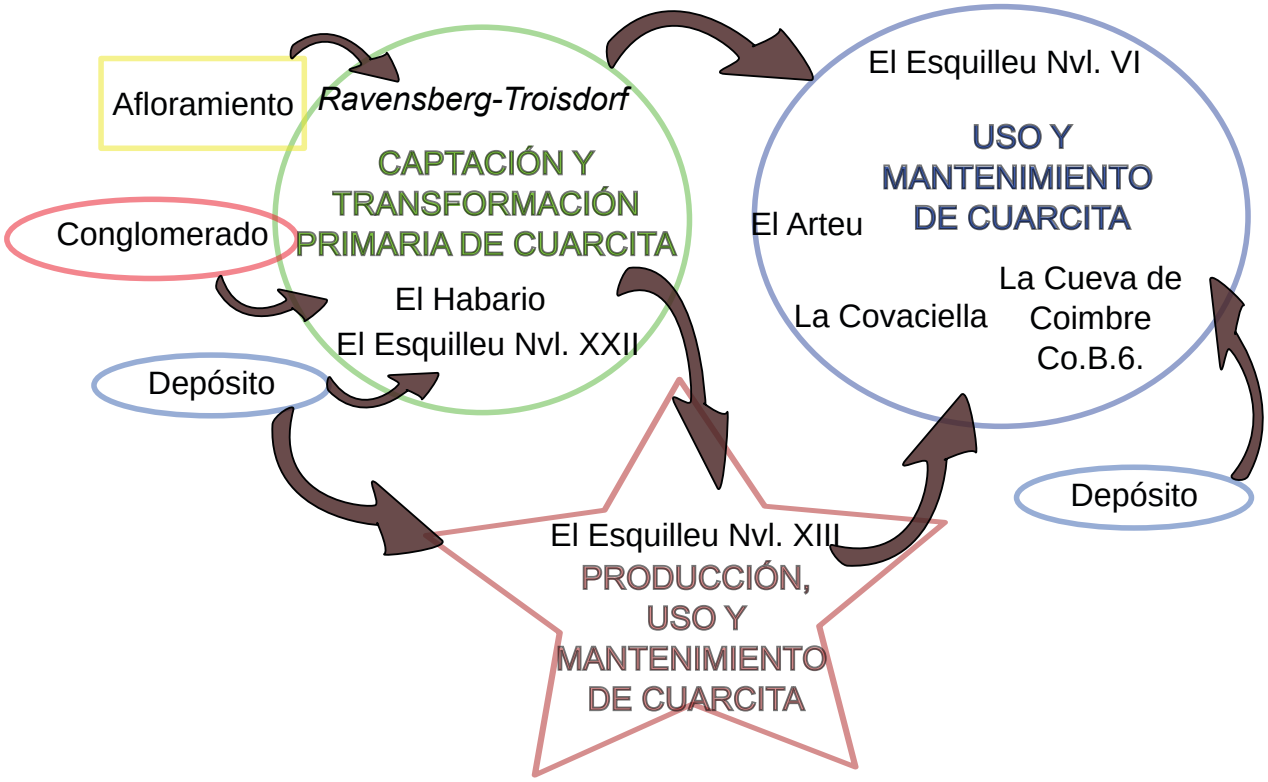

Figura-14.2: Representación esquemática de los modelos de adquisición y gestión de la cuarcita en los yacimientos analizados en este trabajo.

En primer lugar hemos documentado **los contextos relacionados con la captación y transformación inicial de la materia prima** en los yacimientos de Ravensberg-Troisdorf, El Habario y en el nivel-XXII-R de El Esquilleu. A pesar de no tener información numérica del primero, la industria lítica del yacimiento de ***Ravensberg-Troisdorf*** muestra procesos claros de selección de variedades cuarcíticas específicas mediante la talla selectiva y la extracción de los tipos y variedades preferentes. Estos son, por un lado, el tipo CC_MQC, obtenido en la zona circundante al yacimiento como producto principal. Por otro, el tipo OO, posiblemente explotado como producto secundario o subproducto. Finalmente, y apenas sin explotación ni importancia económica, la variedad CC_CM, que es considerada como un desecho de la explotación de la materia prima (desecho). Los procesos que aquí se observan están relacionados con la explotación sistemática de un estrato masivo (en posición primaria o bien los clastos recientemente disgregados del afloramiento) en el que se encuentran los tipos previamente descritos y una gestión del material para ser exportado. Este tipo de proceso ya ha sido atestiguado en otras zonas con cronologías similares (Ortiz and Baena, 2016; Preysler et al., 2015). A pesar de ello, futuros trabajos que determinen los tipos y variedades de todas las evidencias líticas, nos permitirán adentrarnos en los mecanismos complejos de adquisición y gestión de la materia prima en este yacimiento, así como la gestión del medio ambiente circundante.

El segundo de los yacimientos relacionados con la captación y transformación inicial de la materia prima lítica es **El Habario**. Este yacimiento pone de relevancia la importancia que los conglomerados con cantos de cuarcita tuvieron para las sociedades prehistóricas que habitaban la principal zona de estudio. El análisis de las industrias líticas nos ha permitido identificar procesos de captación primaria de materia prima. Las estrategias utilizadas son en la colecta de cantos de cuarcita en la zona, alrededor de los conglomerados de la formación Remoña y la captación directa en el estrato, facilitada por la baja compactación que confiere el cemento arcilloso. La existencia de una alta proporción de los tipos OO, SO y BQ en la zona, determina las litologías mayoritarias talladas en este yacimiento (92% de las cuarcitas arqueológicas son de estos tres tipos). El análisis tecnológico revela que los dos últimos tipos cuarcíticos son el producto principal, mientras que el tipo OO es un producto secundario de la explotación económica de la zona. La presencia de un único nódulo del tipo CC con una única extracción, posiblemente muestre un golpeado de testeo del material,

evidenciando también aquí procesos de selección de cuarcita. El análisis de las industrias líticas nos ha permitido observar procesos de talla completos, que pasan por la creación de *stocks* en forma de núcleos y de lascas para los tipos SO y BQ, y de *stocks* en forma de lascas para el tipo OO. Hemos observado diferencias en la primera configuración de las masas líticas entre los dos primeros tipos y el segundo. Las lascas completamente corticales de los tipos SO y BQ son más finas y más ligeras que las del tipo OO, posiblemente debido a la mayor afección del cemento del conglomerado en el último tipo. Igualmente, hemos observado procesos de creación de herramientas (*toolkit*) en los tres tipos. Finalmente, hemos atestiguado el desecho de los antiguos *stocks* (en forma de núcleos y de lascas) y de herramientas y que posiblemente determinen la alta cantidad de material retocado en el sitio, en contraposición a la idea planteada previamente que relacionaba este hecho a procesos de aprendizaje (Carrión and Baena, 2005; Carrión et al., 2013).

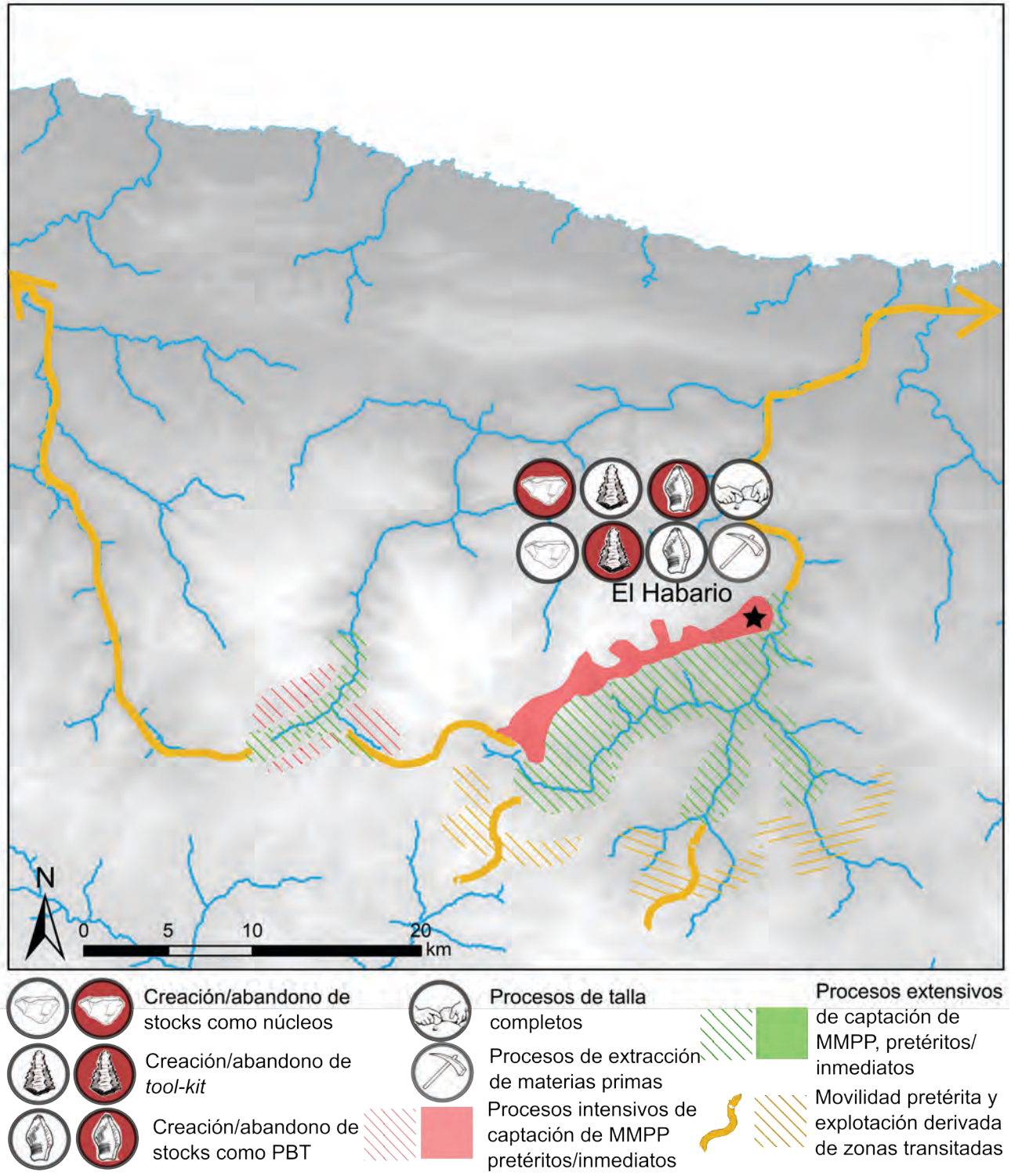

Figura-14.3: Mapa de la zona mostrando los procesos técnicos caracterizados en el yacimiento de El Habario y las zonas explotadas económicamente. PBT es soporte o blank. MMPP son materias primas.

A pesar de que la mayor parte de las rocas provengan de un entorno inmediato, reflejando la explotación intensiva del mismo, también hemos observado cadenas operativas fragmentadas en este yacimiento y que revelan la explotación de otras zonas en momentos pretéritos. Estas áreas son los valles adyacentes mediante una explotación extensiva y las zonas de media montaña y pequeñas mesetas situadas en el nacimiento del río Cares, donde afloran otros conglomerados (Formaciones Remoña, Valdeón y Maraña-Brañas), explotados de forma intensiva. Asimismo, no descartamos la explotación de los múltiples recursos de otras zonas y de forma extensiva, especialmente en las cabeceras de los ríos Deva, Quiviesa y Bullón, como reflejan algunas de las cuarcitas identificadas en el yacimiento (Formaciones Potes y Lechada) Figura-14.3.

El último de los niveles que está relacionado con la captación primaria de cuarcita es **el Nivel-XXII-R de El Esquilleu**. A diferencia de los dos niveles anteriores, relacionados con la explotación masiva y sistemática de afloramientos o conglomerados, la captación de la materia prima se realiza en las playas fluviales cercanas al yacimiento a través de procesos de intensivos de selección de materia prima, donde no sólo se seleccionan nódulos de cuarcita, también de cuarzo, sílex, lutita y radioralita. En este caso, aun existiendo una alta cantidad de los tipos OO y SO, el rol que juega el grupo de las cuarzoarenitas es más importante que el que tienen las cuarcitas *s.s* y el discutido en el yacimiento anterior. Esto se debe a la gran cantidad de este grupo en los depósitos fluviales, especialmente el tipo CC, con mayor representación que el tipo CA. A pesar de la presencia en el yacimiento de estos dos tipos cuarcíticos, ambos juegan un rol complementario en el sitio y su talla y utilización, está ligado a actividades complementarias con bajos requerimientos técnicos y en ausencia de otros tipos cuarcíticos.

El tipo OO es el mejor representado en la colección y es el que relaciona de forma más clara la captación de materia prima en los depósitos fluviales adyacentes al yacimiento. El análisis tecnológico revela la presencia de una gran cantidad de lascas de decorticado, de bajo grosor, posiblemente relacionadas con un primer desbaste de los nódulos de esta ortocuarcita. Este decorticado inicial junto con la sobrerrepresentación de productos brutos de talla revela el acopio directo al yacimiento desde los depósitos fluviales. La útlima característica igualmente revela los cambios de actitudes de talla en función, no sólo del tipo cuarcítico, sino también del tipo de córtex, pues en el yacimiento de El Habario, observamos un decorticado de este tipo de una forma más intrusiva, en respuesta al mayor grosor de la superficie alterada en el conglomerado que en los depósitos fluviales. Los mecanismos selectivos para la obtención de este tipo en playas fluviales son importantes. Además, no descartamos un recorrido de corta distancia para obtener estos tipos hacia el norte, debido a la mayor cantidad del tipo OO presente en las playas fluviales una vez el río Deva erosiona los estratos más meridionales de la Formación de Barrios.

El resto de tipos cuarcíticos también son captados en el río, posiblemente de forma complementaria al producto principal, el tipo OO. A pesar de ello y debido a las características técnicas que en los tipos SO y BQ se han puesto de manifiesto, estos dos son materias primas altamente apreciadas. Esta situación, revela pautas oportunistas de gestión del material lítico y pone de relieve la importancia de los ríos como zonas de alto interés económico debido a la diversidad y cantidad de recursos potencialmente disponibles.

Al igual que en El Habario, observamos cadenas operativas fragmentadas. Estas reflejan, por un lado, la preparación de *stocks* de diferente formato en función del tipo que de cuarcita. Así, algunos tipos cuarcíticos se exportan como núcleos (el tipo OO), mientras que otros, como productos brutos de talla (el tipo SO). Por otro lado las cadenas operativas fragmentadas reflejan la captación y gestión de la cuarcita en momentos pretéritos desde otras zonas (especialmente de la zona más meridional de los valles del Deva y Cares y posiblemente desde zonas fuera del área de estudio). Esto se evidencia en los tipos RQ y MQ, así como otros tipos con córtex de conglomerados, que describen cadenas operativas fragmentadas, especialmente relacionadas con el mantenimiento de diferentes herramientas o *tool-kit*. Todos estos datos, ponen de nuevo en evidencia la utilización complementaria de diferentes biotopos presentes en la zona de estudio. Por un lado, la explotación intensiva y de forma inmediata de las zonas bajas de valle. Por otro, la explotación intensiva y extensiva de zonas amesetadas y de media montaña. Todo ello, está integrado dentro de circuitos de movilidad de media y baja distancia, sin descartar la posibilidad de circuitos más amplios, como refleja la presencia del tipo cuarcítico RQ (Figura-14.4).

Una vez contextualizadas las tres colecciones líticas que muestran los contextos de captación de cuarcitas arqueológicas por parte de las poblaciones paleolíticas, plantearemos una discusión para entender **la gestión integral de esta materia prima lítica en el Nivel-XIII de El Esquilleu**. Este nivel cuenta con la mayor cantidad de restos líticos (únicamente en el cuadro seleccionado

hay 2444), que sumadas al resto de evidencias, como la presencia de hogares, posibles camas realizadas con arbustos y las quemas de carácter sanitario o la alta cantidad de restos faunísticos, hacen ver este nivel como **un lugar de habitación central y continuado en el tiempo**. Este nivel refleja la posición central del yacimiento de El Esquilleu dentro de una red logística de sitios económicos que explotan de forma eficaz el heterogéneo medio ambiente de la zona de estudio.

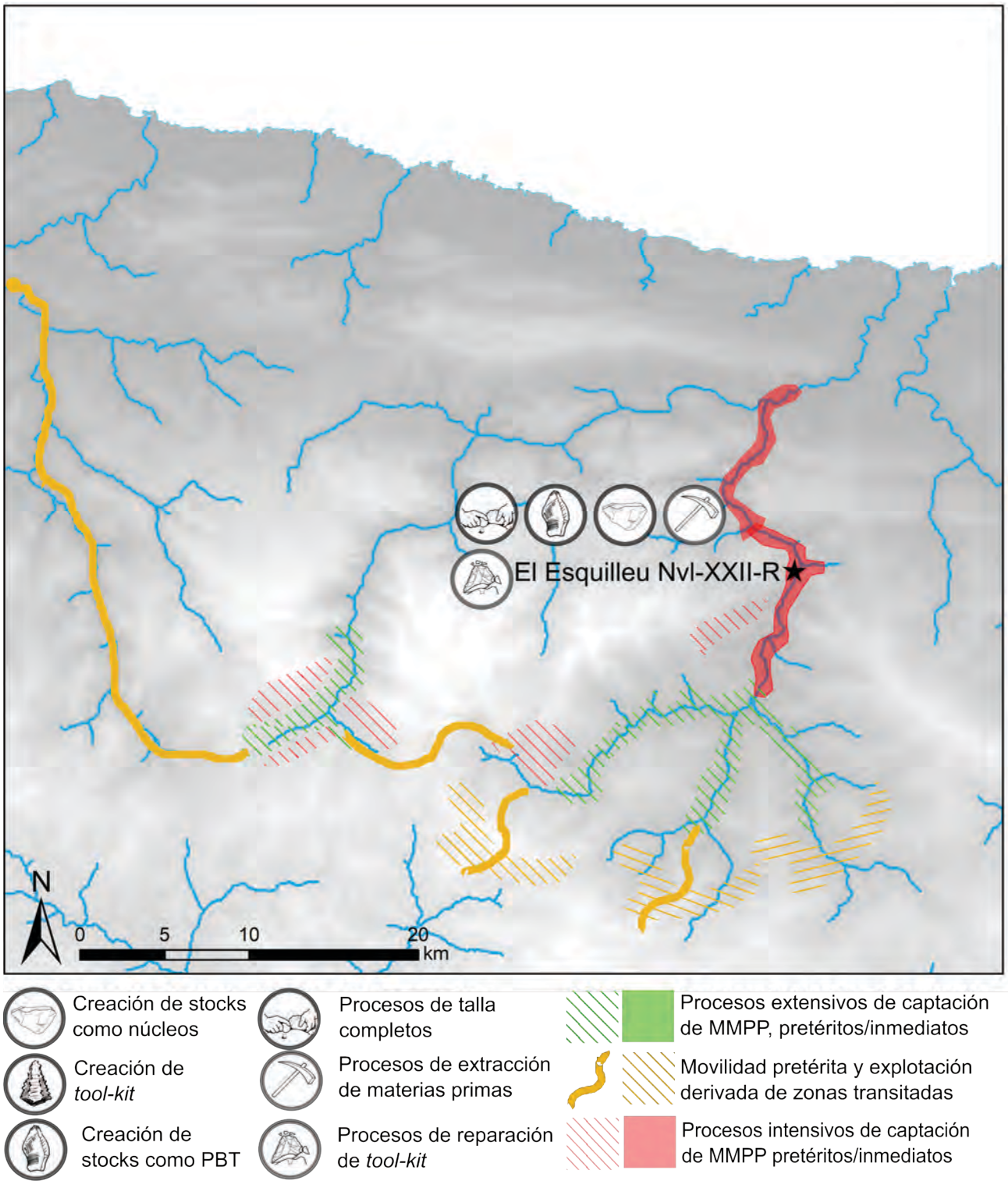

Figura-14.4: Mapa de la zona mostrando los procesos técnicos caracterizados en el nivel-XXII-R del yacimiento de El Esquilleu y las zonas explotadas económicamente.

En este nivel hay una gran cantidad de litologías representadas y todos los tipos cuarcíticos están igualmente caracterizados. Centrándonos en las cuarcitas arqueológicas, observamos que estas se han obtenido en conglomerados y en depósitos fluviales en proporciones similares. Dentro de éstas,

hay una clara tendencia de selección en contextos fluviales del grupo de las cuarzoarenitas y del tipo OO como consecuencia del aprovechamiento económico de los variados recursos de los ríos y en cuyas playas existe presencia de dichos tipos (Figura-14.5). De forma general, estas cuarzoarenitas y ortocuarcitas han sido importadas desde los depósitos fluviales y han sido desbastadas y talladas en el yacimiento. Derivado de la explotación extensiva del río, hemos aportado una nueva prueba a partir del análisis de las litologías de los cantitos existentes en el yacimiento y que pone en evidencia el acopio de las plantas que crecen en las orillas del río Deva (Cabanes et al., 2010; Uzquiano et al., 2012).

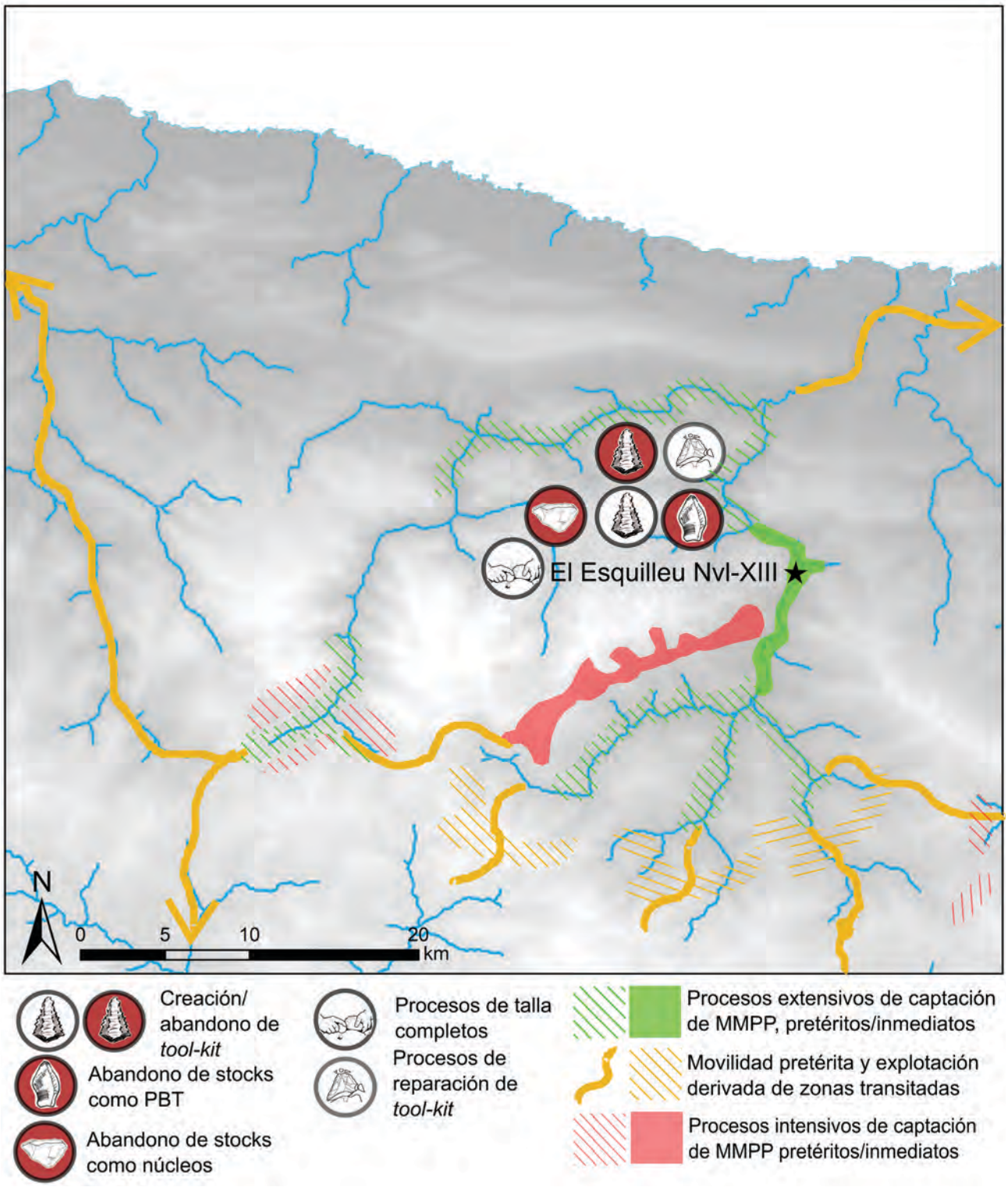

Figura-14.5: Mapa de la zona mostrando los procesos técnicos caracterizados en el nivel-XIII del yacimiento de El Esquilleu y las zonas explotadas económicamente.

La presencia y gran cantidad de cuarcitas con córtex derivados de conglomerados, principalmente de los cercanos afloramientos de la Formación Remoña, ponen en evidencia la captación intensiva de cuarcitas y la explotación de la media montaña y zonas amesetadas a partir de una red de yacimientos satélites similares al yacimiento ya comentado de El Habario (Baena and Carrión, 2014; Baena et al., 2012; Carrión and Baena, 2005; Manzano et al., 2005). La presencia de superficies corticales en núcleos y lascas, refleja que a pesar de que algunos nódulos han sido pre-configurados fuera de El Esquilleu, otros han sido importados directamente.

Finalmente, la presencia de cuarcitas *s.s.* y de córtex no asimilables a la formación Remoña, así como la ocasional fragmentación de las cadenas operativas hacia procesos relacionados con el mantenimiento y la creación del *tool-kit* y su reparación, refleja a su vez el aprovechamiento económico y el tránsito en zonas distantes al yacimiento tanto dentro como fuera de la zona de estudio. Estos últimos elementos reflejan igualmente el lugar central que el yacimiento tiene dentro del poblamiento que en torno al año 40.000 BP. La información que refleja la literatura acerca de los patrones de consumo de capra y capra rupicapra (Yravedra et al., 2005; Yravedra and Gómez-Castanedo, 2014) y la información aportada en este y otros trabajos acerca de El Arteu, muestran igualmente como el Nivel-XIII de El Esquilleu articula también la explotación económica de zonas de roquedo en zonas escarpadas y de media y baja montaña.

Los datos aportados, reflejan la importancia que El Esquilleu jugó en la zona de estudio y que a través de un complejo sistema de yacimientos satélites, aprovechan de forma integral el medio heterogéneo existente. Para entender el rol de estos yacimientos satélites y las relaciones que nos permite plantear la materia prima, en las próximas páginas, discutiremos acerca del yacimiento de El Arteu y, a partir del mismo, platearemos los roles que la cuarcita tuvo como recurso económico en El nivel-VI de El Esquilleu, en el nivel Co.B.6 de La Cueva de Coimbre, y en la Cueva de la Covaciella. Estos roles están relacionados con **la gestión del material en momentos cercanos a su utilización y su desecho**.

El yacimiento de El Arteu está situado en un pequeño abrigo rocoso en los escarpes orientales del desfiladero de la Hermida y se sitúa a escasos kilómetros del yacimiento del Esquilleu. A pesar de carecer de dataciones numéricas precisas, la caracterización de sus industrias líticas lo relaciona con los niveles centrales de El Esquilleu (IX-XIX). A pesar de que los materiales analizados provienen de una recogida en superficie, esta colección refleja la adquisición y gestión de la materia prima de un campamento de baja estabilidad temporal y posiblemente relacionado con la realización de una actividad específica, como la caza de animales de roquedo (Baena et al., 2012; Baena et al., 2005). A pesar de la escasa cantidad de piezas presentes en la colección, existe una gran variabilidad litológica, con representación de sílex, radioralita, caliza, lutita y cuarcita. Dentro de la última categoría aparecen todos los tipos cuarcíticos a excepción del MQ. Los procesos observados de captación de materias primas están relacionados con el aprovisionamiento en el entorno inmediato (a través de los depósitos fluviales) de los tipos OO, CA y CC. El primero es el mejor representado en el yacimiento, no sólo por el aporte obtenido en los depósitos fluviales cercanos, también del proveniente de los conglomerados. Los comportamientos técnicos que reflejan estos tres tipos cuarcíticos reflejan mayoritariamente un comportamiento de utilización inmediatamente posterior a su captación, especialmente los tipos CC y CA. El tipo OO muestra cadenas operativas con un mayor desarrollo debido a la menor cantidad de zonas corticales en los productos brutos de talla, el aumento de artefactos retocados y el tamaño de los núcleos. Por otro lado, observamos comportamientos de adquisición de materias primas pretéritos a partir de las cadenas operativas fragmentadas en los tipos SO, BQ, RQ y parte de las industrias líticas realizadas sobre el tipo OO. En estos tipos cuarcíticos inferimos comportamientos relacionados con el mantenimiento y desecho de herramientas o *tool-kit* o la utilización y abandono de stocks en forma de núcleos o productos brutos de talla. La captación de las mismas se ha realizado en tiempos pretéritos, través de yacimientos centrales (como el Nivel-XIII de El Esquilleu) asentamientos focalizados en la captación primaria de materia prima con los que prima su utilización final (Figura-14.6).

Estos datos nos permiten inferir acerca de la distribución de la cuarcita mediante una red de yacimientos articulados de una forma compleja y que explotan los diferentes biotopos del territorio. En este caso, el yacimiento de El Arteu se relaciona posiblemente con la caza de animales de roquedo. La cantidad y el formato de la industria lítica está adaptada a ello y se ha configurado previamente teniendo en cuenta la funcionalidad de este sitio y la durabilidad de su ocupación. Las materias primas unen, por tanto este yacimiento al Esquilleu, pero también a contextos de captación de materia prima, como El Habario. A pesar de ello, también observamos que la captación de materias primas de una forma inmediata es realizada en este tipo de sitios por las sociedades

paleolíticas. Para ello, estos grupos aplican mecanismos de selección en contextos heterogéneos, como las playas fluviales. Este comportamiento, lejos de mostrar mecanismos de subsistencia poco desarrollados, plantea el aprovechamiento integral del medio ambiente de una forma extensiva obligándonos a replantear los roles simplistas de determinados comportamientos “expeditivos”, como ya afirman recientemente Dibble et al (2017) o Vaquero y Romagnoli (2017).

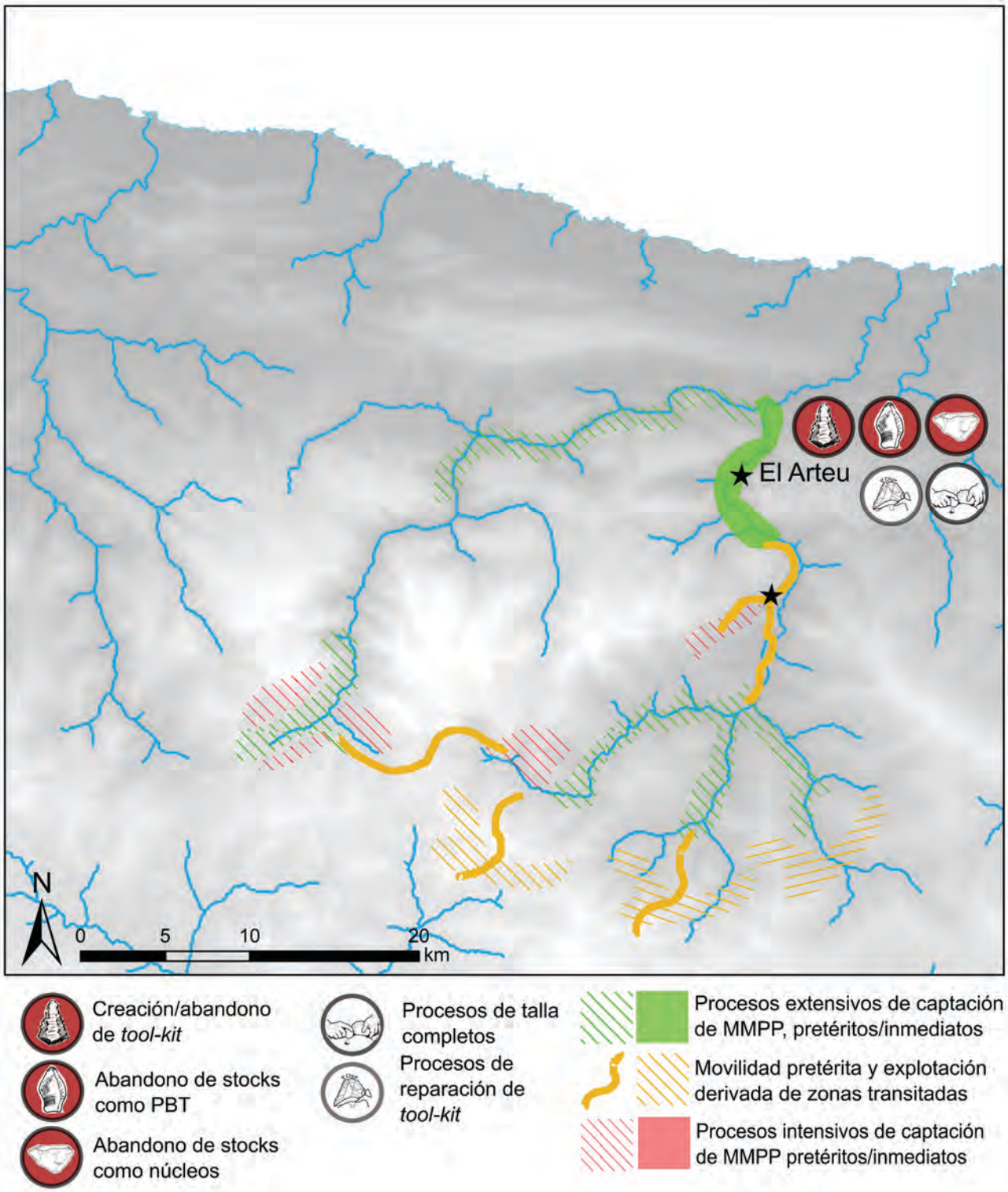

Figura-14.6: Mapa de la zona mostrando los procesos técnicos caracterizados en el yacimiento de El Arteu y las zonas explotadas económicamente.

El siguiente nivel en el que se observan procesos finales de gestión de la materia prima lítica es **el nivel-VIF de El Esquilleu**. La cantidad de industria lítica del nivel es pequeña, y a pesar de ello, la variabilidad de litologías presentes es alta, con cuarcita arqueológica, lutita, sílex, caliza, limonita y cuarzo. Además, todos los tipos de cuarcita están representados en el nivel. Como vimos en el anterior yacimiento, la mayor parte de las superficies corticales identificadas derivan de depósitos fluviales a pesar de la existencia de algunos córtex provenientes de conglomerados. De nuevo, la presencia del grupo de las cuarzoarenitas es importante y todas ellas están recolectadas en depósitos de playas fluviales. El tipo OO, uno de los más numerosos, también ha sido captado en estos de forma mayoritaria en estos mismos contextos. La captación en estos contextos se realizó, posiblemente derivado del tránsito por las riveras del cercano río Deva y debido a la gran cantidad del tipo OO, no descartamos que hayan sido recolectados al norte del yacimiento, una vez el río Deva erosiona los estratos más meridionales de la Formación Barrios. Los tipos CA y OO tienen un comportamiento técnico similar con procesos de talla fragmentada y han sido introducidos en el sitio, posiblemente en forma de productos brutos de talla provenientes de depósitos fluviales cercanos. La explotación del tipo CC muestra procesos aún más claros de este acopio o creación de stocks mediante lascas y no por núcleos. Por su parte, los tipos SO, BQ, RQ y MQ muestran procesos claramente diferenciados debido al aumento en el grado de explotación del material y la disposición del mismo a partir de stocks en forma de núcleo, que son tallados en el yacimiento. La mayor parte de los córtex analizados revelan que provienen de conglomerados cercanos, como el de la Formación Remoña, o lejanos, como la formación Valdeón o Maraña-Brañas. A pesar de ello, los córtex (en pequeñas proporciones) caracterizados como fluviales, revelan que estas materias primas también son captadas en estas zonas, posiblemente como hallazgos puntuales en los tránsitos realizados por los cauces fluviales, o bien derivados de la explotación de las riveras, no sólo del Deva, también del Cares (Figura-14.7).

Los datos obtenidos son similares a los observados en el yacimiento de El Arteu, y reflejan circuitos finales de distribución de la cuarcita. Estudios previos (Baena et al., 2012) plantean un cambio en la funcionalidad del sitio respecto a los niveles analizados con anterioridad. El Esquilleu ha cambiado su relación el resto de yacimientos de la red logística que previamente comentábamos, bien por dejar de ocupar un papel central (ocupado por otro sitio) y ser en estos momentos en torno al 35.000 BP un campamento secundario, o bien por el desmantelamiento completo de la red logística para convertirse en una red de carácter residencial y con ocupaciones más efímeras. A pesar de los procesos de reciclaje de cuarcita de niveles inferiores documentados en los trabajos de Cuartero et al. (2015), consideramos que la primera de las hipótesis planteadas es la más plausible, motivados por la gran cantidad de cuarcitas de contextos lejanos y que han sido configuradas como stocks (de lascas y núcleos) y herramientas complejas con una alta previsión temporal.

La discusión hasta ahora planteada acerca de la variabilidad en los comportamientos de captación, gestión y distribución de la cuarcita, entre los tres tipos de yacimientos propuestos, también nos ha permitido esbozar modificaciones temporales entre los tres niveles seleccionados del yacimiento de El Esquilleu, el único que nos permite establecer una relación crono-estratigráfica. Esto nos permite establecer **un relato histórico acerca de la variabilidad de estos comportamientos en un eje diacrónico**. Hemos observado que la funcionalidad de este sitio ha cambiado. Los momentos más antiguos (en torno al 55.000 BP), analizados a través del Nivel-XXII del yacimiento, muestran que el yacimiento ha sido utilizado como taller en el que se configuran cuarcitas (OO) desde el primer desbaste de la misma hasta la preparación de stocks de formato lasca y núcleo. Además se observan comportamientos pretéritos que hablan acerca de la adquisición de cuarcita en zonas distantes y con diferentes biotopos de forma complementaria. Los datos aportados hacen ver que El Esquilleu, pudo ser uno de los sitios utilizados dentro de una red residencial amplia y de ocupaciones más o menos efímeras en función del tiempo requerido en la explotación de cada biotopo, o bien del momento del año. Por su parte, el Nivel-XIII, cronológicamente más reciente (en torno al 40.000 BP), muestra procesos complejos que lo articulan de forma inevitable en el centro de una red amplia de yacimientos que lo abastecen de diferentes recursos, entre otros, la cuarcita. La articulación de la gestión medioambiental, en este caso está relacionada con una red de carácter logístico, ya planteada en otros trabajos. El rol central como campamento residencial es claro. En el caso del Nivel-VI volvemos a observar un cambio a partir del análisis de las evidencias líticas en torno al 35.000 BP. Estos cambios relacionan al yacimiento de El Esquilleu con una red logística, de carácter similar al observado previamente, si bien, el rol determinado por la adquisición de cuarcitas lo sitúa en la red como un yacimiento periférico y con ocupaciones efímeras, posiblemente relacionado con la captación de recursos cinegéticos de montaña, en relieves escarpados y también de las zonas bajas de valle. Esperamos que futuros trabajos en la zona permitan encontrar nuevos yacimientos que avalen la hipótesis planteada y relacionen este nivel-VI de El Esquilleu con otros yacimientos

de la red. En caso contrario, nos veríamos obligados a aceptar la hipótesis que lo acerca a una red residencial.

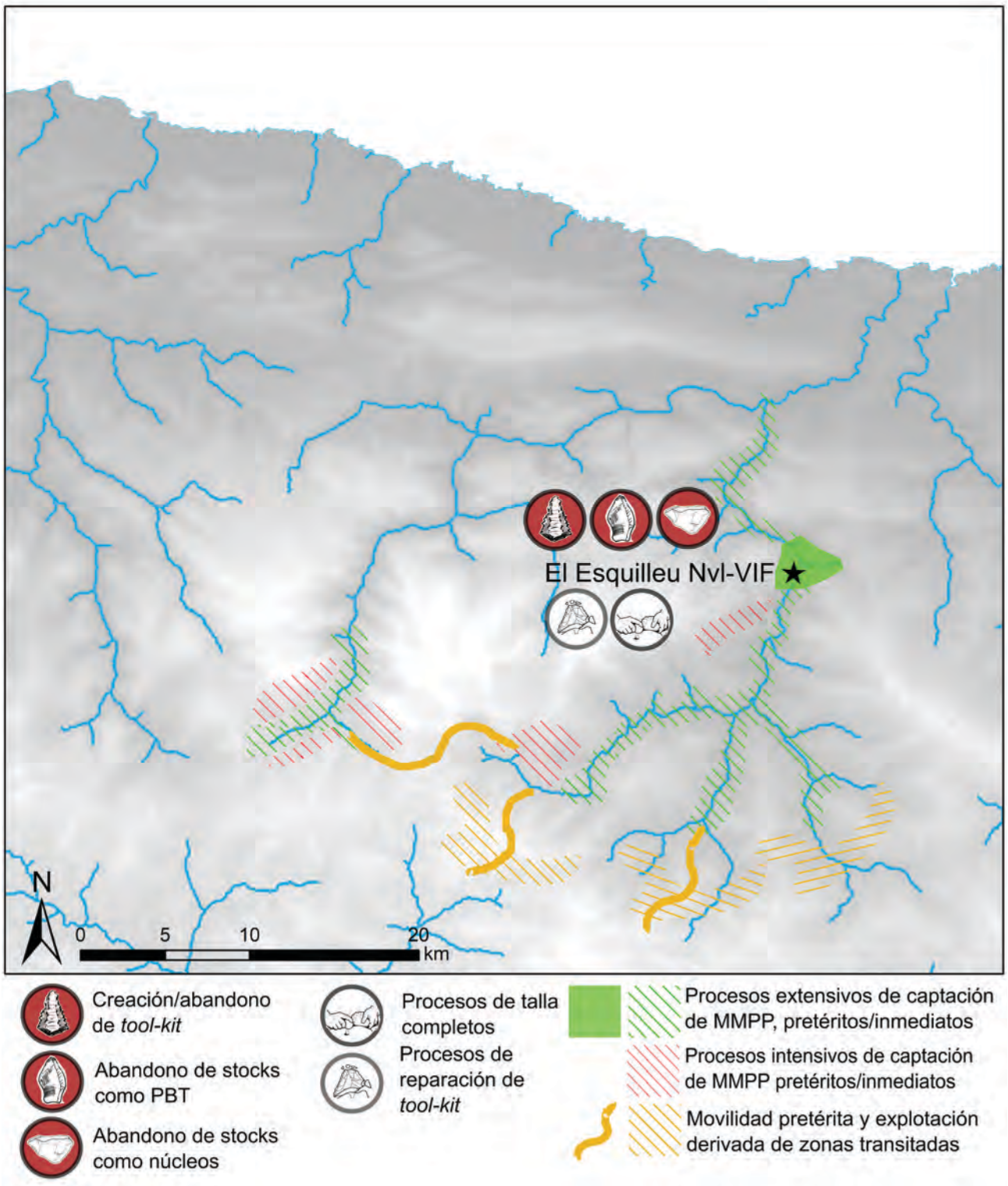

Figura-14.7: Mapa de la zona mostrando los procesos técnicos caracterizados en el nivel-VIF del yacimiento de El Esquilleu y las zonas explotadas económicamente.

Los cambios planteados posiblemente estén condicionados por las modificaciones medioambientales de la zona a lo largo de la horquilla temporal estudiada (aproximadamente 20.000 años). Los estudios paleoclimáticos realizados en el Esquilleu muestran, un enfriamiento paulatino y un desarrollo de vegetación abierta desde el nivel XXII-R, más relacionado con condiciones atemperadas y húmedas en el evento climático H5. El nivel XIII está relacionado con el evento climático frío del H4 que hiciera necesaria la articulación de diferentes biotopos a partir de una red logística de explotación del medio ambiente y que sustituye a la red residencial para la explotación de la zona. Por su parte, el paleoambiente caracterizado en el nivel VI-F está relacionado con un atemperamiento en las condiciones climáticas y la expansión de plantas mesófilas. Esto parece llevar a una modificación de la red logística descrita, o a la explotación del medio a través de una red residencial. Asimismo, este último cambio en el comportamiento puede deberse a los cambios que se están produciendo en la Península Ibérica debido a la entrada de nuevos grupos humanos y que generan modificaciones en la explotación del medio ambiente por parte de los grupos neandertales. Estos cambios, como se ha visto en esta y otras áreas provocan una atomización de los grupos, una descomposición de las redes logísticas previas y una reducción de los territorios explotados por cada grupo (Arrizabalaga, 2009; Baena and Carrión, 2006; Baena et al., 2012; Baena et al., 2005; Finlayson, 2004; Finlayson and Carrión, 2007; Finlayson et al., 2006; Higham et al., 2014; Maroto et al., 2012; Straus, 2005, 2010; Stringer et al., 2003; Zilhao, 2000, 2006; Zilhao and D'Errico, 1999).

Una vez planteadas las modificaciones en el eje diacrónico y sincrónico dentro del Paleolítico medio, en los próximos párrafos, discutiremos acerca de los niveles del Paleolítico superior: el Nivel Co.B6 de la Cueva de Coimbre y la Cueva de La Covaciella.

Los datos aportados por la bibliografía específica del Nivel Co.B6 de la Cueva de Coimbre permiten entender la ocupación de esta localización como un yacimiento secundario integrado dentro de una red logística más amplia de yacimientos y alejada del papel central de una red observada en momentos posteriores y en los que se relaciona con el Arte parietal del yacimiento (Álvarez-Alonso et al., 2017; Álvarez-Alonso et al., 2013b; Álvarez-Alonso et al., 2009; Álvarez-Alonso et al., 2014; Álvarez-Alonso et al., 2013c; Álvarez-Alonso et al., 2016). El estudio realizado en este trabajo a partir de la caracterización de las cuarcitas, principalmente, aporta nuevos datos que robustecen esta asignación. Los mecanismos de adquisición, gestión y distribución de materia prima inferidos son tres.

El primero está relacionado con una captación masiva en contextos fluviales cercanos geográfica y temporalmente (Figura-14.8). Todos los tipos cuarcíticos con presencia de córtex, revelan superficies derivadas de contextos fluviales. Asimismo, caracterizamos este tipo de córtex en el sílex y en la caliza. Todas las cuarzoarenitas y cuarcitas *s.s.* y la mayor parte de las ortocuarcitas tienen este tipo de córtex. A pesar de ello, los procesos técnicos difieren entre las cuarzoarenitas y la mayor parte de las evidencias líticas realizadas en el tipo OO con respecto a los tipos SO, BQ y MQ. Mientras que los tipos CC, CA y OO no están altamente explotados y sólo se observan procesos de talla completos en los dos últimos tipos, los tipos SO, BQ y MQ están más intensamente explotados mediante mecanismos que priman la conservación de la materia prima. El tipo de adquisición de los tipos CC y CA nos recuerda al observado en los yacimientos de El Arteu y el Esquilleu Nivel-VI a través de una captación masiva, una gestión inmediata y una distribución escasa. Por su parte, la adquisición del tipo OO plantea similitudes con el observado en el Nivel-XXIIR de El Esquilleu a través de una captación masiva basada en procesos selectivos, una gestión temporalmente más amplia, y una distribución de mayor recorrido. Por su parte, la gestión de los tipos SO, BQ y MQ derivados de contextos fluviales revela la importancia que estos tipos cuarcíticos tuvieron en las sociedades superopaleolíticas de la región. La captación de ellas, probablemente como actividad complementaria a la adquisición de otros recursos en los lechos fluviales, muestre estrategias de adquisición más oportunistas, pero a la vez intencionadas como las observadas en El Arteu. Asimismo, la gestión de estos tipos muestra procesos conservadores de explotación del material lítico como los observados en el segundo y tercer tipo de captación que expondremos a continuación.

El segundo de los procesos de captación de cuarcita está relacionado con una adquisición en conglomerados y también en playas fluviales, en este caso como consecuencia de una movilidad de medio recorrido. La captación en estos contextos posiblemente se ha realizado en recorridos pretéritos o bien como parte de la gestión territorial de una red de carácter operativa con otros yacimientos especializados y posiblemente primando el eje Este-Oeste en lugar de una movilidad hacia el sur. Los grupos cuarcíticos que reflejan esta captación son las ortocuarcitas y las cuarcitas *s.s.* La cantidad de este material, especialmente el derivado de contextos de conglomerados es bajo y refleja mecanismos de gestión de materia prima de tipo conservador a partir de una distribución

a media escala mediante stocks de formato núcleo y como herramientas. Las últimas son, en ocasiones, reparadas o confeccionadas en el sitio.

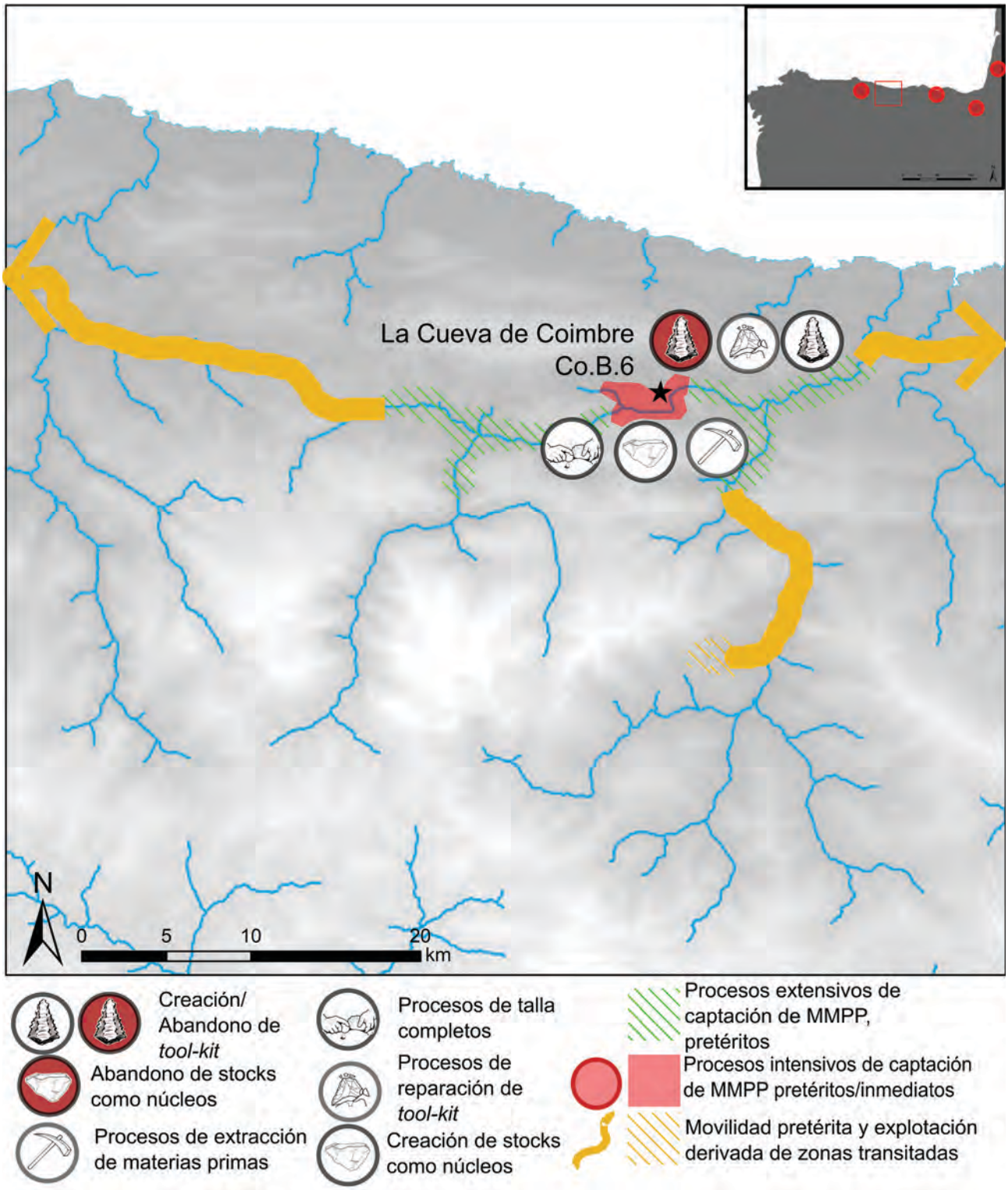

Figura-14.8: Mapa de la zona mostrando los procesos técnicos caracterizados en el nivel Co.B.6. del yacimiento de La Cueva de Coimbre y las zonas explotadas económicamente.

El tercero de los mecanismos de adquisición refleja una gestión de largo recorrido, y en este caso está marcado por los artefactos de sílex caracterizados en otros trabajos (Álvarez-Alonso et al., 2017). Los tipos de sílex caracterizados son los del tipo Piloña, Motepicota/Piedramuelle, Flysch (posiblemente Kurtzia), Urbasa y Chalosse. Estos, reflejan una movilidad a gran escala en un eje Este-Oeste y tanto dentro como fuera de la Cornisa Cantábrica (Rissetto, 2009) ya planteada en otros yacimientos de la región durante el Paleolítico superior y que probablemente una grupos que

habitan regiones distantes geográficamente a través de movimientos anuales de gran escala en lugares de agregación e intercambio de materiales e ideas (Calvo et al., 2016; Corchón et al., 2007; Corchón et al., 2013; Fontes, 2016; Fontes et al., 2016, 2018; Sánchez et al., 2016). Este último elemento nos permite relacionar esta ocupación Gravetiense con los últimos elementos líticos sobre los que discutiremos en este apartado, los presentes en la Cueva con Arte Parietal de la Covaciella.

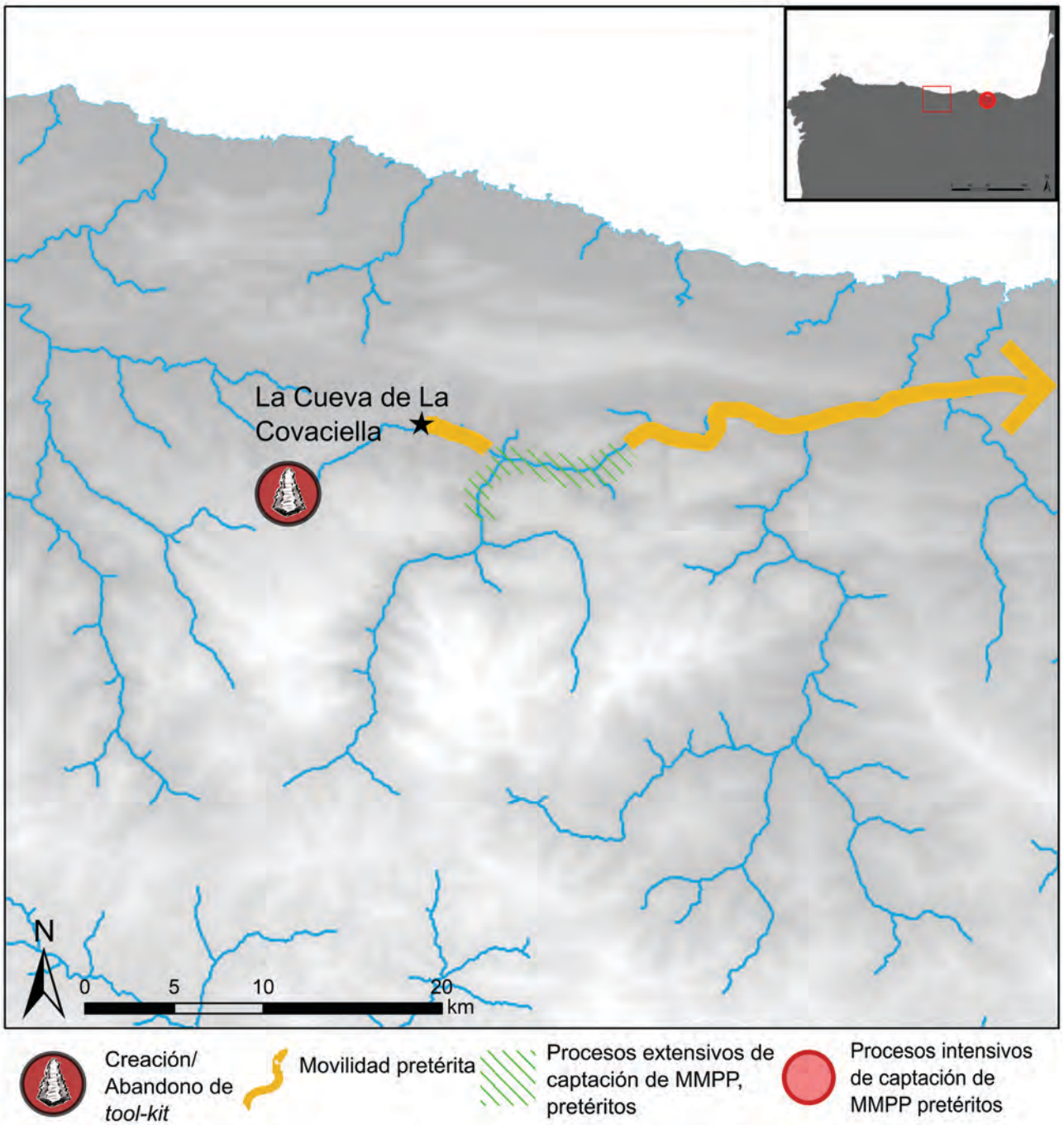

Figure-14.9: Mapa de la zona mostrando los procesos técnicos caracterizados en La Cueva de la Covaciella y las zonas explotadas económicamente.

Los tres objetos líticos analizados en la Cueva de la Covaciella, a pesar de ser muy escasos en número, nos permiten plantear, junto con la colección del nivel Co.B.6 de la Cueva de Coimbre, los mecanismos de captación y distribución de las materias primas en el Paleolítico superior. En este caso, observamos una adquisición de cuarcitas, específicamente del tipo BQ provenientes de depósitos fluviales del río Cares y que han sido obtenidos aplicando mecanismos selectivos muy fuertes. Las características técnicas, al igual que las observadas en la Cueva de Coimbre reflejan un alto grado de explotación y posiblemente sean parte de las herramientas o *toolkit* del grupo que frecuentó y pintó esta cueva. El tercer implemento lítico, posiblemente asociado a los grabados y

pinturas que decoran la cavidad, que hemos caracterizado es un artefacto retocado realizado sobre sílex tipo Flysch Kurtzia. Esto nos permite observar de nuevo las grandes rutas de materiales y también de ideas que a lo largo del Paleolítico superior articularon a las poblaciones del Cantábrico (Barandiarán, 2015; García-Diez et al., 2015) (Figura-14.9).

Una vez evaluadas y contextualizadas todas las colecciones líticas, vamos a dedicar estos últimos párrafos a plantear las diferencias observadas en la captación, gestión y distribución del material lítico entre el Paleolítico medio y el Paleolítico superior.

En el Paleolítico medio hemos observado comportamientos de captación de materias primas complejos y que nos permiten identificar:

1. Procesos de proto-minería con la explotación sistemática de las vetas de interés en el yacimiento alemán de Ravensberg-Troisdorf.
2. Procesos de extracción de materias primas en conglomerados aplicando procesos selectivos de tipos específicos.
3. Procesos selectivos de materia prima.
4. Estrategias intensivas de captación.
5. Estrategias extensivas de captación y aprovechamiento de oportunidades.

A través del estudio de los yacimientos cronológicamente datados en Paleolítico superior hemos observado de forma clara únicamente los tres últimos procesos de captación de materia prima, si bien, no descartamos la posibilidad de extracción de materias primas en conglomerados aplicando procesos selectivos. Por otra parte, en la Región Cantábrica no hemos observado procesos de proto-minería como los observados en el yacimiento de Ravensberg-Troisdof, y estos se sitúan en contextos alejados de la zona de trabajo en el yacimiento burgalés de Araico (Tarriño et al., 2014). En este complejo de yacimientos se ha certificado la explotación del sílex de tipo Treviño mediante la realización de frentes de trinchera que buscan y explotan las variedades de interés mediante el uso de herramientas específicas. Cronológicamente está datado en el Neolítico pleno. La captación de sílex en zonas con alta densidad sí está certificado dentro de la Cornisa Cantábrica, especialmente en el País Vasco. En estas zonas no descartamos que se den procesos proto-mineros similares a los ya comentados en *Ravensberg-Troisdorf* (Arrizabalaga et al., 2014; Barandiarán et al., 2006).

Volviendo al Paleolítico medio, en este caso para comentar las pautas de gestión de las materias primas líticas, hemos observado:

1. Procesos de gestión inmediata de materias primas, captadas y directamente utilizadas con un grado de explotación bajo.
2. Procesos de gestión de las materias primas mediante el *stock* y gestión del material en forma de núcleos.
3. Procesos de gestión de las materias primas mediante el *stock* y gestión del material en forma de productos brutos de talla.
4. Procesos de gestión de las materias primas mediante la creación y el mantenimiento de *tool-kit*.
5. Gestión diferencial de los tipos cuarcíticos en función de las características físicas que determinan su tallabilidad y su uso.
6. Cadenas operativas fragmentadas.

En el Paleolítico superior observamos patrones similares, si bien la gestión mediante productos brutos de talla es más limitada y los procesos de creación y el mantenimiento del *tool-kit*, son más complejos.

Respecto a la distribución de las materias primas líticas, en el Paleolítico medio observamos:

1. Baja distribución de cuarcitas arqueológicas frecuentes dentro del área de estudio (grupo de las cuarzoarenitas, principalmente), por tanto, un comportamiento expeditivo, que refleja la inmediatez en la adquisición.

2. Distribución a media escala de ortocuarcitas y del tipo BQ con grandes aportes de materiales y que suelen constituir el aporte mayoritario en cada colección.

3. Distribución a gran escala de materias primas poco frecuentes en la zona de estudio o inexistentes y que en distancia euclidiana superan los 50 km y las 50 Unidades de Coste.

4. Distribución de materias primas a través de un eje Norte-Sur, principalmente, y de forma secundaria de un eje Este-Oeste. El primero, relacionaría las zonas de la costa cantábrica con las zonas de la Submeseta Norte a través de los Valles del Deva y las zonas de media montaña y meseta baja circundantes a los Picos de Europa.

En el Paleolítico superior, observamos:

1. Distribución similar de las materias primas frecuentes en la zona de estudio.

2. Distribución geográfica más reducida de ortocuarcitas y el tipo BQ. Las cantidades, a priori, también son inferiores.

3. Práctica inexistencia de distribución de cuarcitas poco frecuentes en la zona de estudio o inexistentes, y que no llega a superar las distancias y las cantidades comentadas en el Paleolítico medio.

4. Distribución a gran escala (regional y supra-regional del sílex) a través de un eje Este-Oeste. Este tipo de distribución no se observa en los yacimientos del Paleolítico medio y supone un cambio claro en el hábitat, la movilidad y la estructura social y mental de las sociedades paleolíticas.

Respecto a la gestión y explotación del medio ambiente vemos diferencias claras entre los dos periodos crono-culturales. Por un lado, las sociedades del Paleolítico medio realizaban una gestión y explotación integral del medio ambiente heterogéneo articulando los fondos de los valles, las zonas de media montaña amesetadas y las zonas de relieves escarpados. Para ello, se combinan, bien a través de una red logística o a través de una red de campamentos de movilidad residencial, estrategias de captación de recursos de tipo intensivo y extensivo. La primera se basa en la adquisición de un producto específico en una zona determinada a partir de mecanismos de 1) movilidad hacia el recurso, 2) procesos selectivos intensivos, y 3) gestión específica del material, bien a través de la extracción selectiva, bien a través de la talla diferencial. La segunda estrategia de captación, la extensiva, explota el medio ambiente a través de estrategias flexibles de captación de recursos en zonas más amplias que las primeras. La combinación de ambas se observa claramente en la relación dialéctica entre la captación fluvial a partir de estrategias flexibles y selectivas (estrategia generalmente extensiva) y la captación en conglomerados a partir de estrategias más rígidas y basadas en la movilidad (estrategia intensiva). Las dos redes planteadas, logísticas y residenciales, explotan de forma integral un medio ambiente heterogéneo que les permite a estas sociedades una adaptación a la estacionalidad inter-anual y los cambios climáticos globales.

Por su parte los yacimientos analizados asimilables al Paleolítico superior muestran una gestión y una explotación del medio ambiente de una forma más específica e intensiva. La información derivada del análisis de las cuarcitas en el nivel Co.B.6 y La Cueva de la Covaciella, plantea una adquisición de recursos cercana o muy cercana al asentamiento humano a partir de estrategias intensivas de captación cuarcitas. A pesar de la flexibilidad apreciada en la captación y la gestión de las cuarzoarenitas, observamos una adquisición enfocada a tipos cuarcíticos específicos. La gestión integradora del medio ambiente en una zona más amplia (como la zona de estudio de este trabajo) no ha podido ser documentada. Esto se puede deber al escaso número de yacimientos analizados, o bien a la realidad de la gestión medioambiental de los grupos superopalelíticos, más relacionada con estrategias de adquisición de recursos inmediatos y sobretodo muy intensivos. La ausencia de una explotación integral de este medio más amplio no supone, como se pudiera pensar, una disminución de la movilidad de estos grupos, más bien lo contrario, como demuestran los circuitos de adquisición a escala regional y supra-regional del sílex. Estos circuitos, no movilizan una gran cantidad de materias primas, pero sí de ideas, reflejando una diferencia sustancial que nos diferencia del resto de seres que habitan la tierra y que nos permiten realizar nuestra propia evolución, los memes (Dawkins, 2002).

La discusión que en términos humanas e históricos hemos realizado hasta ahora, nos hacen reflexionar hacia el presente y la gestión del medio por las sociedades que habitan hoy los valles del Deva, Cares y Güeña. Observamos que el campesinado (agrícola y ganadero) explota y gestiona el

medio a partir de la integración de las zonas de valle bajo y montaña alta mediante la transhumancia, bien en red logística, con estabulaciones invernales en el valle y explotaciones extensivas estivales en zonas de media montaña; o bien con red residencial y circuitos de movilidad más largos con campamentos habitacionales estacionales. Esta gestión, no sólo permite obtener beneficios derivados de la actividad principal: la ganadería, también explora y explota recursos variados, como la adquisición de frutos de temporada (véase la recolecta de castañas y que se aprecia en figure-2.24) o los recursos líticos actuales. A lo largo de las prospecciones hemos apreciado una arquitectura tradicional que utiliza de forma casi-exclusiva las litologías del entorno inmediato para la realización de cercado, casas o establos. Por otro lado, la ganadería y agricultura actual de carácter industrial plantea una explotación del medio ambiente de ida y vuelta a través de circuitos de movilidad de carácter suprarregional y que se aleja de esta concepción integral y extensiva de la explotación del medio ambiente para enfocarse más en una explotación ultra-intensiva, generando cambios drásticos en el mismo y las sociedades que lo habitan.

CHAPTER-15

CONCLUSIONES

Tras la discusión, presentamos unas breves conclusiones que sintetizan las principales contribuciones de este trabajo. En esta sección también expondremos de forma clara las limitaciones que esta tesis. Finalmente, enumeraremos una serie de líneas de trabajo que permitan trazar perspectivas de futuro.

15.1. PRINCIPALES CONTRIBUCIONES DE ESTA TESIS

Tres son las principales contribuciones que presenta este trabajo. La primera es de carácter metodológico, y plantea una metodología integral para el estudio de las cuarcitas en contextos arqueológicos. La segunda es de tipo material y está relacionado con la caracterización y definición formal de la cuarcita en contextos arqueológicos. La tercera es de tipo histórica y está orientada hacia la mayor y mejor comprensión de los mecanismos de adquisición, gestión y distribución de las cuarcitas por las sociedades paleolíticas.

La primera, y que consideramos más importante teniendo en cuenta el estado actual en las investigaciones sobre las materias primas líticas utilizadas por los seres humanos prehistóricos, es la contribución metodológica que hemos planteado. En este trabajo de investigación hemos caracterizado y definido la cuarcita en contextos arqueológicos a partir de sus características físicas. Para ello, hemos planteado un protocolo metodológico que aglutina tres escalas: la microscópica, la macroscópica y, finalmente, la regional.

La primera está basada en el análisis petrográfico del material cuarcítico. A partir de ésta, hemos caracterizado las texturas que forman los granos de cuarzo, su empaquetamiento y hemos detectado las características de estos pequeños objetos y que nos permiten la definición y el estudio de las cuarcitas en contextos arqueológicos. Asimismo, la aplicación de técnicas de análisis digital de imagen sobre las fotografías microscópicas de las láminas delgadas nos ha posibilitado conocer los tamaños, las morfologías y las orientaciones de los granos de cuarzo que componen masivamente la cuarcita. Finalmente, y también a partir de la Petrografía, hemos detectado los minerales, matrices y cementos que, adicionalmente a la matriz principal de granos de cuarzo, componen la cuarcita. El establecimiento de tipos petrogenéticos que agrupan buena parte de las características previamente comentadas y de variedades específicas es, sin duda, uno de los aportes más interesantes de este trabajo, pues plantea las bases para desarrollar futuros trabajos. Finalmente, el reflejo de los tipos petrogenéticos y variedades granulométricas y mineralógicas de las cuarcitas mediante la observación microscópica no-destructiva, supone otra contribución interesante de esta tesis. Finalmente, este trabajo ofrece un corpus de datos ilustrado con fotografías de láminas delgadas y fotografías de las superficies de las cuarcitas con un alto detalle que permitirá seguir trabajando en la caracterización de las cuarcitas en la Cornisa Cantábrica y otras zonas.

La metodología que hemos utilizado para entender la realidad visible a partir de una escala macroscópica, a pesar de ser útil para este trabajo, no ha supuesto la novedad que sí ha aportado la escala microscópica. A pesar de ello, este enfoque nos ha permitido establecer criterios de análisis con los que conocer, por un lado, los potenciales contextos de captación de la cuarcita; por otro, los mecanismos de gestión de la materia prima lítica. La descripción de los puntos prospectados a partir de los criterios de análisis especificados en los capítulos tres y cuatro, nos ha permitido entender los contextos geológicos, pero también imaginar los procesos de adquisición de materia prima por parte de los humanos prehistóricos. Por su parte, los criterios de análisis de la industria lítica seleccionados, principalmente desde la Tipología Analítica, nos ha permitido conocer los mecanismos de gestión de la cuarcita, especialmente aquellos relacionados con su explotación.

Finalmente, la metodología que hemos planteado para analizar la zona de estudio a escala regional, nos ha permitido entender espacialmente la distribución de las cuarcitas de la zona de estudio, ha agilizado e implementado las prospecciones y nos ha posibilitado la delimitación de la zona de estudio. Somos conscientes que ninguno de los aportes específicos e individuales es novedoso, pero su aplicación en trabajos geo-arqueológicos en la Región Cantábrica de forma global sí lo es. Por otro lado, la aplicación de la metodología que nos permite entender la movilidad humana a partir de la relación entre la distancia y el relieve, nos ha proporcionado una magnitud con la que valorar de forma más precisa el esfuerzo requerido para llegar de un punto a otro, así como la detección de zonas de tránsito preferencial. La aplicación de esta metodología es igualmente novedosa en la Región Cantábrica, excluyendo los trabajos realizados por mí y otros miembros del Departamento de Geografía, Prehistoria y Arqueología de la Universidad del País Vasco.

La segunda contribución más interesante de este trabajo se relaciona con la definición formal del material: La cuarcita en contextos arqueológicos. La escasa bibliografía científica que ha tratado esta roca desde perspectivas geo-arqueológicas no ha llegado a profundizar en la definición formal del material de una forma similar a la realizada en este trabajo o no han establecido los tipos que permitan entender la gran variabilidad que el término cuarcita abarca. En este trabajo hemos definido la cuarcita a partir de sus características físicas, estableciendo un sistema de siete tipos petrogenéticos agrupados en categorías más amplias, los grupos genéticos. Adicionalmente hemos establecido variedades basadas en el tamaño y la distribución de los granos de cuarzo que componen masivamente la cuarcita. La caracterización de este material a partir de su mineralogía y su reflejo en la coloración de cada una de ellas también ha sido analizada y nos ha permitido establecer nuevas variedades. Todos estos datos nos han permitido caracterizar la roca original, los procesos de consolidación, deformación y/o recristalización metamórfica y los aportes minerales post-deposicionales. El conocimiento adquirido del material nos ha permitido entender también ciertas actitudes que los seres humanos del Paleolítico realizaban, como la selección preferencial de tipos y variedades, la gestión diferencial de las mismas o la talla controlada para el aprovechamiento de ciertos tipos y variedades.

Dentro de esta contribución, también hemos entendido mejor la disposición y la localización de la Cuarcita en la zona centro-occidental de la Región Cantábrica. Hemos definido los pocos afloramientos masivos de cuarcita, los conglomerados en los que encontramos estas rocas y las formaciones cuaternarias en las que se han depositado. Esto nos ha permitido entender el ciclo de esta roca, observando el largo recorrido del material hasta que es captado por las sociedades prehistóricas. Este aporte es igualmente novedoso y supone el establecimiento de un primer corpus de datos que permitirá abordar diferentes investigaciones en la Región Cantábrica.

La última contribución de relevancia que hemos planteado en este trabajo está relacionada con las conclusiones obtenidas en un plano histórico. Por un lado, hemos propuesto procesos de captación de materias primas líticas, especialmente de cuarcitas, en afloramientos masivos, conglomerados y depósitos secundarios, proponiendo la existencia de yacimientos arqueológicos hasta ahora no excavados e imaginando las actividades que allí se realizaban. Dentro de estas, hemos planteado la captación de recursos a partir de la extracción de rocas directamente del afloramiento o el conglomerado. Hemos propuesto la recolección de clastos en las zonas adyacentes a los estratos geológicos con presencia de cuarcitas. Hemos observado la selección de litologías específicas y hemos caracterizado la intensidad de la actividad. Finalmente, hemos observado la creación de reservas de masas líticas (stocks) para futuros usos. Por otro lado, en este trabajo hemos planteado la funcionalidad de cada sitio a partir de los comportamientos de gestión de la cuarcita y otras materias primas líticas. Hemos sido capaces de individualizar cadenas operativas líticas que muestran desde procesos de talla completos hasta procesos fragmentados en el tiempo y en el espacio. Hemos individualizado procesos de creación y reparación de herramientas específicas (*tool-kit*), hemos observado comportamientos flexibles y resolutivos para la realización de actividades, y hemos observado la gestión diferencial de cada uno de los tipos y variedades analizadas. Finalmente, hemos observado la distribución de las cuarcitas por el territorio y hemos planteado los esfuerzos necesarios para su acopio, identificando zonas de paso preferentes frente a otras y el aprovechamiento de forma extensiva e intensiva de las zonas transitadas.

Todos estos datos nos han aportado más pruebas que evidencian la existencia, especialmente en el Paleolítico medio, de redes de yacimientos que permitían a los grupos prehistóricos la explotación de forma sistemática y eficaz del heterogéneo medio ambiente de la zona. Igualmente, hemos aportado nuevos datos que revelan las modificaciones dentro de esta red de yacimientos mediante cambios en las estrategias de adquisición, gestión y distribución de los recursos líticos. Esto se hace especialmente relevante al observar las diferencias entre el Paleolítico medio y el Paleolítico superior. En el primer periodo hemos observado una amplia explotación del medio ambiente que combina los múltiples biotopos de la zona. Por su parte, en el segundo periodo, no hemos sido capaces de observar la amplitud de esta red, y por tanto, la cantidad de biotopos explotados es inferior y geográficamente es más restringido. A pesar de ello, la explotación de estos reducidos biotopos parece ser más intensiva que en el Paleolítico medio. En el Paleolítico superior, hemos aportado más prubas acerca de la existencia de una movilidad supra-regional, una movilidad no detectada durante el Paleolítico Medio. Finalmente, la movilidad observada en último periodo comentado relaciona las zonas de costa, al Norte con las zonas amesetadas del Sur a través de recorridos por los fondos de los valles y de rutas en zonas de media montaña y con relieves poco marcados. La movilidad supra-regional del Paleolítico superior posiblemente tenga una dirección Este-Oeste a través de los corredores paralelos a la actual línea de costa.

Todo ello, nos ha permitido tener un mejor conocimiento acerca de la relación entre el entorno natural y los seres humanos que en el Paleolítico poblaron la región.

15.2. LIMITACIONES ENCONTRADAS DURANTE EL DESARROLLO DE ESTE TRABAJO

Una vez expuestas las principales contribuciones de este trabajo, en esta sección comentaremos las limitaciones que hemos encontrado durante la realización del mismo. Para ello, nos parece relevante volver a remarcar la ausencia de investigadores dentro de este ámbito geográfico y especialmente temático: la geo-arqueología. La cuarcita, a pesar de constituir la segunda materia prima lítica en el registro paleolítico de la Región Cantábrica, no ha recibido el mismo interés y desarrollo que han recibido otras materias primas líticas, especialmente el sílex. Esta realidad, además de generar un déficit de conocimiento histórico en amplias zonas de esta Región, nos ha obligado a entender la cuarcita sin criterios de análisis geo-arqueológicos, haciendo necesaria una formación específica para la comprensión de este material. Adicionalmente, los pocos trabajos arqueológicos que han abordado la caracterización de la cuarcita, lo han hecho mediante de criterios macroscópicos que obviaban la complejidad genética y la antigüedad del material. Esto generó, especialmente en los momentos iniciales de esta investigación, la exploración de líneas de investigación de escasa trascendencia, a pesar de la implementación metodológica pretendida.

Adicionalmente, la diversidad petrológica que el término “cuarcita” lleva aparejado en estudios arqueológicos y parcialmente en trabajos geológicos (principalmente en su utilización como término de campo), favoreció la exploración de líneas de trabajo con escasa trascendencia. Esta ambigüedad terminológica, ha dificultado igualmente el trabajo de campo: las prospecciones. La selección de estratos geológicos con presencia de “cuarcitas” llevó a la prospección de zonas sin relevancia arqueológica debido a la ausencia de materiales “tallables” como areniscas no compactas e incluso rocas calcáreas o arcillosas.

Al igual que en el apartado anterior, hemos organizado este epígrafe en tres apartados. El primero hace referencia a las limitaciones que plantea la metodología utilizada. El segundo, a la caracterización del material: la cuarcita. Finalmente, en el tercer apartado comentaremos las limitaciones que hemos encontrado para elaborar un discurso histórico.

Las principales limitaciones a nivel metodológico, se organizan igualmente mediante los niveles de resolución planteados: el microscópico, el macroscópico y el análisis regional. Comenzando por los criterios microscópicos, ya hemos comentado el escaso desarrollo que esta tesis plantea para la detección mineral y la composición geo-química. Estos dos métodos nos han aportado pocos datos que caractericen las cuarcitas provenientes de contextos arqueológicos y únicamente nos han servido para individualizar cuarcitas en algunos yacimientos arqueológicos y aportar una información más detallada de las mismas. Esto se debe a dos cuestiones, por un lado a la permeabilidad del la cuarcita para absorver pequeños aportes minerales; por otro, a la antiguedad del material que favorece el aporte mineral de multiples áreas fuente. Por otro lado, y dentro de la caracterización de las cuarcitas a partir de técnicas no-destructivas, no hemos llegado a implementar un método de análisis digital de imagen que permita la asignación (con un grado de fiabilidad asociado) a un tipo y/o variedad específica de cada implemento lítico. Esto, creemos que serviría para extender la metodología y el análisis de este material.

Hemos detectado limitaciones metodológicas en el plano macroscópico que, de forma general, se relacionan con el escaso desarrollo en el análisis de las industrias líticas. Éstas son especialmente relevantes en las estructuras modal y morfológica, las dos estructuras de análisis utilizadas para definir los artefactos retocados. Creemos que una mayor y mejor descripción de estos objetos permitiría relacionar ciertas características del retoque con tipos y variedades cuarcíticas específicas. Por otro lado, consideramos que el análisis de los núcleos de forma cualitativa y a partir de esquemas diacríticos, podría haber enriquecido el trabajo, evidenciando procesos de selección de zonas óptimas de cada nódulo mediante la talla o las respuestas técnicas realizadas para optimizar determinados tipos cuarcíticos. Esto se relaciona con las limitaciones en la aplicación de la estructura petrológica. Dentro de ésta, la valoración de las diaclasas y fracturas en las cuarcitas, nos permitirían observar los comportamientos técnicos para evitarlas o gestionarlas eficazmente.

Finalmente, planteamos las limitaciones metodológicas a una escala regional. Por un lado, la optimización de las prospecciones mediante de la información geológica disponible, a pesar de ser una buena herramienta, no nos ha permitido observar toda la variabilidad de estratos y capas

presentes en cada unidad descrita en los mapas MAGNA y SIGECO. Adicionalmente, la falta de correlación de estratos entre mapas diferentes ha limitado la observación horizontal de los mismos. Finalmente, la metodología utilizada para valorar la movilidad paleolítica mediante las unidades de esfuerzo, a pesar de suponer un paso importante a la hora de entender la relación entre el medio físico y los grupos paleolíticos, no tiene en cuenta otros factores físicos como la vegetación o el tipo de suelo, ni factores culturales, económicos y sociales.

El siguiente apartado que valoramos en esta sección está relacionado con la caracterización de las cuarcitas. La limitación más importante se debe a la inexistencia de afloramientos masivos que muestren tipos petrogenéticos altamente deformados y recristalizados. En ellos, podríamos haber documentado estos tipos y, sobretodo, una gradación de los procesos que nos hubieran permitido entender mejor la petrogenia del material más deformado o recristalizado. A pesar de ello, la correlación entre las observaciones en láminas delgadas de la zona con modelos experimentales de la literatura geológica, nos ha permitido entender los procesos formativos de las ortocuarcitas y las cuarcitas s.s. Otra limitación importante en la caracterización de las cuarcitas ha sido el no haber establecido, a partir de las características físicas, el origen último de cada implemento lítico presente en cada yacimiento. A pesar de ello, hemos podido establecer diversos orígenes potenciales a partir de la suma jerárquica de los criterios analizados. Esto, ha enriquecido las perspectivas de este trabajo, evitando una visión simplista de los procesos de adquisición de las materias primas líticas mediante viajes “de ida y vuelta”. Por último, no hemos podido asociar las características físicas de las cuarcitas a determinados métodos de talla y utilización a partir de experimentaciones controladas como hubiéramos deseado debido a limitaciones temporales.

Finalmente, en este párrafo planteamos las limitaciones que muestra este trabajo para la elaboración de un discurso histórico más detallado y profundo. Estas limitaciones se deben principalmente al tiempo de realización de esta tesis, y que determina la cantidad de niveles arqueológicos analizados, la extensión geográfica de la zona de trabajo y la realización de una síntesis conjunta más elaborada. La cantidad de niveles arqueológicos analizados es una clara limitación a la hora de poder comparar las estrategias de captación, distribución y gestión de la cuarcita en otros yacimientos. Por un lado, el análisis numérico de un solo nivel correspondiente al Paleolítico superior condiciona claramente las conclusiones que a nivel histórico aportamos. Por otro lado, consideramos que hubiera sido interesante el análisis de yacimientos en los que se observen procesos de captación en depósitos fluviales para plantear de forma más clara la adquisición y selección de litologías específicas. Por otro lado, las limitaciones temporales también han condicionado la extensión de la zona de estudio, y, por tanto, la amplitud geográfica de las conclusiones obtenidas a toda la Región Cantábrica. Estas son especialmente importantes para elaborar un discurso histórico complejo y que nos permita comparar con otras regiones las conclusiones aportadas.

PERSPECTIVAS DE FUTURO

En esta última sección de las conclusiones y de esta tesis, expondremos una serie de vías de investigación que consideramos pueden ser exploradas. Estas se basan tanto en las conclusiones obtenidas como en las limitaciones previamente comentadas. Estas se pueden resumir a partir de cuatro ejes o vías. El primero está relacionado con la consolidación metodológica. El segundo se basa también en la validación, en este caso de los resultados. La tercera vía es la expansión geográfica del análisis planteado a otros valles de la Región Cantábrica, en especial la zona occidental. La cuarta vía es el salto geográfico para la consolidación metodológica y de resultados, especialmente aquellos relacionados con la caracterización del material.

La primera vía comentada pasa por la mejora de la metodología utilizada. Tres son las formas que consideramos pueden ser más interesantes para esta consolidación. La primera consiste en la realización de más muestras de las cuarcitas seleccionadas en la zona de estudio para su estudio petrográfico, primando la detección de otros minerales que no son el cuarzo y el análisis geo-químico. Los datos aportados, nos permitirían tener una mayor cantidad de muestra con la que analizar la variabilidad mineral y geo-química con el objetivo de encontrar patrones que definan el área fuente de cada cuarcita. La segunda fórmula consiste en la búsqueda de más caracteres con los que relacionar la observación y caracterización de las láminas delgadas y las superficies de las cuarcitas observadas mediante microscopía no-destructiva. La tercera y última fórmula consiste en la exploración, mediante técnicas relacionadas con el *data mining* y el *machine learning*, de las fotografías microscópicas realizadas en este trabajo con el objetivo de obtener una asignación del tipo petrogenético de cada cuarcita analizada, asociándole a su vez un grado de fiabilidad. La aplicación de este proceso para el establecimiento de las variedades granulométricas y minerales,

supondría el último elemento que robusteciera el método de caracterización de cuarcitas realizado en esta tesis.

La segunda vía o perspectiva de futuro de esta tesis es la validación de los resultados en el área seleccionada. Esto pasa, por un lado, por el análisis de más formaciones geológicas en la zona de estudio, y que no se han podido analizar por diferentes cuestiones. Esta vía pasa igualmente por el re-análisis de las formaciones ya trabajadas en este trabajo, incorporando la información de los procesos estructurales que afectan a los estratos rocosos. Por otro lado esta segunda vía podría analizar nuevos niveles arqueológicos de los yacimiento arqueológicos de la zona.

La tercera perspectiva de futuro que plantea este trabajo consiste en la expansión geográfica de hacia otros valles de la Región Cantábrica, especialmente en la zona occidental. Esta vía es necesaria para obtener datos de otras cuencas en contextos similares con las que poder comparar los resultados de este trabajo. Para ello, sería necesaria la aplicación de toda la metodología, desde aquella que permite entender la dispersión de las cuarcitas en el medio ambiente, hasta el análisis de las evidencias líticas de otros yacimientos arqueológicos.

La cuarta y última vía de investigación a desarrollar en el futuro consiste en la aplicación de la metodología de análisis del material hacia otras regiones de Europa. Esto, permitirá apreciar el carácter universal del método a nivel geo-arqueológico y plantear pautas de adquisición, gestión y distribución de la cuarcita en zonas geográficas distantes y que servirán para comparar los patrones observados en esta tesis. El primer paso para desarrollar esta vía de investigación ya está inserto dentro de este trabajo, como se puede observar en el Capítulo-13 a través del análisis de las cuarcitas arqueológicas del yacimiento de *Ravensberg-Troisdorf*.

CHAPTER-16

REFERENCES

Adams, A. E., MacKenzie, W. S., and Guilford, C., 1988, Atlas of sedimentary rocks under the microscope: Essex, ELBS.

Alroy, J., 2001, A Multispecies Overkill Simulation of the End-Pleistocene Megafaunal Mass Extinction, *Science*, **292**(**5523**), 1893-1896.

Altuna, J., Baldeon, A., and Mariezkurrena, K., 1984, La cueva de Amalda (Zestoa, País Vasco). Ocupaciones Paleolíticas y Postpaleolíticas: San Sebastián, Fundación Miguel de Barandiarán.

Álvarez-Alonso, D., 2014, El final del Paleolítico Superior: El Magdaleniense en Asturias, *Entemu*, **XVIII: Los grupos cazadores-recolectores paleolíticos del occidente cantábrico. Estudios en homenaje a Francisco Jordá Cerdá en el centenario de su nacimiento. 1914-2014**, 171-204.

Álvarez-Alonso, D., Arrizabalaga, A., Jordá Pardo, J. F., and Yravedra, J., 2011, La secuencia estratigráfica magdaleniense de la Cueva de Coímbre (Peñamellera Alta, Asturias. España), *Férvedes*, **7**, 57-64.

Álvarez-Alonso, D., and De Andrés, M., 2012, La transición Solutrense-Magdaleniense en la Cueva de El Cierro (Ribadesella, Asturias, España), *Espacio, Tiempo y Forma, Serie I, nueva época Prehistoria y Arqueología*, **5**, 399-411.

Álvarez-Alonso, D., De Andrés, M., and Rojo, J., 2013a, La captación de materias primas líticas durante el Paleolítico en el oriente de Asturias, y su caracterización litológica en la cuenca de los ríos Sella y Cares (Asturias, España), *VIII Reunión de Cuaternario Ibérico, La Rinconada-Sevilla*, **1**, 296-299.

Álvarez-Alonso, D., Yravedra, J., Álvarez-Fernández, E., Calvo, A., Carral, P., Iriarte, M., Jordá, F., Sesé, C., Uzquiano, P., and Arrizabalaga, A., 2017, Subsistencia, movilidad y adaptación al medio de los cazadores-recolectores gravetienses en el sector occidental de la región cantábrica: la cueva de Coímbre (Asturias), *Trabajos de Prehistoria*, **74**(**enero-junio**), 47-67.

Álvarez-Alonso, D., Yravedra, J., Arrizabalaga, A., and Jordá, F., 2013b, Excavaciones arqueológicas en la Cueva de Coímbre (Besnes, Peñamellera Alta). Campañas 2008-2012, in *Excavaciones Arqueológicas en Asturias 2007-2012*, 109-120, P. L. Gasalla, ed., Consejería de Educación, Cultura y Deporte. Dirección General de Patrimonio Cultural, Oviedo.

Álvarez-Alonso, D., Yravedra, J., Arrizabalaga, A., Jordá, J. F., and Heredia, N., 2009, La Cueva de Coimbre (Peñamellera Alta, Asturias, España): su yacimiento arqueológico y su santuario rupestre. Un estado de la cuestión en 2008, *Munibe*, **60**, 139-155.

Álvarez-Alonso, D., Yravedra, J., De Andrés, M., Arrizabalaga, A., García-Díez, M., Garrido, D., and Jordá Pardo, J. F., 2014, La cueva de Coímbre (Asturias, España): Artistas y cazadores durante el Magdaleniense en la Región Cantábrica, in *Cien años de arte rupestre paleolítico. Centenario del descubrimiento de la Peña de Candamo*, 101-108, M. S. Corchón, and M. Menéndez, eds., Ediciones Universidad de Salamanca, Salamanca.

Álvarez-Alonso, D., Yravedra, J., De Andrés, M., Arrizabalaga, A., Jordá, J. F., and Rojo, J., 2013c, La secuencia cronoestratigráfica del Paleolítico superior de la Cueva de Coímbre (Asturias, España), in *Actas de la VIII Reunión del Cuaternarion Ibérico: El cuaternario Ibérico: Investigación en el S. XXI*, 83-86, R. Baena, J. Fernández, and I. Guerrero, eds., G.T.P.E.Q. y AEQUA, Madrid.

Álvarez-Alonso, D., Yravedra, J., Jordá Pardo, J. F., and Arrizabalaga, A., 2016, The Magdalenian sequence at Coímbre cave (Asturias, Northern Iberian Peninsula): Adaptive strategies of hunter–gatherer groups in montane environments, *Quaternary International*, **402**, 100-111.

Alvarez-Marrón, J., Pérez-Estaun, A., Aller, N., and Heredia, H., 2003, Mapa geológico y Memoria de la Hoja nº79 (Puebla de Lillo), in *Mapa Geológico de España Escala 1:50.000, MAGNA*, I. Instituto Geológico y Minero de España, ed., IGME, Madrid.

Álvaro, J. J., Vennin, E., Moreno-Eiris, E., Perejón, A., and Bechstädt, T., 2000, Sedimentary patterns across the Lower–Middle Cambrian transition in the Esla nappe (Cantabrian Mountains, northern Spain), *Sedimentary Geology*, **137**(**1–2**), 43-61.

Álvaro, M., Apalategui, O., Baena, J., Balcells, R., Barnolas, A., Barrera, J. L., Bellido, F., Cueto, L. A., Díaz de Neira, A., Elízaga, E., Fernández-Gianotti, J. R., Ferreiro, E., Gabaldón, V., García-Sansegundo, J., Gómez, J. A., Heredia, N., Hernández-Urroz, J., Hernández-Samaniego, A., Lendínez, A., Leyva, F., López-Olmedo, F. L., Lorenzo, S., Martín, L., Martín, D., Martín Serrano, A., Matas, J., Monteserrín, V., Nozal, F., Olive, A., Ortega, E., Piles, E., Ramírez, J. I., Robador, A., Roldán, F., Rodríguez, L. R., Ruiz, P., Ruiz, M. T., Sánchez-Carretero, R., and Teixell, A., 1994, Mapa geológico de la Península Ibérica, Baleares y Canarias: escala 1.1000.000, I. Instituto Geológico y Minero de España, ed., IGME, Madrid.

Aller, J., Álvarez-Marrón, J., Bastida, F., Bulnes, M., Heredia, N., Marcos, A., Pérez-Estaún, A., Pulgar, J. A., and Rodríguez-Fernández, L. R., 2004, Estructura, deformación y metamorfismo, in *Geología de España*, 42-47, J. A. Vera, ed., SGE-IGME, Madrid.

Andrefsky, W., 1994, Raw-Material Availability and the Organization of Technology, *American Antiquity*, **59**(**1**), 21-34.

Aramburu, C., Méndez-Bedia, I., Arbizu, M., and García-Lópèz, S., 2004, La secuencia preorogénica, in *Geología de España*, J. A. Vera, ed., SGE-IGME, Madrid.

Aramburu, C., Truyols, J., Arbizu, M., Méndez-Bedia, I., Zamarreño, I., García-Ramos, J. C., Suárez de Centi, C., and Valenzuela, M., 1992, El Paleozoico Inferior de la Zona Cantábrica, in *Paleozoico Inferior de Ibero-América*, 397-420, J. C. Gutiérrez Marco, J. Saavedra, and I. Rábano, eds., Universidad de Extremadura, Cáceres.

Arbizu, M., Arsuaga, J. L., and Adán, G., 2005a, La cueva del Forno/Conde (Tuñón, Asturias): un yacimiento del tránsito del Paleolítico medio y superior en la Cornisa Cantábrica, in *Actas de la reunión científica: Neandertales cantábricos, estado de la cuestión. Celebrada en el Museo de Altamira los días 20-22 de Octubre de 2004*, 425-41, R. Montes, and J. A. Lasheras, eds., Monografías del Museo Nacional y Centro de Investigación de Altamira, **20**, Ministerio de Educación y Cultura, Madrid.

Arbizu, M., Arsuaga, J. L., and Adán, G., 2009, La Cueva del Conde 2003-2006 (Proyecto CN 04-218): Neandertales y Cromañones en el Valle de Tuñón (Santo Adriano), *Excavaciones Arqueológicas en Asturias 2003-2006*, 435-446.

Arbizu, M., Arsuaga, J. L., Adán, G., Aramburu, A., Ellwood, B., Fombella, M. A., Álvarez-Laó, D., García-Menéndez, M., and Fernández-Fernández, J., 2005b, Las condiciones ambientales durante la transición del Paleolítico medio al superior en la Cornisa Cantábrica: Del 40000 al 30000 BP en la Cueva del Conde (Tuñón, Asturias, España), in *Cuaternario mediterráneo y poblamiento de homínidos*, 31-32, J. Rodríguez-Vidal, C. Finlayson, and F. Giles, eds., AEQUA, Gibraltar.

Arrizabalaga, A., 2009, The Middle to Upper Paleolithic Transition on the Basque Crossroads: Main Sites, Key Issues, *Mitteilungen der Gesellschaft für Urgeschichte*, **18**, 39-70.

Arrizabalaga, A., 2010, La dialéctica sílex/otras materias primas en la evolución de los recursos líticos durante el Paleolítico vasco. Algunas consideraciones técnicas, económicas y culturales, in *Minerales y rocas en las sociedades prehitóricas*, 83-90, S. Domínguez-Bella, J. Ramos, J. M. Gutiérrez, and M. Pérez, eds., Cádiz.

Arrizabalaga, A., Calvo, A., Elorrieta, I., Tapia, J., and Tarriño, A., 2014, Where to and what for? Mobility Patterns and the Management of Lithic Resources by Gravettian Hunter-Gantherers in the Western Pyrenees, *Journal of Anthropological Research* **70**, 233-261.

Arrizabalaga, A., and Tarriño, A., 2010, Caracterización de los recursos líticos utilizados en el yacimiento paleolítico de Irikaitz (Zestoa, Gipuzkoa). Un nuevo recurso mineral: La vulcanita, in *Minerales y rocas en las sociedades prehistóricas*, 91-97, S. Domínguez-Bella, J. Ramos, J. M. Gutiérrez, and M. Pérez, eds.

Aubry, T., Luís, L., Mangado, J., and Matias, H., 2012, We will be known by the tracks we leave behind: Exotic lithic raw materials, mobility and social networking among the Côa Valley foragers (Portugal), *Journal of Anthropological Science*, **31**, 528-550.

Baceta, J. I., Pujalte, V., Serra-Kiel, J., Robador, A., and Orue-Etxeberria, 2004, El Maastrichtiense final, Paleoceno e Ilerdiense inferior de la Cordillera Pirenáica, in *Geología de España*, 308-313, J. A. Vera, ed., SGE-IGME, Madrid.

Baena, J., and Carrión, E., 2006, Problemas acerca del Final del Musteriense, *Zéphyrus*, **59**, 51-66.

Baena, J., and Carrión, E., 2010, Experimental Approach to the Function and Technology of Quina Side-Scrapers, in *Experiments and Interpretation of Traditional Technologies: Essays in Honor of Errett Callahan*, 171-202, H. Nami, ed., Ediciones de Arqueología Contemporánea, Buenos Aires.

Baena, J., and Carrión, E., 2014, La Cueva de El Esquilleu como nuevo referente para el musteriense Cantábrico, in *Los cazadores recolectores del Pleistoceno y del Holoceno en Iberia y el Estrecho de Gibraltar: Estado actual del conocimiento del registro arqueológico*, 82-87, R. Sala Ramos, ed., Universidad de Burgos, Servicio de Publicaciones e Imagen Institucional y Fundación Atapuerca, Burgos.

Baena, J., Carrión, E., Cuartero, F., and Fluck, H., 2012, A chronicle of crisis: The Late Mousterian in north Iberia (Cueva del Esquilleu, Cantabria, Spain), *Quaternary International*, **247**, 199-211.

Baena, J., Carrión, E., Ruiz, B., Ellwood, B., Sesé, C., Yravedra, J., Jordá, J., Uzquiano, P., Manzano, I., Sánchez-Marco, A., and Hernández, F., 2005, Paleoecología y comportamiento humano durante el Pleistoceno Superior en la comarca de Liébana: La secuencia de la Cueva de El Esquilleu (Occidente de Cantabria, España), in *Actas de la reunión científica: Neandertales cantábricos, estado de la cuestión. Celebrada en el Museo de Altamira los días 20-22 de Octubre de 2004*, 461-487, R. Montes, and J. A. Lasheras, eds., Monografías del Museo Nacional y Centro de Investigación de Altamira, **20**, Ministerio de Cultura, Madrid.

Baldeón, A., 1993, El yacimiento de Lezetxiki (Gipuzkoa, País Vasco). Los niveles musterienses, *Munibe*, **45**, 3-97.

Barandiarán, I., 2015, Contextualización arqueológica de la Covaciella: Una *Koiné* Pirenaico/Cantábrica en el Magdaleniense Medio, in *Arte rupestre paleolítico en la cueva de La Covaciella (Inguanzo, Asturias)*, 125-144, M. García, and J. A. Rodríguez Asensio, eds., Consejería de Educación, Cultura y Deporte y GEA (Gran Enciclopedia Asturiana), Oviedo.

Barandiarán, I., Benéitez, P., Cava, A., and Millán, M. A., 2006, El taller gravetiense de Mugarduia Sur (Navarra): Identificación y cronología, *Zéphyrus*, **60**, 15-26.

Barandiarán, I., Freeman, L., González Echegaray, J., and Klein, R. G., eds., 1987, Excavaciones en la Cueva del Juyo: Monografías del Museo Nacional y Centro de Investigación de Altamira: Madrid, Ministerio de Cultura de España.

Barceló, J. A., 2007, Arqueología y Estadística I: Introducción al estudio de la variabilidad de las evidencias arqueológicas: Barcelona.

Barnolas, A., and Pujalte, V., 2004, La cordillera pirenaica: Definición, límites y división, in *Geología de España*, 233-241, J. A. Vera, ed., SGE-IGME, Madrid.

Bastida, F., 1982, La esquistosidad primaria y las microestructuras de las cuarcitas en la zona Asturoccidental-leonesa, *Trabajos de Geología*, **12**, 159-185.

Bastida, F., 2004, Zona Cantábrica, in *Geología de España*, 25-49, J. A. Vera, ed., SGE-IGME, Madrid.

Bastida, F., Brime, C., García-López, S., Aller, J., Valín, M. L., and Sanz-López, J., 2002, Tectono-thermal evolution of the Cantabrian Zone (NW Spain), in *Palaeozoic conodonts from north Spain*, 105-123, S. García-López, and F. Bastida, eds., Cuadernos del Museo Geominero, IGME, Madrid.

Beroiz, C., Barón, A., Ramírez del Pozo, J., Giannini, G., and Gervilla, M., 2003, Mapa geológico y Memoria de la Hoja nº30 (Villaviciosa), in *Mapa Geológico de España Escala 1:50.000, MAGNA*, I. Instituto Geológico y Minero de España, ed., IGME, Madrid.

Binford, L. R., 1982, The archaeology of place, *Journal of Anthropological Archaeology*, **1**(**1**), 5-31.

Binford, L. R., 1983, Long-term land use patterns: some implications for archaeology, in *Working at Archaeology*, 379-386, L. R. Binford, ed., Academic, New York.

Binns, R. A., and McBryde, I., 1969, Preliminary report on a petrological study of ground-edge artefacts from north-eastern New South Wales, Australia, *Procceding of the Prehistory Society*, **35**(**10**), 229-235.

Blanco-Ferrera, S., Sanz-López, J., García-López, S., and Bastida, F., 2016, Tectonothermal evolution of the northeastern Cantabrian zone (Spain), *International Journal of Earth Sciences*, 1-17.

Block Vagle, G., Hurst, A., and Dypvik, H., 1994, Origin of quartaz cements in some sandsontes from the Jurassic of the Inner Firth (UK), *Sedimentology*, **41**, 363-377.

Blomme, A., Degryse, P., Van Peer, P., and Elsen, J., 2012, The characterization of sedimentary quartzite artefacts from Mesolithic sites, Belgium, *Geologica Belgica*, **15**(**3**), 193-199.

Bocherens, H., 2018, The Rise of the Anthroposphere since 50,000 Years: An Ecological Replacement of Megaherbivores by Humans in Terrestrial Ecosystems?, *Frontiers in Ecology and Evolution*, **6**(**3**).

Boëda, E., 1994, Le Concept Levallois: variabilité des méthodes: Paris, CNRS editions.

Borgerhoff Mulder, M., and Schacht, R., 2012, Human Behavioural Ecology, *eLS*.

Bustos-Pérez, G., and Baena Preysler, J., 2016, Preliminary experimental insights into differential heat impact among lithic artifacts, *Journal of Lithic Studies*.

Bustos-Pérez, G., Chacón, M. G., Rivals, F., Blasco, R., and Rosell, J., 2017, Quantitative and qualitative analysis for the study of Middle Paleolithic retouched artifacts: Unit III of Teixoneres cave (Barcelona, Spain), *Journal of Archaeological Science: Reports*, **12**(**Supplement C**), 658-672.

Butzer, K. W., 1989, Arqueología, una ecología del hombre: Barcelona, Ediciones Bellaterra.

Cabanes, D., Mallol, C., Expósito, I., and Baena, J., 2010, Phytolith evidence for hearths and beds in the late Mousterian occupations of Esquilleu cave (Cantabria, Spain), *Journal of Archaeological Science*, **37**(**11**), 2947-2957.

Cabrera, V., 1984, El yacimiento de la Cueva de"El Castillo"(Puente Viesgo, Santander), Consejo Superior de Investigaciones Científicas, Instituto Español de Prehistoria.

Cabrera, V., Bernaldo de Quirós, F., Maillo, J. M., Pike-Tay, A., and Garralda, M. D., 2005, Excavaciones en El Castillo: Veinte años de reflexiones, in *Actas de la reunión científica: Neandertales cantábricos, estado de la cuestión. Celebrada en el Museo de Altamira los días 20-22 de Octubre de 2004*, 503-526, R. Montes, and J. A. Lasheras, eds., Monografías del Museo Nacional y Centro de Investigación de Altamira, **20**, Ministerio de Educación y Cultura, Madrid.

Cabrera, V., Lloret, M., and Bernaldo de Quirós, F., 1996, Materias primas y formas líticas del Auriñaciense Arcaico de la Cueva del Castillo (Puente Viesgo, Cantabria) *Espacio, Tiempo y Forma, Serie I, Prehistoria y Arqueología* **9**(**9**), 141-158.

Cabrera, V., Maillo, J. M., and Bernaldo de Quirós, F., 2000, Esquemas operativos laminares en el Musteriense final de la Cueva del Castillo (Puente Viesgo, Cantabria), *Espacio, Tiempo y Forma, Serie I, Prehistoria y Arqueología*, **13**, 51-78.

Calvo, A., Bradtmöller, M., Martínez, L., and Arrizabalaga, Á., 2016, Lithic cultural variability during the Gravettian in the Cantabrian Region and the western Pyrenees: State of the art, *Quaternary International*, **406, Part A**, 25-43.

Carreras Suárez, J. F., Ramírez del Pozo, J., Aguilar Tomás, M. J., and Pujalte Navarro, V., 2003, Mapa geológico y Memoria de la Hoja nº57 (Cabezón de la Sal), in *Mapa Geológico de España Escala 1:50.000, MAGNA*, I. Instituto Geológico y Minero de España, ed., IGME, Madrid.

Carrión, E., 1998, El yacimiento al aire libre de El Habario (Pendes, Cantabria), Universidad Autónoma de Madrid, Madrid.

Carrión, E., 2002, Variabilidad técnica en el Musteriense de Cantabria, Universidad Autónoma de Madrid, Madrid.

Carrión, E., and Baena, J., 1999, El Habario, un yacimiento musteriense al aire libre en los Picos de Europa cántabros, *Espacio, Tiempo y Forma, Serie I, Prehistoria y Arqueología*, **12**, 81-101.

Carrión, E., and Baena, J., 2003, La producción Quina del Nivel XI de la Cueva del Esquilleu: Una gestión especializada de la producción, *Trabajos de Prehistoria*, **60**, 35-52.

Carrión, E., and Baena, J., 2005, El Habario: una ocupación musteriense al aire libre en los Picos de Europa, in *Actas de la reunión científica: Neandertales cantábricos, estado de la cuestión. Celebrada en el Museo de Altamira los días 20-22 de Octubre de 2004*, 446-460, R. Montes, and J. A. Lasheras, eds., Monografías del Museo Nacional y Centro de Investigación de Altamira, **20**, Ministerio de Educación y Cultura, Madrid.

Carrión, E., Baena, J., and Conde, C., 1995, Avance sobre los trabajos de excavación realizados en el yacimento de el Habario (Pendes-Cantabria): Procesos técnicos, *CuPAUAM*, **22**, 9-20.

Carrión, E., Baena, J., Conde, C., Cuatero, F., and Roca, M., 2008, Variabilidad técnica del Paleolítico medio en el sudoeste de Europa, *Treballs d'arqueologia*, **14**, 279-318.

Carrión, E., Baena, J., and Torres Navas, C., 2013, Una tecnología en extinción. Procesos técnicos y tecnológicos del final del Musteriense en el Norte Peninsular, *Mainake*, **33**, 251-274.

Castanedo, I., 2001, Adquisición y aprovechamiento de los recursos líticos en la Cueva de la Flecha, *Munibe*, **53**, 3-18.

Castanedo, I., Muñoz, E., and Malpelo, B., 1993, El yacimiento al aire libre de El Habario (Castro Cillórigo, Cantabria) *Nivel Cero*, **3**, 5-29.

Castro, A., 1989, Petrografía básica. Texturas, clasificación y nomenclatura de rocas: Madrid, Paraningo.

Clemente, I., and Gibaja, J., 2011, Formation of use-wear traces in non-flint Rocks: the case of quartzite and rhyolite – differences and similarities, in *Non-flint raw materials use in Prehistory: Old prejudices and New Directions. Proceding of the UISPP XV World Congress*, 93-98, L. Oosterbeek, ed., BAR International Series, Lisbon.

Cnudde, V., Dewanckele, J., De Kock, T., Boone, M., Baele, J. M., Crombé, P., and Robinson, E., 2013, Preliminary structural and chemical study of two quartzite varieties from the same geological formation: a first step in the sourcing of quartzites utilized during the Mesolithic in northwest Europe, *Geologica Belgica*, **16**(**1-2**), 27-34.

Cohen, K. M., Finney, S. C., Gibbard, P. L., and Fan, J.-X., 2013, The ICS International Chronostratigraphic Chart, *Episodes*, **36**(**3**), 199-204.

Colmero, J., Fernández, L. P., Moreno, C., Bahamonde, J. R., Barba, P., Heredia, N., and González, F., 2002, Carboniferous, in *The Geology of Spain*, 93-116, W. Gibbons, and T. Moreno, eds., The Geological Society of London, London.

Corchón, M. S., 1981, Cueva de las Caldas: San Juan de Priorio (Oviedo): Monografías del Museo Nacional y Centro de Investigación de Altamira: Madrid, Ministerio de Cultura.

Corchón, M. S., Martínez, J., and Tarriño, A., 2007, Mobilité, territoires et relations culturelles au début du Magdalénien moyen cantabrique: nouvelles perspectives, in *Le concept de territoires dans le Paléolithique supérieur européen. Actes du XVe Congrès mondial (Lisbonne, 4–9 septembre 2006)*, 217-230, F. Djindjian, J. Kozlowski, and N. Bicho, eds., BAR International Series, Oxford.

Corchón, M. S., Ortega, P., and Vicente, F. J., 2013, Cadenas operativas y suelos de ocupación. El nivel 9 de la cueva de Las Caldas (Asturias, España), *Munibe*, **64**, 17-32.

Cronk, L., 1991, Human Behavioral Ecology, *Annual Review of Anthropology*, **20**, 25-53.

Cross, A. J., Prior, D. J., Stipp, M., and Kidder, S., 2017, The recrystallized grain size piezometer for quartz: An EBSD□based calibration, *Geophysical Research Letters*, **44**(**13**), 6667-6674.

Crutzen, P. J., 2002, Geology mankind, *Nature*, **415**(**23**), 23.

Crutzen, P. J., and Stoermer, E. F., 2000, The "Anthropocene", *IGBP Newsletter*, **41**, 17-18.

Cuartero, F., Alcaraz-Castaño, M., López-Recio, M., Carrión-Santafé, E., and Baena-Preysler, J., 2015, Recycling economy in the Mousterian of the Iberian Peninsula: The case study of El Esquilleu, *Quaternary International*, **361**, 113-130.

Chang, F.-J., and Chung, C.-H., 2012, Estimation of riverbed grain-size distribution using image-processing techniques, *Journal of Hydrology*, **440–441**(**0**), 102-112.

Chung, C.-H., and Chang, F.-J., 2013, A refined automated grain sizing method for estimating river-bed grain size distribution of digital images, *Journal of Hydrology*, **486**(**0**), 224-233.

Dalpra, C. L., and Pitblado, B. L., 2016, Discriminating Quartzite Sources Petrographically in the Upper Gunnison Basin, Colorado: Implications for Paleoamerican Lithic-Procurement Studies, *PaleoAmerica*, 1-10.

Davis, J. C., 1986, Statistics and data analysis in Geology: New York, Chichester, Brisbane, Toronto, Singapore, John Wiley & Sons.

Dawkins, R., 2002, Los memes: Los nuevos replicadores, in *El gen egoista. Las bases biológicas de nuestra conducta*, 247-262, Salvat Editores, Barcelon.

Dayton, L., 2001, Mass extintions pinned on Ice Age hunters, *Science*, **292**(**8**).

De Andrés, M., and Arrizabalaga, A., 2014, El Paleolítico superior inicial en Asturias, *Entemu*, **XVIII: Los grupos cazadores-recolectores paleolíticos del occidente cantábrico. Estudios en homenaje a Francisco Jordá Cerdá en el centenario de su nacimiento. 1914-2014**, 133-156.

De la Rasilla, M., and Fernández de la Vega, J., 2014, El Solutrense en Asturias, *Entemu*, **XVIII: Los grupos cazadores-recolectores paleolíticos del occidente cantábrico. Estudios en homenaje a Francisco Jordá Cerdá en el centenario de su nacimiento. 1914-2014**, 157-169.

De la Rasilla, M., and Llana, C., 1994, La cronología radiométrica del Solutrense en la Península Ibérica y su correlación crono-climática, *Férvedes*, **1**, 57-67.

De la Rasilla, M., Rosas, A., Cañaveras, J. C., and Lalueza-Fox, C., eds., 2011, La Cueva de El Sidrón (Borines, Piloña, Asturias) Investigación interdisciplinar de un grupo neandertal: Excavaciones Arqueológicas en Asturias. Monografías, v. 1, Gobierno del Principado de Asturias.

Demars, P. Y., 1980, Les matières premières utilisées au Paléolithique supérieur dans le Bassin de Brive, Université de Bordeaux, Burdeaux, 173 p.

Demars, P. Y., 1982, L'utilisation du silex au Paléolithique supérieur: choix, approvisionnement, circulation. L'exemple du bassin de Brive: Cahiers du Quaternarie, v. 5: París, CNRS.

Dibble, H. L., Holdaway, S. J., Lin, S. C., Braun, D. R., Douglass, M. J., Iovita, R., McPherron, S. P., Olszewski, D. I., and Sandgathe, D., 2017, Major Fallacies Surrounding Stone Artifacts and Assemblages, *Journal of Archaeological Method and Theory*, **24**(**3**), 813-851.

Dixon, J. E., Cann, J. R., and Renfrew, C., 1968, Obsidian and the origins of trade, *Scientific American*, **218**, 38-46.

Earle, T., and Ericson, J., 1977, Exchange systems in prehistory: New York, Academic Press.

Earle, T., and Ericson, J., eds., 1982, Context for prehistoric exchange: New York, Academic Press, 321 p.

Eixea, A., Villaverde, V., and Zilhão, J., 2016, Not Only Flint: Levallois on Quartzite and Limestone at Abrigo de la Quebrada (Valencia, Spain): Implications for Neandertal Behavior, *Journal of Anthropological Research*, **72**(**1**), 24-57.

Elorrieta, I., 2016, Aprovisionamiento y disponibilidad de las materias primas silíceas en el Pirineo Occidental durante el Paleolítico Superior: PhD thesis, Universidad del País Vasco/Euskal Herriko Unibertsitatea, Vitoria-Gasteiz, 451 p.

Fernández-Eraso, J., García-Rojas, M., Sánchez, A., Prieto, A., Calvo, A., Domínguez-Ballesteros, E., Tarriño, A., López-de-Ocáriz, J., Bradtmöller, M., and Urigoitia, T., 2017, El tecno-complejo del Embalse de Urrúnaga (Álava). Nuevas aportaciones al conocimiento de las sociedades del Paleolítico inferior en el norte de la Península Ibérica, *Munibe*, **68**, 5-31.

Fernández Eraso, J., 2005, Los productos brutos de talla, in *El campamento prehistórico de Mendandia. Ocupaciones mesolíticas y neolíticas*, 237-283, A. Alday, ed., Fundación Barandiarán.

Fernández Eraso, J., 2015, La Tipología Analítica aplicada al estudio de materiales líticos de época histórica, in *Seis décadas de Tipología Analítica. Actas en homenaje a George Laplace*, 167-178, A. Calvo, A. Sánchez, M. García-Rojas, and M. Alonso-Eguíluz, eds., GITA Grupo de Investigación en Tipología Analítica, Vitoria-Gasteiz.

Fernández Eraso, J., and García-Rojas, M., 2013, Tipología Analítica, in *Métodos y técnicas de análisis y estudio en Arqueología prehistórica. De lo técnico a la reconstrucción de los grupos humanos* 479-497, M. García-Díez, ed., Universidad del País Vasco/Euskal Herriko Unibertsitatea, Bilbao.

Fernández, J., 2010, Una aportación desde la arqueología del paisaje al conocimiento del primer poblamiento humano del Valle del Trubia. Estudio geoarqueológico y análisis SIG del territorio: Oviedo, Ediciones de la Universidad de Oviedo.

Fernández, L. P., Bahamonde, J. R., Barba, P., Colmenero, J. R., Heredia, N., L.R., R.-F., Salvador, C., Sánchez de Posada, L. C., Villa, E., Merino-Tomé, O., and Motis, K., 2004, Secuencia sinorogénica, in *Geología de España*, 34-42, J. A. Vera, ed., SGE-IGME, Madrid.

Fernández, V. M., 2015, Arqueo estadística: Métodos cuantitativos en Arqueología: Madrid, Alianza Editorial.

Feynman, R. P., 2015, El carácter de la ley física: Metatemas: Barcelona, Tusquets, 190 p.

Finlayson, C., 2004, Neanderthals and Modern Humans. An Ecological and Evolutionary Perspective: Cambridge Studies in Biological and Evolutionary Anthropology: Cambridge, Cambridge University Press, 255 p.

Finlayson, C., and Carrión, J., 2007, Rapid ecological turnover and its impact on Neanderthal and other human populations, *TRENDS in Ecology and Evolution*, **22**(**4**), 10.

Finlayson, C., Giles, F., Rodríguez-Vidal, J., Fa, D., Gutierrez, J. M., and Santiago, A., 2006, Late survival of Neanderthals at the southernmost extreme of Europe, *Nature*, **443**(**19**), 4.

Fischer, C., Waldmann, S., and von Eynatten, H., 2013, Spatial variation in quartz cement type and concentration: An example from the Heidelberg formation (Teufelsmauer outcrops), Upper Cretaceous Subhercynian Basin, Germany, *Sedimentary Geology*, **291**, 48-61.

Floquet, M., 2004, El Cretácico Superior de la Cuenca Vasco-Cantábrica y áreas adyacentes, in *Geología de España*, 299-306, J. A. Vera, ed., SGE-IGME, Madrid.

Floss, H., 1990, Rohmaterialversorgung im Paläolithikum des Mittelrheingebietes. Dissertation Universität zu Köln: Monographien: Bonn, Habelt, 407 p.

Folk, R., 1980, Petrology of sedimentary rocks: Austin, Texas, Hemphill Publishing Company.

Fontes, L. M., 2016, The Initial Magdalenian mosaic: New evidence from Urtiaga cave, Guipúzcoa, Spain, *Journal of Anthropological Archaeology*, **41**, 109-131.

Fontes, L. M., Straus, L. G., and González Morales, M. R., 2016, Lithic raw material conveyance and hunter-gatherer mobility during the Lower Magdalenian in Cantabria, Spain, *Quaternary International*, **412**, 66-81.

Fontes, L. M., Straus, L. G., and González Morales, M. R., 2018, Lower Magdalenian lithic raw material provisioning: A diachronic view from El Mirón cave (Ramales de la Victoria, Cantabria, Spain), *Journal of Archaeological Science: Reports*, **19**, 794-803.

Fortea, J., 1996, The cave of Covaciella (Carreña de Cabrales, Asturias, Spain), *INORA: International Newslatter on Rock Art*, **13**, 1-3.

Fortea, J., 2007, Cuevas de Covaciella y El Bosque (Cabrales). Campaña de 2000, in *Excavaciones arqueológicas en Asturias 1999-2002*, 221-226, Servicio de Publicaciones del Principado de Asturias, Oviedo.

Fortea, J., De la Rasilla, M., and Rodríguez, V., 1992, La cueva de Llonín (Llonín, Peñamellera Alta). Campañas de 1987 a 1990, in *Excavaciones Arqueológicas en Asturias 1987-1990*, 9-18, Servicio de Publicaciones del Principado de Asturias, Oviedo.

Fortea, J., De la Rasilla, M., and Rodríguez, V., 1995a, La cueva de Llonín (Llonín, Peñamellera Alta). Campañas de 1991 a 1994, in *Excavaciones Arqueológicas en Asturias 1991-94*, 33-43, Servicio de Publicaciones del Principado de Asturias, Oviedo.

Fortea, J., de la Rasilla, M., and Rodríguez, V., 1999, La cueva de Llonín (Llonín, Peñamellera Alta). Campañas de 1995 a 1998, in *Excavaciones Arqueológicas en Asturias 1995-98*, 59-68, Servicio de Publicaciones del Principado de Asturias, Oviedo.

Fortea, J., Rodríguez, V., Hoyos, M., Espeleología, F. A. d., Valladas, H., and Torres, T., 1995b, Covaciella, in *Excavaciones Arqueológicas en Asturias 1991-1994*, 258-270, Servicio de Publicaciones del Principado de Asturias, Oviedo.

French, M., Worden, R., Mariani, E., Larese, R., Mueller, R., and Kliewer, C., 2012, Microcrystalline quartaz generation and the preservation of porosity in sandsontes: Evidence from the Upper Cretaceous or the subhercynian Basin, Germany, *Journal of Sedimentary Research*, **82**, 422-434.

French, M. W., and Worden, R. H., 2013, Orientation of microcrystalline quartz in the Fontainebleau Formation, Paris Basin and why it preserves porosity, *Sedimentary Geology*, **284**, 149-158.

Gamble, C., 2001, Las sociedades paleolíticas de Europa: Barcelona, Ariel.

Gapaist, D., and White, S. H., 1982, Ductile Shear Bands in Naturally Deformed Quartzite, *Textures and Microstructures*, **5**, 1-17.

García-Díez, M., Ochoa, B., Garrido, D., and Vigiola-Toña, I., 2015a, Evidencias de frecuentación: Frecuentación animal, in *Arte rupestre paleolítico en la Cueva de La Covaciella*, 44-45, M. García-Díez, B. Ochoa, and J. A. Rodríguez Asensio, eds., Consejería de Educación, Cultura y Deporte y GEA, Oviedo.

García-Díez, M., Ochoa, B., Garrido, D., and Vigiola-Toña, I., 2015b, Evidencias de frecuentación: Orificios verticales, in *Arte rupestre paleolítico en la Cueva de La Covaciella*, 49-50, M. García-Díez, B. Ochoa, and J. A. Rodríguez Asensio, eds., Consejería de Educación, Cultura y Deporte y GEA, Oviedo.

García-Díez, M., Ochoa, B., Garrido, D., and Vigiola-Toña, I., 2015c, Evidencias de frecuentación: Trazos digitales sobre arcilla, in *Arte rupestre paleolítico en la Cueva de La Covaciella*, 55-60, M. García-Díez, B. Ochoa, and J. A. Rodríguez Asensio, eds., Consejería de Educación, Cultura y Deporte y GEA, Oviedo.

García-Díez, M., Ochoa, B., and Rodríguez Asensio, J. A., eds., 2015d, Arte rupestre paleolítico en la Cueva de La Covaciella (Inguazo, Asturias): Excavaciones Arqueológicas en Asturias. Monografías: Oviedo, Consejería de Educación, Cultura y Deporte y GEA, 151 p.

García-Diez, M., Vigiola-Toña, I., Ochoa, B., Garrido-Pimentel, D., and Rodríguez-Asensio, J. A., 2015, La variabilidad gráfica de La Covacilla y posición en las tradiciones gráficas del Paleolítico del Sudoeste Europea, in *Arte rupestre paleolítico en la cueva de La Covaciella (Inguanzo, Asturias)*, 116-124, M. García, and J. A. Rodríguez Asensio, eds., Consejería de Educación, Cultura y Deporte y GEA (Gran Enciclopedia Asturiana), Oviedo.

García-Mondéjar, J., Fernández-Mendiola, P. A., Agirrezabala, L. M., Aranburu, A., López-Horgue, M. A., Iriarte, E., and Martínez de Rituerto, S., 2004, El Aptiense-Albiense de la Cuenca Vasco-Cantábrica, in *Geología de España*, 291-296, J. A. Vera, ed., SGE-IGME, Madrid.

García-Rojas, M., 2010, Propuesta de descripción y clasificación de los productos de debitado desde la Tipología Analítica, *Zéphyrus*, **66**, 93-107.

García-Rojas, M., 2014, Dinámicas de talla y gestión de las materias primas silíceas a finales del Pleistoceno en el País Vasco: PhD thesis, Universidad del País Vasco/Euskal Herriko Unibertsitatea, Vitoria-Gasteiz, 558 p.

García-Rojas, M., Prieto, A., Sánchez, A., Camarero, C., and Zapata, L., 2017, The Application of GIS to flint management studies during the Pleistocene to Holocene transition: the case of Baltzola (Dima, Bizkaia, Spain), in *Archaeology and Geomatics. Harvesting the benefits of 10 years of training in the Iberian Peninsula (2006-2015)*, 133-148, V. Mayoral Herrera, C. Parcero-Oubiña, and P. Fábrega-Álvarez, eds., Sidestone Press, Leiden.

García, M., Garrido, D., Ochoa, B., Vigiola-Toña, I., and Rodríguez-Asensio, J. A., 2015, El dispositivo iconográfico rupestre, in *Arte rupestre paleolítico en la cueva de La Covaciella (Inguanzo, Asturias)*, 43-62, M. García, and J. A. Rodríguez Asensio, eds., Consejería de Educación, Cultura y Deporte y GEA (Gran Enciclopedia Asturiana), Oviedo.

Geneste, J. M., 1985, Analyse lithique d'industries moustériennes du Périgord: une approche technologique du comportemen des grupes humains au Paléolithique moyen, Université de Bordeaux, Bordeaux.

Ghiasi-Freez, J., Soleimanpour, I., Kadkhodaie-Ilkhchi, A., Ziaii, M., Sedeghi, M., and Hatampour, A., 2012, Semi-automated porosity identification from thin section images using image analysis and intelligent discriminant classifiers, *Computers & Geosciences*, **45**, 36-45.

Gibaja, J., 2007, Estudios de Traceología y funcionalidad, *Praxis Arqueológica*, **2**, 49-74.

González Echegaray, J., 1957, La Cueva de la Mora, un yacimiento paleolítico en la región de los Picos de Europa, *Altamira: Revista del Centro de Estudios Montañeses*, **1-3**, 3-28.

González Echegaray, J., 1980, El yacimiento de la cueva de "El Pendo" (Excavaciones 1953-57): Bibliotheca Praehistorica Hispana: Madrid, Consejo Superior de Investigaciones científicas. Instituto Español de Prehistoria, 270 p.

González Echegaray, J., and Barandiarán, I., 1981, El Paleolítico superior en la Cueva del Rascaño (Santander): Monografías del Museo Nacional y Centro de Investigación de Altamira: Madrid, Ministerio de Educación y Cultura.

González Echegaray, J., and Freeman, L., 1978, Vida y muerte en Cueva Morín: Santander, Institución cultural de Cantabria. Diputación Provincial.

González, J. E., and Ibañez, J. J., 1994, Metodología de análisis funcional de instrumentos tallados en sílex: Cuadernos de Arqueología: Bilbao, Universidad de Deusto, 301 p.

Hames, R., 2001, Human Behavioral Ecology, in *International encyclopedia of the Social and Behavioral Sciences*, 6946-6951, N. Smelser, and P. Baltes, eds., Elsevier Science Ltd.

Hammer, Ø., Harper, D. A. T., and Ryan, P. D., 2001, PAST: Paleontological Statistics Software Package for Education and Data Analysis, *Palaeontologia Electronica*, **4**(**1**), 9.

Heilbronner, R., 2000, Automatic grain boundary detection and grain size analysis using polarization micrographs or orientation images, *Journal of Structural Geology*, **22**, 969-981.

Heilbronner, R., and Tullis, J., 2006, Evolution of c axis pole figures and grain size during dynamic recrystallization: Results from experimentally sheared quartzite, *Journal of Geophysical Research: Solid Earth*, **111**(**B10**), n/a-n/a.

Heredia, H., Alonso, J. L., and Rodríguez Fernández, L. R., 2003a, Mapa geológico y Memoria de la Hoja nº105 (Riaño), in *Mapa Geológico de España Escala 1:50.000, MAGNA*, I. Instituto Geológico y Minero de España, ed., IGME, Madrid.

Heredia, H., and Rodríguez Fernández, L. R., 2003, Mapa geológico y Memoria de la Hoja nº54 (Rioseco), in *Mapa Geológico de España Escala 1:50.000, MAGNA*, I. Instituto Geológico y Minero de España, ed., IGME, Madrid.

Heredia, H., Rodríguez Fernández, L. R., Suárez, A., and Alvarez Marrón, J., 2003b, Mapa geológico y Memoria de la Hoja nº80 (Burón), in *Mapa Geológico de España Escala 1:50.000, MAGNA*, I. Instituto Geológico y Minero de España, ed., IGME, Madrid.

Heredia, N., Navarro, D., Rodríguez Fernández, L. R., Pujalde, V., and García Mondéjar, J., 2003c, Mapa geológico y Memoria de la Hoja nº82 (Tudanca), in *Mapa Geológico de España Escala 1:50.000, MAGNA*, I. Instituto Geológico y Minero de España, ed., IGME, Madrid.

Herrero-Alonso, D., Tarriño, A., Neira-Campos, A., and Fuertes-Prieto, N., 2016, Chert from the Vegamián Formation: A new raw-material supply source in the Cantabrian Mountains (NW Spain) during prehistory, *Journal of Lithic Studies*, **3**(**2**), xxx-xxx.

Higham, T., Douka, K., Wood, R., Ramsey, C. B., Brock, F., Basell, L., Camps, M., Arrizabalaga, A., Baena, J., Barroso-Ruiz, C., Bergman, C., Boitard, C., Boscato, P., Caparros, M., Conard, N. J., Draily, C., Froment, A., Galvan, B., Gambassini, P., Garcia-Moreno, A., Grimaldi, S., Haesaerts, P., Holt, B., Iriarte-Chiapusso, M.-J., Jelinek, A., Jorda Pardo, J. F., Maillo-Fernandez, J.-M., Marom, A., Maroto, J., Menendez, M., Metz, L., Morin, E., Moroni, A., Negrino, F., Panagopoulou, E., Peresani, M., Pirson, S., de la Rasilla, M., Riel-Salvatore, J., Ronchitelli, A., Santamaria, D., Semal, P., Slimak, L., Soler, J., Soler, N., Villaluenga, A., Pinhasi, R., and Jacobi, R., 2014, The timing and spatiotemporal patterning of Neanderthal disappearance, *Nature*, **512**(**7514**), 306-309.

Hirth, G., Teyssier, C., and Dunlap, J., 2001, An evaluation of quartzite flow laws based on comparisons between experimentally and naturally deformed rocks, *International Journal of Earth Sciences*, **90**(**1**), 77-87.

Hirth, G., and Tullis, J., 1989, The effects of pressure and porosity on the micromechanics of the brittle-ductile transition in quartzite, *Journal of Geophysical Research: Solid Earth*, **94**(**B12**), 17825-17838.

Hirth, G., and Tullis, J., 1992, Dislocation creep regimes in quartz aggregates, *Journal of Structural Geology*, **14**(**2**), 145-159.

Howard, J. L., 2000, Provenance of quartzite clasts in the Eocene–Oligocene Sespe Formation: Paleogeographic implications for southern California and the ancestral Colorado River, *GSA Bulletin*, **112**(**11**), 1635-1649.

Howard, J. L., 2005, The Quartzite Problem Revisited, *The Journal of Geology*, **113**(**6**), 707-713.

IGN, 2017, Centro de descargas, **20/01/2016**, Ministerio de Fomento, Gobierno de España, http://centrodedescargas.cnig.es/CentroDescargas/index.jsp.

Jeske, R., 1989, Economies in raw material use by prehistoric hunter-gatherers, in *Time, Energy and Stone Tools*, 34-45, R. Torrence, ed., Cambridge University, Cambridge.

Jordá, J., Baena, J., Carral, P., García-Guinea, J., Correcher, V., and Yravedra, J., 2008, Procesos sedimentarios y diagenéticos en el registro arqueológico del yacimiento pleistoceno de la Cueva de El Esquilleu (Picos de Europa, Norte de España), *Cuaternario y geomorfología*, **22**(**3-4**), 31-46.

Julivert, M., 1971, Decollement tectonics in the Hercynian Cordillera of NW Spain, *American Journal of Science*, **270**, 1-29.

Julivert, M., and Navarro, D., 2003, Mapa geológico y Memoria de la Hoja nº55 (Beleño), in *Mapa Geológico de España Escala 1:50.000, MAGNA*, I. Instituto Geológico y Minero de España, ed., IGME, Madrid.

Kantner, J., 2012, Realism, Reality and Routes. Evaluating Cost-Surface and Cost-Path Algorithms, in *Least Cost Analysis of Social Landscapes Archaeological Case Studies*, 225-238, D. White, and S. Surface-Evans, eds., The University of Utah Press, Salt Lake City.

Kelly, R. L., 1992, Mobility/Sedentism: Concepts, Archaeological Measures, and Effects, *Annual Review of Anthropology*, **21**, 43-66.

Kelly, R. L., 1995, The foraging spectrum. Diversity in hunter-gatherer lifeways: New York, Percheron Press.

Kocks, U. F., C.N., T., and Wenk, H. R., 1998, Texture and Anisotropy: Preferred orientations in polycrystals and their effect on materials properties: Cambridge, Cambridge University Press, 676 p.

Kowalski, B. R., Schatzki, T. F., and Stross, F. H., 1972, Classification of archaeolgical artifacts by applying pattern recognition to trace element data, *Analytical Chemistry*, **44**, 2176-2180.

Kramer, P. A., 2010, The Effect on Energy Expenditure of Walking, *American Journal of Human Biology*, **22**, 497-507.

Kropotkin, P., 2015, La Ciencia moderna y la Anarquía: Madrid, LaMalatesta, 287 p.

Langmuir, E., 1984, Mountaincraft and Leadership: Glasgow, Scottish Sports Council.

Laplace, G., 1972, La typologie analytique et structurale: Base rationelle d'études des industries lithiques et osseuses, *Banques de Données Archéologiques*, **932**, 91-143.

Laplace, G., 1987, Un exemple de nouvelle écriture de la grille typologique, *Dialktikê. Cahiers de Typologie Analytique*, **1985-1987**, 16-21.

Leroi-Gourhan, A., 1964, Le geste et la parole: París, Michel Albin.

Lima, R. D., and De Ros, L. F., 2002, The role of depositional setting and diagenesis on the reservoir quality of Devonian sandstones from the Solimões Basin, Brazilian Amazonia, *Marine and Petroleum Geology*, **19**(**9**), 1047-1071.

Liñán, E., Gonzalo, R., Palacios, R., Gámez, T., Ugidos, J. M., and Mayoral, E., 2002, Cambrian, in *The Geology of Spain*, 17-29, W. Gibbons, and T. Moreno, eds., The Geological Society of London, London.

López, M., and Baena, J., 2001, Captación de recursos líticos durante el Paleolítico medio en la comarca de la Mancha Toledana: El Cerro del Molino de San Cristóbal (Camuñas), in *II Congreso de Arqueología de la Provincia de Toledo*, 11-28, J. Vázquez, and J. A. González, eds., Toledo.

López Romero, R., 2005, Cálculo de rutas óptimas mediante SIG en el territorio de la ciudad celtibérica de Segeda. Propuesta metodológica, *SALDVIE*, **5**, 95-111.

Luedtke, B., 1979, The indentification of sources of chert artifacts, *American Antiquity*, **44**(**4**), 744-757.

Llobera, M., 2000, Understanding movement: a pilot model towards the sociology of movement, in *Beyond the Map.Archaeology and Spatial Technologies*, 65-83, G. Lock, ed., IOS Press.

Mallol, C., Cabanes, D., and Baena, J., 2010, Microstratigraphy and diagenesis at the upper Pleistocene site of Esquilleu Cave (Cantabria, Spain), *Quaternary International*, **214**(**1–2**), 70-81.

Mangado, J., 1998, La arqueopetrología del sílex. Estudio de caracterización de materiales silíceos. Un caso práctico, el nivel II de la Cova del Parco (Alòs de Balaguer, La Noguera), *Pyrenae*, **29**, 47-68.

Manzano, I., 2001, Modelos de captación de materias primas líticas durante el Paleolítico medio en la Comarca de la Liébana (Cantabria): El yacimiento de la Cueva de El Esquilleu, 287, Madrid.

Manzano, I., Baena, J., Lázaro, A., Martín, D., Dapena, L., Roca, M., and Moreno, E., 2005, Análisis de los recursos líticos en la Cueva del Esquilleu: gestión y comportamiento durante el Musteriense (Comarca de la Liébana, Occidente de Cantabria), in *Actas de la reunión científica: Neandertales cantábricos, estado de la cuestión. Celebrada en el Museo de Altamira los días 20-22 de Octubre de 2004*, 285-300, R. Montes, and J. A. Lasheras, eds., Monografías del Museo Nacional y Centro de Investigación de Altamira, **20**, Ministerio de Educación y Cultura, Madrid.

Mardia, K. V., 1975, Statistics of Directional Data, *Journal of the Royal Statistical Society. Series B (Methodological)*, **37**(**3**), 349-393.

Marín, A. B., 2009, The Use of Optimal Foraging Theory to Estimate Late Glacial Site Catchment Areas from a Central Place: The Case of Eastern Cantabria, *Journal of Anthropological Archaeology*, **28**(**1**), 27-36.

Maroto, J., Vaquero, M., Arrizabalaga, A., Baena, J., Baquedano, E., Jordá, J. F., Juliá, R., Montes, R., Van der Plicht, J., Rasines, P., and Wood, R., 2012, Current issues in the late Middle Paleolothic chornology: new assessments from Northern Iberia, *Quaternary International*, **247**, 15-25.

Martin, P., 1990, 40.000 years of extinctions on the “planet of doom”, *Palaegeography, Palaeoclimatology, Palaeoecology*, **82**, 187-201.

Martín, P., Montes, R., and Sanguino, J., 2006, La tecnología lítica del Musteriense final en la región cantábrica: los datos de Covalejos (Velo de Piélagos, Cantabria, España), in *En el centenario de la Cueva del Castillo: El ocaso de los Neandertales*, 231-248, V. Cabrera, F. Bernaldo de Quirós, and J. M. Maillo, eds., UNED, Santander.

Martínez-Torres, L. M., and Eguíluz, L., 2014, Dinámica cortical y pulsos termo-tectónicos alpinos en la Cuenca Vasco-Cantábrica y Pirineo occidental, in *Geología de la Cuenca Vasco-Cantábrica*, 105-118, A. Bodego, M. Mendia, A. Aranburu, and A. Apraiz, eds., Servicio Editorial de la Universidad del País Vasco, Bilbao.

Martínez García, E., 2003, Mapa geológico y Memoria de la Hoja nº32 (Llanes), in *Mapa Geológico de España Escala 1:50.000, MAGNA*, I. Instituto Geológico y Minero de España, ed., IGME, Madrid.

Martínez García, E., Marquínez, J., Heredia, N., Navarro, D., and Rodríguez Fernández, L. R., 2003, Mapa geológico y Memoria de la Hoja nº56 (Careña-Cabrales), in *Mapa Geológico de España Escala 1:50.000, MAGNA*, I. Instituto Geológico y Minero de España, ed., IGME, Madrid.

Masson, A., 1981, Pétroarchéologie des roches siliceuses. Intérêt en Prehistoire, Université Claude Bernard-Lyon I, Lyon, 82 p.

Medina-Alcaide, M. A., Romero, A., Peña, J. A., Perales, U., Ruiz-Márquez, R., and Sanchidrián, J. L., 2014, Descifrando la frecuentación paleolítica de la cueva de Nerja. Ejemplo de estudio arquelógico interdisciplinar, in *Mensajes desde el Pasado*, 63-83, M. A. Medina-Alcaide, and A. Romero, eds., Córdoba.

Medina-Alcaide, M. A., and Zapata, L., 2015, Restos vegetales: Evidencias de frecuentación, in *Arte rupestre paleolítico en la Cueva de La Covaciella (Inguazo, Asturias)*, 50-55, M. García-Díez, B. Ochoa, and J. A. Rodríguez Asensio, eds., Consejería de Educación, Cultura y Deporte y GEA, Oviedo.

Meignen, L., Delagnes, A., and Bourguignon, L., 2009, Patterns of Lithic Material Procurement and Transformation During the Middle Paleolithic in Western Europe, in *Lithic Materials and Paleolithic Societies*, 15-24, Wiley-Blackwell.

Meléndez, M. L., 2015, Marco geológico y geomorfológico, in *Arte rupestre paleolítico en la Cueva de La Covaciella*, 21-25, M. García-Díez, B. Ochoa, and J. A. Rodríguez Asensio, eds., Consejería de Educación, Cultura y Deporte y GEA, Oviedo.

Menéndez, M., 1986, La cueva del Buxu: Estudio del yacimiento arqueológico y de las manifestaciones artísticas, *Boletín del Real Insitituto de Estudios Asturianos*, **111**(**38**), 143-186.

Menéndez, M., 1990, Cueva del Buxu. Excavaciones, campaña 1986, *Excavaciones Arqueológicas en Asturias 1983-86*, 87-99.

Menéndez, M., 1992, Excavaciones arqueológicas en la Cueva del Buxu (Cardes. Cangas de Onís), *Excavaciones Arqueológicas en Asturias 1987-1990*, 69-74.

Menéndez, M., 1999, La cueva del Buxu. Cangas de Onís. Campaña de 1998 y resumen de los trabajos anteriores, in *Excavaciones Arqueológicas en Asturias 1995-1998*, 69-73, Servicio de Publicaciones del Principado de Asturias, Oviedo.

Menéndez, M., 2006, Excavaciones en la Cueva de la Güelga (Cangas de Onís, Asturias), in *En el centenario de la Cueva del Castillo: El ocaso de los Neandertales*, 209-229, V. Cabrera, F. Bernaldo de Quirós, and J. M. Maillo, eds., UNED, Santander.

Menéndez, M., Quesada, J. M., Jordá, J. F., Carral, P., Trancho, G. J., García, E., Álvarez, D., Rojo, J., and Wood, R., 2009, Excavaciones arqueológicas en la Cueva de la Güelga (Cangas de Onís), in *Excavaciones Arqueológicas en Asturias 2003-2006* 209-221, Serivicio de Publicaciones del Principado de Asturias, Oviedo.

Menéndez, M., Weniger, G. C., Álvarez-Alonso, D., de Andrés, M., García, E., Jordá, J., Kehl, M., Rojo, J., Quesada, J. M., and Schmidt, I., 2014, La Cueva de la Güelga. Cangas de Onís. Asturias, in *Los cazadores recolectores del Pleistoceno y del Holoceno en Iberia y El Estrecho de Gibraltar: Estado actual del conocimiento del registro arqueológico*, 60-64, R. Sala Ramos, ed., Universidad de Burgos. Servicio de Publicaciones e Imagen Corporativa y Fundación Atapuerca, Burgos.

Merino-Tomé, O., Suárez Rodríguez, A., and Alonso Alonso, J. L., 2016, Mapa Geológico Digital contínuo E. 1:50.000, Zona Cantábrica (Zona-1000), in *GEODE. Mapa Geológico Digital contínuo de España*, I. Instituto Geológico y Minero de España, ed., IGME, Madrid.

Minnetti, A. E., 1995, Optimum Gradient of Mountain Paths, *Journal of Applied Physiology*, **79**(**5**), 1698-1703.

Montes, L., 1988, El Musteriense en la Cuenca del Ebro, Universidad de Zaragoza.

Montes, R., 2003, El primer poblamiento de la región cantábrica: Monografías del Museo Nacional y Centro de Investigación de Altamira: Madrid, Ministerio de Educación y Cultura.

Montes, R., and Muñoz, E., 1992, Un nuevo yacimiento Paleolítico de superficie en Asturias: Panes II (Peñamellera Baja), *Boletín de Ciencias Naturales*, **42**, 183-197.

Morala, A., 1979, Étude préliminaire de la station aurignacienn des Ardailloux, commune de Soturac (Lot), *Bulletin de la Société des Études du Lot*, **3**(**juillet-septembre**), 195-201.

Morala, A., 1980, Observations sur le Périgordien et l'Aurignacien et leurs matieéres premiéres lithiques en Haute-Agenais, Université de Toulouse, 190 p.

Morala, A., 1983, À propos des matières premières lithiques en Haut-Agenais, *Bulletin de la Société préhistorique française*, **80**(**6**), 169.

Moure, J. A., and Gil, G., 1972, Noticia preliminar sobre los nuevos yacimientos de arte rupestre descubiertos en Peñamellera Alta (Asturias), *Trabajos de Prehistoria*, **29**, 245-465.

Moure, J. A., and Gil, G., 1974, La cueva de Coimbre, en Peñamellera Alta (Asturias), *Boletín del Instituto de Estudios Asturianos*, **28**(**82**), 505-528.

Muñoz, E., 2005, El Musteriense en el centro de la Región Cantábrica, in *Actas de la reunión científica: Neandertales cantábricos, estado de la cuestión. Celebrada en el Museo de Altamira los días 20-22 de Octubre de 2004*, 75-100, R. Montes, and J. A. Lasheras, eds., Monografías del Museo Nacional y Centro de Investigación de Altamira, **20**, Ministerio de Educación y Cultura, Madrid.

Muñoz, E., and Serna, A., 1999, Los niveles solutrenses de la Cueva del Ruso I, *Sautuola: Revista del Instituto de Prehistoria y Arqueología*, **6**, 161-176.

Navarro, D., 2003, Mapa geológico y Memoria de la Hoja nº31 (Ribadesella), in *Mapa Geológico de España Escala 1:50.000, MAGNA*, I. Instituto Geológico y Minero de España, ed., IGME, Madrid.

Normand, C., 1986, Inventaire des gîtes de matières premières de la Chalosse, in *Recherches de Préhistoire dans les Landes*, 121-140, R. L. Arambourou, L. Straus, and C. Normand, eds., Bulletin de la Société de Borda.

Obeso-Amado, R., 2015, Localización y entorno paisajístico, in *Arte rupestre paleolítico en la Cueva de La Covaciella (Inguanzo, Asturias)*, 25-34, M. García-Díez, B. Ochoa, and J. A. Rodríguez Asensio, eds., Consejería de Educación, Cultura y Deporte y GEA, Oviedo.

Ochoa, B., Garrido, D., García-Díez, M., and Vigiola-Toña, I., 2015, Historia del descubrimiento e investigación, in *Arte rupestre paleolítico en la Cueva de La Covaciella*, 35-38, M. García-Díez, B. Ochoa, and J. A. Rodríguez Asensio, eds., Consejería de Educación, Cultura y Deporte y GEA, Oviedo.

Ochoa, B., and Vigiola-Toña, I., 2014, Cueva de Covaciella (Carreña de Cabrales, Asturias), in *Los cazadores recolectores del Pleistoceno y del Holoceno en Iberia y El Estrecho de Gibraltar*, 666-667, R. Sala Ramos, ed., Universidad de Burgos, Servicio de Publicaciones e Imagen Institucional y Fundación Atapuerca, Burgos.

Ortiz, I., and Baena, J., 2016, Did stones speak about people? Flint catchment and Neanderthal behavior from Area 3 (Cañaveral, Madrid-Spain), *Quaternary International*.

Pandolf, K. B., Burse, R. L., and Goldman, R. F., 1977, Role of Physical Fitness in Heat Acclimatization, Decay and Reinduction, *Ergonomics*, **20**, 399-408.

Pastor-Galán, D., Martín-Merino, G., and Corrochano, D., 2014, Timing and structural evolution in the limb of an orocline: The Pisuerga–Carrión Unit (southern limb of the Cantabrian Orocline, NW Spain), *Tectonophysics*, **622**, 110-121.

Pedergnana, A., García-Antón, M. D., and Ollé, A., 2017, Structural study of two quartzite varieties from the Utrillas facies formation (Olmos de Atapuerca, Burgos, Spain): From a petrographic characterisation to a functional analysis design, *Quaternary International*, **433**(**Part A**), 163-178.

Pedergnana, A., and Ollé, A., 2017, Monitoring and interpreting the use-wear formation processes on quartzite flakes through sequential experiments, *Quaternary International*, **427**(**Part B**), 35-65.

Pedergnana, A., Ollé, A., Borel, A., and Moncel, M.-H., 2016, Microwear study of quartzite artefacts: preliminary results from the Middle Pleistocene site of Payre (South-eastern France), *Archaeological and Anthropological Sciences*, 1-20.

Pelayo López, F., and Gonzalo Gutiérrez, R., 2012, Juan Vilanova y Piera (1821-1893), la obra de un naturalista y prehistoriador valenciano: Serie de trabajos varios: Valencia, Diputación de Valencia, 337 p.

Perales, U., 2015, Traceología de la industria lítica de Atxoste (Alava): Aproximación a la gestión económico-social del asentamiento en el final del mesolítico e inicios del neolítico, Universidad del País Vasco, 581 p.

Perales, U., and Prieto, A., 2015, Evidencias de frecuentación: Industria lítica, in *Arte rupestre paleolítico en la Cueva de La Covaciella*, 45-49, M. García-Díez, B. Ochoa, and J. A. Rodríguez Asensio, eds., **3**, Consejería de Educación, Cultura y Deporte y GEA, Oviedo.

Pérez-Estaún, A., 2004, El Precámbrico del Antiforme del Narcea, in *Geología de España*, 26, J. A. Vera, ed., SGE-IGME, Madrid.

Pérez-Estaún, A., Bea, F., Bastida, F., Marcos, A., Martínez Catalán, J. R., Martínez Poyatos, D., Arenas, R., Díaz García, F., Azor, A., Simancas, J. F., and González Lodeiro, F., 2004, La Cordillera Varisca Europea: El Macizo Ibérico, in *Geología de España*, 21-25, J. A. Vera, ed., SGE-IGME, Madrid.

Perkins, D., and Henke, K. R., 2002, Minerales en Lámina Delgada: Madrid, Pearson Edicación, S.A.

Pignatelli, R., Giannini, G., Ramírez del Pozo, J., Beroiz, C., and Barón, A., 2003, Mapa geológico y Memoria de la Hoja nº15 (Lastres), in *Mapa Geológico de España Escala 1:50.000, MAGNA*, I. Instituto Geológico y Minero de España, ed., IGME, Madrid.

Pinto-Llona, A. C., Clark, G., Karkanas, P., Blackwell, B., Skinner, A., Andrews, P., Reed, K., Miller, A., Macías-Rosado, R., and Vakiparta, J., 2012, The Sopeña Rockshelter, a New Site in Asturias, *Munibe*, **63**, 45-79.

Pinto-Llona, A. C., Clark, G., and Miller, A., 2005, Sopeña, un nuevo yacimiento de Paleolítico Medio y Spuerior Inicial en el norte de la Península Ibérica, in *O Paleolítico, Actas do IV Congresso de Arqueología Peninsula, Faro, 2004*, 407-418, N. Bicho, ed., Centro de Estudos de Patrimonio, Departamento de Historia, Arqueologia e Patrimonio, Universidad do Algarve, Faro.

Pinto-Llona, A. C., Clark, G., and Miller, A., 2006, Resultados preliminares de los trabajos en curso en el Abrigo de Sopeña (Onís, Asturias), in *En el centenario de la Cueva de el Castillo: El ocaso de los Neandertales*, 193-207, V. Cabrera, F. Bernaldo de Quirós, and J. M. Maillo, eds., UNED, Santander.

Pinto-Llona, A. C., Clark, G., Miller, A., and Reed, K., 2009, Neanderthals and Cro-Magnons in norther Spain: Ongoing eork at the Sopeña rock-shelter (Asturias, Spain). in *The Mediterranean from 50000 to 25000. Turning points and new directions*, 313-322, M. a. S. Camps, C., ed., Oxbow Books, Oxford.

Pitblado, B., Deheler, C., Neff, H., and Nelson, S., 2008, Pilot Study Experiments Sourcing Quartzite, Gunnison Basin, *Geoarcheology*, **23**(**6**), 741-778.

Pitblado, B. L., Cannon, M. B., Neff, H., Dehler, C. M., and Nelson, S. T., 2012, LA-ICP-MS Analysis of Quartzite from the Upper Gunnison Basin, Colorado, *Journal of Archaeological Science*, **40**, 2196-2216.

Plisson, H., 2007, La fonction des outils de silex dans les grottes orneés paléolithiques, in *Un siécle de construction du dusours scientifique en Préhistoire (Actes du XXVI Congrés Préhisrorique de France*, 125-132, Société Préhistorique Française, Paris.

Polanyi, K., 1957, The economy as instituted process, in *Trade and market in the early empires*, 243-270, K. Polanyi, C. Arensberd, and H. Pearson, eds., Free Press, New York.

Preysler, J. B., Nieto-Márquez, I. O., Navas, C. T., and Cueto, S. B., 2015, Recycling in abundance: Re-use and recycling processes in the Lower and Middle Paleolithic contexts of the central Iberian Peninsula, *Quaternary International*, **361**, 142-154.

Prieto, A., García-Rojas, M., Sánchez, A., Calvo, A., Domínguez-Ballesteros, E., Ordoño, J., and García Collado, M. I., 2016, Stones in Motion: Cost units to understand flint procurement strategies during the Upper Palaeolithic in the south-western Pyrenees using GIS, *Journal of Lithic Studies*, **3**, xx-xx.

Prieto, A., Yusta, I., and Arrizabalaga, A., 2018, Defining and Characterizing Archaeological Quartzite: Sedimentary and Metamorphic Processes in the Lithic Assemblages of El Habario and El Arteu (Cantabrian Mountains, Northern Spain), *Archaeometry*, **0**(**0**).

Pujalte, V., Robles, S., García-Ramos, J. C., and Hernández, J. M., 2004, El Malm-Barremiense no marinos de la Cordillera Cantábrica, in *Geología de España*, 288-291, J. A. Vera, ed., SGE-IGME, Madrid.

Quesada, J. M., and Menéndez, M., 2009, Revisión cronoestratigráfica de la Cueva de la Güelga (Narciandi, Asturias). Del Musteriense al Paleolítico Superior Inicial, *Espacio, Tiempo y Forma. Serie I, Nueva Época. Prehistoria y Arqueología*, **2**, 39-74.

Ramírez del Pozo, J., Portero García, J. M., Olivé Davó, A., Martín Alafont, J. M., and Aguilar Tomás, M. J., 2003, Mapa geológico y Memoria de la Hoja nº33 (Comillas), in *Mapa Geológico de España Escala 1:50.000, MAGNA*, I. Instituto Geológico y Minero de España, ed., IGME, Madrid.

Rasband, W. S., 1997-2016, ImajeJ: Bethesda, Maryland, USA, U.S. National Institutes of Health.

Renfrew, C., 1986, El alba de la civilización: Madrid, Itsmo.

Ríos, J., 2012, Industria lítica y sociedad del Paleolítico medio al superior en torno al Golfo de Bizkaia.

Ríos, J., Garate, D., and Gómez, A., eds., 2013, La cueva de Arlanpe (Lemoa): Ocupaciones humanas desde el Paleolítico Medio Antiguo hasta la Prehistoria Reciente: Kobie, v. 1: Bilbao, Kobie.

Rissetto, J. D., 2009, Late Pleistocene Hunter-Gatherer mobility patterns and lithic exploitation in Eastern Cantabria (Spain), University of New Mexico, Albuquerque.

Rissetto, J. D., 2012, Using Least Cost Path Analysis to Reinterpret Late Upper Paleolithic Hunter-Gatherer Procurement Zones in Northern Spain, in *Least Cost Analysys of Social Landscapes. Archaeological Case Studies*, 11-31, D. A. White, and S. L. Surface-Evans, eds., University of Utah Press, Salt Lake City.

Roberts, R., Flannery, T., Ayliffe, L., Laslett, G., Baynes, A., Smith, M., Jones, R., and Smith, B., 2001, New Ages for the Last Australian Megafauna: Continent-Wide Extinction About 46,000 Years Ago, *Science*, **292**.

Robles, S., 2004, El Pérmico de la Cuenca Vasco-Cantábrica, in *Geología de España*, 269-271, J. A. Vera, ed., SGE-IGME, Madrid.

Robles, S., 2014, Evolución geológica de la Cuenca Vasco-Cantábrica, in *Geología de la Cuenca Vasco-Cantábrica*, 9-104, A. Bodego, M. Mendia, A. Aranburu, and A. Apraiz, eds., Servicio Editorial de la Universidad del País Vasco, Bilbao.

Robles, S., Quesada, S., Rosales, I., Aurell, M., and García-Ramos, J. C., 2004, El jurásico marino de la Cordillera Cantábrica, in *Geología de España*, 279-285, J. A. Vera, ed., SGE-IGME, Madrid.

Rodríguez-Fernández, L. R., 1987, La estratigrafía del Carbonífero y la estructura de la unidad del Pisuerga-Carrión. NO de España, *Cuaderno Laboratoiro Xeoloxico de Laxe*, **12**, 207-229.

Rodríguez Asensio, J. A., and Barrera Logares, J. M., 2012, Las ocupaciones solutrenses de las cuevas de la Lluera, *Excavaciones Arqueológicas en Asturias 2007-2012*, 87-108.

Rodríguez Fernández, L. R., 1992, Estratigrafía y Estructura de la región de Fuentes Carriones y áreas adyacentes, Universidad de Oviedo, Oviedo, 244 p.

Rodríguez Fernández, L. R., Heredia, N., Navarro, D., Martínez, E., and Marquínez, J., 2003, Mapa geológico y Memoria de la Hoja nº81 (Potes), in *Mapa Geológico de España Escala 1:50.000, MAGNA*, I. Instituto Geológico y Minero de España, ed., IGME, Madrid.

Roebroeks, W., 1988, From find scatters to early hominid behaviour: a study of Middle Palaeolithic riverside sttlements at Maastrich-Belvédere (The Neanderlands): Leiden, Sidestone Press.

Roy, M., Mora, R., Plasencia, F. J., Martínez-Moreno, J., and Benito-Calvo, A., 2017, Quartzite selection in fluvial deposits: The N12 level of Roca dels Bous (Middle Palaeolithic, southeastern Pyrenees), *Quaternary International*, **435**, 49-60.

Sánchez, A., Domínguez-Ballesteros, E., García-Rojas, M., Prieto, A., Calvo, A., and Ordoño, J., 2016, Patrones de aprovisionamiento de sílex de las comunidades superopaleolíticas del Pirineo occidental: el "coste" como medida de análisis a partir de los SIG, *Munibe*, **67**, 235-252.

Sanguino, J., and Montes, R., 2005, Nuevos datos para el conocimiento del Paleolítico medio en el centro de la Región Cantábrica: La Cueva de Covalejos, in *Actas de la reunión científica: Neandertales cantábricos, estado de la cuestión. Celebrada en el Museo de Altamira los días 20-22 de Octubre de 2004*, 489-504, R. Montes, and J. A. Lasheras, eds., Monografías del Museo Nacional y Centro de Investigación de Altamira, **20**, Ministerio de Educación y Cultura, Madrid.

Santamaría, D., 2012, La transición del Paleolítico medio al superior en Asturias. El abrigo de La Viña (Oviedo, Asturias) y la cueva de El Sidrón (Borines, Piloña), Servicio de Publicaciones de la Universidad de Oviedo.

Santonja, M., 1986, Valgande (Puebla de Yeltes, Salamanca). Área de talla y sitio de ocupación de Paleolítico medio, *Numantia*, **2**, 33-87.

Sarabia, P., 1993, Las estrategias de aprovisionamiento de materias primas líticas en la transición del Paleolítico medio-superior en Cantabria, in *Actas del XXII Congreso Nacional de Arqueología*, 357-366, Vigo.

Sarabia, P., 1999, Notas sobre los modelos de aprovisionamiento de materioas primas líticas en el Paleolítico superior de Cueva Morín, *Sautuola: Revista del Instituto de Prehistoria y Arqueología*, **6**, 145-154.

Sarabia, P., 2000, Aprovechamiento y utilización de las materias primas líticas en los tecnocomplejos del Paleolítico en Cantabria, Universidad de Santander, Santander.

Schmidt, I., 2013, Solutrean Points of the Iberian Peninsula. Tool making and using behavior of hunter-gatherers during the Last Glacial Maximum.

Schneider, C. A., Rasband, W. S., and Eliceiri, K. W., 2012, NIH Imagen to ImageJ: 25 years of image analysis, *Nature methods*, **9**(**7**), 671-675.

Séronie-Vivien, M., and Séronie-Vivien, M.-R., 1987, Les silex du Mésozoïque nord-aquitain. Approche géologique de l'étude des silex pour servir à la recherche préhistorique, *Bulletin de la Société Linnéenne de Bordeaux*, **Suppl. XV**, 136.

Sieveking, G., Bush, P., Ferguson, J., Craddock, P. T., Hughes, M. J., and Cowell, M. R., 1972, Prehistoric flint mines and their identication as sources of raw material, *Archaeometry*, **14**(**2**), 151-176.

Simonet, R., 1981, Carte des gîtes à silex des Pré-Pyrénées, in *Congrés Préhistorique de France*, 308-323, Quercy.

Skolnick, H., 1965, The quarzite problem, *Journal of Sedimentary Petrology*, **35**(**1**), 12-21.

Soto, A., 2014, Producción y gestión de la industria lítica de Atxoste (Álava): Una aproximación a las sociedades epipaleolíticas y mesolíticas del Alto Ebro, Universidad del País Vasco-Euskal Herriko Unibertsitatea, Vitoria-Gasteiz, 1024 p.

Soto, M., Gómez de Soler, B., and Vallverdú, J., 2017, The chert abundance ratio (CAR): a new parameter for interpreting Palaeolithic raw material procurement, *Archaeological and Anthropological Sciences*.

Steffen, W., Grinevald, J., Crutzen, P., and McNeill, J., 2011, The Anthropocene: conceptual and historical perspectives, *Philosophical Transactions of the Royal Society A: Mathematical, Physical and Engineering Sciences*, **369**(**1938**), 842-867.

Stipp, M., Stünitz, H., Heilbronner, R., and Schmid, S. M., 2002a, Dynamic recrystallization of quartz: Correlation between natural and experimental conditions, *Geological Society London Special Publications*, **200**, 171-190.

Stipp, M., Stünitz, H., Heilbronner, R., and Schmid, S. M., 2002b, The eastern Tonale fault zone: A 'natural laboratory' for crystal plastic deformation of quartz over a temperature range from 250 to 700 °C, *Journal of Structural Geology*, **24**(**12**), 1861-1884.

Straus, L., 1975, El Solutrense de las cuevas del Castillo y Hornos de la Peña (Santander) en el Museo Arqueológico Nacional de Madrid, *Trabajos de Prehistoria*, **32**, 9-19.

Straus, L., 1983, El Solutrense vasco-cantábrico, una nueva perspectiva: Monografías del Museo Nacional y Centro de Investigación de Altamira: Madrid, Ministerio de Educación y Cultura.

Straus, L., 1992, Iberia before the Iberians. The Stone Age Prehistory of Cantabrian Spain: Albuquerque, University of New Mexico Press.

Straus, L., 2001, Solutrean, in *Encyclopedia of Prehistory*, 238-250, P. Peregrine, and M. Ember, eds., Kluwer Academic/Plenum, New York.

Straus, L., 2005, A mosaic of change: the Middle–Upper Paleolithic transition as viewed from New Mexico and Iberia, *Quaternary International*, **137**, 47-67.

Straus, L., 2010, The emergence of modern-like forager capacities & behaviors in Africa and Europe: Abrupt or gradual, biological or demographic?, *Quaternary International*, **30**, 1-8.

Straus, L., 2012, El Solutrense: 40 años de reflexiones por un aqueólogo norteamericano, *Espacio, Tiempo y Forma, Serie I, nueva época Prehistoria y Arqueología*, **5**, 27-36.

Straus, L., and Clark, G., 1986, La Riera Cave, Stone Age hunter-gatherer adaptations in northern Spain: Anthropological Research Papers, v. 36: Arizona, Arizona State University.

Stringer, C., Pälike, H., Van Andel, T., Huntley, B., Valdes, P., and Allen, R. M., 2003, Climatic Stress and the Extinction of the Neanderthals, in *Neanderthals and modern humans in the European landscape during the last glaciation*, 233-240, T. van Andel, and W. Davies, eds., MacDonald Institute for Archaeological Research, Oxford.

Sussanman, C., 1985, Micro-wear on Quartz: fact or fiction?, *World Archaeology*, **28**(**2**), 101-111.

Tarriño, A., 1998, Rocas silíceas sedimentarias. Su composición mineralógica y terminología, *KREI*, **3**, 143-161.

Tarriño, A., 2000, Estudio de la procedencia de los sílex recuperados en el yacimiento de Labeko Koba (Arrasate, País Vasco), *Munibe*, **52**, 345-354.

Tarriño, A., 2006, El sílex en la cuenca vasco-cantábrica y Pirineo navarro: caracterización y su aprovechamiento en la Prehistoria: Monografías del Museo Nacional y Centro de Investigación de Altamira: Madrid, Minesterio de Educación y Cultura.

Tarriño, A., 2011a, Procedencia de los sílex de la cueva de Aitzbitarte-III (Rentería, Gipuzkoa), in *Ocupaciones humanas en Aitzbitarte III (País Vasco) 33.600-18.400 BP*, 353-373, J. Altuna, K. Mariezkurrena, and J. Ríos, eds., EKOB Euskal Kultura Ondare Bilduma, Vitoria-Gasteiz.

Tarriño, A., 2011b, Procedencia de los sílex de la industria lítica del yacimiento en cueva de Santimamiñe, in *La cueva de Santimamiñe: Revisión y actualización (2004-2006)*, 281-290, J. C. López Quintana, ed., Diputación Foral de Bizkaia, Bilbao.

Tarriño, A., 2015, A New Methodology and Classification System for Describing Three-Dimensional Particle Formats: Application to Clastic Lithic Products of Archaeological and Geological Origin, *Archaeometry*, 928-948.

Tarriño, A., and Aguirre, M., 1997, Datos preliminares sobre fuentes de aprovisionamiento de rocas silíceas en algunos yacimientos paleolíticos y postpaleolíticos del sector oriental de la cuenca vasco-cantábrica, *Veleia*, **14**, 101-116.

Tarriño, A., Bon, F., and Normand, C., 2007a, Disponibilidad del Sílex como materia prima en la Prehistoria del Pirineo occidental, in *Frontières culturelles dans les Pyrénées préhistoriques*, 103-123, N. Cazals, J. González Urquijo, and X. Terradas, eds., PubliCan-Ediciones de la Universidad de Cantabria, Cantabria.

Tarriño, A., Cava, A., and Barandiarán, I., 2013a, Recursos líticos en las industrias del Solutrense Cantábrico : El caso de Altamira (Cantabria, España), *Revue Archéologique du Centre de la France* **21**, 261-272.

Tarriño, A., Duarte, E., Santamaría, D., Martínez, L., Fernández de la Vega, J., Suárez, P., Rodríguez, V., Forcelledo, E., and De la Rasilla, M., 2013b, El sílex de Piloña. Caracterización de una nueva fuente de materia prima lítica en la Prehistoria de Asturias, in *F. Javier Fortea Pérez. Universitatis Ovetensis Magister. Estudios en homenaje*, 115-132, M. de la Rasilla, ed., Universidad de Oviedo/Ménsula Ed., Oviedo.

Tarriño, A., Elorrieta, I., and García-Rojas, M., 2015, Flint as raw material in prehistoric times: Cantabrian Mountain and Western Pyrenees data, *Quaternary International*, **364**, 94-108.

Tarriño, A., Elorrieta, I., García-Rojas, M., and Sánchez, A., 2014, Neolithic flint mines of Treviño (Basque-Cantabrian Basin, Western Pyrenees, Spain), *Journal of Lithic Studies*, **1**(**1**), 129-147.

Tarriño, A., Lobo, P. J., García-Rojos, M., Elorrieta, I., Orue, I., Benito-Calvo, A., and Karampanglidis, T., 2011, Introducción al estudio de las minas neolíticas de sílex de la Sierra de Araico (Condado de Treviño): Campaña de excavación del 2011, *Estudios de Arqueología Alavesa*, **27**, 7-48.

Tarriño, A., and Normand, C., 2002, Procedencia de los restos líticos en el Auriñaciense antiguo (C 4b1) de Isturitz (Pyrénées-Atlantiques, Francia), *Espacio, Tiempo y Forma, Serie I, nueva época Prehistoria y Arqueología*, **15**, 135-143.

Tarriño, A., Olivares, M., Etxebarria, N., Baceta, J. I., Larrasoaña, J., Yusta, I., Pizarro, J., Cava, A., Barandiarán, I., and Murelaga, X., 2007b, El sílex de tipo "Urbasa": Caracterización petrológica y geoquímica de un marcador litológico en yacimientos arqueológicos del Suroeste europeo durante el Pleistoceno superior y Holoceno inicial, *Geogaceta*, **43**, 127-130.

Tarriño, A., Yusta, I., and Aguirre, M., 1998, Indicios de circulación a larga distancia de sílex en el Pleistoceno superior. Datos petrográficos y geoquímicos de materiales arqueológicos de Antoliñako Koba, *Boletín de la Sociedad Española de Mineralogía*, **21-A**, 200-201.

Terradas, X., 1995, Las estrategias de gestión de los recursos líticos del Prepirineo catalán en el IX milenio BP: El asentamiento prehistórico de la Font del Ros (Berga, Barcelona), *Treballs d'arqueologia*, **3**.

Terradas, X., 2002, La gestión de los recursos minerales en las sociedades cazadoras-recolectoras, *Treballs D´Etnoarqueologia*, **4**.

Terradas, X., and Ortega, D., 2017, Flint quarrying in north-eastern Iberia: quarry sites and the initial transformation of raw material, *Antiquity*, **91**(**359, e5**), 1-6.

Tobler, W., 1993, Three presentations on geographical analysis and modeling, in *Technical Report 93-1. National Center for Geographic Information and Analysis*, **15/12/2014**, http://www.ncgia.ucsb.edu/Publications/Tech_Reports/93/93-1.PDF.

Turq, A., 1989, Exploitation des matières premières lithiques et esploitation des sols_ l' exemple du Moustérien entre Dordogne et Lot, in *INQUA: Colloque du comité français de l'Union internationale pour l'étude du quaternaire. Variations des paléo-milieux et peuplement préhistorique*, 179-2014, H. Laville, ed., Cahiers du Quaternaire, CNRS, Bordeaux.

Turq, A., 1996, L'approvisionnement en matiere premiere lithique au Mousterien et au début du Paléolithique supérieur dans le nord est du bassin aquitain: Continuité ou discontinuité, in *The Last Neandertals The First Anatomically Modern Humans*, 355-362, E. Carbonell, and M. Vaquero, eds., Fundació catalana per a la recerca.

Turq, A., Faivre, J.-P., Gravina, B., and Bourguignon, L., 2017, Building models of Neanderthal territories from raw material transports in the Aquitaine Basin (southwestern France), *Quaternary International*, **433, Part B**, 88-101.

Turq, A., Roebroeks, W., Bourguignon, L., and Faivre, J.-P., 2013, The fragmented character of Middle Palaeolithic stone tool technology, *Journal of Human Evolution*, **65**(**5**), 641-655.

Uzquiano, P., Yravedra, J., Zapata, B. R., Gil Garcia, M. J., Sesé, C., and Baena, J., 2012, Human behaviour and adaptations to MIS 3 environmental trends (>53–30 ka BP) at Esquilleu cave (Cantabria, northern Spain), *Quaternary International*, **252**, 82-89.

Vagle, G. B., Hurst, A., and Dypvik, H., 1994, Origin of quartz cements in some sandstone from the Jurassic of the Inner Moray Firth (UK), *Sedimentology*, **41**, 363-377.

Valín, M. L., García-López, S., Brime, C., Bastida, F., and Aller, J., 2016, Tectonothermal evolution in the core of an arcuate fold and thrust belt: the south-eastern sector of the Cantabrian Zone (Variscan belt, north-western Spain), *Solid Earth*, **7**, 1003-1022.

Vaquero, M., and Romagnoli, F., 2017, Searching for Lazy People: the Significance of Expedient Behavior in the Interpretation of Paleolithic Assemblages, *Journal of Archaeological Method and Theory*.

Veldeman, I., Baele, J. M., Goemaere, E., Deceukelaire, M., Dusar, M., and De Doncker, H., 2012, Characterizing the hypersiliceous rocks of Belgium used in (pre-)history: a case study on sourcing sedimentary quartzites, *Journal of Geophysics and Engineering*, **9**, 118-128.

Vita-Finzi, C., 1978, Archaeological sites in their setting: Ancient peoples and places: London, Thames & Hudson.

Wallerstein, I., 1974, The Modern World-System, vol. I: Capitalist Agriculture and the Origins of the European World-Economy in the Sixteenth Century: New York/London, Academic Press.

Wallerstein, I., 1979, The Capitalist World-Economy: Cambridge, Cambridge University Press.

Wallerstein, I., 1980, The Modern World-System, vol. II: Mercantilism and the Consolidation of the European World-Economy, 1600-1750: New York, Academic Press.

Waters, C. N., Zalasiewicz, J., Summerhayes, C., Barnosky, A. D., Poirier, C., Gałuszka, A., Cearreta, A., Edgeworth, M., Ellis, E. C., Ellis, M., Jeandel, C., Leinfelder, R., McNeill, J. R., Richter, D. d., Steffen, W., Syvitski, J., Vidas, D., Wagreich, M., Williams, M., Zhisheng, A., Grinevald, J., Odada, E., Oreskes, N., and Wolfe, A. P., 2016, The Anthropocene is functionally and stratigraphically distinct from the Holocene, *Science*, **351**(**6269**).

Weibel, R., Friis, H., Kazerouni, A. M., Svendsen, J. B., Stokkendal, J., and Poulsen, M. L. K., 2010, Development of early diagenetic silica and quartz morphologies — Examples from the Siri Canyon, Danish North Sea, *Sedimentary Geology*, **228**(**3**), 151-170.

Wentworth, C. K., 1922, A scale of grade and class terms for clastic sediments, *Journal of Geology*, **30**, 377-392.

Wilson, C. J. L., 1973, The prograde microfabric in a deformed quartzite sequence, Mount Isa, Australia, *Tectonophysics*, **19**(**1**), 39-81.

Winterhalder, B., and Smith, E. A., 2000, Analyzing adaptive strategies: Human behavioral ecology at twenty-five, *Evolutionary Anthropology: Issues, News, and Reviews*, **9**(**2**), 51-72.

Winterscheid, H., and Kvaček, Z., 2016, Late Oligocene macrofloras from fluviatile siliciclastic facies of the Köln Formation at the south-eastern border of the Lower Rhine Embayment (North Rhine-Westphalia, Germany), *Acta paleobotánica*, **56**(**1**), 4-64.

Worden, R. H., French, M. W., and Mariani, E., 2012, Amorphous silica nanofilms result in growth of misoriented microcrystalline quartz cement maintaining porosity in deeply buried sandstones, *Geology*, **40**(**2**), 179-182.

Yardley, B. W. D., Mackenzie, W. S., and Guilford, C., 1990, Atlas of metamorphic rocks and their textures: Essex, Longman Scientific & Technical.

Yravedra, J., Álvarez-Alonso, D., Estaca-Gómez, V., López-Cisneros, P., Arrizabalaga, A., Elorza, M., Iriarte, M. J., Jordá, J. F., Sesé, C., and Uzquiano, P., 2016, New evidence of bones used as fuel in the Gravettian level at Coímbre cave, northern Iberia Peninsula, *Archaeological and Anthropological Sciences*, **9**, 16.

Yravedra, J., Baena, J., Arrizabalaga, A., and Iriarte, M. J., 2005, El empleo de material óseo como combustible durante el Paleolítico Medio y Superior en el Cantábrico. Observaciones experimentales, in *Actas de la reunión científica: Neandertales cantábricos, estado de la cuestión. Celebrada en el Museo de Altamira los días 20-22 de Octubre de 2004*, 369-383, R. Montes, and J. A. Lasheras, eds., Monografías del Museo Nacional y Centro de Investigación de Altamira, Ministerio de Cultura, Madrid.

Yravedra, J., and Gómez-Castanedo, A., 2014, Taphonomic implications for the Late Mousterian of South-West Europe at Esquilleu Cave (Spain), *Quaternary International*, **337**, 225-236.

Yravedra, J., and Uzquiano, P., 2013, Burnt bone assemblages from El Esquilleu cave (Cantabria, Northern Spain): deliberate use for fuel or systematic disposal of organic waste?, *Quaternary Science Reviews*, **68**, 175-190.

Zilhao, J., 2000, The Ebro Frontier: a model for the late extinction of Iberian Neanderthals, in *Neanderthals on the edge: 150th anniversary conference of Forbes' Quarry discovery, Gibraltar*, 111-121, C. Stringer, R. Barton, and C. Finlayson, eds., Oxbow Books, Oxford.

Zilhao, J., 2006, Genes, fossils and culture. An overview of the evidence for Neandertal-Modern human interaction and admixture, *Procceding of the Prehistory Society*, **72**, 1-20.

Zilhao, J., and D'Errico, F., 1999, The Chronology and Taphonomy of the Earliest Aurignacian and Its Implications for the Understanding of Neandertal Extinction, *Journal of World Prehistory*, **13**(**1**), 1-68.

RESUMEN

El estudio que plasmamos en esta tesis doctoral, tiene por objetivo general conocer los comportamientos de captación, distribución y gestión de la cuarcita por parte de las comunidades humanas que habitaron la Región Cantábrica entre el Paleolítico medio y el Paleolítico superior. Consideramos que este trabajo puede aportar nuevas perspectivas para entendernos hoy como humanos en el cambiante medio ambiente que nosotros estamos modificando (Bocherens, 2018; Crutzen, 2002; Crutzen and Stoermer, 2000; Steffen et al., 2011; Waters et al., 2016) y que tiene su génesis más remota en los comportamientos y los memes (Dawkins, 2002) que le permitieron a nuestra especie la expansión por todos las latitudes de la tierra, excepto en la Antártida.

Para ello, nos serviremos de un doble enfoque metodológico y que combina el método hipotético-deductivo y el método inductivo-deductivo. El primero, parte del análisis histórico de las sociedades del Paleolítico como sujeto de estudio para entender las sociedades del presente. El enfoque aportado en este trabajo tiene un componente eminentemente económico y este se plantea a partir de la captación, gestión y distribución de las materias primas líticas aplicando una visión socio-económica. Hemos utilizado conceptos de diferentes escuelas metodológicas como la arqueología procesualista a partir de los Site Catchment analysis (Binford, 1982, 1983; Butzer, 1989; Kelly, 1992; Kelly, 1995; Vita-Finzi, 1978), la escuela de la Human Behavioural Ecology (Borgerhoff Mulder and Schacht, 2012; Cronk, 1991; Hames, 2001; Winterhalder and Smith, 2000), la Chaîne opératoire (Leroi-Gourhan, 1964) o conceptos derivados de la Tipología Analítica (Fernández Eraso and García-Rojas, 2013; Laplace, 1972, 1987). El segundo, el método inductivo-deductivo está claramente presente en esta investigación a partir de la selección de el objeto de estudio, la cuarcita y con el tratamiento de los datos que se realizan en esta tesis. Partiendo del objeto estático tratamos de conocer las fuerzas y dinámicas que lo generan: Materia/->Fuerza (Feynman, 2015; Kropotkin, 2015). Caracteres petrológicos + Caracteres tecno-tipológicos + Caracterización geográfica /-> Adquisición, gestión y distribución de la cuarcita.

El estudio de las materias primas líticas sobre las que se fabricaron las herramientas prehistóricas es un tema de investigación que ha formado parte de la Arqueología prehistórica desde sus inicios como disciplina científica. Desde finales del siglo XIX, los primeros

prehistoriadores, en muchas ocasiones geólogos de formación, ya realizaban descripciones de las rocas utilizadas por las sociedades prehistóricas. Estas caracterizaciones comienzan a ser cada vez más precisas a partir de los años 50 y 60 del siglo pasado. Estas primeras investigaciones, focalizadas en la obsidiana, permitieron trazar rutas de intercambio de materiales líticos a través del Mediterráneo durante la Prehistoria Reciente. Los llamativos resultados obtenidos en estos trabajos y las mejoras técnicas para la caracterización del material pétreo generaron un aumento de los estudios tanto a nivel cuantitativo como cualitativo durante la década de los 70. Durante los últimos 20 años del siglo XX, los estudios petrológicos sobre las industrias líticas se ampliaron a nivel geográfico y cronológico, aumentando igualmente los tipos de materiales estudiados. Para cronologías paleolíticas, el sílex se ha convertido, sin duda, en la materia prima lítica más estudiada. Complementariamente, la multiplicación de las investigaciones enfocadas al conocimiento de las dinámicas económicas y sociales de las sociedades paleolíticas a partir del análisis tecno-tipológico de la industria lítica, ha permitido entender los complejos mecanismos de adquisición y gestión de esta materia prima. El cambio de milenio supuso la incorporación de nuevas tecnologías, como por ejemplo los Sistemas de Información Geográfica (SIG), que permiten un acercamiento más eficaz a la complejidad económica y social de las sociedades paleolíticas articulada en base a la adquisición y distribución del sílex. Todo ello nos está permitiendo entender y delimitar territorios económicos complejos, así como su articulación a partir de la movilidad humana.

La cuarcita, a pesar de ser la segunda materia prima lítica más empleada durante el Paleolítico en Europa, no ha sido objeto del mismo desarrollo metodológico que la obsidiana o el sílex, como evidencian los escasos y recientes trabajos geo-arqueológicos focalizados al conocimiento de este material (Blomme et al., 2012; Cnudde et al., 2013; Pedergnana et al., 2017; Pitblado et al., 2008; Pitblado et al., 2012; Prieto et al., 2018; Roy et al., 2017; Veldeman et al., 2012). Ello ha generado un vacío científico y un sesgo en el conocimiento de las estrategias de adquisición, distribución y gestión de las materias primas líticas (Arrizabalaga, 2010). Este déficit se puede entender a partir de tres ejes interrelacionados. El primero, de carácter geográfico, evidencia que la distribución de los afloramientos rocosos genera una pérdida de información en las zonas con amplia distribución de cuarcitas. El segundo, de carácter crono-cultural, pone de manifiesto la escasez de datos para periodos históricos en los que el sílex o la obsidiana no son cuantitativamente importantes o no están representados. El tercer eje hace referencia a la pérdida de información a nivel interpretativo, consecuencia de la sobrerrepresentación de la información disponible sobre el sílex y la obsidiana, generalmente relacionadas con la movilidad geográfica de larga distancia. Esto impide entender los complejos mecanismos de adquisición, gestión y distribución dentro de zonas económicas más restringidas y, por tanto, los territorios económicos cotidianos de las sociedades prehistóricas. Estas razones han influido en la seleción de la zona de estudio, los valles del Deva, Cares y Güeña y una selección de yacimientos, principalmente con cronologías correspondientes al Paleolítico medio y al Paleolítico superior. Los yacimientos analizados son El Esquilleu, el Habario, El Arteu, La Cueva de Coimbre y la Cueva con arte parietal de la Covaciella. Además, y con la finalidad de entender la variabilidad de las cuarcitas en contextos aqueológicos, hemos analizado las cuarcitas del yacimiento alemán de *Ravensberg-Troisdorf*.

Este trabajo se estructura en cuatro partes diferenciadas y que se articulan a partir de un sistema de escalas que parten de lo más amplio hacia lo más pequeño, para realizar un camino de vuelta que asciende desde las ideas más básicas hasta las más complejas. La primera de las partes está conformada por el capítulo introductorio y los tres siguientes, correspondientes a métodos y materiales. En este primer bloque planteamos la metodología utilizada en este trabajo a partir de una cuestión de escala y enfoque, desde lo más amplio hasta lo más pequeño. La segunda de las partes cambia esta relación y lanza desde lo concreto y minúsculo, un grano de cuarzo, una mayor complejidad de conceptos, hasta entender la dispersión de las cuarcitas a través del ciclo de las rocas. Esta parte corresponde con los dos primeros capítulos de resultados y que sientan las bases para el análisis de los materiales arqueológicos que compone el tercer bloque de este trabajo. El último,

presenta los resultados obtenidos de la caracterización de la cuarcita desde un punto de vista geo-arqueológico y tecno-tipológico de las ocho colecciones líticas analizadas en los siguientes siete capítulos de esta tesis, ampliando más si cabe esta jerarquía de conceptos. Finalmente, la cuarta parte de este trabajo corresponde a la discusión y las conclusiones del mismo. En este último bloque hemos evaluado la metodología, los resultados y las conclusiones aportadas a partir de la comparación con otros trabajos.

Tres son los principales aportes que presenta este trabajo. El primero es de carácter metodológico, y plantea una metodología fundacional para el estudio de las cuarcitas en contextos arqueológicos. El segundo es de tipo material y está relacionado con la caracterización y definición formal de la cuarcita en contextos arqueológicos. El tercero es de tipo histórico y está orientado hacia la mayor y mejor comprensión de los mecanismos de adquisición, gestión y distribución de las cuarcitas por las sociedades paleolíticas.

El primero y consideramos el más importante, teniendo en cuenta el estado actual en las investigaciones sobre las materias primas líticas utilizadas por los seres humanos prehistóricos, es el aporte metodológico. En este trabajo de investigación hemos caracterizado y definido la cuarcita en contextos arqueológicos a partir de sus características físicas. Para ello, hemos planteado una metodología que se articula a partir de tres niveles de profundidad: la escala microscópica, la macroscópica y finalmente el estudio regional a gran escala.

La primera está basada en el análisis petrográfico del material cuarcítico. A partir de éste, hemos caracterizado las texturas que forman los granos de cuarzo, su empaquetamiento y hemos detectado las características de estos pequeños objetos que nos permiten la definición y el estudio de las cuarcitas en contextos arqueológicos. Asimismo, la aplicación de técnicas de análisis digital de imagen sobre las fotografías microscópicas de las láminas delgadas nos ha posibilitado conocer los tamaños, las morfologías y las orientaciones de los granos de cuarzo que componen masivamente la cuarcita. Finalmente, y también a partir de la petrografía, hemos detectado los minerales, matrices y cementos que, adicionalmente a la matriz principal de granos de cuarzo, componen la cuarcita. El establecimiento de tipos petrogenéticos que agrupan buena parte de las características previamente comentadas y de variedades específicas es, sin duda, uno de los aportes más interesantes de este trabajo, pues plantea las bases para desarrollar futuros trabajos. Finalmente, el reflejo de los tipos petrogenéticos y variedades granulométricas y mineralógicas de las cuarcitas mediante la observación microscópica no-destructiva, supone otro de los aportes más interesantes de esta tesis. Finalmente, este trabajo aporta un corpus de datos ilustrado con fotografías de láminas delgadas y fotografías de las superficies de las cuarcitas con un alto detalle que permitirá seguir trabajando en la caracterización de las cuarcitas en la Cornisa Cantábrica y otras zonas.

La metodología utilizada para entender la realidad visible a partir de una escala macroscópica, a pesar de ser útil para este trabajo, no ha supuesto la novedad que ha aportado la escala microscópica. A pesar de ello, este enfoque nos ha permitido establecer criterios de análisis con los que conocer, por un lado los potenciales contextos de captación de la cuarcita; por otro, los mecanismos de gestión de la materia prima lítica. La descripción de los puntos prospectados a partir de los criterios de análisis especificados en los capítulos tres y cuatro, nos ha permitido entender los contextos geológicos, pero también imaginar los procesos de adquisición de materia prima por parte de los humanos prehistóricos. Por su parte, los criterios de análisis de la industria lítica seleccionados, principalmente desde la Tipología Analítica, nos ha permitido conocer los mecanismos de gestión de la cuarcita, especialmente aquellos relacionados con su explotación.

Finalmente, la metodología utilizada para analizar la zona de estudio a escala regional ha permitido entender espacialmente la distribución de las cuarcitas de la zona de estudio, ha agilizado e implementado las prospecciones y ha posibilitado la delimitación de la zona

de estudio. Somos conscientes que ninguno de los aportes específicos e individuales es novedoso, pero su aplicación en trabajos geo-arqueológicos en la Región Cantábrica de forma global sí lo es. Por otro lado, la aplicación de la metodología que nos permite entender la movilidad humana a partir de la relación entre la distancia y el relieve, nos ha permitido cuantificar de forma más precisa el esfuerzo requerido para llegar de un punto a otro así como la detección de zonas de tránsito preferencial. La aplicación de esta metodología es igualmente novedosa en la Región Cantábrica, excluyendo los trabajos realizados por mí y otros miembros del Departamento de Geografía, Prehistoria y Arqueología de la Universidad del País Vasco.

El segundo aporte más interesante de este trabajo se relaciona con la definición formal del material: La cuarcita en contextos arqueológicos. La escasa bibliografía científica que ha tratado esta roca desde perspectivas geo-arqueológicas no ha llegado a profundizar en la definición formal del material de una forma similar a la aportada en este trabajo o no han establecido los tipos que permitan entender la gran variabilidad que el término cuarcita abarca. En este trabajo hemos definido la cuarcita a partir de sus características físicas, estableciendo un sistema de siete tipos petrogenéticos agrupados en categorías más amplias, los grupos genéticos. Adicionalmente hemos establecido variedades basadas en el tamaño y la distribución de los granos de cuarzo que componen masivamente la cuarcita. La caracterización de este material a partir de su mineralogía y su reflejo en la coloración de cada una de ellas también ha sido analizada y nos ha permitido establecer nuevas variedades. Todos estos datos nos han permitido caracterizar el petrolito original, los procesos de consolidación, deformación y/o recristalización metamórfica y los aportes minerales post-deposicionales. El conocimiento adquirido del material nos ha permitido entender también ciertas actitudes que los seres humanos del Paleolítico realizaban, como la selección preferencial de tipos y variedades, la gestión diferencial de las mismas o la talla controlada para el aprovechamiento de ciertos tipos y variedades.

Dentro de este mismo aporte, también hemos entendido la disposición y la localización de la Cuarcita en la zona centro-occidental de la Región Cantábrica. Hemos definido los pocos afloramientos masivos de cuarcita, los conglomerados en los que encontramos estas rocas y las formaciones cuaternarias en las que se han depositado. Esto nos ha permitido entender el ciclo de esta roca, observando el largo recorrido del material hasta que es captado por las sociedades prehistóricas. Este aporte es igualmente novedoso y supone el establecimiento de un primer corpus de datos que permitirá abordar diferentes investigaciones en la Región Cantábrica.

El último aporte de relevancia planteado en este trabajo está relacionado con las conclusiones obtenidas en un plano histórico. Por un lado, hemos inferido procesos de captación de materias primas líticas, especialmente de cuarcitas, en afloramientos masivos, conglomerados y depósitos secundarios, proponiendo la existencia de yacimientos arqueológicos hasta ahora no excavados e imaginando las actividades que allí se realizaban. Dentro de estas, hemos planteado la captación de recursos a partir de la extracción de rocas directamente del afloramiento o el conglomerado. Hemos propuesto la recolección de clastos en las zonas adyacentes a los estratos geológicos con presencia de cuarcitas. Hemos observado la selección de litologías específicas y hemos caracterizado la intensidad de la actividad. Finalmente, hemos observado la creación de stocks de masas líticas para futuros usos. Por otro lado, en este trabajo hemos planteado la funcionalidad de cada sitio a partir de los comportamientos de gestión de la cuarcita y otras materias primas líticas. Hemos sido capaces de individualizar cadenas operativas líticas que muestran desde procesos de talla completos hasta procesos fragmentados en el tiempo y en el espacio. Hemos individualizado procesos de creación y reparación de tool-kit, hemos observado comportamientos expeditivos para la realización de actividades, y hemos observado la gestión diferencial de cada uno de los tipos y variedades analizadas. Finalmente, hemos observado la distribución de las cuarcitas por el territorio y hemos inferido los esfuerzos necesarios para su acopio, identificando zonas de paso preferentes frente a otras y el aprovechamiento de forma extensiva e intensiva de las zonas transitadas.

Todos estos datos nos han permitido evidenciar la existencia, especialmente en el Paleolítico medio, de redes de yacimientos que explotaban de forma sistemática y eficaz el heterogéneo medio ambiente presente en la zona. Igualmente, hemos observado las modificaciones de esta red de yacimientos así como los cambios en las estrategias de adquisición, gestión y distribución de recursos. Esto se hace especialmente relevante al observar las diferencias entre el Paleolítico medio y el Paleolítico superior. En el primer periodo observamos una explotación del medio ambiente a través de los múltiples biotopos, mientras que en el segundo, no hemos sido capaces de observar la amplitud de esta red, y por tanto, los biotopos explotados son menos y geográficamente más restringidos. A pesar de ello, la explotación de estos reducidos biotopos es más intensiva que en el Paleolítico medio. En el Paleolítico superior, hemos planteado la existencia de una movilidad supra-regional no detectada en las sociedades que habitaban esta región en el Paleolítico Medio. Finalmente, la movilidad observada en último periodo comentado relaciona las zonas de coste al Norte con las zonas amesetadas del Sur a través de recorridos por los fondos de los valles y de rutas en zonas de media montaña con relieves poco marcados. La movilidad supra-regional del Paleolítico superior posiblemente tenga una dirección Este-Oeste a través de los corredores paralelos a la actual línea de costa.

Todo ello, nos ha permitido tener un mejor conocimiento acerca de la relación entre el Medio Ambiente y los seres humanos que en el Paleolítico poblaron la región, planteando interesantes reflexiones para entendernos como especie en el presente.

ABSTRACT

The main aim of the this thesis is to understand the acquisition, distribution and management mechanisms implemented by Palaeolithic societies in the Cantabrian Region in order to exploit quartzite as a raw material. Due to the scarcity of previous research on the properties of this raw material, we characterised quartzite from the geo-archaeological point of view in this Region.

The methodology proposed combines three different approaches: microscopic, macroscopic and regional scales. The first one is based on petrographic, geochemical and binocular characterisation. The second one is the macroscopic approach and it is founded on the analysis of lithic assemblages based on technological, typological, petrological and metric criteria. The same macroscopic approach is used to characterise potential raw material acquisition areas through the geological survey of the geological strata and deposits where quartzites are present. Finally, the regional scale is based on the geographic, geologic and archaeological analysis of landscape using Geographic Information Systems.

The application of this comprehensive methodology to a narrow area, the Deva, Cares and Güeña valleys, allow us to understand quartzite from geological and archaeological perspectives. On one hand, we were able to understand the original source area of the sediment which formed quartzites, their transformations due to sedimentary and metamorphic forces, and the embedded minerals incorporated from the different geological environments where quartzites have been. The understanding of all these phenomena allows us to classify quartzite into seven petrogenetic types and varieties, according to grain size and mineral inclusions. We also describe the geological strata where quartzite is present, characterising both their arrangement and its dispersion based on the types and varieties defined.

On the other hand, we inferred the acquisition, management, and mobility patterns of Prehistoric societies in the Deva, Cares and Güeña valleys during the Middle and Upper Palaeolithics based on the analysis of the lithic assemblages from layers XI, XIII and XXII from El Esquilleu rockshelter, layer Co.B.6 from Coimbre cave, the sites of El Habario and El Arteu and the Cave Art of La Covaciella. This allowed us to understand the different strategies of landscape management of such a heterogeneous and mountainous area as the central Cantabrian Region. Finally, we include the analysis of the lithic assemblage from the German site of Ravensberg-Troisdorf, which gave us the opportunity to test our methodological proposal on a different Europe context.

RESUMEN ABREVIADO

El objetivo general de esta tesis doctoral es conocer los mecanismos de adquisición, gestión y distribución que las sociedades paleolíticas pusieron en práctica para explotar la cuarcita en la Región Cantábrica. Debido al escaso desarrollo en la caracterización de esta materia prima lítica en estudios previos, en este trabajo hemos caracterizado la cuarcita desde un punto de vista geo-arqueológico en este marco geográfico.

La metodología propuesta se articula en torno a tres escalas diferenciadas: la microscópica, la macroscópica y la regional. La primera se basa en la caracterización petrográfica, geoquímica y petrológica detallada mediante lupas de alta resolución. La segunda, la escala macroscópica, se fundamenta en la caracterización de las industrias líticas a partir de criterios tecnológicos, tipológicos, petrológicos y métricos. Dentro de esta misma escala de observación, caracterizamos las potenciales fuentes de adquisición de las cuarcitas en el medio geográfico mediante trabajo de campo a partir de la descripción de los estratos geológicos y los depósitos con presencia de cuarcitas. Finalmente, la escala regional, se basa en el análisis geográfico, geológico y arqueológico del terreno aplicando Sistemas de Información Geográfico.

La aplicación de esta metodología integral en una zona más acotada, los valles del Deva, Cares y Güeña, nos ha permitido entender la cuarcita desde un punto de vista geológico y arqueológico. Por un lado, hemos caracterizado el aporte sedimentario original de las cuarcitas, su transformación y las inclusiones minerales que esta roca ha recibido en los diferentes ambientes geológicos en los que ha estado presente. Esto nos ha permitido clasificar las cuarcitas en siete tipos basados en su génesis y múltiples variedades en función de los tamaños de los granos de cuarzo que componen masivamente la cuarcita y sus aportes minerales. Asimismo, hemos descrito los estratos geológicos en los que aparece y hemos caracterizado tanto su disposición como su dispersión teniendo en cuenta los tipos establecidos.

Por otro lado, a través del análisis de las industrias líticas de los niveles VI, XIII y XXII de El Esquilleu, del nivel Co.B.6 de Coimbre, de los yacimientos de El Habario y El Arteu y las evidencias líticas de la cueva con arte parietal de La Covaciella, hemos podido inferir las pautas de adquisición, gestión y distribución de la cuarcita en los valles del Deva, Cares y Güeña durante el Paleolítico medio y superior. Esto nos ha permitido observar las diferentes estrategias de gestión de un medio ambiente montañoso y heterogéneo como es la zona central de la Región Cantábrica. Finalmente, y con el objetivo de testar la metodología empleada, hemos analizado una parte de la colección lítica del yacimiento alemán de Ravensberg-Troisdorf.

Vitoria-Gasteiz, Septiembre de 2018